BIOCHEMICAL AND BIOPHYSICAL Research Communications

EDITORS

John N. Abelson
Ernesto Carafoli
Pedro Cuatrecasas
I. C. Gunsalus
B. L. Horecker
Yasuo Kagawa
M. Daniel Lane
William J. Lennarz
William D. McElroy
Masami Muramatsu
Claude Paoletti
Alberto Sols

Volume 156 • 1988

ACADEMIC PRESS, INC.
Harcourt Brace Jovanovich, Publishers
San Diego New York Boston
London Sydney Tokyo Toronto

Copyright © 1988 by Academic Press, Inc.

ALL RIGHTS RESERVED

No part of this publication may be reproduced or transmitted in any form, or by any means, electronic or mechanical, including photocopy, recording, or any information storage and retrieval system, without permission in writing from the copyright owner.

The appearance of the code at the bottom of the first page of an article in this journal indicates the copyright owner's consent that copies of the article may be made for personal or internal use, or for the personal or internal use of specific clients. This consent is given on the condition, however, that the copier pay the stated per copy fee through the Copyright Clearance Center, Inc. (27 Congress Street, Salem, Massachusetts 01970), for copying beyond that permitted by Sections 107 or 108 of the U.S. Copyright Law. This consent does not extend to other kinds of copying, such as copying for general distribution, for advertising or promotional purposes, for creating new collective works, or for resale. Copy fees for pre-1988 articles are as shown on the article title pages; if no fee code appears on the title page, the copy fee is the same as for current articles.

0006-291X/88 $1.50

MADE IN THE UNITED STATES OF AMERICA

BIOCHEMICAL AND BIOPHYSICAL RESEARCH COMMUNICATIONS

CONTENTS

Volume 156, Number 1, October 14, 1988

AUTHOR INDEX, Volume 156, Number 1, October 14, 1988 iii

HL-60 Cells Become Resistant toward Antitumor Ether-Linked Phospholipids following Differentiation into a Granulocytic Form *David S. Vallari, Zigrida L. Smith, and Fred Snyder* 1

Bis-Pyridoxal Polyphosphates: A New Class of Specific Intramolecular Crosslinking Agents for Hemoglobin *Ruth E. Benesch and Suzanna Kwong* 9

Physiological Concentrations of Atrial Natriuretic Factor Stimulate Human Erythroid Progenitors *in Vitro* *Eero Niskanen and Alex J. Baertschi* 15

Physicochemical Characterization of [^{3}H]DHEA Binding in Rat Liver *Mohammed Kalimi and William Regelson* 22

Proteolytic Activity in the Insulin Receptor *Eleazar C. Vega-SaenzdeMiera and Boanerges Rubalcava* 30

A Genuine Organ Specific Alcohol Dehydrogenase from Hamster Testes: Isolation, Characterization, and Developmental Changes *Wing-Ming Keung* 38

Anti-HLA Class I Monoclonal Antibody Effect on PKC Kinetics in PHA Activated Human Peripheral Blood Mononuclear and E^+ Cells *Licia Poltronieri, Edon Melloni, Michele Rubini, Rita Selvatici, Cristina Mazzilli, Roberto Baricordi, and Enrico Gandini* 46

Reconstitution of Partially Purified Opioid Receptors with a GTP-Binding Protein *Toshiyuki Fujioka, Fumiko Inoue, Sachiyo Sumita, and Masayuki Kuriyama* 54

Identification of a High-Affinity Receptor for Interleukin-1β in Rat Brain *Goro Katsuura, Paul E. Gottschall, and Akira Arimura* 61

Exon–Intron Organization of a Gene for Pregnancy-Specific β_1-Glycoprotein, a Subfamily Member of CEA Family: Implications for Its Characteristic Repetitive Domains and C-Terminal Sequences *Shinzo Oikawa, Chikako Inuzuka, Goro Kosaki, and Hiroshi Nakazato* 68

High Affinity Receptors for Atrial Natriuretic Factor in PC12 Cells *A. Rathinavelu and G. E. Isom* 78

Evidence for Light-Induced Lysine Conformational Changes during the Primary Event of the Bacteriorhodopsin Photocycle *Earl McMaster and Aaron Lewis* 86

Affinity Purification of Human Deoxycytidine Kinase: Avoidance of Structural and Kinetic Artifacts Arising from Limited Proteolysis *Min-Young Kim, Seiichiro Ikeda, and David H. Ives* 92

A Consensus Sequence in the N-Terminus of Exported Proteins: Resemblance with Metal Binding Domains and Implications in Protein Translocation across Membranes *Panagiotis A. Tsonis, Janusz M. Sowadski, and Paul F. Goetinck* 99

Mitogenic Activity in Ovine Uterine Fluids: Characterization of a Growth Factor Activity Which Specifically Stimulates Myoblast Proliferation *R. Curtis Bird, Frank F. Bartol, Harlow Daron, David A. Stringfellow, and M. Gatz Riddell* 108

Chemical Characterization by Protein Sequence Analysis of the Bovine Estrogen Receptor *Thomas Ratajczak, Martine J. Brockway, Roland Hähnel, Robert L. Moritz, and Richard J. Simpson* 116

Dermorphin Analogs: Resistance to *in Vitro* Enzymatic Degradation Is Not Always Increased by Additional D-Amino Acid Substitutions *Krzysztof Darlak, Deanne E. Benovitz, Arno F. Spatola, and Zbigniew Grzonka* 125

Almost Total Conversion of Pancreas to Liver in the Adult Rat: A Reliable Model to Study Transdifferentiation *M. S. Rao, R. S. Dwivedi, V. Subbarao, M. I. Usman, D. G. Scarpelli, M. R. Nemali, A. Yeldandi, S. Thangada, S. Kumar, and J. K. Reddy* 131

On the Mechanism of the Chromate Reduction by Glutathione: ESR Evidence for the Glutathionyl Radical and an Isolable Cr(V) Intermediate *Xianglin Shi and N. S. Dalal* 137

Rapid Purification of Inositol Monophosphate Phosphatase from Beef Brain *James L. Meek, Timothy J. Rice, and Elizabeth Anton* 143

Spacial Isolation of Protein Kinase C Activation in Thrombin Stimulated Human Platelets
Michael F. Crouch and Eduardo G. Lapetina 149
A Lecithin:Retinol Acyltransferase Activity in Human and Rat Liver
Paul N. MacDonald and David E. Ong 157
Brush Border Membrane Vesicles Formed from Human Duodenal Biopsies Exhibit Na^+-Dependent Concentrative L-Leucine and D-Glucose Uptake
James M. Harig, Konrad H. Soergel, Jeanne Barry, and Krishnamurthy Ramaswamy 164
Three Growth Hormone- and Two Prolactin-Related Novel Peptides of M_r 13,000–18,000 Identified in the Anterior Pituitary *Y. N. Sinha and B. P. Jacobsen* 171
Domain Structure of Cellobiohydrolase II as Studied by Small Angle X-Ray Scattering: Close Resemblance to Cellobiohydrolase I
Peter M. Abuja, Ingrid Pilz, Marc Claeyssens, and Peter Tomme 180
Endothelin and Ca^{2+} Agonist Bay K 8644: Different Vasoconstrictive Properties
Michel Auguet, Sylvie Delaflotte, Pierre-Etienne Chabrier, Eduardo Pirotzky, François Clostre, and Pierre Braquet 186
Calcimedin, Calelectrin: Correlation of Relatedness *Pamela B. Moore* 193
Growth Hormone-Dependent Insulin-like Growth Factor (IGF) Binding Protein Both Inhibits and Potentiates IGF-I-Stimulated DNA Synthesis in Human Skin Fibroblasts
John S. M. De Mellow and Robert C. Baxter 199
Synthesis of Nuclear Lamins in BHK-21 Cells Synchronized with Aphidicolin
Sylvain Foisy and Viviane Bibor-Hardy 205
Potassium Ion-Dependent Proton Efflux and Depolarization from Spleen Lysosomes
Yoshinori Moriyama 211
Release of Peptide Leukotrienes from Rat Kupffer Cells
Yoshihide Sakagami, Yasuhiro Mizoguchi, Shuichi Seki, Kenzo Kobayashi, Seiji Morisawa, and Sukeo Yamamoto 217
DNA-Binding Proteins in Protein Kinase C Preparations
Alessandro Testori, Charles S. T. Hii, Agnes Fournier, Leigh A. Burgoyne, and Andrew W. Murray 222
Water Immersion Increases the Concentration of the Immunoreactive N-Terminal Fragment of Proatrial Natriuretic Factor in Human Plasma
Alexander L. Gerbes and Angelika M. Vollmar 228
The Effect of Cyclosporin A on the Growth and Prolactin Binding to Nb-2 Rat Lymphoma Cells *Shobha Varma and Kurt E. Ebner* 233
Norepinephrine Stimulates the Production of Inositol Trisphosphate and Inositol Tetrakisphosphate in Rat Aorta *Vivian Pijuan and Irene Litosch* 240
Yeast *KEX2* Gene Encodes an Endopeptidase Homologous to Subtilisin-like Serine Proteases *Kensaku Mizuno, Tomoko Nakamura, Takehiro Ohshima, Shoji Tanaka, and Hisayuki Matsuo* 246
The Calcium Channel Antagonist ω-Conotoxin Inhibits Secretion from Peptidergic Nerve Terminals *G. Dayanithi, N. Martin-Moutot, S. Barlier, D. A. Colin, M. Kretz-Zaepfel, F. Couraud, and J. J. Nordmann* 255
Effect of Retinoic Acid on cAMP-Dependent Protein Phosphorylation in Psoriatic Fibroblasts *F. Raynaud, C. Liapi, P. Gerbaud, W. B. Anderson, and D. Evain-Brion* 263
The Transcription of the Interleukin 1β Gene Is Induced with PMA and Inhibited with Dexamethasone in U937 Cells *Tsutomu Nishida, Masaaki Takano, Takuma Kawakami, Naoki Nishino, Satoru Nakai, and Yoshikatsu Hirai* 269
Thyroid Hormone Action on Glucose Transporter Activity in Astrocytes
Lois M. Roeder, Irene B. Hopkins, Jeffrey R. Kaiser, Lea Hanukoglu, and J. Tyson Tildon 275
Purification and Characterization of a Cytochrome P450 Isozyme Isolated from the Liver of Rats Pretreated with Clofibrate *Liliane Kiffel, Chantal Célier, and Jean-Paul Leroux* 282
An Insulin Mediator Preparation Serves to Stimulate the Cyclic GMP Activated Cyclic AMP Phosphodiesterase Rather than Other Purified Insulin-Activated Cyclic AMP Phosphodiesterases *Nigel J. Pyne and Miles D. Houslay* 290
HIV-1 Protease Specificity of Peptide Cleavage Is Sufficient for Processing of gag and pol Polyproteins *Paul L. Darke, Ruth F. Nutt, Stephen F. Brady, Victor M. Garsky, Terrence M. Ciccarone, Chih-Tai Leu, Patricia K. Lumma, Roger M. Freidinger, Daniel F. Veber, and Irving S. Sigal* 297

Amino Acid Composition and Proteolytic Generated Domains of Higher Plant Tubulin
Pascal Picquot, Marylin Vantard, Iradj Amiri, Luc Fausser, and Anne-Marie Lambert 304

Does Endothelin Mobilize Calcium from Intracellular Store Sites in Rat Aortic Vascular Smooth Muscle Cells in Primary Culture?
Nobuco Miasiro, Hiromichi Yamamoto, Hideo Kanaide, and Motoomi Nakamura 312

Characterization of Two Glycoproteins of Human Pancreatic Juice: P35, a Truncated Protease E, and P19, Precursor of Protein X
O. Guy-Crotte, C. Barthe, D. Basso, B. Fournet, and C. Figarella 318

N-Acylated Pentapeptide Antagonists of Substance P on Guinea Pig Ileum
Pascal Schmitt, Michel Mayer, Sylviane Magneney, Robert Michelot, and Pierre Potier 323

Evidence that a GTP Binding Protein Regulates Phosphorylation of the CD3 Antigen in Human T Lymphocytes
Adelina A. Davies, J. Mark Hexham, Doreen A. Cantrell, and Michael J. Crumpton 328

A Novel Action of Activin A: Stimulation of Insulin Secretion in Rat Pancreatic Islets
Yasuo Totsuka, Mari Tabuchi, Itaru Kojima, Hiroshiro Shibai, and Etsuro Ogata 335

RNA Mediated Formation of a Phosphorothioate Diester Bond
Jamal M. Buzayan, Paul A. Feldstein, George Bruening, and Fritz Eckstein 340

Interaction between α1 and β1 Subunits of Human Hemoglobin
Yasuko Kawamura-Konishi and Haruo Suzuki 348

Isolation and Structural Determination of Rat Neuromedin U
Naoto Minamino, Kenji Kangawa, Mayumi Honzawa, and Hisayuki Matsuo 355

Different Types of ADP-Ribose Protein Bonds Formed by Botulinum C2 Toxin, Botulinum ADP-Ribosyltransferase C3, and Pertussis Toxin
Klaus Aktories, Ingo Just, and Walter Rosenthal 361

Identification of Glutathione *S*-Transferase as a Substrate and Glutathione as an Inhibitor of *in Vitro* Calmodulin-Stimulated Protein Methylation in Rat Liver Cytosol
Tom L. Neal, Lynda S. Wright, and Frank L. Siegel 368

Discrepancies between the Affinities of Binding and Action of the Novel β-Adrenergic Agonist BRL 37344 in Rat Brown Adipose Tissue
Patrick Muzzin, Josiane Seydoux, Jean-Paul Giacobino, John-Craig Venter, and Claire Fraser 375

Plasminogen Activator Inhibitor 2: Isolation and Characterization of the Promoter Region of the Gene
E. K. O. Kruithof and E. Cousin 383

Structure of the Human Blood Platelet Membrane Glycoprotein Ibα Gene
Roland H. Wenger, Nelly Kieffer, Andreas N. Wicki, and Kenneth J. Clemetson 389

Different Roles of the Diphosphate Moieties of Allylic and Homoallylic Diphosphates in Prenyltransferase Reaction
Takeshi Gotoh, Tanetoshi Koyama, and Kyozo Ogura 396

Saposin D: A Sphingomyelinase Activator
Satoshi Morimoto, Brian M. Martin, Yasuo Kishimoto, and John S. O'Brien 403

Lectins Inhibit Cell Binding and Spreading on a Laminin Substrate
John W. Dean III, S. Chandrasekaran, and Marvin L. Tanzer 411

Slipped DNA Structures within the Enhancer Region of the Moloney Murine Leukemia Virus
Miguel A. Gama Sosa, Jessica C. Hall, and Ruth M. Ruprecht 417

Cyclic AMP Decreases LDL Catabolism and Cholesterol Synthesis in the Human Hepatoma Cell Line HepG2
Cécile Maziere, Jean-Claude Maziere, Suzanne Salmon, Martine Auclair, Liliana Mora, Martine Moreau, and Jacques Polonovski 424

Antisera to an Amino-Terminal Peptide Detect the Amyloid Protein Precursor of Alzheimer's Disease and Recognize Senile Plaques
Mark R. Palmert, Marcia Berman Podlisny, Dennis S. Witker, Tilman Oltersdorf, Linda H. Younkin, Dennis J. Selkoe, and Steven G. Younkin 432

An Investigation of Human Oxyhemoglobin β Tetramer Dissociation Using Haptoglobin Binding
Linda A. Michalski and Melisenda J. McDonald 438

Partial Amino Acid Sequence Analysis of Human Placenta Monoamine Oxidase A and Bovine Liver Monoamine Oxidase B
Shiuan Chen and Walter Weyler 445

Ribulose 1,5-Bisphosphate-Dependent CO_2 Fixation in the Halophilic Archaebacterium, *Halobacterium mediterranei*
Nenoo Rawal, S. M. Kelkar, and Wijaya Altekar 451

Unregulated Secretion of an Exogenous Glycotripeptide by Rat Islets and HIT Cells
Gerald Gold, Felix T. Wieland, and Gerold M. Grodsky 457

IL1/ETAF Activity and Undetectable IL1β mRNA and Minimal IL1α mRNA Levels in Normal Adult Heat-Separated Epidermis
Stephen Demczuk 463

In Vitro Demonstration by the Rate Assay of the Presence of Small Pores in the Outer Membrane of *Pseudomonas aeruginosa*
Eisaku Yoshihara, Naomasa Gotoh, and Taiji Nakae 470
Fibrinogen Association with Human Monocytes: Evidence for Constitutive Expression of Fibrinogen Receptors and for Involvement of Mac-1 (CD18, CR3) in the Binding
Cristina Trezzini, Thomas W. Jungi, Peter Kuhnert, and Ernst Peterhans 477
Transient Accumulation of Inositol (1,3,4,5)-Tetrakisphosphate in Response to α_1-Adrenergic Stimulation in Adult Cardiac Myocytes
Guy P. Heathers, Peter B. Corr, and Leona J. Rubin 485
Evidence for a Differential Physiological Modulation of Brown Fat Iodothyronine 5′-Deiodinase Activity in the Perinatal Period
M. Giralt, I. Martin, T. Mampel, F. Villarroya, R. Iglesias, and O. Viñas 493
Characterization of Epitopes on the Cationic Peanut Peroxidase by Four Monoclonal Antibodies *Chunfang Hu and Robert B. van Huystee* 500
Paradoxical Protection of Both Protein-Free and High Protein Diets against Acute Ammonium Intoxication *Vicente Felipo, María-Dolores Miñana, and Santiago Grisolía* 506
Abscisic Acid Enhances Aggregation and Fusion of Phospholipid Vesicles
William Stillwell, Blair Brengle, and Stephen R. Wassall 511
Molecular Cloning of the Nosiheptide Resistance Gene from *Streptomyces actuosus* ATCC 25421 *Donald C. Dosch, William R. Strohl, and Heinz G. Floss* 517
15-Hydroxyeicosatetraenoic Acid Dehydrogenase Activity in Microsomal Fraction of Mouse Liver Homogenate *Dai-Eun Sok, Jun Bu Kang, and Hong Dae Shin* 524
Sites of Modification of Human Angiogenin by Bromoacetate at pH 5.5
Robert Shapiro, Daniel J. Strydom, Stanislawa Weremowicz, and Bert L. Vallee 530
Site-Directed Mutagenesis at the Regulatory Site of Fructose-6-phosphate 1-Kinase from *Bacillus stearothermophilus* *B. C. Valdez, S. H. Chang, and E. S. Younathan* 537
Biosynthesis of 12-Oxo-10,15(Z)-phytodienoic Acid: Identification of an Allene Oxide Cyclase *Mats Hamberg* 543
Enterotoxin of *Clostridium perfringens* Type A Forms Ion-Permeable Channels in a Lipid Bilayer Membrane *Nakaba Sugimoto, Masayuki Takagi, Kunihiro Ozutsumi, Shigeko Harada, and Morihiro Matsuda* 551
Excision Repair in Xeroderma Pigmentosum Group C Cells Is Regulated Differently in Transformed Cells and Primary Fibroblasts *James E. Cleaver* 557
Evidence for the Expression of a Primitive Intestinal-like Alkaline Phosphatase in the Intestinal 407 Cell Line *Kazuyuki Hirano, Tomikazu Kusano, Kentaro Asai, Kyozo Hayashi, Torgny Stigbrand, Shiro Iino, and Jose L. Millan* 563
Insulin and Glucose Modulate Protein Kinase C Activity in Rat Adipocytes
Boris Draznin, J. Wayne Leitner, Karl E. Sussman, and Nancy A. Sherman 570
The Complete Nucleotide Sequence of Human Liver Cytochrome b_5 mRNA
Min Yoo and Alan W. Steggles 576
Apolipoprotein B-100 Is the Major Form of This Apolipoprotein Secreted by Human Intestinal Caco-2 Cells *Diana M. Lee, Nassrin Dashti, and Tina Mok* 581
Heterologous Up-Regulation of the 1,25-Dihydroxyvitamin D_3 Receptor by Parathyroid Hormone (PTH) and PTH-like Peptide in Osteoblast-like Cells
H. A. P. Pols, J. P. T. M. van Leeuwen, J. P. Schilte, T. J. Visser, and J. C. Birkenhäger 588
Isolation of the Human Platelet Glycoprotein IIb Gene and Characterization of the 5′ Flanking Region *M. H. Prandini, E. Denarier, P. Frachet, G. Uzan, and G. Marguerie* 595
Purification of the D-2 Dopamine Receptor from Bovine Striatum
Zvulun Elazar, Hannah Kanety, Carol David, and Sara Fuchs 602
ERRATUM
Volume 154, Number 2, July 29, 1988: A. Pietrangelo, A. Cossarizza, D. Monti, E. Ventura, and C. Franceschi, "DNA Repair in Lymphocytes from Humans and Rats with Chronic Iron Overload," pp. 698–704 610

Volume 156, Number 2, October 31, 1988

AUTHOR INDEX, Volume 156, Number 2, October 31, 1988 iii
Basic Fibroblast Growth Factor (FGF) Promotes Cartilage Repair *in Vivo*
Pedro Cuevas, Jesus Burgos, and Andrew Baird 611

rial Natriuretic Peptide Gene Expression and Its Secretion by Pneumocytes Derived from Neonatal Rat Lungs *Hiroaki Matsubara, Yasukiyo Mori, Yukihisa Umeda, Shinzo Oikawa, Hiroshi Nakazato, and Mitsuo Inada* 619

bcellular Distribution of Protein Kinase C in Rat Adrenal Glomerulosa Cells *Anna Faragó, János Seprődi, and András Spät* 628

problast Growth Factor Regulates the Expression of Luteinizing Hormone Receptors in Cultured Rat Granulosa Cells *Florence Oury and Jean-Marie Darbon* 634

23187 and Protein Kinase C Activators Stimulate Phosphatidylinositol Metabolism and Prostaglandin Synthesis in a Human Lung Cancer Cell Line *Bruce E. Rapuano and Richard S. Bockman* 644

odulation of Glycogen Synthase Kinase Activity of Skeletal and Smooth Muscle Casein Kinase I by Spermine *Mohammed G. Hegazy, Keith K. Schlender, Erwin M. Reimann, and Joseph DiSalvo* 653

oning and Characterization of a cDNA Encoding Bovine Endonexin (Chromobindin 4) *Helen C. Hamman, Lynn C. Gaffey, Kevin R. Lynch, and Carl E. Creutz* 660

duction of Follicle Stimulating Hormone Receptor by Erythroid Differentiation Factor on Rat Granulosa Cell *Yoshihisa Hasegawa, Kaoru Miyamoto, Yumiko Abe, Takanori Nakamura, Hiromu Sugino, Yuzuru Eto, Hiroshiro Shibai, and Masao Igarashi* 668

Histone 1-like Antigen Is a Component of the Nuclear Envelope *Jaya T. Venkatraman, J. Gohill, Marvin J. Fritzler, and Yvonne A. Lefebvre* 675

our Species of cDNAs for Cytochrome P450 Isozymes Immunorelated to P450C-M/F Encode for Members of P450IID Subfamily, Increasing the Number of Members within the Subfamily *Nobuhiro Ishida, Yasunori Tawaragi, Chikako Inuzuka, Osamu Sugita, Ichiro Kubota, Hiroshi Nakazato, Teruhisa Noguchi, and Shigeru Sassa* 681

hibitors of Sterol Synthesis. Exogenous Oleate Reduces the Inhibitory Effect of 5α-Cholest-8(14)-en-3β-ol-15-one on the Growth of CHO-K1 Cells *Frederick D. Pinkerton, Nanda Duhé Kirkpatrick, and George J. Schroepfer, Jr.* 689

Mutation Affecting Peptide Bond Formation in Nikkomycin Biosynthesis *P. Engel and A. H. J. Ullah* 695

Mapping of a DNA Sequence that Down-Regulates the Expression of an Interferon-Induced Gene *Hiroaki Akai and Andrew C. Larner* 701

Effect of Diabetes on Guanine Nucleotide Exchange Factor Activity in Skeletal Muscle and Heart *S. R. Kimball and L. S. Jefferson* 706

Retinoic Acid Rapidly Induces Lung Cellular Retinol-Binding Protein mRNA Levels in Retinol Deficient Rats *Riaz ul Haq and Frank Chytil* 712

Diacylglycerol Provides Arachidonic Acid for Lipoxygenase Products that Mediate Angiotensin II-Induced Aldosterone Synthesis *Rama Natarajan, Naftali Stern, and Jerry Nadler* 717

Cloning of a Complete cDNA Encoding Human Aromatase: Immunochemical Identification and Sequence Analysis *Nobuhiro Harada* 725

Control of Misincorporation of *de Novo* Synthesized Norleucine into Recombinant Interleukin-2 in *Escherichia coli* *Larry B. Tsai, Hsieng S. Lu, William C. Kenney, Craig C. Curless, Michael L. Klein, Por-Hsiung Lai, Dennis M. Fenton, Bruce W. Altrock, and Michael B. Mann* 733

The Primary Structure of the Lymphocyte Pore-Forming Protein Perforin: Partial Amino Acid Sequencing and Determination of Isoelectric Point *Pedro M. Persechini and John Ding-E Young* 740

Calcium-Stimulated ATPase Activity in Plasma Membrane Vesicles from Pancreatic Acinar Cells *Duane L. Ochs, Denise M. Belanger, and Joan Kalnitsky-Aliff* 746

Infrared Spectroscopy of a Single Cell: The Human Erythrocyte *Aichun Dong, Robert G. Messerschmidt, John A. Reffner, and Winslow S. Caughey* 752

Immunological Detection of G-Protein α-Subunits in *Dictyostelium discoideum* *B. Ewa Snaar-Jagalska, Fanja Kesbeke, Maureen Pupillo, and Peter J. M. Van Haastert* 757

Variant Apolipoprotein AI as a Major Constituent of a Human Hereditary Amyloid *William C. Nichols, Francis E. Dwulet, Juris Liepnieks, and Merrill D. Benson* 762

ATP-Sensitive K^+ Channels May Control Glucose-Induced Electrical Activity in Pancreatic B-Cells *Jean-Claude Henquin* 769

Prolactin Differentially Affects Bacterial Toxin-Induced ADP-Ribosylation of Nb_2 Lymphoma Cell Membrane Proteins *Ronnie J. Barkey, Juan C. Calvo, and Maria L. Dufau* 776

Recognition of Insulin-like Growth Factor (IGF) Serum Binding Proteins by an Antibody Raised against a Specific IGF-Inhibitor *Guck T. Ooi and Adrian C. Herington* 783

A Simple Formula for Solvent-Accessible Areas of Amino Acid Side-Chains *Richard Cowan* 792

Ouabain Sensitivity of the α 3 Isozyme of Rat Na,K-ATPase *Osamu Urayama and Kathleen J. Sweadner* 796

Differential Sensitivity of Neural and Non-neural Protein Kinase Isozymes to Cyclic AMP *Deepak Bhatnagar, Andrew A. Burton, and Robert Roskoski, Jr.* 801

Identification of Unusual Replacement of Methionine by Norleucine in Recombinant Interleukin-2 Produced by *Escherichia coli* *Hsieng S. Lu, Larry B. Tsai William C. Kenney, and Por-Hsiung Lai* 807

Structure of the Mouse C-Reactive Protein Gene *Shuji Ohnishi, Shuichiro Maeda, Seiji Nishiguchi, Tatsuyoshi Arao, and Kazunori Shimada* 814

Interrelation of Platelet Aggregation, Release Reaction, and Thromboxane A_2 Production *Carlo L. Balduini, Giampiera Bertolino, Patrizia Noris, Fabiola Sinigaglia, Antonella Bisio, and Mauro Torti* 823

Post-transcriptional Control of IL-1 Gene Expression in the Acute Monocytic Leukemia Line THP-1 *Martin Turner, David Chantry, and Marc Feldmann* 830

Age and Sex Related Changes of Plasma Membrane Fluidity in Isolated Rat Hepatocytes *Antonio Benedetti, Gianna Ferretti, Giovanna Curatola, Anne Marie Jézéquel, and Francesco Orlandi* 840

Platelet-Derived Growth Factor (PDGF)-Induced Phospholipase C-Mediated Hydrolysis of Phosphoinositides in Vascular Smooth Muscle Cells: Different Sensitivity of PDGF- and Angiotensin II-Induced Phospholipase C Reactions to Protein Kinase C-Activating Phorbol Esters *Yasuhiro Kawahara, Ken-ichi Kariya, Shun-ichi Araki, Hisashi Fukuzaki, and Yoshimi Takai* 846

Tosyl-lysyl Chloromethylketone Detects Conformational Changes in the Catalytic Unit of Adenylate Cyclase Induced by Receptor and G-Protein Stimulation *Lindsey Needham and Miles D. Houslay* 855

Synthetic Peptides Based on the Calmodulin-Binding Domain of Myosin Light Chain Kinase Inhibit Activation of Other Calmodulin-Dependent Enzymes *Donald K. Blumenthal, Harry Charbonneau, Arthur M. Edelman, Thomas R. Hinds, Gary B. Rosenberg, Daniel R. Storm, Frank F. Vincenzi, Joseph A. Beavo, and Edwin G. Krebs* 860

Rat Liver Carboxylesterase: cDNA Cloning, Sequencing, and Evidence for a Multigene Family *Rochelle M. Long, Hiroko Satoh, Brian M. Martin, Shioko Kimura, Frank J. Gonzalez, and Lance R. Phol* 866

Molecular Cloning and Nucleotide Sequence of Murine 2,3-Bisphosphoglycerate Mutase cDNA *P. Le Boulch, V. Joulin, M-C. Garel, J. Rosa, and M. Cohen-Solal* 874

Muramyl Dipeptide-Elicited Production of PGD_2 from Astrocytes in Culture *Kozo Yamamoto, Toshiaki Miwa, Ryuji Ueno, and Osamu Hayaishi* 882

Small Molecular Weight GTP-Binding Proteins in Human Erythrocyte Ghosts *Kazuto Ikeda, Akira Kikuchi, and Yoshimi Takai* 889

Processing of the Oxytocin Precursor: Isolation of an Exopeptidase from Neurosecretory Granules of Bovine Pituitaries *Ursel Nörenberg and Dietmar Richter* 898

Inhibition of α_2-Adrenergic Receptor-Mediated Cyclic GMP Formation by a Phorbol Ester, a Protein Kinase C Activator *Rama K. Jaiswal and Rameshwar K. Sharma* 905

Facile Analysis and Purification of Deblocked N-Terminal Pyroglutamyl Peptides with a Strong Cation-Exchange Sulfoethyl Aspartamide Column *Dan L. Crimmins, Dave W. McCourt, and Benjamin D. Schwartz* 910

Sucrose Feeding Prevents Changes in Myosin Isoenzymes and Sarcoplasmic Reticulum Ca^{2+}-Pump ATPase in Pressure-Loaded Rat Heart *Heinz Rupp, Vijayan Elimban, and Naranjan S. Dhalla* 917

Differential Effects of Norepinephrine and Phorbol Ester on α-1 Adrenergic Receptor Number and Surface-Accessibility in DDT_1 MF-2 Cells *Wilson S. Colucci, Marjorie Akers, and Gwendolyn M. Wise* 924

Isolation and Characterization of Human Platelet Glycoprotein IX *Gerald J. Roth, Juris Ozols, Diane J. Nugent, and Stuart A. Williams* 931

hanges in Intracellular Redox and Energy Status during Induced Transplasma Membrane Electron Transport in *Cuscuta* Protoplasts *Shalini Revis and Prakash C. Misra* 940

elective Inhibition of Free Arachidonic Acid Production in Activated Alveolar Macrophages by Calmodulin Antagonists *Yasuhito Nakagawa and Keizo Waku* 947

lentification of GTP-Binding Proteins in the Plasma Membrane of Higher Plants *W. Blum, K.-D. Hinsch, G. Schultz, and E. W. Weiler* 954

bsorption of Eicosapentaenoic Acid and Docosahexaenoic Acid from Fish Oil Triacylglycerols or Fish Oil Ethyl Esters Coingested with a High-Fat Meal *Larry D. Lawson and Bronwyn G. Hughes* 960

olation and Characterization of a Bovine Liver Tryosine-O-Sulfate-Binding Protein: A Putative Receptor Molecule for Tyrosine-Sulfated Proteins? *Ming-Cheh Liu, Masahito Suiko, and Xibai Tang* 964

uman Erythrocytes Cross-Linked with Glutaraldehyde: General Properties and Significance as a Blood Substitute *A. Bellelli, P. L. Benedetti, M. Coletta, R. Ippoliti, and M. Brunori* 970

crease in the ADP/ATP Exchange in Rat Liver Mitochondria Irradiated *in Vitro* by Helium–Neon Laser *Salvatore Passarella, Angela Ostuni, Anna Atlante, and Ernesto Quagliariello* 978

loning and Sequencing of a cDNA for Human Mitochondrial Ubiquinone-Binding Protein of Complex III *Hiroshi Suzuki, Yoshitaka Hosokawa, Haruo Toda. Morimitsu Nishikimi, and Takayuki Ozawa* 987

duction of Poly(ADP-Ribose) Polymerase Gene Expression in Lectin-Stimulated Human T Lymphocytes Is Dependent on Protein Synthesis *Marta Menegazzi, Franca Gelosa, Marina Tommasi, Kazuhiko Uchida, Masanao Miwa, Takashi Sugimura, and Hisanori Suzuki* 995

trial Natriuretic Peptide Receptors Are Present in Brown Adipose Tissue *H. Okamura, P. A. Kelly, J. G. Chabot, G. Morel, M. Belles-Isles, and S. Heisler* 1000

dditive Effects of IL-1 and TNF on Induction of Prostacyclin Synthesis in Human Vascular Endothelial Cells *Hirahito Endo, Tohru Akahoshi, and Sadao Kashiwazaki* 1007

M2-Gangliosidosis B1 Variant: A Wide Geographic and Ethnic Distribution of the Specific β-Hexosaminidase α Chain Mutation Originally Identified in a Puerto Rican Patient *Akemi Tanaka, Kousaku Ohno, and Kunihiko Suzuki* 1015

latelet Aggregation Is Inhibited by Long Chain Acyl-CoA *I. Lascu, B. Edwards, M. P. Cucuianu, and D. W. Deamer* 1020

haracterization of Receptor for Granulocyte Colony-Stimulating Factor on Human Circulating Neutrophils *H. Uzumaki, T. Okabe, N. Sasaki, K. Hagiwara, F. Takaku, and S. Itoh* 1026

Photocrosslinking of Calmodulin and/or Actin to Chicken Gizzard Caldesmon *Chih-Lueh Albert Wang* 1033

Isolation of a cDNA Clone for the α Subunit of the Human GABA-A Receptor *Kennon M. Garrett, Ronald S. Duman, Naoaki Saito, Arthur J. Blume, Michael P. Vitek, and John F. Tallman* 1039

Potent and Selective Activity of a New Carbocyclic Nucleoside Analog (Carbovir: NSC 614846) against Human Immunodeficiency Virus *in Vitro* *Robert Vince, Mei Hua, Jay Brownell, Susan Daluge, Fangchen Lee, William M. Shannon, George C. Lavelle, Jeanine Qualls, Owen S. Weislow, Rebecca Kiser, Peter G. Canonico, Robert H. Schultz, V. L. Narayanan, Joseph G. Mayo, Robert H. Shoemaker, and Michael R. Boyd* 1046

Human Placental Endonuclease Cleaves Holliday Junctions *R. Jeyaseelan and G. Shanmugam* 1054

ERRATUM

Volume 154, Number 3, August 15, 1988: Ilona Gruda, Eric Gauthier, Svetlana Elberg, Janina Brajtburg, and Gerald Medoff, "Effects of the Detergent Sucrose Monolaurate on Binding of Amphotericin B to Sterols and Its Toxicity for Cells," pp. 954–958 1061

Volume 156, Number 3, November 15, 1988

AUTHOR INDEX, Volume 156, Number 3, November 15, 1988 iii

Evidence of Gene Amplification in Tunicamycin-Resistant Chinese Hamster Ovary Cells *Jane R. Scocca, Karin O. Hartog, and Sharon S. Krag* 1063

Effects of Atrial Natriuretic Factor on Urinary Concentration of Catecholamines and Renin Secretion in Dogs *J. R. Sowers, P. K. Mohanty, M. D. Thames, D. S. Goldstein, and S. Atlas* 1070
Defective Formation of Inositol 1,4,5-Triphosphate in Bradykinin-Stimulated Fibroblasts from Progressive Systemic Sclerotic Patients *Mariko Seishima, Yukihiro Yada, Seiji Nagao, Shunji Mori, and Yoshinori Nozawa* 1077
NAD(P)H-Dependent Reduction of 12-Ketoeicosatetraenoic Acid to 12(R)- and 12(S)-Hydroxyeicosatetraenoic Acid by Rat Liver Microsomes *Jean-Pierre Falgueyret, Yves Leblanc, Joshua Rokach, and Denis Riendeau* 1083
Phosphatidylethanol Formation in Human Platelets: Evidence for Thrombin-Induced Activation of Phospholipase D *Raphael Rubin* 1090
The Heat Shock Response of *Neurospora crassa:* Stress-Induced Thermotolerance in Relation to Peroxidase and Superoxide Dismutase Levels *M. Kapoor and G. M. Sveenivasan* 1097
Expression and Characterization of Recombinant Human Angiotensinogen in a Heterologous Eukaryotic Cell Line *Lei Wei, Isabelle Gaillard, Pierre Corvol, and Eric Clauser* 1103
Light-Induced Phosphoinositide Degradation and Light-Induced Structural Alterations in the Rat Retina Are Enhanced after Chronic Lithium Treatment *J. Pfeilschifter, Ch. Remé, and C. Dietrich* 1111
Reaction Products of a New Anticancer Agent, Pt(IV)(Cyclohexyldiamine)Cl_4, with Guanosine and 9-Methylguanine: First Crystal Structures of Pt(Cyclohexyldiamine) Complexes with a Nucleobase and a Nucleoside *Hok-Kin Choi, Aristidis Terzis, Raymond C. Stevens, Robert Bau, Rudiger Haugwitz, V. L. Narayanan, and Mary Wolpert-DeFilippes* 1120
Octahedral Complexes of Anticancer Pt(IV)(Cyclohexyldiamine) Agents with 9-Methylguanine *Hok-Kin Choi, Sharon Kuei-Shang Huang, and Robert Bau* 1125
Glutamate Synthase in *Medicago sativa* L. Occurrence and Properties of Fd-Dependent Enzyme in Plant Cell Fraction during Root Nodule Development *Akira Suzuki, Elisa Carrayol, Claire Zehnacker, and Marie-Esther Deroche* 1130
Enhancement of Intracellular Calcium Concentration by Extracellular ATP and UPT in Madin Darby Canine Kidney Cells *M. Paulmichl and F. Lang* 1139
Inhibition of Duck Hepatitis B Virus Replication by Purine 2′,3′-Dideoxynucleosides *Satoru Suzuki, Bonita Lee, Weixing Luo, Dorothy Tovell, Morris J. Robins, and David L. J. Tyrrell* 1144
Spatial Distribution and Temporal Change of Cytoplasmic Free Calcium in Human Platelets *Yasuhiro Tsunoda, Kazuhiko Matsuno, and Yutaka Tashiro* 1152
ADP-Ribosylation of Bovine S-Antigen by Cholera Toxin *Naoka Komori, Maureen A. Rider, Dolores J. Takemoto, Hitoshi Shichi, and Hiroyuki Matsumoto* 1160
Expression of the Rat Growth Hormone Gene in Transfected CV-1 Cells *David S. Howland, W. C. Hymer, and William D. Taylor* 1166
Superoxide Anion Measurement by Sulfonated Phenyl Isothiocyanate Cytochrome C *Françoise Morel, Anne-Christine Dianoux, and Pierre V. Vignais* 1175
Structure-Activity Relationships of Endothelin: Importance of the C-Terminal Moiety *Sadao Kimura, Yoshitoshi Kasuya, Tatsuya Sawamura, Osamu Shinmi, Yoshiki Sugita, Masashi Yanagisawa, Katsutoshi Goto, and Tomoh Masaki* 1182
Isolation and NH_2-Terminal Amino Acid Sequences of Rat Serum Carrier Proteins for Insulin-like Growth Factors *Jürgen Zapf, Walter Born, Jui-Yoa Chang, Peter James, E. Rudolf Froesch, and Jan A. Fischer with the technical assistance of Christina Hauri, Margaretha Waldvogel, and Else-Marie Pedersen* 1187
Role of Calcium in the Potentiating Effect of Phorbol Ester on KC1-Induced Vasocontraction *Ichiro Wakabayashi, Eizo Kakishita, Katsuhiko Hatake, Shigeru Hishida, and Kiyoyasu Nagai* 1195
Carboxyl Residue(s) at the Ligand-Binding Site of Rat Muscarinic Receptors *Ronit Galron and Mordechai Sokolovsky* 1203
Interleukin-1 α and β Induce Interleukin-1 β Gene Expression in Human Dermal Fibroblasts *Alain Mauviel, Nathalie Temime, Dominique Charron, Gérard Loyau, and Jean-Pierre Pujol* 1209
Partial Covalent Labeling with Pyridoxal 5′-Phosphate Induces Bis(sulfosuccinimidyl)suberate Crosslinking of Band 3 Protein Tetramers in Intact Human Red Blood Cells *James M. Salhany and Renee L. Sloan* 1215

mparison of Two Independent cDNA Clones Reported to Encode β1,4 Galactosyltransferase
Linda C. Lopez and Barry D. Shur 1223

ochemical and Immunological Similarity of Soluble Angiotensin II-Binding Proteins in Different Organs *Elizabeth Rosenberg, Carlo Russo, M. A. Ravi Kiron, and Richard L. Soffer* 1230

oactivity of Synthetic Human Pancreastatin on Exocrine Pancreas
Akihiro Funakoshi, Kyoko Miyasaka, Rieko Nakamura, Kenichi Kitani, Susumu Funakoshi, Hirokazu Tamamura, Nobutaka Fujii, and Haruaki Yajima 1237

cumulation of 1-Methyl-4 Phenylpyridinium (MPP^+) into Bovine Chromaffin Granules Results in a Large Restriction of Its Molecular Motion: A ^{13}C and ^{31}P NMR Study
A. J. Daniels, J. F. Reinhard, Jr., and G. R. Painter 1243

e Antiproliferative Effects of Staurosporine Are Not Exclusively Mediated by Inhibition of Protein Kinase C *Charles D. Smith, J. Fraser Glickman, and Kwen-Jen Chang* 1250

orbol Ester Treatment Inhibits Thrombin but Not Stable GTP Analog-Induced Platelet Granule Secretion despite Inhibition of Phosphatidate Formation with Both Agonists
Sushila Krishnamurthi and Vijay V. Kakkar 1257

eletion of a Homeobox Gene in Myeloid Leukemias with a Deletion in Chromosome 2
Cila Blatt and Leo Sachs 1265

vidence for Impaired Subunit Interaction in Chemically Deglycosylated Human Choriogonadotropin *Wolfgang E. Merz* 1271

irect Coupling of a G-Protein to Dihydropyridine Binding Sites
Stefania Bergamaschi, Stefano Govoni, Paola Cominetti, Marco Parenti, and Marco Trabucchi 1279

duction of an *Alu*-Sequence Containing Transcript by Insulin in Human Hepatoma Cells
Lee-Ming Chuang, Boniface J. Lin, Sheng-Chung Lee, Tong-Yuan Tai, and Ding-Shinn Chen 1287

latelet Activating Factor Is a Potent Stimulant of the Production of Active Oxygen Species by Human Monocyte-Derived Macrophages
Mustapha Rouis, Fabienne Nigon, and M. John Chapman 1293

he Effect of Doxorubicin on the Transport of Pyruvate in Rat-Heart Mitochondria
Giuseppe Paradies and Francesca Maria Ruggiero 1302

ynthesis of Prostaglandins and Eicosanoids by the Mast Cell Secretory Granule
Stephen P. Chock and Elsa A. Schmauder-Chock 1308

orskolin and Prostacyclin Inhibit Fluoride Induced Platelet Activation and Protein Kinase C Dependent Responses *M. Gabriella Doni, Renzo Deana, Stefano Bertoncello, Franco Zoccarato, and Adolfo Alexandre* 1316

Targets for Calcium Channel Blockers in Mammalian Skeletal Muscle and Their Respective Functions in Excitation–Contraction Coupling *Georges Romey, Luis Garcia, François Rieger, and Michel Lazdunski* 1324

Phosphorylation of Calmodulin on Threonine Residue(s) by Cytosol Prepared from the Adrenal Cortex *Mitsumasa Kubo and Charles A. Strott* 1333

Monokine-Induced Gene Expression of a Human Endothelial Cell-Derived Neutrophil Chemotactic Factor *R. M. Strieter, S. L. Kunkel, H. J. Showell, and R. M. Marks* 1340

Epidermal Growth Factor and Insulin-like Growth Factor-I Stimulate the Hydrolysis of the Insulin-Sensitive Phosphatidylinositol-Glycan in BC3H-1 Myocytes
Robert V. Farese, Govindan P. Nair, Mary L. Standaert, and Denise R. Cooper 1346

Detection of an ATPase Activity in Rat Liver Peroxisomes
Ruth del Valle, Ubaldo Soto, Cecilia Necochea, and Federico Leighton 1353

Early and Late Heat-Induced Proteins during *Leishmania mexicana* Transformation
Antonio Alcina and Manuel Fresno 1360

Progesterone-Dependent Binding of a *trans*-Acting Factor to the Uteroglobin Promoter
V. Rider and D. W. Bullock 1368

Temperature-Dependent Inhibition of fMet-Leu-Phe-Stimulated Superoxide Generation by C-I and H-7 in Human Neutrophils *Jayasree Nath and Annette Powledge* 1376

A Novel Bombesin Receptor Antagonist Inhibits Autocrine Signals in a Small Cell Lung Carcinoma Cell Line *Jane B. Trepel, James D. Moyer, Frank Cuttitta, Harold Frucht, David H. Coy, Ronald B. Natale, James L. Mulshine, Robert T. Jensen, and Edward A. Sausville* 1383

Nucleolin (C23), a Physiological Substrate for Casein Kinase II
Helge R. Schneider and Olaf-Georg Issinger 1390

Immunoprecipitation of the *in Vitro* Translation Product of Rabbit Muscle Protein Phosphatase C-I MRNA *Shi Yan Zheng and Ernest Y. C. Lee* 1398

Cloning, Nucleotide Sequence, and Molecular Evolution of a Rabbit Processed Metallothionein MT-2 Pseudogene *You C. Tam, Manuel Hassan, Arvind Chopra, and Jean-Paul Thirion* 1403

The Effect of Fetal Calf Serum on Intracellular Calcium in GH_3 Cells *I. J. Wrench, T. J. Brown, B. L. Brown, and P. R. M. Dobson* 1411

ERRATA

Volume 154, Number 3, August 15, 1988: G. A. McClarty, P. N. Tonin, P. R. Scrinivasan, and J. A. Wright, "Relationships between Reversion of Hydrooxyurea Resistance in Hamster Cells and the Co-Amplification of Ribonucleotide Reductase M2 Component, Ornithine Decarboxylase and P5-8 Genes," pp. 975–981 1419

Volume 155, Number 1, August 31, 1988: Kan Tanaka, Hiuga Saito, Motoo Arai, Sawao Murao, and Hideo Takahashi, "Cloning and Expression of the Metalloproteinase Inhibitor (S-MPI) Gene from *Streptomyces nigrescens*," pp. 487–492 1419

Volume 155, Number 3, September 30, 1988: Masanori Tsukuda, Yoshinori Asaoka, Kazuo Sekiguchi, Ushio Kikkawa, and Yasutomi Nishizuka, "Properties of Protein Kinase C Subspecies in Human Platelets," pp. 1387–1395 1420

ISSN 0006-291X

Volume 156, Number 1, October 14, 1988
Pages 1–610

BIOCHEMICAL AND BIOPHYSICAL Research Communications

EDITORS

John N. Abelson
Ernesto Carafoli
Pedro Cuatrecasas
I. C. Gunsalus
B. L. Horecker
Yasuo Kagawa
M. Daniel Lane
William J. Lennarz
William D. McElroy
Masami Muramatsu
Claude Paoletti
Alberto Sols

DICAL
H
01
358
BRARY

[redacted]

ACADEMIC PRESS, INC.
Harcourt Brace Jovanovich, Publishers
San Diego New York Boston

BIOCHEMICAL AND BIOPHYSICAL
RESEARCH COMMUNICATIONS

Manuscripts should be sent to one of the following editors:

JOHN N. ABELSON
Division of Biology 147–75
California Institute of Technology
Pasadena, California 91125

ERNESTO CARAFOLI
Laboratorium für Biochemie
ETH-Zentrum
CH-8092 Zurich, Switzerland

PEDRO CUATRECASAS
Department of Research and
Development
Glaxo, Inc.
5 Moore Drive
Research Triangle Park
North Carolina 27709

I. C. GUNSALUS
420 RAL, 1209 W. California
University of Illinois
Urbana, Illinois 61801

B. L. HORECKER
Room F-104
Cornell University Medical College
1300 York Avenue
New York, New York 10021

YASUO KAGAWA
Department of Biochemistry
Jichi Medical School
Minamikawachi-Machi Kawachi-gun
Tochigi-ken 329-04, Japan

M. DANIEL LANE
Department of Biological Chemistry
The Johns Hopkins University
725 No. Wolfe Street
Baltimore, Maryland 21205

WILLIAM J. LENNARZ
Department of Biochemistry and
Molecular Biology (Box 117)
University of Texas System
Cancer Center
M.D. Anderson Hospital and
Tumor Institute
1515 Holcombe Boulevard
Houston, Texas 77030

WILLIAM D. McELROY
Department of Biology, B-022
University of California,
San Diego
La Jolla, California 92093

MASAMI MURAMATSU
Department of Biochemistry
The University of Tokyo
Hongo, Bunkyo-ku
Tokyo 113, Japan

CLAUDE PAOLETTI
Laboratoire de Biochimie
INSERM-CNRS
Institut Gustave-Roussy
Rue Camille Desmoulins
94805 Villejuif, France

ALBERTO SOLS
Instituto Investigaciones
Biomédicas CSIC
Facultad de Medicina UAM
Arzobispo Morcillo 4
28029 Madrid, Spain

BIOCHEMICAL AND BIOPHYSICAL

RESEARCH COMMUNICATIONS

Volume 156, Number 1, October 14, 1988

Copyright © 1988 by Academic Press, Inc.

ALL RIGHTS RESERVED

No part of this publication may be reproduced or transmitted in any form, or by any means, electronic or mechanical, including photocopy, recording, or any information storage and retrieval system, without permission in writing from the copyright owner.

The appearance of the code at the bottom of the first page of an article in this journal indicates the copyright owner's consent that copies of the article may be made for personal or internal use, or for the personal or internal use of specific clients. This consent is given on the condition, however, that the copier pay the stated per copy fee through the Copyright Clearance Center, Inc. (27 Congress Street, Salem, Massachusetts 01970), for copying beyond that permitted by Sections 107 or 108 of the U.S. Copyright Law. This consent does not extend to other kinds of copying, such as copying for general distribution, for advertising or promotional purposes, for creating new collective works, or for resale. Copy fees for pre-1988 articles are as shown on the article title pages; if no fee code appears on the title page, the copy fee is the same as for current articles.

0006-291X/88 $1.50

MADE IN THE UNITED STATES OF AMERICA

BIOCHEMICAL AND BIOPHYSICAL RESEARCH COMMUNICATIONS
(ISSN 0006-291X)

Published semimonthly by Academic Press, Inc., 1 East First Street, Duluth, MN 55802

1988: Volumes 150–157. Price: $680.00 U.S.A. and Canada: $805.00 all other countries

1989: Volumes 158–165. Price: $712.00 U.S.A. and Canada; $879.00 all other countries

All prices include postage and handling.

Information concerning personal subscription rates may be obtained by writing to the Publishers. All correspondence and subscription orders should be addressed to the office of the Publishers at 1 East First Street, Duluth, MN 55802. Send notices of change of address to the office of the Publishers at least 6 to 8 weeks in advance. Please include both old and new addresses. POSTMASTER: Send changes of address to *Biochemical and Biophysical Research Communications,* 1 East First Street, Duluth, MN 55802.

Second class postage paid at Duluth, MN, and at additional mailing offices.

Copyright ©1988 by Academic Press, Inc.

Vol. 156, No. 1, 1988
October 14, 1988

AUTHOR INDEX
Volume 156, Number 1

Abuja, Peter M., 180
Aktories, Klaus, 361
Altekar, Wijaya, 451
Amiri, Iradj, 304
Anderson, W. B., 263
Anton, Elizabeth, 143
Arimura, Akira, 61
Asai, Kentaro, 563
Auclair, Martine, 424
Auguet, Michel, 186

Baertschi, Alex J., 15
Baricordi, Roberto, 46
Barlier, S., 255
Barry, Jeanne, 164
Barthe, C., 318
Bartol, Frank F., 108
Basso, D., 318
Baxter, Robert C., 199
Benesch, Ruth E., 9
Benovitz, Deanne E., 125
Bibor-Hardy, Viviane, 205
Bird, R. Curtis, 108
Birkenhäger, J. C., 588
Brady, Stephen F., 297
Braquet, Pierre, 186
Brengle, Blair, 511
Brockway, Martine J., 116
Bruening, George, 340
Burgoyne, Leigh A., 222
Buzayan, Jamal M., 340

Cantrell, Doreen A., 328
Célier, Chantal, 282
Chabrier, Pierre-Etienne, 186
Chandrasekaran, S., 411
Chang, S. H., 537
Chen, Shiuan, 445
Ciccarone, Terrence M., 297
Claeyssens, Marc, 180
Cleaver, James E., 557
Clemetson, Kenneth J., 389
Clostre, François, 186
Colin, D. A., 255
Corr, Peter B., 485
Couraud, F., 255
Cousin, E., 383
Crouch, Michael F., 149
Crumpton, Michael J., 328

Dalal, N. S., 137
Darke, Paul L., 297
Darlak, Krzysztof, 125
Daron, Harlow, 108
Dashti, Nassrin, 581
David, Carol, 602
Davies, Adelina A., 328
Dayanithi, G., 255
Dean, John W., III, 411
Delaflotte, Sylvie, 186
Demczuk, Stephen, 463
De Mellow, John S. M., 199
Denarier, E., 595
Dosch, Donald C., 517
Draznin, Boris, 570
Dwivedi, R. S., 131

Ebner, Kurt E., 233
Eckstein, Fritz, 340
Elazar, Zvulun, 602
Evain-Brion, D., 263

Fausser, Luc, 304
Feldstein, Paul A., 340
Felipo, Vicente, 506
Figarella, C., 318
Floss, Heinz G., 517
Foisy, Sylvain, 205
Fournet, B., 318
Fournier, Agnes, 222
Frachet, P., 595
Fraser, Claire, 375
Freidinger, Roger M., 297
Fuchs, Sara, 602
Fujioka, Toshiyuki, 54

Gama Sosa, Miguel A., 417
Gandini, Enrico, 46
Garsky, Victor M., 297
Gerbaud, P., 263
Gerbes, Alexander L., 228
Giacobino, Jean-Paul, 375
Giralt, M., 493
Goetinck, Paul F., 99
Gold, Gerald, 457
Gotoh, Naomasa, 470
Gotoh, Takeshi, 396
Gottschall, Paul E., 61
Grisolía, Santiago, 506
Grodsky, Gerold M., 457

Grzonka, Zbigniew, 125
Guy-Crotte, O., 318

Hähnel, Roland, 116
Hall, Jessica C., 417
Hamberg, Mats, 543
Hanukoglu, Lea, 275
Harada, Shigeko, 551
Harig, James M., 164
Hayashi, Kyozo, 563
Heathers, Guy P., 485
Hexham, J. Mark, 328
Hii, Charles S. T., 222
Hirai, Yoshikatsu, 269
Hirano, Kazuyuki, 563
Honzawa, Mayumi, 355
Hopkins, Irene B., 275
Houslay, Miles D., 290
Hu, Chunfang, 500

Iglesias, R., 493
Iino, Shiro, 563
Ikeda, Seiichiro, 92
Inoue, Fumiko, 54
Inuzuka, Chikako, 68
Isom, G. E., 78
Ives, David H., 92

Jacobsen, B. P., 171
Jungi, Thomas W., 477
Just, Ingo, 361

Kaiser, Jeffrey R., 275
Kalimi, Mohammed, 22
Kanaide, Hideo, 312
Kanety, Hannah, 602
Kang, Jung Bu, 524
Kangawa, Kenji, 355
Katsuura, Goro, 61
Kawakami, Takuma, 269
Kawamura-Konishi, Yasuko, 348
Kelkar, S. M., 451
Keung, Wing-Ming, 38
Kieffer, Nelly, 389
Kiffel, Liliane, 282
Kim, Min-Young, 92
Kishimoto, Yasuo, 403
Kobayashi, Kenzo, 217
Kojima, Itaru, 335
Kosaki, Goro, 68
Koyama, Tanetoshi, 396

0006-291X/88 $1.50
Copyright © 1988 by Academic Press, Inc.
All rights of reproduction in any form reserved.

Kretz-Zaepfel, M., 255
Kruithof, E. K. O., 383
Kuhnert, Peter, 477
Kumar, S., 131
Kuriyama, Masayuki, 54
Kusano, Tomikazu, 563
Kwong, Suzanna, 9

Lambert, Anne-Marie, 304
Lapetina, Eduardo G., 149
Lee, Diana M., 581
Leitner, J. Wayne, 570
Leroux, Jean-Paul, 282
Leu, Chih-Tai, 297
Lewis, Aaron, 86
Liapi, C., 263
Litosch, Irene, 240
Lumma, Patricia K., 297

MacDonald, Paul N., 157
Magneney, Sylviane, 323
Mampel, T., 493
Marguerie, G., 595
Martin, Brian M., 403
Martin, I., 493
Martin-Moutot, N., 255
Matsuda, Morihiro, 551
Matsuo, Hisayuki, 246, 355
Mayer, Michel, 323
Maziere, Cécile, 424
Maziere, Jean-Claude, 424
Mazzilli, Cristina, 46
McDonald, Melisenda J., 438
McMaster, Earl, 86
Meek, James L., 143
Melloni, Edon, 46
Miasiro, Nobuco, 312
Michalski, Linda A., 438
Michelot, Robert, 323
Millan, Jose L., 563
Minamino, Naoto, 355
Miñana, María-Dolores, 506
Mizoguchi, Yasuhiro, 217
Mizuno, Kensaku, 246
Mok, Tina, 581
Moore, Pamela B., 193
Mora, Liliana, 424
Moreau, Martine, 424
Morimoto, Satoshi, 403
Morisawa, Seiji, 217
Moritz, Robert L., 116
Moriyama, Yoshinori, 211
Murray, Andrew W., 222
Muzzin, Patrick, 375

Nakae, Taiji, 470
Nakai, Satoru, 269
Nakamura, Motoomi, 312
Nakamura, Tomoko, 246
Nakazato, Hiroshi, 68
Neal, Tom L., 368
Nemali, M. R., 131
Nishida, Tsutomu, 269
Nishino, Naoki, 269
Niskanen, Eero, 15
Nordmann, J. J., 255
Nutt, Ruth F., 297

O'Brien, John S., 403
Ogata, Etsuro, 335
Ogura, Kyozo, 396
Ohshima, Takehiro, 246
Oikawa, Shinzo, 68
Oltersdorf, Tilman, 432
Ong, David E., 157
Ozutsumi, Kunihiro, 551

Palmert, Mark R., 432
Peterhans, Ernst, 477
Picquot, Pascal, 304
Pijuan, Vivian, 240
Pilz, Ingrid, 180
Pirotzky, Eduardo, 186
Podlisny, Marcia Berman, 432
Polonovski, Jacques, 424
Pols, H. A. P., 588
Poltronieri, Licia, 46
Potier, Pierre, 323
Prandini, M. H., 595
Pyne, Nigel J., 290

Ramaswamy, Krishnamurthy, 164
Rao, M. S., 131
Ratajczak, Thomas, 116
Rathinavelu, A., 78
Rawal, Nenoo, 451
Raynaud, F., 263
Reddy, J. K., 131
Regelson, William, 22
Rice, Timothy J., 143
Riddell, M., Gatz, 108
Roeder, Lois M., 275
Rosenthal, Walter, 361
Rubalcava, Boanerges, 30
Rubin, Leona J., 485
Rubini, Michele, 46
Ruprecht, Ruth M., 417

Sakagami, Yoshihide, 217
Salmon, Suzanne, 424
Scarpelli, D. G., 131
Schilte, J. P., 588
Schmitt, Pascal, 323
Seki, Shuichi, 217
Selkoe, Dennis J., 432
Selvatici, Rita, 46
Seydoux, Josiane, 375
Shapiro, Robert, 530
Sherman, Nancy A., 570
Shi, Xianglin, 137
Shibai, Hiroshiro, 335
Shin, Hong Dae, 524
Siegel, Frank L., 368
Sigal, Irving S., 297
Simpson, Richard J., 116
Sinha, Y. N., 171
Smith, Zigrida L., 1
Snyder, Fred, 1
Soergel, Konrad H., 164
Sok, Dai-Eun, 524
Sowadski, Janusz M., 99
Spatola, Arno F., 125
Steggles, Alan W., 576
Stigbrand, Torgny, 563
Stillwell, William, 511
Stringfellow, David A., 108
Strohl, William R., 517
Strydom, Daniel J., 530
Subbarao, V., 131
Sugimoto, Nakaba, 551
Sumita, Sachiyo, 54
Sussman, Karl E., 570
Suzuki, Haruo, 348

Tabuchi, Mari, 335
Takagi, Masayuki, 551
Takano, Masaaki, 269
Tanaka, Shoji, 246
Tanzer, Marvin L., 411
Testori, Alessandro, 222
Thangada, S., 131
Tildon, J. Tyson, 275
Tomme, Peter, 180
Totsuka, Yasuo, 335
Trezzini, Cristina, 477
Tsonis, Panagiotis A., 99

Usman, M. I., 131
Uzan, G., 595

Valdez, B. C., 537
Vallari, David S., 1
Vallee, Bert L., 530
van Huystee, Robert B., 500
van Leeuwen, J. P. T. M., 588
Vantard, Marylin, 304
Varma, Shobha, 233
Veber, Daniel F., 297
Vega-SaenzdeMiera, Eleazar C., 30
Venter, John-Craig, 375
Villarroya, F., 493
Viñas, O., 493
Visser, T. J., 588
Vollmar, Angelika M., 228

Wassall, Stephen R., 511
Wenger, Roland H., 389
Weremowicz, Stanislawa, 530
Weyler, Walter, 445
Wicki, Andreas N., 389
Wieland, Felix T., 457
Witker, Dennis S., 432
Wright, Lynda S., 368

Yamamoto, Hiromichi, 312
Yamamoto, Sukeo, 217
Yeldandi, A., 131
Yoo, Min, 576
Yoshihara, Eisaku, 470
Younathan, E. S., 537
Younkin, Linda H., 432
Younkin, Steven G., 432

Vol. 156, No. 1, 1988 BIOCHEMICAL AND BIOPHYSICAL RESEARCH COMMUNICATIONS
October 14, 1988 Pages 1-8

HL-60 CELLS BECOME RESISTANT TOWARDS ANTITUMOR ETHER-LINKED PHOSPHOLIPIDS FOLLOWING DIFFERENTIATION INTO A GRANULOCYTIC FORM

David S. Vallari, Zigrida L. Smith, and Fred Snyder

Medical and Health Sciences Division
Oak Ridge Associated Universities
P.O. Box 117
Oak Ridge, Tennessee 37831

Received August 23, 1988

1-O-Alkyl-2-O-methyl-sn-glycero-3-phosphocholine (alkylmethoxy-GPC) exerts a highly selective cytotoxic activity towards a variety of tumor cells that is not seen in normal cells. Human promyelocytic leukemia (HL-60) cells are particularly sensitive to this cytotoxic action. In this report we show that when HL-60 cells are differentiated into a granulocytic form by dimethylsulfoxide (Me_2SO) they become resistant toward the cytotoxic effects of alkylmethoxy-GPC. Also, after short-term exposures of the HL-60 cells to alkylmethoxy-GPC, the uptake of [methyl-^{3}H]choline is inhibited in the undifferentiated cells, but not in those differentiated with Me_2SO. Thus, cellular choline uptake appears to be a useful index for assessing the susceptibility of cells to the cytotoxic effects of antitumor phospholipids. [^{3}H]Alkylmethoxy-GPC is poorly metabolized by both cell populations as is evident by the trace quantities of labeled metabolites formed; also, alkylmethoxyglycerols do not exert any cytotoxic activity toward undifferentiated cells. These results demonstrate that differences in the cytotoxic response of sensitive (undifferentiated) and resistant (differentiated) cells to alkylmethoxy-GPC are not due to differences in their ability to metabolize alkylmethoxy-GPC or to a phospholipase C-generated toxic metabolite. Instead the data support our earlier hypothesis that the antitumor action of alkylmethoxy-GPC is, at least in part, caused by an impaired transport of small molecules across the membrane of sensitive cells. © 1988 Academic Press, Inc.

Extensive studies have clearly shown that a number of unnatural ether-linked phospholipids possess highly selective antineoplastic activity (1). The 2-O-methyl-substituted analog of platelet activating factor, 1-O-alkyl-2-O-methyl-sn-glycero-3-phosphocholine (alkylmethoxy-GPC), exhibits direct antiproliferative and cytotoxic activity towards a variety of tumor cells in culture (2,3), whereas normal cells such as human polymorphonuclear neutrophils are highly resistant (4). Human promyelocytic leukemia (HL-60) cells are particularly sensitive to the lethal effects of alkylmethoxy-GPC (4,5), although resistant lines of cancer cells have also been described (3,6). Also of interest is that sub-cytotoxic levels of alkylmethoxy-GPC can induce differentiation of HL-60 cells into granulocytes and monocytes (7).

A number of investigations with sensitive cells have indicated alkylmethoxy-GPC perturbs membrane structures (8-10), modifies phospholipid

0006-291X/88 $1.50
Copyright © 1988 by Academic Press, Inc.
All rights of reproduction in any form reserved.

metabolism (11-14), and inhibits nutrient transport (14). Moreover, the fact that alkylmethoxy-GPC inhibits protein kinase C activity (13,15-17) and alters cellular protein phosphorylation patterns (13,18) suggests a stimulus-response coupling mechanism might be involved in the response of sensitive cells to the methoxy analog.

Our studies show that when HL-60 cells are differentiated into granulocytes with dimethyl sulfoxide (Me_2SO) they become resistant toward the cytotoxic action of alkylmethoxy-GPC and, therefore, exhibit a response similar to what is seen in normal cells. Also, the inhibition of [^{3}H]choline uptake observed only in the undifferentiated cells treated with the methoxy analog supports the use of choline uptake as an index for measuring the degree of the cytotoxic response elicited by the antitumor phospholipid agents.

MATERIALS AND METHODS

[^{3}H]Alkylmethoxy-GPC (1-[^{3}H]alkyl-2-O-methyl-sn-glycero-3-phosphocholine), containing mixed C-16 and C-18 chain lengths, was purchased from Amersham, Arlington Heights, IL. It was 95% radiopure based on thin-layer chromatography on Silica Gel H layers developed in chloroform/methanol/acetic acid/water;(50/30/8/4, v/v) and was used without further purification. [Methyl-^{3}H]choline chloride was purchased from Dupont (New England Nuclear), Boston, MA. We obtained unlabeled alkylmethoxy-GPC (1-O-octadecyl-2-O-methyl-sn-glycero-3-phosphocholine), choline chloride, formyl-Nle-Leu-Phe-Nle-Tyr-Leu, Silica Gels G and H, and the lipid chromatography standards from Sigma Chemical Co., St. Louis, MO. The 1-octadec-9'-10'-enyl-2,3-diacetyl-sn-glycerol was a gift from Western Chemical Industries, Vancouver, British Columbia. Other commercial products included Vitride [$NaAlH_2(OCH_3CH_2OCH_3)_2$] from Eastman Organic Chemicals, Rochester, NY, Optifluor aqueous counting scintillant from Packard Instrument Company, Downers Grove, IL, and cell culture media from Grand Island Biological Co., Grand Island, NY.

1-Alkyl-2-O-methyl-sn-glycerol, prepared by Vitride reduction (19) of alkylmethoxy-GPC, was purified by chromatography on Silica Gel G layers developed in chloroform/methanol (98/2, v/v). The product migrated close to that of a 1-octadec-9'-10'-enyl-2-acetyl-glycerol standard (20) on Silica Gel G chromatoplates developed in hexane/ether/methanol/acetic acid (70/30/5/1, v/v).

Cell Culture: HL-60 cells from the American Type Culture Collection (Rockville, MD) were propagated at 37°C in a humidified 5% CO_2/95% air atmosphere. The culture density was maintained between 2 x 10^5 and 2 x 10^6 cells/ml by transferring the cells every 3-4 days to fresh RPMI-1640 medium containing 10% fetal bovine serum (heat-inactivated), penicillin (100 units/ml), streptomycin (100 μg/ml), and L-glutamine (4 mM). The doubling time for these cultures was 25-30 h. Cells were induced to differentiate by adding Me_2SO (1.3%) to the cultures (21) and the extent of differentiation assessed by reduction of nitroblue tetrazolium (NBT) dye (22). For the NBT reduction assays, cells were suspended in a Hepes-buffered salt solution (23) at 37°C and exposed to 5 μg/ml cytochalasin B for 10 min followed by 1 μM formyl-Nle-Leu-Phe-Nle-Tyr-Leu for 15 min. The proportion of differentiated cells determined by this method typically increased from approximately 5% before induction to 65-75% after a 5-day exposure to Me_2SO. Trypan-blue dye (0.1%) exclusion (24) revealed greater than 95% cell viability at the start of all experiments. Cells were counted in a hemacytometer; adherent cells were suspended by repeated pipeting immediately before enumeration.

Cytotoxicity Assays: Undifferentiated and Me_2SO-differentiated HL-60 cells were removed from their culture media by centrifugation (700xg for 5 min), washed once, and suspended to 1.0 x 10^6 cells/ml in fresh media

containing fetal bovine serum. The suspensions (1 ml) were placed into 16-mm well culture dishes for treatment with alkylmethoxy-GPC; the concentration of the alkymethoxy-GPC solvent (ethanol) in the incubation did not exceed 1% and had no apparent effects. The IC_{50} value was defined as the concentration of alkylmethoxy-GPC that reduced the viable cell number by one-half during a 24-h period (5).

[^{3}H]Alkylmethoxy-GPC Labeling: Undifferentiated and Me_2SO-differentiated HL-60 cells were removed from the cultures, washed, and suspended to 2.0 x 10^6 cells/ml in fresh media containing fetal bovine serum; 1-ml aliquots were then placed in 16-mm culture wells. [^{3}H]Alkylmethoxy-GPC (0.1-0.2 μCi) plus unlabeled alkylmethoxy-GPC (0.25 - 15.0 μM) were added to the cells in 10 μl ethanol. After a 4-h or 20-h labeling period, the suspensions were centrifuged (11,500xg for 30 s) and the pelleted cells washed three times with phosphate-buffered saline (PBS). The washed cells were suspended in PBS and samples were removed for determination of cell number and radioactivity. For analyses of [^{3}H]alkylmethoxy-GPC metabolites, cells, including the media, were extracted by a modified Bligh and Dyer (25) procedure, with the methanol containing 2% acetic acid. Recovery of tritium in the lipid extracts (84$\pm$3%) was the same for both differentiated and undifferentiated cultures and for incubations with cell-free culture medium.

Phospholipids were separated on Silica Gel H layers developed in chloroform/methanol/acetic acid/water (50/30/8/4, v/v) and neutral lipids were resolved on Silica Gel G layers developed in hexane/ether/methanol/acetic acid (70/30/5/1, v/v). Specific areas of the chromatograms corresponding to lipid standards were removed and the distribution of tritium determined by liquid scintillation spectrometry.

Protein was measured by the procedure of Lowry, et al. (26), with bovine serum albumin as the standard.

[Methyl-^{3}H]choline Uptake: Undifferentiated and Me_2SO-differentiated HL-60 cells were removed from the cultures, washed, and suspended in (1.0 x 10^6 cells/ml) in fresh media containing fetal bovine serum. Equal portions of cells were incubated for 4 h with either 12.5 μM alkylmethoxy-GPC or 0.625% ethanol (control). The suspensions were centrifuged (700xg for 5 min), washed twice in Hank's balanced salt solution, and suspended (2.0 x 10^6 cells/ml) in choline-free RPMI-1640 medium buffered with 20 mM Hepes (pH 7.3). The cells were preincubated at 37°C for 10 min and then [methyl-^{3}H]choline (final concentration, 10 μM; sp. act. 0.2 Ci/mmol) was added to initiate the uptake measurements. Aliquots were removed at 5-min intervals, centrifuged (11,500xg for 30 s), and the pelleted cells washed twice with PBS containing 0.1 mM choline chloride. The washed cells were suspended in PBS and the radioactivity measured; blank values, obtained from identical incubations done in an ice bath were subtracted from each of the experimental values.

RESULTS AND DISCUSSION

Our results show that the increased resistance of HL-60 cells to the cytotoxic effects of alkylmethoxy-GPC is clearly related to the degree of cellular differentiation as seen from the correlation of the recovery of viable cells following a 24-h exposure to alkylmethoxy-GPC with the capacity of the cells to reduce NBT (Fig. 1). Maximum resistance of the HL-60 cells toward alkylmethoxy-GPC cytotoxicity occurred at 5 d after exposure to Me_2SO. A 24-h exposure of undifferentiated cells to alkylmethoxy-GPC in the presence of 10% fetal bovine serum yielded a dose-dependent cytotoxic response with an IC_{50} value of 6 μM (Fig. 2), whereas the IC_{50} value in the Me_2SO-differentiated HL-60 granulocytes was 30 μM. At this high concentration of alkylmethoxy-GPC, greater than 90% of the undifferentiated HL-60 cells were lysed.

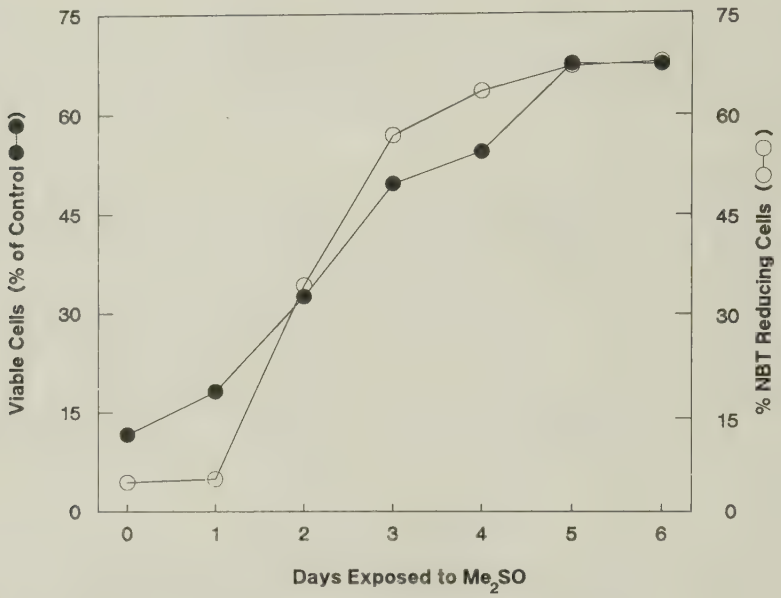

Fig. 1 Development of resistance of HL-60 cells toward alkylmethoxy-GPC-mediated cytotoxicity as a function of differentiation to a granulocytic form by Me_2SO. Cells were removed from culture 1-6 d following the addition of Me_2SO for assay of NBT reduction and cytotoxicity of 25 μM alkylmethoxy-GPC. Each value corresponds to the average of duplicate determinations and is representative of three separate experiments.

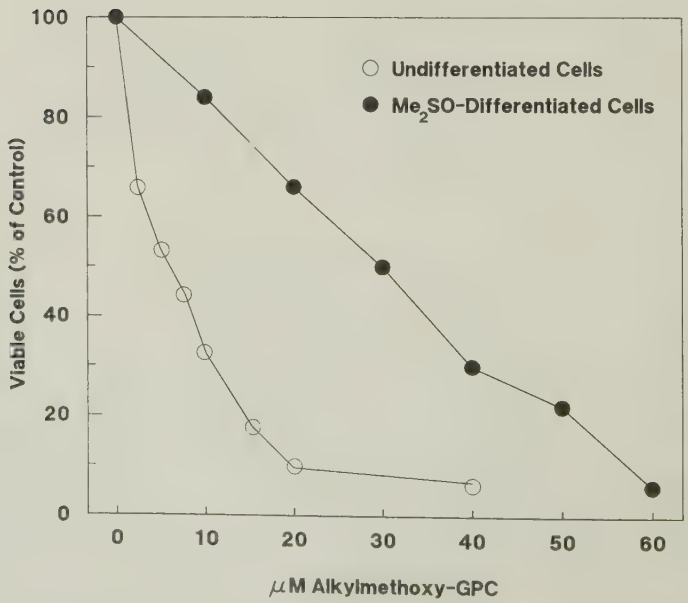

Fig. 2 Cytotoxicity of alkylmethoxy-GPC toward undifferentiated and Me_2SO-differentiated HL-60 cells. Each value corresponds to the average of duplicate determinations and is representative of three separate experiments.

Several reports indicate that the sequestration of ether-linked phospholipids in cell surface membranes is an important contributing factor in the cytotoxic mechanism (9,14,27). We found Me_2SO-differentiated HL-60 granulocytes treated with [3H]alkylmethoxy-GPC (12.5 μM) for 4 h contained smaller amounts ($p<0.05$, based on paired experimental values) of the cytotoxic phospholipid (791 $\pm$ 249 pmol/10^6 cells, n=6) than the undifferentiated HL-60 cells (1547 $\pm$ 480 pmol/10^6 cells, n=8); under these experimental conditions no change in cell viability was apparent. The Me_2SO-differentiated HL-60 cells also contained less tritium when incubated with low concentrations (0.5 μM) of [^{3}H]alkylmethoxy-GPC for either 4 or 20 h. Although statistically significant ($p<0.01$), differences between the undifferentiated and differentiated cells were less apparent for each of the conditions tested when labeling was expressed on either a protein or phospholipid basis since these constituents are considerably lower in the differentiated HL-60 granulocytes in comparison to the undifferentiated cells (23). These results are consistent with those reported earlier for comparisons between polymorphonuclear neutrophils and HL-60 cells (27).

Hoffman, et al. (14,27) reported alkylmethoxy-GPC is poorly metabolized regardless of the cytotoxic response of cells to this phospholipid and also that it is not a substrate for the alkyl monooxygenase that cleaves the ether bond. In addition, they (27) found the activities of the cleavage enzyme in different cell types did not correlate with the cytotoxic response. The current work clearly shows that Me_2SO-induced differentiation does not alter the limited ability of HL-60 cells to metabolize alkylmethoxy-GPC. After an 18-h incubation of HL-60 cell suspensions with either cytotoxic (15 μM) or sub-cytotoxic (0.5 μM) levels of [3H]alkylmethoxy-GPC, greater than 93% of the tritium found in lipid extracts remained with the parent compound in both the undifferentiated and differentiated cells. This result further supports the notion that differences in the metabolism of the antitumor phospholipid between sensitive and resistant cells do not contribute to its highly selective antitumor response.

As detected in earlier experiments (27), labeled 1-alkyl-2-acyl-<u>sn</u>-glycerophosphocholine was formed to a limited extent (<1% of tritium) in both the undifferentiated and Me_2SO-differentiated cells; it presumably orginates after oxidation of the 2-O-methyl moiety and a subsequent acylation step. Trace amounts of labeled 1-alkyl-2-O-methylglycerol also were found in our experiments and could have been formed via a phospholipase C (27) or through the combined actions of a phospholipase D and a phosphohydrolase. Based on indirect evidence, Fleer et al. (28-29) proposed a phospholipase C-dependent cleavage of the methoxy analog is required for its cytotoxic activity. This is an attractive hypothesis since 1-alkyl-2-O-methyl-glycerol has previously been identified as a minor alkylmethoxy-GPC metabolite in HL-60,

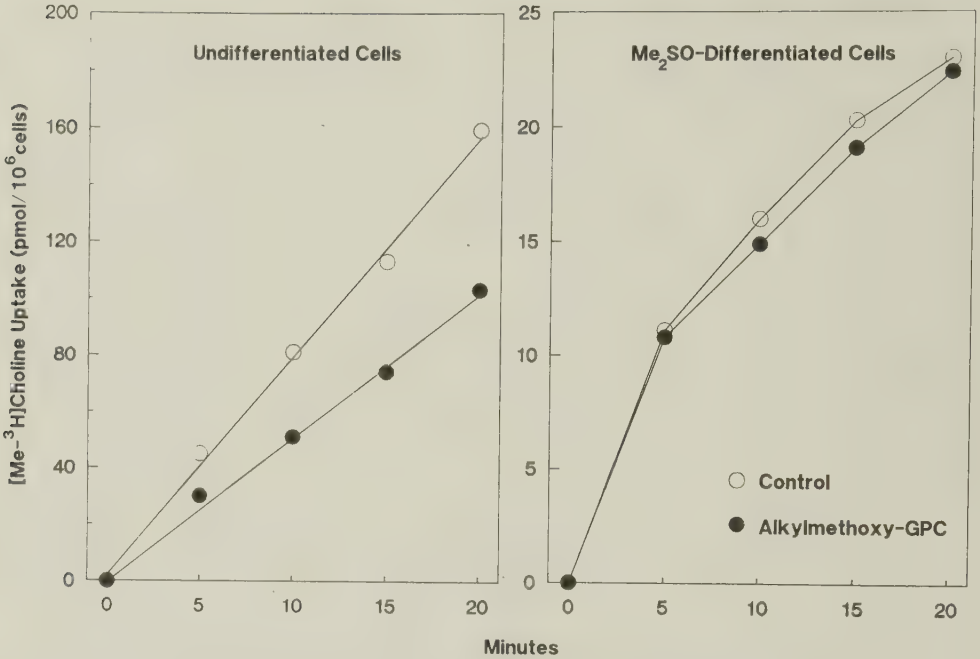

Fig. 3 Effect of alkylmethoxy-GPC on [methyl-^{3}H]choline uptake by undifferentiated and differentiated (granulocytic form) HL-60 cells. These values are representative of two separate experiments.

PMN (27), MDCK, K562 (30), Ehrlich ascites (31) and mouse MO_4 fibrocarcinoma cells (32), and it is known to inhibit protein kinase C in vitro (32). However, in our experiments 1-alkyl-2-0-methyl-glycerol (up to 25 μM) was not cytotoxic toward the undifferentiated HL-60 cells. We believe these data rule out any role for a phospholipase C activity as a factor in the cytotoxic mechanism of the antitumor ether-linked phospholipids.

Inhibition of cell transport processes appears to be a general and early phenomenon observed in sensitive cells exposed to alkylmethoxy-GPC (14). In our studies, treatment of undifferentiated HL-60 cells for 4 h with 12.5 μM of the methoxy analog inhibited the initial rate of [methyl-^{3}H]choline rate by 35% (Fig. 3) without affecting the proportion of cells that excluded Trypan-blue dye. After differentiation of the HL-60 cells into the granulocytic form, [methyl-^{3}H]choline was taken up at a significantly lower rate than the undifferentiated cells, but the uptake was unaffected by the methoxy analog (12.5 μM).

Results from our studies demonstrate that the chemical-induction of differentiation in HL-60 cells to a granulocytic form causes them to become resistant towards the cytotoxic action of alkylmethoxy-GPC. Therefore, since comparisons can be made between sensitive and resistant cells of the same cell line, the HL-60 system described in this report should be an extremely useful

model for future investigations of the detailed molecular mechanism(s) responsible for the selective cytotoxic action of alkylmethoxy-GPC. In addition, inhibition of the uptake of [^{3}H]choline observed in the undifferentiated cells treated with alkylmethoxy-GPC and the lack of inhibition in the differentiated cells further supports our earlier concept that indicates the antitumor action of alkylmethoxy-GPC is, at least in part, due to an impaired transport of molecules across the plasma membrane of sensitive cells.

ACKNOWLEGEMENTS

This work was supported by the Office of Energy Research, US Department of Energy (Contract No. DE-AC05-76CR00033) and the American Cancer Society (BC-70 R).

REFERENCES

1. Berdel, W.E., Andreesen, R., and Munder, P.G. (1985) In Phospholipids and Cellular Regulation (J.F. Kuo, Ed), pp. 42-74. CRC Press, Boca Raton.
2. Andreesen, R., Modolell, M., Weltzien, H.U., Eibl, H., Common, H.H., Lohr, G.W., and Munder, P.G. (1978) Cancer Res. 38, 3894-3899.
3. Berdel, W.E., Greiner, E., Fink, U., Stavrou, D., Reichert, A., Rastetter, J., Hoffman, D.R., and Snyder, F. (1983) Cancer Res. 43, 541-545.
4. Hoffman, D.R., Stanley, J.D., Berchtold, R., and Snyder, F. (1984) Res. Comm. Chem. Pathol. Pharm. 44, 293-306.
5. Hoffman, D.R., Hadju, J., and Snyder, F. (1984) Blood 63, 545-552.
6. Tidwell, T., Guzman, G., and Vogler, W.R. (1981) Blood 57, 794-797.
7. Honma, Y., Kasukabe, T., Hozumi, M., Tsushima, S., and Nomura, H. (1981) Cancer Res. 41, 3211-3216.
8. Storme, G.A., Berdel, W.E., van Blitterswijk, W.J., Bruyneel, E.A., DeBruyne, G.K. and Mareel, M.M. (1985) Cancer Res. 45, 351-357.
9. van Blitterswijk, W.J., Hilkmann, H., and Storme, G.A. (1987) Lipids 22, 820-823.
10. Bolscher, J.G.M., Schallier, D.C.C., van Rooy, H., Storme, G.A., and Smets, L.A. (1988) Cancer Res. 48, 977-982.
11. Vogler, W.R., Whigham, E., Bennett, W.D., and Olson, A.C. (1985) Exp. Hematol. 13, 629-633.
12. Hermann, D.B.J. and Neumann, H.A. (1986) J. Biol. Chem. 261, 7742-7747.
13. Parker, J., Daniel, L.W., and Waite, M. (1987) J. Biol. Chem. 262, 5385-5393.
14. Snyder, F., Record, M., Smith, Z., Blank, M.L., and Hoffman, D.R. (1987) Aktuel. Onkol. 34, 19-26.
15. Helfman, D.M., Barnes, K.C., Kinkade, J.M., Jr., Vogler, W.R., Shoji, M., and Kuo, J.F. (1983) Cancer Res. 43, 2955-2961.
16. Daniel, L.W., Etkin, L.A., Morrison, B.T., Parker, J., Morris-Natschke, S., Surles, J., and Piantadosi, C. (1987) Lipids 22, 851-855.
17. Oishi, K., Raynor, R.L., Charp, P.A., and Kuo, J.F. (1988) J. Biol. Chem. 263, 6865-6871.
18. Kiss, Z., Deli, E., Vogler, W.R., and Kuo, J.F. (1987) Biochem. Biophys. Res. Comm. 142, 661-666.
19. Snyder, F., Blank, M.L., and Wykle, R.L. (1971) J. Biol. Chem. 246, 3639-3645.
20. Renooij, W. and Snyder, F. (1981) Biochim. Biophys. Acta 663, 545-556.
21. Collins, S.J., Ruscetti, F.W., Gallagher, R.E., and Gallo, R.C. (1978) Proc. Natl. Acad. Sci. USA 75, 2458-2462.

22. Collins, S.J., Ruscetti, F.W., Gallagher, R.E., and Gallo, R.C. (1979) J. Exp. Med. 149, 969-974.
23. Billah, M.M., Eckel, S., Myers, R.F., and Siegel, M.I. (1986) J. Biol. Chem. 261, 5824-5831.
24. Patterson, M.K. (1979) Meth. Enzymol. 58, 141-152.
25. Bligh, E.G. and Dyer, W.J. (1959) Can. J. Biochem. Physiol. 37, 911-917.
26. Lowry, O.H., Rosebrough, N.J., Farr, A.L., and Randall, R.J. (1951) J. Biol. Chem. 193, 265-275.
27. Hoffman, D.R., Hoffman, L.H., and Snyder, F. (1986) Cancer Res. 46, 5803-5809.
28. Unger, C., Eibl, H., Kim, D.-J., Fleer, E.A., Kotting, J., Bartoch, H.-H., Nagel, G.A., and Pfizenmaier, K. (1987) JNCI 78, 219-222.
29. Fleer, E.A.M., Unger, C., Kim, D.-J., and Eibl, H. (1987) Lipids 22, 856-861.
30. Wilcox, R.W., Wykle, R.L., Schmitt, J.D., and Daniel, L.W. (1987) Lipids 22, 800-807.
31. Weber, N. and Benning, H. (1988) Biochim. Biophys. Acta 959, 91-94.
32. van Blitterswijk, W.J., van der Bend, R.L., Kramer, I.M., Verhoeven, A.J., Hilkmann, H., and de Widt, J. (1987) Lipids 22, 842-846.

Vol. 156, No. 1, 1988
October 14, 1988

BIOCHEMICAL AND BIOPHYSICAL RESEARCH COMMUNICATIONS

Pages 9-14

BIS-PYRIDOXAL POLYPHOSPHATES: A NEW CLASS OF SPECIFIC INTRAMOLECULAR CROSSLINKING AGENTS FOR HEMOGLOBIN

Ruth E. Benesch and Suzanna Kwong

Department of Biochemistry and Molecular Biophysics
Columbia University, 630 W. 168 St., New York, N.Y. 10032

Received August 23, 1988

A series of compounds related to bis-pyridoxal phosphate has been synthesized and used to crosslink deoxyhemoglobin. The yield of crosslinked hemoglobin increased dramatically from about 15% for the di- or triphosphate to about 70% for the tetraphosphate. The site of attachment of the intramolecular crossbridge was found to be from the N-terminal amino group of one β chain to lysine 82 of the other. Since the distance between these residues is only 11Å, the bis-pyridoxal tetraphosphates probably have a "stacked" conformation. The crosslinked hemoglobins bind oxygen cooperatively but with a greatly decreased affinity. The increased ability to unload oxygen together with the stabilization of the tetramer qualifies them as promising cell-free blood substitutes. © 1988 Academic Press, Inc.

Hemoglobin crosslinked covalently between the αβ dimers is of interest from two points of view. One is to see to what extent dissociation into αβ dimers and especially subunit exchange between these dimers and intact tetramers (1, 2) play a role in the conformational change of the oxygen carrier from the T state to the R state. The second is that in order to use hemoglobin as an emergency blood replacement, dissociation into αβ dimers must be prevented, since these are filtered by the glomerulus and therefore rapidly excreted.

A number of crosslinking agents for this purpose have been described, including diaspirins (3), a dialdehyde derivative of pyridoxal phosphate (4) and most recently 4,4'-diisothiocyanostilbene-2,2'-disulfonate (5).

In this communication we describe a series of new crosslinking reagents consisting of two pyridoxal residues joined covalently by a bridge containing phosphates.

Materials and Methods

These bis-pyridoxal phosphate (bis-PLP) derivatives are listed in Table I. Only No. 1, (bis-PL)P_2 has been described previously (6). All the compounds were synthesized by the anion exchange method of Michelson (7) as modified for pyridoxal derivatives by Fukui et al. (6, 8, 9).

0006-291X/88 $1.50
Copyright © 1988 by Academic Press, Inc.
All rights of reproduction in any form reserved.

The syntheses involved the following steps:

(1) The reactants were converted into their tributylammonium salts by standard methods.

(2) Pyridoxal 5' diphosphate β-diphenyl ester was prepared from tributylammonium pyridoxal phosphate by reaction with diphenylchlorophosphate at room temperature for 3 hours followed by extraction of the excess reagent with ether as described (6,7). It was used in the anion exchange reaction for all the compounds except no. 2, which required pyridoxal-5'-triphosphate γ diphenyl ester. The latter was prepared in the identical manner from pyridoxal diphosphate, synthesized as described by Fukui et al. (6).

(3) Anion exchange was allowed to proceed at room temperature for 1-1½ hours in dry pyridine (~ 1 ml per millimole of the diphenylester). The anions used, as their tributylammonium salts, were pyridoxal phosphate for compounds 1 and 2, pyrophosphate for compound 3, methylene diphosphonate for no. 4, fructose 1,6 diphosphate for no. 5 and 2,3 diphosphoglycerate for no. 6. The ratio of diphenylester to anion in the exchange reaction was 0.6/1 for compounds 1 and 2, and 4/1 for the others.

(4) The products were purified by chromatography on a 1.5 x 17 cm column of Dowex 1-X2 using a gradient of LiCl from 0 to 0.2 M in 0.01N HCl (6,7). After concentration to a small volume and precipitation with acetone, the lithium salts of the bis-pyridoxal polyphosphates were further purified by chromatography on silica gel, using $MeOH/CHCl_3$ (6:4) as the solvent.

Solutions of the bis-pyridoxal polyphosphates were standardized spectrophotometrically using the molar extinction coefficient $\varepsilon_{392} = 9.400$ reported for (bis-PL) P_2 (6). Normal adult human hemoglobin (HbA) was prepared from fresh blood and stored in liquid N_2 as described previously (10).

The reaction with deoxyhemoglobin was carried out in an atmosphere of argon at 10°C exactly as described previously for 2-nor-2-formylpyridoxal 5'-phosphate (4,11). After reduction with $NaBH_4$, the argon was replaced by CO. The yield of crosslinked hemoglobin was determined by passage of the reaction mixture through a 2.5 x 35 cm column of Sephadex G-100 "superfine" in 1.0M $MgCl_2$. Under these conditions uncrosslinked hemoglobin is completely dissociated into αβ dimers (12) and excellent separation between dimers and tetramers is achieved. The methods used to determine the site of substitution on the hemoglobin molecule have been described (10).

Results and Discussion

The bis-pyridoxal polyphosphates used for this study are listed in Table I together with their extinction coefficients in the U.V. It is clear that the introduction of a fourth phosphate between the two pyridoxal rings is accompanied by a decrease in the extinction coefficient of the 392 nm absorption band while the shoulder at 324 nm is replaced by another absorption maximum. These changes in spectrum would be expected if "stacking" of the two pyridine rings occurs in compounds 3-6 but not in compound 1 or 2 (13). In that case there should be a substantial change in the distance between the two aldehyde residues on going from (bis-PL)P_3 to (bisPL) P_4 and this is completely borne out by the results on their reaction with hemoglobin. As can be seen from Table II, there is a dramatic increase in the amount of intramolecular crosslinking with the introduction of a fourth phosphate between the two pyridoxal rings.

TABLE I

Bis-Pyridoxal Polyphosphates

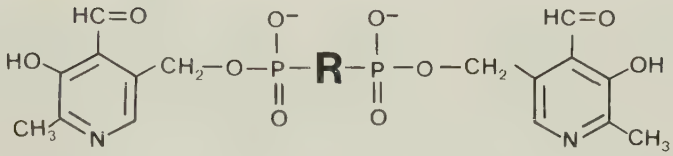

No.	Abbreviation	R	εM 392 nm	εM 324 nm
1.	(bis-PL) P_2	Oxygen	8.800	3.900 (sh)
2.	(bis-PL) P_3	Orthophosphate	9.100	4.400 (sh)
3.	(bis-PL) P_4	Pyrophosphate	6.700	4.700
4.	CH_2 (bis-PL) P_4	Methylene diphosphonate	6.800	4.500
5.	Fructose (bis-PL) P_4	Fructose 1,6-diphosphate	7.100	5.300
6.	PLP-DPG-PLP	2,3-diphosphoglycerate	7.600	5.700

The effect of different ratios of crosslinking agent to hemoglobin on the reaction is shown for two of the compounds in Fig. 1. It is clear that these compounds are remarkably efficient and specific in their reaction with deoxy hemoglobin, since the yield of intramolecularly cross-linked hemoglobin is over 60% when only stoichiometric amounts are used. By contrast, using diaspirins the yield is about 15% (14) and with 4,4'-diisothiocyanostilbene-2,2'disulfonate it is only 5% (5). Furthermore, it should be noted that the tetramer fraction isolated from the reaction

TABLE II

Covalent Intramolecular Crosslinking of Deoxy Hemoglobin by the Bis-Pyridoxal Polyphosphates

Compound	% Tetramer
(bis-PL) P_2	16
(bis-PL) P_3	18
(bis-PL) P_4	68
CH_2 (bis-PL) P_4	53
Fructose (bis-PL) P_4	41
PLP-DPG-PLP	70

The reactions were performed as described (4, 11) using 1.4 moles of bis-pyridoxal compound per mole of deoxy hemoglobin. The proportion of tetramer was determined by gel filtration as described in the text.

of hemoglobin with 1 mole/mole (or less) of these compounds was entirely homogeneous by acrylamide gel electrophoresis (data not shown) whereas higher ratios gave rise to a minor component with a larger anionic mobility.

The site of attachment of the crosslink on the hemoglobin molecule was determined as follows: - The modified hemoglobin was dissociated into α and β chains by chromatography on CM cellulose in urea as described (15). The α chains were normal as judged by their elution volume, U.V. spectrum and the absence of phosphate. The β chains eluted earlier than normal ones, contained all the phosphate and had a U.V. absorption with a maximum at 325 nm, typical of pyridoxylamino acids. The label was further localized by chromatography of a pronase hydrolysate of the globin on a sulfonic acid resin (UR-30) as described previously (10). Equal amounts of pyridoxyl-lysine and pyridoxyl-valylhistidine were found together with a trace of pyridoxyl valine. These results suggest strongly that the bis-pyridoxal polyphosphates crosslink deoxyhemoglobin tetramers at the same site as 2-nor-2-formylpyridoxal 5'-phosphate, i.e. between the N-terminal amino group of one β chain and lysine 82 of the other one.

The distance between these two amino groups is about 11Å in deoxyhemoglobin (16). This is much smaller than the distance between the two aldehyde residues in the bis-pyridoxal tetraphosphate compounds in their extended form. The very high affinity of these compounds for this particular site therefore strongly confirms the idea that their pyridine rings interact. It will be of great interest to see whether the conformational change with ligand binding, which involves a large increase

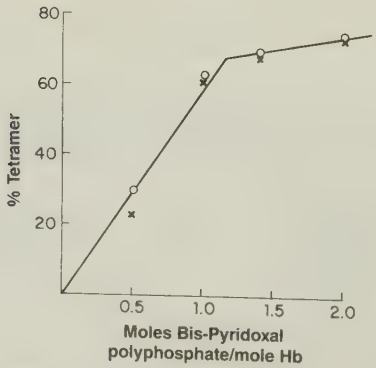

Figure 1. Effect of pyridoxal polyphosphate concentration on the yield of crosslinked hemoglobin.

The reactions were carried out with 2.5×10^{-4}M deoxyhemoglobin as described (4, 11), using the indicated concentrations of pyridoxal polyphosphate.

Crosses = $(bis\text{-}PL)P_4$
Open Circles = PLP-DPG-PLP

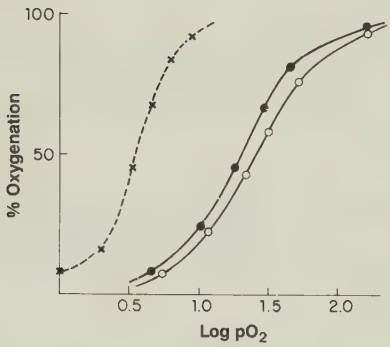

Figure 2. Oxygen Equilibrium Curves of Native and Crosslinked Hemoglobin.
Crosses = native HbA
Filled Circles = tetramer crosslinked with compound 3, Table I
Open Circles = tetramer crosslinked with compound 6, Table I
All measurements at 20°C in 0.05M bisTris pH 7.3, 0.1M Cl^-, 0.1mM EDTA.

in the distance between the two amino groups to which the crosslink is attached, destroys the interaction of the pyridine rings within the crosslinked hemoglobin.

The location of the crosslink in the central cavity between the β chains is also borne out by the oxygenation curves in Fig. 2. The crosslinked hemoglobins have a greatly decreased affinity for oxygen but retain cooperativity. In fact, both the position and the shape of their oxygen binding curves is very similar to that of unmodified hemoglobin in the presence of the most powerful allosteric regulator, inositol hexaphosphate.

In conclusion, the bis-pyridoxal polyphosphates appear to have a number of advantages as intramolecular crosslinking reagents for hemoglobin:

(1) The synthesis by the anion exchange method involves only two steps and can easily be completed in three days including purification of the product.

(2) Other functional groups can be readily incorporated between the two pyridoxal rings. Thus, for example, the fructose compound, no. 5, was invaluable for following the purification by monitoring the fructose/pyridoxal and fructose/phosphate ratio.

(3) The reaction of the compounds with deoxyhemoglobin shows an exceptional degree of specificity and a very high yield of crosslinked tetramer (Fig.1).

(4) Under the conditions used for the reaction with hemoglobin there is no intermolecular crosslinking since no hemoglobin species with molecular weight higher than the tetramer were found.

(5) Crosslinking with bis-pyridoxal polyphosphates simultaneously overcomes the two major disadvantages of hemoglobin as a blood substitute

since it stabilizes the tetramer and at the same time lowers the oxygen affinity and therefore dramatically facilitates oxygen unloading (Fig. 2).

Acknowledgements

We would like to thank Barry Honig of this department for the important suggestion that the pyridine rings could "stack" in some of the bis-pyridoxal polyphosphates.

This work was supported by National Institutes of Health Grant HL-05791.

References

1. Smith, F.R., Gingrich, D., Hoffman, B.M. and Ackers, G.K. (1987) Proc. Natl. Acad Sci. (U.S.) 84, 7089-7093.
2. Benesch, R.E., Benesch, R. and Macduff, G. (1965) Proc. Natl. Acad. Sci. (U.S.) 54, 535-542.
3. Snyder, S.R., Welty, E.V., Walder, R.Y., Williams, L.A. and Walder, J.A. (1987) Proc. Natl. Acad Sci. (U.S.) 84, 7280-7284.
4. Benesch, R., Benesch, R.E., Yung, S. and Edalji, R. (1975) Biochem. Biophys. Res. Commun. 63, 1123-1129.
5. Kavanaugh, M.P., Shih, D.T.B. and Jones, R.T. (1988) Biochemistry, 27, 1804-1808.
6. Shimomura, S. and Fukui, T. (1978) Biochemistry, 17, 5359-5367.
7. Michelson, A.M. (1964) Biochim. Biophys. Acta. 91, 1-13.
8. Tagaya, M. and Fukui, T. (1986) Biochemistry, 25, 2958-2964.
9. Tagaya, M., Nakano, K., and Fukui, T. (1985) J. Biol. Chem. 260, 6670-6676.
10. Benesch, R.E., Benesch, R., Renthal, R.D. and Maeda, N. (1972) Biochemistry, 11, 3576-3582.
11. Benesch, R. and Benesch, R.E. (1981) Methods Enzymol. 76, 147-159.
12. Macleod, R.M. and Hill, R.J. (1970) J. Biol. Chem. 245, 4875-4879.
13. Cantor, C.R. and Schimmel, P.R. (1980) Biophysical Chemistry, p. 396, W.H. Freeman & Co., San Francisco, CA.
14. Walder, J.A. (1986) U.S. Patent no. 4,598,064.
15. Clegg, J.B., Naughton, M.A. and Weatherall, D.J. (1968) Nature, 219, 69-70.
16. Fermi, G. (1975) J. Mol. Biol. 97, 237-256.

Vol. 156, No. 1, 1988 BIOCHEMICAL AND BIOPHYSICAL RESEARCH COMMUNICATIONS
October 14, 1988 Pages 15-21

PHYSIOLOGICAL CONCENTRATIONS OF ATRIAL NATRIURETIC FACTOR STIMULATE HUMAN ERYTHROID PROGENITORS *IN VITRO*

Eero Niskanen[1] and Alex J. Baertschi

Departments of Internal Medicine and Physiology,
Box 502 University of Virginia School of Medicine,
Charlottesville, VA 22908

Received August 25, 1988

Human α-ANF[1-28] potentiated erythroid colony formation up to four-fold in cultures containing erythropoietin. Both early and late erythroid precursor cells responded to α-ANF[1-28] [0.032 to 1 nM] in a dose dependent fashion. Removal of T lymphocytes and macrophages which have been shown to modulate erythropoiesis did not abolish the stimulatory effect. All major circulatory forms of ANF (α-ANF[1-28], α-ANF[4-28] and α-ANF[5-28]) had potent erythropoietic activity. These results indicate that concentrations of ANF reached during hypoxia stimulate erythroid progenitor cells in the presence of erythropoietin. © 1988 Academic Press, Inc.

Stimulation of red cell production by hypoxia has been attributed to enhanced renal synthesis and release of a hormone called erythropoietin (Epo) (1). Epo is a glycoprotein acting on terminal stages of erythroid differentiation (2). Another hormone released in response to low oxygen pressure is atrial natriuretic factor (ANF) (3,4). This recently discovered peptide (5,6) is synthesized in the atria and has powerful diuretic, natriuretic and hypotensive actions (7-9). ANF also allows intravascular fluid to exit across the capillaries which leads to acute hematocrit rise (10). These observations and the increase in plasma ANF during hypoxia (up to 0.2 nM)(4) prompted us to assess whether ANF can control red cell mass by action on erythropoiesis.

The effect of ANF on human early and late erythroid progenitor cells called burst forming unit-erythroid (BFU-E) and colony forming unit-erythroid (CFU-E) cells, respectively, was studied *in vitro*. We report that in the presence of Epo, α-ANF[1-28]

[1]To whom correspondence should be addressed.

0006-291X/88 $1.50
Copyright © 1988 by Academic Press, Inc.
All rights of reproduction in any form reserved.

increases CFU-E and BFU-E numbers up to four-fold. This effect is dependent on the molecular form of ANF and concentration of ANF (0.032 to 0.96 nM), and is not affected by the presence of T cells or macrophages in the culture.

MATERIALS AND METHODS

Cell preparations: Bone marrow cells and peripheral blood cells were collected from normal human volunteers after obtaining informed consent. The cells were suspended in α-medium containing 10% fetal calf serum and separated by Ficoll-Hypaque gradient to obtain an enriched mononuclear cell population. Peripheral blood derived cells were further enriched by incubation in plastic dishes twice for 30 minutes to remove macrophages. Then the majority of T cells were removed by rosetting with sheep red blood cells (Lampire) and centrifugation. The remaining T cells were removed by incubating the cell suspension with Leu-1 antibody (Becton-Dickinson) and rabbit complement. Less than 0.3% of macrophages and T cells could be detected among the total cells in the suspension.

Erythroid progenitor BFU-E and CFU-E assay. Cells (5×10^4 per plate) were cultured in petri dishes using the methylcellulose technique (11). Human Epo (Toyobo) was added to the cultures on day 0. Human ANF analogs (Peninsula) diluted in α-medium were added to the cultures every 3 days starting on day 0. Control cultures were supplemented with α-medium alone. Triplicate plates were incubated at 37°C in a humidified atmosphere of 7% CO_2 in air. On day 8, cell aggregates which contained more than seven erythroid cells were counted as CFU-E. On day 14, aggregates of forty cells or more were counted as BFU-E. Hemoglobinization of the cells was confirmed by using a Soret band. Number of observations are indicated in the bottom part of the bar.

Data analysis: Statistical significances were obtained by using Kruskal-Wallis Analysis of Variance [one way by ranks].

RESULTS

Cell culture techniques have allowed detection of molecules that act on erythropoietic precursor cells. Demonstration of the stimulatory effect on BFU-E and CFU-E *in vitro* requires the presence of erythropoietin in the culture system (12-14). Addition of human α-ANF[1-28] alone at a concentration of 0.32 nM to cultures had no effect on erythroid precursors (Fig. 1). As expected, Epo alone stimulated both erythroid precursors ($p < 0.05$). The highest numbers of both BFU-E and CFU-E were observed in cultures containing Epo plus α-ANF[1-28] ($p < 0.005$). The stimulatory effect was dependent on the doses of α-ANF[1-28] and Epo (Fig. 2). For identical α-ANF[1-28] concentrations, BFU-E and CFU-E yield was higher in cultures containing 2 U of Epo than 0.25 U. A concentration-dependent potentiation of erythropoiesis was observed when α-ANF[1-28] levels were increased from 0.032 nM to

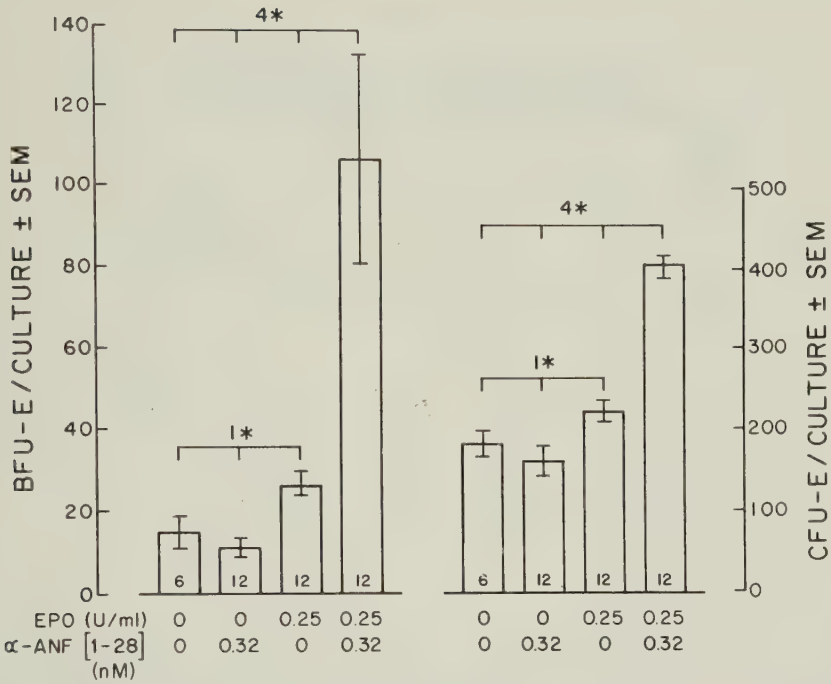

Fig. 1. Effects of α-ANF[1-28] on erythroid progenitors BFU-E and CFU-E in the presence and absence of Epo: 1* = $p < 0.05$; 2* = $p < 0.01$; 3* = $p < 0.005$; 4* = 0.001. Bars represent ± SEM.

0.96 nM. Potentiation usually peaked at 0.96 nM α-ANF[1-28]. Stimulation of erythroid colony formation by α-ANF[1-28] was not dependent on the presence of T lymphocytes or macrophages (Table 1). The number of peripheral blood derived BFU-E colonies increased three-fold in the presence of α-ANF[1-28] in cultures containing 0.25 U of Epo and less than 0.3% of T cells and macrophages. Potentiation of erythropoiesis depended on the molecular form of ANF (Peninsula) (Table 2). The stimulatory effect of Epo on both CFU-E and BFU-E colony formation was enhanced by α-ANF[1-28] as well as α-ANF[4-28] and α-ANF[5-28]. In fact, the number of BFU-E colonies, but not CFU-E colonies, was higher in cultures supplemented with α-ANF[4-28] ($p < 0.05$) and α-ANF [5-28] than in cultures containing α-ANF[1-28] (Table 2). The effect of α-ANF[1-11] and α-ANF-dimer on erythroid precursors was not significant.

DISCUSSION

These results indicate that all major circulatory forms (15) of ANF stimulate erythroid colony formation *in vitro* in the presence of erythropoietin. This newly described bioactivity of ANF does not depend on an intact N-terminal sequence but may

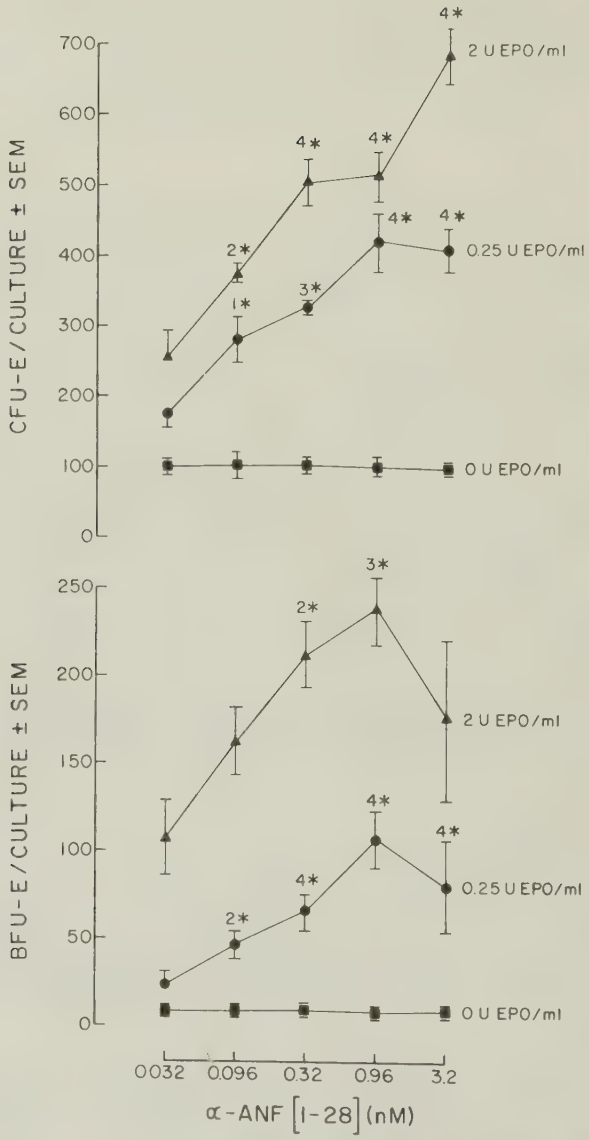

Fig. 2. Relationship between α-ANF[1-28] dose and erythroid progenitor BFU-E and CFU-E numbers in Epo containing cultures. Probabilities (Fig. 1) were determined using the lowest ANF concentration in each group as a reference point. N = 6 observations per group; bars represent ± SEM. Note log scale on abcissa.

require an intact ring structure (Table 2) as do the renal actions of ANF (5-7). Both early (BFU-E) and late (CFU-E) erythroid progenitors respond to α-ANF[1-28] (Fig. 2) at concentrations detectable in hypoxemic rabbits(4). Removal of macrophages and T cells which have been shown to elaborate factors stimulating both CFU-E and BFU-E *in vitro* (16), did not abolish the enhanced colony formation due to α-ANF[1-28] (Table 1). This suggests that the stimulating effect of ANF is not mediated via these cells.

TABLE 1

THE EFFECT OF HUMAN α-ANF[1-28] AND ERYTHROPOIETIN ON PERIPHERAL BLOOD BFU-E IN THE ABSENCE OF T CELLS AND MACROPHAGES

Agent	BFU-E/culture ± SEM
Experiment 1	
Epo 0.25 U/ml	7.0 ± 0.9
Epo 0.25 U/ml + ANF 0.32 nM	22.7 ± 1.9**
Experiment 2	
Epo 0.25 U/ml	14.0 ± 2.0
Epo 0.25 U/ml + ANF 0.32 nM	42.3 ± 6.8*

* = $p < 0.025$;
** = $p < 0.005$; n = 3 observations per group.

It is well established that erythropoietin is important in the latter stages of erythropoietic differentiation by stimulating proliferation of CFU-E and morphologically recognizable erythroid cells (1). Humoral control of the early stages of erythropoiesis is not as well understood. *In vitro* stimulation of BFU-E has been observed in the presence of three species of molecules. Interleukin-3 (IL-3, also called multipotential growth factor, Multi-CSF) acts on many hemopoietic precursors and stimulates BFU-E burst formation *in vitro* (12). Granulocyte-macrophage colony

TABLE 2

POTENTIATION OF ERYTHROPOIETIN-STIMULATED ERYTHROPOIESIS FROM HUMAN BONE MARROW BY ANF-ANALOGS

ANF analog	Potentiation of BFU-E(%)	p^1	p^2	Potentiation of CFU-E (%)	p^1	p^2
ANF [1-28]	100 ± 24.9	0.001	-	100 ± 39.2	0.00003	-
ANF [4-28]	74.8 ± 15.3	0.003	NS	208 ± 41.0	0.00001	0.05
ANF [[5-28]	98.5 ± 38.6	0.003	NS	143 ± 26.7	0.00001	NS
ANF [1-11]	-1.5 ± 8.8	NS	0.001	14.8 ± 4.6	NS	0.003
ANF Dimer	40.2 ± 26.7	NS	0.04	5.4 ± 13.1	NS	0.025

The concentration of ANF analog was 0.32 nM. All cultures were supplemented with 0.25 U/ml of Epo. Potentiation is expressed relative to the effect of α-ANF[1-28] + Epo (100%). The actual numbers of BFU-E and CFU-E in the presence of α-ANF[1-28] and Epo were 103 ± 26 and 440 ± 176, respectively. In cultures containing Epo alone, the number of BFU-E and CFU-E was 54 ± 16 and 265 ± 160, respectively. p^1 = significance relative to Epo alone; p^2 = significance relative to potentiation by α-ANF[1-28]. Numbers are means ±SEM (n=6 observations/group).

stimulating factor (GM-CSF) is thought to act mainly on granulocyte and macrophage precursors and stimulates BFU-E in vitro if cultures are initiated in the presence of this factor and erythropoietin is added 3-5 days later (13). The third factor is erythroid potentiating activity (EPA). EPA stimulates in vitro growth of BFU-E and CFU-E from both human and murine marrow and colony formation by the K-562 human erythroleukemic leukemia line cells (14,17). In vivo enhancement of erythropoiesis was observed after administration of EPA to experimental animals (18). A significant increase in the number of reticulocytes is seen in the peripheral blood and erythroid precursors in the spleen in anemic ICR mice. The significance of EPA effects on erythropoiesis has been challenged since its molecular form is identical to the tissue inhibitor of metalloproteinases (TIMP) that is involved in collagen metabolism (19).

In this study, a fourth species of molecules with major short-term effects on the circulation was shown also to modulate erythroid precursor cell proliferation in vitro. In contrast to EPA, ANF release is controlled by a physiological mechanism that plays a pivotal role in regulation of erythropoiesis, namely, hypoxia (3,4). Production of erythropoietin is increased in response to low tissue oxygen pressure, leading to enhanced red cell production. Our results suggest that ANF may function similarly because ANF at concentrations induced in vivo by hypoxia augmented colony formation in cultures containing erythropoietin. This mechanism may be important in the long-term control of red cell mass and circulatory homeostasis.

ACKNOWLEDGEMENTS

The authors thank Tim Shellem for his technical assistance, Christine Petersen for typing the manuscript, and Drs. R. Murphy and I. McNiece for reviewing the article. This work was supported by grants from the National Institutes of Health (RO1-AM27423), American Cancer Society (CH334) and American Heart Association (Virginia Affiliate).

REFERENCES

1. Jelkmann, W. (1986) Rev. Physiol. Biochem. Pharmacol. 104, 139-215.
2. Iscove, N.N., (1977) Cell Tissue Kinet. 10, 323-34.
3. Baertschi, A.J., Hausmaninger, C., Walsh, R.W., Mentzer, R.M., Jr., Wyatta, D.A., Pence, R.A. (1986) Biochem. Biophys. Res. Comm. 140, 427-33.
4. Baertschi, A.J., Adams, M.J., Sullivan, R.M. (In press, 1988) Am. J. Physiol.

5. de Bold, A.J., Borenstein, H.B., Veress, A.T. Sonnenberg, H. (1981) Life Sci. 28, 89-94.
6. Flynn, T.G. de Bold, M.L. de Bold, A.J. (1983) Biochem. Biophys. Res. Commun. 117, 859-65.
7. Atlas, S.A., Laragh, J.H. (1986) Amer. Rev. Med. 37, 397-414.
8. Ballermann, B.J., Brenner, B.M. (1986) Circ. Res. 58, 619-30.
9. Genest, J., Cantin, M. Circulation 75 (1987) (Suppl I), I-118-24.
10. Fluckiger, J.P., Waeber, B., Matsueda, G., Delaloye, B., Nussberger, J., Brunner, H.R. (1986) Am. J. Physiol. H251, H880-3.
11. Iscove, N.N., Sieber, F., Winterhalter, K.H. (1974) J. Cell. Physiol. 83, 309-20.
12. Sieff, C.A. (1987) J. Clin. Invest. 79, 1549-57.
13. Donahue, R.E., Emerson, S.G., Wang, E.A., Wong, G.G., Clarke, S.C., Nathan, D.G. (1985) Blood 66, 1479-81.
14. Gasson, J.C., Bersch, N., Golde, D.W. (1985) Prog. Clin. Biol. Res. 184, 95-104.
15. Schwartz, D., Geller, D.M., Manning, P.T., Siegel, N.R., Fok, K.F., Smith, C.E., Needleman, P. (1985) Science 229, 397-400.
16. Mangan, K.F., Desforges, J.F. (1980) Exp. Hematol. 8, 717-27; Reid, C.E., Baptista, L.C., Chanarin, I. (1981) Br. J. Haematol. 48, 155-64; Linch, D.C., Nathan, D.G. (1984) Nature 312, 775-7.
17. Gasson, J.C., Golde, D.W., Kaufman, S.E., Westbrook, C.A., Hewick, R.M., Kaufman, R.J., Wong, G.G., Temple, P.A., Leary, A.C., Brown, E.L., Orr, E.C. Clark, S.C. (1985) Nature 315, 768-71; Fraser, J.K., Lin, F.K., Berridge, M.V. (1988) Blood 71, 104-9.
18. Niskanen, E.. Golde, D.W., Teates, D.C., Gasson, J.C. (In press, 1988) Blood.
19. Stricklin, G.P., Welgus, H.G. (1986) Nature 321, 628.

Vol. 156, No. 1, 1988 BIOCHEMICAL AND BIOPHYSICAL RESEARCH COMMUNICATIONS
October 14, 1988 Pages 22-29

PHYSICOCHEMICAL CHARACTERIZATION OF [^{3}H] DHEA BINDING IN RAT LIVER

Mohammed Kalimi* and William Regelson

Departments of Physiology, Microbiology and Medicine, Medical College of Virginia, Virginia Commonwealth University, Richmond, VA 23298

Received August 25, 1988

SUMMARY: Dehydroepiandrosterone (DHEA), the native clinical steroid and steroid precursor, may have a targeted physiologic role. A high affinity (Kd 2.3nM) and steroid specific [^{3}H] DHEA binding macromolecule in male Sprague-Dawley rat hepatic cytosol suggests that DHEA may have receptor mediated physiologic action. ^{3}[H] DHEA binding was highest in the liver followed by kidney and testis cytosols. Sulfhydryl reagents such as N-ethylmalemide and iodoacetamide inhibited the binding of [^{3}H]DHEA by up to 60-70%. The DHEA-macromolecular complex was stable at 35°C. and addition of 5mM molybdate or 0.3M KCl increased stability. Interestingly, rat liver cytosol, specific binding at 4° C increased by almost 40-50% with addition of 0.1M NaSCN or 0.3M KCl. Sucrose gradient analyses showed a 7-8 S macromolecular complex in the low salt and 3-4 S complex under high salt conditions. The [^{3}H] DHEA- macromolecular complex shows minimal temperature dependent activation <u>in vitro</u> at 25°C as judged by binding to DNA-cellulose. The results suggest a specific high affinity macromolecule for DHEA in rat liver cytosol with unique physicochemical properties. © 1988 Academic Press, Inc.

INTRODUCTION: Dehydroepiandrosterone (DHEA) is a major clinical cortical steroid which declines with chronologic age (1). For many years, DHEA has been thought to be important only as an intermediate source for the sex steroids. That DHEA may have alternative roles of primary importance is seen in its wide range of biological activity including anticarcinogenic action (2), anti-obesity (3), anti-diabetic effects (4) and CNS effects (5). Although DHEA is now seen to have many biochemical, physiological and immunological effects in rodents, (6,7) our knowledge regarding how DHEA exerts its broad modulating effects remains very limited. Hardly any information is available regarding DHEA's binding activity in various target tissues and since DHEA is a steroid, it is likely that, like other steroid

*To whom all correspondence should be addressed.

0006-291X/88 $1.50
Copyright © 1988 by Academic Press, Inc.
All rights of reproduction in any form reserved.

hormones, DHEA responses may be mediated by specific high affinity receptors present in the subcellular fractions of target tissues such as cytosol and/or nuclei. This is particularly pertinent to recent data suggesting an affinity of DHEA for rat CNS binding (5). It is possible that there are distinct binding sites for DHEA in target cells which mediate observed physiologic responses. Therefore, the identification and characterization of DHEA binding in target cells is of considerable scientific and potential clinical interest.

Alternatively, DHEA might cross react with other steroid hormone receptors to modulate their activity. In this regard, there is one report suggesting that there is competition by DHEA with the receptor binding of estradiol and estrone in post menopuasal females (8). On the other hand. Poortman et al. (9) detected no DHEA or DHEA sulfate binding activity to estrogen receptors. In this paper, we describe DHEA binding, in vitro activation, and the physicochemical properties of a DHEA high affinity protein in rat hepatic cytosol. The results presented here will help us understand the molecular mechanism by which DHEA may mediate broad biochemical responses during cellular growth, differentiation, transformation and senescence.

MATERIALS AND METHODS: Male Sprague-Dawley rats (200-250 g) were obtained from Charles River Breeding Laboratories. The animals were adrenalectomized 3-5 days before use and were maintained on standard Purina rat chow, 0.9% NaCl (Saline) ad libitum. [1,2,6,7 - ^{3}H [N] Dehydroepiandrosterone (97.3 Ci/mmole) was obtained from New England Nuclear. Its purity was checked by thin-layer chromatography on precoated silica sheets (Eastman, Kodak) using a benzene/ ethyl acetate (60:40 V/V) solvent system. Bovine pancrease deoxyribonuclease type I and bovine pancreas ribonuclease type A were obtained from Sigma. Trypsin, chymotrypsin, papain and wheat germ lipase were from Worthington Co. Inc. Unlabelled steroid were obtained from Sigma. All other reagents used were of analytical grade.
PREPARATION OF CYTOSOL: - Rats were killed by cervical dislocation and livers were perfused with buffer A (10mM Tris, 0.25M sucrose, pH 7.6 at 4°C). The livers were removed, cleansed of adhering tissue and homogenized (1:3 W/V) in buffer A with a Teflon homogenizer. The cytosol fraction was prepared by centrifuging the homogenate at 105,000 x g for 60 min at 0°C. The cytosol was carefully removed, adjusted to approximately 5mg protein/ml cytosol and a final pH of 7.6 at 4°C and used. Protein was determined by the method of Lowry et al using bovine serum albumin as the standard (10). The cytosolic samples were incubated with 1-50nM of [^{3}H] DHEA in the presence or absence of 500 fold excess of unlabeled steroid. After incubation for 4h at 4°C, the specific macromolecular binding was determined using the charcoal-dextran technique (11). The data were evaluated using method of Scatchard (12).

Hepatic cytosol was incubated for 4h at 4°C with 10nM [^{3}H] DHEA with or without 10mM sodium molybdate or 5mM dithiothreitol or 0.3M KCl before

denaturation studies were carried out at 35°C for various times. The samples were then treated with charcoal-dextran and radioactivity was determined using Beckman Ready Solve-EP.

In vitro activation studies were carried out by preincubating cytosol with [^{3}H] DHEA for 4h at 4°C in the presence or absence of 10mM sodium molybdate. Portions of samples were then further incubated for 45min at 25°C. 200μl cytosol samples were mixed with 100μl DNA-cellulose (1.4mg native calf thymus DNA/ml cellulose) and incubated for 60min at 4°C with occasional stirring. The incubation samples were washed thrice with 1ml of buffer A. The pellets were suspended overnight in the Beckman Ready Solve - EP solvent and counted as described before (11), DNA was measured using the diphenylamine assay of Burton (13).

Linear 5-20% sucrose gradients were prepared in 10mM Tris buffer, PH 7.6 containing 30mM KCl (low salt) or 300mM KCl (high salt). Bovine Serum albumin (4.6 S) and human gamma globulin (7.1 S) were used as references to estimate sedimentation coefficients (14). This work was aided by funds from Dr. Susan Mellette and Barbara J. Johnson.

RESULTS: Scatchard plot analysis of data presented in Fig. 1 show that [^{3}H] DHEA was bound to a rat hepatic cytosolic macromolecule having a single class of binding site. With apparent dissociation constant (Kd) of about 2.3nM. Interestingly, addition of either 0.1M NaSCN or 0.3M KCl increased the concentration of the binding sites without effecting the binding affinity (Kd 2.8nM).

Steroid specificity of binding presented in Fig 2 show that [^{3}H] DHEA was displaced effectively (70-80%) with unlabelled DHEA, β etiocholanolone and androsterone. 17β estradiol, progesterone, and testosterone also considerably displaced the binding of [^{3}H] DHEA (40-50%). While dexamethasone and aldosterone were less effective.

Table I represents the effect of various enzyme treatments on the binding of [^{3}H] DHEA to the rat hepatic cytosol. The binding was markedly inhibited by trypsin and chymotrypsin. Deoxyribonuclease, ribonuclease and lipase were found to be without any effect.

The [^{3}H] DHEA - macromolecular complex was found to be stable up to 2 hrs at 35°C and the addition of 5mM dithiothreitol, 10mM molybdate or 0.3M KCl further stabilized the complex at 35°C. (Fig 3).

Data presented in Fig 4 show that pretreatment of hepatic cytosol with sulfhydryl blocking reagents such as N-ethylmalemide or iodoacetamide reduced the [^{3}H] DHEA binding up to 60-70%. Interestingly, p-

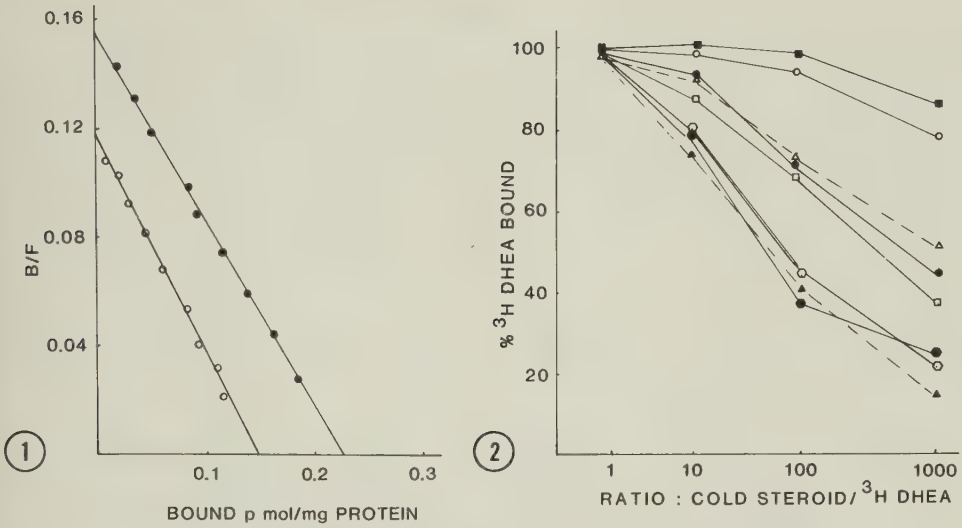

Fig 1. Scatchard analysis of specific [^{3}H] DHEA binding in rat hepatic cytosol. Binding were carreid out as described in Methods. Control (0-0) and 0.1M NaSCN (●-●).

Fig 2. Steroid specificity of [^{3}H] DHEA binding. Samples in triplicate were incubated with 10nM [^{3}H] DHEA alone or in the presence of various concentrations of unlabeled steroids and specific bound radioactivity determined as described in Methods. Each point is the mean value of two experiments. Aldosterone (■-■), Dexamethasone (0-0) Progesterone (Δ-Δ), Testosterone (●-●), 17β estradiol (□), DHEA (⬡), Androsterone (⬢), β etiocholanolone (▲).

TABLE I

Effects of various hydrolytic enzymes on rat hepatic cytosolic [^{3}H] DHEA binding

Enzyme	[^{3}H] DHEA bound	%
Untreated control	3,680	100
Trypsin	256	7
Chymotrypsin	126	4
Lipase	3,460	96
Deoxyribonuclease	3,698	100
Ribonuclease	3,574	97

Samples were incubated for 60 min at 4°C with 0.1ml (1mg per ml) of the appropriate enzymes or with homogenization buffer. The specific binding was determined as described in Methods.

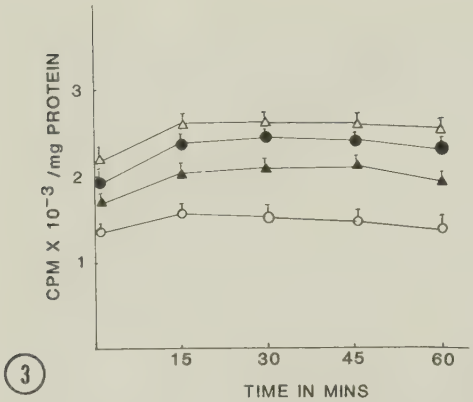

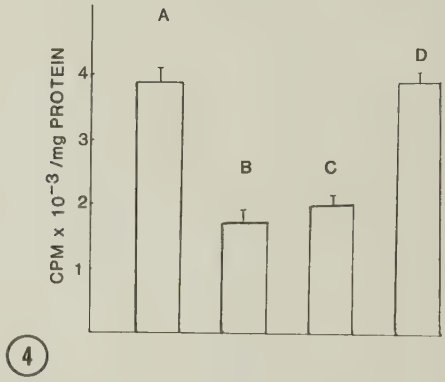

Fig 3. Stability of preformed [^{3}H] DHEA-macromolecular complex. Hepatic cytosol samples were incubated with 10nM [^{3}H] DHEA alone (0-0) or in the presence of 10mM sodium molybdate (Δ-Δ), or 5mM dithiothreitol (▲-▲) or 0.3M KCl (●-●) for 4h at 4°C. At different time intervals, triplicate aliquots were withdrawn and bound radioactivity was determined as described in Methods. Results are mean ± S.E. of four determinations.

Fig 4. Effect of - SH blocking reagents on rat liver [^{3}H] DHEA binding. Control samples (A) or samples treated with 5mM concentration of iodoacetamide (B), 5mM N-ethylmalemimide (c) or, 5mM p-chloromerobenzoate (D) for 30 min at 4°C with 10nM [^{3}H] DHEA. Iodoacetamide, N-ethylamlemide and p-chloromercuribenzoate were prepared in concentrated stock solution (100mM, pH 7.6) before use. The specific binding was determined as described in Methods. Results are mean ± S.E. of three determinations done in triplicate.

chloromercurobenzoate at 5mM concentration was unable to inhibit the [^{3}H] DHEA binding.

[^{3}H] DHEA binding was highest in the liver, followed by kidney and testis, plasma had no detectable amount of [^{3}H] DHEA binding (Table II).

The [^{3}H] DHEA binder was sedimented at 7-8 S macromolecular complex in low ionic strength sucrose density gradients and 3-4 S in high ionic strength sucrose density gradients (Fig 5).

The hepatic cytosolic [^{3}H] DHEA complex when incubated in vitro for 45 min at 25°C bound poorly to the DNA-cellulose. Only 30-40% binding over control untreated samples was noted on thermal activation (Fig 6). The addition of 10mM sodium molybdate completely inhibited DNA-cellulose binding of [^{3}H] DHEA -bound complex.

DISCUSSION: The result described here suggest the presence of high affinity, steroid specific binding for DHEA in the rat hepatic cytosol. In this

TABLE II

Specific [^{3}H] DHEA binding in cytosol of various tissues of rat

Tissue	Specific [^{3}H] DHEA binding cpm/mg protein
Liver	3200 ± 240
Kidney	1300 ± 148
Testis	1108 ± 96
Heart	946 ± 46
Plasma	280 ± 38

Cytosol prepared by homogenizing different tissues (1:3 W/V) in buffer A. The specific binding was determined as described in Methods. The results are mean ± S.E. of two experiments with triplicate determinations.

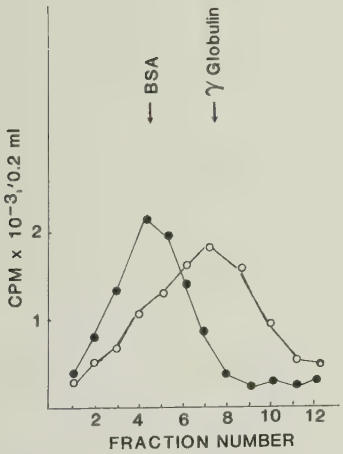

5

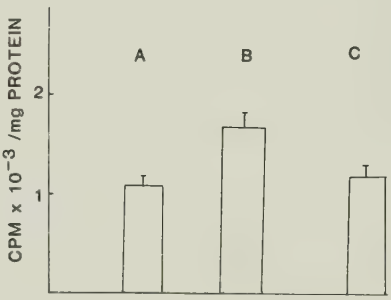

6

Fig 5. Sucrose density gradient analysis of rat liver [^{3}H] DHEA -macro - molecular complex. Cytosol saturated with 10nM [^{3}H] DHEA at 4°C for 4h and then treated with charcoal dextran. 400 μl of supernatant sample was applied to low salt (30mM KCl) (0-0) or high salt (300 mM KCl) gradients (●-●). Samples were centrifuged at 4°C for 18h in a Spinco SW rotor at 35,000 rpm. Gilford Densiflow apparatus was used to collect 8 drop samples, starting from the top of the gradients. Bovine serum albumin (BSA). The details are described in Methods.

Fig 6. DNA-cellulose binding of [^{3}H] DHEA-macromolecular complex. Hepatic cytosol samples were preincubated for 4h at 4°C in the presence of 10nM [^{3}H] DHEA (A). Samples were further incubated for 45 min at 25°C in the absence (B) or presence of (c) 10mM sodium molybdate. DNA-cellulose bound radioactivity was determined as described under Methods. Results are mean ± S.E. of three experiments done in triplicate.

regard, we found some interesting properties of the [^{3}H] DHEA binding protein: (a) [^{3}H] DHEA-macromolecular complex is very stable at 35°C. (b) Increasing the salt concentration (by addition of either 0.1M NaSCN or 0.3M KCl) of the hepatic cytosol resulted in enhanced binding of [^{3}H] DHEA to its cytosolic protein at 4°C without altering the affinity. Thus, it seems that high salt keeps DHEA binding sites in vitro in a configuration which not only enhanced its binding to DHEA, but also imparts stability to the [^{3}H] DHEA protein bound complex. Finally, (c) the [^{3}H] DHEA-macromolecular complex responds poorly to thermal activation in vitro as judged from its DNA-cellulose binding.

In order to assign any physiological revelance to the specific hepatic DHEA binding seen, we have deliberately studied the possible presence of a specific receptor protein utilizing physiologic concentrations of DHEA. In constrast, 0.4% DHEA has been commonly used in rodent feeding experiments (6,7) while from 20-80mg/kg/day have been used in clinical studies (7). In our in vitro studies μM concentration of DHEA have been used in the cell culture experiments (unpublished data), and there is a great dissociation between the in vitro affinity of DHEA reported here compared to reports of DHEA's clinical dosage or its in vivo biological activity or response. (7)

One probable explanation for in vitro and in vivo differences may be attributed to the lower in vitro thermal activation of the [^{3}H] DHEA complex. However, in addition to our observed slower activation of [^{3}H] DHEA - cytosolic complex, it is probable that absorption, distribution and more likely the in vivo metabolism of DHEA may play a crucial role in in vivo biologic responses. In that regard, it is possible that DHEA is probably converted in vivo to an active metabolite. Various researcher have attributed DHEA or DHEA-sulfate (DHEA-S) functions in vivo to its conversion into either androgenic or estrogenic compounds (15,16). As such, DHEA is described in the literature as a weak androgenic 17β ketosteroid and recent observations have shown it to have clinical androgenic effects (7). It is, therefore, important that further systematic work should be carried out using both in vivo and in vitro studies to determine whether the observed in

vitro specific [^{3}H] DHEA hepatic binding reported here is represented by interaction with distinct receptor or that DHEA and its metabolites exert their effects by binding to well characterized estrogen, androgen or progesterone receptors in order to influence various cellular function in normal and transformed cells. This is particularly important to the renewed interest in DHEA and related structures for their potential antidiabetic, antiviral, antiobesity and anticarcinogenic actions. (2,4,6,7,17).

REFERENCES

1. C. Migeon, B. Keller, B. Lawrence, et al., J. Clin. Endocrinol. Metab. 17 051-1062 (1957).
2. A. Schwartz, Cancer Res. 39 1129-1132 (1979).
3. M. Cleary, R. Seidensatt, R. Pearson, et al., Lipids 12 409-413 (1977).
4. D. Coleman, E. Leiter and R. Schwizer, Diabetes 31, 830-835 (1982).
5. C. Corpechot, P. Robel, M. Axelson et al. Brain Res. 270 119-125 (1983).
6. A. Schwartz in Molecular Biology of Aging (A. Woodhead, Ed.) Plenum Press New York, p. 181-191, 1985.
7. W. Regelson, R. Loria and M. Kalimi in Neuroimmunomodulation: Interventions in Aging and Cancer (Eds. W. Pierpaoli and N. Spector) Annals of the New York Academy of Sciences Vol. 521, The New York Academy of Sciences, New York, p. 260-273, 1988.
8. J. Thijssen, J. Poortman and J. Schwarz, J. Steroid Biochem. 6 729-734, (1975).
9. J. Poortman, J. Vroegindewey, J. Thijssen and F. Schwarz, Mol. Cell Endocrinology 8 27-34 (1977).
10. O. Lowry, N. Rosebrough, A. Farr and R. Randall, J. Biol. Chem. 193 265-275 (1951).
11. M. Kalimi, P. Colman and P. Feigelson, J. Biol. Chem. 250 1080-1086 (1975).
12. G. Scatchard, Ann. N.Y. Acad. Sci. 51 660-664 (1949).
13. D. Burton, Biochem. J. 62 315-322, (1956).
14. R. Martin and B. Ames, J. Biol. Chem. 236 1372-1379 (1961).
15. K. Li, D. Chandra, T. Food et al. Steroids 28 561-574 (1976).
16. W. Miller and A. Forrest. Lancet 28 66-868 (1974).
17. R. Loria, T. Inge, S. Cock, A. Szakal and W. Regelson, J. Medical Virology, In Press (1988).

Vol. 156, No. 1, 1988 BIOCHEMICAL AND BIOPHYSICAL RESEARCH COMMUNICATIONS
October 14, 1988 Pages 30-37

PROTEOLYTIC ACTIVITY IN THE INSULIN RECEPTOR

Eleazar C. Vega-SaenzdeMiera(a,b) and Boanerges Rubalcava(a,c#)

(a) Departamento de Bioquimica, Centro de Investigacion y de Estudios Avanzados del Instituto Politecnico Nacional, Apartado Postal 14-740, 07000 Mexico, D.F. (Mexico)

(b) Departamento de Ciencias Fisiologicas, Instituto de Ciencias, Universidad Autonoma de Puebla, Puebla (Mexico)

(c) Molecular Pharmacology Department, Nucleic Acid Research Institute, 3300 Hyland Avenue, Costa Mesa, CA 92626

Received August 29, 1988

SUMMARY. When a highly purified preparation of rat liver insulin receptor is incubated with trypsin, the receptor develops hydrolytic activity towards Nα-benzoyl-L-arginine ethyl ester, Nα-p-tosyl-L-arginine methyl ester, and Nα-benzoyl-DL-arginine-p-nitroanilide, (compounds which are synthetic substrates of trypsin). The activity toward Nα-benzoyl-DL-arginine-p-nitroanilide is inhibited by soybean trypsin inhibitor but not by Nα-p-tosyl-L-lysil chloromethyl ketone. These data are consistent with the presence of proteolytic activity in the insulin receptor specific for the bonds whose carbonyl functions are provided by arginine but not by lysine. Furthermore we found that the esterase activity toward Nα-benzoyl-L-arginine ethyl ester in the presence of trypsin is enhanced by insulin, and that the concentration of insulin that produced the half maximum stimulation is of the same magnitude as the dissociation constant for the soluble receptor. These data suggest that the insulin receptor is a zymogen, activated by trypsin, and based on its specific activity, may be the protease which releases a peptide chemical mediator of intracellular action of insulin. © 1988 Academic Press, Inc.

The mechanism of action of insulin remains unknown although insulin is one of the best studied proteins. There are many hypotheses to explain its multiple effects on the cell.

It has been reported that trypsin at low concentrations, mimics the actions of insulin (1-3), and that trypsin added to adipocyte plasma membranes causes the generation of a chemical mediator for insulin action (2-4).

It is apparent that the binding of insulin to its receptor enhances the release of a low molecular weight glycopeptide that mediates some of the

#To whom correspondence should be addressed at the Nucleic Acid Research Institute.

The abbreviations used are: BAEE, Nα-benzoyl-L-arginine ethyl ester; TAME, Nα-p-tosyl-L-arginine methyl ester; BAPNA, Nα-benzyol-DL-arginine-p-nitroanilide; TLCK, Nα-p-tosyl-L-lysylchloromethyl ketone.

0006-291X/88 $1.50
Copyright © 1988 by Academic Press, Inc.
All rights of reproduction in any form reserved.

intracellular actions of insulin (2-8). An intrinsic plasma membrane protease is involved in the release of this glycopeptide. This protease is inhibited by synthetic substrates with arginine esters but not by lysine or other amino acid esters (2). Therefore, it has been suggested (2) that the insulin-receptor interaction activates an endogenous arginine-specific protease that acts on an unspecified substrate to release the chemical mediator. The nature of this protease, the source of the chemical mediator, as well as the mechanism by which the binding of the hormone to its receptor leads to the release of this putative mediator is not yet known.

The insulin receptor is a tyrosine-specific protein kinase, which is stimulated by insulin (3,9), and it has been suggested that the release of the insulin mediator is stimulated by a phosphorylation reaction, similar to insulin-stimulated receptor tyrosine kinase phosphorylation (10), this phosphorylation is specifically inhibited by the arginine esters BAEE and TAME (11).

Clusters of insulin receptors are required for the hormone response (12-14), therefore, it is conceivable that the clusters are involved in the generation and transport of the chemical mediator, and that the protease responsible for the mediator release may be an activated receptor acting on other receptors in the cluster.

The present study was performed to investigate whether the insulin receptor contains any proteolytic activity, and we report here that the purified insulin receptor incubated with trypsin, hydrolyzes the arginine esters BAEE and TAME and the arginine amido compound BAPNA. These hydrolytic activities are inhibited by soybean trypsin inhibitor but not by TLCK (a specific inhibitor of proteases on the peptide bond whose carbonyl is provided by lysine). We discuss the possibility that the insulin receptor is the protease that releases the glycopeptide mediator, and a possible mechanism involving the tyrosine kinase activity, for triggering this proteolytic effect.

MATERIAL AND METHODS

Materials. Wistar rats (200-250g) were used. ^{125}I was obtained from Amersham. 1,3-diaminodipropylamine and 2,4,6 trinitrobenzensulfonic acid were purchased from Kodak; ethanolamine (scintillation grade) and succinic anhydride were from Fisher Scientific Company; dioxan from Merck; crystalline porcine insulin was a gift from Eli Lilly, Sephadex G10 and Sepharose 4B-CL were from Pharmacia Fine Chemicals. Diethylaminoethyl cellulose microgranular DE52 was from Whatman. All reagents for sodium dodecyl sulphate/polyacrylamide gel electrophoresis and comassie blue G-250 were from Bio-Rad. BAEE, BAPNA, TAME, TLCK, porcine trypsin type IX (15,700 and 16,500 BAEE units[1]) and all the remaining reagents were from Sigma Chemical Corp. The spectrophotometer was a Beckman model 35.

---

[1] One BAEE unit is defined as an increase of 0.001 O.D. per min. per mg of protein, at 253 nm, at pH 7.7 and 35° C, with BAEE as substrate in a reaction volume of 3.2 ml (1 cm light path).

Purification of insulin receptor from rat liver. Liver membranes were prepared by differential centrifugation (15) and solubilized with 2% Triton X-100; insulin receptor was purified by sequential chromatogragy on DEAE cellulose, insulin-agarose and concanavalin A-agarose (16). The [^{125}I]Insulin was prepared according to Posner et al.(17). Protein was measured by the procedure of Bradford (18) using bovine serum albumin as the standard.

Assay of esterase activity. The BAEE assay was performed as described by Schwert and Takenaka (19) (in a quartz microcell) with minor modifications: the mixture to be assayed described in table 1 and fig 1, was added to 500 ul of 1mM BAEE in 50 mM Tris-HCl pH 7.7; the activity was followed spectrophotometrically by recording the changes in absorbance at 253 nm of BAEE over 7.5 minutes and rates were estimated from the recorded slopes. Walsh (20) described the procedure for TAME, that we followed with modifications, and essentially is the BAEE assay described above but with TAME substituting for BAEE and a wave length of 247 nm to follow the activity.

Amidase assay. The rate of reaction was estimated from the slope of electronic recordings. The method of Erlanger et al. (21) was followed using BAPNA as substrate, in the volume and conditions of the precedent assays at a wave length of 410 nm.

RESULTS

Esterase activity could not be detected when mixtures of freshly prepared purified insulin receptor or the receptor plus insulin were assayed with BAEE as the substrate (Table 1). However, if the receptor mixture was first incubated with trypsin, a 2.5 fold increase above the initial activity of trypsin alone was obtained. When insulin was added to the above mixture, an additional

TABLE 1

ESTERASE ACTIVITY OF PURIFIED INSULIN RECEPTOR ON BAEE

Additions	Relative esterase activity			
Trypsin	100	±	12	(3)
Trypsin + Insulin	106	±	3	(3)
Insulin receptor	0			(3)
Insulin receptor + Insulin	0			(3)
Trypsin + Insulin receptor	252	±	52	(5)*
Trypsin + Insulin receptor + Insulin	388	±	60	(5)**

The proteins indicated were added successively to 500 μl of BAEE (1 mM in 50 mM Tris-HCl pH 7.7). After each addition, the spectrophotometric activity was followed for 7.5 min at 253 nm. The additions were: 33 ng of trypsin in 3 μl; 2 μg of insulin receptor in 100 μl; 3 μl of insulin to reach 1 μM final concentration. The results are the mean of the number of experiments (in parenthesis) ± S.D. The insulin receptor was obtained from three independent purifications. The actual values for insulin receptor + trypsin with the values corrected by volume and the basal trypsin activity subtracted were 287 ± 60 BAEE units, which increased to 542 ± 112 BAEE units in the presence of insulin.

* $p < 0.002$ with respect to trypsin.

** $p < 0.001$ with respect to trypsin + insulin receptor.

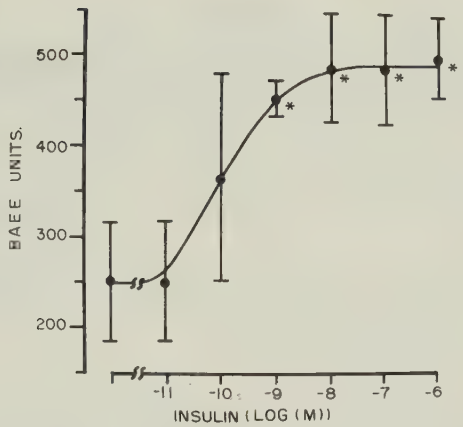

Fig. 1. Dose response of the effect of insulin on esterase activity of the mixture of trypsin + Insulin receptor. Trypsin (33 ng in 3 µl) were added to 500 µl of BAEE (1 mM in Tris-HCl pH 7.7). The trypsin activity was monitored spectrophotometrically by recording the changes in absorbance of BAEE at 253 nm for 7.5 minutes. Then 2 µg of insulin receptor in 100 µl were added and the recording continued for another 7.5 minutes. To the above mixture successive increasing doses of insulin were added, and the activity was recorded at the same time interval after each addition. Each point represents the mean ± S.D. of 5 experiments. The insulin receptor for the experiments shown was from 3 independent purifications. From all points the value of initial trypsin activity has been subtracted.

* $p < 0.001$ with respect to the mixture trypsin + insulin receptor, with no insulin.

increment to 3.9 fold greater than the initial activity with trypsin was achieved. If three week old preparations of the receptor were used, these increases in activity were not observed (data not shown). Insulin by itself (in the absence of the receptor) does not increase the activity of trypsin.

The BAEE esterase activity of trypsinized insulin receptor was determined as a function of insulin concentration (Fig.1). Esterase activity increased with increasing insulin concentrations up to 10^{-8}M; a half maximal response was at 1.2×10^{-10}M.

Purified insulin receptor also increases the esterase activity of trypsin with TAME as a substrate; the increase was rather modest in comparison to the increment described with BAEE. Trypsin (33 ng/500 µl of 1 mM TAME) provided 0.0325 ± 0.001 (S.D.) O.D. after ten minutes; in the presence of 2 µg of insulin receptor this value increased to 0.0485 ± 0.001 (n=3, $p < 0.001$).

TLCK completely abolished the trypsin response in the BAEE esterase assay, but only in the absence of insulin receptor. On the other hand, in the presence of the insulin receptor, 284 units of BAEE esterase activity was observed. This value is very close to that obtained by subtracting the trypsin activity in the absence of receptor in the experiment shown in table 1 (see legend in table). We also used BAPNA as a substrate which overcomes amplitude noise encountered in BAEE esterase assay in the presence of TLCK. With BAPNA

TABLE 2

EFFECT OF TLCK AND SOYBEAN TRYPSIN INHIBITOR ON AMIDASE ACTIVITY OF PURIFIED INSULIN RECEPTOR

ADDITIONS	O.D. (10 min)
Trypsin	0.0076 ± 0.0001
Trypsin + TLCK	0.0018 ± 0.0001
Trypsin + Insulin receptor + TLCK	0.0065 ± 0.0007
Trypsin + Insulin receptor + TLCK + Soybean trypsin inhibitor	0

Either 33 ng of trypsin in 103 μl (Trypsin) or the same amount of trypsin treated for 1 minute with 10 μl of TLCK, final concentration 1 mM (Trypsin + TLCK) or 2 μg of insulin receptor in 100 μl incubated with the above quantity of trypsin for one minute and then treated with TLCK (Trypsin + Insulin receptor + TLCK) were added to 500 μl of BAPNA (1 mM in 50 mM Tris-HCl pH 7.7) The activity was monitored by recording spectrophotometrically the changes in absorbance at 410 nm for 7.5 minutes. To the last group, after the recording, 10 μg of soybean trypsin inhibitor were added. The results are the mean ± S.D. from 3 experiments.

as substrate, TLCK inhibits 78% of trypsin activity (Table 2), however, activity of trypsin plus insulin receptor was not affected. This amidase activity was completely inhibited by soybean trypsin inhibitor. When the mixture of trypsin plus insulin receptor was treated with TLCK, further addition of insulin did not increase the remaining activity of the mixture, either with BAPNA or with BAEE, as substrates (data not shown).

DISCUSSION

The increase in BAEE esterase activity when freshly prepared insulin receptor is added to trypsin, and the lack of this response with an old preparation of insulin receptor, strongly suggests that trypsin is acting on the receptor, and supports the idea that the insulin receptor may be a protease. Furthermore, the coincidence of the esterase activity in the experiments shown in Table 1 and the activity obtained when TLCK inhibits trypsin in the BAEE assay, seems to suggest that the increase in the esterase activity is due to an activation of protease activity in the insulin receptor.

A direct effect of insulin on the esterase activity of the insulin receptor is suggested by the failure of insulin to modify the esterase activity of trypsin unless insulin receptor was present. Also noteworthy is the coincidence between the concentration of insulin that produces a half maximal stimulatory activity in the BAEE assay and the dissociation constant value reported for the soluble insulin receptor (1.3×10^{-10}M, 22).

According to Seals and Czech (2), we may expect that if the insulin receptor is the protease which releases the chemical mediator, the protease

should have hydrolytic activity towards arginine substrates and this activity should not be inhibited by TLCK, but should be inhibited by the soybean trypsin inhibitor. Our results completely support this idea, since we found activity of the insulin receptor towards BAEE, BAPNA and TAME. The insulin receptor activity with BAEE or BAPNA as substrates was not inhibited by TLCK, and disappeared when soybean trypsin inhibitor was added.

That a protective effect of the receptor on trypsin autolysis might have significantly influenced our results seems to us unlikely. In the present study, the activity produced by trypsin was linear with time up to the point when the receptor was added and, in other instances, it also retained its linearity well beyond that point in time. These observations suggest that, under the conditions of our experiments, significant trypsin autolysis did not occur. Moreover, protection against even major trypsin autolysis would at best be expected to restore, not increase the slope produced by trypsin alone. Therefore, modulated trypsin autolysis could not account for the sharply increased curves generated by the addition of receptor and insulin.

BAEE and TAME are inhibitors of the insulin receptor autophosphorylation, and the esters of lysine, alanine or phenylalanine are much less efficient in inhibiting that process (11). The coincident esterase activity of insulin receptor towards BAEE and TAME, with the same abilities of the latter to inhibit the autophosphorylation process, suggests that a relationship may exist between these effects. If the esterase activity of the receptor versus trypsin activity is expressed on a molar basis, we find that the insulin receptor is 4.3 times less active with BAEE and 8.4 times less active with TAME. This represents 1.95 times less active with TAME than with BAEE, a value very close to the ratio of 2.5 found for the inhibition of the insulin receptor autophosphorylation by both substrates at 1.0 mM (11).

Since we did not detect any esterase activity in the receptor, unless preincubated with trypsin, and since the phosphorylation of the receptor is less sensitive to inhibition by TAME, we propose that the autophosphorylation of the receptor occurs first; this in turn activates the proteolytic activity in the receptor which then releases the peptide mediator, either from the receptor itself or from another protein. The mediator may in turn increase the kinase activity of the receptor. Such a mechanism may explain the ability of trypsin to increase the phosphorylation of the insulin receptor (23), the release of the peptide mediator (2, 24, 25), and the stimulated release of the mediator by a tyrosine kinase phosphorylation (10). Also the increased tyrosine kinase activity of the receptor may phosphorylate other plasma membrane proteins, like G protein(s) (26, 27), which in turn may activate other protein(s) like the proposed phospholipase C (28, 29) which releases from membrane several other proteins, linked to phosphatidylinositol by a glycan anchor (30), and all leading to pleiotropic effects.

The insulin receptor is reported to be more sensitive to degradation by trypsin in the presence of insulin (31). We found that once tryspin is inhibited by TLCK no increment of esterase activity of the insulin receptor could be observed. This result suggests that the interaction of insulin with its receptor induces a conformational change that makes a fragment accessible. When the fragment is removed the esterase activity increases. Another possibility is that the interaction of the hormone with inactive receptors exposes particular segments, the scission of these segments induces the proteolytic activity of the cluster.

In conclusion, our results provide the first direct evidence that the insulin receptor is a zymogen, and therefore may be the protease which releases a mediator for insulin action.

ACKNOWLEDGMENTS. We are grateful to Dr. Björn Holmgren and Dr. Randall Willis for the critical reading of the manuscript, and to Dr. E. Soto for his photographical work. Eleazar C. Vega-SaenzdeMiera was a fellow of CONACYT (Mexico).

REFERENCES

1. Kono, T., and Bayham, F.W. (1971) J. Biol. Chem. 246, 6204-6209.
2. Seals, J.R., and Czech, M.P. (1980) J. Biol. Chem. 255, 6529-6531.
3. Leef, J.W., and Larner, J. (1987) J. Biol. Chem. 262, 14837-14842.
4. Kikuchi, K., Schwartz, C., Creacy, S., and Larner, J. (1981) Mol. Cell Biochem. 37, 125-130.
5. Larner, J., Galasko, G., Cheng, K., DePaoli-Roach, A.A., Huang, L., Daggy, P., and Kellog, J. (1979) Science 206, 1408-1410.
6. Seals, J.R., and Jarett, L. (1980) Proc. Natl. Acad. Sci. USA. 77, 77-81.
7. Saltiel, A.R., Doble, A., Jacobs, S., and Cuatrecasas, P. (1983) Biochem. Biophys. Res. Comm. 110, 789-795.
8. Newman, J.D., Armstrong, J. McD., and Bornstein, J. (1985) Endocrinology 116, 1912-1919.
9. Kasuga, M., Zick, Y., Blith, D.L., Karlsson, F.A., Harings, H.U., and Kahn, C.R. (1982) J. Biol. Chem. 257, 9891-9894.
10. Suzuki, S., Toyota, T., Tamura, S., Kikuchi, K., Tsuiki, S., Huang, L., Villar-Palasi, C., Larner, J., and Goto, Y. (1987) J. Biol. Chem. 262, 3199-3204.
11. Tamura, S., Schwartz, C.F.W., Whipple, J.H., Dubler, R.E., Fujita-Yamaguchi, Y. and Larner, J. (1984) Biochem. Biophys. Res. Commun. 119, 465-472.
12. Kahn, C.R., Baird, K.L., Jarret, D.B., and Flier, J.S. (1978) Proc. Natl. Acad. Sci. USA 75, 4209-4213.
13. Schlessinger, J., Van Obberghen, E., and Kahn, C.R. (1980) Nature (London) 286, 729-731.
14. Jarrett, L., and Smith, R.M. (1983) Proc. Natl. Acad. Sci. USA 80, 1023-1027.
15. Cuatrecasas, P., and Parikh, I. (1974) Methods in Enzymol. Vol XXXIV, Part B. ed. W.B. Jacoby and M. Wilchek, pp. 653-670, Academic Press, New York.
16. Jacobs, S., Shechter, Y., Bissell, K. and Cuatrecasas, P. (1977) Biochem. Biophys. Res. Commun. 77, 981-988.
17. Posner, B.I., Josefsberg, Z., and Bergeron, J.J.M. (1978) J. Biol. Chem. 253, 4067-4073.

18. Bradford, M.M. (1976) Analytical Biochem. 72, 248-254.
19. Schwert, G.W., and Takenaka, Y. (1955) Biochem. Biophys. Acta. 16, 570-575.
20. Walsh, K.A. (1970) Methods in Enzymol. Vol XIX, ed. W.B. Jacoby and M. Wilchek, pp. 41-63, Academic Press, New York.
21. Erlanger, B.F., Kokowsky, N. and Cohen, W. (1961) Arch. Biochem. Biophys. 95, 271-278.
22. Cuatrecasas, P. (1972) J. Biol. Chem. 247, 1980-1991.
23. Tamura, S., Fujita-Yamaguchi, Y., and Larner, J. (1983) J. Biol. Chem. 258, 14749-14752.
24. Begum, N., Tepperman, H.M., and Tepperman, J. (1983) Endocrinology 112, 50-59.
25. Begum, N., Tepperman, H.M., and Tepperman, J. (1982) Endocrinology 110, 1914-1921.
26. O'Brien, R.M., Houslay, M.D., Milligan, G., and Siddle, K. (1987) FEBS Lett. 212, 281-288.
27. Gawler, D., Milligan, G., Spiegel, A.M., Unson, C.G., and Houslay, M.D. (1987) Nature 327, 229-232.
28. Saltiel, A.R., and Cuatrecasas, P. (1986) Proc. Natl. Acad. Sci. USA 83, 5793-5797.
29. Fox, J.A., Soliz, N.M., and Saltiel, A.R. (1987) Proc. Natl. Acad. Sci. USA 84, 2663-2667.
30. Low, M.G. (1987) Biochem. J. 244, 1-13.
31. Pilch, P.F., and Czech, M.P. (1980) Science 210, 1152-1153.

Vol. 156, No. 1, 1988 BIOCHEMICAL AND BIOPHYSICAL RESEARCH COMMUNICATIONS
October 14, 1988 Pages 38-45

A GENUINE ORGAN SPECIFIC ALCOHOL DEHYDROGENASE FROM HAMSTER TESTES: ISOLATION, CHARACTERIZATION AND DEVELOPMENTAL CHANGES

Wing-Ming Keung[1]

Department of Biochemistry
The Chinese University of Hong Kong
Shatin, N.T., Hong Kong

Received August 29, 1988

ABSTRACT: Testes of golden hamsters (*Mesocricetus auratus*) contain a unique form of alcohol dehydrogenase. The enzyme purified to homogeneity is a dimer composed of two identical 41000 dalton subunits and was inhibited by 4-methylpyrazole and 1,10-phenanthroline. The enzyme prefers primary over secondary alcohol substrates and oxidizes vitamin A (retinol) most efficiently. Its activity in the testis increases during the prepubertal development and such increase is concomitant with, but preceding slightly, the increase in testicular weight and plasma testosterone. These results may implicate the involvement of this enzyme in the development of male hamsters' reproductive system. © 1988 Academic Press, Inc.

INTRODUCTION: The golden hamster (*Mesocricetus auratus*), in contrast to most outbred strains of laboratory rodents, prefers to drink ethanol under free choice situations (1-4). Sex differences in ethanol preference and sensitivity in golden hamsters have also been reported (5). These species and sex differences correspond very well to the species and sex-differences in the activities of liver alcohol dehydrogenase (ADH), ethanol metabolism in isolated hepatocytes and blood ethanol elimination rates (2-5). In an attempt to characterize the alcohol metabolizing enzymes in golden hamsters, a testis specific form of ADH was discovered.

---

[1] Present address: Center for Biochemical and Biophysical Sciences and Medicine, Harvard Medical School, Seeley G. Mudd Building, 250 Longwood Avenue, Boston, MA 02115.

Abbreviations: ADH, alcohol dehydrogenase; CapGapp-, 4-(3-(N-(6-aminocaproyl)amino)propyl)pyrazole-; $NaDodSO_4$, sodium dodecyl sulfate; OP, 1,10-phenanthroline; 4-MP, 4-methylpyrazole.

0006-291X/88 $1.50
Copyright © 1988 by Academic Press, Inc.
All rights of reproduction in any form reserved.

Organ specific ADH isozymes have been reported in many species including man (6,7), mouse (8) and rat (9). Studies on the catalytic properties of organ specific isozymes in relation to the specialized metabolic function(s) of the particular organs have provided insights to the understanding of the functional role(s) these isozymes played in their specific organs and to the understanding of the physiological function(s) of ADH isozymes in general. The hamster testis ADH reported here is unique not only because it is the only form of ADH found in the testes but also that it is not found in other tissues. This report describes the isolation, characterization of this testis ADH and the changes in its activity during prepubertal development of the golden hamsters.

MATERIALS AND METHODS: Golden hamsters (*Mesocricetus auratus*) were bred in our animal colony from animals originally obtained from Simonson laboratories, Gilroy, California and were maintained from birth in a long photoperiod, 14 h light:10 h darkness. The animals had free access to food and water. Adult male golden hamsters (70-90 days old) were killed by decapitation and testes were removed and frozen immediately in liquid N_2 and stored at -70 °C. The frozen testes were used within one month.

Fresh or frozen and thawed testes were homogenized in 50 mM sodium phosphate buffer, pH 7.5 containing 1 mM NAD^+. The homogenate was centrifuged at 38,000 g for one hour and the supernatant was loaded onto a CapGapp-Sepharose column (2x10 cm). The column was washed and ADH was eluted according to the procedure of Lange & Vallee (10).

Starch gel electrophoresis was performed according to the method of Bosron et al. (11). Electrophoresis in $NaDodSO_4$ polyacrylamide gel was carried out by the procedure of Laemmli and Favre (12). Urea gel electrophoresis was carried out by the system developed by Keung et al. (13). Protein concentration was determined by the method of Lowry et al. (14) using bovine serum albumin as standard. ADH activity was determined spectrophotometrically as the increase in absorbance at 340 nm due to the reduction of NAD^+ in buffers specified in the text. One unit of activity is defined as the amount of enzyme that catalyses the formation of 1 μmole NADH per min at 25 °C.

All alcohol substrates and other reagents used were of analytical grade and used without further purification.

RESULTS AND DISCUSSION: Electrophoresis of adult hamster testis extracts on starch gel revealed only one detectable ADH activity band (ADH-4)(Fig. 1). The electrophoretic pattern of the hamster liver extract containing seven bands is also shown for comparison. While ADH-3, ADH-5, ADH-6, ADH-7 and ADH-8 were stained with ethanol as substrate, ADH-1 and ADH-2 could be visualized only when long chain alcohols, e.g. 1-octanol, were used. ADH-4 was the only ADH detected in the testis, independent

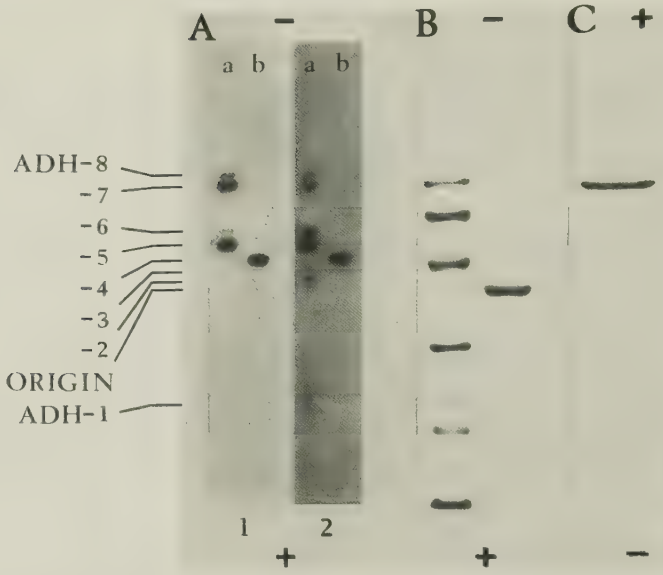

Fig. 1 (A) Starch gel electrophoretic patterns of (a) hamster liver and (b) hamster testis ADH. Gels were stained for ADH activity using (1) ethanol and (2) 1-octanol as substrates. (B) $NaDodSO_4$ gel electrophoresis of purified hamster testis ADH and a standard mixture (Pharmacia) composed of phosphorylase b (Mr. 94,000), bovine serum albumin (Mr. 66,000), ovalbumin (Mr. 45,000), carbonic anhydrase (Mr. 29,000), soybean trypsin inhibitor (Mr. 20,100) and alpha-lactalbumin (Mr. 14,400). (C) Urea gel electrophoresis of hamster testis ADH.

of the staining substrate. None of the other tissues studied including liver, kidney, brain, lung, heart, cecum, spleen, intestine, ovary and stomach, showed any detectable ADH-4 activity (result not shown).

The testis ADH was purified to homogeneity by affinity chromatography on a CapGapp-Sepharose column and the result of the purification procedure is shown in Table 1. The enzyme was purified in satisfactory yield (60-70 %) by this single step procedure which was accomplished in two days. From 60 g of testes, about 18 units of pure ADH-4 was obtained.

Chromatography of the purified testis ADH on a molecular sieving HPLC column yielded a single protein peak which co-eluted with human liver ADH (not shown) indicating that the hamster testis ADH, like the human ADHs (15,16), has a molecular weight around 80,000. $NaDodSO_4$ gel electrophoresis of ADH-4 revealed a single protein band corresponding to a subunit molecular weight of about 41,000 (Fig. 1). Electrophoresis of the urea dissociated ADH-4 on polyacrylamide gels containing 7 M urea also showed a single protein band (Fig. 1). These results not only establish the homogeneity of the enzyme preparation but also

Table 1: Purification of Hamster Testis ADH[a]

Purification step	Total Activity[b] (unit)	Total Protein (mg)	Specific Activity (U/mg)	Yield (%)	Purification Fold
38,000 g supernatant	27	1080	0.025	100	1
CapGapp-Sepharose	18	4.6	4.0	67	160

[a] From 34 testes, about 60 g.

[b] Activity was determined at pH 7.5 in 0.1 M sodium phosphate buffer containing 2.4 mM NAD^+ and 40 mM ethanol.

suggest that ADH-4 is a dimeric enzyme composed of two identical subunits.

Like the human class I ADHs (15,16), hamster testis ADH is extremely sensitive to 4-methylpyrazole and OP inhibition. While 4-methylpyrazole inhibits the enyzme in a competitive fashion (K_i=0.5 μM), OP is a mixed type inhibitor (K_i=0.13 mM)(Fig. 2).

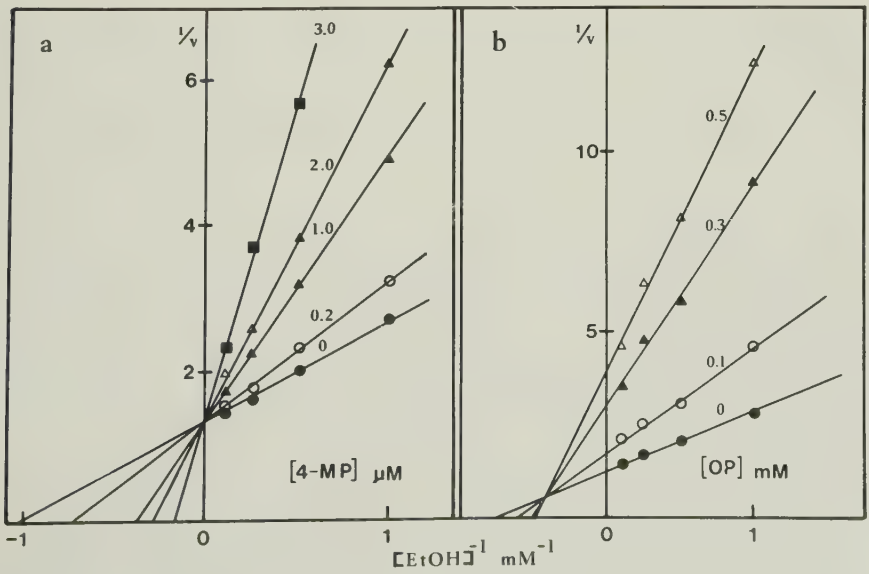

Fig. 2 Lineweaver-Burk plots of (a) 4-MP and (b) OP inhibition of hamster testis ADH catalysed ethanol oxidation. Initial velocities were determined at pH 7.5 in 0.1 M sodium phosphate containing 2.4 mM NAD^+ and varied inhibitor and ethanol concentrations.

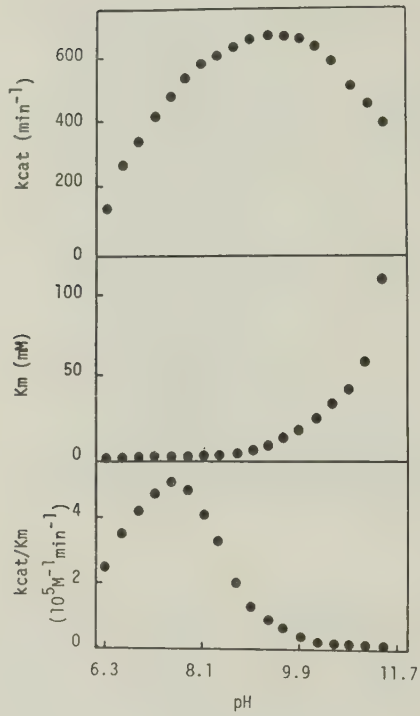

Fig. 3 pH-(a) k_{cat}, (b) K_m, and (c) k_{cat}/K_m profiles for hamster testis ADH catalysed ethanol oxidation. Initial velocities were determined in 0.1 M glycine-NaOH (pH 11.4 to pH 9.3), sodium pyrophosphate (pH 9.3 to pH 7.5) or sodium phosphate (pH 7.5 to 6.3) buffers.

The effect of pH on the kinetic properties of ADH-4 was studied using ethanol as substrate and the pH-K_m, pH-k_{cat}, and pH-k_{cat}/K_m profiles are shown in Fig. 3. The value of k_{cat} is optimal at a pH between 9 and 10 whereas the K_m value decreases logarithmically from 0.11 M at pH 11.4 to 0.52 mM at pH 6.3. The k_{cat}/K_m is maximal at pH 7.5.

The steady state kinetics of ADH-4 was studied at pH 7.5 using a series of primary and secondary alcohol as substrates. The kinetic parameters are shown in Table 2. With the exception of methanol, the enzyme oxidizes all the primary alcohols very efficiently. Both K_m and k_{cat} values decrease as the chain length of the substrate increases. The k_{cat}/K_m values indicate that alcohols with longer chain length are better substrates.

At pH 7.5, 12-hydroxydodecanoate is virtually not oxidized by the testis ADH. However, it is an effective competitive inhibitor of ethanol oxidation with a K_i=1 μM. At pH 10 however, this substrate is oxidized very efficiently. Secondary alcohols are also oxidized by the testis ADH but with much higher K_m's and as a consequence, the k_{cat}/K_m values determined for secondary

Table 2: Kinetic parameters for hamster testis ADH[a]

Substrate	K_m (μM)	k_{cat} (min^{-1})	k_{cat}/K_m (M^{-1} min^{-1})
ethanol	960	480	5.0×10^5
1-butanol	440	450	1.0×10^6
1-hexanol	69	182	2.6×10^6
12-hydroxy-dodecanoate[b]	50	146	2.9×10^6
all-trans-retinol[c]	20	78	3.9×10^6
benzyl alcohol	410	82	2.0×10^5
2-butanol	250000	285	1.1×10^3
cyclohexanol	31000	122	3.9×10^3
NAD^+[d]	57	465	8.2×10^6
$NADP^+$(2.4 mM)		no activity	

[a] Activity was determined at pH 7.5 in 0.1 M sodium phosphate containing 2.4 mM NAD^+ and various concentrations of alcohol substrates. Kinetic parameters were estimated by Lineweaver-Burk plots.

[b] Determined at pH 10 in 0.1 M glycine-NaOH buffer.

[c] Retinol oxidation was studied at pH 7.5 in 0.1 M sodium phosphate containing 0.02% Tween 80 (22).

[d] Kinetic parameters for NAD^+ were estimated at saturating ethanol concentration, 40 mM.

alcohols are about 1000 fold lower than those for the primary alcohols.

The coenzyme requirement for the testis ADH, using ethanol as substrate, indicates that the enzyme requires NAD^+ for activity. $NADP^+$, at a concentration of 2.4 mM yielded no activity.

It is of interest to note that vitamin A (retinol) is oxidized most efficiently by the testis ADH. It is well established that vitamin A is essential for developement and growth(17-19). Vitamin A is ingested as the relatively inactive retinol and is oxidized to the more active retinoic acid or its metabolites in vivo (19-20). The fact that hamster testis ADH oxidizes retinol so efficiently suggests that this enzyme may play an important role in the development of the golden hamsters. To further substantiate this hypothesis, a study on the changes in ADH activity in the golden hamster testes has been carried out and the result is shown in Fig. 4. During prepubertal development in the golden hamster, there is major age-related changes in the testicular ADH activity. Since throughout the prepubertal

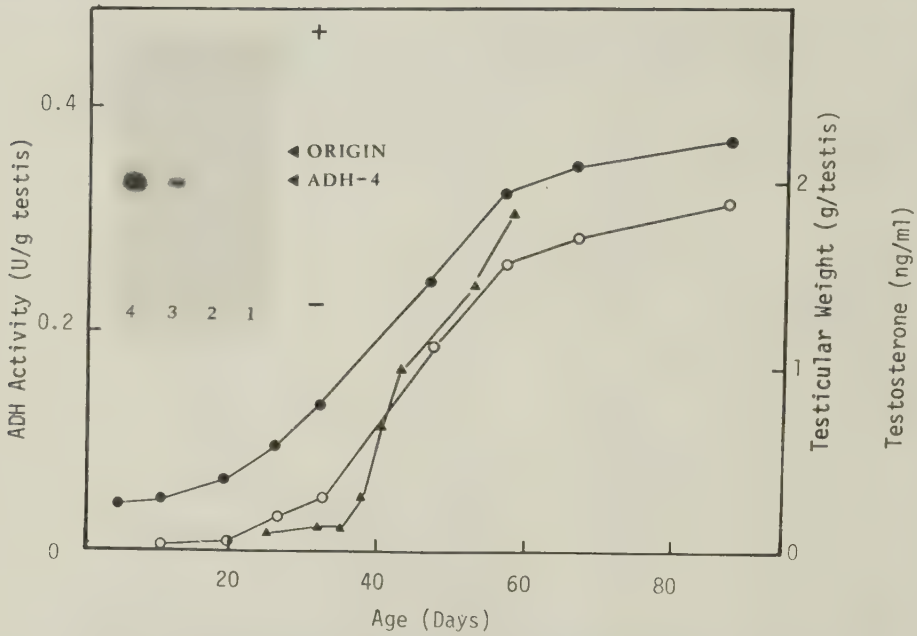

Fig. 4 Changes in testis ADH activity (●), testicular weight (O) and plasma testosterone level (▲) during the development of golden hamsters. Testes from hamsters of different ages were homogenized and centrifuged for 1 h at 38,000 g. ADH activities in the supernatants were determined at pH 7.5 in 0.1 M sodium phosphate containing 2.4 mM NAD^+ and 40 mM ethanol. Background activities, determined in the presence of 1 mM 4-MP, were subtracted from data. Plasma testosterone data were taken from reference 20. Insert: starch gel electrophoretogram of testis extracts from hamsters of different ages: (1) 12 days, (2) 25 days, (3) 41 days and (4) 62 days. Extracts from equal amount (40 μg) of testis were applied to each sample well.

development, no ADH isozyme other than ADH-4 was detected in the testes (Fig. 4 insert), the observed changes in testicular ADH activity reflects the changes in the level of ADH-4. Between 20 and 55 days of age, there is greater than 10 fold increase in testicular ADH activity. Such increase is in general parallel to, but preceding slightly, the increase in testicular weight and plasma testosterone concentrations reported previously (21). These results implicate the involvement of testis ADH in the development of the male hamsters' reproductive system. Further investigation on this subject is in progress.

ACKNOWLEDGEMENT: The author thanks Dr. B.L. Vallee of Harvard Medical School for providing the CapGapp-Sepharose resin. This work was supported by grants from The Chinese University of Hong Kong and the Hopeh & Shantung Native Hong Kong Association Limited.

REFERENCES

(1) Arvola, A. and Forsander, O. A. (1961) Nature 191, 819-820.
(2) Crow, K.E., Cornell, N.W. and Veech, R.L. (1977) In: Alcohol and aldehyde metabolizing systems. Vol. III, Eds Thurman, R.G., Williamson, J.R., Drott, H. and Chance, B. 335-342, Academic Press, New York.
(3) Thurman, R.G., Bleyman, M.A. and McMillan, D.E. (1978) Pharmacologist 20, 160-168.
(4) Kulkosky, P.J. and Cornell, N.W. (1979) Pharmacol. Biochem. & Behav. 11, 439-444.
(5) Moss, H.B., Salin-Pascual, R.J., Rathnagiri, P., Goldman, D. and Tamarkin, L. (1987) Alcohol and Drug Research 7, 301-307.
(6) Pares, X., Farres, J. and Vallee, B.L. (1984) Biochem. Biophys. Res. Commun. 119, 1047-1055.
(7) Dafeldecker, W.P. and Vallee, B.L. (1986) Biochem, Biophys. Res. Commun. 134, 1056-1063.
(8) Algar, E.M., Seeley, T-L. and Holmes, R.S. (1983) Eur. J. Biochem. 137, 139-147.
(9) Julia, P., Farres, J. and Pares, X. (1987) Eur. J. Biochem. 162, 179-189.
(10) Lange, L.G. and Vallee, B.L. (1976) Biochemistry 15, 4681-4686.
(11) Bosron, W.F., Li, T.-K. and Vallee, B.L. (1979) Biochem. Biophys. Res. Commun. 91, 1549-1555.
(12) Laemmli, U.K. and Favre, M. (1973) J. Mol. Biol. 80, 575-599.
(13) Keung, W.M., Ditlow, C.C. and Vallee, B.L. (1985) Anal. Biochem. 151, 92-96.
(14) Lowry, O.H., Rosebrough, N.J., Farr, A.L. and Randall, R.J. (1951) J. Biol. Chem. 193, 265-275.
(15) Vallee, B.L. and Bazzone, T.J. (1983) In Isozymes: Current topics in biological and medical research. Vol. 8, 219-244. Alan R. Liss, New York.
(16) Vallee, B.L. (1985) Proc. Congr. Eur. Brew. Conv. 20, 65-90.
(17) Leathem, J.H. (1970) In: The testes, Eds. Johnson, A.D., Gomes, W.R., Vandermark, N.L., Vol. 3, 188-190, Academic Press,New York.
(18) Steinberg, A. and Steinberg, E. (1966) Exp. Cell Res. 44, 429-435.
(19) Van Thiel, D.H., Gavaler, J. and Lester, R. (1974) Science 186, 941-942.
(20) Sporn, M.B. (1985) In Retinoids, differentiation and disease. Ciba Foundation Symposium 113, p. 92, Pitman, London.
(21) Stallings, M.H., Matt, K.S., Amador, A., Bartke, A., Siler-Khodr, T.M., Soares, M.J. and Talamantes, F. (1985) J. Reprod. Fert. 75, 663-670.
(22) Julia, P., Farres, J. and Pares, X. (1986) Exp. Eye Res. 42, 305-314.

Vol. 156, No. 1, 1988 BIOCHEMICAL AND BIOPHYSICAL RESEARCH COMMUNICATIONS
October 14, 1988 Pages 46-53

ANTI HLA CLASS I MONOCLONAL ANTIBODY EFFECT ON PKC KINETICS IN PHA ACTIVATED HUMAN PERIPHERAL BLOOD MONONUCLEAR AND E' CELLS

Licia Poltronieri*, Edon Melloni**, Michele Rubini*, Rita Selvatici*, Cristina Mazzilli***, Roberto Baricordi* and Enrico Gandini*

*Istituto di Genetica Medica, Universita' degli Studi di Ferrara, Ferrara, Italy

**Istituto Policattedra Chimica Biologica, Universita' degli Studi di Genova, Genova, Italy

***Dipartimento di Biologia Spererimentale, Universita' La Sapienza, Roma, Italy

Received August 11, 1988

SUMMARY: Cytoplasmic protein kinase C (PKC) has been studied in phytohemagglutinin (PHA) activated peripheral blood mononuclear cells (PBMC) and macrophage depleted E' cell culture. Within 10' after contemporanous addition of PHA and anti HLA class I monoclonal antibody 01.65 (MoAb) PKC is depleted in both cell types. Enzyme activity recovers in the following hours however at 72 hours is at control values in E' cultures while in PBMC cultures it is still depleted at 68% of the control. Anti HLA class I MoAb induced tritiated tymidine (^{3}H-TdR) incorporation inhibition appears to be related to low levels of PKC activity. © 1988 Academic Press, Inc.

Anti HLA class I antigens monoclonal antibodies (MoAbs) inhibit the proliferation of T lymphocytes triggered by ligands active on Ca^{2+} dependent pathways such as antigens, lectins, agonistic MoAbs anti T3-T1 complex and ionofores. They are inffective, however, on T cells stimulated by phorbol esthers that activate protein kinase C (PKC) in a Ca^{2+} independent pathway. It has been assumed that HLA class I antigens regulate an early event in the Ca^{2+} dependent pathway of T cell activation (1-5).

ABBREVIATIONS: PKC, Protein Kinase C; PBMC, Peripheral blood mononuclear cells; E', Sheep red cells rosettes purified T cells; PHA, Phytohemagglutinin; MoAb, Monoclonal antibody; SRBC, Sheep red blood cell.

0006-291X/88 $1.50
Copyright © 1988 by Academic Press, Inc.
All rights of reproduction in any form reserved.

According to some reports (3-4) and in our own experience no inhibition is observed in macrophages depleted PHA activated T cell cultures (6). We have provided evidence however that anti HLA class I MoAbs do not affect in activated peripheral blood mononuclear cells (PBMC) early events such as $(Ca^{2+})_i$ rise, and inositol phosphate level, considered essential for PKC activation (6). On the other hand we could show that anti HLA class I MoAb down regulates native protein kinase C (PKC) of PHA stimulated T cell cultures. Within 10' from the addition of PHA and anti HLA class I MoAb to E' cells, PKC is depleted to 80% of the normal value, and in the following 24 hours is 58% of control (7). Furthermore we could show that when HLA Class I MoAb is added to a PHA activated PBMC culture the cell cycle progression is delaied and the number of cell divisions is reduced. As a consequence the number of dividing cells in the MoAb treated cultures is lower and the ammount of ^{3}H-TdR incorporated comparatively decreased (8).

We present in this report cytoplasmatic PKC kinetics during the 72 hours of culture in MoAb treated PHA activated PBMC and E' cells. The data furthermore suggest a direct relationship between cytoplasmatic PKC values and inhibition percent of ^{3}H-TdR incorporation by anti HLA class I MoAb.

MATERIALS AND METHODS

DEAE-cellulose (DE-52) was obtained from Whatman. Phosphatidylserine (bovine brain), Dioleoylglycerol, Histone IIIS, Leupeptin, Phenylmethylsulphonyl fluoride and ATP were purchased from Sigma. (γ-^{32}P) ATP (3000 Ci/mmol) was from Amersham, PHA was from Burroughs Wellcome. MoAb 01.65(15) anti HLA Class I antigens (HLA-A, B and -C) and Mo1 anti monocytes were kindly provided by Dr. F. Malavasi (9).
All other chemicals were reagent grade.

T cell preparation

Pheripheral blood lymphocytes were isolated from buffy coats of normal adults by centrifugation over Fycoll/Hypaque density gradient at 1000xg for 20' at 20° C. Cells were washed twice with RPMI 1640 medium and suspended in RPMI 1640 containing 5% fetal calf serum. Then, cells were incubated in Petri dishes at 37° C for 1 hour in 5% CO_2, for depletion of monocytes/macrophages. The non-adherent cells were colleted in RPMI 1640 at the concentration of $6x10^6$ cells/ml. E rosettes were formed with sheep red blood

cells (SRBC) treated with Neuraminidase (4 ml SRBC treated/100x10^6 cells) and incubated at 37° C for 15'. The mixture was centrifuged at 1000xg at room temperature and incubated on ice for 1 hour. The pellets were resuspended gently and centrifuged over Fycoll at 1000xg for 20'. The B cells were recovered from the interface, and the E' cells were obtained from the pellet by lysis of the SRBC with 5 mM Ammonium Cloride followed by centrifugation at 700xg for 5'. E' cells were resuspended in RPMI 1640 added with antibiotics. E' cell preparation contained less then 3% of Mo1 positive cells.

Cell culture incubation

Cells were suspended at 1x10^{6}cells/ml concentration in RPMI medium containing 5% fetal calf serum and antibiotics and incubated at 37° C with PHA (2 ug/ml) and/or MoAb 01.65 (0.1 mg/ml) at different times. Following incubation, cells were washed and lysed by sonication as described below.

Isolation of Soluble and Particulate Fraction

Lysates were obtained by sonicating the cell suspension (15x10^6 T cells/ml in 0.25 M sucrose, 10 mM Hepes pH 7.5, 5 mM EDTA, 10 mM 2-mercaptoethanol, 2 mM phenylmethyl- sulphonylfluoride and 0,01% leupeptin) with six 10-sec. bursts from a MSE model MK2 sonicator, followed by a centrifugation at 100,000xg for 20'. The supernatant was collected as cytosolic fraction and the pellet was suspended in the same buffer containing 0.1% Triton X-100 as particulate fraction.

Partial purification of PKC from T cells

PKC was partially purified from the cytosolic fraction by a chromatography on a DEAE-cellulose column equilibrated with 10 mM Hepes pH 7.5, 10 mM 2-mercaptoethanol and 5 mM EDTA.
PKC was eluted with a 70 ml linear 0-0.4 M NaCl gradient.

PKC activity

PKC was assayed according to Melloni et al. (10). In the incubation mixture for certains experiments Ca^{2+} and phospholipids were replaced by 5 mM EDTA. PKC activity is expressed as nmol ^{32}P incorporation into Histone under experimental conditions.

Protein determination

According to Lowry (11) using bovine serum albumin as standard protein.

RESULTS

PHA activated PBMC (Fig. 1)

Native cytosolic PKC in the initial 10' after lectin addition is depleted to 47,2 % of total control activity. However the recovery is almost complete at 24 hours and enzymatic activity is completely restored at 72 hours.

In PHA activated PBMC cultured in presence of MoAb 01.65 the drop of cytosolic activity within the initial 10' is observed to 36% of control. The native cytosolic PKC recovers during the following

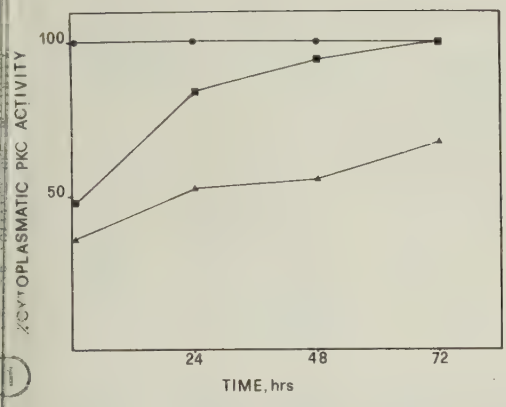

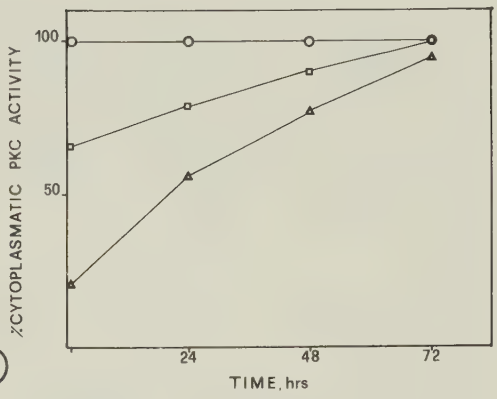

FIG. 1 : TIME COURSE OF THE EFFECT OF PHA AND PHA+MoAb 01.65 TREATMENT ON CYTOSOLIC PKC IN PBMC CULTURE.

Cells were incubated at $1X10^6$/ml concentration with PHA (2 ug/ml) or PHA plus MoAb 01.65 (0.1 mg/ml). Cytosolic PKC activity was determined at different times in PBMC only (●) as control and in PHA (■) or in PHA+MoAb 01.65 (▲).

FIG. 2 : EFFECTS OF PHA AND PHA+MoAb 01.65 ON CYTOSOLIC PKC ACTIVITY IN E^+ CELLS.

E^+ cells were incubated with PHA in presence or absence of MoAb 01.65 at the same conditions described in the legend of Fig. 1. E^+ only (○), PHA (□), PHA+MoAb (△).

hours to about 50% of activity at 24 and 48 hours and 68% of activity at 72 hours.

PHA activated E+ cells (Fig. 2)

Native cytosolic PKC after 10' from the addition of PHA drops to 65% of control and is completely recovered at 72 hours.

When E^+ cells are cultured in presence of MoAb 01.65 the activity drops at 20% of control in the initial 10 minutes progressively recovers to 56% at 24 hours and 94% at 72 hours.

Fig. 3 shows PKC kinetics in PHA activated MoAb 01.65 treated PBMC and E^+ cell cultures.

In PBMC culture PKC depletion at 10' after the addition of lectin and MoAb is lower than in E^+ cells. However the recovery is much faster in E^+ cell cultures where in 48 hours PKC value increases from 20% to 80% of control. PKC recovery in PBMC culture is much slower in the first 24 hours and essentially null between 24 and 48

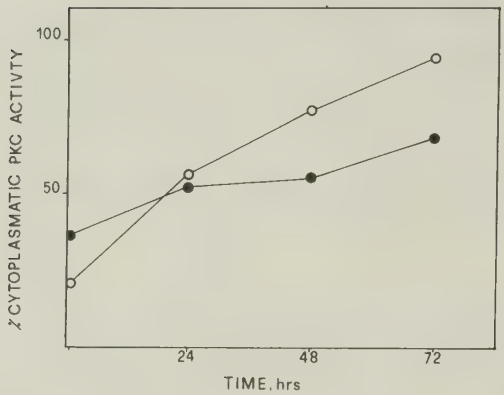

FIG. 3 : TIME KINETIC COMPARISON OF CYTOSOLIC PKC ACTIVITY IN PHA+MoAb 01.65 TREATED CULTURE OF PBMC (●) OR E' (○) CELLS.

hours. Between 48 and 72 hours the rate af increase of cytosolic PKC is apparently similar in the two types of cultures.

DISCUSSION

PKC kinetics in anti HLA class I MoAb treated PBMC and E' cell preparations is different.

Within ten minutes from the addition of PHA to either PBMC or E' cell preparations of cytosolic PKC is depleted. In both systems the depletion is reversible and within 48 hours is back to normal values.

In presence of MoAb 01.65 PBMC remains depleted at about 50% of controls enzimatic activity, while is back to normal value within 24/48 hours in the case of E' cells.

Down regulation of PKC is induced in different cell lines by a variety of external stimula (12-22). The reason of the PKC depletion remains to be established although it can be attributed to the removal of the inhibiting effect of PKC on an unidentified cell function of a short-life activated PKC form by a proteolytic mechanism (10,23,24).

MoAb activates on lymphocytes a proteolytic system wich selectively recognizes and digestes PKC. This process is completed and in few

TABLE I

		HOURS FROM LECTIN PLUS MoAb ADDITION		
		24	30	72
PBMC	PKC depletion%	38		32
	3H-TdR inhibition%		52-57*	30-85***
E+	PKC depletion%	31		6
	3H-TdR inhibition%		53-89*	0-13**

Comparison of PKC depletion percent and 3H-TdR incorporation inhibition percent. PKC depletion is expressed as the ratio

$$\frac{\text{PKC (PHA+MoAb cultures)}}{\text{PKC (PHA cultures)}}$$

*: 3 donors
**: 5 donors
***: 24 donors

minutes ends, then PKC activity reappears in the cells. The macrophages effect may be explaned as a further and prolonged activation of this proteolytic system.

PKC plays a role in PHA stimulated T cell proliferaton (25,26) and it has been suggested that Ca^{2+}/phospholipid dependent PKC is involved in the G1 transit of epithelial cell lines during the transition G0/G1 and G1/S (27).

Our work has shown that anti HLA class I MoAb affects the cell cycle of PHA stimulated PBMC slowing down the cell cycle and induces a significant increase of cell with a G1 DNA content (2C) incorporating 5-Bromo2-deoxyuridine (8).

A possible correlation between PKC activity and prolipherative response of PHA activated T cells is suggested by the comparison of per cent enzymatic depletion and inhibition of ^{3}H-TdR incorporation (Tab. 1). Data have been obtained in independent experiments on

different donors. There is however a clear indication that at the first step in wich in vitro lymphocyte prolipheration triggered by PHA stimulation can be monitored: i.e. 30 hours PKC activity is depleted in both PBMC and E' cell cultures anti HLA class I MoAb inhibits ^{3}H-TdR incorporation. Vice versa at 72 hours of culture when PKC value is normal in E' cells preparation no ^{3}H-TdR incorporation inhibition is detectable. In PHA activated PBMC preparation, containing macrophages, at 72 hours PKC is still depleted to 35% of control and ^{3}H-TdR incorporation inhibition is observed varying in different cases from 35 to 80% (24 experiments).

ACKNOWLEDGMENTS

Dr. Licia Poltronieri is personally supported by the Associazione Italiana per la Ricerca sul Cancro, Milan - Italy.
The autors thank Prof. F. Malavasi, Turin - Italy, for the generous supply of antibody 01.65.
This work was partially supported by C.N.R. Progetto Finalizzato "Oncologia" contratto n.87.01297.44 and Gruppo Immunologia, contributo n.87.01509.04.

REFERENCES

1) Turco, M.C., De Felice, M., Corbo, L., Morrone, G., Mertelsmann, R., Ferrone, S., and Venuta, S. (1985) J. Immunol. 135, 2268-2273.
2) Taylor, S., Nowell, P.C., Kornbluth, J. (1986) Proc. Natl. Acad. Sci. U.S.A. 83, 4446-4450.
3) Dasgupta, J.D., Clunach, K., Dubey, D.P., Yunis, E.J., and Amos, D.B.(1987) Proc. Natl. Acad. Sci. U.S.A. 84, 1094-1098.
4) Dasgupta, J.D., and Yunis, E.J. (1987) J. Immunol. 139, 672-677.
5) De Felice, M., Turco, M.C., Carandente Giarrussa, P., Corbo, L., Pirrano, R, Martinelli, V., Ferrone, S., and Venuta, S. (1987) J. Immunol. 139, 2683-2689.
6) Cavallini, G., Pozzan, T., Selvatici, R., Baricordi, O.R., Mazzilli, C. and Gandini, E. (1988) Biochem. Biophys. Res. Commun. in press.
7) Poltronieri, L., Melloni, E., Rubini, M., Selvatici, R., Mazzilli, M.C., Baricordi, O.R., and Gandini, E. (1988) Biochem. Biophis. Res. Commun. 152 n.3, 951-956.
8) Rubini, M., Panozzo, M., Selvatici, R., Poltronieri, L., Baricordi, O.R., Mazzilli, C. and Gandini, E. (1988) submitted for pubblication.
9) Malavasi, F., Milanesi, C., Fabbi, M., Richiardi, P., Calligaris-Cappio, F., Ferrero, E., Roggero, S., Dellabona, P. and Ceppellini, R. (1984) Diagn. Immunol. 2, 53-62.
10) Melloni, E., Pontremoli, S., Michetti, M., Sacco, O., Sparatore, B., Salamino, F., and Horecker,B.L. (1985) Proc. Natl. Acad. Sci. U.S.A. 82, 6435-6439.

(1) Lowry, O.H., Rosegrough, N.J., Farr, A.L. and Randall, R.J. (1951) J. Biol. Chem. 193, 265-275.
(2) Solanki, V., Slaga, T.J., Callaham, M. and Huberman, E. (1981) Proc. Natl. Acad. Sci. U.S.A. 78, 1722-1725.
(3) Rodriguez-Pena, A. and Rozengurt, E. (1984) Biochem. Biophys. Res. Commun. 120, 1053-1059.
(4) Tapley, P.M. and Murray, A.W. (1984) Biochem. Biophys. Res. Commun. 122, 158-164.
(5) Tapley, P.M. and Murray, A.W. (1985) Eur. J. Biochem. 151, 419-423.
(6) Pontremoli, S., Melloni, E.,Sparatore, B., Salamino, F., Michetti, M., Sacco, O. and Horecker, B.L. (1985) Biochem. Biophys. Res. Commun. 128, 331-338.
(7) Hoshijima, M., Kikuchi, A., Tanimoto, T., Kaibuchi, K. and Takai, Y. (1986) Cancer. Res. 46, 3000-3004.
(8) Murray, A. W., Fournier, A. and Hardy, S.J. (1987) TIBS 12, 53-54.
(9) Edelman, A.M., Blumenthal, D.K., and Krebs, E.G. (1987) Ann. Rev.Biochem. 56, 567-613.
(10) Gopalakrishna, R. and Barsky, S.H. (1988) Proc. Natl. Acad. Sci. U.S.A. 85, 612-616.
(11) Young, S., Rotjbard, J. and Parker, P.J. (1988) Eur. J. Biochem. 173, 247-252.
(12) Ito, M., Takami, Y., Tanabe, F., Shigeta, S., Tsukui, K. and Kawade, Y. (1988) Biochem. Biophys. Res. Commun. 150, 126-132.
(23) Yamada, S., Ohmori, M. and Takayama, H. (1983) J. Biol. Chem. 258, 457-463.
(24) Melloni, E., Pontremoli, S., Michetti, M., Sacco, O., Sparatore, B. and Horecker, B.L. (1986) J. Biol. Chem. 261, 4101-4105.
(25) Nishizuka, Y. (1986) Science 233, 305-312.
(26) Kaibuchi, K., Takai, Y., and Nishizuka, Y. (1985) J. Biol. Chem. 260, 1365-1369.
(27) Boynton, A.L., Kleine, L.P., Whitfield, J.F. and Bossi, D. (1985) Exp. Cell Res. 160, 197-205.

Vol. 156, No. 1, 1988 BIOCHEMICAL AND BIOPHYSICAL RESEARCH COMMUNICATIONS
October 14, 1988 Pages 54-60

RECONSTITUTION OF PARTIALLY PURIFIED OPIOID RECEPTORS WITH A GTP-BINDING PROTEIN

Toshiyuki Fujioka, Fumiko Inoue, Sachiyo Sumita, and Masayuki Kuriyama

Faculty of Pharmaceutical Sciences, Mukogawa Women's University, Nishinomiya, 663 Japan

Received August 16, 1988

SUMMARY: Partially purified opioid receptors, obtained from rat brains using an affinity resin, AF-Amino Toyopearl with [D-Ala^2, Leu^5]enkephalin, were reconstituted with an inhibitory GTP-binding protein (G_i). In the reconstituted system, the displacement curve for the binding of a δ-agonist, [D-Ala^2, D-Leu^5]enkephalin, showed two states, high and low affinity binding ones, with different affinities for the agonist. The high affinity binding was eliminated by the addition of a guanine nucleotide analog to the system. These results directly showed that opioid receptors, at least the δ-type, could interact with G_i.
© 1988 Academic Press, Inc.

The GTP-binding proteins (G proteins) function as transducers in transmembrane signaling systems; G proteins link the activation of receptors to the regulation of effectors. There are several known G proteins, controlling several different intracellular systems that cause the changes of the activities of specific effectors (1-3). In some opioid receptor systems, transformation of the signals is transduced via G proteins. An inhibitory GTP-binding protein G_i links the activation of the receptors to the inhibition of adenylyl cyclase, thus lowering the concentration of cAMP (4-6). A G protein with unknown function G_o and,

Abbreviations: G proteins, guanine nucleotide-binding regulatory proteins; G_i, a G protein that inhibits adenylyl cyclase; G_o, a G protein of unknown function, originally isolated from bovine brain; $G_{pp}(NH)_p$, guanyl-5'-yl imidodiphosphate; Tes, N-tris-[hydroxymethyl]methyl-2-aminomethanesulfonic acid; DALE, [D-Ala^2, Leu^5]enkephalin; DADLE, [D-Ala^2, D-Leu^5]enkephalin; DTT, dithiothreitol; SDS, sodium dodecyl sulfate; PAGE, polyacrylamide gel electrophoresis.

0006-291X/88 $1.50
Copyright © 1988 by Academic Press, Inc.
All rights of reproduction in any form reserved.

to a lesser extent, G_i may be involved in the functional coupling of the receptors to neuronal voltage-dependent calcium channels (7). To more directly clarify the interaction among the components of the transmembrane signaling pathways in the opioid receptor systems, the components need to be isolated and reconstituted.

Opioid receptors have recently been purified using affinity chromatography in several laboratories (8-12). We have reported the purification of opioid-binding materials using an affinity resin with an enkephalin derivative as the affinity ligand for the receptors (13). However, the functional reconstitution of the purified receptors with G proteins has not been reported. Therefore, we attempted to reconstitute partially purified opioid receptors with G_i and to examine the interaction between the receptors and G_i in a membrane state.

MATERIALS AND METHODS

All radiochemicals were purchased from New England Nuclear Co. Guanyl-5'-yl β,γ-imidodiphosphate (Gpp(NH)p) and phosphatidylinositol were obtained from Sigma. AF-Amino Toyopearl was a generous gift from TOSOH Co. Enkephalin derivatives were synthesized as previously reported (14). All other chemicals and chromatographic media were obtained from commercial sources and used as supplied.

An affinity resin, AF-Amino Toyopearl with DALE, was prepared as previously reported (14) except using AF-Amino Toyopearl instead of AH-Sepharose as an insoluble support.

The opioid-binding materials were purified as in our previous study (13) with minor modifications. Details of the preparation of the resin and the purification of the materials will be reported elsewhere (15).

G_i was purified from bovine brain essentially using reported methods (16-18). The concentrations of Gi were determined by [^{35}S]guanosine-5'-[γ-thio]triphosphate binding activities (19). The purified opioid-binding materials and Gi were reconstituted essentially as reported in the literature (20, 21); ten- to twenty-fold excess of G_i over receptors was used in the reconstitution experiments. The brain extract (Folch Fraction I, 0.5 mg) and phosphatidylinositol (1.5 mg) was suspended in 2 ml of a buffer solution (Tes-Mg: 10 mM Tes-KOH (pH 7.5), 10 mM $MgCl_2$) containing 0.3% n-octyl-β-D-thioglucoside. The resulting suspension was sonicated in a bath-type sonicator in an atmosphere of nitrogen. This lipid mixture was added to the concentrated purified receptors (100 μl) and allowed to stand at room temperature (15 min). The resulting mixture was gel filtered, and void-volume fractions were collected. Next, Gi was added to the frac-

tions and the mixture was allowed to stand on ice (1 hr) followed by dilution with two volumes of Tes-Mg. The obtained suspension was used as a reconstituted system.

The binding of [^{3}H]DADLE (2 nM; 43.9 Ci/mmol; NEN) to the purified receptors or the reconstituted mixture was assayed by the membrane filter method, essentially as described previously (13). For the purified materials, the non-specific binding was measured in the presence of 10^{-5} M of cold ligands.

Protein was determined by staining with Amidoblack (22).

RESULTS

AF-Amino Toyopearl with DALE was used in the present study. AF-Amino Toyopearl has two outstanding characteristics; it contains more free amino groups than AH-Sepharose (the ratio of free amino groups of AF-amino Toyopearl to AH-Sepharose, 15:1) and it is more stable to pressure than AH-Sepharose. In the previous studies (14, 15), DALE or DADLE was used as an affinity ligand for opioid receptors. However, the content of DADLE (0.4 μmol/ml resin) was lower than that of DALE (1 μmol/ml resin), because of the solubility of the DADLE derivative in the solvent used in the coupling step to AH-Sepharose. Thus, DALE was used as an affinity ligand in this study. The content of DALE in this resin (10 μmol/ml resin) was ten times more than that in AH-Sepharose (15). The higher ligand content in the affinity resin enables more efficient purification of the receptors, especially in large-scale preparations.

Because the materials showed little or no GTPase activity originating from G protein (data not shown), the partially purified materials were reconstituted with purified G_i in liposome. The addition of G_i to the purified materials resulted in an increase in an apparently high affinity state for an agonist. Fig. 1 shows the displacement of [^{3}H]DADLE from isolated materials by DADLE in the absence or presence of G_i. In its presence, two states with different affinities were observed: a high affinity state with IC_{50} of 1 nM and a low affinity one with IC_{50} of 50

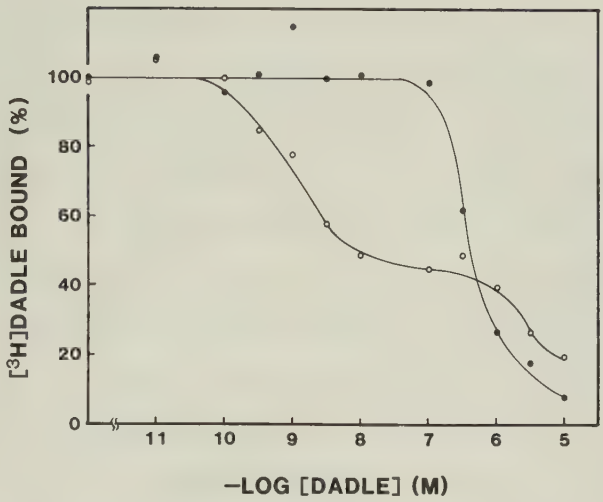

Fig. 1. Displacement of [^{3}H]DADLE binding by DADLE. The purified materials were reconstituted with (o—o) or without G_i (●—●) in liposome and the reconstituted systems were incubated with [^{3}H]DADLE (2 nM) and various concentrations of DADLE at 30°C, 1 hr. The fractions of protein-bound [^{3}H]DADLE were trapped by nitrocellulose membranes (BA-85, S & S). The points are the averages of triplicate determinations.

μM. The latter value was almost the same as in the absence of G_i.

The specific binding activity of the purified materials was ca. 150 pmol/mg protein for [^{3}H]DADLE, which was a little smaller than that of the previously purified materials (13) and much lower than expected for pure receptors (15). However, the activity increased to ca. 2,000-3,000 pmol/mg protein if the materials were reconstituted with G_i in liposome. The same phenomenon of an increase in the agonist-binding activity has been observed in the reconstituted system of muscarinic cholinergic receptors and G proteins (23).

In opioid receptor systems, guanine nucleotides decreased the affinities of agonists for the receptor binding site (24-27). We therefore tested the effect of guanine nucleotides in our system; a nonhydrolyzable analog of GTP, $G_{pp}(NH)_p$, decreased the opioid-binding activity of the reconstituted purified materials

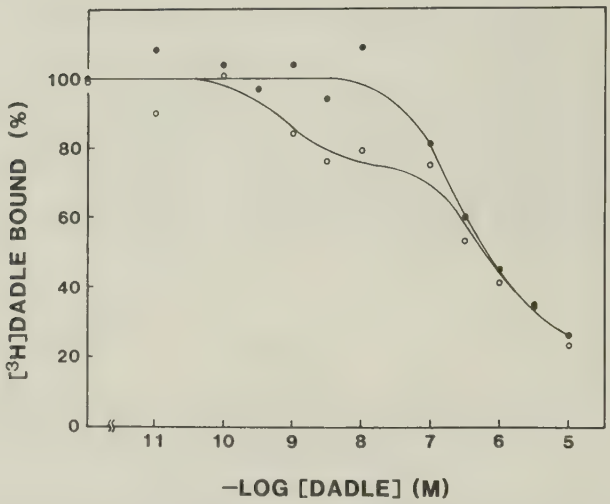

Fig. 2. Effect of $G_{pp}(NH)_p$ on agonist binding to reconstituted receptors. [^{3}H]DADLE binding to the reconstituted system with G_i was assayed in the presence (●—●) and absence (○—○) of 0.1 mM $G_{pp}(NH)_p$. The conditions of the assay were the same as cited in Fig. 1.

with G_i. Fig. 2 shows the effect of $G_{pp}(NH)_p$ in the reconstituted system: addition of $G_{pp}(NH)_p$ to the reconstituted system with G_i eliminated the high affinity state for the agonist. No effect of $G_{pp}(NH)_p$ was observed on the reconstituted system without G_i (data not shown).

DISCUSSION

In the previous study (13), one major polypeptide with specific opioid-binding activity was purified using the affinity resin. However, the opioid-binding activity was the only measure for the materials which might be opioid receptors. To find whether or not the materials were primarily composed of opioid receptors, the purified materials had to be functionally reconstituted with the proposed compornent involved in the state of the cell membrane.

In opioid receptor systems, extracellular signals received with receptors are transformed into intracellular responses produced by effectors, such as adenylyl cyclase (4-6) or ion chan-

nels (7), via the transducers, G_i and/or G_o. Therefore, the purified materials were reconstituted with G_i in liposome; two binding states, a high and low affinity one, for the δ-agonist of opioid receptors were observed in the reconstituted system with G_i, but only a low affinity state was observed without G_i. Because the coupling efficiencies of the receptors and G_i differed in each reconstitution experiment, the percentage of the high affinity state differed (compare Fig. 1, o—o, and Fig. 2, o—o). The low affinity state showed very large IC_{50} value (50 μM), but physiological importance for this state is not clear. From the preliminarily experiments, the reconstituted system with G_i showed no high affinity binding activity to a μ-agonist Tyr-D-Ala-Gly-(N-Me)Phe-Gly-ol (DAGO) and a κ-agonist ethylketocyclazocine. These results indicate that the purified materials contain mainly δ-type opioid receptors.

Guanine nucleotides cause dissociation of the subunits of G_i, simultaneously decoupling of G_i and receptors, resulting in a change in the affinity of the agonists for the receptors from high to low (26-29). In the reconstituted system with G_i, the addition of $G_{pp}(NH)_p$ changed the high affinity state for the agonist to a low one. These results also suggested that the δ-type of opioid receptors could functionally couple with G_i in the membrane state as in other transmembrane signaling pathways transduced with G_i (1-3). We stand at the first step in the elucidation of transmembrane signaling pathways in opioid-signaling systems.

ACKNOWLEDGMENT. We thank Professor M. Ui of University of Tokyo, Dr. T. Katada of the Industrial College of Tokyo and Dr. T. Higashijima of University of Texas Health Science Center at Dallas for their useful suggestions and discussions. This work was supported in part by a Grant-in-Aid for Special Project Research from the Ministry of Education, Science, and Culture, Japan (1987, 1988) and a research grant from the Uehara Memorial Foundation (1986).

REFERENCES

1. Stryer, L. and Bourne, J. (1986) Ann. Rev. Cell Biol. 2, 391-419.
2. Gilman, A. G. (1987) Ann. Rev. Biochem. 56, 615-649.
3. Neer, E. J. and Clapham, D. E. (1988) Nature 333, 129-134.
4. Sharma, S. K., Nirenberg, M., and Klee, W. A. (1975) Proc. Natl. Acad. Sci. USA 72, 590-594.
5. Law, P. Y., Wu, J., Koehler, J. E., and Loh, H. H. (1981) J. Neurochem. 36, 1834-1846.
6. Cooper, D. M. F., Londos, C., Gill, D. L., and Rodbell, M. (1982) J. Neurochem. 38, 1164-1167.
7. Hescheler, J., Rosenthal, W., Trautwein, W., and Schultz, G. (1987) Nature 325, 445-447.
8. Bidlack, J. M., Abood, L. G., Osei-Gyimah, P., and Archer, S. (1981) Proc. Natl. Acad. Sci. USA 78,636-639.
9. Maneckjee, R., Zukin, R. S., Archer, S., Michael, J., and Osei-Gyimah, P. (1985) Proc. Natl. Acad. Sci. USA 82, 594-598.
10. Cho, T. M., Ge, B.-L., and Loh, H. H. (1985) Life Sci. 36, 1075-1085.
11. Gioannini, T. L., Howard, A. D., Hiller, J. M., and Simon, E. J. (1985) J. Biol. Chem. 260, 15117-15121.
12. Cho, T. M., Hasegawa, J., Ge, B.-L., and Loh, H. H. (1986) Proc. Natl. Acad. Sci. USA 83, 4138-4142.
13. Fujioka, T., Inoue, F., and Kuriyama, M. (1985) Biochem. Biophys. Res. Commun. 131, 640-646.
14. Fujioka, T., Inoue, F., and Kuriyama, M. (1985) Chem. Pharm. Bull. (Tokyo) 33, 4633-4636.
15. Fujioka, T., Inoue, F., and Kuriyama, M., submitted.
16. Sternweis, P. C., Northrup, J. K., Smigel, M. D., and Gilman A. G. (1981) J. Biol. Chem. 256, 11517-11526.
17. Bokoch, G. M., Katada, T., Northrup, J. K., Hewlett, E. L., and Gilman, A. G. (1984) J. Biol. Chem. 259, 3560-3567.
18. Sternweis, P. C., and Robinshaw, J. D. (1984) J. Biol. Chem. 259, 13806-13813.
19. Ferguson, K. H., Higashijima, T., Smigel, M. D., and Gilman A. G. (1986) J. Biol. Chem. 261, 7393-7399.
20. Florio, V. A., and Sternweis, P. C. (1985) J. Biol. Chem. 260, 3477-3483.
21. Haga, K., Haga, T., and Ichiyama, A. (1986) J. Biol. Chem. 261, 10133-10140.
22. Schaffner, W. and Weissmann, C. (1973) Anal. Biochem. 56, 502-514.
23. Florio, V. A. and Sternweis, P. C. (1985) J. Biol. Chem. 260, 3477-3483.
24. Childers, S. R. and Snyder, S. H. (1978) Life Sci. 23, 759-762.
25. Childers, S. R. and Snyder, S. H. (1982) J. Neurochem. 34, 583-593.
26. Chang, K.-J., Blanchard, S. G., and Cuatrecasas, P. (1983) 80, 940-944.
27. Law, P.-Y., Hom, D. S., and Loh, H. H. (1985) J. Biol. Chem. 260, 3561-3569.
28. Blume, A. J. (1978) Life Sci. 22, 1843-1852.
29. Blume, A. J., Mullikin-Kilpatrick, D., and Kilian, P. L. (1984) in Methodol. Surv. Biochem. Anal. (Reid, E., Cook, G. M. W., and Morre, D. J., eds.) Vol. 13, pp.151-161, Plenum, New York.

Vol. 156, No. 1, 1988 BIOCHEMICAL AND BIOPHYSICAL RESEARCH COMMUNICATIONS
October 14, 1988 Pages 61-67

IDENTIFICATION OF A HIGH-AFFINITY RECEPTOR FOR INTERLEUKIN-1 *BETA* IN RAT BRAIN

Goro Katsuura, Paul E. Gottschall and Akira Arimura

U.S.-Japan Biomedical Research Laboratories, Tulane University Hebert Center, Belle Chasse, LA 70037; and Departments of Medicine and Anatomy, Tulane University School of Medicine, New Orleans, LA 70112

Received August 18, 1988

SUMMARY: A single type of high-affinity binding sites for IL-1 *beta* was identified in the rat hypothalamus (K_d=1.0 ± 0.2 nM) and cerebral cortex (K_d=1.3 ± 0.2 nM), but not in the pituitary. The maximum binding capacity (B_{max}) in the hypothalamus (B_{max}=75.4 ± 10.8 fmol/mg protein) was 4 times greater than in the cerebral cortex (B_{max}=17.2 ± 1.5 fmol/mg protein). Neither various neuropeptides nor IL-2 appeared to influence the binding of [^{125}I]IL-1 *beta* to the hypothalamic membrane preparations. The potency of unlabeled IL-1 *alpha* to replace the binding of [^{125}I]IL-1 *beta* to the hypothalamic membrane preparations was considerably less than that of unlabeled IL-1 *beta*. These findings indicate that IL-1 *beta* receptors are heterogeneously distributed in the central nervous system and that IL-1 *alpha* does not bind with IL-1 *beta* receptors in the brain © 1988 Academic Press, Inc.

The neuroendocrine and immune systems are now recognized as being intimately linked and bidirectionally communicating (1). A prototypical immunotransmitter interleukin-1 (IL-1), produced by activated monocytes and macrophages which triggers various immune responses, has been reported as modulating the activities of the endocrine organs and the central nervous system (2-4). IL-1 stimulates adrenocortictropic hormone (ACTH) secretion from the pituitary via corticotropin releasing hormone (CRH) in the hypothalamus (5-7). Furthermore, IL-1 exerts other central effects such as induction of fever (2), slow-wave sleep (8), satiety (9) and analgesia (10). IL-1 is synthesized not only in monocytes and phagocytes, but also in astrocytes and glia (11, 12) and can be detected in the cerebrospinal fluid (13). Recent immunohistochemical study has

ABBREVIATIONS

Interleukin (IL), Adrenocorticotropic hormone (ACTH), Corticotropin releasing hormone (CRH), Growth hormone releasing factor (GRF), Somatostatin-14 (SS-14), Thyrotropin releasing hormone (TRH), Neuropeptide Y (NPY), Neurotensin (NT), Luteinizing hormone releasing hormone (LH-RH), Leu-enkephalin (L-Enk), Met-enkephalin (M-Enk), Angiotensin II (A-II), Vasoactive intestinal polypeptide (VIP)

0006-291X/88 $1.50
Copyright © 1988 by Academic Press, Inc.
All rights of reproduction in any form reserved.

shown IL-1-like immunoreactivity in the neurons of the human brain (14) as well. These findings suggest that IL-1 has a physiological role(s) in the brain. If so, the brain tissues may have specific, high affinity receptors for IL-1. Our previous study indicated a clear-cut difference between IL-1 *alpha* and IL-1 *beta* in terms of their potency to stimulate ACTH release *in vivo* in rats (15). In the immune system, IL-1 *alpha* and IL-1 *beta* both exert similar activities and bind the same receptors (16-18); therefore, it is necessary to investigate to determine if that holds true for binding sites in brain tissue as well. The present study has been designed to address two questions: (1) Are there specific, high affiinity receptors for IL-1 in the hypothalamus, cerebral cortex and pituitary?; and, (2) Do both IL-1 *alpha* and IL-1 *beta* bind the brain receptors in a similar manner as they do in T lymphocytes?

MATERIALS AND METHODS

Animals. Male Sprague-Dawley rats, 280-300 g BW, (Charles River Breeding Laboratories, Wilmington, MA) were housed at a constant room temperature of 23° C with a 12 h light/dark cycle (lights on at 0630 h). Food and water were available *ad libitum*.

Preparation of receptor membranes: Immediately following sacrifice of rats by decapitation, brains and pituitary glands were removed. Each brain was placed on a glass plate on ice, and the hypothalamus and cerebral cortex were dissected by the method described by Glowinski and Iversen (19). Dissected tissues were quickly frozen in crushed, solid CO_2, stored at -80° C and analyzed within 3 days. To prepare receptor membranes, tissues were homogenized in freshly prepared, ice-cold 10 mM Tris/HCl buffer (pH 7.5) containing 2.5 mM dithiothreitol with a glass-Teflon homogenizer. The homogenate was centrifuged at 1000 x *g* for 10 min, the pellet was discarded, and the supernatant was centrifuged at 48,000 x *g* for 30 min. The resultant pellet was resuspended and washed twice in Tris buffer. The pellet was then suspended in Tris buffer. All preparation procedures were performed at 4° C.

Iodination of IL-1 *beta*: Recombinant human IL-1 *beta* (Cistron Corporation, Pine Brook, NJ) was iodinated by the lactoperoxidase method and then purified by reverse-phase HPLC on a Vydac C18 column with a linear gradient of acetonitrile from 10 - 60% in 0.1% trifluoroacetic acid. The radioligand was stored at 4° C. Specific activity was 65 μCi/ug.

Binding assay: Binding assay was performed using a slightly modified method described by Srikant and Patel (16). Optimum conditions for radioreceptor assay for IL-1 *beta* were determined from the preliminary experiment. The binding assays were performed using approximately 250 μg protein/tube of membrane preparation for 75 min incubation at 37° C. Membrane homogenates (100 μl) were incubated with [^{125}I]IL-1 *beta* in 50 mM HEPES/KOH buffer (pH 7.5) (assay buffer) containing 5 mM $MgCl_2$, 200 KIU/ml Trasylol, 0.02 μg/ml Bacitracin and 0.02 μg/ml phenylmethylsulfonyl fluoride in 12 x 75 mm glass tubes. Final assay volume was 0.4 ml. Nonspecific binding was determined by the addition of 1 μg unlabeled IL-1 *beta* to assay tubes. The mixture was incubated for 75 min at 37° C in a shaking water bath at 100 strokes/min, unless otherwise indicated. After incubation, 1 ml of 0.125% Celite solution was added, the tubes were centrifuged at 2000 x *g* for 10 min, and the precipitate which contained membrane-bound radioactivity was measured (21). The following reagents were used to test competence in binding: IL-1 *alpha* (a gift of Dr. Steven Gillis, Immunex Corporation, Seattle, WA), IL-2 (Cetus Corporation, Emeryville, CA), growth hormone releasing factor (GRF), CRF, somatostatin-14 (SS-14), thyrotropin releasing hormone (TRH), neuropeptide Y (NPY), neurotensin (NT), luteinizing hormone releasing hormone (LH-RH), Leu-enkephalin (L-Enk), Met-enkephalin (M-Enk), angiotensin II (A-II) and vasoactive intestinal polypeptide (VIP) All neuropeptides were purchased from Bachem Bioscience Inc., Philadelphila, PA and were diluted in the assay buffer. Protein concentrations were determined using a Bio-Rad (Richmond, CA) assay kit.

RESULTS

The binding of [^{125}I]IL-1 *beta* to hypothalamic membrane preparations increased over time during the incubation at 37° C, and reached its maximum level after 75 min when it then began to

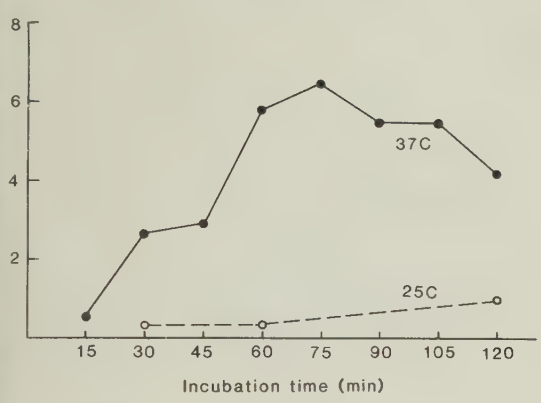

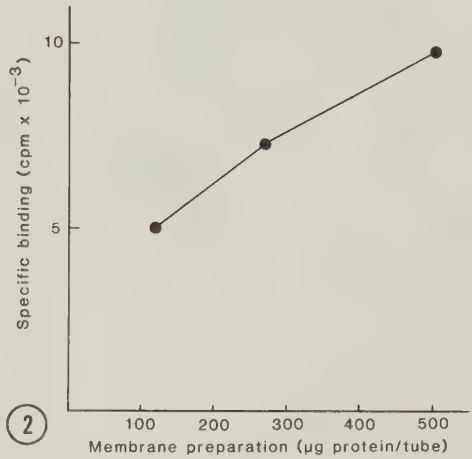

Fig. 1. Time course of [^{125}I]IL-1 *beta* binding to hypothalamic membrane preparations. The membrane preparations (approximately 250 µg protein/tube) were incubated with [^{125}I]IL-1 *beta* (1.8 nM) for the indicated time periods.

Fig. 2. Effect of protein concentrations in hypothalamic membrane preparations on [^{125}I]IL-1 *beta*. Membrane preparations at the indicated protein concentrations were incubated with [^{125}I]IL-1 *beta* (1.8 nM).

decrease. At 25° C the binding remained low for up to 2 h incubation (*Fig. 1*). Therefore, the following experiments were performed at 37° C for 75 min incubation. The binding of [^{125}I]IL-1 *beta* to hypothalamic membrane preparations increased proportional to the amount of membrane (*Fig. 2*). The binding assays were routinely carried out using approximately 250 µg of membrane protein per tube.

Fig. 3 shows specific binding of [^{125}I]IL-1 *beta* to membrane preparations of the rat hypothalamus, cerebral cortex and the pituitary as a function of ligand concentration, and the plot of Scatchard analysis for hypothalamus and brain cortex membranes. [^{125}I]IL-1 *beta* bound to the membrane preparations of the hypothalamus and cerebral cortex increased as the amount of ligand increased toward the level of saturation. Scatchard analysis yielded a single type of high-affinity binding site for IL-1 *beta* in these tissues. On the other hand, the pituitary membrane preparations did not show a dose-related increase in specific binding and therefore K_d value was not determined by Scatchard analysis. A similar study using hypothalamic and certebral cortex membrane preparations and results are shown in Table 1. K_d of [^{125}I]IL-1 *beta* was not different between the hypothalamus and the cerebral cortex. The maximum binding capacity (B_{max}) for IL-1 *beta* receptors in the hypothalamus was, however, 4 times greater than that in the cerebral cortex. Specificity of the binding of [^{125}I]-IL-1 *beta* with the hypothalamic membrane preparations was tested by incubation with 1 µg of IL-1 *alpha*, IL-2 and various neuropeptides. As shown in *Fig. 4*, none of the peptides tested other than IL-1 *beta* and IL-1 *alpha* affected the binding which indicated that the binding was specific to IL-1. In the next experiment, smaller and increasing doses of IL-1 *beta* or IL-1 *alpha* were incubated with [^{125}I]-IL-1 *beta* and the hypothalamic membrane preparation. Although both unlabeled IL-1 *alpha* and IL-1 *beta* decreased the binding of

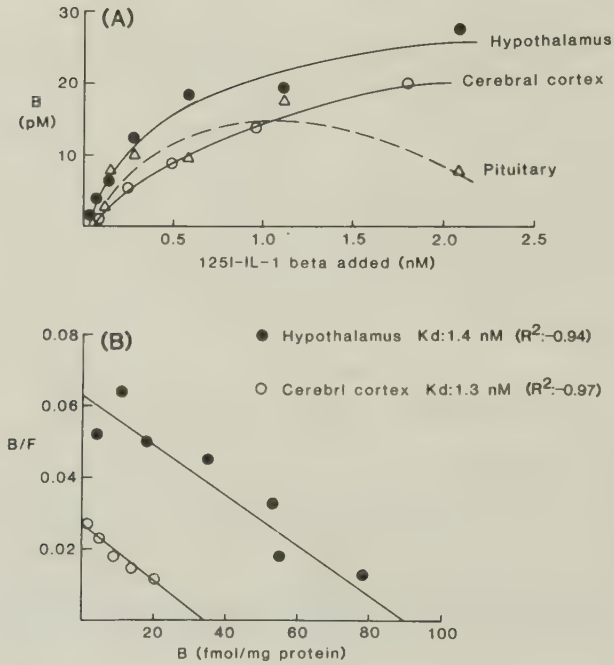

Fig. 3. Specific binding of [^{125}I]IL-1 *beta* as a function of ligand concentration to membrane preparations of the hypothalamus, the cerebral cortex and the pituitary (**A**), and Scatchard plot analysis (**B**). Membrane preparations were incubated with the indicated concentrations of [^{125}I]IL-1 *beta*. The data represent specific binding.

the radioligand with the membrane preparation in a dose-dependent manner, about 100 times greater amount of IL-1 *alpha* than IL-1 *beta* was needed to achieve suppression of binding to the same extent (*Fig. 5*).

DISCUSSION

The present study shows the presence of specific receptors for IL-1 *beta* in the brain tissue with K_d = 1.0 - 1.3 nM. The receptors appeared to be distributed heterogenously, about 4 times richer in the hypothalamus than in the cerebral cortex. On the other hand, no clear-cut saturation

TABLE 1.

Properties of IL-1 *beta* receptors in the hypothalamus and the cerebral cortex

Regions	No. of Exp.	Kd (nM)	Bmax (fmol/mg protein)
Hypothalamus	6	1.0 ± 0.2	75.4 ± 10.8
Cerebral cortex	5	1.3 ± 0.2	17.2 ± 1.5

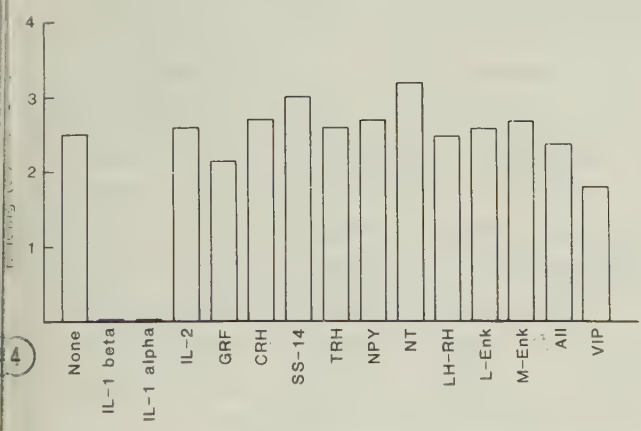

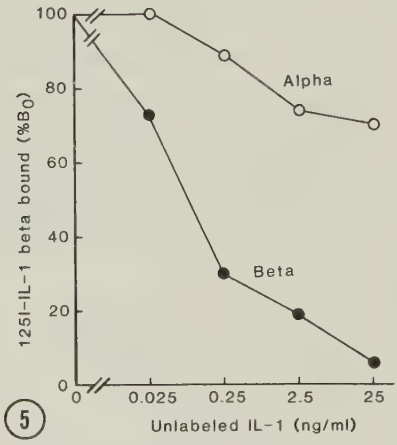

Fig. 4. Effect of IL-1 *alpha*, IL-2, and various neuropeptides on binding of [^{125}I]IL-1 *beta* to hypothalamic membrane preparations. Membrane preparations were incubated with [^{125}I]IL-1 *beta* (1.8 nM) with neuropeptides (2.5 μg/ml) and IL-2 (2.5 μg/ml). Each value represents specific binding in the presence of unlabeled IL-1 *beta* (2.5 μg/ml).

Fig. 5. Effect of unlabeled IL-1 beta and *alpha* on binding of [^{125}I]IL-1 *beta* to hypothalamic membrane preparations. Membrane preparations were incubated with [^{125}I]IL-1 *beta* (1.8 nM) in the binding assay with unlabeled IL-1 *beta* and IL-1 *alpha* at the indicated concentrations. Inhibition of [^{125}I]IL-1 *beta* binding was calculated as percentage of total binding in the absence of competitor.

curve of binding of [^{125}I]-IL-1 *beta* could be obtained using the pituitary membrane preparation, suggesting the absence of high affinity binding sites in the pituitary gland. This is comparable to our previous finding and others that IL-1 *beta* failed to stimulate ACTH release *in vitro* when the monokine was added to monolayer cultures of the rat anterior pituitary cells (6, 7, 22). On the other hand, IL-1 *beta* did stimulate ACTH release *in vivo*, probably by stimulating the release of endogenous CRF from the hypothalamus since IL-1 *beta*-induced ACTH release was completely blocked by prior administration of antiserum against CRH (5-7). It has also been reported that injection of IL-1 increased CRH concentration in the hypophysial portal blood in rats (6).

The present finding may substantiate the view that, in terms of ACTH release, the primary site of action of IL-1 *beta* is the brain. K_d (1.0-1.3 nM) for hypothalamic IL-1 *beta* receptors, however, is at least 5 times greater than that reported for these receptors on lymphocytes or fibroblasts (K_d = 8 - 200 pM)(16, 23, 24). The binding sites in the brain tissue are specific to IL-1 since various neuropeptides as well as IL-2 failed to affect the binding of [^{125}I]-IL-1 *beta* with the hypothalamic membrane preparations. It is conceivable that the IL-1 receptors in brain tissue are different from those in lymphocytes or fibroblasts. A higher K_d in brain tissue suggests that a greater concentration of IL-1 *beta* is necessary for the brain cells to respond to the monokine than for lymphocytes or fibroblasts. It is possible that the concentration of the monokine in certain loci in the brain reaches the nM range by some concentrating or accumulating process for circulating IL-1 or local production of the monokine. Some neurons in the human brain appear to contain IL-1-like substance (14). Astrocytes and glia also synthesize IL-1 (11, 12).

It is interesting that the hypothalamic membrane preparations bind IL-1 *beta* much more efficiently than IL-1 *alpha*. Approximately 100 times greater a concentration of IL-1 *alpha* than IL-1 *beta* was necessary to replace the [^{125}I]-IL-1 *beta* bound with the hypothalamic membrane preparations to the same extent. Such a high concentration of IL-1 *alpha* might be unlikely to occur in the brain tissue, even though it is synthesized and released in a limited area in the tissue. Most reports on IL-1 binding sites in lymphocytes indicated common receptors for IL-1 *alpha* and IL-1 *beta* (16-18), though some showed that IL-1 *beta* has a different affinity for the receptors on immune cells and a different biological activity, such as production of prostaglandin E_2 and IL-2 from IL-1 *alpha* (23-25). Our study suggests that IL-1 *beta* receptors in the brain are different from those for IL-1 *alpha*. This view is in agreement with our previous demonstration that IL-1 *beta*, administered either intravenously or intracerebroventricularly, stimulated ACTH release, whereas IL-1 *alpha* produced little effect (15, 26). The receptors for IL-1 *alpha* in the brain, if present, may have different actions from IL-1 *beta* in the central nervous system.

ACKNOWLEDGMENT

We wish to thank Cistron Corporation, Immunex Corporation and Cetus Corporation for their gifts of interleukin preparations. We would like to gratefully acknowlege the editorial assistance of Mrs. Linda Powell. This study was supported in part by NIH grant DK 09094 and a grant from Shionogi Co. Ltd., Japan.

REFERENCES

1. Cotman, C.W., Brinton, R.E., Galaburda, A., McEwen, B., and Schneider, D.M. (1987) The Neuro-Immune-Endocrine Connection, Raven Press, New York.
2. Dinarello, C.A. (1984) Rev. Infect. Diseas. 6, 51-95.
3. Besedovsky, H., and Sorkin, E. (1977) Clin. Exp. Immunol. 27, 1-12.
4. Weigent, D.A., and Blalock, E. (1987) Immunol. Rev. 100, 79-108.
5. Uehara, A., Gottschall, P.E., Dahl, R.R., and Arimura, A. (1987) Endocrinology 121, 1580-1582.
6. Sapolsky, R., Rivier, C., Yamamoto, G., Plotsky, P., and Vale, W. (1987) Science 238, 522-524.
7. Berkenbosch, F., van Oers, J., del Rey, A., Tilders, F., and Besedovsky, H. (1987) Science 238, 524-526.
8. Krueger, J.M., Walter, J., Dinarello, C.A., Wolff, S.M., and Chedid, A. (1984) Am. J. Physiol. 246, R994-R999.
9. McCarthy, D.O., Kluger, M.J., and Vander, A.J. (1985) Am. J. Clin. Nutr. 42, 1179-1182.
10. Nakamura, H., Nakanishi, K., Kita, A., and Kadokawa, T. (1988) Eur. J. Pharmacol. 149, 49-54.
11. Fontana, A., Kristeinsen, F., Dubs, R., Gemsa, D., and Weber, E. (1982) J. Immunol. 129, 2413-2419.
12. Giulian, D., Baker, T.J., Shih, L.N., and Lachman, L.B. (1986) J. Exp. Med. 164, 594-604.

13. Coceani, F., Lees, J., and Dinarello, C.A. (1988) Brain Res. 446, 245-250.
14. Breder, C.D., Dinarello, C.A., and Saper, C.B. (1988) Science 240, 321-324.
15. Uehara, A., Gottschall, P.E., Dahl, R.R., and Arimura, A. (1987) Biochem. Biophys. Res. Comm. 146, 1286-1290.
16. Killian, P.L., Kaffka, K.L., Stern, A.S., Woehle, D., Benjamin, W.R., Dechiara, T.M., Gubler, U., Farrar, J.J., Mizel, S.B., and Lomedico, T. (1986) J. Immunol. 136, 4509-4514.
17. Bird, T.A., and Saklatvala, J. (1986) Nature 324, 263-266.
18. Dower, S.K., Kronhein, S.R., Hopp, T.P., Cantrell, M., Deeley, M., Gillis, S., Henney, C.S., and Urdal, D.L. (1986) Nature 324, 266-268.
19. Glowinski, J., and Iversen, L.L. (1966) J. Neurochem. 13, 655-669.
20. Srikant, C.B., and Patel, Y.C. (1981) Nature 294, 259-260.
21. Aten, R.F., Williams, A.T., and Behrman, H.R. (1986) Endocrinology 118, 961-967.
22. Uehara, A., Gillis, S., and Arimura, A. (1987) Neuroendocrinology 45, 343-347.
23. Matsushima, K., Akahoshi, T., Yamada, M., Furutani, Y., and Oppenheim, J.J. (1986) J. Immunol. 136, 4496-4502.
24. Chin, J., Cameron, P.M., Rupp, E., and Schmidt, J.A. (1987) J. Exp. Med. 165, 70-86.
25. Bird, T.A., Gearing, A.J.H., and Saklatvala, J. (1987) FEBS Lett. 225, 21-26.
26. Katsuura, G., Gottschall, P.E., Dahl, R.R., and Arimura, A. (1988) Endocrinology 122, 1773-1779.

Vol. 156, No. 1, 1988 BIOCHEMICAL AND BIOPHYSICAL RESEARCH COMMUNICATIONS
October 14, 1988 Pages 68-77

EXON-INTRON ORGANIZATION OF A GENE FOR PREGNANCY-SPECIFIC ß1-GLYCOPROTEIN, A SUBFAMILY MEMBER OF CEA FAMILY: IMPLICATIONS FOR ITS CHARACTERISTIC REPETITIVE DOMAINS AND C-TERMINAL SEQUENCES

Shinzo Oikawa[1], Chikako Inuzuka[1], Goro Kosaki[2] & Hiroshi Nakazato[1]

[1]Suntory Institute for Biomedical Research, Shimamoto-cho, Mishima-gun, Osaka 618, Japan
[2]Tokyo Metropolitan Komagome Hospital, Bunkyo-ku, Tokyo 113, Japan

Received August 18, 1988

A fragment of human gene for pregnacy-specific ß1-glycoprotein(s), recently identified CEA family member(s), has been cloned. Analyses of nucleotide and deduced amino acid sequences revealed that it carried, from 5' to 3' direction, exons IA, IB, IIA, IIB, C3, C1 and C2, the first four encoding peptides distinct from but highly similar to domains of PSßGs. The lack of consensus 3' splice site sequence ahead of IB indicated that it was an abortive exon, which would explain the peculiar domain construction of PSßGs, *i.e.* N-IA-IIA-IIB-C1, 2 or 3. Apparently, the multiple C-terminal sequences for a PSßG were generated by alternative splicing among C1, C2 and C3 exons. Furthermore, sequences which overlapped partly with C exons, were found to be similar to parts of 3'-UTR of CEA and NCA, indicating further the close relationship of CEA/NCA and PSßG subfamily genes. © 1988 Academic Press, Inc.

CEA (1) is one of the most widely used human tumor markers although it lacks absolute tumor specificity because of the presence of a number of immunologically closely related glycoprotein antigens, which comprise CEA family.

Recent success in cloning cDNAs and parts of genomic sequences revealed the existence of multiple genes of highly similar sequences for CEA family (2,3,4,5,6,7,& 8). The characteristic domain structures (2,7) are evident for CEA and NCA of which the former is composed of 108-residue N-domain, three repetitive 178-residue domains I, II and III, and 26-residue hydrophobic M-domain, the latter is composed of 108-residue N-domain, 178 residue domain I and 24-residue M-domain. Domains I, II and III are further subdivided into 92-residue A and 86-residue B subdomains (9). Domain N and subdomains A and B respectively, have been shown to belong to Ig superfamily (9), *i.e.* CEA family belongs to Ig superfamily (3,9,10).

Abbreviations: CEA, carcinoembryonic antigen; NCA, nonspecific crossreacting antigen; PSßG, pregnacy-specific ß1-glycoprotein; UTR, untranslated region; -b, -bases.

0006-291X/88 $1.50
Copyright © 1988 by Academic Press, Inc.
All rights of reproduction in any form reserved.

Recently, primary structure of precursors to two kinds of PSßG was deduced from cloned cDNAs (11), and it was found that the PSßGs belonged to CEA family (12), its domain construction and amino acid sequences being highly similar to CEA and NCA. The precursors comprised, consecutively, 143-residue N-terminal domain including a signal peptide, 93-residue domains IA, IIA and 86 or 88-residue domain IIB and lacked the hydrophobic M-domain. Apparently, domains IA and IIA, and IIB, respectively, are homologous to subdomains A and B of CEA or NCA. The characteristics peculiar to the PSßG is the lack of domain B between IA and IIA, in addition to the lack of M-domain and the presence of two kinds of C-terminal sequences. An apparently identical PSßG with different C-terminus and another PSßG, which was composed of domains N, IA and IIB were recently reported (13).

In this report we will describe cloning and nucleotide sequence of a genomic DNA segment containing introns and exons which encoded sequences highly similar to subdomain As and Bs of PSßGs. The possible mechanisms generating the peculiar domain construction and different C-termini of PSßGs will be discussed.

MATERIALS AND METHODS

Human Genomic Library — A human genomic library which had been prepared from placental DNA using bacteriophage charon 4A vector as described by Lawn *et al.* (14) was kindly provided by Dr. Masabumi Shibuya of Tokyo University.

Screening, Subcloning and DNA Sequence Determination — Approximately one million clones were plated and screened using two ^{32}P-labeled *Pvu* II fragments of CEA cDNA which corresponded to the repetitive domains of CEA (2). Two positive clones were obtained and the one termed λCGM35, was characterized by restriction endonuclease analysis (Fig. 1A). Before subcloning, Southern blot hybridization analysis (15) was performed to locate sequences related to those of cDNA for CEA and NCA using ^{32}P-labeled probes described below. Only the fragments containing sequences related to those were recloned into M13mp18 or M13mp19 (16) and sequenced by the chain termination method (17).

Probes — *Pvu* II-*Acc* I and *Pvu* II-*Pvu* II fragments of pCEA55-2 clone (2) were for N-domain and repetitive domains, respectively. *Rsa* I-*Eco*R I fragment of λKr40 (2) and *Eco*R I-*Hin*d III fragment of NCA15 (7) were for the sequences related to 3'-UTR of CEA and NCA, respectively. Probes were ^{32}P-labelled by the nick translation method (18).

RESULTS AND DISCUSSION

Fig. 1 is a schematic representation of the exon-intron organization of the human genomic clone λCGM35, also depicted is the subcloning and sequencing strategy of the DNA fragment. Amino acid sequences translatable from the three frames of the DNA fragments were deduced and compared with those of CEA and NCA to identify exons. The consensus sequences at 5'- and 3'-splice sites (19, 20) were also referred to in order to locate the exon-intron boundaries. As is shown in Fig. 1, there were seven putative

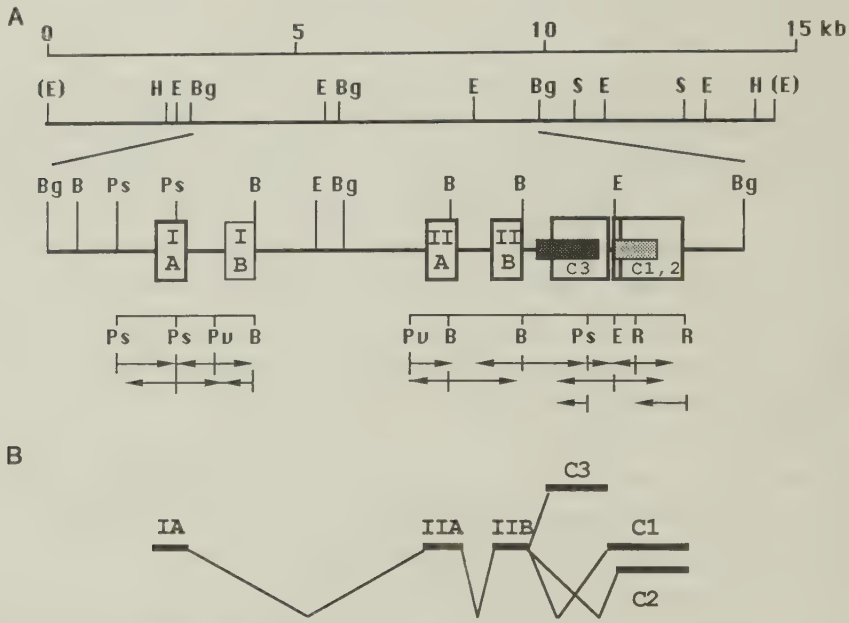

Fig. 1 (A) Sequencing strategy and exon-intron structure of CGM35. The scale is shown at the top in kilobases. Only restriction endonucleases relevant to the present work are shown: B, *Bam* H I; Bg, *Bgl* II; E, *Eco*R I; H, *Hin*d III; Ps, *Pst* I; Pv, *Pvu* II; R, *Rsa* I; S, *Sac* I; (E), *Eco*R I linker. Extent and direction of sequencing are shown by arrows. □, exon, but the sequence shown in thin lines may not be an exon; ■, ▒; sequences similar to parts of CEA and NCA cDNA, respectively. (B) Mode of splicing. Thick horizontal lines denote exons, which correspond to those shown in (A).

exons, four of them being translatable into peptides (Fig. 2) highly similar in size and sequence to subdomain As and Bs of CEA family (Fig. 3). However, it should be noted that 3'-splice site preceding "1B" was not conforming to the consensus sequence, suggesting that "1B" might not be processed into mRNA. Other three exons, two of them almost entirely overlapping except for 86-b, apparently encoded C-terminal sequences of this CEA family member. There was no N-domain coding region within entire length of the DNA insert, for CEA N-domain probe did not hybridize to any of the restriction fragments in Southern blot hybridization analysis.

When peptide sequences encoded by each exon were aligned with those of subdomain As and Bs of the members of CEA family deduced from the cloned cDNAs (Fig. 3), and sequence similarities were calculated (Table 1), high similarity, especially to those of PSßGs was evident. Each peptide was 43 to 63% and more than 82% similar to the corresponding subdomains of CEA and NCA, and PSßG, respectively. Apparently, the present gene was of a member of PSßG subfamily rather than of CEA/NCA subfamily. Furthermore, it is significantly more related to PSßG16/93 and C/D than to E. Interestingly, sequence similarity between As or Bs belonging to different repetitive domains, *i.e.* I and II, of PSßGs was only 44 to 49% while that between As or Bs belonging to the same repetitive domains was 80 to 95%. In contrast, subdomains

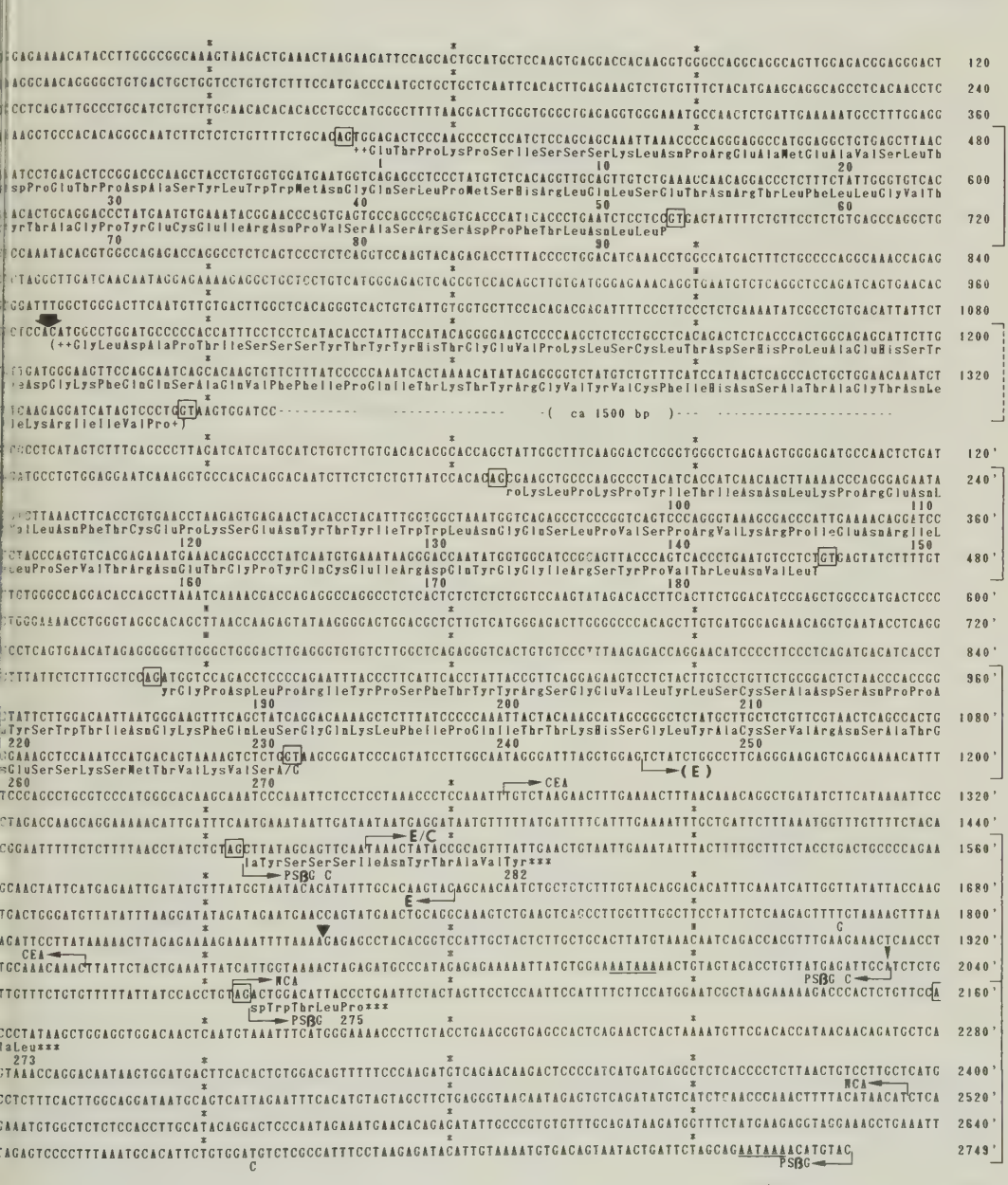

Fig. 2 Nucleotide sequence and deduced amino acid sequence of CGM35. Nucleotides are numbered beginning from *Pst* I site (1-1358) and *Pvu* II site (1'-2749') of the sequenced fragments (Fig. 1A). Sequences containing exons are shown on the right by]. Consensus splice site sequences are boxed, with ◆ being non-conforming sequence. IB which may be an abortive exon is shown by broken], and amino acids deduced are parenthesized. Amino acids are numbered beginning from the first residue of exon IA, throgh the C-terminal residues of exon C1, C2 or C3. ⌐, ⌙; start and end of the sequence resembling to that of a part of the cDNA indicated; PSßG, PSßG16/93 (9); E, C, PSßGE and C(13), respectively; (E), not highly but moderately similar to E, ▼, *Alu* family insert seen in the case of CEA; ▼, poly A addition site. Putative poly A signals are underlined. Nucleotides 1788' and 2676' are ambiguous.

```
                    *         *         *         *         *         *
CEA      I  ELPKPSISSNNSKPVEDKDAVAFTCEPETQDATYLWWVNNQSLPVSPRLQLSNGNRTLTL
CEA     II  -P---F-T-----N----E----L-----I-NT-------------D-----
CEA    III  ---------------------------A-NT-------G-------------
NCA      I  -------------N---------------V-NT-------G-------------M-
CGM35    I  -T-------SKLN-R-AME--SL--D---P--S----M-G----M-H-----ET---F-
CGM35   II PK----Y-TI--L--R-N--VLN-----KSENY-I--L-G--------VKRPIE--I-I-
PSßG     I L-T-------S-LN-R-TME--SL--D---P--S----M-G----MTHS-K--ET---F-
PSßG    II PK----Y-TI--LN-R-N--VLN-----KSENY-I--L-G--------VKRPIE--I-I-
PSßG E   I L-T-------S-LN-R-AMET-IL--D---P-TS-Q--M-G----MTH-F---ET---F-
CONSENSUS    PKP I      P E       TC P      Y WW N QSLP          N  L L

                    *         *         *         *         *         *
CEA      I  FNVTRNDTASYKCETQNPVSARRSDSVILNVLYGPDAPTISPLNTSYRSGENLNLSCHAA
CEA     II  LS-----VGP-E-GI--EL-VDH--P----------D-----SY-Y--P-V--S------
CEA    III  -------ARA-V-GI--S---N--P-T-D------T-I---PDS--L--A-----S-
NCA      I  LS-K---AG--E--I---A--N--P-T--------V-----SKAN--P-------
CGM35    I  LG--KYTAGP-E--IR-----S---PFT--L-H-L------SSY-Y-HT--VPK---LTD
CGM35   II  PS---E-GP-Q--IRDQYGGI--YP-T--------L-R-Y-SF-Y-----V-Y---S-D
PSßG     I  LG--KYTAGP-E--IR-----S---P-T--L-
PSßG    II  PS---E-GP-Q--IRDRYGGV---P-T--------L-R-Y-SF-Y-----V-Y---S-D
PSßG E   I  -G--KYTAGP-E--IR-SG--S---P-T--L-
PSßG E  II                                H---L-R-H-SY-N----D--Y---F-N
CONSENSUS    V       Y C          S    L  L G D P I      Y  G    LSC

                    *         *         *         *         *         *
CEA      I  SNPPAQYSWFVNGTFQQSTQELFIPNITVNNSGSYTCQAHNSDTGLNRTTVTTITVYA
CEA     II  ---------LID-NI--H------S---EK---L-----N--AS-HS----K----S-
CEA    III  ---SP----RI--IP--H--V---AK--P--N-T-A-FVS-LA--R-NSI-KS---S-
NCA      I  ----------I---------------------M------A---------M---SG
CGM35    I  -H-L-EH--LID-K----A-VF---Q--KTYR-V-V-FI---A-AGTNLIIKR-I-P-
CGM35   II  ---------TI--K--L-G-K----Q--TKH--L-A-SVR--A--KESSKSM-VK-SD/E
                                                                    /A
PSßG    II  ---------TI-EK--LPG-K---RH--TKH--L-V-SVR--A--KESSKSM-VE-SD/E
                                                                    /A
PSßG E  II  ---------TI--K----G-N----Q--TKH--L-V-SVR--A--EESSTSL-VK-S-
CONSENSUS   S P    SW      Q   Q  FI  IT    G Y C   N              V
```

Fig. 3 Comparison of the domains of CGM35 with those of CEA family. Only amino acids different from those of CEA I are shown in single notation. Dashes mean identity. Arrow indicates boundary between A and B subdomains. Underlined sequence is probably not expressed in the protein. The last residues of CGM35 II and PSßG are D, E or A due to the presence of three kinds of C-terminal coding sequences. Possible N-glycosylation sites are boxed. PSßG C/D are different from PSßG only at amino acid 82 in II. PSßG stands for PSßG16/93.

belonging to different repetitive domains of CEA/NCA subfamily, were more than 72% similar with the exception of CEA IIIB which were about 60% similar to CEA IB, IIB and NCA IB (Fig. 3). These results clearly indicate that divergence among repetitive domains are greater in PSßG subfamily than in CEA/NCA subfamily. In view of this, CGM35 IB had no counterpart among PSßGs whose primary structure had been deduced from the cloned cDNAs. It was noted that there was no putative N-glycosylation site in subdomain Bs of PSßG, albeit the presence of several of ones in other subdomains (Fig. 3).

Watanabe and Chou isolated two cDNA clones, PSßG16 and 93, encoding human PSßGs of 417 and 419 amino acids, respectively (11). The sequenced portions of these cDNAs were identical with the exception that PSßG93 contained an additional 86-b at the end of the common 3'-coding region. This resulted in the generation of two C-terminal sequences after common 414 amino acids, which were EAL and DWTVP, for PSßG16 and 93, respectively. More recently, three PSßGs deduced from cloned cDNAs were reported (13). PSßGD was virtually identical to PSßG93 with only three amino acids

Table I. Amino acid similarities between subdomain As and Bs of CGM 35, PSßG 16/93(12), PSßG E(13), CEA(2) and NCA(7). PSßG stands for PSßG 16/93 which is virtually identical to PSßG C/D (13). The number of matches is expressed as per cent of the similarity length.

A Subdomain

	CEA		NCA	CGM35		PSßG		PSßG E
	II	III	I	I	II	I	II	I
CEA I	73.9	83.7	81.5	59.8	53.3	58.7	53.3	55.4
CEA II		76.1	79.3	57.6	53.3	56.5	55.4	55.4
CEA III			85.9	58.7	55.4	57.6	55.4	58.7
NCA I				63.0	56.5	62.0	58.7	59.8
CGM35 I					45.7	93.5	47.8	88.0
CGM35II						46.7	95.7	46.7
PSßG I							48.9	88.0
PSßG II								48.9

B Subdomain

	CEA		NCA	CGM35		PSßG	PSßG E
	II	III	I	I	II	II	II
CEA I	72.1	60.5	86.0	46.5	57.0	53.5	59.3
CEA II		58.1	73.3	47.7	57.0	55.8	60.5
CEA III			60.5	43.0	50.0	47.7	51.2
NCA I				46.5	58.1	54.7	60.5
CGM35 I					47.7	44.2	48.8
CGM35II						93.0	82.6
PSßG II							77.9

differences. PSßGCshared 414 N-terminal amino acids with PSßGD but followed by an entirely different C-terminal sequence of 14 amino acids, AYSSSINYTSGNRN. PSßGEwas composed of N-domain and subdomains IA and IIB which were distinct from but highly similar to corresponding domains of other PSßGs.

Interestingly, three exons of CGM35 contained sequences which could generate three kinds of mRNA by differential splicing (Fig. 1B). As is shown in Fig. 2, C3 exon at nucleotides 1475'-2034' encoded 12-residue C-terminal sequence, whose first 9 residues were identical to those of PSßGC. C1 and C2 exons starting at nucleotides 2076' and 2162', respectively, were identical except for the extra 86-nucleotides at 5'-terminus of C1 exon. C1 and C2 exons, respectively, would encode C-terminal sequences, DWTLP and EAL, which were virtually identical to those of PSßG93/D(11, 13) and 16 (11), respectively. In addition to the C-terminal amino acid sequence similarities, C1, C2 and C3 exons are highly similar, *i.e.* >93%, in nucleotide sequence to 3'-end of PSßG93/D, 16 and C, respectively (Fig. 4). The sequence related to 3'-end of PSßGEwas also found but

```
(A)
                                                  *         *         *         *         *
CGM35                                   AGTCTATCTGGCCTTCAGGGAAGAGTCAGGAAAACATTTTTATTCCC
PSßG E                                  CT...TC..CT....A.TCC..C.TAGCA.CTGTG..G.CAT...TG
                     *         *         *         *         *         *         *
CGM35   AGCCTGCGTCCCATGGGCACAAG-CAAATCCCAAATTCTCCTCCTA-AACCCTCCAA---ATTTGTCTAA
PSßG E  TATT.CA.GAAG.CT....GG..ATTT..GGA..GG....T.A.A.GG..T..TG..TAC.AGCTC..G.
CEA                                                                       .....G.
                     *         *         *         *         *         *         *
CGM35   GAACTTTGAAAACTTTAACAAACAGGCTGATATC-TTCATAA----AATTCCCAGCCTAGACCAAGCAG-
PSßG E  T...-..C..G.-.CAT..C.CTG.A..A.G.A.T....A..TTTT...GAA...G..GATA.CTT..T-
CEA     ...T..CC.........TG...TAA....C.G.-.....G.----..C.GT.CA..A...T.......A
                     *         *         *         *         *         *         *
CGM35   GAAAAAC-ATTGATTTCAATGAAATAATTGATAATAAT-GAGGATAATGTTTTTATGA-TTTTCATTTGA
PSßG E  ....TT.A.GAC.AAGA.GAA.....C.CA..GT..T.G..CT.A.TAA.CAAA.G..-.AA.G....C.
CEA     .....TA-...A......TG.G.C...A...-.C....-.........A....C..A.T....T......
                     *         *         *         *         *         *         *
CGM35   AAATTTGCTGATTCTTTAAATGGTTTGTTTTCTACA-TTGACGGAA-TTTTTCTCTTTTAACCTATCTGT
PSßG E  T.....T..-...-.GA.....TGC..A..CT.GG.-A..-TTTC.-..C.C.AGA....TGAACAT.T.
CEA     ..T..................TC......C.C.G.T..C.G.A..C.....T........G.....CAC
                     *         *         *         *         *         *         *
CGM35   AGCTTATAGCAGTTCAATAAACTATACCGCAGTTTATTGAACTGTAATTGAAATATTTACTTTTGCTTTC
PSßG E  TT...-G....-A.TGG....G...-----.C...TG.A...AAA........C....C........C..
CEA     ......C....A..TG.....A...-----.C...TG.....AAA......G.C......A...T..CC.
PSßG C    .......................-----.C..CTGG....C..........C................
                     *         *         *         *         *         *         *
CGM35   TACCTGACTGCCCCAGAATTGGGCAACTATTCATGAGAATTGATATGTTTATGGTAATACACATATTTGC
PSßG E  ..T....G...............A.T...........T...C.............____A.GC.......
CEA     ..TG..GTC..T.....C.....A............AT...T....-.G..........T.GT..-....
PSßG C  ....................................................................
                     *         *         *         *         *         *         *
CGM35   ACAAGTACAGCAACAATCTGCTCTCTTTGTAACAGGACACATTTCAAATCATTGGTTATATTACCAAGGC
PSßG E  ......T.[Poly A]                   ↓↓
CEA     ......T.__AT..A__.........T.G.A.G....A.T......G...A...................A.
PSßG C  ..........T...........T...........T.........G......................T..
                     *         *         *         *         *         *         *
CGM35   TTTGACTGGGATGTTATATTTAAGGATATAGA----TA--GAATGAACCAGTATGAACTGCAGGCAAAGT
CEA     .......A.A....CG.....G........A.CCCA..GGT...A....CAC.G.T...A..AA......
PSßG C  .....T.C..........-....AA.C.....----..--..........A...................
                     *         *         *         * (G)     *         *         *
CGM35   CTGAAGTCAGCCTTGGTTTGGCTTCCTATTCTCAA-GAGTTTTGTAAAAGTTTAATCTCAGATTCCTTAT
CEA     ............................G.G....TT.AAC..C.............G...........
PSßG C  ....................................-...G.....G..GA....................
                     *         *         *         *         *         *         *
CGM35   AAAAACTTAGAGAAAAGAAAATTTTAAAA[---Gap---]GAGAGCCTACACGGTCCATTGCTACTCTTG
CEA     ........CC..C....-C..C.......[Alu 303-b]A.A..T...TGT....AG.CA.........
PSßG C  ........................G..[---Gap---]..C........T..................
                     *         *         *         *         *         *         *
CGM35   CTGCACTTATGTAAACAATCAGACCACGTTTGAAGAAACTCAACCTATTTTGCAAACAAACTTATTCTAC
CEA     .....G.....A...G...G..G...A..C...T...__A.A.__.T.......A....[Poly A]
PSßG C  ...........................A.............C.............................
                     *         *         *         *         *         *         *
CGM35   TGAAATTATCATTGGTAAAACTAGAGATGCCCATAGAGAGAAAAATTATGTGGAAAATAAAAACTGTAGT
PSßG C  ....................G................G.................._____.........
                     *         *         *         *         *         *         *
CGM35   ACACCTGTTATGAGATTGC
PSßG C  .T............C...[Poly A]
```

Fig. 4 Nucleotide alignments of similarities in the 3'-end between CGM 35 and members of CEA family. (A) CGM 35 (nucleotides 1162'-2033'), PSßGE(982-1440) (13), CEA (2499-3468) ((2), nucleotides 2930-3468 are our unpublished data) and PSßGC(1244-1796) (13) are aligned. (B) CGM 35 (2074'-2749'), PSßG16/93 (1310-1906, with additional 86-b seen in PSßG93, which are underlined) (11) and NCA (1074-1520) (7) are aligned. PSßGD(1242-1928) is almost identical to PSßG16/93 except for the portion shown in last line. Identical residues and deletions are shown by dots and dashes, respectively. ↓, poly A addition site. Poly A signals are underlined.

(B)

```
                 *         *         *         *         *         *         *
CGM35   AGACTGGACATTACCCTGAATTCTACTAGTTCCTCCAATTCCATTTTCTTCCATGGAATCGCTAAGAAAA
PSßG16  T.........G.T................A.................C..........A......GC.
NCA     ...T.....CAG............T....C.........C.......A.C........C.A....A..C.
                 *         *         *         *         *         *         *
CGM35   AGACCCACTCTGTTCCAGAAGCCCTATAAGCTGGAGGTGGACAACTCAATGTAAATTTCATGGGAAAACC
PSßG16  ..................................................................
NCA     ..GT.TG.....C...T...........T.......A.............A......A.A.........
                 *         *         *         *         *         *         *
CGM35   CTTGTACCTGAAGCGTGAGCCACTCAGAACTCACTAAAATGTTCGACACCATAACAACAGATGCTCAAAC
PSßG16  ..............A...................C.....A.............................
NCA     ..CAGG.....G.T...T..........---G...----.------....-....T.G...CAG......
                 *         *         *         *         *         *         *
CGM35   TGTAAACCAGGACAATAAGTGGATGACTTCACACTGTGGACAGTTTTTCCCAAGATGTCAGAACAAGACT
PSßG16  ...............C..................................................
NCA     ..C......T.GTG.G..A.T..C...........A.......C................A........
                 *         *         *         *         *         *         *
CGM35   CCCCATCATGATGAGGCTCTCACCCC-TCTTAAC-TGTCCTTGCTCATGCCTGCCTCTTTCACTTGGCAG
PSßG16  ......................C....-........-....................................
NCA     ..T.........A.......T.....C.T....TT..........T...............G........
                 *         *         *         *         *         *         *
CGM35   GATAATGCAGTCATTAGAATTTCACATGTAGTAGCTTCTGAGGGTAAC--AATAGAGTGTCAGATATGTC
PSßG16  ........................................A.....--..C.................
NCA     ...G....T........T........A.A.........A.........TT..C............C.A..
                 *         *         *         *         *         *         *
CGM35   ATCTCAA-CCCAAACTTTTACATAACATCTCAGGGGGAAATGTGGCTCTCTCCACCTTGCATACAGGACT
PSßG16  .......C.T.......................................................G..
NCA     T.G....T.....CG..........A..AAGAGATCCTTTA
                 *         *         *         *         *         *         *
CGM35   CCCAATAGAAATGAACACAGAGATATTGCCCGTGTGTTTGCAGATAAGATGGTTTCTATGAAGAGGTAGG
PSßG16  ............................T.............G..........G........C.....
                 *         *         *         *         *         *         *
CGM35   AAAGCTGAAATTATAATAGAGTCCCCTTTAAATGCACATTCTGTGGATGTCTC--GCCATTTCCTAAGAG
PSßG16  ...............................C......G........G...TT...G...........
                 *         *         *         *         *         *
CGM35   ATACATTGTAAAATGTGACAGTAATACTGATTCTAGCAGAATAAAACATGTAC
PSßG16  .............C..........G..--........................CACCTCCC[EcoR I]
PSßG D  .............C..........G..--.... ...........T...TTGCT[Poly A]
```

Figure 4 - Continued.

it was separable into two portions, the 5'- and 3'-end sequences comprising nucleotides 1164'-1489' and 1490'-1620' were 47.6%and 80.2%similar to corresponding PSßGE sequences, respectively. The 3'-end sequence was where similarity between 3'-end sequences of PSßGCand PSßGEwas found (13). Although 5'-end sequence could encode 35-residue peptide if it was processed into mRNA, the significance of these findings is not clear at this time.

In addition to the similarities found between 3'-end sequences of members of PSßG subfamily, CGM 35 contained sequences highly similar, *i.e.* >76%, to 3'-UTR of CEA and NCA. The CEA and NCA like sequences overlapped partly with exons C3 and C1,2, respectively (Fig. 2). The corresponding CEA sequence started about 40-residue downstream of the first *Alu* sequence, extended beyond the poly A addition site of the shorter cDNA (2) and ended at the poly A addition site of the longer cDNA (Fig. 4A). The second *Alu* sequence of 303-b found in the longer cDNA (details will be published elsewhere) was missing in the CGM 35 sequence (Fig. 2 & 4A). The NCA sequence started from 40-b downstream of the stop codon, *i.e.* where similarity between NCA and CEA cDNA ceased (7). The sequence similarity of parts of 3'-UTR of cDNAs of PSßGDand NCA was already noted (13). In spite of these similarities, sequences similar to those corresponding to M-

domains of CEA or NCA were not found. These results, along with the finding that none of the known PSßGs including CGM 35 has C-terminal hydrophobic M-domain, might indicate that M-domains of CEA/NCA subfamily are encoded by separate exons.

In conclusion, CGM 35 clone carried a sequence which contained most of a gene for a new member of PSßG subfamily within CEA family. As is summarized in Fig. 1A, the N-domain truncated sequence consisted of exons IA, IB, IIA, IIB, C3, C1 and C2, from 5' to 3' direction. As discussed above, exon IB was apparently an abortive exon which would not be processed into mRNA. Alternative splicing will generate at least three kinds of mRNA which encode PSßGs having three different C-terminal sequences. Thus, at least three PSßGs, (N)-IA-IIA-IIB-C1, (N)-IA-IIA-IIB-C2 and (N)-IA-IIA-IIB-C3, which are distinct from but highly similar to PSßG93/D, 16 and C, respectively, will be produced. In addition, it is possible that the fourth PSßG having C-terminal sequence derived from the E-like sequence would be found. Another implication of the present findings is that, PSßGE(13) having N-IA-IIB-CE construction might be encoded by a gene having two consecutive abortive exons, namely "IB" and "IIA", although other mechanisms such as alternative splicing can not be excluded.

Finally, considering the highly conserved domain structures among CEA family members, it is conceivable that genes for the members are similary constructed, *i.e.* each domain and subdomain are encoded by separate exons like in immunoglobulin and T cell receptors, introns between A and B are rather short and those between N and A, and B and A are rather long.

REFERENCES

1. Gold, P. & Freedman, S. O. (1965) J. Exp. Med. 121, 439-462
2. Oikawa, S. Nakazato, H, & Kosaki, G. (1987) Biochem. Biophys. Res. Commun. 142, 511-518
3. Zimmermann, W., Ortlieb, B., Friedrich, R. & von Kleist, S. (1987) Proc. Natl. Acad. Sci. USA. 84, 2960-2964
4. Beauchemin, N., Benchimol, S., Cournoyer, D., Fuchs, A. & Stanners, C P. (1987) Mol. Cell. Biol. 7, 3221-3230
5. Thomson, J. A., Pande, H., Paxton, R. J., Shively, L., Padma, A., Simmer R. L., Todd, C W., Riggs, A. D. & Shively, J. E. (1987) Proc. Natl. Acad. Sci. USA. 84, 2965-2969
6. Oikawa, S., Kosaki, G. & Nakazato, H. (1987) Biochem. Biophys. Res. Commun. 146, 464-469
7. Tawaragi, Y., Oikawa, S., Matsuoka, Y., Kosaki, G & Nakazato, H. (1988) Biochem. Biophys. Res. Commun. 150, 89-96
8. Neumaier, M., Zimmermann, W., Shively, L., Hinoda, Y., Riggs, A. D. & Shively, J. E. (1988) J. Biol. Chem. 263, 3202-3207
9. Oikawa, S., Imajo, S., Noguchi, T., Kosaki, G. & Nakazato, H (1987) Biochem. Biophys. Res. Commun. 144, 634-642

10. Paxton, R. J., Mooser, G., Pande, H., Lee, T. D., & Shively, J. E. (1987) Proc. Natl. Acad. Sci. USA. 84, 920-924
11. Watanabe, S. & Chou, J. Y. (1988) J. Biol. Chem. 263, 2049-2054
12. Watanabe, S. & Chou, J. Y. (1988) Biochem. Biophys. Res. Commun. 152, 762-768
13. Streydio, C., Lacka, K., Swillens, S. & Vassart, G. (1988) Biochem. Biophys. Res. Commun. 154, 130-137
14. Lawn, R. M., Fritsch, E. F., Parker, R. C., Blake, G. & Maniatis, T. (1978) Cell 15, 1157-1174.
15. Southern, E. M. (1975) J. Mol. Biol. 98, 503-517
16. Yanisch-Perron, C., Vieira, J. and Messing, J. (1985) Gene, 33, 103-119
17. Sanger, F., Nicklen, S. & Coulsen, A. R. (1975) Proc. Natl. Acad. Sci. USA, 72, 3961-3965
18. Rigby, P. W. J., Dieckmann, M., Rhodes, C. and Berg, P. (1977) J. Mol. Biol. 113, 237-251
19. Chambon, P. & Breathnach, R. (1981) Ann. Rev. Biochem. 50, 349-383
20. Shapiro, M. B. & Senapathy, P. (1987) Nucl. Acids Res. 15, 7155-7174

Vol. 156, No. 1, 1988 BIOCHEMICAL AND BIOPHYSICAL RESEARCH COMMUNICATIONS
October 14, 1988 Pages 78-85

HIGH AFFINITY RECEPTORS FOR ATRIAL NATRIURETIC FACTOR IN PC12 CELLS

A. Rathinavelu and G.E. Isom

Department of Pharmacology and Toxicology
School of Pharmacy and Pharmacal Sciences
Purdue University, West Lafayette, IN 47907

Received August 1, 1988

Specific receptors for atrial natriuretic factor (ANF) are characterized on PC12 cells (rat pheochromocytoma cell line). Radioiodinated synthetic ANF (Rat, 8-33) bound to a single class of high affinity binding sites with the Kd value of 6.7 X 10^{-10} M. The Bmax value was 29 fmol/10^5 cells and receptor density was calculated as 194,000 ± 20,000/cell. Photoaffinity labelling of ANF receptor specifically labelled two protein bands with apparent m.wt of 70,000 and 130,000. When the cells were incubated with the labelled ligand at 37°C the ligand was internalized. The rate of internalization increased in the presence of increased ligand concentration. ANF receptors on PC12 cells are reported for the first time which would provide a unique model for study of ANF-receptor interaction. © 1988 Academic Press, Inc.

The regulatory role of Atrial Natriuretic Factor (ANF) in fluid volume homeostasis, natriuresis and smooth muscle relaxation (1-2) has been the focus of numerous investigations since the discovery of this new class of peptidic hormone. Specific ANF receptors are localized in various tissues (3) and are found to coexist witn guanylate cyclase enzyme activity, a bifunctional protein with a receptor domain for ANF and a catalytic domain for cyclic GMP (4).

The presence of high affinity receptors for ANF on adrenal cortex (5) and adrenal medullary cells (6) suggest that the adrenal glands serve as the target organ for ANF. Inhibition of aldosterone synthesis and release in the adrenal zona glomerulosa (7) and inhibition of catecholamine synthesis in pheochromocytoma tumor cells (8) by ANF confirms the regulatory effect of this hormone on adrenal function, yet the intracellular mechanisms whereby it elicits its control effect(s) is not known. In this study we report the presence of ANF receptors in PC12 cells, a pheochromocytoma cell line which is widely used for the study of

0006-291X/88 $1.50
Copyright © 1988 by Academic Press, Inc.
All rights of reproduction in any form reserved.

catecholamines biosynthesis and secretion. This cell line offers a unique model to study the interaction of ANF receptor dynamics with catecholamine synthesis and release.

MATERIALS AND METHODS

Materials

Synthetic rat Atrial Natriuretic Factor (ANF 8-33) and [^{125}I]-ANF (Rat, 8-33, specific activity 1200-1500 Ci/mmole) were purchased from Peninsula Laboratories Inc. (Belmont,CA). Electrophoresis materials were purchased from Bethesda Research Laboratories and *bis*(Sulfosuccinimidyl) suberate was obtained from Pierce Chemical Company. All other chemicals used in these experiments were purity grade.

Cell Culture

PC12 cells were obtained from American Type Culture Collection (CRL NO.1721) and maintained in RPMI medium containing 10% heat inactivated horse serum, 5% fetal bovine serum, 50 units/ml penicillin and 50 μg/ml streptomycin at 37°C in a humidified atmosphere containing 5% CO2. Just prior to the binding assay, the cells were harvested from tissue culture flasks and washed three times with serum free RPMI medium containing 0.2% BSA.

Binding Experiments

ANF binding assays in intact PC12 cells was performed by incubating 5x10^{5} cells with [^{125}I]-ANF in the binding medium (RPMI medium containing 0.2% BSA) in a total volume of 200 μl, at 0°C for 2 hrs. All assays were performed in polystyrene tubes. At the end of incubation the bound and free radioligand were separated by rapid filtration using GF/C glass fibre filters treated with 0.02% Tween-20 in PBS for 2 hrs. The filters were washed rapidly with an additional 10 ml of ice cold 0.15 M NaCl and counted in a gamma scintillation counter.

Internalization of ANF-receptors

PC12 cells were washed in prewarmed binding medium three times, loosely pelleted by centrifugation at 300 X g and incubated with [^{125}I]-ANF at 37°C. At the end of incubation period the tubes were drawn from the incubator and placed on ice. The cells were washed by adding ice cold 0.15 M NaCl and centrifuged at 300 X g for 2 min. at 0°C. ANF bound to the cell surface was determined by extraction of the intact cells with 0.5 M NaCl, 0.2 M acetic acid (9). The cells were solubilized in 1 N NaOH and the radioactivity associated with the cells was determined which represented the internalized ligand.

Affinity Cross-linking Studies

Confluent cells from 150 cm^{2} flasks were washed with serum free RPMI medium and homogenized in the ice cold binding medium containing 0.25 M sucrose, 0.4 mM phenymethylsulfonyl fluoride, 1.0 mg/ml bacitracin, 20 μg/ml each leupeptin and aprotinin. The homogenate was centrifuged at 1,500 x g for 10 min. and the supernatant was centrifuged at 100,000 x g for 30 min. The pellet was resuspended in the binding medium and centrifuged again at 100,000 x g for 30 min. to remove sucrose. The washing step was repeated twice and the final pellet obtained was incubated with the labelled ligand in a total volume of 200 μl for 90 min at 37°C. 200 μl of 0.2 mM *bis*(sulfosuccinimidyl) suberate in DMSO was added and the incubation was continued for

another 30 min. At the end of incubation the tubes were transferred to ice, cold binding medium was added and centrifuged at 100,000 x g for 30 min. The pellet was solubilized and electrophoresed according to the method of Laemmli (10) using 10% gel. The gels were dried and exposed to Kodak X-OMAT film at -70°C for 30 days.

RESULTS

ANF Receptor Binding

PC12 cells show high affinity, saturable binding for [^{125}I]-ANF. Scatchard analysis yielded a linear plot (fig.1) indicating a single class of binding sites; the apparent dissociation constant (Kd) for ANF was 6.7 X 10^{-10} M and Bmax was 1.94 X 10^{-10} M (29 fmol/10^5 cells). Based on this data the number of binding sites are calculated as 194,000 ± 20,000/cell. Also binding of [^{125}I-ANF was a time dependent process and equilibrium binding was reached within 120 min.(fig.2). 2 μM concentration of cold ANF displaced almost 80% of labelled ligand binding indicating the specificity of receptor binding.

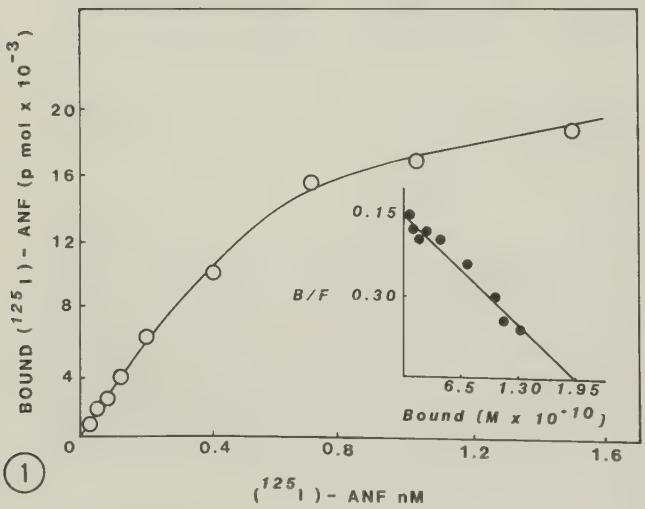

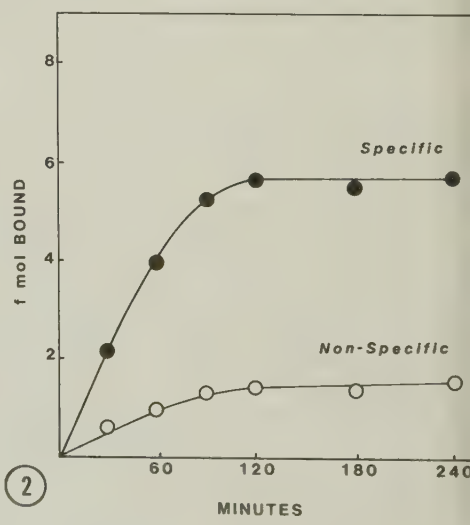

Fig.1: Saturable binding of [^{125}I]-ANF (rat, 8-33) to PC12 cells. The cells (5x10^5 cells/tube) were incubated at 0°C with various concentrations of [^{125}I]-ANF for 2 hrs. in RPMI medium containing 0.2% BSA. Specific binding is the difference between total binding and the non-specific binding in the presence of 2 μM unlabelled ANF (rat,8-33). (Inset) Scatchard plot of the binding data. The calculated Kd is 6.7 x 10^{-10}M and Bmax is 29 fmol/10^5cells.

Fig.2: Binding of [^{125}I]-ANF (rat,8-33) to PC12 cells as a function of time at 0°C with labelled ANF. Non-specific binding was determined in the presence of 2 μM unlabelled ANF (rat, 8-33).

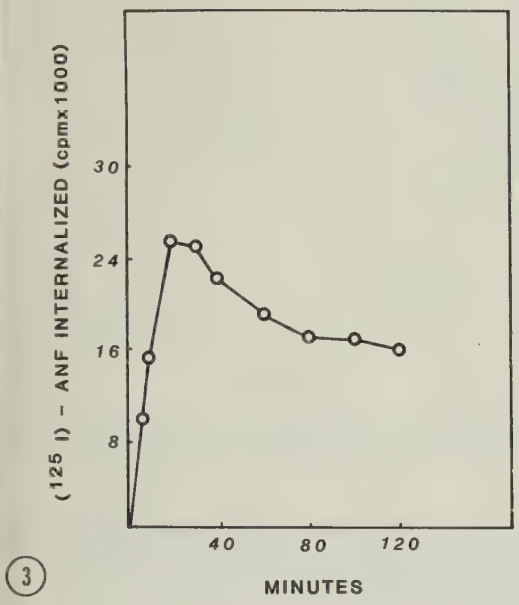

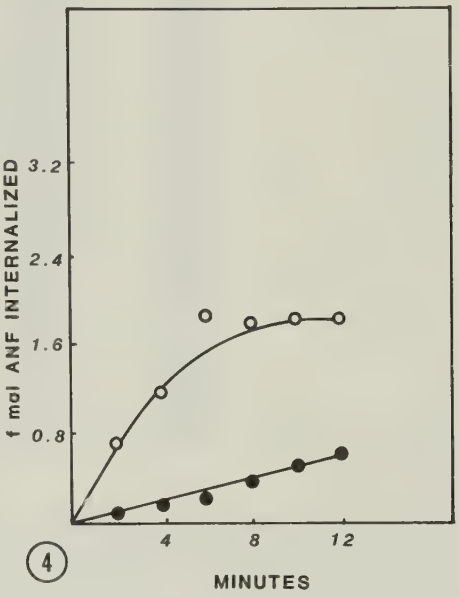

Fig.3: Time course of [^{125}I]-ANF internalization by PC12 cells at 37°C. The cells were incubated for 120 min. with 2 nM [^{125}I]-ANF.

Fig.4: Internalization with 0.25 [●] nM and 2 nM [O] [^{125}I]-ANF concentrations at 37°C.

Internalization of I-125 ANF

When the cells were incubated with [^{125}I]-ANF at 37°C, internalization of ANF was observed. This was indicated by the inability of NaCl/acetic acid to completely remove the cell associated radioactivity. The binding of the ligand was more rapid at 37°C, reaching a maximum at 20 min. (fig.3). When internalization was observed at two different concentrations of [^{125}I]-ANF, the internalization was more rapid at 2 nM ANF as compared to the 0.25 nM concentration (fig.4). The surface binding was also the highest with the 2 nM concentration than the 0.25 nM concentration (fig.5). The endocytic rate constant (Ke) was determined by plotting the ratio of internalized ligand to surface-bound ligand as a function of time of incubation (11). This plot produced a linear curve with a slope of Ke. The calculated Ke for ANF at 0.25 nM concentrations was 0.045 min^{-1} and the endocytic rate constant increased to 0.092 min^{-1} at 2 nM concentrations of ANF (fig.6). The increase in the Ke value at higher concentrations of ANF was concomitant with an increased

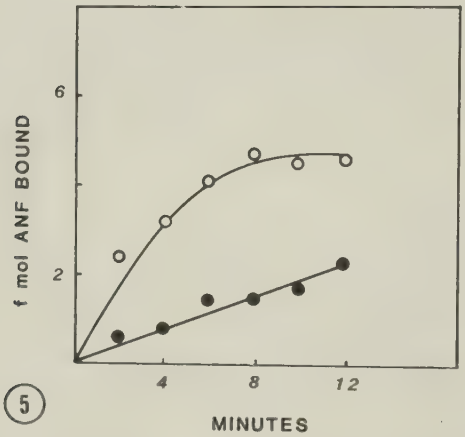

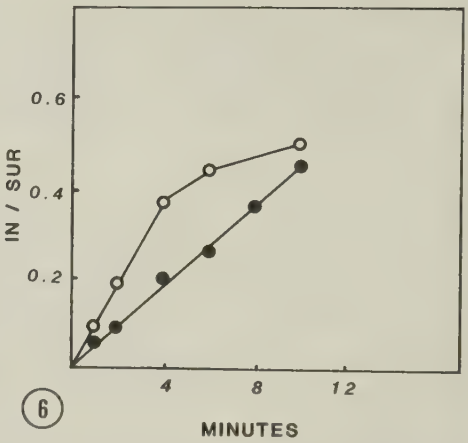

Fig.5: Surface binding of [^{125}I]-ANF on PC12 cells at 37°C with 0.25 nM [●] and 2 nM [O] labelled ANF for different time intervals.

Fig.6: In/Sur analysis in PC12 cells at 37°C with 0.25 nM [●] and 2 nM [O] [^{125}I]-ANF. The ratio of radioactivity associated with the interior to the surface of the cell (In/Sur) was determined. The slope of this curve yielded the endocytic rate constant Ke.

surface binding, thus the observed increase in internalization was apparently due to receptor occupancy.

Affinity Labelling of ANF Receptors

The affinity labelling reaction using *bis*(sulfosuccinimidyl) suberate coupled [^{125}I]-ANF specifically to two protein components of the PC12 cell plasma membrane. The labelled proteins migrated at m.wt of 70,000 and 130,000 on SDS polyacrylamide gel electrophoresis under reducing condition (fig.7). In the presence of 2 μM cold ANF the labelling of both of these proteins was inhibited almost completely, while non-specific labelling of other fractions remained unaltered. This indicated the specificity of ANF binding with 70,000 and 130,000 m.wt proteins in the plasma membrane.

DISCUSSION

A great deal of attention has focused on the influence of ANF on adrenal responses, since the polypeptide inhibits basal aldosterone synthesis and release from the adrenal zona glomerulosa (7). The presence of high affinity receptors for ANF has been reported in adrenal cortex (5), adrenal zona glomerulosa (12), adrenal medullary cells (6) and in human pheochromocytoma cells (8). This suggests that the adrenal glands may be functionally regulated by ANF at various levels. Recent evidence

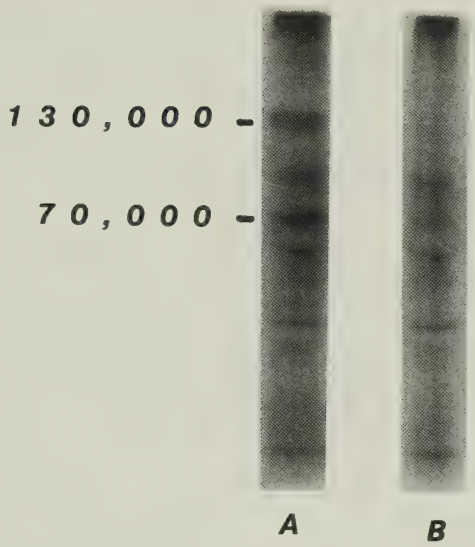

Fig.7: Specificity of [^{125}I]-ANF cross linking to ANF receptors on PC12 cells. The dried gel was exposed to Kodak X-OMAT film at -70°C for 30 days. Specific binding of [^{125}I]-ANF to the receptors in plasma membrane (lane A). Non-specific binding in the presence of 2 μM unlabelled ANF (lane B).

of ANF secretion by adrenal medullary cells (13) indicates that the adrenals may have more complicated roles in mediating the actions of ANF.

The present results demonstrate high affinity receptors for ANF on PC12 cells, a transformed cell line which has served as an interesting model for exploring the functional aspects of chromaffin cells. Binding of ANF to PC12 cells fulfills many of the criteria for specific receptor recognition sites. It was specific, rapid, reversible and saturable. The dissociation constant value (Kd) and Bmax values are comparable to the values reported previously for adrenal medullary (6), renal cortex (14) and cultured vascular smooth muscle cells (15). PC12 cells have been reported to possess high levels of the particulate form of guanylate cyclase which was activated by ANF resulting in the elevation of intracellular cGMP (16). This response is similar to the cGMP elevation observed in rabbit and rat aorta (17), vascular smooth muscle cells (14) and bovine aortic endothelial cells (18). Demonstration of ANF receptors on PC12 cells suggest that the particulate form of guanylate cyclase may be functionally coupled to the ANF receptors, as in many other cells.

Following covalent coupling of radiolabelled ligand to ANF receptors on plasma membranes, two proteins were specifically labelled and migrated at m.wt 70,000 and 130,000 under reducing conditions. These correspond to two classes of receptors reported in bovine adrenocortical cells (5), bovine aortic endothelial cells, aortic smooth muscle cells and human lung fibroblast (19). The high molecular weight protein, isolated from the bovine adrenocortical cells showed both ANF binding and guanylate cyclase activity, which is also believed to exist in reducible and non-reducible forms. The low molecular weight receptors are reported not coupled to particulate guanylate cyclase.

PC12 cells appear to possess two classes of receptors, one linked to the particulate form of guanylate cyclase. Since the high molecular weight receptor was not completely reduced to the low molecular weight protein, as indicated by the presence of two labelled fractions, it is speculated both reducible and non-reducible forms of high molecular weight receptor proteins may be present in PC12 cells. The internalization process is another interesting phenomenon, since the internalization rate varies with the ligand concentration. It is speculated that the internalization process in these cells may perform functions other than receptor-mediated endocytosis, such as transmembrane signal transduction or diminishing the cell responsiveness to the ligand by removing the cell surface receptors (20).

REFERENCES

1. Cantin, M., and Genest, J. (1985) Endocrin. Rev., 6, 107-126.
2. Ingami, T., Misono, K.S., Grammer, R.T., Fukumi, H., Maki, K., Tanaka, I., McKenzie, J.C., Tajayangi, R., Pandey, K.N., and Parmentier, M. (1985) Clin. Exp. Hypertens. Part A theory Pract.,A7, 851-866.
3. Roubert, P., Lonchampt, M.O., Chabrier, P.E., Plas, P., Goulin, J., and Braquet, P. (1987) Biochem. Biophys. Res. Commun., 147, 957-963.
4. Kuno, T., Anderson, J.W., Kamidsaki, Y., Waldman, S.W., Chang, L.Y., Saheki, S., Leitman, D.C., Nakane, M. and Murad, F. (1986) J. Biol. Chem., 261, 5817-5823.
5. Takayanagi, R., Ingami,T., Snajdar, R.M., Imada, T., Tamura,M., and Misono, K.S. (1987) J. Biol. Chem., 262, 12104-12113.
6. Heisler, S. and Morrier, E. (1988) Biochem. Biophys. Res. Commun., 150, 781-787.
7. Goodfriend, T.l., Elliot, M.E., Atlas, S.A. (1984) Life Sci., 35, 1675-1682.

8. Shionoiri, H., Hirawa, N., Takasaki, I., Ishikawa, K., Minamisawa, K., Miyajima, E., Kinoshita, Y., Shimoyama, K., Shimonaka, M., Ishido,M., and Hirose, S. (1987). Biochem. Biophys. Res. Commun., 148, 286-291.
9. Haigler, H.T., Maxfield, F.R., Willingham,M.C., and Pastan, I. (1980) J. Biol. Chem.,255, 1239-1241.
10. Laemmli, U.K. (1970) Nature, 227, 680-685.
11. Wiley, H.S. and Cunningham, D.D. (1982) J. Biol. Chem., 257, 4222-4229.
12. Meloche, S., Ong, H., Cantin, M. and DeLean, A. (1986) J. Biol. Chem., 261, 1525-1528.
13. Pruss, R.M. and Zamir, N. (1987) Neurochem. Int., 11, 299-304.
14. Ogura, T., Mitsui, T., Ogawa, N., Ota, Z. (1985) Res. Commun. Chem. Pathol. Pharmacol., 49, 353-360.
15. Roubert, P., Lonchampt, M.O., Chabrier, P.E., Plas, P., Goulin, J., and Braquet, P. (1987) Biochem. Biophys. Res. Commun., 148, 61-67.
16. Fiscus, R.R., Robles, B.T., Waldman, S.A., Murad, F. (1987) J. Neurochem., 48, 522-528.
17. Rapoport,R.M., Winquist, R.J., Faison, E.P., Waldman, S.A., and Murad, F. (1986) Eur. J. Pharmacol., 120, 123-126.
18. Leitman, D.C. and Murad, F. (1986) Biochem. Biophys. Acta, 885, 74-79.
19. Leitman, D.C., Andresen, J.W., Catalano, R.M., Waldman, S.A., Tuan, J.J. and Murad, F. (1988) J. Biol. Chem., 263, 3720-3728.
20. Minami, Y., Samelson, L.E. and Klausner, R.D. (1987) J. Biol. Chem., 262, 13342-13347.

Vol. 156, No. 1, 1988 BIOCHEMICAL AND BIOPHYSICAL RESEARCH COMMUNICATIONS
October 14, 1988 Pages 86-91

EVIDENCE FOR LIGHT-INDUCED LYSINE CONFORMATIONAL CHANGES DURING THE PRIMARY EVENT OF THE BACTERIORHODOPSIN PHOTOCYCLE

Earl McMaster and Aaron Lewis

Department of Applied Physics, Cornell University, Ithaca, New York 14853

Received August 22, 1988

Fourier transform infrared difference spectroscopy is used to examine the role of lysine in the primary event of the bacteriorhodopsin photocycle. Isotopically labeled lysine is used to tentatively assign the lysine modes in the BR and K species. The results suggest that the lysine side-chain undergoes conformational changes in concert with the known light-induced chromophore structural alterations.
© 1988 Academic Press, Inc.

Bacteriorhodopsin (BR)[1] is a 26,000-dalton pigment in the purple membrane (pm) of *Halobacterium halobium*. BR is composed of an all-trans retinal chromophore bound via a protonated Schiff base to the ε-amino group of a lysine residue of the protein bacterio-opsin. This protein consists of alpha helices that traverse the membrane seven times with the retinal linked to the lysine residue numbered 216 (Lys-216) on the C-terminal helix. Absorption of a visible photon by the retinal chromophore of BR provides the energy which is transduced into the movement of protons across the bacterial cell membrane. The resulting electrochemical gradient is coupled to the synthesis of ATP. The absorption of a photon initiates a series of mutual structural changes in the retinal chromophore and the protein. These changes form a photocycle composed of a series of intermediates (for a review, see reference 1).

The BR photocycle has been established by time-resolved visible absorption spectroscopy. The primary photoproduct is K_{610}[2] followed by the intermediates L_{550}, M_{412}, N_{520} and O_{640}; returning to BR_{570} in ~10ms (2,3). Resonance Raman spectroscopy has been useful in elucidating the retinal chromophore structure and the Schiff base protonation state for each intermediate (4-8). Fourier transform infrared (FTIR) difference spectroscopy has supported many of the conclusions deduced from resonance Raman spectroscopy (9-11). Whereas resonance Raman spectroscopy selectively probes vibrational modes directly coupled to the electronic transition, FTIR difference spectroscopy detects all the IR active modes that change with light. Thus, in addition to detecting retinal alterations, FTIR difference spectroscopy has been able to probe protein structural changes induced by light. Studies on specific amino acids of BR have monitored the protonation state of aspartic acid, glutamic acid, and tyrosine residues (12-17). We report here the first results from FTIR difference spectroscopy which directly probe side-chain vibrational modes of lysine residues in the

[1] Abbreviations: BR = bacteriorhodopsin, pm = purple membrane, FTIR = Fourier transform infrared.
[2] The subscript indicates the visible absorption maximum in nanometers. The K intermediate has a visible absorption maximum near 610nm at room temperature and near 630nm at 80K.

0006-291X/88 $1.50
Copyright © 1988 by Academic Press, Inc.
All rights of reproduction in any form reserved.

BR_{570} and K_{630} species. Our results indicate that, in concert with the well known chromophore structural alterations, there are light-induced conformational changes in lysine.

Materials and Methods

Materials D,L-lysine-3,3,4,4,5,5,6,6-[$^2H_8$] 2HCl (98.8 atom % ^2H) was purchased from MSD Isotopes (Montreal, Quebec) and used without further purification. Native pm was prepared by growing Halobacterium halobium S9 on a modified Onishi medium (18). [$^2H_8$]lysine pm was prepared using an identical procedure except that twice the quantity of D,L-lysine-3,3,4,4,5,5,6,6-[$^2H_8$] 2HCl was substituted for L-lysine HCl. Little, if any, deuterium from the deuterated lysine transfers to other amino acid residues and bacterial synthesis of unlabeled lysine is unlikely (19). Purple membrane (pm) sheets were isolated and washed several times in H_2O.

Wet films were made by depositing several drops of concentrated pm (A_{570}~4, 1 cm pathlength) on a AgCl window (International Crystal Laboratories, Inc., Elizabeth, NJ) and partially drying using N_2 gas. The sample was sealed by adding a second AgCl window with a thin Ag O'Ring and placed in a cryocooler (Cryogenic Technology, Inc., Waltham, MA) suspended in an FTIR spectrometer (IR/98, IBM Instruments Inc., Danbury, CT), equipped with a liquid N_2 cooled HgCdTe detector. Water content of the film was monitored by comparing the integrated intensity of the water band at 3300 cm^{-1} to the amide I band. Ratios of approximately 6 to 1 or higher were considered adequately hydrated (16).

FTIR Spectroscopy The sample is light adapted with yellow light (λ>515nm filter, Esco Products Inc., Oak Ridge, NJ) for at least 15 min. at room temperature and then cooled in the dark to 80K. An FTIR difference spectrum is obtained by:

1) Collecting an FTIR spectrum of BR in the dark (512 scans, 2 cm-1 resolution, ~7 min.)
2) Shining 500 nm light (40 nm bandpass filter, Corion Corp., Holliston, MA) for 10 minutes.
3) Collecting an FTIR spectrum of BR+K in the dark (512 scans, 2 cm-1 resolution, ~7 min.)
4) Subtracting the BR spectrum from the BR+K spectrum to produce a difference spectrum.
5) Shining ~650 nm light (650 nm long-wavelength pass filter in series with an IR absorbing filter (Melles Griot, Irvine, CA)) for ~15 minutes to regenerate BR.

This procedure is repeated at least four times and the resulting difference spectra are averaged to produce a K/BR difference spectrum for both native and [$^2H_8$]lysine pm. The individual difference spectra are highly reproducible in terms of both frequency and relative intensity. Every peak labeled in the results and discussion section is clearly seen in each of the individual difference spectra. The spectra shown are unsmoothed with a resolution of 2 cm^{-1}. The Fourier transforms were computed using Happ-Genzel apodization.

Results and Discussion

Determination of lysine peaks in the K/BR FTIR difference spectrum. In order to detect the vibrational modes in BR_{570} and K_{630} which are due to lysine, FTIR difference spectra were obtained at 80K for hydrated films of both native pm and [$^2H_8$]lysine pm. At this temperature the primary photoproduct, K_{630}, is indefinitely stable and light activated pm samples contain only the species BR_{570} and K_{630}. The K/BR difference spectra obtained for the native pm sample and the [$^2H_8$]lysine pm sample are shown in Figures 1A and 1B, respectively. In these spectra positive peaks originate from K_{630} and negative peaks are due to BR_{570}. The majority of K_{630} and BR_{570} peaks in the two spectra are very similar in intensity and frequency. For example, Figure 1 shows the C=N-H^+ stretching vibration of the Schiff base does not change by more than 2 cm^{-1} as a result of [$^2H_8$]lysine substitution. In fact, most of the clearly identifiable retinylidene chromophore vibrations (e.g. C=N, C=C and C-C stretches) are completely unchanged in frequency and relative intensity by substituting [$^2H_8$]lysine in place of the native amino acid. However, there are numerous bands that either

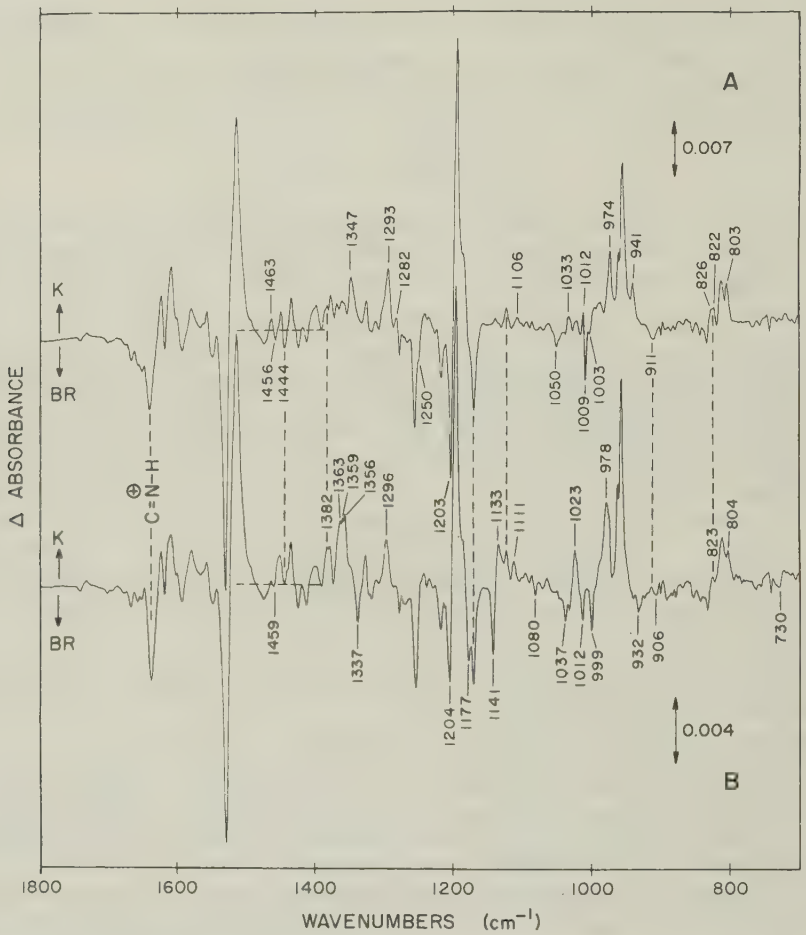

Figure 1. K/BR Fourier transform infrared difference spectra in the range 700 - 1800 cm^{-1} at 80K and 2 cm^{-1} resolution in H_2O. (A) Native purple membrane film. (B) [$^2H_8$]lysine purple membrane film. The arrow indicates the absorbance scale.

completely disappear or are significantly altered by the above replacement. These bands are labeled with their frequencies in Figure 1. All labeled peaks have either reproducibly different frequencies (>2 cm^{-1} difference) or clearly different intensities in the two spectra of Figure 1. The spectral differences can be caused by isotope-induced shifts of lysine vibrational modes in or out of a particular region and/or changes in non-lysine vibrational modes via an isotope-induced alteration in coupling to lysine.

Assignment of lysine modes in the K/BR FTIR difference spectrum. As a first approximation, a vibrational mode may be associated with local symmetry coordinates of the molecule. For the side-chain of lysine the local symmetry coordinates are the CH_2 scissor, CH_2 wag, CH_2 twist, CH_2 rock, C-N stretch and the C-C stretch. Table 1 lists the vibrational frequency range found for each of these modes in fully protonated and fully deuterated compounds similar to lysine.

The region 1438 - 1489 cm^{-1} has been assigned to CH_2 scissor modes (see Table 1). We notice significant alterations in this region as a result of the [$^2H_8$]lysine substitution. A horizontal dashed line has been added in this region as an aid in differentiating positive from negative peaks. Upon

Table 1. The range of vibrational frequencies observed for some modes appropriate to lysine. The data are from analyses on poly-L-lysine (20), n-butylamine (21), n-propylamine (22), hexane, pentane, and butane (23) for the fully protonated compounds and from hexane and pentane (23) for the fully deuterated compounds.

MODE	FREQUENCY RANGE (cm^{-1})	
	Fully Protonated	Fully Deuterated
CH_2 scissor	1438 - 1489	968 - 1152
CH_2 wag	1246 - 1410	727 - 893, 987 - 1042
CH_2 twist	1180 - 1342	726 - 794, 933 - 967
CH_2 rock	725 - 910, 1131 - 1179	520 - 659, 980 - 991
C-N stretch	1030 - 1141	—
C-C stretch	811 - 1124	709 - 892, 1115 - 1246

[$^2H_8$]lysine substitution the 1463 cm^{-1} K_{630} band and the 1444 cm^{-1} and 1456 cm^{-1} BR_{570} bands in native pm have lost intensity. If these are indeed lysine CH_2 scissor modes they would shift to the CD_2 scissor region (968 - 1152 cm^{-1}) upon deuteration (see Table 1). In this region of the [$^2H_8$]lysine pm spectrum we observe numerous new K_{630} and BR_{570} bands which are possible candidates for CD_2 scissor modes.

According to Table 1, CH_2 wag and CH_2 twist modes may be found in the 1180 - 1410 cm^{-1} region of the native pm spectrum. In this region is an intense positive peak at 1347 cm^{-1} which is not found in the deuterated spectrum. According to Table 1, this may be a CH_2 wag mode. If this is the case, the intense positive peak at 1023 cm^{-1} in the [$^2H_8$]lysine pm spectrum is a likely candidate for the shifted CD_2 wag mode. Alternatively, the 1347 cm^{-1} peak has been assigned as an N-H in-plane bending mode (11). The intense positive peak at 1293 cm^{-1} in the native spectrum is probably a chromophore peak which shifts to 1296 cm^{-1} upon [$^2H_8$]lysine substitution.

Other possible CH_2 wag and/or CH_2 twist modes of the lysine side-chain are indicated by losses of intensity at 1282, 1250, and 1203 cm^{-1} in the native pm spectrum. According to Table 1, the corresponding peaks in the [$^2H_8$]lysine pm spectrum may be those at 730 cm^{-1} or in the region from 999 to 1037 cm^{-1} (see Figure 1B).

The 1180 - 1410 cm^{-1} region of the [$^2H_8$]lysine pm spectrum is composed of a triplet of intense peaks between 1356 and 1363 cm^{-1}, flanked by a negative peak at 1337 cm^{-1} and a gain of intensity at 1382 cm^{-1}. The frequencies of these modes are too high to be CD_2 modes and their assignment is, at present, unclear.

We find several candidates for C-N and/or C-C stretch modes in the 1030 - 1141 cm^{-1} region of the native pm spectrum. These occur as K_{630} bands at 1106 and 1033 cm^{-1} and as a BR_{570} band at 1050 cm^{-1}. In the C-C stretch region, a whole sequence of changes due to [$^2H_8$]lysine substitution occur between 1012 and 822 cm^{-1}. Among these are alterations in K_{630} bands at 1012, 974, and 941 cm^{-1} and in BR_{570} bands at 1009, 1003 and 911 cm^{-1}. If these are C-C stretch modes they should either shift up to the 1115 - 1246 cm^{-1} region or down to the 709 - 892 cm^{-1} region upon [$^2H_8$]lysine substitution (see Table 1). Within these regions of the [$^2H_8$]lysine pm spectrum we find new intensity at 1177, 1141, 1133 and 730 cm^{-1}.

The K_{630} peaks at 826, 822, and 803 cm^{-1} are in the region where CH_2 rock modes can occur. If these are CH_2 rock modes, they would most likely shift to the 520 - 659 cm^{-1} CD_2 rock region upon [$^2H_8$]lysine substitution. Unfortunately, our HgCdTe detector cuts off at about 700 cm^{-1}.

Table 2. Tentative assignments for lysine modes in the K/BR difference spectrum of native purple membrane in H_2O (see Figure 1A)

BR_{570}	K_{630}	MODE
1456	1463	CH_2 scissor
1444		"
	1347	CH_2 wag
1250	1293	CH_2 wag, CH_2 twist
	1282	"
1203		CH_2 twist
1050	1106	C-N st., C-C st.
	1033	"
1009	1012	C-C stretch
1003	974	"
911	941	"
	826	C-C st., CH_2 rock
	822	"
	803	CH_2 rock

A complete summary of our tentative assignments for the lysine vibrational modes of the K_{630} and BR_{570} species in native purple membrane appears in Table 2. The reader is reminded that some of the peaks in the K/BR FTIR difference spectrum, which we assigned to lysine, may be chromophore modes coupled to lysine.

From Figure 1 it is apparent that certain regions of the spectrum, such as the 1500-1800 cm^{-1} regime, are completely unaltered by [$^2H_8$]lysine substitution. These regions are clearly assigned to the double bond stretches of the retinylidene chromophore and certain amino acid side-chains (e.g. aspartic acid, glutamic acid and arginine). On the other hand, frequency regimes discussed above where significant alterations are observed by deuterium substitution are associated with previously identified lysine side-chain modes. Although this is encouraging, deuteration of simple molecules indicates that no bands should be observed in certain regions where [$^2H_8$]lysine pm samples show intense vibrations. The precise reason for this observation in not clear. Nonetheless, the simplest explanation of our data is that upon light-induced transformation from BR_{570} to K_{630}, not only the retinylidene chromophore structure is altered but, in addition, the lysine structure is also affected. It is plausible to assume that, in view of the rapid timescale of K_{630} production, the lysine vibrations that are altered are associated with the lysine-216 side chain attached to the retinylidene chromophore. At the present time this is simply an hypothesis. Additional experiments will allow us to test this hypothesis by investigating FTIR difference spectra of bacteriorhodopsin permethylated (24) at all of the lysines other than lysine-216.

References

1. Packer, L., Ed. (1982) Methods Enzymol., Vol. 88, Academic Press, New York.
2. Lozier, R. H., Bogomolni, R. A., and Stoeckenius, W. (1975) Biophys. J. 15, 955-962.
3. Dencher, N., and Wilms, M. (1975) Biophys. Struct. Mech. 1, 259-271.
4. Lewis, A., Spoonhower, J., Bogomolni, R. A., Lozier, R. H., and Stoeckenius, W. (1974) Proc. Nat. Acad. Sci. USA 71, 4462-4466.
5. Aton, B., Doukas, A. G., Callender, R. H., Becher, B., and Ebrey, T. G. (1977) Biochemistry 16, 2995-2999.

6. Stockburger, M., Klusmann, W., Gattermann, H., Massig, G., and Peters, R. (1979) Biochemistry 18, 4886-4900.
7. Terner, J., Hsieh, C.-L., Burns, A. R., and El-Sayed, M. A. (1979) Proc. Natl. Acad. Sci. USA 76, 3046-3050.
8. Smith, S. O., Lugtenburg, J., and Mathies, R. A. (1985) J. Membrane Biol. 85, 95-109.
9. Rothschild, K. J., and Marrero, H. (1982) Proc. Natl. Acad. Sci. USA 79, 4045-4049.
10. Bagley, K., Dollinger, G., Eisenstein, L., Singh, A. K., and Zimanyi, L. (1982) Proc. Natl. Acad. Sci. USA 79,4972-4976.
11. Siebert, F., and Mäntele, W. (1983) Eur. J. Biochem. 130, 565-573.
12. Siebert, F., Mäntele, W., and Kreutz, W. (1982) FEBS Lett. 141, 82-87.
13. Engelhard, M., Gerwert, K., Hess, B., Kreutz, W., and Siebert, F. (1985) Biochemistry 24, 400-407.
14. Rothschild, K. J., Roepe, P., Ahl, P. L., Earnest, T. N., Bogomolni, R. A., DasGupta, S. K., Mulliken, C. M., and Herzfeld, J. (1986) Proc. Natl. Acad. Sci. USA 83, 347-351.
15. Dollinger, G., Eisenstein, L., Lin, S.-L., Nakanishi, K., and Termini, J. (1986) Biochemistry 25, 6524-6533.
16. Roepe, P., Ahl, P. L., DasGupta, S. K., Herzfeld, J., and Rothschild, K. J. (1987) Biochemistry 26, 6696-6707.
17. Eisenstein, L., Lin, S.-L., Dollinger, G., Odashima, K., Termini, J., Konno, K., Ding, W.-D., and Nakanishi, K. (1987) J. Am. Chem. Soc. 109, 6860-6862.
18. Onishi, H., McCance, M. E., and Gibbons, N. E. (1965) Can. J. Microbiol. 11, 365-373.
19. Argade, P. V., Rothschild, K. J., Kawamoto, A. H., Herzfeld, J., and Herlihy, W. C. (1981) Proc. Natl. Acad. Sci. USA 78, 1643-1646.
20. Yu, T.-J., Lippert, J. L., and Peticolas, W. L. (1973) Biopolymers 12, 2161-2176.
21. Teixeira-Dias, J. J. C., Batista de Carvalho, L. A. E., Amorim da Costa, A. M., Lampreia, I. M. S., and Barbosa, E. F. G. (1986) Spectrochimica Acta 42A, 589-597.
22. Sato, N., Hamada, Y., and Tsuboi, M. (1987) Spectrochimica Acta 43A, 943-954.
23. Shimanouchi, T., Matsuura, H., Ogawa, Y., and Harada, I. (1978) J. Phys. Chem. Ref. Data 7, 1323-1443.
24. Longstaff, C., and Rando, R. R. (1987) Biochemistry 26, 6107-6113.

Vol. 156, No. 1, 1988 BIOCHEMICAL AND BIOPHYSICAL RESEARCH COMMUNICATIONS
October 14, 1988 Pages 92-98

AFFINITY PURIFICATION OF HUMAN DEOXYCYTIDINE KINASE: AVOIDANCE OF STRUCTURAL AND KINETIC ARTIFACTS ARISING FROM LIMITED PROTEOLYSIS

Min-Young Kim, Seiichiro Ikeda and David H. Ives

Department of Biochemistry
The Ohio State University
484 West 12th Avenue
Columbus, OH 43210

Received August 25, 1988

Homogeneous deoxycytidine kinase has been isolated from leukemic human T-lymphoblasts by affinity chromatography based on a multisubstrate analog, deoxycytidine 5'-adenosine 5'''-P^1,P^4-tetraphosphate (dCp_4A). Chromatography of extract treated with protease inhibitors yielded a monomeric polypeptide, inasmuch as the M_r of the native protein, 59,300, is comparable to the value of 52,000 from sodium dodecyl sulfate polyacrylamide gel electrophoresis. The isoelectric pH was 6.1. But, enzyme isolated without protease inhibitors exhibited two fragments of M_r = 30,000 and 33,000, suggesting that proteolytic cleavage of the parental polypeptide had occurred during affinity chromatography. Both the parental and proteolyzed enzymes phosphorylated deoxyadenosine and deoxyguanosine, as well as deoxycytidine. However, the proteolyzed enzyme had an increased apparent K_m for deoxycytidine. In consequence of this, a mixture of the two forms produced bimodal kinetic plots, whereas linear kinetics were displayed by each form alone. © 1988 Academic Press, Inc.

The identification and characterization of the enzymes responsible for phosphorylating deoxyadenosine, deoxyguanosine and deoxycytidine in human cells continues to be a challenging and elusive problem. While mutant cells lacking these activities can continue to grow, their resistance to chemotherapeutic nucleosides reveals that one or more of these activities plays an important practical role in the activation of these drugs (1-3). These kinase activities also contribute to the cytotoxic effects of purine deoxynucleosides in cases of impaired catabolism of dAdo (4) or dGuo (5), resulting in immunodeficiency diseases.

Each of the dCyd or purine deoxynucleoside kinases partially purified from the cytosol of human cells has been able to phosphorylate more than one deoxynucleoside substrate, but in varying ratios, and with various K_m values (6-8). It is also unclear how many multispecific kinases are expressed in human cytosol. For example, two fractions having all three activities, but with a different set of apparent K_m values, have been obtained from T-lymphoblasts, in contrast to a single multispecific dCyd kinase from B-lymphoblasts (6). Osborne has reported a dAdo-dGuo kinase from mutant CCRF-CEM T-cells lacking both dCyd and Ado kinase activities (9), and Hurley et al. (7) have identified three fractions from human placental extract as dGuo-dCyd kinase, dCyd-dAdo kinase and Ado-dAdo kinase. Sarup and Fridland purified human T-lymphoblast and myeloblast kinases more extensively (8), and Bohman and Eriksson have recently isolated homogeneous dCyd kinase from human leukemic spleen (10). In each case, the dCyd kinase also phosphorylated dAdo and dGuo. Progress towards a clear understanding of the kinetic and regulatory mechanisms affecting human deoxynucleoside kinases has been impeded by the bi-modal or nonlinear kinetic patterns often obtained when nucleoside or ATP is varied (2, 8, 11). Such results mimic those seen earlier with animal cell preparations (12, 13). Typically, double-reciprocal plots have yielded two slopes, from which two K_m values have been derived. It has not been clear whether this phenomenon is due to cooperative behavior, or to a mixture of enzyme forms. In this paper we will show that limited proteolysis, which can occur during purification of the human enzyme, gives rise to a second active form having kinetic properties which differ from those of the parental enzyme and which may contribute to non-linear kinetic patterns.

0006-291X/88 $1.50
Copyright © 1988 by Academic Press, Inc.
All rights of reproduction in any form reserved.

EXPERIMENTAL PROCEDURES

Materials--Human leukemic lymphocytes, obtained by leukopheresis, were provided by the Tumor Procurement Service of the OSU Comprehensive Cancer Center. The majority of the cells in a bone-marrow biopsy were primitive T-lymphoblasts, as characterized by E-rosette formation and cell-surface antigens, leading to a diagnosis of acute lymphoblastic leukemia (ALL). The bisubstrate affinity column, dCp_4A-Agarose, was synthesized as described previously (14), obtaining 2.6 umol of substituent per ml of gel.

Enzyme preparation and assay--After the lymphocytes were washed and freed of red cells by hypotonic lysis they were disrupted by brief sonication in Seligmann balanced salt solution also containing 0.05 % EDTA and 2 mM dithioerythritol. The 20,000 x g supernatant fraction was quick-frozen and stored at -80 °C. Preliminary to purification of the enzyme, nucleic acids were precipitated with streptomycin sulfate (1 g/g protein, pH 7.0). The supernatant solution was fractionated with ammonium sulfate; the protein precipitating between 30% and 63% saturation was dissolved in equilibration buffer (EB)--20 mM Tris buffer (pH 7.5) containing 20% glycerol and 2 mM dithioerythritol. Kinases were routinely assayed as described previously (15) at pH 7.5 and 37 °C, in 5% glycerol, aided by a disk-washing device (16). One unit of enzyme activity is defined as that amount of enzyme which catalyzes the formation of 1 nmol of deoxynucleotide per minute. Protein concentrations were measured by the Bradford method (17).

Affinity chromatography--A 3-ml column of dCp_4A-Sepharose was equilibrated with EB. Several protease inhibitors were added to the sample before it was passed onto the affinity column, but the column itself was not equilibrated with these inhibitors, because they caused a larger proportion of the activity to run through the column. The final protease inhibitor concentrations in the sample were: 1,10-phenanthroline (5 mM), benzamidine (1 mM) and diphenylcarbamyl chloride (0.1 mM). After adding the sample at 4° over a three-hour period, the column was washed with 10 vol of equilibration buffer (EB), followed by 10 vol of the same plus 0.3 mM ATP and 0.5 M NaCl to remove any nonspecifically-bound proteins. Then, before eluting the enzyme, the ATP and salt were removed by washing again with 5 vol of EB. Finally, flow through the column was reversed, and the dCyd kinase was eluted by adding 0.3 mM dCTP in EB to the column and allowing it to stand overnight before resuming flow and collecting the eluate. (Pronounced tailing of the elution peak occurred unless the column was allowed to equilibrate overnight with the dCTP, presumably because of an unusually slow off-rate for the ligand-bound enzyme.) Mg^{2+} ion was not required either for retention or elution of enzyme.

Electrophoresis and isoelectric focusing--Discontinuous non-denaturing polyacrylamide gel electrophoresis was run according to the procedure of Laemmli (18), but without SDS, using a Bio-Rad mini slab-cell at 4°, and staining with Coomassie Blue or silver (19). Enzyme activies were assayed in unstained parallel channels cut into 2 mm slices as described previously (20). Sodium dodecyl sulfate (SDS) polyacrylamide gel electrophoresis (18) was run at room temperature, with 4% stacking gel and 12% separating gel. Horizontal isoelectric focusing was performed as described by Righetti (21), using a thermoelectrically-cooled Hoefer 950 Isobox electrofocusing unit at 4°, developed at a maximum of 2000 V constant power. Either 5% polyacrylamide or 1% agarose gel was cast on the hydrophilic surface of GelBond film, and contained 2% Ampholite, pH 3-10. A channel was cut into 2 mm slices which were soaked in water, and the pH was measured. Enzyme activity was located in gel slices assayed as above.

Molecular weights--The relative molecular mass (M_r) of the unproteolyzed enzyme was determined by sedimentation equilibrium at 4° in a Beckman Airfuge by the method of Pollet (22), modified as described previously (23). Either bovine serum albumin or Dextran T-40 was added (5 mg/ml) to the dCyd kinase samples to stabilize the density gradients, and glycerol was added to standard tubes to equal its concentration (6.7%) in the diluted enzyme samples. Ten successive 10-ul samples withdrawn from the meniscus of each tube were assayed for enzyme activity or protein content. Molecular weights were also estimated by the observing the effect of polyacrylamide gel concentration (8, 10, 12 and 15%) on electrophoretic mobilities of native proteins (24). Standard proteins included ß-lactoglobulin, carbonic anhydrase, ovalbumin and bovine serum albumin.

RESULTS

Purification of deoxycytidine kinase--Depending on the sample load applied to the dCp_4A-Sepharose affinity column, from 13 to 60% of the dCyd kinase activity applied was recovered in the fraction eluted by its end-product, dCTP, while the amount of activity in the runthrough fraction also increased in proportion to the amount of sample applied. A typical application of 750 mg of protein resulted in recovery of 16-20% of the activity, with a specific activity of 21 $nmol \cdot min^{-1} \cdot mg^{-1}$ (corrected for inhibition by dCTP). This activity was eluted biospecifically in 1-2 column volumes of dCTP (after overnight equilibration), whereas 10 column-volumes of ATP and salt did not displace it from the column. Therefore, enzyme interaction with the column was probably not due to ion-exchange or nonspecific nucleotide interactions with the phosphate-donor site of the enzyme. A mixture of dCyd and ATP was considerably less effective than dCTP as an eluent. Columns were used repeatedly over a period of a year or more, with only a gradual deterioration of performance being noted.

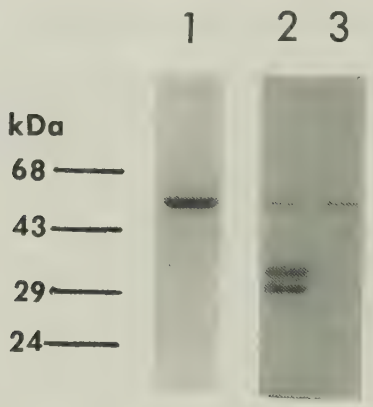

Figure 1. SDS-polyacrylamide gel electrophoresis of dCyd kinase purified with and without protease inhibitors. Lane 1, kinase purified with protease inhibitors; Lane 2, kinase purified without protease inhibitors; Lane 3, diluted kinase purified with protease inhibitors. Arrows denote R_fs of molecular weight marker proteins (Sigma).

Enzyme purity and subunit molecular weight--Judging from the single band obtained with the affinity-purified enzyme in SDS-polyacrylamide gel electrophoresis (Figure 1, lane 1), this preparation was virtually homogeneous, with an M_r of 52,000 ± 2000 for the denatured polypeptide. Only one band of protein was observed upon electrophoresis in nondenaturing gels as well. Assurance that the stained band was, in fact, the enzyme was provided by activity assays in gel slices from a parallel channel. A series of such assays revealed the congruent migration of activity and the protein band at four concentrations of acrylamide monomer. Had the protein bearing the activity and the protein yielding the stained band been different molecular species, they could have been expected to diverge as the gel concentration was changed (24). Since they did not, and since only one band was detected by either procedure, we can conclude that the enzyme was practically homogeneous.

Molecular weight of native enzyme--Sedimentation equilibrium determinations (22), carried out with two batches of dCyd kinase prepared in the presence of protease inhibitors, yielded an average molecular weight of 59,300 ± 3700 for the native protein, assuming a partial specific volume of 0.725. An identical value was obtained from the mobilities of the enzyme activity after electrophoresis in polyacrylamide gels of various concentrations (24), even though the latter determination is affected by the shape as well as the mass of the molecule. Although the M_r estimated for the native enzyme is somewhat larger than the 52,000 value determined for the denatured polypeptide, it seems clear that this enzyme consists of a single polypeptide chain.

Isoelectric pH--Isoelectric focusing of the pure enzyme on a flat-bed polyacrylamide gel system yielded a single peak of activity centered on a pI value of 6.1 ± 0.1. The presence of a slight shoulder on the high-pH side of the peak suggests that a minor polymorphic form of this protein may be present.

Specificity--The pure protein retained the ability to phosphorylate dAdo and dGuo, but dCyd is clearly the preferred substrate in terms of its apparent K_m and efficiency ratio, as may be seen in Table I. Potential phosphate

Table I
SUBSTRATE SPECIFICITY OF HUMAN DEOXYCYTIDINE KINASE

Nucleoside	K_m(app) (uM)	V_{max} ($nmol \cdot min^{-1} \cdot mg^{-1}$)	Efficiency Ratio (V_{max}/K_m)*
dCyd	3.3	21	6400
dAdo	890	41	46
dGuo	640	28	44

*K_m expressed in mM units.

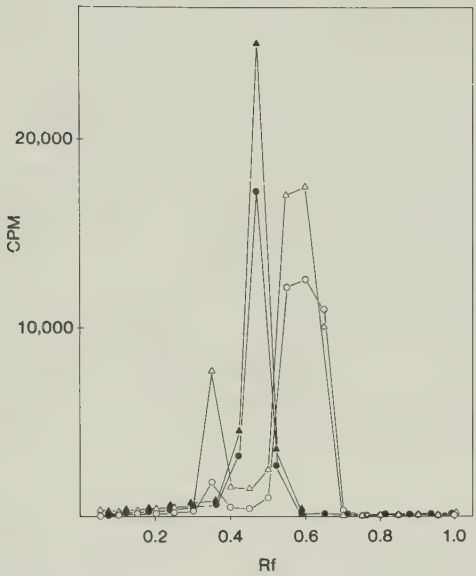

Figure 2. Non-denaturing polyacrylamide gel electrophoresis of parental and proteolyzed dCyd and dAdo kinase. Assays were performed on gel slices from an unstained adjacent channel. The acrylamide monomer concentration was 12%.

●, parental dCyd kinase; ▲, parental dAdo kinase; o, proteolyzed dCyd kinase; Δ, proteolyzed dAdo kinase.

donors were also compared, each at 10 mM (with 12 mM $MgCl_2$). Relative rates were: ATP, 100; GTP, 61; dGTP, 59; dTTP, 37; CTP, 24; dATP, 23; UTP, 6; and dCTP, 0. These nucleotides were used straight from the bottle without any repurification, so it is possible that the relatively low activity seen with UTP could have been due to an inhibitory level of UDP (12). These patterns of specificity are similar to those seen with other human deoxycytidine kinase preparations (8, 10), and it seems highly likely that the purine deoxynucleoside kinase activities are inseparably associated with the dCyd kinase protein.

Conditional proteolytic modification during purification--Enzyme purified in the absence of protease inhibitors showed evidence of substantial proteolysis during affinity chromatography, with the parental (presumably unproteolyzed) 52 kilodalton band giving place to bands of 30 kDa and 33 kDa in SDS electrophoretic gels. Figure 1 (Lane 2) shows very clearly that nearly all of the parental protein in the eluate was replaced by two smaller fragments staining with roughly equal intensity. Lane 3 contains diluted parental protein, which is identical in size to the residual minor band of the proteolyzed fraction. The discrete character of the proteolyzed bands and the complete absence of smearing below the parental band make it appear likely that the 30 and 33 kDa bands are the result of a discrete cleavage event, rather than being due to progressive proteolysis of the 52 kDa polypeptide. No smaller fragment was detectable, either by Coomassie Blue or silver staining.

The proteolyzed enzyme retained activity despite altered molecular properties, but that activity was labile and was soon lost. The electrophoretic R_f of the proteolyzed enzyme activity in nondenaturing gels shifted to about 0.60 (Figure 2), compared with 0.47 for the native enzyme run under the same conditions. A less active minor component was also seen at R_f 0.35, corresponding to a barely-detectable band on the stained gel (not shown). The increased R_f after proteolysis is presumed to be due to a reduced molecular mass, but activity losses prevented the completion of molecular weight determinations. Figure 2 also shows that, for both the parental and proteolyzed enzyme, dAdo kinase activity is exactly congruent with dCyd kinase activity, as would be expected if both substrates were phosphorylated by the same protein in each fraction. However, it should not necessarily be inferred from this figure that the ratio of dCyd/dAdo kinase is constant; since the assay of gel slices extended over a number of hours, differential loss of enzyme activities could have occurred, so the radioactivities plotted should be viewed in

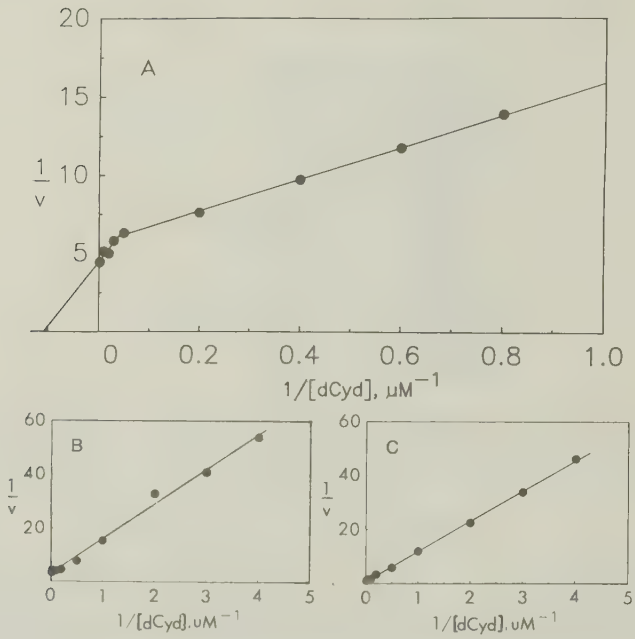

Figure 3. Lineweaver-Burk kinetics of mixture of parental and proteolyzed dCyd kinase. Each 80 ul reaction mixture contained 0.19 ug parental enzyme and/or 0.16 ug proteolyzed enzyme. ATP was 10 mM and $MgCl_2$ was 12 mM.

A. Mixture of parental and proteolyzed enzyme proteins.
(The two slopes were individually fitted by computer.)
B. Parental protein fraction only.
C. Proteolyzed fraction only.

qualitative rather than quantitative terms. The results of comparative isoelectric focusing were less dramatic, in that the principal pI appears to have shifted only slightly in the proteolyzed sample, from pH 6.1 to 6.2 (results not shown). Within the range of experimental error, this pI is unchanged. However, a minor peak was detected at pH 6.9-7.0.

Kinetic effects of proteolysis--We wondered whether a mixture of the parental and proteolyzed enzyme might account for the non-linear kinetics often observed with dCyd kinase. Although other human leukemic cell extracts studied in this laboratory have yielded such broken line kinetics (unpublished work), with this ALL cell preparation we did not succeed in trapping the optimum blend of molecular species which would show this most clearly. Therefore, we mixed approximately equal amounts of proteolyzed and unproteolyzed protein, with the kinetic results shown in Figure 3. Apparent K_m values of 1.8 and 9.3 uM were obtained for dCyd from the slopes of this plot, 7A. Individually (7B & C), each preparation yielded a straight line, but the proteolyzed enzyme appeared to have a significantly larger K_m^{app} (13 uM, compared with 3.3 uM for the parental enzyme).

DISCUSSION

We have described a simple and efficient two-step method for isolating apparently homogeneous deoxycytidine kinase protein by affinity chromatography. It is believed to be the first time an affinity ligand of this degree specificity has been applied to the purification of dCyd kinase from mammalian cytosol. Ligands based on structural analogs of nucleoside triphosphates, including Blue Sepharose, have been useful but not completely selective (8, 10, 25). On the other hand, most modifications of the substrate towards which the enzyme is most specific--the deoxynucleoside--drastically interfere with binding (26).

The enzyme has a small apparent K_m for dCyd, but exhibits much weaker affinities for dAdo and dGuo. If the crude leukemia cell extract should also contain low-K_m versions of dAdo and dGuo kinase activities, as have been reported in T-lymphoblasts (6), they were not recovered from the dCp_4A-Sepharose column. Perhaps the dAp_4A-Sepharose bisubstrate medium (14) would be more specific for this putative isoenzyme.

The discovery that proteolysis can occur on the affinity column--when the enzyme protein is very dilute--highlights the very important concept that, unless suitable precautions are taken, an enzyme isolated from human leukocytes may be a modified protein. Fortunately, a mixture of simple chemical inhibitors appeared to completely eliminate this effect. A similar proteolytic phenomenon was reported for calf thymus terminal deoxynucleotidyl transferase (27, 28). Crude thymus extracts were found to contain 58 and 44 kDa active enzyme peptides, in addition to the 32 kDa peptide species originally isolated as terminal transferase, and it was suggested that the alpha and beta subunits reported in the 32 kDa preparation may have arisen by proteolysis of the 58 kDa monomeric peptide (28). Evidence has also been cited recently that human DNA polymerase δ is modified during isolation from placental extracts (29). By analogy, it seems quite possible that the T-cell specific kinase reported as having a molecular weight of 26.5 kDa, (30), may have been a proteolyzed fraction, with corresponding changes in its kinetic properties, as well.

The proteolysis we have observed appears to have been a discrete cleavage producing two fragments of unequal size. SDS-gel electrophoresis revealed a parental polypeptide unit of about 52 kDa, which is comparable to the sum of the fragments and to the molecular weight of the native protein. These results are in agreement with the other estimates of the M_r of human dCyd kinase, which range from 53-56 kDa (9, 10, 30) to 68 kDa (31).

The kinetic pattern we obtained with a synthetic mixture of parental and proteolyzed proteins bears a striking resemblance to results obtained with dCyd kinase isolated without protease inhibitors from other human T-lymphocytic cells (2, 8), and from calf thymus dCyd kinase (12, 13). There seems to be a distinct possibility, therefore, that limited proteolysis of the kinase may account for the non-linear kinetics obtained in several cases. Further, if the modified protein were the form of the enzyme isolated, the K_m values and other physical properties reported might be subject to error. While we can minimize this possibility by the judicious use of protease inhibitors, we will not be certain that even the 52 kDa polypeptide is unmodified until its terminal sequences are compared with the corresponding genetic sequences.

Acknowledgement. This work was supported in part by National Science Foundation Grant DMB-8416134, Ohio Cancer Research Associates Grant OCRA-88-02-05 and National Institutes of Health Grant P30CA16058.

REFERENCES

1. Verhoef, V., Sarup, J. and Fridland, A. (1981) Cancer Res. **41**, 4478-4483.
2. Hershfield, M. S., Fetter, J. E., Small, W. C., Bagnara, A. S., Williams, S. R., Ullman, B., Martin, D. W., Jr., Wasson, D. B. and Carson, D. A. (1982) J. Biol. Chem. **257**, 6380-6386.
3. Bhalla, K., Nayak, R. and Grant, S. (1984) Cancer Res. **44**, 5029-5037.
4. Carson, D. A., Kaye, J. and Seegmiller, J. E. (1978) J. Immunol. **121**, 1726-1731.
5. Ullman, B., Gudas, L. J., Clift, S. M. and Martin, D. W. (1979) Proc. Natl. Acad. Sci. U.S.A. **76**, 1074-1078.
6. Yamada, Y., Goto, H., and Ogasawara, N. (1983) Biochim. Biophys. Acta **761**, 34-40.
7. Hurley, M. C., Palella, T. D. and Fox, I. H. (1983) J. Biol. Chem. **258**, 15021-15027.
8. Sarup, J. C., and Fridland, A. (1987) Biochemistry, **26**, 590-597.
9. Osborne, W. R. A. (1986) Proc. Natl. Acad. Sci. USA **83**, 4030-4034.
10. Bohman, C. and Eriksson, S. (1988) Biochemistry **27**, 4258-4265.
11. Yamada, Y., Goto, H. and Ogasawara (1983) FEBS Letters **157**, 51-53.
12. Ives, D. H. and Durham, J. P., (1970) J. Biol. Chem. **245**, 2285-2294.
13. Kozai, Y., Sonoda, S., Kobayashi, S. and Sugino, Y. (1972) J. Biochem. 71, 485-496.
14. Ikeda, S., and Ives, D. H. (1985) J. Biol. Chem. **260**, 12659-12664.
15. Ives, D. H. and Wang, S.-M. (1978) in Methods in Enzymology (Hoffee, P. A. and Jones, M. E., Eds.) Vol. 51, pp. 337-345.
16. Ives, D. H. (1984) Anal. Biochem. **136**, 416-420.
17. Bradford, M. (1978) Anal. Biochem. **72**, 248-254.
18. Laemmli, U. K. (1970) Nature, **227**, 680-685.
19. Wray, W., Boulikas, T., Wray, V. P., and Hancock, R. (1981) Anal. Biochem. **118**, 197-203.
20. Gower, W. R., Jr., Carr, M. C. and Ives, D. H. (1979) J. Biol. Chem. **254**, 2180-2183.

21. Righetti, P. G. (1982) Isoelectric Focusing: Theory, Methodology and Application pp.174-178, Elsevier Biomedical Press, New York.
22. Pollet, R. J., Haase, B. A. and Standaert, M. L. (1979) J. Biol. Chem. **254**, 30-33.
23. Chakravarty, R., Ikeda, S. and Ives, D.H. (1984) Biochem. **23**, 6235-6240.
24. Hedrick, J. L. and Smith, A. J. (1968) Arch. Biochem. Biophys. **126**, 155-164.
25. Baxter, A., Currie, L. M. and Durham, J.P. (1978) Biochem. J. **173**, 1005-1008.
26. Ikeda, S., Park, I., Gardner, P. and Ives, D. H. (1984) Biochemistry **23**, 1914-1921.
27. Deibel, M. R., Jr. and Coleman, M. S. (1980) Arch. Biochem. Biophys. **202**, 414-419.
28. Chang, L. M. S., Plevani, P. and Bollum, F. J. (1982) J. Biol. Chem. **257**, 5700-5706.
29. Lee, M. Y. W. T (1988) Biochemistry **27**, 5188-5193.
30. Yamada, Y., Goto, H. and Ogasawara, N. (1985) Int. J. Biochem. **17**, 425-428.
31. Coleman, C. N., Stoller, R. G., Drake, J. C. and Chabner, B. A. (1975) Blood, **46**, 791-803

Vol. 156, No. 1, 1988 BIOCHEMICAL AND BIOPHYSICAL RESEARCH COMMUNICATIONS
October 14, 1988 Pages 99-107

A Consensus Sequence in the N-terminus of Exported Proteins: Resemblance with Metal Binding Domains and Implications in Protein Translocation Across Membranes

Panagiotis A. Tsonis, Janusz M. Sowadski* and Paul F. Goetinck

La Jolla Cancer Research Foundation,
Cancer Research Center, 10901 N. Torrey Pines Road,
La Jolla, CA 92037

*Department of Biology,
University of California, San Diego, La Jolla, CA 92093

Received July 7, 1988

SUMMARY By analyzing and comparing the N-terminus of several exported proteins we identified two consensus sequences that resemble metal binding domains. The consensus sequences are part of the signal peptide and part of the adjacent sequences of the mature protein. Three-dimensional modelling of one such domain suggests a conformation with implication in signal peptide insertion.
© 1988 Academic Press, Inc.

In order for proteins to be secreted they have to be translocated across membranes. For eukaryotes the translocation is across the endoplasmic reticulum and for bacteria it is across the cell membrane. The actual process of translocation across membranes is preceeded by a recognition step which, in eukaryotes, involves, in addition to the protein that is to be transported, a soluble receptor known as the signal recognition particle and a membrane receptor known as the docking protein (1,2). The signal recognition particle is made up of a 7S RNA and six different polypeptides (3). A third component, the signal sequence receptor, may also play a role in this process (4). The

0006-291X/88 $1.50
Copyright © 1988 by Academic Press, Inc.
All rights of reproduction in any form reserved.

nascent protein that is to be secreted contains information that is instrumental for either its targeting to or its translocoation across the ER membrane. There is a great deal of evidence that indicates that this information is contained in the signal peptide, the N-terminus of the primary translation product of secretory proteins that is proteolytically removed to form the mature protein (1,2). Signal peptides range in size from 15 to 30 amino acids and although they share as a common characteristic a centrally located stretch of hydrophobic amino acids, their primary sequences show no homologies that might suggest how they are recognized in the targeting or the translocoation process. Whereas the signal peptide is essential for export of proteins, it is not known if any additional information for this process resides in the mature protein.

In an analysis of the sequence of the primary translation product of cartilage link protein (5) we identified a sequence that resembles the consensus sequence for the metal binding domains of the transcription factor IIIA of Xenopus laevis (6). This sequence of link protein encompasses the signal peptide and the N-terminus of the mature protein. A search of the protein sequence database of the National Biomedical Research Foundation (Georgetown University Medical Center, Washington D.C., 4028 sequences, 963031 residues) indicated that such a sequence involving the signal peptide is not restricted to link protein. Indeed we found such a sequence to be present in the N-termini of the primary translation product of 53 proteins.

Two very similar consensus sequences could be identified. These are: α-X_{0-4}-α-X_{5-17}-α-X_{1-5}-α and α-X_{5-21}-α-X_{1-5}-α, where α is a cysteine or a histidine and X is any amino acid. These sequences resemble the consensus sequence C-X_4-C-X_{12}-H-X_3-H which makes up the metal binding domains of the Xenopus transcription factor IIIA (TFIIIA) (6-10). The alignment of these three consensus sequences is shown in Figure 1. TFIIIA which binds to 5SRNA genes and their transcripts contains 9 homologous repeats of this domain and the binding of Zn^{2+} to these domains has been demonstrated. In those instances where the Zn^{2+} binding activity of such domains has been demonstrated it has

Consensus	(TFIIIA)	$C - X_4 - C - X_{12} - H - X_3 - H$
Consensus I		$\alpha - X_{0-4} - \alpha - X_{5-17} - \alpha - X_{1-5} - \alpha$
Consensus II		$\alpha - X_{5-21} - \alpha - X_{1-5} - \alpha$

Fig. 1. Alignment of the two consensus sequences, I and II, found in the N-terminus, showing a resemblance with the metal binding domain of the TFIIIA. α15, a Cys or His and X any amino acid.

been shown to be determined by the arrangement of the Cys and His ligands rather than by the primary sequence of the protein (6). In Figure 2 we present the sequences of the proteins according to the pattern of alignment presented in Figure 1. For each of the two patterns we list first the proteins whose signal peptide cleavage site is known, followed by those whose cleavage site is not known. Since we have no evidence that the sequences we describe bind metals we will, based on their structural motif, refer to them as putative metal binding domains. Of the 53 N-terminal sequences listed, 27 and 26 follow the type I and the type II consensus sequences respectively. Forty-nine of the sequences are from eukaryotes and 4 from prokaryotes. Of the eukaryotic sequences, 40 are from vertebrates, 4 from invertebrates and 5 from plants. The signal peptide cleavage site is known for ten of the sequences that follow the type I consensus sequence. Seven of these cleavage sites are situated on the N-terminal side of the first α position and 3 are situated between the second and the third α positions. Of the 15 known signal peptide cleavage sites in the sequences that follow the type II consensus sequence, three are situated on the N-terminal side of the first α position, 11 are located between the first and the second α positions and one is located on the C-terminal side of the third α position. Finally, the two most C-terminally located α positions for the type I consensus sequences are most often Cys and Cys (16 out of 27) whereas those for the type II consensus sequences are most often His and His (23 out of 26). The significance of the above observations is not known at the present time.

						α	X_{0-4}	α	X_{5-17}	α	X_{1-5}	α
consensus I	link protein-chicken	9			LISV	C	WAEP	H	PDNSSLE	H	ERII	H IQE
	vasotocin-amphibian	-11				C	FL	C	LLALSSA	C	YIQN	C
	mesotonin-amphibian	1				C	YIQN	C	PIGGKRSVIDFMDVRK	C	IP	C
	vasopresin-amphibian	1				C	YIQN	C	PRGGKRATSDMLRQ	C	LP	C
	oxytosin-amphibian	1				C	YIQN	C	PLGGKRAALDLDMRK	C	LP	C
	fibronectin receptor β-subunit-human	16				C		C	VFAQTDENPCLKANAKS	C	GE	C
	prolactin-human	29			LPI	C	GGAAR	C	QVTLRDLFDRAVVLS	H	YI	H
	purothionin A-I wheat	1			KS	C		C	KSTLGRN	C	YNL	C
	purothionin II-precursor-barley	19			KS	C		C	RSTLGRN	C	YNL	C
	vitronectin precursor-human	20			DQGS	C	KGR	C	TEGFNVDKKCQ	C	DEL	C
	superoxide dismutase-photobacterium	44	F		HI	H	QNGS	C	ASSEKDGKVVLGGAAGG	H	YDPE	H
	bromelain inhibitor-pineapple	14	Y		K	C	Y	C	ADTYSD	C	PGF	C
	follitropin β-human	17				C	RF	C	LTINTTW	C	AGY	C
	trypsin inhibitor-mongolian snake	15				C	W	C	ISRGYLCG	C	MP	C
	keratin feather I-chicken	3	F		DL	C	RP	C	GPTPLANS	C	EP	C
	somatomedin B-human	6			DKK	C	Q	C	DLCSYYQSN	C	T	C
	large γ-3 heavy chain disease protein -human	24				C	PR	C	PEPKSCDTPPP	C	PR	C
	agglutinin isolectin-2 wheat	17				C		C	SQYGYCGMGGDY	C	GKG	C
	vasopresin-meurophysin precursor -bovine	17	F		ISA	C	YFQN	C	PRGGKRAMSDLELRQ	C	LP	C
	creatin kinase M chain chicken	3	F		SST	H	NK	H	KLKFSAEEEFFPDLSK	H	NN	H
	phopholipase A2 eastern cotton moth	24	Y		GFCN	C	GWG	H	RGQPKDATDRC	C	FV	H
	urokinase-type plasminogen activator precursor-pig	7				C	LSL	C	VLVVSDSKGS	H	EL	H
	glutelin 5-maize endosperm	2				H	TSGG	C	GSQPPPPVHLPPPV	H	LPPPV	H
	transaminase β-E. coli	37	F		EGIR	C	YDS	H	KGPVVFRHRE	H	QRL	H
	acrosin inhibitor A_1-(pig bovine)	32	Y		ANP	C	IF	C	SEKGLRNQKFDFG	H	WG	H
	acrosin-inhibitor I-bovine	36	Y		SNE	C	TF	C	NEKMNNDADI	H	FN	H
	cysteine rich intestinal protein-rat	28				C	LK	C	EKCGKTLTSGG	H	AE	H
						■	X_{5-21}			α	X_{1-5}	α
consensus II	L-CAM-chicken	-6	F		PK	H	DPGFLRRQKRDWVIPPIS			C	LEN	H
	chorioamammotropin precursor-human	13	F		ALL	C	LPWLQEAGAVQTVPLSRLFD			H	AMLQA	H
	α-1 antitrypsin precursor-human	15			LC	C	LVPVSLAEDPQGDAAQKTDTS			H	HDQD	H
	parathyroid hormmone precursor -bovine	18				C	FLARSDGKSVKKRAVSEIQFM			H	NLGK	H
	growth hormone-rat	-14	F		SLL	C	LLWPQEAGALPLMPLSSLFANAVLRAQ			H	L	H
	colony stimmulating factor-mouse	-13			LLLV	C	LLMSRSIAKGVSG			H	CS	H
	as1 casein-bovine	-8				C	LVAVALARPK			H	PIK	H
	aminodiphosphoribosyl-tranferase-bacilus subtilis	8			LNEE	C	GVFGIWGHEEAPQITYYGL			H	SLQ	H
	haptoglobin-1-human	5			NDVTDIADDG	C	PKPPEIA			H	GYVE	H
	prothrombin precursor human	1			QLPG	C	LALAALCSLV			H	SQ	H 36
	nerve growth factor receptor-rat	1			KET	C	STGLYTHSGEC			C	KA	C
	angiotensinogen precursor-human	23				C	LLAWAGLAAGDRVYI			H	PF	H
	angiotensinogen precursor-rat	13	F			C	ILTWVSLTAGDRVYI			H	PF	H
	urinary protein-human	-13			LLLV	C	LLASRITEEVSEYCS			H	MIGSG	H
	parathyroid hormone related protein-human	-14				C	GRSVEGLSRRLKRAVSE			H	QLL	H
	azurin - A. denitrificans	26				C	KQFTV			H	LK	H
	factor XII-human	28				C	HFPFQY			H	RQLY	H
	large heavy chain V-III human dob.	22				C	AASGFNF			H	EYNM	H
	large chain V region mouse S107A					C	TASESLYSSK			H	KV	H
	hemoglobin α-chain nile crocodile	34				C	AYPQTKIYFP			H	FDLS	H
	cygnin-swan	5	Y			C	PKVGY			C	SSK	C
	specific body pattern-fruit fly	3			LEDR	C	SPQSAPSPITLQMQ			H	LH	H
	myohemerythrin -T zostericola	33	F			C	DIRDNSAPNLATLVKVTTN			H	FT	H
	nerve growth factor β-chain precursor-mouse	1			ML	C	LKPVKLGSLEVG			H	GQ	H
	superoxide dismutase-horse	6				C	VLKGDGPV			H	GVI	H
	chymotrypsin II-European hornet	25				C	GGSISKRYVLTAAHCLVGKSK			H	QVTV	H

The finding of the presence of putative metal binding domains near or nvolving the signal peptide, suggests a mechanism that might provide a unique onformation for the N-termini of proteins that could be important in signal ecognition and in the translocation process across membranes. An examination f the hydropathy profiles of the sequences in the N-termini of the proteins isted in Table 1 indicated a hydrophobic-hydrophilic-hydrophobic pattern. The ydropathy profiles and secondary structure prediction of link protein, urinary rotein and angiotensinogen are presented as examples in Figure 3. Similar tructural features have been described in zinc binding enzymes such as Cu-Zn uperoxide dismutase and alkaline phosphatase whose three dimensional structure s known. In these enzymes a β-strand motif involving hydrophobic regions is he common structural element that provides the ligand for the zinc atom. istidines are the invariant ligands although the number of histidines binding he zinc atoms may vary (11-13). Based on the stuctural features of these nzymes we aligned and compared the N-terminal signal sequence of link protein ith the sequences within the region of the hydrophobic β-strand-hydrophilic oop-- hydrophobic β-strand motif that provides the histidine ligands to the inc atoms in the three dimensional structure of alkaline phosphatases of E. oli (Fig. 4). It is apparent from Figure 3 that the two highly homologous -strand regions of the alkaline phosphatases can be aligned with the two ydrophobic portions of the N-terminal region of link protein. Conserved igands His-372 and His-412 of the E. coli alkaline phosphatase and correspon- ling ligands of the other alkaline phosphatases can be aligned with His-18 and is-31 of link protein. Using the coordinates of alkaline phosphatase and the bove alignment, we built a three dimensional model of the N-terminal sequence f link protein. The resulting model, presented in Figure 5, has some important eatures. First, the antiparallel β-strands form a hydrophobic twisted surface.

Fig. 2. N-terminus of proteins containing putative metal-binding domains. The sequences of the proteins are arranged according to the two consensus sequences presented in Fig. 1. Numbers correspond to the first amino acid of the sequence. The number preceded with the minus sign represents cases where numbering of the reported sequences starts after the peptidase cleavage. The arrows indicate the cleavage site of the signal peptide. Standard single-letter amino acide abbreviations are used.

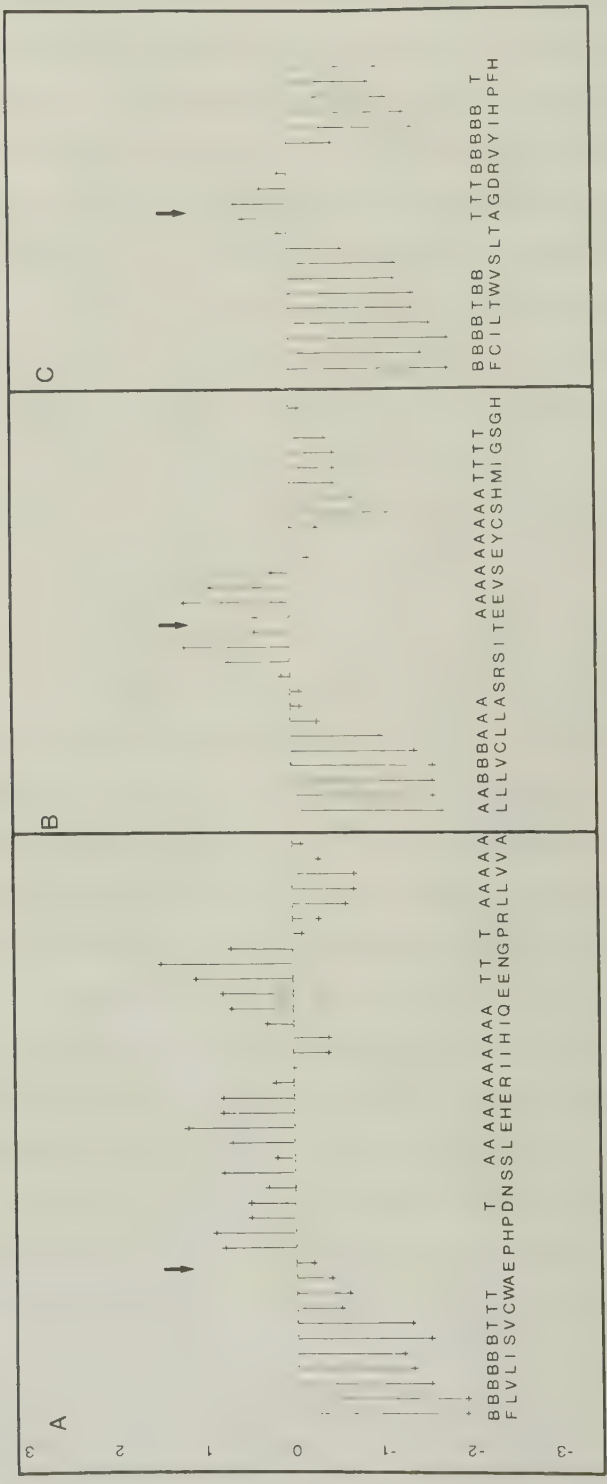

Fig. 3. Hydropathy profiles determined according to the algorithm of Hopp and Woods (14), of the putative metal binding domains found in the N-terminus of link protein (A), urinary protein (B), and rat angiotensinogen (C). The sequences and the secondary structure prediction using the algorithm of Garnier et al. (15) are shown. The arrows indicate the cleavage sites by signal peptidase.

ß strand loop ß strand

E.	362	T L V I V T A D - - H A H	412 H T G S Q - - L R - I A A Y
P.	350	T L S L V T A D - H S H	432 H A G E D - V A - V F A R
L.	354	T L T V V T A D - - H S H	437 H G G E D V A - V F S K
Link.	6	F L V L I S V C W A E P H P D N S S L E H E R I I H I Q E E N G P R L L V V A	

Fig. 4. Sequence alignment of alkaline phosphatases and link protein. Alkaline phosphatase from E. coli whose structure has been solved at 2.8Å resolution contains two closely spaced zinc atoms. The zinc metal doublet is located between N- and C-termini of two antiparallel β-strands. These two antiparallel strands provide three out of four histidine ligands. Alignment of the sequence of the β-strand-loop-β-strand motif is presented for the alkaline phosphatases of E. coli (E) (16), kidney, liver and bone (L) (17) and placental (P) (18). Below is the putative metal binding domain of link protein. The alignment is good with the first β-strand, but less pronounced with the second. Position of cleavage site by signal peptidease is identified with a black dot.

Fig. 5. The three dimensional model of the putative metal binding domain of link protein (color code: blue-histidines, yellow-hydrophobic residues, purple-signal peptidase cleavage site, red-cysteine). The model is based on the coordinates of alkaline phosphatase β-strand-loop-β strand motif and on the sequence alignment with link protein as presented in Fig. 4. His 372 and His 412 of E. coli alkaline phosphatase has been aligned in this model with His 18 and His 31 of link protein. The third histidine ligand, His 26, is proposed to be located in the loop. The link protein loop is shorter than the loop of the alkaline phosphatase family. In the model, the signal peptidase cleavage site is located in the loop close to one of the histidine ligands.

Second, a zinc atom, if present, could lie in the loop formed by the two antiparallel β-strands. Third, the sequence known to be cleaved by the signal peptidase lies in the upper portion within the loop. Fourth, the length of the signal peptide with the proposed conformation might be sufficient to span the membrane (30A) with the N- and C-termini facing the cytoplasm. Finally, we would like to suggest that the putative metal binding domains involving the signal peptides may have nucleic acid binding properties that could allow them to be recognized by the 7S RNA component of the signal recognition particle. The above suggestion is plausible since TFIIIA, which contains homologous zinc binding domains, is known to bind to transcripts of the 5S RNA gene (6-10). The identification of a putative metal binding domain with its possible resulting tertiary structure in the N-termini of several exported proteins described in the present communication may be useful in setting up new experimental approaches to elucidate the mechanism of protein translocation across cell membranes.

ACKNOWLEDGEMENTS

We are grateful to Dr. Van Beveren for advice with the searches, to Jim Cairns for assistance in the modelling studies and to Cindy Clatterbuck for manuscript preparation. This work was supported by grant HD22016 from the National Institute of Child Health and Human Development. P.A.T. is a recipient of an Arthritis Investigator Award.

REFERENCES

1. Walter, P. and Lingappa, V.R. (1986). Ann. Rev. Cell. Biol. 2, 499.
2. Wickner, W.T. and Lodish, H.F. (1985) Science 400-407.
3. Walter, P. and Blöbel, G. (1982). Nature 299, 691.
4. Wiedmann, M., Kurzchalia, T.V., Hartmann, E. and Rapoport, T.A. (1987) Nature 328:830-833.
5. Deák, F. et al. (1986). Proc. Natl. Acad. Sci. USA 83, 3766.
6. Diakum, G.D., Fairall, L. and Klug, A. (1986). Nature 324, 698.
7. Miller, J., McLachland, A.D. and Klug, A. (1985). EMBO J. 4, 1609.
8. Brown, R.S., Sander, C. and Argos, P. (1985). FEBS Lett. 186, 271.
9. Fairall, L., Rhodes, D. and Klug, A. (1986). J. Mol. Biol. 192, 577.
10. Hanas, J.S., Hazuda, D.J., Bogenhagen, D.F., Wu, F.Y.-H. and Wu,. C.-W. (1983). J. Biol. Chem. 258, 1420.
11. Argos, P., Garavito, R.M., Erentohoff, W., Rossmann, M.G., and Bränden. (1978). J. Mol. Biol. 126, 444.

12. Tainer, J.A., Getzaff, E.D., Beern, K.M., Richardson, J.S. and Richardson, D.C. (1982) J. Mol. Biol. 160, 181.
13. Sowadski, J.M., Handschumacher, M.D., Kristina-Murthy, H.M., Foster, B.A. and Wyckoff, H.W. (1985). J. Mol. Biol. 186, 417.
14. Hopp, T.P. and Woods, K.R. (1981). Proc. Natl. Acad. Sci. USA 78, 3824.
15. Garnier, J., Osguthorpoe, D.J. and Robson, B. (1978) J. Mol. Biol. 120, 97.
16. Bradshaw, R.A. et al. (1981). Proc. Natl. Acad. Sci. USA 78, 3473.
17. Weiss, M.J., et al. (1986). Proc. Natl. Acad. Sci. USA 83, 7182.
18. Millán, J.L. (1986). J. Biol. Chem. 261, 3112.
19. Lipscomb, W.N. (1983) Ann. Rev. Biochem. 52:17-34.

Vol. 156, No. 1, 1988 BIOCHEMICAL AND BIOPHYSICAL RESEARCH COMMUNICATIONS
October 14, 1988 Pages 108-115

MITOGENIC ACTIVITY IN OVINE UTERINE FLUIDS: CHARACTERIZATION OF A GROWTH FACTOR ACTIVITY WHICH SPECIFICALLY STIMULATES MYOBLAST PROLIFERATION[$]

R. Curtis Bird[*&], Frank F. Bartol[+], Harlow Daron[+], David A. Stringfellow[*], and M. Gatz Riddell[#]

Departments of Pathobiology[*] and Large Animal Surgery and Medicine[#], College of Veterinary Medicine, and Department of Animal and Dairy Sciences[+], Auburn University, Auburn, AL 36849

Received July 29, 1988

Fluids produced by the uterus of pregnant sheep (OUF-ovine uterine fluids) were assayed for mitogenic activity in a thymidine incorporation assay. A dose-dependent mitogenic activity was observed in OUF which exceeded that of adult ovine plasma or fetal bovine serum. Uterine fluids were capable of stimulating thymidine incorporation in mouse 3T3 fibroblasts, rat L6 myoblasts, ovine trophoblast-derived cells, HeLa S3 cells, and bovine aortic endothelial cells. The greatest stimulation was observed in L6 myoblasts. The name ovine uterine-derived growth factor (ovine UDGF) has been suggested for this activity. © 1988 Academic Press, Inc.

Regulation of proliferative activity in eukaryotic cells is dependent upon the actions of peptide growth factors. Growth factors have generated interest not only because of their role in normal growth (1) but also due to their implication in the development of the transformed phenotype (2,3). The discovery of shared homology between the epidermal growth factor receptor and the oncogene erb-B (4,5) as well as between platelet-derived growth factor and the sis oncogene (6,7) both support this contention.

Until recently little attention has been paid to the mitogenic activities present in fluids produced by maternal and fetal tissues during mammalian development. Although specific proteins have been identified in fluids from maternal (8-10) and embryonic tissues (9,13), little is known concerning the components which stimulate proliferation of fetal cells. The rapid

[$]Publication No. 2001, College of Veterinary Medicine, Auburn University. Supported by the Alabama NSF/EPSCoR Program in Molecular, Cellular and Developmental Biology (#RII-8610669), the state of Alabama Program for Genetic Engineering and Animal Health Research and an Auburn University Grant-in-Aid to C.B. (#85-94).

[&]Author to whom reprint requests and all correspondence should be addressed.

Abbreviations Used: HBS, Hepes-buffered saline, alpha-MEM, alpha modification of Eagle's minimum essential medium, OUF, ovine uterine fluid(s), FBS, fetal bovine serum, GFU, growth factor unit(s), TES, Tris-EDTA-SDS solution, FGF, fibroblast growth factor, SD, standard deviation.

0006-291X/88 $1.50
Copyright © 1988 by Academic Press, Inc.
All rights of reproduction in any form reserved.

proliferation of all tissues during early development suggests that fluids which emanate from the uterine lining and are absorbed by the fetus (9,14) are a likely source of growth factors.

The surgical technique of unilateral ligation of a single uterine horn of ewes allows collection of large volumes of concentrated uterine fluids produced by the endometrium (9,15). These fluids are normally absorbed by the fetal tissues and do not accumulate. Since the maternal side is surgically isolated by the ligature, the fluids which collect and any growth factors residing therein, must be of maternal origin. The large volume and high concentration of this material offer distinct advantages over the dilute products recovered by uterine flushing (15). We have characterized the mitogenic activity(s) found in ovine uterine fluids collected from unilaterally ligated uterine horns at a late stage of pregnancy.

MATERIALS AND METHODS

Cell Lines and Culture - The myoblast cell line, clone L6-5 derived from rat skeletal muscle, was obtained from C.P. Stanners (McGill University)(17) and was originally isolated by D. Yaffe (18). The HeLa S3 cell line of human epithelial carcinoma-derived cells and the mouse 3T3 fibroblasts were obtained from B.H. Sells (University of Guelph) (19). These three cell lines were grown in 25 cm^2 tissue culture flasks or 24-well plates (Corning) in alpha-MEM (Flow Laboratories) supplemented with 10% (v/v) fetal bovine serum (Flow) and the cultures were incubated at 37°C, 100% humidity and 5% CO_2 in air. All cell lines were passaged prior to attaining confluence by trypsinization and diluted 1:3 - 1:5 in fresh growth medium.

Primary cultures of aortic endothelial cells were isolated from bovine aortas by a modification of published procedures (20). Pieces of fresh descending thoracic aorta (approximately 5x5 cm) were obtained at slaughter, and the lumenal surfaces were rinsed 4 times in sterile HBS (10 mM HEPES, pH 7.2, 0.9% NaCl). The lumenal surface was digested with 1 mg/ml collagenase (Worthington, CLSII) in HBS containing 0.15 mg/ml $CaCl_2$ and 0.1 mg/ml $MgCl_2$ at 37°C for 30 min. The endothelial cells were gently scraped from the lumenal surface with a sterile Teflon spatula and rinsed in alpha-MEM containing 20% FBS. Cell suspensions were gently centrifuged for 2 min in a clinical centrifuge and resuspended in alpha-MEM with 20% FBS prior to plating in 25 cm^2 tissue culture flasks coated with sterile 0.1% (w/v) gelatin. Bovine aortic endothelial cells were transferred from coated flasks to uncoated flasks by passage 5. Cell line BA53-90d, used in this study, was derived from a 90 day bovine fetus. The cells were uniformly endothelial in morphology (cobblestone appearance at confluence) and were used between passages 25-35.

The OE-1 cell line was established from a preimplantation ovine embryo as previously described (21). Briefly, a single day 11 ovine embryo was cultured in HEPES-buffered Ham's F-10 medium (Gibco) supplemented with 10% (v/v) FBS, 110 ug/ml sodium pyruvate, and 100 ng/ml epidermal growth factor (Sigma). After 13 days in culture the embryo had attached and an explant growth originating from the trophectoderm covered an area approximately 0.2 cm^2 in the culture well. The explant was dispersed by trypsinization, and cells which grew as a monolayer were expanded through serial passage at dilutions of approximately 1:3. Sufficient numbers of cells were available for study by the 4th passage (25 cm^2 flasks). Cells used in this study were at the 6th to 13th passage.

Collection of Ovine Uterine Fluids - Uterine fluids were collected from the nonpregnant horn of ewes on gestational day 120 as previously described (15). The fluids were immediately divided into aliquots and stored at -70°C. Before use, the aliquotes were thawed, their protein concentration determined (22),

and they were diluted to 2.5 mg/ml total protein with HBS. Suspended particles were removed by centrifugation (14,000Xg, 2 min, 4°C), and the supernatant was sterilized by filtration through a 0.2 um filter (Schleicher & Schuell).

Growth Factor Assay - Growth of the cell lines was determined by the rate of ^{3}H-thymidine incorporation into acid precipitable material as previously described (23) with some modification (17). Each cell line was propagated in the appropriate growth medium and plated at approximately 50% confluence on 24-well tissue culture plates (Corning). The cells were then allowed to become quiescent in one of two ways: (1) allowed to grow to confluence and maintained without a change of medium for 5 days or (2) allowed to grow to confluence and the medium changed to alpha-MEM without serum supplement for 24 hr. At this time the medium was reduced to 150 ul conditioned medium per well, and the growth factor activity assay was conducted. A total of 100 ul of growth supplement and HBS was added to each well. Each plate included a titration of each test OUF (diluted to 2.5 mg/ml and sterilized by filtration) up to 20% (v/v), several negative control wells in which 100 ul of HBS was added, and a positive control titration of up to 20% (v/v) FBS. To each well was added 10 ul of HBS containing 2.5 uCi of ^{3}H-thymidine (10 uCi/ml final, New England Nuclear). The contents of the plates were mixed and incubated for approximately 24 hr at 37°C. The assays were stopped by removing the labeled medium, rinsing out each well with ice-cold HBS (400 ul/well) and lysing the cells with 80 ul/well of TES (10 mM Tris-HCl, pH 7.6, 1 mM Na_2EDTA, 1% w/v sodium dodecyl sulfate). Acid precipitable counts were determined for each lysate as previously described (17). The contents of each well were pipetted onto a Whatman 540 paper disc and allowed to dry. Discs were then batch precipitated and washed at room temperature, sequentially, in 300 ml/50 filters for 20 min, in 20%(w/v) and then 10%(w/v) trichloroacetic acid, absolute ethanol, diethyl-ether, and absolute ethanol and allowed to dry. The filters (including several blanks) were then counted in an LKB liquid scintillation counter in 5 ml of toluene-omnifluor (New England Nuclear). Each titration point was calculated as the mean of the CPMs from 2-4 wells less the mean CPMs obtained with the blank filters. The level of stimulation obtained in the 50 ul point in the FBS titration above the level observed for the HBS negative controls in each individual plate was defined as 2 GFU: ie. FBS was defined as containing 2 GFU in each assay as previously described (23).

Growth Factor Characterization - OUF samples were subjected to ultrafiltration (Amicon centricon microconcentrator) to retain native protein complexes of >30,000 daltons as per manufacturers specifications. OUF samples, diluted to 2.5 mg/ml and centrifuged 5 min at 10,000xg (4°C), were subsequently fractionated by centrifugation through the microconcentrator for up to 2 hr at 5,000xg (4°C) to collect the filtrate of less than 30,000 daltons. HBS was then added to the inverted device, and the whole assembly was recentrifuged to collect the greater than 30,000 dalton fraction off the filter at approximately the original concentration. Both fractions were tested to determine which contained the mitogenic activity.

RESULTS AND DISCUSSION

The amount of mitogenic activity in each OUF sample was determined by titration of the OUF in a growth factor assay based upon the incorporation of ^{3}H-thymidine into quiescent 3T3 cells (Fig.1). On each plate tested the diluted OUF were compared to a test titration of FBS (23). One growth factor unit was defined arbitrarily as 50% of the response of quiescent 3T3 cells to 50 ul of FBS (20% v/v) per 250 ul total of conditioned medium and supplementary HBS. In each case the response was found to be dose dependent.

Six different OUF and plasma from adult sheep were tested for growth factor activity in the thymidine incorporation assay (Table I). The mean GFU in OUF

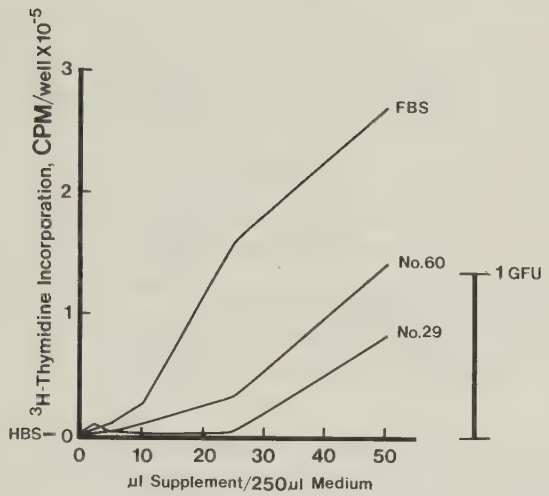

Figure 1: A representative growth factor activity assay including two independent OUF samples as well as both positive and negative controls. A serial titration of OUF samples No.29 and No.60 were tested against a titration of FBS positive and HBS negative controls for their ability to stimulate incorporation of thymidine over 24 hr in quiescent 3T3 cells. Calculation of growth factor unit (GFU) activity for this assay is shown. These two OUF samples were diluted 3.4X (No.29) and 3.1X (No.60) prior to testing, to bring them to a uniform 2.5 mg/ml total protein. SD for each time ranged between 1.5×10^2 and 6.08×10^4 cpm or an average SD of 22% of the mean at each time point.

ranged from 3.2-16.0 GFU/mg protein compared to 1.54 GFU/mg for FBS. In all cases the GFU in OUF were much higher than those found in plasma from adult sheep (0.88 GFU/mg protein) ranging between 3.6 and 18.2 times higher. This suggests that even though OUF contain detectable levels of plasma proteins by electrophoretic analysis (8,24), plasma proteins do not seem to be the source of the growth factor activity observed. Because plasma did contain low GFU activity it is possible that some of the observed activity occurred because serum transferrin or other serum-derived growth factors, while being

TABLE 1

GROWTH FACTOR ACTIVITY IN OVINE UTERINE FLUIDS

OUF	PROTEIN CONC. (mg/ml)	VOLUME RECOVERED (ml)	GROWTH FACTOR ACTIVITY CONC. (GFU/ml)	TOTAL (GFUx10^{-3})	SPECIFIC ACTIVITY (GFU/mg +/-SD)[a]
A	8.4	653	134	87.8	16.0 +/-2.0 (5)
B	7.7	273	105	28.6	13.6 +/-1.6 (5)
C	26.6	677	98	66.3	3.68 +/- 0 (2)
D	73.2	8	252	2.0	3.44 +/-0.05 (3)
E	39.1	ND	428	ND	10.96 +/-0.53 (2)
F	27.3	ND	87	ND	3.2 (1)
PLASMA	64.4	NA	57	NA	0.88 (1)
FBS	26.0	NA	40[b]	NA	1.54

a Values are the mean and SD of n determinations, where n is given in parentheses.

b The GFU/ml for FBS is calculated from the arbitrarily defined value of 2.0 GFU/50 ul FBS therefore no SD is given.

ND - not determined, NA - not applicable, A - OUF No.29, B - OUF No.60.

transported by the uterine lining, undergo significant concentration (25). It seems more likely, however, that most of the observed activity emanates from the uterine lining which has been shown to synthesize a variety of secreted proteins in culture (8).

By definition, FBS contains 1.54 GFU/mg protein in this assay (Table I). When the dilution factor for each OUF is taken into account, the net mean GFU activity for OUF ranged from 3.2-16.0 GFU/mg protein. This is 2.1-10.4 times higher than that observed in FBS per mg protein. OUF protein concentration was not correlated with GFU activity in each sample (data not shown). The bulk of the protein present in each OUF sample was unrelated to the level of GFU activity observed.

Diluted samples of OUF were moderately stable during heat treatment (Table II). Treatment at 60°C for 20 min resulted in a 10%-22% loss of growth factor activity. Treatment at 100°C for 20 min, however, resulted in an 18%-100% loss of activity suggesting a progressive loss of GFU activity. GFU activity was also able to withstand at least 3 cycles of freezing and thawing without being diminished. Preliminary evidence suggests that the GFU activity is not basic-FGF because it has little or no affinity for heparin-agarose in 0.15 M NaCl, 10 mM KH_2PO_4, pH 7.4 (data not shown) (26).

An estimation of the approximate molecular weight limit of the GFU activity in OUF was obtained by ultrafiltration on a 30,000 dalton exclusion filtration device. In three separate experiments from 51.0-99.7% of the growth factor activity was retained by the exclusion filter indicating a size of greater than 30,000 daltons for the native form. The presence of some activity in the fraction which passed through the filter may reflect the presence of other smaller growth factor activities in OUF.

To determine whether OUF possessed any tissue specificity, the thymidine incorporation assay was modified to accommodate a variety of cell lines representing five different cell types (Fig.2). Reducing the period of

TABLE II

HEAT STABILITY OF GFU ACTIVITY

OUF No.	% OF INITIAL GFUs AFTER 20 MIN AT 60°C	% OF INITIAL GFUs AFTER 20 MIN AT 100°C
A	78	ND
B	90	50
C	ND	0
D	96	51
E	ND	35
F	ND	82
FBS	ND	30

Samples of each OUF were diluted and filter sterilized and heat treated immediately prior to assaying for growth factor activity. GFU activity was evaluated after treatment at 60°C or 100°C for 20 min. Duplicate native samples were held on ice during treatment for comparison. ND - not determined.

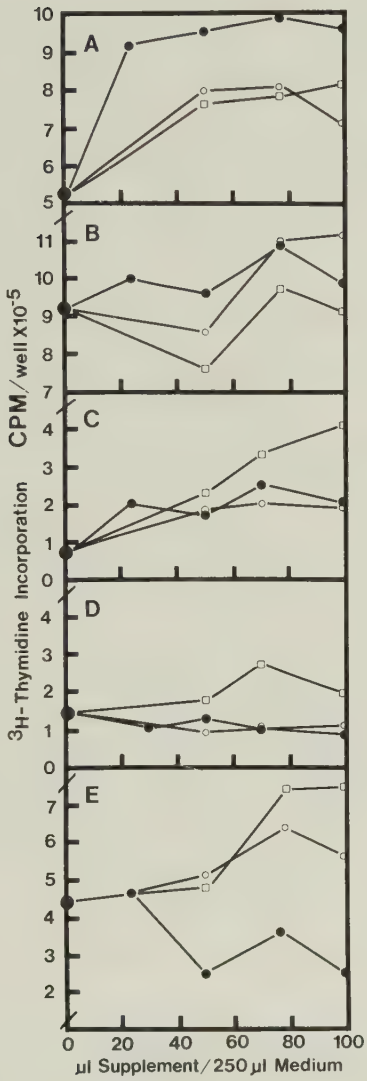

Figure 2: OUF growth factor activity assays on five different cell types. The mitogenic activity of OUF no.29 (open circles) and no.60 (open squares) were compared to that of FBS (small closed circles) in cells which had been grown to confluence and changed to serum-free alpha-MEM for 24 hr. Unstimulated cultures received an equivalent volume of HBS (large closed circles). A) L6-5 rat skeletal muscle myoblasts (SD range 1.9×10^3 to 3.33×10^4 cpm or 11.6% of the mean on average), B) HeLa S3 epidermal carcinoma-derived cells (SD range 3.35×10^4 to 22.4×10^4 cpm or 9.7% of the mean on average), C) OE-1 ovine trophoblast-derived cells (SD range 8.0×10^2 to 36.7×10^4 cpm or 9.3% of the mean on average), D) BA53-90d bovine endothelial cells (SD range 2.7×10^3 to 9.7×10^4 cpm or 17.3% of the mean on average), E) 3T3 mouse fibroblast cell line (SD range 6.6×10^2 to 27.8×10^4 cpm or 18.4% of the mean on average). Note that 3T3 cells were not made fully quiescent in this modified assay.

quiescence from 5 to 1 day increased the residual incorporation observed in HBS treated controls but was necessary because several of the cell lines did not proliferate readily after extended periods of quiescence.

A differential effect of OUF stimulation was observed in different cell types. Mouse 3T3 fibroblasts were not fully quiescent under this modified

treatment and showed only a slight stimulation in thymidine incorporation over FBS. Higher FBS concentrations proved somewhat inhibitory to nonquiescent 3T3 cells. Incorporation was only marginally increased by the presence of FBS over HBS during the next 24 hr. Incorporation by bovine aortic endothelial cells was unaffected by greater amounts of FBS and was only slightly enhanced by one of the OUF samples. Ovine trophoblast-derived cells were moderately stimulated by increased FBS or OUF concentration. HeLa S3 epidermal carcinoma-derived cells were also stimulated by increasing concentrations of FBS and by OUF at higher concentrations. Rat L6-5 skeletal myoblast cells were very sensitive to both FBS and OUF concentration. Myoblasts consistently responded to increasing concentrations of OUF with increased incorporation of thymidine.

The effect of OUF upon skeletal myoblasts was striking compared to its effect upon all other cell types tested. Activity was 1.6 GFU (or 81% of FBS at 50ul) after a 3.1 or 3.4-fold dilution (11.8 or 14.1 GFU/mg protein for OUF compared to 7.2 for FBS in L6 cells). Also, in myoblasts and trophoblasts the effect of OUF on ^{3}H-thymidine incorporation had not come to a plateau. The data suggest that OUF contain a growth factor-like activity which has a marked and specific effect upon trophoblast and myoblast cells in culture. The trophoblast is the first cell type to differentiate in the ovine embryo so that this effect was not unexpected. However, the effect of OUFs upon myoblasts was surprising because few muscle specific growth factors have been reported (25,27).

Due to its unusual characteristics with regard to cell type specificity it is possible that OUF contain a novel growth factor. If so, we suggest the name ovine UDGF: ovine uterine-derived growth factor for this activity (26,27).

ACKNOWLEDGMENTS

The authors wish to acknowledge the assistance of Dr. D. Vaughn with the ultrafiltration experiments and the technical assistance of Mr. R. Young-White and Mrs. A. Church Bird.

REFERENCES

1. Rozengurt, E. (1986) Science 234, 161-166.
2. Helden, C.H., and Westermark, B. (1984) Cell 37, 9-20.
3. Carpenter, G. (1984) Cell 37, 357-358.
4. Schechter, A.L., Stern, D.F., Vaidyanathan, L., Decker, S.J., Drebin, J.A., Greene, M.I., and Weinberg, R.A. (1984) Nature 312, 513-516.
5. Downward, J., Yarden, Y., Mayes, E., Scrace, G., Totty, N., Stockwell, P., Ullrich, A., Schlessinger, J., and Waterfield, M.D. (1984) Nature 307, 521-527.
6. Chiu, I.M., Reddy, E.P., Givol, D., Robbins, K.C., Tronick, S.R., and Aaronson, S.A. (1984) Cell 37, 123-129.
7. Johnsson, A., Heldin, C.H., Wasteson, A., Westermark, B., Deuel, T.F., Huang, J.S., Seeburg, P.H., Gray, A., Ullrich, A., Scrace, G., Stroobant, P., and Waterfield, M.D. (1984) EMBO J. 3, 921-928.
8. Bartol, F.F., Roberts, R.M., Bazer, F.W., Lewis, G.S., Godkin, J.D., and Thatcher, W.W. (1985) Biol. Reprod. 33, 745-759.
9. Moffatt, R.J., Bazer, F.W., Roberts, R.M., and Thatcher, W.W. (1987) J. Anim. Sci. 65, 1400-1410.

10.Hansen, P.J., Ing, N., Moffatt, J., Baumbach, G.A., Saunders, P.T.K., Bazer, F.W., and Roberts, R.M. (1987) Biol. Reprod. 36, 405-418.
11.Bartol, F.F., Roberts, R.M., Bazer, F.W., Lewis, G.S., Godkin,J.D., and Thatcher, W.W. (1985) Biol.Reprod. 32, 681-693.
12.Imakawa, K., Anthony, R.V., Kazemi, M., Marotti, K.R., Polites, H.G., and Roberts,R.M. (1987) Nature 330, 377-379.
13.Sen-Majumdar, A., Murthy, U., and Manjusri, D. (1986) Biochem. 25, 627-634.
14.Renegar, R.H., Bazer, F.W., and Roberts, R.M. (1982) Biol. Reprod. 27, 1247-1260.
15.Bazer, F.W., Roberts, R.M., Basha, S.M.M., Zavy, M.T., Caton, D., Barron, D.H. (1979) J. Animal. Sci. 49, 1522-1527.
16.Moffatt, J., Bazer, F.W., Hansen, P.J., Chun, P., Roberts, R.H. (1987) Biol. Reprod. 36, 419-430.
17.Bird, R.C., Jacobs, F.A., Stein, G., Stein, J., and Sells, B.H. (1985) Biochim. Biophys. Acta 824, 209-217.
18.Yaffe, D. (1968) Proc. Natl. Acad. Sci. USA 61, 477-483.
19.Bird, R.C., and Sells, B.H. (1986) Biochim. Biophys. Acta 868, 215-225.
20.Schwartz, S.M. (1978) In Vitro 14, 966-980.
21.Stringfellow, D.A., Gray, B.W., Lauerman, L.H., Thompson, M.S., Rhodes, P.J., and Bird, R.C. (1987) In Vitro 23, 750-754.
22.Lowry, O.H., Rosebrough, N.C., Farr, A.L., and Randall, R.J. (1951) J. Biol. Chem. 193, 265-275.
23.Hauschka, P.V., Mavrakos, A.E., Iafrati, M.D., Doleman, S.E., and Klagsbrun, M. (1986) J. Biol. Chem. 261, 12665-12674.
24.Anderson, L., and Anderson, N.G. (1977) Proc. Natl. Acad. Sci. USA 74, 5421-5425.
25.Kardami, E., Spector, D., and Strohman, R.C. (1985) Proc. Natl. Acad. Sci. USA 82, 8044-8047.
26.Bohlen, P., Esch, F., Baird, A., and Gospodarowicz, D.(1985) EMBO J. 4, 1951-1956.
27.Ewton, D.Z., and Florini, J.R. (1980) Endocrinology 106, 577-583.
28.Brigstock, D.R., Laurie, M.S., Heap, R.B., and Brown, K.D. (1986) Biol. Reprod. 34(suppl. 1), 133.
29.Ogasawara, M., and Sirbasku, D.A. (1987) J. Cell Biol. 105, 15a.

Vol. 156, No. 1, 1988 BIOCHEMICAL AND BIOPHYSICAL RESEARCH COMMUNICATIONS
October 14, 1988 Pages 116-124

CHEMICAL CHARACTERIZATION BY PROTEIN SEQUENCE ANALYSIS OF THE BOVINE ESTROGEN RECEPTOR

Thomas Ratajczak, Martine J. Brockway, Roland Hähnel, *Robert L. Moritz, and *Richard J. Simpson

Endocrine Research Laboratory
Department of Obstetrics and Gynaecology
University of Western Australia
King Edward Memorial Hospital for Women
Subiaco, Western Australia 6008, Australia

*Joint Protein Structure Laboratory
Ludwig Institute for Cancer Research, and
The Walter and Eliza Hall Institute of Medical Research,
Parkville, Victoria 3050, Australia

Received August 24, 1988

SUMMARY Tryptic peptides generated from bovine estrogen receptor have been fractionated and purified using microbore column high performance liquid chromatography. Sequence analysis performed on six of these peptides, derived from diverse structural regions of the receptor protein, yielded 73 unique assignments corresponding to approximately 12% of the molecule. The amino acid sequences of these peptides displayed a high degree of similarity with corresponding sequences from estrogen receptors of mammalian origin, but were only moderately conserved in receptors from non-mammalian species. The sequenced residues of one tryptic peptide, positioned in the estrogen binding domain, were fully conserved in all estrogen receptors. © 1988 Academic Press, Inc.

Our laboratory has previously described an affinity chromatography-based method for purifying the molybdate-stabilized, 9-10S untransformed estrogen receptor from calf uterus (1). This heteromeric receptor complex is composed of receptor subunits of relative molecular mass (M_r) 65,000 (65K) associated noncovalently with a 90K heat shock protein (hsp 90) which does not bind steroid (2). Similar component structures have been established for the steroid receptors of chick oviduct (3,4), the heteromeric 8S form of the progesterone receptor from rabbit uterus (5) and the untransformed glucocorticoid receptors of uncultured cells from mouse (6,7).

0006-291X/88 $1.50
Copyright © 1988 by Academic Press, Inc.
All rights of reproduction in any form reserved.

In two previous publications we reported on the sequential use of preparative SDS-polyacrylamide gel electrophoresis (SDS-PAGE), electroelution and microbore high performance liquid chromatography (HPLC) techniques to isolate in pure form the bovine hsp 90 component from affinity chromatography-purified estrogen receptor extracts (8, 9). Direct amino-terminal sequence analysis of the protein and sequence determination of peptide fragments generated by trypsin digestion demonstrated regions of high similarity between bovine hsp 90 and a number of previously identified heat-shock proteins (8, 9). We have now employed a similar strategy for the chemical characterization, by sequence analysis, of the estrogen binding subunit. In this report we describe the amino acid sequences of six tryptic peptides derived from the bovine estrogen receptor. These sequences display varying degrees of similarity with the cDNA-deduced amino acid sequences of estrogen receptors from five other species (10-15). One peptide, which by sequence alignment is placed in the putative estrogen binding domain of the protein, is fully conserved in all six estrogen receptors.

MATERIALS AND METHODS

Estrogen Receptor Purification

Bovine estrogen receptor was purified, as previously described (1), by affinity chromatography of calf uterine cytosol. The method, which utilizes sodium molybdate in purification buffers, isolates estrogen receptor associated with a major bovine heat shock protein (hsp 90) (1,8,9) and provides receptor preparations of 5-20% purity. As an aid to receptor detection during preparative SDS-PAGE approximately 1% of the affinity chromatography-purified receptor was recovered and tagged covalently with [^{3}H]tamoxifen aziridine (specific activity 23 Ci/mmol, Amersham) (18). Receptor from batches of these purified extracts was refined to homogeneity by preparative SDS-PAGE (8). The separated proteins were visualized by Coomassie Brilliant Blue staining (19) and the receptor band corresponding to [^{3}H]tamoxifen aziridine labeled protein was excised. The protein was recovered from the polyacrylamide gel by electroelution in 50 mM NH_4HCO_3 containing 0.1% SDS (8) and was shown to be homogeneous by analytical SDS-PAGE (20) after silver stain detection (21).

Preparation of Tryptic Peptides of Estrogen Receptor for Sequence Analysis

The electroeluate (~450 µl) containing purified estrogen receptor (20 µg) was made 10 mM with respect to dithiothreitol and the sample was heated to 100°C for 5 min. After cooling to room temperature the solution was transferred to a polypropylene tube containing 4 mg of recrystallized

iodoacetic acid dissolved in 6 µl of 1 M NaOH (final solution pH 9.0). The sample was kept in the dark at 37°C for 45 min and the S-carboxymethylated (SCM)-estrogen receptor was recovered from this mixture by precipitation with 9 volumes of prechilled (-20°C) methanol. Trypsin (Worthington TRTPCK) (1% w/w) was immediately added and after standing at -20°C overnight the mixture was centrifuged at 16,000 g (Beckman JA-18.1 rotor) for 45 min at -5°C in Beckman microfuge tubes. SCM-estrogen receptor was resuspended in 250 µl of 0.1 M NH_4HCO_3, 2 mM $CaCl_2$ buffer containing 0.02% (v/v) Tween 20 (Pierce Chemical Co.). An additional aliquot of trypsin (1% w/w) was added and the mixture was incubated at 37°C for 24 h.

Purification of Tryptic Peptides for Sequence Analysis

The tryptic digest of estrogen recpetor was fractionated by microbore chromatography employing a two-dimensional purification procedure (16, 17). Selected tryptic peptides were subjected to N-terminal sequence analysis as previously described (8, 9).

RESULTS AND DISCUSSION

Covalent labeling of the estrogen receptor with [^{3}H] tamoxifen aziridine in the endstage of affinity chromatography purification proved to be most useful for identifying the receptor protein after electrophoretic separation on preparative SDS-PAGE gels. After recovery of the protein from the excised gel by electroelution analytical SDS-PAGE showed a single band for the purified sample with a M_r = 65,000 (Fig. 1). This corresponds closely to most published molecular weight values for the estrogen receptor present in a number of target tissues (10-15, 18, 22).

The tryptic digest of SCM-estrogen receptor was fractionated by microbore RP-HPLC in low-pH (0.1 % v/v) aqueous trifluoroacetic acid (pH 2.1) mobile phase into a complex pattern of peptide-containing peaks (Fig. 2A). Fractions 1-5 (see Fig. 2A) were selected for further purification using a second chromatographic step. Chromatographic conditions were as described in Fig. 2A except that the mobile phase was 1% (w/v) aqueous sodium chloride, pH 6.5 (see Fig. 2B, 2C). These refinements yielded six peptides (T_1-T_6) for sequence analysis (Fig. 3A). Figures 2B and 2C show the peptide profiles resulting from rechromatography of peak fractions 4 and 5. The multiple forms of peptides T_4 and T_5 (see different retention times in Fig. 2) are due, presumably, to oxidation of methionine and tryptophan residues.

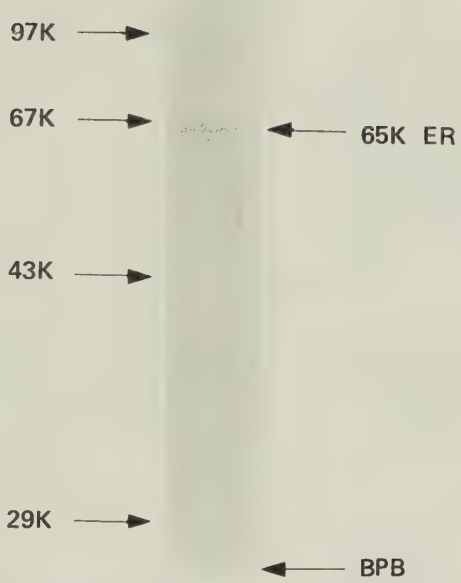

Figure 1 Analytical SDS-PAGE of bovine estrogen receptor recovered from preparative SDS-PAGE by electroelution. Proteins used were silver stained (21) and protein standards used were: 97 K, phosphorylase b, 67 K, bovine serum albumin, 43 K, ovalbumin, 29 K, carbonic anhydrase. BPB-bromophenol blue.

As expected the amino acid sequences of the tryptic fragments derived from the bovine estrogen receptor (T_1-T_6) share structural similarities with the sequences published for estrogen receptors from five different species (10-15) (Fig. 3A). Greatest amino acid sequence similarity was with human estrogen receptor (10,11) which displayed 81% identity with the sequenced residues (Fig. 3A). A slightly less extensive similarity (74%) was observed between the peptides and the estrogen receptors from mouse (15) and rat (13), while the corresponding regions of chicken (12) and frog (14) estrogen receptors were only 60% and 47% identical, respectively (Fig. 3A).

All estrogen receptors have been shown to have a structural organization similar to that initially described for human and chicken

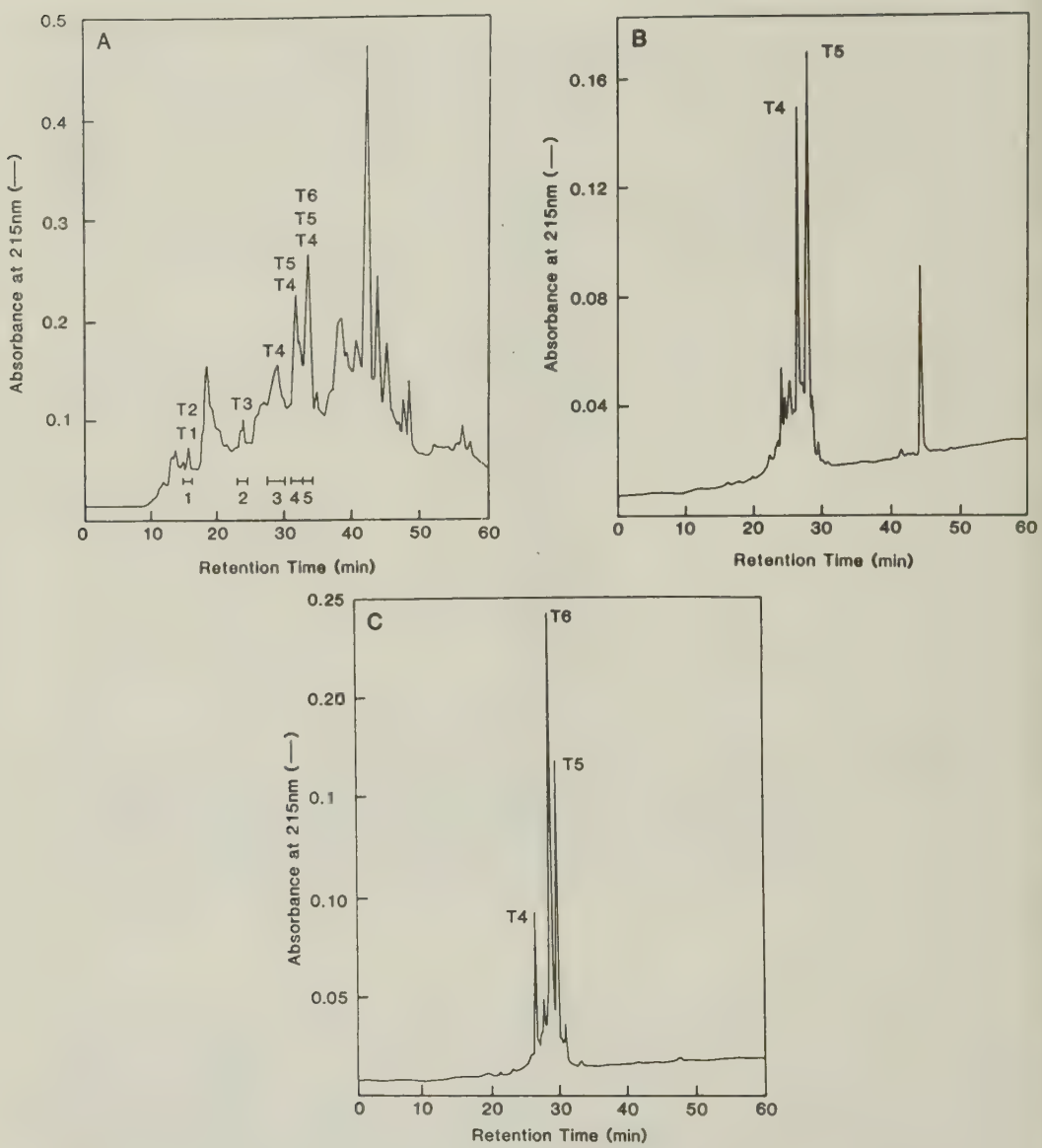

Figure 2A Separation of tryptic peptides of SCM-estrogen receptor by microbore RP-HPLC. Chromatographic conditions: column, Brownlee RP-300 (30 x 2.1 mm i.d.), linear 75-min gradient from 0 to 100% B, where solvent A was 0.1% (v/v) aqueous trifluoroacetic acid and solvent B was 75% acetonitrile/25% water containing 0,085% (v/v) trifluoroacetic acid, flow rate, 100 µl/min, column temperature, 45°C. Peaks (100-150 µl) were collected manually in Eppendorf tubes and stored at -10°C prior to further manipulation.

2B Rechromatography of peak fraction 4 from Fig. 2A by microbore RP-HPLC. Chromatographic conditions: column, Brownlee RP-300 (30 x 2.1 mm i.d.), linear 50-min gradient from 0 to 50% B, where solvent A was 1% (w/v) aqueous sodium chloride pH 6.5 and solvent B was 100% acetonitrile, flow rate, 100 µl/min, column temperature, 45°C.

2C Rechromatography of peak fraction 5 from Fig. 2A by microbore RP-HPLC. Chromatographic conditions were identical to those in Fig. 2B.

A

| | | |

estrogen receptors by Krust et al. (12). Based on sequence homology the receptor can be divided into six structural regions (Fig. 3B). Between species domains A, C and E are highly conserved, while greater variability is displayed by B, D and F (10-15). Alignment of the peptide sequences with the cDNA-deduced amino acid sequence of the human estrogen receptor revealed that the peptides are derived from diverse regions of the bovine receptor protein (Fig. 3B). Peptides T_2 and T_1 are contiguous and are placed towards the carboxyterminus of domain B. Peptide T_5 comes from the D region, close to the dividing line with E, while peptide T_4 originates from the E domain. Peptides T_6 and T_3 are both derived from region F of the protein with T_6 partially overlapping domain E. Peptide T_3 represents the carboxyterminal tryptic peptide of the bovine estrogen receptor.

The homology patterns we have observed for the bovine receptor peptides are consistent with those reported generally for estrogen receptors (10-15). This is particularly evident for peptide T_4 from domain E - the steroid binding domain of the protein (23), and for peptides T_6 and T_3 from the carboxyterminal domain F. The residues of peptide T_4 are fully conserved in all six estrogen receptors (Fig. 3A). A similar trend is observed for the first four residues of peptide T_6 which also reside within the E domain (Fig. 3A,B). The above observations contrast with the generally low level of conservation noted for the residues from region F (part of peptide T_6 and peptide T_3) (Fig. 3A).

Domain E encompasses a stretch of approximately 250 highly conserved amino acids which form the steroid binding hydrophobic pocket in estrogen receptors (10-15). Computer-based studies (24) have defined similar segments within the steroid-binding domains of the estrogen and glucocorticoid (25) receptors and of the α-subunit of $(Na^+ + K^+)$ATPase (26). These studies favour residues 323-395 of the human estrogen receptor as the location of the estrogen binding site (24). Such a

location would place the residues of peptide T_4 close to the centre of the steroid binding region (Fig. 3A).

Region D, a segment containing approximately 40 amino acid residues (10-15), may function as a flexible hinge between the steroid binding (E) and DNA-binding (C) domains of the receptor (12) (Fig. 3B). While the amino acid residues in this region of the human estrogen receptor are 80% identical with the corresponding proteins from mouse and rat (10,11, 13, 15) less extensive homologies exist with the receptors from the non-mammalian species chicken (38%) and frog (30%) (12, 14). Apart from one conservative replacement (leucine for isoleucine) in the human receptor, and the same alteration plus a second substitution (valine for methionine) in the mouse and rat, the sequence of peptide T_5 is all but identical to all three proteins (Fig. 3A). This result from the bovine estrogen receptor therefore, extends the observed differences in region D, between the receptors of mammalian and non-mammalian origin.

The amino acid sequence in the contiguous peptides T_2, T_1 shows similarities with all published estrogen receptor sequences (Fig. 3A). Again, however, the residues were more highly conserved in the human, mouse and rat (Fig. 3A). Although a function for region B in estrogen receptors has not yet been defined (12) White et al., (15) have suggested that two small conserved regions (named B_1 and B_2), existing near the amino- and carboxytermini of the variable B domain, might be involved in the modulation of transcriptional activity. The first five residues of peptide T_2 are included in the B_2 region and are totally conserved in estrogen receptors except for a single substitution (serine for asparagine) in the frog (Fig. 3A).

ACKNOWLEDGEMENT

A portion of this work (T. Ratajczak, M.J. Brockway and R. Hähnel) was supported by the National Health and Medical Research Council of Australia.

REFERENCES

1. Atrache, V., Ratajczak, T., Senafi, S. and Hähnel, R. (1985) J. Biol. Chem. 260, 5936-3941.
2. Redeuilh, G., Moncharmont, B., Secco, C. and Baulieu, E.-E. (1987) J. Biol. Chem. 262, 6969-6975.
3. Joab, I., Radanyi, C., Renoir, M., Bichou, T., Catelli, M.-G., Binart, N., Mester, J. and Baulieu, E.-E. (1984) Nature 308, 850-853.
4. Dougherty, J.J., Puri, R.K. and Toft, D.O. (1984) J. Biol. Chem. 259, 8004-8009.
5. Catelli, M.G., Binart, N., Jung-Testas, I., Renoir, J.M., Baulieu, E.E., Feramisco, J.R. and Welch, W.J. (1985) EMBO J. 4, 3131-3135.
6. Housley, P.R., Sanchez, E.R., Westphal, H.M., Beato, M. and Pratt, W.B. (1985) J. Biol. Chem. 260, 13810-13817.
7. Mendel, D.B., Bodwell, J.E., Gametchu, B., Harrison, R.W. and Munck, A. (1986) J. Biol. Chem. 261, 3758-3763.
8. Ratajczak, T., Comber, M., Moir, R., Hähnel, R., Grego, B., Rubira, M.R. and Simpson, R.J. (1987) Biochem. Biophys. Res. Commun. 143, 218-224.
9. Ratajczak, T., Brockway, M.J., Hähnel, R., Moritz, R.L. and Simpson, R.J. (1988) Biochem. Biophys. Res. Commun. 151, 1156-1163.
10. Green, S., Walter, P., Kumar, V., Krust, A., Bornert, J.-M., Argos, P. and Chambon, P. (1986) Nature 320, 134-139.
11. Greene, G.L., Gilna, P., Waterfield, M., Baker, A., Hort, Y. and Shine, J. (1986) Science 231, 1150-1154.
12. Krust, A., Green, S., Argos, P., Kumar, V., Walter, P., Bornert, J.-M. and Chambon, P. (1986) EMBO J. 5, 891-897.
13. Koike, S., Sakai, M. and Muramatsu, M. (1987) Nucl. Acids Res. 15, 2499-2513.
14. Weiler, I.J., Lew, D. and Shapiro, D.J. (1987) Mol. Endocrinol. 1, 355-362.
15. White, R., Lees, J.A., Needham, M., Ham, J. and Parker, M. (1987) Mol. Endocrinol. 1, 735-744.
16. Simpson, R.J., Moritz, R.L., Lloyd, C.J., Fabri, L.J., Nice, E.C., Rubira, M.R. and Burgess, A.W. (1987) FEBS Lett. 224, 128-132.
17. Simpson, R.J., Moritz, R.L., Rubira, M.R. and Van Snick, J. (1988) Eur. J. Biochem. (in press).
18. Katzenellenbogen, J.A., Carlson, K.E., Heiman, D.F., Robertson, D.W., Wei, L.L. and Katzenellenbogen, B.S. (1983) J. Biol. Chem. 258, 3487-3495.
19. Hunkapiller, M.W., Lujan, E., Ostrander, F. and Hood, E.L. (1983) Meth. Enzymol. 91, 227-236.
20. Laemmli, U.K. (1970) Nature (Lond.) 227, 680-685.
21. Merril, C.R., Goldman, D., Sedman, S.A. and Ebert, M.H. (1981) Science 211, 1437-38.
22. Lubahn, D.B., McCarty, K.S. Jr. and McCarty, K.S. Sr. (1985) J. Biol. Chem. 260, 2515-2526.
23. Kumar, V., Green, S., Staub, A. and Chambon, P. (1986) EMBO J. 5, 2231-2236.
24. Baker, M. (1986) Biochem. Biophys. Res. Commun. 139, 281-286.
25. Hollenberg, S. M., Weinberger, C., Ong, E.S., Carelli, G., Oro, A., Lebo, R., Thompson, E.B., Rosenfield, M.G. and Evans, R.M. (1985) Nature 318, 635-641.
26. Shull, G.E., Schwartz, A. and Lingrel, J.B. (1985) Nature 316, 691-695.

Vol. 156, No. 1, 1988 BIOCHEMICAL AND BIOPHYSICAL RESEARCH COMMUNICATIONS
October 14, 1988 Pages 125-130

DERMORPHIN ANALOGS: RESISTANCE TO IN VITRO ENZYMATIC DEGRADATION IS NOT ALWAYS INCREASED BY ADDITIONAL D-AMINO ACID SUBSTITUTIONS

Krzysztof Darlak,* Deanne E. Benovitz,† Arno F. Spatola,† and Zbigniew Grzonka*

* Institute of Chemistry, University of Gdansk, Gdansk, Poland

† Department of Chemistry, University of Louisville, Louisville, KY 40292

Received August 25, 1988

SUMMARY: Dermorphin (H-Tyr-D-Ala-Phe-Gly-Tyr-Pro-Ser-NH_2) and seven analogs were examined for their biostability towards rat brain homogenate; half-lives for the parent were 127 min and 48 min, respectively, with Gly^4-Tyr^5 cleavage confirmed by collection and identification of the N-terminal fragment. Surprisingly, several analogs with additional D-amino acid substitutions were cleaved more rapidly than the parent, suggesting the importance of remote secondary structural features for differential enzyme susceptibility. © 1988 Academic Press, Inc.

Dermorphin (H-Tyr-D-Ala-Phe-Gly-Tyr-Pro-Ser-NH_2), an opioid heptapeptide, was first isolated from the skin of frogs of the Phyllomedusa species (1). The presence of the unusual D-amino acid residue at the 2 position has been partially credited for dermorphin's very high and long lasting analgesic activity (2). Extensive structure-activity studies of dermorphin analogs have been reported in the literature (3-16).

The first studies of the enzymatic stability of dermorphin (17) confirmed the increased resistance of the molecule toward proteolytic enzymes. This enhanced stability was attributed both to the D-amino acid at position 2 as well as to the proline in position 6, both of which appear to protect dermorphin against exopeptidase action (18). In vivo experiments showed that dermorphin is degraded by the liver and kidney to the N-terminal tripeptide, and by brain enzymes to the N-terminal tetrapeptide (19). Further in vitro experiments demonstrated that both kidney and brain homogenates can inactivate dermorphin by cleaving the peptide bond between position Gly-4 and Tyr-5 (20,21). In contrast,

0006-291X/88 $1.50
Copyright © 1988 by Academic Press, Inc.
All rights of reproduction in any form reserved.

in vitro experiments with plasma showed the very high stability of dermorphin in that environment (17).

We have previously shown that HPLC-based assays of peptides and pseudopeptides can be used to monitor and quantify both half-lives and cleavage patterns in biological fluids (23). Interestingly, the incorporation of amide bond surrogates was sometimes seen to increase the stability of remote scissile bonds. More recently this approach has been expanded to help design more stable and highly potent analogs of cholecystokinin octapeptides as anti-satiety agents (22). In this paper, we report the results of analogous experiments on dermorphin and a series of analogs with modifications at diverse locations throughout the molecule, and we contrast the degradation results with their biological activities.

MATERIALS AND METHODS

Chromatography. Peptides discussed in this study were previously synthesized in our laboratory (15,16). HPLC analyses were performed using an L-6200 Hitachi pump equipped with a solvent gradient system, a temperature controlled column oven, a Varian Model 9090 autosampler, and an LKB 2140 diode array detector, coupled to an IBM AT personal computer using Wavescan software (LKB, Bromma, Sweden, version 1.08). Degradation products were separated on an analytical Zorbax C_{18} column (4.6 x 250 mm) using a gradient made up of two solvents: A, 0.25 M ammonium acetate, pH = 6.5; B, methanol. The gradient used was of 5-20% methanol for 5 min, 20-40% methanol for 25 min, 40-50% methanol for 5 min. The elution program was initiated 1 min after sample injection, at a flow rate of 1 ml/min at 40°C. Degradation products after HPLC fractionation were collected and hydrolyzed in 6N hydrochloric acid for 24 h at 110°C. Amino acid analysis was performed using the PicoTag system (Waters Associates, Milford, MA).

Peptide Degradation. Degradation studies were performed using rat brain or dog duodenal homogenates. Rat brain homogenate was obtained from male Sprague-Dawley rats (350-450 g). Brain tissue was homogenized in 4 parts (w/v) saline at 0°C using a PCU-2 homogenizer (Kinematica GmbH, Luzern) using 3 x 10 sec bursts. Fractions of supernatant (0.5 ml for each peptide) obtained after centrifugation (3000 rpm for 15 min at 0°C) were used for assay. An average amount of 0.7-0.9 mg of peptide was dissolved in 2.0 ml of buffer (0.01 M aqueous ammonium acetate, pH = 7.4, containing 1.26 mM Z-Tyr-OH as internal standard), and 0.5 mL of brain homogenate was added. Incubations were carried out at 37°C. Aliquots of 200 µl were removed at variable time intervals up to 240 min, and the enzymatic reactions terminated by placing tubes into boiling water for 5 min. Samples were filtered through 0.46 µm nylon filters (Millipore, Bedford, MA) and then injected (100 µl) onto the reversed phase column. Degradation studies using dog duodenal homogenate were carried out as follows. The duodenum was surgically removed from a male German shepard, still on a respirator, after the removal of a kidney. The duodenal tissue was washed with saline solution and then homogenized in 9 parts (w/v) saline solution. A portion (200 µl) of this suspension was added to a glass vial containing a weighed sample (0.7-0.9 mg) of the appropriate peptide along with buffer and internal standard. The incubations, and further HPLC analysis were carried out as described above. Half-lives of dermorphin and its analogs were calculated as described previously (23).

RESULTS AND DISCUSSION

In the present study we have carried out in vitro analyses to assess the enzymatic stability of dermorphin and its analogs to rat brain and dog duodenal homogenates. Since it has previously been demonstrated that dermorphin is unusually more stable in blood serum (17,20), these tissues were deemed more suitable for rapidly comparing the relative stability of presumably more stabilized analogs.

The degradation half-lives for dermorphin and the other analogs tested are summarized in Table 1. Dermorphin showed a $t_{1/2}$ = 127 ±26.1 min (n=3) using rat brain homogenates, whereas inactivation using duodenal homogenate was faster ($t_{1/2}$ = 45.7 min). The same relative behavior was observed with the other dermorphin peptide analogs. All compounds modified in positions 1 to 5 showed lower stability than dermorphin. Generally, this finding correlates well with their lower in vitro activities (15,16), although this relationship is not necessarily predictable.

In contrast, [Sar^6]-dermorphin and [D-Ala^7]-dermorphin were found to be 6 and 2 times more stable, respectively, than the parent peptide, and showed in vitro GPI activities closer to the parent. Both of the latter two compounds are more active in vivo than is dermorphin (24). But [Tyr(Me)^5]-dermorphin showed a

TABLE 1. Half-lives of dermorphin and its analogs degraded by rat brain and dog duodenum homogenate

No.	Structure	Half-life (min) Brain (rat)	Half-life (min) Duodenum (dog)	Rel. Activity GPI
1	H-Tyr-D-Ala-Phe-Gly-Tyr-Pro-Ser-NH_2	127	45.7	1
2	Ac-Tyr^1----------NH_2	84.5	-	$3x10^{-5}$
3	H-D-Tyr^1----------NH_2	80.8	26.2	$3x10^{-4}$
4	H----------D-Phe^3----------NH_2	59.4	-	2.5x10-3
5	H----------Ala^5--------NH_2	59.2	54.3	$1.3x10^{-3}$
6	H----------Tyr(Me)^5----NH_2	112	-	4.5
7	H----------Sar^6----NH_2	860	-	0.38
8	H----------D-Ala^7-NH_2	257	-	0.55

TABLE 2. Degradation of dermorphin analogs by brain homogenate

No.	Structure	Peptide HPLC t_R/min	Main Degradation Peak HPLC t_R/min	amino acid analysis Tyr	Ala	Phe	Gly
1	Dermorphin	24.4	18.3	1.00	0.97	0.99	1.02
2	[Ac-Tyr^1]-Der	28.3	19.4	0.99	1.00	1.00	1.04
3	[D-Tyr^1]-Der	25.5	16.3	0.98	1.00	1.03	0.87
4	[D-Phe^3]-Der	23.2	16.2	0.99	1.20	1.02	1.00
5	[Ala^5]-Der	25.4	18.4	1.00	1.00	0.99	1.13
6	[Tyr(Me)^5]-Der	24.2	18.3	0.98	1.00	1.00	1.08
7	[Sar^6]-Der	23.3	18.3	n.d.	n.d.	n.d.	n.d.
8	[D-Ala^7]-Der	27.5	18.5	0.97	1.00	0.89	1.30

somewhat higher in vitro bioactivity, but was slightly less stable to enzymatic attack ($t_{1/2}$ = 112.1 min). Preliminary findings suggest that there is nevertheless an interesting positive correlation between the half-lives reported here and the in vivo analgesic activities of these compounds (24). However, much of this can be considered fortuitous since, for example, the D-Tyr^1 analog, when contrasted with other opioids, is not expected to retain high biological activity. On the other hand, the slightly increased rate of degradation observed both for this compound and for the D-Phe^3 analog is somewhat of a surprise, and reveals the importance of understanding the effects of remote modifications on enzymatic selectivity and substrate turnover rates.

Table 2 contains chromatographic data and amino acid analysis results of several metabolites collected after digestion by brain enzymes. On the basis of the amino acid analysis of the major fragment, all tested compounds gave results consistent with primary cleavage between positions 4 and 5 (Gly-Tyr). The predominant metabolite, the N-terminal tetrapeptide collected after assay appeared to be very stable against further degradation by brain homogenate. On the other hand the second metabolite, the C-terminal tripeptide, was not detected during assay. As reported earlier (20), this tripeptide appears to be further degraded very easily under the experimental conditions.

Our results are thus supportive of data published in the literature regarding both the relative stability and fragmentation patterns that can be expected for various dermorphin analogs. On the basis of the data from these studies, it would appear that analogs containing further stabilizing modifications in the interior portion, such as isosteric amide bond replacements, might increase their half lives and yet be consistent with retention or enhancement of biological potency. In this regard, it is interesting to note that Scalia et al. (20) have recently reported that a dermorphin analog with a retro amide ([NHCO]) replacement between Gly^4 and Tyr^5 blocked 4-5 cleavage, but did not substantially increase biological potency (25). Further efforts to improve both stability and potency are in progress in our laboratories.

ACKNOWLEDGEMENTS

This work was supported by NIH grants GM-33376 and DA-04504, and by CPBR-3.13.4.3.2. Our thanks to Mr. Van Osdol for the amino acid analysis results.

REFERENCES

1. Montecucchi, P. C., de Castiglione, R., Piani, S., Gozzini, L., and Erspamer, V. (1981) Int. J. Pept. Protein Res., 17, 275-283.
2. Broccardo, M., Erspamer, V., Falconieri-Erspamer, G., Improta, G., Linari, G., Melchiorri, P., and Montecucchi, P. C. (1981) Br. J. Pharmacol., 73, 625-631.
3. de Castiglione, R., "Highlights in Receptor Chemistry," C. Melchiorri and M. Giannella eds., Elsevier Biomedical Press, Amsterdam, 1984, pp. 149-168.
4. de Castiglione, R., Faoro, F., Perseo, G., Piani, S., Santangelo, F., Melchiorri, P., Erspamer, V., Falconieri-Erspamer, G., and Guglietta, A. (1981) Peptides, 2, 265-269.
5. Melchiorri, P., Falconieri-Erspamer, G., Erspamer, U., Gulietta, A., de Castiglione, R., Faoro, F., Perseo, G., Piani, S., and Santangelo, F. (1982) Peptides, 3, 745-748.
6. Salvadori, S., Sarto, G., and Tomatis, R. (1982) Int. J. Pept. Protein Res., 19, 536-542.
7. Salvadori, S., Marastoni, M., Balboni, G., Sarto, G., and Tomatis, R. (1985) J. Med. Chem., 28, 769-774.
8. Salvadori, S., Marastoni, M., Balboni, G., Sarto, G., and Tomatis, R. (1986) J. Med. Chem., 29, 889-894.
9. Salvadori, S., Marastoni, M., Balboni, G., Sarto, G., and Tomatis, R. (1985) Int. J. Peptide Protein Res., 25, 526-533.
10. Salvadori, S., Marastoni, M., Balboni, G., Marzola, G., and Tomatis, R. (1986) Int. J. Peptide Protein Res., 28, 254-261.
11. Salvadori, S., Marastoni, M., Tomatis, R., and Sarto, G. (1983) Il Farmaco Ed. Sci., 38, 640-646.
12. Sarto, G., Borea, P. A., Salvadori, S., and Tomatis, R. (1983) Arzneimittel Forsch., 33, 1577-1579.
13. Salvatori, S., Sarto, G., and Tomatis, R. (1984) Arzneimittel Forsch., 34, 410-411.

14. Marastoni, M., Salvadori, S., Balboni, G., Marzola, G., degli Uberti, E., and Tomatis, R. (1986) Int. J. Pept. Protein Res., 28, 274-281.
15. Darlak, K., Grzonka, Z., Janicki, P., and Gumulka, S. W. (1984) Peptides, 5, 687-689.
16. Darlak, K., Grzonka, Z., Janicki, P., Czlonkowski, A., and Gumulka, S. W. (1983) J. Med. Chem., 26, 1445-1447.
17. Erspamer, V., Melchiorri, P., Broccardo, M., Falconieri-Erspamer, G., Falaschi, P., Improta, G., Negri, L., and Renda, T. (1981) Peptides, 2 S2, 7-16.
18. Montecucchi, P. C., de Castiglione, R., and Erspamer, U. (1981) Int. J. Pept. Protein Res., 17, 316-321.
19. Negri, L., and Improta, G. (1984) Pharmacol. Res. Commun., 16, 1183-1191.
20. Scalia, S., Salvadori, S., Marastoni, M., Bortolotti, F., and Tomatis R. (1986) Peptides, 7, 247-251.
21. Sasaki, Y., Hosomo, M., Matsui, M., Fujita, H., Suzuki, K., Sakurada, S., Sakurada, T., Kisara, K. (1985) Biochem. Biophys. Res. Commun., 130, 964-970.
22. Rosamond, J. D., Comstock, J. M., Thomas, N. J., Clark, A. M., Blosser, J. C., Simmons, R. D., Gawlak, D. L., Loss, M. E., Augello-Vaisey, S. J., Spatola, A. F., and Benovitz, D. E., (1988) "Peptides, Chemistry and Biology, Proceedings of the Tenth American Peptide Symposium," Garland Marshall, ed., Escom, Leiden, pp. 610-612.
23. Benovitz, D. E., and Spatola, A. F. (1985) Peptides, 6, 257-261.
24. Grzonka, Z., and Darlak, K., unpublished results.
25. Salvadori, S., Marastoni, M., Balboni, G., Sarto, G., Tomatis R. (1985) Int. J. Peptide Protein Res., 25, 526-533.

Vol. 156, No. 1, 1988 BIOCHEMICAL AND BIOPHYSICAL RESEARCH COMMUNICATIONS
October 14, 1988 Pages 131-136

ALMOST TOTAL CONVERSION OF PANCREAS TO LIVER IN THE ADULT RAT: A RELIABLE MODEL TO STUDY TRANSDIFFERENTIATION

M.S. Rao, R.S. Dwivedi, V. Subbarao, M.I. Usman, D.G. Scarpelli, M.R. Nemali, A. Yeldandi, S. Thangada, S. Kumar, and J.K. Reddy

Department of Pathology
Northwestern University Medical School
303 E. Chicago Avenue
Chicago, Illinois 60611

Received August 25, 1988

Study of transdifferentiation provides an excellent opportunity to investigate various factors and mechanisms involved in repression of activated genes and derepression of inactivated genes. Here we describe a highly reproducible in vivo model, in which hepatocytes are induced in the pancreas of adult rats that were maintained on copper-deficient diet containing a relatively non-toxic copper-chelating agent, triethylenetetramine tetrahydrochloride (0.6% w/w) for 7-9 weeks and then returned to normal rat chow. This dietary manipulation resulted in almost complete loss of pancreatic acinar cells at the end of copper-depletion regimen, and in the development of multiple foci of hepatocytes during recovery phase. In some animals, liver cells occupied more than 60% of pancreatic volume within 6-8 weeks of recovery. Northern blot analysis of total RNA obtained from the pancreas of these rats revealed the expression of albumin mRNA. Albumin was demonstrated in these pancreatic hepatocytes by immunofluorescence. The advantages of this model over the previously described models are: a) low mortality (10%), b) depletion of acinar cells, and c) development of multiple foci of hepatocytes in 100% of rats. © 1988 Academic Press, Inc.

Transdifferentiation is an irreversible process in which one differentiated cell is converted into a completely different cell type (1). During this process, they completely lose the morphological and biochemical characteristics of the original cell and acquire features of an entirely different cell type accompanied by expression of new genes (2). This fascinating phenomenon of transdifferentiation has been clearly documented in in vitro and in vivo conditions, shown to be possible with or without DNA synthesis and cell replication and can occur between cell types belonging to the same cell class, same cell lineage, or different cell lineages (2-5). Although transdifferentiation has been observed in several cell types, the histogenesis still remains controversial. It is not clear whether transdifferentiation involves direct conversion of a fully differentiated cell, conversion of an intermediate cell, or dedifferentiation of a fully differentiated cell followed by

0006-291X/88 $1.50
Copyright © 1988 by Academic Press, Inc.
All rights of reproduction in any form reserved.

redifferentiation. To satisfactorily answer these questions, a reproducible experimental system which does not involve embryonic tissue is required.

Recently, we and others have described the development of hepatocytes in the pancreas of adult hamsters and rats that were either given carcinogens or maintained on a copper-depletion-repletion protocol, or a methionine-deficient diet (6-8). In these species, the induced pancreatic hepatocytes were identical to the liver parenchymal cells both morphologically and functionally (9,10). Although, the exact cell or cells from which pancreatic hepatocytes are derived in rats and hamsters is not established, the process of conversion is referred to as transdifferentiation, since hepatocytes are developing in an organ of an adult animal in which no stem cells are known to exist. The existing rat models are useful to study transdifferentiation and identify various factors that can lead to the development of pancreatic hepatocytes. However, these models are not ideal because of a high incidence of mortality, very low incidence of pancreatic hepatocytes, and the presence of almost all pancreatic acinar cells. In the present study, we describe a highly reproducible model in which hepatocytes are induced in the pancreas of rats that are maintained on a copper-deficient diet supplemented with 0.6% triethylenetetramine tetrahydrochloride (trien) for 50-65 days and returned to normal diet. The advantage of this model is less than 10% mortality of animals and extensive pancreatic hepatization in 100% of the animals in a pancreas which has been depleted of most of its exocrine acinar cells.

Materials and Methods

Twenty male Fischer 344 rats, weighing 80-90 g, were purchased from Charles River Breeding Laboratories (Wilmington, MA). They were housed in individual plastic cages with stainless steel wire bottoms. All rats were fed a copper-deficient diet (United States Biochemical Corp., Cleveland, OH) supplemented with 0.6% triethylenetetramine tetrahydrochloride (trien) (Aldrich Chem.Co.) for 7-9 weeks. During the final two weeks, if the animals were found sick they were returned to a normal diet (Purina rat chow, St.Louis, MO); otherwise, all rats were changed to a normal diet on the 65th day. Ten control rats were maintained on a normal diet throughout the experimental period. Five animals from experimental and five from control group were sacrificed at the end of copper-deficiency regimen. Eight weeks after changing to a normal diet, all rats were sacrificed. The pancreas from all animals was processed for light and electron microscopy. For immunofluorescence localization of albumin, portions of pancreas were fixed in 70% ethanol and processed as described (7). Total RNA was isolated from liver, normal pancreas and pancreas with hepatocytes after homogenization in guanidinium isothiocyanate and centrifugation through cesium chloride (11), and analyzed by Northern blot hybridization using nick translated ^{32}P-labeled albumin cDNA (12).

Results and Discussion

Rats maintained on a copper-deficient diet containing 0.6% trien gained body weight during the first 6 weeks, although at a lower rate than control rats. At 8 weeks of copper deficiency, experimental animals weighed 20% less than controls. The pancreas

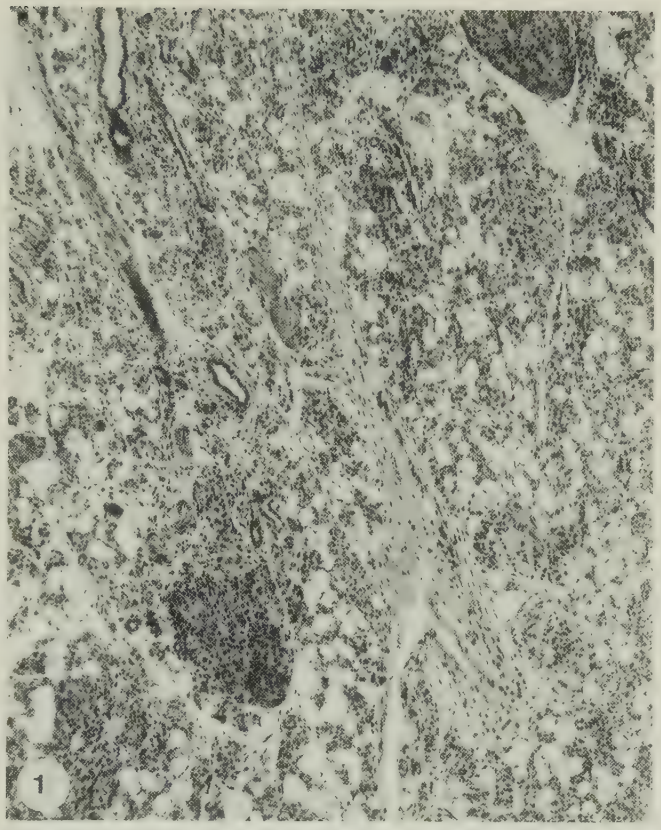

Fig.1 Pancreas of a rat maintained on a copper-deficient diet containing 0.6% trien for 8 weeks, shows total loss of acinar tissue, collapse and fatty infiltration. H&E, X120.

of all of 5 rats that were killed at the end of 8 weeks of copper-deficiency regimen was markedly atrophic and weighed approximately 90 mg/100 g body weight as compared to about 230 mg/100 g body weight in controls. Histologically, there was extensive (>90%) loss of acinar tissue (Fig.1). Islets and ducts appeared unaffected. The interstitial tissue contained increased numbers of spindle or oval-shaped cells.

The pancreas of all 13 rats that were killed 8 weeks after changing to a normal diet showed fatty infiltration along with multiple foci of randomly distributed hepatocytes. Although, there was some variation in the number of hepatic foci between animals, in a majority of rats more than 60% of the pancreas was occupied by hepatocytes (Fig.2). Size of the hepatic foci ranged from groups of few cells to large clusters of several cells. Morphology of pancreatic hepatocytes was indistinguishable from liver parenchymal cells. These cells are polyhedral with a central nucleus containing a prominent nucleolus and substantial eosinophilic cytoplasm. Electron microscopic appearance of pancreatic hepatocytes was indistinguishable from that of liver hepatocytes. Some of the liver cells were seen in continuity with smaller intercalated ducts, or in close association with islets, whereas others were present in the fatty stroma

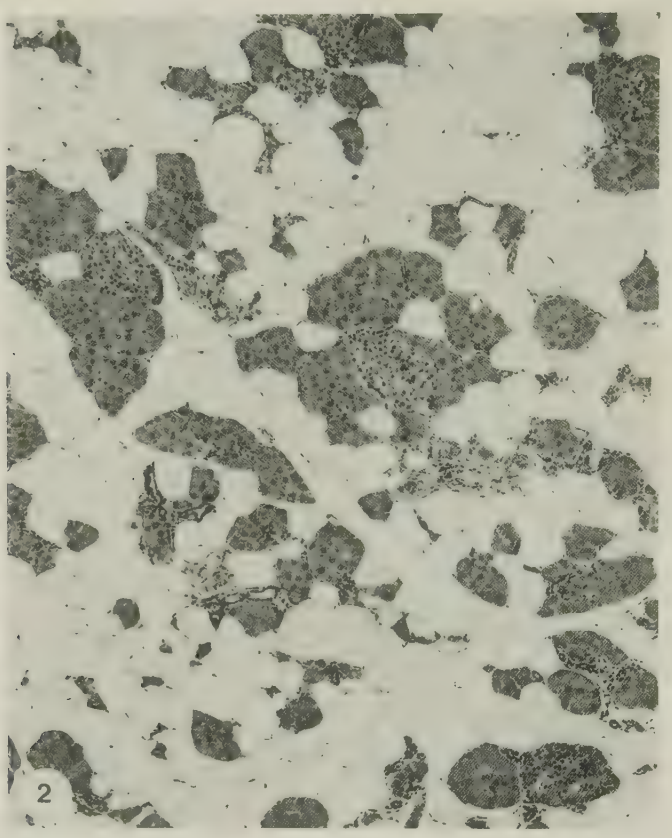

Fig.2 Pancreas of a rat maintained on a copper-deficient diet containing 0.6% trien for 8 weeks and changed to normal diet for 8 more weeks, showing multiple foci of randomly distributed hepatocytes. H&E, X120.

without any apparent relation to either ducts, acini or islets. Detailed analysis of 0.5μm thick sections with light microscopy suggested that hepatocytes appear to originate from epithelium of small ductules (intercalated ducts) and scattered interstitial cells. The amount of acinar tissue in the pancreas of these animals was less than 15% of total volume. Total RNAs were isolated from the pancreas of two rats killed at 8 weeks of recovery from copper-deficiency and analyzed by Northern blot method to ascertain the expression of mRNA for albumin, a liver specific protein. For comparison, total RNA isolated from normal rat liver and pancreas was also analyzed (Fig.3). Albumin mRNA is detected in the pancreas of both rats recovering from copper-deficiency (Fig.3, Lanes 1&2) but not detected in normal rat pancreas (Fig.3, Lane 3). Furthermore, albumin was localized in all hepatocytes in these pancreata by indirect immunofluorescence method (not illustrated).

With this dietary regimen, coupled with a less toxic copper-chelator, trien, only 2 rats (10%) died during the entire experimental procedure, as compared to 50% mortality observed in rats that were made copper-deficient using D-penicillamine as chelator (7). Although penicillamine and trien are equally effective in inducing cupruresis, the

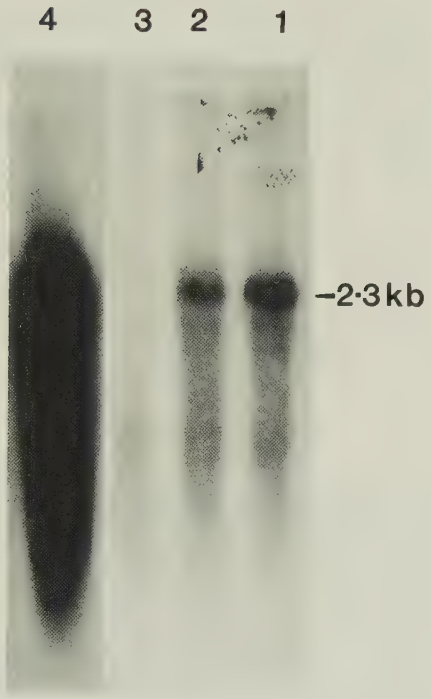

Fig.3 Northern blot analysis of the albumin mRNA in the pancreas of two rats 8 weeks after recovery from copper-depletion-induced atrophy (Lanes 1&2). Lanes 3&4 represent RNA isolated from pancreas and liver respectively from a normal rat. Total RNA (15 μg/Lane) was denatured with glyoxal, electrophoresed, transferred to nylon filter, and hybridized with a ^{32}P-labeled albumin cDNA. The autoradiograph demonstrates a 2·3 kb mRNA in liver and pancreas of two rats with hepatocytes, but not in normal rat pancreas.

increased mortality of rats in experiments using penicillamine is due to its toxic effects in several organs and multiple enzyme systems (13,14). In addition to low mortality, the number of foci and incidence of hepatocytes in the pancreas of rats maintained on copper-deficient diet with trien are high and reproducible. The marked depletion of acinar cells in these pancreata makes this system highly attractive for studying trans-differentiation

The mechanism(s) by which copper deficiency induces hepatic transdifferentiation in pancreas is not clear. The differentiated state of a cell is probably dependent on DNA methylation, chromatin structure, and DNA protein interactions (15,16). Copper is an important trace metal and is essential for the activity of several enzymes (17). Deprivation of cells from copper can lead to macromolecular changes which may result in expression of new genes. In addition to DNA alterations, cell-cell interactions may also play an important role in the maintenance of differentiated state (18). Since copper deficiency leads to almost total ablation of acinar tissue, this may result in loss of feedback mechanism, resulting in proliferation of ductular and interstitial cells with altered differentiation. The experimental model described here should be invaluable in

studying the role of cells lining the intercalated and smaller pancreatic ducts in the histogenesis of hepatocytes and in elucidating the molecular events involved in transdifferentiation of these pancreatic cells to hepatocytes.

Acknowledgment

This research was supported by Grant DK 37958 from The National Institutes of Health.

References

1. Okada, T.S. (1980) Cur. Top. Dev. Biol. 15, 349-390.
2. Okada, T.S. (1986) Dev. Growth Differ. 28, 213-221.
3. Tsunematsu, Y., and Coulombre, A. (1981) Dev. Growth Differ. 23, 297-311.
4. Schmid, V., and Alder, H. (1984) Cell 38, 801-809.
5. Pritchard, D.J., Clayton, R.M., and DePomerai, D.I. (1978) J. Embryol. Exp. Morphol. 48, 1-21.
6. Scarpelli, D.G., and Rao, M.S. (1981) Proc. Natl. Acad. Sci. USA 78, 2577-2581.
7. Rao, M.S., Subbarao, V., and Reddy, J.K. (1986) Cell Differ. 18, 109-117.
8. Hoover, K.L., and Poirier, L.A. (1986) J. Nutr. 116, 1569-1575.
9. Rao, M.S., Scarpelli, D.G., and Reddy, J.K. (1986) Curr. Top. Dev. Biol. 20, 63-78.
10. Reddy, J.K., Rao, M.S., Qureshi, S.A., Reddy, M.K., Scarpelli, D.G., and Lalwani, N.D. (1984) J. Cell Biol. 98, 2082-2090.
11. Chirgwin, J.M., Przybyla, A.E., MacDonald, R.J., and Rutter, W.J. (1979) Biochemistry 18, 5294-5299.
12. Simmons, D.L., Lalley, P.A., and Kasper, C.B. (1985) J. Biol. Chem. 260, 515-521.
13. Sarker, B., Sass-Kortsak, A., and Clarke, R. (1977) Proc. Roy. Soc. Med. 70, Suppl 3, 13-18.
14. Friedman, M. (1977) Proc. Roy. Soc. Med. 70, Suppl 3, 50-60.
15. DiBerardino, M.A., Hoffner, N.J., and Etkin, L.D. (1984) Science 224, 946-952.
16. Brown, D.D. (1984) Cell 37, 359-365.
17. Davis, G.K., and Mertz, W. (1987) In Trace elements in human and animal nutrition (W.Mertz, ed), vol 1, pp 301-364, Academic Press, Inc., San Diego, CA.
18. Wetts, R., and Fraser, S.E. (1988) Science 239, 1142-1144.

Vol. 156, No. 1, 1988 BIOCHEMICAL AND BIOPHYSICAL RESEARCH COMMUNICATIONS
October 14, 1988 Pages 137-142

THE MECHANISM OF THE CHROMATE REDUCTION BY GLUTATHIONE: ESR EVIDENCE FOR THE GLUTATHIONYL RADICAL AND AN ISOLABLE Cr(V) INTERMEDIATE

Xianglin Shi and N.S. Dalal*

Department of Chemistry, West Virginia University
Morgantown, WV 26506

ceived August 25, 1988

With a view of elucidating the role of glutathione (GSH) in the chemical pathways of the chromate-exposure related carcinogenesis, carried out electron spin resonance (ESR) spectroscopic vestigations of the chromate-GSH redox reactions. The ESR asurements, employing spin-traps, provide evidence for the volvement of the glutathione (GS·) radical, as well as an isolable (V)-glutathione intermediate. These results indicate a new chanism for the reduction of chromate by GSH in *in vitro* llular environment and help understand the (unexpected) increase in (VI)-induced DNA strand breaks at elevated GSH levels. © 1988 Academic ss, Inc.

We report here indirect electron spin resonance (ESR) evidence or the involvement of the glutathionyl (GS·) radical and direct vidence for a Cr(V) intermediate in the reactions of glutathione GSH) with chromate for the first time. This work was undertaken to larify the biochemical pathway of the reduction of chromate by GSH, ince this reduction process is thought to be a critical step in the athogenesis of the chromate-exposure related carcinogenesis[1]. This llows from the literature reports which show that (a) Cr(VI) ompounds have been proven to be carcinogens in laboratory animals as ell as in human studies[2-4], (b) Cr(VI) and not Cr(III) compounds are utagenic[5-7], (c) Cr(VI) and not Cr(III) compounds can penetrate cell embranes[8,9], (d) the final state of Cr(VI) in cellular reductions is (III)[1], (e) by itself chromate (or Cr(VI)) cannot be directly utagenic since Cr(VI) is known not to interact with isolated DNA nder physiological conditions[10], suggesting the significance of (VI) reduction processes. One of the major reductants in cellular

uthor to whom correspondence should be addressed.

0006-291X/88 $1.50
Copyright © 1988 by Academic Press, Inc.
All rights of reproduction in any form reserved.

environments is thought to be the GSH, both outside and inside the cells[11-13]. Other evidence for the role of GSH in the chromate toxicity is seen from recent studies showing that exposure of hamster cells to non-toxic levels of added selenite increases the levels of GSH as well as the Cr(VI)-induced DNA strand breaks[14], and that such DNA strand breaks in hepatocytes also change in direct proportion to their GSH content[15,16]. These observations were interpreted as implying that the reduction of chromate by GSH to some reactive intermediate is an important step in the chromate carcinogenicity[15,16]. The following reaction steps were suggested[15,16]:

(A) Initial step:

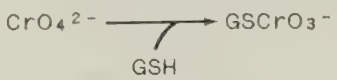

(1)

(B) At high GSH levels:

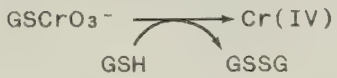

(2)

(C) At low GSH levels:

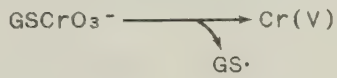

(3)

where $GSCrO_3^-$ is the glutathione-chromate-ester, GSSG the glutathione dimer, and GS· the glutathionyl radical. Thus far, however, in these reactions, the GS· radical has eluded spectroscopic detection, perhaps because of its high reactivity, whereas both positive[17,18] as well as negative[11] evidence for Cr(V) formation has been reported. In the present undertaking, we have used the ESR spin-trap methodology to circumvent the aniticipated high reactivity of GS· and find definitive evidence for the formation of this radical. In addition, we provide unequivocal evidence for the involvement of an intermediate species containing Cr(V).

MATERIALS AND METHODS: ESR spectra were obtained at X-band (~9.7 GHz) using a Bruker ER200D ESR spectrometer. The magnetic field was calibrated with a self-tracking NMR Gaussmeter (Bruker, Model ER035M) and the microwave frequency was measured with a Hewlett-Packard (Mode 5340A) frequency counter. The spin probes, α-(4-pyridyl-1-oxide)-N -tert-butylnitrone (4-POBN) and 5,5-dimethyl-1-pyrroline-1-oxide (DMPO) were purchased from Aldrich, and used without further purification since very weak or no spin adduct signals were obtained

rom the purchased sample when used alone. $K_2Cr_2O_7$ was purchased rom Fisher. All experiments were done at room temperature.

ESULTS AND DISCUSSION: An aqueous solution of 0.1 M spin trap α-(4-yridyl-1-oxide)-N-tert-butylnitrone (4-POBN), either with chromate lone or GSH alone, did not give a detectable ESR spectrum. However, hen chromate, GSH and 4-POBN were mixed, an ESR spectrum was observed hich was a composite of the spin adduct signal (sharp doublets of riplets) and that of Cr(V)[17,18], the broad peak at g = 1.995 (Fig. 1 -c). About ten minutes later, when the signal from Cr(V) had decayed, clear spectrum (g = 2.0061), consisting of only doublets of triplets as obtained (Fig.1 f). This spectrum is assigned to the 4-POBN-GS dduct by its strong similarity to the spectrum reported earlier[19] for he same adduct. The analysis of the spectrum in Fig. 1 f gave the itrogen hyperfine coupling a_N = 15.0 G and proton hyperfine coupling $_H$ = 2.3 G, which compare well with those (a_N = 15.13 G and a_H = .32 G) reported earlier[19].

Additional support for this identification was seen from ESR pectra using 5,5-dimethyl-1-pyrroline-1-oxide (DMPO). The spectrum btained, Fig. 2 a, is composite of that of the spin adduct, a 1:2:2:1 uartet, and that of Cr(V), as evidenced by the broad peak at g = .995. The analysis of the ESR spin adduct spectrum gave a_N = 15.2 G nd a_H = 15.9 G. These values are very similar to those (a_N = 15.4 G nd a_H = 16.2 G) reported[20,21] earlier for the DMPO-GS spin adduct. he spin adduct spectrum shows rapid decay essentially as ecribed[20,21] previously.

An important observation in the spin-trap studies was that an ncrease in the amount of GSH caused an increase in the spin adduct SR signal until the intensity leveled off at a molar ratio of about ifteen to one of GSH to $K_2Cr_2O_7$ (Fig. 1 a-c). No spin adduct SR signal was detected for the molar ratio of less than one Fig. 1 e). This observation is in contradiction to the steps (B) nd (C) as outlined in equations (2) and (3) above.

Fig. 1 and Fig. 2 a-b provide direct evidence for the formation f a fairly long-lived Cr(V) intermediate whe the molar ratios of GSH o $K_2Cr_2O_7$ are higher than one. In agreement with earlier studies[17,18], different kinds of Cr(V) complex are formed depending

on the reaction conditions (Fig. 1 a-d). We were able to isolate the g = 1.995 species with a yield of about 50 percent. A typical ESR spectrum for the powder is shown in Fig. 2 c. The measured g-values are $g_{\parallel}$ = 2.007 and $g_{\perp}$ = 1.989, with little variation with temperature from 115 K to 310 K. These values are typical of Cr(V) solids[22]. When the isolated Cr(V) intermediate was redissolved in water, its ESR spectrum was identical with that from the original solution.

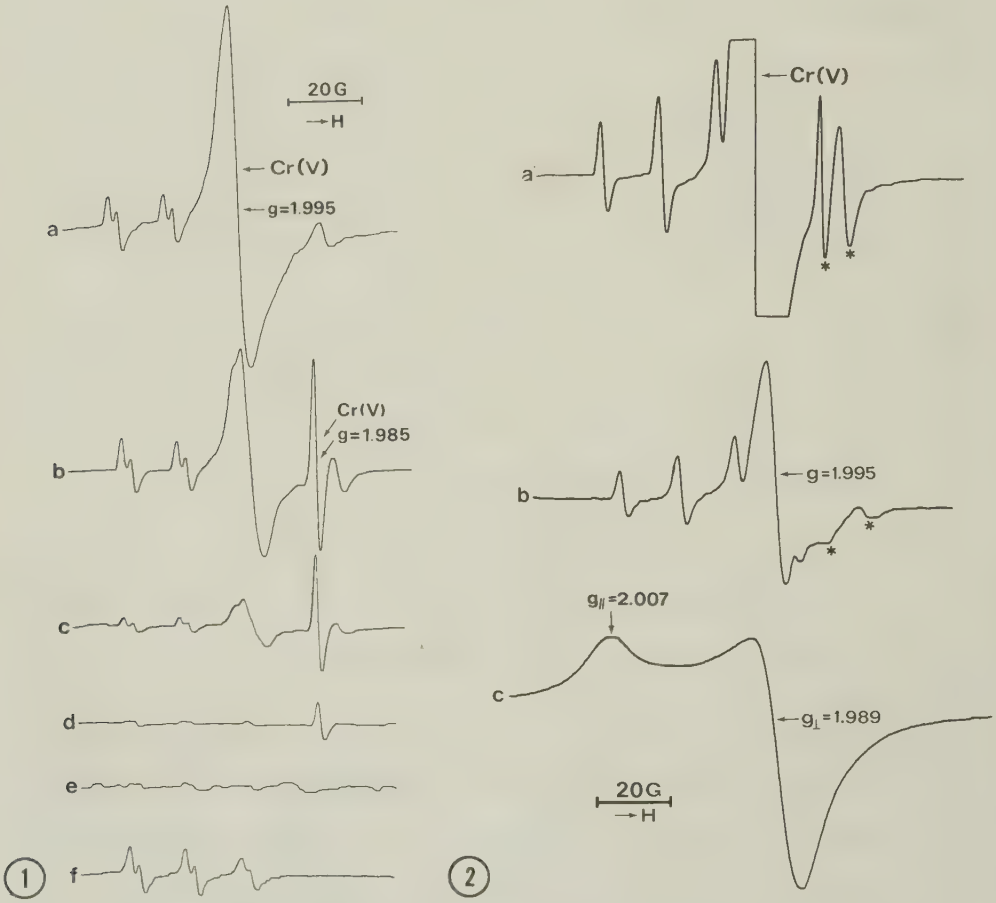

Fig. 1. ESR spectra recorded 2 minutes after mixing a 0.015 M solution of $K_2Cr_2O_7$ with the following concentrations of GSH: (a) 0.375 M, (b) 0.15 M, (c) 0.075 M, (d) 0.03 M, (e) 0.0075 M. The spectrum in (f), corresponding to [GSH] = 0.575 M, was taken after 10 minutes of the mixing, in order to obtain the spin adduct signal free of the Cr(V) signals. The concentration of spin trap used, 4-POBN, was 0.1 M.

Fig. 2. ESR spectra of chromate-glutathione mixtures: [$K_2Cr_2O_7$] = 0.015 M; [glutathione] = 0.375 M; [DMPO] = 0.1 M; (a) pH = 7.2; (b) pH = 4.0 M, recorded 2 minutes after mixing. (c) ESR spectrum of an isolated Cr(V) complex. The astrisks indicate minor Cr(V) species.

Using the isolated Cr(V) complex, as well as K_3CrO_8, a nown Cr(V) compound[22], it was found that the Cr(V) intermediate also erves as an oxidant for the formation of GS·, a result not discussed n any of the earlier studies of the chromate-GSH reaction[1,8-18]. We nus suggest the following alternative mechanisms for the chromate eduction:

) At high GSH levels:

(4)

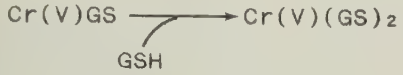

(5)

(6)

(7)

) At low GSH levels:

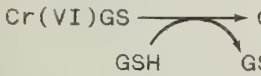

(8)

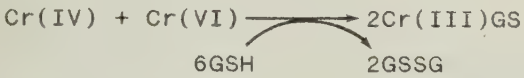

(9)

The above results also help understand the recent reports[15,16] hat increased levels of GSH in the cells result in increased DNA amage by Cr(VI). In the cellular environment the concentration of SH is much higher than that of Cr(VI)[10]. Now this study shows hat the simultaneous formation of GS· and Cr(V) takes place only higher levels of GSH relative to Cr(VI). It thus appears that ncreased Cr(VI)-induced DNA strand breaks noted at higher GSH evels are related to the simultaneous formation of the GS· radicals nd Cr(V) intermediates.

In conclusion, this work shows that both a long-lived, olable, Cr(V) intermediate, and the GS· radical are formed in the eaction between chromate and GSH, but only at high levels of GSH elative to chromate ions, in disagreement with an earlier proposed echanism[15,16]. Thus, a new mechanism has been suggested, which also rovides a plausible explanation for the recent (unexpected) report an increase in Cr(VI)-induced DNA strand breaks at increased GSH evels. Our success in isolating the Cr(V) complex opens up the

possibility of carrying out a detailed single crystal characterization of Cr(V)-$(GSH)_n$ complexation, which may provide clues as to the mechanism of the chromate reduction by cellular thiols. Also a methodology for combating chromate-related carcinogenesis may be available as a results of these investigations.

REFERENCES

1. Connett, P.H., and Wetterhahn, K.E. (1983) Struct. Bond. 54, 93-124.
2. Enterline, P.E. (1974) J. Occup. Med. 16, 523-526.
3. Norseth, T. (1981) Environ. Health Perspect. 40, 121-130.
4. Doll, R. (1981) Environ. Health Perspect. 40, 11-20.
5. Leonard, A., and Lauwerys, R.R. (1980) Mutat. Res. 76, 227-239.
6. Bianchi, V., Celotti, L., Lanfranchi, G., Majone, F., Marin, G., Montaldi, A., Sponza, G., Tamino, G., Venier, P., Zantedesdi, A., and Levis, A.G. (1983) Mutat. Res. 117, 279-300.
7. Löfroth, G., and Ames, B.N. (1978) Mutat. Res. 53, 65-66.
8. Wetterhahn, J.K. (1981) Environ. Health Perspect. 40, 233-235.
9. Jennette, K.W. (1979) Biol. Trace Element Res. 1, 55-62.
10. Tsapakos, M.T., and Wetterhahn, K.E. (1983) Chem.-Biol. Interact. 46, 265-277.
11. Connett, P.H., and Wetterhahn, K.E. (1985) J. Am. Chem. Soc. 107, 4282-4288.
12. Connett, P.H., and Wetterhahn, K.E. (1986) J. Am. Chem. Soc. 108, 1842-1847.
13. Weigand, H.J., Ottenwälder, H., and Bolt, H.M. (1984) Toxicology 33, 341-348.
14. Sugiyama, M., Ando, A., Furuno, A., Furlong, N.B., Hidaka, T., and Ogura, R. (1987) Cancer Lett. 38, 1-7.
15. Wetterhahn, K.E., and Connett, P.H. (1984) Trace Subst. Environ. Health 18, 154-162.
16. Cupo, D.Y., and Wetterhahn, K.E. (1985) Proc. Natl. Acad. Sci. USA 82, 6755-6759.
17. O'Brein, P. (1985) Inorg. Chim. Acta 108, L19-20.
18. Goodgame, D.M.L., and Joy, A.M. (1986) J. Inorg. Biochem. 26, 219-224.
19. Niki, E., Tuschiya, J., Tanimura, R., and Kamiya, Y. (1982) Chemistry Lett. 789-792.
20. Harman, L.S., Carver, D.K., Schreiber, J., and Mason, R.P. (1986) J. Biol. Chem. 261, 1642-1648.
21. Stock, B.H., Schreiber, J. Guenat, C., Mason, R.P., Bend, J.R., and Eling, T.E. (1986) J. Biol. Chem. 261, 15915-15922.
22. Dalal, N.S., Millar, J.M., Jagadeesh, M.S., and Seehra, M.S. (1981) J. Chem. Phys. 74, 1916-23.

Vol. 156, No. 1, 1988 BIOCHEMICAL AND BIOPHYSICAL RESEARCH COMMUNICATIONS
October 14, 1988 Pages 143-148

RAPID PURIFICATION OF INOSITOL MONOPHOSPHATE PHOSPHATASE FROM BEEF BRAIN

James L. Meek,* Timothy J. Rice and Elizabeth Anton

Central Research and Development Department, E. I. Dupont de Nemours & Co.
Wilmington, DE 19898

Received August 26, 1988

A procedure is described for preparation of homogeneous inositol monophosphate phosphatase (EC 3.1.3.25) from beef brain in less than 2 days with an overall recovery of 15-25%. This enzyme, an essential part of the inositol phospholipid cycle in brain, is a proposed site of action of lithium ions in manic-depressive disorders. The major purification steps are:
a) removal of most interfering protein by heat denaturation at 75° C for 1 h,
b) separation by anion exchange at a pH (6.0) near the enzyme's pI (4.9), and
c) adsorption of most remaining impurities on a Procion Red affinity column.
© 1988 Academic Press, Inc.

Many hormones, growth factors and neurotransmitters act on cells via stimulation of hydrolysis of inositol phospholipids, causing the formation of the "second messengers" diacylglycerol and inositol-1,4,5 trisphosphate (IP_3) (1). Resynthesis of inositol phospholipids in brain (which lacks an inositol uptake mechanism) requires that released inositol phosphates be hydrolyzed to form free inositol. Lithium uncompetitively inhibits the monophosphate phosphatase that catalyses the hydrolysis of D-inositol-1-phosphate (which arises from phosphatidylinositol), D-inositol-3-phosphate (from glucose-6-phosphate) and D-inositol-4-phosphate (from breakdown of IP_3) (2-4). This phophatase also catalyses the hydrolysis of a few other compounds including 2'-AMP, and β-glycerophosphate. The latter compound is a convenient inexpensive substrate for routine studies. Although it has recently been suggested that therapeutic concentrations of Li salts also inhibit an inositol polyphosphate phosphatase (5) and a "G protein" (6), the inositol monophosphate phosphatase remains an enzyme of considerable interest. A convenient source of this enzyme would be useful for sequence analysis, kinetic and mechanistic studies, preparation of antibodies, etc. This enzyme has been purified from rat brain (3), and during the course of this work, from beef brain (4). We report here a much simpler isolation procedure.

* To whom correspondence should be addressed.

0006-291X/88 $1.50
Copyright © 1988 by Academic Press, Inc.
All rights of reproduction in any form reserved.

Materials and Methods

Frozen beef brains (250-400 g) were obtained from Pel-Freez, Rogers, AR. Triton X-100, D,L-inositol-1-phosphate and β-glycerophosphate were purchased from Sigma (St. Louis, MO). Triton X-100 was freed of inorganic phosphate by stirring a 10 % solution in water with Dowex 1. For kinetic analyses, the β-glycerophosphate was freed of traces of inorganic phosphate by conversion to the cyclohexylamine form and crystallization from ethanol. Elemental analysis of the resulting needles showed it to be β-glycerophosphate bis-(cyclohexylamine)·1/2 H_2O. Sephacryl S-200 HR, Q Sepharose Fast Flow, and precast "Phastgels" (10-15% gels for SDS-polyacrylamide gel electrophoresis, 8-25% gels for non-denaturing electrophoresis, and pH 4-6.5 isoelectric focusing gels) and Coomassie stain were obtained from Pharmacia (Uppsala). Matrex Red A (Procion Red) agarose and a kit of other dye affinity columns were purchased from Amicon (Danvers, MA).

Inorganic phosphate was assayed with malachite green as described by Lanzetta et al (7) except that instead of 1 ml of Sterox/50 ml of color reagent, we used 100 µl of 10 % Triton X-100/50 ml. The absorbance was linear with phosphate from 0.5-20 nmol. Protein was assayed using Coomassie Blue reagent and γ-globulin standard from Bio Rad (Richmond, CA). Gel filtration of crude preparations was perfomed on a 90 x 1.6 cm Sephacryl S-200 HR column with a flow rate of 1 ml/min and a mobile phase of 0.2 M KCl, 50 mM tris (pH 7.4) and 5 % glycerol. Reverse phase HPLC was performed on a Vydac 5 cm X 4.6 mm "C4" column with a gradient from 10% acetonitrile, 0.1% TFA to 70% acetonitrile, 0.1% TFA in 30 min at 1 ml/min.

INOSITOL MONOPHOSPHATE PHOSPHATASE ASSAY To 50 µl solution of enzyme containing solution (diluted as needed with tris HCl, pH 7.4 at 25°) in 1.5 ml Eppendorf tubes was added 5 µl of 5 mg/ml bovine serum albumin and 5 µl of a solution of 50 mM β-glycerophosphate (cyclohexylamine salt), 20 mM $MgCl_2$ and 2.5 M NaCl in 20 mM tris pH 7.4. After incubation at 37° for 15 min, the reaction was stopped with 5 µl 4 M $HClO_4$. After centrifugation for 2 min, 50 µl of the supernatant solution was assayed for inorganic phosphate.

In initial experiments with gel-filtration and ion exchange columns, a microtiter-plate assay was used to examine large numbers of fractions. Falcon 96-well plates were rinsed with water to remove phosphate, then 50 µl enzyme solution was incubated at 37° with 10 µl substrate/cofactor solution. After 15 min, 12 µl of the mixture was transferred with an 8 channel pipette to wells containing 0.2 ml malachite green reagent. The plates were examined visually or absorbance measured at 660 nm in a Titertek plate reader.

PURIFICATION OF INOSITOL MONOPHOSPHATE PHOSPHATASE

Step 1) 15,000 g Supernatant A frozen brain (300 - 400 g) was thawed for 30 min to allow cutting into pieces. The tissue was homogenized in a Waring blendor in 2 volumes of a solution containing 150 mM KCl, 50 mM tris HCl (pH 7.4) and 0.1 mM EGTA, then centrifuged at 15,000 g for 30 min.

Step 2) 40-60% Ammonium Sulfate Precipitation Ammonium sulfate (242 g/L) was added to the supernatant solution. After 30 min at 4°, the suspension was centrifuged at 15,000 x g for 30 min. Ammonium sulfate (130 g/L) was added to the supernatant solution. The suspension was centrifuged as before.

Step 3) 75° Heat Treatment The resulting pellet was dissolved in homogenization buffer (28 ml/300 g brain weight), and placed in screw capped 25 ml centrifuge tubes. DTT and EDTA were added to a final concentration of 1mM each. The tightly sealed tubes were placed in a preheated 75° C waterbath for 1 hour, then centrifuged at 15,000 x g for 30 min in a Sorvall HB-4 swinging bucket rotor. The clear supernatant solution (with fresh DTT added to 1 mM final concentration) was dialysed first for 1 h, then overnight at 4° against 2 liters of 50 mM tris HCl (pH 7.4 at 25°).

Step 4) Anion Exchange The dialysed enzyme solution was passed at room temperature at 1.0 ml/min over a 1 cm dia. X 25 cm column of Q Sepharose Fast Flow anion exchanger which had been equilibrated with 20 mM tris HCl pH 7.4. The column was eluted with a 55 ml linear gradient of NaCl (0-0.3 M) in 20 mM bis-tris HCl pH 6.0 containing 1 mM DTT, followed by 30 ml 1 M NaCl.

Step 5) Dye Affinity Fractions of eluate containing enzyme activity were combined and concentrated by ultrafiltration to approximately 2 ml on an Amicon YM10 membrane to reduce the amount of salt present. The concentrate was diluted to 8 ml with 20 mM bis-tris acetate pH 6, containing 2 mM $MgCl_2$ and 1 mM DTT and passed at approximately 0.5 ml/min, 4°, over a 0.5 cm dia. x 3 cm Procion Red A column which had been equilibrated with the same buffer.

Step 6) FPLC The column effluent plus a 2 ml wash with the same buffer was adjusted to pH 8 with tris base and loaded via a 10 ml "Superloop" sample injector onto a 5 mm dia. x 5 cm MONO-Q anion exchange column. The enzyme was eluted with a NaCl gradient (0-0.2 M) in 20 min, followed by 0.2 M-.5 M in 10 min) in 20 mM histidine HCl buffer, pH 5.5. The fractions containing enzyme were adjusted to pH 7.4 with tris base and stored frozen at -70°.

Results and Discussion

The remarkable heat resistance of inositol monophosphate phosphatase (2,3,8-10) provided the basis for a most convenient means of precipitating about 99% of interfering proteins while losing only moderate amounts of enzyme activity (Table 1). The heating step eliminates the inositol polyphosphate phosphatase which was a major difficulty in an earlier enzyme preparation (4). Enzyme heated in the presence of DTT and EDTA eluted as a single symmetrical peak on a Sephacryl S-200 HR size exclusion column with an apparent molecular weight of 46,000. Enzyme heated in the absence of DTT gave a broader peak with a higher apparent molecular weight, possibly due to aggregation via disulfide interchange.

Previous preparations of the enzyme (2-4) employed anion exchange separation at pH 8.0. We found that the separation was much better when carried out at a pH closer to the pI of the enzyme (4.9). We examined DEAE Sephacel and Q Sepharose columns. With both columns at pH 6.0, a large degree of purification of protein, and removal of DNA could be rapidly achieved (Fig. 1). The sample was loaded at pH 7.4 in order to maximize the column capacity. SDS-PAGE analysis of the active fractions showed a band with the apparent molecular weight of the enzyme monomer (29,000) contaminated with 1 major and several minor protein bands (Fig. 2).

Table 1. Purification of inositol monophosphate phosphatase

Step	Volume (ml)	Protein (mg)	Total Activity*	Specific Activity*	Purif. (fold)	Yield (%)
15,000 g supernatant	610	8,140	31.6	0.004	1.0	100
40-60% Ammonium SO_4	60	3,330	28.9	0.009	2.2	91
Heat, 75° C, 1 h	40	24.4	17.8	0.73	188	56
Q Sepharose Fast Flow	9	4.9	15.3	3.14	810	48
Procion Red Effluent	10	1.9	8.5	4.49	1150	27
MONO Q	1.8	1.0	6.7	6.66	1710	21

* Total activity = μmol Pi formed per min from β-glycerophosphate.
Specific activity = μmol Pi min^{-1} mg $protein^{-1}$.

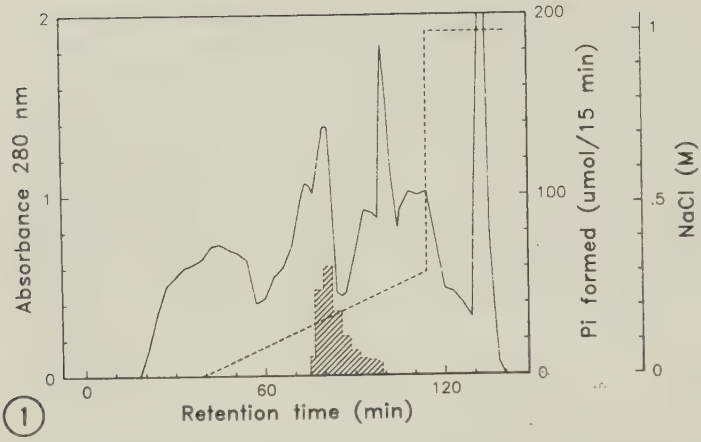

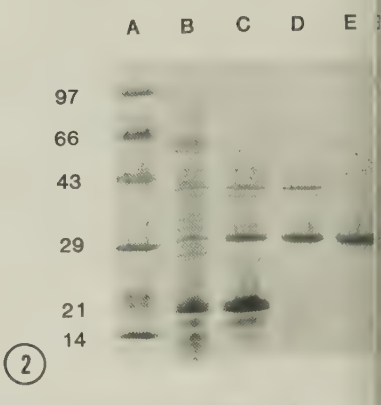

Fig. 1 Anion exchange purification of inositol monophosphate phosphatase. A heat-treated beef brain extract (40 ml, pH 7.4) was loaded onto a Q Sepharose Fast Flow column, then eluted with a NaCl gradient at pH 6.0 The hatched area represents enzyme activity.

Fig. 2. SDS-PAGE of molecular mass markers (lane A), and of proteins present after various purification steps: Lane B, 75° heat treated; Lane C, Q Sepharose eluate; Lane D, Procion Red effluent; Lane E, Mono Q eluate. Samples were heated 15 min at 95° (5 min was insufficient to completely denature the phosphatase) with SDS and mercaptoethanol, and separated on 10-15% "Phastgels". Mass markers (kD): lysozyme (14), soybean trypsin inhibitor (21), carbonic anhydrase (29), ovalbumin (43), bovine serum albumin (66), rabbit muscle phosphorylase B(97). The gel was stained with Coomassie Blue.

Removal of most of the remaining impurities was achieved with a red dye affinity column. The separation was carried out at 4°, pH 6.0, and in the presence of magnesium ions in order to maximize retention of proteins (11). Under these conditions, the monophosphatase was not retained either by the Matrex Red (Procion Red) column, or by any of the other dye affinity columns in the Amicon test kit. The Procion Red column was chosen as the "negative" column, since it adsorbs the most protein from crude tissue extracts (11).

The dye affinity column effluent contained the enzyme contaminated with small amounts of a few other proteins (Fig. 2). These minor contaminants could be effectively removed by chromatography at pH 5.5-6.25 on a MONO Q column. Chromatography at pH 7.4 was much less effective. The enzyme was not retained at pH 5.0

The purified protein gave a single band on SDS-PAGE (with a migration similar to that of carbonic anhydrase, molecular weight 29,000), a single band on non-denaturing gradient gels (with a migration slightly slower than bovine serum albumin), a single band on isoelectric focusing (pI=4.9), and a single peak on reverse phase HPLC, t_r= 23.2 min (ovalbumin= 21.4 min). The strong retention on the reverse phase column indicates that the enzyme is relatively lipophilic. The data obtained by SDS-PAGE and isoelectric focusing are similar

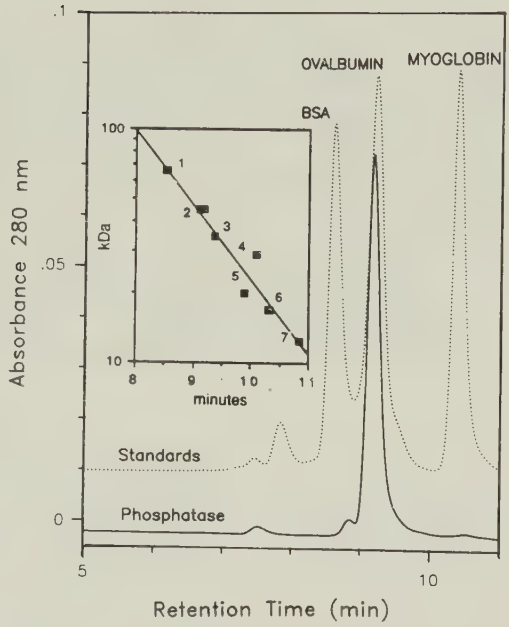

Fig. 3. HPLC-Gel Filtration analysis of the molecular weight of inositol monophosphate phosphatase. The enzyme and standards were chromatographed on a Dupont Bio-series GF250 column (25 x 0.94 cm) with a mobile phase of 0.2 M sodium sulfate, 20 mM tris (pH 7.4) and a flow rate of 1 ml/min. The sample was 20 ul of the MONO Q effluent concentrated approximately 6 fold with an Amicon Centricon 10 centrifugal concentrator. The inset shows the calibration curve: 1, bovine serum albumin; 2, ovalbumin; 3, β-lactoglobulin A; 4, carbonic anhydrase; 5, soybean trypsin inhibitor; 6, myoglobin; 7, cytochrome C.

to that reported previously (4). In non-denaturing and isoelectric focusing gels, monophosphatase activity co-migrated with the protein band as shown by assay of enzyme activity in slices of a lane of the gel adjacent to one subsequently stained with Coomassie blue.

High performance gel filtration chromatography of the enzyme (Fig. 3) indicated a molecular mass of the native enzyme of 46 kDa, a lower value than the 58 and 50 kDa reported previously for the beef brain enzyme (2,4). The value obtained by gel filtration is considerably smaller than twice the apparent 29 kDa mass of monomer given by SDS-PAGE. A better understanding of the correct size of the protein awaits sequence analysis.

The apparent K_m for D,L inositol-1-phosphate was 0.12 mM and 1.0 mM for D,L-β-glycerophosphate. LiCl (20 mM) caused a 90% inhibition of hydrolysis of β-glycerophosphate. In 8 separate preparations of enzyme, the final specific activity for β-glycerophosphate ranged from 2.9 to 6.7 μmol/min/mg protein.

Purified enzyme lost more than 50% of its activity in less than a week at 4°, with or without addition of DTT, β-glycerophosphate, glycerol or $MgCl_2$. The enzyme lost about 10 % activity when stored at -70° for 2 months.

The enzyme was reported to be activated 1.5-2 fold by high concentrations of NaCl, KCl, or NH_4Cl (2). Since the enzyme is inhibited by Li ions, we wondered if there was a requirement for a monovalent metal. We found less than 20% stimulation by addition of 0.25 M NaCl with inositol monophosphate cyclohexylammonium salt as substrate in tris buffer, and no stimulation with β-glycerophosphate as substrate. There was no stimulation by NaCl of β-glycerophosphate hydrolysis even when the cyclohexylammonium ion of the substrate was replaced by the more hindered tetraethylammonium ion, and the incubation buffer was HEPES adjusted to pH 7.4 with tetraethylammonium hydroxide. These data suggest that the effect of NaCl is unlikely to be on a specific mono-cation site.

Purified enzyme was found to be stimulated about 50% by the presence of 0.25-2 mg/ml bovine serum albumin. The stimulation was not due to prevention of enzyme inactivation during incubation since activity was linear with time both with and without albumin addition.

References

1 Berridge, M. J. (1984) Biochem. J. 220, 345-360.
2 Hallcher, L.M., and Sherman, W.R. (1980) J. Biol. Chem. 255, 10896-10901.
3 Takimoto, K., Okada, M., Matsuda, Y., Nakagwa, H. (1985) J. Biochem. 98, 363-370.
4 Gee, N.S., Ragan, C.I., Watling, K.J., Aspley, S., Jackson, R.G., Reid, G.G., Gani, D., and Shute, J.K. (1988) Biochem. J. 249, 883-889.
5 Inhorn, R.C. and Majerus, P.W. (1987) J. Biol. Chem. 262, 15946-15952.
6 Avissar, S., Schreiber, G., Danon, A., and Belmaker, R.H. (1988) Nature 331, 440-442.
7 Lanzetta, P.A., Alvarez. L.J., Reinach.P.S., and Candia, O.A. (1979) Anal. Biochem. 100, 95-97.
8 Chen, I. W., and Charalampous, F.C. (1966) Arch. Biochem. Biophys. 117, 154-157.
9 Eisenberg, F., Jr. (1967) J. Biol. Chem. 242, 1375-1382.
10 Naccarato, W. F., Ray, R.E., and Wells, W. W. (1974) Arch. Biochem. Biophys. 164, 194-201.
11 Scopes, R.K. (1986) J. Chromatogr. 376, 131-140.

Vol. 156, No. 1, 1988 BIOCHEMICAL AND BIOPHYSICAL RESEARCH COMMUNICATIONS
October 14, 1988 Pages 149-156

SPACIAL ISOLATION OF PROTEIN KINASE C ACTIVATION IN THROMBIN STIMULATED HUMAN PLATELETS

Michael F. Crouch* and Eduardo G. Lapetina

Division of Cell Biology,
Burroughs Wellcome Co.,
3030 Cornwallis Road,
Research Triangle Park, NC 27709

Received August 29, 1988

SUMMARY: Thrombin stimulation of human platelets is associated with turnover of inositol phospholipids, mobilization of intracellular Ca^{2+} stores, and activation of protein kinase C. However, within 5 minutes, the thrombin receptor desensitizes, but can be re-coupled to its effectors by stimulation of α_2-adrenergic receptors (Crouch and Lapetina, J. Biol. Chem. 263, 3363- 3371, 1988). This effect of epinephrine was found to be inhibited by preincubation of platelets with phorbol ester, suggesting that protein kinase C was inhibitory. However, since thrombin also activated protein kinase C and epinephrine was active following thrombin stimulation of platelets, this implied that thrombin activation of protein kinase C may have been spacially isolated near the thrombin receptor and could not inactivate α_2-receptor activity. In the present paper, we have tested this possibility, and we present evidence which strongly favours the possibility that protein kinase C activation by receptors induces its local translocation to the cell membrane. © 1988 Academic Press, Inc.

Protein kinase C is critically important in the activation of cells by agonist occupation of a variety of receptors (1). This is particularly true for the class of receptors that stimulate inositol phospholipid turnover (2,3). The activation of platelet receptors, such as those for thrombin, platelet activating factor (PAF), and vasopressin, induces the hydrolysis of phosphatidylinositol-4,5-bisphosphate by phospholipase C (4). The result is the generation of inositol 1,4,5- trisphosphate (IP3) (5,6) and 1,2-diacylglycerol (DAG) (7), which mobilizes intracellular Ca^{2+} stores

*Present address: Department of Pharmacology, Australian National University, Canberra, A.C.T. 2601, Australia

Abbreviations: IP3, inositol 1,4,5-trisphosphate; DAG, 1,2-diacylglycerol; D_iC_8, 1,2-dioctanoyl-sn-glycerol; PAF, platelet activating factor; PDBu, phorbol 12,13-dibutyrate.

0006-291X/88 $1.50
Copyright © 1988 by Academic Press, Inc.
All rights of reproduction in any form reserved.

(3,8) and activates protein kinase C (1), respectively. These initially separate arms of the signalling pathway converge at three points at least. Firstly, DAG reduces the Ca^{2+} requirement for activation of protein kinase C (1). Secondly, there is a more downstream synergism between protein kinase C stimulation and elevation of the cytosolic Ca^{2+} level in which the cellular response, such as platelet secretion, is greater when both occur in parallel than individually (1,4). Thirdly, the actions of protein kinase C in signal transduction are associated with a Ca^{2+}-stimulated translocation of this enzyme to the plasma membrane where the enzyme is activated by DAG (1,2).

This scheme suggests that protein kinase C could conceivably be activated at localized sites at the plasma membrane. Two ways in which this could occur are through the local, receptor-induced DAG production and/or Ca^{2+} mobilization, which could then induce a directed translocation and activation of protein kinase C.

Results from a previous study from this laboratory (9) suggested that such a local activation of protein kinase C may have been occurring. The thrombin-induced mobilization of Ca^{2+} was found to be transient because of an agonist-induced desensitization of the thrombin receptor. However, the thrombin receptor (9) could be recoupled to Ca^{2+} mobilization and phospholipase C by activation of α_2-adrenergic receptors with epinephrine (9). The α-adrenergic receptor is not itself coupled to phospholipase C (9,10). The ability of epinephrine to reactivate thrombin receptors was totally inhibited by pretreating platelets with phorbol ester (9), implying that protein kinase C was phosphorylating and inactivating a component of the α_2-adrenergic receptor coupling system. However, thrombin receptors also activate protein kinase C, but epinephrine was effective after thrombin stimulation. This implied that perhaps protein kinase C activation in response to thrombin was a local event in the cell, but that phorbol ester produced an indiscriminant translocation and activation of this enzyme.

EXPERIMENTAL PROCEDURES

Platelet preparation, measurement of Ca^{2+} mobilization, and protein phosphorylation was as described before (9,11). All experiments are representative of at least two other similar experiments. 1,2-Dioctanoyl-sn-glycerol (D_iC_8) was from Novabiochem.

RESULTS

Phorbol ester and synthetic 1,2-diacylglycerol both desensitize epinephrine action - lack of effect of hormone agonists. As has been shown previously (9,11), activation of human platelets by α-thrombin (10 nM) produces a rapid mobilization of intracellular Ca^{2+} stores (fig 1). This is followed by a

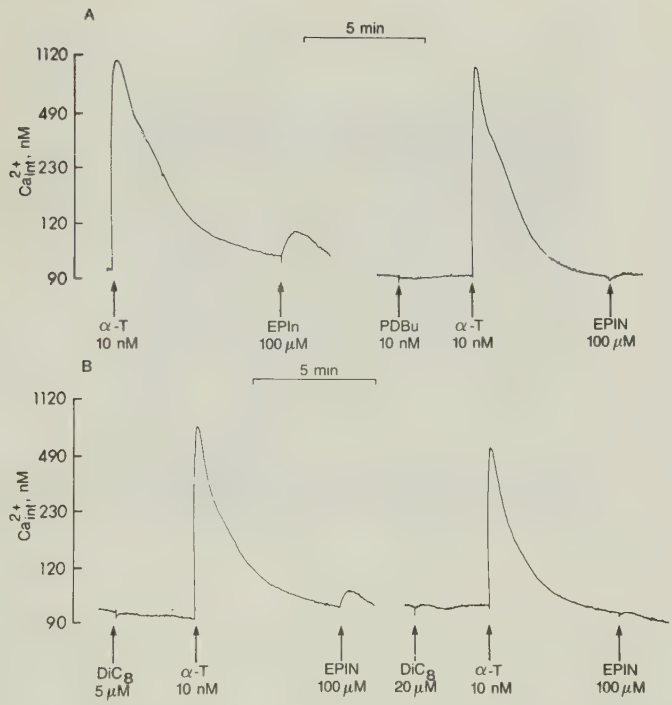

Figure 1 Phorbol 12,13-dibutyrate and 1,2-dioctanoyl-sn-glycerol inhibit epinephrine action on human platelets. Human platelets were loaded with a fluorescent indicator, Indo-1, and the intracellular Ca^{2+} concentration was measured in a fluorescence spectrophotometer. When used, phorbol 12,13-dibutyrate and 1,2-dioctanoyl-sn-glycerol were added 3 min before α-thrombin. α-T, α-thrombin; EPIN, epinephrine; PDBu, phorbol 12,13-dibutyrate; DiC8, 1,2-dioctanoyl-sn-glycerol.

decline of the Ca^{2+} response, which is due to homologous and heterologous desensitization processes (9,11). However, epinephrine will recouple the thrombin receptor to Ca^{2+} mobilization (fig 1A). Preincubating platelets for 3 min with phorbol 12,13-dibutyrate (PDBu) (10 nM) totally inhibited this effect of epinephrine (fig 1A). Similar effects were seen when platelets were preincubated with 1,2-dioctanoyl-sn-glycerol (DiC8), (fig 1 B). The inhibitory effects of DiC8 were half maximal at 5 μM and maximal at 20 μM (fig 1B).

In contrast, if platelets were challenged with endoperoxide analog U44069 (10 μM) and platelet activating factor (PAF, 1 μM) before (not shown) or following thrombin addition, epinephrine was still able to activate a subsequent release of intracellular Ca^{2+} stores (fig 2).

Protein phosphorylation in response to α-thrombin, endoperoxide U44069, PDBu and DiC8. A comparison of the abilities to activate protein kinase C (as shown by phosphorylation of the 47 kDa platelet substrate) showed that α-thrombin (10 nM) and endoperoxide U44069 (10 μM) were much more effective

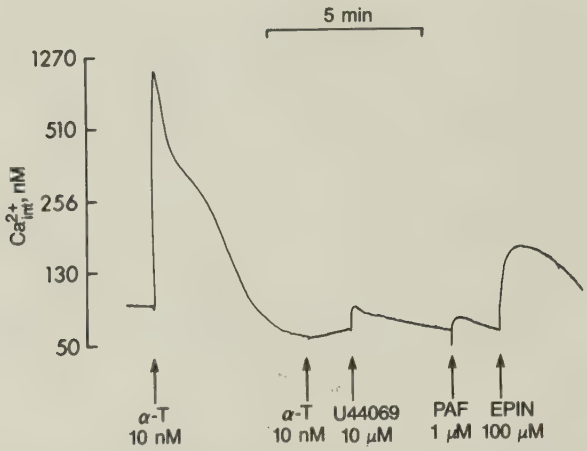

Figure 2 The effect of endoperoxide U44069 and platelet activating factor on epinephrine action. Intracellular Ca^{2+} concentration was measured using Indo-1. Agonists were added at the indicated times. α-T, α-thrombin; U44069, endoperoxide analog U44069; PAF, platelet activating factor; EPIN, epinephrine.

than PDBu (10 nM) (fig 3). Fig 4 compares the abilities of α-thrombin, PAF, endoperoxide U44069, and vasopressin to activate protein kinase C.

We also examined a more extended time course of phosphorylation in response to α-thrombin (10 nM), PDBu (10 nM), and DiC8 (5 and 20 μM)

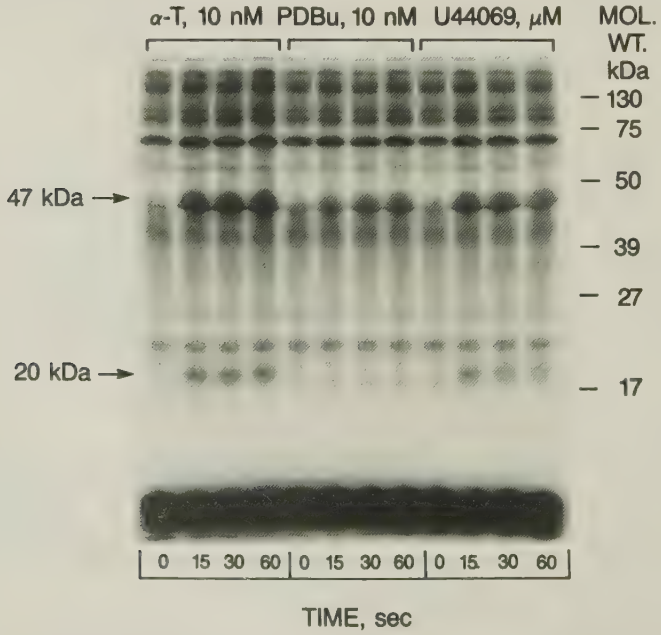

Figure 3 ^{32}P-Protein phosphorylation in response to α-thrombin, phorbol ester and endoperoxide U44069. ^{32}P-Labelled platelets were activated with either α-thrombin (α-T, 10 nM), phorbol 12,13-dibutyrate (PDBu, 10 nM), or endoperoxide U44069 (U44069, 10 μM) for the indicated times. Reactions were stopped by adding aliquots to SDS-PAGE sample buffer, and the proteins were then separated on SDS-PAGE and visualized by autoradiography. Positions of molecular weight standards are indicated.

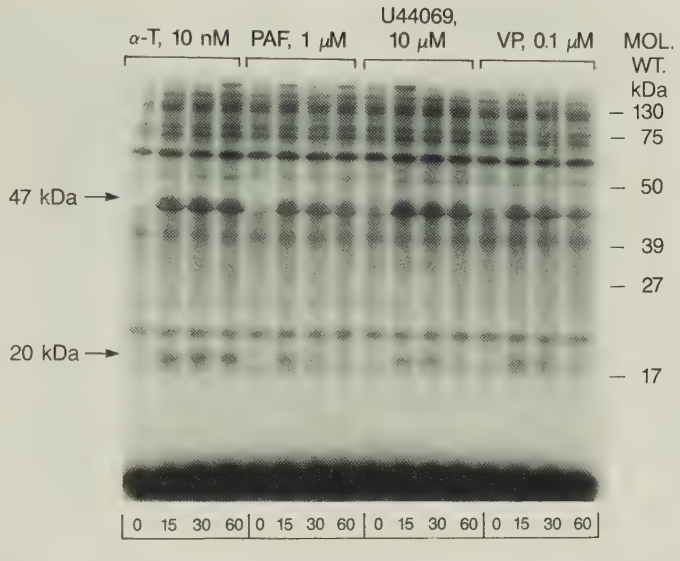

Figure 4 ^{32}P-Protein phosphorylation in response to α-thrombin, platelet activating factor, endoperoxide U44069 and vasopressin. ^{32}P-Labelled platelets were activated with either α-thrombin (α-T, 10 nM), platelet activating factor (PAF, 1 μM), endoperoxide U44069 (U44069, 10 μM) or vasopresin (VP, 0.1 μM) for the indicated times. Reactions were stopped by adding aliquots to SDS-PAGE sample buffer, and the proteins were then separated on SDS-PAGE and visualized by autoradiography. Positions of molecular weight standards are indicated.

(fig 5). Again, α-thrombin was the most potent agonist. Protein kinase C activation in response to PDBu was weaker but was sustained for up to 8 min after addition. DiC8 displayed a biphasic protein kinase C activation, at both 5 and 20 μM concentrations (fig 5). Maximal phosphorylation in response to 20 μM DiC8 was the same as that found in response to PDBu, whereas 5 μM DiC8 induced very little phosphorylation, and after 8 min there was no difference in 47 kDa protein phosphorylation from that found in unactivated samples (fig 5).

DISCUSSION

The steps involved in hormonal activation of protein kinase C have largely been elucidated (1,2,12). They include the receptor-induced degradation of inositol phospholipids (1,3,4) (and perhaps other phospholipids, 13) to form DAG. A rise in the cytosolic Ca^{2+} level then induces the translocation of protein kinase C to the cell membrane where DAG can bind and activate the enzyme (1,2). As discussed in the Introduction, the possibility exists that protein kinase C could be activated in local domains of the cell, based on selective translocation (such as by local increases in Ca^{2+} concentration) or on selective activation (due to localized production of DAG).

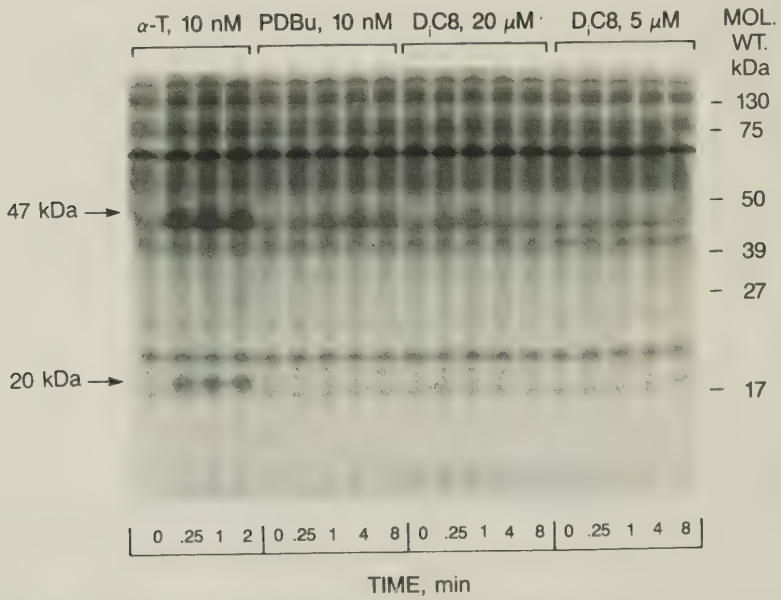

Figure 5 Time course of protein phosphorylation in response to α-thrombin, phorbol ester and 1,2-dioctanoyl-sn-glycerol. ^{32}P-Labelled platelets were activated with either α-thrombin (α-T, 10 nM), phorbol 12,13-dibutyrate (PDBu, 10 nM), or 1,2-dioctanoyl-sn-glycerol (D_iC_8, 20 or 5 μM)for the indicated times. Reactions were stopped by adding aliquots to SDS-PAGE sample buffer, and the proteins were then separated on SDS-PAGE and visualized by autoradiography. Positions of molecular weight standards are indicated.

We have presented a series of findings that suggest that protein kinase C is activated in localized domains of the thrombin-stimulated human platelet. Epinephrine acting on α_2-adrenergic receptors is able to reverse the desensitization of the thrombin receptor, as shown in a previous study (9). This effect was extremely sensitive to phorbol esters (9). The ability of both PDBu and exogenous DiC8 to inhibit epinephrine action strongly implicates protein kinase C activation in this inhibition, rather than another nonspecific mechanism. In addition, a protein kinase C inhibitor, staurosporine, can reverse this effect of PDBu (9,11).

Our present experiments were done because thrombin is itself a potent activator of protein kinase C. That is, how could the effects of epinephrine be inhibited by phorbol esters but not by thrombin. The obvious explanation, which we have explored, is that the protein kinase C, which was activated by thrombin, was not accessible to the α_2-adrenergic receptor, whereas it was in response to phorbol ester .

Our results show that α-thrombin, at the concentration used, was a far better stimulator of protein kinase C than PDBu. However, preincubation of platelets with PDBu was effective at inhibiting epinephrine action. One way in which this could be explained without invoking spacial isolation of protein kinase C activation is that in response to α-thrombin, after 5 min

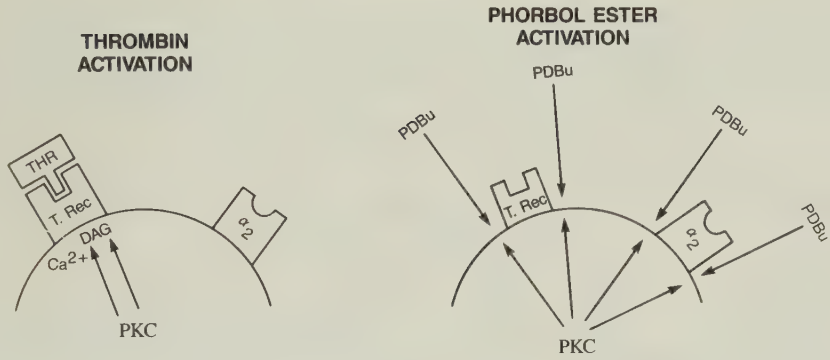

Figure 6 Spacial isolation of protein kinase C activation in thrombin stimulated human platelets. For details see Discussion. THR, thrombin; T. Rec., thrombin receptor; DAG, 1,2-diacylglycerol; PKC, protein kinase C; PDBu, phorbol 12,13-dibutyrate; α_2, α_2-adrenergic receptor.

of stimulation, the receptor has desensitized and protein kinase C activation has returned to basal levels. This could then allow epinephrine action. Because of platelet aggregation, we could not study protein phosphorylation at these late time points in response to thrombin. However, we have answered the question in two other ways.

Firstly, preincubating platelets with DiC8 inhibited subsequent epinephrine action. However, protein phosphorylation in response to DiC8 was biphasic (14 and fig 5), and the level of protein kinase C activation after the same time interval was either very low (20 μM DiC8) or at basal levels (5 μM DiC8). Therefore, inhibition of epinephrine action by DiC8 did not require the sustained activation of protein kinase C, and so a biphasic activation of this enzyme by α-thrombin could not explain a lack of inhibitory action.

Secondly, following α-thrombin desensitization, we challenged platelets with endoperoxide U44069 and PAF before adding epinephrine. Both of these agonists activate protein kinase C, and both were partially active for Ca^{2+} mobilization following the α-thrombin stimulation. However, the epinephrine effect was not diminished by pretreating platelets with these agonists. Thus, not only did α-thrombin-induced protein kinase C activation have no inhibitory effect on epinephrine action, but neither did that in response to endoperoxide U44069 or PAF.

We believe these results are strong evidence in favor of the suggestion that protein kinase C activation in response to α-thrombin, and also endoperoxide U44069 and PAF, is spacially isolated (Fig. 6). This isolation probably would be near the occupied receptors where phospholipase C is activated and DAG is produced (Fig. 6). The generalized desensitization of epinephrine action by PDBu and DiC8 is explained by the nonspecific delivery

of these protein kinase C activators to the plasma membrane and generalized translocation of protein kinase C to the membrane where it could interact with all hormone receptors (Fig. 6).

REFERENCES

1. Nishizuka, Y. (1984) *Nature* **308**, 693-698.
2. Michell, R.H. (1975) *Biochim. Biophys. Acta* **415**, 81-147.
3. Berridge, M.J. (1984) *Biochem. J.* **220**, 345-360.
4. Lapetina, E.G. (1986) in *Phosphoinositides and Receptor Mechanisms* pp 271-286 (Putney, J.W. Jr., ed) Alan R. Liss, Inc. New York.
5. Agranoff, B.W., Murthy, P., and Seguin, E.G. (1983) *J. Biol. Chem.* **258**, 2076-2078.
6. Watson, S.P., McConnell, R.T., and Lapetina, E.G. (1984) *J. Biol. Chem.* **259**, 13199-13203.
7. Rittenhouse-Simmons, S. (1979) *J. Clin. Invest.* **63**, 580-587.
8. O'Rourke, F.A., Halenda, S.P., Zavoico, G.B., and Feinstein, M.B. (1985) *J. Biol. Chem.* **260**, 956-962.
9. Crouch, M.F., and Lapetina, E.G. (1988) *J. Biol. Chem.* **263**, 3363-3371.
10. Siess, W., Weber, P.C., and Lapetina, E.G. (1984) *J. Biol. Chem.* **259**, 8286-8292.
11. Crouch, M.F., and Lapetina, E.G. (1988) *Biochem. Biophys. Res. Commun.* 151, 178-186.
12. Wolf, M., Levine, H., III, May, W.S. Jr., Cuatrecasas, P., and Sahyoun, N. (1985) *Nature* **317**, 546-549.
13. Besterman, J.M., Duronio, V., and Cuatrecasas, P. (1986) *Proc. Natl. Acad. Sci.* U.S.A. **83**, 6785-6789.
14. Lapetina, E.G., Reep, B., Ganong, B.R., and Bell, R.M. (1985) *J. Biol. Chem.* **260**, 1358-1361.

Vol. 156, No. 1, 1988 BIOCHEMICAL AND BIOPHYSICAL RESEARCH COMMUNICATIONS
October 14, 1988 Pages 157-163

A LECITHIN:RETINOL ACYLTRANSFERASE ACTIVITY IN HUMAN AND RAT LIVER

Paul N. MacDonald and David E. Ong

Department of Biochemistry, Vanderbilt University School of Medicine, Nashville, Tennessee 37232

Received August 29, 1988

Summary: This report demonstrates that exogenous phosphatidylcholine will serve as an acyl donor for the esterification of retinol complexed to cellular retinol-binding protein (CRBP) by human and rat liver microsomal preparations. The retinyl ester synthases utilized phosphatidylcholine but had little or no ability to transfer acyl groups from lysophosphatidylcholine, phosphatidylethanolamine, or phosphatidic acid to retinol-CRBP. The human and rat activities also demonstrated positional selectivity as only the fatty acyl group at the sn-1 position of phosphatidylcholine was transferred. This *in vitro* activity may have considerable physiological importance since the fatty acyl composition at the sn-1 position of phosphatidylcholine is remarkably similar to the hepatic retinyl esters observed *in vivo*. © 1988 Academic Press, Inc.

Vitamin A is stored primarily in the liver, where it is present as long-chain fatty acid esters of retinol. A CoA-dependent activity in microsomal preparations obtained from human (1) and rat liver (2) has been suggested to carry out hepatic retinol esterification *in vivo*. This activity, designated acyl-CoA:retinol acyltransferase, was characterized *in vitro* with unbound or free retinol as the substrate. However, both human and rat liver contain a protein that binds retinol with high affinity and specificity, termed cellular retinol-binding protein, or CRBP (reviewed in Ref. 3). When retinol bound to CRBP was examined as a substrate for esterification by rat liver microsomal preparations, it was not available for the reaction catalyzed by acyl-CoA: retinol acyltransferase (4). Instead, the retinol-CRBP substrate was esterified by a different enzyme that used an endogenous acyl donor associated with the microsomal preparation to synthesize mainly retinyl palmitate, the predominant hepatic retinyl ester observed *in vivo* (5). Similar CoA-independent retinyl ester synthases are present in the bovine retina (6-8) and rat small intestine (9,10). Here, we report that the CoA-independent activity

Abbreviations used: CRBP, cellular retinol-binding protein; HPLC, high performance liquid chromatography; NEM, N-ethylmaleimide; PMSF, phenylmethylsulfonyl fluoride.

0006-291X/88 $1.50
Copyright © 1988 by Academic Press, Inc.
All rights of reproduction in any form reserved.

described in rat liver (4) will catalyze acyl transfer from the C-1 position of exogenous phosphatidylcholine to retinol-CRBP to produce retinyl esters. Human liver preparations also catalyzed a similar reaction. These observations suggest that this lecithin:retinol acyltransferase activity may be of considerable importance in the metabolism and storage of vitamin A in the liver of human and rat.

EXPERIMENTAL PROCEDURES

Materials- all-trans-Retinol, all-trans-retinaldehyde, N-ethylmaleimide, phenylmethylsulfonyl fluoride, fatty acyl anhydrides, and all phospholipids were from Sigma. [^{3}H]-Retinol was prepared by reducing all-trans-retinaldehyde with sodium boro-[^{3}H]-hydride (11). 1-Myristoyl-2-lauroylphosphatidylcholine and 1-lauroyl-2-myristoylphosphatidylcholine were prepared and purified as described previously (10). CRBP was purified from rat liver (12). [^{3}H]-Retinol-CRBP was prepared by adding [^{3}H]-retinol to apo-CRBP (9).

Microsomal preparations- Frozen portions from two human livers (weighing approximately 1 and 4 gm) were provided by Dr. F. Peter Guengrich, Department of Biochemistry, Vanderbilt University, Nashville, TN. The material had been obtained at autopsy from two males, ages 22 and 36 years. Collection of the samples was approved by the Vanderbilt University Committee for the Protection of Human Subjects. Microsomal preparations were obtained from human and rat liver in 0.2 M KH_2PO_4, pH 7.2 by methods described previously (4). Protein concentrations were determined by the Pierce BCA protein assay with bovine serum albumin as the standard.

Preparation of phospholipid substrate solutions- Briefly, 400 nmol of phospholipid in chloroform were evaporated to dryness under N_2. The residue was lyophilized for 30-45 min to remove residual solvent and then resuspended in 1 ml of 0.2 M KH_2PO_4, pH 7.2 by sonication with a Branson sonifier fitted with a microtip for 60 x 1 s pulses at a power setting of 2.

Esterification assays- Retinyl ester production from human and rat liver preparations was examined by methods described previously (10). Briefly, 60-120 μg of microsomal protein were incubated for 5 min at room temperature with or without 20-40 nmol of the sonicated phospholipid preparations. The reactions were then initiated with the addition of retinol-CRBP (generally 1.5 nmol) to a final volume of 0.5 ml. Following a 15 min incubation at 37°C, the reactions were quenched with 4 volumes of ice-cold ethanol, extracted into hexane, and the hexane extract analyzed for retinyl esters by reverse-phase HPLC (9). Control incubations used microsomal preparations that were heat-inactivated for 5 min at 100°C. All HPLC results were corrected for the levels of endogenous retinyl esters present in the microsomal preparations as determined in incubations that omitted retinol-CRBP. In some experiments, retinyl ester production was determined with [^{3}H]-retinol-CRBP and the [^{3}H]-retinyl esters were analyzed by batch elution on columns of alumina (9).

Positional selectivity of the acyltransferase activity in human microsomal preparations- The positional selectivity of the acyltransferase activity in human microsomal preparations was examined in 0.22 ml reactions that contained 3.0 μM [^{3}H]-retinol-CRBP and 53 μg of microsomal protein in the presence and absence of 40 nmol of 1-myristoyl-2-lauroylphosphatidylcholine or 1-lauroyl-2-myristoylphosphatidylcholine. Following a 15 min incubation at 37°C, the reactions were stopped with 4 volumes of ice-cold ethanol and then extracted from 44 % ethanol into 3.2 ml of hexane (9). [^{3}H]-Retinyl esters were separated from [^{3}H]-retinol by applying 5 x 0.5 ml aliquots of the hexane extract to 5 x 1.2 gm columns of alumina. The [^{3}H]-retinyl esters were eluted from each column with 5 ml of hexane containing 2% ether (13). The ester fractions were combined, taken to dryness under N_2, redissolved in methanol,

and analyzed by reverse phase HPLC (9). Fractions were collected at 20 s intervals (0.66 ml) and the radioactivity in each fraction was determined by scintillation counting.

Inhibitor Studies- N-Ethylmaleimide and phenylmethylsulfonyl fluoride were examined as chemical inhibitors of the human retinyl ester synthase by methods described previously (10).

RESULTS AND DISCUSSION

Esterification of retinol-CRBP by human liver microsomal preparations- Microsomal preparations obtained from rat liver use an endogenous acyl donor and retinol-CRBP to catalyze the production of retinyl esters (4). Here, we examined whether human liver preparations would esterify retinol-CRBP in a similar fashion.

Microsomal preparations from two separate human livers were observed to catalyze [^{3}H]-retinyl ester production from [^{3}H]-retinol-CRBP. No other factors were required for retinyl ester production. The synthesis of retinyl esters by both human preparations was linear up to at least 120 μg of microsomal protein per ml. Heat-treated microsomes were inactive. Figure 1 illustrates the saturable production of [^{3}H]-retinyl esters with increasing amounts of [^{3}H]-retinol-CRBP from one of these preparations. These data were transformed linearly to calculate the kinetic constants of the microsomal activity (Fig. 1, inset). The average Km and Vmax values for the two preparations were 0.5 μM and 16 pmol per min per mg microsomal protein, respectively. The corresponding kinetic constants reported for the rat liver preparations were 1 μM and 50 pmol per min per mg microsomal protein, respectively (4).

Sensitivity of the human retinyl ester synthase to sulfhydryl and hydroxyl modifying reagents- The CoA-independent esterification of retinol-CRBP by rat liver preparations is sensitive to reagents that modify sulfhydryl or active serine residues (4). Here, the sulfhydryl reagent, NEM, and the anti-esterase, PMSF, were examined as potential inhibitors of the activity in human liver preparations. Retinyl ester production from retinol-CRBP was inhibited when human liver preparations were treated with increasing amounts of either NEM or PMSF (Fig. 2). The human retinyl ester synthase was extremely sensitive to NEM. Preincubating human preparations with 1 μM NEM resulted in essentially complete inhibition of esterifying activity (Fig. 2A). The esterification of retinol-CRBP was also decreased more than 90 % by 2 mM PMSF (Fig. 2B). In contrast, the acyl-CoA:retinol acyltransferase of various tissues is relatively insensitive to millimolar concentrations of PMSF (14,15). Thus, the inhibition observed with PMSF indicated that retinol-CRBP esterification with the endogenous donor was not the result of acyl-CoA:retinol acyltransferase using an endogenous pool of acyl-CoA.

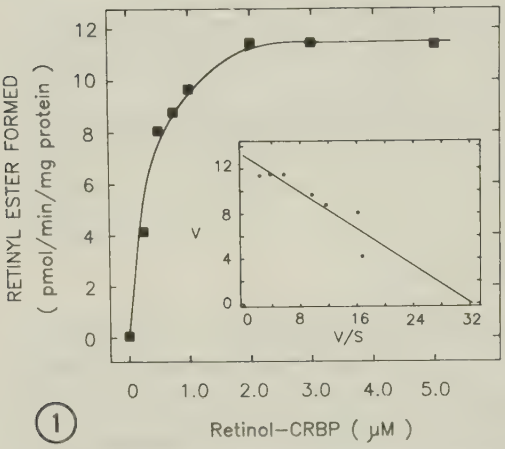

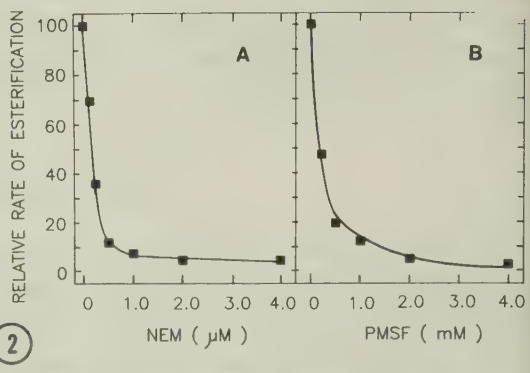

Fig. 1. Concentration dependence of retinol-CRBP esterification by human liver microsomal preparations. Increasing concentrations of [^{3}H]-retinol-CRBP were incubated with 14 μg of microsomal protein in 0.2 M KH_2PO_4, pH 7.2. The reaction volume was 0.12 ml. Following a 10 min incubation at 37°C, 0.1 ml of the reaction was removed into 0.4 ml of ice-cold ethanol and then extracted into hexane (9). The hexane extract was analyzed for [^{3}H]-retinyl esters on 1.2 gm alumina columns (13). Each point is an average of two determinations minus the background radiation obtained in reactions using heat-inactivated microsomal preparations. A linear transformation of this data is shown in the inset.

Fig. 2. Effect of N-ethylmaleimide and phenylmethylsulfonyl fluoride on the esterification of retinol-CRBP by human liver microsomal preparations. Increasing concentrations of either N-ethylmaleimide (panel A) or phenylmethylsulfonyl fluoride (panel B) were incubated in 0.2 M KH_2PO_4, pH 7.2 with 14.4 μg human liver microsomal protein for 10 min at 37°C. Esterification reactions were then initiated with the addition of 0.36 nmol of [^{3}H]-retinol-CRBP (3.5 Ci/mmol) to a final volume of 0.12 ml. Following a 10 min incubation at 37°C, the reactions were analyzed for [^{3}H]-retinyl esters as described in the legend to Figure 1.

Ability of various exogenous phospholipids to participate in retinol-CRBP esterification with human and rat liver preparations- The serum enzyme, lecithin:cholesterol acyltransferase, and the lecithin:retinol acyltransferase activity described in the rat small intestine are also sensitive to reagents that modify active serine and sulfhydryl residues (10,16-18). These activities catalyze the transfer of fatty acids from lecithin to cholesterol or retinol presumably via serine and sulhydryl residues in their active sites. Thus, we examined the ability of the human and rat liver microsomal preparations to catalyze a similar reaction.

In the absence of exogenous phospholipid, only those retinyl esters synthesized from the endogenous acyl donor were observed. These esters were mainly retinyl palmitate/oleate and retinyl stearate (Table 1). Minor amounts of retinyl linoleate and retinyl myristate were also observed (not tabulated). Including dilauroylphosphatidylcholine in the incubation resulted in the appearance of an additional retinyl ester peak in the chromatogram that co-eluted with standard retinyl laurate. Retinyl laurate equalled 30-40 % of the

TABLE I

Selectivity of Hepatic LRAT for Various Exogenous Phospholipids[a]

	Rat Liver Preparations[b]			Human Liver Preparations[b]		
	RL[c]	RP/O	RS	RL	RP/O	RS
NO ADDITION	0	65	27	0	85	15
DLPC	40	41	12	28	61	11
L-PC	4.2	67	20	0	80	20
DLPE	> 2	67	26	0	91	9
DLPA	2.3	69	23	0	88	12

a. Rat and human liver microsomal preparations (60 and 120 μg of microsomal protein, respectively) were incubated with and without 20 nmol of various phospholipid preparations and 1.5 nmol of retinol-CRBP in a volume of 0.5 ml. After 15 min at 37°C, the reactions were extracted into hexane and analyzed by HPLC.
b. All values are expressed as a percentage of the total retinyl ester produced.
c. RL, retinyl laurate; RP/O, retinyl palmitate/oleate; RS, retinyl stearate; DLPC, dilauroylphosphatidylcholine; L-PC, 1-lauroyl-2-lysophosphatidylcholine; DLPE, dilauroylphosphatidylethanolamine; DLPA, dilauroylphosphatidic acid.

total ester generated (Table 1). Boiled microsomal preparations gave no retinyl ester formation from either endogenous or exogenous acyl donors. Other phospholipids such as dilauroylphosphatidylethanolamine, dilauroylphosphatidic acid, or 1-lauroyl-2-lysophosphatidylcholine demonstrated little if any ability to participate in the production of retinyl laurate (Table 1). Thus, of the exogenous lipids examined, both the human and rat activities demonstrated a marked preference for phosphatidylcholine.

Positional selectivity of the acyltransferase- The predominant retinyl ester found in the liver is retinyl palmitate (5). Hepatic phosphatidylcholine contains palmitate almost exclusively at the C-1 position; the C-2 position contains mainly unsaturated fatty acids (19). If the physiological enzyme of the liver is a lecithin:retinol acyltransferase, then one would expect that the transferase is positionally selective for the C-1 fatty acyl moiety. In contrast, lecithin:cholesterol acyltransferase is positionally selective for the fatty acid at the C-2 position (16,20). To examine this possibility, phosphatidylcholines of positionally defined fatty acid composition were synthesized and examined as acyl donors for the esterification of retinol-CRBP.

Figure 3A,D show the retinyl esters generated by the enzyme with acyl moieties derived from the endogenous acyl donor in the absence of exogenous phosphatidylcholine. The retinyl palmitate/oleate peak was the predominant ester peak observed with both human and rat preparations. The radioactivity elution profile of the reaction products from the human preparations also

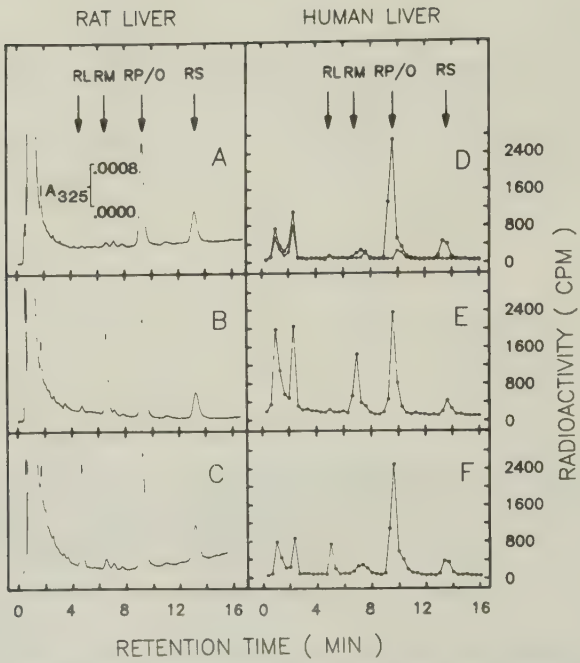

Fig. 3. Positional selectivity of the rat and human retinyl ester synthase for the C-1 moiety of phosphatidylcholine. Rat liver microsomal preparations (60 μg of microsomal protein) were incubated in the absence (panel A) and presence of 40 nmol of 1-myristoyl-2-lauroylphosphatidylcholine (panel B) or 1-lauroyl-2-myristoylphosphatidylcholine (panel C) in 0.2 M KH_2PO_4, pH 7.2 at room temperature for 5 min. Esterification reactions were initiated with the addition of 1.5 nmol of retinol-CRBP to a final volume of 0.5 ml. Following a 15 min incubation at 37°C, the reactions were analyzed for retinyl esters by reverse phase HPLC. Human liver microsomal preparations (40 μg of microsomal protein) were incubated in the absence (panel D) or presence of 18 nmol of 1-myristoyl-2-lauroylphosphatidylcholine (panel E) or 1-lauroyl-2-myristoylphosphatidylcholine (panel F) at room temperature for 5 min. Esterification reactions were initiated with the addition of 0.66 nmol of [^{3}H]-retinol-CRBP to a final volume of 0.22 ml. The reaction time and temperature was 15 min and 37°C, respectively. The [^{3}H]-retinyl esters were isolated on alumina columns and then analyzed by reverse phase HPLC as described in Experimental Procedures.

contained two peaks that eluted in the first three minutes. These peaks were present in the boiled control preparations as well (Fig. 3D, lower tracing). This radioactivity may represent some degradation of the retinol during processing of the extracts.

When human and rat liver preparations were incubated with retinol-CRBP and 1-myristoyl-2-lauroylphosphatidylcholine, the appearance of a new ester peak that coeluted with authentic retinyl myristate was observed (Fig. 3B,E). Only minor amounts of retinyl laurate were detected. Conversely, reactions containing 1-lauroyl-2-myristoylphosphatidylcholine produced retinyl laurate (Fig 2C,F). Thus, both the human and rat retinyl ester synthases displayed a clear positional selectivity for the C-1 acyl moiety of phosphatidylcholine.

Consequently, microsomal preparations from both human and rat liver catalyzed acyl group transfer from the C-1 position of exogenous phosphatidylcholine to retinol-CRBP to produce retinyl esters. The possible physiological relevance of such an activity is indicated by the observations that the predominant fatty acid at the C-1 position of phosphatidylcholine is palmitate and the predominant retinyl ester observed in vivo is retinyl palmitate. In support of this reaction as a general mechanism of retinol esterification is the recent demonstration of a similar, but not identical lecithin:retinol acyltransferase activity in the rat small intestine (10). The results here suggest that hepatic lecithin:retinol acyltransferase may play an important role in the storage of vitamin A in the liver of all species.

ACKNOWLEDGMENTS: We wish to thank Angela Gubitosi and Lee Bullock for excellent technical assistance as well as Dr. Frank Chytil and Dr. Tim Quick for a critical reading of the manuscript.

REFERENCES

1. Rasmussen, M., Helgerud, P., Petersen, L.B., and Norum, K.R. (1984) Acta. Med. Scand. **216**, 403-407.
2. Ross, C.A. (1982) J. Biol. Chem. **257**, 2453-2459.
3. Chytil, F., and Ong, D.E. (1984) in The Retinoids (Sporn, M.B., Roberts, A.B., and Goodman, D.S., Eds.), Vol. II, pp 89-123, Academic Press, New York.
4. Ong, D.E., MacDonald, P.N., and Gubitosi, A.M. (1988) J. Biol. Chem. **263**, 5789-5796.
5. Futterman, S., and Andrews, J.S. (1964) J. Biol. Chem. **239**, 4077-4080.
6. Andrews, J.S., and Futterman, S. (1964) J. Biol. Chem. **239**, 4073-4076.
7. Berman, E.R., Horowitz, J., Segal, N., Fisher, S., and Feeney-Burns, L. (1980) Biochim. Biophys. Acta **630**, 36-46.
8. Saari, J.C., and Bredberg, D.L. (1988) J. Biol. Chem. **263**, 8084-8090.
9. Ong,D.E., Kakkad, B., and MacDonald, P.N. (1987) J. Biol. Chem. **262**, 2729-2763.
10. MacDonald, P.N., and Ong, D.E. (1988) J. Biol. Chem., in press.
11. Liau, G., Ong, D.E., and Chytil, F. (1981) J. Cell. Biol. **91**, 63-68.
12. Ong, D.E., and Chytil, F. (1978) J. Biol. Chem. **253**, 828-832.
13. Helgerud, P., Petersen, L.B., and Norum, K.R. (1982) J. Lipid Res. **23**, 609-618.
14. Ross, A.C. (1982) J. Lipid Res. **23**, 133-144.
15. Torma, H., and Vahlquist, A. (1987) J. Invest. Dermatol. **88**, 398-402.
16. Glomset, J.A. (1962) Biochim. Biophys. Acta **65**, 128-135.
17. Aron, L., Jones, S., and Fielding, C.J. (1978) J. Biol. Chem. **253**, 7220-7226.
18. Jauhiainen, M., and Dolphin, P.J. (1986) J. Biol. Chem. **261**, 7032-7043.
19. Montfoort, A., Van Golde, L.M.G., VanDeenan, L.L.M. (1971) Biochim. Biophys. Acta **231**, 335-342.
20. Sgoutas, P.S. (1972) Biochem. **11**, 293-296.

Vol. 156, No. 1, 1988 BIOCHEMICAL AND BIOPHYSICAL RESEARCH COMMUNICATIONS
October 14, 1988 Pages 164-170

BRUSH BORDER MEMBRANE VESICLES FORMED FROM HUMAN DUODENAL BIOPSIES EXHIBIT NA^+-DEPENDENT CONCENTRATIVE L-LEUCINE AND D-GLUCOSE UPTAKE

James M. Harig, Konrad H. Soergel, Jeanne Barry and Krishnamurthy Ramaswamy

Gastroenterology Division, Medical College of Wisconsin and Zablocki Veterans Administration Medical Center Milwaukee, Wisconsin

Received August 31, 1988

Summary: The human duodenum actively transports L-leucine and D-glucose under Na^+ gradient conditions as demonstrated by uptake studies using brush border membrane vesicles from organ donor duodenum. Brush border membrane vesicles formed from peroral duodenal biopsies likewise demonstrate Na^+ dependent concentrative uptake of D-glucose and L-leucine. This is the first demonstration of active transport processes in human duodenum. A simple microvesiculation method to form these vesicles is described as well as its potential application to clinical medicine in studying diseases of defective intestinal transport.
© 1988 Academic Press, Inc.

Introduction: Human small intestine obtained from organ donors has been used to form brush border membrane vesicles for transport studies (1-5). Vesicles obtained from human jejunum and ileum demonstrate active transport of D-glucose and L-leucine in the presence of a Na^+ gradient (6). However, it is not known whether the human duodenum possesses monosaccharide and amino acid transporters similar to the jejunum and ileum. The purpose of the present study was two-fold: 1) to determine if the human duodenum actively transports amino acids and monosaccharides 2) to develop a technique for obtaining brush border membrane vesicles from routine endoscopic duodenal biopsies in order to assess duodenal transport functions.

Methods

Permission for these studies was obtained from the Human Rights and Research Committee of the Medical College of Wisconsin on August 13, 1984.

Brush Border Membrane Vesicles From Organ Donor Intestine

Human duodenal mucosa was obtained from six organ donors at the time of organ retrieval as previously described (1-3). The mucosa was scraped from the seromuscular layer and was stored at -70° C. Purified brush border membranes were obtained from thawed mucosal scrapings by the $CaCl_2$ precipitation method of

0006-291X/88 $1.50
Copyright © 1988 by Academic Press, Inc.
All rights of reproduction in any form reserved.

Schmitz et al (7). Vesiculation was attained by a modification of the procedure of Hopfer et al (8), as previously described by us (1-3). Uptake studies were performed using 50 uM [^{14}C] D-glucose and 50 uM [^{14}C] L-leucine.

Microvesiculation method for endoscopic biopsies

Once the above transport studies had been performed, we formed brush border membrane vesicles from very small amounts of organ donor mucosa utilizing a microvesiculation method (Figure 1). We could form enough membrane vesicles to get a 3 point time course uptake curve for D-glucose and L-leucine using only 100-200 mg of mucosa. We then obtained biopsies from the descending duodenum of three patients; during fiberoptic endoscopy in two and by fluoroscopically controlled aspiration biopsy in the other. The final diagnosis of these patients was functional gastrointestinal disorder; biopsies from each patient showed no histologic abnormalities. The total biopsy weight ranged from 60 to 200 mg. Membrane vesicles were then formed from these biopsies using the same microvesiculation technique developed for small amounts of organ donor mucosa (Figure 1).

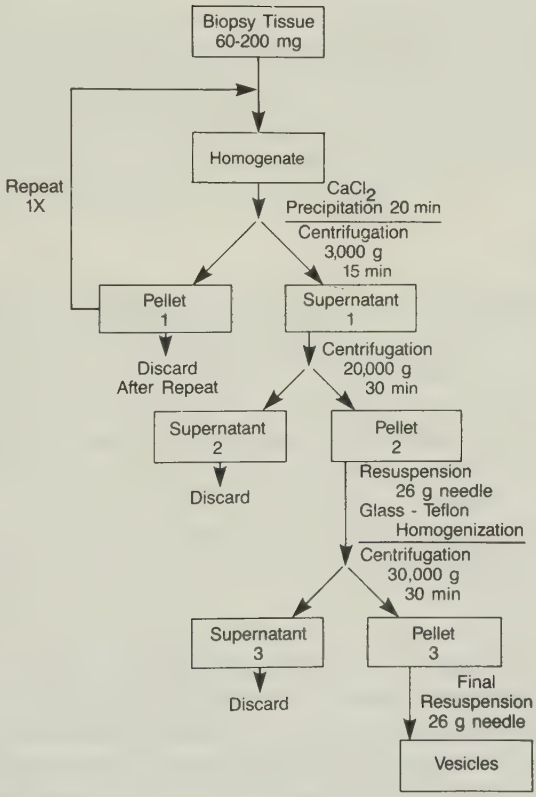

Figure 1: Microvesiculation method for the formation of human intestinal brush border membrane vesicles from peroral endoscopic or suction biopsies. Homogenization is performed in a Polytron homogenizer for 30 seconds at full speed. Homogenization buffer consists of 50 mM mannitol, 2 mM Tris-HCl, (pH 7.0); 1 mM $CaCl_2$ is used for membrane precipitation. Pellet 2 is resuspended in the desired buffer to be loaded into the vesicles.

Uptake Studies

Uptake studies were carried out by the rapid filtration technique of Hopfer et al (8) as previously described (1-3). Briefly, the vesicles were suspended to a final protein concentration of 5-10 mg/ml. Membrane protein was measured by the method of Lowry et al (9). Incubation media contained the following in a 250-ul final volume: 10 mM Tris-HEPES (pH 7.5), 150 mM NaCl, and 50 uM of either radiolabeled D-glucose or L-leucine. Studies were initiated by the addition of vesicles containing 250-750 ug of membrane protein into a tenfold dilution of incubation medium containing 50 uM of radiolabeled substrate and were conducted at room temperature. At specified time intervals, 50-ul aliquots of the reaction mixture were transferred to a cold (0°C) stop solution (composition equal to the incubation media and containing [^{3}H]-L-glucose to correct for incomplete washing of the [^{14}C] substrates) and filtered on wetted 0.45 um membrane filters. The filters were washed with 4 ml of ice-cold rinse solution of the same composition as the stop solution but containing no [^{3}H]-L-glucose and were processed for dual isotope counting as previously described (1). There was negligible nonspecific binding of any of the labeled substrates to either the membranes or the nitrocellulose filters. Results are expressed as picomoles of uptake per milligram of membrane protein (1). Using different membrane preparations, qualitatively identical results are obtained but because of variations in the equilibrium uptake values, results of representative experiments are shown.

Measurement of sucrase enrichment from the mucosal homogenate to the purified membrane vesicle pellets was done by the method of Dahlqvist et al (10). D-[U-^{14}C] glucose, L-[U-^{14}C] leucine and L-[^{3}H] glucose were obtained from New England Nuclear, Boston, MA. All other chemicals were obtained from Sigma Chemical Co., St. Louis, MO.

Results

Sucrase enrichment

Approximate enrichment of sucrase activity from crude mucosal homogenate to final brush border membrane vesicle pellets were as follows: duodenum-20 fold, jejunum-19 fold (both by conventional method); duodenum-16 fold (by microvesiculation method). These enrichments demonstrate excellent purifications of brush border membranes for vesicle studies.

Organ donor membrane vesicles using the standard method: D-glucose and L-leucine uptake

Figures 2 and 3 demonstrate the time course uptakes of representative experiments under sodium gradient conditions for D-glucose and L-leucine respectively into organ donor intestine membrane vesicles. Duodenal brush border membrane vesicles actively transport D-glucose and L-leucine under these conditions. Although the membrane purifications are equivalent, the ratios of duodenal peak uptakes to the final (60 minute) uptakes are somewhat smaller than those in the jejunum. These results, however, demonstrate that there is indeed Na^+-dependent secondary active transport of D-glucose and L-leucine by the human duodenum similar to the human jejunum and ileum (6).

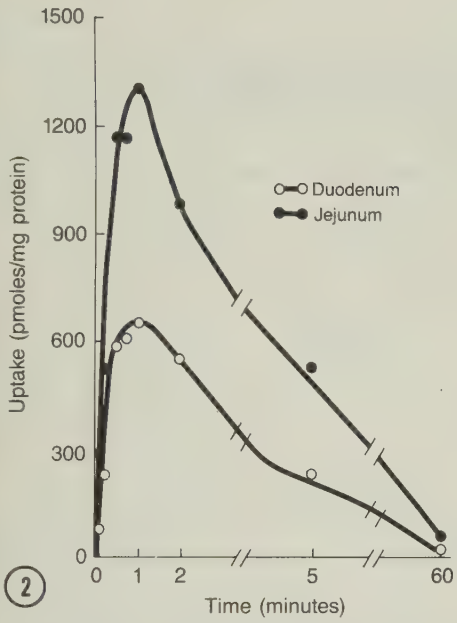

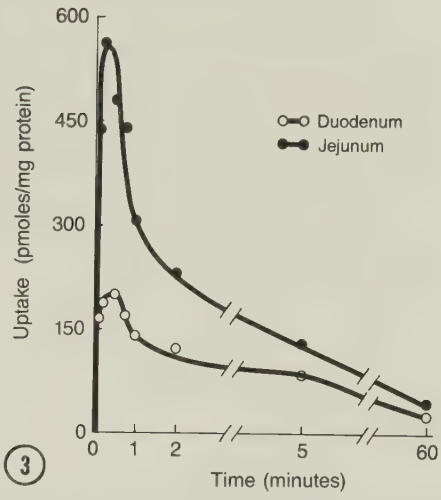

Figure 2: Uptake of [^{14}C] D-glucose into brush border membrane vesicles obtained from organ donor intestine. Vesicles were loaded with 150 mM KCl, 10 mM Tris-HEPES buffer (pH 7.5). Extravesicular incubation medium consisted of 150 mM NaCl, 10 mM Tris-HEPES (pH 7.5) and 50 uM [^{14}C] D-glucose.

Figure 3: Uptake of [^{14}C] L-leucine into brush border membrane vesicles obtained from organ donor intestine. Vesicles were loaded with 150 mM KCl, 10 mM Tris-HEPES buffer (pH 7.5). Extravesicular incubation medium consisted of 150 mM NaCl, 10 mM Tris-HEPES (pH 7.5) and 50 uM [^{14}C] L-leucine.

Duodenal biopsy membrane vesicles using the microvesiculation method: D-glucose and L-leucine uptake

Table 1 shows the uptake of D-glucose and L-leucine into duodenal vesicles prepared from small amounts (200 mg) of organ donor mucosa using the microvesiculation method. The vesicles were loaded with 150 mM choline chloride (instead of KCl) to demonstrate the effects of an inward Na^+ versus a K^+ gradient. All other transport conditions are similar to Figures 2 and 3. The data in Table 1 demonstrate concentrative uptake at 0.5 minutes well above equilibrium (at 60 minutes) with a Na^+ gradient (but not with a K^+ gradient) for D-glucose and L-leucine. Uptakes of D-glucose and L-leucine under Na^+ gradient conditions were actually higher than those obtained using the standard vesiculation method, demonstrating that the microvesiculation technique is suitable for very small amounts of mucosa.

Table 2 shows the time course uptakes for D-glucose and L-leucine, respectively, under sodium gradient conditions into brush border membrane vesicles formed from duodenal biopsies.

Table 1

Na^+ DEPENDENT D-GLUCOSE AND L-LEUCINE INTO HUMAN ORGAN DONOR MUCOSA BRUSH BORDER MEMBRANE VESICLES (MICROVESICULATION TECHNIQUE)

	(4 Different Preparations) Uptake (picomoles/milligram protein)		
Time (minutes)	0.1	0.5	60
D-glucose			
Na^+	345 ± 32	693 ± 66	128 ± 15
K^+	23 ± 1	36 ± 3	102 ± 8
L-leucine			
Na^+	300 ± 38	445 ± 67	183 ± 15
K^+	90 ± 11	181 ± 18	172 ± 12

All three biopsy preparations demonstrated concentrative uptake of D-glucose and L-leucine. The small amount of material allowed only 3 time points to be studied for each substrate, thus no figure is given. The intervals at 0.1, 0.5 and 60 min, were chosen to demonstrate concentrative uptake based on the results shown for organ donor vesicles as in Figs. 2 and 3. Vesicle loading and "incubation" buffers were similar to those in Figures 2 and 3. Concentrative uptake of D-glucose and L-leucine into the membrane vesicles well above the final equilibrium point at 60 minutes is again demonstrated indicating Na^+ activated carrier mediated uptake. In fact, these uptakes using the microvesiculation procedure on biopsies are of equal if not greater magnitude to those obtained with the conventional method using organ donor mucosa (Figures 2,3 and Table 1). These studies show that functional duodenal membrane vesicles can be prepared from clinical biopsy material.

Table 2

Na^+ DEPENDENT D-GLUCOSE AND L-LEUCINE TRANSPORT INTO HUMAN DUODENAL BIOPSY BRUSH BORDER MEMBRANE VESICLES (MICROVESICULATION TECHNIQUE)

	(3 Different Preparations) Uptake (picomoles/milligram protein)		
Time (minutes)	0.1	0.5	60
D-glucose	895 ± 290	1565 ± 300	244 ± 58
L-leucine	440 ± 60	617 ± 36	280 ± 53

Discussion

This study demonstrates that the human duodenum is capable of secondary active transport of neutral amino acids and D-glucose under sodium gradient conditions. This is the first direct demonstration of active transport processes in the human duodenum. The magnitude of these processes at the membrane level is somewhat less in the duodenum than in the jejunum. This data is potentially relevant in the treatment of patients with short bowel syndrome where the duodenum is intact and may serve as an organ for adaptive absorption of nutrients and sodium. The present study also demonstrates that vesicles formed from biopsy material are comparable or superior to organ donor intestinal vesicles prepared from much greater amounts of mucosal tissue.

Endoscopic duodenal biopsies have been shown to be histologically equivalent to proximal jejunal biopsies in their diagnostic accuracy for diseases such as celiac sprue (11). We have demonstrated in this study that these biopsies are qualitatively the functional equivalent of jejunal biopsies. (This has been attempted in one other instance using only jejunal biopsies, but no active transport was demonstrated and the very low uptakes were likely a result of vesicle swelling since the vesicles were loaded with mannitol) (12). These findings have important ramifications for the study of small intestinal dysfunction in conditions such as sprue (13), chronic alcoholism (14) and diabetes (15) where there may be abnormal glucose and amino acid uptake related to altered transporter density or function. This technique may also be applied to the study of patients with inborn defects of amino acid transport such cystinuria (16), Hartnup's disease (17) and dicarboxylic aminoaciduria (18). Recently, the human duodenum has been shown to secrete bicarbonate in vivo thereby protecting the mucosa from damage due to hydrochloric acid. This capacity to secrete HCO_3 appears to be decreased in patients with duodenal ulcer disease (19). Thus, vesicles formed from duodenal ulcer patients may allow the characterization of defects in their HCO_3 transport system. Finally, biopsy-derived brush border membrane vesicles will be useful in assessing functional aspects of small intestinal transplantation in animals (20) and man. In conclusion, we demonstrate active transport processes for glucose and neutral amino acids in human duodenum. Using this information, we present a simple method to assess proximal intestinal transport function in patients using material easily obtained from routine clinical procedures.

Acknowledgments

The authors thank Dr. Mark Adams for procurement of the organ donor intestine, Dr. Michael Weil for his helpful

suggestions and Ms. Lynette McCall for her assistance in manuscript preparation. This study was supported by NIH grants 1-T32-AM07267 and AM33349 and the Veterans' Administration.
Direct reprint requests to: James M. Harig, M.D., Clinical Nutrition Research Unit (Gastroenterology Section), University of Chicago Hospitals, Box 223, 5841 S. Maryland Avenue, Chicago, IL 60637.

References

1. Rajendran, V.M., Ansari, S.A., Harig, J.M., Adams, M.B., Khan, A.H., and Ramaswamy, K. (1985) Gastroenterology 89:1298-1304.
2. Rajendran, V.M., Harig, J.M., Adams, M.B., and Ramaswamy, K. (1987) Am J Physiol 252 (Gastrointest Liver Physiol 15): G33-G39.
3. Harig, J.M., Rajendran, V.M., Barry, J.A., and Ramaswamy, K. (1987) Biochim Biophys Acta 903:358-364.
4. Said, H.M., Ghishan, F.K., and Redha, R. (1987) Am J Physiol 252 (Gastrointest Liver Physiol 15): G229-G236.
5. Barnard, J.A., and Ghishan, F.K. (1987) Gastroenterology 93:925-933.
6. Harig, J.M., Barry, J.A., Rajendran, V.M., Soergel, K.H., and Ramaswamy, K (1986) Gastroenterology 90:1450.
7. Schmitz, J., Preiser, H., Maestracci, D., Ghosh, B.K., Cerda, J.J., and Crane, R.K. (1973) Biochim Biophys Acta 323:98-112.
8. Hopfer, U., Nelson, K., Perotto, J., and Isselbacher, K.J. (1973) J Biol Chem 1973; 248:25-32.
9. Lowry, O.H., Rosebrough, N.J., Farr, A.L., and Randall, R.J. (1951) J Biol Chem 193:265-275.
10. Dahlqvist, A. (1964) Anal Biochem 7:18-25.
11. Mee, A.S., Burke, M., Vallon, A.G., Newman, J., and Cotton, P.B. (1985) Brit Med J 291:769-772.
12. Booth, I.W., Murer, H., Stange, G., Fenton, T.R., and Milla, P.J. (1985) Lancet 1:1066-1069.
13. Cole, S.G., Kagnoff, M.F. (1985) Celiac disease. Ann Rev Nutr 5:241-66.
14. Krasner, N., Cochran, K.M., Russell, R.I., Carmichael, H.A., and Thompson, G.G. (1976) Gut 17:245-8.
15. Vinnik, I.E., Kern, F., and Sussman, K.E. (1965) J Lab Clin Med 66:131-6.
16. Silk, D.B.A., Perrette, D., and Clark, M.L. (1975) Gastroenterology 68:1426-32.
17. Leonard, J.V., Marra, T.C., Addison, J.M., et al. (1976) Pediatr Res 10:246-9.
18. Melancon, S.B., Dallaire, L., Lemieux, B., Robitoille, P., and Rotier, M. (1977) J Pediatr 91:422-7.
19. Isenberg, J.I., Selling, J.A., Hogan, D.L., and Koss, M.A. (1987) N Engl J Med 1316:374-379.
20. Nemeth, M.A., Harris, M.S., Ramaswamy, K. et al. (1987) Dig Dis Sciences 32:923.

Vol. 156, No. 1, 1988 BIOCHEMICAL AND BIOPHYSICAL RESEARCH COMMUNICATIONS
October 14, 1988 Pages 171-179

THREE GROWTH HORMONE- AND TWO PROLACTIN-RELATED NOVEL PEPTIDES of M_r 13,000-18,000 IDENTIFIED IN THE ANTERIOR PITUITARY

Y.N. Sinha and B.P. Jacobsen

The Lutcher Brown Department of Biochemistry
The Whittier Institute for Diabetes and Endocrinology
Scripps Memorial Hospital
La Jolla, CA 92037

Received August 24, 1988

SUMMARY: Electrophoretic analysis of murine anterior pituitary extract revealed five major proteins of M_r 13,000-18,000 (designated P13, P14, P16, P17, and P18 according to M_r), three of which, P16, P17, and P18, were markedly influenced by estradiol benzoate and perphenazine in a manner similar to that of growth hormone, and two, P13 and P14, to that of prolactin. Tyrosine peptide mapping showed partial resemblance of fingerprints for P16 and P17 (and possibly P18) to those for growth hormone, and of P13 and P14 to those for prolactin. Both P14 and P18 bound to Concanavalin A. None of the peptides crossreacted with antibodies to growth hormone or prolactin. The concentrations of P13 and P14 in pituitaries from lactating rats and in a prolactinoma were distinctly higher than normal. All five peptides were secreted into the medium during *in vitro* incubation. These results suggest that P16, P17 and P18 are growth hormone- and P13 and P14 prolactin-related secretory proteins of the pituitary. © 1988 Academic Press, Inc.

GH and PRL are the two major proteins of the anterior pituitary, which together constitute 5-10% of the total adenohypophyseal protein. Analysis of the pituitary tissue by SDS-PAGE shows five other very conspicuous bands that range in M_r from 13,000-18,000. Although these low M_r proteins can be seen in the pituitary glands of a variety of species (1, 2), their identity and chemical nature are not known. Since they are present in such large amounts in the pituitary, and since their concentrations vary among species, we examined them with physiological, structural and immunological means to determine their biological significance. Our findings suggest that these major constituents of the pituitary are secretory peptides, three of which are related to GH, and two to PRL, in regulation and structure.

Abbreviations used are: SDS-PAGE, sodium dodecyl sulfate-polyacrylamide gel electrophoresis; GH, growth hormone; PRL, prolactin; 2-ME, 2-mercaptoethanol; Con A, Concanavalin A; NTC, nitrocellulose; RIA, radioimmunoassay.

0006-291X/88 $1.50
Copyright © 1988 by Academic Press, Inc.
All rights of reproduction in any form reserved.

MATERIALS AND METHODS

Animals and Tissues. S/A strain rats (Simonsen Laboratories, Gilroy, CA) and C3H/St and C57BL/6J strain mice (Scripps Clinic and Research Foundation, La Jolla, CA) were housed in controlled environment (12 hr light, 12 hr darkness; temperature 24 ± 1°C), and fed Wayne Lab Blox and water *ad libitum*. Anterior pituitary glands were obtained after decapitation and were washed 3-4 times with cold normal saline before being homogenized in Laemmli's sample buffer (3) in the ratio of 20 mg/ml. The homogenates were heated in boiling water for 3 min and then centrifuged at 1,000 x *g* for 15 min. The supernatants were stored at -20°C until analyzed by SDS-PAGE.

Physiological experiments.

(i) Effect of sex steroids. Rats and mice were assigned at random to one of the following groups: a) intact males, b) intact females, c) castrated females, d) castrated females plus estradiol benzoate (10 μg for rats, 1 μg for mice), e) intact females plus progesterone (5 mg), f) intact females plus estradiol benzoate and progesterone, g) intact females plus testosterone (500 μg). All steroids were dissolved in sesame oil. Castration was performed under light ether anesthesia. Injections were started 2 weeks after castration and were given once daily, sc, for 2 weeks.

(ii) Effect of perphenazine. Adult female rats of the S/A strain were given a single ip injections of perphenazine (1 μg/g BW) and were killed 0, 0.5, 1, and 2 hr after injection.

(iii) Effect of nursing. Primiparous rats of the S/A strain were separated from their litters for 15 hr on days 10-12 of lactation. Half of the mothers were then decapitated without nursing; the other half were allowed to nurse their young for 1 hr before decapitation.

(iv) Prolactinoma tissue. Normal and adenomatous tissues were obtained by transsphenoidal surgery from a 31 year old woman who had a long history of hyperprolactinemia and galactorrhea.

Gel electrophoresis. SDS-PAGE was performed in 1.5-mm thick and 12-cm long slab gels of 12% acrylamide using the buffer system of Laemmli (3). The gels were stained with Coomassie brilliant blue R.

Quantitation of protein bands. The amount of protein in the gel bands was determined by the method of Ball (4).

Western blotting. The method described by Burnett (5) was used. Murine proteins, electroeluted from gels, were re-electrophoresed, transferred onto NTC, and immunostained. For immunostaining, a highly specific monkey anti-murine GH serum (6) and a rabbit anti-mouse PRL serum that also crossreacts with rat PRL (7) were used at a 1:1,000 dilution. ^{125}I-labeled Protein A was used to visualize GH- and PRL-immunoreactive bands.

Peptide mapping. The method of Elder *et al*. (8) was used. The major peptides revealed are only those that contain tyrosine residues, but the patterns obtained are quite characteristic for a given protein.

In Vitro Incubation. Anterior pituitaries were incubated at 37°C in an atmosphere of 95% O_2 and 5% CO_2 in medium 199 (Grand Island Biological Co., Grand Island, NY), alone or in a 1:10 combination with Krebs-Ringer-Bicarbonate buffer, pH 7.4, using 0.05 ml incubation medium for each mg of tissue. At the end of either 6 or 16 hr, pituitary glands were removed, extracted as described above, and stored at -20°C for electrophoresis. The incubation medium was dialyzed against water to remove salts, lyophilized, and stored at -20°C for electrophoresis or lectin affinity chromatography.

Con A affinity chromatography. Dialyzed and lyophilized incubation medium was reconsituted in 0.01M NH_4HCO_3 and fractionated on a Con A-Sepharose 4B column, as described (9).

Bioassay. Pigeon crop sac-stimulating activity of murine P13 and P14 eluates was tested by the method described by Nicoll (10).

Statistics. Analysis of variance and Duncan's new multiple range test were used for evaluating the significance of differences among treatment means.

RESULTS

Fig. 1a,b shows the effects of sex steroids on GH, PRL, and on each of the five low M_r proteins, designated P13, P14, P16, P17 and P18, the numbers

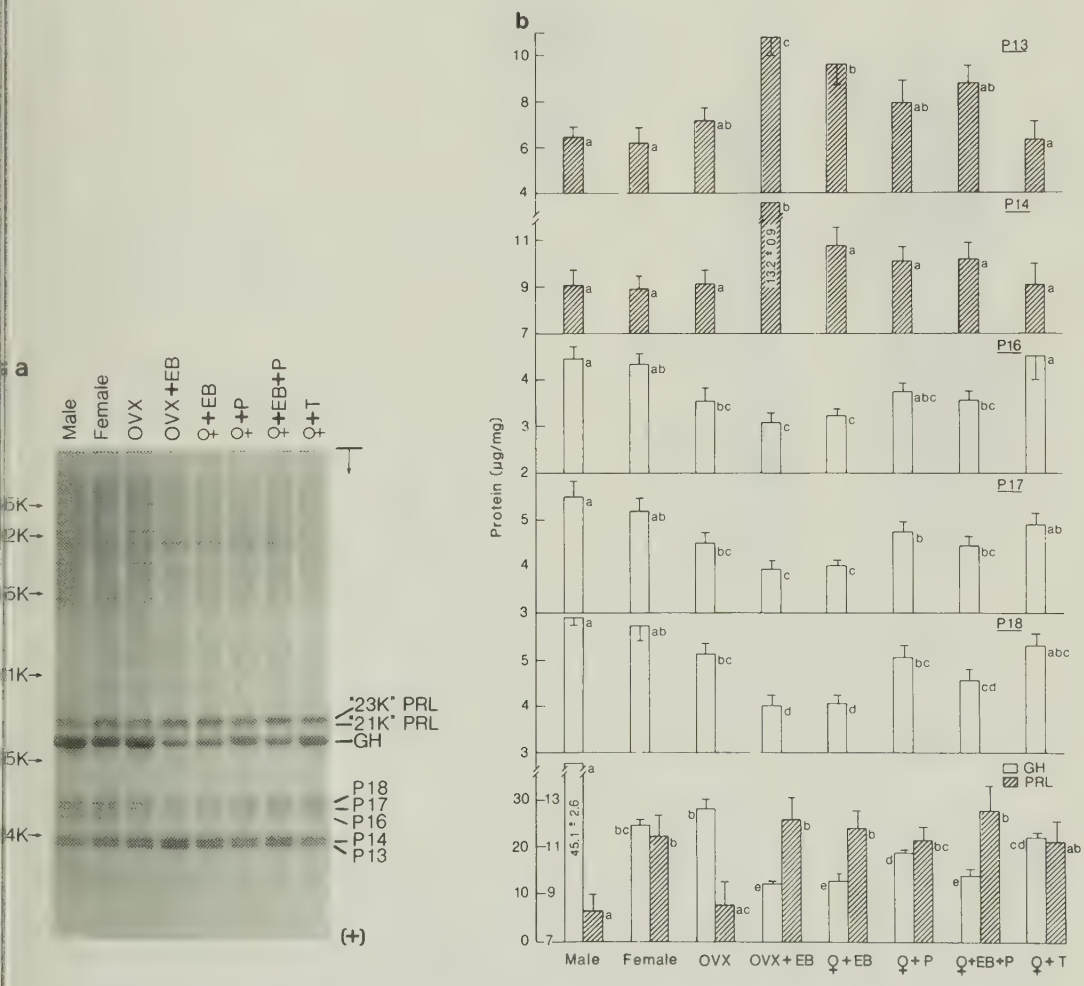

Fig. 1a. Effects of sex steroids on the low M_r proteins of the rat adenohypophysis. A 0.1 mg equivalent sample of tissue from pooled pituitary extract from each group was electrophoresed in a lane. The gel was stained with Coomassie blue. OVX = ovariectomized; EB = estradiol benzoate; P = progesterone; T = testosterone. At the time of sacrifice, the rats were approximately 90 days of age. "21K" PRL refers to a new PRL variant described recently (15).

Fig. 1b. Quantitative data for the results in Fig. 1a. Each bar is the average of 10 rats. The vertical lines represent the standard errors of the means. In the bottom panel, the outside ordinate scale pertains to GH, the inside, to PRL. The alphabetical superscripts at the top of the bars indicate statistical significance; for a given parameter, means with common superscripts are statistically not different from one another ($P > 0.05$).

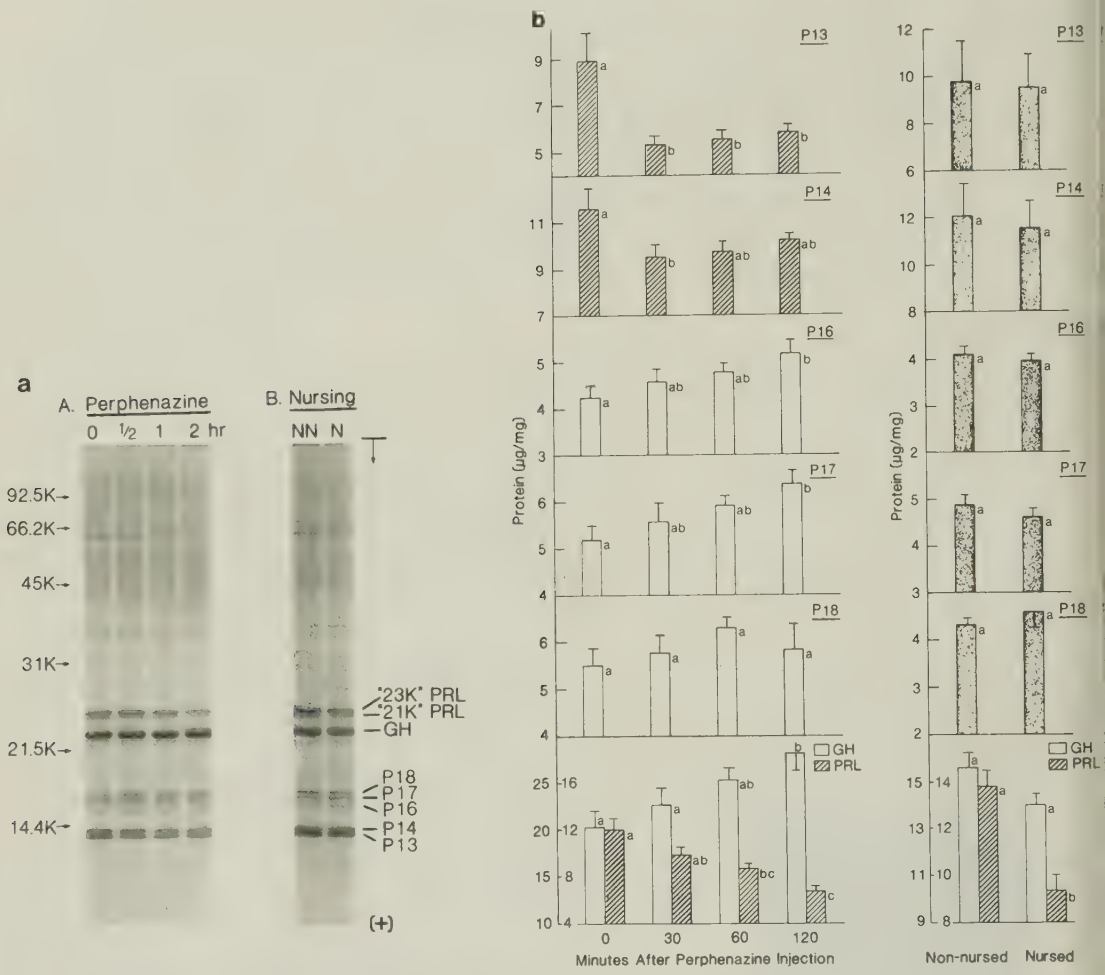

Fig. 2a. Effects of perphenazine and nursing on the low M_r proteins of the rat adenohypophysis. The rats were 108 days old at the time of the experiment. N = nursed; NN = non-nursed.

Fig. 2b. Quantitative data for the results in Fig. 2a. Each bar is the average of 8 rats. Refer to the legend of Fig. 1b for an explanation of the statistical notations.

denoting their approximate molecular mass in kilodaltons. Per mg of tissue, murine pituitary averaged 20-30 µg GH, 8-10 µg PRL, and 4-8 µg low M_r proteins. As is well known from previous work, female pituitaries contained more PRL and less GH than male pituitaries. Ovariectomy decreased the concentrations of PRL in the pituitary glands, with no sigificant changes in GH concentrations. Estradiol benzoate produced opposite effects on the two hormones: either alone or in combination with progesterone, it increased PRL concentrations but at the same time drastically reduced GH concentrations. These converse effects of estradiol benzoate were correspondingly reproduced in the case of the new proteins: the concentrations of P16, P17, and P18 were markedly reduced while those of P13 and P14 were dramatically increased. Progesterone, testosterone, or the sex of the animal had no significant effects on any of the new proteins.

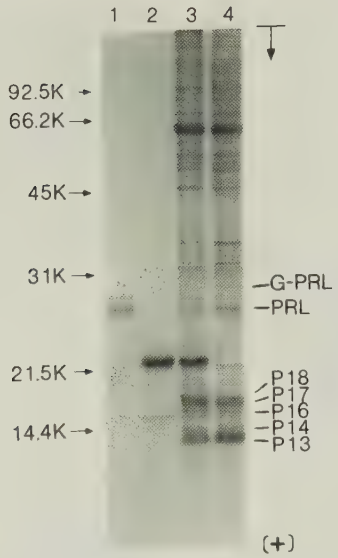

Fig. 3. Concentrations of the low M_r proteins in a human prolactinoma. Lane 1 = human PRL (Lewis 405-63-4), 25 μg; lane 2 = human GH (Lewis 201-86-3), 25 μg; lane 3 = normal pituitary tissue, 0.5 mg equivalent; lane 4 = tumorous pituitary tissue, 0.5 mg equivalent.

Fig. 2a,b shows the effects of perphenazine, a dopamine antagonist, which causes a massive release of PRL and a shut-down of GH release in the mouse (11). As expected, a single injection of the neuroleptic produced a step-wise decrease in PRL and a reciprocal increase in pituitary GH concentrations. Again, the new peptides P16 and P17 beautifully mimicked the changes observed for GH, as peptides P13 and P14 did for PRL. In contrast, acute nursing, which caused a 32% reduction in PRL concentrations and a small (9%) but insignificant drop in GH, had no appreciable effects on any of the five proteins, which speaks for the functional specificity of the new proteins. However, the concentrations of P13 and P14 were significantly greater in lactating (panel B) than in non-lactating (panel A) rats.

Fig. 3 depicts a comparison of these proteins in normal and prolactinoma tissues from a human pituitary. The prolactinoma tissue was characterized by complete absence of a GH band and a greater than normal concentration of PRL. The concentrations of P13 and P14, particularly that of P13, were also higher in the prolactinoma tissue, which indicated a common cellular origin for PRL and the two smaller peptides. On the other hand, despite the absence of a GH band, the GH-related peptides P16, P17, and P18 were present in the prolactinoma tissue, which indicated that these three peptides could be produced in non-GH-producing cells.

Fig. 4 presents the tyrosine peptide maps of the five proteins from murine and human glands and some purified preparations of GH and PRL. The fingerprint of rat P13 was similar to that of rat P14, as was the fingerprint of human P17 to human P18. Furthermore, fingerprints of the murine and human pep-

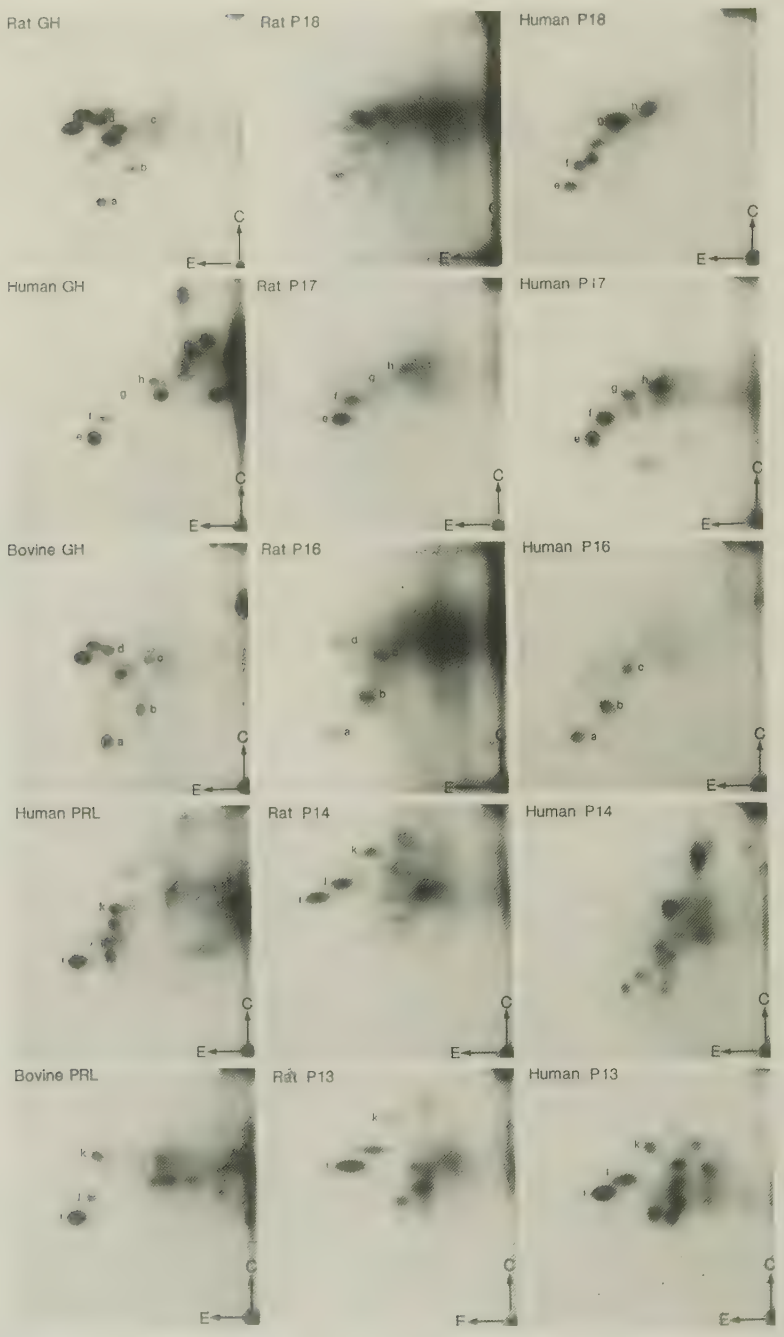

Fig. 4. Tyrosine peptide maps of the low M_r proteins from rat and human pituitaries and some GH and PRL standards. Arrows indicate the directions of electrophoresis (E) and chromatography (C).

tides exhibited easily discernible resemblances to one another in the case of three peptides, P13, P16, and P17; in the case of P14 and P18, the similarity was not so apparent. In comparison to known hormonal proteins, the migration patterns of spots a, b, c, and d of murine and human P16 exhibited striking resemblance to similar spots for bovine and murine GH. The arc-like formation

of spots e, f, g, and h of P17, in both murine and human protein, and of P18 in human protein, showed partial resemblance to a similar arrangement of spots in the human GH fingerprint. The migration patterns of spots i, j, and k of murine and human P13, and of murine P14, matched the migration patterns of similar spots in bovine and human PRL. Fingerprints of murine P18 and human P14 showed no obvious resemblance to the fingerprints of any of the purified hormones examined. Nor did the fingerprints of the new proteins resemble fingerprints of the fragments of cleaved GH or cleaved PRL (data not presented).

We then attempted to determine the immunological crossreactivity of the peptides with GH and PRL antibodies. The electroeluted murine proteins failed to crossreact with RIA-grade polyclonal antibodies to GH and PRL (data not presented). The electroeluted proteins from murine P13 and P14 bands exhibited no biological activity in the pigeon crop sac bioassay for PRL (data not presented).

Fig. 5 shows the results of *in vitro* incubation. Both GH and PRL were secreted into the medium, PRL more so than GH, in agreement with previously well-documented observations. Each of the five peptides also was present in the incubation medium, P13 in visibly greater concentration than the others. Furthermore, as we had observed in Fig. 1a, the concentrations of GH, PRL and the new peptides in the incubation medium appeared variously influenced by the sex of the animal, by ovariectomy, and by estradiol benzoate treatment.

When the incubation medium was fractionated through a Con A-Sepharose B column, P13, P15, and P17 passed unretarded, but P14 and P18 were markedly

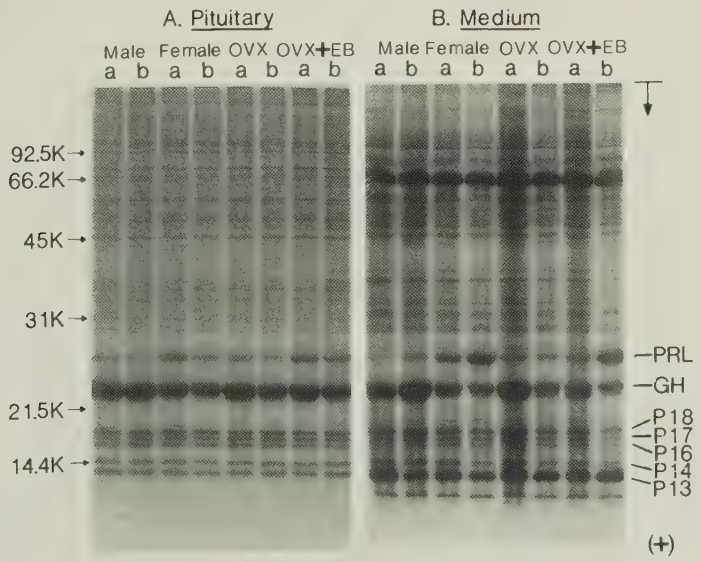

Fig. 5. *In vitro* incubation of murine pituitary for 6 hr. a = C3H/St strain; b = C57BL/6J strain. The mice were 75 days of age at the time of sacrifice. A: extract of 0.5 mg equivalent pooled pituitary tissue from each group was applied in a lane; B: medium from 10 mg anterior pituitary tissue was applied in each lane.

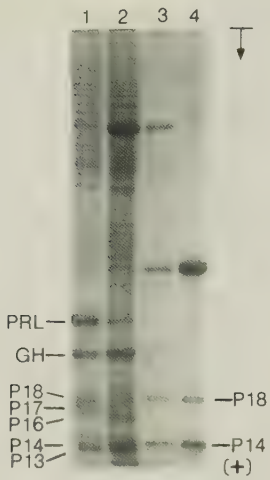

Fig. 6. Determination of the glycoprotein nature of the low M_r proteins by lectin-affinity chromatography. Medium from 16 hr incubation of 10 male rat anterior pituitaries was fractionated on a Con A-Sepharose 4B column. Lane 1 = pituitary extract; lane 2 = starting material; lane 3 = unretained fraction; lane 4 = retained fraction.

retained, and subsequently could be eluted with methyl-α-D-mannopyranoside (Fig. 6). These results indicated a glycoprotein nature for P14 and P18. Since the fingerprint of murine P14 is quite similar to that of P13, P14 may represent glycosylated P13. The same relationship could exist between P17 and P18, but the fingerprint data were not that clear-cut in this case.

DISCUSSION

Although the low M_r proteins described here are always encountered in pituitary extracts during SDS gel electrophoresis, they have remained largely unexplored. Our measurements show that they are present in the pituitary in relatively large amounts, next only to GH and PRL. Furthermore, they are subject to regulatory control, their concentrations varying under the influence of differing physiological and pharmacological stimuli. Also, they seemed to be secreted from the cell, as evidenced by their ample discharge into the medium when the pituitary was incubated *in vitro*, and by the marked drop in the concentrations of P13 and P14 when perphenazine was injected. Thus, these pituitary constituents represent not cytoskeletal proteins, but rather hitherto uncharacterized secretory peptides of the pituitary.

Induction of GH- and PRL-like changes by GH- and PRL-influencing agents, such as estradiol benzoate and perphenzine, and partial resemblance in their tyrosine peptide maps, suggest that P16, P17, and P18 are related to GH, and P13 and P14, to PRL. High concentrations of P13 and P14 in lactating rat pituitaries and in a PRL-secreting adenoma further support this conclusion. Another implicating fact is the Con A-binding property of P14 and P18, one peptide from each of the two hormone groups, which is analogous to the recently

iscovered glycosylated variants of GH (12-14) and PRL (9). Whether the new peptides are fragments of GH and PRL or whether they only share common sequences with them is not clear from our results. Purification and sequencing of the peptides are needed to determine that. However, occurrence of P16, P17, and P18 in prolactinoma tissue devoid of GH and failure of acute nursing to alter P13 and P14 concentrations suggest that they are most likely produced by genes other than those for GH and PRL. The lack of immunological crossreactivity of the peptides with GH and PRL antibodies is also suggestive of this possibility.

It is not known whether the peptides have any biological action. The fact that their pituitary concentrations were altered within a relatively short time, such as only 30 min after an injection of perphenazine, suggests that they are important modulators of physiological function in the organism. Substantial increments in concentrations of the PRL-related peptides during lactation and after neoplastic transformation of the cell also imply a physiological role. The roles most likely differ from the known functions of GH and PRL, however, since the concentrations of the PRL-related peptides P13 and P14 did not change after acute nursing, despite a precipitous drop in PRL concentrations. Nor did these peptides stimulate the crop sac of the pigeon. Further work will shed light on the biological importance of these newly-recognized pituitary secretion products.

ACKNOWLEDGMENTS

This research was supported by NIH grant DK 32311. We are grateful to the NIDDK for the gift of purified GH and PRL preparations and to Dr. K. Ott of Scripps Memorial Hospital for the human prolactinoma tissue used in this study. Our special thanks to Anita Sinha for technical assistance, Eileen F. VanderLaan for editorial work, and Pamela Ann de Lopez for the graphics and typing of the manuscript.

REFERENCES

1. Sinha, Y.N. and Gilligan, T.A. (1985) Proc. Soc. Exp. Biol. Med. 178:505-514.
2. Sinha, Y.N., Ott, K., and VanderLaan, W.P. (1987) Am. J. Med. Sci. 30:15-25.
3. Laemmli, U.K. (1970) Nature (London) 227:680-685.
4. Ball, E.H. (1986) Analyt. Biochem. 155:23-27.
5. Burnett, W.N. (1981) Analyt. Biochem. 112:195-203.
6. Sinha, Y.N., Selby, F.W., Lewis, U.J., and VanderLaan, W.P. (1972) Endocrinology 91:784-792.
7. Sinha, Y.N., Selby, F.W., Lewis, U.J., and VanderLaan, W.P. (1972) Endocrinology 91:1045-1053.
8. Elder, J.H., Pickett II, R.A., Hampaton, J., and Lerner, R.A. (1977) J. Biol. Chem. 252:6510-6515.
9. Lewis, U.J., Singh, R.N.P., Lewis, L.J., Seavey, B.K., and Sinha, Y.N. (1984) Proc. Natl. Acad. Sci., USA 81:385-389.
10. Nicoll, C.S. (1967) Endocrinology 80:641-655.
11. Sinha, Y.N., Salocks, C.B., and VanderLaan, W.P. (1975) Endocrinology 97:1112-1122.
12. Sinha, Y.N. and Lewis, U.J. (1986) Biochem. Biophys. Res. Commun. 140:491-497.
13. Sinha, Y.N. and Jacobsen, B.P. (1987) Biochem. Biophys. Res. Commun. 145:1368-1375.
14. Berghman, L.R., Lens, P., Decuypere, E., Kuhn, E.R., and Vandesande, F. (1987) Gen. Comp. Endocrinol. 68:408-414.
15. Sinha, Y.N. and Jacobsen, B.P. (1988) Endocrinology 123:1364-1370.

Vol. 156, No. 1, 1988 BIOCHEMICAL AND BIOPHYSICAL RESEARCH COMMUNICATIONS
October 14, 1988 Pages 180-185

DOMAIN STRUCTURE OF CELLOBIOHYDROLASE II AS STUDIED BY SMALL ANGLE X-RAY SCATTERING: CLOSE RESEMBLANCE TO CELLOBIOHYDROLASE I

Peter M. Abuja[1], Ingrid Pilz[1*], Marc Claeyssens[2], and Peter Tomme[2]

[1]Institut für Physikalische Chemie, Karl-Franzens Universität Graz, Heinrichstraße 28, A-8010 Graz, Austria

[2]Laboratorium voor Biochemie, Fakulteit Wetenschappen, Rijksuniversiteit Gent, K. L. Ledeganckstraat 35, B-9000 Gent, Belgium

Received June 30, 1988

Evidence for a domain structure of cellobiohydrolase II (CBH II, 58 kDa) from *Trichoderma reesei* (Teeri et al., 1987; Tomme et al., 1988) is corroborated by results from SAXS experiments. They indicate a 'tadpole' structure for the intact CBH II in solution (Dmax = 21.5 ± 0.5 nm; Rg = 5.4 ± 0.1 nm) and a more isotropic, ellipsoid shape for the core protein (Dmax = 6.0 ± 0.3 nm; Rg = 2.1 ± 0.1 nm).

The latter was obtained by partial proteolysis with papain which cleaves the native CBH II to give two fragments (Tomme et al., 1988): the core (45 kDa) with the active (hydrolytic) domain and a smaller fragment (11 kDa) coinciding with the tail part of the model and containing the binding domain for unsoluble cellulose. This peptide fragment is conserved in most cellulolytic enzymes from *Trichoderma reesei* (Teeri et al., 1987). It contains a conserved region (block A) and glycosylated parts (blocks B and B' duplicated and located N-terminally in CBH II).

In spite of different domain arrangements in CBH I (blocks B-A at C-terminals) SAXS measurements (Abuja et al., 1988) indicate similar tertiary structures for both cellobiohydrolases although discrete differences in the tail parts exist.
© 1988 Academic Press, Inc.

*To whom correspondence should be addressed.

Cellobiohydrolase II, core CBH II, small-angle X-ray scattering, functional-structural domains, model for solution structure

Abbreviations: SAXS, small-angle X-ray scattering; cellobiohydrolase (CBH, 1.4-ß-D-glucan cellobiohydrolase, E.C. 3.2.1.91); Dmax: maximum diameter; Rg: radius of gyration

0006-291X/88 $1.50
Copyright © 1988 by Academic Press, Inc.
All rights of reproduction in any form reserved.

The filamentous fungus *Trichoderma reesei* is known to produce a variety of cellulolytic enzymes, among them two types of cellobiohydrolases (CBH I and CBH II, Fägerstam and Pettersson, 1979; van Tilbeurgh et al., 1984). Their primary structures have been elucidated (Shoemaker et al., 1983; ; Teeri et al., 1983; Fägerstam et al., 1984). Both enzymes exhibit a similar action as they adsorb strongly onto insoluble substrates and lack carboxymethylcellulase activity. Differences in specifity may however be noted with respect to the degradation of small, soluble substrates (van Tilbeurgh et al., 1982) and microcrystalline cellulose (Henrissat et al., 1985).

Partial proteolysis of both CBH I and CBH II with papain (van Tilbeurgh et al.,1986, Tomme et al., 1988) cleaves these enzymes in two fragments. The larger fragment (56 kDa for CBH I, 45 kDa for CBH II), called the core protein, contains the catalytic site and the smaller consists of the terminal 35 amino acids long conserved region (block A) and the O-glycosylated regions (B in CBH I,BB' in CBH II). These homologous regions are situated at the C-terminus of CBH I (BA) but at the N-terminus of CBH II (ABB') (Teeri et al., 1987, Tomme et al., 1988). Both cores were fully active against soluble substrates but showed reduced adsorptive and hydrolytic activities against microcrystalline cellulose (Tomme et al., 1988).

SAXS studies on CBH I and its core revealed a tadpole-like structure of the intact enzyme and permitted the identification of the head part of CBH I as the core [Abuja et al., 1988]. The tail part of the tadpole is thus identical with the C-terminal peptide (BA block).

Presently we report on the results obtained with CBH II and its core.

The native CBH II was prepared from the extracellular fluid of *Trichoderma reesei* QM 9414 as reported (van Tilbeurgh et al., 1984) and its core was obtained by partial proteolysis with papain as described (Tomme et al., 1988). The purity of these preparations was checked by SDS-PAGE (CBH II, 58 kDA; core, 45 kDA) and IEF-PAG (CBH II p_i = 5.9; core p_i = 4.4). The molar absorption coefficient (280 nm) is 75000 M^{-1} cm^{-1} for CBH II and is unchanged for the core protein.

Scattering experiments were performed with a Kratky camera (improved compact type) with slit collimation system on a Philips

PW1730 X-ray generator with a copper tube which was operated at 50 kV and 30 mA. Each scattering curve was recorded up to 10 times in the range of h= 0.1 to 5.1 nm^{-1} (h = (4 π sin θ)/ , 2 θ : scattering angle, =0.154 nm , wavelength of the CuK_α - line). Measuring temperature was 4°C. A series of 5 concentrations from 8 to 37 mg/ml was measured for core-CBH II and from 8 to 31 mg/ml for intact CBH II.

Data evaluation, desmearing and indirect Fourier transformation were done as described elsewhere (Glatter, 1977; Glatter and Kratky, 1982; Pilz et al. 1977). Model calculations were performed with the MULTIBODY program (Glatter, 1980).

As for CBH I the intact enzyme is an elongated particle with a head part rich in mass and a long tail. Fig. 1 shows the model and its p(r)-function compared to the experimental p(r)-function (distance distribution function, 4π*p(r) represents the number of distances *r* in a homogenous particle, found by the combination of any volume element with any other within the particle; p(r) becomes zero at Dmax.) . The core protein is more isotropic and about one third of the length of the intact enzyme. The model and its p(r)-function are shown in Fig. 2. Dmax of the intact particle is 21.5 nm ± 0.5 nm, Dmax of the core is 6.0 nm ± 0.3 nm. The radii of gyration found are 5.4 nm ± 0.1 for the intact CBH II and 2.1 nm ± 0.1 for the core. For comparison we give the parameters for

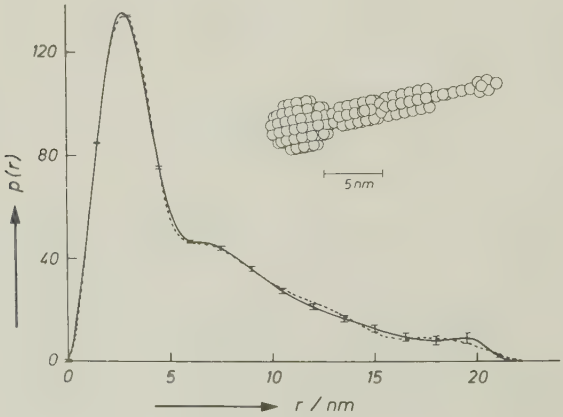

Fig. 1

Model structure and comparison of the experimental and model p(r)-functions of intact CBH II. The functions are normalized to an integral of 10^5.

experimental (———)

model (- - -)

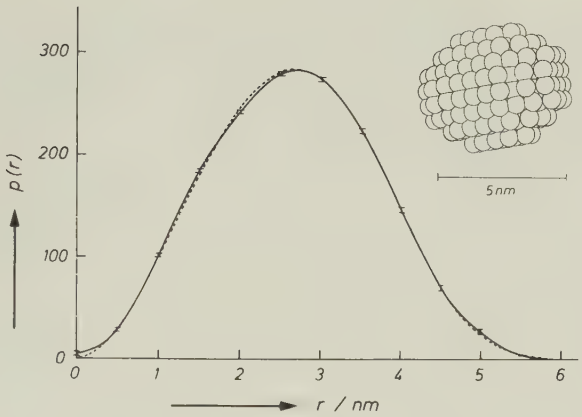

Fig. 2

Model structure and comparison of the experimental and model p(r)-functions of core CBH II. The functions are normalized to an integral of 10^5.

experimental (———)

model (- - -)

CBH I [Abuja et al., 1988]: intact - Dmax = 18.0 ± 0.5 nm, Rg = 4.3 ± 0.2 nm; core - Dmax = 6.5 ± 0.3 nm, Rg = 2.1 ± 0.2 nm.

The resemblance between the CBH II and CBH I models is striking (Fig. 3). Closer examination however reveals significant differences not only in size but also in shape. CBH II is even more elongated with a longer tail part which lacks the distinct "girdle" typical for CBH I. Studies on the primary structure of

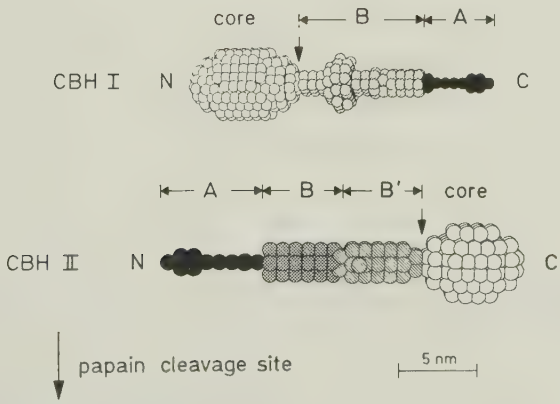

Fig. 3

Comparison between the domain arrangement of CBH I and CBH II. The core part is situated N-teminally in CBH I and C-terminally in CBH II, where block B is duplicated.

both cellobiohydrolases indicate in fact a duplication of the block B in CBH II (Tomme et al., 1988), situated in the tail part. This duplication (BB') is obviously responsible for the additional length of the tail part of CBH II.

For the core best fit was obtained with an ellipsoid with the axial ratios 1.4 : 1.0 : 1.0 which is identical with the head part of intact CBH II and has nearly the same shape and size as the core of CBH I.

Some preliminary function-structure relationships can be deduced from these and previous results. The compact heads (cores) contain the enzymes' active sites, whereas the tails (block BA and ABB') coincide with the binding domains for the insoluble substrate, cellulose.

Since the core proteins have been successfully crystallized (A. Jones, personal communication) more information about the position of the active site relative to these two structurally defined domains may be expected soon. The particular tadpole shape of the intact proteins may then functionally differentiate head (core) domains from the tail parts, the latter operating as 'anchors' to the cellulose. The very strong (nearly irreversible) adsorption of the intact enzymes seem to confirm this hypothesis.

The differences in the shapes of the tails for the two enzymes is a further intriguing observation. Although adsorptive capacities for both enzymes (onto Avicel) are comparable, specific activities are somewhat different. Also CBH I is far more sensitive to product inhibition. The synergistic action of both enzymes on the same substrate is a further peculiarity, which originates undoubtedly from the different adsorptive characteristics and which are presumably linked to the different shapes of the tails. Further investigations of the adsorptive behaviour of these enzymes and their interaction with large soluble substrates, as may be studies by SAXS, are in progress.

Acknowledgements

The work of P.A. was generously supported by the Österreichscher Fonds zur Förderung der Wissenschaftlichen Forschung.

References

Abuja, P.M., Schmuck, M., Pilz, I., Tomme, P., Claeyssens, M. and Esterbauer H., (1988)
Eur. Biophys. J. 15, 339-342

Fägerstam, L.G., Pettersson, L.G. and Engström, J.A. (1984)
FEBS Lett. 167, 309-315

Glatter, O. (1977)
J. Appl. Cryst. 10, 415-412

Glatter, O. (1980)
Acta Phys. Austr. 52, 234-256

Glatter, O. and Kratky, O. eds. (1982)
Small Angle X-rax Scattering
Academic Press London-NewYork

Henrissat, B., Driguez, H., Viet, C. and Schulein, M. (1985)
Bio/Technology 3, 722-726

Pilz, I., Glatter, O. and Kratky, O. (1977)
Meth. Enzymol 61, 148-249

Shoemaker, S., Schweickart, V., Ladner, M., Gelfand, D. Kwok, S., Myambo, K. and Innis, M. (1983)
Bio/Technology 1, 691-696

Teeri, T., Salovuori, I. and Knowles, J. (1983)
Bio/Technology 1, 696-699

Teeri, T., Lehtovaara, P., Kauppinen, S., Salovuori, I. and Knowles, J. (1987)
Gene 51,43-52

van Tilbeurgh, H., Claeyssens, M. and De Bruyne, C.K. (1982)
FEBS Lett. 149, 152-156

van Tilbeurgh, H., Bhikhabhai, R., Pettersson, L.G. and Claeyssens, M. (1984)
FEBS Lett. 169, 215-218

van Tilbeurgh, H., Tomme, P., Claeyssens, M., Bhikhabai, R. and Pettersson, L. G. (1986)
FEBS Lett. 204, 223-227

Tomme, P., van Tilbeurgh, H., Pettersson, G., van Damme, J., Vanderkerckhove, J., Knowles, J., Teeri, T. and Claeyssens, M. (1988)
Eur. J. Biochem. 170, 579,581

Vol. 156, No. 1, 1988 BIOCHEMICAL AND BIOPHYSICAL RESEARCH COMMUNICATIONS
October 14, 1988 Pages 186-192

ENDOTHELIN AND Ca^{++} AGONIST BAY K 8644: DIFFERENT VASOCONSTRICTIVE PROPERTIES

Michel Auguet, Sylvie Delaflotte, Pierre-Etienne Chabrier, Eduardo Pirotzky, François Clostre and Pierre Braquet*

Institut Henri Beaufour

1, avenue des Tropiques, 91952 LES ULIS, France

Received August 25, 1988

The mechanism of vasoconstriction induced by endothelin was investigated in rat isolated aorta in comparison with the Ca^{++} agonist, Bay K 8644. Endothelin (EC_{50}=4 nM) induced a slow and sustained contraction in control medium whereas the one elicited by Bay K 8644 (EC_{50}=14 nM) necessitating a partly K^{+} depolarized medium was fast with superimposed rhythmic contraction. By opposition with Bay K 8644, endothelin contraction was not inhibited by the calcium antagonists (1 μM), nifedipine, diltiazem and D 600, and substantially persisted in Ca^{++} free medium or after depletion of intracellular Ca^{++} by phenylephrine (1 μM). These data show that endothelin does not act as an activator of potential dependent Ca^{++} channels but probably through specific receptor(s) as suggested by its mode of vasoconstriction. © 1988 Academic Press, Inc.

Furchgott and Zawadzki (1) first reported that the relaxing effect of acetylcholine on rabbit aorta was mediated by substance(s) released from the endothelium : the endothelium derived relaxing factor(s) (EDRF). Since this original observation, extensive studies have focused on the role of endothelium in the regulation of the vascular smooth muscle. Recently, Yanagisawa et al. (2) have isolated and identified from porcine aortic endothelial cells a highly potent vasoconstrictor peptide termed endothelin. Considering the properties and the structure of this compound that presents some regional homologies with the amino acid sequence of neurotoxins active on ion channels, it was proposed that endothelin acts as an endogenous agonist of the dihydropyridine sensitive Ca^{++} channels (2). The dihydropyridine derivative Bay K 8644 diametrically opposes the action of calcium antagonists typified by nifedipine and is currently used as slow channel calcium activator (3).

In an attempt to define more precisely the vasoconstriction mechanism of endothelin, we investigated the contractile properties of endothelin in comparison with Bay K 8644 in rat isolated aorta.

*To whom correspondence should be addressed.

0006-291X/88 $1.50
Copyright © 1988 by Academic Press, Inc.
All rights of reproduction in any form reserved.

MATERIALS AND METHODS

Male Sprague Dawley rats (Charles River, Paris, 270 g-360 g) were sacrificed by cervical dislocation and the thoracic aorta removed and cleaned of the surrounding tissue. Rings 2 mm wide were suspended in organ baths containing 10 ml of physiological solution (for composition see below) under a tension of 2 g at 37°C and gassed with 95% O_2 / 5% CO_2. Contractile responses were measured using force displacement transducers (Statham UC2) coupled to a Gould 8000 S polygraph. In some experiments the endothelium was mechanically disrupted by gently rolling a small forceps on the luminal surface of the rings. A 1 h equilibration period was allowed before experimentation.

Normal physiological solution was composed of (mM) : NaCl, 118 ; KCl, 4.7 $CaCl_2$, 2.5 ; KH_2PO_4, 1.2 ; $MgSO_4$, 1.2 ; $NaHCO_3$, 25 ; glucose, 11. The Ca^{++} free-medium, was prepared by substituting $CaCl_2$ with 1 mM EGTA and by reducing Mg_4SO_4 to 0.6 mM. After equilibration in normal medium the preparation was subjected to a near maximal dose (about 95%) of phenylephrine (PE, 1 μM). When the contraction was stable, carbachol (10 μM) was tested in order to test the integrity of endothelium (1).

After this sensitization different procedures were used :

- to study the contraction elicited by endothelin and Bay K 8644 a cumulative dose-response curve was constructed after a rest period of 45 min. In some case KCl (7.3 mM) was added five minutes before the beginning of this cumulative dose-response curve.
- to determine the effects of Ca^{++} channel antagonists four preparations from a given animal were used in parallel. One served as control whereas the three other received calcium antagonists introduced into the bath 30 min before agonist. The maximal contractile effect of each ring that had been subjected to antagonist was determined by comparing the response evoked by the application of sensitizing agent (PE) with that evoked in the control preparation. For experiments using Bay K 8644 as agonist KCl was increased to 12 mM five minutes before the beginning of the cumulative dose-response curve.
- to study the extracellular Ca^{++} dependence of endothelin response, the preparations were washed for 50 min in normal solution followed by 20 min in Ca^{++} free-medium. After agonists induced response $CaCl_2$ (2.5 mM) was added or tissues were washed in Ca^{++} free medium for an additional period of 20 min followed by a second addition of agonist.

Chemicals

Endothelin (human, porcine) corresponding to the 21 amino acid peptidic sequence, was purchased from Peninsula Lab. Inc. (Belmont CA, USA). EGTA, phenylephrine, Angiotensin II, carbachol, diltiazem and nifedipine were from Sigma Chemical Co. (St Louis MO, USA). Bay K 8644 was from Bayer A-G (Leverkusen, FRG) and D600 (gallopamil) was from Knoll A-G (Ludwigshafen, FRG).

Statistics

The data are given as means ± S.E.M. and one way analysis of variance (ANOVA) was used for statistical comparison of the results. CE_{50} were determined graphically.

RESULTS

Contractile responses of endothelin and Bay K 8644

In endothelium denuded rat aorta, the tone induced by endothelin was slow and sustained (Fig. 1). The one elicited by Bay K 8644 was fast with superimposed rhythmic contractions ; moreover high concentrations of Bay K

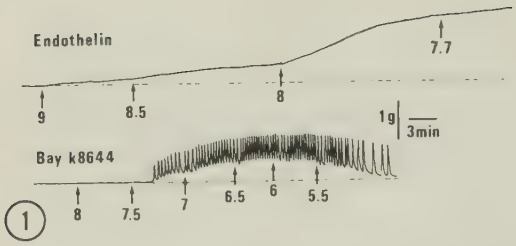

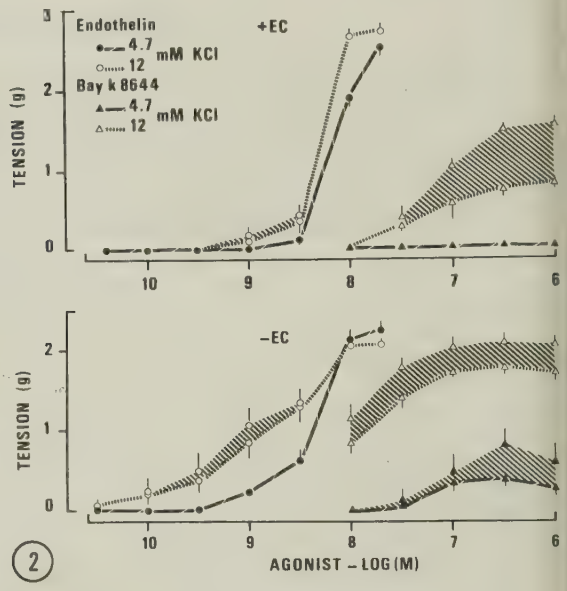

Figure 1 - Representative recordings of contraction produced by endothelin and Bay K 8644 in endothelium free rat aorta incubated in normal medium. Note rhythmic contractions elicited by Bay K 8644.

Figure 2 - Comparison of contraction elicited by endothelin and Bay K 8644 in rat aorta with (+EC, upper panel) and without (-EC, lower panel) endothelial cells. Preparations were incubated in normal (4.7 mM KCl) or partially depolarizing (12 mM KCl) solution. Hatched part indicates rhythmic contractions. Means ± SEM (n = 7).

8644 produced tissue relaxation (Fig. 1). The maximal tension observed with endothelin (2.2 ± 0.11 g, n = 7) was significantly higher than with Bay K 8644 (0.8 ± 0.22 g, n = 7, $p < 0.001$) (Fig. 2). Since full expression of Bay K 8644 required partial membrane depolarization (3,4,5) experiments were also carried out in partially depolarized arteries with K^+ (12 mM). In endothelium free preparations (Fig. 2, -EC), the sensitivity of both agonists was increased. The maximal tension elicited by Bay K 8644 was also greatly enhanced (2.1 ± 0.11 g, n = 7) reaching the level obtained with endothelin. In endothelium intact preparations (Fig. 2, +EC) Bay K 8644 failed to induce any contractile response in normal medium whereas in partly depolarizing medium, it produced a moderate tone superimposed with potent rhythmic contractions. The effect of endothelin was little affected by the presence of endothelium in normal medium or in depolarizing medium.

Effects of Ca^{++} channel antagonists

Fig. 3 shows that on endothelium free aorta Ca^{++} antagonists were very weak inhibitors of the contractile response induced by endothelin (EC_{50} = 4nM). Diltiazem (1 μM), D600 (1 μM) and nifedipine (1 μM) decreased the maximal tension induced by endothelin only by 8 ± 2.7%, 14 ± 1.3% and 16 ±

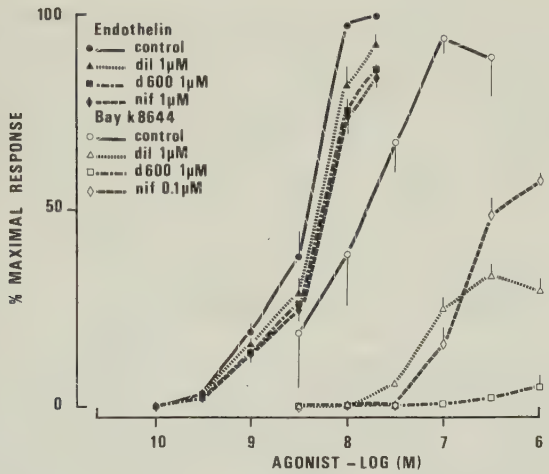

Figure 3 - Effects of diltiazem (dil), D 600 and nifedipine (nif) on the contraction induced by endothelin and Bay K 8644. Experiments using Bay K 8644 as agonist were conducted in partially depolarizing solution. Means ± SEM (n = 5).

2.5%, respectively (n = 5). In contrast, in partly depolarized endothelium free aorta, diltiazem (1 μM) reduced (66 ± 3.0% inhibition, n = 5) and D600 (1 μM) nearly abolished (95 ± 3.5% inhibition, n = 5), the contraction evoked by Bay K 8644 (EC_{50}=14 nM). As expected, nifedipine (0.1 μM) the dihydropyridine derivative shifted to the right the Bay K 8644 dose-response curve. These results are consistent with the mechanism of action of Bay K 8644 that depends upon influx of extracellular Ca^{++} through potential dependent channel (3,4,5,6).

Contractile response of endothelin in Ca^{++} free medium

Since the effect of endothelin appeared different from that of Bay K 8644, we studied the action of endothelin in Ca^{++} free medium. Phenylephrine (PE, 1 μM) induced a phasic contraction which was 27 ± 1.5% (n = 6) of the maximum response obtained in calcium containing solution. Endothelin also developed a slow and sustained contraction (29 ± 1.2%, n = 6 of the maximum PE response in control medium) (Fig. 4). After addition of Ca^{++} to the medium a tonic contraction was obtained (PE : 102 ± 4.4% and endothelin : 107 ± 3.8% of the maximal PE response in control medium).

Effects of repeated challenges with different agonists in Ca^{++} free-medium

Two consecutive exposures to PE (1 μM) in Ca^{++} free medium induced a decline in the contraction. This inhibition was unlikely due to a change in PE sensitivity since it was also observed if PE was replaced by angiotensin II (0.1 μM). Thus, a reduction of intracellular Ca^{++} available for release by PE or angiotensin II could be involved. After first exposure to PE, a second

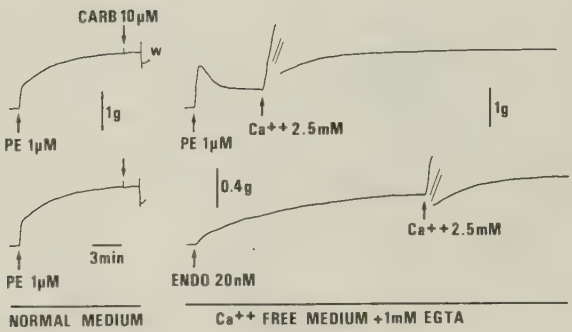

Figure 4 - Contractile response produced by phenylephrine (PE) in normal medium and by PE and endothelin (ENDO) in calcium free EGTA medium. Effect of Ca^{++} introduced to the bath after agonist response in Ca^{++} free medium. The break in the tension recordings denotes a change in scale. Note that, in normal medium, carbachol (CARB) did not induce relaxation of the PE precontracted ring, as there is no endothelium present.

challenge of PE reduced the contraction to 9.5 ± 1.29% (n = 6) of the maximal response of PE obtained in control medium whereas the contraction elicited by endothelin remained to the same 24 ± 1.4% (n = 6)(Fig. 5).

DISCUSSION

The present study reveals a clear dissociation between the contractile properties of endothelin and Bay K 8644 in isolated rat aorta. As previous described (3,4,5) the contraction elicited by Bay K 8644 is dependent on extracellular Ca^{++} in flux through potential dependent channels and is blocked by Ca^{++} antagonists. But as unexpected, Ca^{++} antagonists do not effectively affect the contraction induced by endothelin. Moreover, Bay K

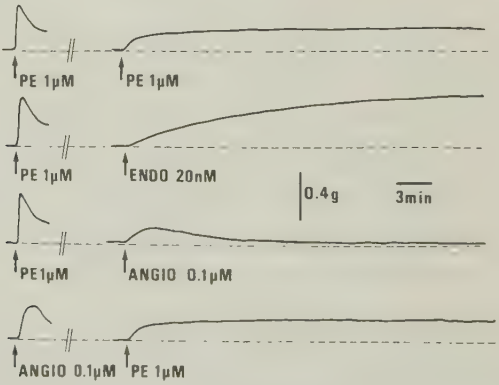

Figure 5 - Representative recordings of effect of repeated challenge with agonists : phenylephrine (PE), Angiotensin II (ANGIO) and endothelin (ENDO) in rat aorta incubated in a Ca^{++} free EGTA medium. Preparations were washed for 20 min in Ca^{++} free medium between the two agonist applications.

8644 requires a partial membrane depolarization which is not necessary to express full effect of endothelin. However, the potentiating effect of partial K^+ depolarization is attenuated for both agonists in presence of endothelium indicating a possible membrane hyperpolarization by EDRF (7,8).

Thus, it is unlikely that endothelin produces rat aorta contraction by a mechanism similar to Bay K 8644, promoting Ca^{++} influx through potential dependent channels as initially postulated (2). In vascular smooth muscle the contractile response induced by agonist in a Ca^{++} free medium can be separated into two components : a fast phase due to a mobilization of intracellular Ca^{++} stores and a tonic phase obtained after readmission of Ca^{++} to the medium which is dependent on extracellular Ca^{++} (9,10,11). Endothelin elicites a slow tonic contraction in rat aorta incubated in a Ca^{++} free medium and after calcium readmission a sustained contraction is obtained. This suggests that the endothelin contractile response consits of two components, one is independent of Ca^{++} influx, the other is dependent on Ca^{++} influx insensitive to potential dependent channel blockers. Regarding the extracellular Ca^{++} independent component the present study also shows that the endothelin contraction is much more resistant to Ca^{++} depletion than PE or angiotensin II. Since this component is probably due to intracellular Ca^{++} release, our results may indicate that endothelin releases Ca^{++} in higher concentration or from different intracellular stores than PE or angiotensin II. Alternatively, it may be postulated that endothelin like the phorbol esters increases the affinity of protein kinase C for Ca^{++} since slowly developing sustained contraction resistant to Ca^{++} depletion was also observed with these compounds (12,13,14). In addition the C-kinase inhibitor H-7 reversed the contraction induced by endothelin on porcine coronary artery (15).

Finally, these results suggest that endothelin acts through specific receptors different from the dihydropyridine recognition sites. Further studies are required to characterize these receptors.

Added Notes

The effects of endothelin presented here were also confirmed in our laboratory by studying $45Ca^{++}$ influx in cultured smooth muscle cells and by C. Chander and D.A. Willoughby (personal communication) who found that isolated superfused rat myofibroblast preparation still contracts to endothelin in presence of Ca^{++} channel blockers and in a Ca^{++} free superfusion system.

REFERENCES

1. Furchgott, R.F. and Zawadzki J.V. (1980) Nature 288, 373-376.
2. Yanagisawa, M., Kurihara, H., Kimura, S., Tomobe, Y., Kobayashi, M., Mitsui Y., Yazaki Y., Goto K. and Masaki T. (1988) Nature 332, 411-415.
3. Schramm, M., Thomas, G., Towart, R. and Franckowiak, G. (1983) Nature 303, 535-538.

4. Su, C.M., Swamy, V.C. and Triggle, D.J. (1984) Can. J. Physiol. Pharmacol. 62, 1401-1410.
5. Salaices, M., Marin, J., Sanchez-Ferrer, C.F. and Reviriego, J. (1985) Biochem. Pharmac. 34, 3131-3135.
6. Yamamoto, H., Hwang, O.K. and Van Breemen, C. (1984) Eur. J. Pharmac. 102, 555-557.
7. De Mey, J. and Vanhoutte, P.M. (1981) in vasodilatation (Vanhoutte P.M. and Leusen I. Eds) pp.331-337. Raven Press, New York.
8. Spedding, M., Schini, V., Schoeffter, P. and Miller, R.C. (1986) J. Cardiovas. Pharmac. 8, 1130-1137.
9. Deth, R. and Van Breemen, C. (1974) Pflügers Arch. 348, 13-22.
10. Hester, R.K. and Carrier, O. Arch. Int. Pharmacodyn. 233, 21-41.
11. Auguet, M. and Defeudis, F.V. (1982). Gen. Pharmac. 13, 343-346.
12. Gleason, M.M. and Flaim S.F. (1986) Biochem. Biophys. Res. Comm. 138, 1362-1369.
13. Singer, H.A. and Baker, K.M. (1987) J. Pharm. Exp. Ther. 243, 814-821.
14. Jim, K.F., Reese, J.B. and Matthews W.D. (1988) J. Cardiovas. Pharmac. 11, 24-28.
15. Kurihara, H., Yanagisawa, M., Yoshizumi, M., Kimura, S., Goto, K., Takaku, F., Masaki, T. and Yazaki, Y. (1988) Abst 614, 12th Scientific Meeting of the International Society of Hypertension (Kyoto, May 22-26, 1988).

Vol. 156, No. 1, 1988 BIOCHEMICAL AND BIOPHYSICAL RESEARCH COMMUNICATIONS
October 14, 1988 Pages 193-198

CALCIMEDIN, CALELECTRIN: CORRELATION OF RELATEDNESS

Pamela B. Moore

The Rockefeller University
New York, New York 10021-6399

Received August 26, 1988

A statistical method has been used to compare the amino acid compositions of several calelectrin proteins and the 67k calcimedin protein. The validity of the method for determining protein relatedness and ancestry has been established with many different proteins. Torpedo calelectrin, p68 brain calelectrin, 67,000 dalton brain calelectrin, 67,000 bovine aorta protein, 32k lipocortin (and probably 67R lung protein) share considerable homology with each other and with calpactin I or lipocortin II, the pp60^{src} tyrosine kinase substrate. The 67k calcimedin appears to be unrelated to these several proteins, in agreement with biochemical evidence, although limited homology may still be present. The lung 67E protein, calregulin and calmodulin, are unrelated to any of the other proteins. © 1988 Academic Press, Inc.

Numerous calcium-binding proteins which bind to synthetic hydrophobic ligands or to biomembranes in the presence of micromolar calcium have been described during the past several years. These proteins include the calcimedins (1), brain calelectrin (2), the chromobindins (3), the 68,000 dalton lymphocyte protein (4) and calregulin or CAB63 (5). Little is known about the relationships or functional homologies of these calcium-binding proteins since well documented comparative data are not available. Statements in the literature have suggested that all these proteins, derived from different sources, are identical with each other (6,7,8) based solely on crossreactivity of antibody. Biochemical data obtained with several of these proteins does not support this identity.

Although sequences of two of these proteins have now been determined (9,10), the amino acid compositions are known for eleven of these proteins. The well established SΔQ method of Marchalonis and Weltman (11,12) allows the determination of protein relatedness based on amino acid composition (11-16). The method calculates SΔQ values for any two proteins being compared. SΔQ is a measure of the diversity of the two proteins. An SΔQ value <50 suggests primary structure homology (11); the stronger the relatedness, the lower the SΔQ value. When analyses of the same protein performed by different laboratories were compared, the maximum SΔQ obtained was 4. Unrelated proteins had SΔQ values >50; and values >50 implied little or no relatedness (11). The validity of this method has been demonstrated with a wide range of proteins, including immunoglobulin μ chains (13), lysozymes (14), membrane glycoproteins and transplantation antigens (15), carotenoid containing lipoglycoproteins (16), and 177 miscellaneous proteins (11,12).

0006-291X/88 $1.50
Copyright © 1988 by Academic Press, Inc.
All rights of reproduction in any form reserved.

Methods

The relatedness coefficient, SΔQ, is a defined as the sum of the squares of each amino acid difference, or $\Sigma (X_{i,j} - X_{k,j})^2$, where X_j is the content of the amino acid j in each of the two proteins (i and k) being compared.

Results and Discussion

Eleven calcium-binding proteins are compared by the SΔQ criterion. Eight of these proteins are about the same size (65,000 daltons to 70,000 daltons); several papers have suggested that these proteins are identical (6,7,8). Three additional proteins, Torpedo calelectrin (M_r = 34,000), 32k lipocortin (M_r = 32,000) and calmodulin (M_r = 17,000), were also compared. The relatedness coefficients were calculated from the amino acid composition literature values reported for these eleven proteins. Table I is a compilation of the calculated amino acid compositions in mole percent used for the subsequent relatedness coefficient (SΔQ) calculations. Table II is a compilation of the calculated coefficients (SΔQ) between these eleven proteins taken two at a time.

TABLE I

AMINO ACID COMPOSITION COMPARISON (Mol %)

Residue	67k Calcimedin	p68 Calelectrin	67,000 Calelectrin	Torpedo Calelectrin	32k Lipocortin	67k Bovine Aorta	Lung 67R	Lung 67E	68,000 Lymphocyte	CAB 63	Brain Calmodulin
Asx	9.5	10.6	10.5	12.8	9.9	11.2	9.6	1.1	12.2	18.6	15.6
Thr	4.6	5.8	5.3	6.2	6.0	5.7	5.1	6.0	6.3	3.7	7.0
Ser	8.7	6.3	8.3	6.9	8.3	5.8	8.9	12.7	6.2	3.3	2.6
Glx	15.7	12.9	13.2	13.5	13.8	13.0	11.8	23.3	14.8	22.0	20.9
Gly	11.9	6.8	9.0	7.3	9.3	8.5	15.0	13.4	5.4	4.3	4.4
Ala	9.8	8.7	8.3	8.8	8.2	9.0	7.0	8.0	6.3	3.5	5.2
Val	3.8	5.0	2.6	5.5	4.0	4.0	3.8	4.6	2.3	4.2	4.6
Met	1.8	2.5	2.6	1.5	1.2	2.3	2.5	0.5	2.9	1.2	7.3
Ile	2.8	6.4	4.9	5.5	4.5	6.2	5.3	2.9	2.7	4.9	5.2
Leu	6.1	11.9	9.8	9.1	10.7	9.5	9.1	5.2	8.3	4.9	6.4
Tyr	2.6	0.49	2.6	2.9	3.8	3.4	4.1	2.0	5.6	5.4	1.8
Phe	3.7	3.6	3.0	2.9	4.0	3.1	3.3	2.3	5.1	6.3	6.5
His	4.3	1.8	1.5	1.8	1.5	1.4	2.1	2.6	5.7	2.5	0.8
Lys	9.0	8.0	9.0	6.6	7.6	7.9	6.8	3.9	9.8	11.8	5.7
Arg	2.3	6.2	5.6	4.4	5.7	5.2	5.6	1.8	6.3	3.4	6.0

Amino acid compositions in mole %: 67k calcimedin [1], p68 calelectrin [21], 67,000 calelectrin and Torpedo calelectrin [2], lipocortin [26], bovine aorta protein [20], lung 67R and 67E proteins [23], 68,000 lymphocyte protein [4], CAB 63 [5], and calmodulin [24]. Proline, tryptophan and cysteine contents were not consistently reported for the eleven proteins and were deleted from the calculations.

TABLE II

COMPARISON OF CORRELATION COEFFICIENTS (SΔQ)

	67k Calcimedin	p68 Calelectrin	67,000 Calelectrin	Torpedo Calelectrin	32k Lipocortin	67k Bovine Aorta	Lung 67R	Lung 67E	68,000 Lymphocyte	CAB 63	Brain Calmodulin
67k Calcimedin	--	119	58	80	63	74	72	186	110	283	267
p68 Calelectrin	119	--	28	27	31	20	105	386	95	301	193
67,000 Calelectrin	58	28	--	29	11	13	50	286	67	277	214
Torpedo Calelectrin	80	27	29	--	26	12	88	344	74	228	163
32k Lipocortin	63	31	11	26	--	17	46	274	72	286	221
67k Bovine Aorta	74	20	13	12	17	--	64	345	71	252	181
Lung 67R	72	105	50	88	46	64	--	277	156	405	327
Lung 67E	186	386	286	344	274	345	277	--	411	602	503
68,000 Lymphocyte	110	95	67	74	72	71	156	411	--	164	156
CAB 63	283	301	277	228	286	252	405	602	164	--	124
Brain Calmodulin	267	193	214	163	221	181	327	503	156	124	--

SΔQ analysis of the twelve calcium-binding proteins. SΔQ is a measure of protein relatedness [9,10]. Values less than 50 have been outlined.

The apparently related proteins (SΔQ <50) include Torpedo calelectrin, lipocortin, the 67,000 and p68 brain calelectrins, and the bovine aorta 67,000 dalton protein. The lung 67R protein appears separate from this group. However, differences in only one amino acid (glycine) accounts for 60-70% of the SΔQ values, suggesting the protein does belong to this group of proteins. Several of these proteins have also been reported to share a 17 amino acid consensus sequence with p36 calpactin I (17), the $pp60^{src}$ tyrosine kinase substrate (18,19). The SΔQ values between these proteins and calpactin I ranged between 16 and 33.

Proteins with SΔQ values between 50 and 100 include the 67k calcimedin (1) and the 68,000 dalton lymphocyte protein (4). These proteins do not appear to belong to the lipocortin/ calelectrin family above. SΔQ values suggest that these two proteins are unrelated to each other and would share only limited homology, if any, with the first group. Despite the apparent non-identity of these proteins based on analysis of the reported amino acid compositions, the lymphocyte 68,000 Da protein has now been reported to be identical to the 67,000 Da calelectrin protein (9,10). Analysis of the compositions predicted from the cDNA sequences of calelectrin and the lymphocyte protein gave an SΔQ of 0.5% (Table III; the 67k calcimedin is included for comparison). The

TABLE III

COMPARISON OF CALELECTRIN SEQUENCE COMPOSITIONS WITH 67k CALCIMEDIN AMINO ACID COMPOSITION

Residue	Human Calelectrin	Lymphocyte Calelectrin	Smooth Muscle Calcimedin
Asx	10.9	10.8	9.5
Thr	5.1	5.2	4.6
Ser	4.7	4.8	8.7
Glx	13.7	13.4	15.7
Pro	2.0	2.0	2.9
Gly	3.6	3.8	11.9
Ala	6.0	6.1	9.8
Val	3.5	3.4	3.8
Met	3.4	3.6	1.8
Cys ½	0.8	0.8	nd
Ile	7.0	7.2	2.8
Leu	10.0	10.1	6.1
Tyr	4.8	4.8	2.6
Phe	4.7	4.4	3.7
Trp	0.5	0.5	0.8
His	2.3	2.1	4.3
Lys	8.7	8.8	9.0
Arg	8.2	7.9	2.3

nd=not determined

Comparison of the amino acid sequence compositions for the human calelectrin and the lymphocyte proteins. The amino acid compositions of the 67k calcimedin is included for comparison.

lymphocyte protein appears to have a true molecular size ranging between 80,000 and 85,000 daltons, rather that the 67,000 Da, estimated from SDS-polyacrylamide gel electrophoresis (PAGE). The sequence data suggest this increased size is accounted for by the linker regions between the repeat residues (9).

The apparent discrepancy between the published amino acid analyses for the 67k Da brain and the p68 lymphocyte calelectrins and the published sequence analyses for the human and lymphocyte calelectrins, may be partially resolved by the following: small amounts of the 67k calcimedin derived from blood vessels may be present in the calelectrin preparations and go undetected on 10-12% SDS-polyacrylamide gels which do not resolve the two proteins. Antibody to the 67k calcimedin does not recognize brain calelectrin (20) and does not crossreact with the lymphocyte protein (21). Additionally, the estimated size of the 67k calcimedin from the amino acid analysis is 65,000 Da (cysteine residues not determined) as compared to the value of 67,000 Da obtained by PAGE. Comparison of the cDNA derived amino acid compositions of calelectrin and

the lymphocyte protein (Table III) with the 67k calcimedin gave SΔQ values of 187 and 183, respectively. Based on the comparisons between the amino acid analysis or sequence analysis data, the 67k calcimedin appears to be distinct from the lymphocyte protein. This conclusion is supported by the lack of 67k calcimedin antibody staining in lymphocytes (21).

The remaining proteins, with SΔQ values greater than 100, include the liver CAB63 protein (calregulin) (5), the lung 67E protein (22), and calmodulin (23). Each of these proteins is clearly unrelated to any of the other calcium-binding proteins tested. Interestingly, the CAB63 protein showed a correlation coefficient of 48 when compared to rabbit skeletal muscle calsequestrin (24) (data not shown). When compared with a one-to-one heterodimer of calsequestrin (M_r = 45,000) and calmodulin (M_r = 17,000), the CAB63 SΔQ value decreased to 9, suggesting near identity. Addition or subtraction of calmodulin did not substantially alter the SΔQ values for any of the other proteins.

The amino acid data are therefore consistent with the following: 1) a major group sharing homology with the 32,000 dalton lipocortin and calpactin I include Torpedo calelectrin, brain calelectrin, the aorta protein and possibly the lung 67R protein; 2) the 67k calcimedin appears to be distinct from this group of proteins and 3) CAB63, lung 67E and calmodulin are totally unrelated proteins. This analysis demonstrates the utility of the SΔQ method for determining relatedness and ancestry of proteins, especially when amino acid or DNA sequences are not yet available. The groupings of these proteins based on SΔQ values do not necessarily coincide with the groupings defined by less specific criteria such as molecular size, mobility on SDS gel electrophoresis, and binding to immobilized ligands. These other criteria are useful, but not fully adequate, to suggest similarities between proteins and may be misleading if solely relied upon.

Acknowledgements

I thank Dr. S. S. Morse, The Rockefeller University, for critical comment on the manuscript. Supported by The American Heart Association, National Program. The author is an Investigator of the American Heart Association, New York City Affiliate.

References

1. Moore, P.B. (1986) Biochem. J. 238:49-54.
2. Südhof, T.C., Ebbecke, M., Walker, J.H., Fritsche, U., and Boustead, C. (1984) Biochemistry 23:1103-1109.
3. Creutz, C.E., Dowing, L.G., Sando, J.J., Vilar-Plasi, C., Whipple, J.H., and Zaks, W.J. (1983) J. Biol. Chem.258:14664-14674.
4. Owens, R.J., and Crumpton, M.J. (1984) Biochem. J. 219:306-316.
5. Waisman, D.M., Salimath, B.P., and Anderson, M.J. (1985) J. Biol. Chem. 260:1652-1660.
6. Dedman, J.R. (1986) Cell Calcium 7:297-307.
7. Martin, F., Derancourt, J., Capony, J.P., and Cavadore, J.D. (1987) J. Muscle Res. & Cell Motil. 8:77.
8. Geisow, M.J., Walker, J.H., Boustead, C., and Taylor, W. (1987) Bioscience Reports 7:289-307.
9. Südhof, T.C., Slaughter, C.A., Leznicki, I., Barjon, P. and Reynolds, G.A. (1988) Proc. Nat. Acad. Sci. USA 85:664-668.
10. Crompton, M.R., Owens, R.J., Totty, N.F., Moss, S.E., Waterfield, M.D. and Crumpton, M.J. (1988) The EMBO J. 7:21-27.
11. Marchalonis, J.J., and Weltman, J.K. (1971) Comp. Biochem. Physiol. 38B, 609-625.
12. Weltman, J.K., and Dowben, R.M. (1973) Proc. Nat. Acad. Sci. USA 70:3230-3234.
13. Marchalonis, J.J. (1972) Nature New Biol. 236, 84-86.
14. Prager, E.M., and Wilson, A.C. (1971) J. Biol. Chem. 246:5978-5989.

15. Robert, L., Sayolle, J., Derovette, F., and Zabriskie, J. (1972) Transplant. Proc. 4:415-418.
16. Zagalsky, P.S. (1972) Comp. Biochem. Physiol. 41B: 385-397.
17. Gerke, V., and Weber, K. (1984) The EMBO J. 3:227-233.
18. Geisow, M.J., Fritsche, U., Hexham, J.M., Dash, B., and Johnson, T. (1986) Nature 320:636-638.
19. Martin, F., Derancourt, J., Capony, J.P., Colete, S., and Cavadore, J.D. (1987) Biochem. Biophys. Res. Commun. 145:961-968.
20. Rhoads, A.R., Lulla, M., Moore, P.B., and Jackson, C.E. (1985) Biochem. J. 229:587-593.
21. Morse, S.S. and Moore, P.B. (1988) Biochem. J. 251:171-174.
22. Fauvel, J., Vicendo, P., Roques, V., Ragab-Thomas, J., Granier, C., Vilgrain, I., Chambaz, E., Rochet, H., Chap, H., and Douste-Blazy, L. (1987) FEBS Lett. 221:397-402.
23. Dedman, J.R., Potter, J.D., Jackson, R.L., Johnson, J.D., and Means, A.R. (1971) J. Biol. Chem. 252:8415-8422.
24. Slupsky, J.R., Ohnishi, M., Carpenter, M.R., and Reitmeier, R.A.F. (1987) Biochem. 26:6539-6544.
26. Rothhut, B., Comera, C., Prieur, B., Errasfa, M., Minassian, G., and Russo-Marie, F. (1987) FEBS Lett. 219:169-175.

Vol. 156, No. 1, 1988 BIOCHEMICAL AND BIOPHYSICAL RESEARCH COMMUNICATIONS
October 14, 1988 Pages 199-204

GROWTH HORMONE-DEPENDENT INSULIN-LIKE GROWTH FACTOR (IGF) BINDING PROTEIN BOTH INHIBITS AND POTENTIATES IGF-I-STIMULATED DNA SYNTHESIS IN HUMAN SKIN FIBROBLASTS

John S. M. De Mellow and Robert C. Baxter

Department of Endocrinology, Royal Prince Alfred Hospital,
Camperdown, NSW 2050, Australia

Received August 26, 1988

SUMMARY: This study investigates the effects of BP-53, the acid-stable IGF-binding subunit of the circulating 150 kDa IGF-binding protein complex, on IGF-I-stimulated thymidine incorporation by neonatal human skin fibroblasts. When cells were incubated for 24 h with IGF-I in serum-free medium, and thymidine incorporation studied over the final 4-h period, maximal stimulation (4- to 7-fold) was seen with 30 ng/ml IGF-I, with a half-maximal effect at 6.8±1.2 ng/ml (SD, n=4). Co-incubation of IGF-I with increasing concentrations of pure BP-53 caused dose-dependent inhibition of IGF-I-stimulated thymidine incorporation, which was complete when IGF-I and BP-53 were equimolar. In contrast, preincubation of cells with BP-53 for 8-48 h before adding IGF-I resulted in a potentiation of the subsequent IGF-I effect. The potentiation was maximal (2-fold) at a BP-53 concentration of 150 ng/ml, and appeared to act by increasing the maximal rate of thymidine incorporation rather than the sensitivity of this process to IGF-I. Since neonatal fibroblasts produce a protein which is identical to BP-53 in size and immunoreactivity, these results suggest an autocrine role for BP-53 in regulating fibroblast responsiveness to IGF-I.
© 1988 Academic Press, Inc.

The existence of binding proteins (BP) for peptides of the insulin-like growth factor (IGF) family has been recognized for over a decade. Several such proteins have been isolated and characterized in recent years, from both human (1-6) and non-primate (5, 7-10) sources. BPs for which an N-terminal amino acid sequence is known appear to fall into two structurally related classes : proteins of approximately 30 kDa, such as those from human amniotic fluid and rat BRL-3A cells (1,3,7,8), and proteins of approximately 50 kDa isolated from adult human and rat serum (5,6). Many other BP species, identified by binding studies in a wide variety of biological fluids, have not yet been classified in this way.

In human serum the major BP species exists as part of a GH-dependent complex of approximately 150 kDa (11-13), which appears to contain, in addition to BP and IGF-I or IGF-II, a non-IGF-binding, acid-labile protein of approximately 100 kDa (13,14). We have previously isolated the binding subunit of this complex, of which the predominant form is a 53 kDa acid-stable glycoprotein (termed BP-53), with high affinity (K_a= 2-3 x 10^{10} L/mol) for both IGF-I and IGF-II (6). A minor BP form of 47 kDa, with apparently identical properties, always co-purifies with BP-53 (6).

Abbreviations: BP, binding protein; IGF, insulin-like growth factor.

0006-291X/88 $1.50
Copyright © 1988 by Academic Press, Inc.
All rights of reproduction in any form reserved.

Impure BP preparations have been found to inhibit various IGF actions *in vitro*, including stimulation of glucose transport by adipocytes, sulfate incorporation by chondrocytes, and thymidine incorporation in fibroblasts (15-18). Pure preparations of a 34 kDa BP isolated from amniotic fluid or human decidua, and the homologous protein from rat BRL-3A cells, have also been shown to inhibit IGF actions in several tissues (19-21) but, interestingly, in one recent study the amniotic fluid protein had a marked potentiating action on IGF-stimulated DNA synthesis in porcine aortic smooth muscle cells and human, mouse and chick embryo fibroblasts (22). Because comparable studies have not previously been performed using a well-characterized preparation of the major BP species from adult human serum, we have now tested the effects of pure BP-53 on DNA synthesis in human fibroblasts. In this report we describe the inhibitory effect of this protein when it is co-incubated with IGF-I, and contrast this with the potentiating effect seen when cells are preincubated with BP-53 prior to the addition of IGF-I.

Materials and Methods

Natural human IGF-I and IGF-II were purified from Cohn Fraction IV of human plasma, as previously described (23). Recombinant DNA-derived human IGF-I (24) was generously donated by Dr. B.D. Burleigh, International Minerals and Chemical Corp., Terre Haute, IN. BP-53 was isolated from Cohn Fraction IV by affinity chromatography and reverse-phase high performance liquid chromatography (6).

Neonatal human fibroblasts were grown from foreskin explants, and maintained at 37°C in 25 cm^2 Corning flasks (Corning, NY) in Ham's F10 medium (Flow Laboratories, Herts, UK) supplemented with 28 mM Na Hepes, 60 mg/liter penicillin, 100 mg/liter streptomycin and 10% fetal bovine serum (Cytosystems, Sydney, Australia). Cells, used between generations 5 and 10, were trypsinized and plated in 4.5 cm^2 12-place multiwells (Flow) at a subconfluent density of 3.0 x 10^4 cells/ml in 2 ml supplemented F10 medium containing 10% serum. After 24 h the medium was replaced with a 1:1 mixture of F10 medium and RPMI 1640 medium (Flow), serum-free and supplemented with Hepes, penicillin and streptomycin as above, plus 1 g/liter bovine albumin (RIA Grade, Sigma, St. Louis, MO). The thymidine concentration of this medium is 1.5 μM. Cells were incubated 48 h under these conditions unless the effect of preincubation with BP-53 was being tested, when the medium was replaced (normally after 24 h) with the same medium containing various concentrations of BP-53, and the incubation continued to a total of 48 h. The medium was again replaced by the same medium without BP-53, containing IGF-I or other substances being tested in the thymidine incorporation assay, and after 20 h [^{3}H]thymidine (Amersham, UK, 40-50 Ci/mmol) was added at 1 μCi/ml. After 4 h of [^{3}H]thymidine incorporation, the medium was removed and the cells were washed in succession with 0.15 M NaCl, 100 g/liter trichloroacetic acid, and methanol, then dissolved in 0.75 ml 0.5% sodium dodecyl sulfate. Aliquots of 0.6 ml were mixed with 8 ml Pico-Fluor 30 scintillant (Packard, Downers Grove, IL) and counted in a Packard Tricarb 300 liquid scintillation counter. DNA concentrations were measured on duplicate 75 μl aliquots of solubilized cells by the method of Cesarone et al. (25). Since correction for cell DNA content did not alter the results, all data are presented uncorrected for DNA content.

Results

Figure 1(a) shows the stimulation of [^{3}H]thymidine incorporation into DNA by increasing concentrations of IGF-I. In 4 similar experiments, maximal stimulation (4- to 7-fold above basal incorporation) was seen at 30 ng/ml IGF-I, with a half-maximal effect at 6.8±1.2 ng/ml IGF-I (mean±SD). These figures are similar to the maximal 3.5-fold stimulation by IGF-I, with a half maximal effect at 9 ng/ml IGF-I, reported by Conover et al. (26) for adult human fibroblasts. Recombinant DNA-derived IGF-I was indistinguishable from the natural peptide in its stimulatory effect (not shown). IGF-II was approximately half as potent as IGF-I in stimulating

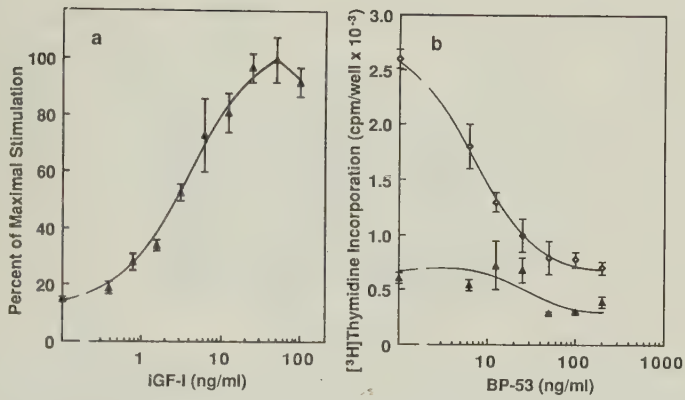

Figure 1. (a) Stimulation of [^{3}H]thymidine incorporation in human skin fibroblasts by increasing concentrations of IGF-I. (b) Inhibition of [^{3}H]thymidine incorporation in the presence of 7.5 ng/ml IGF-I (*open symbols*) or no IGF-I (*solid symbols*) by co-incubation with increasing concentrations of pure BP-53. Data are means ± SEM for triplicate incubations.

[^{3}H]thymidine incorporation (not shown), but was not tested further in this study as it is likely that GF-I and IGF-II act through the same (type I) receptor (26).

The presence of increasing concentrations of pure BP-53 during the 24-h incubation with IGF- resulted in a dose-dependent inhibition of the IGF-I effect. As illustrated in Figure 1(b), imulation of [^{3}H]thymidine incorporation by 7.5 ng/ml IGF-I (i.e. 1 nM) was fully reversed by) ng/ml BP-53, an equimolar concentration. Basal [^{3}H]thymidine incorporation was also hibited slightly by high concentrations of BP-53, suggesting that the basal rate might be due in rt to endogenous IGF-I.

In contrast to the inhibitory effect of BP-53 when co-incubated with IGF-I, preincubation of broblasts with BP-53 prior to the addition of IGF-I resulted in a potentiation of the stimulatory fect of subsequently added IGF-I on [^{3}H]thymidine incorporation. In three similar experiments, preincubation period with BP-53 of at least 8 h was required, with 24-h or 48-h preincubations aving no greater effect, and no effect after only 4 h (Figure 2). The [^{3}H]thymidine incorporation te in the absence of IGF-I was not significantly altered by preincubation for any length of time ith BP-53.

Figure 3(a) shows a dose-response curve for the potentiation of IGF-stimulated incorporation [^{3}H]thymidine by preincubation with increasing concentrations of BP-53. Up to 2-fold otentiation was seen when cells were preincubated with 150 ng/ml BP-53, with a half-maximal otentiation at 20-30 ng/ml. As seen in Figure 3(b), IGF-I at a concentration of 5 ng/ml stimulated H]thymidine incorporation half-maximally regardless of the concentration of BP-53 present uring the preincubation period, indicating that the potentiating effect of BP-53 was on the aximal rate of [^{3}H]thymidine incorporation obtained, rather than on the sensitivity of the cells wards IGF-I.

Discussion

This study demonstrates that a purified preparation of BP-53, the IGF-binding subunit of the irculating 150 kDa IGF-BP complex, can either inhibit or potentiate IGF-stimulated

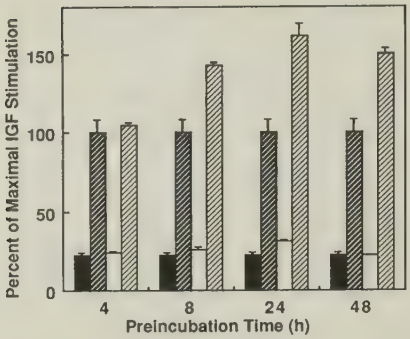

Figure 2. Potentiation of IGF-I-stimulated [^{3}H]thymidine incorporation in human fibroblasts by preincubation for various times with pure BP-53 before the addition of IGF-I. For each time point, the four bars indicate : *black,* no BP in the preincubation (period 1), and no IGF-I present during the final 24-h period (period 2); *dark hatched*, no BP in period 1, 30 ng/ml IGF-I in period 2; *white*, 50 ng/ml BP-53 in period 1, no IGF-I in period 2; and *light hatched*, 50 ng/ml BP-53 in period 1, 30 ng/ml IGF-I in period 2. Data are means ± SEM for triplicate incubations, expressed in terms of the maximal IGF-I stimulated incorporation without BP-53 preincubation. By analysis of variance and Duncan's multiple-range test, IGF-I-stimulated incorporation was significantly higher after 8, 24 or 48 h preincubation with BP-53 than after 4 h ($P<0.001$).

[^{3}H]thymidine incorporation in neonatal skin fibroblasts, depending upon the incubation conditions used. The possibility that these effects might represent physiological mechanisms is strongly suggested by the observation that these cells secrete an IGF-binding protein which is indistinguishable from plasma BP-53, both in its size on sodium dodecyl sulfate polyacrylamide gel electrophoresis and by its immunoreactivity towards an antiserum raised against plasma BP-53 (27). Serum-free medium conditioned by fibroblasts contains over 50 ng/ml immunoreactive BP-53, increasing to over 300 ng/ml in the presence of 10% fetal calf serum (27). Thus the concentrations of BP-53 required to achieve maximal inhibition or potentiation of IGF-stimulated

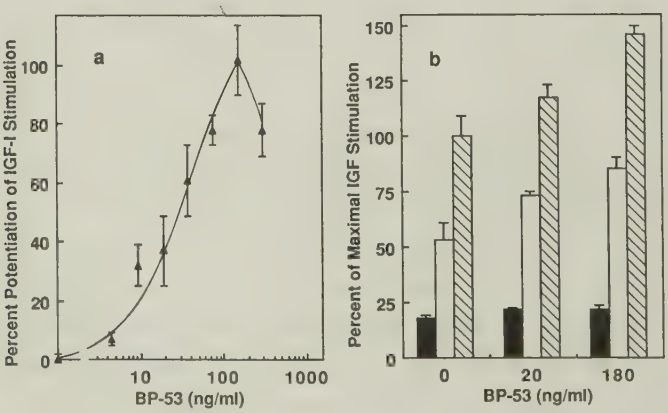

Figure 3. The effect of preincubation with increasing concentrations of pure BP-53 on IGF-I-stimulated [^{3}H]thymidine incorporation. Preincubations were for 24 h, after which cells were changed to fresh medium containing (a) 5 ng/ml IGF-I or (b) no IGF-I (*black bars*), 5 ng/ml IGF-I (*white bars*) or 30 ng/ml IGF-I (*hatched bars*), without BP-53. Data are means ± SEM for triplicate incubations, expressed in terms of the maximal IGF-I stimulated incorporation without BP-53 preincubation.

[^{3}H]thymidine incorporation in neonatal fibroblasts are within the range actually found in culture medium conditioned by these cells.

Since co-incubation of IGF-I and BP-53 resulted in inhibition of the stimulatory effect of IGF-I, it appears that the BP-IGF complex is inactive in this system. This conclusion is in accord with many other reports that various IGF BPs are able to inhibit a range of IGF actions (15-19, 21), but contrasts with the observation by Elgin et al. (22) that a preparation of amniotic fluid BP was able to potentiate IGF-stimulated mitogenesis in several cell types. Other studies also suggest that some IGF-BP complexes may be biologically active. Cornell et al. (28) found that serum subjected to anion-exchange chromatography at pH 8.1 fractionated into a BP-IGF complex rich in IGF-I, with very little activity in a rat adipocyte assay for insulin-like activity, and an IGF-II-rich complex which had strong insulin-like activity. Another recent preliminary report suggests that co-incubation of a plasma BP preparation with IGF-I could potentiate the stimulatory effect of IGF-I on DNA synthesis in hamster kidney fibroblasts (29).

Whereas co-incubation of IGF-I with BP-53 was clearly inhibitory in our study, fibroblasts that had been exposed to BP-53 prior to the addition of IGF-I showed an increased responsiveness to IGF-I action. This potentiation required between 8 and 24 h to reach its maximal effect, a considerably longer time than would be required for BP-53 to bind any free IGFs in the culture medium. Nevertheless, it is possible that the potentiating effect results from the binding of free IGFs by the BP. For example, if endogenous IGFs normally act to desensitize fibroblasts to IGF stimulation, either by receptor down-regulation or by some post-receptor mechanism, then the effective removal of free IGFs for an extended period by complexing them to BP-53 might result in a heightened sensitivity of the cells towards IGFs.

Alternatively, it is possible that BP-53 acts directly on fibroblasts, sensitizing the cells towards IGFs. This might occur independently of the IGF-binding function of the BP, or might be due to a modulation of IGF binding to its receptors on the fibroblast cell surface, resulting from the association of BP-53 with the cells. The latter hypothesis is supported by studies indicating that a 35 kDa IGF BP released by fibroblasts can associate with the cell surface and affect IGF-I binding (30,31). This protein is the same size as an IGF BP which is secreted by neonatal fibroblasts together with the 53 kDa BP and cross-reacts with an antibody raised against plasma BP-53 (27). Whether this protein is a processed form of the 53 kDa protein, or a separate gene product with an epitope in common with BP-53, is not known.

Whichever explanation is correct, this study provides new evidence that the action of IGF-I on fibroblast DNA synthesis can be modified in both inhibitory and stimulatory ways by a 53 kDa IGF BP apparently identical to one released by these cells. This observation therefore strongly suggests an autocrine role for BP-53 in regulating fibroblast responsiveness to IGF-I.

Acknowledgement

This work was supported by the National Health and Medical Research Council, Australia.

References

1. Povoa, G., Enberg, G., Jornvall, H., and Hall, K. (1984) Eur. J. Biochem. 144: 199-204.
2. Drop, S.L.S., Kortleve, D.J., and Guyda, H.J. (1984) J. Clin. Endocrinol. Metab. 59: 899-907.

3. Koistinen, R., Kalkkinen, N., Huhtala, M.-L., Seppala, M., Bohn, H., and Rutanen, E.-M. (1986) Endocrinology 118: 1375-1378.
4. Povoa, G. Isaksson, M., Jornvall, H., and Hall, K. (1985) Biochem. Biophys. Res. Commun. 128: 1071-1078.
5. Baxter, R.C., and Martin, J.L. (1987) Biochem. Biophys. Res. Commun. 147: 408-415.
6. Martin, J.L., and Baxter, R.C. (1986) J. Biol. Chem. 261: 8754-8760.
7. Lyons, R.M., and Smith, G.L. (1986) Molec. Cell. Endocrinol. 45: 263-270.
8. Mottola, C., MacDonald, R.G., Brackett, J.L., Mole, J.E., Anderson, J.K., and Czech, M.P. (1986) J. Biol. Chem. 261: 11180-11188.
9. Romanus, J.A., Terrell, J.E., Yang, Y. W.-H., Nissley, S.P., and Rechler, M.M. (1986) Endocrinology 118: 1743-1758.
10. Szabo, L., Mottershead, D.G., Ballard, F.J., and Wallace, J.C. (1988) Biochem. Biophys. Res. Commun. 151: 207-214.
11. Hintz, R.L., and Liu, F. (1977) J. Clin. Endocrinol. Metab. 45: 988-995.
12. Baxter, R.C., and Martin, J.L. (1986) J. Clin. Invest. 78: 1504-1512.
13. Furlanetto, R.W. (1980) J. Clin. Endocrinol. Metab. 51: 12-19.
14. Baxter, R.C. (1988) J. Clin. Endocrinol. Metab. 67 : 265-272.
15. Chochinov, R.H., Mariz, I.K., Hajek, A.S., and Daughaday, W.H. (1977) J. Clin. Endocrinol. Metab. 44: 902-908.
16. Zapf, J., Schoenle, E., Jagars, G., Sand, I., Grunwald, J., and Froesch, E.R. (1979) J. Clin. Invest. 63: 1077-1084.
17. Drop, S.L.S., Valiquette, G., Guyda, H.J., Corvol, M.T., and Posner, B.I. (1979) Acta Endocrinol. (Copenh.) 90: 505-518.
18. Ooi, G.T., and Herington, A.C. (1986) Biochem. Biophys. Res. Commun. 137: 411-417.
19. Knauer, D.J., and Smith, G.L. (1980) Proc. Natl. Acad. Sci. USA 77: 7252-7256.
20. Clemmons, D.R., Elgin, R.G., Busby, W.H., and McCusker, R.H. Abstract, 69th Annual Meeting of The Endocrine Society, Indianapolis, IN, 1987, p 124.
21. Ritvos, O., Ranta, T., Jalkanen, J., Suikkari, A.-M., Voutilainen, R., Bohn, H., and Rutanen, E.-M. (1988) Endocrinology 122: 2150-2157.
22. Elgin, R.G., Busby, W.H., and Clemmons, D.R. (1987) Proc. Natl. Acad. Sci. USA 84: 3254-3258.
23. Baxter, R.C., and De Mellow, J.S.M. (1986) Clin. Endocrinol. 24: 267-278.
24. Baxter, R.C., De Mellow, J.S., and Burleigh, B.D. (1987) Clin. Chem. 33: 544-548.
25. Cesarone, C.E., Bolognese, C., and Santi, L. (1979) Analyt. Biochem. 100: 188-197
26. Conover, C.A., Rosenfeld, R.G., and Hintz, R.L. (1987) J. Cell Physiol. 133: 560-566
27. Martin, J.L., and Baxter, R.C. (1988) Endocrinology 123: (in press).
28. Cornell, H.J., Enberg, G., and Herington, A.C. (1987) Biochem. J. 241: 745-750.
29. Blum, W.F., Jenne, E., Kietzmann, K., Bierich, J.R., and Ranke, M.B. (1987) J. Endocrinol. Invest. 10 (Suppl 4): 25 (abstract)
30. De Vroede, M.A., Tseng, L.Y.-H., Katsoyannis, P.G., Nissley, S.P., and Rechler, M.M. (1986) J. Clin. Invest.77: 602-613.
31. Clemmons, D.R., Han, V.K., Elgin, R.G., and D'Ercole, A.J. (1987) Molec. Endocrinol. 1: 339 -347.

Vol. 156, No. 1, 1988 BIOCHEMICAL AND BIOPHYSICAL RESEARCH COMMUNICATIONS
October 14, 1988 Pages 205-210

SYNTHESIS OF NUCLEAR LAMINS IN BHK-21 CELLS SYNCHRONIZED WITH APHIDICOLIN

Sylvain Foisy and Viviane Bibor-Hardy

Institut du Cancer de Montréal, 1560 Est Sherbrooke,
Montréal, QC, Canada H2L 4M1

Received August 29, 1988

Lamins A, B and C are the major proteins of mammalian nuclear lamina and have been well studied in BHK-21 cells [1, 2]. By synchronizing BHK-21 cells with aphidicolin, a potent inhibitor of DNA α-polymerase, we were able to detect a differential pattern of synthesis for nuclear lamins during the cell cycle. Lamin B starts to be synthesized only in S phase up to mitosis while synthesis of lamins A and C remain stable throughout the cell cycle. The precursor of lamin A [2] see its half-life increase from a reported 63 min in interphase cells to 103 min in G2/M cells. © 1988 Academic Press, Inc.

The nuclear membranes of eukaryotic cells are underlined with a fibrillar meshwork called nuclear lamina [3-5]. The main proteins of this structure are known as lamins A, B and C in mammalian cells [3-5]. Lamins A and C are synthesized by two different mRNAs [6] but may came from a single gene by differential splicing [7,8]. Immunological cross-reactions show that lamin B is related to the other two lamins [9-16]. Lamin A is synthesized as a precursor of higher molecular weight [2,6,14]; lamin B is also the target of some post-translational modifications [17].

The lamins exhibit striking behavior differences in their distribution during the cell cycle. From G1 to G2 phase, the lamins are polymerized together into the nuclear lamina [5]. During mitosis, lamins A and C become soluble while lamin B is associated with nuclear membranes remains [18]. Although lamins are always present in the cell, the exact timing of their synthesis remains undefined. Conflicting reports have been published: synthesis only in S phase in HeLa cells [19], throughout the cell cycle in CHO cells [14,15], presence of mRNAs for lamins B and C only in S phase in Ehrlich ascites cells [20]. We report in this manuscript that in BHK-21 cells synchronized with aphidicolin, a specific inhibitor of DNA α-polymerase in eukaryotic cells [21-23], lamin B is synthesized only in S phase and afterward while levels of synthesis of lamins A and C remain stable in all phases. We also observe variation in the half-life of the lamin A precursor during the cell cycle.

0006-291X/88 $1.50
Copyright © 1988 by Academic Press, Inc.
All rights of reproduction in any form reserved.

MATERIALS AND METHODS

Cell culture and synchronization

Baby hamster kidney cells (BHK-21) were grown at 37°C in α-medium (Gibco) supplemented with 10% fetal calf serum (Gibco) (standard medium). Cell synchronization was done according to Pedrali-Noy [22]: cells grown in standard medium for 24 h were washed with α-medium without serum and incubated for 24 h. After a second 24 h serum starvation period, cells were incubated for 24 h in standard medium containing 5 μg/ml aphidicolin (Sigma; freshly prepared at 5 mg/ml in DMSO), to block the cells in G1/S interphase. The cells were released from the aphidicolin block by washing with PBS prior to incubation in standard medium.

Cell cycle analysis

For cell cycle analysis, 24-well trays (Corning) were plated with 5 x 10^4 cells/well and the cells synchronized as described above. Each hour after release from the aphidicolin block, cells from 3 wells were labelled for 15 min with 10 μCi/ml of [^{3}H]thymidine (117 Ci/mmol, Amersham) in standard medium. The cells were washed twice with ice-cold PBS and scraped off with a rubber policeman in 500 μl of PBS. Labelled DNA was precipitated with 5% trichloroacetic acid and filtered on GF/A filters (Whatman Ltd). The filters were washed twice with cold 5% TCA, twice with ethanol and dried. The radioactivity was counted for each filter.

Cell cycle phases were established according to the [^{3}H]thymidine incorporation and data from other laboratories [22]: G1 and G1/S, respectively 5 h and 24 h after release from serum starvation, during aphidicolin block; S, G2 and G2/M, respectively 6 h, 9 h and 11 h after release from the aphidicolin block.

Protein synthesis studies

BHK-21 cells were plated in 60 mm culture dishes at 2 x 10^5 cells/dish and synchronized. At each pre-established cell cycle phase, the cells were washed twice with methionine-free α-medium containing 10% dialyzed fetal bovine serum, either with 5 μg/ml aphidicolin for G1 and G1/S phases or without for S, G2 and G2/M. After a 20 min incubation in the same medium, [^{35}S]methionine (1100 Ci/mmol, Amersham) was added at either 25 μCi/ml or 40μCi/ml for pulse-chase labelling experiments [2]. After labelling, the cells were washed twice with cold PBS, scraped off with a rubber policeman in cold PBS and microfuged at 15000 rpm at 4°C for 15 min. The pellets were frozen on dry ice and kept at -20°C prior to immunoprecipitation.

Immunoprecipitations were performed using a serum against BHK lamins [2]. Additional protease inhibitors were added to the immunoprecipitation buffer (1 mM benzamidine, 25 μg/ml leupeptin, 25 μg/ml aprotinin). The samples were frozen on dry ice and kept at -20°C prior to electrophoresis.

SDS-PAGE and autoradiographies were done as described in previous papers [1,2]. For the pulse-chase experiments, the same amount of radioactivity was applied in each well of the gel. Quantitative data was obtained with an UltroScan XL densitometer and GelScan XL densitometry analysis software (LKB, Uppsala) linked to a IBM XT-compatible computer.

RESULTS AND DISCUSSION

The cell cycle kinetics of BHK cells synchronized with aphidicolin was determined by [^{3}H]thymidine incorporation into DNA (fig. 1). A maximum of incorporation was observed 6 h after the removal of the aphidicolin block identifying the S phase. Synchronization by aphidicolin was spread over two full cycles since a second peak of synthesis of DNA was observed after 24 to

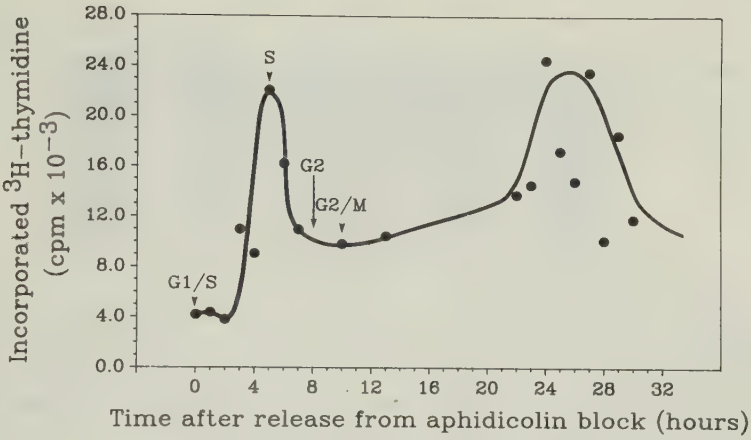

Fig. 1. Incorporation of [^{3}H]thymidine in DNA of synchronized BHK-21 cells. BHK-21 cells were plated in 24-well tissue culture plates, synchronized, labelled and their DNA precipitated as described in MATERIALS AND METHODS. Each point represents the average value from 3 wells.

26 h; this second maximum was however much broader indicating a progressive lost of the synchronization. With Pedrali-Noy's data [22], these results enabled us to establish four of the phases of the cell cycle: G0, during serum starvation; G1, when most of the cells are out of G0, 5 h after release from serum starvation with standard medium containing aphidicolin; G1/S, after a 24 h aphidicolin block; S, 6 h after the release from the aphidicolin block, at the first burst of DNA synthesis. G2 and G2/M phases were arbitrarily fixed at 3 h (G2) and 5 h (G2/M) after the S phase. That last point contains an increasing number of mitotic cells on the basis of the mitotic index (data not shown). Some difficulties to pinpoint an accurate position for G2 phase is in accordance with results from other groups [24].

Variations in lamins synthesis during the cell cycle were assessed by labelling of synchronized cells with [^{35}S]methionine for 10 and 60 min followed by immunoprecipitation of lamins with a specific antibody [2]. The newly synthesized lamins were visualized after autoradiography of SDS-PAGE gels. In G0 cells, no lamins were detected (data not shown) suggesting that the synthesis of lamins A, B and C is growth-regulated. As shown in Fig. 2, we observed an almost total lack of lamin B synthesis in G1 phase although newly synthesized lamins A and C were detected during this phase. All three lamins were detected in all phases afterward. Quantitative studies of SDS-PAGE autoradiograms were obtained by densitometry as shown in fig. 3. Since actin and vimentin, detected by our anti-lamin serum [1,2], are cell cycle dependant [25,26], no internal standard could be used. Therefore, the relative abundance of each lamin was calculated as the ratio of the total amount of lamins A, B and C. In normal non-synchronous cells, lamins are produced in almost equal amounts. During synchronization, we observed that the relative abundance of

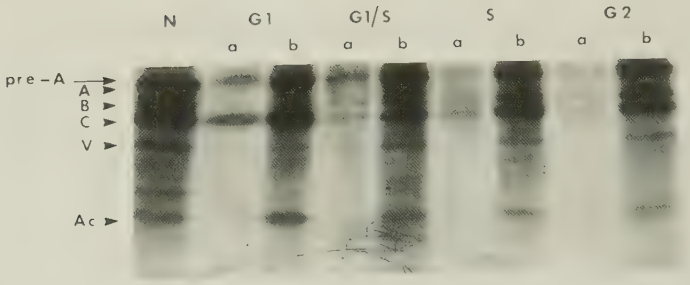

Fig. 2. Autoradiograph of SDS-PAGE of immunoprecipitated lamins labelled with [^{35}S]methionine in synchronized cells. BHK-21 cells were plated in 60 mm tissue culture petris, synchronized and labelled with [^{35}S]methionine as described in MATERIALS AND METHODS. Lane 1 represents normal non-synchronous cells labelled for 60 min. Lanes 2, 4, 6 and 8 represent immunoprecipitated lamins from cells labelled 10 min; lanes 3, 5, 7 and 9 represent immunoprecipitated lamins from cells labelled 60 min. A: lamin A; B: lamin B; C: lamin C; V: vimentin; Ac: actin.

pre-lamin A/lamin A and lamin C is fairly constant throughout the cell cycle; this is a very different situation from the ones previously reported by Jost and Johnson [19] on HeLa cells and Bludau et al. [20] on Ehrlich ascites cells but is in accordance with the results of Gerace et al. [14] and Ottaviano and Gerace [15]. In G1/S, we observed a low level of synthesis of lamin B with a maximum in S phase and a continuous synthesis at lower level in phases afterward. The presence of lamin B synthesis in G1/S phase can be explained by the fact that aphidicolin does not suppress in the G1/S interphase the

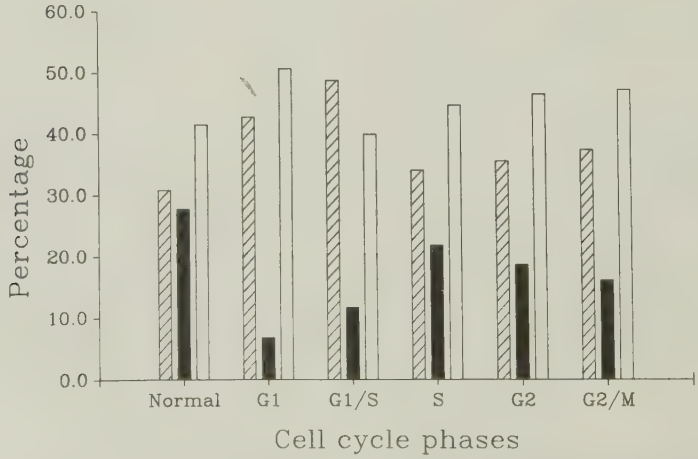

Fig. 3. Abundance of each lamin in the different phases of the cell cycle. Autoradiographs from SDS-PAGE of labelled immunoprecipitated lamins were scanned with a LKB Ultroscan XL and the lamins quantified. The value for each lamin represents its ratio of the total amount of immunoprecipitated lamins, for each phase of the cell cycle determined as described in MATERIALS AND METHODS. The hatched box represents pre-lamin A/lamin A, the open box, lamin B and the filled box, lamin C.

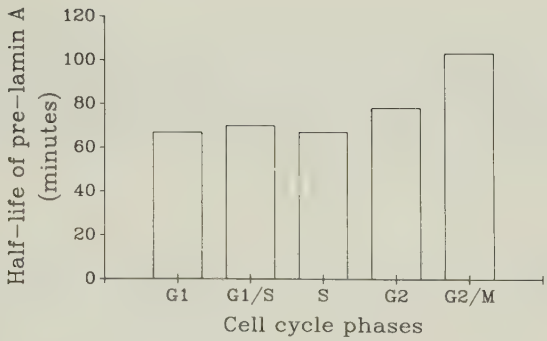

Fig. 4. Variation of the half-life of the precursor of lamin A during the cell cycle. BHK-21 cells plated in 60 mm tissue culture petri dishes were synchronized as described in MATERIALS AND METHODS. For each phase of the cell cycle, cells were pulse-labelled for 10 min with [^{35}S]methionine and chased with radioactivity-free medium for 0, 30, 60, 90 and 120 min. Lamins were immunoprecipitated and separated on SDS-PAGE, visualized by autoradiography and quantified using a LKB Ultroscan XL. The half-life was determined according to Dagenais et al. [2] by dividing the quantity of the pre-lamin A (74 kD) by the total amount of pre-lamin A (74 kD) and lamin A (72 kD).

synthesis of proteins normally synthesized in S phase [22]. The fact that lamin B is mainly produced in S phase may indicate that its synthesis is related to the expansion phase of the nucleus associated with the DNA synthesis that characterized that phase.

We examined also if there were variations in the half-time of the precursor of lamin A by pulse-chase experiments. Previous experiments using normal non-synchronized BHK-21 [2] cells have shown a half-life of 63 minutes, a very long time compared to other known precursors suggesting a post-transcriptional processing. The half-time determined for the conversion of pre-lamin A into lamin A at each phase is shown in fig. 4. We observed that the half-life of the pre-lamin A remains constant for most of the cell cycle. However, we observed a sharp increase in G2 to 78 min with a maximum in G2/M of 103 min. This increase suggests that the protease responsible for the processing of pre-lamin A is not present nor active prior to mitosis, allowing an accumulation of the precursor for lamin A in pre-mitotic cells. Although a precursor for lamin A has been observed in many different cells [27], no role has been suggested for this protein. This difference in half-life during the cell cycle is the first indication that pre-lamin A may play an important function during cell growth.

We report an effective approach to synchronize fibroblasts in culture by using aphidicolin to inhibit DNA synthesis therefore stopping the cells in a G1/S interphase. The analysis of the synthesis of lamins in such cells shows that general synthesis of lamins A, B and C is related to cell growth with differences in individual synthesis pattern. Lamin B is not synthesized in G1 cells but is produced in the phases afterward with a peak of synthesis in S

phase whereas pre-lamin A/lamin A and lamin C are produced throughout the cell cycle. We also observed that in cells synchronized with aphidicolin, the half-life of the precursor for lamin A is increased in pre-mitotic cells. The studies of differential patterns of synthesis and variations in half-life on other cell lines are underway.

ACKNOWLEDGMENTS: We thank Dr. Ivan Todorov, Institute of Cell Biology, Bulgaria, for helpful discussions. This work was supported by the Medical Research Council of Canada and the National Cancer Institute of Canada.

REFERENCES

1. Dagenais, A., Bibor-Hardy, V. & Simard, R. (1984) Exp. Cell Res. 155, 435-447.
2. Dagenais, A., Bibor-Hardy, V., Laliberté, J.-F., Royal, A. & Simard, R. (1985) Exp. Cell Res. 161, 269-276.
3. Gerace, L., Blum, A. & Blobel, G. (1978) J. Cell Biol. 79, 546-566.
4. Gerace, L. & Blobel, G. (1980), Cell 19, 277-287.
5. Aebi, U., Cohn, J., Buhle, L. & Gerace, L. (1986) Nature 323, 560-564.
6. Laliberté, J.-F., Dagenais, A., Filion, M., Bibor-Hardy, V., Simard, R. & Royal, A. (1984) J. Cell Biol. 98, 980-985.
7. McKeon, F. D., Kirshner, M. W. & Caput, D. (1986) Nature 319, 463-468.
8. Fisher, D. Z., Caudhary, N. & Blobel, G. (1986) Proc. Natl. Acad. Sci. USA 83, 6450-6454.
9. Shelton, K. R., Higgins, L. L., Cochran, D. L., Ruffolo, J. J. & Egle, P. M. (1980) J. Biol. Chem. 255, 10978-10983.
10. Shelton, K. R., Guthris, V. H. & Cochran, D. L. (1980) Biochem. Biophys. Res. Commun. 93, 867-872.
11. Kaufmann, S. H., Gibson, W. & Shaper, J. H. (1983) J. Biol. Chem. 258, 2710-2719.
12. McKeon, F. D., Tuffanelli, D. L., Fukuyama, K. & Kirshner M. W. (1984) Proc. Natl. Acad. Sci. USA 67, 4374-4378.
13. Maul, G. G., Baglia, F. A., Newmeyer, D. D., Ohlsson-Wilheim, B. M. (1984) J. Cell Sci. 67, 69-85.
14. Gerace, L., Comeau, C. & Benson, M. (1984) J Cell Sci. suppl. 1, 137-160.
15. Ottaviano, Y. & Gerace, L. (1985) J. Biol. Chem. 260, 624-632.
16. Raymond, Y., Gagnon, G. (1988) Biochemistry 27, 2590-2597.
17. Wolda, S. L., Glomset, J. A. (1988) J. Biol. Chem. 263, 5997-6000.
18. Gerace, L. & Blobel, G. (1980) Cell 19, 277-287.
19. Jost, E. & Johnson, R. T. (1981) J. Cell Sci. 47, 25-53.
20. Bludau, H., Kopun, M. & Werner, D. (1986) Exp. Cell Res. 165, 269-282.
21. Ikegami, S., Tagushi, T. & Ohashi, M. (1978) Nature 275, 458-460.
22. Pedrali-Noy, G., Spadari, S., Miller-Faurès, A., Miller, A. O. A., Kruppa, J. & Koch, G. (1980) Nucl. Ac. Res. 8, 377-387.
23. Huberman, J. A. (1981) Cell 23, 647-648.
24. Hoy, C. A., Rice., G. C., Kovacs, M., Schimke, R. T. (1987) J. Biol. Chem. 262, 11927-11934.
25. Ferrari, S., Battini, R., Kaczmarek, L., Rittling, S., Calabretta, B., Kim de Riel, J., Philiponis, V., Wei, J.-F., Baserga, R. (1986) Mol. Cell. Biol. 6, 3614-3620.
26. Masibay, A. S., Qasba, P. K., Sengupta, D. N., Damewood, G. P., Sreevalsan, T. (1988) Mol. Cell. Biol. 8, 2288-2294.
27. Franke, W. (1987) Cell 48, 3-4.

Vol. 156, No. 1, 1988 BIOCHEMICAL AND BIOPHYSICAL RESEARCH COMMUNICATIONS
October 14, 1988 Pages 211-216

POTASSIUM ION DEPENDENT PROTON EFFLUX AND DEPOLARIZATION FROM SPLEEN LYSOSOMES

Yoshinori Moriyama

Roche Institute of Molecular Biology,Roche Research Center,
Nutley, New Jersey 07110

Received August 30, 1988

SUMMARY: Lysosomes, isolated from various organs, exhibited an acidic interior (≅ pH 5.2) when incubated in a buffer at neutral pH. K^+-induced proton efflux was observed in spleen lysosomes, but not in liver or kidney lysosomes. The initial velocity of the proton efflux showed saturation kinetics with Km value of about 15 mM K^+. Rb^+ and Cs^+ have an effect similar to K^+, while Na^+, Li^+ or divalent cations have little or no effect. The properties of the K^+ induced proton efflux correlated with the K^+-induced depolarization of the lysosomes, suggesting the presence of K^+-transport system(s) in lysosomal membranes. © 1988 Academic Press, Inc.

INTRODUCTION: Lysosomes, one of the vacuolar organelles in mammalian cells, play an important role in intracellular digestion (1). Since nutrients are hydrolyzed inside and reutilized outside of the organelles, transport systems for the metabolites have been postulated in lysosomal membranes (2). Some sugars and amino acids are extruded from lysosomes via specific transport systems (2). Amino acid efflux might be coupled with proton motive force which is formed by lysosomal H^+-ATPase (3,4). Moreover, it has been proposed that some genetic disorders are due to defective lysosomal transport systems (3,5). Lysosomal ion transport systems may function in processes such as regulation of electrochemical potential, osmotic pressure, and volume changes. Although such ion transport systems were found in various vacuolar systems (6,7,8), little is known about ion transport in lysosomes.

Fluorescein isothiocyanate dextran (FITC-dextran) has been used to measure the internal pH of lysosomes (9). FITC-dextran is taken up via endocytosis and trapped in lysosomes, allowing measurement of intralysosomal pH specifically, even in the presence of other organelles. Using this method, the effect of various salts on internal pH of lysosomes prepared from various organs was studied. It was found that K^+ induced proton efflux and depolarization in spleen lysosomes.

MATERIALS AND METHODS

Materials. FITC-dextran (FD-70S) and Triton WR 1339 (tyroxapol) were purchased from Sigma. 3,3'dipropylthiadicarbocyanine iodide (diS-C3(5)) was obtained

0006-291X/88 $1.50
Copyright © 1988 by Academic Press, Inc.
All rights of reproduction in any form reserved.

from Molecular Probes. Animals (rats, Wistar male, 200-250 g body weight, mouse, ddY male, about 20 g body weight) were supplied from Charles River Co.

Analytical procedures. Fluorescence change of FITC-dextran and diS-C3(5) were measured with Perkin Elmer MPF66 fluorescence spectrometer as described previously (9,10,11). The assay solution consisted of 20 mM MOPS-tris pH 7.0, 0.3 M sucrose and lysosomes. Lysosomal latency and marker enzyme activities for lysosomes, mitochondria and plasma membrane were measured as described previously (12). Protein concentration was estimated by the method of Lowry et al. (13).

Preparations. FITC-dextran (20 mg/ml) was introduced into lysosomes as described previously (9). After overnight starvation, animals were decapitated and various organs were isolated. Crude lysosomes from liver or kidney were prepared by differential centrifugation according to the published procedures (9,10). Crude lysosomes from spleen were prepared as follows: Isolated spleen was homogenized in 3 vol of 0.3 M sucrose containing 1 mM EDTA and 0.1% v/v ethanol pH 7.0 (SVE). The homogenate was centrifuged at 270 g for 10 min and the supernatant was diluted twice with SVE and centrifuged at 500 g for 5 min to remove erythrocytes. This step was repeated a few times if necessary. The supernatant was then centrifuged at 12000 g for 10 min, and the pellets (crude spleen lysosomes) were washed twice with SVE, suspended in the same solution, and kept on ice until use.

Highly purified lysosomes from liver or kidney were prepared by the published procedures (9,10). Highly purified lysosomes from rat spleen were prepared as follows: Triton WR 1339 (0.85 mg/g of body weight) was injected intraperitoneally into rats 1 week before preparation. After overnight starvation, rats were killed and spleens were isolated. Crude spleen lysosomes were prepared as described above and suspended in 45% (w/w) sucrose and layered onto 60% (w/w) sucrose. A discontinuous sucrose density gradient was made by adding 12 ml of 34.5% (w/w) sucrose and 8 ml of 14.3% (w/w) sucrose. The gradient was centrifuged at 90000 g for 2 h. Lysosomes which were recovered from the interface between 34.5% and 14.3% sucrose were taken by pipetting and kept on ice until use. Lysosomal purity was estimated from marker enzymes to be about 30-35 fold over the homogenate, which is the highest purity achieved for lysosomes from lymphoid tissues (14). In addition, the latency of the purified lysosomes was greater than 80%.

RESULTS AND DISCUSSION

Internal pHs of lysosomes from various organs. FITC-dextran was found to be present in various organs following intraperitoneal injection. Appreciable amounts of FITC-dextran were found in liver, spleen, kidney, adrenal and testis as shown in Table 1. Subcellular fractionation studies revealed that almost all FITC-dextran was present in the particulate fraction corresponding to lysosomes (not shown). Thus, the lysosomal pH of these organs can be measured using the FITC-dextran fluorescence technique developed for liver lysosomes (9). All lysosomes prepared from these organs maintained an acidic pH (≅ pH 5.2) when suspended in the buffer at neutral pH. In lysosomes from all organs addition of MgATP (1 mM) resulted in decreased FITC-dextran fluorescence, indicating acidification by H^+-ATPase. The properties of the MgATP-induced acidification (divalent cation requirement, substrate specificity, sensitivity to inhibitors) were essentially the same as those from previous reports (9-12), suggesting that the same type of H^+-ATPase operates in lysosomes from various organs.

K^+-induced H^+ efflux in spleen lysosomes. It is well known that plant vacuoles contain cation/proton antiporters (6-8), which take up cations at the expense of proton motive force established by the H^+-ATPase. The effect of cations on lysosomal pH was measured to identify similar systems in lysosomes.

Fig. 1 shows the effect of KCl on rat lysosomal pH. Addition of KCl significantly enhanced the fluorescence intensity of FITC-dextran (Fig. 1-a), without changing the

TABLE I

Distribution of FITC-dextran into Various Organs from Rat and Mouse

Organ	Content of FITC-dextran (relative fluorescence intensity per weight of organ)	
	rat	mouse
liver	100	100
spleen	30	24
kidney	15	7
adrenal	5	5
testis	4	7
brain	< 0.5	< 0.5
lung	< 0.5	< 0.5
heart	ND	3

ND: not detected.

FITC-dextran was injected into animals and the organs were isolated and homogenized as described in "Materials and Methods". After removing nucleous and unbroken cells by centrifugation, content of FITC-dextran in the post-nuclear supernatant was estimated by its fluorescence in 20 mM MOPS-tris pH 7.0 containing 0.05% Triton X-100. Content of FITC-dextran was expressed as relative fluorescence intensity per wet weight of organ with that of liver taken as 100%.

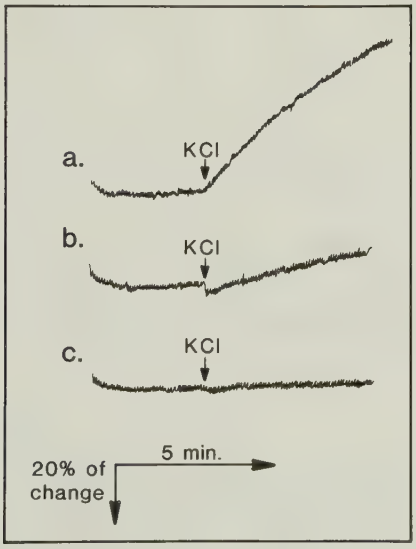

Figure 1. KCl-induced proton efflux from lysosomes. Changes in intralysosomal pH were measured by FITC-dextran fluorescence as described in "Materials and Methods". KCl was added at final concentration of 25 mM as indicated. a, lysosomes from rat spleen, 40 μg protein; b, lysosomes from rat liver, 80 μg protein; c, lysosomes from rat kidney, 40 μg protein.

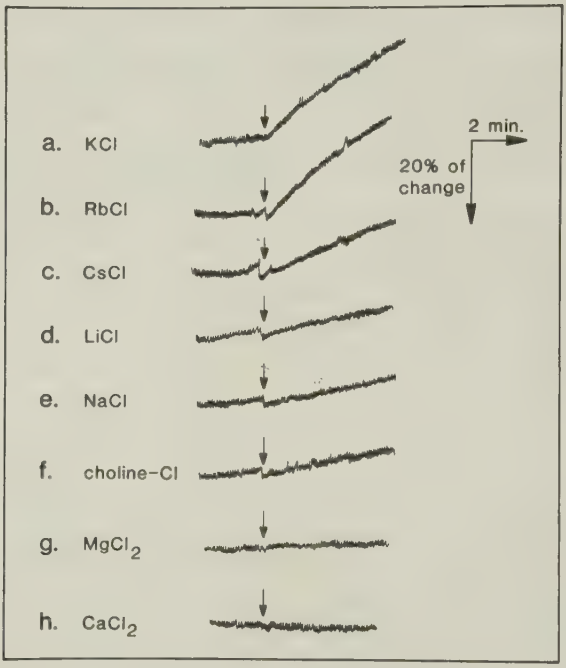

Figure 2. Cation specificity of proton efflux. Changes in the internal pH of spleen lysosomes following the addition of various salts were measured as described in "Materials and Methods". Fifty µl of 1 M salt were added to give a final concentration of 25 mM as indicated. Fifty µg protein of lysosomes were used per assay.

latency of the lysosomes, indicating alkalization of intralysosomal space. The KCl induced proton efflux was predominantly observed in spleen lysosomes. However, KCl had little effect on lysosomes from liver or kidney (Fig. 1-b,c). Essentially the same phenomena were observed in lysosomes prepared from mouse organs. The KCl induced proton efflux showed typical saturation kinetics with a half maximum effect at 15 mM KCl giving maximum change of initial velocity (ΔpH 0.02/min). Fig. 2 shows the effect of various salts on spleen lysosomal pH. Rb^+ and Cs^+ were also effective, however, other monovalent or divalent cations have no significant effect. Anions (Cl^-,Br^-, SO_4^{2-}, I^-, NO_3^-, F^- and SCN^-) have essentially no effect on K^+ induced proton efflux (data not shown). These results indicated that K^+ induced efflux of protons from spleen lysosomes and suggested the presence of K^+-transport system(s) in lysosomal membranes, most probably K^+/H^+ exchange system.

K^+-induced depolarization of lysosomes. Lysosomes have been shown to be polarized inside negative when suspended in K^+-free buffer (10,11,15). Addition of K^+ depolarized the membrane potential. To see the correlation between the K^+-induced depolarization and proton efflux, changes in membrane potential of spleen lysosomes was measured. DiS-C3(5) fluorescence can be used to measure lysosomal membrane potential semiquantitatively (10,11). As shown in Fig. 3, similar amounts of fluorescence quenching was attained after several minutes incubation following the addition of

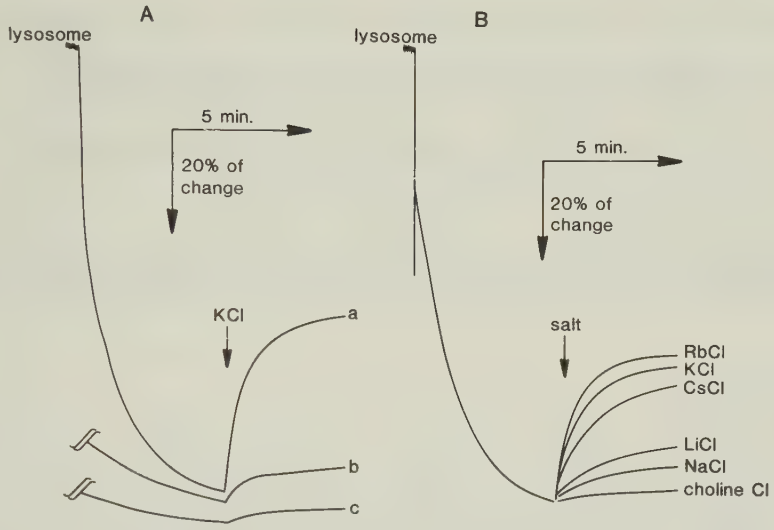

Figure 3. K^+-induced depolarization of lysosomes. The membrane potential of lysosomes was measured as described previously (11) in buffer containing 20 mM MOPS-tris pH 7.0, 0.3 M sucrose and 1 μM diS-C3(5). (A) Depolarization by K^+ in various lysosomes. KCl was added at 25 mM. Lysosomes from rat liver, kidney and spleen were purified as described in "Materials and Methods". (a) Spleen lysosomes (20 μg), (b) liver lysosomes (35 μg) and (c) kidney lysosomes (20 μg) were used for assay. (B) Cation specificity. Various salt solutions (25 mM) were added as indicated. Spleen lysosomes (20 μg) were used per assay.

lysosomes from all sources. Therefore, all lysosomes tested maintained nearly the same membrane potential (about 100 mV to 120 mV (10,11)). Addition of KCl decreased quenching, indicating depolarization of membrane potential. As expected, the initial velocity of depolarization in spleen lysosomes was about 5-fold and 20-fold faster than those of liver and kidney lysosomes, respectively (Fig. 3-A). Depolarization exhibited the same cation specificity as that of proton efflux (Fig. 3-B) and the same order of Km (10 mM, K^+) (not shown). These results indicated the close relationship between K^+-induced proton efflux and depolarization, and suggest that both activities are catalyzed by the same enzyme. It is concluded that an electrogenic K^+/H^+antiport may operate in lysosomal membrane. Of course, the possibility that influx of K^+ results in secondary movement of protons cannot be excluded. These activities are more pronounced in spleen in comparison with lysosomes from other sources (Fig. 1 and 3-A). This may be due to different activities or number of carriers in lysosomes from various organs. Thus, spleen lysosomes may be useful to study the K^+ transport system.

The physiological role of K^+-induced proton efflux and depolarization is not known. One possible role is in the regulation of intralysosomal pH. Chromaffin granule H^+-ATPase, which is one of the vacuolar H^+-ATPases, is regulated by anions and membrane potential (16,17). Similar mechanisms may be present to regulate lysosomal H^+-ATPase. *In vivo*, electrogenic K^+/H^+ transport or K^+ transport presented in this paper may cancel part of the membrane potential formed by H^+-ATPase, which helps to form a

larger ΔpH across the lysosomal membrane. In fact, the initial velocity of MgATP dependent acidification was accelerated about twice in the presence of K^+ (not shown). Recently, a similar K^+ conductance has been reported in various endomembrane systems where vacuolar type H^+-ATPase operates (18-21). It will be interesting to see the structural and functional relationship among these activities.

ACKNOWLEDGEMENTS: I wish to thank Dr. Nathan Nelson for encouragement, support during the study and critical reading of the manuscript. I also thank Dr. Patricia Reilly, Dr. Miloslav Boublik and Dr. John P. Reeves for critical reading of the manuscript.

REFERENCES

1. De Duve, C. (1983) *Eur. J. Biochem.* **137,** 391-397.
2. Docherty, K., Maguire, B.A., and Hales, C.N. (1983) *Biosci. Rep.* **3,** 207-216.
3. Jonas, A.J., Smith, M.L., Allison, W.S., Laikind, P., Greene, A.A., and Schneider, J.A. (1983) *J. Biol. Chem.* **258,** 11727-11730.
4. Pisoni, R.L., Thoene, J.G., and Christensen, H.N. (1985) *J. Biol. Chem.* **260,** 4791-4798.
5. Rosenblatt, D.S., Hosack, A., Matiaszuk, N.V., Cooper, B.A., and Laframboise, R. (1985) *Science* **228,** 1319-1321.
6. Ohsumi, Y., and Anraku, Y. (1983) *J. Biol. Chem.* **258,** 5614-5617.
7. Bush, D.R., and Sze, H. (1986) *Plant Physiol.* **80,** 549-555.
8. Blumwald, E., and Poole, R.J. (1985) *Plant Physiol.* **78,** 163-167.
9. Ohkuma, S., Moriyama, Y., and Takano, T. (1982) *Proc. Natl. Acad. Sci. U.S.A.* **79,** 2758-2762.
10. Harikumar, P., and Reeves, J.P. (1983) *J. Biol. Chem.* **2581,** 10403-10410.
11. Ohkuma, S., Moriyama, Y., and Takano, T. (1983) *J. Biochem. (Tokyo)* **94,** 1935-1943.
12. Moriyama, Y., Takano, T., and Ohkuma, S. (1984) *J. Biochem. (Tokyo)* **95,** 995-1007.
13. Lowry, O.H., Rosebrough, N.J., Farr, A.L., and Randall, R.J. (1951) *J. Biol. Chem.* **193,** 265-275.
14. Bowers, W.E. (1974) *Methods Enzymol.* **31,** 353-356.
15. Cretin, H. (1982) *J. Memb. Biol.* **65,** 175-184.
16. Moriyama, Y., and Nelson, N. (1987) *Biochem. Biophys. Res. Commun.* **149,** 140-144.
17. Moriyama, Y., and Nelson, N. (1988) In The Ion Pumps - Structure, Function and Regulation (Stein, W., Ed.), pp. 387-392, Alan R. Luis, Inc., New York, NY.
18. Wada, Y., Ohsumi, Y., Tanifuji, M., Kasai, M., and Anraku, Y. (1987) *J. Biol. Chem.* **2621,** 17260-17263.
19. Klein, U., Weerth, S., Schindlbeck, M., Schweikl, H., and Wieczorek, H. (1988) *Verh. Dtsch. Zool. Ges.* **81,** in press.
20. Schmalzing, G. (1987) *Eur. J. Biochem.* **168,** 27-35.
21. Kolb, H.-A., Köhler, K., and Martinoia, E. (1987) *J. Memb. Biol.* **95,** 163-169.

Vol. 156, No. 1, 1988 BIOCHEMICAL AND BIOPHYSICAL RESEARCH COMMUNICATIONS
October 14, 1988 Pages 217-221

RELEASE OF PEPTIDE LEUKOTRIENES FROM RAT KUPFFER CELLS

Yoshihide Sakagami*, Yasuhiro Mizoguchi*, Shuichi Seki*, Kenzo Kobayashi*, Seiji Morisawa**, and Sukeo Yamamoto***

*The Third Department of Internal Medicine, **The First Department of Biochemistry, Osaka City University Medical School, Osaka, Japan

***Osaka Socio Medical Center, Osaka, Japan

Received August 30, 1988

SUMMARY : Kupffer cells isolated from the normal rat liver were incubated with calcium ionophore A23187, and the levels of peptide leukotrienes (LTC_4, LTD_4, and LTE_4) contained in the culture supernatant were determined by the combined technique of reverse-phase high-performance liquid chromatography and radioimmunoassay. In response to A23187, Kupffer cells released LTC_4, LTD_4, and LTE_4. After 10 min-preincubation of Kupffer cells with AA861, a 5-lipoxygenase inhibitor, the generation of LTC_4, LTD_4, and LTE_4 from A23187-stimulated Kupffer cells was significantly suppressed. Platelet activating factor (PAF), a phospholipid mediator, significantly enhanced the release of LTC_4, LTD_4, and LTE_4 from Kupffer cells stimulated with A23187. These results suggested that Kupffer cells may participate in inflammatory and immunologic events in the liver tissue by the release of peptide leukotrienes.
© 1988 Academic Press, Inc.

Kupffer cells, as resident macrophages of the liver, are part of the organism's mononuclear phagocyte system and show many typical functions common to macrophages of different provenance (1-3). It is also reported that Kupffer cells may have the capacity to influence immunologic and inflammatory events in chronic liver diseases (4-6).

Peptide leukotrienes (LTC_4, LTD_4, and LTE_4) are derived from arachidonic acid via the lipoxygenase pathway (7) and are potent mediators of inflammatory and allergic reactions. LTC_4, LTD_4, and LTE_4 may contribute significantly to the pathogenesis of various inflammatory and ischemic disorders (8). Leukotrienes are known to be produced from macrophages, polymorphonuclear leukocytes, and mast cells (9). Although Kupffer cells stimulated with certain substances release prostaglandin E_2, prostaglandin I_2, thromboxane A_2, and a variety of other inflammatory mediators (10), how

0006-291X/88 $1.50
Copyright © 1988 by Academic Press, Inc.
All rights of reproduction in any form reserved.

LTC_4, LTD_4, and LTE_4 are formed by Kupffer cells is as yet unknown. In this study, we examined the production of LTC_4, LTD_4, and LTE_4 from rat Kupffer cells.

MATERIALS AND METHODS

Chemicals: Calcium ionophore A23187, Hank's balanced salt solution, Tyrode's solution, medium RPMI 1640, pronase, collagenase, L-serine, and gelatin were obtained from Sigma, Tokyo, Japan. AA861 (2-[12-hydroxy-dodeca-5,10-diynyl]-3,5,6-trimethyl-1,4-benzoquinone) was a generous gift from Takeda Chemical Industries, Osaka, Japan. Platelet activating factor, synthetic LTC_4, LTD_4, and LTE_4 were kindly supplied by Ono Pharmaceuticals, Osaka, Japan. The radioimmunoassay kit for LTC_4, LTD_4, and LTE_4 was purchased from Amersham Japan, Osaka, Japan.

Preparation and incubation of rat Kupffer cells: Kupffer cells were isolated from the Wistar rat liver as previously reported (6). Kupffer cell suspension in Tyrode's solution containing 20mM L-serine and 1% gelatin was prepared. Based on histochemical staining, 95% of the adherent cells from the rat liver were found to be Kupffer cells. The Kupffer cell suspension ($5x10^5$ cells/ml) was incubated with calcium ionophore A23187 (2.5 μM) with or without 10^{-9}M PAF. The Kupffer cell suspension was also incubated with 10^{-6}M AA861, a specific inhibitor of 5-lipoxygenase (11), which was added to the cell suspensions 10 min before the addition of calcium ionophore. Immediately after the incubation of Kupffer cells, a four-fold amount of ice-cold ethanol was added, and the supernatant was obtained by centrifugation.

Purification and assay of LTC_4, LTD_4, and LTE_4: LTC_4, LTD_4, and LTE_4 in the culture supernatant were fractionated by reverse-phase high-performance liquid chromatography (HPLC) and determined by radioimmunoassay as follows. The ethanol-extracted leukotriene-rich supernatant was evaporated to dryness under nitrogen gas in a water bath at 37°C. This was then suspended in 1.5 ml of 40% methanol and used as the sample for the fractionation by HPLC. One milliliter of the above sample was injected into a pre-column (YMC-BBC-5 S-5 ODS; Yamamura Chemical Lab., Osaka, Japan), and this was washed with distilled water (flow rate: 1 ml/min) for 4 min. The flow was then changed by the column switching method using a system controller (SCL-6A; Shimazu, Osaka, Japan), and the mobile phase (acetonitrile/methanol/water/acetic acid : 1500/500/1500/1, adjusted to pH 5.6 with triethylamine) was injected from the opposite side of the pre-column at a flow rate of 1 ml/min and drawn into the main column. Develosil (ODS 5k; 4.6x150 mm; Nomura Chemicals, Aichi, Japan) was used as the main column, and the absorbance of elutes at 280 nm was measured using a spectrophotometer (SPD-6A; Shimazu) and monitored using Chromatopac (C-R4A; Shimazu). Each fraction corresponding to the standard preparation of LTC_4, LTD_4, and LTE_4 was collected by a fraction collector (FRAC-100; Pharmacia Japan, Osaka, Japan). These fractionated materials were evaporated to dryness and resuspended in Tyrode's solution. LTC_4, LTD_4, and LTE_4 in the HPLC-purified sample were measured by radioimmunoassay according to the method of Levi-Schaffer et al (12).

RESULTS

When incubated with calcium ionophore A23187 (2.5 μM), Kupffer cells generated LTC_4, LTD_4, and LTE_4 (Fig. 1, Fig. 2, and Fig. 3). LTC_4 level in the culture supernatant of Kupffer cells reached the peak at 5 min after the addition of A23187 with a decline thereafter (Fig. 1). AA861, a specific 5-lipoxygenase inhibitor, had an inhibitory effect on leukotriene release

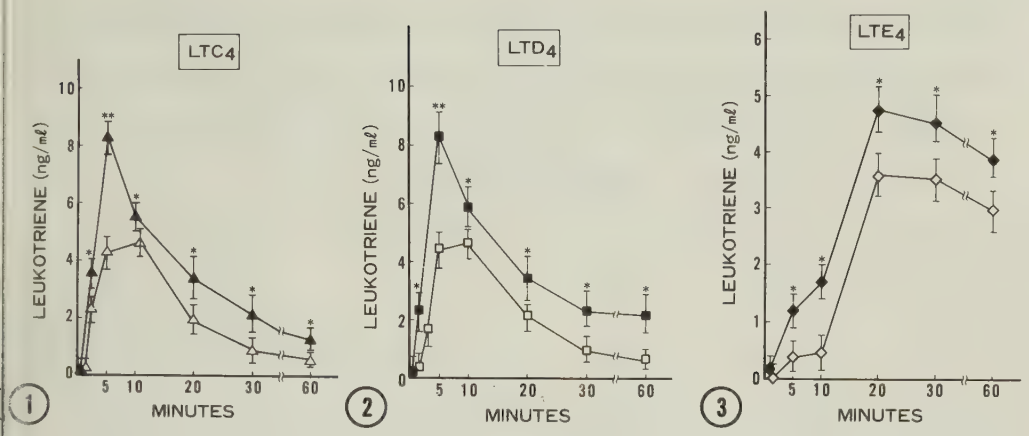

Fig. 1 Release of LTC_4 from rat Kupffer cells.
Kupffer cells were treated with 2.5 μM A23187 (▲) or with 2.5 μM A23187 and 10^{-6}M AA861 (△). The values are means of five independent experiments, and bars indicate SD. At each time point, the difference between A23187-stimulated cells and A23187-stimulated cells pretreated with AA861 was significant (*p<0.01, **p<0.001).

Fig. 2 Release of LTD_4 from rat Kupffer cells.
Kupffer cells were treated with 2.5 μM A23187 (■) or with 2.5 μM A23187 and 10^{-6}M AA861 (□). The values are means of five independent experiments, and bars indicate SD. At each time point, the difference between A23187-stimulated cells and A23187-stimulated cells pretreated with AA861 was significant (*p<0.01. **p<0.001).

Fig. 3 Release of LTE_4 from rat Kupffer cells.
Kupffer cells were treated with 2.5 μM A23187 (◆) or with 2.5 μM A23187 and 10^{-6}M AA861 (◇). The values are means of five independent experiments, and bars indicate SD. At each time point, the difference between A23187-stimulated cells and A23187-stimulated cells pretreated with AA861 was significant (*p<0.01).

from rat Kupffer cells stimulated with calcium ionophore A23187. As shown in Fig. 1, pretreatment of Kupffer cells at 37°C for 10 min with 10^{-6}M AA861 caused a significant inhibition of LTC_4 release. LTD_4 release by rat Kupffer cells was essentially similar to that noted in LTC_4 (Fig. 2). On the other hand, LTE_4 level in the culture supernatant of Kupffer cells reached the peak at 20 min after the addition of A23187 with a decline thereafter (Fig. 3). In addition, AA861 significantly inhibited the release of LTE_4 from A23187-stimulated Kupffer cells.

When Kupffer cells were incubated in the presence of both 10^{-9}M PAF and 2.5 μM calcium ionophore A23187 at 37°C, PAF enhanced the production of peptide leukotrienes from Kupffer cells (Table 1). No leukotriene was detectable in the culture supernatant of Kupffer cells not stimulated with A23187 or PAF.

Table 1 Enhancement of the release of peptide leukotrienes from rat Kupffer cells by PAF

A23187 (μM)	PAF (M)	LTC_4[a]	LTD_4[a]	LTE_4[b]
		(ng/5x10^5cells)		
0	0	<0.01	<0.01	<0.01
0	10^{-9}	<0.01	<0.01	<0.01
2.5	0	8.21±0.42[c]	8.12±0.64[e]	4.76±0.45[g]
2.5	10^{-9}	10.56±0.51[d]	11.4±0.78[f]	6.72±0.66[h]

Incubation time : (a) 5 min, (b) 20 min. Significant difference between (c) and (d) at $p<0.01$, (e) and (f) at $p<0.005$, (g) and (h) at $p<0.01$.

DISCUSSION

It has been suggested that leukotrienes may be the key mediators in inflammatory liver diseases (9). Since Kupffer cells produce various chemical mediators (10) and have the capacity to influence immunologic events (6), they are thought to be closely related to inflammatory and immune responses in the liver.

Since LTC_4 is converted to LTD_4 and then to LTE_4, there is a prolongation of the biological effects of the peptide leukotrienes as they undergo metabolism. In many systems, LTD_4 is more biologically active than LTC_4, so that, at least initially, the metabolism of LTC_4 enhances the effects of peptide leukotrienes. However, LTE_4 is usually less active than LTD_4, although it still has appreciable biological activity (13). Moreover, since LTE_4 accumulates during leukotriene metabolism in Kupffer cells, LTE_4 may play a more important role in the pathogenesis of liver diseases than was previously thought. Our results show the possibility that Kupffer cells may affect inflammatory cell infiltration and the immune response in the liver through the production of LTC_4, LTD_4, and LTE_4.

PAF is a phospholipid mediator produced from macrophages and polymorphonuclear leukocytes, and is involved in anaphylaxie shock and various inflammatory responses (14). PAF is known to increase the production of prostaglandin E_2 from polymorphonuclear leukocytes (15). In this study,

the production of LTC_4, LTD_4, and LTE_4 from Kupffer cells was enhanced by PAF, suggesting that PAF may also be involved in inflammatory liver diseases by causing the increase in LTC_4, LTD_4, and LTE_4 production.

ACKNOWLEDGMENTS

We would like to thank Dr. Toshio Amano and Dr. Yasuji Terao of Takeda Chemical Industries Co. for their help with the techniques of high-performance liquid chromatography.

REFERENCES

1. Toh, K., Yamamoto, N., and Kikuchi, K. (1981) J. Reticuloendothel. Soc. 29, 265-273.
2. Birmelin, M. and Decker, K. (1983) Eur. J. Biochem. 131, 539-543.
3. Birmelin, M., Marme, D., Ferber, E., and Decker, K. (1984) Eur. J. Biochem. 140, 55-61.
4. Arthur, M.J.P., Kowalski-Saunders, P., and Wright, R. (1986) Gastroenterology 91, 174-181.
5. Hell, M.F. and Garvey, J.S. (1982) J. Reticuloendothel. Soc. 32, 287-296.
6. Richman, L.K., Klingenstein, R.J., Richman, J.A., Strober, W., and Berzofsky, J.A. (1979) J. Immunol. 123, 2602-2609.
7. Payman D.G., Goldman D.W., and Goetzl E.J. (1984) In The Leukotrienes. Chemistry and Biology (L.W. Charkrin and D.M. Bailey, Ed.), pp. 231-245. Academic Press, Orlando, FL.
8. Samuelsson, B. (1983) Science 220, 568-575.
9. Keppler, D., Hagmann, W., Rapp, S., Denzlinger, C., and Koch, H.K. (1985) Hepatology 5, 883-891.
10. Decker, K. (1985) Seminars in Liver Disease 5, 175-190.
11. Ashida, Y., Saijo, T., Kuriki, H., Makino, H., Terao, S., and Maki, Y. (1983) Prostaglandins 26, 955-972.
12. Levi-Schaffer, F., Dayton, E.T., Austen, F., Hein, A., Caulfield, J.P., Gravallese, P.M., Liu, F., and Stevens, R.L. (1987) J. Immunol. 139, 3431-3441.
13. Lewis, R.A. and Austen, K.F. (1984) J. Clin. Invest. 73, 889-897.
14. Valone, F.H. (1988) J. Immunol. 140, 2389-2394.
15. Dahl, M.L. (1985) Int. Archs. Allergy. Appl. Immun. 76, 145-150.

Vol. 156, No. 1, 1988 BIOCHEMICAL AND BIOPHYSICAL RESEARCH COMMUNICATIONS
October 14, 1988 Pages 222-227

DNA-BINDING PROTEINS IN PROTEIN KINASE C PREPARATIONS

Alessandro Testori, Charles S.T.Hii, Agnes Fournier, Leigh A.Burgoyne and Andrew W. Murray

School of Biological Sciences, Flinders University, Bedford Park, South Australia, 5042

Received August 31, 1988

Summary: Human DNA enriched in repetitive sequences specifically bound to a component(s) in purified preparations of rat brain protein kinase C (PKC). DNA which bound to protein was cloned in pUC-19 and one clone characterized as containing an approx. 140 bp insert. The band containing this insert (separated by acrylamide gel electrophoresis) was lost when the DNA was incubated with purified PKC preparations. Thus a protein in relatively pure PKC preparations is a sequence-selective DNA-binding protein. The results raise the possibility that PKC or a fraqment of PKC binds selectively to specific DNA sequences.

© 1988 Academic Press, Inc.

Identification of protein kinase C (PKC) as a binding protein for the tumor-promoting phorbol esters was a major advance in understanding promotion at the molecular level (1,2). Although the question of whether PKC activation is the only mechanism mediating the effects of the phorbol esters is still controversial (3,4), there is considerable interest in PKC as a target for phorbol esters because of its role in transmembrane signaling systems associated with the turnover of inositol phospholipids (2,5). Phorbol esters such as 12-0-tetradecanoylphorbol-13-acetate (TPA) act as structural analogs of 1,2-diacylglycerol and cause a massive translocation of PKC to membrane and the subsequent phosphorylation of specific proteins.

Although many of the early responses to TPA occur at the cell surface, these are followed by a programmed series of changes in gene expression (6,7). While it is generally assumed that the role of PKC in these changes is indirect (i.e. via phosphorylation), the enzyme contains a conserved cysteine-rich

0006-291X/88 $1.50
Copyright © 1988 by Academic Press, Inc.
All rights of reproduction in any form reserved.

tandem repeat near its amino terminus characteristic of some metalloproteins and DNA-binding proteins (8,9). In the present report we show that a component(s) in highly purified rat brain PKC preparations binds specifically to human DNA enriched in repetitive sequences.

Materials and Methods

Preparation of PKC. Rat brain PKC was purified by adsorption to and elution from inside-out red cell vesicles essentially as described (10). The eluted enzyme was further purified by DE-52 cellulose chromatography (11). Peak fractions of Ca^{2+}/phosphatidylserine-dependent activity were pooled and stored at 4°. Such preparations were stable for about 2 weeks. Typically, 18 g of rat brain yielded about 300 μg of protein with a specific activity of about 600 pmoles/min/μg protein when assayed as described (11). Protein was determined by the method of Bradford (12).Following electrophoresis on 12% SDS-polyacrylamide gels, the preparations showed a protein doublet of approx. 80kD and minor bands between 50-67 kD after Coomassie Blue (Fig.1) or silver staining (not shown). Both doublet bands and the more rapidly migrating material were detected by immunoblotting after electrophoretic transfer to nitrocellulose and probing with a rabbit antiserum to a peptide corresponding to amino acids 279-292 of bovine α-PKC (Fig.1). This antiserum detects all of the three major PKC isozymes present in rat brain (unpublished). Sheep anti-rabbit was used as the secondary antibody and detection was carried out with rabbit anti-sheep coupled to alkaline phosphatase. The bands were also detected by a sheep polyclonal antibody to mouse brain PKC (13) and a monoclonal antibody to rat brain PKC (Amersham). A similar doublet has previously been observed in purified preparations of rat brain PKC (14,15), and it has been concluded that the two bands are not a consequence of proteolysis or phosphorylation. The bands presumably represent partial resolution of the three major, closely related, isozymes of PKC known to be present in purified rat brain PKC preparations (16).

Human repetitive DNA. Human DNA was sonicated, denatured, renatured under slowly decreasing stringency and digested with S1 nuclease. After phenol extraction, those fragments larger than approx. 100 bp were selected by gel filtration. The final product represented approx. 10% of the original DNA, and on agarose gel electrophoresis it showed a near-random smear ranging from 0.1kb to 0.4kb, except for a pronounced band in the region of 0.3-0.4kb that was presumably the small interspersed repeat, ALU. Repeated cloning from this material has demonstrated that all of the common repetitive species of human DNA are well represented. The DNA was labelled using Klenow polymerase and [α-^{32}P]ATP.

Cloning of sequences binding to PKC preparations. PKC (4 μg) was dot-blotted onto nitrocellulose, hybridised with repetitive DNA (200 ng) and washed with binding buffer (20mM Tris,pH 7.6, 50mM KCl,0.05% Nonidet P40, 5% glycerol, 50μg/ml BSA, 10mM 2-mercaptoethanol, 1mM EDTA). The nitrocellulose was incubated for 5 h in 0.2% tris dodecyl sulphate- 5mM EDTA containing proteinase K (6 μg/ml). The mixture was phenol extracted, the DNA precipitated with alcohol and resuspended in 10mM Tris,pH 8, 1mM EDTA. The DNA was ligated to dephosphorylated pUC-19 (100ng) cut

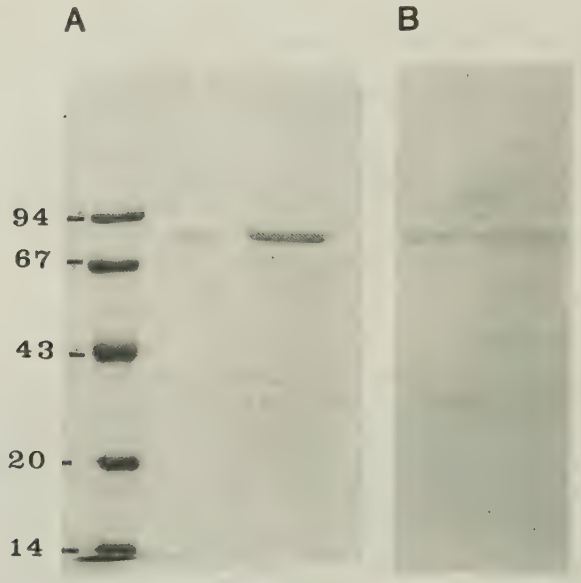

Figure 1. Characterization of purified PKC.
A. SDS-acrylamide gel of PKC stained with Coomassie blue. Left lane, molecular weight markers; centre lane, 0.35 μg protein; right lane, 3.5 μg protein. B. Western blot of parallel gel stained with anti-PKC (see Materials and Methods).

with Sma I, and the ligation mixture used to transform competent JM-101 cells. The inserts were cut out with EcoR1 and Sal 1, Klenow-labelled and used as probes in mobility-shift assays.
DNA-binding assay. Purified PKC (0.1-1 μg protein) was mixed with the probe (approx.0.5μC_i) in binding buffer and incubated for 30 min in the presence of up to 1μg of poly(d[I-C]). Reaction mixtures were loaded onto 5% polyacrylamide gels and electrophoresed for 3 h in 40mM Tris-borate, pH 7.8, 1mM EDTA. Gels were dried and autoradiographed.

Results and Discussion

Incubation of PKC preparations (see Materials for characterization) with labelled DNA enriched in repetitive sequences followed by gel electrophoresis, resulted in the appearance of labelled bands with slower electrophoretic mobility (see arrows in Fig.2). These anomalous bands were not abolished by an excess of poly(d[I-C]), indicating that a component(s) of the DNA specifically bound proteins in the PKC preparation. In these preliminary experiments it was noted that the majority of the PKC preparation protein did not enter the gel. This was established by both Coomassie Blue staining and by loading gels with autophosphorylated PKC. However, a minor proportion of intact PKC, of a PKC fragment or of a non-PKC contaminant did enter the gel resulting in poly (d[I-C]) competition-resistent DNA-binding bands.

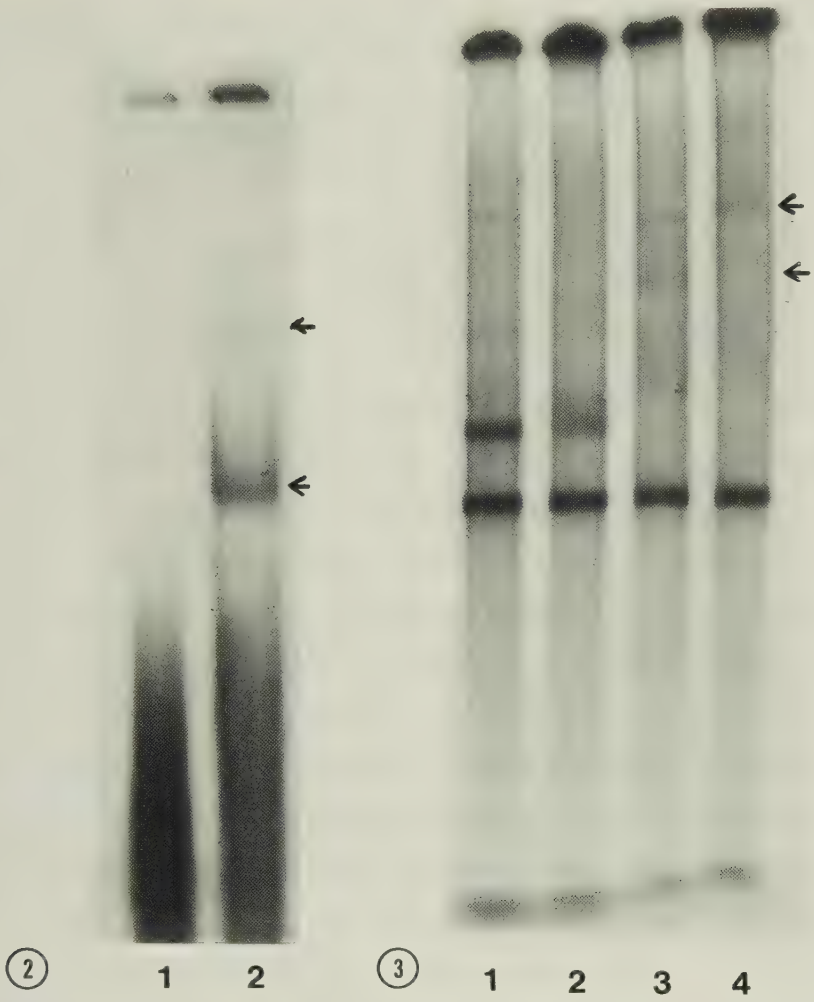

Figure 2. Binding of human repetitive DNA to PKC preparations. Unfractionated repetitive DNA (10 ng) was incubated in the absence (lane 1) or presence (lane 2) of PKC preparation (1 μg protein) and electrophoresed on an acrylamide gel.

Figure 3. Binding of cloned DNA to PKC preparations. Clone C-11 (5 ng DNA) was cut with EcoRI and Sal 1 and incubated in the absence (lane 1) and presence (lanes 2-4) of purified PKC (0.1, 0.5 and 1 μg protein respectively).

DNA which bound to the PKC preparations was extracted and the DNA fragments cloned in pUC-19. This gave 4 clones containing inserts which bound to PKC preparations in the presence of poly (d[I-C]). One of these clones (C-11) was used in further experiments. Incomplete cleavage of C-11 with EcoR1 and Sal gave two bands on acrylamide gels (Fig.3). The more slowly migrating band (approx. 170 bp, including 33 bp derived from the pUC polylinker) reacted with protein and had one uncleaved Sal 1

site within it.The faster, unreactive band (approx. 150 bp) is the same species, but with the internal Sal 1 site cleaved. Only this latter band was observed after complete cleavage with Sal 1 and EcoR1 or with Sal 1 alone. Clearly, incubation with PKC preparations resulted in the selective removal of the 170 bp band (Fig.3), and we therefore conclude that the binding sequence is close to the internal Sal 1 site. The unreactive, fully cleaved, species served as a closely related control. The experiment shown in Fig.3 was carried out in the absence of competitor except for the high molecular weight DNA derived from the vector. Similar results were obtained if up to 1 μg poly (d[I-C]) was included in the incubations (data not shown). Faint mobility shift bands were routinely observed in these experiments (eg see arrows in Fig 3). It is not, however, clear that these were responsible for the band disappearance. Although the band disappearance is an unequivocal proof of the existence of specificity in binding, it does not identify which protein(s) is the source of this specificity. A number of technical ambiguities unavoidably arise from the bulk of the protein not entering the gel. The results are compatible with one of the minor mobile species being responsible for the specific binding, but can not rule out the participation of other species that have not entered the gel.

Despite the high purity of the PKC preparations, we recognise the difficulties in unambiguously attributing the DNA-binding observed in these experiments to PKC or a fragment derived from PKC (17), and are currently using DNA-affinity chromatography to resolve this question. It will, however, be of great interest to determine whether the DNA sequence we have identified is associated with the regulatory elements of genes known to be regulated by phorbol esters and therefore with a suspected involvement of PKC.

Acknowledgements: This work was supported by grants from the National Health and Medical Research Council and the Anti-Cancer Foundation of the Universities of South Australia. We thank Elizabeth Isaac and Kathy Clark for expert assistance.

References

1. Castagna,M., Takai,Y., Kaibuchi,K., Sano,K., Kikkawa,U. and Nishizuka,Y. (1982) J. Biol. Chem. 257, 7847-7851.
2. Nishizuka,Y. (1986) Science, 233, 305-311.
3. Morin,M.J., Kreutter,D., Rasmussen,H. and Sartorelli,A.C. (1987) J. Biol. Chem. 262, 11758-11763.
4. Burch,R.M., Ma,A.L. and Axelrod,J. (1988) J. Biol. Chem. 263, 4764-4767.
5. Berridge,M.J. (1987) Ann. Rev. Biochem. 56, 159-193.
6. Chiu,R., Imagawa,M., Imbra,R.J.,Bockoven,J.R. and Karin,M. (1987) Nature, 329, 648-651.
7. Angel,P., Imagawa,M., Chui,R., Stein,B., Imbra,R.J., Rahmsdorf,H.J., Jonat,C., Herrlich,P. and Karin,M. (1987) Cell, 49, 729-739.
8. Parker,P.J., Coussens,L., Totty,N., Rhee,L., Young,S., Chen,E., Stabel,S., Waterfield,M.D. and Ullrich,A. (1986) Science, 233, 853-859.
9. Murray,A.W., Fournier,A. and Hardy,S.J. (1987) Trends Biochem. Sci. 134, 53-54.
10. Wolf,M., Cuatrecasas,P. and Sahyoun,N. (1985) J. Biol. Chem. 260, 15718-15722.
11. Tapley,P.M. and Murray,A.W. (1984) Biochem. Biophys. Res. Commun. 118, 835-841.
12. Bradford,M.M. (1976) Analyt. Biochem. 72, 248-254.
13. Cambier,J.C., Newell,M.K., Justerment,L.B., McGuire,J.C., Leach,K.L. and Chen,Z.Z. (1987) Nature, 327, 629-632.
14. Woodgett,J.R. and Hunter,T. (1987) Molec. Cell. Biol. 7, 85-96.
15. Woodgett,J.R. and Hunter,T. (1987) J. Biol. Chem. 262, 4836-4843.
16. Huang,K.P., Nakabayashi,H. and Huang,F.L. (1986)Proc. Natl. Acad.Sci. USA, 83, 8535-8539.
17. Fournier,A. and Murray,A.W. (1987) Nature, 330, 767-769.

Vol. 156, No. 1, 1988 BIOCHEMICAL AND BIOPHYSICAL RESEARCH COMMUNICATIONS
October 14, 1988 Pages 228-232

WATER IMMERSION INCREASES THE CONCENTRATION OF THE IMMUNOREACTIVE N-TERMINAL FRAGMENT OF PROATRIAL NATRIURETIC FACTOR IN HUMAN PLASMA

Alexander L. Gerbes and Angelika M. Vollmar *

Department of Medicine II, Klinikum Grosshadern and * Institute of Pharmacology, Toxicology and Pharmacy, University of Munich, Munich, Federal Republic of Germany

Received August 31, 1988

Atrial natriuretic factor (ANF) N-terminal (ANF 1-98) and C-terminal (ANF 99-126) fragments were determined by radioimmunoassay in human plasma. Mean basal plasma ANF N-terminal concentrations in 9 healthy subjects were 461 ± 58 fmol/ml, significantly ($p<0.0001$) higher than ANF C-terminal concentrations (4.8 ± 0.5 fmol/ml). Central volume stimulation by one hour head-out water immersion (WI) induced a significant ($p<0.01$) increase of the C-terminal peptide levels to 11.6 ± 2.3 fmol/ml, paralleled by a significant ($p<0.001$) increase of the N-terminal fragment levels to 749 ± 96 fmol/ml. Increases of plasma concentrations of both fragments upon WI correlated significantly ($r=0.71; p<0.05$). These data suggest cosecretion of the N-terminal fragment with the C-terminal fragment of pro ANF 1-126 following a physiological stimulus of ANF release in man. © 1988 Academic Press, Inc.

Atrial natriuretic factor (ANF) is stored in atrial granules as 126 amino acid prohormone (for review, see 1). Upon appropriate stimulation, such as atrial stretch (2), it is released and cleaved, and in the plasma the biologically active form has been identified as the 28 amino acid C-terminal fragment ANF 99-126 (3-7). Recently, presence of the N-terminal fragment ANF 1-98 has also been demonstrated in plasma of both, rat and man (8,9). This finding together with the observation of increased concentrations of both, N-terminal and C-terminal immunoreactivity following morphine stimulation in rats, suggested cosecretion of both fragments (8,9). The present study addresses the issue of cosecretion in man, applying water immersion (WI) as a physiological stimulus of ANF release (10-12).

0006-291X/88 $1.50
Copyright © 1988 by Academic Press, Inc.
All rights of reproduction in any form reserved.

MATERIALS AND METHODS

Subjects

9 healthy subjects, 5 men and 4 women, aged 30 to 65 (mean 47 ± 3) years were investigated after their informed consent had been obtained. The subjects had a normal physical examination and normal routine laboratory tests. They showed no evidence of cardiovascular,renal,pulmonary or endocrine diseases. The subjects were on a regular diet,containing approximately 150 meq sodium and took no medications.

Water immersion

The protocoll has been specified before (10,12).Briefly: In the morning of the experiment,an intravenous catheter was placed into a forearm vein and subjects sat down comfortably on a chair next to the immersion tank. After 1 hour,they were immersed to their neck into thermoneutral (34.5 ± 0.2 ^{o}C) water for one hour,maintaining the same seated position. This was followed by a 1 hour period of sitting outside the tank. Plasma samples were collected before ,after 1 hour WI and 1 hour after the end of WI.

Determination of ANF by radioimmunoassay

C-terminal ANF was determined by RIA, using antiserum Toni III,as described in detail before (6). The RIA procedure for the N-terminal fragment with antibody GT 23 has been reported elsewhere in detail (9).

Chromatographic analysis of ANF immunoreactivity (ir)

Serum was applied to a Spherogel TM TSK,2000 SW column (10 m,7.5 mm x 300 mm;Beckman Instruments,San Ramon,Ca.,USA) and eluted with 0.09 % TFA containing 0.005 M Na_2SO_4,0.002 M NaH_2PO_4 and 30% acetonitrile; flowrate was 0.3 ml/min. Calibration of the column was performed with bovine serum albumin,MW 66 KD (V_o), cytochrome C,MW 12.5 KD, vitamin B 12, MW 0.7 KD (V_t), rat pro ANF 2-126,MW 15 KD and human ANF 99-126,MW 3 KD. Fractions (0.3 ml) were lyophilized and tested for ir ANF by both RIA procedures.

Statistical evaluation

Differences between N-terminal and C-terminal concentrations as well as concentrations of the same fragment before and after WI were compared by paired t-test. The Pearson correlation coefficient was determined by the usual linear least squares test. Data are presented as mean and standard error.

RESULTS AND DISCUSSION

Concentrations and HPLC analysis of N-terminal and C-terminal immunoreactivity in human plasma

The mean plasma concentration of the N-terminal fragment in basal conditions was significantly ($p<0.0001$) higher than the mean concentration of C-terminal ANF: 461 ± 58 fmol/ml as compared to 4.8 ± 0.5 fmol/ml. This finding is in accordance

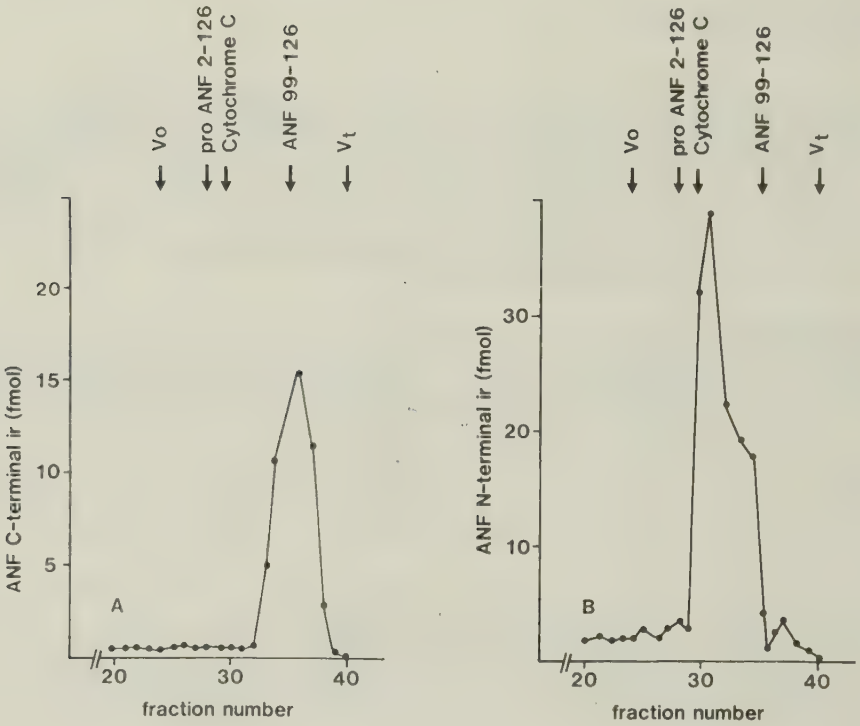

Figure 1
HPLC analysis of C-terminal (panel A) and N-terminal (panel B) ANF immunoreactivity.
The void (V_o) and total volumes (V_t) of the column were determined by BSA and vitamin B 12, respectively. Arrows indicate the elution positions of rat pro ANF 2-126, cytochrome C and human ANF 99-126. C-terminal immunoreactivity elutes in the molecular weight range of ANF 99-126, N-terminal immunoreactivity in the range of ANF 1-98.

with recent observations (9) and may be due to a longer elimination half-life of the N-terminal fragment.
Figure 1 shows a HPGPC analysis of C-terminal (panel A) and N-terminal (panel B) ANF immunoreactivity. The C-terminal ir was detected as a single peak coeluting with synthetic ANF 99-126. The N-terminal ir was eluted as a single peak in the molecular weight range of ANF 1-98.

N-terminal and C-terminal plasma concentrations after stimulation of ANF release

Following immersion plasma concentrations of C-terminal ANF increased significantly ($p<0.01$) from 4.8 ± 0.5 fmol/ml to 11.6 ± 2.3 fmol/ml,returning to 5.7 ± 0.7 fmol/ml post immersion

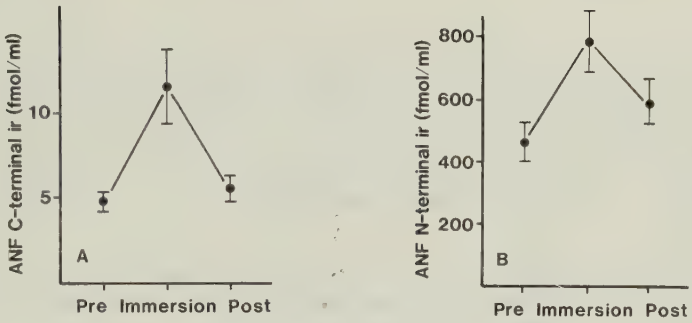

Figure 2
Plasma concentrations of C-terminal and N-terminal ANF immunoreactivity after stimulation of ANF release.
Plasma concentrations (mean ± standard error) of C-terminal (panel A) and N-terminal (panel B) ANF immunoreactivity before ("Pre"), after one hour water immersion ("Immersion") and one hour after the end of water immersion ("Post") of nine healthy subjects. Immersion induced a significant ($p<0.01$) increase of both, C-terminal and N-terminal ANF.

(figure 2a). This finding is in accordance with previous observations of our (10,12) and of other groups (11,13-15) and supports the contention that central volume stimulation stimulates ANF release. Interestingly,the concentration of the counterpart of the C-terminal fragment,the N-terminal fragment also was found increased upon immersion: plasma levels rose from 461 ± 58 fmol/ml to 749 ± 96 fmol/ml ($p<0.001$) during WI,returning to 590 ± 83 fmol/ml in the recovery period (figure 2b). The augmentations of plasma concentration of both fragments by immersion were correlated significantly ($r=0.71, p<0.05$).

The observation of an increase of the N-terminal in parallel with the C-terminal fragment of pro ANF 1-126 suggests cosecretion of both peptides in man following a physiological stimulus of ANF release.

ACKNOWLEDGMENTS

Drs. M. Cantin and G. Thibault,Clinical Research Institute of Montreal,Canada are thanked for providing antiserum GT 23 and for their help in establishing the RIA. Dr. R.Arendt,Dept. of Medicine I,Klinikum Grosshadern,Univ. of Munich,FRG is gratefully acknowledged for donating antiserum Toni III and for his support.Drs. Schöne,Preibisch and Seipke,Hoechst AG,Frankfurt,FRG provided synthetic rat pro ANF 2-126. M.Bauch,G.Hach,F.Höpker and R.Witthaut are thanked for technical assistance.

REFERENCES

1. Cantin, M. and Genest, J. (1985) Endocrin. Rev. 6, 107-127.
2. Lang, R.E., Thölken, H., Ganten, D., Luft, F.C., Ruskoaho, H. and Unger, T. (1985) Nature 314, 264-265.
3. Schwartz, D., Geller, D.M., Manning, P.T., Siegel, N.R., Fok,K.R., Smith, C.E. and Needleman, P. (1985) Science 229, 397-400.
4. Sugawara, A., Nakao, K., Morii, N., Sakamoto, M., Suda, M., Shimokura, M., Koso, Y., Kihara, M., Yamori, Y., Nishimura, K., Someda, J., Ban, T. and Imura, H. (1985) Biochem. Biophys. Res. Comm. 129, 439-446.
5. Thibault, G., Lazure, E.L., Schiffrin, J., Gutkowska, L., Chartier, R., Garica, R., Seidah, N.G., Chretien, M., Genest, J. and Cantin, M. (1985) Biochem. Biophys. Res. Comm. 130, 981-986
6. Arendt, R.M., Gerbes, A.L., Ritter, D. and Stangl, E. (1986) Klin. Wochenschr. 64(suppl VI), 97-102.
7. Needleman, P.J. and Greenwald, J.E. (1986) N. Engl. J. Med. 314, 828-834.
8. Thibault, G., Murthy, K.K., Gutkowska, J., Seidah, N.G., Lazure, C., Chretien, M. and Cantin, M. (1988) Peptides 9, 47-53.
9. Sundsfjord, J.A., Thibault, G., Larochelle, P. and Cantin, M. (1988) J. Clin. Endocr. Metab. 66, 605-610.
10. Gerbes, A.L., Arendt, R.M., Schnizer, W., Silz, S., Jüngst, D., Zähringer, J. and Paumgartner, G. (1986) Klin. Wochenschr. 64, 666-667.
11. Epstein, M., Loutzenhiser, R., Friedland, E., Aceto, R.M., Camargo, M.I.F. and Atlas S.A. (1987) J. Clin. Invest. 79, 738-745.
12. Gerbes, A.L., Arendt, R.M., Gerzer, R., Schnizer, W., Jüngst, D. and Paumgartner, G. (1988) Eur. J. Clin. Invest., in press.
13. Anderson, J, Struthers, A., Christofides, N. and Bloom, S. (1986) Clin. Sci. 70,327-331.
14. Ogihara, T., Shima, J., Hara, H., Tabuchi, Y., Hashizume, K., Nagano, M., Katahira, K., Kangawa, K., Matsuo, H. and Kumahara, Y.(1986) Life Sci. 38, 2413-2418.
15. Pendergast, D.R., De Bold, A.J., Pazik, M. and Hong, S.K. (1987) Proc. Soc. Exp. Biol. Med. 184, 429-435.

Vol. 156, No. 1, 1988 BIOCHEMICAL AND BIOPHYSICAL RESEARCH COMMUNICATIONS
October 14, 1988 Pages 233-239

THE EFFECT OF CYCLOSPORIN A ON THE GROWTH AND PROLACTIN BINDING TO Nb-2 RAT LYMPHOMA CELLS

Shobha Varma and Kurt E. Ebner

Department of Biochemistry & Molecular Biology
University of Kansas Medical Center
39th and Rainbow Blvd.
Kansas City, Kansas 66103

Received September 2, 1988

Cyclosporin A, an immunosuppressive agent, inhibited the prolactin stimulated growth of rat lymphoma Nb-2 cells. In the presence of 1 ng/ml of prolactin, 50% inhibition of growth was at 5 x 10^{-6} M and the inhibition was reversible. The K_d of cyclosporin A binding to the Nb-2 cells was 10^{-7} M and was independent of prolactin. The K_d of prolactin binding to the Nb-2 cells was 2 x 10^{-10} M. Cyclosporin A did not influence the binding of prolactin to the cells and vice-versa. The inhibitory effect of cyclosporin A on the growth of Nb-2 cells is due to some step other than the binding of prolactin to the cells. © 1988 Academic Press, Inc.

Cyclosporin A is a potent immunosuppressive agent preferentially active against proliferating T cells (1). It is postulated that immunosuppression is the result of reversibly blocking early mitogenic events in T cell activation (2) though the exact mechanism of this action is not clearly understood. Some evidence suggests that cyclosporin acts on activated T lymphocytes by blocking the transcription of the interleukin-2 gene (3-4) and other studies suggest that cyclosporin A might act by inhibiting calmodulin dependent cellular events (5).

Russell and coworkers (6,7) have demonstrated prolactin receptors on human peripheral blood lymphocytes and shown that cyclosporin inhibits the prolactin stimulated induction of ornithine decarboxylase in a variety of rat tissues, including the thymus and the spleen (8). These studies suggested that cyclosporin might be regulating the prolactin stimulated events by competing with prolactin for binding to its receptors (6,7). Similar observations in rat lymphocytes (9) suggested that the immunosuppressive effects of cyclosporin may be mediated by the displacement of prolactin from its binding site on rat lymphocytes.

In contrast, cyclosporin A did not affect the binding of ovine prolactin to isolated rabbit mammary gland membranes which have well characterized prolactin receptors (10). The Nb-2 rat lymphoma cell line requires lactogenic hormones for

Abbreviations: CsA, cyclosporin A; oPRL, ovine prolactin

0006-291X/88 $1.50
Copyright © 1988 by Academic Press, Inc.
All rights of reproduction in any form reserved.

growth (11-13) and has well characterized prolactin receptors (14). This cell line then provides an excellent system for studying prolactin binding and biochemical events resulting from the interaction of prolactin with its receptor (15-19).

In this study, the effect of cyclosporin A on the prolactin induced mitogenic stimulation of the Nb-2 cells was examined as well as the effect of cyclosporin A on the binding of prolactin to the Nb-2 cells. The results showed that cyclosporin A inhibited reversibly the prolactin growth stimulation of the Nb-2 cells and that the binding of prolactin and cyclosporin A was independent of each other.

MATERIALS AND METHODS

Measurement of Cell Growth

The Nb-2 rat lymphoma cells were a gift from Dr. C. T. Beer (Vancouver, Canada). CsA was a gift from Sandoz Pharmaceutical Ltd. and [^{3}H]-CsA (0.05 μCi/μg) was purchased from the same manufacturer. Ovine prolactin was provided by the National Institute of Arthritis, Metabolism and Digestive Diseases (Bethesda, MD). [^{125}I] Ovine PRL was prepared as previously described (20). Fetal calf serum and horse serum were purchased from Dutchland Laboratories, (Denver, PA).

Nb-2 lymphoma cells were maintained as suspension culture in Fisher's medium (K.C. Biologicals, Lenexa, KS) supplemented with 10% fetal calf serum (FS), 10% horse serum (HS), 10^{-4} M 2-mercaptoethanol, 50 u/ml penicillin and 50 μg/ml streptomycin (21). Incubation was at 37°C in an atmosphere of 5% CO_2-95% air. Under these conditions, the cell numbers doubled every 20 hours reaching a maximum at 72 hours. Nb-2 cells were made quiescent by incubation at 37°C for 24 hours in Fisher's medium containing 10% horse serum and 1% fetal calf serum (slow down media). The cells were then transferred at a concentration of 10^5 cells/ml into Fisher's medium containing 10% horse serum (stationary media). In stationary media the cell population did not increase substantially, but following the addition of 1 ng/ml of ovine PRL, it doubled every 20 hours.

In the experiments measuring the inhibitory effect of CsA on the oPRL stimulated proliferation of the Nb-2 cells, CsA was added at the onset of culture along with oPRL and incubation was continued for 72 hours unless otherwise indicated. At the end of this time period, 0.4 ml of the cell suspension were removed and diluted to 10 ml with Hematol (Fisher Scientific Company). The number of cells was determined in the Sysmex cell counter.

Measurement of Binding [^{125}I] oPRL and [^{3}H] CsA to Nb-2 Lymphoma Cells

The effect of CsA on the binding of [^{125}I] oPRL to the Nb-2 cells (and vice versa) was examined using similar protocols. Actively growing cells (in maintenance media) were slowed down for 24 hours. At the end of the 24 hour incubation period, the cells were removed by centrifugation and resuspended in stationary media at 2 x 10^6 cells/ml. Assays were carried out in duplicate in 1.5 ml Eppendorf tubes. For each data point, two tubes were used. Both tubes contained the same amount of radiolabeled ligand (100,000 cpm of [^{125}I] oPRL or 80,000 cpm of [^{3}H] CsA) but only one tube received the cold ligand. For each determination, 2 x 10^6 cells/ml were used in a total volume of 1.1 ml. Incubations with labeled ligand were at 37°C for 1 hour. At the end of this time period, the cells were pelleted and washed three times with phosphate buffered saline solution. The radioactivity in the cell pellet was measured using a gamma counter for [^{125}I] oPRL binding , and the liquid scintillation counter for [^{3}H] CsA binding.

Specific binding was the difference between the binding of the labeled ligand (total) and that in the presence of cold ligand (non specific binding). Under these conditions, the nonspecific binding was 12-20% of the total binding for [^{125}I] oPRL in presence of 10 μg/ml cold PRL where as it was 45% for [^{3}H] CsA in the presence of 10^{-5} M CsA.

RESULTS

Prolactin is a potent mitogen for the Nb-2 cells (11-13) with maximum growth occurring at 1 ng/ml of prolactin. When cyclosporin A was added at the onset of culture along with 1 ng/ml oPRL, a marked decrease in the prolactin stimulated proliferation of the cells occurred over the total growth period. The inhibition of growth by CsA was dose-dependent Fig. 1, and the concentration of CsA required for 50% inhibition of cell growth (the IC_{50}) was 5 x 10^{-6} M while the EC_{50} or the concentration of prolactin required for a 50% increase in cell growth was 0.05 ng/ml (2.3 x 10^{-12} M). CsA at 10^{-5} M completely inhibited growth.

Cyclosporin A by itself had no effect on cell numbers since they were the same as those obtained in control samples maintained in stationary media. The viability of the cells, incubated with cyclosporin A, as determined by trypan blue staining experiments showed that CsA was non-toxic to the cells.

The inhibition of cell growth by cyclosporin A was completely reversible under the conditions used (data not shown). Cells which were held in the presence of 10^{-5} M CsA for 3 days did not grow but after washing with media to remove the CsA and then placed in media containing 1 ng/ml oPRL exhibited a normal growth curve.

Binding of [^{125}I] oPRL to the cells was saturable and specific. About 80-88% of the total binding was specific while only 12-20% of [^{125}I] oPRL bound non-specifically. Displacement of [^{125}I] oPRL from its receptor by varying concentrations of ovine prolactin (1 ng/ml to 10 μg/ml) showed that the apparent Kd (defined as the concentration of the unlabeled hormone required to displace 50% of the specifically bound radiolabeled prolactin) was 2 x 10^{-10} M [Fig. 2]. This was in good agreement with the Kd (1.4 x 10^{-10}) obtained by Scatchard analysis

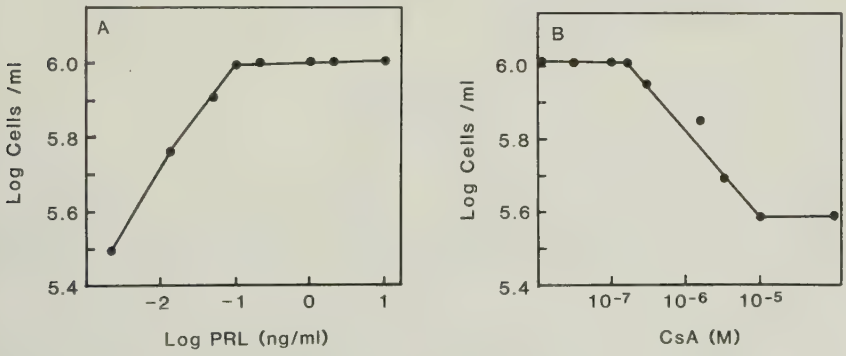

Fig. 1 Dose dependent inhibition of oPRL stimulated proliferation of Nb-2 cells by CsA

(A) Standard curve for the growth of Nb-2 cells at different concentrations of oPRL (from 0.01 ng/ml to 1 ng/ml). The EC_{50} for 50% stimulation of cell growth is 0.05 ng/ml oPRL.

(B) Inhibition of Nb-2 cells stimulated by 1 ng/ml oPRL by 5 x 10^{-6} M.

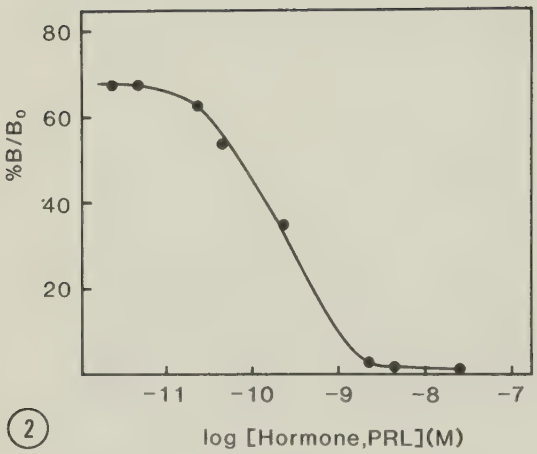

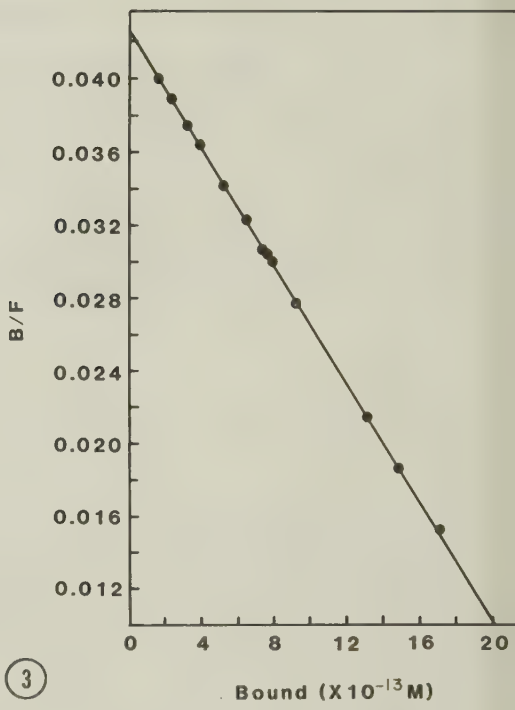

Fig. 2 Displacement curve for the binding of ^{125}I-oPRL to Nb-2 cells. Binding of [^{125}I]-oPRL to Nb-2 cells was carried out at varying concentrations of oPRL (from 0.05 ng/ml to 10 μg/ml). B represents specific binding of [^{125}I]-oPRL in the presence of 10 μg/ml of oPRL. B_0 is the maximum binding of [^{125}I]-oPRL. The data represent an average of two experiments.

Fig. 3 Scatchard analysis of [^{125}I]-oPRL binding to the Nb-2 cells. Data represents an average of two experiments

[Fig. 3]. Cyclosporin A over the concentration range 10^{-10} M to 10^{-5} M did not have any effect on the binding of [^{125}I] oPRL to the prolactin receptors on the Nb-2 cells [Fig. 4B]. Tritiated cyclosporin, however, bound to the cells with a Kd of 10^{-7} M. Competition with cold prolactin (up to 10 μg/ml had no effect on the binding of [^{3}H] CsA [Fig. 4A]. These results show that CsA and PRL do not compete for a common binding site on the Nb-2 cells.

Changes in the number and/or affinity of receptors can modulate the responsiveness of the cell to extracellular mitogenic signals. Also, the binding of structurally unrelated ligands to the cell can control the cellular affinity for the hormone. The possibility that cyclosporin A, by binding at a distinct site of its own on the Nb-2 cells, might somehow destabilize the binding of [^{125}I] oPRL to its receptor on the Nb-2 cells was explored. This was done by examining the Kd of [^{125}I] oPRL binding to the cells in the presence and absence of CsA by Scatchard analysis. No change was noted in the Kd of oPRL binding which was 1.4 to 2 x 10^{-10} in the absence of cyclosporin A and 2.7 x 10^{-10} in the presence of CsA at 10^{-5} M.

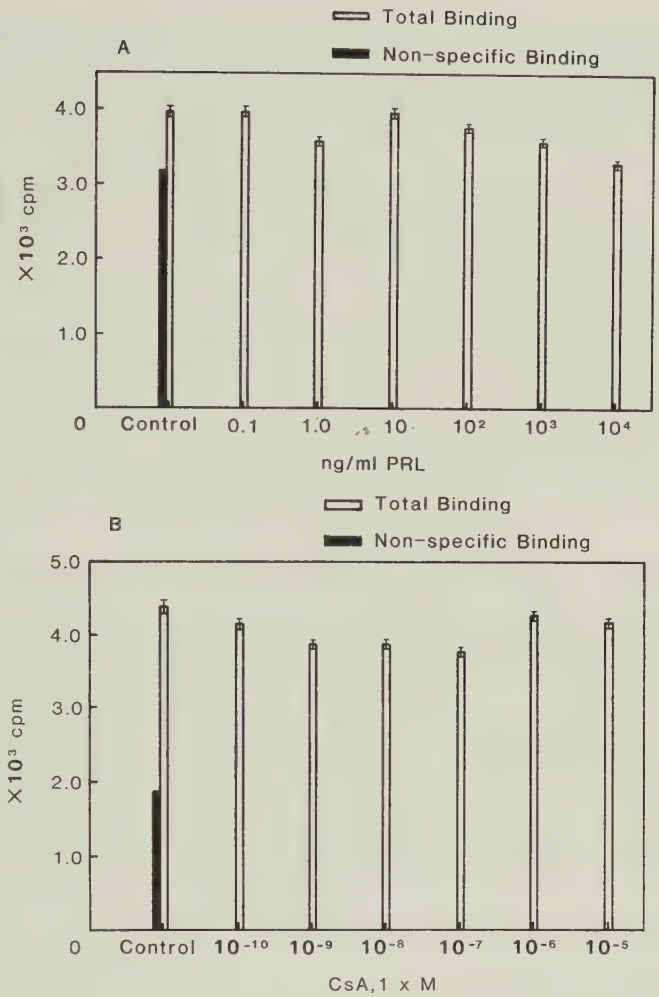

Fig. 4 Effect of ovine prolactin on the binding of [^{3}H]CsA (Fig. 5A) and of cyclosporin A on the binding of [^{125}I]-oPRL [Fig. 5B] to the Nb-2 rat lymphoma cells. Vertical bars represent an average of two experiments.

DISCUSSION

Previous studies (6,7) relating to the inhibitory action of cyclosporin A on human lymphocytes have implicated the prolactin receptor by competing for prolactin receptors. Such studies were difficult since these cells have low numbers of prolactin receptors which is in contrast to the Nb-2 rat lymphoma cells which have well characterized prolactin receptors and require prolactin for growth. Accordingly, the effects of cyclosporin A on the prolactin dependent growth and binding of prolactin to the Nb-2 rat lymphoma cells was examined in this study.

The results showed that cyclosporin A reversibly inhibited the prolactin stimulated growth of the Nb-2 cells with 50% growth inhibition at 5 x 10^{-6} M CsA. The K_d of binding of tritiated cyclosporin A to the Nb-2 cells was 1 x 10^{-7} M which is comparable to that found in other systems (22,23). In contrast, the K_d of

prolactin binding to the cells was 1.4 x 10^{-10} M and the concentration of prolactin to effect a 50% increase in growth was 2.3 x 10^{-12} M. These results are similar to binding constants observed for the binding of CsA (K_d = 2.2 x 10^{-6} M) and prolactin (K_d = 2 x 10^{-10} M) to isolated rabbit mammary gland membranes (10). Neither prolactin nor cyclosporin A competed with each other for binding suggesting that the sites were distinct. It is possible the CsA could modulate the binding of prolactin to the cells which occurred with the EGF receptor where PDGF which bound at a separate and distinct site deceased the affinity of EGF for its receptor (24-27). However, the presence of CsA did not change the K_d of prolactin binding to the Nb-2 cells indicating no evidence for transmodulation.

The results of this study show that in the Nb-2 rat lymphoma cell, cyclosporin A does not exert its action by interfering with the binding of prolactin to its receptor but acts at some point distal in the intracellular signal transduction pathway.

This concept is supported by the recent work of Bijsterbosch and coworkers (28) who have shown that in thymocytes or B cells, CsA does not interfere with the second messenger production initiated by PIP_2 breakdown, which is a receptor mediated event responsible for cell growth in many systems (29) including the Nb-2 cells (30). Cyclosporin A may inhibit an early step in lymphocyte activation by mitogens that induce PIP_2 degradation and Ca^{+2} mobilization (31-34).

ACKNOWLEDGEMENT

This work was supported by grant HD 18584 from the N.I.H.

REFERENCES

1. White, D.J.G., Plumb, A.M., Pawelec, G., Brons, G. (1979) Transplantation 27, 55-58.
2. Wiesinger, D. and Borel, J.F. (1979) Immunobiology 156, 454-463.
3. Elliot, J.F., Lin, Y., Mizel, S.B., Bleackley, R.C., Harnish, D.G. and Paetkau, V., (1984) Science 226, 1439-1441.
4. Kronke, M., Leonard, W.J., Depper, J.M., Arya, S.K., Wong-Stall, F., Gallo, R.C., Waldmann, T.A. and Greene, W.C. (1984) Proc. of Natl. Acad. Sci. USA 81, 5214-5218.
5. Colombani, P.M., Robb, A. and Hess, A.D. (1985) Science 228, 337-339.
6. Russell, D.H., Matrisian, L., Kibler, R., Larson, D.F., Poulos, B. and Magun, B.E. (1984) Biochemical and Biophysical Research Communications 121, 899-906.
7. Russell, D.H., Kibler, R., Martisian, L., Larson, D.F., Poulos, B. and Manun, B.E (1985) The Journal of Immunology 134, 3027-3031.
8. Russell, D.H., Larson, D.F., Cardon, S.B. and Copeland, J.G. (1984) Molecular and Cellular Endocrinolgy 35, 159-166.
9. Hiestand, P.C., Mekler, P., Nordmann, R., Grieder, A. and Permmongkol, C. (1986) Proc. Natl. Acad. Sci. USA 83, 2599-2603.
10. Mahajan, P.B. and Ebner, K.E. (1985) Biochem. Biophys. Res. Comm. 133, 753-758.
11. Gout, P.W., Beer, C.T. and Noble, R.L. (1980) Cancer Res. 40, 2433-2436.
12. Noble, R.L., Beer, C.T. and Gout, P.W. (1980) Cancer Res. 40, 2437-2440.
13. Tanaka, T., Shiu, R.P.C., Gout, P.W., Beer, C.T., Noble, R.L. Friesen, H.G., (1980) J Clin. Endocrinol. Metab. 51, 1058-1063.

14. Shui, R.P.C., Elsholtz, P., Tanka, T., Friesen, H.G., Gout, P.W., Beer, C.T., and Noble, R.L. (1983) Endocrinology 113, 159-164.
15. Bunjes, D., Hardt, C., Rollinghoff, M. and Wagner, H. (1981) Eur. J. Immunol., 11, 657-661.
16. Richards, J.F., Beer, C.T., Bourgeault, C., Chen, K. and Gout, P.W. (1982) Molecular and Cellular Endocrinology 26, 41-49.
17. Friesen, H.G., Cowden, E.A., Rowe, R.C., Klindt, J. and Kato, N. (1983) Prolactin and Prolactinomas, (Tolie, G. Ed.) Rowen Press, New York.
18. Gout, P.W., Juntze, W., Rennie, P.S. and Bruchovshi, N. (1984) Clinica Chemica Acta 139, 23-27.
19. Lawson, D.M., Sensui, N., Haisenleder, D.H. and Gala, R.R. (1982) Life Sciences 31, 3063-3070.
20. Necessary, P.C., Humphrey, P.A., Mahajan, P.B. and Ebner, K.E. (1984) J. Biol. Chem. 259, 6942-6946.
21. Necessary, P.C., Andersen, T.T., and Ebner, K.E. (1985) Molecular and Cellular Endocrinology, 39, 247-254.
22. Ryffel, B., Gotz, U. and Heuberger, B. (1982) J. Immunol. 129, 1978-1982.
23. Ryffel, B., Donatsch, P., Crotz, U. and Tschopp, M. (1980) Immunology 41, 913-919.
24. Rozenqurt, E. (1986) Science, 234, 161-166.
25. Heldin, C.H., Westermark, A., Wastrson, A. (1981) Proc. Natl. Acad. Sci. USA, 78, 3664-3668.
26. Collins, M.K.L., Sinnett-Smeth, J.W., Rozenqurt, E. (1983) J. Biol. Chem. 258, 11689-11693.
27. Bowen-Pope, D.F., DiCorletto, P.E., Ross, R. (1983) J. Cell Biol. 96, 679-683.
28. Bijsterbosch, M.K., Klaus, G.G.B (1985) Immunology, 56, 435-440.
29. Berridge, M.J. (1984) Biochemistry Journal, 220, 345-360.
30. Ofenstein, J.P. and Rillema, J.A. (1987) Proc. of the Society for Experimental Biology and Medicine, 185, 147-152.
31. Bijsterbosch, M.K., Meade, C.J.M., Turner, G.A., and Klaus, G.G.B. (1985) Cell, 41, 999-1006.
32. Kay, J.E., Meehan, R.T., Benzie, C.R. (1983) Immunol letter, 7, 151-156.
33. Kay, J.E., Benzie, C.R., Borghetti, A-F., (1983) Immunology, 50, 441-446.
34. Handschumacher, R.E., Harding, M.W., Rice, J., Dreugge, R.J. and Speicher, D.W. (1984) Science 226, 554-547.

Vol. 156, No. 1, 1988 BIOCHEMICAL AND BIOPHYSICAL RESEARCH COMMUNICATIONS
October 14, 1988 Pages 240-245

NOREPINEPHRINE STIMULATES THE PRODUCTION OF INOSITOL TRISPHOSPHATE AND INOSITOL TETRAKISPHOSPHATE IN RAT AORTA

Vivian Pijuan and Irene Litosch

Department of Pharmacology, University of Miami
School of Medicine, Miami, Florida 33101

Received September 6, 1988

SUMMARY Norepinephrine stimulated the rapid hydrolysis of [^{3}H]phosphatidylinositol-4,5-bisphosphate in rat aorta with a maximal decrease of 30% within 60 sec of stimulation. Levels of [^{3}H]phosphatidylinositol-4,5-bisphosphate returned to control by 5 min despite the continued presence of agonist. Hydrolysis of [^{3}H]phosphatidylinositol-4,5-bisphosphate occurred concurrently with the formation of inositol phosphates. Inositol-tris and tetrakisphosphate levels were increased within 30 sec of agonist stimulation. Increases in inositol phosphate levels due to agonist were dose-dependent with half-maximal activation at 1 μM norepinephrine. © 1988 Academic Press, Inc.

The primary stimulus needed to promote contraction in smooth muscle is an increase in the cytosolic Ca^{2+} concentration (1). A number of agonists including norepinephrine, vasopressin and angiotensin II increase cytosolic Ca^{2+} through stimulation of Ca^{2+} release from intracellular stores as well as by promoting Ca^{2+} influx through putative receptor operated channels (1,2). The phosphoinositide-phospholipase C system appears to have an important role in the regulation of these events in vascular smooth muscle (3). Inositol-1,4,5-trisphosphate, derived from phospholipase C-mediated hydrolysis of phosphatidylinositol-4,5-bisphosphate, has been shown to elicit the release of Ca^{2+} from sarcoplasmic reticulum in permeabilized vascular smooth muscle cells (4,5,6) and muscle strips (7,8). Products of inositol-1,4,5-trisphosphate metabolism also appear to have an important role in regulation of cytosolic Ca^{2+} concentration. Inositol-1,3,4,5-tetrakisphosphate, generated from the phosphorylation of inositol-1,4,5-trisphosphate, may regulate Ca^{2+} influx (9).

In cultured smooth muscle cells obtained from rat aorta, both vasopressin and angiotensin II stimulated production of inositol-trisphosphate has been demonstrated to occur (10,11,12). There are limited studies in non-cultured vascular smooth muscle systems. In rabbit mesenteric artery, α_1-adrenergic amine-stimulation of inositol-trisphosphate has been shown to occur within 30 sec (5). In rat aorta, a system used to study regulation of vascular smooth muscle contraction, only production of inositol-monophosphate in response to agonist stimulation has been reported (13,14). Norepinephrine (NA)-stimulated an increase in inositol-monophosphate levels within 30 sec and a 20% decrease in phosphatidylinositol-4,5-bisphosphate levels within 10

Abbreviations: KHB, Krebs-Henseleit Buffer; GPI, glycerophosphorylinositol; $InsP_1$, inositol-monophosphate; $InsP_2$, inositol-bisphosphate; $InsP_3$, inositol trisphosphate; $InsP_4$, inositol-tetrakisphosphate; NA, norepinephrine; PIP_2, phosphatidylinositol-4,5-bisphosphate.

0006-291X/88 $1.50
Copyright © 1988 by Academic Press, Inc.
All rights of reproduction in any form reserved.

sec (13). The inability to measure changes in inositol-trisphosphate levels despite the hydrolysis of phosphatidylinositol-4,5-bisphosphate could reflect a rapid phosphatase-mediated hydrolysis of inositol-trisphosphate as has been observed in numerous systems (15). The purpose of the present studies was to ascertain whether rapid changes in inositol-trisphosphate occurred in rat aorta in response to NA stimulation.

MATERIALS AND METHODS

Thoracic aortas from male rats (Sprague-Dawley) weighing 150-200 g were excised and cleansed of extraneous fatty tissue. Each aorta was cut into 4 or 6 pieces of equal sizes (approx. 1 cm in length). The tissue was labeled for 4-5 h with [^{3}H]inositol, as indicated, at 37°C in modified Krebs-Henseleit Buffer (KHB), equilibrated with 95% O_2/5% CO_2 consisting of 118 mM NaCl, 4.7 mM KCl, 3.0 mM $CaCl_2$, 1.2 mM $MgCl_2$, 1.2 mM KH_2PO_4, 0.5 mM EDTA, 25 mM $NaHCO_3$, 3.3 mM Hepes, 10 mM glucose and 20 mM Tris/HCl, (pH 7.4). Labeled tissue was transferred to test tubes containing one ml fresh KHB. LiCl and agonist were added for the indicated time. The incubations were terminated by the addition of 3 ml ice-cold methanol/chloroform (2:1 v/v) containing 0.1% HCl to the incubation tubes followed by the addition of 1 ml chloroform. The tissue was sonicated in the extraction medium for 1 h in an ice bath and extracted overnight at 5°C. Aqueous and lipid phases were separated by the addition of H_2O (2 ml). The upper phase was neutralized, applied to 0.5 ml Dowex-Formate resin slurry (AG1-X8) and poured into small columns. [^{3}H]Inositol was eluted with 40 ml H_2O followed by 4 ml each of 5 mM sodium tetraborate/60 mM ammonium formate to elute glycerophosphorylinositol (GPI) and 0.1 M formic acid containing 0.2, 0.4 and 1.0 M ammonium formate to elute inositol-monophosphate ($InsP_1$), inositol-bisphosphate ($InsP_2$), inositol-trisphosphate ($InsP_3$), respectively. In experiments in which inositol-tetrakisphosphate ($InsP_4$) was measured, $InsP_3$ was eluted with 0.1 M formic acid/0.8 M ammonium formate followed by the elution of $InsP_4$ with 0.1 M formic acid/1.0 M ammonium formate (16). Analysis of the elution profile for the individual inositol phosphates indicated that they eluted as separate and distinct peaks in regions corresponding to the elution of standards as documented (16). The lipid phase was evaporated in vacuo, resuspended in 50 μl chloroform and applied to silica gel plates for thin layer chromatographic separation of the labeled phosphoinositides. The solvent system used was methanol/chloroform/4N NH_4OH/water (90:90:9:19; v/v) (17). The labeled lipids were detected by fluorography using [^{3}H]Enhance. Lipids were scraped from the plates and radioactivity determined.

Norepinephrine (bitartrate salt) and phosphatidylinositol-4,5-bisphosphate were from Sigma Chemical Co. Myo-[2-^{3}H]-inositol (15 Ci/mmol) was obtained from American Radiolabeled Chem, Inc. and Amersham Corp. (19 Ci/mmol). AG1-X8 (formate form) was from Bio-Rad. Uniplate Silica-Gel HL plates were from Analtech. [^{3}H]Enhance was from New England Nuclear.

RESULTS AND DISCUSSION

The time course for production of inositol phosphates in response to NA stimulation in the presence of 25 mM LiCl is shown in Fig. 1. NA stimulated the rapid production of $InsP_1$, $InsP_2$ and $InsP_3$ within 60 sec. $InsP_3$ levels continued to increase slowly during a 15 min incubation. $InsP_1$ and $InsP_2$ increased at a greater rate than $InsP_3$. At 15 min, approximately five times as much labeled $InsP_1$ as $InsP_3$ was formed in response to agonist stimulation. These results demonstrate that rapid increases in $InsP_3$ do occur in rat aorta in response to NA stimulation.

In most tissues, at least two isomers of $InsP_3$ are generated in response to agonist stimulation. Ins-1,4,5-P_3 is the immediate product of phospholipase C-mediated hydrolysis of phosphatidylinositol-4,5-bisphosphate. An Ins-1,4,5-P_3-3-kinase mediates the phosphorylation of Ins-1,4,5-P_3 to form Ins-1,3,4,5-P_4 which is subsequently dephosphorylated to Ins-1,3,4-P_3 (18,19). The next series of experiments were designed to ascertain whether $InsP_4$ was generated in response to NA stimulation. Rat aorta were prelabeled with 150 μCi/ml

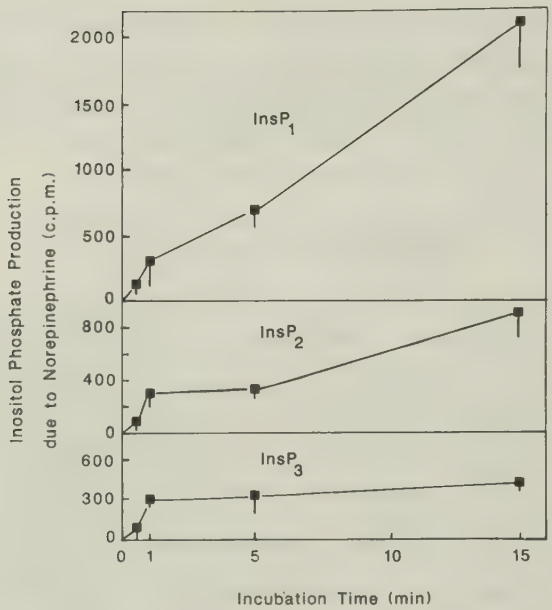

Figure 1 Norepinephrine Stimulated Production of Inositol Phosphates. Rat aortic strips were labeled with 45-55 μCi/ml [^{3}H]inositol for 4 h. Strips were transferred to fresh KHB to which 25 mM LiCl was added 2.5 min prior to the addition of agonist. Buffer control or norepinephrine (10 μM) was added for the indicated times. Each point represents the mean ± S.E.M for 4 experiments.

[^{3}H]inositol and the water soluble products of phosphoinositide hydrolysis were analyzed for production of $InsP_3$ and $InsP_4$. As shown in Fig. 2, NA stimulated an increase in the levels of $InsP_3$ and $InsP_4$ within 30 sec. The amount of $InsP_4$ produced was approximately half that of

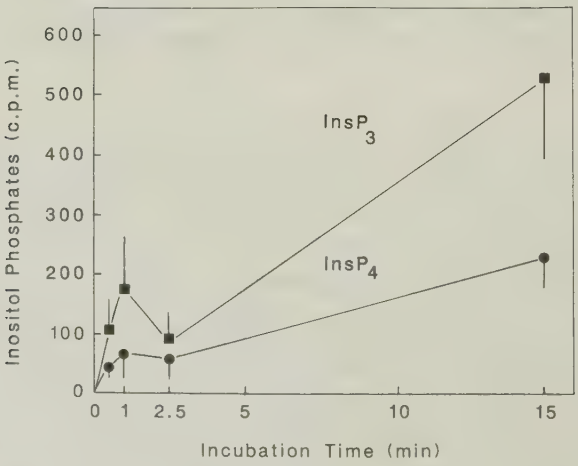

Figure 2 Norepinephrine Stimulated Production of Inositol Tris- and Tetrakisphosphate. Rat aortic strips were labeled for 4 h with 150 μCi/ml [^{3}H]inositol. The tissue was transferred to fresh KHB and subsequently incubated with or without 10 μM norepinephrine for the indicated times. 25 mM LiCl and 3 μM propranolol were present in the buffer. Each point represents the mean ± S.E.M. for 8 experiments.

TABLE I. Effect of LiCl on Basal and Norpinephrine Stimulated Inositol Phosphate Production

	(c.p.m.)			
Inositol Phosphates	Basal		Norepinephrine	
	-LiCl	+LiCl	-LiCl	+LiCl
$InsP_1$	150	260	230	430
$InsP_2$	140	300	290	420
$InsP_3$	160	260	230	360

Rat aortic strips were incubated for 3 h with 65 μCi/ml [^{3}H]inositol. The tissue was transferred to fresh KHB and incubated with or without 25 mM LiCl for 2.5 min followed by the addition of buffer control or 33 μM norepinephrine for 1 min.

$InsP_3$. Since $InsP_4$ is rapidly dephosphorylated to Ins-1,3,4-P_3, it is likely that the $InsP_3$ fraction contains both Ins-1,4,5-P_3 and Ins-1,3,4-P_3 (15).

The ability to detect $InsP_3$ and $InsP_4$ production in the present study as compared to other published studies may be a consequence of several factors. The amount of [^{3}H]inositol used to label the tissue was 45-150 μCi/ml as compared to 8-40 μCi/ml (13). Secondly, LiCl, at 25 mM was added to the incubation medium to inhibit phosphatase-mediated hydrolysis of $InsP_3$ (15). The effect of 25 mM LiCl on basal and NA-stimulated inositol phosphate production is shown in Table I. LiCl increased the basal levels of inositol phosphates by approximately 75%. LiCl did not markedly affect the distribution of label in the individual phosphates or the response to stimulation by NA. However, the increased radioactivity in the individual phosphates facilitated the detection of these compounds. LiCl was therefore used in subsequent experiments. Finally, it was observed that excessive handling of the labeled tissue resulted in an increase in basal $InsP_3$ levels. Under these conditions, it was difficult to consistently measure agonist-stimulated increases in $InsP_3$ levels. Thus, in all experiments, the incubation was terminated by the direct addition of ice-cold extraction medium rather than by removal of tissue from the medium as described in other studies (13,14).

The NA-stimulated production of inositol phosphates occurred concurrently with degradation of [^{3}H]phosphatidylinositol-4,5-bisphosphate (Fig. 3). A maximal decrease of 30% was observed within 60 sec of stimulation. After 60 sec, levels of [^{3}H]phosphatidylinositol-4,5-bisphosphate increased despite the continued presence of agonist. By 5 min, levels of [^{3}H]phosphatidylinositol-4,5-bisphosphate had returned to control. These results demonstrate that in rat aorta, as in many tissues including cultured vascular smooth muscle cells (10,11), the initial agonist-stimulated hydrolysis of [^{3}H]phosphatidylinositol-4,5-bisphosphate is followed by resynthesis. Whether the resynthesized lipid contributes to the continued agonist-stimulated production of $InsP_3$ remains to be determined.

Stimulation of inositol phosphate production due to NA was dose dependent (Fig. 4). Maximal accumulation of inositol phosphates was obtained with 100 μM NA. The EC_{50} was approximately 1 μM. Legan et al. (14) observed maximal stimulation of [^{3}H]inositol monophosphate production at 10 μM NA with an EC_{50} of 100 nM.

A slow increase in the levels of labeled glycerophosphorylinositol was also observed after 60 sec of incubation with NA (Fig. 5). An increase in glycerophorylinositol has also been

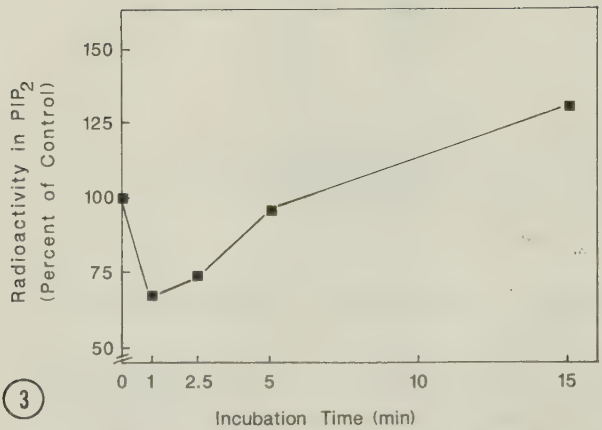

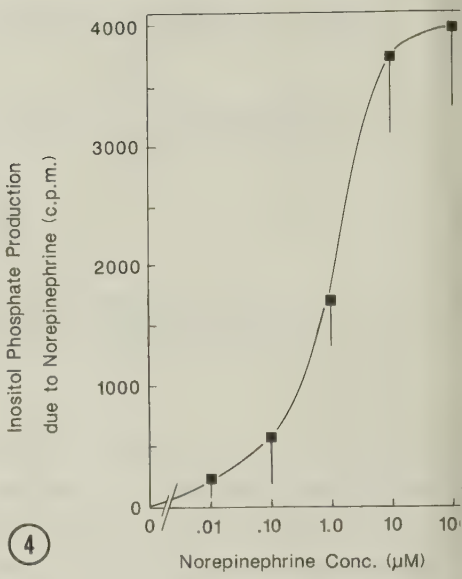

Figure 3 Time Course for Norepinephrine Stimulated Hydrolysis of [^{3}H]Phosphatidylinositol-4,5-Bisphosphate. Rat aortic strips were labeled with [^{3}H]inositol and incubated with or without 10 μM norepinephrine as described in the legend to Fig. 1. Changes in [^{3}H]phosphatidylinositol-4,5-bisphosphate (PIP_2) were analyzed by thin layer chromatography. Results are the mean of 6 experiments. The average S.E.M. was ± 27%. The average basal level of radioactivity in PIP_2 was 2000 c.p.m.

Figure 4 Dose Dependent Stimulation of Inositol Phosphate Production by Norepinephrine. Rat aortic strips were labeled with 45 μCi/ml [^{3}H]inositol for 4 h. The tissue was transferred to fresh KHB and 25 mM LiCl was added 2.5 min prior to the addition of agonist. Strips were subsequently incubated for 5 min with or without the indicated concentrations of norepinephrine. Each point represents the mean ± S.E.M. for 3-4 experiments.

observed in response to stimulation by vasopressin and angiotensin II in cultured rat aortic smooth muscle cells (10). The significance of this increase in glycerophosphorylinositol is presently unknown.

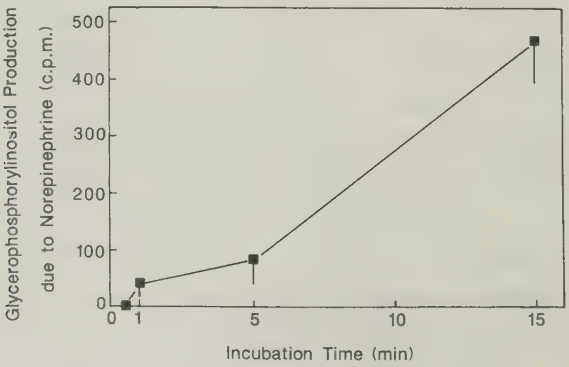

Figure 5 Norepinephrine Stimulated Production of Glycerophosphorylinositol. Rat aortic strips were labeled with 45-55 μCi/ml [^{3}H]inositol for 4 h. The tissue was transferred to fresh KHB to which 25 mM LiCl was added 2.5 min prior to the addition of agonist. Buffer control or norepinephrine (10 μM) was added for the indicated times. Each point represents the mean ± S.E.M. for 4 experiments.

Recent findings have shown that the agonist-stimulated accumulation of Ins-1,4,5-P_3 appears to be slower than the rise in intracellular free Ca^{2+} in a number of cells including GH_4C_1 cells (20), BC3H-1 cells (21) and 1321N1 cells (21). This apparent disparity in the kinetics of Ins-1,4,5-P_3 accumulation relative to the increase of Ca^{2+} may be due to 1) a localized effect of $InsP_3$ such that a small increase in Ins-1,4,5-P_3 is needed to elicit a maximal Ca^{2+} signal (20,21) or 2) multiple mechanisms may mediate the receptor-coupled increase in cytosolic Ca^{2+} (21,22). Characterization of the relationship of $InsP_3$ and $InsP_4$ production to Ca^{2+} elevation in rat aorta will allow further assessment of the role of the phosphoinositide pathway in Ca^{2+} elevation and vascular smooth muscle function.

ACKNOWLEDGEMENTS

This work was supported by an Established Investigator Award from the American Heart Association and with funds contributed from the AHA Florida Affiliate as well as by NIH DK-37007 and Lucille P. Markey Foundation.

REFERENCES

1. Somlyo, A.P. and Somlyo, A.V. (1986) In The Heart and Cardiovascular System (H.A. Fozzard et al., Ed.), pp. 845-864. Raven Press, New York.
2. Rasmussen, H. and Barrett, P.Q. (1984) Physiol. Rev. 64, 938-984.
3. Berridge, M.J. (1987) Ann. Rev. Biochem. 56, 159-193.
4. Yamamoto, H. and van Breemen, C. (1985) Biochem. Biophys. Res. Commun. 130, 270-274.
5. Hashimoto, T., Hirata, M., Itoh, T., Kanmura, Y. and Kuriyama, H. (1986) J. Physiol. 370, 605-618.
6. Suematsu, E., Hirata, M., Hashimoto, T. and Kuriyama, H. (1984) Biochem. Biophys. Res. Commun. 120, 481-485.
7. Somlyo, A.V., Bond, M., Somlyo, A.P. and Scarpa, A. (1985) Proc. Nat'l. Acad. Sci. (U.S.A.) 82, 5231-5235.
8. Walker, J.W., Somlyo, A.V., Goldman, Y.E., Somlyo, A.P. and Trentham, D.R. (1987) Nature 327, 249-252.
9. Irvine, R.F. and Moor, R.M. (1986) Biochem. J. 240, 917-920.
10. Nabika, T., Velletri, P.A., Lovenberg, W. and Beaven, M.A. (1985) J. Biol. Chem. 260, 4661-4670.
11. Smith, J.B., Smith, L., Brown, E.R., Barnes, D., Sabir, M.A., Davis, J.S. and Farese, R.V. (1984) Proc. Nat'l. Acad. Sci. (U.S.A.) 81, 7812-7816.
12. Alexander, R.W., Brock, T.A., Gimbrone, M.A. and Rittenhouse, S.E. (1985) Hypertension 7, 447-451.
13. Rapoport, R.M. (1987) J. Pharmacol. Exp. Ther. 242, 188-194.
14. Legan, E., Chernow, B., Parrillo, J. and Roth, B.L. (1985) Eur. J. Pharmacol. 110, 389-390.
15. Majerus, P.W., Connolly, T.M., Bansal, V.S., Inhorn, R.C., Ross, T.S. and Lips, D.L. (1988) J. Biol. Chem. 263, 3051-3054.
16. Batty, I.R., Nahorski, S.R. and Irvine, R.F. (1985) Biochem. J. 232, 211-215.
17. Litosch, I., Lin, S-H. and Fain, J.N. (1983) J. Biol. Chem. 258, 13727-13732.
18. Putney, J.W. (1987) Trends in Pharmacol. Sci. 8, 481-485.
19. Rossier, M.F., Capponi, A.M. and Vallotton, M.B. (1987) Biochem. J. 245, 305-307.
20. Tashjian, A.H., Jr., Heslop, J.P. and Berridge, M.J. (1987) Biochem. J. 243, 305-308.
21. Ambler, S.K., Thompson, B., Solski, P.A., Brown, J.H. and Taylor, P. (1987) Mol. Pharmacol. 32, 376-383.
22. Hughes, B.P., Crofts, J.N., Auld, A.M., Read, L.C., Barritt, G.J. (1987) Biochem. J. 248, 911-918.

Vol. 156, No. 1, 1988 BIOCHEMICAL AND BIOPHYSICAL RESEARCH COMMUNICATIONS
October 14, 1988 Pages 246-254

YEAST KEX2 GENE ENCODES AN ENDOPEPTIDASE HOMOLOGOUS TO SUBTILISIN-LIKE SERINE PROTEASES

Kensaku MIZUNO, Tomoko NAKAMURA, Takehiro OHSHIMA*, Shoji TANAKA* & Hisayuki MATSUO

Department of Biochemistry, Miyazaki Medical College, Kiyotake, Miyazaki 889-16, Japan

*Suntory Institute for Biomedical Research, Shimamoto, Mishima, Osaka 618, Japan

Received August 8, 1988

SUMMARY: Yeast Saccharomyces cerevisiae KEX2 gene previously isolated, was characterized as the gene encoding a calcium-dependent endopeptidase required for processing of precursors of α-factor and killer toxin. In this study, we report the amino acid sequence of the KEX2 gene product deduced from nucleotide sequencing. Our results indicate that the KEX2 gene contains a 2,442-bp open reading frame encoding a polypeptide of 814 amino acids. The deduced amino acid sequence contains a region extensively homologous to the members of subtilisin-like serine protease family near the N-terminus. A putative membrane-spanning domain near the C-terminus was also detected. These facts indicate that the KEX2-encoded protein may function as a membrane-bound, subtilisin-like serine protease. © 1988 Academic Press, Inc.

Many bioactive peptides are processed from their precursors by proteolytic cleavage at paired basic residues. However, little is known about the endopeptidases that are physiologically involved in precursor processing (1). Yeast Saccharomyces cerevisiae cells synthesize and secrete α-factor and killer toxin, which are also processed from larger precursors by specific cleavage at paired basic residues (2,3). Therefore, yeast may provide a simple model system for the study of prohormone processing in higher eukaryotic cells. Yeast kex2 mutants are defective in proteolytic processing of precursors for α-factor and killer toxin (4). Reintroduction of the normal KEX2 gene into deficient strains restored both processing activity and endopeptidase activity specific for cleaving on the carboxyl side of paired basic residues, indicating that the KEX2 gene product may be an endopeptidase involved in precursor processing (4,5). The KEX2 gene product was found to exhibit unique enzymatic properties, including membrane-association, Ca^{2+}-dependency, and substrate specificity toward paired basic residues (4,5).

Abbreviations: MCA, 4-methylcoumaryl-7-amide; AMC, 7-amino-4-methylcoumarin; PMSF, phenylmethylsulfonyl fluoride; DFP, diisopropyl fluorophosphate; pAPMSF, p-amidinophenylmethylsulfonyl fluoride.

0006-291X/88 $1.50
Copyright © 1988 by Academic Press, Inc.
All rights of reproduction in any form reserved.

Enzymes with properties similar to those of the KEX2 protease were partially purified by Wolf's group (6,7) and ours (8). To understand the molecular mechanisms of this unique proteolytic action of the enzyme, it was essential to elucidate its primary structure. In a recent review, Fuller, et al. showed the schematic depiction of the structure of the KEX2-encoded protease (9); however, no data regarding its primary structure had as yet been available. In this paper, we report the complete amino acid sequence of the KEX2-encoded protein deduced from nucleotide sequencing.

MATERIALS AND METHODS

Strains and DNA: Saccharomyces cerevisiae K16-57C (MATα leu2 trp1 ura3 kex2-8) was used for the kex2 mutant host. The kex2-8 mutation of K16-57C derived from strain 399 was obtained from Dr. Reed Wickner. R27-7C (MATα leu2 trp1 ura3 his3) was used for the KEX2 wild type strain. The genomic DNA used for isolation of the KEX2 gene was prepared from X2180-1B (10).
Recombinant DNA techniques: Ligation, T4 DNA polymerase and restriction endonuclease treatment were performed according to Maniatis, et al. (11).
Plasmid: pYE vector, carrying the selection marker gene TRP1 and one of the inverted repeat sequence of 2μm DNA which contains the replication origin, was used for the high copy number plasmid. YCpLe vector, carrying the selection marker gene LEU2, CEN4 and ARS1, was used for the single copy number plasmid. Both vectors have pBR322 replication origin and ampicillin-resistant gene.
Transformation: Transformation of yeast was carried out by using the lithium acetate technique (12). Transformation of E.coli was performed as described before (13).
Bioassay for killer activity: To isolate the KEX2 gene, the transformants were screened for the secretion of active killer toxin. Agar diffusion assay for killer activity was performed on a lawn of the sensitive indicator 5 x 47 (MATa/MATα his1/+ trp1/+ ura3/+) (14), according to the procedure of Wickner and Leibowitz (15).
Assay for protease activity: Permeabilization of yeast cells with Brij 58 was carried out by the methods described previously (4). Protease activity was measured as follows (8): Twenty nanomoles of Boc-Gln-Arg-Arg-MCA were incubated for 1 hr at 37°C with the permeabilized cells in 250 μl of 0.4 M Tris-HCl buffer (pH 7.0) containing 0.1% Lubrol, 1 mM EGTA, pepstatin (1mg/ml), and bestatin (1mg/ml) in the presence or absence of 2 mM $CaCl_2$. The amounts of AMC released from the substrate were measured by a fluorescence spectrophotometer with excitation at 380 nm and emission at 460 nm. Calcium-dependent endopeptidase activity was evaluated after the addition of $CaCl_2$.
Sequencing: DNA sequence analysis was carried out by the dideoxy method after subcloning suitable restriction fragments into M13mp18 and M13mp19 vectors (16). The DNA sequence was determined for both strands, and across all restriction sites used for subcloning.

RESULTS AND DISCUSSION

The KEX2 gene was previously isolated by Julius, et al. (4). They described that the functional KEX2 gene was located on a 3.5Kb EcoRI fragment. According to their description, we isolated the 3.5Kb EcoRI fragment capable of complementing the kex2-8 mutation from X2180-1B genomic DNA (Fig.1A). However, the nucleotide sequence analysis revealed that the 3.5 Kb EcoRI fragment contained one long open reading frame without a stop codon. To determine the complete coding sequence of the KEX2 gene product, the 5.0 Kb EcoRI-SalI fragment capable of complementing the kex2-8 mutation was newly

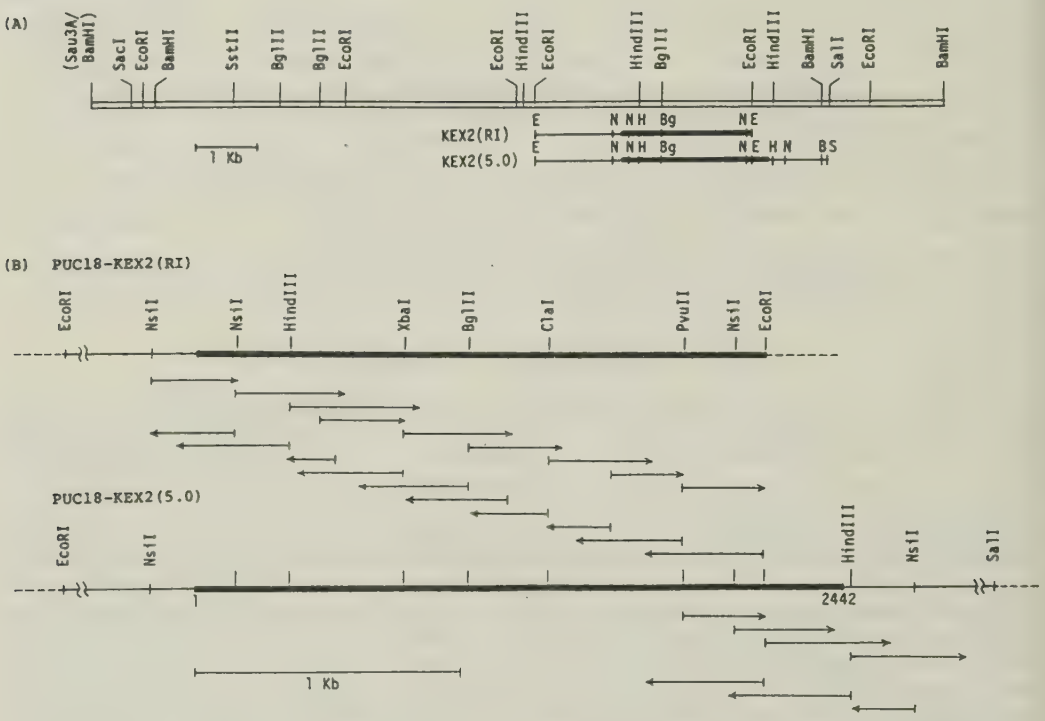

Fig.1 (A) Upper: Physical map of KEX2 gene previously reported (4). Middle and lower: Physical maps of KEX2(RI) and KEX2(5.0) isolated in this study. E;EcoRI, N;NsiI, H;HindIII, B;BamHI, S;SalI, Bg;BglII. (B) Strategy for sequencing cloned DNA. The restriction map shows only the relevant restriction sites. Protein coding region is indicated by a closed box. Arrows under each clone indicate direction and extent of sequence determination. Dashed line indicates the region of PUC18.

isolated. As shown in Fig.1A, the restriction maps of these two isolated genes (named KEX2(RI) and KEX2(5.0)) were identical to that of the KEX2 gene previously reported (4). Transformants of the kex2-8 mutants containing the cloned genes on a single- or multi-copy number plasmid regained both killer activity and Ca^{2+}-dependent endopeptidase activity (Table 1). Hence, these genes probably encode a Ca^{2+}-dependent endopeptidase required for maturation

Table 1. Killer and endoprotease activity of the normal and kex2 mutant cells

Strain	Inserting direction of KEX2 gene	Killer activity	Endoprotease activity
K16-57C (non)	——	-	0.5
K16-57C[pYE-KEX2(RI)a]	KEX2(RI) → IRI	+	22.9
K16-57C[pYE-KEX2(RI)b]	← KEX2(RI) IRI	++	50.3
K16-57C[pYE-KEX2(5.0)b]	← KEX2(5.0) IRI	++	78.8
K16-57C[YCpLe-KEX2(RI)a]	KEX2(RI) → CEN4	+	5.0
K16-57C[YCpLe-KEX2(RI)b]	← KEX2(RI) CEN4	+	11.1
R27-7C (non)	——	+	7.2

of active killer toxin. Two plasmids containing overlapping segments of the yeast genome were analyzed for nucleotide sequence by the dideoxy method, according to the strategy indicated in Fig.1B.

Fig.2 shows the 2,848-nucleotide sequence of the KEX2 gene and the deduced amino acid sequence of the KEX2 gene product. The sequence contains one long open reading frame corresponding to 814 amino acid residues. The translational initiation site is tentatively assigned to the methionine codon at nucleotides 1 to 3, because this is the first ATG triplet that appears downstream from the nonsense codon TAA (nucleotides -57 to -55) found in-frame. A translation stop codon (TGA) occurs in-frame after the 814th codon specifying serine. A putative polyadenylation site AATAAA is present at position 2,616 to 2,621. Thus the KEX2 gene appears to encode a polypeptide of 814 amino acid residues with a calculated molecular weight of 89,997.

The hydropathicity profile of the deduced amino acid sequence revealed two hydrophobic segments. One is at the N-terminus of the protein and may function as a signal sequence to direct the KEX2 protein into endoplasmic reticulum. The other segment, consisting of 21 hydrophobic residues (residue 679 to 699) near the C-terminus of the protein, may function as a membrane-spanning domain, as was generally found in many transmembrane proteins. There are five potential sites for N-linked glycosylation, that is, Asn-X-Ser/Thr, where X can be any amino acid except proline (Fig. 2).

When the amino acid sequence deduced for the KEX2 gene product was compared with the known polypeptide sequences stored in the NBRF data bank, significant homology was found with members of subtilisin-like serine protease family (17). Fig.3A shows an alignment of the respective amino acid sequences of the KEX2 gene product and subtilisin BPN' (18). When the region of amino acid residues [152-410] of KEX2 gene product was compared with the sequence [9-246] of subtilisin BPN', 28% was found to be occupied by identical residues and 22% by conservative residues. The active site of subtilisin BPN' was assigned to the triad consisting of residues Asp-32, His-64, and Ser-221 (18). The KEX2 protein also contains these three residues at homologous positions (Asp-175, His-213 and Ser-385). The extensive homology of the amino acid sequence observed between KEX2 protein and subtilisins, especially in the region around the active site residues (Fig.3B), strongly suggests that the KEX2 protein may physiologically function as a serine protease in a manner similar to that of the subtilisins. Subtilisins are classified into a serine-

---

Fig.2 Nucleotide sequence of KEX2 gene and predicted amino acid sequence of KEX2 gene product. Nucleotides are numbered from the presumed initiator ATG. Amino acid residues are numbered starting at Met-1. The potential N-glycosylation sites are underlined. The residues corresponding to the active site of subtilisin are boxed. Two hydrophobic domains situated at the N-terminus and near the C-terminus are indicated by dashed lines. The AATAAA sequence is doubly underlined.

```
                                        T GCA TAA TTC TGT CAT AAG CCT GTT   -145
-144  CTT TTT CCT GGC TTA AAC ATC CCG TTT TGT AAA AGA GAA ATC TAT TCC    -97
 -96  ACA TAT TTC ATT CAT TCG GCT ACC ATA CTA AGG ATA AAC TAA TCC CGT    -49
 -48  TGT TTT TTG GCC TCG TCA CAT AAT TAT AAA CTA CTA ACC CAT TAT CAG     -1

   1  Met Lys Val Arg Lys Tyr Ile Thr Leu Cys Phe Trp Trp Ala Phe Ser     16
   1  ATG AAA GTG AGG AAA TAT ATT ACT TTA TGC TTT TGG TGG GCC TTT TCA     48

  17  Thr Ser Ala Leu Val Ser Ser Gln Gln Ile Pro Leu Lys Asp His Thr     32
  49  ACA TCC GCT CTT GTA TCA TCA CAA CAA ATT CCA TTG AAG GAC CAT ACG     96

  33  Ser Arg Gln Tyr Phe Ala Val Glu Ser Asn Glu Thr Leu Ser Arg Leu     48
  97  TCA CGA CAG TAT TTT GCT GTA GAA AGC AAT GAA ACA TTA TCC CGC TTG    144

  49  Glu Glu Met His Pro Asn Trp Lys Tyr Glu His Asp Val Arg Gly Leu     64
 145  GAG GAA ATG CAT CCA AAT TGG AAA TAT GAA CAT GAT GTT CGA GGG CTA    192

  65  Pro Asn His Tyr Val Phe Ser Lys Glu Leu Leu Lys Leu Gly Lys Arg     80
 193  CCA AAC CAT TAT GTT TTT TCA AAA GAG TTG CTA AAA TTG GGC AAA AGA    240

  81  Ser Ser Leu Glu Glu Leu Gln Gly Asp Asn Asn Asp His Ile Leu Ser     96
 241  TCA TCA TTA GAA GAG TTA CAG GGG GAT AAC AAC GAC CAC ATA TTA TCT    288

  97  Val His Asp Leu Phe Pro Arg Asn Asp Leu Phe Lys Arg Leu Pro Val    112
 289  GTC CAT GAT TTA TTC CCG CGT AAC GAC CTA TTT AAG AGA CTA CCG GTG    336

 113  Pro Ala Pro Pro Met Asp Ser Ser Leu Leu Pro Val Lys Glu Ala Glu    128
 337  CCT GCT CCA CCA ATG GAC TCA AGC TTG TTA CCG GTA AAA GAA GCT GAG    384

 129  Asp Lys Leu Ser Ile Asn Asp Pro Leu Phe Glu Arg Gln Trp His Leu    144
 385  GAT AAA CTC AGC ATA AAT GAT CCG CTT TTT GAG AGG CAG TGG CAC TTG    432

 145  Val Asn Pro Ser Phe Pro Gly Ser Asp Ile Asn Val Leu Asp Leu Trp    160
 433  GTC AAT CCA AGT TTT CCT GGC AGT GAT ATA AAT GTT CTT GAT CTG TGG    480

 161  Tyr Asn Asn Ile Thr Gly Ala Gly Val Val Ala Ala Ile Val Asp Asp    176
 481  TAC AAT AAT ATT ACA GGC GCA GGG GTC GTG GCT GCC ATT GTT GAT GAT    528

 177  Gly Leu Asp Tyr Glu Asn Glu Asp Leu Lys Asp Asn Phe Cys Ala Glu    192
 529  GGC CTT GAC TAC GAA AAT GAA GAC TTG AAG GAT AAT TTT TGC GCT GAA    576

 193  Gly Ser Trp Asp Phe Asn Asp Asn Thr Asn Leu Pro Lys Pro Arg Leu    208
 577  GGT TCT TGG GAT TTC AAC GAC AAT ACC AAT TTA CCT AAA CCA AGA TTA    624

 209  Ser Asp Asp Tyr His Gly Thr Arg Cys Ala Gly Glu Ile Ala Ala Lys    224
 625  TCT GAT GAC TAC CAT GGT ACG AGA TGT GCA GGT GAA ATA GCT GCC AAA    672

 225  Lys Gly Asn Asn Phe Cys Gly Val Gly Val Gly Tyr Asn Ala Lys Ile    240
 673  AAA GGT AAC AAT TTT TGC GGT GTC GGG GTA GGT TAC AAC GCT AAA ATC    720

 241  Ser Gly Ile Arg Ile Leu Ser Gly Asp Ile Thr Thr Glu Asp Glu Ala    256
 721  TCA GGC ATA AGA ATC TTA TCC GGT GAT ATC ACT ACG GAA GAT GAA GCT    768

 257  Ala Ser Leu Ile Tyr Gly Leu Asp Val Asn Asp Ile Tyr Ser Cys Ser    272
 769  GCG TCC TTG ATT TAT GGT CTA GAC GTA AAC GAT ATA TAT TCA TGC TCA    816

 273  Trp Gly Pro Ala Asp Asp Gly Arg His Leu Gln Gly Pro Ser Asp Leu    288
 817  TGG GGT CCC GCT GAT GAC GGA AGA CAT TTA CAA GGC CCT AGT GAC CTG    864

 289  Val Lys Lys Ala Leu Val Lys Gly Val Thr Glu Gly Arg Asp Ser Lys    304
 865  GTG AAA AAG GCT TTA GTA AAA GGT GTT ACT GAG GGA AGA GAT TCC AAA    912

 305  Gly Ala Ile Tyr Val Phe Ala Ser Gly Asn Gly Gly Thr Arg Gly Asp    320
 913  GGA GCG ATT TAC GTT TTT GCC AGT GGA AAT GGT GGA ACT CGT GGT GAT    960

 321  Asn Cys Asn Tyr Asp Gly Tyr Thr Asn Ser Ile Tyr Ser Ile Thr Ile    336
 961  AAT TGC AAT TAC GAC GGC TAT ACT AAT TCC ATA TAT TCT ATT ACT ATT   1008

 337  Gly Ala Ile Asp His Lys Asp Leu His Pro Pro Tyr Ser Glu Gly Cys    352
1009  GGG GCT ATT GAT CAC AAA GAT CTA CAT CCT CCT TAT TCC GAA GGT TGT   1056

 353  Ser Ala Val Met Ala Val Thr Tyr Ser Ser Gly Ser Gly Glu Tyr Ile    368
1057  TCC GCC GTC ATG GCA GTC ACG TAT TCT TCA GGT TCA GGC GAA TAT ATT   1104

 369  His Ser Ser Asp Ile Asn Gly Arg Cys Ser Asn Ser His Gly Gly Thr    384
1105  CAT TCG AGT GAT ATC AAC GGC AGA TGC AGT AAT AGC CAC GGT GGA ACG   1152

 385  Ser Ala Ala Ala Pro Leu Ala Ala Gly Val Tyr Thr Leu Leu Leu Glu    400
1153  TCT GCG GCT GCT CCA TTA GCT GCC GGT GTT TAC ACT TTG TTA CTA GAA   1200

 401  Ala Asn Pro Asn Leu Thr Trp Arg Asp Val Gln Tyr Leu Ser Ile Leu    416
1201  GCC AAC CCA AAC CTA ACT TGG AGA GAC GTA CAG TAT TTA TCA ATC TTG   1248
```

```
417   Ser Ala Val Gly Leu Glu Lys Asn Ala Asp Gly Asp Trp Arg Asp Ser    432
1249  TCT GCG GTA GGG TTA GAA AAG AAC GCT GAC GGA GAT TGG AGA GAT AGC   1296

433   Ala Met Gly Lys Lys Tyr Ser His Arg Tyr Gly Phe Gly Lys Ile Asp    448
1297  GCC ATG GGG AAG AAA TAC TCT CAT CGC TAT GGC TTT GGT AAA ATC GAT   1344

449   Ala His Lys Leu Ile Glu Met Ser Lys Thr Trp Glu Asn Val Asn Ala    464
1345  GCC CAT AAG TTA ATT GAA ATG TCC AAG ACC TGG GAG AAT GTT AAC GCA   1392

465   Gln Thr Trp Phe Tyr Leu Pro Thr Leu Tyr Val Ser Gln Ser Thr Asn    480
1393  CAA ACC TGG TTT TAC CTG CCA ACA TTG TAT GTT TCC CAG TCC ACA AAC   1440

481   Ser Thr Glu Glu Thr Leu Glu Ser Val Ile Thr Ile Ser Glu Lys Ser    496
1441  TCC ACG GAA GAG ACA TTA GAA TCC GTC ATA ACC ATA TCA GAA AAA AGT   1488

497   Leu Gln Asp Ala Asn Phe Lys Arg Ile Glu His Val Thr Val Thr Val    512
1489  CTT CAA GAT GCT AAC TTC AAG AGA ATT GAG CAC GTC ACG GTA ACT GTA   1536

513   Asp Ile Asp Thr Glu Ile Arg Gly Thr Thr Thr Val Asp Leu Ile Ser    528
1537  GAT ATT GAT ACA GAA ATT AGG GGA ACT ACG ACT GTC GAT TTA ATA TCA   1584

529   Pro Ala Gly Ile Ile Ser Asn Leu Gly Val Val Arg Pro Arg Asp Val    544
1585  CCA GCG GGG ATA ATT TCA AAC CTT GGC GTT GTA AGA CCA AGA GAT GTT   1632

545   Ser Ser Glu Gly Phe Lys Asp Trp Thr Phe Met Ser Val Ala His Trp    560
1633  TCA TCA GAG GGA TTC AAA GAC TGG ACA TTC ATG TCT GTA GCA CAT TGG   1680

561   Gly Glu Asn Gly Val Gly Asp Trp Lys Ile Lys Val Lys Thr Thr Glu    576
1681  GGT GAG AAC GGC GTA GGT GAT TGG AAA ATC AAG GTT AAG ACA ACA GAA   1728

577   Asn Gly His Arg Ile Asp Phe His Ser Trp Arg Leu Lys Leu Phe Gly    592
1729  AAT GGA CAC AGG ATT GAC TTC CAC AGT TGG AGG CTG AAG CTC TTT GGG   1776

593   Glu Ser Ile Asp Ser Ser Lys Thr Glu Thr Phe Val Phe Gly Asn Asp    608
1777  GAA TCC ATT GAT TCA TCT AAA ACA GAA ACT TTC GTC TTT GGA AAC GAT   1824

609   Lys Glu Glu Val Glu Pro Ala Ala Thr Glu Ser Thr Val Ser Gln Tyr    624
1825  AAA GAG GAG GTT GAA CCA GCT GCT ACA GAA AGT ACC GTA TCA CAA TAT   1872

625   Ser Ala Ser Ser Thr Ser Ile Ser Ile Ser Ala Thr Ser Thr Ser Ser    640
1873  TCT GCC AGT TCA ACT TCT ATT TCC ATC AGC GCT ACT TCT ACA TCT TCT   1920

641   Ile Ser Ile Gly Val Glu Thr Ser Ala Ile Pro Gln Thr Thr Thr Ala    656
1921  ATC TCA ATT GGT GTG GAA ACG TCG GCC ATT CCC CAA ACG ACT ACT GCG   1968

657   Ser Thr Asp Pro Asp Ser Asp Pro Asn Thr Pro Lys Lys Leu Ser Ser    672
1969  AGT ACC GAT CCT GAT TCT GAT CCA AAC ACT CCT AAA AAA CTT TCC TCT   2016

673   Pro Arg Gln Ala Met His Tyr Phe Leu Thr Ile Phe Leu Ile Gly Ala    688
2017  CCT AGG CAA GCC ATG CAT TAT TTT TTA ACA ATA TTT TTG ATT GGC GCC   2064

689   Thr Phe Leu Val Leu Tyr Phe Met Phe Phe Met Lys Ser Arg Arg Arg    704
2065  ACA TTT TTG GTG TTA TAC TTC ATG TTT TTT ATG AAA TCA AGG AGA AGG   2112

705   Ile Arg Arg Ser Arg Ala Glu Thr Tyr Glu Phe Asp Ile Ile Asp Thr    720
2113  ATC AGA AGG TCA AGA GCG GAA ACG TAT GAA TTC GAT ATC ATT GAT ACA   2160

721   Asp Ser Glu Tyr Asp Ser Thr Leu Asp Asn Gly Thr Ser Gly Ile Thr    736
2161  GAC TCT GAG TAC GAT TCT ACT TTG GAC AAT GGA ACT TCC GGA ATT ACT   2208

737   Glu Pro Glu Glu Val Glu Asp Phe Asp Phe Asp Leu Ser Asp Glu Asp    752
2209  GAG CCC GAA GAG GTT GAG GAC TTC GAT TTT GAT TTG TCC GAT GAA GAC   2256

753   His Leu Ala Ser Leu Ser Ser Ser Glu Asn Gly Asp Ala Glu His Thr    768
2257  CAT CTT GCA AGT TTG TCT TCA TCA GAA AAC GGT GAT GCT GAA CAT ACA   2304

769   Ile Asp Ser Val Leu Thr Asn Glu Asn Pro Phe Ser Asp Pro Ile Lys    784
2305  ATT GAT AGT GTA CTA ACA AAC GAA AAT CCA TTT AGT GAC CCT ATA AAG   2352

785   Gln Lys Phe Pro Asn Asp Ala Asn Ala Glu Ser Ala Ser Asn Lys Leu    800
2353  CAA AAG TTC CCA AAT GAC GCC AAC GCA GAA TCT GCT TCC AAT AAA TTA   2400

801   Gln Glu Leu Gln Pro Asp Val Pro Pro Ser Ser Gly Arg Ser ***
2401  CAA GAA TTA CAG CCT GAT GTT CCT CCA TCT TCC GGA CGA TCG TGA TTC   2448

2449  GAT ATG TAC AGA AAG CTT CAA ATT ACA AAA TAG CAT TTT TTT CTT ATA   2496
2497  GAT TAT AAT ACT CTC TCA TAC GTA TAC GTA TAT GTG TAT ATG ATA TAT   2544
2545  AAA CAA ACA TTA ATA TCC TAT TCC TTC CGT TTG AAA TCC CTA TGA TGT   2592
2593  ACT TTG CAT TGT TTG CAC CCG CGA ATA AAA TGA AAA CTC CGA ACC GAT   2640
2641  ATA TCA AGC ACA TAA AAG GGG AGG GTC CAA TTA ATG CAT
```

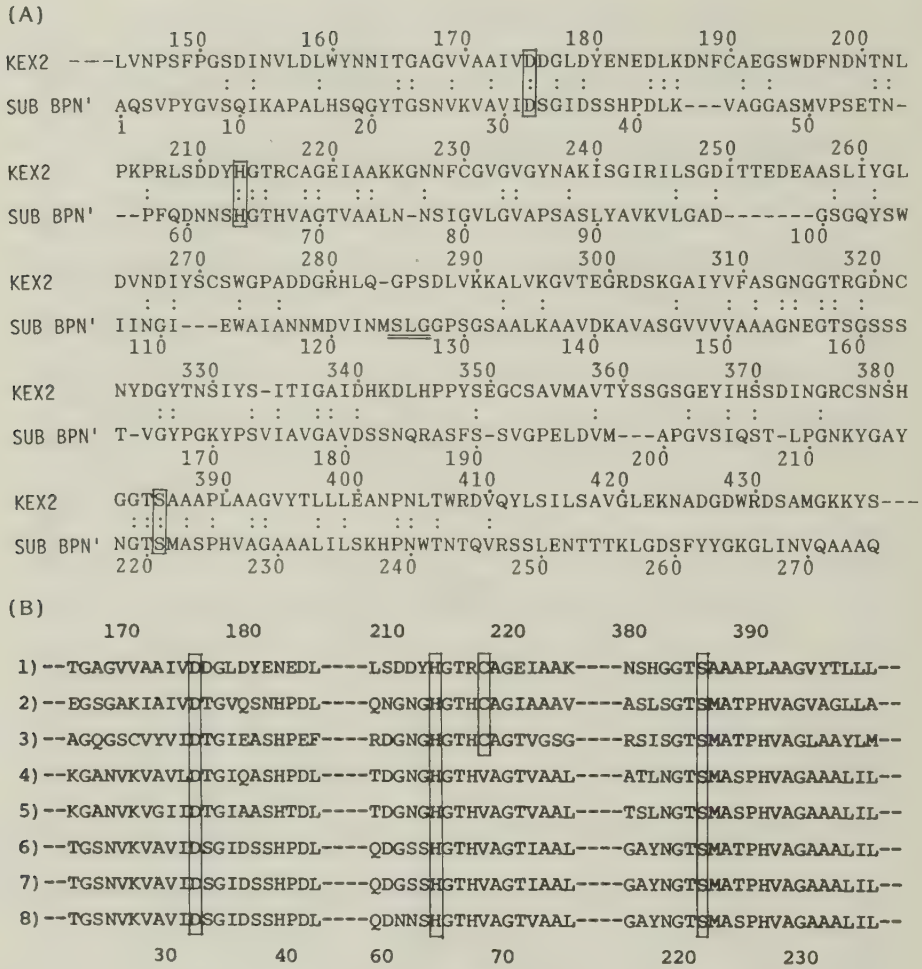

Fig.3. (A) Alignment of the amino acid sequences of the KEX2 protein (upper) and subtilisin BPN' (lower) (19). Sets of identical residues are marked with two dots. Gaps (-) have been inserted to achieve maximum homology. The residues constructing the active site are boxed and the substrate binding site of subtilisin is doubly underlined. (B) Comparison of the amino acid sequences around the active site residues. The residues constructing the active site and the putative free cysteine residues are boxed. Only the residue numbers of KEX2 protease and subtilisin BPN' are specified in the figure. 1) KEX2 protease, 2) thermitase, 3) proteinase K, 4) subtilisin Carlsberg, 5) subtilisin DY, 6) subtilisin I168, 7) subtilisin from *Bacillus amylosaccariticus*, 8) subtilisin BPN'.

protease superfamily, but are not related to the chymotrypsin-like serine-protease family, the latter being considered to have evolved independently. Sequence comparison led us to classify the KEX2 protease as a subtilisin-like serine-protease.

It has been reported that KEX2 protease activity was inhibited by thiol-directed reagents such as monoiodoacetate and heavy metal ions but not by PMSF, a general serine-protease inhibitor (4,5). Similar results were obtained with membrane-bound proteases in yeast, as reported by Wolf's group

and by ours (6-8). As had been known, two fungal subtilisin-like serine proteases, proteinase K and thermitase, are inactivated by thiol-directed reagents. They have a free cysteine residue located immediately adjacent to a histidine residue in the active site (19). KEX2 protein contains eight Cys residues, one of which (Cys-217) is situated in a homologous position (Fig.3B). Inactivation of KEX2 protease by thiol-reagents may be due to the blockage of this free Cys residue. Our preliminary study showed that KEX2 protease was inactivated by inhibitors for serine protease, such as PMSF, DFP, and pAPMSF, at a high concentration of 10 mM. (Details will be reported elsewhere.) These results, taken together, further support the conclusion that KEX2 protease belongs to the serine protease family, as also suggested by Fuller, et al. (9).

KEX2 protease activity exhibits Ca^{2+}-dependency (5-8), analogous to calcium-activated neutral protease (calpain) found in mammalian tissues. However, the KEX2 product does not contain sequences with obvious resemblance to calpains or other calcium-binding proteins. Further studies are necessary to understand the molecular mechanisms by which calcium regulates the enzyme.

The structural organization of KEX2 protein is similar to those of other processing enzymes ever characterized, including yeast KEX1-encoded carboxypeptidase B-like protease (20), and peptide C-terminal α-amidating enzymes from Xenopus laevis skin (21) and bovine pituitary (22). These enzymes have in common two hydrophobic regions, a putative signal sequence at the N-terminus and a putative membrane-spanning domain near the C-terminus, both of which may function to localize and anchor them to the intracelluler target organelles. The active domain of each enzyme, situated at the N-terminal side of the membrane-spanning domain, should be oriented inside the secretory vesicles.

Paired basic residues are conserved on various bioactive peptide precursors to serve as sites of proteolytic processing in a wide range of eukaryotic species from yeast to mammals. This fact suggests a possibility that endopeptidases similar to KEX2 gene product may be involved in precursor processing in mammalian tissues (23,24). The cloned KEX2 gene may serve as a probe for searching these enzymes, which have not yet been well-characterized.

ACKNOWLEDGEMENTS

We thank Dr. Reed Wickner for providing the strain carrying kex2-8 mutation, Miss Kumiko Matsubara for technical assistance. We also thank Drs. Tatsuo Nakayama, Yoshiko Setoguchi, and Naoya Akizuki for valuable comments.

REFERENCES

1. Docherty,K. & Steiner,D.F. (1982) Ann.Rev.Physiol. 44, 625-638.
2. Kurjan,J. & Herskowitz,I. (1982) Cell 30, 933-943.

3. Bostian,K.A., Ellott,Q., Bussey,H., Burn,V., Smith,A. & Tipper,D.J. (1984) Cell 36, 741-751.
4. Julius,D., Brake,A., Blair,L., Kunisawa,R. & Thorner,J. (1984) Cell 37, 1075-1089.
5. Fuller,R., Brake,A. & Thorner,J.(1986) in Microbiology 1986, ed. Levine,L. (American Society for Microbiology, Washington,DC), pp. 273-278.
6. Achstetter,T. & Wolf,D.H. (1985) EMBO J. 4, 173-177.
7. Wagner,J.C., Escher,C. & Wolf,D.H. (1987) FEBS Lett. 218, 31-34.
8. Mizuno,K., Nakamura,T., Takada,K., Sakakibara,S. & Matsuo,H. (1987) Biochem.Biophys.Res.Commun. 144, 807-814.
9. Fuller,R.S., Sterne,R.E. & Thorner,J. (1988) Ann.Rev.Physiol. 50, 345-362.
10. Davis,R.W. et al. (1980) Methods in Enzymology 65, 404-411.
11. Maniatis,T., Fritsch,E.F. & Sambrook,J. (1982) in Molecular Cloning: A Laboratory Manual (Cold Spring Harbor Laboratories, New York).
12. Ito,H., Fukuda,Y., Murata,K. & Kimura,A. (1983) J.Bacteriol. 153, 163-168.
13. Hanahan,D. (1983) J.Mol.Biol. 166, 557-580.
14. Wickner,R.B. (1974) Genetics 76, 423-432.
15. Wickner,R.B. & Leibowitz,M.J. (1976) Genetics 82, 429-442.
16. Messing,J. (1983) Methods in Enzymology 101, 20-78.
17. Kraut,J. (1971) in "The Enzymes", vol.3, ed. Boyer, P.D., (Academic Press, New York), pp. 547-560.
18. Wells,J.A., Ferrari,E., Henner,D.J., Estell,D.A. & Chen,E.Y. (1983) Nucl. Acids Res. 11, 7911-7925.
19. Betzel,C., Pal,G.P., Struck,M., Jany,K-D. & Saenger,W. (1986) FEBS Lett. 197, 105-110.
20. Dmochowska,A., Dignard,D., Henning,D., Thomas,D.Y. & Bussey,H. (1987) Cell 50, 573-584.
21. Ohsuye,K., Kitano,K., Wada,Y., Fuchimura,K., Tanaka,S., Mizuno,K. & Matsuo,H. (1988) Biochem. Biophys. Res. Commun. 150, 1275-1281.
22. Eipper,B.A. et al. (1987) Mol. Endocrinol. 1, 777-790.
23. Davidson,H.W., Peshavaria,M. & Hutton,J.C. (1987) Biochem. J. 246, 279-286
24. Brennan,S.O. & Peach, R.J. (1988) FEBS Lett. 229, 167-170.

ol. 156, No. 1, 1988 BIOCHEMICAL AND BIOPHYSICAL RESEARCH COMMUNICATIONS
ctober 14, 1988 Pages 255-262

THE CALCIUM CHANNEL ANTAGONIST ω-CONOTOXIN INHIBITS SECRETION FROM PEPTIDERGIC NERVE TERMINALS

G.Dayanithi*, N. Martin-Moutot+, S. Barlier*, D.A. Colin*,
M. Kretz-Zaepfel*, F. Couraud+ and J.J. Nordmann*

* Centre de Neurochimie, 5, rue Blaise Pascal, 67084 Strasbourg, Cédex, France
+ Laboratoire de Biochimie, Bd. Pierre-Dramard,13326 Marseille Cédex 15, France

eceived August 1, 1988

UMMARY - The binding of ω-conotoxin to isolated rat neurohypophysial nerve erminals, its effect on the depolarization-induced increase of cytoplasmic Ca^{2+} and on he potassium and electrically-induced release of vasopressin (AVP) have been tudied. The results show that isolated neurosecretory nerve endings have calcium hannels with a high affinity for ω-CgTx and that this toxin inhibits neurohormone elease at very low concentration (IC_{50}= 0. 1nM). Although secretion of vasopressin is nhibited to a great extent by the toxin it is shown that a small but significant amount f the depolarization-induced AVP release is insensitive to ω-CgTx and to the lihydropyridine molecule nicardipine. © 1988 Academic Press, Inc.

A new class of toxins isolated from the venom of the fish-hunting snail *Conus geographus* has recently been described (1). One of these toxins, ω-conotoxin GVIA hereafter abbreviated ω-CgTx) has been shown to block voltage-sensitive calcium hannels at the frog neuromuscular junction (2) as well as two distinct calcium urrents (termed N and L) in chick sensory neurons (3). In brain synaptosomes, the peptide ω-conotoxin fraction GVIA inhibits only a small percentage of the depolarization-induced $^{45}Ca^{2+}$ uptake and neurotransmitter release (4). In the present study we have analyzed the binding of ω-conotoxin to isolated rat neurohypophysial nerve terminals, its effects on the depolarization-induced increase of cytoplasmic Ca^{2+} and on the potassium and electrically-induced release of vasopressin (AVP).

MATERIALS AND METHODS

AVP release from neural lobes and isolated neurohypophysial nerve terminals. The neural lobes were prepared as described earlier (5, 6). They were perfused with normal saline containing (mM):NaCl, 140; $KHCO_3$, 5; $CaCl_2$, 2.2; $MgCl_2$, 1; glucose, 10; HEPES, 10; pH 7.2 and to which bovine serum albumine at a final concentration of 0.01 % was

0006-291X/88 $1.50
Copyright © 1988 by Academic Press, Inc.
All rights of reproduction in any form reserved.

added. The saline was continuously gassed with 5 % CO_2 in O_2. After 60 min of perfusion, at a flow rate of 100 µl x min^{-1}, the neurohypophyses were perfused for 20 min with Na-free saline containing 140 mM choline chloride. Depolarization, for a period of 10 min, was induced with 100 mM potassium, choline being decreased accordingly in order to maintain the osmolarity constant. The evoked AVP release was calculated by subtracting the mean basal release determined in the fractions preceding the onset of the stimulus from the amount of hormone found in each fraction.

Electrical stimulation of the neural lobe. The neural lobes were obtained from male rats (250-300 g body weight) and the pars intermedia carefully dissected out. The neural lobe was impaled on one of a pair of electrodes which were inserted in a small perspex chamber which had an internal volume of about 50 µl. The gland was continuously perfused with normal saline (See Fig. 2 legend) in the presence or absence of ω-CgTx (1 nM). Fractions (100 µl x min^{-1}) were collected every 2 min. and AVP in the perfusate was determined. The neurohypophyses were stimulated electrically with biphasic electrical pulses which had a pattern of discharge similar to the bursting activity of AVP cells (see ref. 6). Briefly the electrical activity of vasopressin cell recorded *in vivo* was used as a command pulse to trigger the stimulator and thus generate a series of pulses (2 ms duration, 2 mA) similar to the bursting pattern observed *in vivo*. The neural lobes were stimulated with four"AVP-like" bursts separated by intervals of 21 s.

Binding of ω-CgTx. ω-CgTx (Peptide Institute, Osaka, Japan) was iodinated by the lactoperoxydase method (7,8) and the monoiodinated derivative was obtained by HPLC 7,8). Membranes (8 µg protein per assay) were prepared by lysing the isolated nerve endings and by further centrifugation of the disrupted membranes. They were incubated with ω-CgTx for 60 mn at 37° in a final volume of 150 µl of a medium containing (mM) : NaCl, 140; KCl, 5; $MgSO_4$, 0.8; glucose, 10; HEPES, 20 and 0,5% bovine serum albumin adjusted to pH 7.2 with Tris-base. Bound toxin was separated by rapid filtration over polyethyleneimine pretreated glass fiber filters (Whatman GF/C).

Binding of (3H) PN 200-110. The binding of (^{3}H)PN 200-110 (85 Ci/mmole, Amersham Corp.) was measured in 170 mM Tris, 1 mM $CaCl_2$ (pH 7.4) in a final volume of 150 µl containing membranes equivalent to three neural lobes. (^{3}H) PN200-110 (2 nM) was incubated with membranes for 30 min at 37°C under red light. Non specific binding was measured in the presence of 100 nM nifedipine (Sigma). Binding was terminated by rapid filtration over polyethyleneimine pretreated glass fiber filter (Whatman GF/C).

RESULTS

Binding of ω-CgTx and PN 200-110 to nerve endings.

Figure 1a shows the results of typical experiments demonstrating a saturable binding of ω-CgTx to nerve terminal membranes. As already demonstrated (7,8), the binding of the toxin with its receptor is irreversible and thus the ligand-receptor interaction can be described by the following equation : $R + L \xrightarrow{k} RL$ where k is the association kinetic constant. After linearization of the results (Fig. 1b; see ref. 8) the association kinetic constant had a value of 5.6 x 10^6 $M^{-1}s^{-1}$ at 37°C and the total number of binding sites was 85 fmoles x mg^{-1} of protein. In an other series of experiments we looked if the calcium channel antagonists diltiazem (0.1 µM) and nifedipine (0.1 µM) could compete with the toxin for its binding site. Both on membranes isolated from

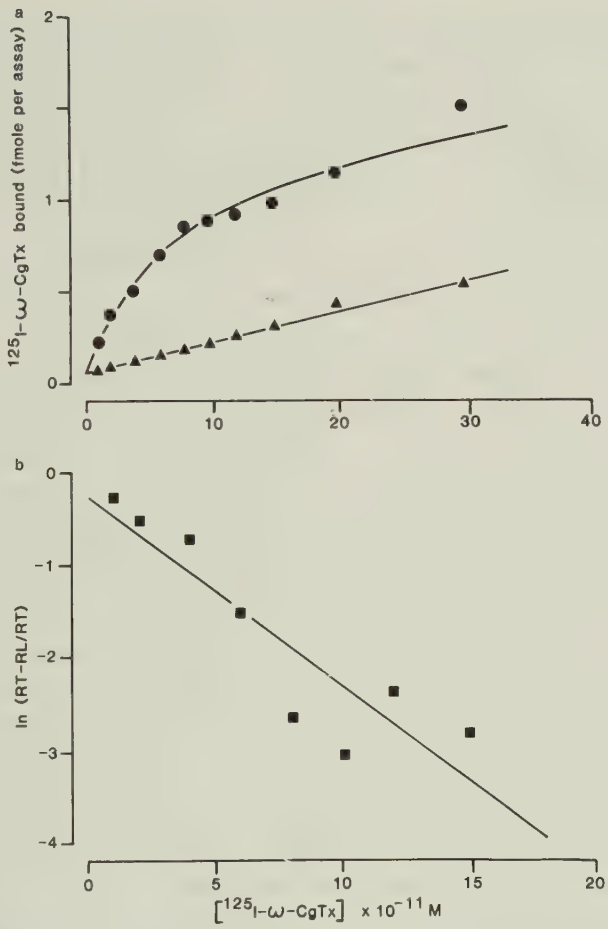

Figure 1. Binding of ω-CgTx to isolated rat neurohypophysial nerve terminal membrane. **a**, the membranes were incubated with increasing concentrations of (^{125}I)-ω-CgTx in the presence (▲ , non specific binding) or in the absence of 0.1 μM native toxin (●, total binding). A saturable binding is observed. **b**,the specific binding (i.e. the difference between total and non specific binding illustrated in a) was linearized according to Ref. 8.

he neurohypophysial nerve endings and on synaptosomes from the cortex the antagonists did not affect significantly (less than 10%) the binding of ω-CgTx to its receptor (not illustrated). We also found that ω-CgTx up to a concentration of 0.1 μM did not compete with (^{3}H)-labeled dihydropyridine PN 200-110. In two sets of experiments the number of sites (fmol/neural lobe) was determined for both ω-CgTx and PN 200-110. The mean values were 4.4 (4.8-4.0) and 0.6 (0.6-0.6) respectively. This suggests that the number of binding sites for ω-CgTx is 6.7 to 8.0 larger than that of the dihydropyridines binding sites. Similarly, in lysed brain synaptosomes isolated from the rat, the number of binding sites for the toxin and PN 200-110 were 500 and 88 fmol x mg^{-1} respectively; thus the ratio of 5.7 between the two categories of sites is very similar to that measured in the neurosecretory nerve endings.

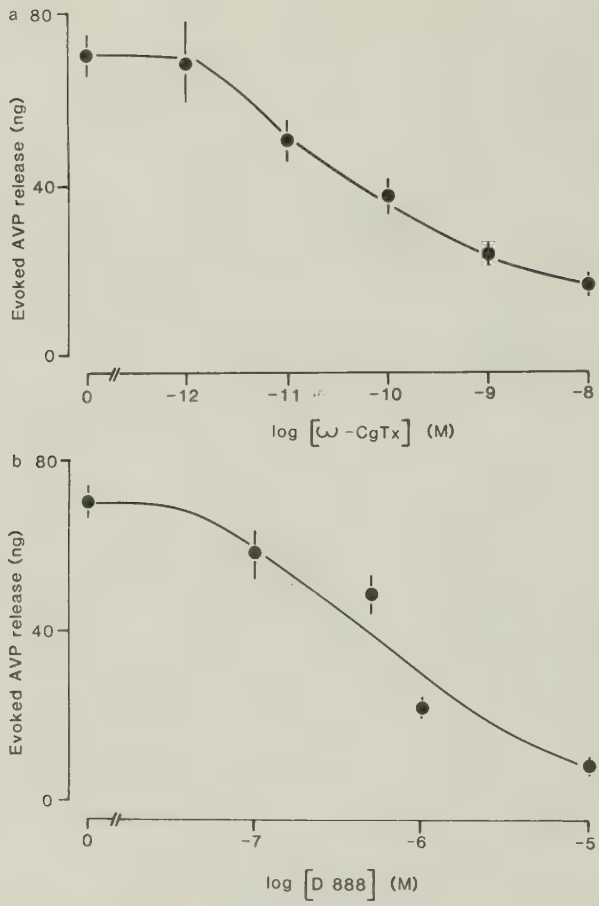

Figure 2. The effects of increasing concentrations of ω-CgTx (**a**) and D888 (**b**) on high potassium evoked AVP release from isolated neural lobes. ω-CgTx and D888, at concentrations indicated on the abcissa were present 10 min before and during the K+ stimulation. The results are given as mean ± S.E.M. (4<n<7).

K^+-induced AVP release.

Figure 2 shows the dose-response curves of high K+-evoked AVP release from isolated neural lobes in the presence of ω-CgTx (Fig. 2a) or in the presence of another calcium channel antagonist, D 888 (desmethoxyverapamil; Fig. 2b); half-maximal hormone release was observed at concentrations of 0.1 nM and 1 μM respectively. In another series of experiments we studied the effect of the toxin on AVP release from isolated nerve endings. These were obtained from rat neural lobes by methods already described (5). Depolarization of the nerve terminals with 100 mM potassium evoked an AVP release of 3.8 ± 0.3 ng (n=4) whereas in the presence of 0.1 μM ω-CgTx there was a 80% inhibition of the evoked AVP release. Thus, although verapamil derivatives (Fig. 2b) and some dihydropyridines can inhibit depolarization-induced release from the neural lobe, ω-CgTx is the most potent inhibitor of secretion so far described. From the data presented in Figs. 1 and 2 it is possible to correlate the degree

occupancy of the toxin receptors and the extend of hormone release inhibition. One n calculate that, during a 10 min incubation period, the ω-CgTx concentration ecessary for half of its membrane receptors to be occupied is 0.2 nM. On the other and half maximal K^+-evoked AVP release is observed following 10 min exposure of e neural lobes to 0.1 nM ω-CgTx (Fig. 2a). The fact that these two values are very milar suggest strongly that ω-CgTx interacts with the voltage-sensitive calcium annels involved in the mechanism leading to neuropeptide release. However K^+-duced AVP release is never completely abolished by the toxin. Similarly, although e have already presented data on the potent inhibitory effect of nitrendipine and cardipine on AVP release (5), depolarization-induced secretion could not be totally olished in the presence of 5 μM nicardipine. Whereas in the presence of 0.3 μM ω-gTx the K^+ induced AVP release was inhibited by 78±6 % (n=4), in the presence of 5 M nicardipine the degree of inhibition was 58 ± 6 % (n=9). In order to analyze further e inhibition of AVP release by ω-CgTx and the dihydropyridine, neurosecretory erve terminals were incubated in the presence of 30 μM nicardipine and hormone lease was triggered with 100 mM K^+ for a period of 10 min. The neurohypophyses ere then allowed to rest for a period of 30 min in the presence of dihydropyridine olecule. Hormone release was induced a second time with 100 mM potassium but in e presence of nicardipine and 30 nM ω-CgTx. Thus the effect of the toxin in the resence of nicardipine on the evoked hormone release could be calculated by omparing the amount (S_2) released during the second stimulation with that (S_1) bserved during the first exposure to elevated potassium concentration. Neural lobes timulated twice with K^+ in the presence of nicardipine were used as controls. We ound that ω-CgTx inhibited by 22.0 + 2.4 % (n=6) the release of AVP induced in the resence of nicardipine.

Electrically-induced AVP release.

Figure 3 shows that ω-CgTx also reduced electrically induced AVP release from he neurohypophysis. The neural lobe was stimulated with a pattern of firing nimicking the electrical activity of magnocellular neurons of the hypothalamus(9). ω-CgTx (1 nM) considerably decreased the electrically-evoked release. Four AVP-like ursts induced the release of 1.74 ± 0.34 ng (n=3) of AVP whereas in the presence of the oxin the amount of hormone secreted was 0.50 ± 0.07 ng (n=3). In another series of experiments we used the S_2/S_1 paradigm (see above) to analyze further the effects of ω-CgTx and nicardipine on the electrically induced AVP release. The neural lobes were first stimulated with four AVP like bursts in the absence of the drug. The neurohypophyses were then let to rest for a period of 30 min. The neural lobes were then stimulated with four AVP like bursts in the presence of nicardipine (5 μM) or ω-CgTx (30 nM) which were added 10 min before the onset of stimulation. In control experiments the neural lobes were stimulated twice in the absence of the calcium channel blockers. Figure 4 summarizes the data obtained for both the electrically and

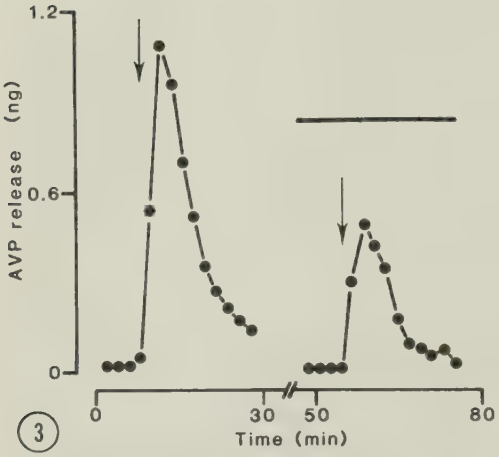

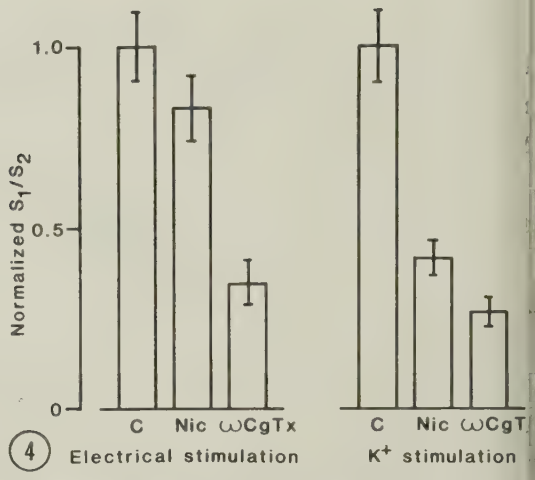

Figure 3. Effects of ω-CgTx on vasopressin release from electrically stimulated rat neural lobe. The neural lobe was stimulated (arrows) with four bursts of pulses mimicking the electrical activity of vasopressin-containing cells during haemorrhage. AVP in the perfusate was measured by radioimmunoassay. ω-CgTx (10 nM) was present, as indicated by the bar, 10 min before, during and after the second stimulus.

Figure 4. Effects of ω-CgTx and nicardipine on the electrically and potassium-induced AVP release. The neural lobes were stimulated twice with four AVP-like bursts (see Materials ands Methods). A period of 30 min was given between the two stimuli and the toxin (30 nM) or nicardipine (5 μM) were added 10 min before the onset of the second stimulation. Similarly isolated neurosecretory nerve terminals were stimulated with 100 mM potassium for two periods of 10 min separated by 30 min and the calcium channel blockers were added 10 min before the onset of the depolarization. The results are given as the ratio between the amount of AVP released during the second stimulation (S_2) and during the first (S_1). They have been normalized in such a way that for control experiments this ratio was 1.0. The results are given as mean ± S.E.M.(16<n<4).

potassium-induced AVP release. Whereas ω-CgTx greatly inhibited AVP release in both cases, nicardipine was much more potent when hormone release was triggered with an increase of external K^+ concentration then when stimulated with electrical pulses. This may be due to the well-known voltage dependency of dihydropyridine binding, the affinity being higher on depolarized membranes.

Depolarization-induced $(Ca^{2+})_i$ increase.

The effect of the toxin on the depolarization-induced increase in internal (Ca^{2+}) was measured using the Ca^{2+} indicator fura-2 (10) as described in ref. 11. Under basal conditions the resting Ca^{2+} concentration in control and toxin-treated (1 nM) terminals was 422 ± 90 nM (n=7) and 504 ± 117 nM (n=7), respectively. Depolarization of the nerve terminals with 50 mM potassium gave rise to an increase of 341 ± 4 nM (n=7) whereas in the presence of the toxin the change of internal Ca^{2+} was 209 ± 28 nM (n=7). Using a higher toxin concentration (10 nM) the K^+- induced $(Ca^{2+})_i$ was inhibited by 50 ± 8% (n=7).Thus ω-CgTx inhibits but does not abolish totally the rise in free internal Ca^{2+}concentration induced by the activation of the voltage dependent calcium channels.

To see if the toxin could also act at a step following the increase in ionized toplasmic Ca^{2+} concentration induced by the activation of the voltage-dependent lcium channels, it was added before and during a period when internal calcium was tificially increased without depolarizing the membrane. This involves making the rve terminals permeable, with digitonin, in a medium containing micromolar ncentrations of calcium (12). ω-CgTx (1 nM) did not modify the total evoked AVP ease. In controls, AVP levels were 1.5 ± 0.3 ng (n=4) whereas in the presence of the xin the amount secreted was 1.3 ± 0.1 ng (n=4). These data show that the toxin does t act at a step following the opening of calcium channels.

SCUSSION

The present study shows that ω-CgTx is an extremely potent inhibitor of polarization-induced secretion from the neurohypophysis. Electrophysiological udies on other excitable tissues have shown that the toxin acts on the N- and L-types calcium channels as defined in ref. 13. Furthermore it has been found in chick nsory neurons that the L-type calcium channel is sensitive to dihydropyridines hereas the N and T types are not (3,13). Because AVP release from the nerve endings highly sensitive to dihydropyridines (5) and can be greatly inhibited by ω-CgTx, we n reasonably assume that in the neural lobe activation of the L-type calcium nannels is mainly responsible for inducing an increase of $(Ca^{2+})_i$ and subsequent ecretion. This conclusion is supported by the recent findings showing that in the olated neurohypophysial nerve endings a predominant Ca-inward current orresponds to L-type channels and is sensitive to dihydropyridines (14). In contrast ith our findings, the $^{45}Ca^{2+}$ uptake (15) and the release of the noradrenalin and erotonin from brain synaptosomes are only slightly inhibited by ω-CgTx at oncentrations higher than those used in the present study (4). Furthermore, in ontrast to what has been observed in the neural lobe, calcium influx and transmitter elease from synaptosomes are insensitive to dihydropyridines (4, 16, 17) (but see ref. 8). However it is interesting to note that in a paper published very recently it was hown that the release of (^3H)-labeled noradrenalin from superior cervical ganglion eurons in culture was inhibited by concentrations of ω-CgTx relatively similar to hose used in the present study (19). Thus, the sensitivity to ω-CgTx varies among lifferent preparations used. Our results suggest that neuropeptide release from the eurohypophysis can be modulated by the activation of both N and L-type channels whereas the results obtained from brain synaptosomes suggest that neurotransmitter elease is mostly triggered by the opening of the N-type calcium channels.

ACKNOWLEDGEMENTS : We thank Jose Lemos and Martha Nowycky for helpful comments on the manuscript and for being so cute communicating their results before publication. We also thank Ruud Buijs for the AVP antiserum serum. D888 was a gift from Knoll A.G. Supported by grants from CNRS and INSERM.

REFERENCES

1. Olivera, B.M., Gray, W.R., Zeikus, R., McIntosh, J.M., Varga, J., Rivier, J., de Santos, V. & Cruz, L.J.(1985) Science **230**, 1338-1343.
2. Kerr, L.M. & Yoshikami, D. (1984) Nature **308**, 282-284.
3. Fox, A.P., Nowycky, M.C. & Tsien R.W.(1987) J. Physiol. Lond. **394**, 173- 200.
4. Reynolds, I.J., Wagner, J.A., Snyder, S.H., Thayer, S.A., Olivera, B.M. & Miller, R.J. (1986) Proc. Natl. Acad. Sci. USA **83**, 8804-8807.
5. Cazalis, M., Dayanithi, G. & Nordmann, J.J. (1987) J. Physiol. Lond. **390**, 55- 70.
6. Cazalis, M., Dayanithi, G. & Nordmann, J.J. (1985) J. Physiol. Lond. **369**, 45-60.
7. Cruz, L.J. & Olivera, B. M. (1986) J. Biol. Chem. **261**, 6230-6233.
8. Marquèze, B., Martin-Moutot, N., Levêque, C. & Couraud, F., Mol. Pharmacol., in press.
9. McCleskey, E.W., Fox, A.P. Feldman, D.H., Cruz, L.J.,Olivera, B.M., Tsien, R.W. & Yoshikami, D. (1987) Proc. Natl. Acad. Sci. USA. **84**, 4327-4331.
10. Grynkievicz, G., Poenie, M. & Tsien, R.Y. (1985) J. Biol. Chem. **260** 3340- 3350.
11. Brethes, D., Dayanithi, G., Letellier, L. & Nordmann, J.J. (1987) Proc. Natl. Acad. Sci. USA, **84**, 1439-1443.
12. Cazalis, M., Dayanithi, G. & Nordmann, J.J. (1987) J. Physiol. Lond. **390**, 71-91.
13. Nowycky, M.C., Fox, A.P. & Tsien, R.W. (1985) Nature **316**, 440-443.
14. Lemos, J.R. & Nowycky, M.C. Neuros. Abst. **13**, in press.
15. Suszkiw, J.B., Marawsky, M.M. & Fortner, R.C. (1987), Biochem. Biophys. Res. Commun. **145**, 1283-1286.
16. Suszkiw, J.B., O'Leary, M.E., Murawsky, M.M. & Wang, T. (1986) J. Neuroscience, **6**, 1349-1357.
17. Rampe, D., Janis, R.A. & Triggle, D.J. (1984) J. Neurochem. **43**, 1688-1691.
18. Turner, T.J. & Goldin, S.M. (1985) J. Neuroscience **5**, 841-849.
19. Hirning, L.D., Fox, A.P., McCleskey, E.W., Olivera, B.M., Thayer, S.A., Miller, R.J. and Tsien, R.W. (1988) Science, **239**, 57-61.

Vol. 156, No. 1, 1988 BIOCHEMICAL AND BIOPHYSICAL RESEARCH COMMUNICATIONS
October 14, 1988 Pages 263-268

EFFECT OF RETINOIC ACID ON cAMP DEPENDENT PROTEIN PHOSPHORYLATION IN PSORIATIC FIBROBLASTS

F. RAYNAUD°, C. LIAPI*, P. GERBAUD°, W. B. ANDERSON*, AND D. EVAIN-BRION°

° Laboratoire de Physiopathologie du Développement, CNRS ENS
46 rue d'ulm 75230 Paris Cedex 05 France

* Laboratory of Cellular Carcinogenesis and Tumor Promotion, N.I.H.,
Bethesda, MD 20205

Received August 3, 1988

Retinoic acid treatment of psoriatic fibroblasts increases the activity of cyclic AMP dependent protein kinase. In this study we report that retinoic acid treatment of cultured psoriatic fibroblasts modifies their subsequent cAMP dependent protein phosphorylation. In the soluble fraction of normal fibroblasts cAMP clearly enhances the in vitro phosphorylation of proteins of MW 37,49,54,56,68,83 kD while retinoic acid treatment of the same cells results in a decrease of the cAMP dependent phosphorylation of the first five of the same proteins. In contrast, in psoriatic fibroblasts from psoriatic patients retinoic acid either has no effect or increases the cAMP dependent phosphorylation of some of these proteins. Moreover the phosphorylation of a protein of MW 54 kD, undetectable in untreated psoriatic cells, is more phosphorylated in the presence of cAMP after retinoic acid treatment. The appearance of this phosphorylated proteins is time dependent and dose dependent upon the addition of retinoic acid. These in vitro phosphorylation results suggest that retinoic acid treatment of psoriatic fibroblasts change the level of cAMP dependent phosphorylation of some cytosolic proteins. These specific phosphorylations could be implicated in a variation of cell functions.
© 1988 Academic Press, Inc.

Retinoids, derivatives of vitamin A, play an essential role in regulation of growth of many different cell types (1-3) and are required for normal epithelial cell differentiation (4).

Retinoic acid derivatives have been used with success as therapy in psoriasis. These compounds have been shown to increase cAMP dependent protein kinase activity during differentiation of tumoral cells (5,6) and to change the protein phosphorylation pattern in these cells (7).

We recently showed in psoriatic fibroblasts a deficiency of cAMP dependent protein kinase and reported that this deficiency in psoriatic erythrocytes was correlated with the severity of the disease (8).

ABBREVIATIONS RA: Retinoic Acid
cAMP: cyclic Adenosine Monophosphate

0006-291X/88 $1.50
Copyright © 1988 by Academic Press, Inc.
All rights of reproduction in any form reserved.

In vitro treatment of psoriatic fibroblasts with retinoic acid induces an increase either in cAMP dependent protein kinase activity or in the photoaffinity labelling with 8-Azido[^{32}P]cAMP of both regulatory subunits RI and RII of these enzymes (9). For this reason we were interested in the in vitro cAMP dependent phosphorylation of proteins from normal and psoriatic fibroblasts before and after retinoid acid (RA) treatment.

MATERIALS AND METHODS

Trypsin (2X crystallised, collagenase (type II-5), cAMP, and kemptide were purchased from Sigma (St. Louis, Missouri). Ham's F12 medium and glutamine were from Flow Laboratories (Puteaux, France) and fetal calf serum from Seromed (Berlin, F.R.G.). All-trans-vitamin A (retinoic acid), was a generous gift from Hoffman-LaRoche (Basel-Swizerland). [γ^{32}P]ATP (30 Ci/mmol) was obtained from Amersham (Les Ulis, France), and [8-Azido^{32}P]cAMP (20 Ci/mmol) from ICN Pharmaceuticals (Cleveland, Ohio). Low and high molecular weight standarts were from Biorad (Richemond, California).

Fibroblast cultures were established as previously described (8). The cells were used after their fourth and fifth passage. Where indicated RA dissolved in absolute ethanol was added one day after plating to give a final concentration of 1μM. The final concentration of ethanol in the medium did not alter cell growth, morphology or in vitro protein phosphorylation.

Preparation of cells for in vitro protein phosphorylation: Control and RA treated cells were harvested at various times following the RA addition. Growth medium was aspirated from the dishes and the cells washed three times with ice cold buffer (50 mM MES, 10 mM $MgCl_2$, 0.25 M sucrose pH 6.2) and scraped into this buffer with the addition of leupeptin (20μg/ml). The cells were then homogeneized in a Dounce homogenizer (27 strokes) and the homogenate centrifuged at 12 000 g for 15 minutes. Aliquots of both supernatant and particulate fractions from all samples were assayed for protein content using a fluorometric assay with bovine serum albumin as standard(10).

Protein phosphorylation and gel electrophoresis: Supernatant or particulate fractions (50 μg of protein) were autophosphorylated in a total volume of 100 μl containing 50 mM MES, pH 6.2, 10 mM Mg Cl_2 , 5.5 μM [γ^{32}P] ATP, 10μM cAMP and 1mM 3 isobutyl-1-methylxanthine for 3 minutes. The reaction was stopped by the addition of 20 μl of SDS sample buffer (9% SDS, 15% glycerol, 3 mM EDTA, 30 mM Tris buffer pH 8). Samples were treated at 100°C for 2 minutes and 2 μl of 2 mercaptoethanol and 5 μl of 0.1% bromophenol blue in 50% glycerol were then added. Samples were analyzed by SDS-polyacrylamide gel electrophoresis using a 6% to 15% gradient separating gel and 2% stacking gel. Gels were stained for proteins with Coomassie blue, destained and dried and exposed against Amersham MP films for one to three days at -80°C. Densitometric scannig of the autoradiograms was performed using a Beckmann densitometer.

RESULTS

We showed in previous studies that RA treatment of psoriatic fibroblasts (uninvolved and involved skin) in culture induced an increase in cAMP dependent protein kinase activity (9) and also an increase of the amount of 8-Azido[^{32}P]cAMP bound to the soluble regulatory subunits RI and RII (9). In contrast either no change or a decrease in cAMP dependent protein kinase activity occured upon RA treatment of normal fibroblasts. These results led us to investigate

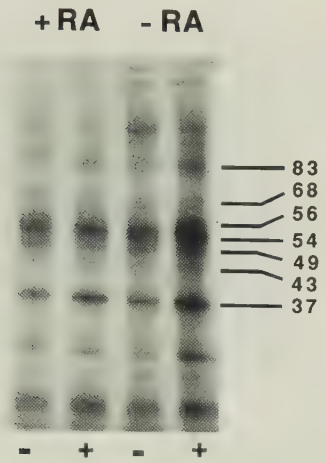

Figure 1: The effect of RA treatment of normal fibroblasts on subsequent in vitro phosphorylation. Normal fibroblasts were treated or not for 48 h with 1μM RA. Cells were then harvested and in vitro phosphorylation performed with 12 000 g supernatant in presence (+) or absence (-) of 1μM cAMP.

whether some cellular proteins were phosphorylated in a cAMP dependent manner in the presence or absence of RA.

In our experimental conditions we could not detect any change in phosphorylation in the presence of cAMP in the particulate fractions either in normal or in psoriatic cells and no modification after RA treatment.

In the 12 000 g supernatant of normal fibroblasts seven bands were phosphorylated more intensively in the presence of cAMP, three prominent bands of MW respectively 37, 56, 83 kD, and four weaker bands of MW 43,49,54,68 kD (Fig 1).When normal fibroblasts were treated with RA cAMP decreased the subsequent in vitro phosphorylation of four bands (37,43,49,56 kD) or slighty modified the phosphorylation of three bands (54,68,83 kD).(Fig 1 and 2).

In psoriatic fibroblasts, only five bands (37,43,56,68,83 kD) are phosphorylated in the presence of cAMP. In contrast to normal cells the RA treatment of all type of psoriatic fibroblasts induced the phosphorylation of protein at 54 kD and in one patient at 49 kD (Fig 2 and 3).

We previously showed that the changes of cAMP dependent protein kinases in psoriatic fibroblasts were dependent upon the concentration of RA used in treating the cells (9). We therefore studied whether the changes in protein phosphorylation were also dependent upon RA concentration. Psoriatic fibroblasts were treated for 2 days with either 0.01, 0.1, 1μM RA. The

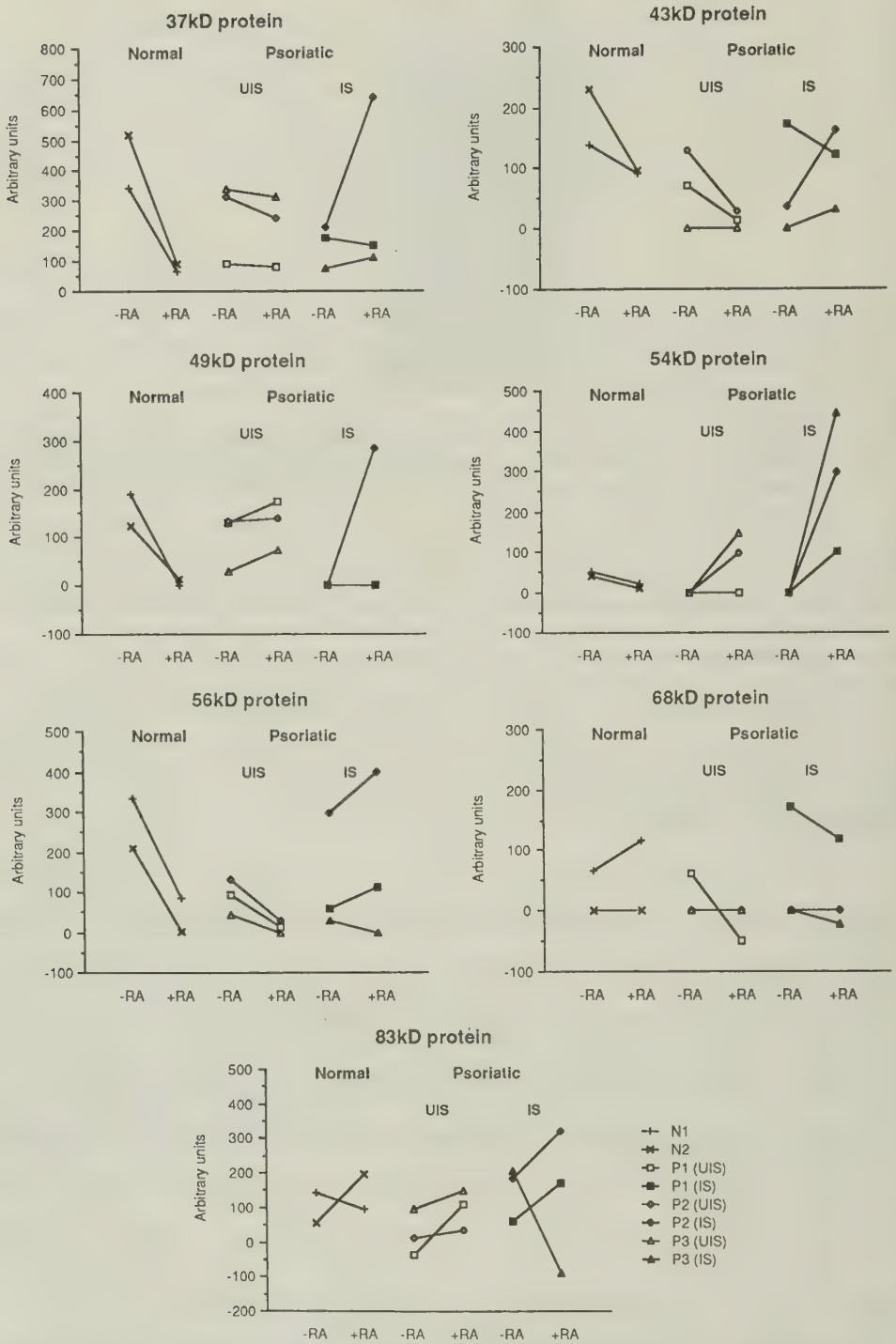

Figure 2: cAMP dependent phosphorylation of soluble proteins of normal and psoriatic fibroblasts in presence (+RA) and absence (-RA) of RA treatment after SDS PAGE. An arbitrary quantitation of the cAMP dependent phosphorylation of the seven protein bands which is calculated from the scanner integration of the intensity of the autoradiograph. The value represents the amount of P^{32} incorporated in the protein band in presence of cAMP minus the amount in absence of cAMP. N = Normal(2 subjects), P = Psoriatic (3 patients).
UIS = UnInvolved Skin, IS = Skin

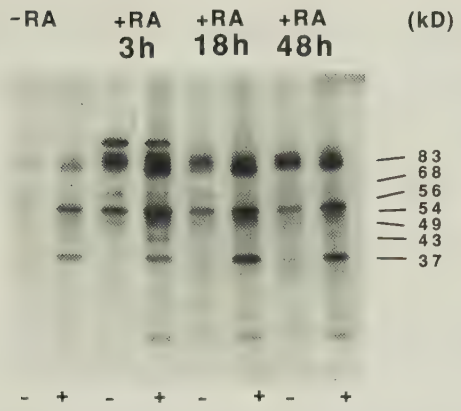

Figure 3: Time couse of the effect of RA treatment of psoriatic fibroblasts on subsequent in vitro cAMP dependent phosphorylation. Cells were treated with 1μM RA for 3, 18 or 48 hours in involved fibroblasts in presence (+) or in absence (-) of 1μM cAMP during in vitro phosphorylation.

phosphorylation changes were maximal at a RA concentration of 1μM and did not occur at a concentration of 0.01μM (data not shown). In addition studies on the time course of RA action (1μM RA) on the pattern of the cAMP dependent protein kinases revealed that the increase was observed as early as three hours after RA addition to the cell culture medium. Similarly we explored whether alterations in in vitro protein phosphorylation were dependent upon the duration of RA treatment (Fig 2). The 54 kD phosphorylated protein appeared in the soluble fractions of psoriatic cells after three hours of RA treatment and was not further increased with longer periods of RA treatment. In some cases, (for example the 54 kD proteins and 49 kD), similar changes in phosphorylation were observed in uninvolved and involved skin fibroblasts of psoriatic patients. However since the pattern of change was not consistent amongst all the proteins it is not possible to draw further conclusions concerning effects in the two situations.

DISCUSSION

This study demonstrates that RA treatment of human fibroblasts can alter their subsequent in vitro cAMP dependent phosphorylation.

RA induced the phosphorylation of a protein band of MW 54 kD in the three psoriatic patients studied, which was enhanced by cAMP. The effect of RA on the phosphorylation of the 54 kD protein was time and dose dependent. It will be of interest to indentify further the 54 kD protein(s) and to assess its precise role in psoriatic fibroblasts.

Although these results do not establish definitively that the increase in cAMP dependent phosphorylation in retinoic acid treated psoriatic cells is due to increased activity of cAMP dependent protein kinases, it is interesting to note the similarity in time course and dose dependency of the action of RA on cAMP dependent protein kinase activities and on subsequent in vitro cAMP dependent phosphorylation of cytosolic proteins.

Among the numerous biochemical effects of RA on cells in culture (10), the changes in cAMP dependent phosphorylation observed in psoriatic cells is one of the earliest. As soon as three hours after the initiation of RA treatment, changes in phosphorylation of cytosolic proteins were observed. These effects may have a critical role in regulating psoriatic fibroblast functions which in turn have a preeminent role in the appearance of psoriatic lesions (11).

REFERENCES

1. Sporn, M.B., and Roberts, A.B. (1983). Canc. Res., 43: 3034-3040.

2. Moon, R.C., McCormick, D.L., and Mehta, R.G. (1983). Cancer Res., 43 sup: 2469-2475.

3. Adamo, S., DeLuca, L.M., Akalovsky, I., and Bhat, P.V. (1979). J.N.C.I., 62: 1473-1481.

4. Kubilus, J. (1983). J. Invest. Dermatol., 81sup: 55-58.

5. Plet, A., Evain, D., and Anderson, W.B. (1982). J. Biol. Chem., 889-893.

6. Ludwig, K.W., Loewy, B., and Niles, R.M. (1980). J. Biol. Chem., 255: 5999-6002.

7. Niles, R.M., Loewy, B., and Rogeys, S. (1986). Exp. Cell Res., 164: 437-448.

8. Evain-Brion, D., Raynaud, F., Laurent, P., Plet, A., Leduc, B., and Anderson, W.B. (1986). Proc. Natl. Acad. Sci. USA, 83: 5272-5276.

9. Raynaud, F., Leduc, C., Anderson, W.B., and Evain-Brion, D. (1987). J. Invest. Dermatol., 89: 105-110.

10. Chytil, F. (1986). J. Amer. Acad. Dermatol., 15: 741-745.

11. Saiag, P., Coulomb, B., Lebreton, C., Bell, E., and Dubertret, L. (1985). Science, 230: 669-672.

Vol. 156, No. 1, 1988 BIOCHEMICAL AND BIOPHYSICAL RESEARCH COMMUNICATIONS
October 14, 1988 Pages 269-274

THE TRANSCRIPTION OF THE INTERLEUKIN 1β GENE IS INDUCED WITH PMA AND INHIBITED WITH DEXAMETHASONE IN U937 CELLS

Tsutomu Nishida, Masaaki Takano, Takuma Kawakami, Naoki Nishino, Satoru Nakai and Yoshikatsu Hirai

Cellular Technology Institute, Otsuka Pharmaceutical Co., Ltd.
463-10 Kagasuno Kawauchi-cho Tokushima, 771-01, Japan

Received August 8, 1988

SUMMARY: Interleukin 1β mRNA was induced with phorbol ester, not LPS, in the human histiocytic lymphoma cell line U937, but interleukin 1α mRNA was not induced. Nuclear run-on analysis showed that phorbol ester induced the transcription of interleukin 1β but did not induce it in the presence of cycloheximide. This indicates that the induction of the transcription with PMA requires de novo protein synthesis. Dexamethasone, an immunosuppressive and anti-inflammatory agent, decreased the level of interleukin 1β mRNA induced with phorbol ester. The transcriptional analysis showed that dexamethasone inhibits the transcription of the interleukin 1β gene. © 1988 Academic Press, Inc.

Interleukin 1(IL-1) is a mediator of immunologic and inflammatory responses (1). Two distinct forms of IL-1 are produced by monocytes and macrophages (2 - 5). These two forms of IL-1, termed IL-1α and IL-1β, have been cloned in humans (6 - 9). Both forms of IL-1 have identical biological activities (1,10) and bind to the same receptor(11). The production of IL-1 can be induced in culture cells by various stimuli and in most cases, IL-1β mRNA is induced predominantly(7,9,12,13). It has been reported that IL-1β mRNA is rapidly induced and falls to a low, but constant level within 6 hours in THP-1 human monocytic leukemia cells stimulated with LPS (14). However the regulatory mechanism of IL-1β gene expression as well as IL-1α gene expression remains to be elucidated.

Glucocorticoids are used clinically as immunosuppressive and anti-inflammatory agents. Snyder and Unanue have reported that glucocorticoids inhibit IL-1 production from murine peritoneal macrophages (15).

In order to examine the regulatory mechanism of IL-1 gene expression including effects of glucocorticoids, we studied the expression of IL-1

Abbreviations: IL-1, interleukin 1; LPS, lipopolysaccharide; PMA, phorbol-12-myristate-13-acetate; Dex, dexamethasone; CHX, cycloheximide.

0006-291X/88 $1.50
Copyright © 1988 by Academic Press, Inc.
All rights of reproduction in any form reserved.

mRNA using human histiocytic lymphoma cell line U937 (16) which is known to differentiate to macrophages (17). In this paper, we describe that PMA induced the transcription of IL-1β which required de novo protein synthesis, and dexamethasone(DEX) inhibited the transcription induced with PMA.

MATERIALS AND METHODS

Cell culture : The human histiocytic lymphoma cell line U937 was cultured to 4×10^5 cells/ml in RPMI 1640 medium (Gibco) supplemented with 10% fetal calf serum (FCS) (Gibco). Cells were induced and treated as follows: cells were washed and resuspended in fresh RPMI 1640 medium supplemented with 10% FCS and 25 ng/ml of phorbol-12-myristate-13-acetate (PMA) (Pharmacia) in the presence or absence of 10^{-6} M dexamethasone (Dex) (Sigma) or 10 μg/ml of cycloheximide, and incubated at 37°C in 5% CO_2 and 95% air for the indicated period.

RNA isolation and hybridization : Total cellular RNA was isolated by the guanidine isothiocyanate - cesium chloride method (18). RNA samples (10 μg) were denatured with glyoxal-DMSO, electrophoresed in 1.2% agarose and blotted onto nitrocellulose membrane (Schleicher & Schuell) (19). Cytoplasmic RNA was isolated from the post-nuclear supernatant (20) and transferred to nitrocellulose membranes as described (21). Prehybridization and hybridization were carried out as described (19) with nick-translated IL-1β cDNA probe (PstI - PvuII fragment of pcD-GIF-16 (9)).

Nuclear run-on transcription : Nuclei were isolated from U937 cells treated as indicated by lysing the cells in NP40 lysis buffer as described (20). Nuclear transcription and RNA extraction were performed essentially as decribed (22) except that [α-^{32}P]GTP (400 Ci/mmol, Amersham) was used to label elongating RNA chains. RNA samples of equal radioactivity were hybridized with 2 μg of linearized plasmid DNA immobilized on nitrocellulose filters. Prehybridization, hybridization and washing of the filters were performed as described (23).

RESULTS AND DISCUSSION

Expression of IL-1β gene in U937 cells induced with PMA

We have previously reported that both IL-1α and IL-1β cDNAs were isolated from mRNA derived from U937 cells, which were differentiated to adhered cells with PMA and ConA, and then stimulated with LPS, MDP, and PMA (9). In the process of our investigation of the kinetics of IL-1 mRNAs, we found that IL-1β mRNA accumulates in U937 cells treated with only PMA, but IL-1α mRNA does not. IL-1β mRNA can be observed within 4 hours after PMA induction while no IL-1β mRNA can be detected in uninduced U937 cells (Fig.1, left). The levels of IL-1β mRNA remain essentially unchanged from 8 hours to 3 days after PMA induction (Fig.1). This is in contrast to the transient expression of IL-1β mRNA in THP-1 human monocytic leukemia cells reported by Fenton et al., (14). It may be due to a difference in mRNA stability since PMA treatment induces the stable expression of c-fos mRNA in U937 cells (24) and GM-CSF mRNA in T

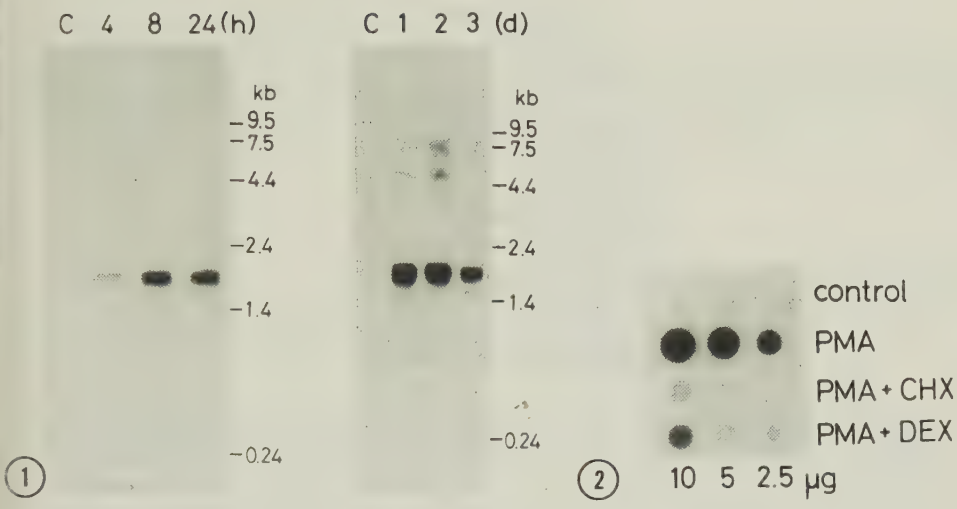

Figure 1. Time course of IL-1β mRNA expression in U937 cells. Cells were treated with PMA at 25 ng/ml for the indicated periods. Total cellular RNA was blotted on each lane (10 μg). Control (C) represents the total cellular RNA from uninduced U937 cells. Molecular size markers of RNA (BRL) are shown on the right. h,hours; d,days.

Figure 2. Accumulation of IL-1β mRNA in U937 cells after various treatments. Cells were treated with indicated reagents for 8 hours. Cytoplasmic RNA was extracted and the indicated amounts of cytoplasmic RNA was applied onto nitrocellulose filter. Control shows cytoplasmic RNA from non-treated U937 cells.

lymphocytes (25). Next we examined whether IL-1β mRNA expression induced with PMA requires the newly synthesized proteins. Dot blot analysis using cytoplasmic RNA 8 hours after PMA treatment showed that IL-1β mRNA is induced with PMA only, but is not induced with PMA in the presence of 10 μg/ml of cycloheximide(CHX), the inhibitor of de novo protein synthesis (Fig. 2). The run-on analysis using nuclei showed that CHX inhibits the transcription of IL-1β (Fig. 3). Our data indicate that PMA induces the transcription of IL-1β, which requires the newly synthesized proteins in U937 cells. Recently S.W.Lee et al., have reported that IL-1β mRNA induced with PMA and LPS is not inhibited with CHX in U937 cells (26). Therefore, it may be suggested that the additional signal by LPS replaces the newly synthesized proteins which are required in the transcription of IL-1β induced with PMA. Since IL-1β mRNA was not induced with LPS only in U937 cells (data not shown), the signal with PMA is essential for the induction of IL-1β mRNA.

Inhibition of the transcription of the IL-1β gene by dexamethasone

In order to examine the effect of Dex on the expression of IL-1β mRNA induced with PMA, we isolated cytoplasmic RNA from PMA-induced and

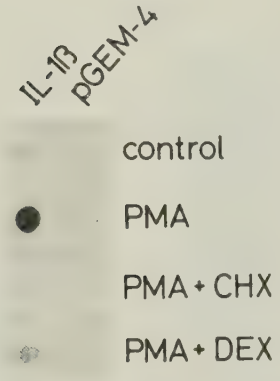

Figure 3. Transcriptional analysis of the IL-1β gene in U937 cells after various treatments. Cells were treated as indicated in Figure 2 legend and their nuclei were isolated. Equal counts of radiolabeled RNAs synthesized in run-on transcription assays were hybridized to the linearized and denatured IL-1β (pcD-GIF-16) and pGEM-4 plasmid DNA immobilized on nitrocellulose filters.

PMA/Dex-treated cells. Dot blot anlysis showed that the expression of IL-1β mRNA induced with PMA was inhibited with Dex (Fig. 2). Nuclear run-on analysis showed that the transcription of IL-1β was inhibited in the presence of PMA and Dex (Fig. 3). This indicates that the transcription of IL-1β induced with PMA is inhibited by Dex in U937 cells. Recently P.J.Knudsen et al., have reported that the expression of IL-1β mRNA in bacterial toxin-stimulated U937 cells is inhibited with Dex (27), and S.W.Lee et al., have shown that the transcription of IL-1β induced with PMA and LPS is inhibited with Dex (26). Our data and their reports show that Dex inhibits the expression of IL-1β mRNA in U937 cells although IL-1β mRNA was induced with the different stimuli, respectively.

Glucocorticoids have been shown to stimulate the transcription of various genes by mechanisms involving the interaction of the glucocorticoid hormone receptor with glucocorticoid response elements (GRE) (28). Recent evidence demonstrates that glucocorticoids can also negatively regulate specific gene expression (29 - 31). The IL-1β gene has been reported to have a sequence homologous to GRE in intron 5 (32). However two more homologous sequences to the GRE consensus sequence (33,34) can be seen in 5'-flanking region (position -588 to -574) and in exon 6 (position 5344 to 5358). Whether these GRE sequences are involved in the negative regulation of transcription by Dex is presently unknown.

It has been reported that IL-1 induces glucocorticoids and that they inhibit the production of IL-1 in vivo (35). Our data suggest that the block of IL-1 production by glucocorticoids occur at the transcriptional level in vivo.

ACKNOWLEDGEMENTS

We thank Dr.Shunsuke Ishii (The Institute of Physical and Chemical Research) for his helpful discussion. We also thank Dr.Michael M. Seidman (Maryland Research Laboratories, Otsuka Pharmaceutical Co., Ltd.) for critical reading of the manuscript.

REFERENCES

1. Dinarello, C.A. (1987) In Inflammation: Basic Principles and Clinical Correlates (J.I. Gallin, I.M. Goldstein and R. Snyderman, Ed.) pp.195 - 208, Raven Press, New York.
2. Lachman, L.B., Hucker, M.P., and Handschumacher, R.E. (1977) J. Immunol. 119, 2019 - 2023.
3. Kraukauer, T. (1984) Arch. Biochem. Biophys. 234, 371 - 376.
4. Wood, D.D., Bayne, E.K., Goldring, M.B., Gowen, M., Hamerman, D., Humes, J.L., Ihrie, E.J., Lipsky, P.E., and Staruch, M-J. (1985) J. Immunol. 134, 895 - 903.
5. Matsushima, K., Bano, M., Kidwell, W.R., and Oppenheim, J.J. (1985) J. Immunol. 134, 904 - 909.
6. Auron, P.E., Webb, A.C., Rosenwasser, L.J., Mucci, S.F., Rich, A., Wolff, S.M., and Dinarello, C.A. (1984) Proc. Natl. Acad. Sci. USA 81, 7907 - 7911.
7. March, C.J., Mosley, B., Larsen, A., Cerretti, D.P., Braedt, G., Price, V., Gillis, S., Henny, C.S., Kronheim, S.R., Grabstein, K., Conlon, P.J., Hopp, T.P., and Cosman, D. (1985) Nature 315, 641 - 647.
8. Furutani, Y., Notake, M., Yamayoshi, M., Yamagishi, J., Nomura, H., Ohue, M., Furuta, R., Fukui, T., Yamada, M., and Nakamura, S. (1985) Nucl. Acids Res. 13, 5869 - 5882.
9. Nishida, T., Nishino, N., Takano, M., Kawai, K., Bando, K., Masui, Y., Nakai, S., and Hirai, Y. (1987) Biochem. Biophys. Res. Commun. 143, 345 - 352.
10. Hirai,Y., Masui, Y., Nakai, S., Kikumoto, Y., Nishida, T., and Hong, Y-M. (1988) In Gann Monograph on Cancer Research (Y. Hashimoto and T. Hamaoka, Ed.), vol. 34, pp.155 - 166. Japan Scientific Societies Press, Tokyo.
11. Dower, S.K., and Urdal, P.L. (1987) Immunol. Today 8, 46 - 51.
12. Libby, P., Ordovas, J.M., Birinyi, L.K., Auger, K.R., and Dinarello, C.A. (1986) J. Clin. Invest. 78, 1432 - 1438.
13. Warner, S.J.C., Auger, K.R., and Libby, P. (1987) J. Exp. Med. 165, 1316 - 1331.
14. Fenton, M.J., Clark, B.D., Collins, K.L., Webb, A.C., Rich, A.D., and Auron, P.E. (1987) J. Immunol. 138, 3972 - 3979.
15. Snyder, D.S., and Unanue, E.R. (1982) J. Immunol. 129, 1803 - 1805.
16. Sundstrom, C., and Nilsson, K. (1976) Int. J. Cancer 17, 565 - 577.
17. Nilsson, K., Forsbeck, K., Gidlund, M., Sundstrom, G., Toterman, T., Sallstrom, J., and Venge, P. (1981) Hematol. Blood Transfus. 26, 215 - 221.
18. Chirgwin, J.M., Przybyla, A.E., MacDonald, R.J., and Rutter, W.J. (1979) Biochemistry 18, 5294 - 5299.
19. Thomas, P.S. (1980) Proc. Natl. Acad. Sci. USA 77, 5201 - 5205.
20. Greenberg, M.E., and Ziff, E.B. (1984) Nature 311, 433 - 438.
21. Davis, L.G., Dibner, M.D., and Battey, J.F. (1986) Basic Methods in Molecular Biology, pp.147 - 149, Elsevier, New York.
22. Groudine, M., Peretz, M., and Weintraub, H. (1981) Mol. Cell. Biol. 1, 281 - 288.
23. Tyagi, J.S., Hirano, H., Merlino, G.T., and Pastan, I. (1983) J. Biol. Chem. 258, 5787 - 5793.
24. Mitchell, R., Zokas, L., Schreiber, R.D., and Verma, I.M. (1985) Cell 40, 209 - 217.
25. Shaw, G., and Kamen, R. (1986) Cell 46, 659 - 667.

26. Lee, S.W., Tsou, A-P., Chan, H., Thomas, J., Petrie, K., Eugui, E.M., and Allison, A.C. (1988) Proc. Natl. Acad. Sci. USA 85, 1204 - 1208.
27. Knudsen, P.J., Dinarello, C.A., and Strom, T.B. (1987) J. Immunol. 139, 4129 - 4134.
28. Evans, R.M. (1988) Science 240, 889 - 895.
29. Turcott, B., Gueqtin, M., Chevrette, M. and Belanger, L. (1985) Nucl. Acids Res. 13, 2387 - 2398.
30. Nechushtan, H., Benvenisty, N., Brandeis, R., and Reshef, L. (1987) Nucl. Acids Res. 15, 6405 - 6417.
31. Collart, M.A., Belin, D., Vassalli, J-D., and Vassalli, P. (1987) J. Immunol. 139, 949 - 955.
32. Clark, B.D., Collins, K.L., Gandy, M.S., Webb, A.C., and Auron, P.E. (1986) Nucl. Acids Res. 14, 7897 - 7914.
33. Scheidereit, C., Westphal, H.M., Carlson, C., Bosshard, H., and Beato, M. (1986) DNA 5, 383 - 391.
34. Jantzen, H-M., Strahle, U., Gloss, B., Stewart, F., Schmid, W., Boshart, M., Miksicek, R., and Schutz, G. (1987) Cell 49, 29 - 38.
35. Besedovsky, H., Del Rey, A., Sorkin, E., and Dinarello, C.A. (1986) Science 233, 652 - 654.

Vol. 156, No. 1, 1988 BIOCHEMICAL AND BIOPHYSICAL RESEARCH COMMUNICATIONS
October 14, 1988 Pages 275-281

THYROID HORMONE ACTION ON GLUCOSE TRANSPORTER ACTIVITY IN ASTROCYTES

Lois M. Roeder, Irene B. Hopkins, Jeffrey R. Kaiser, Lea Hanukoglu and J. Tyson Tildon

Department of Pediatrics, University of Maryland
School of Medicine, Baltimore, Maryland

Received August 8, 1988

In astrocytes from rat brain cultured in thyroid hormone-deficient media cytochalasin B-binding was decreased 80%; addition of L-T3 increased binding to 75% of control levels. Saponin-treatment of controls increased accessibility of binding sites to 60% above untreated cells. Saponin also increased binding in deficient cells; however, the level was less than in treated controls, suggesting L-T3 deficiency decreases total glucose transporters. Addition of L-T3 appeared to convert most (90%) of the binding sites from unavailable to accessible status. Changes in binding to plasma membranes in response to L-T3 level were similar to those in intact cells. No binding to Golgi was detectable, thus no evidence for translocation of carriers was obtained. L-T3 may activate the glucose transporter by increasing its accessibility in brain cells. © 1988 Academic Press, Inc.

Data from our laboratory showed that primary cultures of rat brain astrocytes maintained in the absence of 3, 5, 3'-triiodo-thyronine (L-T3) exhibited low rates of uptake of 2-deoxyglucose (1). The addition of L-T3 to the deficient cells quickly (in minutes) restored uptake rates to those observed in control cells. The rapidity of the effect indicated that synthesis of new carrier protein would not account for this action of L-T3. Rather, the mechanism may involve translocation of existing glucose transporters to more available sites as proposed for the effect of insulin on adipocytes (2-4) and diaphragm (5,6) and for L-T3 action on thymocytes (7) and cardiac cells (8). Alternatively, L-T3 may activate glucose tranporters residing in the brain cells plasma membrane. To further investigate the mechanism of L-T3 action in brain cells, cytochalasin B binding was used to detect glucose transporters in control, L-T3 deficient, and L-T3 replenished rat brain astrocytes. Since saponin has been shown to increase permeability of plasma membranes (9) and has been used effectively to distinguish plasma membrane-associated from intracellularly-located Ca^{++}-pump mechanisms (10).

0006-291X/88 $1.50
Copyright © 1988 by Academic Press, Inc.
All rights of reproduction in any form reserved.

we employed this agent to aid in delineating the mechanisms of L-T3 action. In addition to intact cells, plasma and Golgi membranes isolated from the astrocytes were also used for these binding studies.

MATERIALS AND METHODS

Cell Cultures and Treatments

Pregnant rats of the Sprague-Dawley strain were obtained from Zivic Miller Laboratories (Allison Park, PA, U.S.A.). They were maintained in a facility accredited by the American Association for the Accreditation of Laboratory Animal Care in strict accordance with USDA regulations and NIH guidelines.

Brains were removed from 1 to 2 day-old pups and astrocytes prepared as previously described (1). The cells were plated in 35 mm dished (9 dished per brain) and incubated at 37°C in an atmosphere of 95% air-5% CO_2, with 90-95% humidity. The culture medium was replaced after 3 days; after an additional 3 days, medium containing 10% fetal calf serum was used and replaced twice weekly thereafter. Thyroid hormone-deficient cells were prepared by changing the medium to one containing thyroid-hormone-free serum prepared by an anion-exchange method (11). Some of the cells grown in L-T3-deficient serum were incubated with 50 uM L-T3 for 10 minutes either prior to cytochalasin B binding measurement or before isolation of the membrane fractions.

Plasma membranes were isolated from these cells as follows: plated cells were washed 3 times with phosphate-buffered saline (PBS) and then TES buffer (10 mM Tris-HCl, 5 mM EDTA, 0.32 M sucrose, pH 7.4) containing 24 m units of Aprotinin per ml was added (1.0 ml per 35 mm dish). Cells were harvested by scraping the dish with a rubber policeman and homogenized for 2 minutes using a motor-driven teflon pestle in an ice-jacketed tube. Nuclei and cell debris were removed by centrifugation at 250 x g for 5 minutes. Plasma membranes were obtained from the resulting supernatant by centrifugation at 13,000 x g for 10 minutes. Golgi membranes were pelleted from the post 13,000 x g supernatant by spinning at 100,000 x g for 30 minutes. The membranes were gently resuspended in 0.32 M sucrose and aliquots of each used to determine cytochalasin B-binding. In some experiments, the plated cells were permeabilized by incubation in the presence of saponin (0.0025%) for 10 minutes at room temperature prior to assay.

Measurements

Glucose binding sites were detected in suspensions of the membrane preparations and in plated cells using the cytochalasin B binding method (2,12). Siliconized glassware and pipet tips were used throughout the procedure. Cytochalasin B (approximately 10^{-4} M was dissolved in 100% ethanol and the molarity determined by absorbance at 210 nm. Various dilutions of this stock solution were mixed with ^3H -cytochalasin B, evaporated to dryness under N_2 and diluted in the appropriate volume of H_2O. Each of these solutions was used to prepare 2 reaction mixtures, one with and one without D-glucose. All other components were prepared in TES buffer (10 mM Tris HCl, 5 mM EDTA and 0.32 M sucrose). The final mixtures contained ^3H -cytochalasin B (concentrations ranged from 1.67 x 10^{-5} mM to 8 x 10^{-4} mM), 2.1 uM cytochalasin E and, either 500 mM D-glucose or TES buffer. All samples were pre-incubated with 2.1 uM cytochalasin E for 10 minutes at 0° to suppress cytochalasin B binding to non-D-glucose inhibitable sites (2).

For plated cells, 1 ml of each reaction mixture (containing the same final concentrations of components as for membrane assays) was added to triplicate samples (35 mm dishes) which were then incubated for 10 minutes at 0°C. The reaction mixture was then removed by suction, and the cells were washed 3 times with PBS. After drying the cells were dissolved in 1.5 ml of 0.1 M NaOH. An aliquot (0.5 ml) was transferred to a scintillation vial, and 1 drop of glacial acetic acid plus 4.5 ml of fluor was added. The radioactivity was determined in a liquid scintillation spectrometer.

When binding was measured using isolated membrane preparations, 500 ul of each suspension was pre-incubated with 40 ul cytochalasin E (final concentration = 2.1 uM) for 10 minutes at 0°C. Two aliquots (250 ul each) were mixed with 200 ul of either D-glucose or TES buffer and then distributed into 4 cellulose propionate tubes (100 ul per tube). The various concentrations of ^{3}H -cytochalasin B (40 ul each) were added and the samples incubated for 30 minutes at 0°C. Samples were centrifuged in a 42.2 Ti rotor in a Beckman model G; plasma membrane samples were spun at 20,000 rpm for 30 minutes and Golgi membrane samples at 42,000 rpm for 2 hours. Two aliquots (50 ul each) of each supernatant were transferred to scintillation vials for determination of free ^{3}H -cytochalasin B. To each aliquot was added 110 ul of a 1:5:5 mixture of 7% acetic acid, H_2O and 0.2 M NaOH plus 50 ul of glacial acetic acid and 4.5 ml of fluor. The remainder of the supernatant was carefully removed by suctioning and discarded. The pellet was dissolved in 50 ul of 0.2 M NaOH with vortexing and incubation in a shaking water bath for 1 hour at 55°C. The entire tube was transferred, with inversion, to a scintillation vial, 60 ul of a 5:1 mixture of H_2O and 7% acetic acid plus 50 ul of glacial acetic acid and 4.5 ml fluor were added. Radioactivity was determined in a liquid scintillation spectrometer.

Protein contents were determined by the method of either Lowry et al. (13) or Smith et al. (14).

RESULTS

Fig. 1 is a typical curve for D-glucose inhibitable, non-cytochalasin E, cytochalasin B-binding with increasing concentrations of the ^{3}H-labelled ligand in rat brain astrocytes. Transformation of the data to a Scatchard plot (INSET) yielded a linear

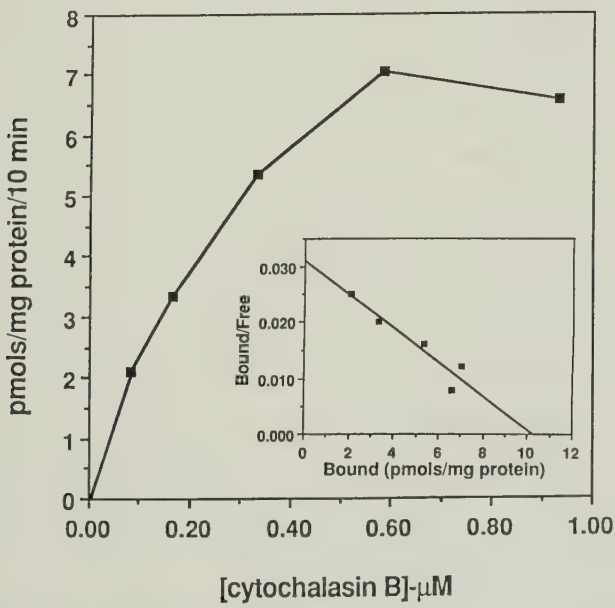

Fig. 1 Cytochalasin B-binding in primary cultures of rat brain astrocytes. Cells plated on 35 mm dishes were pre-incubated with 2.1 uM cytochalasin E for 10 min at 0°C and then incubated in various concentrations of ^{3}H -cytochalasin B (Specific activity approximately 900 DPM per pmol) for 10 min at 0°C. Radioactivity and protein content were determined in separate aliquots of cells from each dish after dissolving in 0.1 M NaOH. Inset shows transformation of the data to a Scatchard plot.

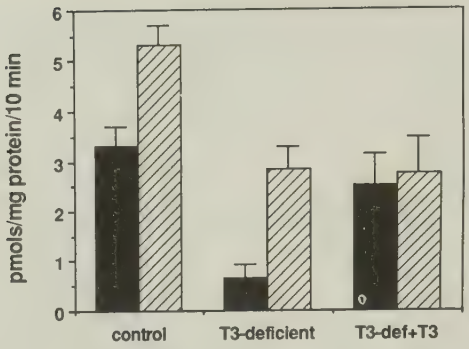

Fig. 2 Effect of L-T3 deficiency and replenishment on cytochalasin B-binding in intact (■) and saponin-treated (▨) rat brain astrocytes. Cells were plated and maintained in medium with complete serum for 7 days. L-T3 deficient cells were prepared by changing the serum in the medium to thyroid hormone-free serum for 6 days. L-T3 (50 uM) was added to the medium of half of the deficient cells for 10 minutes prior to exposure to saponin (0.0025% for 10 min at room temperature). Subsequent determination of cytochalasin B-binding was carried out by incubation in cytochalasin E and ^{3}H -cytochalasin B (0.167 uM) as described in Fig. 1. Vertical bars represent SEM; N = 3 per group.

relationship (r = 0.95) with values for kinetic parameters estimated to be 300 pM for Kd and 9.8 pmol/mg protein for Bmax.

The cytochalasin B-binding assay was carried out in plated control, L-T3 deficient and L-T3 replenished cells using a single concentration of the ligand (0.167 uM); other concentrations of the ligand yielded essentially the same pattern of results . Data were obtained on both untreated and saponin-treated cells. The results are summarized in Fig. 2. In control cultures, exposure to saponin was accompanied by an increase in cytochalasin B-binding of about 60%, suggesting that a large portion of the glucose-binding sites were made more accessible by this treatment. In L-T3-deficient cells, there was a loss (80%) of binding. Saponin treatment increased accessibility of glucose binding sites in L-T3 deficient cells (more than 3-fold). However, the level was less than in saponin-treated controls, suggesting a decrease in total numbers of transporters due to L-T3 deficiency. In the third group of experiments, when L-T3 was added to the cells for 10 minutes prior to the assay, there was an increase in binding and the level achieved was essentially the same after saponin treatment.

In order to determine whether glucose binding sites were associated with Golgi membranes and whether the absence of thyroid hormone in the culture media affected their distribution between plasma and Golgi membranes, cytochalasin-B binding was determined in membranes prepared from control, L-T3 deficient and L-T3 replenished

TABLE 1
Cytochalasin B-Binding to Plasma Membranes and Golgi Preparations
From Rat Brain Astrocytes

Group	N	Plasma Membrane	Golgi
Control	4	2.78 ± 1.10	0
T_3-Deficient	3	0.07 ± 0.07	0
T_3-Deficient + T_3	4	2.10 ± 1.34	0

Cells were prepared as described in the Methods section and for Fig. 2. Cells were harvested and homogenized; the plasma and Golgi membranes were obtained as the 13,000 x g and 100,000 x g pellets from the post 250 x g supernatant and used in a cytochalasin B-binding assay as described under Methods. Results are expressed as mean pmol/mg protein ± SEM.

cells. Table 1 shows that binding to the plasma membrane was markedly reduced in T-3 deficiency and was essentially restored when L-T3 was replaced. However, no net binding in the Golgi membrane preparations was detectable within the limits of this assay.

DISCUSSION

The data obtained using the cytochalasin B-binding assay in cultured rat astrocytes showed saturable binding of the ligand and yielded a single-slope plot when transformed for Scatchard analysis (Fig.1). The application of this technique to cultured cells should be useful for studies on the development and regulation of the glucose transport system in specific cell types that can be grown in vitro and exposed to various potential effectors.

Astrocytes cultured in L-T3 deficient media showed less binding of ^{3}H-cytochalasin B than control cells maintained in complete media. This agrees with the effect of L-T3 deficiency on the uptake of ^{3}H -2-deoxyglucose in these cells previously reported from our laboratory (1). Furthermore, the 10 minute exposure of the deficient cells to L-T3 increased binding to 75% control levels. The previous study (1) showed that the uptake of 2-deoxyglucose was equal to or greater than that of controls when the L-T3 deficient cells were replenished with L-T3 for only 60 seconds. Thus, cytochalasin B-binding was not as completely restored as uptake rates. Similarly, in fat cells of diabetic rats, the insulin-stimulated increase in uptake of 3-0 methylglucose exceeded the increase in number of cytochalasin B binding sites (15). These and other studies may indicate that there are 2 forms of the transporter, of which only 1 is translocated (15, 16). These

workers and others (17) have proposed that the stimulation of glucose transport by insulin in insulin-responsive tissues is a 2-step process involving both recruitment of inactive glucose transporters to the plasma membrane and activation of the carrier itself. Our data on L-T3 action in brain cells are consistent with activation of the glucose transporter by the hormone, and further suggest that translocation of carriers from a sub-cellular site such as Golgi is not involved in this process.

The results comparing the cytochalasin B-binding in intact and saponin-treated cells suggest that a portion of the glucose binding sites on the plasma membrane of astrocytes may be unavailable to, or in some way "protected" from, the substrate. When L-T3 was added to thyroid-homone-deficient cells, there was an increase (greater accessibility) of glucose binding sites. The difference in binding between intact and saponin-treated cells (an estimate of "protected" sites) indicated that L-T3 replenishment had made most of these sites accessible to cytochalasin B. The mechanism involved may be similar to that proposed by Karahasanoglu et al (18) for the increased availability of dopamine beta hydroxylase in the presence of acetylcholine in brain. These workers showed that treatment with a detergent increased the activity of the enzyme to the same level seen after addition of the neurotransmitter.

The initial steps in the interaction of L-T3 with these brain cells are unknown. The binding of L-T3 to its receptor on thymocyte plasma membranes seems to be functionally important to the action of the hormone in increasing 2-deoxyglucose uptake in these cells since mild trypsin-treatment which did not affect basal uptake rates, produced dose-dependent decreases in both L-T3 binding and L-T3 stimulated 2-deoxyglucose uptake (7). Thyroid hormones bind to plasma membranes of cells in several tissues (19), but at present, no data are available to indicate a similar receptor system for L-T3 on the plasma membrane of brain cells.

Information about the glucose transporter and its regulation has been facilitated by the determination of its sequence and structure and the model proposed for its orientation in the plasma membrane by Mueckler et al. (20). The high degree of homology for the glucose transporter protein between species and among tissues (21, 22) suggests that uniqueness of function is regulated by specific effectors that influence recruitment of the carrier molecules and/or their activation. These effectors may be

hormones or intermediates generated in the cascade of events that follow interaction of the hormone with its receptor. On the basis of data from the present study, we propose that, in brain tissue, L-T3 may signal cellular events that promote an increased accessibility of glucose binding sites, perhaps by an activation or shift in the orientation of the glucose transporter in the plasma membrane.

ACKNOWLEDGMENTS: This work was supported in part by NIH Grant HD 16596. We gratefully acknowledge Ms. Bernadette Pasko and Ms. Laura Nasrallah for preparing the typescript and Ms. Dena Yvers for suggestions on the cytochalasin B-binding assay, and we thank Dr. Stephen R. Max for his helpful comments.

REFERENCES

1. Roeder, L.M., Williams, I.B., and Tildon, J.T. (1985) J. Neurochem. 45, 1653-1657.
2. Cushman, S.W. and Wardzala, L.J. (1980) J. Biol. Chem. 255, 4758-4762.
3. Suzuki, K. and Kono, T (1980) Proc. Nat. Acad. Sci. 77, 2542-2545.
4. Gorga, J.C. and Lienhard, G.E. (1984) Fed. Proc. 43, 2237-2241.
5. Wardzala, L.J. and Jeanrenaud, B. (1981) J. Biol. Chem. 256, 7090-7093.
6. Wang, C. (1985) Proc. Nat. Acad. Sci. 82, 3621-3625.
7. Segal, J. and Ingbar, S.H. (1986) Endocrinology 118, 1863-1868.
8. Gordon, A., Schwartz, H., and Gross, J. (1986) Endocrinology 118, 52-57.
9. Seeman, P. (1974) Fed. Proc. 33, 2116-2124.
10. Gill, D.L. and Chueh, S-H. (1985) J. Biol. Chem. 260, 9289-9297.
11. Samuels, H.H., Stanley, F., and Casanova, J. (1979) Endocrinology 105, 80-85.
12. Wardzala, L.J., Cushman, S.W. and Salans, L.B. (1978) J. Biol. Chem. 253, 8002-8005.
13. Lowry, O.H., Rosebrough, N.J., Farr, A.L., and Randall, R.J. (1951) J. Biol. Chem. 193, 265-275.
14. Smith, P.K., Krohn, R.I., Hermanson, G.T., Mollia, A.K., Gartner, F.H., Provenzano, M.D., Fujimoto, E.K., Goeke, N.M., Olson, B.J., and Klenk, D.C. (1985) Anal.Biochem. 150, 76-85.
15. Kahn, B.B. and Cushman, S.W. (1986). Ann. N.Y. Acad. Sci. 488, 356-369.
16. Horuk, E., Matthaei, S., Olefsky, J.M., Baly, D.L., Cushman, S.W. and Simpson, I.A. (1986) J. Biol. Chem. 261, 1823-1828.
17. Houslay, M.D. (1985) IN Molecular Mechanisms of Transmembrane Signalling (P. Cohen and M.D. Houslay, Eds.) p. 279-334. Elsevier, New York.
18. Karahasanoglu, A.M., Edwards, E.H., Tildon, J.T. and Ozand, P.T. (1976) J Neurosci. Res. 2:401-412.
19. Krenning, E.P. and Docter, R. (1986) In: Thyroid Hormone Metabolism (G. Henneman, Ed.) p. 107-131, Marcel Dekker, New York.
20. Mueckler, M., Caruso, C., Baldwin, S.A., Ponico, M., Blench, I., Morris, H.R., Allard, W.J., Lienhard, G.E., and Lodish, H.F. (1985) Science 229, 941-945.
21. Birnbaum, M.J., Haspel, H.C., and Rosen, O.M. (1986) Science 5784-5788.
22. Flier, J.S., Mueckler, M., McCall, A.L., and Lodish, H.F. (1987) J. Clin. Invest. 79, 657-661.

Vol. 156, No. 1, 1988 BIOCHEMICAL AND BIOPHYSICAL RESEARCH COMMUNICATIONS
October 14, 1988 Pages 282-289

PURIFICATION AND CHARACTERIZATION OF A CYTOCHROME P-450 ISOZYME ISOLATED FROM THE LIVER OF RATS PRETREATED WITH CLOFIBRATE

Liliane Kiffel[1], Chantal Célier and Jean-Paul Leroux

INSERM U 75, CHU Necker, 156 rue de Vaugirard,
F-75730 Paris Cedex 15, France

Received August 9, 1988

1- Using a methodology of purification consisting of only one chromatographic step (phenyl-Sepharose) we have purified a cytochrome P-450 isozyme from liver of clofibrate - treated rats. It was called cytochrome P-450 clo. 2- A single polypeptide of mol.wt. 50,000 was visible after sodium dodecyl sulphate polyacrylamide gel electrophoresis. 3- Antiserum raised against the pure enzyme specifically recognized P-450 clo and inhibited more than 90% of the 11- and 12- laurate hydroxylase activities present in clofibrate - treated rats. 4- Clofibrate treatment of the rats resulted in a six fold increase in microsomal cytochrome P-450 clo as judged by immunochemical quantification. This result is in agreement with the increase of laurate hydroxylase activity after treatment by clofibrate. © 1988 Academic Press, Inc.

Several compounds including hypolipidaemic drug clofibrate have been shown in rodents to produce hepatic peroxisome proliferation (1), increases in the enzymes of peroxisomal fatty acid β- oxidation and microsomal cytochrome P-450 dependent hydroxylations (2,3). Lauric acid is hydroxylated at the 11- and 12- positions by microsomes from liver. Preferential induction of 11- hydroxylation by phenobarbital treatment and preferential inhibition by CO, SKF 525 A and metyrapone suggest that different cytochrome P-450 isozymes catalyse the 11- and 12- hydroxylations in the liver (4). Nevertheless, a cytochrome P-450 dependent laurate 12- hydroxylase has been recently isolated from rats given clofibrate by two different groups (5,6). The identity of both these isoenzymes is not yet established. The present paper reports the purification and characterization of a form of cytochrome P-450 from clofibrate - treated rat liver microsomes.

[1] To whom correspondence should be addressed.

0006-291X/88 $1.50
Copyright © 1988 by Academic Press, Inc.
All rights of reproduction in any form reserved.

MATERIALS AND METHODS

Sprague Dawley male rats weighing 180-200g were given clofibrate by an intraperitoneal injection at a dose of 400mg/Kg/day for 4 days. Liver microsomes used for catalytic and immunochemical studies were prepared as previously described (7).

Purification. The first step of the enzyme purification (microsomal preparation, membrane solubilization and ammonium sulphate precipitation) corresponded to the procedure of Knowles and Burchell (8). The ammonium sulphate precipitate was dissolved in a minimal volume of buffer (100mM potassium phosphate, pH 7.4 containing 1mM EDTA, 1mM DTT, 20% glycerol, and 0.05% Lubrol PX) and subjected to phenyl-Sepharose CL-4B chromatography. A linear gradient of 0.05 to 1% of Lubrol was applied to the column. Ten milliliter fractions were collected and an aliquot was checked on SDS-PAGE for homogeneity and assessed by 417nm absorption for cytochrome P-450 content. As a result of this procedure, a fraction of cytochrome P-450 was eluted by 1% Lubrol.

General assays and reconstitution experiments. Cytochrome P-450 content was determined as described by Omura and Sato (9). Protein determination was performed according to Lowry et al. (10) and to Dulley and Grieves for detergent containing fractions (11). Lauric acid hydroxylation and analysis of 11- and 12- hydroxylated products were performed as described by Fan et al. (12) and modified as in (13). Fractions were assayed for laurate 11- and 12-hydroxylase activities after removal of 90% of the non ionic detergent with Bio-Beads SM-2 column (1g beads per mg protein) (14,15). The reconstituted lauric acid hydroxylation assay system contained 0.2 nmol of cytochrome P-450, 0.2 nmol of NADPH - cytochrome P-450 reductase, 0.1mg of dilauroyl phosphatidyl choline, 0.05 mg of sodium cholate and was preincubated for 10 min in presence of substrate before starting the assay (16).

Preparation of polyclonal antibodies. Female New Zealand white rabbits were inoculated subcutaneously with 50µg of antigen mixed 1:1 (v/v) with complete Freund's adjuvant. Two similar booster injections were given every week for 2 weeks. Antisera were collected during the 4th week. IgG were purified using a protein A-Sepharose CL-4B column according to the procedure described by Weatherill et al. (17). The other rat cytochromes P-450 i.e. UT-A, PB-B, BNF-B (the major hepatic cytochromes P-450 from untreated rats, phenobarbital and benzo-β-naphthoflavone - treated rats respectively) and corresponding antisera were kindly provided by Ph. Beaune and J. P. Flinois, and were prepared as previously described (18).

Electrophoresis, immunoblot and Ouchterlony double - diffusion analysis. 10 - 20µg of microsomal proteins or 0.5 - 5 pmol of purified cytochrome P-450 were separated in the discontinuous Laemmli system (19) with a 9% concentration of acrylamide instead of 7.5%. Proteins were either revealed by silver nitrate (20) or transferred to nitrocellulose sheets according to previously described procedures (21-24). Immunoblots were stained with 4-chloro-1-naphthol. (23-24) Ouchterlony double - diffusion analysis (25) were carried out in culture dishes containing 1% agarose in 0.9% Nacl.

Immunoinhibition. Microsomes from control or clofibrate - treated rats were incubated for 20 min at 25° with various amounts of IgG from sera of immunized or non immunized rabbits before starting the reactions. Activities are expressed as percentages of the activity determined without IgG fractions.

RESULTS

Purification of P-450 clo. After hydrophobic affinity chromatography of ammonium sulphate precipitate on a phenyl-Sepharose CL-4B column, a cytochrome P-450 - containing fraction was isolated in fractions eluted with a buffer

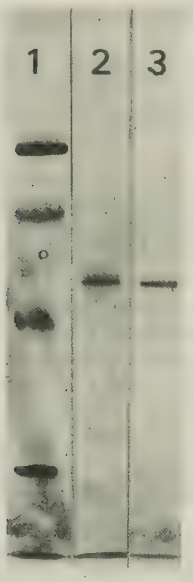

Fig 1. SDS polyacrylamide gel electrophoresis. Migration proceeds from top to bottom. lane 1, LMW calibration Kit proteins from Pharmacia including phosphorylase b (Mr = 94,000), Albumin (Mr = 67,000), ovalbumin (Mr = 43,000), trypsine inhibitor (Mr = 20,000); lane 2 , P-450 clo (5μg) lane 3 , P-450 UT-A (5μg).

containing 1% Lubrol PX. This fraction contained a major polypeptide of monomeric Mr 50kD as judged by Na Dod SO4-polyacrylamide gel electrophoresis (Fig. 1). Fractions containing the protein band of apparent Mr 50 kD were designated as P-450 clo. The overall yield of P-450 clo on the basis of the spectrally determined P-450 present in clofibrate-treated rat liver microsomes was 7.5%. A specific content of 3.0 nmol P-450. mg^{-1} protein was determined by a CO-difference spectrum and Lowry protein determination. Several possibilities may explain this low specific activity, namely loss of prosthetic heme during purification, insufficient reduction of oxidized heme iron (26), over estimation of the protein content by the Lowry procedure (27) or contamination by proteins with the same molecular weight. On the basis of subsequent immunochemical estimations of the level of P-450 clo in clofibrate rat liver microsomes (Table I), P-450 clo was purified about 2.5 fold during this procedure. The absorption maximum in reduced carbon monoxide difference spectra was at 450nm.

TABLE I- CYTOCHROME P-450 clo CONTENT IN CONTROL AND CLOFIBRATE - TREATED RAT MICROSOMES

	Control	Clofibrate treated	fold increase
cytochrome P-450 [a] ($nmol.mg^{-1}$ Protein) n = 6	0.87 ± 0.08	1.60 ± 0.13	1.85
11-hydroxylation [b] ($nmol.min^{-1}.mg^{-1}$ Protein) n = 6	0.43 ± 0.10	1.38 ± 0.29	3.20
12-hydroxylation [b] ($nmol.min^{-1}.mg^{-1}$ Protein) n = 6	0.56 ± 0.17	5.27 ± 1.30	9.40
Cytochrome P-450 clo [c] ($nmol.mg^{-1}$ Protein) (triplicate determination)	0.12	0.75	6.40

[a] spectral determination

[b] enzymatic determination of laurate hydroxylase activity

[c] immunochemical determination

Reconstitution of lauric acid hydroxylase activity. P-450 clo catalyzed the 11- and 12- hydroxylations of lauric acid in a reconstituted system, respectively 0.11nmol and 0.25nmol $.min^{-1}$ per nmol P-450. It is generally acknowledged that microsomal cytochrome P-450 dependent hydroxylations can not be directly compared to in vitro reconstituted activities. Residual detergents, solvent effects and/ or complexities of the interactions between the different components may be involved (28). Because of the low level of activity in the reconstituted system, inhibition studies using the antibody anti-P-450 clo have not been performed.

Electrophoretic and immunochemical characterization. By comparison to known molecular weight standards, the molecular weight of P-450 clo is estimated to be 50kD and is similar in electrophoretic mobility to P-450 UT-A (Fig 1). As judged by Ouchterlony double-diffusion the anti P-450 clo gave a single immunoprecipitation line on reaction with its homologous antigen. In addition, there was no cross-reaction with P-450 UT-A or P-450 PB-B (Fig.2). With the

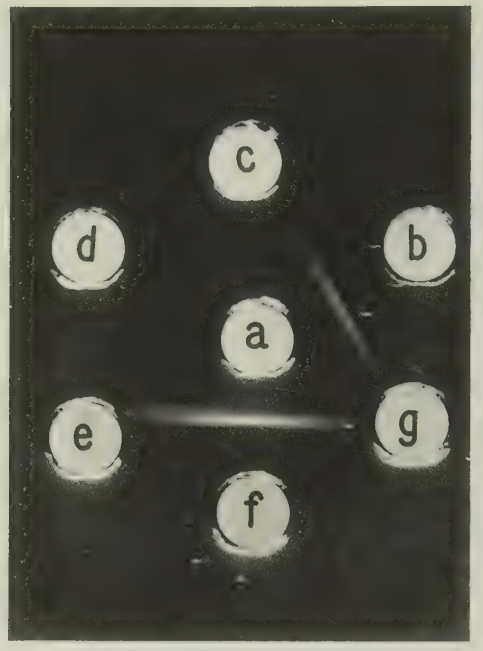

2

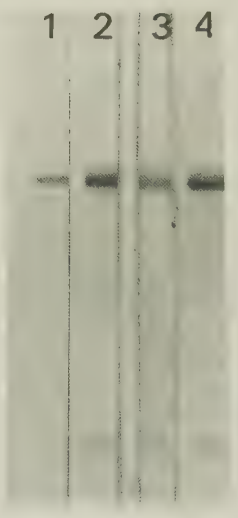

3

Fig 2. Double-immunodiffusion analysis of P-450 clo. a, anti P-450 clo serum (2.5μl); b and f, P-450 clo (40 pmoles); c, P-450 PB-B (40 pmoles); d and g, P-450 UT-A (40 pmoles); e, Epoxide hydrolase (5μg).

Fig 3. Immunnoblot of rat liver microsomal proteins and cytochrome P-450 clo immunoreactive with anti P-450 clo. Lane 1 and 2, 0.75 and 3.75 pmoles of cytochrome P-450 clo; lane 3 and 4, 9 pmoles of rat liver microsomal cytochrome P-450 were loaded (lane 3 untreated rats, lane 4 clofibrate treated rats). the nitrocellulose sheet was incubated with a 1/100 dilution of rabbit antiserum raised to P-450 clo. The bands were densitometered.

Western blotting technique, anti P-450 clo was found to recognize only the homologous antigen but not other cytochrome P-450 isozymes including P-450 UT-A, P-450 PB-B, and P-450 BNF-B confirming the results of Ouchterlony technique. In liver microsomes from untreated or clofibrate - treated rats, anti P-45 clo recognized a single protein band of the same apparent molecular weight as that of purified P-450 clo (Fig. 3). By comparison with a standard curve, the content of P-450 clo was 0.12nmol P-450 per mg protein in untreated rat microsomes and 0.75nmol per mg protein in clofibrate - treated rat microsomes (Table I). The increase observed in P-450 clo content after clofibrate treatment, is in agreement with the raise of total (11 + 12) lauric acid hydroxylase activity (Table I). P-450 clo constitutes respectively about 14% and 47% of the spectrally determined cytochrome P-450 in control and clofibrate - treated rat microsomes (Table I).

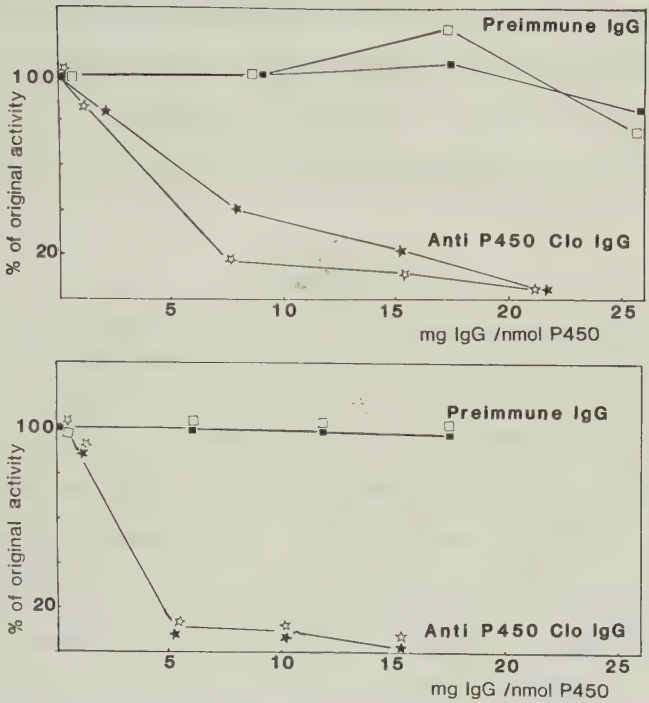

Fig 4. Inhibition of laurate hydroxylation by an antibody raised to cytochrome P-450 clo. Microsomes isolated from control (A) or clofibrate treated (B) rats were incubated with various amounts of anti cytochrome P-450 clo IgG and the enzymatic activity was determined as described in Materials and Methods.
☆---□ 11- hydroxylation and ★---■ 12- hydroxylation

Immunoinhibition of laurate hydroxylase activity. To determine the contribution of P-450 clo to the microsomal laurate hydroxylase activity, an IgG fraction prepared from rabbit antisera raised against P-450 clo was examined for its ability to inhibit the laurate hydroxylase activity catalysed by microsomes prepared from clofibrate -treated rats and untreated rats. Anti P-450 clo inhibited the 11- and 12- laurate hydroxylations in a concentration-dependent manner (Fig.4). In microsomes from clofibrate - treated rats, anti P-450 clo was able to inhibit the 11- and 12- laurate hydroxylations by 90% at a ratio of 5mg IgG per nmol P-450. A residual activity of 35% and 40% for the 11- and 12-hydroxylation respectively was observed at the same ratio in untreated rats microsomes. Rabbits preimmune IgG fractions have no effect on the enzyme activity catalysed by liver microsomes. Thus these immunoinhibition experiments indicated that P-450 clo is responsible for almost all of the

laurate hydroxylase activity in clofibrate - treated rats. However in control rats, the contribution of other cytochrome P-450 isozymes to hydroxylation of lauric acid is more important. Moreover the pattern of the inhibition is similar for 11- and 12- hydroxylations.

DISCUSSION

Using electrophoresis method as the basis for microsomal P-450 purification, we have obtained a form of hepatic cytochrome P-450, designated as P-450 clo, that is involved in the 11- and 12- hydroxylations of lauric acid. This cytochrome P-450 is present in non induced rat liver and its level is markedly elevated after clofibrate administration in agreement with the increase in lauric acid hydoxylase activity. (Table I). Two different groups have recently reported the purification of hepatic cytochrome P-450 isozymes involved in the 11- and 12- hydroxylations of lauric acid and induced by clofibrate treatment (5,6). Using the immunoquantification by Western blotting technique, we determined the amount of P-450 to be 14% of the total cytochrome P-450 population in control rats and 47% in clofibrate - treated rats. These results are similar to those reported by Bains et al. (29) Moreover in agreement with these authors, we have displayed only a single polypeptide band by Western blotting with microsomes from either control or clofibrate treated rats. This pattern is different from that reported by Hardwick et al. (6) who showed the presence of two clofibrate - induced proteins recognized by their antibodies in the liver of control and clofibrate treated rats. On the other hand, Bains et al. (29) and Hardwick et al. (6) reported a differential inhibition in the 11- and 12- hydroxylations of lauric acid. In contrast, our studies showed a similar inhibition for the 11- and 12-hydroxylations, suggesting that anti-cytochrome P-450 clo recognizes either an unique cytochrome P-450 or antigenic sites common to two or more cytochromes P-450 involved in the 11- and 12-hydroxylations of lauric acid. In conclusion, on the basis of the immunochemical characteristics of cytochrome P-450 clo, we believe that it is probably different from the previously isolated forms (5,6). However the final evidence

of difference or similarity should be brought by the protein sequence determination.

ACKNOWLEDGMENT: We thank Michèle TAIEB for typing the manuscript.

REFERENCES

1. Hess, R., Staubli, W. and Reiss, W. (1965) Nature Lond. 208, 856-858.
2. Lazarow, P.B. and De Duve, C. (1976) Proc. Natl. Acad. Sci. USA 73, 2043-2046.
3. Orton, T.C. and Parker, G.L. (1982) Drug. Metab. Dispos. 10, 110-115.
4. Okita, R.T. and Masters, B.S.S. (1980) Drug. Metab. Dispos. 8, 147-151.
5. Tamburini, P.P., Masson, H.A., Bains, S.K., Makowski, R.J., Morris, B and Gibson, G.G. (1984) Eur. J. Biochem. 139, 235-246.
6. Hardwick, J.P., Song, B.J., Huberman, E. and Gonzalez, F.J. (1987) J. Biol. Chem. 262, 801-810.
7. Cresteil, T., Flinois, J.P., Pfister, A. and Leroux, J.P. (1979) Biochem. Pharmacol. 28, 2057-2063.
8. Knowles, R.G. and Burchell, B. (1977) Biochem. J. 163, 381-383.
9. Omura, T. and Sato, R. (1964) J. Biol. Chem. 239, 2370-2378.
10. Lowry, O.H., Rosenbrough, N.J., Farr, A.L. and Randall, R.J. (1951) J. Biol. Chem. 193, 265-275.
11. Dulley, J.R. and Grieves, P.A. (1975) Anal. Biochem. 64, 136-141.
12. Fan, L. F. and Masters, B.S.S. (1976) Anal. Biochem. 71, 265-272.
13. Cresteil, T., Beaune, P., Célier, C., Leroux, J.P., Guengerich, F.P. (1986) Pharmacol. Exp. Ther. 236, 269-276.
14. Holloway, P.W. (1973) Anal. Biochem. 53, 304-308.
15. Magdalou, J., Kiffel, L., Balland, M., Thirion, C., Le Meste, M. and Siest, G. (1982) Chem. Biol. Interactions 39, 245-256.
16. Okita, R.T., Parkhill, I.K., Yasukochi, Y., Masters, B.S.S., Theoharides, A.D., Kupfer, D. (1981) J. Biol. Chem. 256, 5961-5964.
17. Weatherill, P.J., Kennedy, S.M.E. and Burchell, B. (1980) Biochem. J. 191, 155-163.
18. Le Provost, E., Flinois, J.P., Beaune, P. and Leroux, J.P. (1981) Biochem. Biophys. Res. Commun. 101, 547-554.
19. Laemmli, U.K. (1970). Nature 227, 680-685.
20. Wray, W., Boulikas, T., Wray, V.P. and Hancock, R. (1981) Anal. Biochem. 118, 197-203.
21. Towbin, H.T., Staehelin, I. and Gordon, J.(1979) Proc. Natl. Acad. Sci. USA 76, 4350-4354.
22. Guengerich, F.P., Wang, P.P. and Davidson, N.K. (1982) Biochemistry 21, 1698-1706.
23. Wang, P.P., Beaune, P., Kaminsky, L.S., Dannan, G.A., Kadlubar, F.F., Larrey, D. and Guengerich, F.P. (1983) Biochemistry 22, 5375-5382.
24. Beaune, P., Flinois, J.P., Kiffel, L., Kremers, P. and Leroux, J.P. (1985) Biochem. Biophys. Acta 840, 364-370.
25. Ouchterlony, O. (1949) Ark-kemi 1, 43-54.
26. Philpot, R.M. (1974) Chem. Biol. Interactions 9, 169-180.
27. Distlerath, K.M., Reilly, P.E.B., Martin, M.V., Davis, G.G., Wilkinson, G.R. and Guengerich, F.P. (1985) J. Biol. Chem. 260, 9057-9067.
28. Backes, W.L. and Canady, W.J. (1980) in "Hepatic cytochrome P-450 monooxygenase system" (Shenkmann, J.B. and Kupfer, D., eds), Pergamon Press, Oxford.
29. Bains, S.K., Gardiner, S.M., Mannweiler, K., Gillette, D. and Gibson, G.G (1985) Biochem. Pharmacol. 34, 3221-3329.

Vol. 156, No. 1, 1988 BIOCHEMICAL AND BIOPHYSICAL RESEARCH COMMUNICATIONS
October 14, 1988 Pages 290-296

AN INSULIN MEDIATOR PREPARATION SERVES TO STIMULATE THE CYCLIC GMP ACTIVATED CYCLIC AMP PHOSPHODIESTERASE RATHER THAN OTHER PURIFIED INSULIN-ACTIVATED CYCLIC AMP PHOSPHODIESTERASES

Nigel J. Pyne & Miles D. Houslay

Molecular Pharmacology Group, Department of Biochemistry, University of Glasgow, GLASGOW G12 8QQ, Scotland, U.K.

Received September 6, 1988

SUMMARY An insulin mediator preparation was obtained from rat hepatocytes which had been treated with insulin. This preparation inhibited adenylate cyclase activity. It stimulated the activity of homogeneous preparations of both the cytosolic and membrane-bound forms of rat liver cyclic GMP-activated cyclic AMP phosphodiesterase. It failed to activate homogeneous preparations of both the peripheral plasma membrane and 'dense-vesicle' cyclic AMP phosphodiesterases. The insulin mediator preparation stimulated cyclic GMP-activated cyclic AMP phosphodiesterase activity in a dose-dependent fashion with a hill coefficient of 0.46. Insulin caused the dose-dependent production of mediator activity in intact hepatocytes with a K_a of 9 pM, although concentrations of insulin greater than 10 nM progressively reduced stimulatory activity.
© 1988 Academic Press, Inc.

INTRODUCTION. It is well-established that the purified insulin receptor exhibits a functional tyrosine kinase activity and there is compelling evidence to suggest that this plays a pivotal role in the signal transduction mechanism (1-3). However, there is, as yet, no clear indication as to the nature and function of the physiological substrates for this activity other than the insulin receptor itself. Furthermore, no well-defined sequence of events appear to connect this function of the receptor with biochemical changes within the cell. For some time now a number of laboratories (see e.g 4-6) have provided tantalizing evidence which suggests that insulin may act on target cells to release soluble 'second messengers' or 'mediators' within the cell. These have yet to be fully characterized, although recent evidence suggests that such species may include inositol glycans, perhaps with associated peptide material, and also particular forms of diacyl glycerol (7-9). Such species have been suggested to be capable of activating pyruvate dehydrogenase activity , inhibiting cyclic AMP-dependent protein kinase inhibiting adenylate cyclase activity and activating cyclic AMP phosphodiesterase activity (see 10).

In hepatocytes, insulin antagonizes the ability of glucagon to increase cyclic AMP production (11). At subnanomolar glucagon concentrations this effect is achieved by both

0006-291X/88 $1.50
Copyright © 1988 by Academic Press, Inc.
All rights of reproduction in any form reserved.

inhibiting adenylate cyclase activity and by activating cyclic AMP phosphodiesterase activity (12,13). However, at nanomolar concentrations and above, the predominant effect of insulin is to increase cyclic AMP phosphodiesterase activity (11). We (11,12) have shown that in hepatocytes insulin can elicit the stable activation of two membrane-bound cyclic AMP phosphodiesterases. In one instance at least this effect seems to be carried out by insulin eliciting the phosphorylation of the enzyme (11). However, by selectively preventing insulin activating these two enzymes we have been able to show that insulin's activation of these two enzymes cannot account in full for the ability of insulin to decrease intracellular cyclic AMP concentrations (14). Thus insulin must activate at least one other cyclic AMP phosphodiesterase which can exert a major effect in lowering intracellular cyclic AMP concentrations. Hepatocytes, which have been pre-treated with insulin, yield subcellular fractions which show evidence of activation of only the two previously described enzymes. This suggests that the additional enzyme(s) must be activated by a rapidly reversible process. We have purified to homogeneity both cytosolic and membrane bound forms of the other major cyclic AMP metabolizing phosphodiesterase in hepatocytes, the so-called cyclic GMP-activated cyclic AMP phosphodiesterase (15). This particular enzyme is characterise by the unique ability of low (μM) concentrations of cyclic GMP which serve to stimulate the cyclic AMP hydrolysis effected by this enzyme. Here we show that this enzyme, and not the other insulin-regulated phosphodiesterases, is activated by a soluble 'mediator' preparation.

MATERIALS AND METHODS. All biochemicals, including insulin (porcine) were from either Sigma (Poole, UK) or from Boehringer (Lewes, UK); general chemicals were of AR grade or higher (BDH, UK) and radiochemicals were from Amersham International (Amersham, UK). The 'dense-vesicle' (16,17) and peripheral plasma membrane (17) cyclic AMP phosphodiesterases and the cytosolic and membrane bound forms of the cyclic GMP-activated cyclic AMP phosphodiesterase (15) were purified to apparent homogeneity as described in detail before by us. Assay of cyclic AMP phosphodiesterase activity was performed as before (15-17) and initial rates were taken from linear time-courses. Assays were done in a total volume of 100μl and, unless specified otherwise, at 1μM cyclic AMP substrate. Adenylate cyclase assays were carried out for 10min. at 30°C in a total volume of 100μl as described before by us (13). A mediator preparation was obtained essentially as described by Larner et al. (4). Briefly this involved the preparation and pre-incubation of intact hepatocytes, as done before by us (13). Five flasks, each containing 5ml. of Krebs-Hensleit buffer and 5-6 mg. dry weight of cells were incubated for 10min. at 37°C in either the presence or absence of insulin. At the end of this time 5ml. of 'stopping' buffer (0.25M-sucrose, 1mM-EDTA, 10mM-tris HCl final pH7.4) was added to each flask and the cells were harvested by centrifugation at 4°C at 500rpm for 2min. in an MSE Minor centrifuge. The resultant pellets were each resuspended in 5ml. of 'stopping' buffer prior to centrifugation as above. This washing procedure was repeated one further time. The final pellets were pooled and resuspended in 1ml of 'stopping' buffer. 2ml. of 'extraction' solution at 100°C (0.1mM-EDTA, 0.1mM-cysteine, 50mM-formic acid final pH3.5) was added to the resuspended pellets and samples kept at this temperature for 4min. prior to cooling and centrifugation at 14,000g_{av} for 10min. to yield a supernatant fraction (S1). This fraction was treated with activated charcoal (5mg/ml), vortexed for 2min and centrifuged again. The resultant supernatant (S2) was lyophilized and then resuspended in 0.5ml of sample buffer (0.1mM-2-mercaptoethanol, 0.1mM-EDTA, 50mM-formic acid, final

pH3.5). This material was applied, at a flow rate of 0.3ml/min to a 25x1.5 column of Sephadex G25 which had been equilibriated in sample buffer. Fractions (1ml) were collected and immediately lyophilized prior to resuspension in 20µl of 20mM-tris-HCl buffer final pH7.4. Routinely 4/5 fractions were obtained which activated the cyclic GMP-activated cyclic AMP phosphodiesterase. These were pooled to give 80-100µl per preparation and it is with respect to this volume that 'activity' of the mediator is expressed. Comparable fractions from the column were taken for examining 'basal' effects. For chloroform treatment, 20µl fractions were vortexed for 15min with 20µl chloroform. Phases were separated by centrifugation, lyophilized and resuspended in 20mM-tris-HCl buffer final pH7.4.

RESULTS AND DISCUSSION. Mediator preparations were extracted from hepatocytes which had been pre-treated with insulin (10nM) for 10min. at 37°C. Extracts were also made from untreated cells to provide control extracts. The method of extraction and partial purification employed was essentially the same as that described by Larner et al. (4,18). These investigators showed that such a 'mediator' preparation could inhibit adenylate cyclase activity. We confirm this here as the addition of 10µl of such a mediator preparation to adenylate cyclase assays (100µl) gave rise to a 21.6-34.0% (range, n=6) inhibition of the glucagon (10nM) plus GTP (0.1mM) stimulated activity.

The addition of either such a 'mediator' preparation or control extracts, to assays containing either the 'dense-vesicle' or peripheral plasma membrane cyclic AMP phosphodiesterases elicited no change in their activities (<7%) when assayed over a range of mediator concentrations(1-10µl/100µl assay volume) and over a range of substrate concentrations (0.1-1.0µM cyclic AMP). In contrast this 'mediator' preparation elicited a profound activation of both the soluble and membrane-bound forms of cyclic GMP activated cyclic AMP phosphodiesterase (table 1). These two enzymes are almost identical and appear to differ only in the expression of a what is presumed to be a small hydrophobic region which serves to anchor this enzyme to the plasma membrane

Table 1. Selective stimulation of the cyclic GMP activated cyclic AMP phosphodiesterase by insulin 'mediator'

cell treatment	cG-act-sol. PDE	cG-act-membr PDE	'dense-vesicle' PDE	PPM PDE
none	35±5	28±6	3±5	3±6
insulin (10nM)	114±10	173±12	-4±4	5±8
glucagon (10nM)	30±7	25±8	-2±6	3±4
insulin + glucagon	109±12	177±14	1±3	-2±6

Intact hepatocytes were incubated for 10 min. in the presence or absence of the above ligands prior to a mediator fraction being prepared. A portion (10µl) of this fraction was added to assays (100µl)containing the specific phosphodiesterases (PDE) in the presence of 1µM cyclic AMP as substrate. PPM-peripheral plasma membrane. The cytosolic (sol) and membrane (membr) forms of the cyclic GMP activated cyclic AMP phosphodiesterase were used here. Activities are expressed as a percentage increase of the control activity. Errors are S.D., n=4.

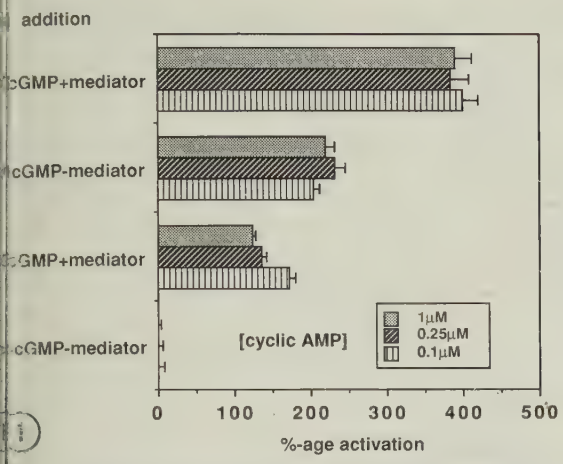

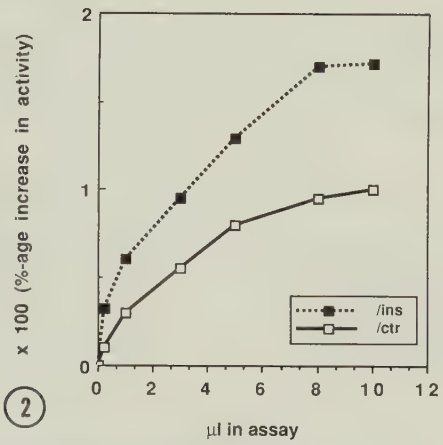

Figure 1. Stimulation of the cyclic GMP activated cyclic AMP phosphodiesterase by mediator fractions occurs in both the presence and absence of cyclic GMP. Cyclic GMP activated cyclic AMP phosphodiesterase was assayed using the indicated concentrations of cyclic AMP as substrate. In some instances mediator (10μl/100μl assay) and maximally stimulating (unlabelled) cyclic GMP (2.5μM) were added to these assays. The %-age increase in activity elicited by these compounds is shown compared to enzyme activity monitored in the absence of either ligand. Errors are S.D., n=4).

Figure 2. Alteration in mediator concentration on cyclic GMP activated cyclic AMP phosphodiesterase activity. Data showing the effect of increasing concentration of 'mediator' extracts on enzyme activity. This is done for 'mediator' produced in response to insulin (10nM) treatment of hepatocytes and also for extracts from control incubations done in the absence of insulin. The 'concentration' indicated is that volume (μl) of extract added to phosphodiesterase assays (100μl) done with 1μM cyclic AMP as substrate. The data is shown for a typical experiment (see text for analysis).

(15). Further studies focussed on the soluble enzyme where we noted that in the absence of cyclic GMP then stimulation by the mediator preparation was somewhat larger at low substrate concentrations (fig 1). In the presence of maximally activating concentrations of cyclic GMP (2.5μM) then mediator preparation yield further activation which appeared to be additive to that elicited by cyclic GMP (fig 1). This indicates that the 'mediator' was not cyclic GMP, which indeed we could show to be completely removed by the charcoal absorption step of the purification. Activation, by the 'mediator' preparation in the presence of cyclic GMP was of a similar magnitude over the range of substrate concentrations examined (0.1-1.0μM cyclic AMP).

Increasing amounts of mediator preparation in the enzyme assay increased activity in an apparently saturatable fashion which was reversible upon dilution (fig. 2). Hill plot analysis of this process showed that control extracts stimulated the enzyme with an EC_{50} of 0.24±0.04 μl/100μl assay whilst observing Michaelis kinetics yielding a Hill coefficient of 1.07±0.05. In contrast, the insulin-stimulated 'mediator' fraction exhibited a Hill coefficient of 0.72±0.06 and an EC_{50} of 0.29±0.05 μl/100μl assay. A hill coefficient of less than unity could indicate either heterogeneity of binding sites or apparent negative co-operativity. In this regard it is of note that

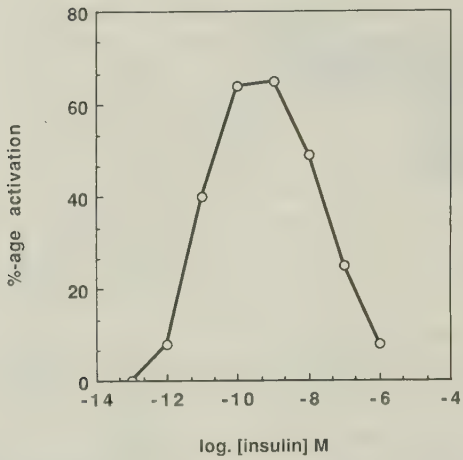

Figure 3. Insulin causes a dose-dependent effect on 'mediator' production. A dose-effect curve for treatment of hepatocytes with increasing concentrations of insulin. Activation has been corrected for 'basal' stimulatory effects and shows the percentage increase in cyclic GMP activated cyclic AMP phosphodiesterase activity. In this experiment material was used which had not been subjected to gel filtration. The data is shown for a typical experiment (see text for analysis).

substrate and activator regulation of this enzyme does not obey Michaelis kinetics (15), indicating that it is subject to complex multisite regulation. In any event, such observations show that the basal activating substance(s) is distinct from the insulin elicited 'mediator'. Indeed, this is all too apparent from data showing (fig. 2) that at 10µl of extract /100µl assay activation by the basal activating substance(s) has been saturated yet it is still possible to elicit further activation using extracts from insulin-treated cells. Analysis of the net stimulatory effect of insulin then yields an EC_{50} of 0.19±0.06 µl/100µl assay and a Hill coefficient of 0.46±0.07.

Production of mediator by the intact hepatocytes was dose-dependent upon insulin, with an apparent K_a of 0.9 x 10^{-11}M (fig. 3). However, stimulatory activity was progressively reduced when hepatocytes were challenged with concentrations of insulin greater than 10^{-9}M. Such an observation has been noted before with a variety of other mediator controlled systems (6) including the cyclic AMP phosphodiesterase activity of adipocyte membranes (7) and is evident when insulin inhibits adenylate cyclase activity in broken membrane preparations (13).

The mediator activity which stimulated the cyclic GMP activated cyclic AMP phosphodiesterase chromatographed as a single peak of activity on Sephadex G25 with an apparent M_r in the range of 1000-2000. This result is similar to that reported by others (18) using adenylate cyclase inhibition to follow mediator activity. We noted that this mediator preparation was essentially hydrophilic in character and was not extracted into chloroform. Analysis of the mediator by isoelectric focussing indicated that the isoelectric point (P_I) was in the range 6.4-6.6 and showed that the mediator activity did not co-chromatograph with the bulk of the ninhydrin reacting material in the extract, which was more acidic. The nature of the biologically active

substances in the mediator fraction has not been identified. However, our previous studies (15) on the cyclic GMP activated cyclic AMP phosphodiesterase showed that its activity was not affected by inositol trisphosphate, inositol bisphosphate and fructose 2,6-bisphosphate. Furthermore, the polyamines spermine, spermidine and putrescine, which have been suggested might mediate certain of insulin's actions (see 1), cause inhibition of both forms of this enzyme (15).

It has been demonstrated (6,7) that mediator/inositol glycan preparations could activate cyclic AMP phosphodiesterase activity in crude membrane preparations but were unable to exert any effect on a phosphodiesterase activity purified from such membranes (19). However, it appears that the enzyme isolated by these investigators was akin to the 'dense-vesicle' enzyme from hepatocytes which is activated in a stable fashion by insulin and not one which is reversed by dilution (see 10, 20 for discussion). Thus failure to observe any effect of a mediator on this species would be in accord with the observations made here. As adipocyte membrane preparations contain cyclic GMP activated cyclic AMP phosphodiesterase activity (20), such an enzyme may have provided the target for activation by the insulin produced mediator.

We also noted that treatment of hepatocytes with glucagon failed to elicit the production of mediator activity (table 1), indicating a specificity for insulin. This is of importance for two reasons, firstly because it clearly shows a difference with the 'dense vesicle' enzyme which can be activated by both insulin and glucagon (12), albeit by distinct mechanisms (21). Secondly, it was clear from our earlier studies that insulin must be capable of activating a cyclic AMP phosphodiesterase which is distinct from both the 'dense vesicle' and peripheral plasma membrane forms (14). The properties of such a enzyme demanded that it be capable of being activated by insulin in the presence of glucagon. Clearly, stimulation of the cyclic GMP activated cyclic AMP phosphodiesterase by the mediator preparation satisfies such criteria and indicates that this may be the prime route through which insulin decreases intracellular cyclic AMP concentrations in hepatocytes.

ACKNOWLEDGEMENTS

We thank the Medical Research Council and the California Metabolic Research Foundation for financial support.

REFERENCES

1. Denton, R.M. (1986) Adv. Cyclic Nucl. Prot. Phosph. Res. 20, 295-341.
2. Kahn, C.R. (1985) Ann. Rev. Med. 36, 429-451.
3. Houslay, M.D. (1985) Mol. Asp. Cellul. Reg. 4, 279-333.
4. Larner, J., Galasko, G., Cheng, K., DePaoli-Roach, A.A., Huang, L., Daggy, P. & Kellog, J.(1979) Science, 206, 1408-1410.
5. Kiechle, F.L., Jarett, L., Kotagal, N. & Popp, D.A. (1981) J.Biol.Chem. 256, 2945-2951.
6. Saltiel, A., Siegel, M.I., Jacobs, S. & Cuatrecasas, P. (1982) Proc. Natl. Acad. Sci. USA 79, 3513-3517
7. Saltiel, A.R. & Cuatrecasas, P. (1986) Proc. Natl. Acad. Sci. USA 83, 5793-5797.

8. Saltiel, A.R., Fox, J.A., Sherline, P. & Cuatrecasas, P. (1986) Science 233, 967-972
9. Kelly, K.L., Merida, I., Wong, E.H.A., DiCenzo, D. & Mato, J.M. (1987) J.Biol.Chem. 262, 15285-15290.
10. Houslay, M.D., Wakelam, M.J.O. & Pyne, N.J. (1986) Trends Biochem. Sci. 11, 393-394.
11. Houslay, M.D. (1986) Biochem. Soc. Trans. 14, 183-193.
12. Heyworth, C.M., Wallace, A.V. & Houslay, M.D. (1983) Biochem. J. 214, 99-110.
13. Heyworth, C.M. & Houslay, M.D. (1983) Biochem. J. 214, 547-552.
14 Heyworth, C.M., Wallace, A.V., Wilson, S.R. & Houslay, M.D. (1983) Biochem. J. 222, 183-187.
15 Pyne, N.J., Cooper, M.E. & Houslay, M.D.(1986) Biochem. J. 234, 325-334.
16. Pyne, N.J., Cooper, M.E. & Houslay, M.D. (1987) Biochem. J. 242, 33-42.
17. Houslay, M.D., Pyne, N.J. & Cooper, M.E. (1988) Methods in Enzymol. 159, 751-760.
18. Malchoff, C.D., Huang, L., Gillespie, N., Palsai, C.V., Schwartz, C.F.W., Cheng, K., Hewlett, E.L. & Larner, J. (1987) Endocrinology 120, 1327-1337.
19. Saltiel, A.R. & Steigerwalt, R.W. (1986) Diabetes 35, 698-704.
20. Pyne, N.J.,, Anderson, N., Lavan, B.E., Milligan, G., Nimmo, H.G. & Houslay, M.D. (1987) Biochem. J. 248, 897-901.
21. Wilson, S.R., Wallace, A.V. & Houslay, M.D. (1983) Biochem. J. 216, 245-248.

Vol. 156, No. 1, 1988 BIOCHEMICAL AND BIOPHYSICAL RESEARCH COMMUNICATIONS
October 14, 1988 Pages 297-303

HIV-1 PROTEASE SPECIFICITY OF PEPTIDE CLEAVAGE IS SUFFICIENT FOR PROCESSING OF GAG AND POL POLYPROTEINS

Paul L. Darke[†]*, Ruth F. Nutt**, Stephen F. Brady**, Victor M. Garsky**, Terrence M. Ciccarone**, Chih-Tai Leu*, Patricia K. Lumma**, Roger M. Freidinger**, Daniel F. Veber** and Irving S. Sigal*

Departments of Molecular Biology* and Medicinal Chemistry**
Merck Sharp and Dohme Research Laboratories
West Point, Pennsylvania 19486

Received July 18, 1988

The mature proteins of retroviruses originate as a result of proteolytic cleavages of polyprotein precursors. Retroviruses encode proteases responsible for several of these processing events, making them potential antiviral drug targets. A 99-amino acid HIV-1 protease, produced by chemical synthesis or by expression in bacteria, is shown here to hydrolyze peptides corresponding to all of the known cleavage sites in the HIV-1 gag and pol polyproteins. It does not hydrolyze peptides corresponding to an env cleavage site or a distantly related retroviral gag cleavage site. © 1988 Academic Press, Inc.

Retroviral proteins are initially translated in the form of large precursor fusions, gag, pol and env that are proteolytically processed to give the viral structural proteins and the virally encoded enzymes (1). Homologous virally encoded proteases have been partially characterized for several retroviruses (2-5) and similar proteases have been inferred from the DNA sequence of known retroviruses (6,7). Although the identities of the cleavages produced by these proteases have not been fully determined, in the case of murine leukemia virus a deletion of the protease gene resulted in unprocessed gag proteins and the loss of viral infectivity (8).

The genome organization for HIV-1 is shown in Fig. 1 with the genes encoding the 3 major viral precursor proteins outlined. The sites for in

[†] To whom correspondence should be addressed.

0006-291X/88 $1.50
Copyright © 1988 by Academic Press, Inc.
All rights of reproduction in any form reserved.

vivo processing of the precursors to give the mature gag p17 (MA), p24 (CA), p7(NC) and p6, the reverse transcriptase, the integrase and the 2 envelope proteins gp41 and gp120 are known from amino acid sequencing of the polypeptides found in the HIV particles and are designated in Fig. 1 as I-IX (9-13). From the literature of retroviral cleavage site specificities (14), the mature HIV-1 protease would be expected to result from cleavages at positions V and VI in Fig. 1 (pol 69-167, numbering according to ref. 15). A protein having the expected N-terminus has been observed to be produced during E. coli expression of portions of the pol gene product (16). We have found that a polypeptide having the sequence pol 69-167 made by expression in E. coli cells (17, 18) or by chemical synthesis (19) has the ability to cleave HIV-1 gag p55 to give the gag p24 and p17 products. In this report we describe the ability of this protease to cleave peptides having sequences that correspond to the known in vivo cleavages of the virus. To ensure that the activities are intrinsic to the HIV-1 protease, we have used the chemically synthesized protease for all of the data reported, although the same specificity was observed for the microbially expressed enzyme. The 99 amino acid HIV-1 protease hydrolyzes peptides with a substrate specificity diverse enough to account for all of the known cleavage sites for the HIV-1 gag and pol precursors, but specific enough so as not to result in cleavage of the env precursor nor a gag precursor from the distantly related avian myeloblastosis virus (AMV).

MATERIALS AND METHODS

HIV Protease. The protease was synthesized by solid phase methods, purified and folded into the active form as described in ref. 19. HIV-1 protease was also purified from an E. coli (18) expression system. Both protease preparations were in 50 mM NaOAc, pH 5.5, 10% glycerol, 1 mM EDTA and 1 mM DTT prior to assay.

Peptide Hydrolysis assays. Synthetic peptides were purified by reverse phase HPLC and hydrolyzed by the protease (0.2 μg) at various concentrations in 50 mM Na acetate, pH 5.5. The reactions (40 μl) were initiated by addition of 5 μl protease and quenched after 30 min at 30°C with 160 μL 12% acetic acid. Peptides were separated on either a 15 cm or a 5.0 cm reverse phase C-18 column with linear gradients of water to acetonitrile (both 0.1% in trifluoroacetic acid), detected by absorbance at 220 nm and the peak areas integrated. In the case of peptides GAG 124-138, GAG 128-135, POL 59-72 and POL 162-174, synthetic product standards were independently

synthesized and shown to comigrate with the products observed. For peptides listed in Table II, large scale reactions were performed to greater than 33% hydrolysis and the resulting mixture subjected to gas phase sequencing to identify the cleavage sites (20). For each of the peptides SQNYPIV and SQNYPIVQ, there were 2 products of the enzyme reaction, one of which had the same retention time on HPLC and a UV absorption characteristic of tyrosine. In the case of SQNYPIV, the second product was shown to comigrate with synthetic PIV, thus the identity of the second product for SQNYPIVQ was assumed to be PIVQ.

Kinetic parameters were determined from assays performed in duplicate at 7 different concentrations of peptide. At least 2 but no more than 3 of the concentrations employed were above the Km values reported. The extent of loss of substrate was in no case greater than 7%. The extinction coefficient for a product on HPLC was either determined by comparison with a known quantity of synthetic product standard, or by preparing a reaction mixture in which more than half of the substrate was hydrolyzed. The quantity of the 2 products appearing in that mixture was calculated from the loss of substrate.

RESULTS AND DISCUSSION

Initial studies of peptide hydrolysis activity by the synthetic protease were conducted with a substrate peptide (gag 124-138, HSSQVSQNYPIVQNI) representing the cleavage site between p17 and p24 (I in Fig. 1). Following incubation of the peptide with the protease, HPLC analysis of the reaction mixture revealed two novel peaks which comigrated with the anticipated products, HSSQVSQNY and PIVQNI (Fig. 2). Gas phase sequencing (20) of the reaction mixture confirmed the generation of the predicted (10) PIVQNI sequence.

The minimal substrate recognition site for the HIV-1 protease was explored by synthesizing a series of consecutively smaller peptides having sequences that span cleavage site I (Table 1). The rates of cleavage reactions listed in Table 1 are relative to that observed for the 15 residue substrate, with all peptides tested at 1 mM. Only a 10% reduction in rate

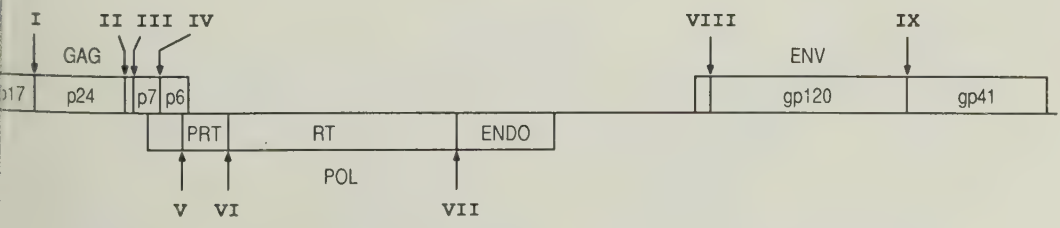

Figure 1. The major open reading frames of HIV-1. Numbered arrows indicate proteolytic processing sites within the polyprotein products.

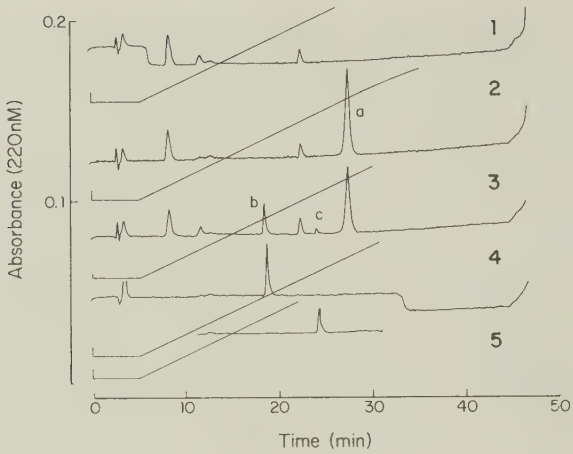

Figure 2. HPLC elution profile for the hydrolysis of a peptide by the synthetic HIV-1 protease. Tracing 1 represents a sample of protease in a reaction solution, in the absence of substrate. Tracing 2 represents GAG 124-138 (peak a) in the absence of enzyme. In tracing 3, the peak area of the substrate is decreased following treatment with the protease, and 2 new peaks (b and c) appear that have mobilities identical to those of the predicted products, GAG 124-132 (tracing 4) and 133-138 (tracing 5). Additional small peaks are due to components of the buffer in the protease preparation.

was observed when the 7 residue peptide corresponding to gag 129-135 (SQNYPIV) was used as a substrate. Removal of residues from either end of this minimal substrate resulted in the elimination of detectable activity. Peptides in which the serine of the 7 amino acid substrate was replaced with an acetyl group or the seryl-glutamine dipeptide with pyroglutamic acid were also not substrates. The Km for the hydrolysis of VSQNYPIV was determined to be 2.5 mM with a Vmax of 275 nmol/min/mg.

Having observed that the 99 amino acid HIV-1 protease had the ability to cleave a peptide of the sequence corresponding to the known cleavage site

Table 1. Length dependence of Hydrolysis Rates for Gag p17/p24 Peptide Substrates

Sequence	Relative Rate of Hydrolysis
HSSQVSQNY-PIVQNI	1.0
VSQNY-PIV	1.0
SQNY-PIVQ	0.95
SQNY-PIV	0.90
SQNY-PI	<0.05
QNY-PIV	<0.10
Acetyl-QNY-PIV	<0.10

Table 2. Hydrolysis of peptides corresponding to peptide cleavage sites

	Site	Sequence	Km (mM)	Vmax (nmol/min/mg)
PEPTIDES HYDROLYZED				
	HIV-1 sites[a]			
I	GAG 124-138	HSSQVSQNY-PIVQNI	N.D.[b]	>275
II	GAG 357-370	GHKARVL-AEAMSQV	2.3	100
III	GAG 370-383	VTNTATIM-MQRGNF	0.16	682
IV	GAG 440-453	SYKGRPGNF-LQSRP	13.9	382
V	POL 59-72	DRQGTVSFNF-PQIT	0.70	954
VI	POL 162-174	GCTLNF-PISPIET	N.D.	>120
VII	POL 721-734	AGIRKIL-FLDGIDK	6.1	145
	HIV-2 site			
	GAG 129-142	SEKGGNY-PVQHVGG	2.3	295
PEPTIDES NOT HYDROLYZED				
	HIV-1 site			
IX	ENV 511-524	RVVQREKR-AVGIGA	-	<2
	AMV site			
	p12/p15[c]	PAVS-LAMTMEHK	-	<2

[a] Numbering according to ref. 15.
[b] Km not determined due to low solubility.
[c] Sequence from ref. 22.

between gag p17 and gag p24, we examined its activity against a series of peptides listed in Table 2, where the peptides designated I-IX have sequences corresponding to several residues on either side of each of the cleavage sites I-IX shown in Fig. 1. Sequences were chosen to favor aqueous solubility while including at least 4 residues N-terminal and 3 residues C-terminal to the *in vivo* cleavage site. The protease was capable of cleaving all of the peptides corresponding to the 4 cleavages of gag (I-IV), the site at the N-terminus of the protease (V), the sites between the protease, reverse transcriptase and integrase (VI, VII), but not the site between env gp120 and gp41 (IX). Because of low solubility, we were unable to examine the peptide that corresponds to the cleavage of the signal peptide of the env precursor (VIII).

The specificity of the protease was further explored using peptides that had sequences for known *in vivo* cleavage sites of the closely related HIV-2 (21) and the more distantly related AMV virus (Table 2). The HIV-2 peptide was a substrate comparable to some of the HIV-1 substrates, while the AMV peptide, shown to be cleaved by the AMV protease (22), was not. The peptides where no cleavage was observed were tested at 2 mM. Increasing the

quantity of protease 10 fold (to 2 μg) or the time of reaction to 6 hr produced no loss of substrate or detectable products.

The peptide cleavages observed are efficient enough to suggest that all of these sites are processed by the HIV protease in vivo. Similarity among the retroviral polyprotein cleavage sites has been noted previously, with the deduction of a consensus sequence Ser(or Thr)-Xaa-Xaa-Tyr(or Phe)-Pro (7). We confirm that peptides (I and V) sharing this sequence are substrates, while noting that the dissimilar peptide III is also very effective. It is unusual that a single peptidase is able to cleave N-terminal to proline as well as N-terminal to primary amino acids. In this study, the utilization of enzyme derived by chemical synthesis avoids possible artifacts arising from contaminating activities and offers convincing evidence that the diverse cleavages are intrinsic to the HIV-1 protease sequence. Although a common feature of the cleavage site is the occurrence of hydrophobic amino acids on either side of the scissile bond, protease treatment of HIV-1 gag p55, which contains numerous hydrophobic residue pairs, has been previously shown to result in the highly specific cleavage at sites I and II (19).

On the basis of limited sequence similarity, the retroviral proteases have been compared to the family of aspartyl proteases that include pepsin and renin (14). The minimal length of 7 residues that we observe for an HIV protease substrate agrees closely with the minimal length for a renin substrate (23). In addition, a recent report on the peptide substrate specificity of avian sarcoma-leukosis virus protease (24) demonstrates that while a decamer is a substrate, a hexamer is not. Whereas renin has a high degree of sequence specificity for peptides as substrates, pepsin is much less stringent (25). The HIV protease activity characterized here is much less specific in its substrate sequence than renin, but a more detailed analysis is necessary before the structure-function determinants of an HIV-1 protease substrate will be known.

In conclusion, we have shown for the first time that the 99 amino acid HIV protease will function in vitro to cleave peptide substrates having the

sequences for 7 of the 9 known processing sites of HIV-1 polyproteins. The versatility of this protease reflects its importance in the life cycle of the virus and highlights its potential as an anti-viral target.

REFERENCES

1. Coffin, J. in Molecular Biology of Tumor Viruses (eds. Weiss, R. et al.) p. 261-268 (Cold Spring Harbor Laboratory, New York, 1982).
2. Sauer, R.T., Allen, D.W.,and Niall, H.D. (1981) Biochem. 20, 3784-3791.
3. Katoh, I., Yasunaga, T., Ikawa, Y., and Yoshinaka, Y. (1987) Nature 329, 654-656.
4. Yoshinaka, Y., Katoh, I., Copeland, T.D., Smythers, G.W., and Oroszlan, S. (1986) J. Virol. 57, 826-832.
5. Vogt, V.M., Wight, A., and Eisenman, R. (1979) Virology 98, 154-167.
6. Shimotohno, K., Takahashi, Y., Shimizu, N., Gojobori, T., Golde, D.W., Chen, I.S.Y., Miwa, M., and Sugimura, T. (1985) Proc. Nat. Acad. Sci. 82, 3101-3105.
7. Pearl, L.H., and Taylor, W.R. (1987) Nature 329, 351-354.
8. Crawford, S. and Goff, S.P. (1865) J. Virol. 53, 899-907.
9. Wain-Hobson, A., Sonigo, P., Danos, O., Cole, S., and Alizon, M. (1985) Cell 40, 9-17.
10. Sanchez-Pescador, T., Power, M.D., Barr, P.J., Steimer, K.S., Stempien, M.M., Brown-Shimer, S.L., Gee, W.W., Renard, A., Randolph, A., Levy, J.A., Dina, D., and Luciw, P. (1985) Science 227, 484-492.
11. Lightfoote, M.M., Coligan, J.E., Folks, T.M., Fauci, A.S., Martin, M.A., and Venkatesan, S. (1986) J. Virol. 60, 771-775.
12. Veronese, F.D., DeVico, A.L., Copeland, T.D., Oroszlan, S., Gallo, R.C., and Sarngadharan, M.G. (1985) Science 229, 1402-1405.
13. Veronese, F.D., Rahman, R., Copeland, T.D., Oroszlan, S., Gallo, R.C. and Sarngadharan, M.G. (1987) Aids Res. and Human Retroviruses 3, 253-264.
14. Pearl, L.H. and Taylor, W.R. (1987) Nature 328, 482.
15. Ratner, L., Haseltine, W., Patarca, R., Livak, K.J., Starcich, B., Josephs, S.F., Doran, E.R., Rafalski, J.A., Whitehorn, E.A., Baumeister, K., Ivanoff, L., Petteway Jr., S.R., Pearson, M.L., Lautenberger, J.A., Papas, T.S., Ghrayeb, J., Chang, N.T., Gallo, R.C. and Wong-Stall, F. (1985) Nature 313, 277-284.
16. DeBouck, C., Gorniak, J.G., Strickler, J.E., Meek, T.D., Metcalf, B.W., and Rosenberg, M. (1987) Proc. Nat. Acad. Sci. 84, 8903-8906.
17. Kohl, N.E., Emini, E.A., Schleif, W.A., Davis, L.J., Heimbach, J.C., Dixon, R.A.F., Scolnick, E.M., and Sigal, I.S. (1988) Proc. Nat. Acad. Sci. USA 85, 4686-4690.
18. Darke, P.L. manuscript in preparation.
19. Nutt, R.F., Brady, S.F., Darke, P.L., Ciccarone, T.M., Colton, C.D., Nutt, E.M., Rodkey, J.A., Bennett, C.D., Waxman, L.H., Sigal, I.S., Anderson, P.S., and Veber, D.F. (1988) Proc. Nat. Acad. Sci. USA in press.
20. Hunkapillar, M.W. and Hood, L.E. (1978) Biochem. 17, 2124-2133.
21. Guyader, M., Emerman, M., Sonigo, P., Clavel, F., Montagnier and Alizon, M. (1987) Nature 326, 662-669.
22. Copeland, T.D. and Orozslan, S. in Peptides: Synthesis, Structure and Function (eds. Rich, D.H. and Gross, E.) 497-500 (Pierce, Rockford, IL 1981).
23. Skeggs, L.T., Lentz, K.E., Kahn, J.R. and Hochstrasser, H. (1968) J. Exp. Med. 128, 13-34.
24. Kotler, M., Katz, R.A., Dahno, W., Leis, J., and Skalka, A.M. (1988) Proc. Nat. Acad. Sci. 85, 4185-4189.
25. Powers, J.C., Harley, A.D. and Myers, D.V. (1977) Adv. in Exp. Med. and Biol. 95, 141-147.

Vol. 156, No. 1, 1988 BIOCHEMICAL AND BIOPHYSICAL RESEARCH COMMUNICATIONS
October 14, 1988 Pages 304-311

AMINO ACID COMPOSITION AND PROTEOLYTIC GENERATED DOMAINS OF HIGHER PLANT TUBULIN

Pascal Picquot, Marylin Vantard, Iradj Amiri*, Luc Fausser and Anne-Marie Lambert

Laboratoire de Biologie Cellulaire Végétale,
Centre National de la Recherche Scientifique, Unité Associée 1182,
Université Louis Pasteur, Institut de Botanique, 67083 Strasbourg Cedex, France
* ALTERGENE laboratoires, 67300 Strasbourg-Schiltigheim
France

Received July 18, 1988

Summary : The molecular architecture of tubulin from higher plant remains unknown. In this report we have made an attempt to identify higher plant tubulin domains using total and limited proteolysis of Haemanthus endosperm tubulin. The tubulin was previously purified and characterized (Picquot and Lambert 1988). The amino acid composition revealed a high content of basic residues, such as arginine and lysine. Tubulin domains were probed by tryptic and chymotryptic cleavage and analyzed by immunoblotting using specific monoclonal antibodies against alpha or beta subunits. These data shed light on specific properties of the higher plant tubulin. © 1988 Academic Press, Inc.

Tubulin is one of the most conserved protein during evolution. This protein consists of two similar monomers, alpha and beta each having a molecular weight of 50 kDa. Alpha-beta dimers polymerise into microtubules. In the living cell, microtubules are involved in chromosome transport during cell division, cell wall formation in higher plants, and intracytoplasmic movement of organelles as reviewed in **(1)**. Plant tubulin is distinguished from neurotubulin in its alkaloïd binding characteristics **(2)**. Plant microtubules are resistant to colchicine and vinblastine while animal microtubules are very sensitive **(3)**. This indicates important physiological variability between animal and plant tubulins. Data concerning plant tubulin are still incomplete mainly due to difficulties encoutered in its isolation. Almost no report is yet available concerning the amino acid composition and molecular architecture of higher plant tubulin. It is in this background that we present here results on amino acid composition of higher plant tubulin. We used Haemanthus (Monocotyledons) endosperm tubulin, purified from young fruits as described previously **(4)**. This protein **(4)** is highly homologous to other higher plant tubulin such as the tubulin obtained from coleoptyls **(5)** or derived from plant cell culture **(2,5)**.

0006-291X/88 $1.50
Copyright © 1988 by Academic Press, Inc.
All rights of reproduction in any form reserved.

This manuscript deals with three essential analyses : (I) the determination of amino acid composition, (II) total cleavage by trypsin followed by analysis of the amino acid content of the tryptic peptides, and (III) a combination of limited proteolysis (using trypsin and chymotrypsin) and immunoblotting (using monoclonal antibodies specific for alpha or beta subunit). This allowed us to study the domain structure of endosperm tubulin with due comparison with neurotubulin.

MATERIALS AND METHODS

Tubulin extraction

Tubulin was extracted from endosperm cells of Haemanthus Katherinae Bak. and Clivia nobilis Lindl., as described previously **(4)**. The crude extract (100,000g supernatant) is fractionnated by ion-exchange chromatography on DEAE Sephadex A50. The tubulin fraction is then concentrated by ammonium sulfate precipitation. After dialysis and centrifugation of the dialysate, tubulin dimers are able to polymerise into microtubules in vitro, using Taxol as stabilizing agent.

Total tryptic proteolysis

The plant endosperm tubuline (alpha - beta dimers) was cleaved by trypsin. For this, the protein was reduced, aminoethylated, and citraconylated using the methods described in **(6)** and **(7)** which were modified and adapted to microquantities. The so modified protein was desalted by gel filtration on Sephadex G25 with 0.1 M ammonium bicarbonate as eluent and recovered by lyophilisation. The modified tubulin was then subjected to tryptic hydrolysis in 0.1 M ammonium bicarbonate at 37°C for 3 hours. The tubulin/trypsin ratio was 50:1 (w/w). The action of protease was stopped by freeze-drying of sample. The tryptic peptides were separated, after decitraconylation on a HPLC apparatus using a reverse phase column (Waters C18 u-Bondapack 3.9 X 300 mm, at a flow rate of 1.2 ml/min) in an acetonitryl gradient (0-60%). Because of the large number of tryptic fragments obtained, a second separation was performed on the same column in an isocratic gradient.

Amino-acid composition

The amino-acid composition was performed on a HPLC apparatus, using precolumn derivatization procedure with phenylisothiocyanate. Tryptic peptides or endosperm tubulin (alpha-beta dimers) were previously hydrolysed with HCl 5.7 N at 110°C. In the case of endosperm tubulin, cystein was not determined, and results were expressed as residues per dimer.

Limited proteolytic digestion of plant endosperm tubulin as compared to neurotubulin

Haemanthus endosperm tubulin was digested with trypsin and chymotrypsin at room temperature (20-22°C) for up to 30 min. The reaction was stopped by addition of 2 mM-PMSF. Enzyme/tubulin molar ratio was 1/50, 1/25, 1/12. Similar digestion was done using purified pig brain tubulin (tubulin dimers) obtained by phosphocellulose chromatography (PC-tubulin) according to **(8)**.

Proteolytic fragments were separated by SDS-PAGE using 12.5 % polyacrylamide, 0.1 % SDS gel. After electrophoresis one portion of the gell was silver-stained, the other part was transferred onto nitrocellulose according to **(9)**. The nitrocellulose sheet was soaked in 5 % BSA in TBS, and incubated with monoclonal antibodies to alpha and to beta chickbrain tubulin (Amersham 356 and 357) at a dilution of 1/1000 in TBS/ 0,1 % - BSA buffer.

The first antibody was detected by a second antibody conjugated with colloidal gold, and silver enhanced (Auroprobe BL plus GAM IgG and IntenSE II Kit, Janssen Pharamaceutica).

RESULTS AND DISCUSSION

Amino-acid composition of Haemanthus endosperm tubulin

Haemanthus endosperm tubulin was purified as described in Material and Methods. Purity of the tubulin is shown **Fig. 1**. Results presented here correspond to the total tubulin (alpha + beta) fraction. Attempt to obtain separate alpha and beta subunits by electroelution did not met with success since enough material could not be made available, and therefore analysis of individual alpha, beta amino acid composition could not be possible. As shown **table 1**, the higher plant tubulin is characterized by rich amino acids content as lysine and arginine, and in this respect it is distinct from neurotubulin. Lower content of threonine and methionine was observed in plant tubulin, however, further investigations are needed as these two residues can be underestimated by the technique. The differences that we found between higher plant tubulin and neurotubulin are summarized in **Fig. 2**. These data are the first attempt to study amino-acid composition of higher plant tubulin. On the SDS-PAGE electrophoresis, the higher plant alpha tubulin migrates faster than alpha neurotubulin **(4, 5)**. Furthermore the alpha subunit of plant tubulin also migrates faster than beta subunit of neurotubulin. Such a pattern of electrophoretic mobility may be partly attributed to the high content [illegible]ic residues in plant tubulin. As non polar residues are of comparable amou[illegible], [illegible]

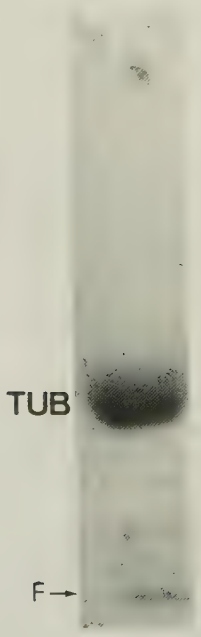

Figure 1 : SDS-PAGE loaded with a large amount (24ug) of plant endosperm tubulin used for amino-acid determination : therefore and are not resolved. The gel was stained with Coomassie blue. No other band than tubulin are detectable. **F** : dye front ; **TUB** : tubulin.

Table 1 : Amino-acid composition of plant endosperm tubulin compared to neurotubulin : the amino-acid composition of pig brain tubulin was deduced form the sequence published by Ponstingl (1981). The relative difference (%) between the two tubulins is calculated for each amino-acid, using pig brain tubulin as a standard (endosperm tubuline - pig brain tubulin)/pig brain tubulin X 100. ASx and GLx represent respectively ASP + ASN and GLU + GLN, which were not differentiated by the technique.

AMINO ACIDS	NUMBER OF RESIDUES		RELATIVE DIFFERENCE (%)
	pig brain tubulin	Haemanthus albumen tubulin	
ASx	92	92	0
GLx	111	97	12,6
SER	50	57	14
GLY	72	85	18
HIS	23	26	13
ARG	43	75	74
THR	59	42	28,8
ALA	65	74	13,8
PRO	40	49	22,5
TYR	35	29	17
VAL	65	57	12,3
MET	28	12	57,4
CYS	20	ND	ND
ILE	45	42	6,6
LEU	63	69	9,5
PHE	43	34	21
TRP	44	ND	ND
LYS	34	57	67,6

increase of basicity could result in enhanced hydrophilic properties of intracellular plant microtubules.

Tubulin domains

In the absence of complete amino-acid sequence data of higher plant tubulin, we have compared neurotubulin and endosperm tubulin after proteolytic cleavage in order to define higher plant tubulin domains. Peptides were generated by tryptic digestion of the total tubulin fraction. After separation

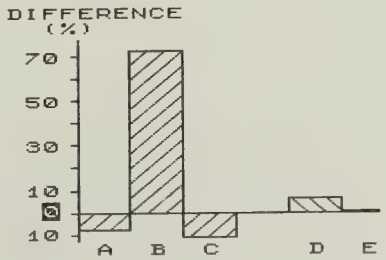

Figure 2 : Relative difference between pig brain tubulin and plant endosperm tubulin for 5 amino-acid families. Difference (%) = ((pig brain tubulin - endosperm tubulin) / pig brain tubulin) X 100. **A** : acidic residues ; **B** : basic residues ; **C** : alcohol residues ; **D** : polar residues ; **E** : non-polar residues. Importance of basic residues was the main difference between the two tubulins.

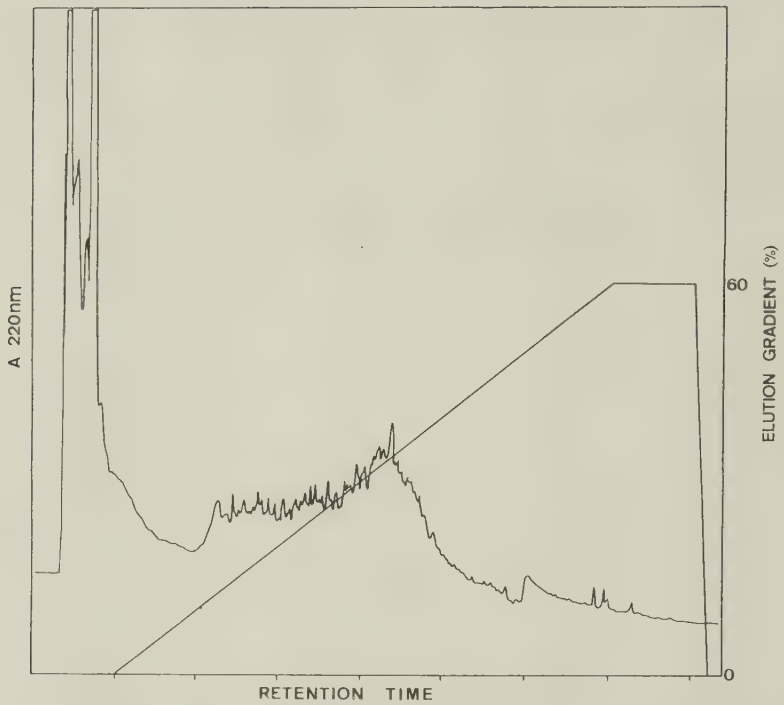

Figure 3 : Peptides of endosperm tubulin obtained by total proteolytic cleavage by trypsin. Separation is processed by HPLC reverse phase chromatography in an acetonitryl gradient (0-60%). Some of the peaks were further purified by reverse phase chromatography, and their amino-acid composition determined. (column : C18 u-Bondapack (Waters) 3.9 X 300 mm, Flow-rate : 1.2 ml/min).

by HPLC (**Fig.** 3), their amino-acid composition was determined. **Fig. 3** indicates a high quantity of peptides that could be related to the elevated level of arginine and lysine residues. Homology with neurotubulin domains was investigated using known neurotubulin sequences **(10,11)**. For each peptide, an homologous domain was searched on neurotubulin using a computer programm set up for this study. Conclusions are given in **Fig. 4**. Most of the homologous domains were found on the beta tubulin subunit, particularly in the regions 50-150 and 250-350 residues.

Limited proteolysis

Trypsin and chymotrypsin limited digestion of endosperm tubulin and neurotubulin was performed concomitantly. Results are given in **Fig. 5**. According to Mandelkow et al. **(12)**, peptides were analysed after Western-blotting using monoclonal antibodies to alpha or beta chicken brain tubulin (Amersham 356 and 357) that recognized the C-terminal region. Therefore, detected peptides (**Fig.5**) represent peptides that contain the C-terminal region. Under the same conditions, the higher plant endosperm tubulin is less sensitive than neurotubulin to the proteolytic cleavage, and

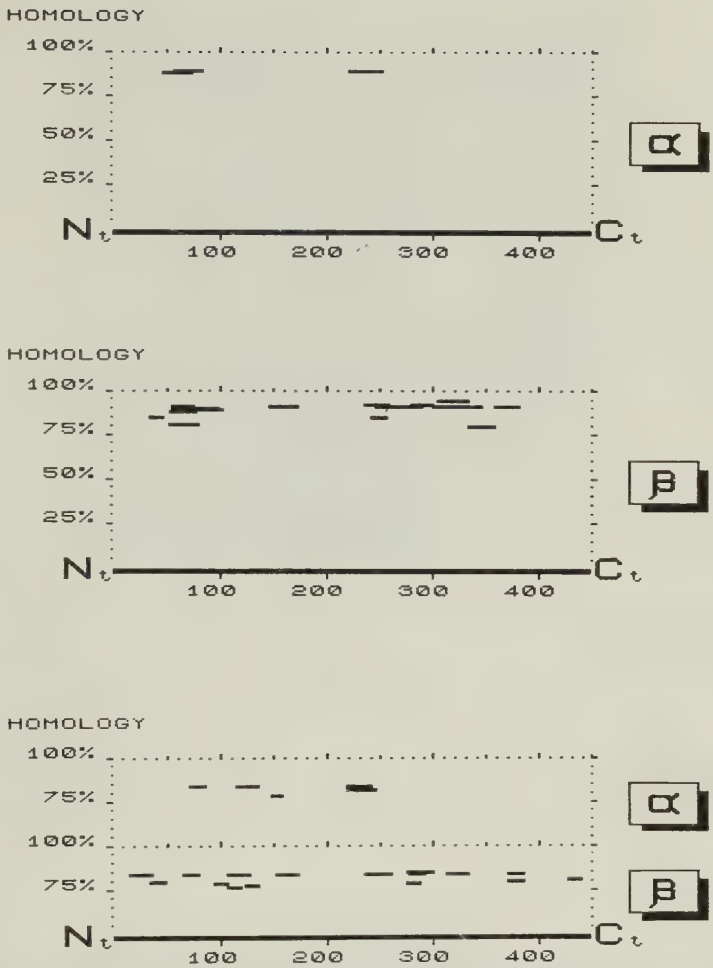

Figure 4 : Domains of pig brain tubulin showing an homology with tryptic peptides of endosperm tubulin : the homology is based on amino-acid composition, as explained in the text. The 2 upper graphs refer to peptides which show an homology restricted to one tubulin subunit, or . The lower graph concerns the peptides which have an homology with both subunits. On each grah, pig brain tubulin is represented as a straight bold line with N- and C- terminals indicated.

some of the peptides are only weakly labelled after immunoblotting. Data are summarized **Fig. 5** and **6.** Increased enzyme/tubulin ratio or incubation time, resulted in progressive loss of these peptides.

The **chymotryptic peptides** that contain the C-terminal region are comparable for neuro and plant tubulins, particularly for the alpha subunit, where similar peptides are found (41, 33 kDa). The plant beta subunit is less sensitive : one 21 kDa neuropeptide is only weakly detected in plant tubulin, while 3 peptides are seen between 33 and 43 kDa in both cases as a result of proteolysis.

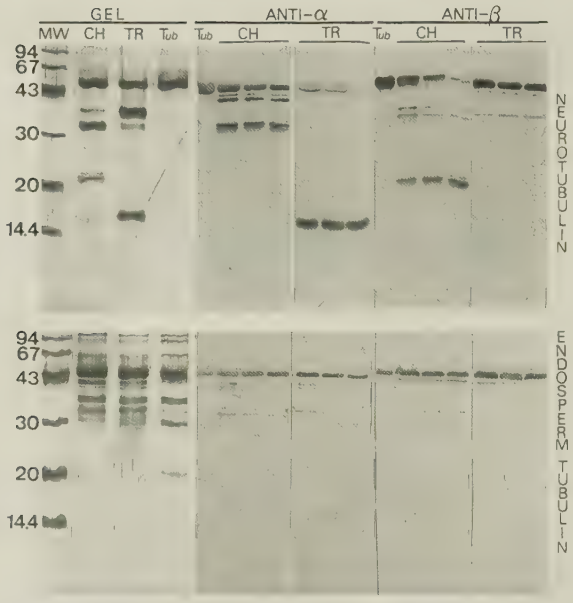

Figure 5 : Partial enzymatic cleavage of plant endosperm tubulin with chymotrypsin and trypsin : comparison with neurotubulin. After SDS-PAGE, part of the gel was stained with silver nitrate (GEL), the remaineder was electrotransfered onto nitrocellulose and probed with antibodies. The peptides containing the C-terminal domain are revealed using monoclonal antibodies specific for alpha (anti-) or (anti-) tubulin subunit. **MW** : molecular weight markers ; **Tub** : non digested tubulin ; **CH** : tubulin hydrolysed with chymotrypsin ; **TR** : tubulin hydrolyzed with trypsin. Neurotubulin and endosperm tubulin are indicated on the right.

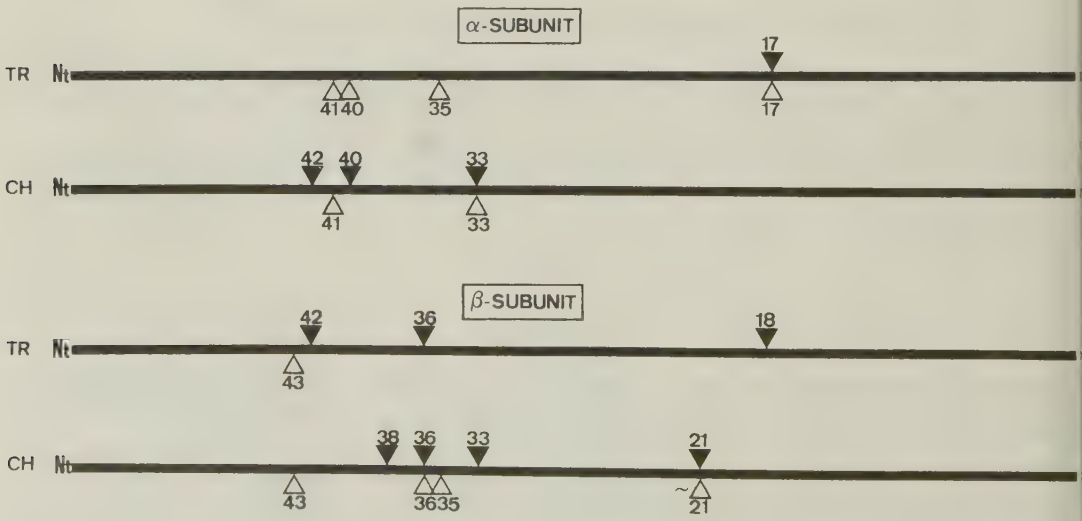

Figure 6 : Chymotrypsin and trypsin cleavage sites as determined by limited proteolysis followed by immunoblotting (the corresponding immuno-blots are shown in **Fig. 5**). **TR** : trypsin cleavage sites ; **CH** : chymotrypsin cleavage sites. : neurotubulin . : endosperm tubulin. For each cleavage site, the molecular weight of the resulting C-terminal peptide is indicated in kDa. Numbers : molecular weight in kDa.

Differences are obtained using **tryptic digestion.** For the alpha neurotubulin only one peptide of 17 kDa was obtained that is hardly detected in plant alpha tubulin, while 3 peptides of higher molecular weight (41, 40 and 35 kDa) are produced from endosperm tubulin. For beta subunits, one fragment only is obtained from plant beta tubulin (42 kDa) and this fragment is found common to neurotubulin, while 2 others (36 and 18 kDa) from neurotubulin are not detected in plant tubulin.

These data indicate that chymotrypsin cleavage sites are mostly common between neurotubulin and Haemanthus endosperm tubulin, while trypsin cleavage sites are highly different. The major drawback is the lower amount of peptide that is obtained with plant tubulin.

These observations provide novel informations on the structure of the higher plant tubulin. As endosperm tubulin was shown to be highly homologous to other plant tubulins **(4)**, the present data point out certain characteristics that could be directly related to specific microtubule functions in the living cell of higher plants.

ACKNOWLEDGEMENTS

This work was supported by the Ministère de la Recherche et de l'Enseignement Supérieur and the Centre National de la Recherche Scientifique (Paris), which are gratefully acknowledged.

REFERENCES

1. Lloyd, C.W., and Barlow, P.W. (1982) In : The Cytoskeleton in Plant Growth and Development (C.W. Lloyd, Ed.), pp.10-28. Academic Press, London.
2. Morejohn, L.C., Bureau, T.E., Tocchi, L.P., and Fosket, D.E. (1984) Proc. Nat. Acad. Sci. USA 81, 1440-1444.
3. Morejohn, L.C., Bureau, T.E., Tocchi, L.P., and Fosket, D.E. (1987) Planta 170, 230-241.
4. Picquot P., and Lambert, A.M. (1988) J. Plant Physiol. 32, 561-568.
5. Mizuno, K. (1985) Cell. Biol. Int. Rep. 9, 13-21.
6. Raftery, M.A., and COle, R.D. (1966) J. Biol. Chem. 241, 3457-3462.
7. Dixon, H.B.F., and Pernam, R.N. (1968) Biochem. J. 109, 312-314.
8. Weingarten, M.D., Lockwood, A.H., HWO, S.Y., and Kirschner, M.W. (1975) Proc. Nat. Acad. Sci. USA 72, 1858-1862.
9. Towbin, H., Stakelin, T., and Gordon, J. (1979) Proc. Nat. Acad. Sci. USA 76, 4350-4354.
10. Krauhs, E., Little, M., Kempf, T., Hofer-Warbinek, R., Ade, W., and Ponstingl, H. (1981) Proc. Nat. Acad. Sci. USA 78, 4156-4160.
11. Ponstingl, H., Krauhs, E., Little, M., and Kempf, T. (1981) proc. Nat. Acad. Sci. USA 78, 2757-2761.
12. Mandelkow, E.M., Hermann, M., and Ruhl, U. (1985) J. Mol. Biol. 185, 311-327.

Vol. 156, No. 1, 1988 BIOCHEMICAL AND BIOPHYSICAL RESEARCH COMMUNICATIONS
October 14, 1988 Pages 312-317

DOES ENDOTHELIN MOBILIZE CALCIUM FROM INTRACELLULAR STORE SITES IN RAT AORTIC VASCULAR SMOOTH MUSCLE CELLS IN PRIMARY CULTURE ?

Nobuco Miasiro, Hiromichi Yamamoto, Hideo Kanaide and Motoomi Nakamura

Research Institute of Angiocardiology , Faculty of Medicine,
Kyushu University, Fukuoka 812, Japan

Received August 23, 1988

SUMMARY: In the presence of endothelin, there was a rapid increase in the $^{45}Ca^{++}$ efflux from primary cultured rat vascular smooth muscle cells, both in physiological salt solution and in calcium free medium containing 2 mM EGTA . The $^{45}Ca^{++}$ influx was not affected. The endothelin-induced, transient increase in cytosolic calcium concentration is probably mainly due to release of calcium from the intracellular store in vascular smooth muscle cells. © 1988 Academic Press, Inc.

Yanagisawa et al (1) isolated a potent vasoconstrictor peptide, endothelin, from the conditioned medium of cultured porcine aortic endothelial cells, determined its amino-acid sequence and molecularly cloned the peptide precursor (2). Since it is generally accepted that the contraction of vascular smooth muscle cells (VSMC) is initiated by mobilization of Ca^{++} into the cytosol (3), we considered that endothelin may mobilize Ca^{++} from the extracellular space and/or intracellular Ca^{++} stores to induce contraction of VSMC. To test this hypothesis we examined the effects of endothelin on $^{45}Ca^{++}$ fluxes in primary cultured rat aortic VSMC, a preparation which is suitable for investigating Ca^{++} homeostasis (4,5). We found that, even in the absence of extracellular Ca^{++}, endothelin induced a rapid increase in $^{45}Ca^{++}$ efflux from cultured VSMC in a concentration-dependent manner. Thus, endothelin probably mobilizes Ca^{++} from intracellular store sites.

ABBREVIATIONS : VSMC, vascular smooth muscle cells; PSS, physiological salt solution; EGTA, ethylene glycol-bis (β-aminoethylether) N,N,N',N'-tetraacetic acid; HEPES, N-2-Hydroxyethyl-piperazine-N'-2-ethane sulfonic acid.

0006-291X/88 $1.50
Copyright © 1988 by Academic Press, Inc.
All rights of reproduction in any form reserved.

MATERIALS AND METHODS

Primary cultures were obtained from the aortic media of male Wistar rats, as described(6). The cells were used at confluence after 10-11 days.

$^{45}Ca^{++}$ Efflux. After rinsing five times with PSS, the cultured VSMC were equilibrated with $^{45}Ca^{++}$ (15 μCi/ml) in 1 ml of PSS for 3 hours at 37°C. The cells were then incubated in 1.4 ml of PSS or Ca^{++}-free PSS containing 2 mM EGTA at 37°C, which was changed every minute for 25 min and trapped in a vial. Endothelin was added at 10 min of the efflux time. The amount of $^{45}Ca^{++}$ released by the cells in each time interval was measured by liquid scintillation counting with 10 ml of ACS II (Amersham Corporation, Arlington Heights, IL,USA). The radioactivity of $^{45}Ca^{++}$ remaining in the cells was also counted, using trypsin and collagenase solution. The number of cells per dish was counted in separate dishes from those cultured at the same time. Fractions lost or $^{45}Ca^{++}$ released per minute per 10^6 cells were calculated and plotted as a function of incubation time (7).

$^{45}Ca^{++}$ Influx. To measure the $^{45}Ca^{++}$ influx the cultured VSMC were rinsed five times with PSS and incubated for 15 min in PSS at 37°C. The cells were then preincubated with endothelin (10^{-7} M) for 0, 2, 5 and 10 min. After the preincubation, the cells were incubated in 1 ml of the solution containing endothelin and $^{45}Ca^{++}$ (1 μCi/ml) for 2 min. To terminate $^{45}Ca^{++}$ uptake and remove external $^{45}Ca^{++}$ the cells were rinsed with Ca^{++}-free PSS containing 2 mM EGTA at 4°C for 10 min (7).

Solutions. The millimolar composition of the normal PSS (pH 7.4 at 25°C) was: NaCl, 140; KCl, 5; $CaCl_2$, 1.5; $MgCl_2$, 1; glucose, 10; HEPES, 10. The composition of Ca^{++}-free PSS was similar to normal PSS, except that it contained 2 mM EGTA instead of 1.5 mM $CaCl_2$. High K^+ solution was prepared by replacing NaCl with KCl isosmotically.

Chemicals. Collagenase (type I), elastase (type I) and trypsin (type III) were purchased from Sigma Chemical Co.,St. Louis, MO, USA, endothelin was purchased from Peptide Institute Inc., Osaka, Japan, Dulbecco's modified Eagle's medium was purchased from Gibco Laboratories, Grand Island, NY, USA, and $^{45}CaCl_2$ (32 mCi/mg) was purchased from NEN Research Products (Billerica, MA, USA). All other reagents were of the highest grade commercially available.

RESULTS AND DISCUSSION

The effect of endothelin on $^{45}Ca^{++}$ efflux from cultured VSMC in the presence of 1.5 mM extracellular Ca^{++} (PSS) is shown in Fig. 1. In the control cells, a nearly constant fraction of $^{45}Ca^{++}$ was released from the cells in each 1 min interval from 10-25 min. Addition of 10^{-7}M endothelin at 10 min markedly increased the $^{45}Ca^{++}$ efflux, which reached the maximum within a 1 min interval. Thereafter, the $^{45}Ca^{++}$ efflux rate gradually returned to control levels. This result suggests that endothelin induced the movement of $^{45}Ca^{++}$ in the cultured VSMC.

To determine whether the increase in $^{45}Ca^{++}$ efflux rate from VSMC by endothelin was due to either the release of intracellular Ca^{++} or

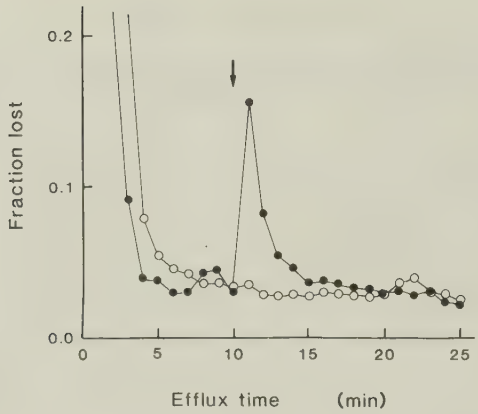

Figure 1. Effect of endothelin on $^{45}Ca^{++}$ efflux from primary cultured rat aortic VSMC in PSS containing 1.5 mM Ca^{++}. 10^{-7} M endothelin was added at 10 min as indicated by the arrow (closed circles). Open circles represent the control cells.

extracellular Ca^{++} influx or both , $^{45}Ca^{++}$ efflux was also determined in Ca^{++}-free medium in the presence of 2 mM EGTA, to chelate the external Ca^{++}. The high extracellular K^{+} (100 mM) under this condition had no effect on $^{45}Ca^{++}$ efflux (data not shown). On the other hand, endothelin (10^{-7}M) under this condition, did increase the $^{45}Ca^{++}$ efflux (Fig. 2). In the first 1 min interval after the addition of endothelin, the amount of $^{45}Ca^{++}$ appearing in the external medium increased three fold over the control and reached a peak. Thereafter, the $^{45}Ca^{++}$ efflux rapidly reverted to control levels. As shown in Fig. 3, this rapid increase in the $^{45}Ca^{++}$ efflux was dose-dependent.

The total amount of $^{45}Ca^{++}$ releasable by endothelin was calculated as a sum of the difference between $^{45}Ca^{++}$ released in the presence of endothelin and that in the control cells. 10^{-6} M endothelin released approximately 238 pmol/10^{6} cells or 79 µmol/liter cells when the volume of 10^{6} cells was assumed to be approximately 3 µl (4). Bond and co-workers reported that the increase in cytoplasmic Ca^{++} during maintained maximal contractions was 1.0 ± 0.2 mmol/kg dry cytoplasm or approximately 235 µmol/liter cell water(8). Thus, the above value estimated as the endothelin-releasable $^{45}Ca^{++}$ seems reasonable.

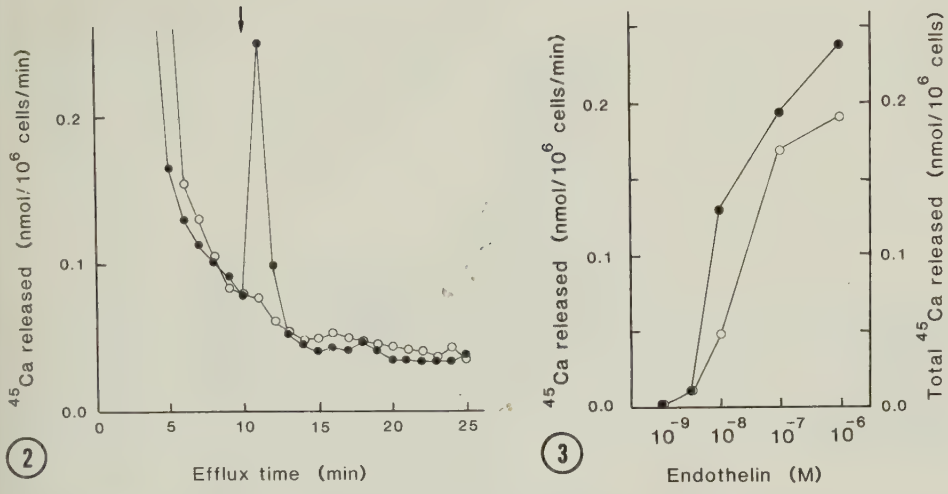

Figure 2. Effect of endothelin on $^{45}Ca^{++}$ efflux from primary cultured rat aortic VSMC in Ca^{++}-free PSS containing 2 mM EGTA. 10^{-7} M endothelin was added at 10 min as indicated by the arrow (closed circles). Open circles represent the control cells.

Figure 3. Dose-response curve for endothelin-stimulated $^{45}Ca^{++}$ efflux. The amount of $^{45}Ca^{++}$ released by endothelin within 1 min after addition was calculated as the difference between $^{45}Ca^{++}$ released into the Ca^{++}-free medium in the presence and absence (the control cells) of various concentrations of endothelin and plotted as a function of endothelin concentration (open circles). The total $^{45}Ca^{++}$ releasable by endothelin was also calculated as a sum of $^{45}Ca^{++}$ released by endothelin every minute (closed circles). The data are means of 2 experiments.

On the other hand, in the presence of 1.5 mM extracellular Ca^{++}, the $^{45}Ca^{++}$ influx of VSMC observed after 2 min of treatment with 10^{-7} M endothelin (including 0, 2, 5 and 10 min of pre-incubation) showed no increase, as compared to findings with the control cells (Fig. 4). The high K^+ depolarization increased significantly ($p<0.005$) the $^{45}Ca^{++}$ influx (Fig. 4), a finding consistent with the presence of voltage-dependent Ca^{++}-channels in cultured rat aortic VSMC (5).

Yanagisawa et al (1) reported that the endothelin-induced contraction was marked and long lasting and was completely inhibited when it was given in Ca^{++}-free Krebs-Ringer solution containing 1 mM EGTA. The vasoconstriction was markedly attenuated with nicardipine, a Ca^{++}-channel blocker. These findings suggested to them that the influx of extracellular Ca^{++} was required for the action of endothelin. However, we found no detectable increase in Ca^{++} permeability of the plasma membrane, even with a long exposure to endothelin.

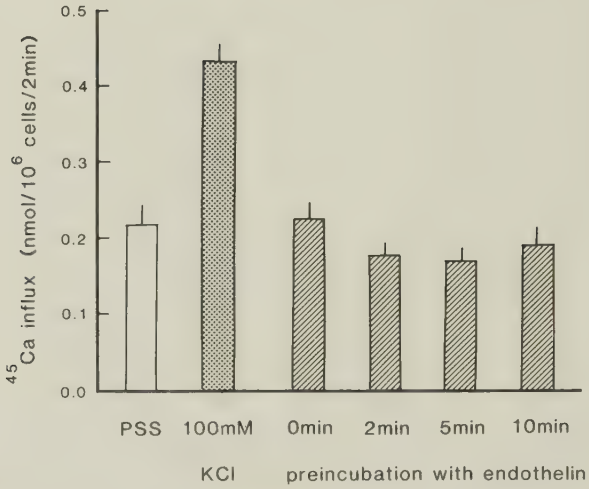

Figure 4. Effect of 10^{-7} M endothelin and 100 mM KCl on $^{45}Ca^{++}$ influx. The cell cultures were pre-incubated with endothelin for 0, 2, 5 and 10 min in normal PSS and then exposed to solution containing both 10^{-7} M endothelin and $^{45}Ca^{++}$ (1 μCi/ml) for 2 min. For 100 mM KCl, the cells were exposed to $^{45}Ca^{++}$ in 100 mM KCl-PSS for 2 min. 100 mM KCl significantly increased ^{45}Ca influx ($p<0.005$ by Student t-test). Each column represents mean ± SD of 6-7 experiments.

The present study shows that endothelin dose-dependently stimulates $^{45}Ca^{++}$ efflux in Ca^{++}-free medium containing 2 mM EGTA (Fig. 3). There are several possible interpretations for this increase in $^{45}Ca^{++}$ efflux by endothelin, including: 1) mobilization of Ca^{++} from intracellular store sites followed by extrusion, 2) primary activation of Ca^{++} extrusion or 3) release of extracellularly bound Ca^{++} not removed by EGTA containing solution. However, the primary activation of Ca^{++} extrusion by endothelin itself is not likely because we observed that the porcine coronary artery contracted and did not relax, in Ca^{++}-free medium containing 2 mM EGTA (unpublished observations). In addition, the endothelin-induced increase in $^{45}Ca^{++}$ efflux depended on temperature with a Q_{10} of 5 (data not shown), hence may be mediated by energy dependent cellular mechanisms. We tentatively conclude that endothelin elevates cytosolic Ca^{++} level mainly by releasing Ca^{++} from intracellular Ca^{++} stores, which in turn activates Ca^{++} extrusion mechanisms and contractile proteins.

The contraction induced by the release of Ca^{++} from the intracellular store, without Ca^{++} influx from extracellular spaces is usually not marked

and is transient (9), thereby differing from that reported in case of endothelin (1). To clarify mechanisms related to the characteristic contraction induced by endothelin, processes of contraction other than a Ca^{++}-mediated ones will have to be given attention.

ACKNOWLEDGEMENTS

We thank M. Ohara for comments. This work was supported in part by a Grant-in-Aid for Scientific Research (N° 61570422), for Scientific Research on Priority Areas (N° 63624510) and for Special Project Research (N 63113001) from the Ministry of the Education, Science and Culture, Japan, a Research Grant for Cardiovascular Disease (61 A-1) from the Ministry of Health and Welfare, Japan, and a Grant from the "Research Program on Cell Calcium Signals in the Cardiovascular System ", and a fellowship grant (M.N.) from the Japan International Cooperation Agency.

REFERENCES

1. Yanagisawa, M., Kurihara, H., Kimura, S., Tomobe, Y., Kobayashi, M., Mitsui, Y., Yazaki, Y., Goto, K., and Masaki, T. (1988) Nature 332, 411-415.
2. Itoh, Y., Yanagisawa, M., Ohkubo, S., Kimura, C., Kosaka, T., Inoue, A., Ishida, N., Mitsui, Y., Onda, H., Fujino, M., and Masaki, T. (1988) FEBS Lett. 231, 440-444.
3. Webb, R.C., and Bohr, D.F. (1981) Prog. Cardiovasc. Dis. 24, 213-242.
4. Yamamoto, H., and van Breemen, C. (1985) Biochem. Biophys. Res. Comm. 130, 270-274.
5. Kobayashi, S., Kanaide, H., and Nakamura, M. (1985) Science 229, 553-556.
6. Yamamoto, H., Kanaide, H., and Nakamura, M. (1983) Br. J. exp. Pathol. 64, 156-165.
7. van Breemen, C., Hwang, O., and Meisheri, K.D. (1981) J. Pharmacol. exp. Ther. 218, 459-463.
8. Bond, M., Shuman, H., Somlyo, A.P., and Somlyo, A.V. (1984) J.Physiol., Lond. 357, 185-201.
9. Casteels, R., Raeymaekers, L., Suzuki, H., and van Eldere, J. (1981) Pflügers Archiv 392, 139-145.

Vol. 156, No. 1, 1988 BIOCHEMICAL AND BIOPHYSICAL RESEARCH COMMUNICATIONS
October 14, 1988 Pages 318-32

CHARACTERIZATION OF TWO GLYCOPROTEINS OF HUMAN PANCREATIC JUICE: P35, A TRUNCATED PROTEASE E AND P19, PRECURSOR OF PROTEIN X

O. Guy-Crotte*§ , C. Barthe*, D. Basso**, B. Fournet*** and C. Figarella*

* Groupe de Recherche sur les Glandes Exocrines, 27 Boulevard Leï Roure, BP 156, 13273 Marseille Cedex 09, France

** Istituto di Medicina Interna, Università di Padova, Padova, Italia

*** Laboratoire de Chimie Biologique et Unité Associée au CNRS n° 217 (Directeur : Prof. J. Montreuil) Université des Sciences et Technique de Lille Flandres-Artois, 59655 Villeneuve d'Ascq Cedex, France

Received August 26, 1988

Four glycoproteins were separated by SDS-polyacrylamide gel electrophoresis of proteins of human pancreatic juice devoid of free proteolytic activity. The two low molecular weight glycoproteins were isolated and characterized. Protein P19, the precursor family of protein X, was analyzed by its carbohydrate content which seemed to play an important role in protein solubility at pH 8.0. Protein P35was found to be a Con A-binding protein rich in mannose. Its N-terminal amino acid sequence covering 33 residues revealed a strong homology with human protease E without the dipeptide Val-Val. Is P35 a protein homologous to the subunit III of bovine procarboxypeptidase A ? © 1988 Academic Press, Inc.

If the protein composition of human pancreatic juice has been extensively studied and is now well elucidated (1), little is known about glycoproteins. During the purification of pancreatic proteins, we have characterized two lipolytic enzymes as glycoproteins : carboxylester hydrolase of 100 kDa which presents a high content of sugars (20 % in weight) (2) and lipase of 48 kDa which separates in two glycosylated isolipases containing only glucosamine and neutral sugars (3). Moreover, human pancreatic kallikrein, a minor component of pancreatic juice of 35 kDa was found to give a positive staining with the Schiff reagent (4). By two dimensional gel electrophoresis, Scheele et al. have separated five glycoproteins giving a positive staining with the Schiff reagent (5)but except lipase, the four other glycoproteins were not identified.

In this paper we report the characterization of two glycoproteins, a protein of 19 kDa (P19) whose carbohydrates content seems to play an important role in protein solubility and a protein of 35 kDa (P35) not yet identified in human pancreatic juice.

§ To whom correspondence should be sent.

0006-291X/88 $1.50
Copyright © 1988 by Academic Press, Inc.
All rights of reproduction in any form reserved.

MATERIAL AND METHODS

Material. Human pancreatic juice was collected by catheterization of the main pancreatic duct after urgery for biliary or pancreatic diseases and lyophilise . Only samples devoid of free proteolytic ctivty measured by chymotrypsin assay on N-acetyl-L- tyrosine ethylester as substrate, were sed.

Polyacrylamide gel electrophoresis. Gel electrophoresis was performed in slab gel in 15 % olyacrylamide in the presence of 0.1 % sodium dodecyl sulfate according to the method of aemmli (6) without treatment with 2-mercaptoethanol. Proteins were stained by Coomassie Blue 250. Glycoproteins were identified with periodic acid Schiff reagent according to the method of acharius et al. (7). Glycoproteins with affinity for Con A were detected by affinoblotting after lectrophoretic separation followed by transfer to nitrocellulose paper and specific reaction with on A as described by Faye et al. (8).

arbohydrate analysis The identification and estimation of carbohydrates were performed after ethanolysis (methanol/0.5M HCl,80°C, 24 h) by gas-liquid chromatography of trifluoroacetylated ethyl glycosides (9).

equence determination. Amino acid sequencing was performed with an Applied Biosystem (model 70 A) gas phase sequencer.Phenylthiohydantoin derivatives of amino acids were analyzed by HPLC using a C-18 column (Brownlee, 5 µm, 2.1 x 220 mm) (10).

urification of proteins P19 and P35 .The first step of purification of proteins P19 and P35 was a hromatography of human pancreatic juice on DEAE-Trisacryl at pH 8.0 in the presence of high mounts of trypsin inhibitors (1 mM benzamidine and lima bean inhibitor, 5 % of protein weight) s described before (11). Then, fractions containing P19 and P35 determined by SDS olyacrylamide gel electrophoresis were purified separately. Fractions containing P19 were ubmitted to a chromatography on CM-Sephadex at pH 6.5 as described for protein X purification 11). Purified P19 migrated like a family of proteins of close molecular weight, heterogeneity due o the presence of carbohydrates . P35 was purified by an affinity chromatography on Con A-Ultrogel (IBF) equilibrated in a 20 mM Tris, 0.5 M NaCl buffer pH 7.6 containing 1 mM $CaCl_2$ and 1 mM $MnCl_2$. Protein P35 was eluted by the addition of 0.2 M α-D-mannopyranoside o the chromatography buffer, but with a low yield. In some cases, fractions containing P35 eluted from DEAE-Trisacryl were purified using the Pharmacia FPLC system in a Mono-S column equilibrated in a 50 mM Mes buffer pH 6.5 and eluted by a NaCl concentration gradient.

RESULTS

Characterization of glycoproteins of human pancreatic juice

Fig. 1 shows the electrophoresis pattern of proteins of human pancreatic juice separated on polyacrylamide slab gel in the presence of SDS. As shown by Coomassie staining, 11 protein bands were separated according to their molecular weight. After staining with the Schiff reagent, a pink reaction was observed with four protein bands with the respective molecular weights of 100 kDa, 48 kDa, 35 kDa and 19 kDa. When glycoproteins were characterised by affino-blotting with Con A, two out of the four glycoproteins were positive, one of them corresponded to lipase with a molecular weight of 48 kDa and the other glycoprotein was a protein of 35 kDa.

Carbohydrate content of P19 and P35

The carbohydrate analysis of proteins P19 and P35 is given in table I, calculated on the basis of 3 mannoses. While P19 contains all neutral and amino sugars, P35 contains only mannose, galactose and glucosamine.

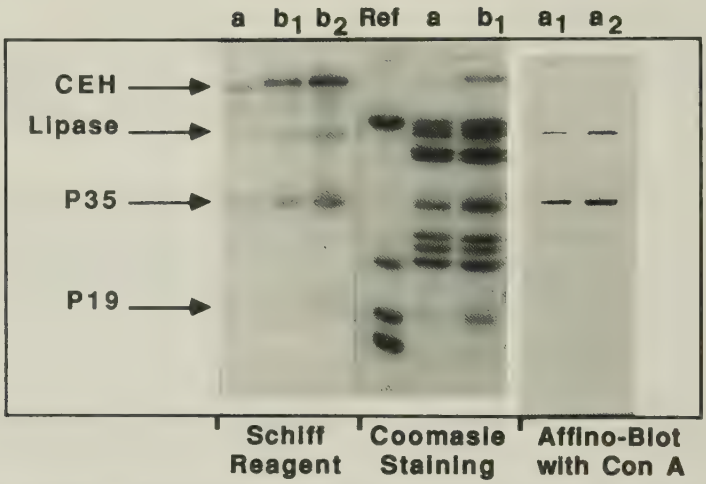

Figure 1 : Polyacrylamide slab gel of proteins of human pancreatic juice after electrophoresis in the presence of SDS and different stainings.
a and *b* are two samples of pancreatic juice loaded with different amounts: *a* , 14 µg ; a_1 , 1 µg ; a_2 , 2 µg ; b_1 , 18 µg ; b_2 , 36 µg. *Ref.* represents the reference proteins: albumin (66 kDa), bovine trypsinogen (24 kDa), β-lactoglobulin (18.4 kDa) and lysozyme (14.3 kDa).

N-terminal sequence of P35

The N-terminal sequence of P35 determined on 33 residues is given in fig. 2 with five unidentified residues in position 1, 23, 26, 27, 28. The N-terminal residue could not be identified because of the presence of some free amino acids in the sample of protein.

DISCUSSION

Four glycoprotein bands have been characterized after separation by SDS polyacrylamide gel electrophoresis of proteins of human pancreatic juice devoid of free proteolytic activity. The same pattern was obtained by Scheele et al. after one dimensional analysis of human pancreatic proteins.

Table I

Carbohydrates Analysis of Proteins P 19 and P 35

Carbohydrates	P 19	P 35
Mannose	3.00	3.0
Galactose	2.00	2.1
Fucose	2.00	-
Glucose	2.80	-
Galactosamine	1.20	-
Glucosamine	0.45	2.7
Sialic acid	0.00	0.0

(calculated on the basis of 3 mannose residues)

X - Gly - Glu - Asp - Ala - Val - Pro - Tyr - Ser - Trp - Pro- Trp - Gln -
1 10

Val - Ser - Leu- Gln - Tyr - Glu - Lys - Ser - Gly - X - Phe - Tyr - X -
20

X - X - Gly - Gly - Ser - Leu - Ile -
30

Figure 2 : N-terminal sequence of protein P35.

After a two-dimensional urea isoelectric focusing/SDS gel electrophoresis (5) the authors have separated one additional minor component with a molecular weight slightly lower than that of P35 . may correspond to kallikrein (4). The two high molecular weight glycoproteins of 100 kDa and 88 kDa that we have separated correspond to carboxyl ester hydrolase and lipase characterized before (2, 3) .

The band of 19 kDa contains the family of glycoproteins P19 that are the precursors of the protein X of 14 kDa which was isolated from slightly autoactivated pancreatic juice (11) and which was found homologous to pancreatic thread protein (12) and to a form of pancreatic stone protein (13). Glycoproteins P19 present in native pancreatic juice (devoid of free proteolytic activity) generate protein X by proteolysis after normal or pathological spontaneous trypsinogen activation (11, 14). The results of carbohydrate analysis indicate that the transformation of P19 into protein X corresponds to the liberation of a small glycopeptide of approximately 5 kDa since protein X was found devoid of sugars by the Schiff reagent as well as by carbohydrate analysis. The carbohydrate moiety seems inefficient to protect proteins P19 from proteolytic degradation as reported for many glycoproteins (15). However it could play an important role in protein solubility at pH 8.0 since P19, the native proteins are soluble in pancreatic juice and chromatography fractions while proteinX precipitates easily after its liberation in activated pancreatic juice or chromatography fractions (11).

The Con A-binding glycoprotein P35 has been characterized by its N-terminal sequence determined on 33 residues. It corresponds to the N-terminal sequence of human protease E recently determined by Shen et al. (16) without the dipeptide Val-Val. This is the first characterization of a truncated protease E in human pancreatic juice. In this respect P35 is highly homologous to the subunit III of procarboxypeptidase AS6 complex present in bovine (17) and some other ruminants (18) but with a higher molecular weight probably due to the presence of carbohydrates . The characterization of this novel human pancreatic protein suggests the coexistence, in human like in bovine, of two proteins closely related, protease E and the protein P35 homologous to the subunit III of procarboxypeptidase A which would be free in human juice.

ACKNOWLEDGMENTS: The authors are glad to thank J. Bonicel (Centre de Biochimie et de Biologie Moleculaire, CNRS, Marseille) for the determination of the N-terminal sequence and P. Timmerman (Laboratoire de Chimie Biologique et Unité Associée an CNRS n°217, Villeneuve d'Ascq) for the analysis of carbohydrates. M. Amouric is gratefully acknowledged for fruitful discussion and E. Rubio and C. Gianfilippo for their skillful technical assistance .

REFERENCES

1 - Figarella, C., Guy-Crotte, O., Barthe, C. and Amouric, M. (1987) Gastroenterol. Clin.Biol. 11, 891-897.
2 - Guy, O. Lombardo, D. and Brahms, I.G. (1981) Eur. J. Biochem. 117, 457-460.
3 - De Caro, A., Figarella, C., Amic, J., Michel, R. and Guy, O. (1977) Biochim. Biophys.Acta. 490, 411-419.
4 - Amouric, M. and Figarella, C. (1980) Hoppe-Seyler's Z. Physiol. Chem. 361, 85-90.
5 - Scheele, G., Bartelt, D. and Bieger, N. (1981) Gastroenterology 80, 461-473.
6 - Laemmli, U.K. (1970) Nature (London) 227, 680-685.
7 - Zacharius, R.M., Zell, T.E., Morrison, J.H. and Woodlock, J.J. (1969) Anal. Biochem. 30, 148-152.
8 - Faye, L. and Chrispeels, M.J. (1985) Anal. Biochem. 149, 218-224.
9 - Zanetta, J.P., Breckenridge, W.C. and Vincendon, G. (1972) J. Chromatogr. 69, 291-304.
10 - Foglizzo, E., Bonicel, J., Kerfelec, B., Granon, S. and Chapus, C. (1988) Biochim. Biophys. Acta. 954, 183-188.
11 - Guy-Crotte, O., Amouric M. and Figarella, C. (1984) Biochem. Biophys. Res. Comm. 125, 516-523.
12 - Gross, J.G., Rolf, I.C., Brauer, A.W., Margolies, M.N., Warshaw, A.L. and Wands, J.R. (1985) J. Clin. Invest. 76, 2115-2126.
13 - Montalto, G., Bonicel, J., Multigner, L., Rovery, M., Sarles, H. and De Caro, A. (1986) Biochem. J. 238, 227-232.
14 - Figarella, C., Amouric, M. and Guy-Crotte, O. (1988) Internat. J. Pancreatol. 3, S9-S18.
15 - Olden, K., Bernard, B.A., Humphries, M.J., Yeo, T.K., Yeo, K.T., White, S.L., Newton, S.A., Bauer, H.C. and Parent, J.B. (1985) TIBS, 10, 78-82.
16 - Shen, W.F., Fletcher, T.S. and Largman, C. (1987) Biochemistry 26, 3447-3452.
17 - Venot, N., Sciaky, M., Puigserver, A., Desnuelle, P. and Laurent, G. (1986) Eur. J. Biochem. 157, 91-99.
18 - Kerfelec, B., Chapus, C. and Puigserver, A. (1985) Eur. J. Biochem. 151, 515-519.

.l. 156, No. 1, 1988 BIOCHEMICAL AND BIOPHYSICAL RESEARCH COMMUNICATIONS
tober 14, 1988 Pages 323-327

N-ACYLATED PENTAPEPTIDES ANTAGONISTS OF SUBSTANCE P ON GUINEA-PIG ILEUM

Pascal Schmitt, Michel Mayer, Sylviane Magneney, Robert Michelot* and Pierre Potier

Institut de Chimie des Substances Naturelles, CNRS 91198, Gif sur Yvette, France

eceived August 8, 1988

UMMARY: Pentapeptides X-D.Trp-Phe-D.Trp-Leu-Y-NH_2 (X = H, Boc, para-ydroxyphenylacetyl, Y = Met,Leu,Nle,Phe) were tested as antagonists against ubstance P and against a specific agonist of the muscular receptor of eurokinins on the guinea-pig ileum . Weak antagonist or agonist activities ould be observed with the free or the Boc-protected pentapeptides whilst the cylated compounds could be compared favorably with the best antagonists lready described. © 1988 Academic Press, Inc.

The three neurokinins identified in mammals : Substance P (SP), eurokinin A (NKA) and neurokinin B (NKB) are widely distributed in the entral and peripheral nervous system and are known to act on specific eceptors to exert various biological functions (1,2). Both pharmacological nd biochemical studies using neurokinin analogs, as well as their C-terminal iologically active fragments have permitted the identification of three istinct neurokinin receptors (3,4).

In view of the numerous roles attributed to these peptides in hysiology and physiopathology (5,6), the synthesis of neurokinin antagonists rovides a promising new type of pharmacological tool. Over the last five ears, a fairly large number of antagonists analogs (undeca-, octa-, hepta- or exapeptides) have been developed (7,8,9) and the common structural features, onsidered as minimal requirements for activity can be summarized as follows :

a/ the presence of at least two D-Trp residues generally at the ositions 7 and 9;

b/ N-terminal residues replaced with D-isomers (D-Arg^1,D-Pro^2 in he undecapeptide, D-Pro^4 in the octapeptide) to protect the peptide from nzymatic degradation, or with L-isomers (Arg^1 in the hepta- and hexapeptides) o improve the solubility;

c/ C-terminal methionine changed for either an aliphatic residue ($NleNH_2$, $LeuNH_2$) or an aromatic residue ($PheNH_2$).

*To whom correspondence should be addressed

0006-291X/88 $1.50
Copyright © 1988 by Academic Press, Inc.
All rights of reproduction in any form reserved.

Many reports have established that modifications starting from the C-terminal hexapeptide SP(6-11) sequence may lead to active agonists (10,11); these data seem to rule out the possibility that shorter fragments afford valuable agonists or antagonists. In fact, the C-terminal pentapeptide of neurokinins (Phe-X-Gly-Leu-MetNH$_2$, X = Phe, Val), although a weak agonist, is the minimal fragment able to promote a full spasmogenic activity on smooth muscle preparations. Extending the size of the fragments towards the N-terminus induces a rapid increase in potency. Larger fragments such as the heptapeptide SP(5-11) or the octapeptide SP(4-11) are more active than SP (12,13) and these results have been frequently explained by a privileged role of Gln^5 and Gln^6 in binding to the receptor (14). Interestingly, some N-acylated C-terminal pentapeptides SP(7-11) have revealed equal or even more activity than SP on smooth muscle (15) and it was thus tempting to evaluate N-acylated pentapeptides for their neurokinin antagonist activity.

In the present communication, we would like to discuss some data, which confirm the hypothesis that active antagonists can also be obtained by modification of a typical pentapeptide structure containing D-Trp residues in positions 7 and 9.

Isolated organs suspended *in vitro* are among the most useful pharmacological assays for characterizing new synthetic peptides,particularly antagonists, related to neurokinins. Activities were measured on the guinea-pig ileum in the presence of atropine against SP and against Septide : (pGlu^6,Pro^9) SP(6-11) (11).

MATERIALS AND METHODS

The SP pentapeptides antagonists (Table I) and Septide were prepared in our laboratory by the classic stepwise solution method and by fragment coupling (16). SP was purchased from Bachem, Switzerland.

Experiments were performed on guinea-pig ileum in the presence of atropine (5.2 µM). Segments of the ileum (2-3 cm length) were suspended in a 10 ml organ bath of Tyrode solution oxygenated by 95 % O_2, 5 % CO_2 at 37 °C (17). The preparation was kept under a resting load of 1 g and longitudinal contractions of the ileum were recorded isometrically after an equilibrium period of 60 min during which the bath medium was changed repeatedly. Before each test of a new analog, the peptide was tested alone to detect any spasmogenic activity. Then the antagonist was applied to the bath 5 min prior to the addition of the agonist (SP or Septide) ; maximum inhibition was observed in this interval.

Between the applications of agonists, a latency period of 15 min and careful washing cycles were performed to avoid tachyphylaxis and to overcome the inhibitory action of previously applied antagonists.

Affinities of antagonists were calculated in terms of pA$_2$ (-log of the concentration of antagonist that reduces the effect of a double dose of agonist to that of a single dose), according to Schild (18). Ratios of the response elicited by 8 nM agonist in the presence of antagonists versus the response produced by 4 nM agonist was plotted as a function of the logarithm of the antagonist concentration. Calculations were performed from a minimum of six experiments and values were given as means with 95 % confidence intervals.

RESULTS AND DISCUSSION

Results are summarized in Table 1 and indicate that :

a/ all compounds are better antagonists against Septide than against SP;

b/ N-protection with a Boc group does not result in great changes in ctivity;

c/ the pentapeptide with D-Trp residues in positions 7 and 9 is, by itself, weak antagonist (pA_2 near 5) and the N-acylation of the peptide leads to an mportant increase of the antagonist activities.

The primary objectives of this study were to examine to what xtent a short C-terminal sequence in a neurokinin antagonist might be onsidered as the site of activity on the smooth muscle and to verify if the ame acylations of the SP C-terminal pentapeptide would also result in some ntagonist activities of the parent pentapeptide.

TABLE 1

Some Pentapeptides Antagonists

	COMPOUND	ACTIVITY ON GUINEA-PIG ILEUM (pA_2)[1]	
		against Septide[2]	against SP
1	DTrp-Phe-DTrp-Leu-Met-NH_2	5.34 ± 0.12	5.20 ± 0.32
2	DTrp-Phe-DTrp-Leu-Leu-NH_2	5.60 ± 0.05	5.05 ± 0.20
3	DTrp-Phe-DTrp-Leu-Nle-NH_2	5.94 ± 0.05	5.31 ± 0.18
4	DTrp-Phe-DTrp-Leu-Phe-NH_2	full agonist	
5	Boc[3]-DTrp-Phe-DTrp-Leu-Met-NH_2	5.26 ± 0.39	5.06 ± 0.32
6	Boc-DTrp-Phe-DTrp-Leu-Leu-NH_2	4.80 ± 0.30	4.75 ± 0.19
7	Boc-DTrp-Phe-DTrp-Leu-Nle-NH_2	5.64 ± 0.05	4.42 ± 0.25
8	Boc-DTrp-Phe-DTrp-Leu-Phe-NH_2	5.01 ± 0.17	4.54 ± 0.27
9	PHPA[4]-DTrp-Phe-DTrp-Leu-Met-NH_2	6.51 ± 0.21	5.69 ± 0.16
10	PHPA-DTrp-Phe-DTrp-Leu-Leu-NH_2	6.79 ± 0.21	5.73 ± 0.14
11	PHPA-DTrp-Phe-DTrp-Leu-Nle-NH_2	6.23 ± 0.12	5.72 ± 0.16
12	PHPA-DTrp-Phe-DTrp-Leu-Phe-NH_2	6.41 ± 0.07	5.72 ± 0.17

[1] pA_2 = -log of the concentration of antagonist that reduced the effect of a double concentration of agonist to that of a single dose.
[2] Septide = (pGlu[6],Pro[9])SP (6-11)
[3] Boc = tertiobutyloxycarbonyl -
[4] PHPA = 4-hydroxyphenylacetyl -

Of the more than one hundred neurokinin analog antagonists, the more efficient contain D-Trp residues in positions 7 and 9 or 7,9 and 10 (19) and methionine amide replaced by other hydrophobic aminoacid amides (8) . In this study, we found that pentapeptides X-D.Trp-Phe-D.Trp-Leu-Y-NH_2 (Y = Met, Leu,Nle,Phe) are weak antagonists whenever the N-terminus is free or blocked with a bulky and hydrophobic tertiobutyloxy radical (pA_2 near 5). We could also observe that this structure represents a minimum prerequisite for activity, since some pentapeptides act as very weak partial agonists (less than 5 % of the maximal activity at 10^{-6} M, for peptides 1,2 and 6) or as weak but full agonist (peptide 4).

The elongation of the pentapeptide antagonist minimal sequence towards the N-terminus with two aminoacid residues has been shown to improve the activity if this modification increases the solubility (9) and hexapeptide analogs containing N-methylated aminoacids and N-terminal Pro are more resistant to proteolysis and are better antagonists (pA_2 near 6.4)(20). In this study, we could confirm a previous observation that acylation of the C-terminal pentapeptide (15,16) by 4-hydroxyphenylacetic acid is a very reinforcing modification which exemplifies some important structural requirements controlling the affinity of the peptide for its binding sites. The gain in activity afforded by this acylating group is of the same order of magnitude as the two Gln residues in positions 5 and 6 of some synthetic antagonists (21).

The guinea-pig ileum, despite its lack of specificity (22), is the most commonly used pharmacological assay (7,23). In this preparation, atropine eliminates the cholinergic presynaptic component of the response to SP or to Septide, which has been reported as a selective agonist for the muscular receptor (11).

Our results, obtained against Septide with compounds 9-12, may thus be compared to those obtained on the same preparation against SP with an undecapeptide (D-Arg^1,D-$Trp^{7,9}$,Leu^{11}) SP = Spantide, pA_2 = 7.1) (24), with an octapeptide (D-Pro^4,D-$Trp^{7,9}$,Nle^{11}) SP(4-11), pA_2 = 7.1) (25) or with an heptapeptide (Arg^5,D-$Trp^{7,9}$,Nle^{11}) SP(5-11), pA_2 = 6.71) (26). Since activities of SP (ED_{50} = 1.75 10^{-9} M (7)) and of Septide (ED_{50} = 2.2 10^{-9} M (11)) are equivalent, the highest activities recorded against this latter agonist could be explained by a better selectivity of compounds 9-12 for a muscular receptor subtype (probably NK-1). Nevertheless, a selective degradation and/or different diffusion rates in the tissue may also account for this apparent selectivity.

It would be of great interest to compare these data to the affinities (K_i) in competition binding experiments performed with guinea-pig ileum (27). It appears unfortunately that naturally occuring peptides are

ather non selective for each receptor subtype. More selective radiolabelled igands based on the structure of recently described selective agonists (28) hould afford, when available, adequate correlations between pharmacological nd biochemical data.

Further studies are in progress in our laboratory to define the ew structural relationships implicated by these results.

REFERENCES

MAGGI C.A., GIULIANI S., SANTICIOLI P., REGOLI D. and MELI A.(1987) J.Auton.Pharmac. 7, 11-32.

PERNOW B. (1983) Pharmacological Review, 35, 85-141.

BUCK S.H., BURCHER E., SCHULTS C.W., LOVENBERG W. and O'DONOHUE T.L. (1986) Science 226, 987-999.

REGOLI D., DRAPEAU G., DION S. and D'ORLEANS-JUSTE P. (1987) Life Sciences 40, 109-117.

POST C.and FOLKERS K. (1985) Eur. J. Phamacol. 113,335-343.

LEANDER S., HAKANSON P., ROSELL S., FOLKERS K., SUNDLER F. and TORNQVIST K. (1981) Nature 294, 467-469.

REGOLI D., MIZRAHI J., D'ORLEANS-JUSTE P., DION S., DRAPEAU G. and ESCHER E. (1986) in Neural and Endocrine Peptides and Receptors (T.W.Moody Ed.) Plenum Press pp.501-511.

FOLKERS K., ROSELL S., JIE-CHENG X., BJORKROTH U., YI-AN L. and YIN-ZENG L. (1983) Acta Chim. Scand. 37B, 623-627.

HÖRIG J. and SCHULTHEISS H. (1984) Pharmacology 105, 65-72.

10. POULOS C., BROWN J.R. and JORDAN C.C. (1986) J.Med.Chem. 29, 1281-1284.

11. LAUFER R., GILON C., CHOREV M. and SELINGER Z.(1986) J.Med.Chem.29 1284-1288.

12. BURY R.W. and MASHFORD M.L. (1976) J. Med. Chem. 19, 854-856.

13. BERGMAN J., BIENERT M., NIEDRICH H., MEHLIS B. and P.OEHME P. (1974) Experientia 15(4), 401-403.

14. THEODOROPOULOS D., PINAS N., POULOS C., COUTURE R., MIZRAHI J., ESCHER E. and REGOLI D. (1982) Eur. J. Med. Chem. 17, 527-530.

15. BIENERT M., FORNER K., MEHLIS B. and NIEDRICH H. (1983) in Peptides 1982 (Blaha K.& Malon P. Ed.) Walter de Gruyter N.Y. p.517-520.

16. MICHELOT R., MAYER M., MAGNENEY S., PHAM VAN CHUONG P., SCHMITT P. and POTIER P. (1988) Eur. J. Med. Chem. 23, 243-247.

17. CALAS B., MICHELOT R., LECAER J.-P., CAVE A., PARELLO J. and POTIER P. (1987) Int. J. Peptide Protein Res. 29, 170-176.

18. SCHILD H.O. (1949) Brit. J. Pharmacol. 4, 277.

19. DUTTA A.S. (1987) Drugs Future 781-792.

20. BAIZMAN E.R., BENTLEY H., GORDON T.D., HANSEN P.E., KIEFER D., McKAY F.C., PERRONE M.H., MORGAN B.A., ROSI D., SINGH J., STEVENSON J. and WARD S.J. (1984) in Peptides (Ragnarsson U.E. Ed.) Almqvist and Wiksell international Stockholm p.359-364.

21. MATHISON R., ESCHER E., HUGGEL H., MIZRAHI J. and REGOLI D. (1985) Eur. J. Pharmacol.114, 147-155.

22. LEE C.M., CAMPBELL N.J., WILLIAMS B.J. and IVERSEN L.L. (1986) Eur. J. Pharmacol. 130, 209-217.

23. REGOLI D., D'ORLEANS-JUSTE P., ESCHER E. and MIZRAHI J. (1984) Eur. J. Pharmacol. 97, 161-170.

24. FOLKERS K., HAKANSON R., HÖRIG H., XU J.C. and LEANDER S. (1984) Br. J. Pharmacol. 83,449-456.

25. REGOLI D., ESCHER E. and MIZRAHI J. (1984) Pharmacology 28, 301-320

26. HÖRIG H. and SCHULTHEISS (1984) Eur. J. Pharmacol. 105, 65-72

27. BURCHER E.,BUCK S.H.,LOWENBERG W. and O'DONOHUE T.L. (1986) J. Pharmacol. Exp. Ther. 236, 819-831.

28. DRAPEAU G., D'ORLEANS-JUSTE P., DION S.,RHALEB N.-E., ROUISSI N.-E. and REGOLI D. (1987) Neuropeptides, 10, 43-54.

Vol. 156, No. 1, 1988 BIOCHEMICAL AND BIOPHYSICAL RESEARCH COMMUNICATIONS
October 14, 1988 Pages 328-334

EVIDENCE THAT A GTP BINDING PROTEIN REGULATES PHOSPHORYLATION OF THE CD3 ANTIGEN IN HUMAN T LYMPHOCYTES

Adelina A. Davies, J. Mark Hexham, Doreen A. Cantrell and Michael J. Crumpton

Cell Surface Biochemistry Laboratory,
Imperial Cancer Research Fund,
P.O. Box 123,
Lincolns Inn Fields,
London, WC2A 3PX, UK

Received August 26, 1988

Summary The role of guanine nucleotide binding regulatory proteins (G proteins) in the regulation of phosphorylation of the γ subunit of the CD3 antigen has been examined. CD3 γ chain phosphorylation in isolated T cell microsomes was stimulated by the G protein activator guanosine 5′-O thiotriphosphate (GTPγS), but cyclic adenosine monophosphate and guanosine 5′-diphosphate were ineffective at inducing γ chain phosphorylation. The effect of GTPγS was rapid and transient; a half maximal effect was observed with 50μM of the nucleotide. γ polypeptide phosphorylated *in vitro* in GTPγS stimulated microsomes incorporated phosphate on Serines 123 and 126. These data are consistent with the involvement of a G protein in the signalling mechanisms that regulate the phosphorylation of the CD3 γ chain. © 1988 Academic Press, Inc.

T lymphocyte activation is regulated by the T cell antigen receptor/CD3 (Ti/CD3) complex (1). Ti has been identified as an idiotypic disulphide linked heterodimer comprising two glycosylated polypeptides (α and β) of *Mr* 50,000 and 43,000 respectively (1). The CD3 antigen which is invariant, is noncovalently associated with Ti and consists of 3 chains: two glycosylated polypeptides of *Mr* 26000 and 21000 (γ and δ respectively)

Abbreviations

Guanosine 5′-O thiotriphosphate: GTPγS, Guanosine 5′ diphosphate: GDPβS
Cyclic adenosine monophosphate: cAMP, 4-(2-hydroxyethyl)-1-piperazineethane sulphonic acid: Hepes, Phorbol 12,13 dibutyrate: Pdbu

0006-291X/88 $1.50
Copyright © 1988 by Academic Press, Inc.
All rights of reproduction in any form reserved.

and one non-N-glycosylated polypeptide of Mr 19000 (ε) (2,3). Recently we have shown that an immediate consequence of antigen activation of T cells is a selective phosphorylation of the CD3 γ subunit (4-7). The proposed role for this phosphorylation is that it controls the cell surface expression and functions of the Ti/CD3 complex (7,8).

Two cell surface receptors are known to initiate the phosphorylation of CD3 γ chains in intact cells, namely the Ti/CD3 complex and CD2 antigen (4,9). There are also two candidates for the immune regulated kinase that mediates CD3 γ subunit phosphorylation, namely protein kinase C (pkC) and an unidentified calcium regulated kinase (7,10). The products of phosphoinositide metabolism are thought to act as intracellular signals coupling the Ti/CD3 complex and CD2 antigens to the CD3 γ chain kinase (11). Thus, triggering of both Ti/CD3 and CD2 molecules initiates an immediate breakdown of phosphatidylinositol biphosphate generating inositol phospholipids that regulate intracellular Ca^{2+} and diacylglycerols that collectively or separately control pkC and the other kinase. In T cells, as in many cells, the turnover of phosphoinositides is apparently controlled by guanine nucleotide binding (G) proteins (12-16). G proteins are activated when GTP is bound and inactivated when bound GTP is hydrolysed. Accordingly, non hydrolysable analogues of GTP can retain G proteins in a functional state and allow an assessment of the role of G proteins in a particular signal transduction pathway. In the present study we have explored the role of G proteins in the mechanisms that control the phosphorylation of the CD3 γ chain. We demonstrate that guanosine 5′-O-[3 thiotriphosphate] can modulate the phosphorylation of the CD3 γ subunit. This demonstration suggests that a G protein(s) is involved in the intracellular pathways that couple the CD3 γ chain to cellular kinases and/or phosphatases.

Materials and Methods

Reagents. Phorbol 12,13 dibutyrate (Pdbu) was purchased from Calbiochem (Behring Diagnostics), Guanosine and adenosine nucleotides were purchased from Boehringer Mannheim.

Phosphorylation. Human T lymphocyte microsomal membranes were prepared from exponentially growing T lymphocytes as described previously (10). Microsomal pellets were resuspended at 10mg protein/ml in Hepes buffer pH 7.5 using a Dounce homogeniser and stored in 1ml aliquots at -70°C. Microsomes (80-100μg) were phosphorylated at 30°C in a final volume of 50μl containing 10mM $MgCl_2$, 20mM Hepes buffer pH 7.5, 25 μM [γ-^{32}P] ATP (5μCi, Amersham) and guanosine nucleotides as indicated. The reaction was timed from the addition of the ATP and stopped with 500μl of ice cold NP40 lysis buffer containing 1mg/ml bovine serum albumin.

CD3 antigen was isolated by immunoprecipitation using the monoclonal antibody UCHT1 and the subunits were separated by SDS/PAGE under reducing conditions (7,10). ^{32}P-incorporation into the γ chain was quantitated by scanning autoradiographs densitometrically using a Joyce-Loebl Chromoscan 3. The relative intensities of the bands were compared on the basis of peak areas (arbitary units). Tryptic peptide analysis of the γ subunit for location of the phosphate group(s) by anion exchange was as described previously (10).

Results

GTPγS regulates CD3 γ chain phosphorylation. Microsomal membranes were incubated at 30°C with ^{32}P-labelled ATP in the presence or absence of 100μM GTPγS and immunoprecipitates of the CD3 antigen were subsequently analysed by SDS-PAGE. The data (Fig 1A) show that incorporation of ^{32}P into the Mr 26000 γ subunit was enhanced by the presence of GTPγS but not 100μM GDPβS in the incubation mixture. Fig 1B shows that 100μM cAMP did not stimulate CD3 γ chain phosphorylation. In 5 separate experiments the GTPγS enhancement of γ chain phosphorylation ranged from 4 to 10 fold. As shown in Fig. 1 three predominant phosphorylated bands were observed in CD3 immunoprecipitates prepared from microsomes phosphorylated *in vitro*. These include the Mr 26000 γ chain but also bands of Mr 55000 and 20000. The Mr 20000 band comprises an endoglycosidase F resistant component and a component that reduces to Mr 14000 after the removal of N-linked sugars (data not shown) and probably represents a mixture of phosphorylated CD3 ε and δ chains. The identity of the Mr 55000 polypeptide is, however, unknown. The effects of GTPγS on phosphorylation were rapid and transient, peaking within 30 seconds exposure to the guanine nucleotide and declining to baseline levels within 5 minutes (Fig 1C). A half maximal effect was observed with 50μM GTPγS (Fig 1D).

Tryptic peptide analysis of ^{32}P-labelled γ chain. Anion exchange chromatographic analyses of tryptic peptides of CD3 γ subunits phosphorylated *in vivo*, and of phosphorylated synthetic peptides corresponding to portions of the cytoplasmic domain of the γ chain, have identified two major phosphorylation sites in the CD3 α chain at serine residues number 123 and 126 (10), (Fig 2). The data in Fig 2 depict the anion exchange elution profile of the tryptic peptides derived from the γ polypeptide phosphorylated *in vitro* in GTPγS stimulated microsomes. The elution pattern comprises 3 peaks of radioactivity (A, B and C) and is consistent with multiple sites phosphorylation of the γ chain. Peaks B and C elute in identical positions with those expected for peptides phosphorylated on serine residues 123 and 126 respectively. The ratio of phosphorylation between serine residues 123 and 126 is approximately 1:1.

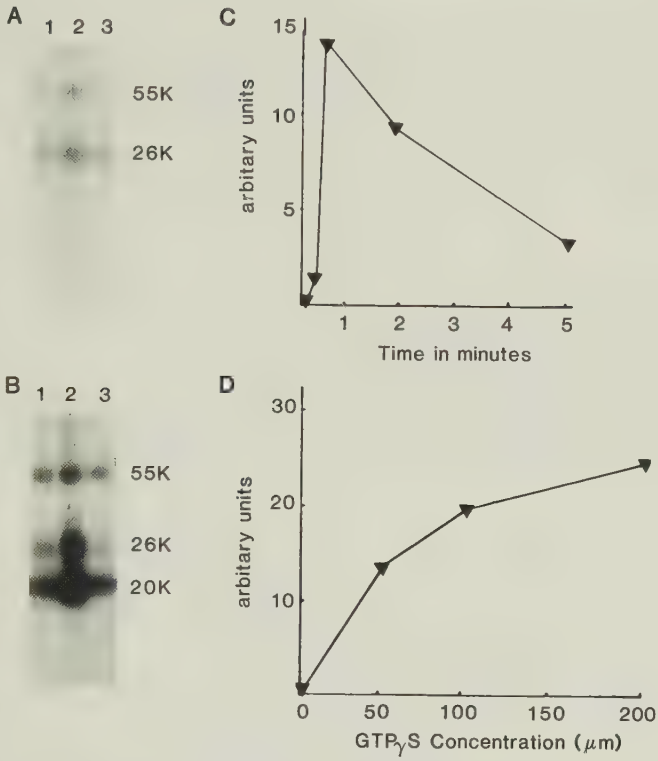

Fig 1. GTPγS regulates CD3 γ chain phosphorylation.

A),B) SDS/PAGE analyses of ^{32}P labelled CD3 antigen immunoprecipitates prepared from T cell microsomes which had been A) unstimulated (track 1), exposed to 100μM GTPγS (track 2) or 100μM GDPβS (track 3) for 2 minutes. B) unstimulated (track 1) or exposed to 100μM GTPγS (track 2) or 100μM cAMP (track 3) for 2 minutes.

C) Kinetics of GTPγS stimulated γ chain phosphorylation. CD3 immunoprecipitates were prepared from T cell microsomes phosphorylated *in vitro* in the presence of 100μM GTPγS for the indicated time.

D) Concentration dependence of GTPγS effects on γ chain phosphorylation. T cell microsomes were phosphorylated *in vitro* in the presence of the indicated concentration of GTPγS for 2 minutes. Data in C,D show ^{32}P incorporation into the γ chain as quantitated by densitometry (arbitary units) of autoradiographs of SDS/PAGE analyses of CD3 immunoprecipiates.

The identity of the more acidic peptide which elutes in peak D is unknown, although it could represent γ chains phosphorylated on both Ser 123 and 126.

The effect of phorbol esters on γ chain phosphorylation. GTPγS could effect γ chain phosphorylation in T cell microsomes via stimulation of pkC. The experiment shown in Fig 3 compares the effects of GTPγS and the pkC activator Pdbu on CD3 antigen phosphorylation. The data indicate that Pdbu enhanced γ chain phosphorylation, but its maximum effect was not as great as that induced by GTPγS.

A Intra-cellular region of T3 γ chain

QDGVR|QSR|ASDK|QTLLPNDQLYQPLK|DR|EDDQYSHLQGNQLRRN

123 126 150

membrane

|Tryptic cleavage sites

Peptides QS^{123}-PO_4R, QS^{123}-$PO_4AS^{126}DK$ elute in peak B.

Peptide AS^{126}-PO_4DK elutes in peak C.

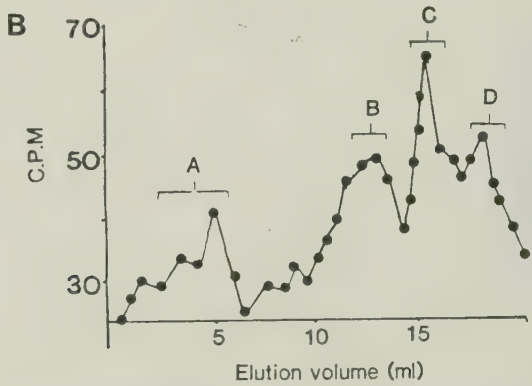

Fig 2. Anion exchange chromatographic analyses of tryptic peptides derived from in vitro ^{32}P labelled γ chain.

A) Amino acid sequence of the cytoplasmic domain of the CD3 γ subunit; vertical arrows indicate potential sites of tryptic cleavage.

B) Tryptic peptide analyses of the γ chain phosphorylated in vitro in T cell microsomes stimulated with GTPγS for 2 minutes. Previous studies have demonstrated that peak A represents radioactivity that does not bind to the column.

Peptides QS^{123}-PO_4R, QS^{123}-$PO_4AS^{126}DK$ elute in peak B.

Peptide AS^{126}-PO_4DK elutes in peak C.

The identity of peak D is unknown.

Discussion

The present data demonstrate that exposure of microsomes from T-lymphocytes to GTPγS leads to the phosphorylation of the γ subunit of the CD3 antigen, and that this effect is not mimiced by other nucleotides such as GDPβS and cAMP. GTPγS irreversibly activates G proteins and, thus, the present data provide indirect evidence for the involvement of a G protein(s) in the regulation of CD3 γ chain phosphorylation. This conclusion is compatible with the data of O'Shea et al who observed that aluminium fluoride complexes, which are thought to interact with G

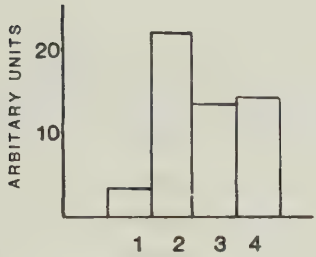

Fig 3. Effect of Pdbu on γ chain phosphorylation in T cell microsomes.

Data show ^{32}P incorporated into the γ chain, quantitated by densitometry (arbitary units) of autoradiographs of CD3 immunoprecipitates prepared from T cell microsomes phosphorylated *in vitro* for 2 minutes. Histograms 1-4 represent control, GTPγS (100μM), Pdbu (5ng/ml) Pdbu (50ng/ml) treated cells respectively.

proteins, modulated the phosphorylation of CD3 γ subunits (14). Protein phosphorylation is determined ultimately by a balance of kinase and phosphatase activities and, therefore, the enhancing effects of GTPγS can be explained in terms of the stimulation of kinase(s) and/or inhibition of phosphatase(s). One kinase that is known to regulate CD3 γ subunit phosphorylation *in vivo* is pkC (7). As GTPγS can activate phospholipase C in T lymphocytes (15,16), it is possible that GTPγS stimulates pkC in T cell microsomes via the breakdown of polyphosphoinositides and the subsequent generation of diacylglycerols. However, if the simple model of diacylglycerol activated pkC accounts for the enhancing effects of GTPγS on CD3 phosphorylation, then phorbol esters, which mimic the effect of diacylglycerols and activate pkC, should also enhance γ chain phosphorylation. Although Pdbu enhanced CD3 phosphorylation in T cell microsomes (Fig 3), it was much less effective than GTPγS, suggesting that GTPγS regulates CD3 γ chain phosphorylation via an alternative pathway or perhaps via a combination of pkC dependent and independent mechanisms. A further indication that pkC is not the only regulatory factor controlling the effects of GTPγS on CD3 phosphorylation in T cell microsomes, comes from the observation that in intact cells, serine residue 126 of the γ chain is the major target for pkC regulated phosphorylation, whereas GTPγS induced phosphorylation of residues 123 and 126. The latter pattern of phosphorylation is similar to that observed in intact cells following stimulation with ionomycin (10). As a result, it is possible that GTPγS modulates γ chain phosphorylation similarly to ionomycin via a calcium regulated kinase.

There are major differences between the pattern of phosphorylation of the CD3 antigen in T cell microsomes compared with intact cells. For example, in intact cells, the basal level of CD3 γ chain phosphorylation is

below the limits of experimental detection and induction of phosphorylation by external stimuli is both rapid and transient (7,8). In contrast, in T cell microsomes, phosphorylation of the γ chains was readily detected in the absence of known external stimuli. Another difference is that in intact cells the γ chain is the preferential target for phosphorylation, the δ chain is phosphorylated weakly and there is no detectable phosphorylation of the ε chain (7), whereas, in microsomes, there is marked phosphorylation of both the ε and δ chains. A possible explanation for the differences between the phosphorylation patterns in vivo and in vitro is that in intact cells the conformation of the CD3 antigen - T cell antigen receptor complex permits an interaction between a kinase and the γ chain, but prohibits a similar interaction with the δ and ε chains. It is also possible that in vitro, there is a breakdown in the restraints imposed by subcellular compartmentalisation on the localisation of the kinase with the result that potential phosphorylation sites in the extracellular domains of the δ and ε subunits become accessible to kinases.

References

1) Moller,G. (ed) (1984) Immunological Review 81
2) Borst,J., Alexander,S., Elder,J. and Terhorst,C. (1983) J.Biol.Chem. 258:5135-5141
3) Kanelopoulous,J.M., Wigglesworth,N.M., Owen,M.J. and Crumpton,M.J. (1983) EMBO J. 2:1807-1814
4) Cantrell,D.A., Davies,A.A., Londei,M., Feldman,M. and Crumpton,M.J. (1987) Nature 325:540-542
5) Samelson,L.E., Halford,J.B., Klausner,R.D. (1985) Cell 43:223-231
6) Samelson,L.E., Patel,M., Weissman,A., Harvard,J.B. and Klausner,R.D. (1986) Cell 46:1083-1090
7) Cantrell,D.A., Davies,A.A. and Crumpton,M.J. (1985) Proc.Nat.Acad.Sci.U.S.A 82:8158-8163
8) Krangel,M.J. (1987) J.Exp.Med. 165:1141-1159
9) Breightmeyer,J.B., Daly,J.F., Levine,H.B. and Schlossman,S.F. (1987) J.Immunol. 139:2899-2905
10) Davies,A.A., Cantrell,D.A., Hexham,J.M., Parker,P., Rothbard,J. and Crumpton,M.J. (1987) J.Biol.Chem. 262:10918-10921
11) Panteleo,G., Olive,D., Hogg,A., Kozumbo,W.J., Moretta,L., and Moretta,A. (1987) Eur.J.Immunol. 17:55-59
12) Zilberman,Y., Howe,L.R., Moore,J.P., Hesketh,T.R. and Metcalfe,S.C. (1987) Embo J. 6:957-962
13) Imboden,J., Shoebuck,D.M., Paterson,G. and Stobo,J.D. (1986) Proc.Nat.Acad.Sci.U.S.A 83:5673-5682
14) O'Shea,J.J., Urdahl,K.B., Luang,H.T., Chused,T.M., Samelson,L.E. and Klausner,R.D. (1987) J.Immunol. 139:3463-3469
15) Stryer,L. and Bourne,H.R. (1986) Annual Review of Cell Biology 2:391
16) Mire-Sluis,A.R., Hoffbrand,V., and Wickremasinghe,R.G. (1987) Biochemical and Biophysical Research Communications 148:1223-1231

ol. 156, No. 1, 1988
ctober 14, 1988

BIOCHEMICAL AND BIOPHYSICAL RESEARCH COMMUNICATIONS
Pages 335-339

A NOVEL ACTION OF ACTIVIN A: STIMULATION OF INSULIN SECRETION IN RAT PANCREATIC ISLETS

Yasuo Totsuka, Mari Tabuchi, Itaru Kojima,
Hiroshiro Shibai* and Etsuro Ogata

Fourth Department of Internal Medicine
University of Tokyo School of Medicine
Tokyo, Japan
*Central Research Laboratory, Ajinomoto,CO.
Kawasaki, Japan

Received August 26, 1988

The present study was conducted to examine an action of activin A on insulin secretion from rat pancreatic islets. In a batch incubation system, activin A stimulated insulin secretion in a dose-dependent manner at concentrations higher than 1 nM. Furthermore, activin A greatly potentiated glucose-induced insulin release. When islets were perifused with 1 nM activin A, insulin secretion was barely affected in this system. However, the insulin response to 16.7 mM glucose was greatly enhanced. Both the first and second phases of insulin response were enhanced by 1 nM activin A. These results indicate that, in addition to its known actions on pituitary-gonadal and hematopoietic systems, activin A modulates the function of pancreatic islets and stimulates insulin secretion. © 1988 Academic Press, Inc.

Activin A is a polypeptide with a molecular weight of 25,000 Da purified from ovarian fluid as a stimulator of follicle-stimulating hormone (FSH) secretion (1). It is a homodimer of the β -subunit of inhibin A, an inhibitory peptide of FSH secretion isolated from ovarian fluid (2). A related polypeptide activin, which is a heterodimer of β -subunits of inhibin A and inhibin B (3), also increases FSH secretion (see ref. 4 for review).

Address correspondence to: Etsuro Ogata, M.D., Ph.D.; Fourth Department of Medicine; University of Tokyo School of Medicine; 3-28-6 Mejirodai; Bunkyo-ku; Tokyo 112, Japan

0006-291X/88 $1.50
Copyright © 1988 by Academic Press, Inc.
All rights of reproduction in any form reserved.

Independent of these studies, Eto et al. isolated a polypeptide which causes differentiation of Friend erythroleukemia cells from conditioned medium of a phorbol ester-treated human monocytic leukemia cell line (5). The primary structure of this polypeptide, erythroid differentiation factor, is identical to that of activin A (6) and was shown to stimulate FSH secretion from primary culture of rat pituitary cells (7). Since activin A acts on at least pituitary, gonadal and erythroid cells (5), and since mRNA for activin A is found in several tissues (8), it is possible that activin A modulates various cell functions as a local regulator or a cytokine.

In the present study, we examined the effect of activin A on insulin secretion in rat pancreatic islets. The results indicate that activin A is a potent stimulator of insulin secretion.

Materials and Methods

Pancreatic islets were isolated from male Wistar rats weighing 200 g by using collagenase as described by Lacy et al. (9,10). Islets were suspended in a solution containing 115 mM NaCl, 5 mM KCl, 2.2 mM $CaCl_2$, 1 mM $MgCl_2$, 24 mM $NaHCO_3$, and 2.8 mM glucose equilibrated with 95% O_2 and 5% CO_2 gas. For batch incubation, an islet was incubated in 1 ml medium for 120 min at 37 °C. Perifusion of islets was performed as described by Zawalich et al. (11). Insulin was measured by radioimmunoassay using rat insulin (Novo Research Institute, Copenhagen, Denmark) as standard. Activin A was purified as described previously (5).

Results

To determine the effect of activin A on insulin secretion in pancreatic islets, we incubated islet with varying concentrations of activin A in the presence of a nonstimulatory concentration of glucose. As depicted in Figure 1, activin A increased insulin secretion at concentrations higher than 1 nM. Activin A-induced insulin release increased in a concentration-dependent manner and was almost saturated at 10 nM.

Figure 2 demonstrates the effect of activin A on glucose-mediated insulin secretion. In the absence of activin A, 16.7 mM glucose induced approximately 14-fold stimulation of insulin release. In the presence of 10

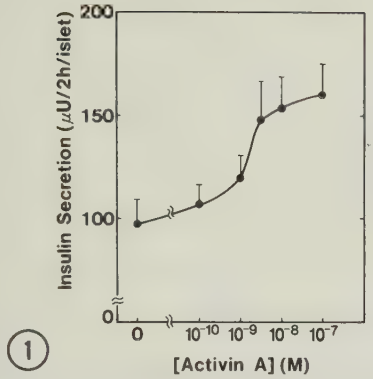

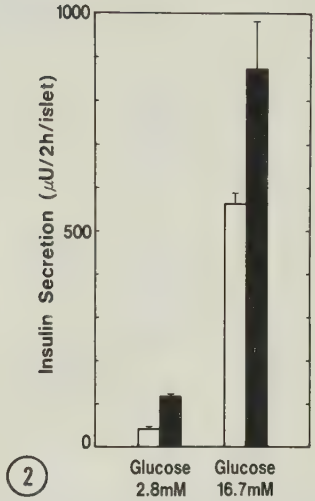

Figure 1. Dose Response Curve for Activin A-induced Insulin Secretion

An islet was incubated with various concentrations of activin A in the presence of 2.8 mM glucose for 120 min. Data are the mean ± S.E. for six determinations and the representative of three experiments with similar results.

Figure 2. Effect of Activin A on Glucose-induced Insulin Secretion

An islet was incubated with either 2.8 or 16.7 mM glucose in the presence and absence of 10 nM activin A for 120 min. Data are the mean ± S.E. for five determinations and the representative of three experiments with similar results.

nM activin A, glucose-mediated insulin secretion was greatly potentiated. The action of activin A was more than additive.

In the next set of experiments, we examined the effect of activin A on insulin secretion in perifusion system. As reported previously, 16.7 mM glucose induced a biphasic increase in insulin release. When 1 nM activin A was added in the presence of 2.8 mM glucose, it did not stimulate insulin secretion significantly. In the presence of 1 nM activin A , however, the insulin response to 16.7 mM glucose was greatly enhanced. The enhancement was evident in both first and second phases of insulin response. In particular, the second phase of glucose-mediated secretion was approximately 200% of that in the absence of activin A (Figure 3). It should be mentioned that the action of activin A was greater in the perifusion system than in the static incubation system.

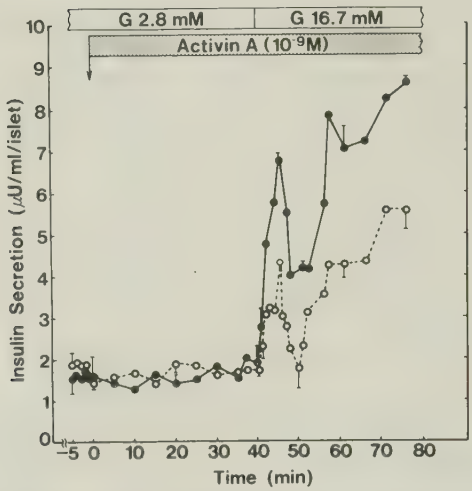

Figure 3. Effect of Activin A on Glucose-induced Insulin Secretion in Perifusion System

Islets were stimulated by 16.7 mM glucose as indicated in the presence (●) and absence (○) of 1 nM activin A . Values are the mean ± S.E. for three experiments.

Discussion

Results obtained in the present study clearly indicate that activin A acts on rat pancreatic islets to stimulate insulin secretion. Although concentrations of activin A which increase insulin secretion are relatively high, the results in Figure 3 demonstrate that a relatively low concentration of activin A (1 nM) enhances glucose-mediated insulin secretion. It should be emphasized that the action of activin A and glucose are synergic rather than additive. Hence, activin A potentiates glucose-mediated secretion. The mode of action of activin A resembles, in some aspect, that of cholecystokinin (CCK), which by itself is a weak stimulator but greatly potentiates glucose-mediated secretion (12). At present the mechanism by which activin A potentiates glucose action is not known. It is tempting to speculate that activin A causes phosphoinositide turnover in β -cells since activin A causes hydrolysis of phosphoinositide in Friend erythroleukemia cells (13) and since CCK potentiates glucose action by causing phosphoinositide turnover (14). It is possible that, in addition to phosphoinositide turnover, activin A may activate an additional transduction mechanism.

The present results are in agreement with our unpublished observation that intraperitoneal administration of activin A results in a marked decrease in plasma glucose concentration in mice. It is quite likely that activin A modulates insulin secretion both in vivo and in vitro. At present the physiological significance of activin A-induced insulin secretion is not certain. It is presumed that both inhibin and activins are present in plasma (4). It is thus possible that activin A in plasma affects insulin secretion in vivo. More importantly, it is also possible that activin A exists in pancreatic islets and modulates insulin secretion as a local regulator. Studies are now in progress in our laboratory to examine this possibility.

Acknowledgment

This work was supported by grants from The Ministry of Education, Science and Culture of Japan and Workshop on Cell Calcium Signal in Cardiovascular System.

References

1) Vale,W.,Rivier,J.,Vaughan,J.,McClintock,R.,CorriganmA.,Woo,W.,Karr,D. and Spiess,J. (1986) Nature 321,776-778.
2) Ling,N.,Ying,S-Y.,Ueno,N.,Esch,F.,Denoroy,L. and Guillmin,R. (1985) Proc.Natl.Acad.Sci.USA. 82,7217-7222.
3) Ling,N.,Ying,S-Y.,Ueno,N.,Shimasaki,S.,Esch,F.,Hotta,M. and Guillmin,R. (1986) Nature 321, 779-781.
4) Ying,S-Y. (1988) Endocrine Review 9, 267-293.
5) Eto,Y.,Tsuji,T.,Takegawa,M.,Takano,S.,Yakagawa,Y. and Shibai,H. (1987) Biochem.Biophys.Res.Commun. 142, 1095-1099.
6) Murata,M.,Eto,Y.,Shibai,H.,Sakai,M. and Muramatsu,M. (1988) Proc.Natl.Acad.Sci.USA. 85,2434-2438.
7) Kitaoka,M.,Yamashita,N.,Eto,Y.,Shibai,H. and Ogata,E. (1987) Biochem. Biophys.res.Commun. 146,1382-1386.
8) Yu,J.,Shao,L.,Lemas,V.,Yu,A.L.,Vaughan,J.,Rivier,J. and Vale,W. (1987) Nature 330, 765-767.
9) Lacy,P.E. and Kostianovski,M., (1967) Diabetes 16, 35-39.
10) Sharp,D.W.,Kemp,C.B.,Knight,M.J.,Ballinger,W.F. and Lacy,P.E. (1973) Transplantation 16, 686-689.
11) Zawalich,W.,Brown,C. and Rasmussen,H. (1983) Biochem.Biophys.Res. Commun. 117,448-455.
12) Zawalich,W. and Daiz,V.A. (1987) Diabetes 36, 118-122.
13) Shibata,H.,Ogata,E.,Eto,Y.,Shibai,H. and Kojima,I. (1987) Biochem.Biophys.Res.Commun. 146,187-193.
14) Zawalich,W.,Daiz,V.A. and Zawalich,K.C. (1987) Diabetes 36, 1420-1424.

Vol. 156, No. 1, 1988 BIOCHEMICAL AND BIOPHYSICAL RESEARCH COMMUNICATIONS
October 14, 1988 Pages 340-347

RNA MEDIATED FORMATION OF A PHOSPHOROTHIOATE DIESTER BOND

Jamal M. Buzayan*, Paul A. Feldstein*, George Bruening* and Fritz Eckstein+

* Department of Plant Pathology, College of Agricultural and Environmental Sciences, University of California, Davis, California 95616

+ Max-Planck-Institut für experimentelle Medizin, Abteilung Chemie, Hermann-Rein-Strasse 3, D-3400 Göttingen, West Germany

Received September 6, 1988

Summary: Previous results showed that multimeric, tandemly sequence-repeated forms of satellite tobacco ringspot virus RNA of the encapsidated polarity (STobRV (+)RNA) autolytically process at a specific phosphodiester bond, the junction. Substituting a phosphorothioate diester bond for the STobRV (+)RNA junction drastically slowed autolytic processing. Here we show that for the complementary STobRV (-)RNA, in contrast, replacing sets of phosphodiester bonds with phosphorothioate diester bonds, even at the junction, did not greatly slow autolytic processing or spontaneous ligation, the usual reactions of the unmodified RNA. In the ligation reaction STobRV (-)RNA directed the formation of an ApG phosphorothioate diester bond. © 1988 Academic Press, Inc.

STobRV RNA, like other plant virus satellite RNAs (1-5), replicates only in association with a specific supporting virus, TobRV. STobRV RNA reduces the TobRV titer and symptom severity and thus has potential as a practical antiviral agent (6). The nucleotide sequences of known STobRV RNA isolates (7) comprise 359 or 360 nucleotide residues (nt). Multimeric forms (8) of STobRV RNA have this "monomeric" sequence tandemly repeated, the repeats joined at a specific phosphodiester bond designated as the junction. Autolytic processing, at CpA junctions in the encapsidated, or (+), polarity sequence (9) and at the ApG junctions in the complementary, or (-), sequence (10,11), releases the respective monomeric RNAs.

"P-M-D" designates the transcript of a circularly permuted, dimeric STobRV RNA cDNA sequence from an appropriately linearized plasmid, with the hyphens representing the phosphodiester bond junctions. P-M-D autolytically processes into P, M, and D and its partial autolysis products P-M and M-D. The terminal groups generated during processing of STobRV (-)RNA sequences are a guanosine-5'-hydroxyl group and an adenylate-2':3'-cyclic phosphodiester (10). As reported (10), the reverse of the autolytic processing reaction of

Abbreviations: **STobRV RNA**, satellite tobacco ringspot virus RNA; **TobRV**, tobacco ringspot virus; **P**, promoter proximal region of transcript; **D**, promoter distal region of transcript; **M**, monomeric STobRV RNA; **cM**, circular monomeric STobRV RNA; **[αS]rNTP**, nucleoside-5'-O-(1-thiotriphosphate); **PAGE**, polyacrylamide gel electrophoresis.

0006-291X/88 $1.50
Copyright © 1988 by Academic Press, Inc.
All rights of reproduction in any form reserved.

STobRV (-)RNA also proceeds to a significant extent, generating P-D from P and D as well as cM from M (e.g., Fig. 1, lane 1). The autolytic processing and spontaneous ligation reactions are possible steps in proposed schemes for the replication of STobRV RNA (9,10,12,13).

That phosphorothioate diester bonds may only slightly alter the conformation and reactivities of some RNA molecules is indicated by their recognition by enzymes and activity in cells (14-16). Each phosphorothioate diester bond has a non-bridging oxygen atom of the corresponding phosphodiester replaced stereospecifically by a sulfur atom. RNA polymerases (EC2.7.7.6) accept as substrates the Sp diastereomers of [αS]rNTPs. The resulting phosphorothioate diester bonds have the Rp configuration (14). We report properties of STobRV (-)RNA sequences synthesized in reaction mixtures with up to four of the rNTPs replaced by the corresponding [αS]rNTPs.

Materials and Methods

Plasmids and transcripts: Plasmids pSP641 (10) and p20SD(-)3 (17) have circularly permuted STobRV RNA dimeric cDNA inserts oriented for transcription of STobRV (-)RNA from bacteriophage SP6 and T7 promoters, respectively. Bacteriophage SP6 RNA polymerase is expected to transcribe from restriction endonuclease (EC3.1.21.4) SmaI-linearized pSP641 a 759 nt P-M-D with 199 and 165 nt of STobRV RNA sequences in the P and D portions. An additional vector-derived 34 and 2 nt are at the 5' and 3' ends, respectively. The bacteriophage T7 RNA polymerase-catalyzed, 807 nt transcript of HindIII-linearized p20SD(-)3 is similar, but with 48 and 36, respectively, 5' and 3' vector derived nt.

Reactions of 1 hr duration were at 40° with SP6 RNA polymerase (1 U/μl) and 0.09 μCi/μl [α^{32}P]rCTP or at 37° with T7 RNA polymerase (3.6 U/μl) and 0.25 μCi/μl [α^{32}P]rGTP in 1X transcription buffer (40 mM Tris-HCl, pH 7.5, 20 mM NaCl, 6 mM $MgCl_2$, 2 mM spermidine-HCl) containing 10 mM dithiothreitol and 0.5 mM of each rNTP. The mixed diastereomers of [αS]rUTP and [αS]rCTP, at 0.5 mM and 1.0 mM, respectively, were substituted for the corresponding rNTPs. The substitutions for rATP and rGTP were by the corresponding Sp-[αS]rNTPs at 0.5 mM. The buffer for PAGE in 7 M urea was 90 mM Tris, 90 mM boric acid, 2.5 mM disodium EDTA. Gel zones for each P-M-D and its corresponding autolytic processing and spontaneous ligation products were soaked for 24 hr, and the suspension was subjected to Cerenkov counting as described (20). The percentage of processing was calculated from T, the combined radioactivity of all zones, and S, the radioactivity of the P-M-D zone, from the formula 100 x (T-S)/T.

Spontaneously-ligated RNA and its junction-containing fragment: RNA cM, spontaneously formed from M (10), was hybridized to the oligodeoxyribonucleotide d35-68(+), which has the nucleotide sequence dGGACGAAACAGGACTGTCATGTGGCCGAAAGCCA. d35-68(+) is complementary to the sequence variant of cM used here except at position 54 (11), as indicated by the break in the vertical bar in Fig. 3. The molecular hybrid of d35-68(+) and cM was partially digested (21) by incubation with ribonuclease T_1 (EC3.1.27.3). The DNA-RNA hybrids were melted, and the oligoribonucleotide products were separated by 20% PAGE.

Oligoribonucleotides, located by autoradiography, were eluted from gel slices, 5'-^{32}P-labeled in a bacteriophage T4 polynucleotide kinase-catalyzed (EC.2.7.1.78) reaction, and electrophoretically purified before being partially degraded by ribonucleases and base (22,23). Oligoribonucleotides also were cleaved partially at phosphorothioate diester bonds by incubation with iodoethanol at 95° for 3 min under conditions similar to those described by Gish and Eckstein (24) except that iodoethanol was dissolved in the 95% formamide solution of dyes to a concentration of 6% rather than 7%. This solution was

added directly to dried oligoribonucleotide. Analyses of products was by 20% PAGE and autoradiography.

Results

Effects of [αS]rNTPs on transcription and autolytic processing of transcripts: Transcription catalyzed by 3.6 U/μl bacteriophage T7 RNA polymerase gave little variation in the extent of P-M-D synthesis in 1 hr regardless of the set of rNTPs and [αS]rNTPs in the reaction mixtures. Substituting [αS]rGTP for rGTP or [αS]rCTP for rCTP reduced the extent of synthesis catalyzed by 1 U/μl bacteriophage SP6 RNA polymerase to 85% or less of the control value. Replacing rGTP with [αS]rGTP to modify the ApG junction and other NpG bonds did not decrease the autolytic processing of P-M-D as observed at the end of a 1 hr incubation (Fig. 1, lane 2). Substitution of all four

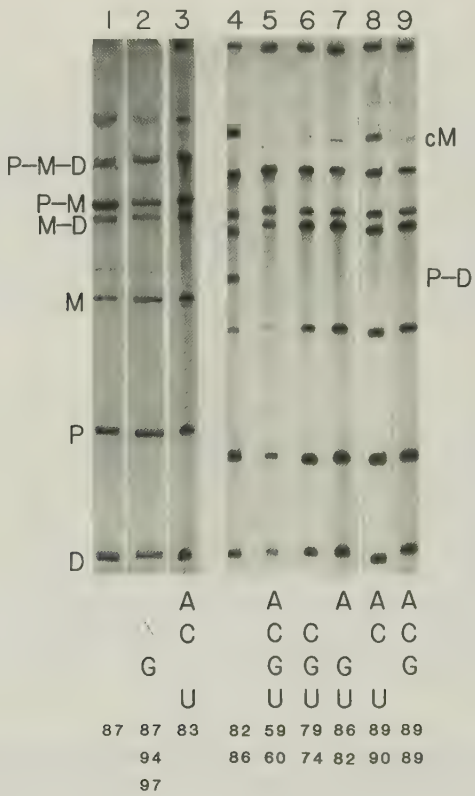

FIGURE 1. Autolytic processing of STobRV (-)RNAs that contain phosphorothioate diester bonds. The transcripts of plasmids pSP641 (lanes 1-3) and plasmid p20SD(-)3 (lanes 4-9) partially autolytically processed and spontaneously ligated during the time of incubation of the transcription reaction mixtures. Products were resolved by 6.5% PAGE and were detected by autoradiography. The zones for the transcript P-M-D and its autolytic processing products are marked to the left of the lanes; zones for the spontaneous ligation products P-D and circularized monomer, cM, are indicated to the right. The letters below each lane designate the rNTPs that were replaced by the respective [αS]rNTPs in the transcription reaction mixtures: no substitution for the samples applied to lanes 1 and 4, [αS]rGTP for rGTP in lane 2, etc. Each of the 17 numbers below the lanes is the result of a separate determination of the percentage of the transcript that was converted to products of autolytic processing and spontaneous ligation. The first line of percentages corresponds to the gel of the autoradiogram shown.

rNTPs did signficantly reduce processing (lane 5), but even the most inhibitory tri-substitution, for rCTP, rGTP and rUTP (lane 6), still allowed more than 70% of the autolytic processing observed for the control with no substitutions of rNTPs by [αS]rNTPs.

Effects of phosphorothioate diester bonds on spontaneous ligation: The ligation of M to cM is more robust than the joining of P and D, occurring even in buffered solution of the metal ion chelator EDTA (10). The conversion of M to cM during the 1 hr transcription in a solution containing either all rNTPs or rATP, rCTP, rUTP and [αS]rGTP gave, respectively, cM values, as a percentage of total monomer, of 64 +/- 5% and 15 +/- 12% (average and standard deviation from three experiments). M and cM from the [αS]rGTP-derived transcript were electrophoretically purified and incubated in 1X transcription buffer for 150 min at room temperature, giving percentages of cM of 45% and 60%, respectively. Apparently phosphorothioate substitution had less effect on the M to cM equilibrium than on the rate of cM formation. Synthesis from all four [αS]rNTPs greatly reduced but did not prevent cM formation (Fig. 2, lanes 1 and 2). Of the four tri-substitutions of [αS]rNTPs tested, substitution of

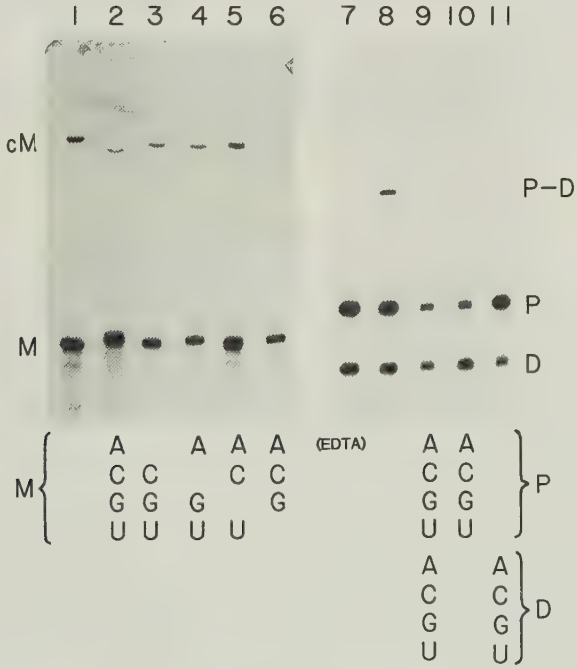

FIGURE 2. Spontaneous ligation of STobRV (-)RNAs that contain phosphorothioate diester bonds. RNAs P, M and D were purified by 6.5% PAGE, from reaction mixtures in which HindIII-linearized p20SD(-)3 was transcribed by bacteriophage T7 RNA polymerase. From 0.5 to 1 μg of monomeric RNA M was incubated in 7 μl of 1X transcription buffer for 150 min at room temperature (lanes 1-6). From 0.4 to 1.2 μg each of P and D were incubated in 10 μl of 1X transcription buffer (lanes 8-11) or 1X transcription buffer with 10 mM EDTA in place of $MgCl_2$ and spermidine (lane 7) for 90 min at room temperature. Reactions were stopped by an addition of 1 μl of 200 mM EDTA and 5 μl of tracking dye solution in formamide. Detection of reactants and products was by 6.5% PAGE and autoradiography. The letters below each lane designate the rNTPs that were replaced by the respective [αS]rNTPs in the source transcription reaction mixtures.

all but rGTP allowed the greatest accumulation of cM (Fig. 2, lanes 3-6). Fig. 2, lanes 7-11 shows the effects of synthesis from four [αS]rNTPs on the ligation of P to D.

Formation of a phosphorothioate diester bond during RNA-directed spontaneous ligation. Monomeric STobRV (-)RNA, derived from transcript synthesized from [αS]rGTP, was allowed to circularize. An RNA fragment recovered from the junction region of cM was too small to be capable of autolytic processing (21). Two such oligoribonucleotide preparations were purified, end-labeled, and partially degraded to determine their structure (Fig. 3, panels A and B). Within the range of digestion products resolved in Fig. 3., ribonucleases T_1 and U_2 (EC3.1.27.4) cleaved to the 3' side of the guanylate and purine (adenylate > guanylate) residues, except at those positions that have phosphorothioate diester bonds derived from [αS]rGTP, corresponding to A49 and G60. The phosphodiester bond to the 3' side of G59, which is next to two phosphorothioate diester bonds, cleaved inefficiently (lanes 6 and 2). The phosphodiester forms of these three bonds are known to be cleaved efficiently by ribonucleases U_2, T_1 and T_1, respectively (21; Fig. 4 of 13).

Iodoethanol is expected to cleave bonds to the 5'-side of guanylate residues in RNA synthesized from [αS]rGTP, rATP, rCTP and rUTP (24). The family of oligoribonucleotides generated by iodoethanol thus should migrate more rapidly than the family generated by ribonuclease T_1. The locations of guanylate residues in the sequence and a relationship between the mobilities of ribonuclease T_1- and iodoethanol-generated zones are indicated in lane 3, Fig. 3.

Discussion

Several small RNAs that replicate in plants, including plant virus-associated satellite RNAs (25) and one viroid (26), exhibit autolytic processing to generate cleavage products which have as their new ends a 5'-hydroxyl group and a 2':3'-cyclic phosphodiester bond. Of these RNAs, including STobRV (+)RNA, only STobRV (-)RNA has exhibited an extensive back reaction, i.e., spontaneous, not enyzme-catalyzed ligation. We found that even STobRV (-)RNA synthesized from all four [αS]rNTPs processed efficiently (Fig. 1, lane 5). In contrast, autolytic processing of circularly-permuted, dimeric STobRV (+)RNA was not detected when the transcript was synthesized in the presence of [αS]rATP as the only [αS]rNTP, which introduces phosphorothioate diester bonds at the CpA junction and other NpA bonds (20).

Ribonucleases A (EC3.1.27.5), T_1 and T_2 (EC3.1.27.1) cleave Rp phosphorothioate diester bonds more slowly than the corresponding phosphodiester bonds (14,27). The two curved arrows in Fig. 3 define the ends of the oligoribonucleotide as expected from the combined effects of resistant phosphorothioate diester bonds and the hybridized d35-68(+). The phosphorothioate diester junction, at nt 49-48, resisted cleavage by ribonuclease U_2 under conditions of partial digestion and was specifically cleaved by iodoethanol (Fig. 3). We conclude that the STobRV (-)RNA sequence directed the spontaneous formation of an ApG phosphorothioate diester bond, which presumably is 3'-to-5' (21). Since the spontaneous ligation reaction is expected to be the reverse of autolysis, ligation should stereospecifically

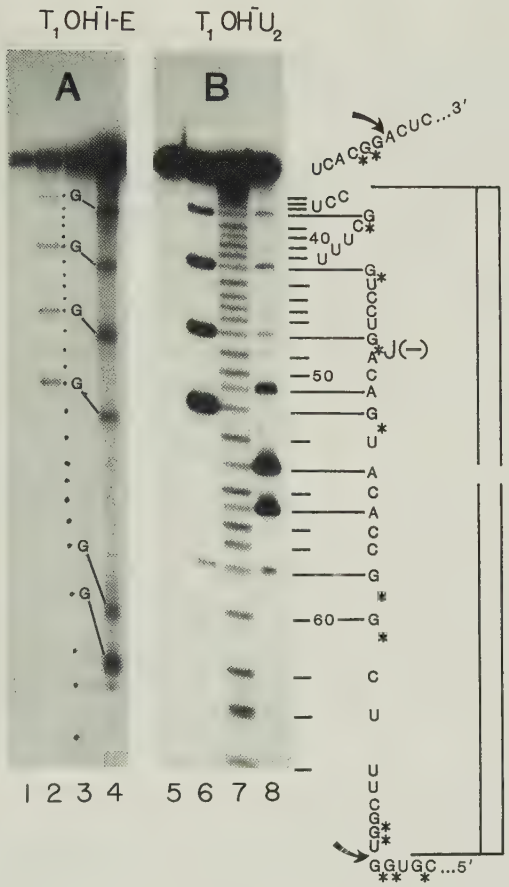

FIGURE 3. A phosphorothioate diester bond in the junction of spontaneously formed STobRV (-)RNA circles. STobRV (-)RNA was transcribed from p20SD(-)3 in the presence of [αS]rGTP, in place of rGTP, and 80 μCi [α^{32}P]rCTP per 200 μl reaction mixture. Electrophoretically purified RNA M circularized spontaneously when incubated as described in the Fig. 2 legend. A ribonuclease T_1-resistant oligoribonucleotide, protected by hybridization of cM to oligodeoxyribonucleotide d35-68(+), was electrophoretically purified, 5'-terminally labeled, and subjected to sequence analysis (21). Partial degradations were with the guanylate specific ribonuclease T_1 (lanes 2 and 6), the phosphorothioate diester bond-specific reagent iodoethanol (lane 4), base (lanes 3 and 7), and the purine-specific (adenylate > guanylate) ribonuclease U_2 (lane 8). The controls (lanes 1 and 5) were incubated as for the ribonuclease T_1 reaction but with no enzyme. Dots in lane 3 locate zones generated by partial base hydrolysis, which were insufficiently exposed to photographically reproduce. The bar on the right corresponds to the region of the RNA sequence that is complementary to oligodeoxyribonucleotide d35-68(+) and J(-) locates the ApG junction phosphodiester bond. Asterisks indicate phosphorothioate diester bonds expected to be derived from [αS]rGTP. The long horizontal lines to the right of the autoradiograms designate the nt identified by combining information from the partial degradations of the oligoribonucleotide by ribonucleases and by iodoethanol. A secondary indication of the locations of guanylate residues in the sequence is the exceptionally wide spacing between the zones for oligoribonucleotides that differ by removal of a 3'-terminal guanylate residue (compare Fig. 1 of ref. 30).

generate the Rp configuration of a phosphorothioate diester bond as the newly formed junction (14,28).

Results in lanes 10 and 11 of Fig. 2 show that, for RNA synthesized from all four [αS]rNTPs, ligation was reduced less by phosphorothioate diester

bonds to the 3' side of the junction than to those of RNA P, which are to the 5' side of, and actually form, the junction. RNA M synthesized from [αS]rATP, [αS]rCTP, rGTP and [αS]rUTP apparently circularized as readily as M with all phosphodiester bonds (Fig. 2, lanes 5 and 1) and more readily than any of the RNA M molecules sythesized from [αS]rGTP and two other [αS]rNTPs (Fig. 2, lanes 3-6). These results imply that the [αS]rGTP substitution was the most influential in retarding cM formation. RNA M molecules with phosphorothioate diester bonds derived from [αS]rGTP and any other two or the other three [αS]rNTPs had a reduced electrophoretic mobility (Fig. 1, lanes 4-9; Fig. 2, lanes 1-6). Thus, although incorporation from [αS]rGTP alone did not cause a detected decrease in the mobility of M (Fig. 1, lanes 1 and 2), phosphorothioate diester bonds derived from [αS]rGTP may influence the conformation of RNA M as well as the chemical structure of the junction.

The phosphorothioate P-S bond is expected to be longer than the corresponding non-bridging phosphodiester P-O bond, and the bond angles of the two 2':3'-cyclic ester compounds are different (29). Our results show that the substitution of phosphorothioate diester bonds for phosphodiester bonds resulted in no detected slowing of base-catalyzed chain cleavage (Fig. 3), little alteration of the equilibrium between the unligated and ligated forms of the monomeric STobRV (-)RNA, and a slight slowing of the rate-limiting step in the ligation (and presumably the autolysis) reactions.

Acknowledgments: This paper is dedicated to the memory of Dr. Irving R. Schneider, the discoverer of satellite tobacco ringspot virus RNA, who died 26 February, 1988. P.A.F. is a McKnight Foundation Training Program Fellow. This research was supported by the United States Public Health Service, under NIH grant GM37627, and by the Agricultural Experiment Station of the University of California.

References

1. Schneider, I.R. (1977) In Beltsville Symposia in Agricultural Research. I. Virology in Agriculture, J.A. Romberger, Ed. (Allenheld, Osmun & Co., Montclair, New Jersey), pp. 201-219.
2. Murant, A.F., and Mayo, M.A. (1982) Annu. Rev. Phytopathol. 20, 49-70.
3. Kaper, J.M., and Tousignant, M.E. (1984) Endeavour (New Series) 8, 194-200.
4. Francki, R.I.B., Randles, J.W., Chu, P.W.G., Rohozinski, J., and Hatta, T. (1985) In Subviral Pathogens of Plants and Animals: Viroids and Prions (K. Maramorosch and J.J. McKelvey, eds.), Academic Press, New York. pp. 265-297.
5. Francki, R.I.B. (1985) Annu. Rev. Microbiol. 39, 151-174.
6. Gerlach, W.L., Llewellyn, D., and Haseloff, J. (1987) Nature 328, 802-805.
7. Buzayan, J.M., McNinch, J.S., Schneider, I.R., and Bruening, G. (1987) Virology 160, 95-99.
8. Kiefer, M.C., Daubert, S.D., Schneider, I.R., and Bruening, G. (1982) Virology 121, 262-273.
9. Prody, G.A., Bakos, J.T., Buzayan, J.M., Schneider, I.R., and Bruening, G. (1986) Science 231, 1577-1580.
10. Buzayan, J.M., Gerlach, W.L., and Bruening, G. (1986) Nature (London) 323, 349-353.
11. Buzayan, J.M., Gerlach, W.L., Bruening, G., Keese, P., and Gould, A.R. (1986) Virology 151, 186-199.

12. Symons, R.H., Haseloff, J., Visvader, J.E., Keese, P., Murphy, P.J., Gill, D.S., Gordon, K.H.J., and Bruening, G. (1985) In **Subviral Pathogens of Plants and Animals: Viroids and Prions** (K. Maramorosch and J.J. McKelvey, Jr., eds.), Academic Press, Inc., New York. pp. 235-263.
13. Bruening, G., Buzayan, J.M., Hampel, A., and Gerlach, W.L. (1988) Chapter 6 in RNA Genetics, Book I: RNA Replication (J. Holland, E. Domingo and P. Ahlquist, Eds.), CRC Press Inc., Boca Raton, Florida. (in press)
14. Eckstein, F. (1985) Annu. Rev. Biochem. 54, 367-402; 15. DeClercq, E., Eckstein, F., Sternbach, H., and Merigan, T.C. (1970) Virology 42, 421-428.
16. Nicholson, A.W., Niebling, K.R., McOsker, P.L., and Robertson, H.D. (1988) Nucleic Acids Res. 16, 1577-1591.
17. Ponz, F., Rowhani, A., Mircetich, S.M., and Bruening, G. (1987) Virology 160, 183-190.
18. Green, M.R., Maniatis, T., and Melton, D.A. (1983) Cell 32, 681-694.
19. Davanloo, P., Rosenberg, A.H., Dunn, J.J., and Studier, F.W. (1984) Proc. Nat. Acad. Sci. USA 81, 2035-2039.
20. Buzayan, J.M., Feldstein, P.A., Segrelles, C., and Bruening, G. (1988) Nucleic Acids Res. 16, 4009-4023.
21. Buzayan, J.M., Hampel, A., and Bruening, G. (1986) Nucleic Acids Res. 14, 9729-9743.
22. Donis-Keller, H., Maxam, A.M., and Gilbert, W. (1977) Nucleic Acids Res. 4, 2527-2538.
23. Krupp, G. and Gross, H.J. (1979) Nucleic Acids Res. 6, 3481-3490.
24. Gish, G., and Eckstein, F. (1988) Science 240, 1520-1522.
25. Forster, A.C. and Symons, R.H. (1987) Cell 50, 9-16.
26. Hutchins, C.J., Rathjen, P.D., Forster, A.C., and Symons, R.H. (1986) Nucleic Acids Res. 14, 3627-3640.
27. Burgers, P.M.J., and Eckstein, F. (1979) Biochemistry 18, 592-596.
28. Eckstein, F., Romaniuk, P.J., Connolly, B.A. (1982) Meth. Enzymol. 87, 197-212.
29. Saenger, W., and Eckstein, F. (1970) J. Am. Chem. Soc. 92, 4712-4723.
30. Haseloff, J., and Symons, R.H. (1981) Nucl. Acids Res. 9, 2741-2752.

Vol. 156, No. 1, 1988 BIOCHEMICAL AND BIOPHYSICAL RESEARCH COMMUNICATIONS
October 14, 1988 Pages 348-354

INTERACTION BETWEEN α1 AND β1 SUBUNITS OF HUMAN HEMOGLOBIN

Yasuko Kawamura-Konishi* and Haruo Suzuki

Department of Biophysical Chemistry, Kitasato University School of Medicine, Sagamihara, Kanagawa 228, Japan

Received September 8, 1988

We prepared normal and modified α and β globin chains in which C-terminal residues were enzymatically removed. The CD spectra of the deoxy form of these chains and the reconstituted modified Hb's were measured in the Soret region. The CD spectra of the modified Hb's were markedly different from the arithmetic means of respective spectra of their constituent chains. This difference was ascribed to the interaction between α1 and β1 subunits to make the α1β1 dimer. The peak wavelength of the difference CD spectra could be classified into two groups, one was 433±1 nm and the other 437±1 nm. A comparison of this classification with the previously identified quaternary structures revealed that the R and T structures showed a maximum of the difference CD spectra at 437±1 nm and 433±1 nm, respectively. These results indicated that the R and T structures differed in the interaction between α1 and β1 subunits. © 1988 Academic Press, Inc.

Hemoglobin (Hb) is a tetrameric protein composed of two α and two β chains. The quaternary structure of deoxy Hb is known to be different from that of oxy Hb [1,2]: the former is a so-called "T structure", the latter is a "R structure". In both the structures, α1β1 dimer has a very similar conformation and the intersubunit contacts at the α1β1 interface are identical [1-3]. Therefore, it has been generally accepted that the interaction between α1 and β1 subunits (the α1 β1 interaction) did not change during the R-T transition of quaternary structure.

The C-terminal residues of deoxy Hb form salt bridges and hydrogen bonds with specific residues [1]. These interactions help to stabilize

* To whom correspondence should be addressed.
Abbreviations: des-, modified by proteolytic removal of C-terminal residue(s) from α and/or β chains; IHP, inositol hexaphosphate; Tris, tris(hydroxymethyl)aminomethane; Bis-Tris, bis(2-hydroxyethyl)imino-tris(hydroxymethyl)methane.

0006-291X/88 $1.50
Copyright © 1988 by Academic Press, Inc.
All rights of reproduction in any form reserved.

the deoxy Hb quaternary structure. Chemically modified Hb's, in which C-terminal residues are removed by carboxypeptidases A and B, are capable of undergoing the R-T structural interconversion within the deoxy state [1,4-10]. On the other hand, the CD spectra in the Soret resion are known to be changed upon assembling of isolated α and β chains to reconstitute Hb molecule [11]. The Soret CD change reflects the interaction between α1 and β1 subunits to make the α1β1 dimer from α and β chains [12-15].

In order to clarify whether the α1β1 interaction is really identical in the R and T quaternary structures, we investigated the Soret CD change upon assembling of the modified α and β chains to reconstitute the modified Hb's. The results indicate that the R and T structures differ in the α1β1 interaction.

MATERIALS AND METHODS

Human Hb and its isolated α and β chains were prepared as previouly reported [12]. The modified chains were prepared from the isolated chains in the CO form by carboxypeptidases A and B (Cooper Biomedical Inc., New Jersey) as described by Kilmartin [16]. The digestion was monitored with a PICO-TAG amino acid analysis system (Waters Ltd., Massachusetts). Carbon monoxide was removed from the modified chains in a rotary evaporator under a stream of oxygen and strong illumination. Deoxygenation was achieved by addition of minimal amounts of sodium dithionite. Reconstitution was performed by mixing of equimolar concentrations of the α and β chains. All the protein concentrations were expressed on a heme basis, which was determined by the pyridine hemochromogen method. CD spectra and stopped-flow traces were measured at 15°C in a Union Giken Dichrograph III-J coupled with a NEC PC-9801F computer. The path of the observation cell was 10 mm.

RESULTS AND DISCUSSION

CD Spectra in the Soret Region The Soret CD spectra of normal and modified α and β chains and those of reconstituted Hb's were measured under three conditions : pH 6.0 ± 1mM IHP or pH 9.0. The difference CD between the spectra of the reconstituted Hb's and the arithmetic means of the spectra of the corresponding constituent chains was obtained.

Figure 1A shows the Soret CD spectra of isolated α (spectra a), β chains (spectra b), des-Argα141 α chain (spectra c) and des-Hisβ 146 β chain (spectra d) in the presence and absence of IHP at pH 6.0 or at pH 9.0. The intensity of the CD band was affected by modification of the chain or buffer conditions, while the peak position of the CD band was not.

Figure 1B shows the Soret CD spectra of reconstituted normal Hb (spectra e) and reconstituted des-Argα141-des-Hisβ146 Hb (spectra

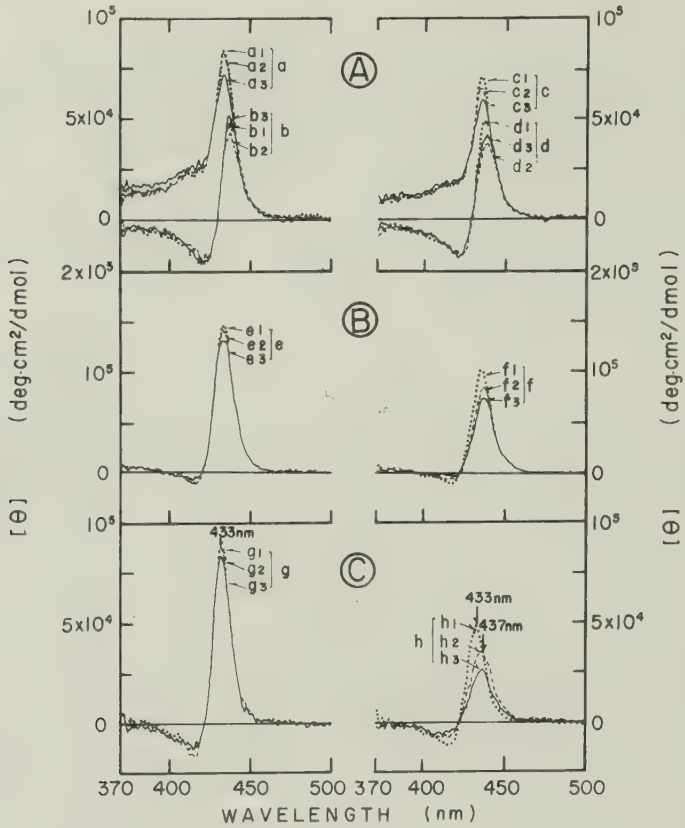

Figure 1. Soret CD spectra of chemically modified hemoglobins under three conditions : 0.1 M Bis-Tris, 0.1 M Cl^- at pH 6.0 in the presence (----; a1,b1,c1,d1,e1,f1,g1 and h1) and absence (-- ; a2,b2,c2,d2,e2,f2, g2 and h2) of 1 mM IHP ; 0.1 M Tris, 0.1 M Cl^- at pH 9.0 (—; a3,b3,c3, d3,e3,f3,g3 and h3). The ellipticity was expressed in molar ellipticity on a heme basis.
A; α chain (spectra a), β chain (spectra b), des-Arg α 141 α chain (spectra c), and des-His β 146 β chain (spectra d). B; Reconstituted normal Hb (spectra e), and reconstituted des-Arg α 141-des-His β 146 Hb (spectra f). C; The difference between the CD spectra of normal Hb and the arithmetic means of respective spectra of α and β chains (spectra g ; g1=e1-(a1+b1)/2, g2=e2-(a2+b2)/2, and g3=e3-(a3+b3)/2), and the difference between the CD spectra of reconstituted des-Arg α 141-des-His β 146 Hb and the arithmetic means of respective spectra of their constituent chains (spectra h ; h1=f1-(c1+d1)/2, h2=f2-(c2+d2)/2, and h3=f3-(c3+d3)/2).

f), which are equimolar mixtures of normal α and β chains for the former and of des-Arg α 141 α chain and des-His β 146 β chain for the latter. The intensity of the CD band of des-Arg α 141-desHis β 146 Hb was much smaller than that of normal Hb. The peak position of the CD band for normal Hb was not affected by buffer conditions. But des-Arg α 141-des-His β 146 Hb in the presence of IHP showed a blue-shift by about 1.5 nm relative to the spectrum in the absence of IHP (compare f1 with f2 and f3 spectra).

Figure 1C shows the difference CD spectra between the CD spectra of reconstituted normal Hb and the arithmetic means of the spectra of normal α and β chains (spectra g = e - (a+b)/2), and between the CD spectra of reconstituted des-Argα141-des-Hisβ146 Hb and the arithmetic means of the spectra of des-Argα141 α chain and des-Hisβ146 β chain (spectra h = f - (c+d)/2). The intensity of the difference CD band for normal Hb was somewhat affected by buffer conditions, while their peak position was not. A blue-shift in the peak position induced by IHP was found in des-Argα141-des-Hisβ146 Hb (compare h1 with h2 and h3 spectra) : the wavelengths of the CD peak in the presence and absence of IHP were 433±1 nm and 437±1 nm, respectively.

It is well-known that the Soret CD spectrum of reconstituted normal Hb is remarkably different from the arithmetic mean of respective spectra of its constituent chains [11]. This difference has been shown to be due to the interaction between α1 and β1 subunits to make the α1β1 dimer [12-15]. However, it is not clear that the difference between the CD spectra of reconstituted modified Hb and the arithmetic means of those of their constitutent chains is ascribed to the same interaction. In order to elucidate this problem, the Soret CD change after mixing of modified α and β chains was investigated kinetically with a CD stopped-flow apparatus.

CD Stopped-Flow Measurements Figure 2 shows a typical trace of the CD change in the Soret region after mixing of equimolar concentrations of des-Argα141 α chain and des-Hisβ146 β chain in the absence of IHP at pH 6.0. The time course gave a straight line in the second-order plots as shown in Figure 2 inset. The value of the slope of the straight line in the second-order plots increased linearly with an increase in the protein concentration, giving one straight line (Fig.3). The value of the second-order rate constant was obtained as $2.75 \times 10^5\ M^{-1}s^{-1}$ regardless of kinds of modified chains or addition of IHP (Fig.3). This value is comparable with a value of $6.4 \times 10^5\ M^{-1}s^{-1}$ for normal Hb at pH 7.5 and 25°C [12]. These results indicate that the Soret CD change after mixing of modified α and β chains obeyed the second-order reaction rate law, that is, the difference between the Soret CD spectra of the reconstituted modified Hb's and the arithmetic means of respective spectra of their constituent chains was induced by the interaction between α1 and β1 subunits to make the α1β1 dimer. Therefore, the difference CD spectra for modified Hb's which have been identified previously as the R or T structures will provide significant informations about the relationship between the quaternary structure and the α1β1 interaction. Then, we investigated the difference CD spectra

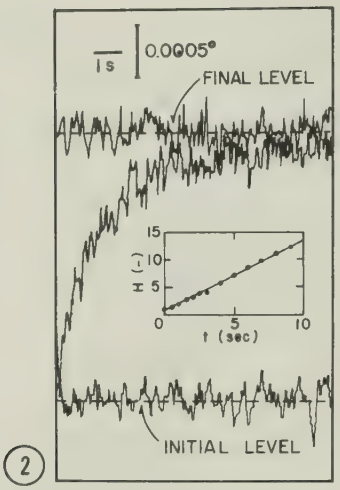

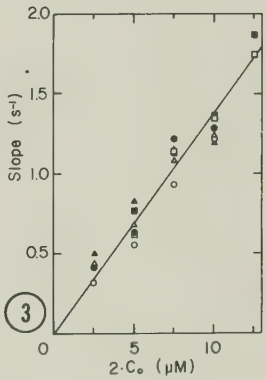

Figure 2. Time course of the CD change at 437 nm after mixing of equimolar concentrations of des-Argα141 α chain and des-Hisβ146 β chain in 0.1 M Bis-Tris (pH 6.0), 0.1M Cl^- at 15°C. The CD traces are of the average of 16 runs. The initial concentrations of both the chains (after mixing), C_0, were 10 μM. Initial level is the arithmetic mean of the CD of des-Argα141 α chain and des-Hisβ146 β chain, obtained with a computer. The inset shows second-order plots of the time course in Fig. 2. The ordinate H is given by $\Delta CD_f/(\Delta CD_f - \Delta CD)$ where ΔCD_f is total CD increases, ΔCD is the CD increase at time t.

Figure 3. Relationship between the slope of the second-order plots of the CD change and the concentation of the chains (after mixing), C_0. (○ , ●); normal Hb, (△ , ▲);des-Argα141-des-Hisβ146 Hb, (□ , ■); des-Argα141-Tyrα140-des-Hisβ146-Tyrβ145 Hb.
The Buffer conditions are 0.1 M Bis-Tris (pH 6.0), 0.1 M Cl^- in the absence of IHP (open symbols), and in the presence of 1 mM IHP (closed symbols).

of eight kinds of modified Hb's in the presence and absence of IHP at pH 6.0 and at pH 9.0, as follows.

The Difference CD Spectra The peak wavelength of the difference CD spectra could be classsified into two groups, one was 433±1 nm and the other 437±1 nm (Table I). The peak intensity of the difference CD spectra decreased with an increase in the number of removed residues (data not shown). The quaternary structures previously identified [4-10] are also given in Table I. A comparison of the classification with the quaternary structures revealed that the R and T structures showed a maximum of the difference CD spectra at about 437 nm and 433 nm, respectively, except des-Hisβ146-Tyrβ145 Hb at pH 6.0. Since the difference CD between the CD spectra of the reconstituted modified Hb's and the arithmetic means of those of their constitutent chains can be ascribed to the $\alpha 1\beta 1$ interaction as mentioned above, the difference in the peak wavelength of the difference CD spectra must reflect the difference in the $\alpha 1\beta 1$ interaction. Hsu and Woody showed [17] that the

Table I. The wavelength of maximum of the difference CD spectra between the CD spectra of reconstituted modifed Hb's and the arithmetic means of respective spectra of their constituent chains. Each wavelength includes an error of ± 1 nm. R and T indicate the quaternary structure of the modified Hb characterized previously. (R) and (T) are the quaternary structure predicted from the present work.

α chain	β chain	pH 6.0 + IHP	pH 6.0 - IHP	pH 9.0 - IHP	ref.
normal	normal	433 T	433 T	433 T	7
	des-His	433 T	433 T	433 T	5,6,7,10
	des-His-Tyr	433 T	433 R	433 (T)	5,8,9
des-Arg	normal	433 T	433 T	437 R	6,7,9,10
	des-His	433 T	437 R	437 (R)	6,7,10
	des-His-Tyr	433 (T)	437 (R)	437 (R)	
des-Arg-Tyr	normal	433 T	437 R	437 R	4,7,9
	des-His	433 (T)	437 (R)	437 (R)	
	des-His-Tyr	437 (R)	437 (R)	437 (R)	

Soret CD spectra of Hb originate from the interaction between $\pi - \pi^*$ transitions of heme and aromatic residues located at a distance of about 12 Å from the heme. Therefore, the difference in the peak wavelength may be ascribed to the difference in the tertiary structural changes in the regions including these residues upon assembling of α and β chains to make the α1β1 dimer. On the basis of the peak wavelength of the difference CD spectrum in the modified Hb's whose quaternary structures are unknown, we predicted their quaternary structures and added them in Table I.

It has been emphasized that the interaction between the α1 and β2 subunits is more important than that between the α1 and β1 subunits for the quaternary structure of Hb molecule, because on oxygenation larger movements occur at the former [18,19]. Our results suggest that the tertiary structure in the heme vicinity, which are characteristic of R and T structures, is mostly achieved upon the formation of α1β1 dimer before the construction of $\alpha_2\beta_2$ tetramer. This implies that the α1β1 interaction is also of great importance to understand the structure-function relationship of Hb molecule.

ACKNOWLEDGEMENTS

Thanks are due to Dr. Kazuhiko Ishihara and Miss Tsukiko Urata for advices about amino acid analysis, Dr. Hideyo Hasumi for programing of CD measurements, and Prof. Shigeo Horie for his valuable discussion during the course of this work. This wark was partly supported by grants from the Ministry of Education of Japan (No.60304099).

REFERENCES

1. Baldwin,J. & Chothia,C. (1979) J.Mol.Biol. 129, 175-220
2. Perutz,M.F. & TenEyck,L.F. (1971) Cold Spring Harbor Symp.Quant. Biol. 36, 295-310

3. Lesk,A.M., Janin,J., Wodak,S., & Chothia,C. (1985) J.Mol.Biol. 183, 267-270
4. Perutz,M.F., Ladner,J.E., Simon,S.R., & Ho,C. (1974) Biochemistry 13, 2163-2173
5. Geraci,G. & Sada,A. (1972) J.Mol.Biol. 70, 729-734
6. Nagai,K., Kitagawa,T., & Morimoto,H. (1980) J.Mol.Biol. 136, 271-289
7. Kilmartin,J.V., Hewitt,J.A., & Wootton,J.F. (1975) J.Mol.Biol. 93, 203-218
8. Viggiano,G., Wiechelman,K.J., Chervenick,P.A., & Ho,C. (1978) Biochemistry 17, 795-799
9. Miura,S. & Ho,C. (1984) Biochemistry 23, 2492-2499
10. Nagai,K., La Mar,G.N., Jue,T., & Bunn,H.F. (1982) Biochemistry 21, 842-847
11. Sugita,Y., Nagai,M., & Yoneyama,Y. (1971) J.Biol.Chem. 246, 383-388
12. Kawamura,Y., Hasumi,H., & Nakamura,S. (1982) J.Biochem. 92, 1227-1233
13. Kawamura,Y. & Nakamura,S. (1983) J.Biochem. 93, 1159-1166
14. Mawatari,K., Matsukawa,S., & Yoneyama,Y. (1983) Biochim.Biophys. Acta 745, 219-228
15. Mawatari,K., Matsukawa,S., & Yoneyama,Y. (1983) Biochim.Biophys. Acta 748, 381-388
16. Kilmartin,J.V. (1981) Methods in Enzymology, vol.76, pp.167-171, Academic Press, New York
17. Hsu,M.-C. & Woody,R.W. (1971) J.Am.Chem.Soc. 93, 3515-3525
18. Perutz,M.F., Muirhead,H., Cox,J.M., & Goaman,I.C.G. (1968) Nature 219, 131-139
19. Perutz,M.F. (1970) Nature 228, 726-734

Vol. 156, No. 1, 1988 BIOCHEMICAL AND BIOPHYSICAL RESEARCH COMMUNICATIONS
October 14, 1988 Pages 355-360

ISOLATION AND STRUCTURAL DETERMINATION OF RAT NEUROMEDIN U

Naoto Minamino*, Kenji Kangawa, Mayumi Honzawa and Hisayuki Matsuo

Department of Biochemistry and Department of Anesthesiology*,
Miyazaki Medical College, 5200 Kihara, Kiyotake, Miyazaki 889-16, Japan

Received September 8, 1988

SUMMARY: Rat neuromedin U was isolated from the small intestine using mainly immunoaffinity chromatography and radioimmunoassay for pig neuromedin U-8. The amino acid sequence of rat neuromedin U was determined by microsequence analysis to be Tyr-Lys-Val-Asn-Glu-Tyr-Gln-Gly-Pro-Val-Ala-Pro-Ser-Gly-Gly-Phe-Phe-Leu-Phe-Arg-Pro-Arg-Asn-NH_2, and this structure was confirmed by synthesis. Although the C-terminal heptapeptide amide structure of pig neuromedin U is completely conserved in rat neuromedin U, the remainder of the peptide reveals nine amino acid replacements and two amino acid deletions when compared to pig neuromedin U-25. Rat neuromedin U exerts two-fold potent uterus stimulant activity as compared to pig neuromedin U-25. © 1988 Academic Press, Inc.

Neuromedin U-8 (NMU-8) and neuromedin U-25 (NMU-25) are novel bioactive peptides isolated from pig spinal cord using a bioassay for a stimulant effect on rat uterus (1). These two peptides induce hypertension in anesthetized rat in addition to exerting potent uterus contractile activity. NMU-8 is an octapeptide having an amide structure at its C-terminus, while NMU-25 is an N-terminally extented form of NMU-8 carrying paired Arg residues just before the NMU-8 sequence. In our systematic survey for unknown neuropeptides in pig spinal cord, we already isolated a series of new bioactive peptides: two tachykinins, two bombesin-like peptides and their big forms, and neurotensin-like peptide (2-7). Although these peptides have their counterparts in known peptides, neither NMU-8 nor NMU-25 shows significant structural homology to known members of neuropeptides or hormones (1). In order to elucidate the physiological significance of NMU-8 and NMU-25, we raised antisera against these peptides and investigated the regional distribution in rat brain and peripheral tissue using radioimmunoassay (RIA) and immunohistochemical method. The results demonstrated that rat small intestine contained neuromedin U (NMU)-like immunoreactivity (NMU-LI) at much higher concentration than any regions of rat brain or other peripheral tissue (8,9). However, chromatographic properties of NMU-LI from rat intestine and brain suggested that rat NMU may be different from pig NMU-25 and NMU-8 (to

0006-291X/88 $1.50
Copyright © 1988 by Academic Press, Inc.
All rights of reproduction in any form reserved.

be reported elsewhere). Based on these results, we undertook the isolation of rat NMU from the rat intestine and determined its amino acid sequence.

MATERIALS AND METHODS

Materials: Pig NMU-8 and NMU-25 were synthesized and purified in our laboratory, as reported in the previous paper (1). Bradykinin was purchased from Protein Research Foundation (Osaka, Japan).

Isolation of rat NMU: Small intestines of male Wistar rats, including the duodenum, jejunum and ileum, were collected soon after decapitation and washed with cold saline. Rat intestines (117 g) from 17 animals were boiled in 5 volumes of water for 10 min to inactivate intrinsic proteases. After addition of glacial acetic acid (final concentration = 1.0 M), the boiled tissue was homogenized by a Polytron mixer for 10 min at 4°C. The supernatant obtained by centrifugation at 20,000 x g for 30 min was precipitated by addition of acetone (final acetone concentration = 75%). After removal of the precipitates by centrifugation, the supernatant was evaporated, diluted two-fold with water, and pumped onto a C_{18} silica column (90 ml, LC-SORB ODS, Chemco). The column was washed with 0.5M acetic acid, and then eluted with a solution of 60% CH_3CN containing 0.1% trifluoroacetic acid (TFA). The eluate was evaporated, reconstituted with 1M acetic acid, and then loaded onto a SP-Sephadex C-25 column (H^+-form, 1.7 x 13 cm, Pharmacia). Successive elutions with 1M acetic acid, 2M pyridine, and 2M pyridine-acetate (pH 5.0) yielded three respective fractions: SP-I, SP-II and SP-III. SP-III fraction containing basic materials was lyophilized and then subjected to Sephadex G-50 gel filtration (fine, 1.8 x 135 cm, Pharmacia). The fractions containing NMU-LI were pooled and loaded onto an anti-pig NMU-8 immunoaffinity column (see details below). The peptides eluted from the affinity column were finally purified by reverse phase HPLC on a μ-Bondasphere C_{18} column (3.9 x 150 mm, Waters) at a flow rate 1.0 ml/min with a linear gradient elution of CH_3CN in 0.1% TFA for 120 min. Column effluents from HPLC were monitored by measuring absorbance at 210 nm and at 280 nm.

Immunoaffinity chromatography: Immunoglobulin G (IgG) fraction was purified from 2 ml of antiserum #139-8 against pig NMU-8 by using a Protein A-Sepharose CL-4B column (0.8 x 5 cm, Pharmacia). IgG fraction thus obtained was coupled with 2 ml of AFFI-GEL 10 (BIO-RAD) in 0.1M sodium phosphate buffer (pH 7.4) at 4°C for 4hr. The NMU-LI fraction in the gel filtration was dissolved in 0.1M sodium phosphate buffer (pH 7.4), loaded onto the column (gel volume = 500 μl), and washed with the same buffer. The adsorbed peptides were then eluted with a solution of 1M CH_3COOH containing 10% CH_3CN.

RIA for NMU-8: Details for RIA of NMU-8 will be reported elsewhere. In brief, antiserum #139-8 could be used for RIA at a final dilution of 1:800,000, and the peptides were measurable in a range of 2-200 fmol/tube in this RIA system. The antiserum mainly recognized the C-terminal pentapeptide amide structure of NMU-8, and NMU-25 and N-terminal amino acid shortened NMU-8s had comparable affinities with the antiserum.

Sequence analysis: Sequence analysis was performed mainly by a gas phase sequencer (Model 470A/120A, Applied Biosystems). The resulting PTH-amino acids were analyzed by reverse phase HPLC in concert with the gas phase sequencer. PTH-amino acids were measurable as low as 1 pmol. Amino acid analysis was carried out with an amino acid analyzer (A-5550, IRICA) after hydrolysis of the peptide (ca. 250 pmol) in 6N HCl containing 0.1% phenol and 0.02% 2-mercaptoethanol at 110°C for 24 hr. Carboxy-terminal amino acid amide was determined by the method of Tatemoto and Mutt (10). Asparagine amide generated upon tryptic digestion was identified as its dansyl derivative on a polyamide sheet.

Synthesis: Rat NMU was synthesized by solid phase techniques conducted on p-methyl-benzhydrylamine resin with a peptide synthesizer (430A, Applied Biosystems) and purified by reverse phase HPLC. Correct synthesis was confirmed by amino acid analysis and sequencing.

Bioassay: The effect of rat NMU on the contractility of freshly isolated rat uterus was examined according to the reported method (11).

RESULTS AND DISCUSSION

From the acid extracts of 17 rat small intestines, the basic peptide fraction, which contained almost all of the NMU-LI, was effectively condensed through acetone precipitation, followed by step-wise chromatographies on reverse phase C_{18} silica gel column and on SP-Sephadex C-25 ion exchange column. The basic peptide fraction (dry weight; 91 mg) was then subjected to gel filtration on a Sephadex G-50 column, as shown in Fig. 1. More than 95% of the total NMU-LI were eluted in fractions #53-56 corresponding to synthetic pig NMU-25. A minor NMU-LI peak emerged around fraction #60, but was much earlier than that of pig NMU-8. Fractions #53-55 were pooled, lyophilized (dry weight; 4.5 mg), and subjected to anti-pig NMU-8 immunoaffinity chromatography. The adsorbed peptides on the immunoaffinity column were then subjected to reverse phase HPLC on a C_{18} column, and rat NMU was finally purified to a homogeneous state (Fig. 2). Purification by anti-pig NMU-8 immunoaffinity chromatography was highly efficient; about 70% of the peptides eluted from the affinity column was rat NMU, as calculated from the absorbance at 210 nm on reverse phase HPLC at the next purification step.

The amino acid composition of rat NMU thus isolated was determined after acid hydrolysis to be Asp, 1.96(2); Ser, 0.92(1); Glu, 1.97(2); Pro, 3.17(3); Gly, 3.07(3); Ala, 0.98(1); Val, 1.86(2); Leu, 1.11(1); Tyr, 1.94(2); Phe, 2.90(3); Lys, 1.18(1); Arg, 1.94(2). Thus, rat NMU was found to consist of 23 amino acid residues, i.e., two amino acids less than pig NMU-25. Based on the

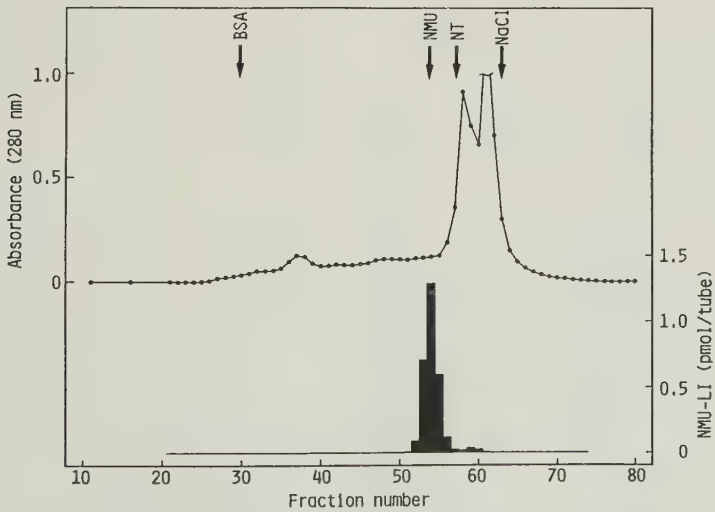

Figure 1. Sephadex G-50 gel filtration of the basic peptide fraction purified from rat small intestine.
Sample: Basic peptide fraction purified from 117g of rat small intestine.
Column: Sephadex G-50 fine (1.8 x 135 cm, Pharmacia).
Solvent: 1M acetic acid. Fraction size: 5 ml/tube. Flow rate: 8 ml/hr.
Arrows indicate the elution positions of bovine serum albumin (BSA), pig NMU-25 (NMU), neurotensin (NT) and NaCl, respectively.
Black columns represent NMU-LI of each fraction.

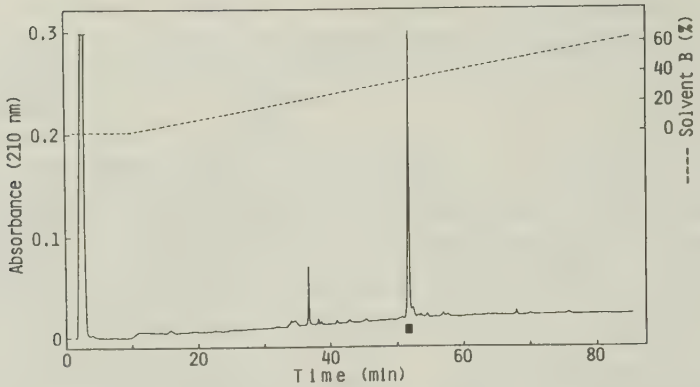

Figure 2. Final purification of rat neuromedin U by reverse phase HPLC.
Sample: Half of anti-pig NMU-8 immunoaffinity chromatography purified fraction obtained from fractions #53-55 in Sephadex G-50 gel filtration.
Column: μ-Bondashere C_{18} (100A, 3.9 x 150 mm, Waters).
Flow rate: 1.0 ml/min. Temperature: ambient.
Solvent system: Linaer gradient elution from (A) to (B) for 120 min.
H_2O:CH_3CN:10%TFA = (A) 90:10:1, (B) 40:60:1 (v/v).
NMU-LI was observed only at the black bar region.

amino acid analysis data, 2.60 nmol of rat NMU were purified from 117 g of rat small intestine. The average tissue concentration of NMU-LI in the rat duodenum, jejunum and ileum was about 35 pmol/g wet tissue. The yield of rat NMU in the present purification indicated that 65% of rat NMU in the small intestine was isolated as a pure peptide. This total recovery yield of rat NMU was significantly higher than those of our previous isolation of a series of neuromedins (5-20%) (2-7).

Amino acid sequence analysis was performed by a gas-phase sequencer and PTH-amino acid liberated at each cycle of Edamn degradation was successfully identified up to the C-termianl residue, as shown in Fig. 3a. Carboxy-terminal Asn-NH_2 was also clearly identified as its dansyl derivative by the method of Tatemoto and Mutt (10). Thus, the amino acid sequence of rat NMU was determined, as shown in Fig. 3b. Positive confirmation of the sequence thus determined was provided by chemical synthesis of rat NMU. The native and synthetic rat NMUs were co-eluted as a single peak on reverse phase HPLC under identical conditions used for Fig. 2.

Biological activity of rat NMU was measured by a bioassay for the stimulant effect on rat uterus. Figure 4 shows that rat NMU also elicits a repeated and sustained uterus contraction in a manner similar to that of pig NMU-25. Furthermore, potency of rat NMU was about twice as high as that of pig NMU-25, when rat uterus was used for the assay.

In order to maximize the sequence homology between rat NMU and pig NMU-25, spaces must be inserted in rat NMU at position 6 and at position 11, respectively, of the pig NMU-25 numbering system (Fig. 3b). Except for these amino acid deletions, the other amino acid replacements observed between rat

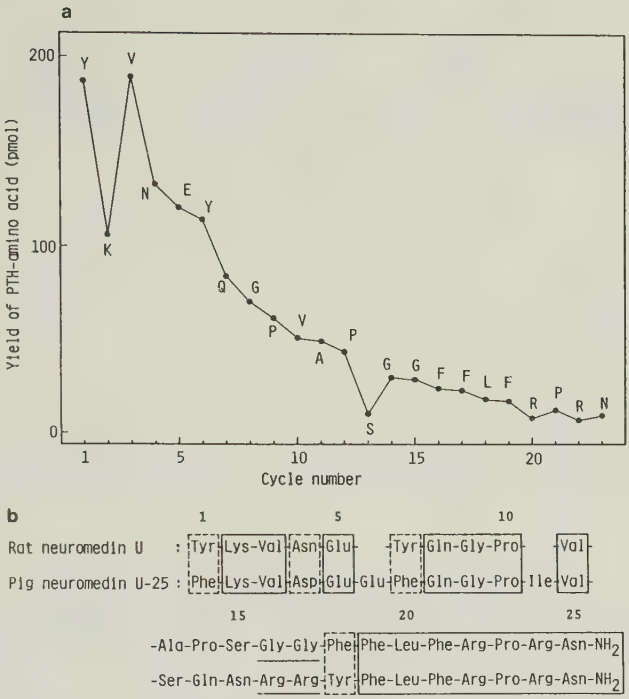

Figure 3. (a) Yield of PTH-amino acid at each cycle of Edman degradation. (b) Amino acid sequences of rat neuromedin U and pig neuromedin U-25. Identical residues and homologous residues are boxed with solid lines and dashed lines, respectively.

NMU and pig NMU-25 could occur by one base substitution of each amino acid codon. The carboxy-terminal heptapeptide sequence of pig NMU-25, which is essential for biological activity, is completely conserved in rat NMU.

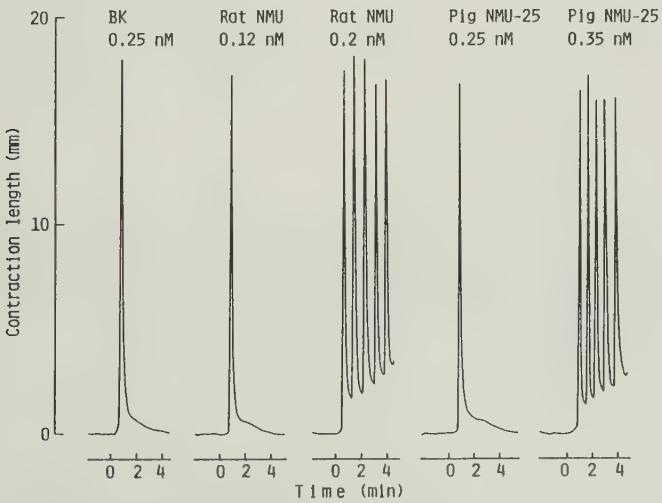

Figure 4. Rat uterus stimulant activity of rat neuromedin U, pig neuromedin U-25 and bradykinin.
Freshly isolated rat uterus was bathed at 32-35°C in modified Locke-Ringer solution with a tension of 0.5-1.0 g. Peptides dissolved in 0.9% saline were added at 0 min. BK: bradykinin.

Moreover, the 8th residues from the C-terminus are aromatic amino acids in both peptides. In the N-terminal region, amino acid sequences are homologous up to the 12th residue. However, five amino acid residues at the middle portion are quite different. Of note is that the Arg-Arg of paired basic amino acids, often observed as a signal for proteolytic processing, is replaced by Gly-Gly. The absence of a low molecular weight form in rat corresponding to pig NMU-8 and the relatively large difference in the elution time between rat NMU-LI and pig NMU-25 on reverse phase HPLC are probably due to these replacements (9,12).

NMU is a novel type of brain-gut peptide, and its physiological function has not been elucidated as yet. The present identification of rat NMU indicates that the C-terminal heptapeptide amide structure may be conserved among mammalian species and is essential in eliciting bioactivity. Therefore, this heptapeptide amide structure can be recognized as the minimum unit to exert the physiological functions of neuromedin U.

ACKNOWLEDGEMENTS: This work was supported in part by a Grant-in-Aid from the Ministry of Education, Science and Culture of Japan. The authors are grateful to Miss T. Hatoh for synthesis of peptides.

REFERENCES

1. Minamino, N., Kangawa, K. & Matsuo, H. (1985) Biochem. Biophys. Res. Commun., 130, 1078-1085.
2. Kangawa, K., Minamino, N., Fukuda, A. & Matsuo, H. (1983) Biochem. Biophys. Res. Commun., 114, 533-540.
3. Minamino, N., Kangawa, K., Fukuda, A. & Matsuo, H. (1984) Neuropeptides, 4, 157-166.
4. Minamino, N., Kangawa, K. & Matsuo, H. (1984) Biochem. Biophys. Res. Commun., 122, 542-549.
5. Minamino, N., Kangawa, K. & Matsuo, H. (1983) Biochem. Biophys. Res. Commun., 114, 541-548.
6. Minamino, N., Kamgawa, K. & Matsuo, H. (1984) Biochem. Biophys. Res. Commun., 119, 14-20.
7. Minamino, N., Sudoh, T., Kangawa, K. & Matsuo, H. (1985) Biochem. Biophys. Res. Commun., 130, 685-691.
8. Honzawa, M., Sudoh, T., Minamino, N., Tohyama, M. & Matsuo, H. (1987) Neuroscience, 23, 1103-1122.
9. Sudoh, T., Honzawa, M., Minamino, N., Kangawa, K. & Matsuo, H. (1986) Seikagaku (in Japanese), 58, 987.
10. Tatemoto, K. & Mutt, V. (1978) Proc. Natl. Acad. Sci. USA, 75, 4115-4119.
11. Carraway, R. & Leeman, S.J. (1973) J. Biol. Chem., 248, 6854-6861.
12. Domin, J., Ghatei, M., Chohan, P. & Bloom, S.R. (1986) Biochem. Biophys. Res. Commun., 140, 1127-1134.

Vol. 156, No. 1, 1988 BIOCHEMICAL AND BIOPHYSICAL RESEARCH COMMUNICATIONS
October 14, 1988 Pages 361-367

DIFFERENT TYPES OF ADP-RIBOSE PROTEIN BONDS FORMED BY BOTULINUM C2 TOXIN, BOTULINUM ADP-RIBOSYLTRANSFERASE C3 AND PERTUSSIS TOXIN

Klaus Aktories[1], Ingo Just[1] and Walter Rosenthal[2]

[1]) Rudolf-Buchheim-Institut für Pharmakologie der Justus-Liebig Universität Giessen, Frankfurter Str. 107, D-6300 Giessen, F.R.G.

[2]) Institut für Pharmakologie, Freie Universität Berlin, Thielallee 69/73, D-1000 Berlin 33, F.R.G.

Received September 9, 1988

SUMMARY: We attempted to characterize ADP-ribose-amino acid bonds formed by various bacterial toxins. The ADP-ribose-arginine bond formed by botulinum C2 toxin in actin was cleaved with a half-life of about 2 h by treatment with hydroxylamine (0.5 M). In contrast, the ADP-ribose-cysteine bond formed by pertussis toxin in transducin and the ADP-ribose-amino acid linkage formed by botulinum ADP-ribosyltransferase C3 in platelet cytosolic proteins were not affected by hydroxylamine. $HgCl_2$ cleaved the ADP-ribose-amino acid bond formed by pertussis toxin in transducin but not those formed by botulinum C2 toxin or botulinum ADP-ribosyltransferase C3 in actin and platelet cytosolic proteins, respectively. NaOH (0.5 M) cleaved the ADP-ribose-amino acid bonds formed by botulinum C2 toxin and pertussis toxin but not the one formed by botulinum ADP-ribosyltransferase C3. The data indicate that the ADP-ribose bond formed by botulinum ADP-ribosyltransferase C3 differs from those formed by the known bacterial ADP-ribosylating toxins.
© 1988 Academic Press, Inc.

Various bacterial toxins such as diphtheria, cholera and pertussis toxin affect the metabolism of the eukaryotic cell by ADP-ribosylation of proteins [1]. These ADP-ribosyltransferases differ in their protein substrate specificity and with respect to the amino acid residue modified by the respective toxin. While diphtheria toxin ADP-ribosylates diphthamide [2], a posttranslationally modified histidine, cholera toxin ADP-ribosylates arginine residues [3], and pertussis toxin modifies cysteine residues [4].

0006-291X/88 $1.50
Copyright © 1988 by Academic Press, Inc.
All rights of reproduction in any form reserved.

Recently, it was shown that Clostridium botulinum type C produces two distinct ADP-ribosyltransferases, botulinum C2 toxin and botulinum ADP-ribosyltransferase C3 [5-7]. Whereas botulinum C2 toxin ADP-ribosylates actin in arginine-177 [8], the substrate for botulinum ADP-ribosyltransferase C3 appears to be a GTP-binding protein [9]; the ADP-ribose-amino acid bond of this protein has not yet been characterized.

Hilz and coworkers showed that ADP-ribose-protein bonds can be characterized by their stability towards neutral hydroxylamine [10], dilute alkali [10] and mercury ions [11]. The mono-ADP-ribosylation of a glutamate residue catalyzed by poly-ADP-ribose synthase is characterized by its instability towards neutral hydroxylamine or dilute alkali [10,18]. This type of ADP-ribose bond was, therefore, called hydroxylamine-"labile" (half-life 3-10 min). The ADP-ribose-arginine bond formed by mono-ADP-ribosyltransferase purified from turkey erythrocytes is reportedly more stable against hydroxylamine [19]. Similarly, the ADP-ribose-arginine bond formed by cholera toxin in G-proteins, G_s and transducin, has a half-life of 1-2 h in the presence of hydroxylamine [20].

We studied the stability of the ADP-ribose protein bond formed by botulinum C2 toxin, botulinum ADP-ribosyltransferase C3 and pertussis toxin and report here that the ADP-ribosylation catalyzed by botulinum ADP-ribosyltransferase C3 is more stable than the ADP-ribose-arginine bonds formed by botulinum C2 toxin or the ADP-ribose-cysteine bond formed by pertussis toxin.

MATERIALS AND METHODS

Materials

Botulinum C2 toxin and botulinum ADP-ribosyltransferase C3 were purified as described [12,13]. Transducin was prepared according to Kühn [14]. Pertussis toxin was a gift of Dr. M. Yajima (Kobe, Japan). [^{32}P]NAD was prepared according to Cassel and Pfeuffer [15]. Hydroxylamine-HCl was obtained from Sigma (Deisenhofen, FRG) and $HgCl_2$ from Merck (Darmstadt, FRG). All other reagents were from commercial sources.

Preparation of human platelet membranes and cytosol

Platelets were isolated as described [16] and lysed by freezing and thawing in a hypotonic medium containing 10 mM triethanolamine/HCl (pH 7.5) and 5 mM EDTA. Platelet membranes and cytosol were obtained by centrifugation of the lysate for 15 min at 30.000 xg and kept at -20°C until use.

N-ethylmaleimide treatment of platelet membranes and cytosol

Membranes and cytosol of human platelets were incubated with the indicated concentrations of N-ethylmaleimide for 15 min at 25°C. After termination of the reaction by addition of dithiothreitol (10 mM, final concentration), membranes and cytosol were immediately used in the ADP-ribosylation assay.

ADP-ribosylation assay

ADP-ribosylation was carried out in a medium containing 10 mM thymidine, 0.5 mM ATP, 6 mM $MgCl_2$, 0.1 µM [^{32}P]NAD (about 1 µCi/tube), ADP-ribosylating toxins at the indicated concentrations and 50 mM triethanolamine/HCl (pH 7.5) with about 100-300 µg of platelet membranous or cytosolic protein or 1 µg transducin in a total volume of 200 µl. ADP-ribosylation with pertussis toxin (activated by 20 mM dithiothreitol) was performed in the presence of 0.01% Lubrol PX. After 30 min of incubation at 37°C, reactions were terminated by the addition of 2% SDS and 100 mM HEPES, pH 7.5 (final concentrations each).

Studies on the stability of ADP-ribose-protein bonds with hydroxylamine, NaOH and $HgCl_2$

After termination of the ADP-ribosylation with SDS/HEPES, 50 µl aliquots of the reaction mixture were added to the same volume of 2 mM or 1 M NaCl, 1 M NH_2OH (pH 7.5), 1 N NaOH or 2 mM $HgCl_2$, and incubated for the indicated periods of time at 37°C or as indicated. Thereafter, proteins were precipitated by addition of trichloroacetic acid (20%, final concentration). The formed pellet was washed with diethylether and dissolved in 50 µl of electrophoresis buffer. SDS-PAGE was performed according to Laemmli [17]. Gels were stained with Coomassie Blue, destained and subjected to autoradiography for 24-48 h.

RESULTS AND DISCUSSION

The stability of ADP-ribose bonds formed by botulinum C2 toxin, botulinum ADP-ribosyltransferase C3 and pertussis toxin were studied under denaturing conditions in order to prevent any shielding effects of the native proteins. As is shown in Fig. 1A, in the presence of 0.5 M hydroxylamine (pH 7.5) ^{32}P-ADP-ribose-arginine residues formed by botulinum C2 toxin in actin were degraded by about 50% after an incubabation of 2 h. A similar stability has been reported for ADP-ribose-arginine bonds formed by endogenous ADP-ribosyltransferases and cholera toxin [19,20]. The ADP-ribose-amino acid bond formed by botulinum ADP-ribosyltransferase C3 was not affected by hydroxylamine. In accordance with a previous report [20], pertussis toxin-catalyzed ADP-ribosylation of a cysteine residue in transducin was stable towards treatment with hydroxylamine (Fig. 1B). It was recently reported that the substrate of botulinum ADP-ribosyltransferase C3 is

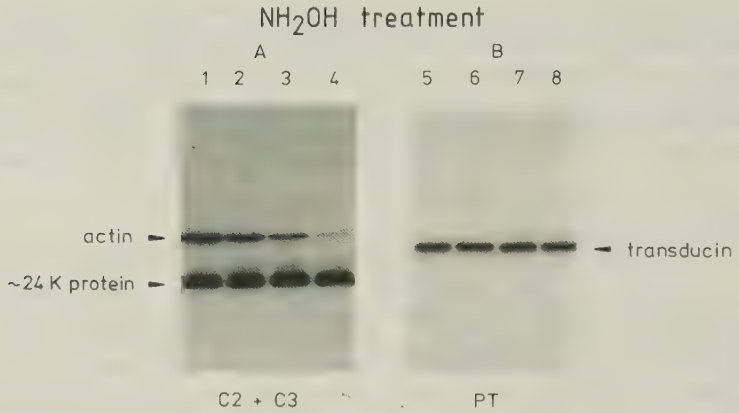

Fig. 1: Stabilities towards NH_2OH of ^{32}P-ADP-ribose-amino acid bonds formed by botulinum C2 toxin, botulinum ADP-ribosyltransferase C3 and pertussis toxin. Platelet cytosol (A) was incubated with [^{32}P]NAD and botulinum C2 toxin (C2, 0.1 µg/ml) and botulinum ADP-ribosyltransferase C3 (C3, 3 µg/ml); purified transducin (B) was incubated with [^{32}P]NAD and pertussis toxin (PT, 20 µg/ml). Thereafter, samples were treated with 0.5 M NaCl for 180 min (lanes 1, 5) or with 0.5 M NH_2OH for 30 min (lanes 2, 6) 60 min (lanes 3, 7), 120 min (lane 8) or 180 min (lane 4). SDS PAGE of samples was performed (15% acrylamide in A, 11% acrylamide in B), and ^{32}P-ADP-ribosylated peptides were analyzed by autoradiography. The M_r values of radiolabelled peptides were 43 kDa (corresponding to the M_r of actin), 22-24 kDa (corresponding to the M_r of GTP-binding proteins ADP-ribosylated by botulinum ADP-ribosyltransferase C3) and 39 kDa (corresponding to the M_r of the α-subunit of transducin) in panels A and B, respectively.

sensitive towards the sulfhydryl-group-alkylating reagent, N-ethylmaleimide, employed at a high concentration (200 mM) [21]. In platelet membranes and cytosol, ADP-ribosylation of 21-24 kDa proteins by ADP-ribosyltransferase C3 was inhibited by N-ethylmaleimide at a concentration as low as 100 µM (Fig. 2) Since pertussis toxin-induced ADP-ribosylation of cysteine residues is also prevented by N-ethylmaleimide at low concentrations [22], one might assume that ADP-ribosyltransferase C3, too, modifies cysteine residues. In order to test this hypothesis, we took advantage of the recent finding that the ADP-ribose-cysteine bond is sensitive to mercury ions [11]. As shown in Fig. 3C, treatment of ADP-ribosylated transducin with 1 mM $HgCl_2$ for 10 min largely removed the ADP-ribose residue; after 1 h of incubation, the loss of ADP-ribose appeared to be complete. Neither the ADP-ribose-arginine bond in actin (Fig. 3A) nor the ADP-

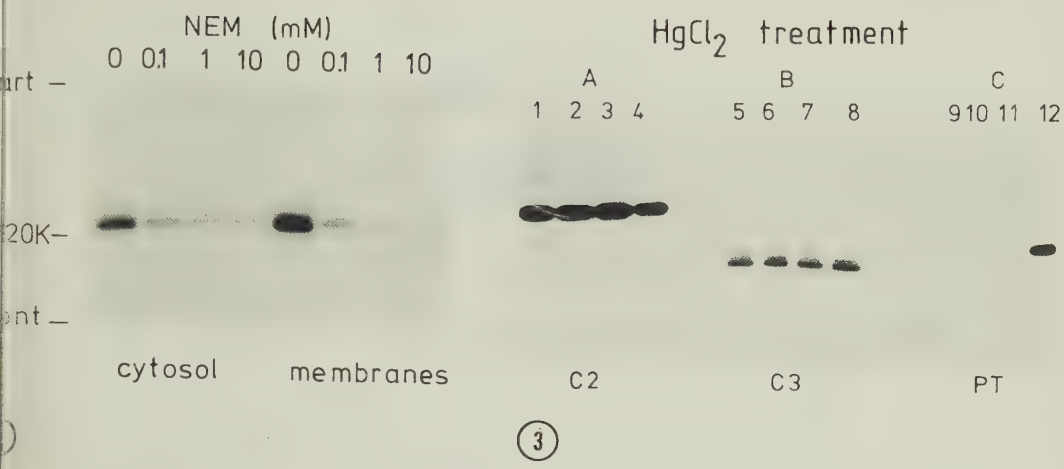

3

Fig. 2: Influence of N-ethylmaleimide on ADP-ribosylation by botulinum ADP-ribosyltransferase C3. Membranes and cytosol of human platelets were pretreated with N-ethylmaleimide (NEM) at the indicated concentrations as described. After incubation with botulinum ADP-ribosyltransferase C3 (3 μg/ml) and [^{32}P]NAD, samples were subjected to SDS PAGE and ^{32}P-ADP-ribosylated peptides were analyzed by autoradiography.

Fig. 3: Stability towards $HgCl_2$ of ^{32}P-ADP-ribose-amino acid bonds formed by botulinum C2 toxin, botulinum ADP-ribosyltransferase C3 and pertussis toxin. Platelet cytosol (A,B) was incubated with [^{32}P]NAD and botulinum C2 toxin (C2, 1 μg/ml) or botulinum ADP-ribosyltransferase C3 (C3, 3 μg/ml); purified transducin (C) was incubated with [^{32}P]NAD and pertussis toxin (PT, 20 μg/ml). Thereafter, samples were treated with 1 mM NaCl for 60 min (lanes 4, 8, 12) or with 1 mM $HgCl_2$ for 10 min (lanes 1, 5, 9), 30 min (lanes 2, 6, 10) and 60 min (lanes 3, 7, 11), respectively. Samples were subjected to SDS PAGE (11% acrylamide), and ^{32}P-ADP-ribosylated peptides were analyzed by autoradiography. The M_r values of the respective ^{32}P-ADP-ribosylated substrates were as in Fig. 1.

ribose-amino acid linkage in the botulinum ADP-ribosyltransferase C3 substrate (Fig. 3B) was affected by mercury ions after incubations for up to 1 h. The high resistence towards dilute alkali of the ADP-ribose-amino acid bond formed by botulinum ADP-ribosyltransferase C3 is depicted in Fig. 4. While treatment with 0.5 M NaOH at 37°C resulted in a time-dependent cleavage of the ADP-ribose-amino acid bonds in actin and in transducin, the ADP-ribose-amino acid bond of the botulinum ADP-ribosyltransferase C3 substrate remained almost unaffected.

Taken together, the data presented indicate that the ADP-ribose-amino acid bond formed by botulinum ADP-ribosyl-

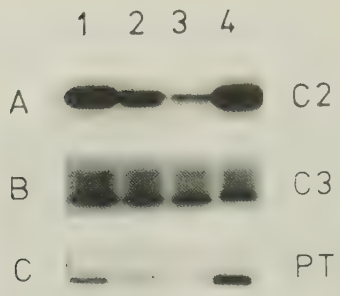

Fig. 4: Stability towards NaOH of ^{32}P-ADP-ribose-amino acid bonds formed by botulinum C2 toxin, botulinum ADP-ribosyltransferase C3 and pertussis toxin. Platelet cytosol (A,B) was incubated with [^{32}P]NAD and botulinum C2 toxin (C2, 1 µg/ml) or botulinum ADP-ribosyltransferase C3 (C3, 3µg/ml); purified transducin (C) was incubated with [^{32}P]NAD and pertussis toxin (PT, 20 µg/ml). Thereafter, samples were treated with 0.5 M NaCl for 60 min (lane 4) or with 0.5 M NaOH for 10 min (lane 1), 30 min (lane 2) and 60 min (lane 3). Samples were subjected to SDS PAGE (11 % acrylamide) and ^{32}P-ADP-ribosylated peptides were analyzed by autoradiography. The M_r values of the respective ^{32}P-ADP-ribosylated substrates were as in Fig. 1.

transferase C3 differs in its stability towards hydroxylamine, mercury ions and dilute alkali from ADP-ribose-amino acid bonds formed by botulinum C2 and pertussis toxins. So far, a similarly stable ADP-ribose-amino acid bond has only been observed in the elongation factor 2, in which diphtheria toxin catalyzes ADP-ribosylation of a diphthamide residue [24]. As diphthamide is an amino acid unique for the elongation factor [1,2] our findings suggest a novel type of ADP-ribose bond formed by botulinum ADP-ribosyltransferase C3.

ACKNOWLEDGEMENTS: The authors are indebted to Dr. M. Yajima for supplying pertussis toxin and to Mrs. M. Laux for excellent technical assistance. This work was supported by grants of the Deutsche Forschungsgemeinschaft and the Fonds der Chemischen Industrie.

REFERENCES

1. Foster, J.W., and Kinney, D.W. (1985) CRC Critical Rev. Microbiol. 11, 273-298.
2. Van Ness, B.G., Howard, J.B., and Bodley, J.W. (1980) J. Biol. Chem. 255, 10710-10716.
3. Moss, J., and Vaughan, M. (1978) Proc. Natl. Acad. Sci. USA 75, 3621-3624.
4. West, R.E., Moss, J., Vaughan, M., Liu, T., and Liu, T.-Y. (1985) J. Biol. Chem. 260, 14428-14430.

5. Aktories, K., Bärmann, M., Chhatwal, G.S., and Presek, P. (1986) TIPS 8, 158-160.
6. Aktories, K., Bärmann, M., Ohishi, I., Tsuyama, S., Jakobs, K.H., and Habermann, E. (1986) Nature (Lond.) 322, 390-392.
7. Aktories, K., Weller, U., and Chhatwal, G.S. (1987) FEBS Lett. 212, 109-113.
8. Vandekerckhove, J., Schering, B., Bärmann, M., and Aktories, K. (1988) J. Biol. Chem. 262, 696-700.
9. Aktories, K., and Frevert, J. (1987) Biochem. J. 247, 363-368.
10. Bredehorst, R., Wielckens, K., Gartemann, A., Lengyel, H., Klapproth, K., and Hilz, H. (1978) Eur. J. Biochem. 92, 129-135.
11. Meyer, T, Koch, R., Fanick, W., and Hilz, H. (1988) Biol. Chem. Hoppe Seyler, in press.
12. Ohishi, I., Iwasaki, W., and Sakaguchi, T. (1980) Infect. Immun. 30, 668-673.
13. Aktories, K., Rösener, S., Blaschke, U., and Chhatwal, G.S. (1988) Eur. J. Biochem. 172, 445-450.
14. Kühn, H. (1980) Nature (Lond.). 283, 587-589.
15. Cassel, D., and Pfeuffer, T. (19787) Proc. Natl. Acad. Sci. USA 75, 2669-2673.
16. Jakobs, K.H., Lasch, P., Minuth, M., Aktories, K., and Schultz, G. (1982)J. Biol. Chem. 257, 2829-2833.
17. Laemmli, U.K. (1970) Nature (Lond.) 227, 680-685.
18. Burzio, L.O. (1982) In: ADP-Ribosylation Reactions (Hayaishi, O., and Ueda, K., eds.) pp. 103-116, Academic Press, New York.
19. Moss, J., Yost, D.A., and Stanley, S.J. (1983) J. Biol. Chem. 258, 6466-6470.
20. Hsia, J.A., Tsai, S.-C., Adamik, R., Yost, D.A., Hewlett, E.L., and Moss, J. (1985) J. Biol. Chem. 260, 16187-16191.
21. Rubin, E.J., Gill, M., Boquet, P., and Popoff, M.R. (1988) Mol. Cell. Biol. 8, 418-426.
22. Aktories, K., Hungerer, K.D., Robbel, L., and Jakobs, K.H. (1984) IUPHAR 9th Intern. Congress of Pharmacology, London, Abstr. Vol. 1655 P.
23. Payne, D.M., Jacobson, E.L., Moss, J., and Jacobson, M.K. (1985) Biochemistry 24, 7540-7549.

Vol. 156, No. 1, 1988 BIOCHEMICAL AND BIOPHYSICAL RESEARCH COMMUNICATIONS
October 14, 1988 Pages 368-374

IDENTIFICATION OF GLUTATHIONE S-TRANSFERASE AS A SUBSTRATE AND GLUTATHIONE AS AN INHIBITOR OF IN VITRO CALMODULIN-STIMULATED PROTEIN METHYLATION IN RAT LIVER CYTOSOL

Tom L. Neal, Lynda S. Wright and Frank L. Siegel

Departments of Physiological Chemistry and Pediatrics and the Waisman Center, University of Wisconsin Medical School, Madison, Wisconsin 53706

Received September 9, 1988

SUMMARY: This report describes the isolation of the major calmodulin-stimulated methyl acceptor protein of adult rat liver cytosol. This M_r 29,000 methyl acceptor protein (MeAP29) has been purified to apparent homogeneity using ammonium sulfate precipitation and chromatography on DEAE-cellulose, phosphocellulose, hydroxylapatite and Sephadex G-75. Affinity chromatography on glutathione-Sepharose and assays of enzyme activity indicate that MeAP29 is a member of the glutathione S-transferase family. We further show that glutathione can act as an inhibitor of calmodulin-stimulated in vitro methylation of MeAP29 and that MeAP29 methylation is enhanced in non-dialyzed liver cytosol from rats with lowered glutathione levels. © 1988 Academic Press, Inc.

INTRODUCTION: A previous report from this laboratory (1) showed that calmodulin, a major intracellular calcium-binding protein in eucaryotes, stimulates the in vitro methylation of three proteins (M_r 29,000, 32,000 and 45,000) in liver cytosol from adult rats. Calmodulin stimulated the methylation of the M_r 29,000 methyl acceptor protein (MeAP29) to a greater extent than for either MeAP32 or MeAP45. Dialysis also stimulated the methylation of these three proteins. The addition of calmodulin to methylation incubations containing dialyzed liver cytosol produced additive effects on the methylation of MeAP29, without significantly affecting the methylation of either MeAP32 or MeAP45. Calmodulin-stimulated MeAP29 methylation occurs in cytosol of liver and to a lesser extent in kidney and lung cytosol. This stimulation of protein methylation represented a previously unreported activity of calmodulin.

While the significance of protein methylation in eucaryotes is not yet known, a number of proteins have been shown to be post-translationally modified by methylation, including calmodulin (2), histones (3) and cytochrome c (4). This laboratory presented evidence (5) that calmodulin exists in both methylated and non-methylated states in some rat tissues. It has been shown that the N-methylation of calmodulin modulates its activation of NAD kinase (6). Other enzymes, such as cyclic nucleotide phosphodiesterase (7) and myosin light chain kinase (8), are activated to the same degree by either methylated or non-methylated calmodulins.

The observation that calmodulin could stimulate the methylation of specific proteins led to our interest in the possible significance of these events, especially in relation to calcium fluxes and subsequent calcium-calmodulin interactions within cells. To better understand protein methylation and the effects of calmodulin on this post-translational modification, we sought to isolate and characterize the calmodulin-dependent methyl acceptor protein MeAP29 and to

0006-291X/88 $1.50
Copyright © 1988 by Academic Press, Inc.
All rights of reproduction in any form reserved.

determine the identity of the dialyzable inhibitor of this in vitro methylation. We report here the purification of MeAP29 to apparent homogeneity, as indicated by its appearance as a single band on 12.5% SDS-polyacrylamide gels. The retention of MeAP29 on glutathione-Sepharose affinity columns and its elution with buffer containing glutathione identified MeAP29 as a member of the glutathione S-transferase family; enzyme activity studies confirmed this classification. We also show that glutathione, a substrate of glutathione S-transferases, can act as an inhibitor of the calmodulin-stimulated methylation of MeAP29 and that methylation of MeAP29 is enhanced in non-dialyzed liver cytosol from rats with lowered hepatic glutathione levels.

MATERIALS AND METHODS

Materials: [^{3}H]-S-adenosyl-L-methionine was obtained from the NEN Division of DuPont Corporation. DEAE-cellulose (DE-52) was purchased from Whatman; Sephadex G-75 from Pharmacia Fine Chemicals; and, phosphocellulose (Cellex-P) and hydroxylapatite (HTP) from BioRad Laboratories. Ultrafiltration units and filters are products of Amicon. Holtzmann rats (Sprague-Dawley Corp., Madison, WI) were reared in our breeding colony. All other materials were obtained from Sigma Chemical Company.

Purification of MeAP29: The presence of MeAP29 in fractions was determined by the existence of an M_r 29,000 Coomassie Blue-stained protein band following electrophoresis on 12.5% SDS-polyacrylamide gels and the ability of this protein to be methylated in the presence of calmodulin, partially purified methyltransferase and [^{3}H]-S-adenosyl-L-methionine under in vitro methylation conditions.

Liver cytosolic fractions were obtained as described (1) from 200-300 gram male Holtzmann rats. These cytosolic fractions were brought to 75% ammonium sulfate saturation by the gradual addition of solid ammonium sulfate, followed by one hour of gentle stirring at 4°C. The suspension was then centrifuged at 100,000 x g for 30 minutes. The resulting supernatant was brought to 90% ammonium sulfate saturation, stirred for 1 hour, and then centrifuged as before. The 75-90% ammonium sulfate pellet was dissolved in Buffer A (20 mM Tris-HCl, pH 7.3) and then dialyzed overnight against this buffer.

The dialyzed ammonium sulfate fraction was clarified by a 30 minute centrifugation (100,000 x g) and then pumped (1 ml/min) onto a DEAE-cellulose column (21.5 cm x 3.5 cm), which had been previously equilibrated in Buffer A. The washthrough fraction from this column was immediately pumped (1 ml/min) onto a phosphocellulose column (20 cm x 2.5 cm), previously equilibrated in Buffer A. The washthrough fraction from the phosphocellulose column was dialyzed overnight against 50 mM sodium phosphate, pH 7.0 (Buffer B), reduced in volume by ultrafiltration (YM10 filter) and pumped (20 ml/h) onto a hydroxylapatite column (15 cm x 2.5 cm), previously equilibrated in Buffer B. The column was washed with Buffer B until the 280nm absorbance returned to baseline. Bound proteins were eluted with a linear, six column volume gradient to 300 mM sodium phosphate, pH 7.0. Fractions containing a methyl accepting 29,000 dalton protein were pooled and dialyzed overnight against 20 mM Tris-HCl, pH 7.4, 150 mM NaCl (Buffer C); MeAP29 eluted from hydroxylapatite during the latter half of the gradient. The dialyzed pool was reduced in volume by ultrafiltration to less than two ml and pumped (10 ml/h) onto a Sephadex G-75 column (90 cm x 2.5 cm), previously equilibrated with Buffer C. MeAP29 eluted from this sizing column with an apparent molecular weight of 50,000 daltons (data not shown), suggesting that it exists as a dimer in solution.

Partial purification of MeAP29 methyltransferase : The rat liver cytosol methyltransferase(s), which methylate(s) MeAP29, was isolated by a 35-55% ammonium sulfate precipitation followed by chromatography on DEAE-cellulose. The 35-55% ammonium sulfate pellet was dissolved in Buffer A, dialyzed overnight against this buffer, and then chromatographed on DEAE-cellulose. MeAP29 methyltransferase was eluted from DEAE-cellulose with a step-wise gradient of Buffer A containing 75 mM NaCl. Neither MeAP29 nor calmodulin was detectable in this enzyme preparation.

In vitro methylation : Methylation incubations, followed by SDS-PAGE and fluorography, were carried out essentially as described (1), and were scaled-up for some experiments. Glutathione was added to some incubations, as described in the figure legends.

Glutathione affinity chromatography : Glutathione was attached to epoxy-activated Sepharose as described (9). Glutathione S-transferases were purified using this column (10).
Glutathione S-transferase assay : Glutathione S-transferase activity was assayed by the method of Habig and Jakoby (11), using 1-chloro-2,4-dinitrobenzene (CDNB) as substrate.
Buthionine sulfoximine treatment : Buthionine sulfoximine (BSO) was used to lower hepatic glutathione levels in rats by the method of Meister and Griffith (12). Animals were injected intraperitoneally with 4 mmoles BSO/kg body weight at time zero and again after 2 h, and sacrificed 2 h later. Control animals received injections of 0.9% sodium chloride.
Glutathione levels : Glutathione levels were assayed by the method of Tietze (13).

RESULTS AND DISCUSSION : MeAP29 was purified, to a single stained protein band on 12.5% SDS-polyacrylamide gels, through the successive use of ammonium sulfate precipitation and chromatography on DEAE-cellulose, phosphocellulose, hydroxylapatite and Sephadex G-75 (Fig. 1). Identification of fractions containing MeAP29 was determined by : 1) the presence of an M_r 29,000 protein on 12.5% SDS-polyacrylamide gels, and 2) its ability to accept methyl groups in methylation incubations containing calmodulin, partially purified methyltransferase and [^{3}H]-S-adenosyl-L-methionine. Amino acid sequence determination of the N-terminus of the purified MeAP29 suggested that it is a member of the glutathione S-transferase (GST) family (manuscript in preparation).

Others have shown that the members of the GST family can be purified by glutathione-Sepharose affinity chromatography (9,10). To further characterize MeAP29 as a member of the GST family, a scaled-up methylation assay was incubated under standard conditions using dialyzed liver cytosol and added calmodulin, followed by isolation of GSTs on GSH-Sepharose. Methylated MeAP29 bound to this column and was eluted with buffer containing GSH (Fig. 2). The GSH eluate from the GSH-Sepharose column contained both methylated MeAP29 (Fig. 2) and GST activity (TABLE I), indicating that MeAP29 is a glutathione S-transferase.

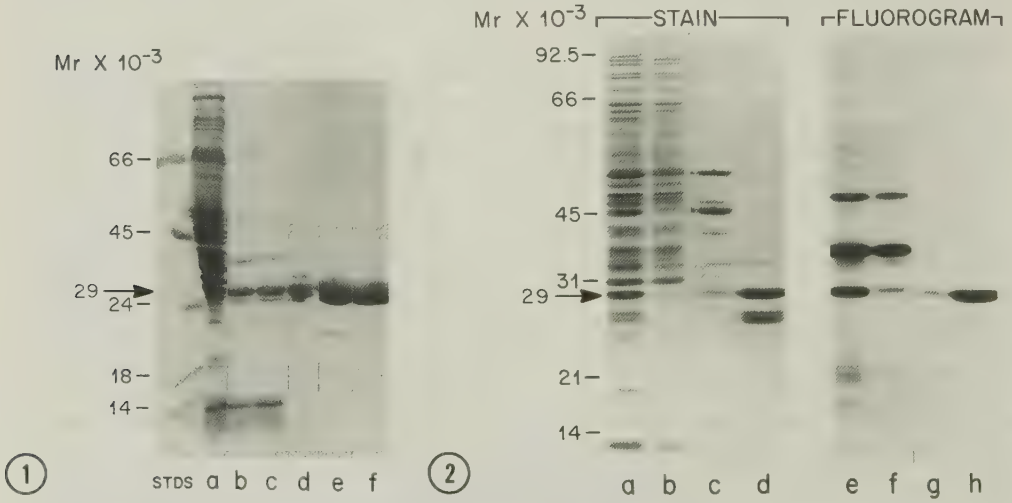

Figure 1. Purification of MeAP29 from adult rat liver cytosol. MeAP29 was isolated from liver of adult male rats, as described in Materials and Methods. Lane a, total liver cytosol; lane b, 75-90% ammonium sulfate pellet; lane c, DEAE-cellulose washthrough; lane d, phosphocellulose washthrough; lane e, hydroxylapatite pool and lane f, Sephadex G-75 pool.

Figure 2. Affinity purification of methylated MeAP29 on GSH-Sepharose. Left panel, Coomassie blue stain; right panel, fluorograph. Lanes a and e, total liver cytosol; lanes b and f, washthrough from GSH-Sepharose; lanes c and g, 50 mM Tris-HCl, pH 9.6 eluate from GSH-Sepharose; and lanes d and h, GSH eluate.

TABLE I

Affinity Purification of Liver Glutathione S-Transferase Following Calmodulin-Stimulated Methylation

Fraction	mg Protein	Specific Activity (nmol/min•mg)	Total GST Activity
Dialyzed Cytosol	20.0	380	7,600
Post Methylation	12.7	534	6,800
Column Washthrough	6.6	28.3	187
pH 9.6 Eluate	0.32	438	142
Glutathione Eluate	0.51	9,160	4,670

Glutathione S-transferase activity was determined with CDNB as substrate.

Dialyzed rat liver cytosol was chromatographed on glutathione-Sepharose following in vitro methylation in the presence of calmodulin. Nonspecifically bound proteins were eluted from the column with 50 mM Tris-HCl, pH 9.6. Bound proteins were eluted with 50 mM Tris-HCl, pH 9.6 containing 5 mM glutathione.

This laboratory (1) had shown that calmodulin-dependent methylation of MeAP29 was subject to inhibition by a dialyzable inhibitor. Since GSH serves as a substrate in reactions catalyzed by GSTs, we decided to determine the effects of GSH on MeAP29 methylation in vitro. The methylation of MeAP29 was stimulated by dialysis or added calmodulin (Fig. 3). The combination of dialysis and added calmodulin resulted in additive effects on MeAP29 methylation. Inclusion of 0.1 mM GSH in the incubation slightly inhibited the methylation of MeAP29 in dialyzed cytosol compared to control; 1.0 mM GSH almost completely inhibited

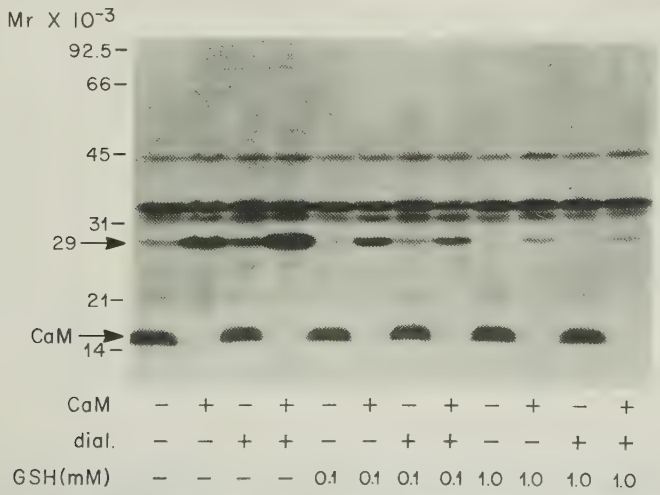

Figure 3. Effect of glutathione on in vitro methylation of MeAP29; fluorograph of SDS-polyacrylamide gel. GSH and/or calmodulin were added to methylation incubations, as indicated. MeAP29 source was either dialyzed or non-dialyzed liver cytosol, as shown. Methylation conditions as described in Materials and Methods.

MeAP29 calmodulin-stimulated methylation. Glutathione had no apparent effect on the in vitro methylation of any other protein.

Glutathione levels in normal adult rat liver cytosol are approximately 5 mM (14). Under a number of stresses, the level of GSH may drop substantially (for review, see 15). To determine the effect of lowered GSH levels on MeAP29 methylation, we injected rats with buthionine sulfoximine (BSO) (12). Rats injected with BSO showed only approximately 30% of the control levels of GSH (TABLE II). Fig. 4 shows the effect of lowered in vivo GSH levels on in vitro MeAP29 methylation (individual animals are shown; a typical control animal and four experimental animals). Lowered GSH levels resulted in enhanced methylation of MeAP29 in non-dialyzed liver cytosol. In the non-dialyzed cytosol plus added calmodulin lanes, there is a negative correlation between GSH levels and MeAP29 methylation (e.g., BSO-4 had the highest GSH level and under these in vitro conditions MeAP29 methylation was the lowest for this animal). Once again, no significant changes were observed in methylation of any of the other methyl acceptor proteins as a result of this drug treatment. The increased in vitro methylation of MeAP29 from BSO-injected animals was probably not due to an increase in GST levels, as there was actually a slight decrease in GST activity in the experimental animals compared to controls (TABLE III). These data suggest that GSH is the dialyzable inhibitor of calmodulin-stimulated in vitro MeAP29 methylation.

We classify MeAP29 as a member of the GST family from the following evidence: 1) retention of MeAP29 on GSH-Sepharose columns and its elution with buffer containing

TABLE II

Effect of Buthionine Sulfoximine Injection on Glutathione Levels in Rat Liver

Treatment		μmoles GSH/g tissue
Control	C-1	4.72
	C-2	6.25
	C-3	6.35
	C-4	7.10
		$\bar{X}$ = 6.10 ± 1.00
BSO-Injected	BSO-1	1.67
	BSO-2	1.12
	BSO-3	2.04
	BSO-4	2.88
		$\bar{X}$ = 1.93 ± 0.74 * (31.6% of control)

Male Holtzmann rats (200-300 g) were injected with 4 mmoles BSO/kg body weight at time zero and again after 2 hours, and sacrificed 2 hours later. Control rats received injections of 0.9% sodium chloride in a volume equal to those received by the experimental animals. Injections were made intraperitoneally. Data for individual animals is shown. * Using a two sample t test for independent samples $p < .0001$, indicating a significant difference between the control and BSO-injected data.

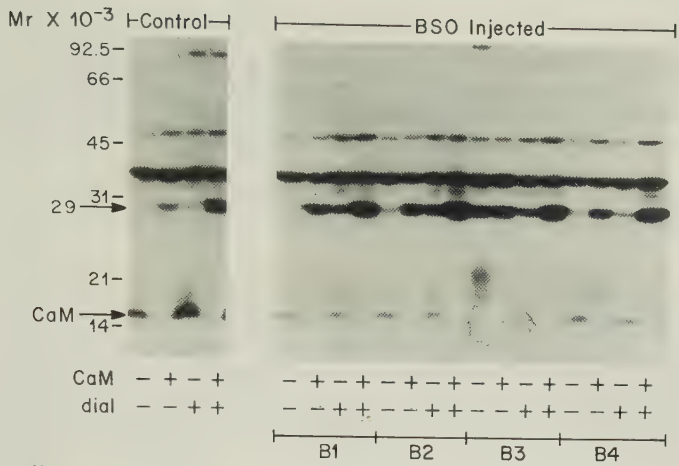

Figure 4. Effect of BSO-injection on in vitro MeAP29 methylation; fluorograph of SDS-polyacrylamide gel. Left panel, typical control; right panel, individual BSO-injected animals. Sample source was either dialyzed or non-dialyzed liver cytosol, as indicated. Alternate incubations contained 20 μg calmodulin.

glutathione; 2) comparable monomer molecular weights of the GSTs and MeAP29 (14, Fig. 2); 3) formation of dimers in solution (14) and 4) MeAP29 fractions purified through the Sephadex G-75 step contained GST activity (data not shown). Partial N-terminal amino acid sequence analysis supports this classification (manuscript in preparation).

Further studies point to GSH as the dialyzable inhibitor of MeAP29 calmodulin-dependent methylation. GSH added to dialyzed liver cytosol affected only the methylation of MeAP29 and not of other methyl acceptor proteins. Also, lowering GSH levels in liver enhanced the methyl

TABLE III

Glutathione S-Transferase Activity in Livers of Control and Buthionine Sulfoximine Injected Rats

Treatment		Specific Activity (nmol/min•mg)
Control	C-1	359
	C-2	379
	C-3	330
	C-4	406
		$\bar{X}$ = 367 ± 31.7
BSO-Injected	BSO-1	318
	BSO-2	195
	BSO-3	277
	BSO-4	292
		$\bar{X}$ = 270 ± 53.1 * (73.6% of control)

Glutathione S-transferase activity was determined with CDNB as substrate. Data for individual animals is shown. Assays were run in duplicate for individual animals. * Using two sample t test for independent samples, control and BSO-injected results are not significantly different.

accepting activity of MeAP29 in non-dialyzed cytosol. Since glutathione levels in normal rat liver are high enough to inhibit MeAP29 methylation, this post-translational modification may only occur during times when glutathione levels are reduced and thus the methylation may constitute a stress response. Our current efforts to further characterize MeAP29 include studies of GST isoforms, the identification of methylated amino acid residue(s) and the determination of the physiological significance of this methylation.

ACKNOWLEDGEMENTS : We thank Dr. J. Collins (University of Maryland Medical School) for partial amino acid sequence analysis of MeAP29 and the Univ. of Wisconsin Enzyme Institute for computer search of N-terminal amino acid sequences. This research was supported by NIH grants GM 38497, NS 24969 and HD 03352. TLN is supported by a pre-doctoral grant from the Lucille P. Markey Charitable Trust, Miami, Florida. We thank P. Rowe for early insight in MeAP29 purification; B. Rogers for preparation of tables and Y. Slusser for graphic artistry.

REFERENCES

1. Siegel, F. L. and Wright, L. S. (1985) Arch. Biochem. Biophys. 237, 347-353.
2. Jackson, R. L., Dedman, J. R., Schreiber, W. E., Bhatnagar, P. K., Knapp, R. D. and Means, A. R. (1977) Biochem. Biophys. Res. Commun. 77, 723-729.
3. Paik, W. P. and Kim, S. (1970) J. Biol. Chem. 245, 6010-6015.
4. Durban, E., Nochumson, S., Kim, S., Paik, W. K. and Chan, S. K. (1973) J. Biol. Chem. 253, 1427-1435.
5. Rowe, P. M., Wright, L. S. and Siegel, F. L. (1986) J. Biol. Chem. 261, 7060-7069.
6. Roberts, D. M., Rowe, P. M., Siegel, F. L., Lukas, T. J. and Watterson, D. M. (1986) J. Biol. Chem. 261, 1491-1494.
7. Marshak, D. R., Clarke, M., Roberts, D. M. and Watterson, D. M. (1984) Biochemistry 23, 2891-2899.
8. Roberts, D. M., Burgess, W. H. and Watterson, D. M. (1984) Plant Physiol. 75, 796-798.
9. Simons, P. C. and Vander Jagt, D. L. (1981) Methods in Enzymol. 77, 235-237.
10. Vander Jagt, D. L., Hunsaker, L. A., Garcia, K. B. and Royer, R. E. (1985) J. Biol. Chem. 260, 11603-11610.
11. Habig, W. H. and Jakoby, W. B. (1981) Methods in Enzymol. 77, 398-405.
12. Meister, A. and Griffith, O. W. (1979) Proc. Natl. Acad. Sci. 76, 5606-5610.
13. Tietze, F. (1969) Anal. Biochem. 27, 502-522.
14. Jakoby, W. B. and Habig, W. H. (1980) Enzymatic Basis of Detoxication, Acad. Press, vol. 2, pp. 63-94.
15. Meister, A. (1983) Science 220, 472-477.

Vol. 156, No. 1, 1988 BIOCHEMICAL AND BIOPHYSICAL RESEARCH COMMUNICATIONS
October 14, 1988 Pages 375-382

DISCREPANCIES BETWEEN THE AFFINITIES OF BINDING AND ACTION OF THE NOVEL β-ADRENERGIC AGONIST BRL 37344 IN RAT BROWN ADIPOSE TISSUE

Patrick Muzzin[1], Josiane Seydoux[2], Jean-Paul Giacobino[1], John-Craig Venter[3] and Claire Fraser[3]

Départements de Biochimie Médicale[1] et de Physiologie[2], Centre Médical Universitaire, 9 Avenue de Champel, 1211 Genève 4 Switzerland

Section of Receptor Biochemistry[3] NINCDS, National Institutes of Health, Park Building, Room 405, Bethesda, MD 20892

Received August 29, 1988

The novel brown adipose tissue (BAT) selective β-adrenergic agonist, BRL 37344, is 31-fold more potent than (-)-isoproterenol in stimulating the respiratory rate of interscapular BAT fragments. BRL 37344 is also more potent (9-fold) than (-)-isoproterenol in stimulating adenylate cyclase activity of IBAT purified plasma membranes whereas, in the same preparation, it is 81-fold less potent than (-)-isoproterenol in competition displacement studies with the β-adrenergic ligand, [^{125}I]cyanopindolol. We have previously demonstrated that the photoaffinity reagent [^{125}I]cyanopindolol-diazirine selectively labels a 62 kDa protein in IBAT plasma membranes that displays pharmacological properties of a β_1-adrenergic subtype. Relatively high concentrations of BRL 37344 (10 μM) are required to displace [^{125}I]cyanopindolol-diazirine binding to the 62 kDa protein. Taken together, the results suggest that two different populations of β-adrenergic receptors may co-exist in BAT plasma membranes: a small population (about 15 %) of atypical β-receptors and a large population of β_1-receptors that exhibit high and low affinities for BRL 37344, respectively. © 1988 Academic Press, Inc.

Brown adipose tissue (BAT), which is the main effector of cold-induced and diet induced-thermogenesis in rodents (1, 2), is under the control of the sympathetic nervous system (3) which acts through β-adrenergic receptors (4). The characterization of this receptor, however, is still a matter of controversy. Various studies performed with labeled β-adrenergic ligands suggest that the BAT β-receptor consists mostly of the β_1 subtype (5 - 7). The use of a novel group of β-adrenergic agonists, however, has shown that BAT β-receptor might not conform to the β_1/β_2 classification (8). These β-agonists stimulate brown adipocyte lipolysis much more selectively than atrial rate (β_1) or tracheal relaxation (β_2). The possible atypy of BAT β-receptor is supported by another puzzling feature i.e. its unusually low affinity for β-adrenergic antagonists (8).

To date, the binding characteristics of the novel group of β-adrenergic agonists to BAT plasma membranes have to our knowledge not

0006-291X/88 $1.50
Copyright © 1988 by Academic Press, Inc.
All rights of reproduction in any form reserved.

been studied. It thus seemed of interest to perform binding competition studies using the β-adrenergic ligand [^{125}I]cyanopindolol (CYP) and one of these novel β-agonists, BRL 37344, in order to determine if the high affinity of BRL 37344 for β-adrenergic action in BAT could be correlated with a high affinity for binding to the BAT β-receptor. Binding competition studies were also performed using the photoaffinity ligand [^{125}I]CYP-diazirine and labeled proteins were analyzed by SDS polyacrylamide gel electrophoresis in an attempt to characterize BRL 37344 binding proteins. The results demonstrate that BRL 37344 is much less potent in displacing the binding of β-adrenergic radioligands to IBAT receptors than in activating IBAT metabolism. These data extend previous reports on the nature of β-adrenergic responses in IBAT and suggest a new insight into the possible β-receptor subtypes of BAT plasma membranes.

MATERIALS AND METHODS

All organic and inorganic chemicals were of analytical grade and were purchased from Merck (Darmstadt, F.R.G.), Sigma (St.Louis, MO, USA) and Fluka (Buchs, Switzerland). [^{32}P]ATP, 410 Ci/mmol, [^{125}I]CYP, 2,000 Ci/mmol and [^{125}I]CYP-diazirine, 2,000 Ci/mmol were purchased from Amersham (Amersham, U.K.). (-)-Isoproterenol was obtained from Sigma (St. Louis, MO, USA) and BRL 37344 was a gift from Beecham Pharmaceuticals (Epsom, UK). Premixed SDS-polyacrylamide gel electrophoresis standards (phosphorylase b, 92.5 kDa; albumin, 66.2 kDa; ovalbumin, 45.0 kDa; carbonic anhydrase, 31.0 kDa; soybean trypsin inhibitor, 21.5 kDa; lysozyme, 14.4 kDa) were from Bio-Rad (Richmond, CA, USA). X-ray films (XAR-5) were from Eastman Kodak (Rochester, NY, USA).

Sprague-Dawley male rats weighing 200-250 g, kept at room temperature (22°C) with 12 hrs of illumination per day and fed ad libitum with Provimi Lacta chow (Cossonay, Switzerland), were used in these studies. The respiratory rate (MO_2) of IBAT fragments was measured under basal conditions and in response to increasing concentrations of β-agonists. Tissue fragments of about 12 mg were perifused with Krebs-Ringer bicarbonate solution at 30°C, and the respiratory rate measured as described in detail by Barde et al. (9). The IBAT plasma membranes were prepared as previously described (7) and atrium plasma membranes by using the same technique. Protein concentrations were determined by the method of Lowry et al. (10). The adenylate cyclase activity was measured on purified IBAT plasma membranes according to the technique described by Salomon et al. (11) as modified by Cooper et al. (12).

In ligand binding studies, IBAT and atrium plasma membranes were incubated 30 min at 37°C in 20 mM PO_4 buffer at pH 7.4 containing [^{125}I]CYP alone or in the presence of increasing concentrations of β-agonists (total volume: 0.5 ml). The binding of the radioligand to the membranes was determined by the polyethylene glycol precipitation technique (13). Specific binding was defined as the difference between total binding obtained in the absence of competing ligand and the non specific binding value obtained in the presence of an excess of (-)-isoproterenol. The mean specific binding represented 88 % of the total binding. Estimation of the K_i as well as that of the maximal number of binding sites at saturation were calculated from a Scatchard plot (14) using the LIGAND program (15). Plasma membranes were photoaffinity labeled as described previously (7). SDS-polyacrylamide

gel electrophoresis was performed according to the method of Laemmli (16) using 9-15 % acrylamide gradient slab gels as described previously (7).

RESULTS

Oxygen consumption of IBAT fragments

As shown in Fig. 1, (-)-isoproterenol and BRL 37344 produce dose-dependent increases in the MO_2 values of rat IBAT fragments. Maximal stimulation of MO_2 by both agonists is similar (7.8-fold over the basal value) however BRL 37344 is 31-fold more potent ($p<0.001$) than (-) -isoproterenol in stimulating MO_2 in IBAT fragments (Fig. 1 and Table). When BRL was added in the presence of (-)-propanolol (1 μM) a 9-fold shift to the right in the dose-response curve for MO_2 was observed (Fig. 2).

Adenylate cyclase activity of IBAT plasma membranes

Fig. 3 shows the adenylate cyclase activity of rat IBAT plasma membranes in the presence of increasing concentrations of (-)-isoproterenol or of BRL 37344. Maximal stimulations of adenylate cyclase activity are 5.8- and 4.1-fold over basal levels for (-)-isoproterenol and BRL 37344, respectively. The maximally stimulated values are 340 ± 31 and 232 ± 16 pmol of $_c$AMP formed per mg protein per min for (-)-isoproterenol and BRL 37344, respectively. The difference between these two values is significant ($p<0.05$). As found for MO_2, BRL 37344 is more potent than (-)-isoproterenol in stimulating adenylate cyclase activity in IBAT membranes ($p<0.005$). Comparison of the K_{act} values (see Table) demonstrates that the potencies differ by a factor of 9.

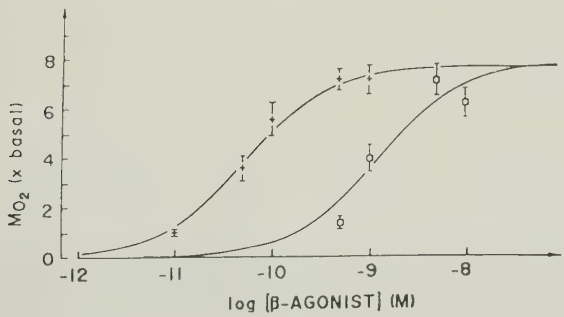

Fig. 1: Steady state increase of MO_2 in IBAT fragments in the presence of increasing concentrations of (-)-isoproterenol (□) or BRL 37344 (+). The values are the means ± SEM of 5 experiments. Mean basal value is 40 ± 2 nmol O_2 per mg wet weight per hour.

TABLE

EC_{50}, K_{act} and K_i values of BRL 37344 and of (-)-isoproterenol on MO_2, adenylate cyclase activity and [^{125}I]CYP binding

	MO_2	Adenylate cyclase	[^{125}I]CYP binding
(-)-isoproterenol	1.4 ± 0.1	2,130 ± 230	140 ± 50
BRL 37344	0.045 ± 0.010	230 ± 7	11,300 ± 1,800

The results are expressed in nmol/L and represent the mean of the number of experiments in the corresponding figures.

[^{125}I]CYP and [^{125}I]CYP-diazirine binding in IBAT plasma membranes

As illustrated in Fig. 4, the binding of 50 pM [^{125}I]CYP to IBAT plasma membranes can be displaced by increasing concentrations of BRL 37344 or (-)-isoproterenol. (-)-Isoproterenol is a more potent inhibitor of [^{125}I]CYP binding to IBAT plasma membranes than BRL 37344. Comparison of the K_i values (see Table) shows that the binding affinities of these ligands for the IBAT β-receptor differ by a factor of 81.

Analysis of the competition displacement curves by the LIGAND program suggests the existence of two populations of binding sites for BRL 37344 with K_i of 5.9 and 14,000 nM, respectively. The high affinity BRL 37344 binding sites represent only 14 % of the total BRL 37344 binding sites of the IBAT plasma membranes. In contrast, although two populations of binding sites for (-)-isoproterenol are present in IBAT, the majority of these sites (86 %) are of high affinity with a K_i of 92 nM. It is of note that the small population

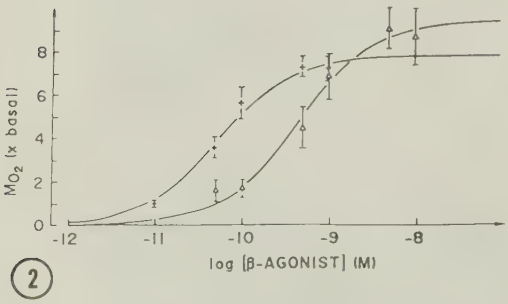

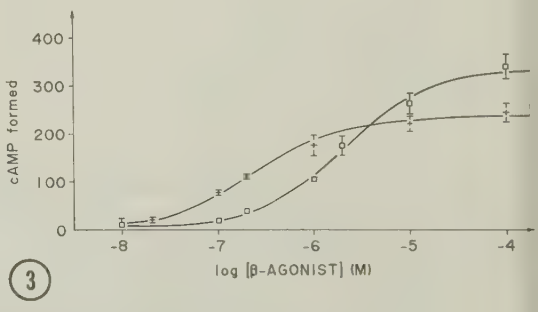

Fig. 2: Steady state increase of MO_2 in IBAT fragments in the presence of increasing concentrations of BRL 37344 alone (+) or with 1 μM (-)-propranolol (Δ). The values are the means ± SEM of 3 experiments.

Fig. 3: Stimulation of adenylate cyclase activity in IBAT plasma membranes by increasing concentrations of (-)-isoproterenol (□) or BRL 37344 (+). The values which are the mean of 3 experiments ± SEM are expressed in pmol of cAMP formed per mg protein per min. Mean basal value is 58 pmol per mg protein per min.

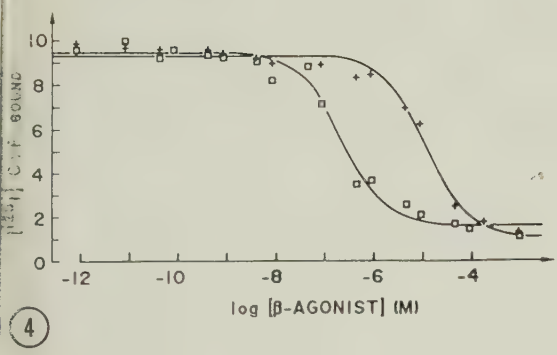

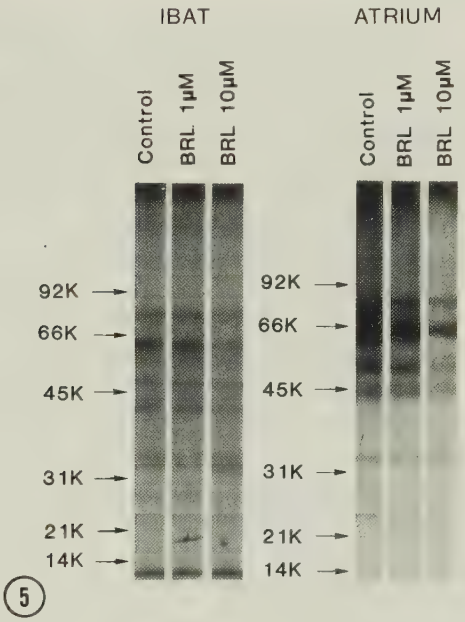

Fig. 4: Displacement of [^{125}I]CYP to IBAT plasma membranes by increasing concentrations of (-)-isoproterenol (□) or BRL 37344 (+). Membranes were incubated with 50 pM [^{125}I]CYP and the indicated concentrations of agonist for 30 min at 37°C. Assays were stopped and binding determined as described. The values, which are the means of duplicates, were obtained in 3 separate experiments and are expressed in fmol of ligand bound per mg of protein.

Fig. 5: Displacement of the specific binding of 0.5 nM [^{125}I]CYP diazirine to IBAT or atrium plasma membranes by BRL 37344. The figure shows autoradiograms obtained after incubation of the plasma membranes with [^{125}I]CYP-diazirine followed by photolysis and polyacrylamide gradient SDS gel electrophoresis (see Methods). The mobility of the protein standards is shown to the left of the figures.

of high affinity BRL 37344 binding sites has an affinity for BRL 37344 16-fold higher than the high affinity (-)-isoproterenol binding sites.

Fig. 5 shows the result of a typical experiment performed with the photoaffinity ligand [^{125}I]CYP-diazirine. A protein of 62 kDa as well as others at 50 and 42 kDa are specifically labeled with [^{125}I] CYP-diazirine. A recent study from our laboratory suggested that these proteins most likely represent the intact β-adrenergic receptor and two major proteolytic fragments (7). In the atrium the pattern of photoaffinity labeling is comparable; specific labeling of peptides at 65, 50 and 45 kDa are observed. It can be seen that BRL 37344 is no more potent in displacing the specific binding of 0.5 nM [^{125}I]CYP-diazirine to the β-receptor in the IBAT than in the atrium In fact, at a concentration of 1 μM BRL 37344, no displacement of [^{125}I]CYP-diazirine binding is seen in plasma membrane proteins of either tissue. It is only when the concentration of BRL 37344 is increased to 10 μM that displacement of the stereoselectively labeled bands is seen in the plasma membranes of both tissues.

DISCUSSION

The MO_2 value measured in BAT fragments is a good index of thermogenesis in this tissue. The β-agonist BRL 37344 was found to be more potent in stimulating MO_2 in brown adipose tissue fragments than (-)-isoproterenol. This result extends the finding by Arch et al. (8) that BRL 37344 was more potent in stimulating lipolysis in brown adipocytes than (-)-isoproterenol. The EC_{50} of BRL 37344 for the stimulation of thermogenesis was even lower than the EC_{50} described by Arch et al. (8) for stimulation of lipolysis in brown adipocytes by a factor of 38-fold, confirming that BRL 37344 is a very powerful thermogenic agent in BAT. The inhibition of BRL 37344-stimulated MO_2 by (-)-propanolol confirms that BRL 37344 acts through the β-receptor.

Adenylate cyclase activity and β-adrenergic binding were both measured on the same purified IBAT plasma membrane system to allow for a more valid comparison of the results. The K_{act} of (-)-isoproterenol and BRL 37344 were 3 orders of magnitude higher than the EC_{50} for MO_2 observed in tissue fragments. Such a change in potency has already been described by Svartengren et al. (17). The K_{act} and the activity at maximal stimulation obtained in the present study are very close to those reported in the literature (17, 18). The main finding of these experiments is that the K_{act} of BRL 37344 for adenylate cyclase activity in IBAT plasma membranes is lower than the K_{act} of (-)-isoproterenol. It is interesting to note that BRL 37344 stimulates less adenylate cyclase activity than (-)-isoproterenol. The reason for this difference is currently under study.

The situation is quite different when the K_i of (-)-isoproterenol and of BRL 37344 for $[^{125}I]$CYP displacement are studied. It was found that BRL 37344 is much less potent that (-)-isoproterenol in competing with $[^{125}I]$CYP for binding to IBAT β-receptors. Analysis of the curves using the LIGAND program (15) suggests that a small population of binding sites (14 %) has a high affinity for BRL 37344. This population would represent the atypical β-receptor proposed by Arch et al. (8) which mediates the selective thermogenic effect of BRL 37344 in BAT. The major part of the binding sites i.e. the (-)-isoproterenol binding sites have a low affinity for BRL 37344. It cannot be determined from these data wether the thermogenic effect of (-)-isoproterenol is mediated by the atypical β-receptor displaying high affinity for BRL 37344 and/or by the other β-receptors present in IBAT.

The autoradiograms reveal that the concentration of BRL 37344 required for displacement of $[^{125}I]$CYP-diazirine binding to the IBAT β-receptor is significantly higher than that which elicits maximal adenylate cyclase activation. Furthermore, the tissue selectivity described for BRL 37344 action is not observed, since BRL 37344 is no more potent in inhibiting $[^{125}I]$CYP-diazirine binding to the β-receptor in IBAT plasma membranes than in atrium. It should be noted

that the labeled 62 kDa protein has the characteristics of a β_1 adrenergic receptor subtype since the β_1-antagonist, betaxolol, was found to be 100 times more potent in displacing the labeling of this protein than the β_2-antagonist ICI 118,551 (7). One interpretation of these data is that both the atypical β-receptor and the β_1-receptor have the same molecular weight of 62 kDa. The small population of atypical β-receptors with a high affinity for BRL 37344 would be displaced by low concentrations of BRL 37344 but, since they represent only a small percentage of the labeled receptor this displacement would not be detectable. The binding of [^{125}I]CYP-diazirine to the large population of β_1-receptors, having a low affinity for BRL 37344, is only displaced by high concentrations of BRL 37344 and to the same extent in IBAT and in atrium. Another interpretation of these data is that, due to the low affinity of the atypical receptor for β-antagonists (8), [^{125}I]CYP-diazirine does not bind to the atypical receptor and thus cannot be detected on the autoradiograms.

Taken together the results of this study suggest that two different populations of β-adrenergic receptors may co-exist in IBAT plasma membranes: a small population of atypical β-receptor that exhibit high affinity for BRL 37344 but that is difficult to detect by competition displacement studies with radiolabeled β-adrenergic antagonists and a large population of β_1-receptor that exhibit low affinity for BRL 37344. The cloning and sequence analysis of β-adrenergic receptors in brown adipose tissue will provide the most definitive evidence for the existence of more than one receptor subtype.

ACKNOWLEDGEMENTS

We greatly appreciated the excellent technical help of Miss C. Colomb and Mrs. D. Rohrer and we thank Mr. R. Schumacher for the illustrations. This work was supported by grants N° 3.567.087 and 3.638-087 from the Swiss National Science Foundation and by grants-in-aid from Sandoz Stiftung zur Förderung der Medizinisch-Biologischen Wisenschaften (Basel) and from the Carlos et Elsie de Reuter Foundation.

REFERENCES

1. Foster, D.O., and Frydman, M.L. (1978) Can.J. Physiol. Pharmacol. 56, 110-122.
2. Rothwell, N.J., and Stock, M.J. (1979) Nature 281, 31-35.
3. Seydoux, J., and Girardier, L. (1978) Experientia Suppl. 32, 153-167.
4. Bukowiecki, L.J., Folléa, N., Lupien, J., and Paradis, A. (1981) J. Biol. Chem. 256, 12840-12848.
5. Rothwell, N.J., Stock, M.J., and Sudera, D.K. (1985) Amer. J. Physiol. 248, E397-E402.

6. Levin, B.E., and Sullivan, A.C. (1986) J. Pharmacol. Exp. Ther. 236, 681-688.
7. Muzzin, P., Colomb. C., Giacobino, J.-P., Venter, J.C., and Fraser, C.M. (1988) J. Rec. Res. 8, 713-729.
8. Arch, J.R.S., Ainsworth, A.T., Cawthorne, M.A., Piercy, V., Sennitt, M.V., Thody, V.E., Wilson, C., and Wilson, S. (1984) Nature 309, 163-165.
9. Barde, Y.A., Chinet, A., and Girardier, L. (1975) J. Physiol. 252, 523-536.
10. Lowry, O.H., Rosebrough, N.J., Farr, A.L., and Randall, R.J. (1951) J. Biol. Chem. 193, 265-275.
11. Salomon, Y., Londos, C., and Rodbell, M. (1974) Anal. Biochem. 58, 541-548.
12. Cooper, D.M.F., Schlegel, W., Lin, M.C., and Rodbell, M. (1979) J. Biol. Chem. 254, 8927-8931.
13. Strauss, W.L., Ghai, G., Fraser, C.M., and Venter, J.C. (1979) Arch. Biochem. Biophys. 196, 566-573.
14. Scatchard, G. (1949) Ann. N.Y. Acad. Sci. 51, 660-672.
15. Munson, P.J., and Rodbard, D. (1980) Anal. Biochem. 107, 220-229.
16. Laemmli, U.K. (1970) Nature 227, 680-686.
17. Svartengren, J., Svoboda, P., Drahota, Z., and Cannon, B. (1984) Comp. Biochem. Physiol. 78C, 159-170.
18. Granneman, J.G., MacKenzie, R.G., Fluharty, S.J., Zigmond, M.J., and Stricker, E.M. (1985) J. Pharmacol. Exp. Ther. 233, 163-167.

Vol. 156, No. 1, 1988 BIOCHEMICAL AND BIOPHYSICAL RESEARCH COMMUNICATIONS
October 14, 1988 Pages 383-388

PLASMINOGEN ACTIVATOR INHIBITOR 2. ISOLATION AND CHARACTERIZATION OF THE PROMOTER REGION OF THE GENE

E.K.O. Kruithof and E. Cousin

Hematology Division, Department of Medicine, University Hospital,
1011 Lausanne, Switzerland

Received August 29, 1988

Summary We have isolated the promoter region and part of the coding region of the human plasminogen activator inhibitor 2 gene. The first two exons (65 and 177 base pairs, respectively) are separated by a 3.6 kilo base pair intron. More than 2 kilo base pair of the promoter region was sequenced and analyzed. The promoter region is characterized by: a) a TATAAA box located 31 base pairs upstream of the trancription initiaton site; b) a 123 base pair stretch (-598 to -720) that is homologous (>90% identity) to the inverted sequence of -1268 to -1380; c) a 24 base pair inverted repeat at -276 to -299 and three direct repeats; and d) several sequences that are homologous (up to 1 mismatch) to the cAMP responsive element or to binding sites for the transcription factors AP1 and AP2. © 1988 Academic Press, Inc.

Plasminogen activator inhibitor 2 (PAI-2) is one of the principal inhibitors of the fibrinolytic system, an enzyme cascade system that generates localized proteolysis. Two forms of PAI-2 have been recognized: a glycosylated and a nonglycosylated form. The majority (over 90%) is nonglycosylated and intracellular, whereas only a small part is glycosylated and secreted (1,2). Release of intracellular PAI-2 by cell death in the context of wound healing or inflammation may provide a means to block local fibrinolysis. Several lines of evidence suggest that indeed PAI-2 plays a role in local inflammatory processes. Thus, PAI-2 is a major constituent of monocytes and macrophages (3-5) and is also present in endothelial cells and fibroblast like cells; in these cells, biosynthesis and release of PAI-2 is stimulated by phorbol ester, endotoxin and the inflammatory mediator tumor necrosis factor (1,5-9). Induction by phorbol ester in the promonocyte cell line U-937 or by tumor necrosis factor in fibrosarcoma cells is followed by an up to 50 fold increase in the rate of gene transcription (7,8). As a first step to understand the molecular mechanisms underlying the response of the PAI-2 gene to tumor necrosis factor or other inflammatory mediators we have isolated the gene and sequenced more than two kilobase pair of the promoter region.

MATERIALS AND METHODS

Enzymes and chemicals - Restriction endonucleases, T4 DNA polymerase and T4 polynucleotide kinase were obtained from New England Biolabs (Beverly, MA, USA) and labelled nucleotides from New England Nuclear (Boston, MA, USA).

0006-291X/88 $1.50
Copyright © 1988 by Academic Press, Inc.
All rights of reproduction in any form reserved.

Screening of human genomic DNA library - One million recombinant phage of a human genomic Charon 4A library (10) were plated on Escherichia coli LE 392 at a density of approximately 50'000 plaque-forming units/15 cm diameter petri dish and screened by hybridization with a random primer labelled (11) insert of PAI-2 cDNA (pPAI J7, ref.7). Duplicate plaque lifts were made on nitrocellulose filters and hybridized with the labelled insert. Hybridization and washing conditions were as described (12). Phage that hybridized on both filters were replated and rescreened until all phage hybridized with the cDNA probe.

Preparation of phage DNA and subcloning in pUC 18 - Phage DNA was prepared as described (11), digested with one or more restriction enzymes, subjected to electrophoresis in agarose, transferred (13) to Gene Screen plus membranes (New England Nuclear, Boston, MA) and probed with random primer labelled fragments of PAI-2 cDNA or with end labelled oligonucleotides (11), complementary to different regions of PAI-2 cDNA. Two Eco R1/Pst 1 fragments were subcloned into the pUC18 plasmid, analyzed by restriction enzyme digestion and partially sequenced by the chemical method (14) or by the dideoxy chain termination method (15) on supercoiled plasmid DNA (16) using synthetic oligonucleotides.

Primer extension analysis - A single stranded oligomer (TCTGAGTTGCTGTCTGAC) complementary to the 5' region of the PAI-2 cDNA (17,18) was labelled with [$-^{32}$P]dATP and polynucleotide kinase to a specific radioactivity of 10^8 cpm per nmol. Ten µg of poly A+ RNA obtained from phorbol ester stimulated U-937 cells (7) was coprecipitated with 1 pmol of the labelled primer. The pellet was dissolved in 12.5 µl of 0.5 mM EDTA, denatured at 90 °C for 3 min and 38 U (1µl) of RNAse inhibitor (RNA guard, Pharmacia, Uppsala, Sweden) and 2.5 µl of 0.5 M Tris-HCl (pH 8.3) - 0.5 M KCl - 0.05 M $MgCl_2$ - 0.4 M dithiotreitol added. After 10 min hybridization at 37 °C, 6 µl of the mRNA/primer mixture was mixed with 3 µl of 2.5 mM each of the four deoxynucleotide triphosphates and 1 µl (16 U) of reverse transcriptase (Super RT, Staehelin, Basel, Switzerland). The primer extended DNA product was extracted with phenol, ethanol precipitated and run on a 6% sequencing gel alongside a dideoxy sequencing ladder obtained on a supercoiled plasmid using the same primer.

RESULTS AND DISCUSSION

Isolation of PAI-2 genomic clones - Two recombinant phages were isolated from the Charon 4A human gene library and plaque purified. The DNA of both phages was subjected to restriction enzyme digestion and probed with labelled oligonucleotide probes complementary to ten different regions of the cDNA. Only two probes, representing the 5' end of the coding region, reacted with the DNA. The rfestriction enzyme pattern of both phages was identical. Screening of a second library (human leukocyte genomic in EMBL3, Clontech Laboratories, Palo Alto, CA, USA) did not yield additional positive clones. One of the Charon 4A clones was analyzed in detail. A 9 kbp EcoR1 fragment of its DNA reacted with the two probes complementary to the 5' end of the cDNA. This fragment was additionally cut with Pst 1 and the resulting two subfragments of 7.6 and 1.4 kilo base pair inserted into pUC 18, yielding two plasmids: pPAI-2/52 and pPAI-2/38, respectively. DNA sequencing and restriction enzyme analysis of both plasmids revealed that pPAI-2/52 contains the first (65 base pair) exon, 4.8 kilo base pair of upstream sequences and 2.8 kilo base pair of the first intron and that pPAI-2/38 contains the second (177 base pair) exon, 0.8 kilo base pair of the first intron and 0.4 kilo base pair of the second intron (Fig. 1). The sequence of the two exons was

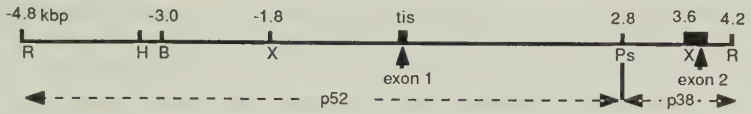


```
-2080 CTAAGGGCTC TCTGAATTAA TACCCGAAGA AAATTAGGAA GAAGGGTAGC AGAAAGGCAT TGATTGGGGT AGGCAATCAA
-2000 CAGTACCAGC TGTATAGAAT TATTAGAAAA TTAGAAGTTA GAGTAGTTGA GAAATACGTG CAAGATTATA CAACTAGTAA
-1920 ATGGCAAAAA GAAGATTCTG AGTCTGAGAC TTTTCTGAGT CTCTCAGTAT TCATATCCTT GTTCACCACA GTATAGGGCC
-1840 TCTCTAGAGA GTTTTAGCAT GTTACTCCAC CCATTAAAAA TATTTGGTAA GAATTTGCTT GATGCTCACC ACTGTTCTTG
-1760 CTGCTCAAGG GAAACCAAGT ATATATTTGT GGATAGATCC TAACTCAGAT GATACTGTCA GAATATATAA GATTCCTATA
-1680 CCACATCCTG AACTCTGAAA GTTGCAGTTC TACGTAGAAG TTCACTGAGG GTTGTAAGAG TCAGAATGGA CTCCATGGAA
-1600 GTTATGGGGT GTGAATCAAA CCTCACAGGT GAGTCAGTGG GGAGAAAGAA GCATGACATT CCTCTTGAGA ATAACTGGAA
-1520 TGAAAATAAT ACGGTGAGAA AGAGTAGCAC CTGAAAAGTG AGTGAAGGAA AGGGTGGTGG AAGTTCTAGG TACATTGATA
 1440 TCTGTCCAAC TTGTTGAGCT GTCAATGTGT GGTTAAAAAA CAGTTAAACA GGCCAGGCCC GGTGGCTCAC ACCTGTAATC
-1360 CCAGCACTTT GGGAGGCCGA GGTGGGCGGA TTGCCTGAGG TCAGGAGTTT GAGACCAGCC TGGCCAACAT GGTGAAACCC
-1280 CGTCTCTACT AAAAATACCA AAAATTAGCC AGTCGTAGTG GTTGGGCACC TGTAATCCCA GCTATTCAGG AGGCTGAGGC
-1200 AGGAGGATCA CTTGAACCCA AGAGGCGGGA GTTGCAGTGA GCAGAGATCA CGCCATTGCA CCCCAGCCTG GGCAACAAGA
-1120 GTGAAACTCG ATCTCAAAAA AACAAAAACA AAAACAAAAA ACGTTAAACG TGGTTGGTCA CATAGACATT ACCAGAGGGG
-1040 TCTTCTTGGA CAGAGGCTGA AAAGAAAGAA GGGACTTAGC TCACCACCAG ACTCCTCAGC ACTCACGGGA GAAGAGCACT
 -960 AAGGACAAAG GGGCACTTAA CACGTGTAAA AGGGCAATGG CTCCTAATAA AGGATAAGAT CTGTTTTCTT TTTATTTTAT
 -880 TTTTTGTTTT TGAGATGGAG TCTCACTCTG TCACCCAGGC TGGAGTGCAG TGGCACAGTC TCAGCTCAAT GCAACCTCCA
 -800 CCTCCCAGGT TCAAGTGATT CTTCTGCCTC AGCCTCTCAA GTAGCTGGAA CTGGAGATGT GTGCCACCAC GTGCAGCTAA
 -720 TTTTTGTATT TTTAGTAGTG ACAGGGTTTC ACCATGCTGG CCAGGCTGGT CTCAAACTCC TGACCTCAAG TGATCCTCCC
 -640 GCCTCGGCCT CCCAAAGTGC TGGGATTACA TGCATGAGCC ACCACACCCG GCCATAAGAT CTATTTTATA ATCAAGAGAA
 -560 GATGAAAAAT TCTTCTTGTG TCAGGATATT AGGGTAGAAT CCGAGTTATT TCGAAAATTA CAGCTTGAGA CAATGTAAGA
 -480 CAGATTAAAA TAGAGAATTT CTAAGACAGA AAATGGATTT TTTCTTCCCT TCCCATGCCC TAAGCATCGC TTGGGTCTCC
 -400 CTAGGCTCAA AAGAGAGAGT AAATCTCATT ATATTTATAT ATTGGAAGAA GCCCACAGGC CATGGTTGTC CAAAGCTAGA
 -320 AGAAGTATTG TAGAATTTGA TACTATCCTT GAGCACAAGT ATAGTGGGGG AAATCTTGAA ACTGGGGCTG ACAGATTTTA
 -240 GCTAACTTTC ACAGGCATGT GTAGATATTG ACAAATTCTT AAGTTTCAGA GTGACCTCAT CCTCCCCCAA AATTTCTTAA
 -160 ACCATGCCTT TACAAACAAG TATTTCTATT CTAATGATGT CTTCCTGAGT AAAATGTTGA ATCACTCAAA GGACACAGAT
  -80 CAAAAGACAG AGGGAGAAAA AAAAATGCCA TGTGGGAGGG GCAAACCTGT ATAAAACCAG TCATTACCAT GTCTGAACTG
tis TAACAACTCT CAGAGGAGCA TTGCCCGTCA GACAGCAACT CAGAGAATAA CCAGAGAACA ACCAGgtatt tcaatgattt
    ccatgccatg ......intron A (3.6 kbp)......ttcttcctctcttgcttctagATTGAAACA ATG GAG GAT CTT
    TGT GTG GCA AAC ACA CTC TTT GCC CTC AAT TTA TTC AAG CAT CTG GCA AAA GCA AGC CCC ACC CAG
    AAC CTC TTC CTC TCC CCA TGG AGC ATC TCG TCC ACC ATG GCC ATG GTC TAC ATG GGC TCC AGG GGC
    AGC ACC GAA GAC CAG ATG GCC AAG gtgagtttgagctgagctcacatttgggcgagtag .....intron B......
```

Fig. 1 **Structure of the 5' end of the PAI-2 gene.** A: restriction map of the cloned region (R: EcoRI; H: Hind III; B: Bam HI; X: XbaI; P: PstI). The positions are given in kilo base pair with respect to the transcription initiation site (tis). B: DNA sequence of the promoter region of the PAI-2 and of the first two exons with their flanking sequences. Note the tataaa box at position -31 to -26, a long inverted repeat starting at -1258 and -598, a short inverted repeat between-299 to -276 and two direct repeats at -1219 and -1356 and at -1124 and -1292 (underlined with arrows). In the region up to -600 are also marked the sequences that are homologous to binding sites (maximum 1 mismatch) for the transcription factors AP1 (////) and AP2 (\\\\), as well as the cAMP responsive element (═). DNA sequences coding for the PAI-2 protein are given as triplets. Intron sequences are given in lower case.

identical with that of the cDNA (7,17,18). The 3.6 kilo base pair first intron is located 9 base pairs upstream of the start codon of PAI-2, in a region where all known members of the serpin family of proteins have an intron. The second intron is located after a secondary structure element (Helix C) where PAI-2 has, compared to the other serpins, an additional 23 aminoacids inserted in the loop structure between helices C and D. To determine the size of the second intron two oligonucleotides were prepared

complementary to the cDNA sequence just downstream of the second exon, but no hybridization of these probes with phage DNA was obtained.

Determination of the transcription initiation site - To locate the transcription initiation site a labelled 18-mer complementary to the 5' end of the PAI-2 cDNA was hybridized to mRNA isolated from phorbol ester stimulated U-937 cells and extended as described in the methods section. One major extended DNA product was observed (Fig. 2). Alignment with the DNA sequence run alongside revealed the most likely position of the transcription initiation site. As expected for an eukaryotic gene, a TATAAA consensus sequence is situated at 26 to 31 base pair upstream (Fig.1).

Sequence and analysis of the promoter region of the PAI-2 gene - As a first step to the identification of structural elements involved in the regulation of the PAI-2 gene we have sequenced and analyzed more than 2 kilo base pair of the promoter region. Several repeats and inverted repeats were noted (Fig. 1). Particularly noteworthy is the 123 base pair stretch from -598 to -720 that is almost identical (> 90% identity) to the inverted sequence of -1258 to -1380. Interestingly, two direct repeats (a 16 base pair repeat at -1219 and -1356; and a 15 base pair repeat, 1 mismatch, at -1124 and -1292) are located within the 123 base pair inverted repeat region -1258 to -1380. An almost perfect (1 mismatch) contigouous inverted repeat is located at position -276 to -299.

In recent years a number of transcription factors have been identified. We therefore searched the promoter region for homologies with sequences known to interact with

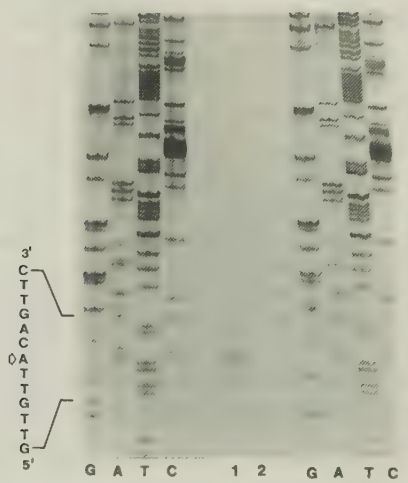

Fig. 2 Primer extension analysis of the 5' end of the human PAI-2 gene. An 18 base pair synthetic oligomer (TCTGAGTTGCTGTCTGAC) was end-labelled, hybridized to 10 μg of poly (A^+) mRNA from phorbol ester stimulated U-937 cells and extended on the mRNA as described in the methods section (lane 1). The reaction product and the labelled primer alone (lane 2) were electrophoresed between the products of dideoxy chain termination sequencing reactions performed on the plasmid containing the transcription initiation site (pPAI 2-52) using the same primer. The sequence at the right of the figure represents the complement of the coding strand sequence: GAACTGTAACAAC; underlined is the most likely position of the transcription initiation site.

these factors. From their complete or almost complete (1 mismatch) identity with such sequences several putative binding sites for the transcription factors AP1 and AP2 as well as cAMP responsive elements were identified (Fig. 1). Some of these elements may be involved in PAI-2 gene regulation. Thus one or more of the putative binding sites for AP1, also known as the phorbol ester responsive element (19,20) may be implicated in the induction by phorbol ester of of PAI-2 gene transcription in U-937 cells (7). The presence of several potential AP2 binding sites, that mediate induction by protein kinase C dependent or cAMP induced signal transduction pathways (21,22) as well of two putative binding sites for the cAMP responsive element binding factor (23) render it worthwile to investigate whether PAI-2 gene transcription can be induced also via cAMP dependent pathways. Deletion and mutation studies need to be undertaken to determine which of the potential regulatory elements are implicated in the regulation of PAI-2 gene transcription.

The isolation of the promoter region of the PAI-2 gene will allow a detailed analysis of the molecular mechanisms underlying the regulation of this inhibitor. As PAI-2 is strongly transcriptionally induced by tumor necrosis factor (8), the PAI-2 promoter region will provide a model system to study the elements involved in gene regulation by this cytokine.

ACKNOWLEDGMENTS

This work was supported by a grant from the Swiss National Fund for Scientific Research (No. 3.387-0.86) and by the Foundation for Research on Atherosclerosis and Thrombosis (FRAT). We thank E. Ayala and J.P. Vögeli for synthesizing the oligonucleotides, Dr. R.L. Medcalf for providing the mRNA from phorbol ester stimulated U-937 cells and Drs. E. Kawashima, D. Jenne and W.D. Schleuning for helpful discussions.

REFERENCES

1. Genton, C., Kruithof, E.K.O., and Schleuning, W.D. (1987) J. Cell Biol. 104, 705 - 712
2. Wohlwend, A., Belin, D., and Vassalli, J.D. (1987) J. Exp. Med.165, 320 - 339
3. Golder, J.P., and Stephens, R.W. (1983) Eur. J. Biochem. 136, 517 - 522
4. Vassalli, J.D., Dayer, J.M., Wohlwend, A., and Belin, D. (1984) J. Exp. Med. 159, 1653 - 1688
5. Chapman, H.A., and Stone, O.L. (1985) Am. Rev. Respir. Dis. 132, 569 - 575
6. Kruithof, E.K.O., Vassalli, J.D., Schleuning, W.D., Mattaliano, R.J., and Bachmann, F. (1986) J. Biol. Chem. 261, 11207 - 11213
7. Schleuning, W.D., Medcalf, R.L., Hession, C., Rothenbühler, R., Shaw, A., Kruithof, E.K.O. (1987) Mol. Cell. Biol. 7, 4564 - 4567
8. Medcalf, R.L., Kruithof, E.K.O., and Schleuning, W.D. (1988) J. Exp. Med. (in press).
9. Sadler, J.E., Ye, R.D., Wun, T.C., and Scarpati, E.M. (1988) FASEB J. 2, A1736, (abstr.)
10. Lawn, R.M., Fritsch, E.F., Parker, R.C., Blake, G., and Maniatis, T. (1978) Cell 15, 1157 - 1174
11. Maniatis, T., Fritsch, E.F., and Sambrook, J. (1982) Molecular cloning. A laboratory manual. Cold Spring Harbor Laboratory.
12. Benton, W.D., and Davis, R.W. (1977) Science 196, 180 - 182

13. Southern, E. (1975) J. Mol. Biol. 98, 503 - 517
14. Maxam, A.M., and Gilbert, W. (1977) Proc. Natl. Acad. Sci. USA 74, 560 - 564
15. Sanger, F., Nicklen, S., and Coulson, A.R. (1977) Proc. Natl. Acad. Sci. USA 74, 5463 - 5467
16. Chen, E.Y., and Seeburg, P.H. (1985) DNA 4, 165 -170
17. Ye, R.D., Wun, T.C., and Sadler, J.E. (1987) J. Biol. Chem. 262, 3718 - 3725
18. Webb, A.C., Collins, K.L., Snyder, S.E., Alexander, S.J., Rosenwasser, L.J., Eddy, R.L., Shows, T.B., and Auron, P.E. (1987) J. Exp. Med. 166, 77 - 94
19. Lee, W., Mitchell, P., Tjian, R. (1987) Cell 49, 741 - 752
20. Angel, P., Imagawa, M., Chiu, R., Stein, B., Imbra, R.J., Rahmsdorf, H.J., Jonat, C., Herrlich, P., and Karin, M. (1987) Cell 49, 729 - 739
21. Imagawa, M., Chiu, R., and Karin, M. (1987) Cell 51, 251 - 260
22. Mitchell, P.J., Wang, C., and Tjian, R. (1987) Cell 50, 847 - 861
23. Montminy, M.R., Sevarino, K.A., Wagner, J.A., Mandel, G., and Goodman, R.H. (1986) Proc. Natl. Acad. Sci. USA 83, 6682 - 6686

Vol. 156, No. 1, 1988 BIOCHEMICAL AND BIOPHYSICAL RESEARCH COMMUNICATIONS
October 14, 1988 Pages 389-395

STRUCTURE OF THE HUMAN BLOOD PLATELET MEMBRANE GLYCOPROTEIN Ibα GENE

Roland H. Wenger*, Nelly Kieffer**, Andreas N. Wicki* and Kenneth J. Clemetson*†

* Theodor Kocher Institute, University of Berne, Freiestrasse 1, CH-3012 Berne, Switzerland

** Institut National de la Santé et de la Recherche Médicale U.91, Hôpital Henri Mondor, F-94010 France

Received September 1, 1988

Summary: The gene for human platelet glycoprotein Ib α-chain has been cloned from a genomic cosmid library using a partial cDNA clone as probe. 3530 bp were sequenced including the entire transcribed part, as well as additional 5' and 3' regions. A single intron was found 6 bp upstream of the ATG initiation codon. An exceptionally long exon was identical to the recently published cDNA sequence (1). The 5' upstream promoter region is atypical for eukaryotic genes with only a weak homology to the characteristic promoter consensus sequences. The 3' region contains two repetitive Alu elements, belonging to distinct subfamilies, connected by an oligo(dA) linker. © 1988 Academic Press, Inc.

Human blood platelet glycoprotein (GP) Ib is the receptor on unactivated platelets for von Willebrand factor (vWf), a large multimeric plasma component. As such it plays a critical role in adhesion of platelets to the subendothelium of damaged blood vessels in the primary stages of haemostasis (reviewed in refs. 2 and 3). GPIb consists of two subunits, α and β, with masses of 150 kDa and 25 kDa, respectively, joined by disulphide bonds (4). cDNA coding for both these subunits has been cloned and sequenced (1,5) and both contained leucine-rich repeats. In platelet membranes GPIb exists as a 1:1 complex with another glycoprotein, GPIX (6). The α subunit of GPIb contains a

† To whom correspondence should be addressed.

Abbreviations: GP: glycoprotein; vWf: von Willebrand factor; bp: base pair; kb: kilobase pair.

0006-291X/88 $1.50
Copyright © 1988 by Academic Press, Inc.
All rights of reproduction in any form reserved.

thrombin binding site which is involved in the kinetics of platelet activation by thrombin (7). Several bleeding disorders are known in which there is an inherited deficiency or defect in GPIb. These include Bernard-Soulier syndrome (8,9), pseudo von Willebrand disease (10) and Bolin-Jamieson syndrome (11). In Bernard-Soulier syndrome both subunits of GPIb, GPIX and a further glycoprotein, GPV, are all missing or affected (12), suggesting an association between the genetic control or cellular expression of these components. As a step towards understanding the factors controlling expression of the GPIb complex in the megakaryocyte and in platelets we have isolated and sequenced the gene for GPIbα, which contains several unusual features.

MATERIALS AND METHODS

Preparation of a cDNA probe. Human platelet mRNA was isolated and used for the construction of a λgt11 expression library as described (13,14). Polyclonal antibodies against GPIbα were used for screening this library. A partial cDNA clone for GPIbα, identical to nucleotide sequence 661 to 1444 of the full length cDNA (1), was isolated and sequenced (13). The probe was labelled with [α^{32}P]dCTP by the random primed labelling method (Amersham).

Screening of genomic library. This cDNA probe was used for screening a pCV105 cosmid library (15,16). Colonies that hybridized positively were rescreened and the cosmid DNA isolated by the alkaline extraction procedure (17). DNA (25 μg) was digested with EcoRI (Boehringer Mannheim), separated by 0.8% agarose gel electrophoresis and blotted onto nitrocellulose membranes (BA 85, Schleicher & Schuell). The EcoRI fragment that hybridized with the cDNA probe on Southern blots, was isolated from agarose gels by electroelution in a membrane trap (Bio-Trap, Schleicher & Schuell), phenol extracted and precipitated with ethanol.

Nucleotide sequencing. This fragment was subcloned into M13 Bluescript (+) and (-) (Stratagene) by ligation to the linearized plasmid with T4 ligase (New England Bio-Labs) and transformation into *E. coli* strains JM 101, JM 107 and JM 109 by the $CaCl_2$ method (18). Single stranded DNA templates were prepared by superinfection with M13K07 helper phage. Alternatively, double stranded templates were used as described (19). The DNA sequence was determined by the dideoxy-chain-termination method (20) using [α^{35}S]dATP (New England Nuclear) and either the modified T7 DNA polymerase (Sequenase, United States Biochemicals) or the unmodified form (Pharmacia). The sequencing strategy involved synthetic primers and restriction mapping. Universal M13 and reversed M13 primer were purchased from Pharmacia, 18 to 24 bp oligodeoxynucleotides were prepared on a Applied Biosystems 381A DNA synthesizer and purified by gel filtration on NAP-10 columns (Pharmacia). Restriction enzymes were from Boehringer-Mannheim and New England Bio-Labs. Restriction fragments were isolated and subcloned for sequencing

as above. Sequences were assembled and analysed using the MicroGenie program (Beckmann).

RESULTS AND DISCUSSION

A pCV105 cosmid library (15,16) was screened (200,000 colonies) with a 783 bp partial cDNA probe (Fig. 1A) encoding human platelet GPIbα. Fifteen colonies gave a positive signal with this probe and secondary screenings identified 4 clones containing a 6.5 kb EcoRI fragment which hybridized to the same probe on Southern blots. Since genomic Southern blotting also revealed an EcoRI fragment of 6.5 kb (21), one of them (N10) was chosen for sequencing. 3530 bp were sequenced (Fig. 1B) including 261 bp of the 5' non-transcribed region, a single, 233 bp long intron 6 bp upstream of the ATG initiation codon and 646 bp downstream of the polyadenylation site at the 3' end (Fig. 2).

The 5' untranscribed region of the GPIbα gene has some unusual features. No typical TATA or CAAT consensus sequences, which play an important role in promotion of transcription in many eukaryotic genes (22), were found. However, there are two uncharacteristic sequences at relative positions where TATA and

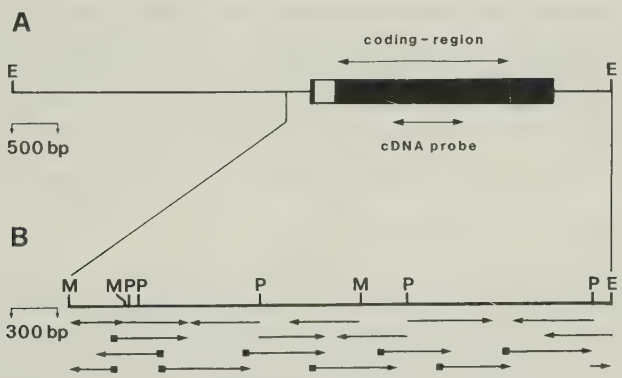

Figure 1: Cloning and sequencing strategy of the GPIbα gene.

Fig. 1A: The line represents the 6,5 kb EcoRI fragment of the GPIbα gene. 3530 bp were sequenced, including the transcribed part (filled bar) and a single intron (open bar). The lengths of the coding region and the cDNA probe used for screening the genomic library are indicated.

Fig. 1B: Restriction map and sequencing strategy. The extent and direction of sequencing are indicated by arrows. Solid boxes associated with the arrows indicate that the sequences were determined by using synthetic primers. The restriction sites are: E: EcoRI; M: MseI; P: PstI.

A

```
5'- TTAAAAGATGGCAGAAGGCTGTTTGGAGGAGTCCACCCCCATCTCCCCTGTGTAAA 56
AGGAAAGCGGAAGAGAGAACCACAAAGAGGGCCTGGGGGAAAGCCGTGGAGTGAGGCGAT 116
AAGGGCTTGTGTCCAGGGGATTCCCGGTCACTGGAATCCCTATCAGGCCTGCATTTCCTC 176
CTCACCCCCATCCCCTTCCTTGCCACTGGCTTAGTCCTCCATGGGGCTAGAAGAGAGAAG 236
                              ↓
GACGGAGTCGAGTGGCACCCTAGAAGACGCTCTGTGCCTTCGGAGGTCTTTCTGCCTGCC 296
Tgtaagccggggttggtgctggggcaggagaggggtctgagggaggggaaagagccaagg 356
acctggagctagtagttttaagttctgcaggcaagggtgggagatgggagtagggaggac 416
aggaggtgtggatgctgtttctggaagcgaagctgcagggggaagggggctggggcctgg 476
ggggatgcttccaggggatgcagggggatccactcaaggctcccttgcccacagGTCCTC 536
 M  P  L  L  L  L  L  L  L  L  P  S  P  L  H  P  H  P  I  C  20
ATGCCTCTCCTCCTCTTGCTGCTCCTGCTGCCAAGCCCCTTACACCCCCACCCCATCTGT 596
 E  V  S  K  V  A  S  H  L  E  V  N  C  D  K  R  N  L  T  A  40
GAGGTCTCCAAAGTGGCCAGCCACCTAGAAGTGAACTGTGACAAGAGGAATCTGACAGCG 656
 L  P  P  D  L  P  K  D  T  T  I  L  H  L  S  E  N  L  L  Y  60
CTGCCTCCAGACCTGCCGAAAGACACAACCATCCTCCACCTGAGTGAGAACCTCCTGTAC 716
 T  F  S  L  A  T  L  M  P  Y  T  R  L  T  Q  L  N  L  D  R  80
ACCTTCTCCCTGGCAACCCTGATGCCTTACACTCGCCTCACTCAGCTGAACCTAGATAGG 776
 C  E  L  T  K  L  Q  V  D  G  T  L  P  V  L  G  T  L  D  L  100
TGCGAGCTCACCAAGCTCCAGGTCGATGGGACGCTGCCAGTGCTGGGGACCCTGGATCTA 836
 S  H  N  Q  L  Q  S  L  P  L  L  G  Q  T  L  P  A  L  T  V  120
TCCCACAATCAGCTGCAAAGCCTGCCCTTGCTAGGGCAGACACTGCCTGCTCTCACCGTC 896
 L  D  V  S  F  N  R  L  T  S  L  P  L  G  A  L  R  G  L  G  140
CTGGACGTCTCCTTCAACCGGCTGACCTCGCTGCCTCTTGGTGCCCTGCGTGGTCTTGGC 956
 E  L  Q  E  L  Y  L  K  G  N  E  L  K  T  L  P  P  G  L  L  160
GAACTCCAAGAGCTCTACCTGAAAGGCAATGAGCTGAAGACCCTGCCCCCAGGGCTCCTG 1016
 T  P  T  P  K  L  E  K  L  S  L  A  N  N  N  L  T  E  L  P  180
ACGCCCACACCCAAGCTGGAGAAGCTCAGTCTGGCTAACAACAACTTGACTGAGCTCCCC 1076
 A  G  L  L  N  G  L  E  N  L  D  T  L  L  L  Q  E  N  S  L  200
GCTGGGCTCCTGAATGGGCTGGAGAATCTCGACACCCTTCTCCTCCAAGAGAACTCGCTG 1136
 Y  T  I  P  K  G  F  F  G  S  H  L  L  P  F  A  F  L  H  G  220
TATACAATACCAAAGGGCTTTTTTGGGTCCCACCTCCTGCCTTTTGCTTTTCTCCACGGG 1196
 N  P  W  L  C  N  C  E  I  L  Y  F  R  R  W  L  Q  D  N  A  240
AACCCCTGGTTATGCAACTGTGAGATCCTCTATTTTCGTCGCTGGCTGCAGGACAATGCT 1256
 E  N  V  Y  V  W  K  Q  G  V  D  V  K  A  M  T  S  N  V  A  260
GAAAATGTCTACGTATGGAAGCAAGGTGTGGACGTCAAGGCCATGACCTCTAACGTGGCC 1316
 S  V  Q  C  D  N  S  D  K  F  P  V  Y  K  Y  P  G  K  G  C  280
AGTGTGCAGTGTGACAATTCAGACAAGTTTCCCGTCTACAAATACCCAGGAAAGGGGTGC 1376
 P  T  L  G  D  E  G  D  T  D  L  Y  D  Y  Y  P  E  E  D  T  300
CCCACCCTTGGTGATGAAGGTGACACAGACCTATATGATTACTACCCAGAAGAGGACACT 1436
 E  G  D  K  V  R  A  T  R  T  V  V  K  F  P  T  K  A  H  T  320
GAGGGCGATAAGGTGCGTGCCACAAGGACTGTGGTCAAGTTCCCCACCAAAGCCCATACA 1496
 T  P  W  G  L  F  Y  S  W  S  T  A  S  L  D  S  Q  M  P  S  340
ACCCCCTGGGGTCTATTCTACTCATGGTCCACTGCTTCTCTAGACAGCCAAATGCCCTCC 1556
 S  L  H  P  T  Q  E  S  T  K  E  Q  T  T  F  P  P  R  W  T  360
TCCTTGCATCCAACACAAGAATCCACTAAGGAGCAGACCACATTCCCACCTAGATGGACC 1616
 P  N  F  T  L  H  M  E  S  I  T  F  S  K  T  P  K  S  T  T  380
CCAAATTTCACACTTCACATGGAATCCATCACATTCTCCAAAACTCCAAAATCCACTACT 1676
 E  P  T  P  S  P  T  T  S  E  P  V  P  E  P  A  P  N  M  T  400
GAACCAACCCCAAGCCCGACCACCTCAGAGCCCGTCCCGGAGCCCGCCCCAAACATGACC 1736
```

Figure 2: Sequence of the GPIbα gene.

5' region: The intron is indicated by lower case letters. The stretch with a certain homology to the CAAT consensus is double underlined and the direct repeated stretches with weak homology to the TATA consensus are single underlined. The beginning of the cloned full length cDNA (1) is represented by an arrow.

3' region: The polyadenylation signal is double underlined and the polyadenylation site is marked with a triangle. The two Alu repetitive elements are underlined.

CAAT boxes have usually been found. These are the GGCCTGCAT and the repeated CTAGAAGA stretch starting at position -100, -39 and -6 respectively, relative to the estimated beginning of the cDNA

B

```
 T  L  E  P  T  P  S  P  T  T  P  E  P  T  S  E  P  A  P  S   420
ACCCTGGAGCCCACTCCAAGCCCGACCACCCCAGAGCCCACCTCAGAGCCCGCCCCCAGC 1796
 P  T  T  P  E  P  T  P  I  P  T  I  A  T  S  P  T  I  L  V   440
CCGACCACCCCGGAGCCCACCCCAATCCCGACCATCGCCACAAGCCCGACCATCCTGGTG 1856
 S  A  T  S  L  I  T  P  K  S  T  F  L  T  T  T  K  P  V  S   460
TCTGCCACAAGCCTGATCACTCCAAAAAGCACATTTTTAACTACCACAAAACCCGTATCA 1916
 L  L  E  S  T  K  K  T  I  P  E  L  D  Q  P  P  K  L  R  G   480
CTCTTAGAATCCACCAAAAAAACCATCCCTGAACTTGATCAGCCACCAAAGCTCCGTGGG 1976
 V  L  Q  G  H  L  E  S  S  R  N  D  P  F  L  H  P  D  F  C   500
GTGCTCCAAGGGCATTTGGAGAGCTCCAGAAATGACCCTTTTCTCCACCCCGACTTTTGC 2036
 C  L  L  P  L  G  F  Y  V  L  G  L  F  W  L  L  F  A  S  V   520
TGCCTCCTCCCCCTGGGCTTCTATGTCTTGGGTCTCTTCTGGCTGCTCTTTGCCTCTGTG 2096
 V  L  I  L  L  L  S  W  V  G  H  V  K  P  Q  A  L  D  S  G   540
GTCCTCATCCTGCTGCTGAGCTGGGTTGGGCATGTGAAACCACAGGCCCTGGACTCTGGC 2156
 Q  G  A  A  L  T  T  A  T  Q  T  T  H  L  E  L  Q  R  G  R   560
CAAGGTGCTGCTCTGACCACAGCCACACAAACCACACACCTGGAGCTGCAGAGGGGACGG 2216
 Q  V  T  V  P  R  A  W  L  L  F  L  R  G  S  L  P  T  F  R   580
CAAGTGACAGTGCCCCGGGCCTGGCTGCTCTTCCTTCGAGGTTCGCTTCCCACTTTCCGC 2276
 S  S  L  F  L  W  V  R  P  N  G  R  V  G  P  L  V  A  G  R   600
TCCAGCCTCTTCCTGTGGGTACGGCCTAATGGCCGTGTGGGGCCTCTAGTGGCAGGAAGG 2336
 R  P  S  A  L  S  Q  G  R  G  Q  D  L  L  S  T  V  S  I  R   620
AGGCCCTCAGCTCTGAGTCAGGGTCGTGGTCAGGACCTGCTGAGCACAGTGAGCATTAGG 2396
 Y  S  G  H  S  L TER                                         626
TACTCTGGCCACAGCCTCTGAGGGTGGGAGGTTTGGGGACCTTGAGAGAAGAGCCTGTGG 2456

GCTCTCCTATTGGAATCTAGTTGGGGGTTGGAGGGGTAAGGAACACAGGGTGATAGGGGA 2516

GGGGTCTTAGTTCCTTTTTCTGTATCAGAAGCCCTGTCTTCACAACACAGGCACACAATT 2576

TCAGTCCCAGCCAAAGCAGAAGGGGTAATGACATGGACTTGGCGGGGGGACAAGACAAAG 2636

CTCCCGATGCTGCATGGGGCGCTGCCAGATCTCACGGTGAACCATTTTGGCAGAATACAG 2696

CATGGTTCCCACATGCATCTATGCACAGAAGAAAATCTGCAAAGTGATTTATCAGGATGT 2756

GAGCACTCGTTGTGTCTGGATGTTACAAATATGGGTGGTTTTATTTTCTTTTTCCCTGTT 2816

TAGCATTTTCTAGTTTTCCACTATTATTGTATATTATCTGTATAATAAAAAATAATTTTA 2876
        ▽
GGGTTGGGAGTGATGGCTCATGCCTGTAATCCTAGCACTTTGGGAGGCCGAGGCGGGTGG 2936

AATCACCAGAGGTAGGGAGTTCAAGACCAGCCTGGCAAACATGGTGAAACCCTGGTCTCT 2996

ACTAAAAATACAAAAATTAGGCCAGGCGTGGTGGTGCACACCTATAACCCCAGCTACTCG 3056

GGAGGGTGGGGCAGGAGAATCGCTTGAACCTGGGAGGCGGAAGTTGCCGTGAGCCAAGAT 3116

CGTACCACTGAACTCCAGCCTGGGTAACAGAGTGAGACTCCGTCTAAAAAAAAAAAAAAA 3176

AAAAAAAAAAACTTCTGGCCGGGTGCAGGGGCTCATGCCTGTAATTCCAGCACTCTGGAA 3236

GGCTGAGGCGGGTGGGTTGCTTGAACCCAGGAGTTTGGCCCAGGCTTGGCAACATGGCAA 3296

AACCCGACCTCTACAAAAAATACAAAACATTAGCCAGGTGTGGTGGCATGCACCTGTGGT 3356

CCCAGGTACCCGGGTGGCTGAGGAGGGAGGATCACCTGAGCCTGGGAGATGGAGGCTGCA 3416

GTGAGCCCTGAAGGTGCCACTGTACTCCAGCCTGGGTGACAGAGTGAGAGCCTGTCTCAA 3476

AACAACTTGGCTTCTTTTGGTGAAGAGTGGCTGGGGCACCTGTCATGAGAATTC  - 3' 3530
```

Figure 2 - Continued.

(1) (Fig. 2). Further investigations will show whether the homology to the TATA$^{A}/_{T}$A$^{A}/_{T}$ and GG$^{T}/_{C}$CAATCA consensus sequences (22) is mere chance or if there exists a new family of promoter sequences controlling the expression of platelet GPIb complex proteins.

The exon-intron structure of the GPIbα gene is also rather uncommon for eukaryotic genes. The whole precursor of GPIbα (626 amino acids) is expressed by a single, exceptionally large exon of 2,4 kb. No difference in the nucleotide sequences was found between our genomic clone and the published cDNA (1). The gene

contains a single intron of 233 bp, 6 bp upstream from the ATG translation initiation codon in the 5' non-translated region. This intron has an unusually high content of guanosine (46% of total). A computer-assisted search of the GeneBank (DNAstar, release 55) revealed no significant homology to any other known sequence. The exon-intron splice junctions are in good agreement with the consensus sequences determined for correct splicing of the precursor mRNA (23). Interestingly, von Willebrand factor, for which GPIbα is the receptor on platelets, also contains an intron just before the initiation site (24,25). Whether this is important for cell specific expression of GPIbα, as has been suggested for vWf, remains to be shown.

The 3' region of the GPIbα gene contains two Alu repeats (Fig. 2). An alignement of the first of these (293 bp) with the published Alu-S consensus sequence (26,27) revealed 88% homology. The second (291 bp) is 83% homologous to the Alu-J subfamily, matching 11 of 15 diagnostic identification points determined for this subfamily, which is more similar to the 7SL DNA (28) in these positions (27). In contrast the Alu-S element did not match in any of these positions. These two repetitive Alu elements are connected by a 26 bp oligo(dA) linker, an element that is characteristic for Alu repeats. It should be noted that the first Alu consensus already starts 6 bp upstream from the polyadenylation site of the determined cDNA (Fig. 2), excluding the possibility of further mRNA processing signals downstream of the first polyadenylation signal.

While the origin of the genetic defect in Bernard-Soulier syndrome, which affects not only GPIbα, but also GPIbβ, GPV and GPIX, is not yet established the information supplied here on the structure of the GPIbα gene is a necessary step on the way to understanding how the biosynthesis of the GPIb complex is regulated. The sequences of the genes for the other members of the complex will be required to determine whether there are common regulatory elements or whether concerted expression is a post transcriptional event as has been postulated for the GP IIb/IIIa complex (29).

ACKNOWLEDGMENTS

We wish to thank Dr. T. Seebeck, Dr. H.-P. Amstutz and Dr. A. Walz for helpful discussions. This work was supported by the Swiss National Science Foundation grant number 3.232-0.85.

REFERENCES

1. Lopez, J.A., Chung, D.W., Fujikawa, K., Hagen, F.S., Papayannopoulou, T. and Roth, G.J. (1987) Proc. Natl. Acad. Sci. USA 84, 5615-5619.
2. George, J.N., Nurden, A.T. and Phillips, D.R. (1984) N. Engl. J. Med. 311, 1084-1098.
3. Clemetson, K.J. and Lüscher, E.F. (1988) Biochim. Biophys. Acta 947, 53-73.
4. Phillips, D.R. and Poh-Agin, P. (1977) J. Biol. Chem. 252, 2121-2126.
5. Lopez, J.A., Chung, D.W., Fujkawa, K., Hagen, F.S., Davie, E.W. and Roth, G.J. (1988) Proc. Natl. Acad. Sci. USA 85, 2135-2139.
6. Du, X., Beutler, L., Ruan, C., Castaldi, P.A. and Berndt, M.C. (1987) Blood 69, 1524-1527.
7. Wicki, A.N. and Clemetson, K.J. (1985) Eur. J. Biochem. 153, 1-11.
8. Nurden, A.T. and Caen J.P. (1975) Nature 255, 720-722.
9. Jenkins, C.S.P., Phillips, D.R., Clemetson, K.J., Meyer, D., Larrieu, M.-J. and Lüscher, E.F. (1976) J. Clin. Invest. 57, 112-124.
10. Miller, J.L., Kupinski, J.M., Castella, A. and Ruggeri, Z.M. (1983) J. Clin. Invest. 72, 1532-1542.
11. Bolin, R.B., Okumura, T. and Jamieson, G.A. (1977) Nature 269, 69-70.
12. Clemetson, K.J., McGregor, J.L., James, E., Dechavanne, M. and Lüscher, E.F. (1982) J. Clin. Invest. 70, 304-311.
13. Wicki, A.N., Walz, A., Gerber-Huber, S., Vornhagen, R. and Clemetson, K.J., in preparation.
14. Wenger, R.H., Wicki, A.N., Walz, A., Kieffer, N. and Clemetson, K.J., submitted for publication.
15. Lau, Y.-F. and Kan, Y.W. (1983) Proc. Natl. Acad. Sci. USA 80, 5225-5229.
16. Lau, Y.-F. and Kan, Y.W. (1984) 81, 414-418.
17. Birnboim, H.C. and Doly, J. (1979) Nucl. Acids Res. 7, 1513-1522.
18. Maniatis, T., Fritsch, T.F. and Sambrook, J. (1982) Molecular Cloning, Cold Spring Harbor, New York.
19. Zhang, H., Scholl, R. and Somerville, C. (1988) Nucl. Acids Res. 16, 1120.
20. Sanger, F., Nicklen, S. and Coulson, A.R. (1977) Proc. Natl. Acad. Sci. USA 74, 5463-5467.
21. Wicki, A.N. and Drouin, J., personal communication.
22. Hejine, G. (1987) Sequence Analysis in Molecular Biology, Academic Press, New York.
23. Mount, S.M. (1982) Nucl. Acids Res. 10, 459-472.
24. Bonthron, D. and Orkin, S.H. (1988) Eur. J. Biochem. 171, 51-57.
25. Assouline, Z., Kerbiriou-Nabias, D.M., Piétu, G., Thomas, N., Bahnak, B.R. and Meyer, D. (1988) Biochem. Biophys. Res. Comm. 153, 1159-1166.
26. Britten, R.J., Baron, W.F., Stout, D.B. and Davidson, E.H. (1988) Proc. Natl. Acad. Sci. USA 85, 4770-4774.
27. Jurka, J. and Smith, T. (1988) Proc. Natl. Acad. Sci. USA 85, 4775-4778.
28. Ullu, E. and Tschudi, C. (1984) Nature 321, 171-172.
29. Wautier, J.L. and Caen, J.P. (1987) Nouv. Rev. Fr. Hematol. 29, 277.

Vol. 156, No. 1, 1988 BIOCHEMICAL AND BIOPHYSICAL RESEARCH COMMUNICATIONS
October 14, 1988 Pages 396-402

DIFFERENT ROLES OF THE DIPHOSPHATE MOIETIES OF ALLYLIC AND HOMOALLYLIC DIPHOSPHATES IN PRENYLTRANSFERASE REACTION

Takeshi Gotoh, Tanetoshi Koyama, and Kyozo Ogura

Chemical Research Institute of Non-Aqueous Solutions,
Tohoku University, Katahira 2-1-1, Sendai 980, Japan

Received August 22, 1988

SUMMARY: In contrast to the reactivity of geranyl methylenediphosphonate in the reaction catalyzed by farnesyl diphosphate synthase, that of isopentenyl methylenediphosphonate showed an optimum at a more acidic pH than that of isopentenyl diphosphate, and it was inhibited by magnesium ions under certain conditions. These facts suggest that isopentenyl diphosphate is engaged in the enzyme reaction in the form of metal-free substrate contrary to the allylic substrate, which reacts in the form of metal-complexed substrate. Thus the diphosphate moieties of allylic and homoallylic substrates have different roles in the prenyltransferase reaction. © 1988 Academic Press, Inc.

As seen in nucleotidyl transfers, there are many enzyme-catalyzed reversible reactions in which bond formations take place with concomitant liberation of inorganic pyrophosphate (PPi). In general, intracellular hydrolysis by pyrophosphatase of the inorganic pyrophosphate thus liberated brings forth a thermodynamic driving force in the direction of bond formation.

The prenyltransferase reaction, however, proceeds with the release of inorganic pyrophosphate in spite of the irreversibility of the reaction (1). This has led us to be interested in the significance of the diphosphate moiety of the substrates of prenyltransferase. In our previous studies with allylic methylenediphosphonates, we showed that the replacement of the

Abbreviations: PPi, inorganic pyrophosphate; -POP, diphosphate moiety; -PCP, methylenediphosphonate moiety; DMAPP, dimethylallyl diphosphate; GPP, geranyl diphosphate; GPCP, geranyl methylenediphosphonate; IPP, isopentenyl diphosphate; IPCP, isopentenyl methylenediphosphonate; FPP, farnesyl diphosphate.

0006-291X/88 $1.50
Copyright © 1988 by Academic Press, Inc.
All rights of reproduction in any form reserved.

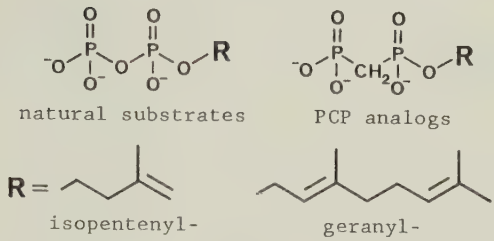

Scheme 1.

diphosphate (-POP) moiety of dimethylallyl diphosphate (DMAPP) or geranyl diphosphate (GPP) by a methylenediphosphonate (-PCP) moiety resulted in a marked decrease of V_{max} without significant change of Km (2). This fact was explained as a reflection of the poor leaving nature of the methylenediphosphonate group, which is similar in shape to the diphosphate group (Scheme 1) (2-5). This led us to expect that the -POP linkage of isopentenyl diphosphate (IPP) could be replaced by a -PCP linkage without marked loss of reactivity, because PPi is released from allylic substrates but not from IPP.

This paper, however, reports unexpected behavior of isopentenyl methylenediphosphonate (IPCP) in the reaction catalyzed by farnesyl diphosphate (FPP) synthase.

EXPERIMENTAL PROCEDURES

MATERIALS

[1-^{14}C]Isopentenyl diphosphate was a product of Amersham. Nonlabeled allylic diphosphates and [1-^{3}H]Isopentenyl methylenediphosphonate were synthesized essentially according to the method of Davission *et al.*(6) except that tris(tetra-*n*-butyl) ammonium hydrogen methylenediphosphonate was employed instead of tris(tetra-*n*-butyl)ammonium hydrogen diphosphate. [1-^{3}H] Isopentenol (3-methyl-3-butenol) was prepared by reduction of methyl 3-methyl-3-butenoate with sodium borotritiride (specific activity 359 mCi/mmol) (Amersham) in the presence of ethanedithiol (7).

Enzyme Reaction

Farnesyl diphosphate synthase was partially purified from pig liver as described previously (8). The enzyme reaction was followed by determination of the amount of [1-^{14}C]IPP or [1-^{3}H] IPCP incorporated into acid-labile materials. In a standard experiment with [1-^{3}H]IPCP as the homoallylic substrate, the incubation mixture contained, in a final volume of 1.0 ml, 20 μmol of Tris-maleate buffer (pH 6.6), 5 μmol of $MgCl_2$, 10 μmol of 2-mercaptoethanol, 100 nmol of [1-^{3}H]IPCP (spec, act. 0.45 Ci/mol), 25 nmol of GPP and 3.5 units of pig liver FPP synthase. The mixture was incubated at 37 C for 1.5 h, and then made acidic by addition of 0.3 ml of 1 M hydrochloric acid. The radioactive alcohols liberated by acid treatment were extracted

with hexane after the mixture was made alkaline. The radioactivity in the hexane extracts was counted with a liquid scintillation counter.

RESULT

The homoallylic methylenediphosphonate, IPCP was found to be active as substrate for FPP synthase. Kinetic parameters of IPCP are shown in Table 1 along with natural substrates and an allylic analog, geranyl methylenediphosphonate (GPCP). Contrary to our expectation, the V_{max} value of IPCP was only 5.4% of that of IPP. The Km value of IPCP was not so small as that of IPP or GPCP.

In addition, marked differences were observed between IPCP and GPCP with respect to the effects of pH and metal ion concentration. The optimal pH of the reaction of IPCP was around 6.6, whereas that of GPCP was 8.2. Figure 1 shows the effect of magnesium ion concentration on the rate of IPCP reaction at pH 6.6 and 8.2. At pH 6.6 the IPCP reaction showed a hyperbolic curve as a function of magnesium chloride concentration, but at pH 8.2 it showed a maximum at about 0.5 mM of magnesium chloride and declined markedly as the magnesium ion concentration was increased.

IPCP inhibited the enzymatic reaction of natural substrates. Figure 2 shows two sets of double-reciprocal plots of initial velocities for the condensation of IPP and DMAPP. IPCP is a competitive inhibitor against DMAPP with Ki of 0.56 mM, but it is an uncompetitive inhibitor against IPP with Ki of 0.48 mM.

DISCUSSION

Divalent cations such as Mg^{2+} and Mn^{2+} are essential for the prenyltransferase reaction. It is assumed that substrates complexed with metal ions are true substrates for the enzyme. It

Table 1. Kinetic parameters of IPCP in FPP synthase reaction

	IPP	IPCP	GPP*	GPCP*
Km/μM	7.1	36.0	8.1	2.6
V_{max}/nmol min^{-1} mg^{-1}	44.3	2.4	44.0	0.6

* The data are those of our previous study (2).

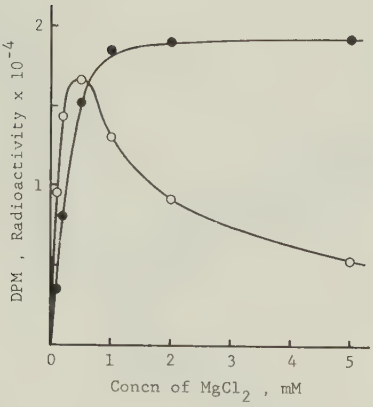

Figure 1. Effect of concentration of magnesium ion on the enzymatic reaction of IPCP at pH 6.6 (●) and pH 8.2 (○).

has been reported that methylenediphosphonic acid, compared with pyrophosphoric acid, has larger pKa values and a stronger affinity for metal ions (4). The reactivity of GPCP, reflecting such characters of the methylenediphosphonate moiety, support the above assumption (2,3).

The results with IPCP, however, are not consistent with the assumption. The reaction with IPCP showed an optimum pH at about 6.6, which was more acidic by 1.1 and 1.4 units than those for the natural substrate and GPCP, respectively. An acidic pH

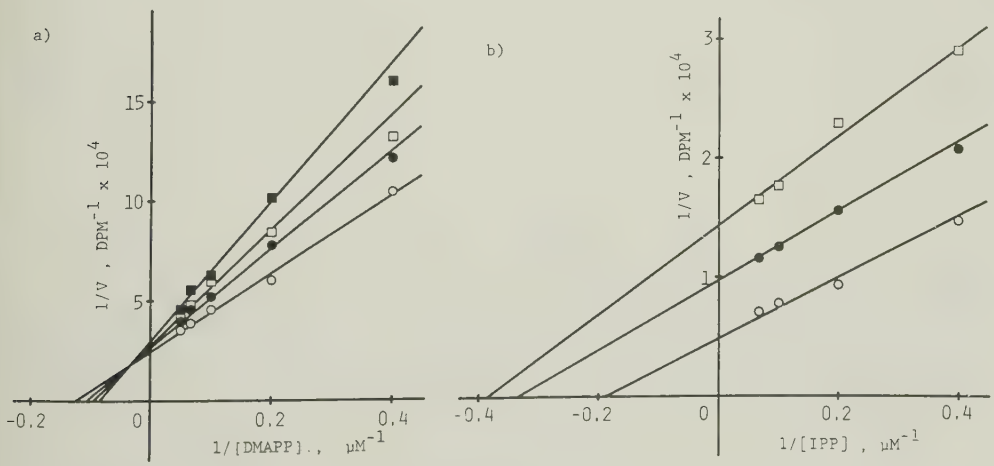

Figure 2. Inhibitory effect of IPCP against DMAPP or IPP. a) The varied substrate was DMAPP. IPCP concentration; 0 (○), 0.1 (●), 0.2 (□), 0.5 mM (■). b) The varied substrate and the allylic substrate were IPP and GPP, respectively. IPCP concentration; 0 (○), 2.0 (●), 3.5 mM (□).

should be disadvantageous to the substrates in forming metal complexes. In addition, the reactivity of IPCP at pH 8.2 was strongly inhibited when the concentration of magnesium ion was raised, whereas such inhibition was not observed at pH 6.6 (Figure 1). These unexpected properties of IPCP against pH and metal ion concentration can not be well interpreted without assuming that the homoallylic substrate, IPP, does react in the metal-free form. Since all the substrate molecules should take the metal complexed forms in the presence of a large excess of magnesium ions, it is necessary to assume a mechanism that involves the capture by the enzyme of the metal ion from the IPP-metal complex. Thus, the magnesium of the IPP-Mg complex is captured by the IPP binding site of the enzyme, and then transferred again to the newly formed allylic diphosphate, which is the product of condensation between the allylic diphosphate complexed with Mg^{2+} and the IPP molecule free of Mg^{2+}. During the condensation reaction, the enzyme may dynamically interact with the substrates and the products including inorganic pyrophosphate to attain an efficient turnover of catalysis. For example, the inorganic pyrophosphate liberated may bind to the enzyme, causing a conformational change of the enzyme in such a way that the captured magnesium is released (Scheme 2). An activation by a small amount of inorganic pyrophosphate was actually observed at an initial stage of the enzymatic reaction (date not shown). Based on the above mechanism, it is explainable that the reaction of IPCP, which has a stronger affinity for metal ions than the natural POP substrate, is strongly inhibited by high concentrations of metal ions. It is likely that the essential role of metal ions in the prenyl-transferase reaction is to form the complex with allylic diphosphates and also probably with the enzyme itself.

Inhibitory effects of IPCP also confirm the difference in behavior of the diphosphate moieties between allylic and homoallylic substrates against metal ion. IPCP was a competitive inhibitor against an allylic substrate, DMAPP, but was an uncompetitive inhibitor against IPP.

Why should the diphosphate moieties of allylic and homoallylic substrates behave so differently with regard to the metal complex formation in the enzymatic reaction ? The complex formation is favorable for the allylic substrate because it accelerates the release of PPi to form the carbonium ion, but it

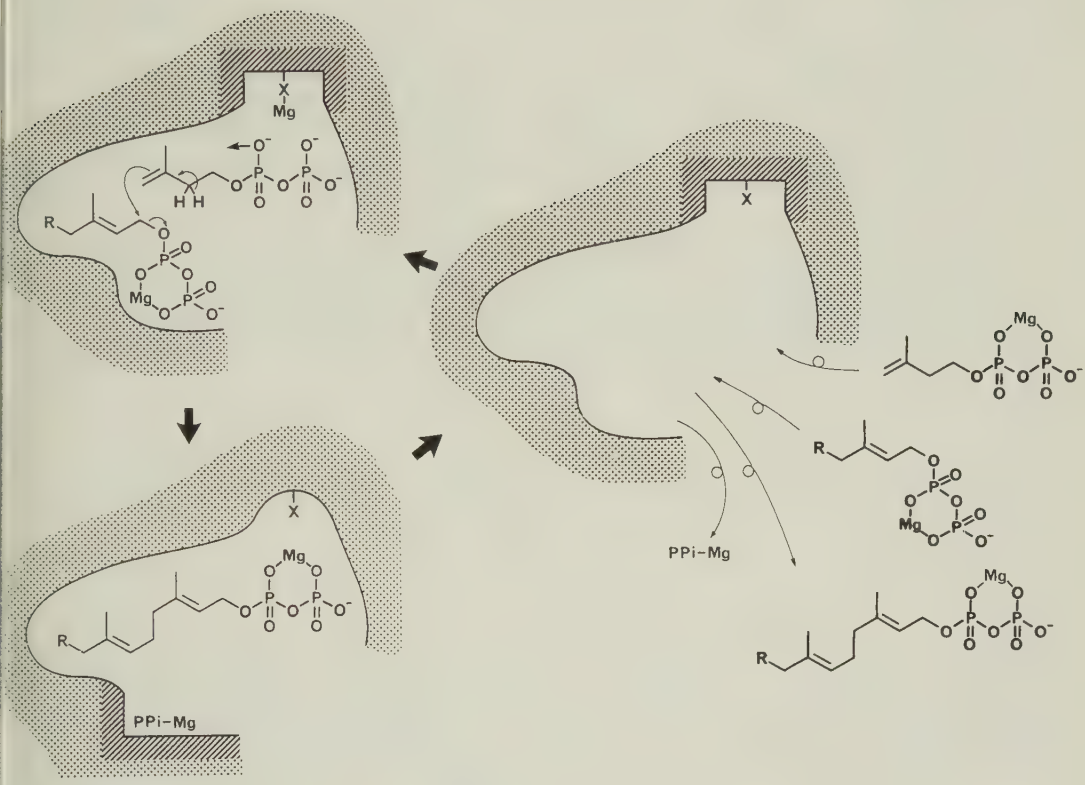

Scheme 2.

seems unnecessary for IPP to be complexed with Mg^{2+} because PPi is not released from IPP during the condensation. It must be rather advantageous for the IPP to be free of Mg^{2+}, because the negatively charged diphosphate moiety can assist the nucleophilic attack of IPP to the carbonium ion formed from the allylic substrate. It may be the reason why nature uses the diphosphate moiety in prenyltransferase reactions that this moiety can play such dual functions.

ACKNOWLEDGEMENTS

This work was supported by Grants-in-Aid for Scientific Research from the Ministry of Education, Science and Culture of Japan, the Asahi Glass Foundation for the contribution to industrial technology, and special coordination funds of the science and technology agency of the Japanese Government.

REFERENCES

1. Poulter, C.D. and Rilling, H.C. (1981) In Biosynthesis of Isoprenoid Compounds (J.W.Porter and S.L.Spurgeon, Eds) Vol.1, pp.161-224.

2. Gotoh, T., Koyama, T., and Ogura, K., *Chem. Lett.* **1987**, 1627-1630.
3. Stremler K.E. and Poulter, C.D. (1987) *J. Am. Chem. Soc.* **109**.5542-5544.
4. Irani, R.R. and Moedritzen, K. (1962) *J. Phys. Chem.* **66**,1349-1353.
5. Larsen, M.L., Willett, R., and Yount, R.G. (1969) *Science* **166**, 1510-1511.
6. Davisson, V.Jo, Woodside, A.B., and Poulter, C.D. (1985) In Methods Enzymol. (J.H.Law and H.C.Rilling, Eds) **110**, 130-144.
7. Maki, Y., Kikuchi, K., Sugiyama, H., and Seto, S. (1975) *Tetrahedron Lett.* **38**, 3295-3296.
8. Koyama, T., Saito, Y., Ogura, K., and Seto, S. (1977) *J. Biochem.* **82**, 1585-1590.

Vol. 156, No. 1, 1988 BIOCHEMICAL AND BIOPHYSICAL RESEARCH COMMUNICATIONS
October 14, 1988 Pages 403-410

Saposin D: A Sphingomyelinase Activator

Satoshi Morimoto*, Brian M. Martin#, Yasuo Kishimoto*[1] and John S. O'Brien*

*Department of Neurosciences, Center for Molecular Genetics, School of Medicine, University of California San Diego, La Jolla, California 92093

#National Institutes of Health, National Institute for Mental Health, Molecular Neurogenetics Unit, Building 10, Room 3D16, Bethesda, Maryland 20892

Received August 25, 1988

SUMMARY: Saposin D, a newly discovered heat-stable, 10 kDa glycoprotein, was isolated from Gaucher spleen and purified to homogeneity. Chemical sequencing from its amino terminus demonstrated colinearity between its amino acid sequence and the deduced amino acid sequence of the fourth domain of prosaposin, the precursor of saposin proteins. Saposin D specifically stimulates acid sphingomyelinase but has no significant effect on the other hydrolases tested.

© 1988 Academic Press, Inc.

INTRODUCTION: The lysosomal hydrolysis of sphingolipids is catalyzed by the sequential action of acid hydrolases. Several enzymatic hydrolytic steps are stimulated by small heat-stable proteins which interact with either the substrate or the enzyme or both. Two of the heat-stable proteins have been structurally defined. The first protein, named saposin B in this report and previously designated an activator of cerebroside sulfatase (1), G_{M1} activator (2), sphingolipid activator protein 1 (3), and dispersin (4), stimulates the hydrolysis of galactocerebroside sulfate (sulfatide) by arylsulfatase A (1,5,6), G_{M1} ganglioside by ß-galactosidase (2,7) and globotriaosylceramide ($Gb0se_3Cer$) by α-galactosidase A (8). Immunological and genetic evidence has demonstrated that saposin B activates all three reactions (3,8). In a recent study, Li *et al.* (9) showed that this protein has an even broader substrate specificity than reported previously, promoting the hydrolysis of the above three glycosphingolipids, as well as G_{M2} ganglioside, sulfate esters of lactosylceramide and asialo G_{M2}, globoside, three neolacto-type glycolipids and two glycerylglycolipids. From these results, Li *et al.* (9) concluded that the hydrolysis of these lipids is

[1] To Whom Correspondence Should Be Addressed.

0006-291X/88 $1.50
Copyright © 1988 by Academic Press, Inc.
All rights of reproduction in any form reserved.

promoted by a nonspecific detergent action of saposin B and called it "nonspecific activator protein". The primary structure of saposin B was determined by sequencing of a cDNA encoding it (10). The physiological significance of saposin B is underscored by the discovery of its absence in a variant form of metachromatic leucodystrophy (8).

The second protein, called saposin C in this paper and previously termed factor P (11), glucocerebrosidase activator (12), coglucosidase (13), sphingolipid activator protein 2 (3), and A_1 activator (14), stimulates the hydrolysis of glucosylceramide by glucosylceramidase (11-14), that of galactocerebroside by galactosylceramide ß-galactosidase (15) and that of sphingomyelin by sphingomyelinase (15). Unlike saposin B, saposin C appears to interact with enzymes to exert its stimulatory effect (16). The primary structure of saposin C was determined by chemical sequencing of its amino acids (17, 18) and by deducing its sequence from nucleotide sequencing of a cDNA encoding prosaposin, its precursor (19). The physiological significance of saposin C was demonstrated by discovery of its deficiency in a variant form of Gaucher's disease (20).

Recently, this laboratory has elucidated the complete nucleotide sequence of a cDNA coding for prosaposin, the precursor protein of both saposin B and C (19). Prosaposin was found to contain 4 saposin domains, two of which are saposin B and C; these are flanked by two additional domains we call saposin A and saposin D. Each saposin domain (A,B,C,D) is approximately 80 amino acid residues in length, has nearly identical placement of cysteine residues, glycosylation sites and helical regions and is flanked by proteolytic cleavage sites. Molecular models indicate that the proteins derived from each domain can fold to give rise to a conformationally rigid hydrophobic pocket held together by 3 disulfide bridges. We predicted that proteolytic cleavage of prosaposin at each domain boundary should give rise to all 4 saposins. We have recently isolated saposin D, the protein arising from domain 4. Saposin D appears to specifically stimulate sphingomyelinase to hydrolyze the phosphorylcholine moiety of sphingomyelin.

METHODS

Isolation of Saposin D. Techniques used for the isolation of saposin D were, in general, similar to those used for the isolation of coglucosidase by Sano and Radin (18). Briefly, 201 grams of spleen from a patient with adult type Gaucher's disease was homogenized with 800 ml of water and the homogenate was heated at 100°C for 10 min. The mixture was then centrifuged at 10,000 x g for 15 min. and the supernatant was fractionated by ammonium sulfate precipitation. The precipitates which appeared between 45 and 80% saturation, were collected and dialyzed. The dialysate was then fractionated by column chromatography on DEAE-cellulose (DE-52, Whatman). The column was eluted with a 0-0.5M NaCl linear gradient in 10 mM sodium phosphate buffer, pH 7.0. Fractions positive for stimulation of hydrolysis of 4-methylumbelliferone (4-MU) ß-D-glucoside (see below) were pooled, dialyzed and lyophilized. The residue, after dissolving in a small volume of water, was fractionated

by gel filtration using Sephadex G-75. The fractions containing stimulating activity for 4-MU glucoside hydrolysis were pooled and further fractionated by HPLC. A Varian model 5000 HPLC equipped with a Vydac protein C4 column (4.6 mm by 25 cm) was used and fractions were eluted with a linear gradient of water containing 0.1% trifluoroacetic acid and acetonitrile-water (4:1) containing 0.1% trifluoroacetic acid. Peaks were detected by measuring absorbance at 220 nm. A typical chromatogram is shown in Fig. 1. The effluent comprising the saposin D peak which eluted later than saposin B and C (shown in Fig. 1) was collected and evaporated to dryness.

Immunological Procedures: Antibodies against saposin D were prepared in a rabbit as described by Crowle (21) and purified with an affinity column which contained purified saposin D linked to Affi-Gel 10 Activated Affinity Support (Bio-Rad) as described previously (10). Rabbit antibodies against saposin B and C were provided by Dr. Arvan Fluharty and Dr. David Wenger, respectively. Dot and Western blots with these antibodies were performed as described previously (10).

Assays for Lysosomal Enzyme Activities: Sphingomyelinase activity was assayed as described by Wenger (22). [Methyl-^{14}C]sphingomyelin obtained from Dr. D. A. Wenger or from NEN/DuPont, was used as substrate. Human placental sphingomyelinase purchased from Sigma Chemical Co. or a Triton X-100 extract of a particulate fraction of human liver, as described by Radin and Berent (23) was used as an enzyme source. Galactoceramide ß-galactosidase and ß-glucosylceramidase were assayed as described by Wenger *et al.* (15). [G-^{3}H]Galactosylceramide was prepared as described previously (24). [G-^{3}H]Glucosylceramide was a gift from Dr. D. A. Wenger. Human spleen was homogenized with two volumes of water and centrifuged at 12,500 x g for 10 min and the supernatant obtained was used as an enzyme source of galactosylceramide ß-galactosidase. The same human liver preparation used for sphingomyelinase activity was used as enzyme source for ß-glucosylceramidase assay. G_{M1} ganglioside ß-galactosidase activity was assayed as described previously (25). The substrate [galactose-^{3}H] ganglioside G_{M1} which was synthesized as described (26) and purified human liver acid ß-galactosidase were provided by Dr. Yoshimi Yamamoto of this laboratory. The hydrolysis of 4-MU ß-D-glucoside or ß-D-galactoside was performed as described previously (27).

Other Analytical Methods: Peptide sequencing was accomplished using an Applied Biosystems model 470A gas-phase sequencer equipped with a model 120A on-line PTH analyzer using standard procedures supplied by the manufacturer. Protein concentration and carbohydrate content were determined by the method of Lowry *et al.* (28) and by the phenol sulfuric acid method (29).

RESULTS

Isolation and Characterization of Saposin D. Saposin D was isolated from Gaucher spleen by taking advantage of its heat-stability, acidity, small molecular size, and hydrophobicity. Since saposin B and C were also present in the DEAE column fractions containing saposin D its final purification was achieved by preparative hydrophobic HPLC. The yield of pure saposin D was 16.1 mg from 201 g of Gaucher spleen. Saposin D was eluted with a higher acetonitrile percentage than saposin B or C indicative of its greater hydrophobicity (Fig. 1). Saposin D contains a single glycosylation site (19) and was found to contain 16% carbohydrate by phenol-sulfuric acid analysis. Polyacrylamide gel electrophoresis in SDS (Fig. 2) gave a subunit molecular weight of approximately 10 kDa for saposin D similar to saposin B and C. Antibodies raised against saposin D did not cross react with saposin B or C (Fig. 2). Conversely, antibodies against saposin B or C did not cross react with saposin D

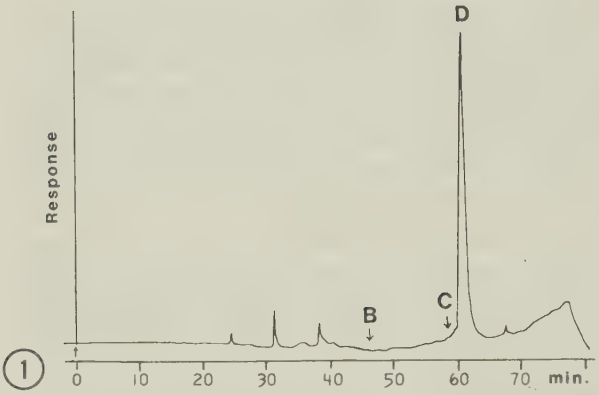

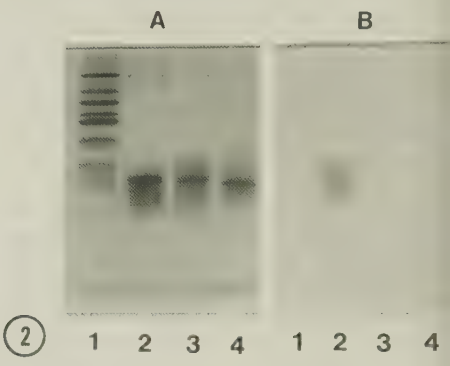

Figure 1. HPLC of Saposin D. Purified saposin D was analyzed by HPLC as described in Methods. Under the same conditions, saposin B and C appear with retention times as indicated by arrows.

Figure 2. SDS-Polyacrylamide Gel Electrophoresis and Immunoblotting of Saposin D. The purified saposin D (8.6 µg, lane 2 and 6) was electrophoresed together with saposin C (7.6 µg, lane 3 and 7) and saposin B (13.6 µg, lane 4 and 8) on 17.5% polyacrylamide slab gels containing SDS. Lanes 1 and 5 contained a protein standard mixture (Sigma Chemical Co.). The lowest protein marker is α-lactalbumin (14,200 Da). Section A was stained with Coomassie brilliant blue and B was immunoblotted with anti-saposin D antiserum as described in Methods.

(data not shown). Chemical sequencing of the N-terminal amino acids of saposin D revealed the first 19 amino acids to be identical to the polypeptide predicted to arise from proteolysis of domain 4 of prosaposin (amino acids 392 to 474) (19).

Specificity of Sphingomyelinase Stimulation by Saposin D. In the presence of Triton X-100, sphingomyelinase activity was stimulated 100% by as little as 2 µg (less than 1 µM) of saposin D as shown in Fig. 3. Stimulation was not increased when the amount of saposin D was increased indicating near saturation at this concentration. Stimulation was not likely due to a nonspecific detergent nature of saposin D because the assay mixture contained sufficient Triton X-100 to solubilize the sphingomyelin present in the assay. In addition, saposin C, which stimulates ß-glucosylceramidase activity (16, 30) and has a structure similar to saposin D (17,18,19,31) did not possess stimulatory activity in the assay. With addition of Triton X-100, 27 µg and 54 µg of Saposin D increased the sphingomyelinase activity 3- and 5-fold, respectively. However, the activity obtained with 54 µg was only 10% of that in the presence of Triton X-100. Saposin D did not stimulate ß-glucosylceramidase activity (Fig. 3), galactosylceramide ß-galactosidase activity or G_{M1} ganglioside ß-galactosidase activity (Table 1). The hydrolysis of 4-MU ß-D-glucoside was slightly enhanced when saposin D was present (also shown in Table 1). Saposin D did not stimulate hydrolysis of the other 4-MU derivative substrates including pyrophosphate, α-galactoside, ß-galactoside, α-glucoside, α-mannoside, ß-fucoside, ß-glucuronide, and ß-N-acetylglucosamide (data not shown).

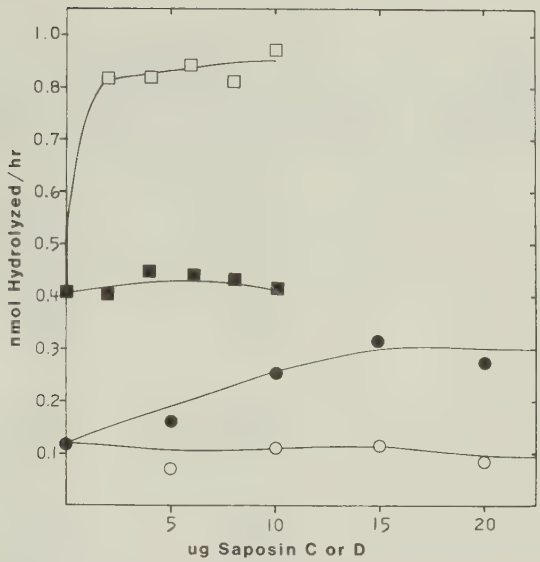

Figure 3. Effect of Saposin D on Sphingomyelinase and Glucocerebrosidase. Various amounts of saposin D were added to an assay mixture of sphingomyelinase and ß-glucosylceramidase activities and its effect was compared with that of saposin C. Sphingomyelinase activity assay mixture contained 20 nmol [methyl-^{14}C] sphingomyelin (830 cpm/nmol), 10 µg Triton X-100, and 50 µmol acetate buffer pH 5.0 in 200 µl. Crude sphingomyelinase prepared from human placenta (Sigma Chem. Co.) was used as enzyme source. Incubation was conducted at 37°C for 1 hr. ß-Glucosylceramidase assay mixture contained 5.25 nmol to [gluco-^{3}H) glucocerebroside (1358 cpm/nmol) and 20 µmol citrate-phosphate buffer pH 4.2 in 200 µl. Human liver particulate preparation solubilized by 0.1% Triton X-100 was used as enzyme source. The activities for sphingomyelinase with saposin D is shown by open squares (□) and that with saposin C is shown by closed squares (■). The activity for ß-glucosylceramidase with saposin D is expressed by open circle (○) and that with saposin C is expressed by closed circle (●). No further increase of ß-glucosylceramidase activity was observed by increasing saposins up to 35 µg each.

DISCUSSION

In accordance with our recent prediction that the proteolytic processing of prosaposin generates 4 saposin proteins of similar structure (19) we report here the isolation of a third saposin protein, saposin D, which stimulates the hydrolysis of sphingomyelin. Proof that saposin D arises from domain 4 of prosaposin was obtained by demonstrating colinearity between its first 19 chemically determined amino acids and the deduced sequence obtained from domain 4 of the prosaposin cDNA. In addition, saposin D has the correct predicted molecular weight (10 kDa) from proteolytic processing of domain 4. While this work was in progress Fürst *et al.* (31) isolated the same protein from Gaucher spleen termed component C; its amino acid sequence is identical to saposin D except for the absence of the first two N-terminal amino acids which may have been removed by peptidase action. No activating properties were reported for component C.

Saposin D has a remarkably high specificity in stimulating sphingomyelinase activity. Activation of sphingomyelinase activity by saposin C has also been reported

Table 1.

Effect of Saposin D on GM_1 Ganglioside ß-Galactosidase, Galactocerebroside ß-Galactosidase and 4-Methylumbelliferyl Glucoside ß-Glucosidase

	Saposin (µg)	nmol hydrolyzed/hr	
		- Saposin	+ Saposin
GM_1 Ganglioside ß-galactosidase	B (42)	0	0.44
	D (45)	0	0.00
Galactosylceramidase	C (8)	0.41	0.57
	(16)	0.41	1.24
	(24)	0.41	1.48
	D (14)	0.41	0.34
	(54)	0.41	0.44
	(95)	0.41	0.44
4-Methylumbelliferyl glucoside ß-glucosidase	C (4)	3.70	9.00
	(10)	3.70	13.80
	(25)	3.70	13.80
	D (4)	3.70	5.50
	(10)	3.70	5.00
	(25)	3.70	5.00

(15); but in our hands saposin C failed to stimulate sphingomyelinase activity. Christomanou and her colleagues (20) purified two proteins, named A_1 and A_2, which stimulated sphingomyelinase activity; their A_1 protein was found by chemical sequencing to be identical to saposin C (17). It is possible that our HPLC-purified saposin C lost its sphingomyelinase activating property while retaining its ß-glucosylceramidase stimulating property. Alternatively, previous preparations of saposin C may have been contaminated with saposin D since their properties are very similar and extremely small amounts of saposin D are required for activation. Another explanation is the detergent-like property of saposin C which helped to solubilize sphingomyelin in the absence of Triton X-100.

Prior to the discovery that saposin B and C are both derived from the same precursor protein (19), these proteins were named nonsystematically. The isolation of saposin D reported here has prompted us to propose a new systematic nomenclature for the saposin proteins. As mentioned the precursor protein (prosaposin) contains 4 domains comprised of similar 80 amino acid modular units which are released upon proteolysis. We propose that those proteins which are derived from the first, second, third and fourth domains be named saposin A, B, C and D. Of the four, saposin A has yet to be isolated. Partial proteolysis of prosaposin also

yields intermediate cleavage products and these have been detected in most human tissues (19). We propose that proteins possessing two saposin domains with subunit molecular weights of 25-30 kDa be called disaposin A, B and C; containing domains 1 and 2, 2 and 3, and 3 and 4 respectively. Similarly, cleavage products containing three saposin domains with subunit molecular weights of approximately 48 and 43 kDa, be named trisaposin A and B; containing domains 1,2 and 3 and domains 2, 3, 4 respectively. In line with this proposal, we have recently isolated a glycoprotein from Gaucher spleen which appears to be disaposin A.

ACKNOWLEDGEMENTS

We are grateful to Dr. David Wenger for providing us with antibodies against saposin C and radioactive sphingolipid substrates, to Dr. Arvan Fluharty for giving us antibodies against saposin B, to Dr. Yoshimi Yamamoto for purified ß-galactosidase and radioactive ganglioside GM_1, and to Dr. Norman Radin for showing us an unpublished manuscript. We also thank Susan O'Brien for her assistance in preparation of this manuscript. This study was supported in part by NIH research grants NS-13559 (YK) and HD-18983 and NS-08682 (JOB).

REFERENCES

1. Fisher, G. and Jatzkewitz, H. (1975) Hoppe-Seyler's Z. Physiol. Chem. 356, 605-613.
2. Li, S.-C. and Li, Y.-T. (1976) J. Biol. Chem. 251, 1159-1163.
3. Wenger, D.A. and Inui, K. (1984) In The Molecular Basis of Lysosomal Storage Disorders (R. O. Brady and J.A. Barranger, Eds.) pp. 61-78. Academic Press, New York.
4. Li, S.-C. and Li, Y.-T. (1986) NATO ASI Ser. A. Life Sci. 116, 307-314.
5. Mehl, E. and Jatzkewitz, H. (1964) Hoppe-Seyler's Z. Physiol. Chem. 339, 260-276.
6. Fischer, G. and Jatzkewitz, H. (1978) Biochim. Biophys. Acta 528, 69-76.
7. Li, S.-C., Wan, C.C., Mazzotta, M.Y. and Li, Y.-T. (1974) Carbohydr. Res. 34, 189-193.
8. Li, S.-C., Kihara, H. Serizawa, S., Li, Y.-T., Fluharty, A.L., Mayes, J.S., and Shapiro, L.J. (1985) J. Biol. Chem. 260, 1867-1871.
9. Li, S.-C., Sonnino, S., Tettamanti, G., and Li, Y.-T. (1988) J. Biol. Chem. 263, 6588-6591.
10. Dewji, N., Wenger, D., Fujibayashi, S., Donoviel, M., Esch, F., Hill, F., O'Brien, J.S. (1986) Biochem. Biophys. Res. Comm. 134, 989-994.
11. Ho. M.W. and O'Brien, J.S. (1971) Proc. Natl. Acad. Sci. USA 68, 2810-2813.
12. Peters, S.P., Coffee, C.J., Glew, R.H., Kuhlenschmidt, M.S., Rosenfeld, L., Lee, Y.C. (1977) J. Biol. Chem. 252, 563-573.
13. Berent, S.L. and Radin, N.S. (1981) Arch. Biochem. Biophys. 208, 248-260.
14. Christomanou, H. and Kleinschmidt, T. (1985) Biol. Chem. Hoppe-Seyler 366, 245-256.
15. Wenger, D.A., Sattler, M., Roth, S. (1982) Biochim. Biophys. Acta 712, 639-649.
16. Radin, N.S. (1984) In Molecular Basis of Lysosomal Storage Disorders (R.O. Brady and J.A. Barranger Eds.), pp. 93-112. Academic Press, New York.
17. Kleinschmidt, T., Christomanou, H., and Braunitzer G. (1987) Biol. Chem. Hoppe-Seyler 368, 1571-1578.
18. Sano A., and Radin, N.S. (1988) FESEB J. 2: A1779.
19. O'Brien, J.S., Kretz, K.A., Dewji, N.N., Wenger, D.A., Esch, F. and Fluharty, A.L. (1988) Science, in press.

20. Christomanou, H., Aignesberger, A. and Linke, R.P. (1986) Biol. Chem. Hoppe Seyler 367, 879-890.
21. Crowle, A.J. (1972) Immunodiffusion, 2nd Edition, pp. 78-96. Academic Press, New York.
22. Wenger, D.A. (1977) In Practical Enzymology of the Sphingolipidoses (R.H. Glew and S.P. Peters, Eds.) pp. 39-70. Alan R. Liss Inc., New York.
23. Radin, N.S. and Berent, S.L. (1982) Meth. Enzymol. 83, 596-603.
24 Hajra, A.K., Bowen, D.M., Kishimoto, Y. and Radin N.S. (1966) J. Lipid Res. 7, 379-386.
25. Norden, A.G.W. and O'Brien, J.S. (1973) Arch. Biochem. Biophys. 159, 383-392.
26. Suzuki, Y. and Suzuki, K. (1972) J. Lipid Res. 13, 687-690.
27. Ho, M.W. and O'Brien, J.S. (1973) Biochem. J. 131, 173-176.
28. Lowry, O.H., Rosenbrough, N.J., Farr, A.L. and Randall, R.J. (1951) J. Biol. Chem. 193, 265-275.
29. Ashwell, G. (1966) Meth. Enzymol. 8, 93-95.
30. Glew, R.H., Basu, A., LaMarco, K.L., and Prence, E.M. (1988) Lab. Invest. 58, 5-25.
31. Fürst, W., Machleidt, W., and Sandhoff, K. (1988) Biol. Chem. Hoppe-Seyler 369, 317-328.

Vol. 156, No. 1, 1988 BIOCHEMICAL AND BIOPHYSICAL RESEARCH COMMUNICATIONS
October 14, 1988 Pages 411-416

Lectins Inhibit Cell Binding and Spreading on a Laminin Substrate

John W. Dean III*§, S. Chandrasekaran* and Marvin L. Tanzer*

Departments of BioStructure and Function* and Periodontology§
School of Dental Medicine
University of Connecticut Health Center
Farmington, CT 06032

Received August 29, 1988

Summary: This study examined the effects on cell binding and spreading of the exposure of laminin substrates to the lectins Wheat Germ Agglutinin or Concanavalin A. Exposure of laminin to Wheat Germ Agglutinin inhibited binding of mouse B16 F1 melanoma cells in a dose dependent manner. Exposure to Concanavalin A had no deleterious effects on binding but did inhibit cell spreading. Both effects were completely prevented by the specific sugars for each lectin. These effects may be due to the proximity of N-linked oligosaccharides to the known cell binding sites of laminin.
© 1988 Academic Press, Inc.

Laminin is a large glycoprotein which is a prominent component of basement membranes. It is composed of three polypeptide chains, A (MW = 400,000), B1 (MW = 210,000) and B2 (MW = 200,000), held together in a cruciform shape by disulfide bonds (1). The laminin molecule is known to be about 15% carbohydrate by weight (2). Many different epithelial, neural and malignant cell lines are known to bind or otherwise respond to laminin. At least three different cell surface receptors for this large glycoprotein have been found (3,4,5) as well as two high-affinity cell adhesion sites (6,7). In this study we have attempted to examine some of the ways in which the carbohydrate components of laminin may influence its biological properties.

MATERIALS AND METHODS

Preparation of Laminin Substrates:

Laminin was isolated from Englebreth-Holm-Swarm (EHS) sarcoma by the method of Timpl et al (8). In Tris-buffered saline solution it was allowed to dry overnight at various concentrations (1 to 25 ug per well), in non-tissue culture treated 96 well flat-bottom plates (Becton Dickinson, Oxnard, CA).

Lectin Treatment of Laminin Substrates:

The laminin coated wells were rinsed twice with phosphate buffered saline (PBS), and then incubated for 2 hours at room temperature on a shaking platform with either of the two lectins

0006-291X/88 $1.50
Copyright © 1988 by Academic Press, Inc.
All rights of reproduction in any form reserved.

tested, Wheat Germ Agglutinin (WGA) or Concanavalin A (Con A) (Sigma, St. Louis, MO), at various concentrations in PBS. As controls the laminin coated wells were incubated for 2 hours with PBS alone, a lectin plus its specific sugar in PBS, a lectin plus a non-specific sugar in PBS, or sugar alone in PBS. These solutions were dumped out of the wells which were then washed three times with PBS (binding experiments with [^{125}I] labeled laminin indicated that less than 10% of the glycoprotein was washed away under these conditions (data not shown). To each well was added 100 ul of serum-free Dulbecco's modified Eagle medium (DMEM; GIBCO, Grand Island, NY).

Cell Culture and Binding Assay:

Cells used in all assays were mouse B16 F1 melanoma (the generous gift of Dr. I. Fidler, Univ. Texas Cancer Center), grown in DMEM (GIBCO) supplemented with 10% fetal bovine serum (CC Laboratories, Cleveland, OH) and 1% antibiotic-antimycotic (GIBCO) in 100mm plastic petri dishes (Becton Dickinson) under standard temperature and atmospheric conditions.

Cells were released from culture plates using an Earle's basic salt solution containing 2mM EDTA. Cells were counted using a Coulter counter (Coulter Electronics, Hialeah, FL) and seeded 5000 cells per well, in serum-free DMEM, in triplicate. Plates were placed back in the incubator for 1 hour under standard culture conditions. Cell viability was assessed on the basis of trypan blue exclusion and was found to be >85%. Medium was dumped out of the plates and all wells were washed 2 times with PBS. The adherent cells were then fixed, stained, and counted essentially by the method of Ruoslahti et al (9). Briefly, the cells were fixed overnight at 4^{0}C with 3% formaldehyde in PBS, cells were then stained with 1% toluidine blue for 2 hours at room temperature, rinsed 3 times with PBS and counted using an inverted microscope (Olympus, Japan)with a video camera (Optomax, Hollis, NH) connected to a digital image analyzer(Optomax).

RESULTS

In Figures 1a and 1b it is evident that exposure of laminin-coated plastic to WGA for 2 hours has a marked effect upon cell binding. This effect seems to be dependent upon the amount of WGA, from 25 to 100 ug per well (data not shown). Use of N-acetylglucosamine, a specific sugar for WGA, completely reverses the inhibition of B16 F1 melanoma cell binding.

Figures 2a and 2b indicate that Con A has essentially no effect on cell binding, as measured by our assay system, at any concentration tested (from 25 to 250 ug per well). However, upon examination of the fixed, stained cells it was found that Con A treatment of the laminin substrates had prevented cell spreading as compared with controls, as shown in Figures 3a and 3b. Addition of the specific sugar for Con A completely reversed the anti-spreading effect.

In all experiments, incubation of the laminin substrates with either PBS or lectin-specific sugar alone gave the same cell

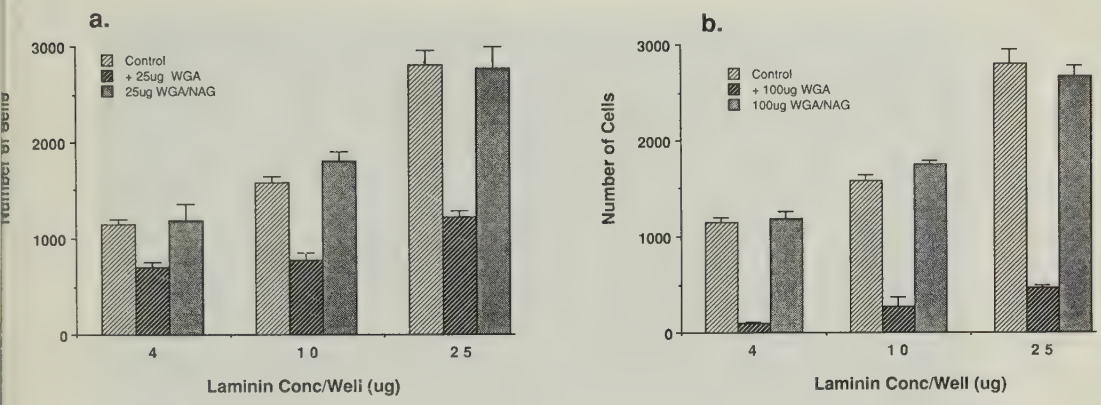

Figure 1. Number of mouse B16 F1 melanoma cells bound to laminin coated plastic (Control) or laminin coated plastic incubated with Wheat Germ Agglutinin (WGA) or incubated with WGA and N-acetylglucosamine, in triplicate wells (see Materials and Methods for detailed procedures). a. Lectin concentration is 25 ug WGA, with standard deviation bars. b. Lectin concentration is 100 ug WGA with standard deviation bars.

binding as the untreated controls (data not shown). Incubation of the lectin-treated laminin substrates with non-specific sugars gave the same results as found for lectin treatment alone (data not shown).

DISCUSSION

The laminin isolated from EHS sarcoma has been shown to possess approximately 40 N-linked oligosaccharides (10,11). We have examined how these carbohydrate moieties may influence cell

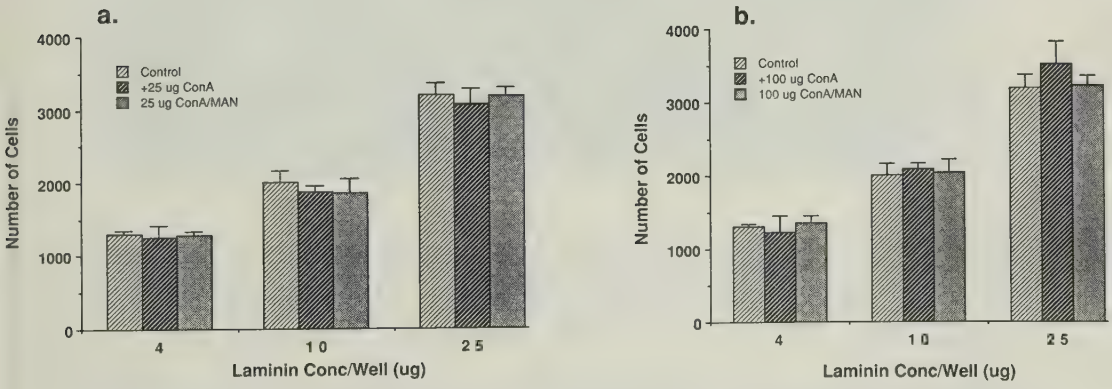

Figure 2. Number of mouse B16 F1 melanoma cells bound to laminin coated plastic (Control) or laminin coated plastic incubated with Concanavalin A (Con A) or incubated with Con A and alpha-methyl mannoside, in triplicate wells (see Materials and Methods for detailed procedures). a. Lectin concentration is 25 ug Con A, with standard deviation bars. b. Lectin concentration is 100 ug Con A, with standard deviation bars.

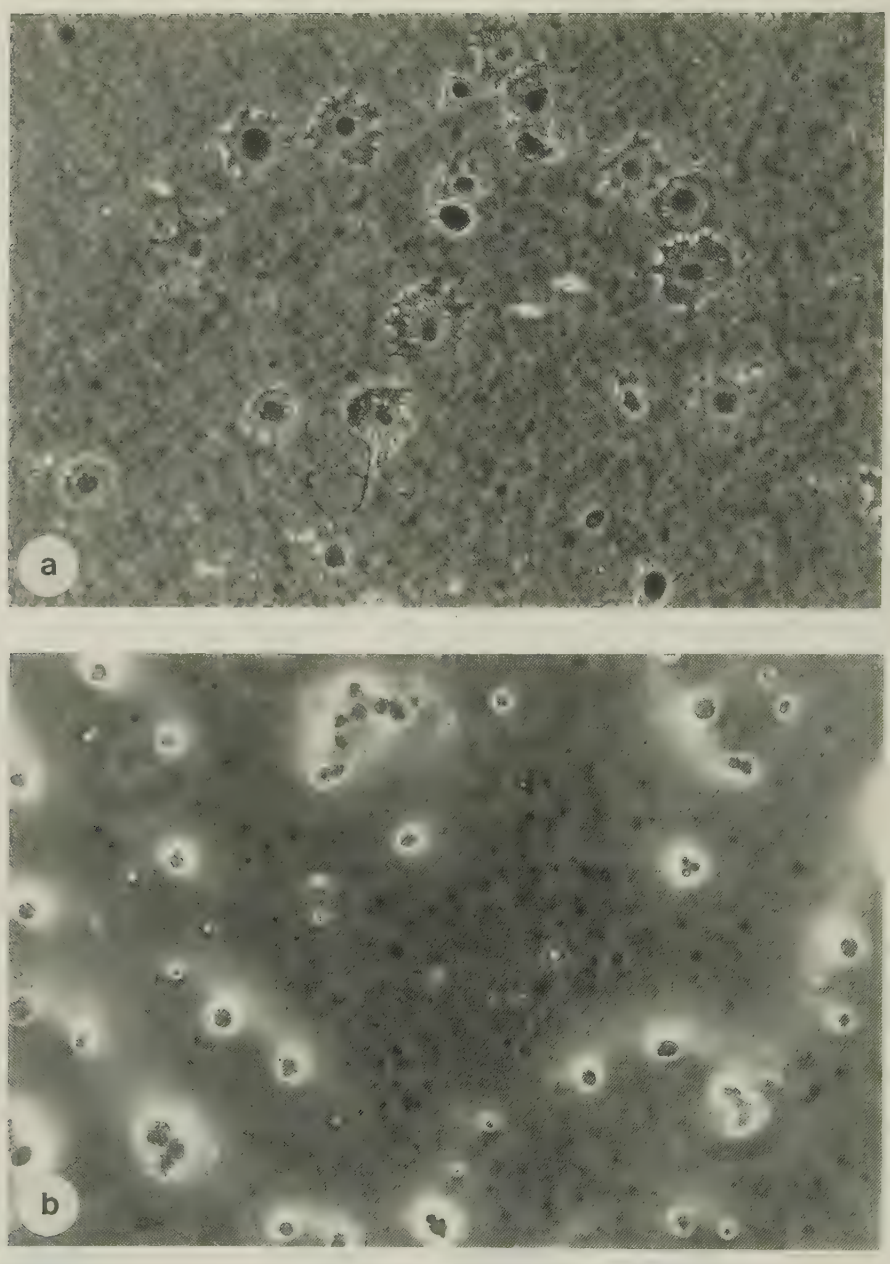

Figure 3. a. Photomicrograph of B16 F1 cells attached and spread on laminin coated plastic, 400x (appearance was the same when lectin plus its specific sugar was added). b. Photomicrograph of B16 F1 cells on laminin coated plastic that has been incubated with Con A, 400x.

binding to laminin. The results indicate that WGA, when bound to laminin substrates, blocks cell attachment sites. This interference is reversed only by N-acetylglucosamine, the specific sugar recognized by WGA. In contrast, Con A does not inhibit cell adhesion, but does prevent cell spreading. The effect is only

reversed by alpha-methyl mannose, the specific sugar recognized by Con A.

Work with fibronectin has shown that the type and extent of glycosylation of this glycoprotein can affect the way it binds to gelatin (12). Jones et al reported that lack of carbohydrates significantly enhanced fibroblast adhesion and spreading on fibronectin coated surfaces (13).

Our results correlate well with the findings of Trinkaus-Randall et al (14) on the effects of different lectins on the binding of rabbit basal corneal epithelial cells to freshly denuded corneal basal lamina. Their work indicates that WGA incubation of corneal basal lamina inhibits cell attachment, while Con A has no effect on cell binding, but prevents extensive cell spreading. The laminin present in the corneal basal lamina used in those experiments may account for their findings.

A possible explanation for the effects that we report on cell binding and spreading is that the bound lectin sterically blocks cell surface receptor binding sites on the laminin molecule. This argument is strengthened by the fact that the amino acid sequence of the laminin B1 chain (15) reveals a potential N-glycosylation site only ten amino acid residues away from the well known YIGSR cell binding domain (6). Further work may reveal the precise location of specific oligosaccharide chains on the native laminin molecule and how they might modulate cell attachment and spreading. The results presented suggest that the lectin, Con A, may be useful in separating these two phenomena of the cellular response to laminin substrates.

ACKNOWLEDGEMENT

This work has been supported by USPHS grants DE-00157 and AR-17220.

REFERENCES

1. Martin, G.R. and Timpl, R. (1987) Ann. Rev. Cell Biol. 3, 57-85.
2. Howe, C.C. (1984) Mol. Cell. Biol. 4, 1-7.
3. Malinoff, H.L. and Wicha, M.S. (1983) J. Cell Biol. 96, 1474-1479.
4. Smallheiser, N.R. and Schwartz, N.B. (1987) Proc. Natl. Acad. Sci. 84, 6457-6461.
5. Kleinman, H.K., Ogle, R.C., Cannon, F.B., Little, C.D., Sweeney, T.M. and Luckenbill-Edds, L. (1988) Proc. Natl. Acad. Sci. 85, 1282-1286.

6. Graf, J., Iwamoto, Y., Sasaki, M., Martin, G.R., Kleinman, H.K., Robey, F.A., and Yamada, Y. (1987) Cell 48, 989-996.
7. Aumailley, M., Nurcombe, V., Edgar, D., Paulsson, M. and Timpl,R. (1987) J. Biol. Chem. 262, 11532-11538.
8. Timpl, R., Rohde, P., Gehron Robey, P., Rennard, S.I., Foidart,J.M. and Martin, G.R. (1979) J. Biol. Chem., 254, 9933-9940.
9. Ruoslahti, E., Hayman, E.G., Pierschbacher, M. and Engvall, E. (1982) Methods In Enzymology, 82, 803-831.
10. Aramugham, R.G., Hsieh, T.C.-Y., Tanzer, M.L. and Laine, R.A. (1986) Biochim. Biophys. Acta 883, 112-126.
11. Fujiwara, S., Shinkai, H., Deutzmann, R., Paulsson, M. and Timpl, R. (1988) Biochem. J. 252, 453-461.
12. Zhu, B.C.R. and Laine, R.A. (1985) J. Biol. Chem. 260, 4041-4045.
13. Jones, G.E., Arumugham, R.G. and Tanzer, M.L. (1986) J. Cell Biol. 103, 1663-1670.
14. Trinkaus-Randall, V., Newton, A.W., Gipson, I.K. and Franzblau, C. (1988) Cell Tissue Res. 251, 315-323.
15. Sasaki, M., Kato, S., Kohno, K., Martin, G.R. and Yamada, Y. (1987) Proc. Natl. Acad. Sci. 84, 935-939.

Vol. 156, No. 1, 1988 BIOCHEMICAL AND BIOPHYSICAL RESEARCH COMMUNICATIONS
October 14, 1988 Pages 417-423

SLIPPED DNA STRUCTURES WITHIN THE ENHANCER REGION OF THE MOLONEY MURINE LEUKEMIA VIRUS

Miguel A. Gama Sosa*, Jessica C. Hall and Ruth M. Ruprecht†

Dana-Farber Cancer Institute, *Department of Pathology
and †Department of Medicine, Harvard Medical School
Boston, MA 02115

Received August 31, 1988

We have examined the S1 nuclease sensitivity of supercoiled plasmids harboring the Moloney Murine Leukemia Virus (MoMuLV) long terminal repeat (LTR). S1 sensitivity was found within the LTR enhancer direct repeats. Transformation of E. coli DH5 cells with a construct containing most of the MoMuLV LTR yielded the precise deletion of one direct repeat and loss of S1 sensitivity. The dependence of S1 sensitivity on the presence of both direct repeats, together with the exact excision of one direct repeat by E. coli, suggests the presence of slipped DNA within the enhancer. Such structures may represent targets for effector proteins which mediate vital functions during viral propagation. © 1988 Academic Press, Inc.

Increasing evidence suggests that DNA conformational microheterogeneity due to the presence of unusual structures plays a central role in cellular processes such as replication, recombination, transcription, mutagenesis and DNA repair (1,2). Such unusual DNA structures include left handed Z DNA (3,4), H DNA (5), cruciforms (6), Pur-Pyr structures (7,8,9), anisomorphic DNA (10), bent DNA (11) and slipped DNA structures (12,13). Although the biological significance of such DNA structures is not understood, they may constitute targets for specific regulatory DNA binding proteins. Many unusual DNA structures are sensitive to the single-strand specific S1 nuclease. Pur-Pyr structures in the major late promoters of adenovirus (7), cruciform structures of Col E1 plasmids (14), and B to Z transitions have been found to be cleaved by S1 nuclease in a site-specific manner (4). We have analyzed the DNA conformational organization of the enhancer region of the Moloney Murine Leukemia Virus (MoMuLV) long terminal repeat (LTR) by S1 nuclease analysis, and we present evidence for the presence of slipped DNA structures within the enhancer region of this LTR.

0006-291X/88 $1.50
Copyright © 1988 by Academic Press, Inc.
All rights of reproduction in any form reserved.

MATERIALS AND METHODS

Bacterial Strains: Escherichia coli strains DH5 (endA1, recA1, hsdR17 (r_k^-, m_k^+), sup E44, thi-1,λ-, gyrA96, relA1, F^-) and HB101 (F^-, hsdS20 (r_B^-, m_B^-), supE44, ara14, galK2, lacY1, proA2, rpsL20(str^R), xyl5, leu, mtl1,λ-, recA13) were obtained from Bethesda Research Laboratories (Gaithersburg, MD).

Plasmid Constructions: Plasmid pLTRM6 was prepared by subcloning a 2.4 kB EcoRI fragment harboring the complete MoMuLV 3'LTR from pZIPneoSV(x)1 (15) into a 1.4 kB EcoRI-AvaI fragment from pBR322 harboring the tetracycline resistance gene, after converting the AvaI site to an EcoRI site. Following propagation in E. coli HB101 cells, pLTRM6 DNA was partially digested with NheI. The plasmid was then end-repaired with T_4 DNA polymerase in the presence of all four deoxyribonucleoside triphosphates, ligated to PstI linkers with T_4 DNA ligase, and digested with PstI. The DNA was self-ligated with T_4 DNA ligase, and the resulting plasmid pLTRM6ΔPst was used to transform E. coli HB101 cells (Fig. 1). Plasmid pLTRM6ΔXho was prepared by double-digestion of pLTRM6ΔPst DNA with XhoI and PstI under standard conditions, end-repaired as described above, ligated with XhoI linkers, XhoI digested, and self-ligated (Fig. 1). The ligated pLTRM6ΔXho DNA was propagated in E. coli DH5 cells. Plasmids pLTRM6ΔPst and pLTRM6ΔXho were extensively characterized by restriction enzyme analysis including EcoRV, whose recognition sites lie within the 75bp direct repeats of the MoMuLV enhancer (Fig. 2). Plasmid pMCAT was prepared by subcloning the 0.4 kB XhoI-HindIII fragment from pLTRM6ΔXho upstream from the chloramphenicol acetyl transferase (CAT) gene sequences of pSVIXCAT (Fig. 1). pMCAT was propagated in E. coli DH5 cells. pACAT was obtained from Dr. W. Haseltine (16).

S1 Nuclease Analysis: Approximately 10 µl of each pLTRM6ΔPst and pLTRM6ΔXho DNAs were digested with 1200 units of S1 nuclease (Boehringer Mannheim,IN) in a 500 µl reaction mixture containing 200mM sodium chloride, 50mM sodium acetate, pH 4.5, 1 mM $ZnSO_4$, 0.5% glycerol, and 10 µg/ml yeast

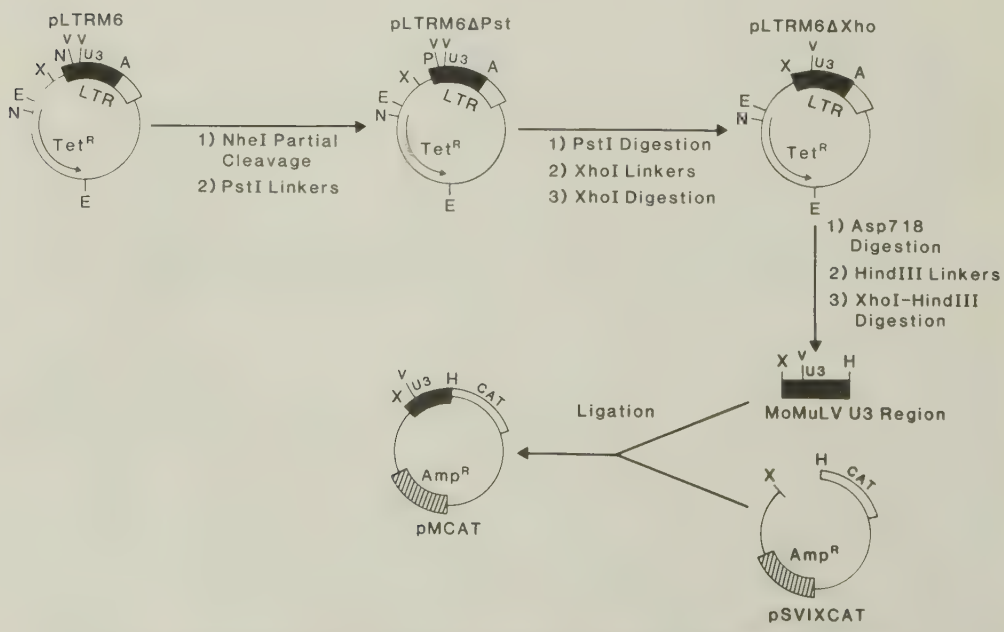

Figure 1. Construction of plasmids harboring MoMuLV enhancer sequences. E (EcoRI), N (NheI), X (XhoI), A (Asp718), P (PstI), H (HindIII), V (EcoRV).

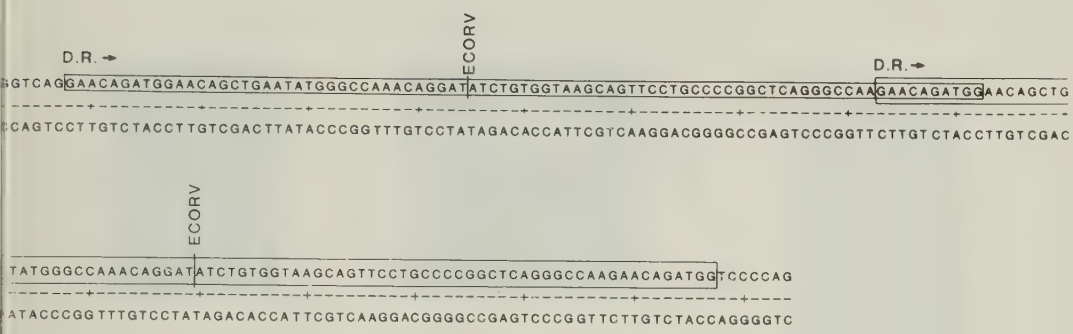

Figure 2. Nucleotide sequence of the MoMuLV enhancer region. D.R. (direct repeat).

tRNA, for 10 min at 10° C. The reaction was stopped by the addition of 6 µl of 0.5 M EDTA, and the S1 nuclease-digested DNA was purified by chromatography through Elutip columns (Schleicher and Schuell, NH) followed by ethanol precipitation. After centrifugation, each DNA pellet was resuspended in 20 µl of 10 mM Tris-HCl, pH 7.6, 1 mM EDTA. Aliquots of 1 µl of pLTRM6ΔPst and pLRTM6ΔXho DNAs treated with S1 nuclease were further digested with 10 units of NcoI, EcoRI or NheI under standard conditions. The products were analyzed by 0.7 or 1.4% agarose gel electrophoresis in the presence of lambda DNA digested with HindIII and OX174 RF DNA digested with HaeIII as molecular weight markers.

DNA Sequence Analysis: Plasmid pLTRM6ΔXho was digested with Asp718, end-repaired as previously described, ligated with HindIII linkers, and digested with both XhoI and HindIII. A DNA fragment of approximately 0.4 kB containing most of the MoMuLV U3 region was purified by agarose gel electrophoresis followed by electrolution, Elutip chromatography, and ethanol precipitation. The purified fragment was subcloned into the plasmid vector Bluescript M13 (Strategene, CA) which had been previously digested with HindIII and XhoI, and dephosphorylated with calf intestine alkaline phosphatase. This construct was propagated in DH5 cells. Sequencing of the XhoI-HindIII insert was performed by the double-stranded sequencing method (17,18,19).

Chloramphenicol Acetyl Transferase (CAT) Activity Directed By pMCAT and pACAT. Murine cell lines M12 (B-cell leukemia) and L691-6 (T-cell lymphoma) (16) were grown in RPMI 1640 medium supplemented with L-glutamine, penicillin, streptomycin, 10% fetal calf serum and 5×10^{-5}M β-mercaptoethanol. Each cell line was transfected with equivalent molar amounts (1 µg) of pMCAT and pACAT as previously described (16). After 72h, the cells were washed with cold phosphate buffered saline, pH 7.2, and resuspended in 150 µl of 0.25M Tris-HCl, pH 8.0. Cell extracts were prepared by 3 cycles of freezing (-70°C) and thawing (37°C), centrifuged, and the supernatants were assayed for protein concentration and CAT activity. Results are expressed as relative percentage conversion of ^{14}C-chloramphenicol to ^{14}C-chloramphenicol acetate by extracts standardized for the same amount of protein.

RESULTS AND DISCUSSION

Restriction Endonuclease and S1 Nuclease Analysis of pLTRM6ΔPst and pLTRM6ΔXho DNAs: Both pLTRM6ΔPst and pLTRM6ΔXho contained the predicted restriction endonuclease sites. However, upon EcoRV digestion, the 75bp DNA

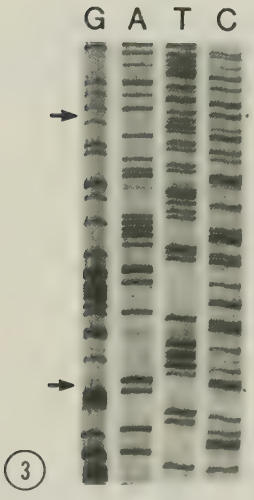

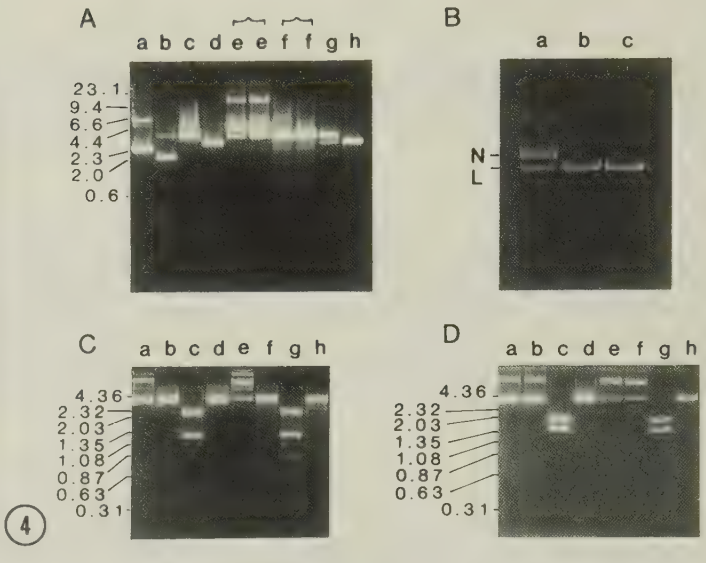

Figure 3. Nucleotide sequence analysis of the enhancer region of pLTRM6ΔXho. Arrows denote the sequence boundaries of the unique enhancer direct repeat found within this plasmid.

Figure 4. A. S1 nuclease sensitivity of pLTRM6ΔPst and pLTRM6ΔXho. 0.7% Agarose gel electrophoresis. a) pLTRM6ΔPst uncut, b) pLTRM6ΔXho uncut, c) pLTRM6ΔPst + NheI, d) pLTRM6ΔXho + NheI, e) pLTRM6ΔPst + S1 nuclease, f) pLTRM6ΔPst + S1 nuclease + NheI, g) pLTRM6ΔXho + S1 nuclease, h) pLTRM6ΔXho + S1 nuclease + NheI. B. S1 nuclease sensitivity of linearized pLTRM6ΔPst. a) pLTRM6ΔPst + S1 nuclease, b) pLTRM6ΔPst + NheI, c) pLTRM6ΔPst + NheI followed by S1 nuclease. C. and D. Mapping of S1 nuclease hypersensitive sites in pLTRM6ΔPst and pLTRM6ΔXho respectively. 1.4% Agarose gel electrophoresis. a) uncut plasmids, b) NcoI, c) EcoRI, d) NheI, e) S1 nuclease, f) S1 nuclease + NcoI, g) S1 nuclease + Eco RI, h) S1 nuclease + NheI .

fragment spanning 38 nucleotides of the enhancer's first and 37 nucleotides of its second direct repeat was present only in pLTRM6ΔPst but not in pLTRM6ΔXho. This suggests that a small deletion of enhancer sequences occurred in pLTRM6ΔXho. DNA sequence analysis of the U3 region of pLTRM6ΔXho showed a deletion within the enhancer region of the MoMuLV LTR. One of the two 75 bp direct repeat units contained within the enhancer had been deleted precisely (Fig. 3) during propagation in E. coli DH5 cells. The same phenomenon has been observed previously when MoMuLV proviruses were cloned into lambda Charon 21A and propagated in E. coli DP50 sup F (20,21).

Specific S1 nuclease sensitive sites were observed preferentially in pLTRM6ΔPst as compared to pLTRM6ΔXho (Figs. 4A,4C,4D). Mapping of these sites in pLTRM6ΔPst showed an S1 sensitive region within the LTR enhancer element (Fig. 5). In contrast, no specific S1 nuclease hypersensitivity was observed within the pLTRM6ΔXho LTR enhancer region (Figs. 4A,4D). S1 sensitivity was observed only in supercoiled and not in previously linearized plasmid of either construct (Fig. 4B).

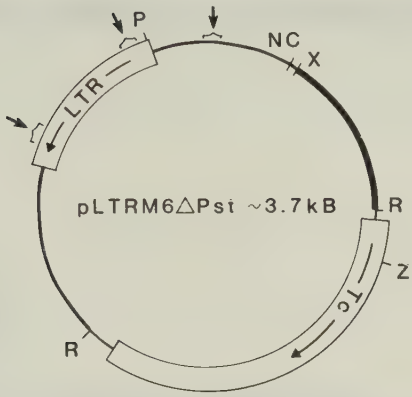

Figure 5. S1 nuclease hypersensitive regions of pLTRM6ΔPst. P(PstI), NC(NcoI), R (EcoRI), N (NheI), X (XhoI). Arrows denote the location of the main S1 hypersensitive regions.

The presence of an S1 nuclease sensitive region within the enhancer LTR region in pLTRM6ΔPst, together with the deletion of a complete enhancer direct repeat in pLTRM6ΔXho, suggests the existence of unusual DNA structures within the MoMuLV LTR enhancer element in supercoiled pLTRM6ΔPst. Sequence analysis of the MoMuLV LTR enhancer direct repeats does not reveal consensus sequences capable of adopting Z-DNA configuration, such as alternating purine-pyrimidine sequences. In addition, the lack of inverted repeats within the enhancer element argues against the presence of cruciform structures. However, the precise deletion of one direct repeat could have arisen from a slipped DNA structure (12,13). Such a model predicts the formation of single-stranded structures within direct repeats, contained within supercoiled DNA. Slipped DNA structures have been proposed for the chicken and mouseα2 (1) collagen promoter (13). We propose a similar phenomenon in the MoMuLV enhancer region of supercoiled pLTRM6ΔPst DNA (Fig. 6). The first repeat on one strand base-pairs with the second repeat on the other strand, or vice versa, producing two staggered single-stranded loops.

Partially single-stranded regions are known to occur in supercoiled DNA plasmids. The energy requirements for stabilizing partially single stranded sequences are offset by relieving stress introduced by DNA supercoiling. As in the extrusion of cruciforms in supercoiled plasmid DNA, where the disruption of the plasmid double helix is partially compensated by basepairing of the stem and thus leads to stabilization of the partially single-stranded DNA structures, the basepairing occurring between direct repeat 1 and direct repeat 2 can stabilize the slipped DNA structure. Therefore, the formation of the staggered single-stranded loops could account for the S1 nuclease sensitivity of the MoMuLV LTR enhancer region in protein-free plasmid preparations.

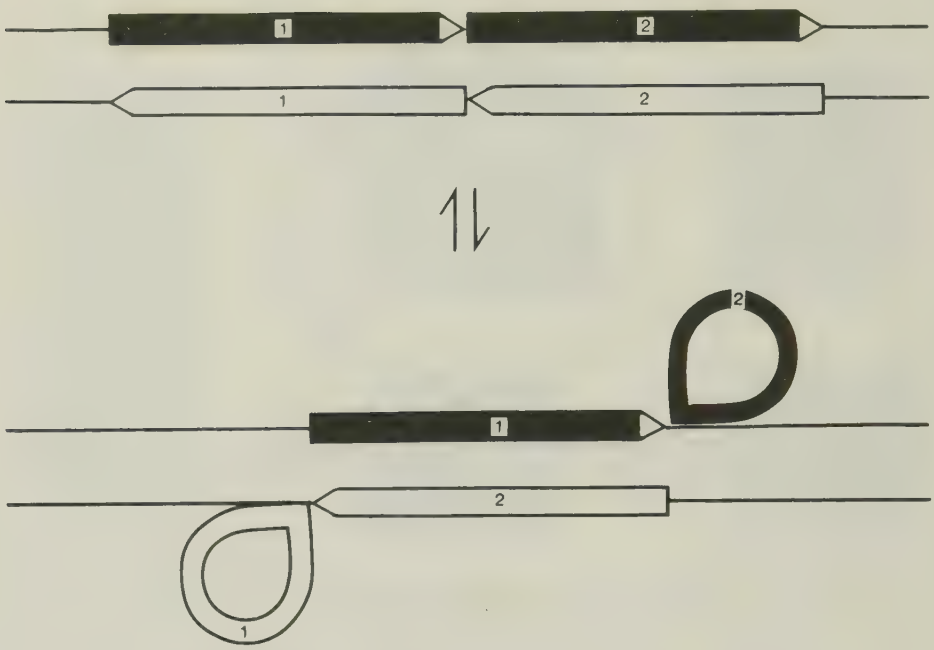

Figure 6. Schematic model representing slipped DNA structures within the enhancer region of MoMuLV LTR.

It has been suggested that slipped DNA structures may be important in the regulation of transcription (1,13). Transfection of pMCAT into murine cell lines resulted in the appearance of chloramphenicol acetyl transferase activity which was expressed in a cell lineage-specific manner (Table 1). Higher activity was observed in the T-cell derived L691-6 cell line and lower activities in the B-cell derived M12 cell line compared to the activities showed by pACAT (harboring the Akv virus U3 region with both enhancer 99bp direct repeats) transformed cell lines. These results confirm a previous report that one direct repeat within the enhancer element is sufficient for cell-lineage specific enhancer activity (22). In addition, MoMuLV with a single enhancer direct repeat has been shown to be infectious; however, the onset of the virus-induced disease was delayed significantly (23).

TABLE 1

Expression of chloramphenicol acetyl transferase (CAT) directed by pMCAT and pACAT promoter-enhancer regions

Plasmid	Parental Virus for U3 Region	% Relative CAT Activity	
		T Cells (L691-6)	B Cells (M12)
MCAT	MoMuLV	100	100
ACAT	Akv	62	753

The single-stranded loops may have been excised by enzymes of the E. coli DNA repair system such as those carrying out mismatch repair (24). In eukaryotes, slipped DNA structures may be stabilized by specific DNA binding proteins, and such structures may be targets for other effector regulatory proteins.

ACKNOWLEDGEMENTS

The authors wish to thank Drs. Dan Celander and William Haseltine for the gift of plasmids pLTRM6 and pACAT and Rita Antonelli for the preparation of this manuscript. Supported by NSF Grant # DMD-8509459.

RMR is the recipient of a Faculty Development Award of the Pharmaceutical Manufacturers Association Foundation (PMAF) and a Science Scholar of the Mary Ingraham Bunting Institute of Radcliffe College.

REFERENCES

1. Wells, R.D. (1988) J. Biol. Chem. 263, 1095-1098.
2. Jaworski, A., Hsieh, W-T., Blaho, J.A., Larson, J.E., and Wells, R.D. (1987) Science 238, 773-777.
3. Rich, A., Nordeim, A., and Wang, H-J. (1984) Annu. Rev. Biochem. 53, 791.
4. Singleton, C.K., Klysik, J., Stirdivant, S.M., and Wells, R.D. (1982) Nature 299, 312-316.
5. Mirkin, S.M., Lyamichev, V.I., Drushlyak, K.N., Dobrynin, V.N., Filippov, S.A., and Kamenetskii, F. (1987) Nature 330, 495-497.
6. Sinden, R.R., and Pettijohn, D.E. (1984) J. Biol. Chem. 259, 6593-6600.
7. Kilpatrick, M.W., Torri, A., Kang, D.S., Engler, J.A., and Wells, R.D. (1986) J. Biol. Chem. 261, 11350-11354.
8. Pulleyblank, D.E., Haniford, D.B., and Morgan, A.R. (1985) Cell 42, 271-280.
9. Evans, J., and Efstratiadis, A. (1986) J. Biol. Chem. 261, 14771-14780.
10. Wohtraub, F., McLean, M.J., and Wells, R.D. (1987) J. Biol. Chem. 262, 6407-6416.
11. Wells, R.D., and Harvey, S.C. (eds) (1987) Unusual DNA Structures, Springer-Verlag New York Inc., New York.
12. Mace, H.A.T., Pelham, H.R.B., and Travers, A.A. (1983) Nature 304, 555-557.
13. McKeon, C., Schmidt, A., and deCrombrugghe, B. (1984) J. Biol. Chem. 259, 6636-6640.
14. Lilley, D.M.J. (1980) Proc. Nat. Acad. Sci. USA 77, 6468-6472.
15. Cepko, C.L., Roberts, B.E., and Mulligan, R.C. (1984) Cell 37, 1053-1062.
16. Celander, D., and Haseltine, W.A. (1984) Nature 312, 159-162.
17. Sanger, F., Miklen, S., and Coulson, A.R. (1977) Proc. Nat. Acad. Sci. USA 74, 5463-5467.
18. Hattori, M. and Sakaki, Y. (1986) Anal. Biochem. 152, 232-238.
19. Chen, E.J. and Seeburg, P.H. (1985) DNA 4, 165-170.
20. Berns, A.J.M., Lai, M.H.T., Bosselman, R.A., McKennett, M.A., Bacheler, L.T., Fan, H., Robanos Maandag, E.C., Putten, H.v.d. and Verma, I.M. (1980) J. Virol. 36, 254-263.
21. Van Beveren, C., Rands, E., Chattopadhyay, S.K., Lowy, D.R., and Verma, I.M. (1982) J. Virol. 41, 542-556.
22. Jolly, D.J., Esty, A.E., Subramani, S., Friedmann, T., and Verma, I.M. (1983) Nucleic Acids Res. 11, 1855-1872.
23. Li, Y., Golemis, E., Hartley, J.W., and Hopkins, N. (1987) J. Virol. 61, 693-700.
24. Friedberg, E.C. (1985) DNA Repair, W.H. Freeman and Co., New York.

Vol. 156, No. 1, 1988 BIOCHEMICAL AND BIOPHYSICAL RESEARCH COMMUNICATIONS
October 14, 1988 Pages 424-431

CYCLIC AMP DECREASES LDL CATABOLISM AND CHOLESTEROL SYNTHESIS IN THE HUMAN HEPATOMA CELL LINE HepG2

Cécile MAZIERE, Jean-Claude MAZIERE, Suzanne SALMON, Martine AUCLAIR, Liliana MORA, Martine MOREAU and Jacques Polonovski

Faculté de Médecine Saint-Antoine, 27 rue Chaligny, 75012 Paris, France

Received September 1, 1988

SUMMARY: A 24h pretreatment of the human hepatoma cell line HepG2 with dibutyryl cyclic AMP in the presence of theophylline induced a dose dependent decrease in low density lipoprotein binding, uptake and degradation. This effect is most likely due to a reduction of the LDL receptor number. Sterol synthesis from sodium acetate is markedly inhibited, either in the presence or absence of LDL, whereas synthesis from mevalonic acid is unchanged. Cyclic AMP also induced a decrease in hydroxy methyl glutaryl coenzyme A reductase activity. These effects of cyclic AMP might be involved in some hormonal regulation of the LDL pathway and cholesterol metabolism in the liver.
© 1988 Academic Press, Inc.

The control of plasma LDL cholesterol level is of importance because it is closely related to coronary heart diseases. LDL is cleared from peripheral tissus by means of the high affinity LDL receptor pathway first reported by Goldstein and Brown in fibroblasts [1], which delivers cholesterol for cell membrane constitution and down regulates cholesterol synthesis by decreasing HMGCoA reductase activity [2]. The liver also plays a central role in LDL removal: in vivo studies demonstrated that more than 60% of LDL in humans is catabolized by the liver [3,4].

Abbreviations: LDL: low density lipoprotein, dbcAMP: dibutyryl cyclic AMP, th: theophylline, HMGCoA: Hydroxy Methyl Glutaryl Coenzyme A.

0006-291X/88 $1.50
Copyright © 1988 by Academic Press, Inc.
All rights of reproduction in any form reserved.

However, in hepatocytes, the down regulation of cholesterol synthesis by LDL appears to be less effective than in fibroblasts [5,6]. Furthermore, it has been suggested that the expressed human hepatic receptor for LDL differs from the fibroblast LDL receptor, both in molecular weight and in Ca^{2+} dependency [7] .

We [8] and others [9] demonstrated that the second messenger cyclic AMP decreases the LDL receptor pathway in human cultured fibroblasts. Since the regulation of the LDL receptor pathway might be different in fibroblasts and in hepatocytes, we investigated the effects of this second messenger in hepatocytes of human origin. The human hepatoma cell line HepG2 was chosen because different authors reported the presence of specific high affinity LDL receptors in these cells [10-13]. Since it was also demonstrated that in HepG2 cells, the LDL receptor and cholesterol synthesis are subject to metabolic regulation, this cell line provides a valuable model for the studies of human hepatocyte metabolism in vitro. It was demonstrated that cyclic AMP decreases the LDL receptor number and HMGCoA reductase activity in HepG2 cells.

MATERIALS AND METHODS

Materials. All chemicals were from Sigma, St.Louis, MO, USA. [2-^{14}C] sodium acetate 55 mCi/mmol, [5-^{14}C] mevalonic acid 50mCi/mmol, were from CEA, Saclay, France; ^{125}INa 13-17 Ci/mg, 3-hydroxy-3-methyl [3-^{14}C] glutaryl Coenzyme A 52mCi/mmol were from Amersham, Buckinghamshire U.K. Dulbecco's modified Minimum Essential Medium with Earle's salts (DMEM) and foetal calf serum were from Gibco, Grand Island, N.Y., U.S.A. The HepG2 cell line was from the American Type Culture Collection, Rockville, Maryland, USA. The serum substitute Ultroser G was purchased from Industries Biologiques Françaises, Villeneuve La Garenne, France.

Cell culture. Cells were cultured in 35 mm Nunc Petri dishes containing 2 ml DMEM medium supplemented with 20 mM Hepes buffer (pH 7.4), 100 units/ml penicillin, 100 µg/ml

streptomycin and 10 % (v/v) foetal calf serum, at 37°C in a humidified atmosphere of 5% CO_2. Experiments were performed on confluent cells.

LDL preparation and labeling. LDL was prepared from normal human serum by the technique of Havel et al. [14], and labeled according to Bilheimer et al. [15]. The specific radioactivity was 200-300 dpm/ng.

Effect of cyclic AMP on LDL binding, internalization and degradation. Cells were pretreated 24h with dbcAMP in the presence of theophylline 10^{-3}M in lipoprotein deficient medium supplemented with 2% Ultroser G for induction of LDL receptors. LDL binding, internalization and degradation were studied according to Goldstein and Brown [1], using ^{125}I-LDL 10µg / ml. Results are expressed in ng LDL/mg of cell protein, and calculated in percentages of control. Protein determination was done by the Lowry method.

Effect of cyclic AMP on cholesterol metabolism. Cells were preincubated 24h with dbcAMP in the presence of theophylline in medium supplemented with Ultroser G or with foetal calf serum. The radioactive precursors were then added. After a further 4 h incubation, lipid analysis is performed by thin layer chromatography after application of a cell suspension aliquot on silicagel plates as previously described [16]. Results are expressed in pmol of precursor incorporated / mg cellular protein.

Hydroxy-Methyl-Glutaryl-Coenzyme A reductase activity. Cells were pretreated with drugs during 24h in medium supplemented with 2% Ultroser G for induction of the enzyme. After harvesting, the enzyme activity was analyzed immediately as described by Beg et al.[17].

RESULTS AND DISCUSSION

The effects of dbcAMP on high affinity LDL binding, uptake and degradation are shown in Figure 1. It can be noted that dbcAMP reduces the three parameters in a dose dependent manner. At 10^{-4} M of dbcAMP, a 30% decrease was observed for binding as well as uptake and degradation. The fact that the three parameters were inhibited to a similar extent by cyclic AMP suggests that the latter exerts its action at the step of LDL binding to its receptor. This hypothesis is further confirmed by the results of Scatchard plot analysis presented in Figure 2: cyclic AMP apparently decreases the LDL high affinity receptor number. The

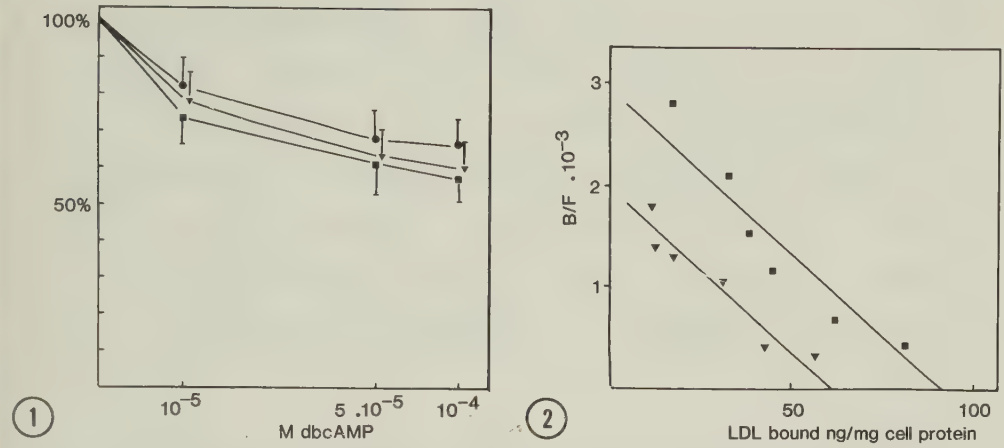

Figure 1. Effect of cyclic AMP on LDL metabolism. Cells were pretreated 24h in medium supplemented with the serum substitute Ultroser G with dbcAMP at the indicated concentrations in the presence of theophylline 10^{-3}M. After washing, LDL binding, uptake and degradation were determined as described [1], with 10µg/ml ^{125}I-LDL. Non specific values, determined in the presence of a 100 fold excess of non labelled LDL, were substracted from total values in order to obtain specific binding, uptake and degradation. Results are expressed in percentages of control values. Absolute values are 61 ± 7, 407 ± 35, 691 ± 57 ng/mg cell protein for LDL binding (■), uptake (▼), and degradation (●) respectively. Means of six determinations ± s.d.

Figure 2. Scatchard plot analysis of the effect of cyclic AMP on LDL binding. Cells were pretreated 24h in 2% Ultroser G supplemented medium with dbcAMP 10^{-4}M + theophylline 10^{-3}M. After washing, LDL binding was performed during 1h at 4°C, with 10µg/ml ^{125}I-LDL in the presence of increasing amounts of unlabeled LDL. ■ :control; ▼ :cAMP.

calculated maximum binding was 91 ngLDL/mg protein for the control and 61 ng/mg for cAMP treated cells.

In the next experiments, the effects of cyclic AMP on cholesterol synthesis were investigated. As in vivo, hepatocytes are exposed to plasmatic concentrations of LDL, the rates of sterol synthesis from sodium acetate were studied in two experimental conditions: in medium devoid of lipoproteins supplemented with the serum substitute Ultroser G, and in medium containing lipoproteins provided by foetal calf serum. The results of Table I show that cholesterol synthesis from sodium acetate is higher in

cells incubated in lipoprotein deficient medium, as expected. Furthermore, cyclic AMP decreased cholesterol synthesis in both conditions, either in the presence or in the absence of lipoproteins, with however a somewhat more marked effect in the absence of lipoproteins. At 10^{-4} M dbcAMP, the rate of sterol synthesis accounted for 10% of control in the absence of lipoproteins and 30% in their presence.

As it is well known that the cholesterol synthesis is under the control of the key enzyme HMGCoA reductase , the enzyme which catalyses the conversion of HMGCoA to mevalonic acid, we decided to comparatively investigate the effects of cyclic AMP on sterol synthesis from sodium acetate and mevalonic acid, in lipoprotein deficient medium. From the results presented in Table I, it can be

Table I. Effect of cyclic AMP on cholesterol synthesis

Precursor	Sodium acetate		Mevalonic acid
Preincubation in:	Ultroser G	Foetal calf serum	Ultroser G
Addition			
None :	2451 ± 221	1727 ± 153	264 ± 25
dbcAMP 10^{-5}M + th 10^{-3}M:	1152 ± 109 ***	1053 ± 98 **	287 ± 27
dbcAMP 5.10^{-5}M + th 10^{-3}M:	711 ± 68 ***	639 ± 57 ***	265 ± 19
dbcAMP 10^{-4}M + th 10^{-3}M:	244 ± 23 ***	518 ± 48 ***	240 ± 21

Cells were pretreated 24h either in lipoprotein-deficient medium supplemented with the serum substitute Ultroser G for induction of sterol synthesis or in foetal calf serum supplemented medium for repression of sterol synthesis. [1-^{14}C] sodium acetate (20 µCi/ml) or [5-^{14}C] mevalonic acid (5µCi/ml) were then added during 4h. Sterol separation was performed by thin layer chromatography. Results are expressed in pmol precursor incorporated per mg protein. Means of 4 experimental values ± s.d. Statistical analysis was performed by the Student's t test. **:p<0,01; ***:p<0,001.

Table II. Effect of dbcAMP on Hydroxy Methyl Glutaryl Coenzyme A reductase activity

Addition	HMGCoA reductase activity (pmol/h/mg)
None	532 ± 51
dbcAMP 10^{-5}M + th 10^{-3}M	133 ± 10 ***
dbcAMP 5.10^{-5}M + th 10^{-3}M	90 ± 7 ***
dbcAMP 10^{-4}M + th 10^{-3}M	52 ± 5 ***

Cells were pretreated 24h in medium supplemented with Ultroser G for induction of the enzyme. After washing, the enzymatic activity was determined as described [17]. Means of 4 experimental values ± s.d. ***: p<0,001 by Student's t test.

concluded that cyclic AMP most probably exerts its action on the activity of the key enzyme, since cholesterol synthesis from mevalonic acid was not impaired. This observation is further confirmed by the data given in Table II, concerning the direct effect of cyclic AMP on HMGCoA reductase activity. The activity of this enzyme is strongly decreased in the presence of cyclic AMP: the lower concentration 10^{-5} M already induced a 75% reduction of activity in our conditions.

This work demonstrates a reduction of LDL binding, uptake and degradation in the hepatoma cell line HepG2 by cyclic AMP, a result already reported in human cultured fibroblasts [8, 9], but not yet described for hepatocytes. This effect is of importance, in view of the fact that many hormones, especially insulin , might act through the activity of adenylate cyclase. Insulin, which decreases cyclic AMP intracellular level, has been reported to increase LDL binding by rat hepatocytes [18]. Results from our laboratory on the hepatoma cell line HepG2 also confirm

this effect (unpublished data). It is also of note that the direct stimulation of adenylate cyclase by the diterpene forskolin induced an effect similar to the cAMP effect on LDL metabolism (data not shown).

Our studies also pointed out that the second messenger cyclic AMP reduces cholesterol synthesis from sodium acetate by decreasing the HMGCoA reductase activity. It is well known that this enzyme is regulated by a short-term phosphorylation-dephosphorylation process [19], the reductase kinase itself is activated by a phosphorylation mechanism in the presence of reductase kinase kinase [20]. However, neither of the kinase enzymes have been identified with cAMP dependent protein kinase in rat liver [21]. Thus, it is most likely that the observed effect of cAMP on HMGCoA reductase activity results from a long term effect on the enzyme level. Kinetic studies of the effect of cAMP on the enzyme activity show that the decrease in activity became evident only after 4-5h of preincubation with the second messenger (data not shown), which confirms the absence of a short term effect. It can be concluded that cyclic AMP most likely act on the rate of enzyme synthesis or degradation.

ACKNOWLEDGMENT: We thank La Ligue Nationale Française contre le Cancer, Comité de Paris, for financial support.

REFERENCES

1. Goldstein, J.L., and Brown, M.S. (1974) J.Biol.Chem., 249: 5153-5162.
2. Brown, M.S. and Goldstein, J.L. (1973) Proc.Natl.Acad. Sci. USA, 70: 2162-2166.
3. Langer, T., Strober, W. and Levy, R.Y. (1972) J.Clin. Invest., 51:1528-1536.

4. Bilheimer, D.W., Stone, N.J. and Grundy, S.M. (1979) J.Clin.Invest., 64: 524-533.
5. Bilheimer, D.W., Goldstein, J.L., Grundy, S.M., Starzl, T.E. and Brown, M.S. (1984) N.Engl.J.Med., 311: 1658-1664.
6. Havekes, L.M., Schouten, D., DeWit, E.C.M., Cohen, L.H., Griffioen, M., Van Hinsbergh, V.W.M., and Princen, H.M.G. (1986) Biochim. Biophys. Acta, 875: 236-246.
7. Hoeg, J.M., Demosky, S.J.Jr., Lachner, K.J., Osborne, J.C.Jr., Oliver, C. and Brewer, H.B.Jr. (1986) Biochim.Biophys.Acta, 876:13-21.
8. Mazière, J.C., Mazière, C., Gardette, J., Mora, L. and Polonovski, J. (1983) Biochem.Biophys.Res.Commun., 112: 795-800.
9. Stout, R.W. and Bierman, E.L. (1983) Atherosclerosis, 46:13-20.
10. Havekes, L., Van Hinsbergh, V., Kempen, H.J. and Emeis, J. (1983) Biochem.J., 214,951-958.
11. Illingworth, D.R., Lindsey, S. and Hagemenas, F.C. (1984) Exp.Cell Res., 155:518:526.
12. Leichtner, A.M., Krieger, M. and Schwartz, A.L. (1984) Hepatololy, 4:1274-1278.
13. Wu, G.Y., Wu, C.H., Rifici, V.A. and Stockert, R.J. (1984) Hepatology, 4:1190-1194.
14. Havel, R.J., Eder, H.A. and Bragdon, J.H. (1955) J.Clin.Invest., 34:1345-1353.
15. Bilheimer, D.W., Eisenberg, S. and Levy, R.I. (1972) Biochim.Biophys.Acta, 260:212-221.
16. Mazière, C., Mazière, J.C., Mora, L. and Polonovski, J. (1987) J.Biochem.Biophys.Methods, 14:267-272 .
17. Beg, Z.H., Reznikov, D.C. and Avigan, J. (1986) Arch. Biochem.Biophys., 244:310-322.
18. Salter, A.M., Fisher, S.C. and Brindley, D.N. (1987) FEBS Lett.,220:159-162.
19. Rodwell, V.W., Nordstrom, J.L. and Mitschelen, J.J. (1976) Adv.Lip.Res., 14:1-74.
20. Beg, Z.H. and Brewer, H.B.Jr. (1981) Curr.Top.Cell. Regul., 20:139-184.
21. Ingebritsen,T.S., Parker,R.A. and Gibson,D.M. (1981) J.Biol.Chem., 256:1138-1144.

Vol. 156, No. 1, 1988 BIOCHEMICAL AND BIOPHYSICAL RESEARCH COMMUNICATIONS
October 14, 1988 Pages 432-437

ANTISERA TO AN AMINO-TERMINAL PEPTIDE DETECT THE AMYLOID PROTEIN PRECURSOR OF ALZHEIMER'S DISEASE AND RECOGNIZE SENILE PLAQUES

Mark R. Palmert[1], Marcia Berman Podlisny[2], Dennis S. Witker[1], Tilman Oltersdorf[3], Linda H. Younkin[1], Dennis J. Selkoe[2], and Steven G. Younkin[1*]

[1]Division of Neuropathology, Institute of Pathology, and Department of Pharmacology, Case Western Reserve University School of Medicine, Cleveland, OH 44106

[2]Department of Neurology (Neuroscience), Harvard Medical School, and Center for Neurologic Diseases, Brigham and Women's Hospital, Boston, MA 02115

[3]Athena Neurosciences, Inc., San Carlos, California 94070

Received August 30, 1988

SUMMARY: The cerebral amyloid deposited in Alzheimer's disease (AD) contains a 4.2 kDa ß amyloid polypeptide (ßAP) that is derived from a larger ß amyloid protein precursor (ßAPP). Three ßAPP mRNAs encoding proteins of 695, 751, and 770 amino acids have previously been identified. In each of these, there is a single membrane-spanning domain close to the carboxyl-terminus of the ßAPP, and the 42 amino acid ßAP sequence extends from within the membrane-spanning domain into the large extracellular region of the ßAPP. We raised rabbit antisera to a peptide corresponding to amino acids 45-62 near the amino-terminus of the ßAPP. We show that these antisera detect the ßAPP by demonstrating that they (i) label a set of ~120 kDa membrane-associated proteins in human brain previously detected by antisera to the carboxyl-terminus of ßAPP and (ii) label a set of ~120 kDa membrane-associated proteins that are selectively overexpressed in cells transfected with a full length ßAPP expression construct. The $ßAPP_{45-62}$ antisera specifically stain senile plaques in AD brains. This finding, along with the previous demonstration that antisera to the carboxyl-terminus of the ßAPP label senile plaques, indicates that both near amino-terminal and carboxyl-terminal domains of the ßAPP are present in senile plaques and suggests that proteolytic processing of the full length ßAPP molecule into insoluble amyloid fibrils occurs in a highly localized fashion at the sites of amyloid deposition in AD brains. © 1988 Academic Press, Inc.

In the brains of patients with Alzheimer's disease (AD), proteinaceous amyloid fibrils are deposited in senile plaque cores and blood vessel walls. A 4.2 kDa polypeptide, referred to as A4 or the beta amyloid protein (ßAP), has been isolated from the amyloid in vessels (1) and plaque cores (2,3). Using oligonucleotides based on the ßAP sequence, several groups (4-7) have isolated cDNAs that encode ßAP as part of a 695 amino acid ß amyloid protein precursor (ßAPP). Two additional ßAPP mRNAs encoding proteins of 751 and 770 amino acids have subsequently been identified (8-10). Based on the sequence of $ßAPP_{695}$ cDNA, Kang *et al.* (4) have developed a model which predicts that, in each of the three ßAPPs,

ABBREVIATIONS: AD, Alzheimer's disease. **ßAP**, beta amyloid polypeptide islolated from the amyloid in AD brain. **ßAPP**, beta amyloid protein precursor. **$ßAPP_{45-62}$**, synthetic peptide corresponding to amino acids 45-62 in the ßAPP. **C_1**, synthetic peptide corresponding to the 20 amino acids at the carboxyl-terminus of the ßAPP. **SP28**, synthetic peptide corresponding to amino acids 1-28 in the ßAP.

*To whom correspondence should be addressed.

0006-291X/88 $1.50
Copyright © 1988 by Academic Press, Inc.
All rights of reproduction in any form reserved.

there is a single membrane-spanning domain close to the carboxyl-terminus and that the 42 amino acid ßAP sequence extends from within the membrane-spanning domain into the putative extracellular region of the ßAPP. Thus, two cleavages, one at the amino-terminus and one at the carboxyl-terminus of the ßAP, appear to be required to release the ßAP from the ßAPP.

As part of an effort to evaluate the cellular location and post-translational processing of the ßAPP, antisera were prepared to a peptide corresponding to amino acids 45-62 of the ßAPP ($ßAPP_{45-62}$). While these antisera were being characterized, (i) two reports were published showing that an antiserum to a cytoplasmic domain ($ßAPP_{666-676}$ in $ßAPP_{695}$) labels a 92 kDa protein in human muscle (11) and mouse muscle and brain (12); (ii) Selkoe *et al.* reported that antisera to the carboxyl-terminus of the predicted ßAPP (anti-C_1) specifically detect a set of ~110-135 kDa membrane-associated proteins in brain, a variety of peripheral tissues, and cultured cells (13,14); and (iii) Tabaton *et al.* (15) reported that an antiserum to synthetic ßAP specifically detects a 130 kDa protein in human brain and fibroblasts. Moreover, Selkoe *et al.* (14) showed that the set of ~120 kDa proteins labeled by anti-C_1 represent the ßAPP by transfecting cells with a full-length ßAPP expression construct and showing marked augmentation of specifically immunolabeled proteins in the appropriate size range. In this report, we describe the initial results of a collaboration designed to compare $ßAPP_{45-62}$ antisera with anti-C_1.

MATERIALS AND METHODS

The synthetic peptide used in this study corresponds to amino acids 45-62 ($ßAPP_{45-62}$) of the 695-residue protein predicted from the full length cDNA isolated by Kang *et al.* (4). The $ßAPP_{45-62}$ peptide was prepared by Peninsula Laboratories and generously provided by P. Gambetti and G. Perry. The data in this report are based on antisera from two of the three rabbits that we immunized with $ßAPP_{45-62}$ peptide linked to keyhole limpet hemocyanin. These two antisera labeled the same proteins on immunoblots but with different intensities. Antiserum to SP28, a synthetic peptide homologous to the first 28 amino acids of the ßAP [amino acids 597-624 of the Kang sequence (4)], was generously provided by B. Frangione. The antiserum raised to a synthetic peptide corresponding to 676-695 (C_1) of the Kang sequence has been described previously (14).

Immunoblots and immunocytochemistry were performed using frozen tissue from histologically confirmed AD (age = 72 years, post-mortem interval = 8.5 hours) and control (age = 89 years, post-mortem interval = 3 hours) brains obtained at autopsy. Selkoe *et al.* (14) previously described the human 293 embryonic kidney cells employed here. Transcription in these cells, which express recombinant $ßAPP_{695}$ cDNA, is driven by the human cytomegalovirus immediate early gene enhancer/promoter unit. The construct also contains the SV40 t-splice and late polyadenylation signal.

Membrane-associated proteins were prepared as described by Selkoe *et al.* (14). Tissue was homogenized in 2 volumes of TS buffer (50 mM Tris, 150 mM NaCl, 5 mM EDTA, 2 mM PMSF, 1 μg/ml leupeptin, 10 μg/ml aprotinin, 0.1 μg/ml pepstatin, and 1 μg/ml TLCK, pH 7.6), and membrane-associated proteins were extracted from the 100,000 g pellet with TS containing 2% Triton X-100. Immunoblot analysis was performed on nitrocellulose blots of 7% SDS-polyacrylamide gels using 5% defatted milk to block non-specific binding of primary antibody and goat anti-rabbit IgG coupled to alkaline phosphatase (Promega) for immunodetection. Immunocytochemistry employed the Vectastain-Elite ABC kit (Vector laboratories) and was carried out conventionally on cryostat sections from tissue blocks that had been rapidly frozen in isopentane cooled with liquid nitrogen. Cryostat sections were fixed 10 min in 10% phosphate-buffered formalin (Fisher) prior to immunostaining.

Specificity of immunochemical reactions was confirmed by peptide absorption. Fifty μg of unconjugated peptide were incubated at 4°C overnight with 1 μl of antiserum diluted (1:100 or 1:300) in Tris buffered saline containing either (i) 0.05% Tween 20 and 1 mg/ml bovine serum albumin for immunoblots or (ii) 1% normal goat serum for immunocytochemistry. After centrifugation at 16,000 x g for 5-10 min, the supernatant was applied to blots or tissue sections.

RESULTS AND DISCUSSION

Fig. 1A shows immunoblots of membrane-associated proteins from human cerebral cortex stained with antisera to C_1 and to βAPP_{45-62}. As previously reported, anti-C_1 labels a set of ~110-135 kDa proteins in human brain (lane 2) that are not detected after absorption with C_1 (14). Anti-βAPP_{45-62} labels a set of proteins that comigrates with the set of ~120 kDa proteins detected by anti-C_1 as well as a ~55 kDa protein (lane 1). Anti-βAPP_{45-62} does not, however, label the ~11 kDa protein previously reported to react with anti-C_1 (14), as expected from its carboxyl-terminal location (data not shown). Absorption with

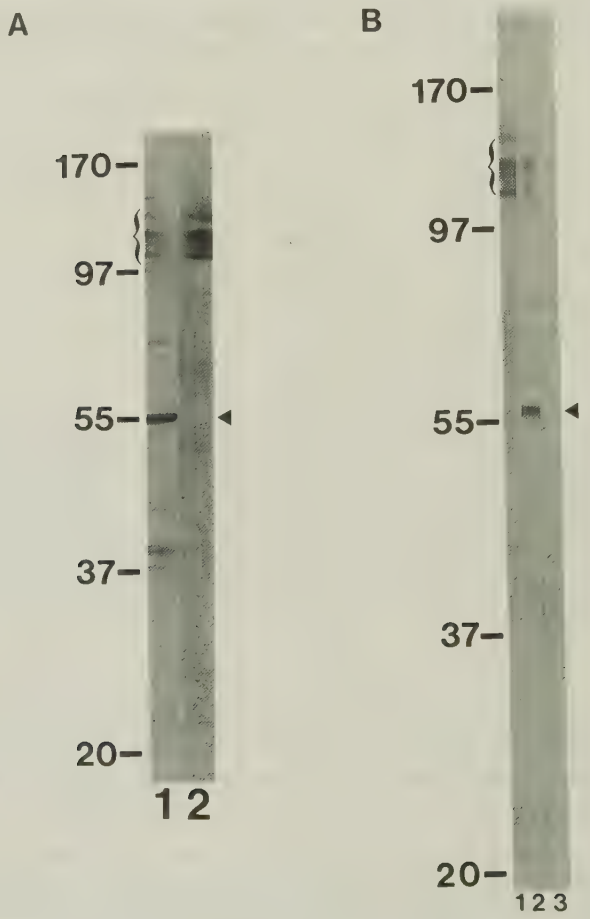

Fig. 1. Immunoblots of membrane-associated proteins in human cerebral cortex. **A**. Comparison of anti-C_1 and anti-βAPP_{45-62} staining. Lane 1, anti-βAPP_{45-62} (1:100); lane 2, anti-C_1 (1:150). The ~55 kDa protein detected by anti-βAPP_{45-62} in lane 1 may represent a fragment of the βAPP containing the amino-terminal region. **B**. Staining of membrane-associated human cerebral cortical proteins with anti-βAPP_{45-62} before and after absorption with βAPP_{45-62}. Lane 1 is stained with anti-C_1 (1:150) to aid in visualizing the proteins in lane 2, which are stained with anti-βAPP_{45-62} (1:100). Lane 3 is stained with anti-βAPP_{45-62} (1:100) that was absorbed with the βAPP_{45-62} peptide. Gels are 7% SDS-polyacrylamide; all lanes loaded with 70 μg protein. Molecular weight markers (bars) are 170, 97, 55, 37, and 20 kDa. The proteins identified in these blots (brackets, arrows) are those that have been shown by peptide absorption to be specifically labeled (Fig. 1B). The proteins that continue to be labeled after peptide absorption are presumably unrelated to the βAPP. The four membrane-associated proteins (brackets) detected by both anti-C_1 and anti-βAPP_{45-62} have calculated molecular weights of 131, 121, 115, and 111 kDa that are essentially identical to those previously reported by Selkoe *et al.* (14). The prominent membrane associated protein labeled by anti-APP_{45-62} (arrow) and not detected by anti-C_1 has a calculated molecular weight of 54 kDa.

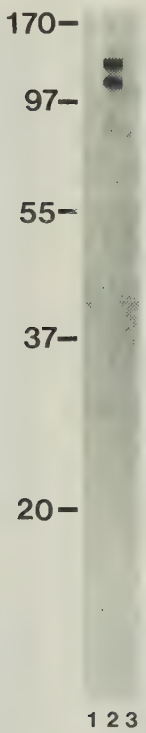

Fig. 2. Membrane-associated proteins labeled by anti-ßAPP$_{45-62}$ in human 293 embryonic kidney cells transfected with a full length ßAPP$_{695}$ expression construct. Lane 1 shows protein from control 293 cells stained with anti-ßAPP$_{45-62}$ (1:300), lane 2 shows protein from transfected 293 cells stained with anti-ßAPP$_{45-62}$ (1:300), and lane 3 shows protein from transfected cells stained with anti-ßAPP$_{45-62}$ (1:300) after absorption with ßAPP$_{45-62}$. Gels are 7% SDS-polyacrylamide; all lanes loaded with 20 μg protein. Molecular weight markers (bars) as in Fig. 1. The two intensely labeled proteins in lane 2 have calculated molecular weights of 130 and 117 kDa.

ßAPP$_{45-62}$ abolishes the immunolabeling of both the 120 kDa complex and the ~55 kDa protein (Fig. 1B, compare lanes 2 and 3). Anti-ßAPP$_{45-62}$ detects similar ~120 kDa and ~55 kDa membrane-associated proteins in rat brain and in human nucleus basalis of Meynert, hippocampus, and cerebellum (data not shown). Preliminary comparison of AD and control brains revealed no obvious qualitative differences in the proteins labeled by anti-ßAPP$_{45-62}$.

Fig. 2 shows immunoblots of membrane-associated proteins in control human 293 embryonic kidney cells and in 293 cells transfected with a full length ßAPP$_{695}$ expression construct. Anti-ßAPP$_{45-62}$ stains two proteins in the 110-135 kDa range that are intensely labeled in the transfected cells (lane 2) and not detected in control cells (lane 1). As shown in lane 3, the immunostaining of these proteins in the transfected cells is completely abolished by absorption with ßAPP$_{45-62}$.

The data in Figs. 1 and 2 demonstrate that, in brain and cDNA-transfected cells, anti-ßAPP$_{45-62}$ labels the set of ~110-135 kDa membrane-associated proteins previously identified as ßAPP using anti-C$_1$. Selkoe *et al.* (14) observed that anti-C$_1$ stains senile plaques in the hippocampus of patients with AD. Fig. 3 shows that anti-ßAPP$_{45-62}$ also stains senile plaques (A) and demonstrates that this staining is removed by absorption with ßAPP$_{45-62}$ (B). For comparison, plaques stained with anti-C$_1$ (C) and anti-SP28 (D) are

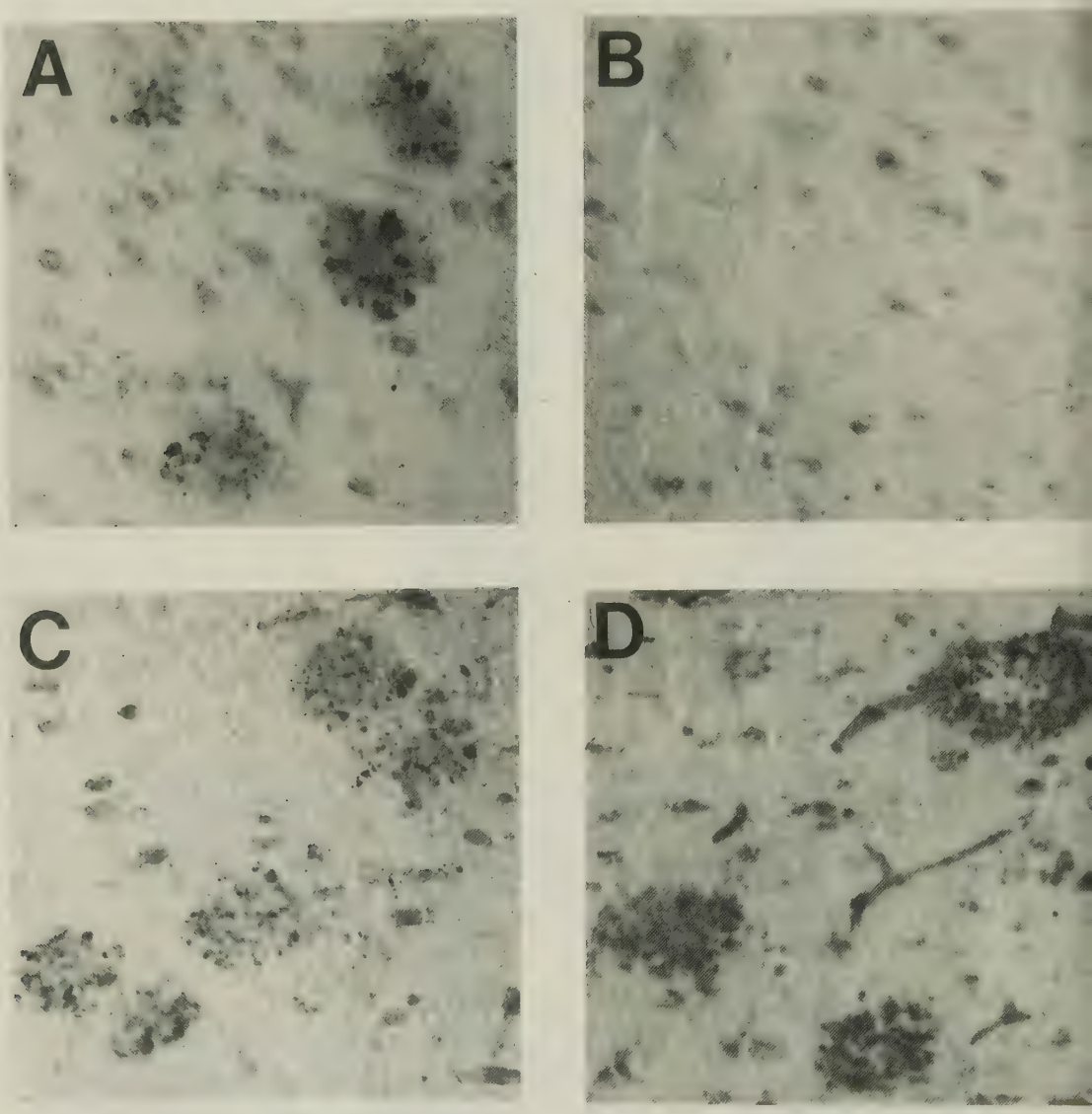

Fig. 3. Immunocytochemistry of various antibodies on cryostat sections of temporal cortex from a patient with Alzheimer's disease. **A**. Anti-ßAPP$_{45-62}$ (1:300). **B**. Anti-ßAPP$_{45-62}$ (1:300) after absorption with ßAPP$_{45-62}$. **C**. Anti-C_1 (1:150). **D**. Anti-SP28, an antiserum corresponding to amino acids 1-28 in the ßAP (1:150). Magnification 200x.

also shown. Overall, both anti-C_1 and anti-ßAPP$_{45-62}$ appear to stain fewer plaques than anti-SP28 (although this is not apparent in Fig. 3).

The fact that antiserum to C_1 labels senile plaques in AD brain indicates that the carboxyl-terminal portion of the ßAPP (which is located approximately 60 amino acids distal to the amyloidogenic ßAP domain) is present in the immediate vicinity of the amyloid fibrils within plaques (14). Our demonstration here that antiserum to ßAPP$_{45-62}$ stains plaques indicates that the near amino-terminal portion of the ßAPP is also located with the ßAP fibrils in senile plaques and suggests that proteolytic processing of the entire ßAPP molecule into insoluble fibrils occurs, at least in part, in a highly localized fashion directly at the sites of amyloid deposition in AD brains.

In a study that will be reported separately, we have found that, in addition to the ~120 kDa membrane-associated proteins, our antisera to βAPP_{45-62} detect a set of large, soluble proteins in brain and βAPP_{695}-transfected cells that are not detected by anti-C_1. For this reason, the immunostaining of senile plaques with anti-βAPP_{45-62} reported here could be due not only to membrane-associated forms of the βAPP detected by anti-C_1 but also to soluble forms of the βAPP not detected by antisera to the carboxyl-terminus.

ACKNOWLEDGEMENTS. We thank M. Usiak and A. Grombeck for assisting with the experimentation and Dr. T. Rosenberry for his excellent technical advice. We thank Drs. P. Gambetti and G. Perry for providing the βAPP_{45-62} peptide and Dr. B. Frangione for providing antiserum to SP28. Supported by USPHS grants AG06656, MH43444, 5T32GM0250, AG06173, AG07911 (Lead Award), AG00795, and a grant from the State of Ohio.

REFERENCES

1. Glenner, G.G. and Wong, C.W. (1984) Biochem. Biophys. Res. Commun. **120**, 885-890.
2. Masters, C.L., Simms, G., Weinmann, N.A., Multhaup, G., McDonald, B.L. and Beyreuther, K. (1985) Proc. Natl. Acad. Sci. U.S.A. **82**, 4245-4249.
3. Selkoe, D. J., Abraham, C.R., Podlisny, M.B., and Duffy, L.K. (1986) J. Neurochem. **146**, 1820-1834.
4. Kang, J., Lemaire, H.-G., Unterbeck, A., Salbaum, J.M., Masters, C.L., Grzeschik, K.-H., Multhaup, G., Beyreuther, K. and Muller-Hill, B. (1987) Nature (London) **325**, 733-736.
5. Goldgaber, D., Lerman, M.I., McBride, O.W., Saffiotti, U. and Gajdusek, D.C. (1987) Science **235**, 877-880.
6. Tanzi, R.E., Gusella, J.F., Watkins, P.C., Bruns, G.A.P., St. George-Hyslop, P., Van Keuren, M.L., Patterson, D., Pagan, S., Kurnit, D.M. and Neve, R.L. (1987) Science **235**, 880-884.
7. Robakis, N.K., Ramakrishna, N., Wolfe, G., and Wisniewski, H.M. (1987) Proc. Natl. Acad. Sci. U.S.A. **84**, 4190-4194.
8. Ponte, P., Gonzalez-DeWhitt, P., Schilling J., Miller, J., Hsu, D., Greenberg, B., Davis, K., Wallace, W., Lieberburg, I., Fuller, F., and Cordell, B. (1988) Nature (London) **331**, 525-527.
9. Tanzi, R.E., McClatchey. A.I., Lamperti, E.D., Villa-Komaroff, L., Gusella, J.F., and Neve, R.L. (1988) Nature (London) **331**, 528-530.
10. Kitaguchi, N., Takahashi, Y., Tokushima, Y., Shiojiri, S., and Ito, H. (1988) Nature (London) **331**, 530-532.
11. Zimmermann, K., Herget, T., Salbaum, J.M., Schubert, W., Hilbich, C., Cramer, M., Masters, C.L., Multhaup, G., Kang, J., Lemaire, H-G., Beyreuther, K., and Starzinski-Powitz, A. (l988) EMBO J. **7** (2), 367-372.
12. Shivers, B.D., Hilbich, C., Multhaup, G., Salbaum, M., Beyreuther, K., and Seeburg, P.H. (l988) EMBO J. **7** (5), 1365-1370.
13. Selkoe, D., Podlisny, M., Vickers, E. (1988) J. Neuropathol. Exp. Neurol. **47** (3), 355 (abstract).
14. Selkoe, D.J., Podlisny, M.B., Joachim, C.L., Vickers, E.A., Lee, G., Fritz, L.C., and Oltersdorf, T. (1988) Proc. Natl. Acad. Sci. U.S.A. (in press).
15. Tabaton, M., Morandi, A., Masters, C., Beyreuther, K., Perry, G., Gambetti, P., and Autilio-Gambetti, L. (1988) J. Neuropathol. Exp. Neurol. **47** (3), 336 (abstract).

Vol. 156, No. 1, 1988 BIOCHEMICAL AND BIOPHYSICAL RESEARCH COMMUNICATIONS
October 14, 1988 Pages 438-444

AN INVESTIGATION OF HUMAN OXYHEMOGLOBIN BETA TETRAMER DISSOCIATION USING HAPTOGLOBIN BINDING*

Linda A. Michalski and Melisenda J. McDonald

Biochemistry Program, Department of Chemistry,
University of Lowell, Lowell, MA 01854

Received August 15, 1988

Haptoglobin was used as a macromolecular probe to investigate the formation of human oxyhemoglobin beta chain dimers from tetramers in 0.1 M potassium phosphate buffer, 20° C at pH 7 and pH 8. Monitoring of spectral changes upon mixing haptoglobin with beta heme chains (2.5 and 5 micromolar) revealed an overall decrease in absorbance accompanied by a shift of the Soret spectral peak from 415 to 417 nm. The magnitude of the absorbance decrease was proportional to the beta concentration; the time courses consistently yielded greater color at pH 8 than at pH 7. At pH 8, two exponential phases of 0.47 min^{-1} and 0.084 min^{-1} were seen whose rates remained invariant with concentration. In contrast, only one exponential process was evident at pH 7, yielding a first order rate constant of 0.21 min^{-1}. We have spectrophotometrically followed the beta chain tetramer to dimer dissociation reaction, thus providing information about the contribution of this step to hemoglobin assembly.
© 1988 Academic Press, Inc.

Hemoglobin is a model system for understanding protein-protein interactions (1). Previous investigations of human oxyhemoglobins have used visible spectroscopy to monitor subunit assembly *in vitro* (2,3). Native subunit alpha and beta chains can be isolated which recombine to produce fully functional hemoglobin tetramers via an alpha-beta dimer intermediate (4-6). Over the protein concentration range previously studied, alpha chains are monomeric, while beta subunits are self-associated (7,8). Indeed, the beta tetramer dissociation can be the rate-limiting step in the reconstitution of hemoglobin (2).

The uncoupling of beta tetramers has been fitted to a tetramer-monomer equilibrium based on gel permeation studies (7) and absorbance changes accompanying dissociation (8). No attempt has been made to assess the role of an intermediate dimer species in this overall process, even though evidence for the existence of the beta chain dimer comes from sedimentation studies (9) and

*Supported by National Institutes of Health Grant HL-38456.

0006-291X/88 $1.50
Copyright © 1988 by Academic Press, Inc.
All rights of reproduction in any form reserved.

more recently from ligand binding studies (10). Furthermore, Atassi's group has demonstrated that beta chains combine with haptoglobin (11, 12), which is known to bind a dimer species of hemoglobin (13-15). By following Soret spectral changes upon mixing of human oxyhemoglobin beta chains with haptoglobin, we have succeeded in defining the beta tetramer to dimer reaction, a probable intermediate step in hemoglobin assembly *in vitro*.

MATERIALS AND METHODS

Preparation of reagent proteins - Isolated beta heme chains were purified from human adult hemoglobin by modifications (5,6) of the method of Bucci and Fronticelli (4). Prior to use in these experiments, the beta chains were stripped of phosphate ions (2) and subsequently buffered to the appropriate pH in 0.1 M potassium phosphate. To minimize stability problems, a fresh micromolar dilution was prepared for each Cary run and for each series of stopped flow traces. Concentration on a heme basis was verified spectrophotometrically at 414 nm (ϵ = 131 $mM^{-1}cm^{-1}$). The human haptoglobin was phenotype 1:1 and > 98% pure (Sigma, St. Louis, MO). Its concentration was maintained at a stoichoimetric excess (0.2 mg/ml before mixing) in 0.1 M potassium phosphate buffer at the desired pH. Multiple preparations of haptoglobin and beta chains were employed.

Static and kinetic spectrophotometric measurements - A Cary 2200 recording spectrophotometer maintained at 20° C was used to make all successive spectroscopic measurements. The mixing experiments were performed in rectangular tandem mixing cuvettes. The sample cell held equal volumes of beta and haptoglobin solutions, whereas the reference cell contained equal volumes of beta solution and buffer. For some trials, successive scans from 380-450 nm at 1 nm/sec were repeated after mixing at intervals sufficient to provide resolution of individual traces. In addition, the change in absorbance as a function of time was followed at 415 nm in either the Cary 2200 or a Kinetic Instruments stopped-flow apparatus integrated by the 4120AT microcomputer-based system (On-Line Instrument Systems, Inc., Jefferson, GA). A minimum of four traces was collected and analyzed for each experimental condition.

Data reduction - All spectral data were corrected to 1 cm path length cell and for small variations in beta chain concentration (< 10%). Data from the successive spectral measurements and absorbance profiles were analyzed using the Guggenheim approximation. Stopped-flow data were fitted directly by the routines in the 4120AT software to obtain first order rate constants.

RESULTS AND DISCUSSION

Since the alpha monomer binds essentially irreversibly to the beta monomer (16,17), our previous studies of subunit assembly utilizing alpha chains as the probe allowed investigation of the rate limiting beta chain tetramer dissociation step (2,3). However, in the presence of alpha chains, the pseudo steady-state approximation with respect to the beta dimer was necessary since the relative absorbance contributions of the tetramer to dimer and the dimer to monomer steps were unknown. The present approach addresses the formation of the beta dimer *in vitro*.

Human oxyhemoglobin beta chains were mixed with human haptoglobin, phenotype 1:1, and the change in absorbance as a function of wavelength and time was monitored on a Cary 2200 recording spectrophotometer. A typical experiment employing the spectral overlay technique is shown in Figure 1 for beta chains at 5 micromolar in heme prior to mixing, 0.1 M potassium phosphate buffer, pH 8 and 20° C. By spectrally monitoring the region from 380 to 450 nm, it was evident that a small but definite Soret absorption peak shift from 415 to 417 nm occurs during the course of the reaction. Such a red shift has been previously reported in 0.1 M Tris, 0.1 M NaCl, 1 mM Na_2EDTA, pH 7.4 and 10° C for beta chain concentration difference spectra and has been assigned to a tetramer dissociation step (8). Presumably, since haptoglobin binding allows the tetramer to dimer reaction to be isolated, our studies suggest that this dissociation step contributes to the overall spectral shift.

The haptoglobin binding reaction resulted in an overall decrease in absorbance of 0.071 at 415 nm, consistent with a beta chain tetramer to dimer dissociation (8). If this reaction is indeed analogous to that of hemoglobin (14), a homogeneous first order dissociation profile should be seen. Successive spectral scans allowed initial inspection of kinetic parameters; however,

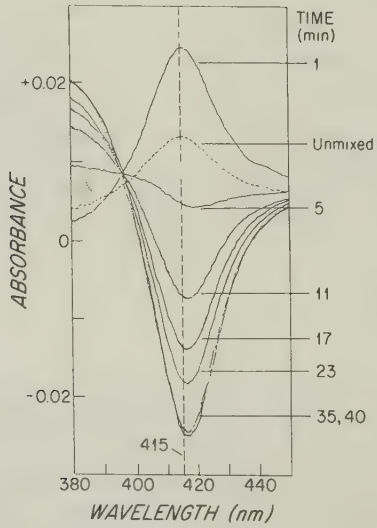

Figure 1: Successive spectra recorded on a Cary 2200 spectrophometer after mixing haptoglobin with oxygenated beta chains in 0.1 M potassium phosphate buffer, pH 8 and 20° C. Kinetics were analyzed at 415 nm. Beta chain concentration on a heme basis prior to mixing was 5 micromolar. Only experimental data demonstrating isosbesty at 395 (±1) nm were used in the present studies. Lack of a clean isosbestic point was inevitably due to methemoglobin formation of beta chains, as revealed by absolute spectra taken immediately following the mixing experiment.

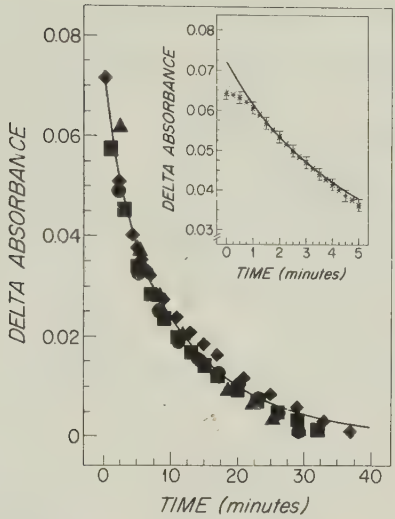

Figure 2: Overall time course for the reaction of beta heme chains with haptoglobin. The figure displays the results of successive scan experiments and absorbance profiles together with the fitted two exponential rate plot. The inset superimposes the same fitted curve with stopped flow data points obtained as the average of four individual traces; average points rather than individual data from each experimental run are shown in the interest of clarity. Conditions are the same as Figure 1. (An initial deviation from the fitted curve is seen and was not further analyzed in the present study.)

to better define the overall profile, the reaction was further monitored on either a Cary 2200 spectrophotometer or a Kinetic Instruments stopped-flow apparatus (Figure 2). Surprisingly, resultant time courses could be fitted to a two exponential process yielding first order rate constants of 0.47 and 0.084 min^{-1} for the fast and slow phases, respectively (See Table I). When the concentration of beta chains was halved to 2.5 micromolar in heme prior to mixing, the fast phase alone contributed the majority of the color change and yielded a rate of

Table I
Absorbance changes and rate constants for the reaction of oxyhemoglobin beta chains with haptoglobin. Results determined as described in text in 0.1 M potassium phosphate buffer and 20° C.

pH	[BETA] before mixing	TOTAL DELTA ABSORBANCE	k_1 min^{-1}	DELTA ABSORBANCE RXN#1	k_2 min^{-1}	DELTA ABSORBANCE RXN#2
8	2.5 uM	0.031	0.49 (±.021)	0.031	*	*
8	5.0	0.071	0.47 (±.035)	0.017	0.084 (±.0033)	0.054
7	2.5	0.016	0.24 (±.098)	0.016		
7	5.0	0.035	0.21 (±.020)	0.035		

* Slow phase contributed less than 10% of overall delta absorbance and was not further evaluated.

tetramer dissociation identical to that seen at 5 micromolar. The slow phase was only marginally detectable at 2.5 micromolar. The unexpected result of a two phase reaction may be explained by recently reported evidence for heterogeneity in the beta tetramer population (10, 18). More probably, this heterogeneity can be accounted for by differential phosphate binding to beta tetramers. Crystallographic evidence from Arnone's laboratory (19,20) demonstrates the existence of two phosphate binding sites on the beta chain tetramer. In addition, our work (2,3,21) as well as that of McGovern *et. al* (22) indicates a strong effect of phosphate on beta chain tetramer dissociation kinetics.

Further studies were conducted in a more physiologically relevant system, 0.1 M potassium phosphate buffer at pH 7 and 20° C at identical protein concentrations. The Soret spectral shift seen at pH 8 was also apparent at pH 7, strongly suggesting that beta chain binding to haptoglobin at both pH's involves a similar mechanism. The results of the spectral and kinetic analyses are shown in Figure 3 and Table I. The color change of the reaction was, again, directly proportional to initial heme concentration. However, the magnitude of the absorbance change at pH 7 was consistently less than that at pH 8. In addition, the overall time course could be fitted to a single exponential curve yielding a rate of 0.21 min^{-1}. This slower rate of beta tetramer to dimer

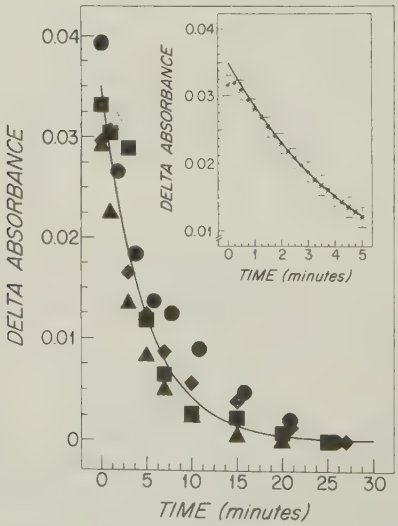

Figure 3: Overall time course for the reaction of beta heme chains with haptoglobin, similar to Figure 2 with conditions of: beta chain concentration of 5 micromolar in heme prior to mixing, 0.1 M potassium phosphate, pH 7 and 20° C. (The initial deviation from the fitted curve is again observed, but not evaluated.)

dissociation at pH 7 is consistent with the proposed stabilization of the beta tetramer by protons (21). Overall beta tetramer to monomer dissociation has been shown spectrophotometrically to be rate limiting in hemoglobin reconstitution (2,3,21-25). We have isolated the tetramer to dimer reaction of oxygenated beta chains and have demonstrated that this step contributes to the Soret absorbance change. Furthermore, the first order rates measured were in the range of those defined as rate limiting in assembly.

The studies reported here are exciting because this method potentially allows monitoring of the tetramer-dimer dissociation in isolated human beta chains by a spectrophotometric technique traditionally used to analyze this dissociation in hemoglobin (26-28). Our findings should encourage further investigations aimed at analyzing the intriguing phenomenon of beta chain self-association, a key reaction in human hemoglobin assembly.

REFERENCES

1. Perutz, M.F. (1987) in The Molecular Basis of Blood Diseases (Stamatoyannopoulos, G., Nienhuis, A.W., Leder, P., and Majerus, P.W., Eds.) pp. 127-178. W.B. Sanders Co., Philadelphia, PA.
2. McDonald, M.J. (1981) J. Biol. Chem. 256, 6487-6490.
3. McDonald, M.J., Turci, S.M., Mrabet, N.T., Himelstein, B.P., and Bunn, H.F. (1987) J. Biol. Chem. 262, 5951-5956.
4. Bucci, E. and Fronticelli, C, (1965) J. Biol. Chem. 240, PC551-PC555.
5. Geraci, G., Parkhurst, L.J., and Gibson, Q.H. (1969) J. Biol. Chem. 244, 4664-4667.
6. McDonald, M.J. and Noble, R. W. (1972) J. Biol. Chem. 247, 4282-4285.
7. Valdes, R. and Ackers, G.K. (1977) J. Biol. Chem. 252, 74-81.
8. Philo, J.S., Adams, M.L. and Schuster, T.M. (1981) J. Biol. Chem. 256, 7917-7924.
9. Tainsky, M. and Edelstein, S.J. (1973) J. Mol. Biol. 75, 735-739.
10. Philo, J.S., Lary, J.W. and Schuster, T.M. (1988) J. Biol. Chem. 263, 682-689.
11. Kazmin, A.L. and Atassi, M.Z. (1980) Biochem. J. 185, 285-287.
12. Yoshioka, N. and Atassi, M.Z. (1986) Biochem. J. 234, 453-456.
13. Nagel, R.L., Rothman, M.C., Bradley, T.B. and Ranney, H.M. (1965) J. Biol. Chem. 240, 4543-4545.
14. Nagel, R.L. and Gibson, Q.H. (1967) J. Biol. Chem. 242, 3428-3434.
15. Nagel, R.L. and Gibson, Q.H. (1971) J. Biol. Chem. 246, 69-73.
16. Shaeffer, J.R., McDonald, M.J., Turci, S.M., Dinda, D.M. and Bunn, H.F. (1984) J. Biol. Chem. 259, 14544-14547.
17. Mrabet, N.T., Shaeffer, J.R., McDonald, M.J. and Bunn, H.F. (1986) J. Biol. Chem. 261, 1111-1115.
18. La Mar, G.N., Yamamoto, Y., Jue, T., Smith, K.M. and Pandey, R.K. (1985) Biochemistry 24, 3826-3831.
19. Arnone, A. and Briley, P.D. (1978) in Biochemical and Clinical Aspects of Hemoglobin Abnormalities (Caughey, W.S., Ed.) pp. 93-107. Academic Press, New York.
20. Arnone, A., Briley, P.D., Rogers, P.H., and Hendrickson, W.A. (1982) in Hemoglobin and Oxygen Binding (Ho, C., Ed.) pp. 127-133. Elsevier North Holland, Inc., New York.

21. Turci, S.M. and McDonald, M.J. (1983) Biochem. Biophys. Res. Comm. 111, 55-60.
22. McGovern, P., Reisberg, P., and Olsen, J.S. (1976) J. Biol. Chem. 251, 7871-7879.
23. Kawamura, Y., Hasumi, H., and Nakamura, S. (1982) J. Biochem. (Tokyo) 92, 1227-1233.
24. Kawamura, Y. and Nakamura, S. (1983) J. Biochem. (Tokyo) 93, 1159-1166.
25. Kawamura, Y. and Nakamura, S. (1983) J. Biochem. (Tokyo) 94, 1851-1856.
26. Kellett, G.L. and Gutfreund, H. (1970) Nature (London) 227, 921-926.
27. Gray, R.D. (1974) J. Biol. Chem. 249, 2879-2885.
28. Ip, S.H.C., Johnson, M.L. and Ackers, G.K. (1976) Biochemistry 15, 654-660.

Vol. 156, No. 1, 1988 BIOCHEMICAL AND BIOPHYSICAL RESEARCH COMMUNICATIONS
October 14, 1988 Pages 445-450

Partial Amino Acid Sequence Analysis of Human Placenta Monoamine Oxidase A and Bovine Liver Monoamine Oxidase B

Shiuan Chen[1+] and Walter Weyler[2]

[1]Division of Immunology, Beckman Research Institute of the City of Hope, Duarte, CA 91010

[2]Molecular Biology Division, VA Medical Center San Francisco, CA 94121

Received August 15, 1988

We have prepared peptide maps from human placenta monoamine oxidase type A (MAO-A) and bovine monoamine oxidase type B (MAO-B) and determined the amino acid sequences of 21of these peptides. These sequences have been compared to the cDNA deduced amino acid sequences of human MAO-A and -B. A result of special interest is the identification of two sets of MAO-A peptides which have sequences different from those deduced from cDNA sequences. This observation is consistent with the notion that MAO-A may be composed of at two subunits which are similar but not identical in primary amino acid sequence. © 1988 Academic Press, Inc.

Monoamine oxidase (MA0) [monoamine: oxygen oxidoreductase (deaminating), EC 1.4.3.4.], a covalent FAD flavoenzyme, is of considerable pharmacological interest because of its central position in the metabolism of monoamine neurotransmitters. Based on their specificity for substrates and inhibitors, particularly the selective suicide inhibitors clorgyline and deprenyl, two types of MAO have been described, MAO-A and B [1-3]. Although the human brain contains both types of MAO, MAO-B, but not MAO-A, has recently been found to be directly involved in the induction of Parkinsonism by the neurotoxin, 1-methyl-4-phenyl-1,2,3,6-tetrahydropyridine (MPTP) [4-6].

Recently, we have prepared tryptic peptides of both purified human placenta MAO-A and bovine liver MAO-B. A significant number of peptides from these two preparations have been purified and sequenced. This is the first time that amino acid sequences of two types of MAO other than that of the FAD penta peptide have been determined. These sequences are

+Correspondence should be addressed to this author.

0006-291X/88 $1.50
Copyright © 1988 by Academic Press, Inc.
All rights of reproduction in any form reserved.

important not only in illustrating the structural difference between two types of MAO, but also in designing oligonucleotide probes for the identification of MAO clones. These sequences are also very important in confirming cDNA sequences, especially frame shift errors [7], and for the detection of a frame shift in cDNA clones [8].

Materials and Methods

Enzyme Isolation. Bovine liver MAO-B was purified from bovine liver mitochrondia according to the procedure described by Salach [9] and further purified by sucrose density centrifugation as previously reported [10]. Human placenta MAO-A was purified as previously reported [11].

Amino Acid Composition. Amino acid composition was determined on a Beckman 121 MB amino acid analyzer after hydrolysis in 5.7N HCl at 110^0 C for 24 hours and cysteine content was determined as cysteic acid after performic acid oxidation.

Carboxymethylation and Trypsin Digestion of MAO. Enzyme (1 mg) in 1 ml of 100 mM phosphate buffer, pH 7.4, containing 6 M guanidine hydrochloride, was incubated with 0.96 mM 2-mercaptoethanol for 6 hours at room temperature, followed by an overnight incubation in the presence of 60 mg of iodoacetic acid. The sample was dialyzed for 24 hr against 4 liters of water and for 24 hr against 4 liters of 100 mM ammonium bicarbonate. The dialyzed sample was digested overnight in the presence of trypsin (40 μl) at 37^0 C.

Separation of peptides by reverse-phase HPLC. The peptides were separated on a Vydac C-18 (Western Analytical Labs) analytical column and rechromatographed with an Altex ultrasphere ODS (Beckman Instruments) analytical column. Chromatographic conditions were similar to those described by Yuan et al. [12].

Analysis of isolated peptides. The isolated peptides were characterized by amino acid analysis, sequence analysis and fast atom bombardment mass spectral (FAB/MS) analysis. Automated sequence analysis was performed on a gas phase sequencer built at the City of Hope [13]. Positive ion FAB/MS was used to confirm our results as previously described [14].

Results and Discussion

The tryptic maps of the human placenta MAO-A and bovine liver MAO-B generated by reverse phase HPLC are shown in Figure 1 and are clearly not the same,indicating that the primary structures of these two MAOs are substantially different from each other. The cysteine-containing peptides (identified by [^{14}C] iodoacetic acid labeling) are also different for the two MAOs. The amino acid sequences of seven tryptic peptides of human placental MAO-A were determined and used to identify a cDNA clone encoding for human MAO-A [15]. The amino acid sequences of fourteen tryptic peptides of bovine liver MAO-B were also determined. These bovine MAO-B sequences are compared to the sequences deduced from human MAO-A and -B cDNA [15, 16]. It has been reported that the amino acid sequences of

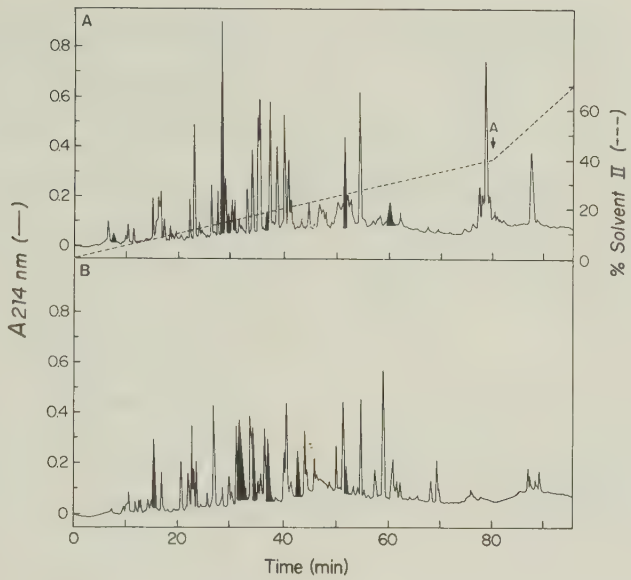

Fig.1. Fractionation of tryptic digest of [^{14}C]-carboxymethylated human placenta MAO-A (A) and bovine liver MAO-B (B) by reverse phase HPLC.

The peptides were separated on a Vydac C-18 column (25 cm x 5 mm) with an 80-min linear gradient from 100% solvent I (0.1% TFA) to 40% solvent II (TFA-water-acetonitrile = 0.1:9.9:90, V/V/V). The flow rate was 0.8 ml/min. One ml of 50% 1-propanol was injected to the column at the end of 80 min. gradient program, indicated as "A" on the chromatogram, to elute the core peptides. Fractions were manually collected and 10µl of aliquot from each peak fraction was counted for [^{14}C] radioactivity. The shaded peaks represent the radioactive fractions.

human MAO-A and -B are ~ 70% identical [16]. Figure 2 shows that those amino acid residues that are identical between human MAO-A and -B are usually conserved in bovine MAO-B sequences as well. More interestingly, among those amino acid residues that differ between human MAO-A and -B, the corresponding residues in bovine MAO-B peptides are identical to those of human MAO-B in most cases. These results show that the primary structures among the same type of MAO from different species are more conserved than those of the two types of MAO from the same species. These results suggest that the genes for MAO-A and -B are derived from a common progenitor gene that probably diverged very early during the revolution.

During amino acid sequence analysis of peptides isolated from the placenta MAO-A, we found that two peptides have eight residues identical to each other over 10 residues (Figure 3). They contain one conservative substitution from Asn to Gln and one substitution from Asp to Tyr. These sequences are different from the amino acid sequence deduced from

```
31                          41
L L T E Y G V S V L V L E A R
* *       *     *   * * * * *
L L H D S G L N V V V L E A R
* * * * * * * * *   * * * * *
L L H D S G L N V I V L E A R

62                                  79
Y V D V G G A Y V G P T Q N R I L R
* * *   * *   * * * * * * * * * * *
Y V D L G G S Y V G P T Q N R I L R
* * * * * * * * * * * * *   * * *
Y V D L G G S Y V G P T Q N H I L R

110                                 129 268                                 288
G A F P P V W N P I A Y L D Y N N L W R   Y V I N A I P P T L T A K I H F R P E L P
*   * * *   * *   * *   * * *   * *   * *   * * *   * * * * * *     * * * *   * * *
G P F P P V W N P I T Y L D H N N F W R   Y V I S A I P P T L G M K I H F N P P L P
*   * *   * * * * * * * * *   * * * * *   * * * * *   * *   * *   * * * * * * * * *
G S F P S V W N P I T Y L D Y N N F W R   Y V I S A V P P V L G G K I H F N P P L P

298           305                         306                 316
L P M G A V I K                           C M M Y Y K E A F W K
  *   *   * * *                           *     * * * *   * *
V P L G S V I K                           C I V Y Y K E P F W R
* * * * * * *                               * * * * * * * *
V P L G S V I K                           (P)I V Y Y K E P F W K

319                       332             336                             352
D Y C G C M I I E D E D A P               T L D D T K P D G S L P A I M G F
* * * *   * * *     *   * *               * * * * * * *   *       * * * * *
D Y C G T M I I D G E E A P               T L D D T K P E G N Y A A I M G F
* * * *   * * *   * * * * *                 * * * * * *   *   *   * *   * *
D Y C G S M I I E G E E A P               A L D D T K P D G S Y P A I I G F

372           379                         380                         395
K I C E L Y A K                           V L G S Q E A L H P V H Y E E K
*   * * * * * *                           * * * *   * * *   * * * * * * *
K L C E L Y A K                           V L G S L E A L E P V H Y E E K
* * *   * * * *                           * * * * * * * * * * * * * * *
K L C D L Y A K                           V L G S L E A L E P V H Y E E K

396                           412         430                 440
N M C E E Q Y S G G C Y T A Y F P         I F F A G T E T A T K
* * * * * * * * * * * * *   * * *         *   * * * * * * * *
N M C E E Q Y S G G C Y T T Y F P         I Y F A G T E T A T H
* * * * * * * * * * * *   * * *           * * * * * * * * * *
N M C E E Q Y S G G C Y T A Y F P         I Y F A G T E T A T(H)

458           465       466                                         493
E V L N G L G K         V T E K D I W V Q E P E S K D V P A V E I T H T F W E R
*   *       * *           *     * *     * * * *   * * * *     * *   * *   * *
E I L H A M G K         I P E D E I W Q S E P E S V D V P A Q P I T T T F L E R
* * * * * * *             * * * * * *     * * * *   * * * *   * *   *
E I L H A M G K         L P E D E I W L P E P E S V D V P A K P I S T S S M(M)(M)
```

Fig. 2. Comparison of amino acid sequences of bovine liver MAO-B peptides with the sequences deduced from human MAO-A and -B.

In each set, the deduced sequence of human MAO-A, the deduced sequence of human MAO-B, and the determined amino acid sequences of bovine MAO-B are shown in lanes 1, 2, and 3, respectively. The numbering of amino acids of human MAO-A peptides is shown according to Hsu et al. [15]and used to indicate the positions of these peptides. The asterisks indicate positions occupied by identical amino acids.

cDNA ^{230}I M D L L G D Q V K^{239}. Furthermore, we determined the sequence of one peptide from human placenta MAO-A as E V L H A V G K. This sequence has strong homology to that of one peptide from bovine liver MAO-B, E I L H A M G K. As shown in Figure 2, the

```
230                 239
 I M D L L G D Q V K
 I E D L L G D Q V K
 I Q D L L G Y Q V K
```

Fig. 3. Comparison of amino aicd sequences of two human placenta MAO-A peptides (lanes 2 and 3) with a sequence deduced from human MAO-A cDNA (lane 1).

sequence of this bovine liver MAO-B peptide is completely identical to that of the corresponding peptide in human MAO-B. However, the sequence of the mentioned human placenta MAO-A peptide is different from that of the corresponding peptide region deduced from the cDNA sequence, ^{458}E V L N G L G K^{465}. These results are consistent with the notion that human placenta MAO-A consists of two subunits which are very similar, and possibly arose by gene duplication. Our results can also be explained by DNA polymorphism as suggested by Ozelius et al. (17).

In summary, this communication we have presented data including peptide mapping and amino acid sequences information of human placenta MAO-A and bovine liver MAO-B. We have compared the sequences of bovine liver MAO-B peptides with those of human MAO-A and -B. We have also provided results indicating sequence heterogeneity for human placenta MAO-A.

Acknowledgments: This work was supported by the Veterans Administration and NIH Grants (MH42462, NS25786 and CA33572) to Shiuan Chen. The authors would like to thank Dr. Terry D. Lee and Mr. Kassu Legesse for assistance with FAB Mass Spectral analysis of the isolated peptides.

References

1. Fuller, R.W., (1968) Biochem. Pharmac., 17, 2097.

2. Johnston, J.P. (1968) Biochem. Pharmac., 17, 1285.

3. Knoll, J.P. and Magyar, K., (1972) Adv. Biochem. Pyschopharmac., 5, 393.

4. Chiba, K., Trevor, A., and Castagnoli, Jr., N., (1984) Biochem. Biophys. Res. Commun., 120, 574-578.

5. Langston, J.W., Irwin, J., Langston, E.B., and Bomo, L.S. (1984) Science, 225, 1480-1482.

6. Markey, S.P., Johannessen, J.N., Chiueh, C.L., Burns, R.S., and Herkenham, M.A., (1984) Nature, 311, 464-467.

7. Bienkowski, M.J., Haniu, M., Nakajin, S., Shinoda, M., Yanagibashi, K., Hall, P.F., and Shively, J.E., Biochem. Biophys Res. Commun., (1985) 25, 734-740.

8. Chen, S., Besman, M.J., Sparkes, R.S., Zollman, S., Klisak, I., Mohandas, T., Hall, P.F., and Shively, J.E. (1988), DNA, 7, 27-38.

9. Salach, J.I., (1979) Arch. Biochem. Biophys., 192, 128-137.

10. Weyler, W. and Salach, J.I., (1981) Arch. Biochem. Biophys., 212, 147-153.

11. Weyler, W. and Salach, J.I., (1985) J. Biol. Chem., 260, 13199-13207.

12. Yuan, P.-M., Pande, H., Clark, B.R., and Shively, J.E., (1986) Anal. Biochem., 120, 289-320.

13. Hawke, D.H., Harris, D.C., and Shively, J.E. (1985) Anal. Biochem., 147, 315-320.

14. Chen, S., Lee, T.D., Legesse, K., and Shively, J.E. (1986) Biochemistry, 25, 5391-5395.

15. Hsu, Y.-P.P., Weyler, W., Chen, S., Sims, K.B., Rinehart, W.B., Utterback, M., Powell, J.F., and Breakefield, X.O. (1988), J. Neurochem., in press.

16. Bach, A.W.J., Lan, N.C., Johnson, D.L., Abell, C.W., Bembenek, M.E., Kwan, S.-W., Seeburg, P.H., and Shih, J.C. (1988) Proc. Natl. Acad. Sci. USA, 85, 4934-4938.

17. Ozelius, L., Hsu Y.-P.P., Bruns, G., Powell, J.F., Chen, S., Weyler, W., Uttenback, M., Zucker, D., Haines, J., Trofatter, J.A., Conneally, P.M., Gusella, J.F., and Breakefield, X.O. (1988), Genomics, in press.

Vol. 156, No. 1, 1988 BIOCHEMICAL AND BIOPHYSICAL RESEARCH COMMUNICATIONS
October 14, 1988 Pages 451-456

RIBULOSE 1,5-BISPHOSPHATE DEPENDENT CO_2 FIXATION IN THE HALOPHILIC ARCHAEBACTERIUM, HALOBACTERIUM MEDITERRANEI

NENOO RAWAL, S.M. KELKAR AND WIJAYA ALTEKAR*

Biochemistry Division
Bhabha Atomic Research Centre, Bombay 400 085, India

Received August 15, 1988

The cell extract of Halobacterium mediterranei catalyses incorporation of $^{14}CO_2$ into 3-phosphoglycerate in the presence of ribulose bisphosphate suggesting the existence of ribulose bisphosphate carboxylase activity in this halophilic archaebacterium. © 1988 Academic Press, Inc.

Light dependent CO_2 assimilation in the surface water samples from Dead Sea was observed by Oren (1) and was attributed to the activity of purple membrane-containing halobacteria. Propionate-stimulated CO_2 fixation was also demonstrated in Halobacterium halobium cells grown anaerobically (2). Their assumption that α-ketobutyrate was formed from propionate and CO_2 was questioned by Kerscher and Oesterhelt (3) since the reaction products were not identified and no electron donor was added.

Halobacteria which are described as chemoheterotrophs (4) have never been shown capable of autotrophic growth. Carbohydrate metabolism in halophilic archaebacteria is a subject of study in our laboratory (manuscript communicated) and at least in one strain ribulose bisphosphate (RuBP) dependent CO_2 fixation was observed after growth in heterotrophic conditions. While we were examining the details of CO_2 fixation, an analytical study by Javor (5) on CO_2 fixation in halobacteria was published. α-ketobutyrate was not detected and the product of NH_4. propionate stimulated CO_2 fixation was identified as glycine and that from pyruvate as pyruvate. However, no RuBP carboxylase activity could be detected in H. halobium. This note presents preliminary data on the RuBP dependent CO_2 fixation which could be attributed to the activity of RuBP carboxylase in the cell extracts of H. mediterranei.

Materials & Methods

RuBP and ribulose 5-phosphate (Ru5P) were purchased from Sigma Chemical Co., U.S.A. $NaH^{14}CO_3$ (48.1 mCi/mmol) was purchased from Isotope Division,

*To whom correspondence should be addressed.

0006-291X/88 $1.50
Copyright © 1988 by Academic Press, Inc.
All rights of reproduction in any form reserved.

Bhabha Atomic Research Centre, India and was diluted suitably with cold $NaHCO_3$. The following archaebacterial halophiles: Halobacterium mediterranei, H. vallismortis, H. halobium and Halobacterium strain R-113 were grown as shake cultures at 37°C in a complex medium containing 20-25% concentrations of NaCl and 0.5% glucose. Glucose was not added to H. halobium growth medium. The details of conditions for growth, harvest and preparation of cell extracts by sonication as well as the source of culture were described in our earlier paper (6, 7). The method of Bowien et al (8) was used for the assay of RuBP carboxylase (EC 4.1.1.39). Protein was estimated by the method of Lowry et al (9).

Results & Discussion

$^{14}CO_2$ fixation reactions

Preliminary tests with cell extracts of halobacteria grown on complex medium showed signs of CO_2 incorporation at least in case of H. mediterranei. Subsequently H. mediterranei was grown on a synthetic medium with glucose (7), and factors affecting CO_2 incorporation by the extracts were tested (Table 1). Incorporation of $^{14}CO_2$ into an acid soluble component took place in the presence of RuBP. The incorporation detected in the absence of added Mg^{2+}

Table 1. RuBP dependent $^{14}CO_2$ incorporation in cell extracts of halobacteria

Strains	Conditions	$^{14}CO_2$ incorporated CPM*
(a) H. mediterranei	Complete	3371
	- $NaHCO_3$	0
	- RuBP	137
	- Enzyme	56
	- Mg^{2+}	3136
	+ EDTA, - Mg^{2+}	200
H. halobium	Complete	ND
H. vallismortis	"	ND
Halobacterium R-113	"	ND
(b) H. mediterranei	Complete with Ru5P*	3276

For (a) reaction mixture in 250 µl contained: $MgCl_2.6H_2O$, 10 mM; $NaH^{14}CO_3$, 33.3 mM (0.17 µCi/µM) Tris-HCl (pH 7.8), 150 mM and 1 M with respect to NaCl. Cell extract was used after 30 min activation with bicarbonate at 25°C, reaction was initiated by addition of 2 mM RuBP and stopped after 1 hr at 30°C with 100 µl of 50% TCA. Following removal of any labile CO_2, precipitate was removed by centrifugation. Radioactivity present in supernatant was measured in a 100 µl aliquot which was added to 15 ml scintillation fluid consisting of POPOP and PPO and counted on a LKB Rackbeta Liquid Scintillation Counter. Protein values: H. mediterranei, 0.35 mg and others, 2-4 mg.

ND = Not detected after 4 h incubation.

For (b), RuBP was replaced by Ru5P, 1.6mM and ATP, 5 mM. Other conditions as in (a).

was attributed to endogenous Mg^{2+}, the concentration of which is known to be high in halobacteria (10). This was confirmed by the addition of 10 mM EDTA to the reaction mixture which resulted in suppression of $^{14}CO_2$ incorporation. Addition of 15 mM $MgCl_2$ to EDTA treated extract restored the activity. In contrast in the extracts of H. halobium, H. vallismortis and Halobacterium R-113, the incorporation of $^{14}CO_2$ could not be detected in complete assay systems even when the incubation time was prolonged to 4 h (Table 1).

The dependence of $^{14}CO_2$ incorporation on RuBP was further confirmed in the reactions when RuBP was replaced by Ru5P and ATP (Table 1"b") since Ru5P kinase activity was detected in H. mediterranei and other halobacteria (manuscript communicated). Thus the coupled activities of Ru5P kinase and RuBP carboxylase in H. mediterranei extract were considered responsible for the incorporation of $^{14}CO_2$ shown in reaction "b", Table 1.

Rate of $^{14}CO_2$ incorporation and effect of salt

The rate of $^{14}CO_2$ incorporation in H. mediterranei extract and the effect of protein concentration on the rate are shown in Fig. 1a and 1b.

The enzymatic activity was halophilic for KCl and NaCl. No activity could be detected in the absence of salt though the low concentration of 0.3 M salt carried over in the assay mixture was adequate for activity. The activity declined slowly in higher concentrations of salt. However, 60% activity was evident in 3 M KCl or NaCl (Fig. 2) and remained unaltered in 4 M salt (data not shown). The activity was lost upon storage of extract without salt.

Identification of the product of $^{14}CO_2$ incorporation

The TCA supernatant obtained after termination of the enzyme reaction was concentrated after desalting and analysed initially by 2-dimensional

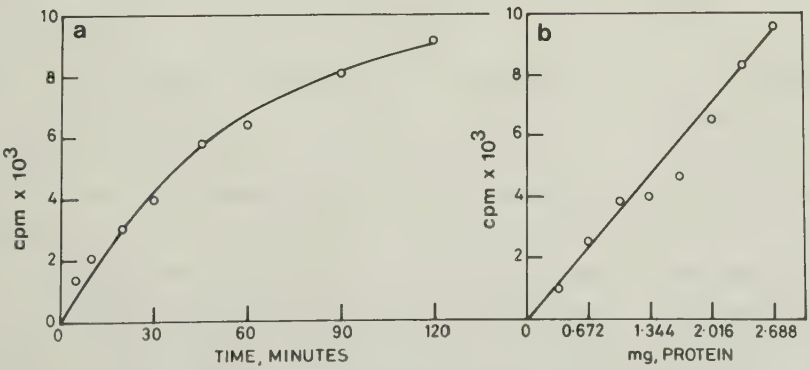

Fig. 1. CO_2 incorporation by extracts of H. mediterranei, conditions as in Table 1. (a) shows the rate of reaction (1.3 mg protein). (b) shows incorporation after 30 min at varying protein concentration.

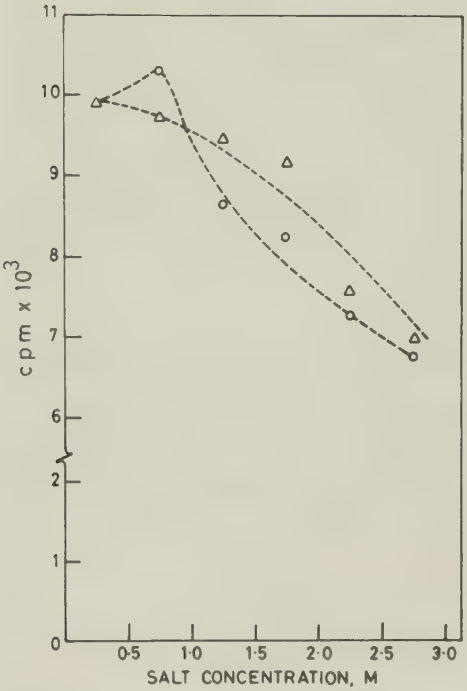

2

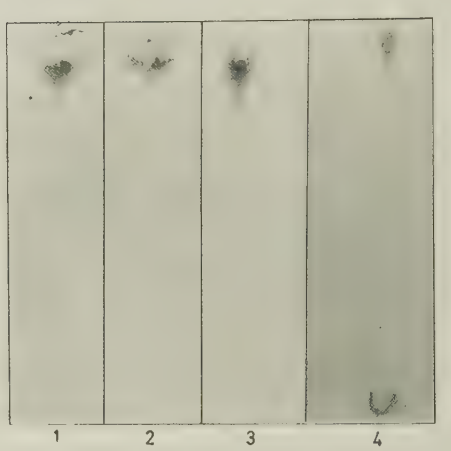

3

Fig. 2. Effect of salt on RuBP dependent CO_2 incorporation in H. mediterranei. Conditions as in Table 1. Protein, 1.3 mg. Values are corrected for carried over salt. Symbols: O, NaCl, Δ , KCl.

Fig. 3. Identification of product of RuBP dependent $^{14}CO_2$ incorporation in H. mediterranei. Reaction conducted as in Table 1 and TCA supernatant desalted by passage through Sephadex G-10. Radioactive fractions pooled and used. Results of chromatography in descending fashion (Ref. 11) on Whatman paper No. 4, solvent, propionic acid : n-butanol : H_2O = 5:10:7. After drying, paper sprayed with ammonium molybdate reagent (Ref. 12) when phosphate esters turned blue. Lane 1, halobacterial reaction product; Lane 2, 3PGA standard; Lane 3, reaction product of pure spinach RuBP carboxylase, reaction being run for 5 min as in Table 1; Lane 4, autoradiogram of halobacterial reaction product run only in single direction in above solvent, not sprayed, after exposure to Kiran X-ray film for 21 days at 4°C.

chromatography (11) when a major spot corresponding to authentic 3-phosphoglyceric acid (3PGA) was observed. The area of this spot was eluted with water and subsequently rechromatographed in single direction (Fig. 3). The unknown spot on paper showed positive test for phosphate with molybdate spray (12) and its R_f value corresponded to that of authentic 3PGA as well as to the reaction product obtained from the assay of pure RuBP carboxylase from spinach. A second chromatogram run similarly, was autoradiographed when the above halobacterial phosphorylated reaction product i.e. 3PGA was found to be radioactive (Fig. 3). Occasionally minor active spots in the area of sugar phosphates were noticed which are not seen in this Fig.

Though CO_2 fixation due to pyruvate carboxylase activity was present in the extract, it was strictly dependent on the presence of acetyl CoA (data not shown).

The RuBP dependent CO_2 incorporating activity was, however inhibited in the presence of 100 μM 3-keto-2-carboxyarabinitol 1,5-bisphosphate, an inhibitor of the plant enzyme (W. Altekar and R. Rajagopalan, unpublished work). Several metabolites are known to inhibit RuBP carboxylases from plant and microbial sources (13) and the effects of a few were tested on the halobacterial activity. A 30% loss of original activity due to 10 mM fructose disphosphate or sedoheptulose disphosphate was seen, while 10 mM 6-phosphogluconate was not inhibitory.

Thus it is evident from our results that the formation of 3PGA as a result of CO_2 fixation into RuBP, attributable to the activity of ribulose bisphosphate carboxylase indeed took place in the cell extract of H. mediterranei. This activity could not be detected in H. halobium, H. R-113 or H. vallismortis. The halobacterial activity for RuBP carboxylase is low (0.5-1 nMoles/mg/min) as compared to that found for CO_2 fixation in autotrophic eubacteria (e.g. 67 nMoles/mg/min for Hydrogenomonas facilis) (13-15). The low activity could be attributed to the aerobic chemoheterotrophic mode of growth of H. mediterranei and the enzyme may not be required for biosynthetic purposes. Though other carboxylation reactions yielding pyruvate or glycine as the products were demonstrated, Javor (5) could not detect RuBP carboxylase activity in H. halobium, nor could we. The metabolic abilities of H. mediterranei and H. halobium which produces bacteriorhodopsin are very different (7, 16), and while the former can utilize sugars, the latter cannot. Besides RuBP carboxylase, we have detected the activities of rest of the enzymes required for the operation of reductive pentose phosphate pathway to be present in heterotrophically grown H. mediterranei, along with activities of the modified Entner-Doudoroff pathway (manuscript communicated). Rodrigue-Valera's group (17) has shown that H. mediterranei accumulates considerable amount of poly-(β-hydroxybutyrate) while H. halobium does not. The situation is very much reminiscent of the reduced levels of RuBP carboxylase noted by several workers when facultative autotrophic bacteria with metabolic make-up similar to H. mediterranei, are grown organotrophically (14, 18, 19). As a matter of fact RuBP carboxylase from H. facilis and H. entrophus was purified from fructose grown cells (20). Ribulose bisphosphate carboxylase activity has not so far been demonstrated in halobacteria, or indeed in any archaebacteria and it provides the basis for comparing the enzyme from archaebacteria with those from eubacteria and eukaryotes and its evolution. Currently, we are examining the factors affecting its formation in halobacteria.

Acknowledgement

We are grateful to Dr. Anil S. Bhagwat for the gift of spinach RuBP carboxylase.

References

1. Oren, A. (1983) Limnon Oceanogr. 28: 33-41.
2. Danon, A. and S.R. Caplan (1977) FEBS Letts. 74: 255-258.
3. Kerscher, L. and D. Oesterhelt (1977) FEBS Letts. 83: 197-201.
4. Kushner, D.J. (1985) The Halobacteriaceae. In the Bacteria, Vol. III (Woese, C.R. and R.S. Wolfe, eds.) pp. 171-214.
5. Javor, B.J. (1988) Arch. Microbiol. 149: 433-440.
6. Dhar, N.M. and W. Altekar (1986) FEBS Letts. 199: 151-154.
7. Dhar, N.M. and W. Altekar (1986) FEMS Microbiol. Letts. 35: 177-181.
8. Bowien, B., F. Mayer, G.A. Codd and H.G. Schlegel (1976) Arch. Microbiol. 110: 157-166.
9. Lowry, O.H., N.J. Rosenbrough, A.L. Farr and R.J. Randall (1951) J. J. Biol. Chem. 193: 265-275.
10. Kushner, D.J. (1968) Adv. Appl. Microbiol. 10: 73-99.
11. Tyszkiewiez, E. (1962) Anal. Biochem. 3: 164-172.
12. Bandurski, R.S. and B. Axelrod (1951) J. Biol. Chem. 193: 405-410.
13. McFadden, B.A. (1973) Bacteriol. Rev. 37: 1289-1319.
14. McFadden, B.A. and C.L. Tu (1986) J. Bacteriol. 93: 886-893.
15. Anderson, L. and R.C. Fueller (1967) Plant Physiol. 42: 497-502.
16. Torsvik, R. and I. Dundas (1982) Methods in Enzymol. 88: 360-368.
17. Fernandez-Castillo, R., F. Rodriguez-Valera, J. Gonzales-Romos and F. Ruiz-Berraquero (1986) Appl. Environ. Microbiol. 51: 214-216.
18. Dijkhuizen, L., M. Knight and W. Harder (1978) Arch. Microbiol. 116: 77-83.
19. Schlegel, H.G. (1966) Adv. Comp. Physiol. Biochem. 2: 185-236.
20. Kuehn, G.D. and B.A. McFadden (1969) Biochemistry 8: 2394-2402.

Vol. 156, No. 1, 1988 BIOCHEMICAL AND BIOPHYSICAL RESEARCH COMMUNICATIONS
October 14, 1988 Pages 457-462

UNREGULATED SECRETION OF AN EXOGENOUS GLYCOTRIPEPTIDE BY RAT ISLETS AND HIT CELLS

Gerald Gold[1], Felix T. Wieland[2] and Gerold M. Grodsky[3]

[1]Eli Lilly and Company
Lilly Corporate Center, 88/4
Indianapolis, IN 46285

[2]Institut fur Biochemie I
In Neuenheimer Feld 328
G-6900 Heidelberg, West Germany

[3]Metabolic Research Unit
University of California
San Francisco, CA 94143

Received August 25, 1988

SUMMARY: Freshly isolated rat islets and cultured hamster insulinoma cells (HIT T15) were incubated with a membrane-permeable octanoyl tripeptide (N-octanoyl-ASN-TYR-THR-NH_2), which contains an acceptor sequence for ASN-linked glycosylation. Labeled octanoyltripeptide (^{125}[I]TYR) was glycosylated by both islets and HIT cells. The carbohydrate moiety of this glycotripeptide was removed by N-glycanase indicating that glycotripeptide was formed in the lumen of endoplasmic reticulum and, subsequently was secreted via the route for secretory protein. Secretion of glycotripeptide began more rapidly than that of insulin newly synthesized from ^{3}[H]leucine. At 30 min glycotripeptide secretion was already significant but, over a 3-h period, it never represented more than 21% of glycotripeptide produced. Glycotripeptide secretion was not affected by compounds shown to regulate insulin secretion (glucose, forskolin, EGTA and streptozotocin). Thus in beta cells, it appears that glycotripeptide secretion is unregulated and that its cellular secretory pathway is different from that for insulin. © 1988 Academic Press, Inc.

INTRODUCTION: In normal rat islets we and others have previously reported that little, if any, newly synthesized insulin was secreted for the first 45 minutes after a ^{3}[H]leucine pulse and, once secretion of newly synthesized insulin began, its release was highly regulated by known secretagogues of pancreatic beta cells (1,2,3). Although unregulated, constitutive release of secretory proteins has been demonstrated in a variety of transformed endocrine cells (4,5), we and others have found that the constitutive pathway represents <1% of insulin released by rat islets (3,6). However, whether or not this stringent secretory regulation in rat islets is unique for insulin or is the case for every protein secreted from islets was unknown.

A simple method to address this problem has recently been described (7). It is based on introduction of an exogenous membrane-permeable peptide,

0006-291X/88 $1.50
Copyright © 1988 by Academic Press, Inc.
All rights of reproduction in any form reserved.

which get trapped inside the endoplasmic reticulum after addition of a high mannose chain by the luminal, oligosaccharyl-N-transferase (8). This procedure has been used to trap exogenously added lipophilic peptides inside the endoplasmic reticulum of live cells from which the glycosylated product can only reach the cell surface via the secretory pathway (7). In two transformed cells, HepG2 and CHO, unregulated secretion of glycosylated product began after only 10 minutes and was sufficiently rapid that after 2 h, more glycosylated product was in the media than in the cells (7). We report here that octanoyltripeptide (N-octanoyl-ASN-TYR-THR-NH_2) is also N-glycosylated to glycotripeptide by normal islet cells, that onset of secretion of glycotripeptide occurs more rapidly than of newly synthesized insulin, that secretion rate is unaffected by secretagogues of insulin and that unlike HepG2 and CHO cells, in both rat islets and HIT cells, the majority (~80%) of glycotripeptide remains associated with the cells for at least 3 h.

EXPERIMENTAL PROCEDURE

Preparation of Rat Islets. Islets were prepared from 300-350 g, male Long-Evans rats that had free access to both food and water. After pentobarbital anesthesia, rat pancreases were inflated with Hanks buffer, removed, diced with a scissor and digested at 37°C with collagenase (Boehringer-Mannheim) using a three-step procedure (9,10). Digests were pipetted onto a discontinuous Percoll gradient, centrifuged 10 minutes at 1,000 g and a crude islet preparation was removed from the 38/60% Percoll interface. Islets were manually selected under a dissecting microscope and groups of 100-150 were put in 12 x 75 mm Falcon plastic tubes for labeling experiments.

Streptozotocin Treatment. Freshly isolated islets were exposed to streptozotocin (0.5 to 1.5 mg/ml) for 20 minutes at 37°C in Krebs-Ringer Bicarbonate (KRB), which contained 20 mM glucose and was gassed with 95% air:5% CO_2. Before experiments, streptozotocin-treated islets were washed twice with fresh KRB.

HIT Cells. HIT T15 cells (passage 77-78) were maintained at 37°C in RPMI 1640 + 10% fetal bovine serum + penicillin/streptomycin and were gassed with 95% air:5% CO_2 (11,12). Twenty-four hours before an experiment, 0.3-1.0 x 10^6 HIT cells were plated in the two centermost wells of a 12-well plate and returned to the incubator.

Iodination of Octanoyltripeptide. Five to 50 nmol of octanoyltripeptide in 50 µl acetonitrile was mixed with 100 µl of 0.5 M NaPi (pH 7.5). Between 0.5 to 10 mCi of ^{125}[I]NaI (carrier free, ICN) was added. To this solution, 100 µl of chloramine T (Sigma) (2 mg/ml) in 0.5 M NaPi (pH 7.5) was added. After two minutes at room temperature, the reaction was stopped by introduction of 400 µl of a solution of sodium bisulfite (2.4 mg/ml) in 0.05M NaPi (pH 7.5) followed by 600 µl water. This solution was loaded onto a Sep-Pak C18 cartridge (Waters) and washed sequentially with 20 ml of 0.1% TFA and 20 ml of 5% acetonitrile in 0.1% TFA. Iodinated octanoyltripeptide was eluted with 60% acetonitrile in 0.1% TFA, concentrated in a speed-vac centrifuge and dissolved and stored in DMSO. Iodination yields were between 25 and 50% and specific radioactivities were between 0.1 and 4.0 x 10^8 cpm/nMol (7).

Labeling of Cells with ^{125}[I]Octanoyltripeptide. After medium was removed, cells were preincubated at 37°C in KRB: islets (Dubnoff metabolic shaker bath, 50-60 cycles/minute, 95% O_2:5% CO_2); and HIT cells (incubator, 95% air:5% CO_2). After 45 min of preincubation, medium was removed and replaced with fresh KRB containing ^{125}[I]octanoyltripeptide (1% final concentration of DMSO) and other specified additions. At indicated times, incubation medium and cells were separated. An aliquot of incubation medium was taken for insulin radioimmunoassay and both the cells and the remainder of each incubation medium were rapidly frozen on dry ice.

Extraction and Purification of Glycotripeptides. Cells were thawed and extracted in 440 µl of ice-cold buffer A (10 mM Tris HCl [pH 7.4], 0.15 M NaCl, 1 mM $CaCl_2$, 1 mM $MnCl_2$, 0.5% Triton X-100). Medium was thawed and brought to 0.5% Triton X-100, 1 mM $MnCl_2$ and 1mM $CaCl_2$ by additions from concentrated stock solutions. Extracts were centrifuged for 1 minute in a microfuge and supernatants loaded on Con A-Sepharose (Pharmacia) columns (approximately 250 µl bed volume). Columns were washed with buffer A (5 x 1 ml) then eluted with 0.5 M α-methylmannoside in buffer A (3 x 0.5 ml). Quantitation of eluted ^{125}[I]glycotripeptide was done in a gamma counter (Tracor).

Immunoassay of insulin. Insulin was extracted from islets with ice-cold ethanol:water:HCl, 83.3:14.9:1.8 (v/v/v). Extracted cellular insulin and insulin in the incubation medium were quantitated by radioimmunoassay using tubes coated with guinea pig anti-insulin serum (Linco) and rat insulin as standard (13). Interference by residual ^{125}[I]octanoyltripeptide was eliminated by two additional washing of immunoassay tubes with water (2 x 1 ml).

Statistical Analysis. Numbers represent mean ± SEM for (n) experiments done on separate days. Data were analyzed with student's paired t-test and 1-way ANOVA.

RESULTS AND DISCUSSION

Rat islets were incubated for 3 h with ^{125}[I]-labeled substrate peptides and glycosylated products isolated on Con A-Sepharose columns. Membrane pearmeability of substrate peptides was absolutely necessary for glycosylation; only 57 cpm was recovered on a Con A-Sepharose column with a charged and membrane-impermeable ^{125}[I]hexapeptide while 11,488 cpm was recovered with an equal amount of ^{125}[I]octanoyltripeptide (both had the same glycosylation acceptor sequence).

Synthesis of ^{125}[I]glycotripeptide was saturable, i.e. inhibited 90 to 100% by addition of unlabeled octanoyltripeptide 20 to 40 µg/0.4 ml (data not shown). To determine if carbohydrate moieties were N-linked, glycosylated products were incubated with or without N-glycanase (an enzyme which hydrolyzes only N-linked carbohydrate bonds) and then run on a silica-gel, thin-layer chromatographic system. Figure 1 is a radioautogram from such an experiment. For both untreated (lane 1) and mock incubated (without N-glycanase) (lane 2) controls, there were several slowly migrating bands indicating synthesis and subsequent processing of glycotripeptide had occurred in rat islets. After incubation with N-glycanase (lane 3), slowly migrating bands were converted to broad bands that migrated as

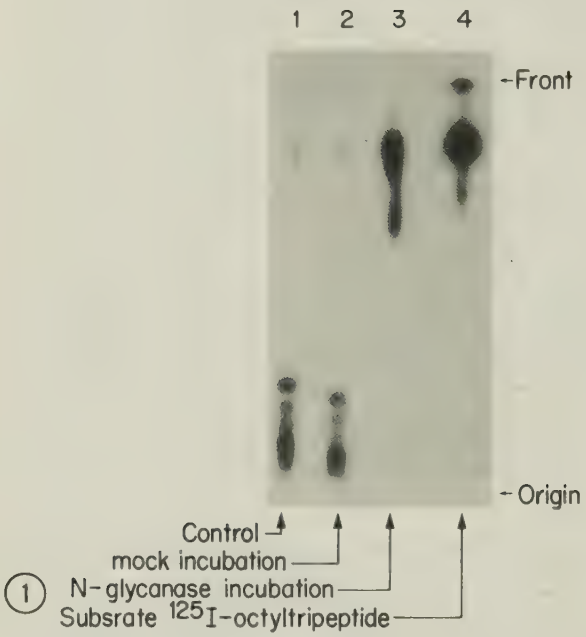

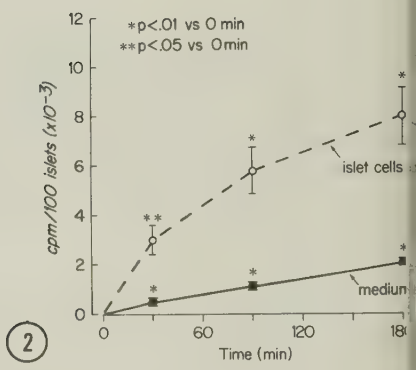

Fig. 1. Characterization of ^{125}[I]glycotripeptide synthesized by rat islets. Glycotripeptide was purified from extracts of rat islets by Con A-Sepharose and aliquots were incubated with or without N-glycanase, an enzyme which hydrolyzes only N-glycosidic linkages. Samples were applied to silica-gel thin-layer plates, chromatographed with butanol:acetic acid:water [5:2:2 (v/v/v)] as the mobile phase and then exposed to X-ray film. Lanes on autoradiograph are: 1. Control, untreated glycotripeptide; 2. Control, mock-digested (without N-glycanase) glycotripeptide; 3. N-glycanase-digested glycotripeptide; and 4. the original substrate octanoyltripeptide.

Fig. 2. Cumulative appearance of ^{125}[I]glycotripeptide in rat islet cells and their medium.

*P <.01 vs. 0 min.
**P <.05 vs. 0 min.

In four experiments, freshly isolated rat islets were continuously incubated in 0.4 ml KRB (20 mM glucose) containing 22.5 ± 1.3 x 10^6 cpm ^{125}[I]octanoyltripeptide. At indicated times, media and cells were separated and glycotripeptide in each fraction was purified (Con A-Sepharose) and quantitated.

rapidly as the substrate ^{125}[I]octanoyltripeptide (lane 4) and only 8% (754 of 9749 cpm) was recovered on a subsequent Con A-Sepharose column; after mock digestion, 95% (9252 of 9749 cpm) was recovered. Thus, octanoyltripeptide must penetrate islet membranes to be glycosylated and the site of glycosylation is the lumen of endoplasmic reticulum (the only organelle known in which N-glycosylation occurs).

With islets continuously incubated with ^{125}[I]octanoyltripeptide, synthesis of glycotripeptide occurred for 3 h (Figure 2) and rate was not affected by glucose concentration (data not shown). Like results reported for HepG2 and CHO cells (7), glycotripeptide was both stored and secreted by

rat islets. However in islets, unlike these other two cell lines, after 3 h secreted glycotripeptide never represented more than 21% of the total glycotripeptide produced. Partitioning of glycotripeptide predominantly in the cellular fraction of islets does not represent an underestimation of extracellular glycotripeptide due to extracellular degradation because when purified ^{125}[I]glycotripeptide was incubated with islets under the same conditions, it was completely recovered (16,092 cpm at 0 min vs. 17,202 cpm at 180 min).

Partioning of glycotripeptide predominantly in the cellular fraction also occurred with transformed hamster beta cells (HIT T15); in three experiments, only 8% of glycotripeptide was secreted after 3 h (secreted, 1080 ± 260 cpm vs. cell, 14,500 ± 3,500 cpm per million cells).

Although islets secreted less than 1/4 of the newly synthesized glycotripeptide in 3 hr, onset of secretion was surprisingly rapid. Glycotripeptide in media was significantly elevated at 30 min, the first measured time point, and for 3 h, it was secreted at a nearly constant rate (Figure 2). Under near identical conditions, we and others previously reported that newly synthesized insulin required more than 30 min to transit from endoplasmic reticulum to secretory granules or plasma membrane (1,3,14,15). Thus, it is likely that glycotripeptide and insulin diverge at some point along the cellular secretory route, suggesting that there is more than one secretory pathway in normal islets.

As a test of whether or not glycotripeptide and insulin were localized in the same secretory granules, islets were first loaded with ^{125}[I]glycotripeptide and then tested for secretory regulation by glucose, forskolin and EGTA (Table 1). Rates of insulin secretion were significantly faster with 20 mM glucose + 10 nM forskolin than with any other condition tested and observed secretory rates spanned a more than 8-fold range from 1.96 to 17.5%/h. In contrast, rates of glycotripeptide secretion were not significantly affected by any of these compounds indicating that, as reported for HepG2 and CHO cells (7), there also is an unregulated secretory pathway in islets.

In summary, this is the strong evidence that: 1. exogenous octanoyltripeptide can be glycosylated and secreted by normal islet cells; 2. there is an unregulated secretory pathway in islets; and 3. both islets and HIT cells differ from HepG2 and CHO cells in that they store, rather than secrete, most of the newly synthesized glycotripeptide.

Table 1
Effects of Glucose, Forskolin and EDTA on Secretion Rates of Insulin and ^{125}[I]Glycotripeptide

Regulators of Insulin Secretion	Secretion Rate of Insulin (% IRI/h)	Secretion Rate of ^{125}[I]Glycotriptide (cpm/h)
20 mM glucose + 10 uM forskolin	17.5 ± 3.1	730 ± 35
20 mM glucose	7.98 ± 1.6*	723 ± 136
20 mM glucose + 3 mM EGTA	3.93 ± 1.4*	613 ± 66
2 mM glucose + 10 uM forskolin	4.82 ± 1.5*	777 ± 109
2 mM glucose	1.96 ± 0.66*	785 ± 57

* p <.01 vs. 20 mM glucose + 10 uM forskolin; all other comparisons are not significant;
Numbers represent mean + SEM for three experiments. One hundred percent immunoreactive insulin was 53.6 ± 14 ng/islet.
Prior to measurement of secretion rates of insulin and ^{125}[I]glycotripeptide, islets were:

1. Incubated 45 min in 0.4 ml Krebs-Ringer bicarbonate buffer containing 20 mM glucose;
2. Incubated 2 hr in 0.4 ml Krebs-Ringer bicarbonate buffer containing 20 mM glucose and 21.0 ± 10 x 10^6 cpm ^{125}[I]-octyltripeptide; and
3. Washed once and returned to incubation for 1 hr with 0.4 ml Krebs-Ringer bicarbonate containing specified regulators.

ACKNOWLEDGMENT We thank Dr. James E. Rothman for his suggestions and critical review of the manuscript.

REFERENCES

1. Jain, K., and Logothetopoulos, J. (1977) Diabetes 26, 650-566.
2. Gold, G., Gishizky, M. L., and Grodsky, G. M. (1982) Science 218, 56-58.
3. Gold, G. Landahl, M. D., Gishizky, M. L., and Grodsky, G. M. (1982) J. Clin. Invest. 69, 554-563.
4. Moore, H-P., Gumbiner, B., and Kelly, R. B. (1983) Nature 302, 434-436.
5. Kelly, R. B. (1985) Science 230, 25-32.
6. Rhodes, C. J., and Halban, P. A. (1987) J. Cell Biol. 105, 145-153.
7. Wieland, F. T., Gleason, M. L., Serafini, T. A., and Rothman, J. E. (1987) Cell 50, 289-300.
8. Welphy, J. K., Shenbagamurthi, P., Lennarz, W. J., and Naider, F. (1983) J. Biol. Chem. 258, 11856-11863.
9. Lacy, P. E., and Kostianovsky, M. (1967) Diabetes 16, 35-39.
10. Gold, G., Pou, J., Gishizky, M. L., Landahl, H. D., and Grodsky, G. M. (1986) Diabetes 35, 6-12.
11. Hill, R. S., and Boyd, A. E. III (1981) Diabetes 34, 115-120.
12. Gold, G., Qian, R. L., and Grodsky, G. M. (1988) Diabetes 37, 160-165.
13. Lundquist, I., Fanska, R., and Grodsky, G. M. (1976) Endocrinology 99,1304-1
14. Orci, L, Lambert, A. E., Kanazawa, Y., Amherdt, M., Rouiller, C., and Renold, A E. (1971) J. Cell Biol. 50, 565-582.
15. Nagamatsu, S., and Grodsky, G. M. (1987) Biochem. Biophys. Res. Commun. 148, 1418-1424.

Vol. 156, No. 1, 1988 BIOCHEMICAL AND BIOPHYSICAL RESEARCH COMMUNICATIONS
October 14, 1988 Pages 463-469

IL1/ETAF ACTIVITY AND UNDETECTABLE IL1 β mRNA AND MINIMAL IL1 α mRNA LEVELS IN NORMAL ADULT HEAT-SEPARATED EPIDERMIS

Stephen Demczuk

Division of Immunology and Allergy, Department of Medicine,
University of Geneva, Hospital Cantonal, CH-1211 Geneva Switzerland

Received August 29, 1988

SUMMARY: Interleukin 1 (IL 1), a cytokine expressed from a number of cell types, plays a vital part in immune and inflammatory processes. Epidermal IL1-like activity, also known as epidermal cell thymocyte-activating factor (ETAF), is associated with whole skin, epidermis, Langerhans cells and cultured keratinocytes and keratinocyte cell lines. We show that preparations of heat-separated epidermis possess abundant IL1/ETAF activity as indicated by PGE/collagenase induction in cultured synovial cells and proliferation of mouse thymocytes. However, using cDNA probes to interleukin-1 α and β we show that freshly isolated heat-separated epidermis from healthy adult donors contains only a slight detectable level of IL1 α mRNA by dot blot analysis and no IL1 β and IL1 α mRNA by Northern blot analysis. The implications of these observations will be discussed. © 1988 Academic Press, Inc.

In addition to lymphoid tissues and resident lymphoid cells, immune systems consist also of cells and tissues of nonlymphoid origin. Only recently, has it become evident that the epidermis plays a vital role in many complex immune reactions. The predominant cells of the epidermis include the keratinocyte, melanocyte and Langerhans cells. Ontogenetically and functionally, bone-marrow-derived Langerhans cells appear as descendants from the monocyte-macrophage-histiocyte linage (1,2). The keratinocyte, which comprises the vast majority of the epidermal cell population, has recently received considerable attention as a participant in the immune response (1,3,4).

IL1 is an important regulator hormone of immune and inflammatory responses (5,6). The predominant source of IL1 is the peripheral monocyte-macrophage. Several names have been given to IL1 or IL1-like activity that reflect the cell-type from which it originates or the physiological response attributed to it. The sources of IL1-like/ETAF activity in the epidermis have been linked to the keratinocyte and the Langerhans cells (7,8,9,10). Although these studies focused on IL1/ETAF release from the epidermis, enriched populations of cultured keratinocytes and Langerhans cells, and keratinocyte cell lines under various culture conditions and stimuli, no study has addressed whether IL1/ETAF is expressed from freshly isolated heat-separated adult epidermis.

Abbreviations: poly(A)$^+$ RNA, polyadenylated RNA; cDNA, complementary DNA; IL1, interleukin-1; ETAF, epidermal thymocyte activating factor; PMA, phorbol myristic acetate; MCF, mononuclear cell factor; LAF, lymphocyte-activating factor; DMEM, Dulbecco's modified Eagle's medium; PHA, phytohemagglutinin; IFN, interferon.

Current Address: Department of Microbiology and Immunology, Bowman Gray School of Medicine, Winston-Salem, NC 27103.

0006-291X/88 $1.50
Copyright © 1988 by Academic Press, Inc.
All rights of reproduction in any form reserved.

In this report, we demonstrate that even though abundant IL1/ETAF activity was present in freshly isolated heat-separated epidermis, only a low level of IL1 α mRNA and no IL1 β mRNA were detected by hybridization analysis of total or poly(A)$^+$ epidermal RNA.

MATERIALS AND METHODS

Human Peripheral Mononuclear Cells (PBMC): Human donor blood (Blood Transfusion Unit, University Hospital, Geneva) was prepared from buffy coats, centrifuged through Ficoll-Hypaque gradients and stimulated or not for 12 to 16 h with 3 ug/ml phytohemagglutinin (PHA) and 12 ug/ml concanavalin A (ConA) as previously described (11). Blood mononuclear cells were also obtained from a female acute monocytic leukemia patient (M5 of the French, American, British classification). Following centrifugation through Ficoll-Hypaque gradients patient mononuclear cells were stimulated for 16 h with 50 ng/ml phorbol myristic acetate (PMA).

Human Monocytic Lymphoma Cell Line U937: U937 cells were first differentiated for 3 days in RPMI-1640, 10% FCS, 2 mM glutamine, 100 U/ml penicillin and 100 ug/ml streptomycin and 250 U/ml human recombinant γ-interferon (rγ-IFN) (Biogen S.A., Geneva). The cells were then washed 2 times in sterile PBS, resuspended in media containing 0.1 ug/ml Con A and 0.05 ug/ml PMA at a cell density of 2 x 10^6 cells/ml and cultured for an additional 24 h. These cells were later determined to be contaminated with mycoplasmas (see ethidium bromide stained gel (Fig 1d), 16S and 23S bands and reference 10).

Heat-Separated Epidermis: Normal epidermis from the upper arms and back of patients with plastic surgery was isolated as described (12). Briefly, skin was received on ice minutes after surgery, placed in 0.9% NaCl (containing 2 mM ZnCl in two cases) at 60°C for 60 sec. The epidermal layer was scraped off using a scalpel and quenched in liquid N_2 for RNA extraction and intracellular IL1 activity.

Human Squamous Carcinoma Cell Line A431: Squamous epidermal carcinoma A431 cells were cultured in Dulbecco's modified Eagles medium (DMEM; Gibco), 10% FCS, 2 mM glutamine and penicillin/streptomycin. Cells were washed two times in cold phosphate buffered saline and quenched in liquid N_2 for RNA extraction (10).

IL1/ETAF Bioassays: Freshly isolated synovia from rheumatoid arthritis patients were the source of target cells in the IL1/ETAF-MCF (PGE_2 and collagenase induction) bioassay (13). Lymphocyte activating factor activity (IL1/ETAF-LAF) was performed on cultured (66 h) thymocytes from 6 to 8 week old C3H/HeJ mice as described (14).

RNA Extraction: Frozen (-80°C) pellets of PBMC, heat-separated epidermis and A431 cells were extracted in 4 M guanidine thiocyanate/0.2 M β-mercaptoethanol (15). Total RNA and poly(A)$^+$RNA were isolated as previously described (16).

Cell-associated IL1 and IL1/ETAF Activities: Cell-associated material was prepared by washing isolated cells and epidermal tissue 3 times with phosphate buffered saline followed by freezing (liquid N_2) and thawing two times in 3 ml DMEM-10% FCS. The resuspended cells were homogenized in a Polytron homogenizer three times on ice, cleared by centrifugation at 4°C, filter-sterilized and assayed for IL1/ETAF activities.

Northern Blot Analysis: Human IL1 α and β cDNA clones were isolated from cDNA gene banks prepared from PMA-induced monocytic cell line U937 as previously described (10,17,18). The β_2-microglobulin cDNA clone (19) was a gift from S. Suggs. RNA gel electrophoresis and Northern blot analysis were performed with 3.0 μg of poly(A)$^+$RNA and 10 μg or 20 μg of total RNA as described (11). After 18-20 h of hybridization at 65°C membranes were washed reaching a stringency of 0.1 x sodium chloride sodium citrate (SSC), 0.1% SDS at 68°C.

RESULTS

IL1 and IL1/ETAF activities in PBMC and heat-separated epidermis: Freshly isolated (non adhered) PBMC possessed little if any detectable cell-associated IL1 activity (Table I). However, after stimulation with PHA/ConA, significant extracellular IL1/MCF and IL1/LAF activities were observed. On the contrary, cell-associated IL1-MCF/ETAF and IL1-LAF/ETAF activities were present in freshly isolated heat-separated human epidermis.

IL1 α and β mRNA steady-state levels in PBMC and heat-separated epidermis: The significant level of cell-associated IL1/ETAF activity in nonstimulated heat-separated epidermis suggested that IL1 α and β mRNA would be abundant provided that either contributed to this activity. Northern blot analyses using cDNA probes to IL1 α and β mRNA were performed to verify this hypothesis. However, as seen in Fig 1a (lanes 7,8) no detectable hybridization was observed by the IL1 β probe to total or poly(A)$^+$RNA from heat-separated epidermis. This is in contrast to the significant hybridization to RNA

Table 1

IL1/MCF and IL1/LAF Activities in Mononuclear Cells and Heat-Separated Epidermis

	Mononuclear Cells		H-S Epidermis
	NS[a]	S[b]	NS
PGE_2 (ng/ml)	3.0	278 ± 17	105 ± 5
Collagenase (U/ml)	< 0.1	1.9 ± 0.2	1.20 ± 0.1
LAF (cpm x 10^{-4})	1.0	3.4 ± 0.2	1.9 ± 0.3

[a]Nonstimulated freshly isolated mononuclear cells were centrifuged through Ficoll' Hypaque and assayed for intracellular IL 1 activity.

[b]Stimulation with PHA/ConA; Data are Mean ± SEM.

from stimulated PBMC (lane 2), an enriched population of stimulated monocytes (lane 4) from a monocytic leukemia patient and stimulated U937 cells (lane 6). Even after extensive film exposure to membrane (Fig. 1b), there was no indication of IL1 β probe hybridization to heat-separated epidermal RNA, suggesting that adult epidermis is void of any detectable level of IL1 β messenger. Figure 1c shows that in each lane intact RNA was transferred to the membrane prior to hybridization with the β_2-microglobulin cDNA probe. As seen in lane 7, β_2-microglobulin mRNA levels in total applied RNA from heat-separated epidermis is lower than that found in enriched mRNA of total poly(A)$^+$RNA (lane 8). Furthermore, nearly equivalent levels of intact total RNA were added to each lane as indicated by the ethidium bromide stained gel in Fig. 1d, an example of the RNA transferred to each membrane.

The cell-associated IL1/ETAF activity from heat-separated epidermis may have resulted from IL1 α encoded by its cognate mRNA. However, as seen in Fig. 2 (lanes 1,2), no detectable mRNA was evident following hybridization to a nick-translated cDNA

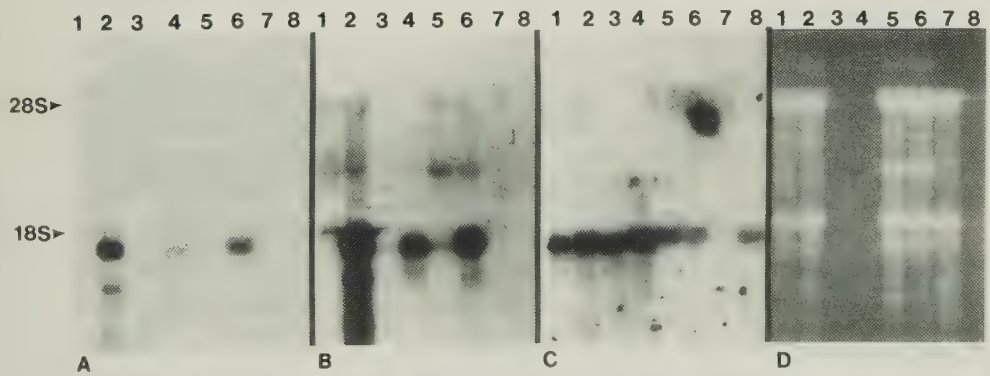

Fig. 1. Northern blot analysis of IL1 β mRNA. Total RNA (20 μg) from PBMC (lanes 1 and 2), polyA$^+$ RNA (3.0 μg) from mononuclear cells of a monocytic leukemia patient (lanes 3,4) and 20 μg total U937 RNA (lanes 5 and 6), and 20 μg total RNA and 3.0 μg polyA$^+$ RNA (lanes 7 and 8) from heat-separated adult epidermis were electrophoresed, transferred to membrane and hybridized to nick translated cDNA probes to IL1 β (a,b) and β_2-microglobulin (c). RNA in lanes 2 and 4 were from cells stimulated with PHA/ConA and PMA, and RNA from lanes 5 and 6 were extracted from cells exposed to γIFN; and γIFN followed by ConA and PMA. The photo in (b) is an overexposure of the same membrane in (a). (d) shows an example of an ethidium bromide stained gel prior to RNA transfer.

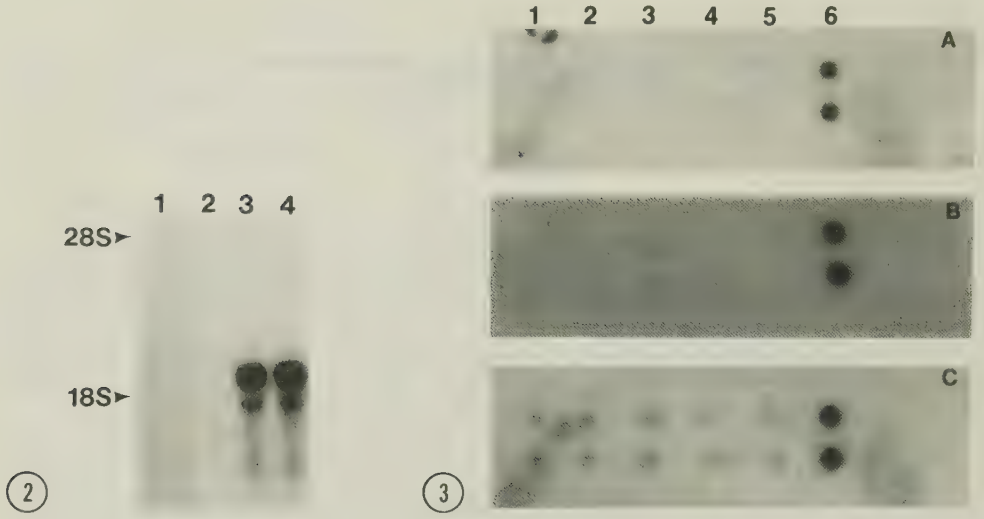

Fig. 2. Northern blot analysis of IL1 α mRNA. Total RNA (10 μg) from heat-separated adult epidermis preparations 5 and 6 (lanes 1 and 2), and control and PMA-stimulated A431 cells (lanes 3 and 4) were hybridized to a nick translated probe to IL1 α.

Fig. 3. Dot blot hybridization of RNA from heat-separated epidermis employing a nick-translated cDNA probe to IL1 β (a) and to IL 1 α (b). Total RNA was spotted in duplicate from epidermal preparation 4 (1) 1.0 μg (2) 2.0 μg (3) 4.0 μg and from preparation 1 (4) 2.5 μg and (5) 5.0 μg and (6) 1.0 μg poly(A)$^+$ RNA from PHA/ConA stimulated PBMC. Panel (c) is the same dot blot as (b) but the membrane was washed at a lower stringency to show that RNA was added as indicated.

IL1 α probe, even after 25 days of membrane-film exposure (long exposure not shown). Parallel lanes contain IL1 α mRNA from the constitutive IL1 producing squamous carcinoma cell line A431 (lanes 3,4). Again, an ethidium bromide staining showed that the RNA was intact prior to blotting and that transfer was complete (data not shown).

Even though RNA dot blots give less information concerning RNA quality and mRNA size distribution and produce a higher signal to noise ratio than that of Northern gel blot analysis, the level of sensitivity is greater. As seen in Fig. 3a, a probe to IL1 β mRNA did not hybridize to RNA from freshly isolated heat-separated epidermis. In Fig. 3b, there occurred a faint amount of hybridization to RNA using a probe to IL1 α mRNA. Figure 3c is the same membrane as 3b, but washed at a lower stringency to show that RNA was added to each point. In all, five tissue preparations were tested in Northern blot and dot blot analysis and only in dot blot analysis was IL1 α mRNA slightly detected.

DISCUSSION

This communication is the first to compare the level of IL1 mRNA to IL1/ETAF activity in freshly isolated adult heat-separated epidermis. In this study skin was not taken from areas that were likely exposed to UV light from the sun. *In vivo* exposed murine epidermis and cultured human and murine keratinocytes exposed to UV light contain elevated levels of IL1/ETAF activity and IL1 mRNA (4,20,21) and UV-irradiated mice and rabbits have increased serum IL1 levels (22,23). Although the epidermis is composed mainly of three major cell types, the keratinocyte is the predominant cell comprising

over 90% of the epidermal population. Keratinocytes that undergo differentiation while surfacing from the lower to the upper epidermal layer in forming the stratum corneum also exhibit considerable changes in gene expression (24). Several reports have demonstrated that cultured keratinocytes (4,25,26), keratinocyte cell lines (4,10,26) and keratinocytes isolated from newborn mice (4) express detectable and at times abundant messenger to IL1 α or β or both, whereas terminally differentiated keratinocytes had no detectable steady-state IL1 messenger RNA (4).

However, in this report we show that adult human heat-separated epidermis in which considerable IL1/ETAF activity is present possesses a slight detectable level of IL1 α mRNA. Even after five epidermal samples were analyzed no IL1 β mRNA was detected. Although, Ansel *et al.* (4) have detected abundant IL1 α levels in normal epidermal keratinocytes of newborn mice, this may be due to the undifferentiated state of the keratinocytes in this tissue. In addition, their results may have resulted from the method of prolonged isolation and trypsin digestion of keratinocytes (27). Others who have shown IL1 α and β expression from cultured keratinocytes have utilized longterm cultures of infant foreskin keratinocytes (26). Under these conditions keratinocytes do not differentiate as *in vivo*, requiring a feeder layer of 3T3 cells, (24,28) and were cultured in the absence of hydrocortisone. The absence of hydrocortisone may increase IL1 mRNA steady-state levels. Glucocorticoids suppress IL1 mRNA expression through decreased IL1 transcription and mRNA stability (29,30,31).

We have utilized skin isolated from mid-winter to early spring months from the upper arm and back which would minimize epidermal exposure to UV radiation. RNA degradation was further minimized by employing heat-separation as a rapid method of isolating the epidermal layer of skin without the contamination from cells of the dermal layer. As evident by the intact RNA bands in the stained gel Fig. 1d, the intact hybridized band of β_2-microglobulin mRNA in Fig. 1c, lane 6, and the high molecular weight (~100 kD) rabbit reticulocyte translation products of heat-separated keratinocytes RNA (data not shown), the absence of IL1/ETAF mRNA in these cells was not due to RNA degradation.

The substantial amount of cell-associated IL1/ETAF activity in these preparations may indicate that 1) another IL1/ETAF factor exists, 2) IL1/ETAF is expressed from perhaps the dermis but accumulates in the epidermis and 3) although the level of IL1 β mRNA is below detection by the current methodologies employed, the efficient translation of IL1 α or β mRNA coupled with a low IL1 turnover could generate conditions which facilitate the detection of IL1 activities. This may possibly be the case since Hsu and Zhao (8) have detected by immunohistological staining a "paucity" of IL1 in Langerhans cells in epidermal skin samples but did not report any evidence of IL1 in the surrounding keratinocytes. Oxholm et al. (32) have detected by immunohistological staining IL1 α and β on human epidermal cell membranes. However, they could not block the staining by preincubating the antisera with excess purified recombinant or native IL1. They suggested that ETAF/IL1 and peripheral blood monocyte derived IL1 are the products of different genes.

Protein turnover is dramatically affected by the age and differentiation of keratinocytes and other cell types (33). For example, the reduction with age of ubiquitin in lens epithelium is in concert with enhanced levels of modified proteins (34). Ubiquitin is a required cofactor for initiation of cytoplasmic degradation of damaged and/or rapidly turned over proteins (35,36). Through cellular aging and development, there occurs an increased inactivation of exopeptidase and endopeptidase activity (34,37). Such conditions could explain the IL1/ETAF activity where the level of IL1 β mRNA is below detection and that IL1 α is minimal but their rate of translation and reduced IL1 turnover allow for IL1/ETAF assayable activity.

In conclusion, we show that heat-separated adult epidermis from normal donors does not possess detectable IL1 β mRNA and only a slight detectable level of IL1 α mRNA by dot blot and not by Northern blot analysis, but does contain readily detectable IL1/ETAF activity. These data suggest the possibility that another IL1/ETAF molecule(s) other than an IL1 α or β product elicits the IL1/ETAF activity in adult epidermal tissue. Recently, IL6, formerly called B-cell stimulatory factor 2, which is expressed in many cell types has been shown to possess LAF activity (38) and other biological activities associated with IL1. It will be critical to determine if the high IL1-ETAF and IL1-MCF activities are due to this multibiological faceted cytokine.

ACKNOWLEDGEMENTS

From the Geneva University Hospital Cantonal I am indepted to C. Hauser and L. Didierjean for assistance in acquiring human epidermis and especially to J.-M. Dayer and C. Baumberger for assistance, suggestions and critical reading of the manuscript. Also, I wish to thank A. Claiborne and B. Pollok, Bowman Gray School of Medicine, for critical reading of the manuscript.

REFERENCES

1. Choi, K.L., and Sauder, D.N., (1986) J. Leukocyte Biol. 39:343-358.
2. Stingl, G. and Wolff, K. (1987) The Langerhans cells and their relation to other dendritic cells and mononuclear phagocytes. Fitzpatrick, T.B., Eizen, A.Z., Wolff, K., Freedberg, I.M. and Austen, K.F., eds. Dermatology in General Medicine. pp. 410-426.McGraw Hill, New York,
3. Tron, V.A., Rosenthal, D. and Sauder, D.N. (1988) J. Invest. Dermatol. 90:378-381.
4. Ansel, J.C., Luger, T.A., Lowry, D., Perry,. P., Roop, D.R. and Mountz, J.D. (1988) J. Immunol. 140:2274-2278.
5. Dinarello, C.A. (1984) Rev. Inf. Dis. 6:51-95.
6. Dayer, J.-M. and Demczuk, S. (1984) Springer Semin. Immunopathol. 7:387-413.
7. Sauder, D.N., Carter, C.S, Katz, S.I. and Oppenheim, J.J. (1982). J. Invest. Dermatol. 79:34-39.
8. Hsu, S.-M. and Zhao, X. (1987) Lymphokine Res. 6:13-17.
9. Hauser, C., Dayer, J.-M., Jaunin, F., DeRochemonteix, B. and Saurat, J.-H. (1986) Cell. Immunol. 100:89-96.
10. Demczuk, S., Baumberger, Mach, B. and Dayer, J.-M. (1988) J. Biol. Chem. 263:In press.
11. Demczuk, S., Baumberger, C., Mach, B. and Dayer, J.-M. (1987) J. Mol. Cell Immunol. 3:255-265.
12. Kassis, V. and Sondergaard, J. (1982) Arch. Dermatol. Res. 273:301-306.
13. Dayer, J.-M., Breard, J., Chess, L. and Krane, S.M. (1979) J. Clin. Invest. 64:1386-1392.
14. Mizel, S.B., Dayer, J.-M., Krane, S.M. and Mergenhagen, S.E. (1981) Proc. Natl. Acad. Sci. USA 78:2471-2477.
15. Chirgwin, J.M., Przybyla, A.E., MacDonald, R.J. and Rutter, W.J. (1979). Biochem. 18:5294-5299.
16. Demczuk, S., Mach, B. and Dayer, J.-M. (1985) Br. J. Rheumatol. 24(Suppl. 1):77-81.
17. Wingfield, P., Payton, M., Tavernier, J., Barnes, M., Shaw, A.R., Rose, K., Simona, M.G., Demczuk, S., Williamson, K. and Dayer, J.-M. (1986) Eur. J. Biochem. 160:491-497.

18. Wingfield, P., Payton, M., Graber, P., Rose, K., Dayer, J.-M., Shaw, A.R. and Schmeissner, U. (1987) Eur. J. Biochem. 165:537-541.
19. Suggs, S.V., Wallace, R.B., Hirose, T., Kawashima, E. and Itakura, K. (1981) Proc. Natl. Acad. Sci. USA 78:6613-6617.
20. Kupper, T.S., Chua, A.O., Flood, P., McGuire, J. and Gubler, U. (1987) J. Clin. Invest. 80:430-436.
21. Ansel, J.C., Lugar, T.A. and Green, I. (1983) J. Invest. Dermatol. 81:519-523.
22. Gahring, L., Baltz, M., Pepys, M.B. and Daynes, R. (1984) Proc. Natl. Acad. Sci. USA 81:1198-1202.
23. Ansel, J.C., Lugar, T.A. and Green, I. (1987) J. Invest. Dermatol. 89:32-37.
24. Freedberg, I.M. (1987) Epidermal Differentiation and Keratinization. Fitzpatrick, T.B., Eizen, A.Z., Wolff, K., Freedberg, I.M. and Austen, K.F., eds. Dermatology in General, pp. 174-184. McGraw Hill, New York.
25. Kupper, T.S., Ballard, D.W., Chua, A.O., McGuire, J.S., Flood, P.M., Horowitz, M.C., Langdon, R., Lightfoot, L. and Gubler, U. (1986) J. Exp. Med. 164:2095-2100.
26. Koide, S. and Steinman, R.M. (1987) Proc. Natl. Acad. Sci. USA 84:3802-3806.
27. Sauder, D.N., Carter, C.S., Katz, S.I. and Oppenheim, J.J. (1982) J. Invest. Dermatol. 79:34-39.
28. Rheinwald, J.G. and Green, H. (1977) Cell 6:331-344.
29. Besedovsky, H., Rey, A.D., Sorkin, E. and Dinarello, C.A. (1986) Science 233:652-654.
30. Synder, D.S. and Unanue, E.R. (1982) J. Immunol. 129:1803-1805.
31. Lee, S.W., Tsou, A.-P., Chan, H., Thomas, J., Petrie, K., Eugut, E.M. and Allison, A.C. (1988) Proc. Natl. Acad. Sci. USA 85:1204-1208.
32. Oxholm, A., Oxholm, P., Staberg, B. and Bendtzen, K. (1988) Brit. J. Dermatol. 118:369-376.
33. Fuchs, E. and Green, H. (1980) Cell 19:1033-1042.
34. Jahngen, J.H., Haas, A.L., Ciechanover, A., Blondin, J., Eisenhauer, D. and Taylor, A. (1986) J. Biol. Chem. 261:13760-13767.
35. Chin, T., Kuehl, L. and Rechsteiner, M. (1982) Proc. Natl. Acad. Sci. USA 79:5857-5861.
36. Ciechanover, A. (1986) J. Cell Biochem. 34:81-100.
37. Taylor, A., Brown, M.J., Daims, M.A. and Cohen, J. (1983) Invest. Ophalmol. Visual Sci. 24:1172-1180.
38. Wong, G.C. and Clark, S.C. (1988) Immunol. Today 9:137-139.

Vol. 156, No. 1, 1988 BIOCHEMICAL AND BIOPHYSICAL RESEARCH COMMUNICATIONS
October 14, 1988 Pages 470-476

IN VITRO DEMONSTRATION BY THE RATE ASSAY OF THE PRESENCE OF SMALL PORE IN THE OUTER MEMBRANE OF *Pseudomonas aeruginosa*

EISAKU YOSHIHARA[1], NAOMASA GOTOH[2] and TAIJI NAKAE[1]

[1]Department of Cellular Information Sciences, School of Medicine, and Institute of Medical Sciences, Tokai University, Isehara 259-11, Japan
[2]Department of Microbiology, Kyoto Pharmaceutical University, Yamashina 607, Japan

Received August 29, 1988

SUMMARY Determination of the rates of saccharide diffusions by the proteoliposomes showed that the outer membrane of *Pseudomonas aeruginosa* only possesses small diffusion pores and that protein F might have not been involved in the pore formation. Proteoliposomes containing stachyose or Dextan T-10 showed the same relative diffusion rates as measured by the liposome swelling method. Slopes of the lines, diffusion rate vs saccharide M_r, in the liposomes made of the *P. aeruginosa* and *E. coli* B outer membranes appeared to be -7.4 and -3.5, respectively. Intercepts of the lines with x-axis in the liposomes containing the *P. aeruginosa* and *E. coli* B outer membrane appeared to be about M_r, 220 and 320, respectively. Relative diffusion rates of saccahrides through the liposome membranes reconstituted from the protein F-deficient outer membrane were superimposable with that of the protein F-sufficient outer membrane.
© 1988 Academic Press, Inc.

P. aeruginosa known as a problem pathogen for immunocompromised patients is highly resistant to a number of structurally unrelated antibiotics (1,2). One of the important factors contributing to this intrinsic drug resistance has been thought to be the poor antibiotic permeability across the outer membrane (2,3). A puzzling results reported earlier were that protein F of *P. aeruginosa* formed a large diffusion pore through which polysaccharides of M_r, 3,000 to 7,000 could penetrate (4,5). On the other hand, Caulcott et al. (6) and Yoneyama et al. (7,8) presented lines of evidence that the outer membrane of *P. aeruginosa* only allows free diffusion of saccharides less than about di- to trisaccharides by measuring the equilibrium of test solutes in the intact outer membrane.

Present study was conducted to verify the presence of small diffusion pores in the outer membrane and explain the intrinsic drug resistance of

0006-291X/88 $1.50
Copyright © 1988 by Academic Press, Inc.
All rights of reproduction in any form reserved.

P. aeruginosa. To do so, the diffusion rates of uncharged saccharides were determined by using the proteoliposomes reconstituted from the purified outer membrane of the protein F-sufficient or -deficient strains. The results fully supported the notion that the P. aeruginosa outer membrane contains small diffusion pores and did not support the notion that protein F is the porin and forms a large pore.

MATERIALS AND METHODS

Bacterial strains and growth conditions P. aeruginosa PAO1 is a wild type laboratory strain and KG1077 (9) is a protein F-deficient mutant derived from a substrain of PAO1. E. coli B was also used. Cells were grown in 1 l of L-broth containing 5 mmol of $MgCl_2$, pH7.4 at 37° C for 4 h with vigorous aeration (200 rpm) after dilution of a fully grown 100 ml of preculture. The outer membranes were purified from P. aeruginosa and E. coli B according to the procedures described by Mizuno and Kageyama (10) or Smit et al. (11) and Mizushima and Yamada (12), respectively.

Reconstitution of the proteoliposomes and the liposome swelling assay Proteoliposomes were reconstituted by the procedure described earlier (13) by using the mixture of 97 parts of phosphatidylcholine (PC) and 3 parts of dicetylphosphate (DCP) (14) or using crude phospholipids extracted from Salmonella typhimurium LT2M1 (13,15), and the outer membrane.

The diffusion rate was calculated from the swelling rate of the proteoliposome as described earlier (13,14). Proteoliposomes (0.26 μmol lipids/ 35 μl) were diluted into 665 μl of the isotonic test solute and a optical density at 450 nm was recorded at range 0.2 with a chart speed 120 mm/min for 60 sec.

Materials Reagents used were the best grades commercially available.

RESULTS AND DISCUSSION

Experiments with the proteoliposomes containing stachyose or Dextran T-10. In order to clarify the discrepancy of the reported pore sizes, the proteoliposomes were prepared entrapping either Dextran T-10 (average M_r, 10,000) or stachyose (M_r, 666), and the diffusion rates of pentoses, hexoses, disaccharides and trisaccharide were determined by the liposome swelling method. If the outer membrane possesses small pores only allowing the diffusion of trisaccharides or less, the diffusion rates of the above listed saccharides should be measurable with either proteoliposomes regardless of the intraliposomal solutes. On the other hand, if the pores are large enough to allow free diffusion of large oligosaccharides, entrapped stachyose should readily leak out of the liposomes resulting in little change

in optical density. While, the diffusion of the above listed solutes should be measurable using the proteoliposomes containing Dextran T-10. The results of such experiments showed that the relative diffusion rates of hexoses in the stachyose or the Dextran T-10 entrapped proteoliposomes appeared to be 40 to 60% or 70 to 75%, respectively, of the rate of ribose (Fig. 1). Relative diffusion rates of methylhexoses and N-acetylglucosamine in both liposomes appeared to be about 10 to 35% of the rate of ribose. Diffusion rates of di- and trisaccharides were undetectably low under the conditions. Slopes of the lines appeared to be -7.4 and -7.3 for the stachyose and Dextran T-10 containing proteoliposomes, respectively and intercepts with x-axis of both lines appeared to be about M_r, 210 to 220, respectively. These results clearly indicated that the pore(s) in the outer membrane of P. aeruginosa is smaller than that of E. coli as was shown in intact cells (6,7,8). Both bacterial crude phospholipids and PC/DCP showed essentially the same results (data not shown). Rate of optical density change of the stachyose or Dextran T-10 entrapped proteoliposomes for glucose appeared to be 56 and 36 arbitrary units, respectively. Methods of outer membrane preparation (refs. 10 or 11) did not affect on the result.

Comparison of the size of the outer membrane pore of P. aeruginosa with that of E. coli B In order to compare the size of the P. aeruginosa pore with that of E. coli B, diffusion rates of saccharides were determined using the liposomes reconstituted from the outer membrane of E. coli B. A slope of the line of diffusion rates vs log M_r appeared to be -3.52 and an intercept of the line with x-axis was close to saccharide M_r, about 320 (Fig. 2). These data essentially confirmed the earlier results reported from this and other laboratories (15,16). Since a slope of the line for the permeability of P. arugninosa was shown to be -7.4 (Fig. 1), comparison of the slope with that of E. coli B clearly indicated that the size of the P. aeruginosa outer membrane pore is smaller than that of the outer membrane pore of E. coli B. The intercepts for P. aeruginosa and E.

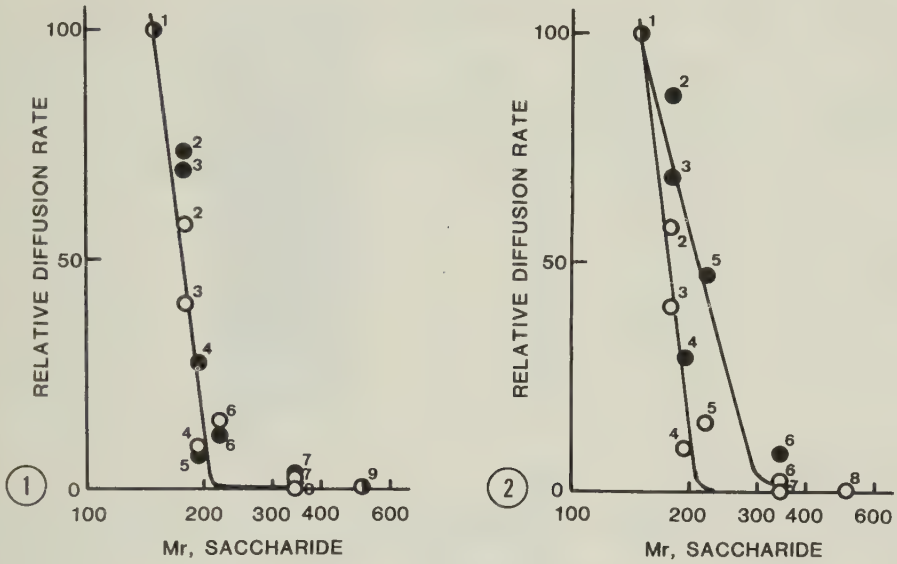

Fig. 1. Diffusion rates of saccharides through the liposome membranes containing stachyose or Dextran T-10. Proteoliposomes were reconstituted from 1 μmol of phospholipid from S. typhimurium LT2M1 and 50 μg of proteins of the P. aeruginosa PAO1 outer membrane in the presence of 40 mosM stachyose or 6% of Dextran T-10 in 1 mM Mops, pH 7.2. The liposome swelling assay was performed as described in Materials and Methods. Diffusion rates were normalized to that of ribose of the respective proteoliposomes. Saccharides used were; (1), ribose; (2), glucose; (3), galactose; (4), α-methylmannoside; (5) α-methylgalactoside; (6), N-acetylglucosamine; (7), lactose; (8), sucrose; and (9), raffinose. Symbols; ○, liposomes containing stachyose; ●, liposomes containing Dextran T-10.

Fig. 2. Diffusion rates of saccharides through the liposome membranes reconstituted from the outer membranes of P. aeruginosa PAO1 or E. coli B. Proteoliposomes were reconstituted from 1 μmol of phospholipid from S. typhimurium and 5 and 50 μg of outer membrane proteins of E. coli B and P. aeruginosa PAO1, respectively, in the presence of 40 mosM stachyose in 1 mM Mops, pH 7.2. Diffusion rates were determined by the liposome swelling assay as described in Materials and Methods. Data for P. aeruginosa PAO1 are taken from Fig. 1. Saccharides used were; (1), ribose; (2), glucose; (3), galactose; (4), α-methylmannoside; (5), N-acetylglucosamine; (6), lactose; (7), sucrose; and (8), raffinose. Symbols; ○, P. aeruginosa PAO1; ●, E. coli B.

coli obtained from Fig. 1 and 2 appeared to be about M_r, 210 and 320, respectively. These results suggested again that the outer membarane pore(s) of P. aeruginosa is substancially smaller than that of E. coli B, supporting the previously reported conclusion (6,7,8). The same result to Fig. 1 was obtained with the octylglucoside soluble materials obtained from the outer membrane of P. aeruginosa as reconstituted into the liposomes after removing the surfactant (data not shown).

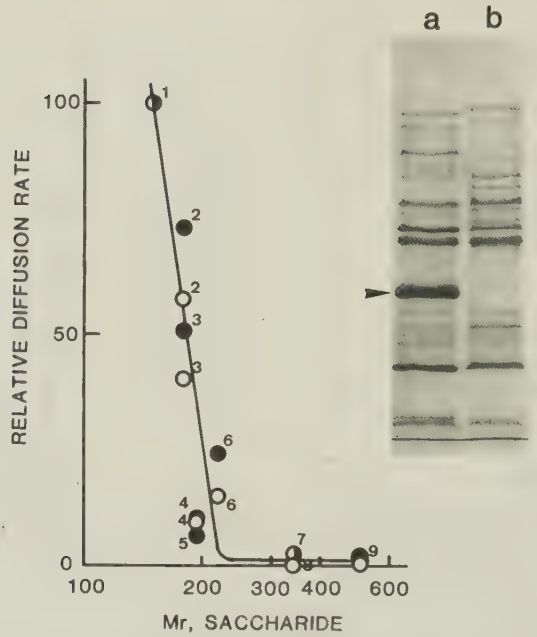

Fig. 3. Diffusion rates of saccharides through the liposomes containing the protein F-deficient and -sufficient outer membranes of P. aeruginosa. Proteoliposomes were reconstituted from 50 μg of proteins of the outer membranes purified from P. aeruginosa PAO1 or KG1077 and 1 μ mol of phospholipid purified from S. typhimurium in the presence of 40 mosM stachyose in 1 mM Mops, pH 7.2. Diffusion rates were determined as described in Materials and Methods and that was normalized to the diffusion rate of ribose. Saccharides used were; (1), ribose; (2), glucose; (3), galactose; (4), α-methylmannoside; (5), α-methylgalactoside; (6), N-acetylglucosamine; (7) lactose; (8), sucrose; and (9), raffinose. Data in PAO1 are taken from Fig. 1. Symbols; ○, PAO1; ●, KG1077.

Inset, Acrylamide gel electrophoregram of the outer membrane proteins. The purified outer membrane was solubilized in the sample buffer, heated at 95° C for 5 min and applied 40 μ g of proteins per lane. The buffer system employed was the Laemmli's formula (23). a, PAO1 (wild type); b, KG1077 (a protein F-deficient mutant). A arrow head indicated the position for protein F. Five other mutants showd the same protein profiles to that of KG1077.

Permeability of the liposome membranes reconstituted from the protein F-free outer membrane A question to be asked now is whether the previously reported pore-forming protein, F forms the diffusion pore of small size. We had isolated 6 protein F-deficient mutants of P. aeruginosa (9). Polyacrylamide gel electrophoregrams of the outer membrane proteins showed no visible band of protein F (Fig. 3, inset). Permeability assay using the proteoliposomes reconstituted from such outer membrane indicated that the membranes allowed the diffusion of pentoses, and hexoses well but did not allow the diffusion of saccahrides larger than di- or trisaccharide

(Fig. 3). The outer membranes from five other protein F-deficient mutants showed the same results (data not shown). The slope of the plots and the intercept with x-axis are indistinguishable from that of the experiment using the protein F-sufficient outer membrane (Fig. 1). These data did not favor the previously published results (4,14,17).

The reason why the previous data suggested the presence of large pore is not clear. However, the following interpretations of the previous data may be possible. (i) Sucrose had been used as a smallest test solute in most experiments (4,5,18) except ref. 14 that was shown to be poorly permeable across the P. aeruginosa outer membrane (6-8). Therefore, earlier data might not be reliable. (ii) Permeability of the intact outer membrane of P. aeruginosa was shown to be roughly close to that of enteric bacteria as mentioned by the investigators themselves (18), yet the in vitro permeability assays in the same laboratory showed the presence of large pores (4,5,14). The investigators provided no clear interpretation for this discrepancy. (iii) Dialysis of the purified proteins against 5% of ethanol solution for 22 days (4) might have caused denaturation of genuine porin(s) and possibly created the artifact by protein F. We experienced that the purified P. aeruginosa porins are relatively sensitive to prolonged storage at 4° C (unpublished result). Following lines of evidence support our conclusion. The imipenem resistant strains from the imipenem-treated patients or by the in vitro selection were missing protein D but fully retained protein F (19,20,21). The deduced amino acid sequence from the DNA sequencing of the gene coded for protein F showed no apparent homology with the known amino acid sequences of E. coli porins, Omp F, Omp C. Pho E or Lam B, but that showed the closest homology to the Omp A proteins of different enteric bacteria (22). All these results suggested that protein F of P. aeruginosa might have not been the porin.

ACKNOWLEDGMENTS This study was suported in part by grants from the Ministry of Education of Japan, Culture and Science of Japan, Ohyama Foundation Inc. and Medical research aids from Tokai University School of Medicine. This was also supported by the General Organization of Research of Tokai University.

REFERENCES

1 Angus, B.L., Carey, A.L., Caron, D.A., Kropinsky, A.M.B., and Hancock, R.E.W. (1982). Antimirob. Agents Chemother. 21: 299-309.
2 Yoshimura, F., and Nikaido, H. (1982) J. Bacteriol. 152: 636-642.
3 Nikaido, H., and Hancock, R.E.W. (1986) Outer membrane permeability of Pseudomonas aeruginosa. p.145-193. In (ed.), The Bacteria vol. X. Academic Press, London.
4 Hancock, R.E.W., Decad, G.M., and Nikaido, H. (1979) Biochim. Biophys. Acta 554; 323-331.
5 Hancock, R.E.W., and Nikaido, H. (1978) J. Bacteriol. 136: 381-390.
6 Caulcott, C.A., Brown, M.R.W., and Gonda, I. (1984) FEMS Microbiol. Lett. 21: 119-123.
7 Yoneyama, H., Akatsuka, A., and Nakae, T. (1986) Biochem. Biophys. Res. Commun. 134: 106-112.
8 Yoneyama, H., and Nakae, T. (1986) Eur. J. Biochem. 157: 33-38.
9 Gotoh, N., Wakebe, H., Nishino, T., and Tanino, T. (1987) J. Microbiol. Methods 6: 265-271.
10 Mizuno, T., and Kageyama, M. (1978) J. Biochem. 84: 179-191.
11 Smit, J., Kamio, Y., and Nikaido, H. (1975) J. Bacteriol. 124: 942-958.
12 Mizushima, S., and Yamada, H. (1975) Biochim. Biophys. Acta 375: 44-53.
13 Nakae, T., Ishii, J., and Ferenci, T. (1986) J. Biol. Chem. 261: 622-626.
14 Yoshimura, F., Zalman, L.S., and Nikaido, H. (1983) J. Biol. Chem. 258: 2308-2314.
15 Nakae, R., and Nakae, T. (1982) Antimicrob. Agents Chemother. 22: 554-559.
16 Nikaido, H., and Rosenberg, E.Y. (1981) J. Gen. Physiol. 77: 121-135.
17 Benz, R., and Hancock, R.E.W. (1981) Biochim. Biophys. Acta 646: 293-308.
18 Decad, G.M., and Nikaido, H. (1976) J. Bacteriol. 128, 325-336.
19 Büscher, K.-H., Cullmann, W., Dick, W. and Opferkuch, W. (1987) Antimicrob. Agents Chemother. 31: 703-708.
20 Lynch, M.J., Drusano, G.L. and Mobley, H.L.T. (1987) Antimicrob. Agents Chemother. 31: 1892-1896.
21 Quinn, J.P., Dudek, E.J., DiVincenzo, C.A., Lucks,D.A., and Lerner, S.A. (1986) J. Infect. Dis. 154: 289-294.
22 Duchêne, M., Schweizer, A., Lottspeich, F., Krauss, G, Marget, M. Vogel, K., von Specht, B.-U., and Domdey, H. (1988) J. Bacteriol. 170: 155-162.
23 Laemmli, U.K. (1970) Nature, 227, 680-685.

Vol. 156, No. 1, 1988 BIOCHEMICAL AND BIOPHYSICAL RESEARCH COMMUNICATIONS
October 14, 1988 Pages 477-484

FIBRINOGEN ASSOCIATION WITH HUMAN MONOCYTES: EVIDENCE FOR CONSTITUTIVE EXPRESSION OF FIBRINOGEN RECEPTORS AND FOR INVOLVEMENT OF MAC-1 (CD18, CR3) IN THE BINDING

Cristina Trezzini, Thomas W. Jungi, Peter Kuhnert and Ernst Peterhans

Institute of Veterinary Virology, Länggass-Str. 122, CH-3012 Berne, Switzerland

Received August 31, 1988

Radiolabeled fibrinogen (Fg) specifically binds to mononuclear leukocytes (MNL) and to purified monocytes, but not to nylon-nonadherent lymphocytes. The association is rapid, Ca^{++}-dependent and reversible. MNL containing Fg-binding monocytes had not been exposed to endotoxin (<4 pg/mL) during the isolation and the binding test, and Fg binding was not altered by preincubation of MNL with lipopolysaccharide. The binding of Fg was inhibited by anti-Mac-1 antibodies (OKM1). Antibodies to surface-bound Fg were able to induce luminol-dependent chemiluminescence, indicating that Fg binding sites have receptor function. Emission of a signal depended on MNL exposure to Fg, on specific, divalent antibodies, but not on the antibody Fc portion. These data show that human monocytes constitutively express specific Fg receptors and suggest that Mac-1, a member of the integrin superfamily, is involved in Fg recognition.
© 1988 Academic Press, Inc.

Mononuclear phagocytes (MP) are not only of key importance in host defense, tissue repair and regeneration; they also have a role in coagulation and hemostasis (1-7). Activated MP express strong procoagulant activity (1); MP may be a focus of deposition of fibrinogen (Fg) and/or fibrin (Fb) in vivo (2) and in vitro (3,4) and are involved in Fb degradation and clearance (5). A role for Fg has recently been implicated in the differentiation of monocytes into macrophages (6). It may be assumed that such responses involve specific binding sites for Fg or Fb on the MP membrane. However, a search for binding sites to the unique amino acid sequence exposed on monomeric Fb after thrombin cleavage, glycyl-prolyl-arginine (GPR), provided no evidence for high-affinity binding sites on human MP for either the GPR sequence or the Fb fragment E (C.

Abbreviations: MP, mononuclear phagocytes; Fg, fibrinogen; Fb, fibrin; Fn, fibronectin; SDS-PAGE, sodium dodecyl sulfate polyacrylamid gel electrophoresis; PBS-A, phosphate-buffered saline containing azide; LAL, limulus amoebocyte lysate; fMLP, formyl-methionyl-leucyl-phenylalanine; PMA, phorbol 12-myristate 13-acetae; MNL, mononuclear leukocytes; HBSS, Hanks' balanced salt solution; IgG-agg, heat-aggregated IgG; CL, chemiluminescence; LPS, lipopolysaccharide.

0006-291X/88 $1.50
Copyright © 1988 by Academic Press, Inc.
All rights of reproduction in any form reserved.

Trezzini, unpublished). In contrast, the present report shows that specific binding sites for intact Fg are constitutively expressed on human peripheral blood monocytes, that crosslinking of bound Fg transduces a signal and that the Mac-1 antigen is involved in Fg binding.

MATERIALS AND METHODS

Reagents: Fibrinogen was purchased from Sigma, St. Louis, Mo (Cat. Nr. 4883) and from KabiVitrum (Stockholm, Sweden) and iodinated by use of chloramine T (8) to a specific activity of 10^3 cpm/ng, followed by dialysis against phosphate-buffered (10 mM, pH 7.4) saline containing 0.02 % sodium azide (PBS-A). It was nondegraded as assessed by sodium dodecyl sulfate polyacrylamid gel electrophoresis (SDS-PAGE) (9) both before and after iodination. Fibronectin (Fn) was from Serva (Heidelberg, F.R.G.), human serum albumin (HSA) from Behringwerke, goat anti-Fn and anti-Fg IgG were from Calbiochem (Lucerne). F(ab')2 and Fab fragments were prepared according to standard methods (10) and dialysed against PBS. Purity was checked by SDS-PAGE (9). RPMI 1640 was provided by Seromed (Munich). OKM1 monoclonal antibodies (Ortho, Raritan. N.J.), were kindly provided by Dr. M. Spycher, Central Laboratory of the S.R.C. Blood Transfusion Service, Berne. Also from the Central Laboratory was standard human gammaglobulin (IgG). The colorimetric limulus amoebocyte lysate (LAL) test kit for endotoxin quantitation (11) (KabiVitrum) was used in a microtiter plate assay adapted to semiautomated photometry. The following reagents were from Sigma: ADP, E. coli lipopolysaccharide (B111:04) (LPS), formyl-methionyl-leucyl-phenylalanine (fMLP), several arginyl-glycyl-asparagyl- (RGD) containing oligopeptides, cytochalasin B, hirudin, luminol, phorbol 12-myristate-13 acetate (PMA) and zymosan. Bovine thrombin (61 NIH units/mg) was from Hoffmann-La Roche, Basel, all other chemicals were purchased from Merck (Darmstadt, F.R.G.).

Monocyte isolation: Mononuclear leukocytes (MNL) were isolated from buffy coats of whole blood donations by a ficoll-hypaque procedure (7), aimed at minimizing platelet contamination and using pyrogen-free ficoll-hypaque. Monocytes were purified from MNL by centrifugation-elutriation as described (12). Pooled monocyte fractions were between 92 and 98 % pure, as assessed by morphology and by nonspecific esterase staining (7); viability was 99 %.

Radioligand binding test: Cell aliquots (2-4 x 10^6 monocytes per ml) were incubated with ^{125}I-Fg either in the presence or absence of excess ($\geq$100fold) cold Fg in a volume of 200 µl. ^{125}I-Fg concentration varied between 73.5 and 0.14 nM, but was usually 36.7 nM. The medium was RPMI 1640 containing HEPES (30 mM), HSA (0.5 % w/v) and azide (0.02 %). Incubation was performed for 60 min in a shaking 37°C waterbath, unless noted otherwise. Then, 80 µl aliquots were layered onto phthalate oil in 400 µl polypropylene tubes (Beckman) as described (13). Tubes were spun for 3 min at 9'000xg, and aliquots of supernatants and cellular pellets were counted separately in a gamma counter.

Chemiluminescence assay: MNL were preincubated for 60 min at 37°C, in Hanks' balanced salt solution (HBSS) either in the absence or presence (3 µM) of Fg. They were resuspended in HBSS at 4°C after 3 washes and kept on ice. These cells, or MNL prepared without pretreatment, were diluted to 0.4 x 10^6 monocytes/ml with cold HBSS containing luminol (5 µM/ml), distributed to polystyrene tubes (0.25 ml/tube), dark-adapted for 25-40 min on ice and warmed up for 4 min in a 37°C waterbath. They then were stimulated with 50 µl of antibodies (0.2 mg /ml) or with heat-aggregated (11 min 63°C) human IgG (1 mg/ml; IgG-agg.), prior to recording of chemiluminescence (CL) for 3 min in a Biolumat LB 950 luminometer (Berthold, Wildbad, F.R.G.) interphased to an IBM XT 286 personal computer. CL stimulated with PMA (10^{-7} M) or opsonized zymosan (200 µg/ml) was determined as described elsewhere (14).

RESULTS AND DISCUSSION

Peripheral blood MNL specifically bind ^{125}I-labeled Fg: Fig. 1 shows that human MNL specifically bind radiolabeled Fg, that the association occurs rapidly and can be reversed by the addition of either excess unlabeled Fg or EDTA. Studies with varying concentrations of Ca^{++} and Mg^{++} suggested that Ca^{++} but not Mg^{++} was required, having its optimum at physiological Ca^{++} concentrations (2.5 mM). Similar amounts of Fg were bound in the presence of cytochalasin B (12 ug/ml) or hirudin (0.2 U/ml). MNL bound similar amounts of Fg as did elutriation-purified monocytes, on a per-monocyte basis, whereas nylon wool-nonadherent cells bound little, if any, Fg (not shown). This suggests that the monocyte is the major cell within MNL which specifically binds Fg in a Ca^{++} dependent and reversible manner.

Monocytes require no exogenous stimulation for binding Fg: In earlier studies (15, 16) monocytes did not specifically bind Fg unless stimulated either with ADP, with thrombin or with fMLP (15,16). In our hands, none of these stimuli increased the amount of Fg binding to elutriated monocytes (not shown) or to unseparated MNL (Table 1). It was therefore considered that monocytes were inadvertently stimulated by LPS contaminating either monocyte or Fg preparations, thereby inducing expression of Fg binding sites. Using a colorimetric LAL-test detecting as little as 4 pg/ml standard endotoxin activity, it was assured that iodination of Fg and isolation of MNL was performed under strictly pyrogen-free conditions. We so far did not achieve elutriating monocytes in the absence of endotoxin in the high-pg range, a problem to be addressed in another study. However, MNL exposed to LPS prior to or during interaction with

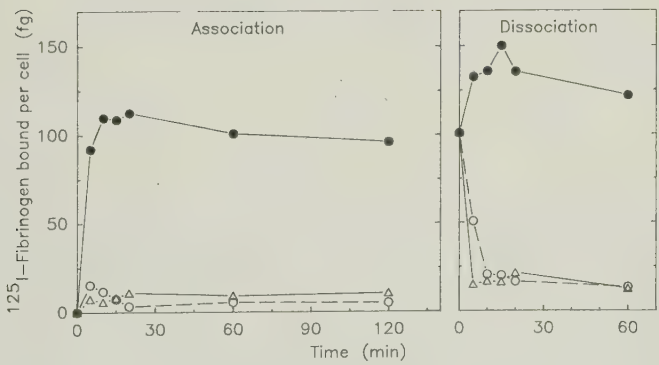

Figure 1: Kinetics of association with and dissociation from monocytes of ^{125}I-Fg. Association: MNL were exposed to labeled Fg, either alone (●) or together with cold Fg (□) or with EDTA (△), and free from bound activity was separated at the indicated time. Dissociation: To MNL pre-exposed to labeled Fg, either medium (●) or excess unlabeled Fg (□) or EDTA (△) was added, and bound Fg was determined at the indicated time. In this figure and the tables the amount of ^{125}I-Fg was calculated per monocyte, since lymphocytes also present in MNL were found to bind negligible amounts of Fg.

Table 1: Expression of Fg binding sites does not require prestimulation of monocytes

Agent used for prestimulation	^{125}I-Fg bound (fg per monocyte)	
	Total binding	Nonspecific binding
-	71.9	11.2
ADP (10 uM, 10 min)	96.2	26.7
fMLP (0.1 ug/ml, 10 min)	60.2	6.1
Thrombin (1 U/ml, 10 min) then hirudin (5 U/ml, 10 min)	68.9	17.8
LPS (10 ug/ml, 1 hr)	68.9	18.0
" (10 ug/ml, 2 hr)	80.2	6.8
Polymyxin B (5 ug/ml, added during binding test	60.9	16.5

After stimulation whith each agent, MNL were washed twice with PBS.

Fg bound similar amounts of Fg as did unexposed control cells (Table 1 and data not shown). Polymyxin B, an antibiotic neutralizing some of the effects of endotoxin (17), did not influence Fg binding to monocytes (Table 1). Moreover, the MNL used were shown to express no detectable procoagulant activity and to secrete no measurable IL-1 (P. Kuhnert and T.W. Jungi, unpublished) which would be sensitive hallmarks for priming by endotoxin (1,18). This argues against a requirement of LPS or any other stimulatory agent for expression of Fg binding sites on monocytes. Altieri et al. used monocytes purified by selective adherence and subsequent dislodgement (15) for determining Fg binding to monocytes. This procedure alters monocyte functions (19) and impairs the capacity to bind Fg (C. Trezzini, unpublished).

Involvement of Mac-1 in monocyte Fg receptor function: Other reports have previously described Fg binding sites on hematopoietic cells. These include an Fg receptor expressed on certain cell lines (20), the platelet Fg receptor, GPIIb/IIIa (21), a monocyte Fg receptor related to GPIIb/IIIA (15) and other related molecules referred to as integrins (22). Mac-1 (CR3, CD18), a member of the integrin family, is expressed on monocytes (23). The binding of integrins to their ligands often involves a conserved amino acid sequence RGD (23, 24). The effect of synthetic peptides containing RGD, and of anti-Mac-1 antibodies, on the binding of ^{125}I-Fg were therefore investigated. Table 2 shows that OKM1, an anti-Mac-1 antibody, significantly reduces binding of Fg to monocytes, thus confirming a recent abstract (16). This suggests that Mac-1 has either a Fg binding site itself, or is closely associated with a Fg binding site. Although the binding of another physiological ligand of Mac-1, C3bi, involves the RGD sequence (23), Fg binding to monocytes was not prevented by any of the RGD peptides (RGD, RGDS, GRGDS, GRGDSPK, and fibronectin-related peptide) tested at concentrations up to 1 mM. This leaves open

Table 2: Inhibition by OKM1 andibodies of Fg binding to monocytes

Exp.	OKM1[a]	^{125}I-Fg bound (fg per monocyte) after incubation with	
		^{125}I-Fg (37 nM)	^{125}I-Fg + EDTA (5 mM)
1	-	270.5	11.3
	10 ug/ml	63.9 (79 %)[b]	11.0
2	-	95.0	12.0
	25 ug/ml	28.6 (82 %)	13.6

a) Cells were preincubated with or without OKM1 for 30 min at 37°C before ^{125}I-Fg (either alone or with EDTA) was added for a 60 min incubation.
b) Percentages in brackets refer to inhibition of specific binding.

whether the RGD sequence within Fg is involved in Fg association with its binding site on monocytes. It has been reported that a Fg receptor is absent from monocytes of thrombasthenia Glanzmann patients which also lack GPIIb/IIIa on platelets (15). However, our preliminary evidence suggests that Fg normally binds to monocytes in these subjects (C. Trezzini et al., in preparation).

Crosslinking of bound Fg induces a respiratory burst: It was next determined whether Fg binding sites have receptor properties, capable of transducing a signal. As an effector system, triggering of a respiratory burst, as indicated by luminol-enhanced CL, was chosen for several reasons. Firstly, CL emission requires protein kinase C activation, phospholipase A2 activation, calcium mobilisation and other biochemical events associated with the triggering of many receptor systems of leukocytes (25). Secondly, the signal is specific for monocytes within MNL as lymphocytes fail to express luminol-enhanced CL (14). Thirdly, CL is observed within minutes after stimulation, thus establishing a close temporal relationship between stimulation and response. Fig. 2 shows that Fg-pretreated MNL responded within <1 min to stimulation by goat anti-Fg IgG, and the signal was even stronger than that induced by non-immune IgG-agg which stimulated cells via Fc receptors and served as a positive control. Anti-Fg Fab'2 also mediated a CL signal, albeit of lower magnitude than complete antibodies. This ruled out an obligatory role for Fc receptors in signal transduction although antibodies stimulating the cells by interacting with both antigen and Fc receptor induced more CL than by interacting with the FcR or the recognized ligand only. Specific antibodies were required, since anti-Fn IgG (Fig. 2) and goat IgG (not shown) did not induce a CL response. MNL preincubated in medium did not respond to anti-Fg, but did respond to IgG-agg (Fig. 2). Monovalent Fab fragments failed to elicit a respiratory burst (Fig. 2). The magnitude of the CL peak depended on the Fg concentration used for preincubation, 1 mg/ml being

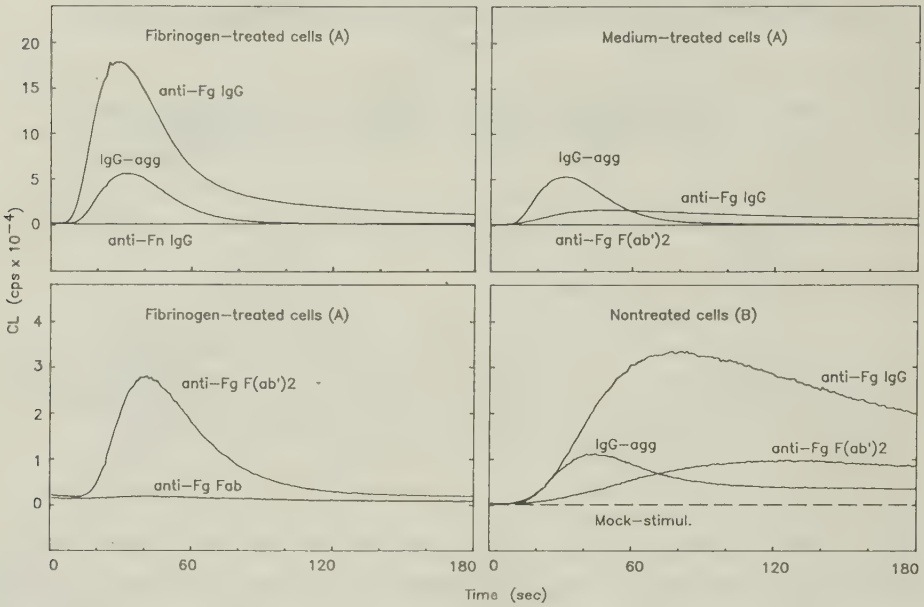

Figure 2: Temporal traces of chemiluminescence recordings from MNL stimulated with antibodies. MNL had been preincubated for 1 hr in the presence of HBSS alone or of of 1 mg/ml Fg. Cells referred to as nontreated had been isolated in the cold under pyrogen-free conditions, dark-adapted, warmed up (4 min) and then stimulated with antibodies or IgG-agg. The other cells had been incubated for 60 min with or without Fg prior to washing and dark-adaption at 4°C. Representative experiments are shown. (A) and (B) allude to two MNL donors.

optimal. After removal of Fg by washing, the intensity of the CL signal was inversely related to the time for which cells had been incubated at 37°C prior to stimulation. Warming up cells for 3-5 min was optimal However, when keeping them for 1 hr at this temperature, the response to anti-Fg F(ab')2 was lost, that to anti-Fg IgG markedly reduced, but that to IgG-agg only lightly reduced. MNL not exposed to Fg in vitro, but isolated in the cold also responded to triggering with either anti-Fg IgG and anti-Fg F(ab')2 (Fig. 2), although much weaker than Fg-exposed counterparts. Taken together, these results suggest that two requirements had to be met: (i) Monocytes had to be covered with Fg; (ii) divalent, Fg-specific antibodies were necessary. That the stimulation is mediated by complexes forming between anti-Fg Fab'2 and Fg shed from the cells is unlikely, since antibody-inducible CL disappears after prolonged incubation of Fg-covered cells at 37°C. It thus appears that CL is induced by antibody-mediated crosslinking of receptor-bound Fg on the monocyte surface. While our studies monitor for an immediate consequence of receptor stimulation, later sequelae of cell exposure to Fg have been reported. These include enhancement of procoagulant activity in monocytes (15), induction of proliferation in hematopoietic cells (20) and promotion of differentiation

from monocytes to macrophages (6). Future studies have to search for the physiological function(s) of monocyte Fg receptors.

Preincubation of MNL with Fg in the presence of anti-Mac-1 prevented a CL signal upon antibody-crosslinking (not shown). This could be due to an inhibition by anti-Mac-1 of Fg binding to its receptor. However, OKM1 pretreatment interfered also with the generation of CL induced by IgG-agg (reduction 50-90 %), zymosan and PMA (reduction 20-60 %). This is compatible with the anti-Mac-1-induced inhibition of Fc receptor-mediated phagocytosis (26,27) and with the down-modulation of the respiratory burst upon ingestion of C3b-coated Leishmania parasites (28). The exact relationship of Mac-1 and the constitutive Fg receptor on monocytes remains to be determined.

ACKNOWLEDGEMENTS

This work was supported by the Swiss National Science Fund, grant 3.858-85, and by the Central Laboratory of the Swiss Red Cross Blood Transfusion Service, Berne. The expert technical assistance of Mrs. M. Brčić and the gift of OKM1 monoclonal antibodies from Dr. M.O. Spycher, Central Laboratory, Swiss Red Cross Blood Transfusion Service, are gratefully appreciated.

REFERENCES

1. Edwards, R.L., and Rickles, F.R. (1984) Progr. Hemostas Thrombos. 7, 183-209.
2. Colvin, R., Dvorak, H.F. (1975) J. Exp. Med. 142, 1377-1390
3. Hopper, K.E., Geczy, C.L., and Davies, W.A. (1981) J. Immunol. 126, 1052-1058.
4. Shelley, W., and Juhlin, L. (1977) Nature 270, 343-344.
5. Rajagopolan, S., and Pizzo, S.V. (1986) Blood 67, 1224-1228.
6. Akiyama, Y., Griffith, R., Miller, P., Stevenson, G.W., Lund, S., Kanapa, D.J., and Stevenson, H.C. (1988) J. Leukocyte Biol. 3, 224-231.
7. Jungi, T.W., Spycher, M.O., Nydegger, U.E., and Barandun, S. (1986) Blood 67, 629-636.
8. Greenwood, F.C., Hunter W.M., and Glover, J.S. (1963) Biochem. J. 89, 114-123.
9. Lämmli, U.K. (1970) Nature 227, 680-685.
10. Fey, H., Pfister, H., Messerli, J., Sturzenegger, M., and Grolimund, F. (1976) Zbl. Vet. Med. B 23, 269-300.
11. Thomas, L.L.M., Sturk, A., Kahlé, L.H., and ten Cate, J.W. (1981) Clin. Chim. Acta 116, 63-68.
12. Clemetson, K.J., McGregor, J.L., McEver, R., Jacques, Y.V., Bainton, D.F., Domzig, W., and Baggiolini, M. (1985) J. Exp. Med. 161, 972-983.
13. Segal, D.M., and Hurwitz, E. (1977) J. Immunol. 118, 1338-1342.
14. Jungi, T.W., and Peterhans, E. (1988) Blut 56, 213-220.
15. Altieri, D.C, Manuccio, P.M. and Capitanio A.M.(1986) J. Clin. Invest. 78, 968-976.
16. Altieri, D.C., and Edgington, T.S. (1988) FASEB J. 2, 6788 (abstract).
17. Weinberg, J.B. (1981) In Methods for Studying Mononuclear Phagocytes (D.O. Adams, P.J. Edelson, and H. Koren, Eds.), pp. 139-154. Academic Press, New York, London.
18. Van der Meer, J.W.M., Endres, S., Lonnemann, G. Cannon, J.G., Ikejima, T., Okusawa, S., Gelfand, J.A., and Dinarello, C.A. (1988) J. Leukocyte Biol. 43, 216-223.

19. Jungi, T.W., von Below, G., Lerch, P.G., and Spaeth, J. (1987) Immunology 60, 261-268.
20. Levesque J.-P., Hatzfeld A., Hudry-Clergeon G., Wilner, G.D., and Hatzfeld J. (1987) J. Cell. Physiol. 132, 303-310.
21. Parise, L.V., and Philips, D.R. (1985) J. Biol. Chem. 260, 10698-10707.
22. Ginsberg, M.H., Loftus, J.C., and Plow, E.F. (1988) Thrombos Haemostas 59, 1-6.
23. Wright, S, Reddy, P.A., Jong, M.T.C., Erickson, B.W. (1987) Proc. Natl. Acad. Sci. U.S.A. 84, 1965-1968.
24. Ruoshlahti, E., and Pierschbacher, M.D. Science 238, 491-497.
25. Rush, D.N., and Keown, P.A. (1984) Cell. Immunol. 87, 252-258.
26. Arnaout, M.A., Todd III, R.F., Dana, N, Melamed, J., and Schlossman, S.F. (1983) J. Clin. Invest. 72, 171-179.
27. Brown, E.J., Bohnsack J.F., and Gresham H.D. (1988) J. Clin. Invest. 81, 365-375.
28. Mosser, D.M., and Edelson, P.J. (1987) Nature 327, 329-331.

Vol. 156, No. 1, 1988 BIOCHEMICAL AND BIOPHYSICAL RESEARCH COMMUNICATIONS
October 14, 1988 Pages 485-492

TRANSIENT ACCUMULATION OF INOSITOL (1,3,4,5)-TETRAKISPHOSPHATE IN RESPONSE TO α_1-ADRENERGIC STIMULATION IN ADULT CARDIAC MYOCYTES

Guy P. Heathers*, Peter B. Corr*+, and Leona J. Rubin+

Department of Medicine* and Pharmacology+

Washington University School of Medicine

St. Louis, Missouri

Received September 9, 1988

To investigate the response to catecholamine stimulation of adult cardiac myocytes and the metabolism of inositol (1,4,5)-trisphosphate (1,4,5-IP_3) and inositol (1,3,4,5)-tetrakisphosphate (IP_4), we have employed a procedure developed in our laboratory to directly measure the mass of inositol phosphates after separation of individual isomers of inositol phosphates by high performance liquid chromatography. Control, unstimulated myocytes, contained low levels of inositol (1,4)-bisphosphate (1,4-IP_2), inositol (1,3)-bisphosphate (1,3-IP_2), inositol (3,4)-bisphosphate (3,4-IP_2), inositol (1,3,4)-trisphosphate (1,3,4-IP_3), 1,4,5-IP_3 and IP_4. Stimulation with norepinephrine for 30 seconds produced peak 1,4,5-IP_3 and IP_4 levels which rapidly returned to basal values by 60 seconds of norepinephrine stimulation. 1,4-IP_2, 1,3-IP_2 and 1,3,4-IP_3 were increased markedly but only after stimulation with norepinephrine for 60 seconds. These results indicate a rapid yet transient increase in 1,4,5-IP_3 and IP_4 in response to norepinephrine stimulation and are the first quantitative measurements of the isomers of inositol phosphates in cardiac tissue. © 1988 Academic Press, Inc.

In many tissues, the physiologic second messenger mediating the intracellular response to α_1-adrenergic stimulation is 1,4,5-IP_3 (1). The metabolism of 1,4,5-IP_3 has been studied extensively in many types of tissues and results demonstrate that dephosphorylation to 1,4-IP_2 (2) or phosphorylation to 1,3,4,5-IP_4 (3,4) are the immediate routes of metabolism. 1,4-IP_2 is further dephosphorylated to inositol 4-monophosphate (5) while 1,3,4,5-IP_4 is dephosphorylated to form another isomer of inositol trisphosphate, 1,3,4-IP_3 (3).

1,4,5-IP_3 mobilizes intracellular Ca^{++} (6) and as such produces the physiologic alterations characteristic of specific hormonal stimulation. Although 1,4,5-IP_3 appears to be the most physiologically active metabolite formed after hormone-stimulated breakdown of phosphoinositides, other inositol phosphates may also have a physiologic "second messenger" role. For example, 1,3,4,5-IP_4 enhances Ca^{++} entry into some cells (7) and potentiates the Ca^{++} mobilizing effect of 1,4,5-IP_3 (8). Therefore, 1,3,4,5-IP_4 may have an important role in controlling Ca^{++} levels in response to hormonal stimulation.

Please address all correspondence to: Peter B. Corr, Ph.D., Washington University School of Medicine, Cardiovascular Division, Box 8086, 660 South Euclid Avenue, St. Louis, Missouri 63110

0006-291X/88 $1.50
Copyright © 1988 by Academic Press, Inc.
All rights of reproduction in any form reserved.

In cardiac tissue, evidence has been presented that 1,4,5-IP_3 is also produced after α_1-adrenergic stimulation (9). However, 1,3,4,5-IP_4 has not been demonstrated in cardiac tissue and the existence of the 1,3,4,5-IP_4/1,3,4-IP_3 pathway in cardiac tissue appears controversial (10,11). Some of the difficulties in defining the metabolic fate of 1,4,5-IP_3 in cardiac tissue may stem from methodologic problems which include the relatively long incubation times with radiolabeled precursors required to sufficiently label phosphoinositides. Therefore, we have developed a method, based on that of Rittenhouse and Sasson (12), to directly measure the mass of inositol phosphates without the use of labeled precursors. Furthermore, the increased sensitivity of this method, enabled the determination of the mass of the isomers of IP_2 and IP_3, as well as the mass of IP_4 in isolated adult canine myocytes before and after stimulation with norepinephrine. We report a transient increase in the concentration of 1,4,5-IP_3 and 1,3,4,5-IP_4 within 30 seconds of stimulation with norepinephrine. In contrast 1,3,4-IP_3 and IP_2 isomers do not accumulate in cardiac myocytes until 60 seconds of stimulation with norepinephrine. The transient accumulation of IP_4 after hormonal stimulation suggests a physiologic role for this inositol polyphosphate, possibly by alteration of Ca^{++} levels in cardiac tissue.

METHODS

Extraction of Inositol Phosphates: Isolated adult canine ventricular myocytes were prepared as described previously (13) and incubated in HEPES buffer (115 mm NaCl, 5 mM KCl, 5 mM $MgCl_2$, 500 μm Ca^{2+}, 35 mM sucrose, 10 mM glucose, 10 mM HEPES, 4 mM Taurine, pH=7.2). Four tubes, 1800 μl of myocyte suspension each (approximately 5 million cells total), were incubated in the presence of 200 μl of norepinephrine (final concentration, 10^{-5} M) or vehicle (HEPES + 1 mg/ml ascorbic acid, pH=7.2). After 0, 30, or 60 seconds, incubations were terminated by addition of an equal volume of ice-cold 15% (w/v) trichloroacetic acid (TCA), vortexed and placed on ice for 10 minutes. At this stage, D-myo-(2-[^{3}H]inositol (1,4) bisphosphate, D-myo-(2-[^{3}H]inositol (1,4,5) trisphosphate, and D-myo-(2-[^{3}H]inositol (1,3,4,5) tetrakisphosphate (approximately 2,500 DPM) was added to assess subsequent recovery. The precipitate was removed by centrifugation and the supernatant decanted and placed in 17 x 100 mm polypropylene or siliconized glass test tubes. TCA was extracted with 2 ml of H_2O-saturated diethyl ether. The extraction was repeated four times and the samples were lyophilized to dryness, resuspended in 1 ml of distilled water and pooled.

Separation of Isomers by HPLC: The pooled aqueous extracts of adult myocytes were loaded onto Supelclean LC-NH_2 columns (1 ml), washed with 5 ml of distilled water followed by elution with 1 ml of 1.5 M NH_4OH to elute inositol phosphates. The eluate was resuspended in 7 ml of distilled water, lyophilized to dryness and resuspended in 1 ml of distilled water. Samples were then applied to a Partisil 10 SAX HPLC column (0.46 cm x 25 cm) equipped with a 2 μm precolumn filter and a 5 μm Adsorbosphere SAX guard column (0.46 cm x 1 cm). In addition, the mobile phase, prior to reaching the injector, passed through a silica (50 μm) saturator column (0.46 cm x 25 cm). This approach saturated the aqueous phase with silica reducing solubilization of the analytical column, and thereby extending column life (14). The column was equilibrated with water and following elution of free inositol (20 minutes with water), inositol phosphates were eluted with a linear gradient of phosphate-buffered ammonium formate, pH=3.8, from 0 to 1.0 M over 20 minutes at 2.0 ml/min. This procedure provided separation of inositol phosphates, as well as the isomers of IP_2 and IP_3. The ammonium formate concentration was held at 1.0 M for 3 min and then IP_4 was eluted from the column by extending the gradient to 1.8 M over 5 minutes. After an additional 5 min at 1.8 M, the column was returned to H_2O. No attempt was made to separate isomers of IP_4 (15). Individual fractions (0.5 ml) containing each inositol phosphate were pooled as were fractions between peaks. The location of inositol phosphates (1,4IP_2, 1,4,5IP_3, 1,3,4IP_3 and 1,3,4,5IP_4) was determined using authentic radiolabeled compounds and radioactivity in each 0.5 ml fraction assessed (Fig. 1). Samples were concentrated using Supelclean LC-NH_2 columns and resuspended in Tris buffer, pH=8.5, prior to dephosphorylation with alkaline phosphatase. The recovery of

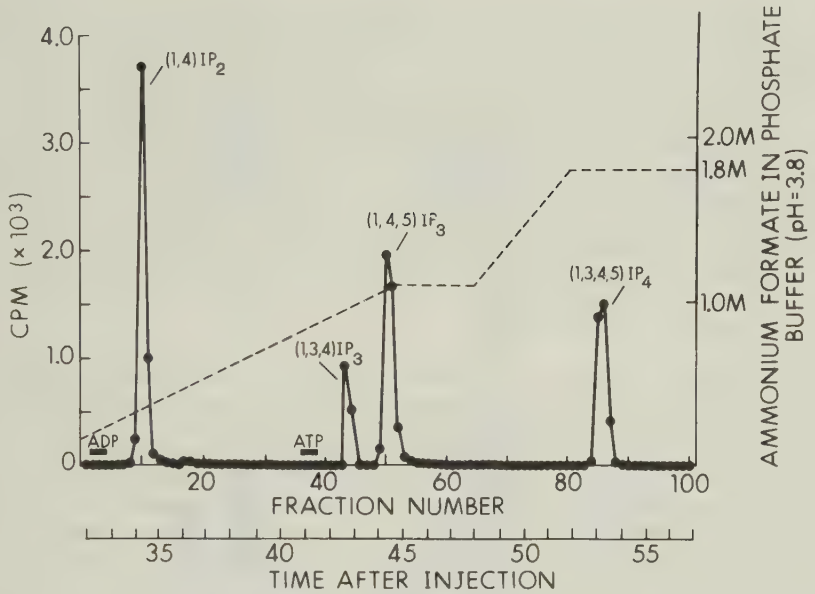

Figure 1. Elution of radiolabelled 1,4-IP_2, 1,3,4-IP_3, 1,4,5-IP_3 and 1,3,4,5-IP_4 from the Partisil 10 SAX column. Ammonium formate gradient (dotted line) was corrected for system void volume (5.4 ml). 0.5 ml fractions were pooled for 1,3-IP_2 (fractions 4-7), 1,4-IP_2 (fractions 9-13), 3,4-IP_2 (fractions 14-17), 1,3,4-IP_3 (fractions 42-46), 1,4,5-IP_3 (fractions 49-54) and 1,3,4,5-IP_4 (fractions 84-89). In addition, fractions between peaks were pooled and subsequently analyzed; no inositol mass was detected in the interpeak fractions (limit of detection 2.0 pmoles/mg protein).

each isomer was assessed by determining the amount of radiolabel eluted for each radiolabeled isomer added (approximately 10,000 dpm each).

Quantification of Inositol Phosphate Isomers: Samples were concentrated prior to dephosphorylation by one of two methods. In one method, samples were lyophilized to dryness and resuspended in 1 ml of Tris buffer, pH=8.5. Alternatively, samples were loaded onto Supelclean LC-NH_2 columns (1 ml), washed with 1 ml of distilled water and inositol phosphates were eluted with 1 ml of 1.5 M NH_4OH. The eluate was lyophilized, effecting removal of most of the NH_4OH, and resuspended in Tris buffer, pH=8.5.

To dephosphorylate the samples, $MgCl_2$ (5 mM) and alkaline phosphatase (Sigma Chemical Co., type VIIS, 100 units) were added to each tube. Samples were incubated for 48 hours at 37°C, followed by boiling for 3 minutes to terminate the reaction. The extent of dephosphorylation was assessed using 10^4 dpm of D-myo-(2-[^{3}H]inositol (1,4,5)-trisphosphate and D-myo-(2-[^{3}H]inositol (1,3,4,5)-tetrakisphosphate (1.0 Ci/mmol) with subsequent ion exchange chromatography (16) to determine the amount of radioactivity in the individual inositol fractions. Following dephosphorylation, 1 nmol of chiro-inositol was added to each sample to serve as an internal standard for gas chromatographic analysis.

Samples were desalted using an extensively washed mixed-bed anion-cation exchange resin (Bio-Rad MSZ 501, 20-50 mesh). Inositol was eluted with 16 mls of distilled water. The eluate was collected in two 13 x 100 mm siliconized glass tubes. Recovery after desalting was assessed by determining the amount of radioactivity in the eluate. After desalting, samples were lyophilized to dryness under vacuum followed by derivatization to the hexatrimethylsilyl derivatives. This was achieved by the addition of 25 μl of anhydrous pyridine (Aldrich Chemical Co.) and 25 μl of bis-(trimethylsilyl) trifluoroacetamide with 1% trimethylchlorosilane (BSTFA) (Pierce Chemical Co.) to each dried residue. Samples were vortexed and transferred to 0.3 ml glass reactivials (Pierce Chemical Co.). Reactivials were capped and placed in a heating block at 60°C overnight. Separation of chiro- and myo-inositol was achieved by gas chromatography using a Varian 3700. The derivatized sample (0.5 μl) was injected onto a Hewlett Packard Ultra 1 column of cross-linked methyl silicone (25 m length, 0.20 mm internal diameter, 0.11 μm film thickness). Gas chromatographic conditions were as follows: injection temperature = 180°C, detection temperature = 240°C, column temperature = 110°C to 210°C at

25°C/min. Helium was used as the carrier gas at a flow rate of 1.0 ml/min. The injections were made in the splitless mode (splitter flow = 150 ml/min) with a 20 sec period between sample injection and opening of the splitter solenoid valve. Products were detected by flame ionization. Myo- and chiro-inositol peaks were identified by co-migration with authentic standards and quantified by integration of peak area using a Varian 4270 integrator. The detector response ratio to chiro- and myo-inositol derivatives was determined by analysis of equal quantities of each inositol derivative. The linearity of the detector response to derivatives of myo-inositol was validated for the range of 1 to 100 pmols. Derivatized samples from standard or tissue preparations were injected onto the column and the amount of myo-inositol from a particular inositol phosphate isomer fraction was determined from the ratio of chiro-to myo-inositol peak areas corrected for the detectors response ratio. The mass of myo-inositol was corrected for recovery and was expressed as pmols/mg protein. Protein was measured by the method of Lowry (18).

Materials: Myo-(2-[^{3}H])-inositol (14.3 Ci/mmole), D-myo-(2-[^{3}H])-inositol 1-phosphate (1.0 Ci/mmole), D-myo-(2-[^{3}H])-inositol 1,4-bisphosphate (1.0 ci/mmole), D-myo-(2-[^{3}H])-inositol 1,4,5-trisphosphate (1.0 Ci/mmole) and D-myo-(2-[^{3}H])-inositol 1,3,4,5-tetrakisphosphate (1.0 Ci/mmole) were obtained from Amersham, Arlington Heights, IL. Authentic myo-(2-[^{3}H])-inositol 1,3,4-trisphosphate was prepared by enzymatic hydrolysis of [^{3}H]-IP_4 according to the procedure of Bansal et al (17) and was kindly supplied by Dr. A. Morrison (Washington University School of Medicine, St. Louis, MO). Alkaline phosphatase (Type VII S) was purchased from Sigma Chemical Co., St. Louis, MO and pyridine from Aldrich Chemical Co., Milwaukee, WI. Bis-(trimethylsilyl) trifluoroacetamide with 1% trimethylchlorosilane (BSTFA) was purchased from Pierce Chemical Co., Rockford, IL. The ultra-1 (0.11 μM, 25 M, 0.2 mm i.d.) capillary gas chromatography columns were purchased from Hewlett Packard, Avondale, PA. Partisil 10 SAX columns and Adsorbosphere SAX guard columns were purchased from Alltech Associates, Inc., Deerfield, IL. Anion exchange resin (AG-1x8 formate form) and mixed bed ion exchange resin (MSZ 501) were obtained from Supelco, Inc., Bellefonte, PA. Chiro-inositol was a kind gift from Dr. William Sherman (Washington, University School Medicine, St. Louis, MO).

RESULTS

The recovery of exogenous [^{3}H]-inositol phosphate isomers through the HPLC column in the absence or presence of sample extract exceeded 95%. Recovery of [3H]-1,4,5-IP_3 through the concentration step prior to dephosphorylation was 100%. Dephosphorylation for 48 hours at 37°C with 100 units of alkaline phosphatase resulted in the complete dephosphorylation of [^{3}H]-1,4,5-IP_3 and ^{3}H-1,3,4,5-IP_4 as assessed by subsequent ion exchange chromatography (16). Desalting of inositol samples resulted in the greatest loss of sample (recovery = 70%) but was accounted for by the presence of chiro-inositol as an internal standard. One nmol standards of chiro- and myo-inositol were derivitized and injected onto the GC column. Integration of subsequent peaks of detection yielded a peak area ratio (chiro-peak area/myo-peak area) of 1.51. This ratio depends on the retention times of the two peaks and was used in subsequent calculations of the mass of myo-inositol from each inositol phosphate isomer fraction.

The myocyte preparation was assessed for viability and physiological characteristics as described previously (13). Cells were found to be intact, Ca^{++} tolerant and with physiologic and electrophysiologic characteristics similar to those of intact cardiac tissue. As shown in the top portion of Figure 2, low levels of several isomers of IP_2, as well as 1,3,4-IP_3 (11.69 $\pm$ 1.44 pmols/mg protein) and 1,4,5-IP_3 (14.15 $\pm$ 0.80 pmols/mg protein) could be measured in control, unstimulated adult myocytes. However, IP_4 levels were barely detectable (3.39 $\pm$ 3.39 pmols/mg protein). Of the IP_2 isomers, most of the mass resides in the 1,4-IP_2 peak (20.02 $\pm$ 5.81 pmols/mg protein) (confirmed by spiking the sample with authentic ^{3}H-inositol-labelled 1,4-IP_2 and by cochromatography with $^{32}PO_4$-1,4-IP_2 made in human erythrocytes according to the

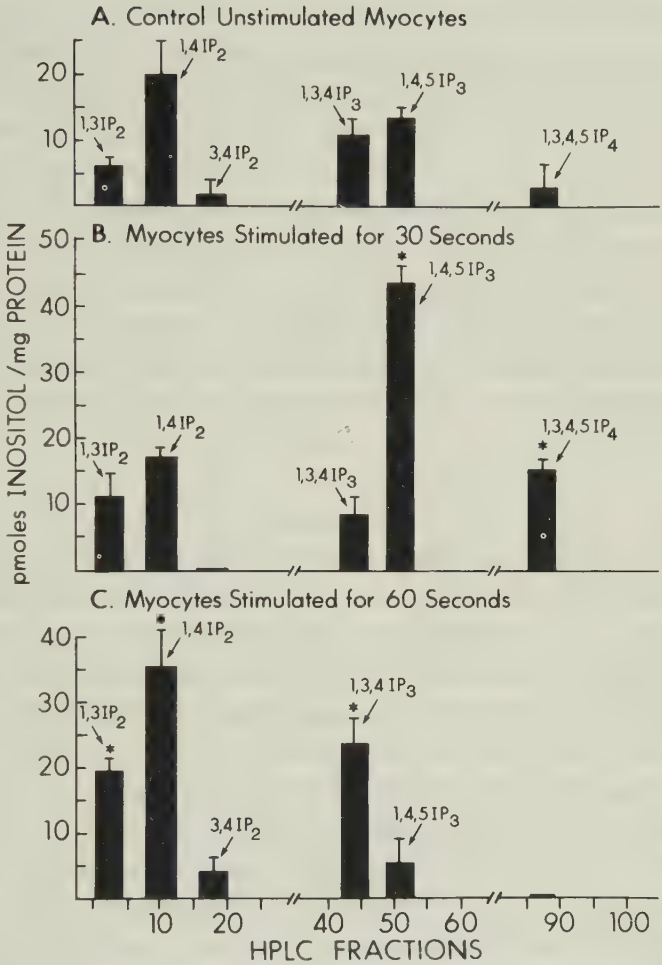

Figure 2. Mass of inositol phosphates in TCA extracts of adult canine myocytes. Inositol mass was determined for the pooled fractions (described in Fig 1) obtained following HPLC separation and corresponding to 1,3-IP_2, 1,4-IP_2, 3,4-IP_2, 1,3,4-IP_3, 1,4,5-IP3 and 1,3,4,5-IP_4. Myocytes were stimulated with 10μM norepinephrine for 30 sec (B) or 60 sec (C) and the levels of inositol mass in each combined fraction compared to that obtained from control, unstimulated myocytes (A). Values are the mean $\pm$ SEM for 3 separate experiments. * indicates $p<0.05$ compared to the control values as assessed by analysis of variance and the Tukey-Kramer multiple comparisons test.

method of Downes and Michell (18). Although we have not confirmed the identity or purity of the other IP_2 isomers for cardiac tissue, under the chromatographic conditions employed here, 3,4-IP_2 elutes after 1,4-IP_2 (20,21) while 1,3-IP_2 elutes prior to 1,4-IP_2 (17,21). Both 3,4-IP_2 and 1,3-IP_2 are hydrolysis products resulting from the dephosphorylation of 1,3,4-IP_3 by separate phosphatases (17,21).

Previous measurements from our laboratory obtained in adult canine myocytes indicated that the total mass of IP_3 peaked 30 seconds after norepinephrine stimulation and was selectively blocked by the α_1-adrenergic antagonist, BE-2254 (22). As shown in Figure 2, 30 seconds of stimulation with norepinephrine induced a 3 fold increase in the mass of 1,4,5-IP_3 (43.66 $\pm$ 2.53 pmols/mg protein) and in addition, a 5 fold increase in IP_4 (15.13 $\pm$ 1.74 pmols/mg protein).

The levels of 1,4-IP_2 (17.12 ± 1.29 pmols/mg protein), 1,3-IP_2 (11.57 ± 3.16 pmols/mg protein), 3,4-IP_2 and 1,3,4-IP_3 (8.45 ± 2.79 pmols/mg protein) were unchanged. Therefore, the increase in IP_3 mass observed after 30 seconds of stimulation with norepinephrine was due entirely to an increase in the 1,4,5-IP_3 isomer. Following 60 seconds stimulation with norepinephrine (Fig 2), the level of 1,4,5-IP_3 returned to values below control. However, the levels of 1,3,4-IP_3 increased significantly (24.41 ± 3.64 pmols/mg protein) as did both 1,3-IP_2 (19.94 ± 3.39) and 1,4-IP_2 (35.17 ± 6.20). IP_4 levels were undetectable following 60 seconds of stimulation with norepinephrine. Furthermore, IP_4 returned to control levels within 45 seconds after stimulation with norepinephrine (data not shown). These data are consistent with rapid formation of 1,4,5-IP_3 and IP_4 following stimulation with norepinephrine. The delay in accumulation of IP_2, as well as, 1,3,4-IP_3 is also consistent with their being dephosphorylation products of 1,4,5-IP_3 and 1,3,4,5-IP_4, respectively.

DISCUSSION

The appearance of IP_4 in response to hormonal stimulation of a number of different tissue types has been well documented (for review, see (23)). However, these results are the first evidence demonstrating the production of IP_4 in cardiac tissue. IP_4 accumulated in adult canine myocytes after only 30 seconds of norepinephrine stimulation but was not measured in either unstimulated myocytes or in myocytes stimulated with norepinephrine for 45 or 60 seconds. Thus accumulation and removal of IP_4 occurs rapidly. Although IP_4 most likely results from phosphorylation of 1,4,5-IP_3 we cannot exclude the possibility that phosphatidylinositol 3,4,5-trisphosphate (PIP_3) exists in cardiac tissues. Preliminary studies of ^{3}H-inositol and $^{32}PO_4$ labelled adult and neonatal rat cardiac myocytes demonstrated a polyphosphoinositide more polar than phosphatidyinositol 4,5-bisphosphate that chromatographed on TLC similar to PIP_3 reported in neutrophils (24) (Rubin, unpublished observations). The absence of IP_4 at times longer than 30 seconds of norepinephrine stimulation suggests that IP_4 is rapidly removed, probably by dephosphorylation to 1,3,4-IP_3 as has been demonstrated in other tissues; 1,3,4-IP_3 accumulated only after 60 seconds of norepinephrine stimulation consistent with its formation from IP_4.

Although we have made no attempt to separate the isomers of IP_4 (15), the kinetics of the appearance of 1,3,4-IP_3 and disappearance of IP_4 suggests that the IP_4 measured in these studies is 1,3,4,5-IP_4 and not 1,4,5,6-IP_4 (15). The enzyme that cleaves the 5-phosphate from 1,4,5-IP_3 also cleaves the 5-phosphate from 1,3,4,5-IP_4, forming 1,3,4-IP_3 (25). This enzyme, 5-phosphomonoesterase, dephosphorylates 1,3,4,5-IP_4 at a slower rate than 1,4,5-IP_3 but has a higher affinity for 1,3,4,5-IP_4. Therefore, at low concentrations of 1,3,4,5-IP_4, as measured in this study, 1,3,4,5-IP_4 is dephosphorylated more rapidly than 1,4,5-IP_3 and may competitively inhibit the dephosphorylation of 1,4,5-IP_3 (8).

Both 1,4-IP_2 and 1,3-IP_2 accumulated after 60 seconds of stimulation with norepinephrine indicating dephosphorylation of 1,4,5-IP_3 and 1,3,4-IP_3 by 5-phosphomonoesterase (25) and inositol polyphosphate 4-phosphomonoesterase (20) respectively. Although small amounts of 3,4-IP_2 were detected, these levels did not change with norepinephrine stimulation suggesting either that dephosphorylation of 1,3,4-IP_3 by inositol 1-phosphomonoesterase is slow or that the

hydrolysis of 3,4-IP_2 to inositol monophosphate is so fast that this metabolite does not accumulate. No attempt was made to measure IP_1 isomers. As discussed above for IP_4, we cannot exclude the possibility that either the 1,4-IP_2 and/or the 1,3-IP_2 isomer could be derived from diesteratic cleavage of either phosphatidylinositol 4-phosphate or phosphatidylinositol 3-phosphate (26) respectively.

Previous work with cardiac tissue has indicated that there is (11) or is not (10) a 1,3,4,5-IP_4/1,3,4-IP_3 pathway of inositol phosphate metabolism following hormonal stimulation. These studies used ^{3}H-inositol to prelabel the inositol pools and subsequently determined the radiolabel appearing in different inositol phosphate fractions. This method has several disadvantages. Adequate and equilibrium labelling of phosphatidylinositol pools is rarely achieved such that a quantitative assessment of inositol phosphate production is unattainable. In addition, pharmacologic interventions, such as inhibition of inositol phosphate degradation by LiCl are required to produce measurable accumulations of inositol phosphates. The method used in the present study and detailed previously (16) circumvents these problems by directly determining the mass of each isomer of inositol phosphates. Thus, previous difficulties in determining 1,3,4,5-IP_4 production may have been due either to inadequate labeling of polyphosphoinositides or the rapid removal of 1,3,4,5-IP_4 may have precluded detection.

Although an important physiologic role for 1,3,4,5-IP_4 has not been firmly established, a number of interesting possibilities have been reported. In xenopus oocytes 1,3,4,5-IP_4 increases Ca^{++} entry (7), while this isomer has also been shown to prolong the Ca^{++}-mobilizing activity of 1,4,5-IP_3 (8), possibly by acting as a competitive inhibitor for 5-phosphate dephosphorylation (25). In addition, 1,3,4,5-IP_4 acts synergistically with 1,4,5-IP_3 in activating a Ca^{++}-dependent K^+ conductance (27). In cardiac tissue, 1,3,4,5-IP_4 may play an important role in modulating the second messenger activities of 1,4,5-IP_3, particularly the Ca^{++} mobilizing abilities. Therefore, the identification of 1,3,4,5-IP_4 in cardiac tissue has significant implications for our understanding of intracellular "second messenger" mechanisms.

ACKNOWLEDGEMENTS

This work was supported by NIH grant HL-34161 to Jeanne Nerbonne, NIH grant HL-17646 SCOR in Ischemic Heart Disease and NIH grants HL-28995 and HL-36773 to Peter B. Corr. Guy P. Heathers was supported by a Research Fellowship from the American Heart Association, Missouri Affiliate. The authors wish to thank Alex S. Evers for instrumental discussions, Evelyn M. Kanter for preparation of the myocytes and Ava Ysaguirre for preparation of the manuscript.

REFERENCES

1. Berridge, M.J., and Irving, R.F. (1984) Nature 312, 315-321.

2. Downes, C.P., Mussat, M.C., and Michell, R.H. (1982) Biochem. J. 203, 169-177.

3. Batty, I.R., Nahorski, S.R., and Irvine, R.F. (1985) Biochem. J. 232, 211-215.

4. Irvine, R.F., Letcher, A.J., Heslop, M.J., and Berridge, M.J. (1986) Nature (London) 320, 631-634.

5. Inhorn, R.C., Bansal, V.S., and Majerus, P.W. (1987) Proc. Natl. Acad. Sci. U.S.A> 84, 2170-2174.

6. Streb, H., Irvine, R.F., Berridge, M.J., Schulz, I. (1983) Nature 306, 67-69.

7. Irvine, R.F., and Moor, R.M. (1986) Biochem. J. 240, 917-920.

8. Joseph, S.K., Hansen, C.A., and Williamson, J.R. (1987) FEBS Lett. 219, 125-129.

9. Woodcock, E.A., White, L.B.S., Smith, A.I., and McLeod, J.K. (1987) Circ. Res. 61, 625-631.

10. Woodcock, E.A., Smith, I.A., Wallace, C.A., and White, L.B.S. (1987) Biochem. Biophys. Res. Commun. 148, 68-77.

11. Renard, D., and Poggioli, J. (1987) FEBS Lett. 217, 117-123.

12. Rittenhouse, S.E., and Sasson, J.P. (1985) J. Biol. Chem. 260, 8657-8660.

13. Heathers, G.P., Yamada, K.A., Kanter, E.M., and Corr, P.B. (1987) Circ. Res. 61, 735-746.

14. Atwood, J.G., Schmidt, G.J., and Slavin, W. (1979) J. Chromat. 171, 109-115.

15. Shears, S.B., Parry, J.B., Tang, E.K.Y., Irvine, R.F., Michell, R.H., and Kirk, C.J. (1987) Biochem. J. 246, 139-147.

16. Heathers, G.P., Juehne, T., Rubin, L.J., Corr, P.B., and Evers, A.S. (1988) Anal. Biochem. (submitted).

17. Bansal, V.S., Inhorn, R.C., and Majerus, P.W. (1987) J. Biol. Chem. 262, 9444-9447.

18. Lowry, O.H., Rosebrough, N.J., Farr, A.L., and Randall, R.J. (1951) J. Biol. Chem. 193, 265-275.

19. Downes, C.P. and Michell, R.H. (1981) Biochem. J. 198, 133-140.

20. Shears, S.B., Storey, D.J., Morris, A.J., Cubitt, A.B., Parry, J.B., Michell, R.H. and Kirk, C.T. (1987) Biochem. 242, 393-402.

21. Inhorn, R.C., Bansal, V.S., and Majerus, P.W. (1987) Proc. Natl. Acad. Sci. U.S.A. 84, 2170-2174.

22. Heathers, G.P., Evers, A.S. and Corr, P.B. (1988) (submitted).

23. Majerus, P.W., Connolly, T.M., Bansal, V.S., Inhorn, R.C., Ross, T.S., and Kips, D.L. (1988) J. Biol. Chem. 263, 3051-3054.

24. Traynor-Kaplan, A.E., Harris, A.L., Thompson, B.L., Taylor, P. and Sklar, L.A. (1988) Nature 334, 353-356.

25. Connolly, T.M., Bansal, V.S., Bross, T.E., Irvine, R.F., and Majerus, P.W. (1987) J. Biol. Chem. 262, 2146-2149.

26. Whitman, M., Downes, C.P., Keeler, M., Keller, T., and Cantley, L. (1988) Nature, 332, 644-646.

27. Morris, A.P., Gallacher, D.V., Irvine, R.F. and Peterson, O.H. (1987) Nature 330, 653-655.

Vol. 156, No. 1, 1988 BIOCHEMICAL AND BIOPHYSICAL RESEARCH COMMUNICATIONS
October 14, 1988 Pages 493-499

EVIDENCE FOR A DIFFERENTIAL PHYSIOLOGICAL MODULATION OF BROWN FAT IODOTHYRONINE 5'-DEIODINASE ACTIVITY IN THE PERINATAL PERIOD

M.Giralt, I.Martin, T.Mampel, F.Villarroya,
R.Iglesias and O.Viñas

Unitat de Bioquimica i Biologia Molecular B,
Departament de Bioquimica i Fisiologia. Universitat de Barcelona,
Diagonal 645, 08071-Barcelona. Spain

Received July 26, 1988

SUMMARY: Brown adipose tissue iodothyronine 5'-deiodinase increases progressively in fetuses from the day 17 of pregnancy on, it reaches peak values on the 20th day of gestation and declines in the last days of fetal life as well as during the first day of life. Birth of premature fetuses causes a sudden drop in the enzyme activity. Postmaturity is associated to a decrease in brown fat 5'-deiodinase similar to that found after birth in fetuses born at term. In the first hours of life brown fat iodothyronine 5'-deiodinase is essentially insensitive to the cold-stimulus. Present data indicates that, differently from adult rats, brown fat iodothyronine 5'-deiodinase activity during the perinatal period is dissociated from the thermogenic activity of the tissue. It is suggested that factors different from the action of the sympathetic nervous system may play a main role in brown fat iodothyronine 5'-deiodinase activity modulation in the fetal and neonatal life. © 1988 Academic Press, Inc.

INTRODUCTION: Since iodothyronine 5'-deiodinase activity was first described in brown adipose tissue a few years ago (1,2), an active research has been developed on its physiological significance and regulation. Similarly to what occurs with the thermogenic activity of the tissue, brown fat iodothyronine 5'-deiodinase in the adult rat is mainly modulated by the action of the noradrenaline coming from the sympathetic innervation to the tissue (2,3). This fact explains the concurrence between brown fat thermogenesis and iodothyronine 5'-deiodinase activity in different physiological situations (4,5,6) and it has been proposed that "in situ" T_3 generation, thanks to the 5'-deiodination of T_4, may be an important event related to the biochemical mechanisms of brown fat thermogenesis and specially to the modulation of uncoupling protein gene expression (7).

Brown fat thermogenesis is specially active during the neonatal period (8) .When we previously studied the changes in iodothyronine 5'-

0006-291X/88 $1.50
Copyright © 1988 by Academic Press, Inc.
All rights of reproduction in any form reserved.

deiodinase activity in rat brown adipose tissue during development, an increase in the enzyme activity was found a few days after birth with respect to the immediately postnatal levels (9). This neonatal increase was closely parallel with the augmented brown fat thermogenesis in this period (10). However, values of brown fat iodothyronine 5'-deiodinase in fetuses two days before birth were found to be extremely high, much more than those of the postnatal peak and in the range of the values corresponding to maximally cold-stimulated brown fat iodothyronine 5'-deiodinase in adult rats (9). This was a surprising finding as fetal brown fat does not show a high thermogenic activity nor it is subjected to physiological stimulus, such as cold environment, that stimulate the enzyme activity in adult rodents (8). Thus, fetal life appeared to be probably the first physiological, not-pathological, situation when a dissociation between brown fat thermogenesis and iodothyronine 5'-deiodinase activity was found.

The aim of the present work has been to study the main physiological modulation of iodothyronine 5'-deiodinase in the perinatal period, in order to assess its differential features with respect to the adult animals. The sequential changes in brown fat iodothyronine 5'-deiodinase activity during the fetal and a few hours postnatal life of the rat have been determined. The role of birth, pre- and post-maturity, and postnatal environment temperature have been also studied.

METHODS: Female Wistar rats (200-210 g b.w.) were mated with adult males and the day of pregnancy was determined by the presence of spermatozoals in vaginal smears. They were fed with a stock diet (A03 type, Panlab, Spain) and kept in a controlled environment (12 h light-dark cycles), environment temperature being 21 ºC unless otherwise stated. When the profile of prenatal changes in brown fat iodothyronine 5'-deiodinase activity was studied, caesarian sections of pregnant rats in the day 17, 18, 19, 20, 21 or 21.5 of gestation were performed in a thermostatized chamber (37 ºC). Fetuses were extracted and the interscapular brown adipose tissues of each litter were removed and pooled . When the postnatal period was studied, pups remained with their mother after spontaneous delivery and they were sacrificed at 0 (considered as when all pups are born but they have not still initiated suckling) 2, 6, 12 and 24 hours after birth. For studies on the effects of postnatal environment temperature, fetuses were extracted by caesarian section in the thermostatized chamber (37 ºC). Two-three pups were sacrificed immediately (0 hours) and half the remaining litter was placed at 21 ºC whereas the other half was kept at 37ºC. This study was performed in at-term (day 21.5 of pregnancy) premature (day 20.5 of pregnancy) and postmature (day 22.5 in pregnant rats treated daily with 7 mg of subcutaneous progesterone from the day 20 of pregnancy, on) fetuses. Pups were sacrificed 2, 12 and 24 hours after birth, with the exception of the postmature group that was studied only at 2 and 12 hours of extrauterine life. In all the cases, fetuses or pups were killed by beheading, interscapular brown adipose tissue was extracted, immediately frozen in dry-ice and kept at -80ºC until further processing. Frozen brown adipose tissue samples were weighed and homogenized in ice cold

0.32 M sucrose, 10 mM HEPES (Sigma), 10 mM DTT (Calbiochem), pH 7.0. Homogenates were centrifuged at 80 x g for 10 min, the fat supernatants were discarded and the infranatants were used for the iodothyronine 5'-deiodinase assay. The protein content was determined as already reported (11). Outer-ring (5') deiodinating activity was assayed by quantifying the $^{125}I^-$ liberated from L-(5'-^{125}I)-rT_3 as previously described (1,12). The enzymatic activity was assayed at a final concentration of 2 nM rT_3, 0.2 nM purified L-(5'-$^{123}I^-$)-rT_3 (5000 cpm/fmols), 20 mM DTT, 0.1 M potassium phosphate buffer (pH 7.0), 1 mM EDTA. Incubations had a final volume of 100 µl containing 0.2-0.3 mg of infranatant protein and they were performed on a shaking bath, at 37 ºC under nitrogen atmosphere during 60 min and were stopped by adding 50 µl ice-cold diluted calf serum/10 mM propylthiouracil (1:1) and 350 µl 10% trichloroactetic acid. Separation of iodine from iodothyronines was done by ion-exchange chromatography on Dowex-50W-X2 (Biorad) columns equilibrated in 10% acetic acid (12). Assays were performed in triplicate. Non enzymatic I^- production was assessed by incubations of free tissue medium and used as blank control. High specific activity L-(5'-^{125}I)-rT_3 was obtained by radio-iodination with $^{125}I^-$(IMS-30, Amersham) using 3,3'-diiodothyronine as substrate (13). Statistical significance of comparisons between groups were performed by means of the Student's t test.

RESULTS AND DISCUSSION: The pattern of pre- and immediately postnatal levels of iodothyronine 5'-deiodinase activity in rat brown adipose tissue is depicted in Fig. 1. Brown fat iodothyronine 5'-deiodinase activity is already detectable in the day 17 of the fetal life, it increases progressively from the day 18 on and reaches its maximum in fetuses at the day 20 of gestation. The 5'-deiodinase activity declines

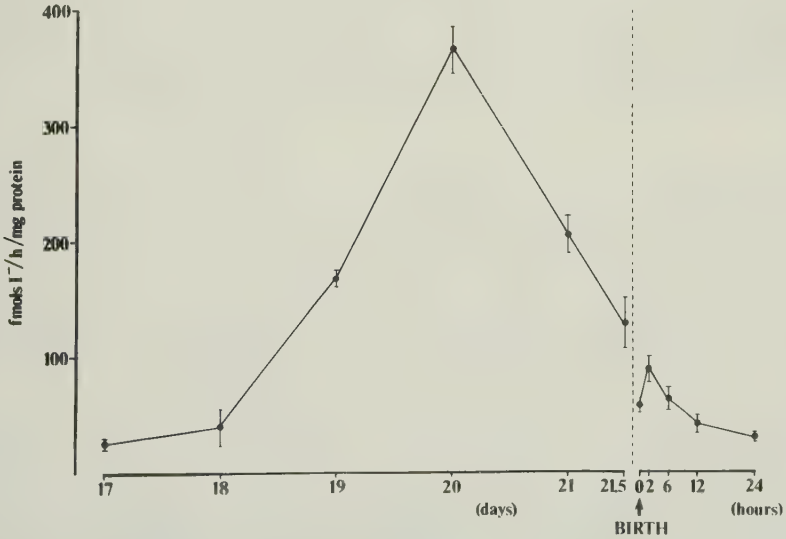

Figure 1
Iodothyronine 5'-deiodinase activity (fmols I^-/h/mg protein) in rat brown adipose tissue during the fetal and immediately postnatal life. Each point represents the means ± SEM of 5-8 litters of the age indicated. For each litter individual fetal or neonatal brown adipose tissues had been pooled.

during the last days of the fetal life and pups at birth show enzyme activity levels similar to those found in fetuses from 18-day pregnant rats. Brown fat iodothyronine 5'-deiodinase activity continues to decrease throughout the first day of life. The peak values of 5'-deiodinase activity in the day 20 of gestation are quantitatively important, in the range of those reported for adult rats in situations of maximally stimulated brown fat 5'-deiodinase activity, such as cold exposure (2,5).

Table 1 summarizes the effects of birth and environment temperature on brown fat iodothyronine 5'-deiodinase activity. Caesarian sections of fetuses in the day 20.5 of gestation (premature birth) cause a sudden drop in brown fat 5'-deiodinase activity which attain, after two hours of extrauterine life, levels similar than those found in two-hour old pups born at-term. Postmature fetuses (day 22.5 of gestation in progesterone-treated mothers) show a lowered iodothyronine 5'-deiodinase activity when compared with at-term fetuses whereas their enzyme activity levels are not significantly different from 24 hours-old pups born at-term. Fetuses from progesterone-treated mothers sacrificed at term showed levels of 5'-deiodinase activity (115 ± 14 fmols I^-/h/mg

Table 1

Iodothyronine 5'-deiodinase activity in brown adipose tissue from rat pups different hours after caesarian section. Effect of gestational age and environment temperature

Hours after caesarian section		Premature	At-term	Postmature
0		226 ± 35 +	122 ± 17 +	51 ± 6 +
2	37ºC	71 ± 14	72 ± 7	40 ± 8 +
	21ºC	70 ± 6	54 ± 8	36 ± 3
12	37ºC	35 ± 5	48 ± 10	67 ± 13
	21ºC	74 ± 16	79 ± 11	80 ± 8
24	37ºC	23 ± 7	28 ± 8	-
	21ºC	46 ± 11	49 ± 5 *	-

For experimental details see Methods section. Results are expressed as fmols I^-/h/mg protein. They are means ± SEM of samples corresponding to 5-8 litters. Statistical significance ($p < 0.05$) of comparisons between pups of the same postnatal age but maintained at different environment temperatures is shown by *. Statistical significance ($p < 0.05$) of comparisons between premature or postmature pups of the same age and environment temperature, and at-term pups is shown by +

protein) that were not significantly different from those in fetuses from untreated dams. Concerning the effects of environment temperature in neonatal brown fat 5'-deiodinase, data in Table 1 indicate that a substantial cold-stress (21ºC) during the first day of extrauterine life does not cause important changes in the brown fat 5'-deiodinase activity of neonates born at-term nor in premature or postmature fetuses, when compared with pups maintained at 37ºC. Only 24 hours after birth, pups born at-term and kept at 21 ºC showed a significant but slight increase in the enzyme activity.The profile of decay in brown fat 5'-deiodinase during the first day of extrauterine life in at-term fetuses extracted by caesarian section was essentially the same than the observed in spontaneously born pups (see Fig 1). These last data can be summarized as that birth appears not to be necessary for the decrease in brown adipose tissue 5'-deiodinase that occurs perinatally but, if birth occurs in a moment of intrauternine life when brown fat 5'-deiodinase is high, it causes a sudden decrease in the enzyme activity.

The overall results presented here on brown fat 5'-deiodinase in the pre- and immediately postnatal life of the rat point to a differential behavior of this enzyme activity in the perinatal period when compared with the adult, specially when its relationship with the thermogenic activity of the tissue is considered. Thus, a very high 5'-deiodinase activity occurs in the fetal life when thermogenesis is not activated. whereas after birth, when the mechanisms of brown fat thermogenesis and specially the uncoupling protein gene expression are rapid and highly increased (14), iodothyronine 5'-deiodinase activity declines progressively. Furthermore iodothyronine 5'-deiodinase in brown fat appears to be considerably insensitive to the cold stimulus in the first hours of life, differently from what occurs in adults and even in 15-day old pups (9).

This characteristic behavior of iodothyronine 5'-deiodinase activity in brown fat during the pre and immediately postnatal life raises the question of which can be the mechanisms that induce such a profile of enzyme activity changes during the perinatal period. First it is considered that the sympathetic nervous system innervating brown adipose tissue is not fully developed neither in the fetal life nor in the first hours after birth (8). Thus, noradrenaline, the main physiological modulator of brown fat 5'-deiodinase in adult rats (4) would not be probably the responsable for the changes in the enzyme activity reported here and specially for the high prenatal activity levels. Among the other hormonal factors known to influence brown fat 5'-deidoinase activity ,the recent report of insulin as a powerful stimulator of brown fat iodothyronine 5'-deiodinase in adult rats (15) probablv needs

special atention. The pattern of changes of fetal and neonatal brown fat 5'-deiodinase levels, the ability of premature birth to cause a sudden decline in the enzyme activity and the lowered brown fat iodothyronine 5'-deiodinase in postmature fetuses are in a striking good parallelism with the known changes in circulating insulin levels in these situations (16,17). Thus, further research will be necessary to elucidate if insulin action would play a main role in the modulation of fetal and neonatal brown fat iodothyronine 5'-deiodinase activity.

Concerning the possible functional role of brown fat iodothyronine 5'-deiodinase activity in the periods studied here, the lack of concurrence between thermogenic and 5'-deiodinase activities seems to exclude the possibility of a direct role of the locally produced T_3 in the modulation of the degree of uncoupling protein gene expression during the perinatal period, differently from what has been suggested for adult animals (7). However, the question of the possible functional role of the prenatal peak in the enzyme activity remains to be solved. Recently it has been proposed that a high fetal "in situ" T_3 generation may be involved in the prenatal differentiation of brown adipose tissue and specially in the induction of the uncoupling protein gene expression. This proposal has been formulated from the comparison between the profile of iodothyronine 5'-deiodinase activity and the sequential appearance of the mRNAs corresponding to mitochondrial proteins in the prenatal development of brown fat in bovines (Giralt et al. manuscript sent for publication). Our present data suggest that this hypothesis may be extended to the prenatal development of brown fat in rodents, that would be good models for future research on the relationships between prenatal iodothyronine 5'-deiodinase activity and brown fat differentiation.

ACKNOWLEDGEMENTS

This work has been supported in part by Direccion General de Investigación Científica y Técnica. Ministerio de Educación y Ciencia (Grant PB-577/86) and CIRIT. Generalitat de Catalunya. Spain.

REFERENCES

1. Leonard, J.L., Mellen, S.A. and Larsen, P.R. (1983) Endocrinology 112, 1153-1155 .
2. Silva, J.E. and Larsen, P.R. (1983) Nature 305, 712-713.
3. Jones, R., Henschen, L., Mohell, N. & Nedergaard, J. (1986) Biochim. Biophys. Acta. 889, 366-373.
4. Silva, J.E. and Larsen, P.R. (1985) J. Clin. Invest. 76, 2296-2305.
5. Fernandez, J.A., Mampel, T., Villarroya, F. and Iglesias, R. (1987) Biochem. J. 243, 281-284.

6 Giralt,M., Villarroya,F., Mampel,T., and Iglesias,R. (1986) Biochem. Biophys. Res. Commun. 138, 1315-1321.
7 Bianco,A.C. and Silva,J.E. (1987) J. Clin. Invest. 249, 5421-5427.
8 Nedergaard,J., Connolly,E. and Cannon,B. (1986) Brown Adipose Tissue. P.Trayhurn and D.G.Nicholls, eds. pp 152-213. Edward Arnold. London.
9 Iglesias,R., Fernandez,J.A., Mampel,T., Obregón,M.J. and Villarroya,F. (1987) Biochim. Biophys. Acta 923, 233-240.
10 Sundin,U. and Cannon,B. (1980) Comp. Biochem. Physiol. B 65, 463-471.
11 Wang,S. and Smith,L.R. (1975) Anal. Biochem. 63, 414-417.
12 Leonard,J.L. and Rosenberg,I.N. (1980) Endocrinology 107, 1376-1383.
13 Kochupillai,N. and Yallow,R.S. (1978) Endocrinology 102, 128-135.
14 Ricquier,D., Bouillaud,F., Toumelin,P., Mory,G., Bazin,R., Arch,J., Pénicaud,L. (1986) J. Biol. Chem. 30, 13905-13910.
15 Silva,J.E. and Larsen,P.R. (1986) Am. J. Physiol.251, E639-E643.
16 Sodoyez-Goffaux,F., Sodoyez,J.C. and De Vos,C.J. (1979) J. Clin. Invest. 63, 1095-1102.
17 Portha,B., Rosselin,G. and Picon,L. (1975) Diabetologia 11, 370-371.

Vol. 156, No. 1, 1988 BIOCHEMICAL AND BIOPHYSICAL RESEARCH COMMUNICATIONS
October 14, 1988 Pages 500-505

CHARACTERIZATION OF EPITOPES ON THE CATIONIC PEANUT PEROXIDASE BY FOUR MONOCLONAL ANTIBODIES

Chunfang Hu and Robert B. van Huystee

Department of Plant Sciences, The University of Western Ontario, London, Ontario N6A 5B7, Canada

Received August 15, 1988

The epitope sites on the cationic peanut peroxidase were characterized by four monoclonal antibodies raised against this isozyme. Evidence is presented showing that the epitope for monoclonal antibody 1B is located on the polypeptide. Sensitivity of the epitopes recognized by 1M and 2F to 0.1M HCl, boiling, 10 mM periodate and trifluoromethane sulfonic acid treatment indicate that they occur at regions where oligosaccharides are linked to the polypeptide backbone. The antigenic specificity of 2A is, in addition, dependent on the conformation of the epitope site which is destroyed after partial proteolysis of the peroxidase. © 1988 Academic Press, Inc.

Proteins are multideterminant antigens. They elicit in the immunized animals a variety of heterogeneous antibody families, each family being comprised of members able to recognized one particular epitope on the surface of the protein (1,2,3). The advent of hybridoma technology (4) to produce monoclonal antibodies (McAb), each of which recognizes a specific antigenic site or epitope, has provided a powerful tool for elucidating the complex antigenic structures of proteins (2).

The cationic peanut peroxidase is a glycohemoprotein (5) containing about 20% N-linked oligosaccharides (manuscript submitted). Ten McAbs were previously produced against this peroxidase and were divided into four groups according to their binding specifities to the antigen (6). In the present study, the molecular nature of the epitopes recognized by McAbs 1M, 1B, 2A and 2F, each representing an antibody group, was determined by the reactivities of the antibodies towards chemically modified or

0006-291X/88 $1.50
Copyright © 1988 by Academic Press, Inc.
All rights of reproduction in any form reserved.

partially fragmented cationic peroxidase in enzyme-linked immunosorbent assay (ELISA) or Western blotting.

Materials and Methods

Isolation of the cationic peroxidase and production of McAbs. The peroxidase was isolated from the spent medium of peanut cell suspension culture according to Chibbar and van Huystee (7). Fusion of spleen cells from mice immunized with purified cationic peroxidase and myeloma cells, cloning of hybridomas for McAb production and preliminary characterization of the specific McAbs were reported (6).

Chemical modification of the cationic peroxidase. The peroxidase was deglycosylated by trifluoromethane sulfonic acid (TFMS, Aldrich Chemical Company) according to Edge *et al* (8) or modified by treatment with 10 mM Na metaperiodate, 0.1 M HCl or boiling essentially as described by Homan *et al* (9). Briefly, purified cationic peanut peroxidase at 1 mg/ml was incubated with 10 mM $NaIO_4$ in 50 mM Na acetate buffer pH 4.5 at 4°C for 1 or 18 h in the dark. At the end of this period, the mixture was neutralized with addition of ethylene glycol to a final concentration of 16% and/or 10 times concentrated PBS (phosphate buffered saline). For acid treatment, the cationic peroxidase (1 mg/ml) was incubated with 0.1 M HCl for 24 h at room temperature and neutralized by addition of 3 N NaOH. Alternatively, the peroxidase was kept at 100°C over a water bath for 5 h. The samples were then dialyzed against (for samples treated with periodate or acid)or resuspended in (for the boiled sample) the coating buffer for ELISA (0.05 M Na bicarbonate pH 9.6) for latter assay of antibody activities. The controls were not boiled or were kept under the same conditions with omission of the chemicals.

Partial proteolysis. The purified cationic peroxidase was digested under denaturing conditions by incubation with *S. aureus* V_8 protease (Miles Laboratory), trypsin or chymotrypsin (Boehringer Mannheim Biochemica) at a substrate:enzyme ratio of 15:1 at 37°C for 15 minutes according to Cleveland *et al* (10).

SDS polyacryamide electrophoresis (PAGE) and Western blotting. The TFMS deglycosylated cationic peroxidase or partially proteolytically cleaved peroxidase peptides were separated on SDS-PAGE and blotted to nitrocellulose membranes as described (6).

Others. ELISA was performed as described (6). Protein contents were measured according to Lowry *et al* (11).

Results

To elucidate the molecular nature of the epitope sites recognized by these antibodies, the effects of treatments of the cationic peroxidase with reagents destroying protein or carbohydrate structure on binding abilities of the McAbs were studied. The peroxidase was treated with 10 mM periodate, which oxidizes the vicinyl hydroxyl groups of carbohydrate residues while leaving the polypeptide intact (12,13), with 0.1 M HCl or boiling, which destroys the protein structure (9). Or it was deglycosylated by TFMS. Of the four McAbs tested, only 1B clearly

Table 1. Reactivities of monoclonal antibodies to chemically modified peanut cationic peroxidase as determined by ELISA. The hybridoma culture supernatants (1B 10^{-2}, 1M 10^{-1}, 2F 10^{-1}, 2A 10^{-0}) were assayed against control and treated cationic peanut peroxidase. Antibody binding was detected by the enzyme reaction of alkaline phosphatase conjugated to goat anti-mouse IgGs secondary antibodies. Each datum represents the mean±s.d. (n=3). The absorbance obtained with non-immune mouse IgGs has been substracted.

Treatment	A_{405}			
	1B	1M	2F	2A
10 mM $NaIO_4$				
Control	1.281±0.160	1.538±0.024	0.763±0.070	1.219±0.122
Treatment	1.303±0.149	0.703±0.065	0.153±0.022	0.653±0.055
% of Control	102	46	20	54
0.1 M HCl				
Control	1.201±0.098	1.456±0.103	0.831±0.075	1.266±0.250
Treatment	0.998±0.092	1.002±0.064	0.190±0.030	0.680±0.065
% of Control	83	69	23	54
Boiling				
Control	1.314±0.341	1.610±0.335	0.919±0.103	1.005±0.152
Treatment	0.641±0.231	0.605±0.025	0.005±0.001	0.153±0.054
% of Control	49	38	1	15

recognized a protein-defined epitope. This epitope was insensitive to either periodate oxidation (Table 1) or to TFMS-deglycosylation (Fig 1). On the other hand, the antibody activity of 1B was reduced to about half of the control when the peroxidase was boiled, and also slightly affected by acid treatment of the antigen, suggesting that 1B-epitope is located on the protein moiety of the peroxidase (Table 1).

The results obtained with McAbs 1M, 2F and 2H indicated that their epitopes seemed to be composed of both protein and carbohydrate groups. Pre-treatment of the cationic peroxidase with 10 mM periodate reduced the binding of these three antibodies. Results after 18 h incubation with periodate were presented in Table 1. Essentially the same effects were achieved with 1 h incubation (data not shown). Similarly, the antibody activities were abolished when the carbohydrate moiety was removed from the peroxidase by TFMS (Fig 1). Moreover, the epitopes recognized by these antibodies were sensitive to acid treatment and boiling (Table 1). However, the degree of involvement of carbohydrate seemed to vary among different epitopes. The antibody activity of 2F was decreased to approximately 20% that of control after periodation of the antigen, a two times greater reduction than that achieved when 2A

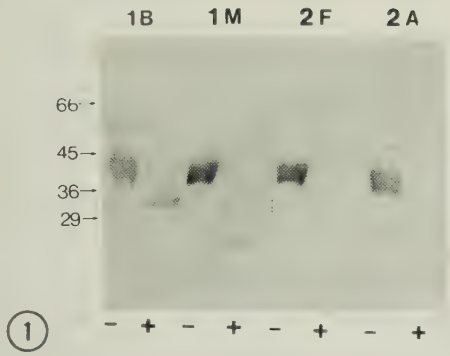

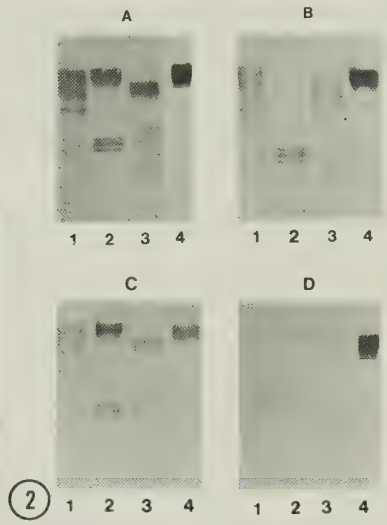

Fig 1. Western blotting of the deglycosylated cationic peanut peroxidase. The cationic peroxidase was incubated with TFMS for 3 h at 0°C. The protein recovered form the mixture and the control was electrophoresed and transferred to nitrocellulose membranes. The membranes were probed with McAbs 1B, 1M, 2F and 2A, respectively. -, control; +, deglycosylated peroxidass.

Fig 2. Western blotting of peptide fragments of the cationic peroxidase after partial proteolysis. Lane 1, digested with trypsin; 2, with V_8 protease; 3, with chymotrypsin and 4, control. Panel A, probed with 1B; B, 1M; C, 2F; D, 2A.

or 1M was used. In addition, the 2A-epitope was sensitive to all protease treatments suggesting that it is conformation- as well as protein-dependent (Fig 2D). On the other hand, some of the fragmented peptides were recognized by 1B, 1M and 2F (Fig 2A, B and C).

Discussion

We have investigated the molecular nature of the epitopes recognized by anti-cationic peanut peroxidase McAbs with the intention of determining the involvement, if any, of the carbohydrate side chains. Of the four McAbs studied, 1B recognized a protein- defined epitope. The results for McAb 1M was of particular interest. The 1M-epitope was affected by periodate oxidation, TFMS-deglycosylation as well as by boiling and acid treatment (Table 1, Fig 1). Thus, it appeared that 1M recognized a region on the cationic peroxidase that comprised of both protein and carbohydrate. This region must be in the vicinity of the enzyme active site, since 1M was previously shown to be inhibitory of peroxidase activity (6). This is not

impossible considering that there are two carbohydrate chains close or in the substrate access channel in the structural model suggested for plant peroxidase (14). Besides, carbohydrates were shown to be essential for the expression of peroxidase activity (manuscript submitted).

Similar to 1M, 2A and 2F seemed to recognized carbohydrate-containing epitopes. The binding of these antibodies were sensitive to treatments that modified protein or carbohydrate structure (Table 1, Fig 1). These results suggest that carbohydrate residues, in combination with protein sequences, form the reactive epitopes. Alternatively, removal of carbohydrate might induce considerable conformational changes such that protein-defined epitopes could no longer be recognized by these McAbs, since carbohydrates may interact with domains of the protein and thus modulate the conformation of a glycoprotein (15). To test these possibilities, the cationic peroxidase was partially digested with V_8 protease, trypsin or chymotrypsin. The fragmented peptides were subjected to SDS-PAGE and Western blotting (Fig 2). No staining of the peptides were observed by using 2A, suggesting that 2A-epitope is conformation- and protein-dependent. The peptide patterns recognized by 1B, 1M and 2F were similar. Because only relatively large fragments (>19 kD) were detected, no distinctions could be made between the binding specificities of 1M, 1B and 2F from Western blotting. At this time, it is uncertain whether the sensitivity of the 2A-epitope to carbohydrate-modifying treatments was due to a direct involvement of carbohydrate in the epitope or to a conformational change caused by the treatments. Nevertheless, it is clear from above that the four McAbs studied here belong to four antibody groups, which is in accordance with previous classification by competition experiment (6). In conclusion, both protein and carbohydrate moieties are antigenic in peanut peroxidase, as was true for many other glycoproteins (9,16,17,18). Monoclonal antibodies are well suited as probes for the surface structures of the enzyme.

Acknowledgment:This work was supported by a grant from Natural Sciences and Engineering Research Council of Canada.

References

1. Atassi, M.Z. (1984) Eur. J. Biochem. 145, 1-20

2. Benjamin, D.C., Berzofsky, J.A., East, I.J., Gurd, F.R.N., Hannum, C., Leach, S.J., Margoliash, E., Michael, J.G.,

Miller, A., Prager, E.M., Reichlin, M., Sercarz, E.E., Smith-Gill, S.J., Todd, P.E. and Wilson, A.C. (1984) Ann. Rev. Immunol. 2, 67-101

3. Geysen, H.M., Tainer, J.A., Rodda, S.J., Mason, T.J., Alexandeer, H., Getzoff, E.D. and Lerner, R.A. (1987) Science 235, 1184-1190

4. Köhler, G. and Milstein, C. (1975) Nature 256, 495-497

5. van Huystee, R.B. (1987) Ann. Rev. Plant Physiol. 38, 205-219

6. Hu, C., Carbonera, D. and van Huystee, R.B. (1987) Plant Physiol. 85, 299-3036.

7. Chibbar, R.N. and van Huystee, R.B. (1984) Plant Physol. 75, 294-298

8. Edge, A.S., Faltynak, C.R., Hof,L., Reichert, L.E.,Jr. and Weber, P. (1981) Anal. Biochem. 118, 131-137

9. Homan, W.L., van Kalshoven, H., Kolk, A.H.J., Musgrave, A., Schuring, F. and van den Ende, H. (1987) Planta 170, 328-335

10. Cleveland, D.W., Fischer, S.G., Kirschner, M.W. and Laemmli, U.K. (1977) J. Biol. Chem. 252, 1102-1106

11. Lowry, O.H., Rosebrough, N.L., Farr, L. and Randall, R.J. (1951) J. Biol. Chem. 193, 265-275

12. Woodward, M.P., Young, W.W. and Bloodgood, R.A. (1985) J. Immunol. Methods 78, 143-153

13. Dyer, J.T. (1956) Methods Biochem. Anal. 3, 112-152

14. Welinder, K.G. (1985) Eur. J. Biochem. 57, 497-504

15. Schwarz, R.T. and Datema (1982) In The Glycoconjugates (M.I. Horowitz,Ed), Vol. III,pp.47-79. Academic Press, New York London Toronto

16. Roberts, K., Phillipa, J., Shaw, P. and Smith, E. (1985) In Biochemistry of Plant Cell Walls (C.T. Brett & R. Hillman,Eds), pp.125-154. Cambridge University Press, Cambridge London New York

17. Stafstorm, J.P. and Staehelin, L.A. (1988) Planta 174, 321-332

18. Frelinger, A.L. and Rutishauser, U. (1986) J. Cell Biol. 103, 1729-1737

Vol. 156, No. 1, 1988 BIOCHEMICAL AND BIOPHYSICAL RESEARCH COMMUNICATIONS
October 14, 1988 Pages 506-510

PARADOXICAL PROTECTION OF BOTH PROTEIN-FREE AND HIGH PROTEIN DIETS AGAINST ACUTE AMMONIUM INTOXICATION

Vicente Felipo, María-Dolores Miñana and Santiago Grisolía

Instituto de Investigaciones Citológicas de la Caja
de Ahorros de Valencia, Centro Asociado del CSIC
Amadeo de Saboya 4, 46010 Valencia, SPAIN

Received August 12, 1988

SUMMARY. Rats were fed standard (20% protein), protein-free or high protein (80%) diets for 15 days and then injected intraperitoneally with ammonium acetate (7 mmol/Kg). Survival was 6%, 75% and 100%, respectively, for rats fed standard, protein-free and high protein diets. After injection of 6 mmol/Kg of ammonium acetate, blood ammonia reached a peak (at ca. 2 mM) after 7, 25 and 30 min for rats fed high protein, protein-free and standard diets, respectively. The results presented indicate that protection in the high protein group is due to faster detoxication of ammonia via a more active urea cycle while the tolerance of the protein-free group to higher levels of ammonia remains to be clarified. © 1988 Academic Press, Inc.

Hyperammonemia is thought to have an important role in encephalopathy. It has been reported that chronically hyperammonemic rats (porta-caval shunted) are more susceptible to ammonia challenge (1). However, we have shown recently that rats made hyperammonemic by feeding them ammonium are more resistant to acute ammonia intoxication (2). It appeared of interest, therefore, to test if rats fed a protein-free or a high protein diet would also have an altered susceptibility to acute ammonia intoxication. It is shown that ingestion of either the protein-free or the high protein diet protects the rats against a highly toxic intraperitoneal injection of ammonium acetate. The results presented suggest that for the high protein diet the protective effect is due to an accelerated elimination via a more active urea cycle, while the remarkably increased tolerance of rats fed a protein-free diet is puzzling and remains a subject for further study.

MATERIALS AND METHODS

Animals and diets. Male Wistar rats weighing 250-280 g were fed the following diets: standard, protein-free and high protein.

ABBREVIATION: CPS, carbamylphosphate synthase I

0006-291X/88 $1.50
Copyright © 1988 by Academic Press, Inc.
All rights of reproduction in any form reserved.

Standard diet (20% protein) was from PanLab, Spain; protein-free diet was protein depletion diet USP XV from ICN Biochemicals and high protein (80%) diet was prepared by mixing 1 part of standard diet with 3.8 parts of casein and 0.2 parts of mineral mixture (AIN mineral mixture 76, ICN Biochemicals). The drinking water was supplemented with 6 g/l of vitamin mixture (AIN vitamin mixture 76, ICN Biochemicals).

Metabolite and enzyme determinations. Blood was taken from the tail vein before and at different intervals after i. p. injection of 6 mmol/Kg of ammonium acetate. Ammonia was determined using glutamate dehydrogenase as in (3). Urea was determined colorimetrically as in (4). Tissues were removed and freeze-clamped immediately. Glutamine was determined as in (5) and acetylglutamate as in (6). Carbamyl phosphate synthase was assayed as in (7).

RESULTS AND DISCUSSION

ats were made chronically hyperammonemic by feeding them a protein-free or a high protein (80%) diet. The ammonia levels in blood after 15 days on diet were 177 ± 16 μM for rats on the control diet and 280 ± 11 and 416 ± 20 μM for rats on protein-free and high protein diets, respectively. Rats were then injected i. p. with 7 mmol/Kg of ammonium acetate. As shown in Table 1 survival was 6% for rats on standard diet but 75% and 100% for rats on protein-free and high protein diets, respectively. Moreover, of the non survivors,control rats died at 18 ± 5 min while those (three) on the protein-free diet died at 56 ± 4 min. It is therefore evident that ingestion of either protein-free or high protein diets had a marked protective effect against injection of high doses of ammonia.

This higher resistance to the ammonia challenge could be due to an increase in the ability to detoxicate ammonia. The main mechanism

TABLE 1. Effect of dietary protein on survival of rats following an ammonia challenge

Protein in diet %	Blood ammonia μM	Died	Survived	Survival time* min
0	280 ± 11	3	9	56 ± 4
20	177 ± 16	17	1	18 ± 5
80	416 ± 20	0	12	

Rats were fed the indicated diets for 15 days and then injected with 7 mmol/Kg of ammonium acetate. 18 rats were used in the control group and 12 rats in protein-free and high protein groups. Body weights at the time of injection were 199 ± 4 for rats on protein-free diet, 330 ± 12 for controls and 308 ± 10 for rats on high protein diet. Samples for blood ammonia determinations were taken at 9:00 a. m.
* Mean survival times of the rats which died.

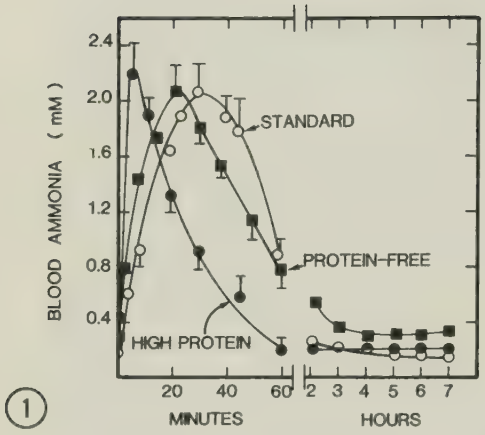

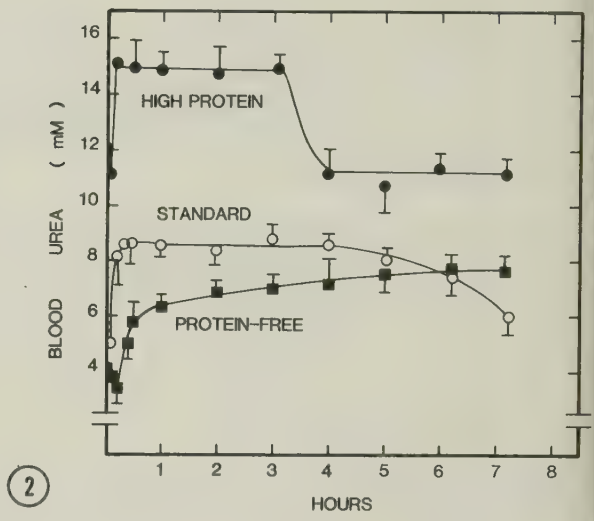

Figure 1. Ammonia levels in blood. Rats fed standard (○), protein-free (■) or high protein (●) diets for 15 days were injected i.p. at 9:00 a. m. with 6 mmol/Kg of ammonium acetate. Blood was taken from the tail vein at indicated times and ammonia levels in blood were determined as indicated in Materials and Methods. The standard deviations for the more relevant points are given.

Figure 2. Urea levels in blood. Experiments were carried out as in Fig. 1. Urea was determined as indicated in Materials and Methods. The standard deviations for the more relevant points are given.

of ammonia detoxication in ureotelic animals is the formation of urea in the liver. To assess if the experimental rats had an increased ability to detoxicate ammonia, control and experimental rats were injected with 6 mmol/Kg of ammonium acetate and the levels of ammonia and urea in blood were determined at various intervals. As shown in Fig. 1 the ammonia levels in blood reached similar values (ca. 2 mM). The maximums were reached after 30 min for controls and 7 min for high protein fed rats, suggesting that these rats were able to detoxicate ammonia more rapidly than controls. As shown in Fig. 2 rats fed the high protein diet also produced urea more rapidly than controls. This is not surprising since the carbamyl phosphate synthase activities were 4.9 and 10.6 U/mg of mitochondrial protein for rats fed standard and high protein diets, respectively. Also the basal levels of acetylglutamate (the physiological activator of CPS) which is thought to regulate urea formation (8-10) were 7, 43 and 170 pmol/g liver for rats on protein-free, standard and high protein diets, respectively, while 15 min after injection these levels rose to 211, 258 and 352 pmol/g liver. The rapid return of blood urea to basal levels could be explained by their greater glomerular filtration rate

which is known to occur in high protein diets (11). The protective effect of ingestion of a high protein diet against an acute ammonia challenge can therefore be attributed to its greater ability to rapidly detoxicate ammonia via a more active urea cycle. On the other hand, as shown in Fig. 1, rats on the protein-free diet reached blood ammonia levels similar to the controls (ca. 2 mM) with a maximum at nearly the same time (25 min). As also shown in Fig. 2, the increase in urea formation was less in rats on protein-free diet than in controls but the increase seems to have been maintained a longer time. Blood urea returned to basal levels in controls after 8 hours while at that time those of the rats fed the protein-free diet were still maximum. The increase of urea synthesis is due to both an increase of the substrate (ammonia) and of acetylglutamate. As shown above, the hepatic acetylglutamate in rats fed the protein-free diet was only 16% of controls and after injection of ammonium, reached 82% that of controls. Under these conditions the lower amount of CPS in livers of rats fed the protein-free could explain the slower formation of urea.

The above results show that both protein-free and high protein diets had a protective effect against acute intoxication with ammonium. However, while the protection by the high protein diet can be explained by a rapid detoxication of ammonia due to an increased activity of the urea cycle, this does not apply to the protein-free diet.

Possibly, ammonia in tissues is transiently sequestered by being incorporated into a non toxic metabolite which could gradually channel the ammonia to the urea cycle. A likely candidate is glutamine. The results shown in Table 2 indicate that ammonia is not

TABLE 2. Effect of ammonium ingestion on glutamine content in liver, brain and muscle

Protein in diet %	Injection	Liver	Brain μmol/g tissue	Muscle
20	No	6.64 ± 0.74	4.19 ± 0.46	4.37 ± 0.29
20	Yes	3.46 ± 0.32	7.99 ± 0.26	5.58 ± 0.56
0	No	5.13 ± 0.78	4.96 ± 0.53	4.88 ± 0.48
0	Yes	4.68 ± 0. 46	9.22 ± 0.46	5.03 ± 0.31

The experiments were carried out as in Table 1 and glutamine was determined as indicated in Materials and Methods.

stored as glutamine in the protein-free group. Experiments to assess if the protective effect of the protein-free diet is due to tolerance to higher ammonia levels or to a transient sequestration of ammonia as a non toxic metabolite need to be carried out.

ACKNOWLEDGEMENTS

Supported in part by Glaxo, the FISS of Spain and the IIC-KUMC International Cytology Program. Vicente Felipo is a "Severo Ochoa" fellow of the Fundación Ferrer.

REFERENCES

1. Cooper, A.J.L. and Lai, J.C.K. (1987) Neurochem. Pathol. 6, 67-95
2. Miñana, M.D., Felipo, V. and Grisolía, S. (1988) Biochem. Biophys. Res. Commun. 153, 979-984
3. Grisolía, S., Quijada, C.L. and Fernández, M. (1964) Biochim. Biophys. Acta 81, 61-70
4. Hunninghake, C. and Grisolía, S. (1966) Anal. Biochem. 16, 200-205
5. Lund, P. (1985) in Methods of Enzymatic Analysis (Bergmeyer, H.U., ed.) Vol. VIII, 3rd edition, pp 357-363 Verlag Chemie Weinheim
6. Cohen, N.S. (1984) Arch. Biochem. Biophys. 232, 38-46
7. Nuzum, C.P. and Snodgrass, P.J. (1976) in "The urea cycle" (Grisolía, S., Báguena, R. and Mayor, F., eds.) pp 325-355 John Wiley and Sons, New York
8. Cohen, P.P. and Grisolía, S. (1948) J.Biol.Chem. 174, 389-390
9. Grisolía, S. and Cohen, P.P. (1953) J.Biol.Chem. 204, 753-757
10. Caravaca, J. nad Grisolía, S. (1959) Biochem. Biophys. Res. Commun. 1, 94-97
11. Hostetter, T.H., Meyer, T.W., Rennke, H.G. and Brenner, B.M. (1986) Kidney Int. 30, 509-517

Vol. 156, No. 1, 1988 BIOCHEMICAL AND BIOPHYSICAL RESEARCH COMMUNICATIONS
October 14, 1988 Pages 511-516

Abscisic Acid Enhances Aggregation and Fusion of Phospholipid Vesicles

William Stillwell[1], Blair Brengle[1] and Stephen R. Wassall[2]

Departments of Biology[1] and Physics[2]
Indiana University-Purdue University at Indianapolis
Indianapolis, IN

Received August 15, 1988

SUMMARY: The plant hormone abscisic acid (ABA) is shown to enhance the aggregation and fusion of small unilamellar lipid vesicles composed of 80 mol% dimyristoylphosphatidylcholine (DMPC) and 20 mol% dimyristoylphosphatidylcholine (DMPE). Aggregation and fusion did not occur with single component (100 mol%) DMPC vesicles. Fusion was followed by two fundamentally different techniques, fluorescence resonance energy transfer which monitors intermixing of bilayers and ANTS-DPX which monitors intermixing of the sequestered aqueous interiors. It is suggested that a previously unreported role of ABA may be as a membrane fusagen. © 1988 Academic Press, Inc.

The plant hormone abscisic acid (ABA) participates through poorly understood mechanisms in a large variety of physiological processes (1). Among the rapid time responses affected by ABA are events clearly associated with membranes (2). The best defined of these are the ABA-induced closure of stomates (3) and ABA alteration in membrane permeability of various root tissues (4,5). Recently we have been studying the effect of ABA on phospholipid bilayer model membranes to elucidate the mode of action of ABA on natural membranes (6-11). Using a variety of biophysical techniques we have demonstrated that ABA significantly enhances membrane permeability to anions, cations and neutral solutes only if the hormone is in its undissociated state (pKa 4.85) and the membranes are composed of at least two different types of lipids. Despite the large effects of ABA on permeability, we could not demonstrate by ESR, NMR and fluorescence polarization significant binding of ABA to any bilayer membrane. From these observations we proposed that ABA is not affecting the entire membrane but instead is acting at regions of bilayer defects found between either two

Abbreviations: DMPC, dimyristoylphosphatidylcholine; DSPC, distearoylphosphatidylcholine; DMPE, dimyristoylphosphatidylethanolamine; DLPE, dilauroylphosphatidylethanolamine; RET, fluorescence resonance energy transfer; NBP-PE, N-4-nitrobenzo-2-oxa-1,3-diazole phosphatidylethanolamine; Rho-PE, lissamine rhodamine-B-Sulfonyl dioleoylphosphatidylethanolamine; ANTS, 8-aminonaphthalene-1,3,6-trisulfonic acid; DPX, p-xylene-bis-pyridinium bromide, ABA, abscisic acid.

0006-291X/88 $1.50
Copyright © 1988 by Academic Press, Inc.
All rights of reproduction in any form reserved.

different phospholipid head group types or between gel and liquid crystalline states with mixed acyl chain PC's. We also reported that ABA enhances membrane aggregation with bilayers of similar composition to those displaying ABA induced permeability (10). Since membrane aggregation is a necessary prerequisite to membrane fusion (12), and the process of fusion has been proposed to occur at regions of membrane defects (13), it is reasonable to propose that ABA may cause the fusion of membranes composed of the appropriate types of phospholipids. Experiments confirming this potential, unique role for ABA are presented here.

MATERIALS AND METHODS

Materials: The phospholipids DMPC, DMPE, DSPC and DLPE, and the fluorescent labeled lipids NBD-PE and Rho-PE were purchased from Avanti Polar Lipids, Birmingham, AL. The aqueous fluorescent molecule ANTS and its quencher DPX were bought from Molecular Probes, Eugene, OR. ±, *cis-trans* abscisic acid was from Sigma Chemical Co., St. Louis, MO.

Vesicle Preparation and Aggregation: Multilamellar vesicles (MLV's) were made as described by Bangham (14) from 90 mol% DMPC/10 mol% DMPE (10.3 mM) in 10 mM sodium acetate, pH 5.0. Small unilamellar vesicles (SUV's) were made by sonicating the MLV's for 6 min on ice at level 7 of a Heat Systems 220-F Cell Disruptor. After a brief centrifugation to remove titanium particles, the SUV's were rapidly mixed with appropriate amounts of ABA, also in 10 mM sodium acetate, pH 5.0. Vesicle aggregation was followed by an increase in turbidity at 350 nm (19°C) on a Beckman DU-8 Computing Spectrophotometer. Results are expressed as the change in absorbance as a function of time.

Fluorescence Resonance Energy Transfer: Fusion of vescicular membranes is followed by fluorescence resonance energy transfer (RET) which monitors the exchange of energy from a light absorbing membrane bound "donor" (NBD-PE) to an acceptor (Rho-PE)(15). Tow populations of SUV's containing 0.3 mol% NBD-PE and Rho-PE, respectively, were made as described above and were mixed at time zero. Lipid content was 2.5 mM in 40 mM sodium acetate, pH 5.0. RET was followed by exciting the mixed vesicles at 464.2 nm and measuring emission at 593.9 nm on a Perkin-Elmer MPF-66 Fluorescence Spectrophotometer. Results, expressed as the percentage of membranes fused over time, are calculated as described by Wang and Huang (16).

Aqueous Compartment Mixing: Fusion of vesicles was also followed with an ANTS-DPX assay that measures the intermixing of the aqueous sequestered compartments of vesicles (17). The highly fluorescent ANTS, initially sequestered in one population of vesicles, is quenched upon fusion by DPX initially trapped in a second vesicle population. SUV's were made as described above in buffers containing either 25 mM ANTS, 40 mM NaCl, 10 mM sodium acetate, pH 5.0 or 90 mM DPX, 10 mM sodium acetate, pH 5.0. Lipid concentration was 10 mM. Excitation was at 420 nm and emission at 513.6 nm. Results are expressed as the percentage of fusion as a function of time. A control experiment measuring fluorescence quenching due to vesicle leakage showed that less than 2.7% DPX diffused during the length of the presented experiments.

RESULTS

The results presented here demonstrate that ABA can induce aggregation and fusion of a mixed component bilayer membrane. The experiments are all

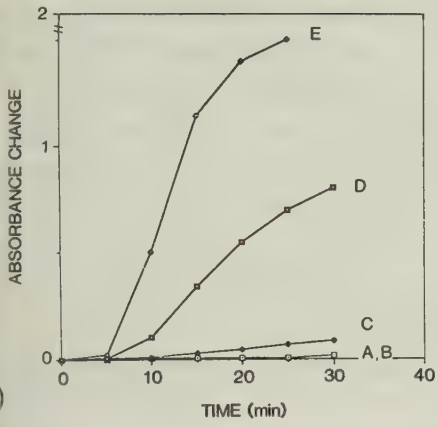

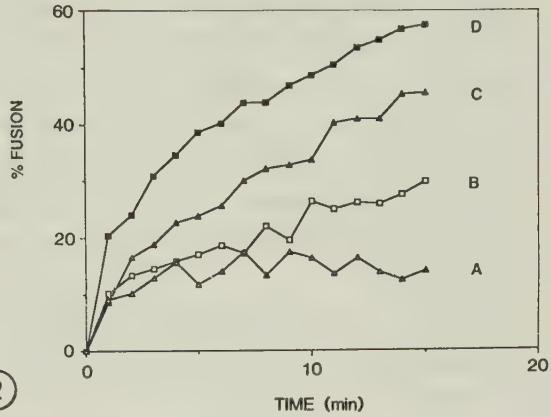

Figure 1. Effect of ABA on inducing aggregation of 90 mol% DMPC/10 mol% DMPE unilamellar vesicles at 19°C. Results are expressed as the increase in absorbance (turbidity) at 350mm. ABA:lipid molar ratios: A. 0.0; B. 0.0054; C. 0.054; D. 0.27; and E. 0.54.

Figure 2. Effect of ABA on inducing fusion of 90 mol% DMPC/10 mol% DMPE vesicles at 10°C as followed by the fluorescence resonance energy transfer method. ABA:lipid molar ratios: A. 0.0; B. 0.125; C. 0.25; and D. 0.50.

run at pH 5.0 which is close to the pKa of ABA, 4.85 (18). This pH is chosen because at lower pH's the solubility of ABA becomes limiting and our previous work measuring bilayer permeability showed that at higher pH's dissociated ABA was not very membrane active.

The ability of ABA to enhance aggregation of lipid vesicles composed of 90 mol% DMPC/10 mol% DMPE is presented in Figure 1. Clearly aggregation is ABA dependent as no increase in turbidity could be detected over 30 min without ABA. Experiments were also run with 20 mol% DMPE but, in the presence of ABA, they became turbid too rapidly for meaningful data to be obtained. Also 100 mol% DMPC bilayers were stable in the presence of ABA and did not aggregate (results not shown).

Fluorescence resonance energy transfer was used to follow the fusion of vesicles by observation of the intermixing of bilayer membranes. ABA did not enhance fusion at all with 100 mol% DMPC bilayers (results not shown). However, when a second component (DMPE) was included at 10 mol%, substantial ABA enhanced fusion was measured (Figure 2). A second mixed component membrane consisting of 90 mol% DSPC/10 mol% DLPE was also tested and, as shown in Figure 3, this membrane also demonstrated considerable ABA dependent fusion.

Finally, fusion was confirmed by the ANTS-DPX method which measures mixing of the vesicles aqueous cores. ABA did not enhance fusion for 100 mol% DMPC vesicles (results not shown) but demonstrated considerable fusion with the mixed component (90 mol% DMPC/10 mol% DMPE) vesicles (Figure 4).

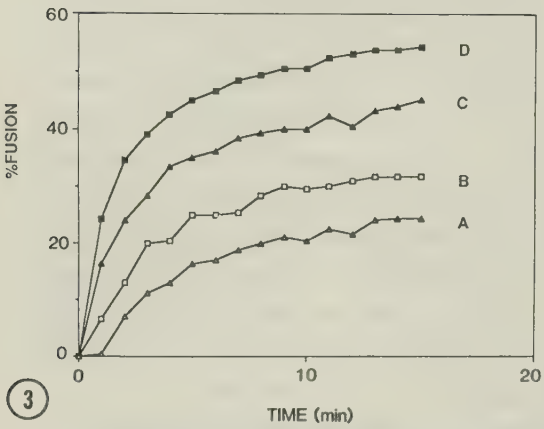

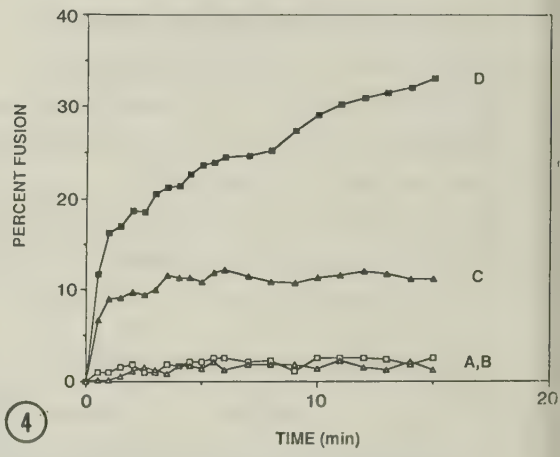

Figure 3. Effect of ABA on inducing fusion of 90 mol% DSPC/10 mol% DLPE vesicles at 15°C as followed by the fluorescence resonance energy transfer method. ABA:lipid molar ratios: A. 0.0; B. 0.125; C. 0.25; and D. 0.50.

Figure 4. Effect of ABA on inducing fusion of 90 mol% DMPC/10 mol% DMPE vesicles at 10°C as followed by the ANTS-DPX method. ABA:lipid molar ratios: A. 0.0; B. 0.125; C. 0.25; D. 0.50.

DISCUSSION

Fusion of various cellular membranes is essential for many physiological processes including membrane biogenesis, endocytosis, secretion and fertilization (19). This important mechanism has been studied for years without producing a clear picture of the sequence of molecular events. By use of protein free lipid bilayer model membranes some basic properties common to all membrane fusions have emerged. The process of fusion must: a. kinetically follow that of membrane aggregation (12); b. occur only over a very small portion of the coalescing membranes (20,21); and c. occur in regions of defects associated with fluctuations in lipid packing (22).

From our previous work with ABA and various phospholipid membranes we demonstrated that the hormone can greatly alter basic membrane properties such as permeability (6-9) and vesicle aggregation (10). Without significantly binding to any portion of the tested membranes from the aqueous interface all the way through to the membrane interior (11). From these experiments we proposed that ABA must be acting at regions of membrane defects where either differing lipid head groups do not pack properly or two different physical states coexist. Therefore conditions necessary for ABA-induced permeability and aggregation clearly parallel the conditions required for general membrane fusion.

In the experiment presented here for the first time we have investigated the possible role of a plant hormone in the process of membrane fusion. In Figure 1 we report the effect of ABA on promoting aggregation of a mixed

component DMPC/DMPE phospholipid membrane. More detailed results comparing ABA-induced aggregation for a variety of mixed phospholipid membranes have been published elsewhere (10). The DMPC/DMPE membranes that undergo aggregation also fuse as followed by two techniques, one monitoring the intermixing of the membranes themselves (Figures 2 and 3) and the other following the intermixing of the aqueous interiors of the vesicles (Figure 4). Since mixing of membrane components does not necessarily imply core mixing and *vica versa* (23), both methods were required.

Our experiments establish that for DMPC/DMPE mixed membranes, ABA induces vesicle aggregation and fusion. Although they by no means prove ABA is inducing these processes *in vivo*, it is emphasized that model membranes have produced most of the basic understanding of how fusion may occur (24). Since ABA meets at least some of the criteria of a membrane fusagen and is shown here to fuse phospholipid vesicles, its potential role in inducing fusion in plant cells should be given serious consideration.

In related experiments Hartung (personal communication) has recently employed a laser light scattering technique to demonstrate that non-dissociated ABA increases the size of particles formed from large unilamellar phospholipid vesicles. ABA-induced particle size changes were attributed to vesicle aggregation and (or) fusion. In addition Behl and Hartung (25) have shown, when stressed, ABA concentrations may rise to the mM range in the acidic apoplast surrounding guard cells. Therefore, the fusion conditions reported here (pH 5.0, mM ABA) are not reasonable and may be of physiological significance.

ACKNOWLEDGMENT: This work was supported by a National Science Foundation Grant, DMB-8607071, to W. Stillwell.

REFERENCES

1. Addicott, F.T., Ed. (1983) Abscisic Acid. Praeger, pp. 607, New York.
2. Van Steveninck, R.F.M. and Van Steveninck, M.E. (1983) in Abscisic Acid (Addicott, F.T., Ed.) pp. 171-235, Praeger, New York.
3. Zeiger, E. (1983) Ann. Rev. Plant Physiol. 34, 441-475.
4. Glinka, Z. and Reinhold, L. (1971) Plant Physiol. 48, 103-105.
5. Cram, W.J. and Pitman, M.G. (1972) Aust. J. Biol. Sci. 25, 1125-1132.
6. Stillwell, W. and Hester, P. (1984) Z. Pflanzenphysiol. 114, 65-76.
7. Stillwell, W. and Hester, P. (1984) Phytochem. 23, 2187-2192.
8. Wassall, S.R., Hester, P. and Stillwell, W. (1985) Biochim. Biophys. Acta 815, 519-522.
9. Stillwell, W., Brengle, B., Belcher, D. and Wassall, S.R. (1987) Phytochem. 26, 3145-3150.
10. Brengle, B., Wassall, S.R. and Stillwell, W. (1988) Plant Sci. 54, 245-249.
11. Stillwell, W., Brengle, B. and Wassall, S.R. (1986) Plant Physiol. 80s, 93.
12. Nir, S., Bentz, J., Wilschut, J. and Duzgunes, N. (1983) Progr. Surf. Sci. 13, 1-124.
13. Wilschut, J. and Hoekstra, D. (1986) Chem. Phys. Lipids 40, 145-166.

14. Bangham, A.D. (1968) Progr. Biophys. Mol. Biol. 18, 29-95.
15. Struck, D.K., Hoekstra, D. and Pagano, R.E. (1981) Biochem. 20, 4093-4099.
16 Wang, C. and Huang, L. (1984) Biochem. 23, 4409-4416.
17. Duzgunes, N., Straubinger, R.M., Baldwin, P.A., Friend, D.S. and Papahadjopoulos, D. (1985) Biochem. 24, 3091-3098.
18. Hipkins, M.F. and Hillman, J.R. (1981) Z. Pflanzenphysiol. 104s, 217-224.
19. Duzgunes, N., Wilschut, J. and Papahadjopoulos, D. (1985) in Physical Methods on Biological Membranes and Their Model Systems (Conti, F., Ed.) pp. 193-218, Plenum Press, New York.
20. Ornberg, R.L. and Reese, T.J. (1981) J. Cell Biol. 90, 40-54.
21. Rand, R.P., Reese, T.J. and Miller, R.H. (1981) Nature 293, 237-238.
22 Hui, S.W., Stewart, T.P., Boni, L.T. and Yeagle, P.L. (1981) Science 212, 921-923.
23 Morris, S.J., Gibson, C.C., Smith, P.D., Grief, P.C., Stirk, C.W., Bradley, D., Haynes, D.H. and Blumenthal, R. (1985) J. Biol. Chem. 260, 4122-4127.
24. Rand, R.P. and Parsegian, V.A. (1986) Ann. Rev. Physiol. 48, 201-212.
25. Behl, R. and Hartung, W. (1986) Planta 168, 360-368.

Vol. 156, No. 1, 1988 BIOCHEMICAL AND BIOPHYSICAL RESEARCH COMMUNICATIONS
October 14, 1988 Pages 517-523

MOLECULAR CLONING OF THE NOSIHEPTIDE RESISTANCE GENE FROM *STREPTOMYCES ACTUOSUS* ATCC 25421

DONALD C. DOSCH[1,2], WILLIAM R. STROHL[1,*], and HEINZ G. FLOSS[2,3]

[1]Departments of Microbiology and [2]Chemistry,
The Ohio State University, Columbus, OH 43210

[3]Department of Chemistry, University of Washington, Seattle, WA 98195

Received August 22, 1988

An 8.5 kb BamHI DNA fragment conferring resistance to nosiheptide, a peptide antibiotic of the 'thiostrepton group', was cloned from *Streptomyces actuosus* ATCC 25421 in *Streptomyces lividans* 1326. Two BamHI fragments of *S. actuosus*, the 8.5 kb fragment and an additional 3.0 kb fragment, hybridized with a thiostrepton resistance gene probe (pIJ30). The 8.5 kb fragment showed a relatively low degree of homology with the thiostrepton resistance gene. The restriction map of the nosiheptide resistance gene isolated here was significantly different from the map of the thiostrepton resistance gene previously published. © 1988 Academic Press, Inc.

Nosiheptide, also known as multhiomycin, is a peptide antibiotic produced by *Streptomyces actuosus* (1) and is used commercially as an animal feed additive to promote weight gain (2). Nosiheptide belongs to the 'thiostrepton group' of antibiotics which includes thiostrepton, siomycin, sporangiomycin and thiopeptin (3). Nosiheptide acts by binding to the 23S ribosomal RNA and ribosomal protein L-11 to inhibit the activities of elongation factors Tu and G (3). *S. actuosus* is resistant to the nosiheptide it produces by methylating an adenosine residue of the 23S ribosomal RNA to produce 2'-O-methyladenosine (3), similar to the mechanism of thiostrepton resistance by the thiostrepton producer, *S. azureus* (3). We describe the isolation and preliminary characterization of a DNA fragment cloned from *S. actuosus* which confers resistance to both nosiheptide and thiostrepton in *Streptomyces lividans*.

*Author to whom correspondence should be addressed.

ABBREVIATIONS: SSC, standard saline citrate; SDS, sodium dodecyl sulfate; aph, aminoglycoside phosphotransferase (neomycin resistance); tsr, thiostrepton resistance.

0006-291X/88 $1.50
Copyright © 1988 by Academic Press, Inc.
All rights of reproduction in any form reserved.

MATERIALS AND METHODS

Streptomyces actuosus, *Streptomyces azureus*, and *Streptomyces laurentii* were obtained from the American Type Culture Collection as ATCC 25421, 14921, and 31255, respectively. *Streptomyces lividans* 1326 was used as the nosiheptide and thiostrepton sensitive recipient in shot-gun cloning experiments. *Escherichia coli* JM83 was used to propagate plasmids for restriction endonuclease digestion analyses. The *Streptomyces* strains normally were grown in YEME (4) supplemented with 34% sucrose. *E. coli* was grown in LB and plasmids were introduced into *E. coli* by transformation using standard procedures (5). For strains harboring plasmids, the appropriate antibiotics were added to the media as follows (in μg/ml): thiostrepton, 50; nosiheptide, 50; neomycin, 10; ampicillin, 100; tetracycline, 15.

Chromosomal DNA, purified from *S. actuosus* according to the procedure of Kieser (6), was digested with BamHI for 60 min using 2 units of enzyme per μg of DNA. Plasmid pANT29, purified from *S. lividans* 1326, was digested with BamHI for 2 h, using 1 unit of enzyme per μg of DNA and treated for 15 min with 1 unit of calf intestine alkaline phosphatase (Boehringer Mannheim, Indianapolis, IN). The DNA preparations in an insert to vector ratio of 4:1 were ligated overnight at 4°C using T4 DNA ligase (Boehringer-Mannheim) as described previously (7). Protoplasts of *S. lividans* were formed as described by Hopwood *et al.* (4). The ligated DNA was introduced into protoplasts of *S. lividans* by transformation and the protoplasts were regenerated to mycelia on R2YE medium as described previously (7). After 18 h of incubation on R2YE at 30°C, the transformants were challenged with a soft agar overlay of R2YE containing 50 μg of nosiheptide per ml. After 72 h of growth, nosiheptide-resistant colonies containing pANT29 with *S. actuosus* DNA inserts were picked over to fresh plates of YEME containing 50 μg of nosiheptide per ml.

Plasmids were obtained using the small scale preparation procedure described by Birnboim and Doly (8). Restriction analyses were carried out according to the specification of the enzyme supplier (Bethesda Research Laboratories, Gaithersburg, MD). DNA fragment sizes were determined by electrophoresis through 0.7% agarose gels. Plasmids to be used as probes were labelled by the ^{32}P-oligolabelling procedure described by Feinberg and Vogelstein (9) using 50 μCi of [α-^{32}P]dCTP per μg of DNA. For hybridization analyses, chromosomal DNA was purified from *S. actuosus*, *S. laurentii*, and *S. azureus* according to the procedure of Kieser (6), and was digested with BamHI for 12 h using 2 units of enzyme per μg of DNA. Southern blots and hybridizations were performed as described by Maniatis *et al.* (5).

RESULTS AND DISCUSSION

Construction of pANT29. Most available streptomycete plasmid vectors use the thiostrepton resistance gene from *Streptomyces azureus* as a selective marker (4). This resistance gene also confers resistance to nosiheptide. To construct a vector which could be used to clone the nosiheptide resistance gene in the absence of an active thiostrepton resistance gene, fragments of bacteriophage lambda DNA generated by restriction with EcoRV were ligated with EcoRV-digested pIJ61 (4) and this mixture was introduced into *S. lividans* 1326 by transformation. A neomycin-resistant, thiostrepton-sensitive transformant yielded plasmid pANT29 (Fig. 1) which carried the EcoRV fragment of lambda from 26821 to 28198 bp of the phage genome (10). This fragment added several restriction sites to the vector, in particular BamHI (Fig. 1).

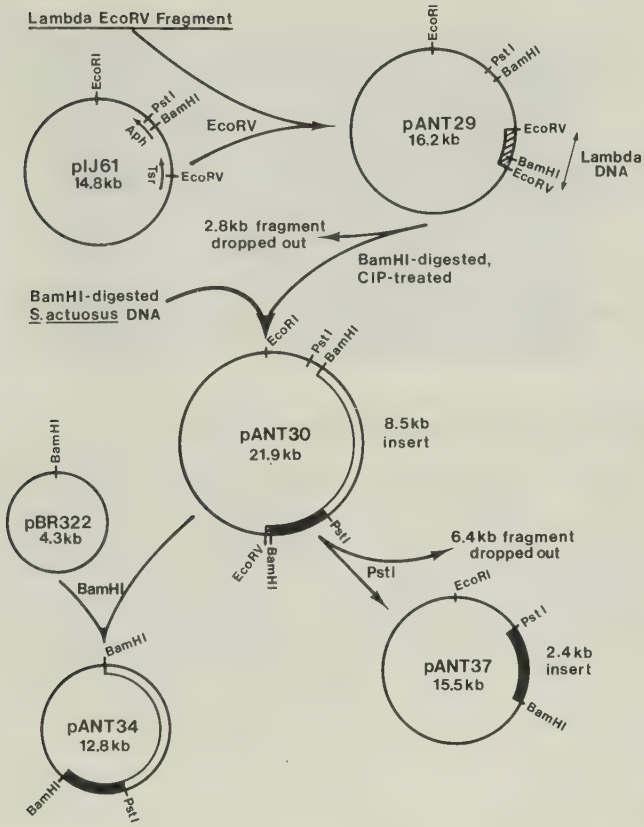

Figure 1. Construction of plasmids used in this study and cloning scheme for the nosiheptide resistance gene. Plasmids pANT30 and pANT37 both conferred resistance to nosiheptide and thiostrepton in *S. lividans* 1326.

Cloning of the nosiheptide resistance gene. Two nosiheptide-resistant transformants were obtained after transformation of *S. lividans* 1326 protoplasts with a BamHI-digested *S. actuosus* library in pANT29. The plasmids isolated from both of the nosiheptide-resistant *S. lividans* transformants contained an 8.5 kb BamHI insert. During the ligations, part of pANT29, including the 3′ half of the thiostrepton resistance gene, was deleted (Fig. 1). When these new plasmids were digested with BamHI and probed with pIJ30 (11), the remaining part of the thiostrepton resistance gene and the 8.5 kb DNA insert from *S. actuosus* showed homology with the probe (data not shown). Plasmid pANT30, which contained the 8.5 kb BamHI *S. actuosus* DNA insert that shared homology with pIJ30, was introduced into *S. lividans* 1326 by transformation and again this plasmid conferred resistance to nosiheptide, as well as to thiostrepton. Plasmid pANT30 also restored thiostrepton and nosiheptide resistance to *S. azureus* AZ-6Y, a thiostrepton-sensitive, blocked (thiostrepton nonproducing) mutant of *S. azureus* ATCC 14921. Further subcloning of pANT30 indicated that the DNA which conferred

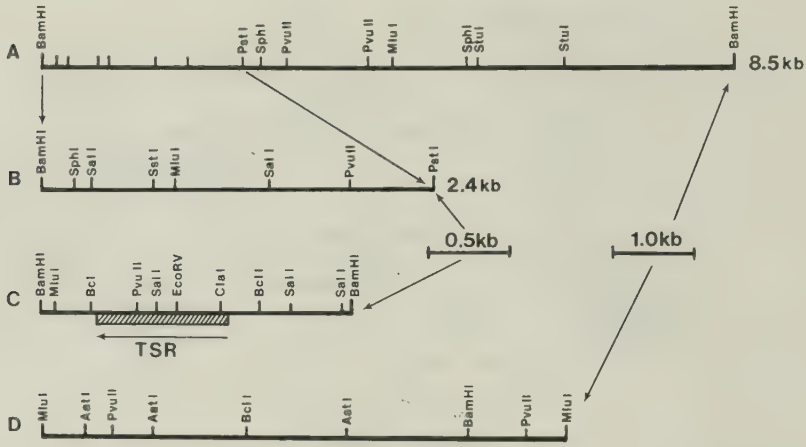

Figure 2. Comparison of restriction maps of the 8.5 kb DNA fragment cloned from *S. actuosus* (A), the 2.4 kb sub-clone of that fragment which confers resistance to nosiheptide (B), the thiostrepton resistance gene from *S. azureus* (C; ref. 11), and the 6.4 kb MluI DNA fragment described by Ohkishi *et al.* (15) which conferred nosiheptide resistance on *S. lividans* (D). Restriction endonucleases which did not cleave the 8.5 kb fragment were: BclI, BglII ClaI, EcoRI, EcoRV, HindIII, HpaI, KpnI, XbaI, and XhoI. Please note that AatI and StuI are isoschizomers.

resistance to nosiheptide resided wholly on a 2.4 kb BamHI-PstI restriction fragment of pANT37 (Fig. 1).

Structural characterization of nosiheptide resistance gene. The 8.5 kb BamHI fragment was subcloned in the *Escherichia coli* vector pBR322 to construct pANT34 from which a detailed restriction map of the insert was determined (Fig. 2). Because thiostrepton and nosiheptide are similar in chemical structure (12) and activities (3), and are cross-resistant, we originally hypothesized that the resistance genes might have a high degree of homology. As shown in Figure 2, the restriction map of the nosiheptide resistance gene was found to be very different from that of the thiostrepton resistance gene previously published (11).

Hybridization of chromosomal DNA preparations with pIJ30 and pANT34. Although the restriction maps of the nosiheptide and thiostrepton resistance genes showed no apparent similarities, there was sequence homology demonstrated by Southern blotting of the plasmids pANT30, pANT34, pANT37 with ^{32}P-labelled pIJ30 (data not shown). When we confirmed this by probing BamHI-digested DNA isolated from *S. actuosus* with ^{32}P-labelled pIJ30, the expected 8.5 kb fragment, as well as an additional 3.0 kb fragment, hybridized to the probe under moderate stringency conditions (Fig. 3). When BamHI-digested DNA from *Streptomyces azureus* was probed with ^{32}P-labelled pIJ30, DNA fragments of ca. 6.1 and 9.0 kb in length hybridized with the plasmid (Fig. 3). The thiostrepton resistance gene of *S. azureus* was

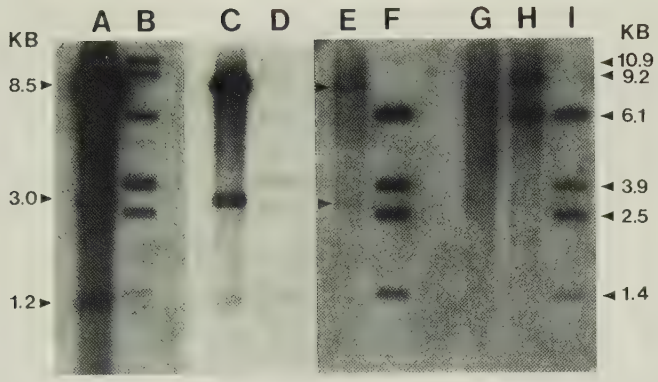

Figure 3. Southern blot analysis of BamHI-digested DNA isolated from *S. laurentii*, *S. azureus*, and *S. actuosus*. The Southern blots were hybridized with ^{32}P-labelled plasmids, and washed twice for 15 min each at room temperature with 2x SSC and 0.1% SDS, followed by a third wash at 45°C with 0.4x SSC and 0.1% SDS. Lanes B, D, F, and I are standards made from digestions of pIJ941 which yield DNA fragments which contain the thiostrepton resistance gene; fragment sizes are given in the figure in kb (kilobases). Lanes A and C: *S. azureus* DNA digests probed with pANT34 and exposed to film for 17 and 3 days, respectively, showing DNA fragments of 1.2, 3.0, an 8.5 kb which hybridize with the probe. Lanes E, G, and H: DNA digests from *S. actuosus* (E), *S. laurentii* (G), and *S. azureus*, respectively, probed with pIJ30. The following amounts of BamHI-digested DNA were loaded into the respective lanes: A, C, and E, 2.5 μg of *S. actuosus* DNA; lane G, 1.0 μg of *S. laurentii* DNA; lane H, 1.0 μg of *S. azureus* DNA.

originally isolated on a 6.9 kb insert generated from an MboI partial digest of *S. azureus* chromosomal DNA which was ligated into BamHI-digested SLP1.2 to make pIJ6 (13). The MboI-BamHI junctions between the insert and vector DNA in pIJ6 were able to be cleaved with BamHI. Plasmid pIJ30 was formed by subcloning a 1.9 kb BamHI DNA fragment, containing the thiostrepton resistance gene from pIJ6, into pBR322 (11). Our data showing that pIJ30 hybridizes to 6.1 and 9.0 kb BamHI DNA fragments of *S. azureus* (Fig. 3) indicate that only one of the BamHI sites of the 1.9 kb insert in pIJ30 originated from *S. azureus* DNA.

S. laurentii ATCC 31255 is capable of producing 10.5 g of thiostrepton per liter in high-density fed-batch fermentations (14). Thus, it was very interesting that *S. laurentii* did not have DNA which was homologous with the thiostrepton resistance gene from *S. azureus*, especially since only moderately stringent conditions were used for these hybridizations (Fig. 3). This suggests that the thiostrepton resistance gene in *S. laurentii* has a markedly different sequence from the thiostrepton and nosiheptide resistance genes described here.

When BamHI-digested *S. actuosus* chromosomal DNA was probed with pANT34 (which contained the 8.5 kb BamHI fragment conferring nosiheptide

resistance), the 8.5 kb cloned fragment hybridized with itself strongly and also hybridized to DNA fragments of 3.0 and 1.2 kb in length (Fig. 3). The presence of hybridizing BamHI DNA fragments in *S. actuosus*, other than the 8.5 kb fragment, is intriguing because it suggests that there may be multiple copies of DNA which confer resistance to (and perhaps production of) nosiheptide. Ohkishi *et al.* (15) recently isolated a 6.4 kb MluI DNA fragment from *S. actuosus* NRRL 2954 (the same strain as ATCC 14921) which conferred nosiheptide resistance in *S. lividans* 1326. Their DNA fragment also shared homology with the thiostrepton resistance gene (15), but it had a markedly different restriction endonuclease pattern from that shown for the nosiheptide resistance-conferring 8.5 kb DNA fragment or the 2.4 kb subclone shown in Fig. 2. The restriction map of the nosiheptide resistance gene determined by Ohkishi *et al.* (15; Fig. 2D) is consistent with our data which showed that the 3.0 kb BamHI DNA fragment hybridized with both pIJ30 and pANT34 (Fig. 3). If the nosiheptide resistance gene isolated by Ohkishi *et al.* (15) is indeed present on the 3.0 kb BamHI hybridizing fragment (Fig. 3), then the entire gene would necessarily reside within the ca. 1.2 kb BamHI-MluI fragment shown at the right end of the restriction map (Fig. 2D). It is probable that the 1.2 kb BamHI fragment is DNA which hybridized to sequences flanking the resistance gene on the probe (pANT34).

The apparent redundancy of nosiheptide resistance genes in *S. actuosus* is interesting, particularly in light of recent reports showing the potential for gene duplication in streptomycetes. Recently, Henderson *et al.* (16) cloned and sequenced two protease genes from *Streptomyces griseus*. These two protease genes were homologous by Southern analysis but contained different restriction maps and had only a 54% amino acid sequence homology. This prompted them to suggest that the presence of a second gene was the result of gene duplication (16). Moreover, Stutzman-Engwall and Hutchinson (submitted to Proc. Natl. Acad. Sci.) recently found that four separate segments of DNA from *Streptomyces peucetius* ATCC 29050 hybridized to an actI (polyketide synthase) gene probe. Their data indicated that each DNA fragment contained a cluster of genes which could encode functions required for biosynthesis of anthracyclines (Stutzman-Engwall and Hutchinson, submitted). Hopwood also recently reported that four separate DNA clusters from the chlorothricin producer, *Streptomyces antibioticus*, hybridized to the actI gene probe (D.A. Hopwood, Plenary Lecture, Seventh International Symposium on the Biology of the Actinomycetes, Tokyo, Japan). It is tempting to suggest that a similar situation exists with the nosiheptide-thiostrepton resistance (and production?) genes of *S. actuosus*. We currently are attempting to clone the other pIJ34-hybridizing BamHI DNA fragments from *S. actuosus* for comparison to the nosiheptide resistance gene already cloned.

ACKNOWLEDGMENTS

We wish to thank David Hopwood for supplying us with several of the vectors and strains used in this study, and Robert Woodman for use of *S. azureus* mutant AZ-6Y. We also thank C. Richard Hutchinson for supplying us with his manuscript prior to publication and H. Ohkishi for sharing his data with us. This material is based on work supported by the National Science Foundation under Grant No. #DMB-8607619.

REFERENCES

1. Prange, T., A. Ducroix, C. Pascard, and J. Lunel. 1977. Nature (London) **265**:189-190.
2. Keppens, L., and G. DeGrote. 1979. Rev. Agric. (Brussels) **32**:159.
3. Cundliffe, E. and J. Thompson. 1981. J. Gen. Microbiol. **126**:185-192.
4. Hopwood, D.A., M.J. Bibb, K.F. Chater, T. Kieser, C.J. Bruton, H.M. Kieser, D.J. Lydiate, C.P. Smith, J.M. Ward, and H. Schrempf. 1985. Genetic manipulation of *Streptomyces*: a laboratory manual. The John Innes Foundation, Norwich.
5. Maniatis, T., E.F. Fritsch, and J. Sambrook. 1982. Molecular cloning: a laboratory manual. Cold Spring Harbor Laboratory, Cold Spring Harbor, New York.
6. Kieser, T. 1984. Plasmid **12**:19-36.
7. Lampel, J.S., and W.R. Strohl. 1986. Appl. Environ. Microbiol. **51**:126-131.
8. Birnboim, H.C., and J. Doly. 1979. Nucl. Acids Res. **7**:1513-1523.
9. Feinberg, A.P., and B. Vogelstein. 1983. Analyt. Biochem. **132**:6-13.
10. Daniels, D.L., J.L. Schroeder, F.R. Blattner, W. Szybalski, and F. Sanger. 1983. In R.W. Hendrix, J.W. Roberts, F.W. Stahl, and R.A. Weisberg (eds), Lambda II: Appendix. Cold Spring Harbor, New York.
11. Thompson, C.J., T. Kieser, J.M. Ward, and D.A. Hopwood. (1982) Gene **20**:51-62.
12. Pascard, C., A. Ducroix, J. Lunel, and J. Prange. 1977. J. Amer. Chem. Soc. **99**:6418.
13. Thompson, C. J., J. M. Ward, and D. A. Hopwood. 1980. Nature (London) **31**:525-527.
14. Suzuki, T., T. Yamane, and S. Shimizu. 1987. Appl. Microbiol. Biotechnol. **25**:526-531.
15. Ohkishi, H., T. Horisaka, K. Miyasaka, and S. Morioka. 1988. Mitsubishi Chemical R & D Rev. **2**:45-52.
16. Henderson, G., P. Krygsman, C.J. Liu, C.C. Davey, and L.T. Malek. 1987. J. Bacteriol. **169**:3778-3784.

Vol. 156, No. 1, 1988 BIOCHEMICAL AND BIOPHYSICAL RESEARCH COMMUNICATIONS
October 14, 1988 Pages 524-529

15-HYDROXYEICOSATETRAENOIC ACID DEHYDROGENASE ACTIVITY IN MICROSOMAL FRACTION OF MOUSE LIVER HOMOGENATE

Dai-Eun Sok, Jung Bu Kang, and Hong Dae Shin*

R.N. 1-4, Agency for Defense Development, DaeJeon P.O. BOX 35, KOREA

*Dept. of Chem., College of Natural Sci., Pusan National Univ., Pusan, KOREA

Received August 25, 1988

Summary. The microsomal fraction of mouse liver homogenate showed NAD(P)-dependent dehydrogenase activity involved in the conversion of 15-hydroxyeicosatetraenoic acid to 15-ketoeicosatetraenoic acid, which was determined quantitatively by HPLC assay. This enzyme, tightly bound to membranes and relatively stable, possessed apparent values of Km of 8.3 μM and Vmax of 2.8 nmoles /mg.min in the oxidation of 15-HETE ,and gave an optimum pH of 9.8. Additionally, the enzyme, not susceptible to the inhibition by indomethacin and showing a similar cosubstrate specificity between NAD and NADP, utilized other hydroxylated eicosanoids as substrates, based on HPLC analyses. © 1988 Academic Press, Inc.

In mammalian cells, arachidonic acid is known to be oxygenated to generate the bioactive metabolites , prostaglandins (1), leukotrienes (2), etc.. Subsequently, 5,15-diHETE (3), 14,15-diHETE and lipoxins (4), which include 15-hydroxyl group commonly, were also reported as bioactive products derived from 15-lipoxygenase-catalyzed oxidation of arachidonic acid.

Whereas the inactivation pathways of prostaglandins and leukotrienes are well defined (5,6), little is known about the metabolism of other 15-hydroxylated eicosatetraenoic acids, 15-HETE, 5,15-diHETE , 14,15-diHETE and lipoxins. Previously (7,8), 15-hydroxyprostaglandin dehydrogenase responsible for the inactivation of prostaglandins by oxidizing the 15-hydroxyl group of prostaglandins was reported to be present in the cytosol fractions of prostate, kidney etc.. Recently (9), 3α-hydroxysteroid dehydrogenase from liver cytosol was also reported to possess the activity to oxidize 15-hydroxy-prostaglandins, although the activity toward the other 15-hydroxylated eicosatetraenoic acids was not investigated. In this study,we show that a microsomal membrane-bound dehydrogenase activity responsible for the oxidation of 15-HETE is determined quantitatively by RP-HPLC assay, and we propose that the enzyme may be involved in the NAD(P)-dependent oxidative metabolism of some 15-hydroxylated eicosanoids

Abbreviations : PGB_2, prostaglandin B ; 15-HETE , 15(S)-hydroxy-5,8,11-cis-13-trans-eicosatetraenoic acid ; 15-KETE , 15-oxo-5,8,11-cis-13-trans-eicosatetraenic acid ; 5,15-diHETE, 5(S),15(S)-dihydroxy-6,13-trans-8,11-cis-eicosatetraenoic acid ; 8,15-diHETE , 8(S),15(S)-dihydroxy-5,11-trans-9,13-cis-eicosatetraenoic acid ; 14,15-diHETE , 14(R),15(S)-dihydroxy-5,8-cis-10,12-trans-eicosatetraenoic acid ; 11-trans-lipoxin A, 5(S),6(S,R),15(S)-trihydroxy-7,9,11,13-trans-eicosatetraenoic acid ; RP-HPLC , reverse phase-HPLC ; TLC , thin layer chromatography.

0006-291X/88 $1.50
Copyright © 1988 by Academic Press, Inc.
All rights of reproduction in any form reserved.

Materials and Methods

Hydroxysteroid dehydrogenase (Grade II), soybean lipoxygenase (Type I), NAD, NADP, PGB_2 and arachidonic acid were products of Sigma Chemical Co.. Methanol and ethyl ether were from Aldrich and Tedia Chemical Co., respectively. 15-HETE, 5,15-diHETE, 8,15-diHETE and 11-trans lipoxin A were prepared as described, respectively (10,11). 15-Ketoeicosatetraenoic acid (15-KETE) was non-enzymatically produced as reported (12), and enzymatically prepared by 30 min-incubation of 15-HETE (1 mM) with microbial hydroxysteroid dehydrogenase (10 units) in 30 ml of 0.1 M pyrophosphate buffer, pH 8.9 containing 2 mM NAD, followed by extraction with ether, separation by TLC (petroleum ether : ethyl ether : acetic acid = 50 : 50 : 1), methylation, hydrogenation over PtO_2 and GC/MS analysis by a JEOL JMS-DX spectrometer equipped with a 1 % OV-1 column as described (12). Separately, liver homogenate(1 g) in 30 ml of 0.1 M phosphate buffer, pH 7.0 including 2 mM NAD was incubated with 15-HETE (1 mM) , and the reaction product was analysed as above.

Development of the RP-HPLC assay for the quantitative determination of 15-KETE was conducted as follows ; various concentrations of 15-KETE were added to 1 ml of 50 mM phophate buffer, pH 7.4 (sample A) and the buffer containing 1 % albumin (sample B). Then, each mixture was acidified with 50 ul of 1 M citric acid , admixed with PGB_2 (2.5 μg) as an internal standard, and then extracted with 5 ml of ether. The extract was concentrated and injected into RP-HPLC system as described (11). The concentration of 15-KETE (λmax at 278 nm, ca. 30,000) (13) was determined from the calibration curve, which was constructed by plotting the peak area ratios versus the concentrations. The percentage recovery was determined by comparing the amounts of 15-KETE extracted from sample A and B.

For enzyme preparation , the frozen mouse liver was homogenized in cold 0.25 M sucrose solution containing 50 mM Tris buffer and 1 mM EDTA. Subcellular fractions were prepared by differential centrifugation (14). The microsomal fraction was sonicated for 30 sec (ARTEK dismembrator), sedimented at 120,000 X g for 30 min , and the pellet was used for the enzyme study. The amount of protein was determined by Lowry method (15).

15-HETE dehydrogenase activity was determined by RP-HPLC assay. Unless otherwise noted, assays were conducted in a final volume of 1 ml containing 50 mM phosphate buffer (pH 7.4), 200 μM 15-HETE and 2 mM NAD. The reaction was started by adding the sonicated microsome, continued for 10 min at 37°C under shaking , and stopped by the addition of 50 μl of 1 M citric acid . The enzyme activity was expressed in nmoles of 15-KETE produced every min, and the kinetic parameters and properties of the dehydrogenase were obtained as reported (14).

To examine the oxidation of the multiple-hydroxylated eicosanoids by dehydrogenases , the dihydroxy acids (200 μM) or lipoxin (10 μM) was incubated with the microsomal preparation (1 mg protein) or microbial hydroxysteroid dehydrogenase (2 units) at 37°C for 30 min in 1 ml of 50 mM Tris buffer, pH 8.8 including 2 mM NAD. The reaction products were extracted as described in RP-HPLC assay except the acidification with 100 μl of 1 M citric acid, and applied onto C_{18} column (11). Separately, the absorbance change at 340 nm during the incubation with hydroxysteroid dehydrogenase was monitored over 30 min at r.t. with a Gilford spectrophotometer.

Results and Discussion

When 15-HETE was incubated with liver homogenate , a more non-polar product (Rf, 0.44) than 15-HETE (Rf, 0.37) appeared as a major product in TLC analysis (12). The product (λ max, 278 nm) , which was also formed from the incubation of 15-HETE with microbial hydroxysteroid dehydrogenase , was methylated with diazomethane, hydrogenated over PtO_2, and then subjected to GC/MS analysis . The characteristic ions were observed at m/e 340 (M), 227 [$\cdot(CH_2)_{12}-CO_2CH_3$] 114 (M - 226) , 99 [$O{=}\dot{C}-(CH_2)_4-CH_3$] and 71 [$\cdot(CH_2)_4-CH_3$], in good agreement with the spectrum as reported (12). The structure of this product was also confirmed by the preparation of standard specimen (12). After having established the structure of the product, we turned to the development of RP-HPLC assay to determine quantitatively the activity of 15-HETE dehydrogenase .

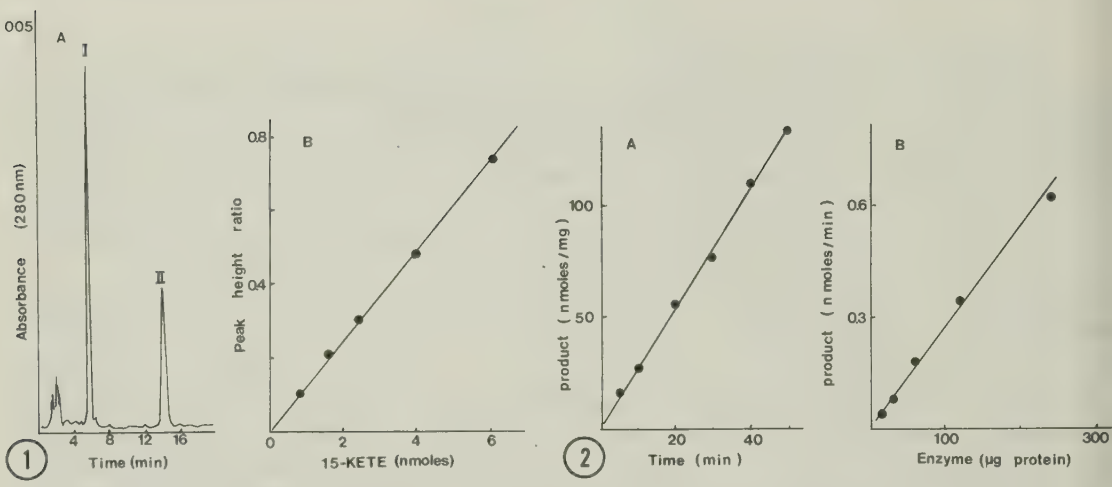

Fig. 1. A) RP-HPLC chromatogram of PGB_2(I) and 15-KETE (II) on the μ Bondapak column (3.9 X 300 mm) , eluted at a flow rate of 1 ml per min with the mobile phase (methanol : water : acetic acid = 75 : 25 : 0.01).
B) Calibration curve for 15-KETE.
Fig. 2. A) Time course of 15-KETE formation with the microsomal fraction.
B) Effect of the enzyme amount on the rate of 15-KETE formation.

Fig. 1 illustrates the typical chromatogram of PGB_2 as an internal standard and 15-ketoeicosatetraenoic acid (15-KETE) , which eluted at 6 min and 14 min , respectively. As shown in Fig.2 , a good linear relationship between amount of 15-KETE and the peak height ratio of 15-KETE to internal standard was observed. The range of coefficient of variance for this method was within 5 % for intraday assay. Recovery determined by comparing the yields of 15-KETE added to the albumin-including buffer and to the buffer only ranges between 95 and 98 %. No appreciable degradation of 15-KETE was seen up to 3 days at 4° C .

When the 15-HETE dehydrogenase activity was measured by RP-HPLC assay, the total activity in the frozen liver amounts to 150-250 nmoles/min .

Table 1 demonstrates the distribution of 15-HETE dehydrogenase activity in the three fractions of liver homogenate. Interestingly, it was observed that the enzyme of the microsomal fraction was very stable, whereas the enzyme activities in both cytosol and mitochondrial portions decreased gradually during storage at 4° C and less than 10 % of total activity remained after one day, respectively.

In this investigation , the emphasis was on the microsomal fraction. Attempts to solubilize the enzyme from microsomes using sonication, papain or 0.2 % Triton X-100 were unsuccessful, while microsomal esterase (> 90 %) was easily solubilized by sonication. These observations suggest that the 15-HETE dehydrogenase activity is tightly bound to the membrane. In time course studies (Fig. 2A) the formation of 15-ketoeicosatetraenoic acid increased linearly with the incubation time for at least

Table 1

Subcellular distribution of the 15-HETE dehydrogenase activity in mouse liver homogenate

Fraction	Total Protein	Total Activity (nmoles.min)	Specific Activity (nmoles.min .mg)
Microsome	28.2 (16.8)	47.7	1.69 (2.8)
Mitochondria	16.4	29.1	1.77
Cytosol	36.6	163.4	4.46

Values are the average of triplicate assays, and the parentheses show the specific activity of the sonicated microsomal pellet.

60 min. Fig. 2B demonstrates that the amount of 15-ketoeicosatetraenoic acid produced from 15-HETE by the microsomal fraction increased proportionally to the protein concentration. The effect of 15-HETE concentration on the 15-HETE dehydrogenase is illustrated in Fig. 3A. The apparent Km and Vmax for 15-HETE were determined to be 8.3 µM and 2.8 nmoles /mg.min. No great difference of specificity between NAD and NADP was observed. At a high concentration (200 µM) of 15-HETE , apparent Michaelis constant (Km) for NAD were determined to be 60 µM. Bioconversion of 15-HETE was negligible in the absence of added pyridine nucleotide. The pH dependence of this dehydrogenase was examined using three different buffer system, 0.05 M sodium phophate (7.6 - 8.4), 0.05 M Tris-HCl (8.4 - 9.2) and 0.05 M glycine-NaOH (pH 9.6 - 11.2). The optimal pH of the enzyme for the oxidation of 15-HETE was found to be around 9.8 (Fig. 3B). The properties of the microsomal dehydrogenase seem to be similar to those of prostaglandin dehydrogenase (9). However, this enzyme was not inhibited significantly by 10 µM indomethacin, though indomethacin is known to inhibit the 9-hydroxy-prostaglandin dehydrogenase strongly (9). Besides, the microsomal localization and NAD(P)-specificy

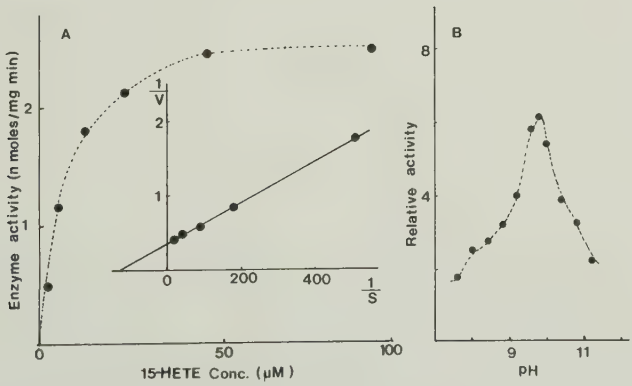

Fig. 3. A) Effect of 15-HETE concentration on the rate of 15-KETE formation. Inset , Lineweaver-Burk plot of 1/15-HETE concentration (mM) against 1/velocity (nmoles / mg.min).
B) Effect of pH on the rate of 15-KETE formation.

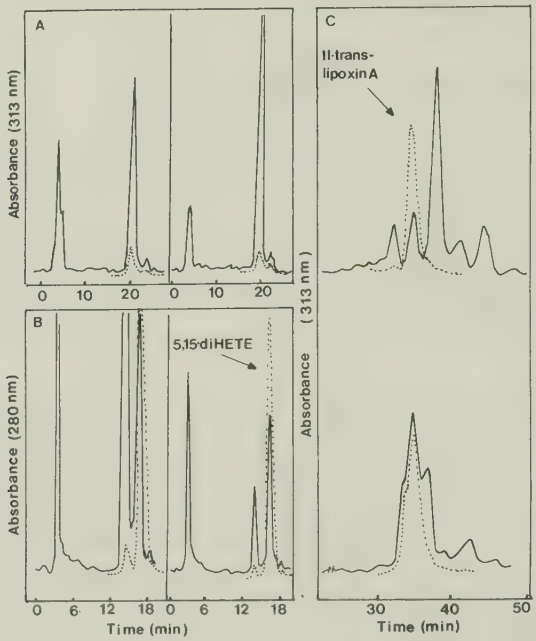

Fig. 4. A) RP-HPLC profile of products derived from the oxidation of 8,15-diHETE by dehydrogenases. Left, oxidation by hydroxysteroid dehydrogenase (——) and nonenzymatic oxidation (-----). Right, oxidation by microsomal dehydrogenase (——) and nonenzymatic oxidation (-----). Non-enzymatic oxidation was performed in the absence of NAD or with boiled enzyme. HPLC was carried out with μ Bondapak column (3.9 X 300 mm), eluted at a flow rate of 1 ml with a mobile phase (methanol : water : acetic acid = 65 : 35 : 0.01).

B) RP-HPLC profile of products formed from enzymatic oxidation of 5,15-diHETE. Experimental procedures are the same as described above.

C) RP-HPLC profile of products formed, the oxidation of 11-trans-lipoxin A. Upper, oxidation by hydroxysteroid dehydrogenase (——). Downer, oxidation by microsomal dehydrogenase (——) and non-enzymatic oxidation with boiled enzyme (-----). HPLC was performed with a Resolve column (3.9 X 150 mm), eluted with a mobile mixture (methanol : acetonitrile : water : acetic acid = 100 : 100 : 270 : 0.2) at 1 ml/min.

of this enzyme are in contrast to the cytosolic localization and NAD-specificity of 15-hydroxyprostaglandin dehydrogenase from placenta (7). Based on these observations, it is assumed that the 15-HETE dehydrogenase of the microsomal fraction was different from prostaglandin dehydrogenase. To see whether the microsomal dehydrogenase can oxidize other 15-hydroxylated eicosatetraenoic acids, the various eicosanoic acids were incubated with the microsomal enzyme , and then the reaction products were subjected to RP-HPLC analysis (Fig. 4 A,B and C). The microsomal dehydrogenase-catalyzed oxidation of these eicosanoic acids was evaluated by comparison with the oxidation of the respective acid by the microbial hydroxysteroid dehydrogenase, which exhibited the time-dependent increment of absorbance at 340 nm during the incubation with the respective hydroxylated acid.

Fig. 4 demonstrates that there is a similarity between the HPLC profiles of oxidation products generated from the incubation of the respective acid with two different enzymes , suggesting that the microsomal dehydrogenase oxidizes the hydroxylated eicosanoic acids in the same way as does

the hydroxysteroid dehydrogenase, although the positional selectivity in the oxidation of hydroxyl groups of the hydroxylated eicosanoic acids was not established. It is thus conceivable that the microsomal dehydrogenase-catalized oxidation pathway may correspond to one of the metabolic pathways of the bioactive multiple-hydroxylated eicosatetraenoic acids. In a separate experiment, it was found unexpectedly that PGB_2 was not utilized by microsomal dehydrogenase, whereas it was easily oxdized by microbial hydroxysteroid dehydrogenase.

Based on these results , it is supposed that the microsomal dehydrogenase , which can be determined quantitatively by RP-HPLC assay , is one of the enzymes involved in the oxidative metabolism of 15-hydroxylated eicosatetraenoic acids other than prostaglandins.

References

1. Vane, J.R. (1969) Br. J. Pharmacol. 35 , 209.
2. Samuelsson, B. (1983) Science, 220 , 568 .
3. O' Flaherty, J. T. and Thomas, M.J. (1985) Prostaglandins Leukotrienes Med. 17, 199.
4. Samuelsson, B., Dahlen, S.-E., Lindgren, J.A., Rouzer, C.A. and Serhan, C.N. (1987) Science, 237, 1171.
5. Anggard, E. and Larsson, C. (1971) Eur. J. Pharmacol., 14, 66.
6. Shak, S., Reich, N.O., Goldstein, I.M. and Ortiz de Montellano, P.R. (1985) J. Biol. Chem., 260 (24), 13023.
7. Westbrook, C., Lin, Y.-M. and Jarabak, J. (1977) Biochem. Biophys. Res. Comm. 110 , 273.
8. Lin, Y.-M. and Jarabak, J. (1978) Biochem. Biophys. Res. Comm. 81 , 1227 .
9. Penning, T.M. and Sharp, R.B. (1987) Biochem. Biophys. Res. Comm. 148, 646 .
10. Van Os, C.P.A., Rijke-Schilder, G.P.M., Halbeek, H.V., Verhagen, J. and Vliegenthart, J.F.G. (1981) Biochem. Biophys. Acta, 663 , 177 .
11. Sok, D.-E., Phi, T.S., Jung, C.H., Chung, Y.U. and Kang, J.B. (1988) Biochem. Biophys. Res. Comm. 153, 840 .
12. Narumiya, S., Salmon, J.A., Cottee, F.H., Weatherley, B.C. and Flower, R.J. (1981) J. Biol. Chem. 256, 9583.
13. Mathews, W.R., Rokach, J. and Murphy, R.C. (1981) Anal. Biochem. 118, 96.
14. Mendoza-Hernandez, G., Lopez-Solache, I., Rendon, J. L., Diaz-Sanchez, V. and Diaz-Zagoya, J.C. (1988) Biochem. Biophys. Res. Comm. 152, 376 .
15. Lowry, O.H., Rosebrough, N.J., Farr, A.L. and Randall, R.J. (1951) J. Biol. Chem. 193, 265.

Vol. 156, No. 1, 1988 BIOCHEMICAL AND BIOPHYSICAL RESEARCH COMMUNICATIONS
October 14, 1988 Pages 530-536

SITES OF MODIFICATION OF HUMAN ANGIOGENIN BY BROMOACETATE AT pH 5.5

Robert Shapiro, Daniel J. Strydom, Stanislawa Weremowicz, and Bert L. Vallee

Center for Biochemical and Biophysical Sciences and Medicine and Department of Pathology, Harvard Medical School, Boston, MA 02115

Received August 25, 1988

Summary: Human angiogenin is inactivated by treatment with bromoacetate at pH 5.5. Use of [^{14}C]bromoacetate and tryptic peptide mapping have identified the sites of carboxymethylation as His-13 and His-114, with His-114 reacting ~1.5-fold more rapidly than His-13. At later stages in the reaction, both His-13 and -114 become modified with His-114 in part forming a bis derivative. Comparison with carboxymethylhistidine derivatives of known structure obtained from bovine pancreatic ribonuclease A indicates that the reaction order is N-1 of His-114 > N-3 of His-13 > N-3 of His-114. © 1988 Academic Press, Inc.

Human angiogenin, a potent inducer of neovascularization, is a single-chain polypeptide of molecular mass 14,124 (1). Its amino acid sequence displays extensive similarity to that of the pancreatic RNases (2,3) and includes their three major active site residues, His-12, Lys-41, and His-119 (bovine RNase A numbering). Recognition of this homology led to the finding that angiogenin is a ribonucleolytic enzyme, albeit with a characteristic activity differing markedly from that of the digestive RNases (4,5). Chemical modification of angiogenin, based on methods previously applied to bovine pancreatic RNase A, subsequently revealed that histidine, lysine, and arginine residues are critical for enzymatic activity and suggested the involvement of histidines in angiogenic activity (4,6). Identification of essential lysines and arginines by chemical modification techniques is made difficult by the lack of

Abbreviations: RNase(s), ribonuclease(s), 3-CM-His, N-3 carboxymethylhistidine; 1-CM-His, N-1 carboxymethylhistidine; HPLC, high performance liquid chromatography; PTC, phenylthiocarbamoyl.

0006-291X/88 $1.50
Copyright © 1988 by Academic Press, Inc.
All rights of reproduction in any form reserved.

specificity of these reactions; in both cases, inactivation is accompanied by modification of several residues. In contrast, carboxymethylation of only 1.5 histidines decreases ribonucleolytic activity by 95% (6). In the present report, we identify His-13 and -114 (corresponding to His-12 and -119 of RNase A) as the residues modified and N-3 carboxymethylhistidine (3-CM-His) and N-1 carboxymethylhistidine (1-CM-His), respectively, as the primary derivatives formed. Although the sites of modification and the adducts generated are the same as with RNase A (7,8), the relative reaction rates differ significantly, and the preference for His-114 over His-13 in angiogenin is much smaller than that found for the corresponding residues in RNase.

MATERIALS AND METHODS

Angiogenin was isolated from human plasma (9). Bovine pancreatic RNase A was obtained from Cooper Biomedical. Carboxymethylation of angiogenin and RNase A (20-30 μM) was performed in the dark using 30 mM bromoacetate in 100 mM sodium acetate at pH 5.5, 27°C. Reaction mixtures (0.3-1.0 mL) contained 80-250 μCi bromo[1-^{14}C]acetic acid (Amersham). Reactions were terminated and unincorporated reagent removed by passage through a C18 HPLC column (2). Aliquots of fractions eluting from this column were taken for amino acid analysis and for ^{14}C measurements by scintillation counting. Amino acid analyses were performed by the method of Bidlingmeyer et al. (10) using a 3.9 x 150 mm PICO·TAG C18 column and a Waters Associates HPLC system. In most cases, a 10-min gradient (curve 5, convex) from 10% to 49% solvent B was employed at 39°C, where solvent A was 0.14 M sodium acetate, pH 6.4, containing 0.06% triethylamine and solvent B was 60% acetonitrile. Eluates were monitored at 254 nm. In this method, amino acids are detected as their phenylthiocarbamoyl (PTC) derivatives. In some cases, noted in the text, a modified HPLC gradient of 5% B to 52% B in 10 min was employed. For determination of radiolabelled amino acids, 0.2 min fractions were collected and counted. Digestion with trypsin, peptide mapping on a C3 HPLC column, and N-terminal amino acid sequencing were performed as described (2). For angiogenin tryptic peptide nomenclature (T-7, T-11) see Strydom et al. (2). Measurements of enzymatic activity of angiogenin and RNase A were performed using tRNA as substrate (6).

RESULTS AND DISCUSSION

Identification of Sites of Carboxymethylation of Angiogenin. Treatment of angiogenin with [^{14}C]bromoacetate for 15.5 h at pH 5.5 decreases its enzymatic activity by 95%, and results in the incorporation of 1.6 carboxymethyl groups. C3 HPLC of a tryptic digest of the modified protein reveals four major peaks of radioactivity (Fig. 1). Material eluting in peak A (column breakthrough), containing 11% of the total radioactivity, was rechromatographed on a C18 HPLC column. Radioactivity eluting

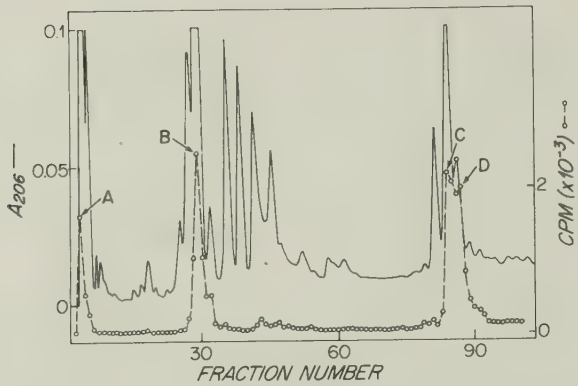

Figure 1: C3 HPLC elution pattern of radioactive tryptic peptides from angiogenin treated with [^{14}C]bromoacetate. HPLC was performed as described previously (2). Half-minute fractions were collected and 50 μL aliquots were counted.

from this column did not cochromatograph with any 206 nm absorbing material, suggesting that it is not peptide-associated.

Amino acid analysis of material in peak B from the C3 column (Table 1), containing 27% of the total counts, indicates that it derives from peptide T-7 (amino acids 6-21). The three fractions analyzed - 28, 29, and 30 - show a loss of ~0.2-0.6 histidine together with the appearance of a new peak at 2.68 min, between PTC-Glu (2.07 min) and PTC-Ser (3.78 min). Assuming that the new derivative has the same molar absorptivity as PTC-His,

Table 1. Amino Acid Compositions of Radiolabeled Tryptic Peptides of Bromoacetate-Modified Angiogenin

Amino Acid	Peak B	T-7	Peak C	T-11	Peak D
Asx	1.88	1	3.90	4	3.89
Glx	2.00	2	2.92	3	2.78
Ser	0.17		1.03	1	1.39
Gly	1.24	1	1.16	1	1.75
His	1.67	2	0.10	1	0.13
Arg	1.05	1	1.06	1	1.07
Thr	2.14	2			0.24
Ala	0.95	1	2.02	2	2.02
Pro	1.10	1	1.31	1	1.47
Tyr	2.00	2			
Val			3.03	4	2.88
Met					
Ile	0.57		2.00	2	1.81
Leu	1.01	1	2.24	2	2.29
Phe	1.25	1	1.01	1	0.99
Lys	0.98	1	0.97	1	0.96
1-CM-His			0.85		0.24
3-CM-His	0.50				
pmol analyzed	93		58		27

Peaks B, C, and D represent fractions 29, 84, and 87, respectively, from the peptide map in Fig. 1. 1-CM-His and 3-CM-His are amino acids whose PTC adducts elute at 2.36 min and 2.68 min, respectively. These identifications are based on a comparison with derivatives obtained from RNase A as discussed in the text.

Table 2. Release of ^{14}C During Edman Degradation of CM-Peptide from Tryptic Digest

Step:	1	2	3	4	5	6	7	8
^{14}C, cpm:	22	33	47	59	38	11	50	3125

One nmol of peptide from fraction 29 (Fig. 1) was sequenced.

0.25, 0.50, and 0.45 residue are present in fractions 28, 29, and 30, respectively. This is in reasonable agreement with the stoichiometries of radioactivity incorporation for the three fractions: 0.3, 0.6, and 0.6, respectively.

Angiogenin peptide T-7 contains two histidines, His-8 and His-13. In order to establish which histidine was carboxymethylated, the modified peptide (fraction 29) was subjected to Edman degradation. Table 2 shows that there was no significant release of ^{14}C until cycle 8, indicating that carboxymethylation occurred exclusively at His-13.

Radioactive peaks C and D (~25% and 21% of the total counts, respectively), elute slightly after peptide T-11 and are not well resolved. Amino acid analysis (Table 1) reveals that both peaks represent derivatives of peptide T-11, containing residues 55-60 and 102-121 in disulfide linkage. In both cases the histidine content is decreased by about 0.9 residue. Based on the 206 nm absorbance peak area of each, unmodified T-11, peak C, and peak D are present in a ratio of 1:2.3:0.9. The stoichiometry of ^{14}C incorporation is 0.8 for peak C and 1.7 for peak D. Amino acid analysis shows that both peaks yield a new absorbance peak eluting at 2.36 min, different from that seen for peak B. Assuming that this derivative has the same molar absorptivity as PTC-His, 0.8-0.9 residue is present for peak C and ~0.2 for peak D.

Radioactivity measurements were performed on amino acid analyzer eluates from peak C (fraction 84) and peak D (fraction 87). With the former, virtually all of the radioactivity coelutes with the new absorbance peak at 2.36 min. With peak D, 19% of the radioactivity elutes at this same time, but the remainder elutes somewhat earlier together with PTC-Asp.

Angiogenin peptide T-11 contains only a single histidine, at position 114. Thus, the peptides in peaks C and D must both be modified at this site. The stoichiometries of radioactivity incorporation suggest that for peak C, His-114 has been monocarboxymethylated while for peak D both imidazole nitrogens have been carboxymethylated.

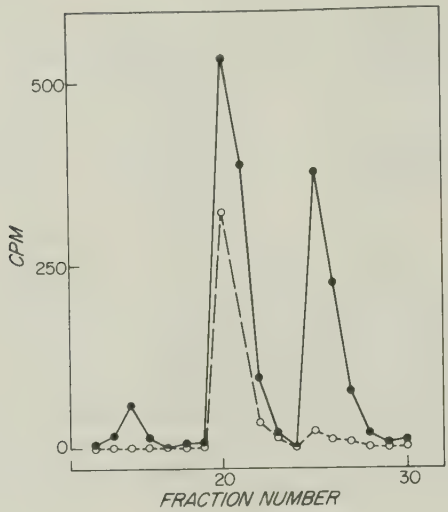

Figure 2: C18 HPLC elution patterns of radioactive PTC-amino acids from RNase A (dotted line) and angiogenin (solid line) treated with [^{14}C]bromoacetate. Modifications and chromatography were performed as described in the text. Fractions (0.2 mL) were collected and counted in their entirety.

Identification of Histidine Derivatives Formed During Reaction of Angiogenin with Bromoacetate. The above results indicate that a bis-CM derivative and two distinct mono-CM derivatives of histidine are formed during the reaction of angiogenin with bromoacetate. The structures of the two mono-CM adducts were determined by chromatographic comparison with derivatives of known structure obtained from RNase A. RNase A was modified with [^{14}C]bromoacetate under conditions (30 mM bromoacetate, 48 min., 27°C) expected to yield an ~8:1 ratio of 1-CM-His-119 to 3-CM-His-12 (8). To facilitate kinetic comparisons of the two proteins, angiogenin was treated under conditions (as with RNase, but for 4 h) producing a similar degree of inactivation (65%). After removal of free [^{14}C]bromoacetate by C18 HPLC, both proteins were hydrolyzed and subjected to amino acid analysis using a modified HPLC gradient (see Materials and Methods) that gives improved separation of the CM-His derivatives. Radioactivity measurements performed on HPLC effluents show two peaks for RNase and three for angiogenin (Fig. 2). The predominant peak from RNase A elutes in fractions 20-21 and should represent the PTC adduct of 1-CM-His. A peak containing ~7-fold less ^{14}C elutes in fractions 25-27 and should represent the PTC adduct of 3-CM-His. Both peaks are generated from the angiogenin sample, although in this case the earlier peak contains only a 1.5-fold larger amount of ^{14}C than the later

one. Based on results described in the previous section, the earlier peak derives from His-114 while the later is from His-13. The additional peak of radioactivity eluting in fractions 14-15 contains only ~4% of the total radioactivity and probably represents bis-CM-His.

In conclusion, inactivation of angiogenin by bromoacetate is associated with carboxymethylation of His-13 and His-114. At times relatively early in the reaction (4 h), modification occurs almost exclusively at N-3 of His-13 and N-1 of His-114. The ratio of the two adducts formed is 1:1.5, in contrast to the 1:8 ratio observed with RNase A. We have previously reported that angiogenin is inactivated by bromoacetate 5-fold more slowly than is RNase A (6). The present findings indicate that this decreased rate reflects largely a slower reaction at His-114 vs. His-119 of RNase A, with little difference in the reaction rates at His-13 of angiogenin vs. His-12 of RNase.

At somewhat later stages in the reaction of bromoacetate with angiogenin, His-114 becomes doubly modified; by 15.5 h, 28% of the modified His-114 residues are biscarboxymethylated, comparable with results reported for RNase A (11). Also, at this time in the reaction, it becomes apparent that both His-13 and His-114 of the same angiogenin molecule are carboxymethylated, since 45% of His-13 and 76% of His-114 have been modified. While it was originally thought that carboxymethylation at the two sites in RNase A were mutually exclusive (8), it was later shown that this is not the case (12).

Finally, it should be noted that the degree of angiogenin inactivation observed is greater than the extent of modification of either His-13 or His-114 separately. Therefore both residues must be important for activity.

ACKNOWLEDGMENTS: We thank Dr. James F. Riordan for helpful discussions and Nazik Sarkissian for excellent technical assistance. This work was supported by funds from Hoechst, A.G., under an agreement with Harvard University.

REFERENCES

1. Fett, J. W., Strydom, D. J., Lobb, R. R., Alderman, E. M., Bethune, J. L., Riordan, J. F., and Vallee, B. L. (1985) Biochemistry 24, 5480-5486.

2. Strydom, D. J., Fett, J. W., Lobb, R. R., Alderman, E. M., Bethune, J. L., Riordan, J. F., and Vallee, B. L. (1985) Biochemistry 24, 5486-5494.
3. Kurachi, K., Davie, E. W., Strydom, D. J., Riordan, J. F., and Vallee, B. L. (1985) Biochemistry 24, 5494-5499.
4. Shapiro, R., Riordan, J. F., and Vallee, B. L. (1986) Biochemistry 25, 3527-3532.
5. St. Clair, D. K., Rybak, S. M., Riordan, J. F., and Vallee, B. L. (1987) Proc. Natl. Acad. Sci. USA 84, 8330-8334.
6. Shapiro, R., Weremowicz, S., Riordan, J. F., and Vallee, B. L. (1987) Proc. Natl. Acad. Sci. USA 84, 8783-8787.
7. Crestfield, A. M., Stein, W. H., and Moore, S. (1963) J. Biol. Chem. 238, 2413-2420.
8. Crestfield, A. M., Stein, W. H., and Moore, S. (1963) J. Biol. Chem. 238, 2421-2428.
9. Shapiro. R., Strydom, D. J., Olson, K. A., and Vallee, B. L. (1987) Biochemistry 26, 5141-5146.
10. Bidlingmeyer, B. A., Cohen, S. A., and Tarvin, T. L. (1984) J. Chromatogr. 336, 93-104.
11. Goren, H. J., and Barnard, E. A. (1970) Biochemistry 9, 959-973.
12. Bello, J., and Nowoswiat, E. F. (1971) Eur. J. Biochem. 22, 225-234.

Vol. 156, No. 1, 1988 BIOCHEMICAL AND BIOPHYSICAL RESEARCH COMMUNICATIONS
October 14, 1988 Pages 537-542

SITE-DIRECTED MUTAGENESIS AT THE REGULATORY SITE OF FRUCTOSE 6-PHOSPHATE-1-KINASE FROM *Bacillus stearothermophilus*

B. C. Valdez, S. H. Chang and E. S. Younathan[1]

Department of Biochemistry, Louisiana State University, Baton Rouge, LA 70803

Received August 29, 1988

We have mutated Arg-25, Asp-59 and Arg-211 to alanine; and Asp-59 also to methionine, in fructose 6-phosphate-1-kinase from *B. stearothermophilus* (designated as RA25, DA59, RA211 and DM59 respectively). All four mutants did not change the affinity of the enzyme for ATP. RA25 has half the affinity for fructose 6-phosphate and exhibits sigmoidicity with respect to this substrate (Hill # = 2.0). DA59 has the same affinity for phosphoenolpyruvate (PEP) as the wild type whereas DM59 has 3-fold the affinity for this modulator and the inhibition is reversed by GDP. RA25 and RA211 are 100-fold less sensitive to PEP inhibition which is not relieved by GDP. It is concluded that Arg-25 and Arg-211, but not Asp-59, are involved in the direct binding of PEP and GDP.
© 1988 Academic Press, Inc.

Fructose 6-phosphate-1-kinase (EC.2.7.1.11) catalyzes the phosphorylation of β-fructose 6-phosphate to β-fructose 1,6-bisphosphate. The activity of this enzyme is regulated by many physiological effectors depending on its source (1-5). *Bacillus stearothermophilus* PFK (BsPFK), with subunit molecular weight of 34,000, is activated by ADP or GDP and inhibited by phosphoenolpyruvate (PEP). These modulators bind to the same site (4,6). The amino acid residues involved in binding the substrates and certain

[1]To whom correspondence should be addressed.

Abbreviations: PFK, fructose 6-phosphate-1-kinase; BsPFK, PFK from *Bacillus stearothermophilus*; PEP, phosphoenolpyruvate; SDS-PAGE, sodium dodecylsulfate polyacrylamide gel electrophoresis; YT, yeast extract-tryptone broth; Tris-Cl, Tris-(hydroxymethyl)aminomethane chloride; DTT, dithiothreitol; EDTA, ethylenediaminetetraacetic acid; Fru 6-P, fructose 6-phosphate; Km, Michaelis-Menten constant; K_{PEP}, dissociation constant of PEP.

0006-291X/88 $1.50
Copyright © 1988 by Academic Press, Inc.
All rights of reproduction in any form reserved.

modulators have been identified from the crystallographic structure of BsPFK (6). We report here the results of mutation of some of these proposed residues to prove unequivocally the ones involved in the binding of the modulators. Our results also indicate that certain mutations at the regulatory site seem to change the allosteric characteristics of BsPFK in the absence of an effector. We have reported recently the use of this approach to study the fructose 6-phosphate binding residues at the active site of BsPFK (7).

EXPERIMENTAL PROCEDURES

Enzymes and Chemicals. Enzymes for subcloning and *in vitro* mutagenesis were obtained from BRL, Bethesda, MD, and New England Biolabs, Inc., Beverly, MA. Other enzymes and chemicals were purchased from Sigma Chemical Co. [α-^{35}S]thio-dATP was obtained from New England Nuclear, Inc. *Bacillus stearothermophilus* NCA 1503 (ATCC 7954) was obtained from the American Type Culture Collection (Rockville, MD). Oligodeoxynucleotides used for site-directed mutation were synthesized by solid support phosphite chemistry in an automated DNA synthesizer (Applied Biosystems Model 380A).

Site-Directed Mutagenesis. BsPFK gene cloned in λgt10 vector (8) was double-digested with *Eco*RI and *Cla*I. The isolated 2.5 kb Bspfk fragment was subcloned into the *Eco*RI-*Acc*I sites of M13mp18. The ligation product was used to transform DH5α competent cells (BRL, Bethesda, MD) with *E. coli* JM109 as lawn cells. The recombinant M13/Bspfk phage was used to prepare the uracil-containing single-stranded template for the oligodeoxynucleotide-directed *in vitro* mutagenesis as described by Kunkel (9). M13 infection was done at 37°C for not more than 5.5 hrs to prevent any undesirable deletion of the insert. Mutants were identified either by screening plaques with ^{32}P-labeled mutagenic oligodeoxynucleotides as hybridization probes or by sequencing representative recombinants. Each entire mutated BsPFK gene was sequenced using a "Sequenase Kit" (USBC, Cleveland, OH) to check that no other mutations had occured. The 2.5 kb fragment containing the mutated BsPFK gene was subcloned into the *Eco*RI-*Hin*dIII sites of pBR322 and expressed in the PFK-deficient *E. coli* DF1020 as reported for the wild type BsPFK (10).

Purification of Cloned BsPFK. The transformed DF1020 host was grown to stationary phase in 2X YT broth (16 g tryptone, 10 g yeast extract, and 5 g NaCl per liter pH 7.5) containing 100 ug/ml ampicillin at 37°C. Cells were pelleted by centrifugation at 4°C, 5,000 Xg for 10 min, resuspended at 10 % and sonicated for 5 min at 0°C in sonication buffer (50 mM Tris-Cl, pH 7.4, 1 mM DTT, 1 mM EDTA, 1 mM phenylmethylsulfonyl fluoride). The crude lysate was centrifuged for 1 hr at 12,000 Xg, 4°C. The clear supernatant solution was heated at 70°C for 15 min, cooled on ice and recentrifuged. The wild type enzyme and the mutants were purified at 4°C using Cibacron Blue 3GA-Agarose Type 3000-CL-L (Sigma Chemical Co.) equilibrated with sonication buffer containing 0.1 M NaCl. The enzyme samples were made to 0.1 M NaCl, loaded on the

column, washed with at least two bed volumes of equilibration buffer, and eluted using a 0.1 M - 1.5 M NaCl gradient. BsPFK which eluted at approximately 1.1 M NaCl was desalted by dialysis against sonication buffer and concentrated by dialysis against 50 % glycerol in same buffer. The concentrated enzyme solution was stored at -20°C. Prior to enzyme assay it was dialyzed against 0.1 M Tris-Cl, pH 7.4, 1 mM DTT. The final enzyme preparations appeared pure as shown by SDS-PAGE (11) stained with Coomassie Blue. Protein concentrations were determined using the BIO-RAD Protein Assay reagent (BIO-RAD, Richmond, CA).

Enzyme Assay. BsPFK activity was measured by an assay coupled to NADH oxidation (12,13). One ml of reaction mixture contained 0.1 M Tris-Cl (pH 8.2), 10 mM $MgCl_2$ 5 mM NH_4Cl, 0.2 mM $NADH_2$, 100 ug aldolase (Type IV), 18 ug triose-phosphate isomerase and 2.4 ug glycerol 3-phosphate dehydrogenase (Type III). ATP and Fru 6-P concentrations were as indicated under Results and Discussion section. To prevent ADP-mediated effects, ATP was regenerated with 1 mM creatine phosphate and 10 ug/ml creatine phosphokinase. This regenerating system was omitted whenever the effects of ADP or GDP were studied. The NADH oxidation was monitored at 340 nm using Gilford Response I spectrophotometer at 29°C.

Determination of Kinetic Parameters. Km and Hill coefficients were calculated using the Enzfitter Program by Leatherbarrow (14) on a personal computer. The dissociation constant for PEP was calculated according to Blangy et al. (15).

RESULTS AND DISCUSSION

Site-directed mutation, expression and purification. Figure 1 shows the nucleotide sequences for the four mutants. We designate Arg-25 → Ala as RA25, Arg-211 → Ala as RA211, Asp-59 → Ala as DA59 and Asp-59 → Met as DM59. Similar to the wild type, these four mutants are all stable at 70°C for 15 min. Increased purity can be obtained by longer heating in the presence of Fru 6-P. Fru 6-P, but not Mg-ATP, renders BsPFK more heat stable. The four mutants have the same mobility in SDS-PAGE as the wild type BsPFK.

Kinetic comparison of the wild type and mutants. The wild type BsPFK and the mutants, except RA25, follow hyperbolic Michaelis-Menten kinetics with respect to ATP and Fru 6-P and exhibit the same affinity for these substrates. RA25 has the same affinity for ATP as the other mutants but has half the affinity for Fru 6-P (Table 1). It exhibits sigmoidal kinetics with respect to Fru 6-P concentrations (Figure 2) with a Hill number of 2.0.

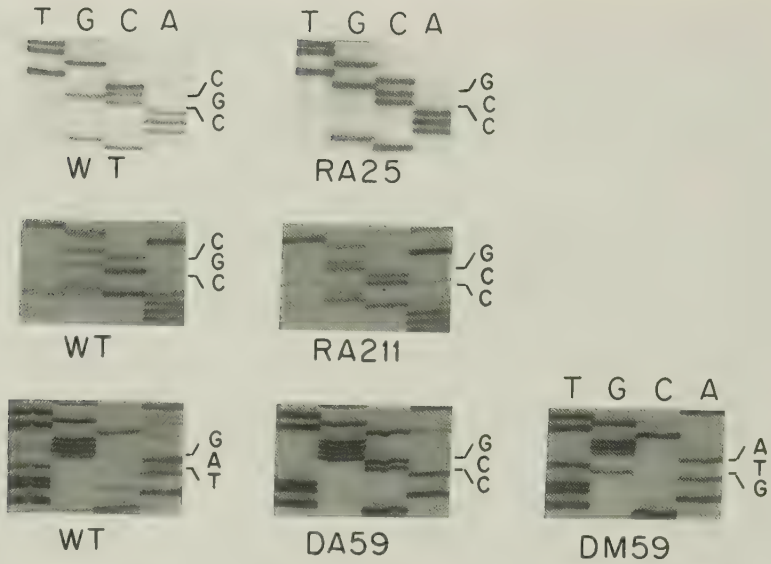

Figure 1. DNA sequence showing the mutations of Arg-25, Arg-211 and Asp-59. *In vitro* mutation was carried out according to Kunkel's protocol (9). Sequencing was performed by dideoxy chain termination method as described under the Experimental Procedures. WT, wild type; RA25, Arg-25 → Ala; RA211, Arg-211 → Ala; DA59, Asp-59 → Ala; DM59, Asp-59 → Met.

Previous kinetic studies in our laboratory have shown that the wild type BsPFK is allosterically different from the major *E. coli* PFK (7). The former exhibits a hyperbolic curve with respect to Fru 6-P whereas the latter shows sigmoidal behavior. Our data on RA25 illustrate the dramatic change in the degree of cooperativity between the subunits of BsPFK by mutating a single residue at the regulatory site, namely Arg-25 → Ala.

Effects of PEP and GDP. PEP is a potent inhibitor of the wild type BsPFK. Mutation of Asp-59 to alanine or methionine

Table 1. Kinetic parameters of the mutants and wild type BsPFK

Enzyme form	Km, Fru 6-P (mM)	K_{PEP} (mM)
Wild Type	0.029 ± 0.002	0.44 ± 0.02
RA25	0.06 ± 0.01	45 ± 9
RA211	0.029 ± 0.003	50 ± 10
DA59	0.027 ± 0.003	0.42 ± 0.07
DM59	0.028 ± 0.003	0.16 ± 0.02

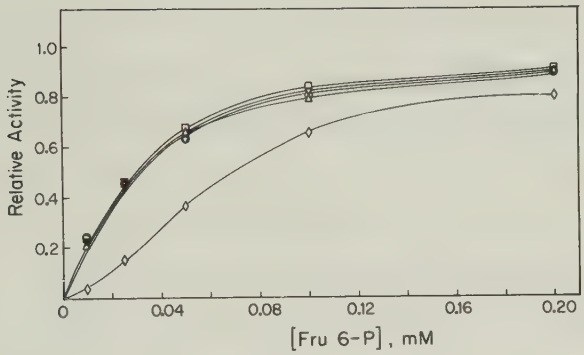

Figure 2. Comparison of the effect of Fru 6-P concentration on the activity of the wild type BsPFK and the four mutants. Activities were measured as described under the Experimental Procedures using 1 mM ATP and the indicated concentrations of Fru 6-P. ○—○, wild type; ◇—◇, RA25; ▽—▽, RA211; □—□, DA59; △—△, DM59.

renders BsPFK slightly more sensitive to PEP inhibition. The dissociation constants of PEP are 0.44, 0.42 and 0.16 mM for wild type, DA59 and DM59, respectively (Table 1). GDP reverses the inhibition by PEP (Figure 3A). These results suggest that the side chain of Asp-59 is not directly involved in the binding of PEP and GDP. This is consistent with the X-ray structure of BsPFK which shows that the polypeptide part of Asp-59, but not its side chain, binds to the β-phosphate of ADP or GDP (6).

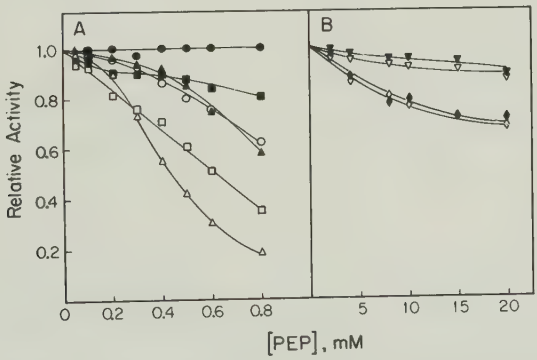

Figure 3. Effect of PEP concentrations on the activity of BsPFK. Activities were measured as described under the Experimental procedures in the presence of 1 mM ATP, 1 mM Fru 6-P and indicated concentrations of PEP in the absence (open marks) or presence (closed marks) of 0.5 mM GDP. (A) Wild Type, with (●—●) and without (○—○) GDP; DA59, with (■—■) and without (□—□) GDP; DM59, with (▲—▲) and without (△—△) GDP. (B) RA25, with (◆—◆) and without (◇—◇) GDP; RA211, with (▼—▼) and without (▽—▽) GDP.

RA25 and RA211 exhibit 100-fold less sensitivity to PEP than does the wild type (Table 1). This insensitivity to PEP inhibition and the inability of GDP to reverse this effect (Figure 3B) prove unequivocally that Arg-25 and Arg-211 are involved in the binding of both modulators. This is consistent with the crystallographic structure of BsPFK which shows that Arg-25 binds to the α- and β-phosphates of ADP or GDP and Arg-211 binds to the β-phosphate and adenine group of ADP or GDP (6).

The above-mentioned mutations define the role of Arg-25, Arg-211 and Asp-59 in BsPFK. Currently, we are conducting certain other mutations to gain more information on the mechanism of regulation of BsPFK and the interaction between its subunits.

ACKNOWLEDGMENTS: We thank M. Shirley for synthesizing the oligonucleotides. This work was supported by the National Institutes of Health Grant # DK31676.

REFERENCES

1. Sanwal, B. D. (1970) Bact. Rev. 34, 20-39.
2. Abrahams, S. L., and Younathan, E. S. (1971) J. Biol. Chem. 246, 2464-2467.
3. Younathan, E. S., Voll, R. J., and Koerner, T. A. W., Jr. (1981) in The Regulation of Carbohydrate Formation and Utilization in Mammals (Veneziale, C. M., ed) pp. 69-98, University Park Press, Baltimore, MD.
4. Evans, P. R., Farrants, G. W., and Hudson, P. J. (1981) Phil. Trans. R. Soc. Lond., B. 293, 53-62.
5. Kemp, R. G., and Foe, L. G. (1983) Mol. Cell. Biochem. 57, 147-154.
6. Hellinga, H. W., and Evans, P. R. (1985) Eur. J. Biochem. 149, 363-373.
7. Valdez, B. C., French, B. A., Younathan, E. S. and Chang, S. H. 1988 FASEB Annual Meeting, May 1-5, Las Vegas, Nevada. Abstract # 1482.
8. French, B. A., and Chang, S. H. (1987) Gene. 54, 65-71.
9. Kunkel, T. A. (1985) Proc. Natl. Acad. Sci. USA. 82, 488-492.
10 French, B. A., Valdez, B. C., Younathan, E. S., and Chang, S. H. (1987) Gene. 59, 279-283.
11. Laemmli, U. K. (1970) Nature. 227, 680-685.
12. Babul, J. (1978) J. Biol. Chem. 253, 4350-4355.
13. Lau, F. T. K., Fersht, A. T., Hellinga, H. W., and Evans, P. R. (1987) Biochemistry. 26, 4143-4148.
14. Leatherbarrow, R. J. 1987) Enzfitter: A Non-linear Regression Data Analysis Program for the IBMPC. Elsevier Science Publishers BV, The Netherlands.
15. Blangy, D., Buc, H., and Monod, J. (1968) J. Mol. Biol. 31, 13-35.

Vol. 156, No. 1, 1988 BIOCHEMICAL AND BIOPHYSICAL RESEARCH COMMUNICATIONS
October 14, 1988 Pages 543-550

BIOSYNTHESIS OF 12-OXO-10,15(Z)-PHYTODIENOIC ACID: IDENTIFICATION OF AN ALLENE OXIDE CYCLASE*

Mats Hamberg

Department of Physiological Chemistry,
Karolinska Institutet, S-104 01 Stockholm, Sweden

Received September 2, 1988

Incubation of 13(S)-hydroperoxy-9(Z),11(E),15(Z)-octadecatrienoic acid with corn (Zea mays L.) hydroperoxide dehydrase led to the formation of an unstable allene oxide derivative, 12,13(S)-epoxy-9(Z),11,15(Z)-octadecatrienoic acid. Further conversion of the allene oxide yielded two major products, i.e. α-ketol 12-oxo-13-hydroxy-9(Z),15(Z)-octadecadienoic acid, and 12-oxo-10,15(Z)-phytodienoic acid (12-oxo-PDA). 12-Oxo-PDA was formed from allene oxide by two different pathways, i.e. spontaneous chemical cyclization, leading to racemic 12-oxo-PDA, and enzyme-catalyzed cyclization, leading to optically pure 12-oxo-PDA. The allene oxide cyclase, a novel enzyme in the metabolism of oxygenated fatty acids, was partially characterized and found to be a soluble protein with an apparent molecular weight of about 45,000 that specifically catalyzed conversion of allene oxide into 9(S),13(S)-12-oxo-PDA. © 1988 Academic Press, Inc.

In recent work from our laboratory, formation of allene oxide derivatives from unsaturated fatty acid hydroperoxides has been described. Thus, corn (Zea mays, L.) hydroperoxide dehydrase was found to catalyze the conversion of 13(S)-hydroperoxy-9(Z),11(E)-octadecadienoic acid (13(S)-HPOD) into the allene oxide 12,13(S)-epoxy-9(Z),11-octadecadienoic acid (12,13(S)-EOD), which was characterized by chemical and physical methods (1). 9(S)-HPOD underwent an analogous type of transformation into allene oxide 9(S),10-EOD (2). The allene oxides were rapidly hydrolyzed ($t_{1/2}$, 33-34 sec at 0°) in aqueous

*Part no. IV in a series of papers dealing with the chemistry and biochemistry of fatty acid allene oxides.

Abbreviations: 13(S)-HPOD, 13(S)-hydroperoxy-9(Z),11(E)-octadecadienoic acid; 13(S)-HPOT, 13(S)-hydroperoxy-9(Z),11(E),15(Z)-octadecatrienoic acid; 9(S)-HPOD, 9(S)-hydroperoxy-10(E),12(Z)-octadecadienoic acid; 12,13(S)-EOD, 12,13(S)-epoxy-9(Z),11-octadecadienoic acid; 9(S),10-EOD, 9(S),10-epoxy-10,12(Z)-octadecadienoic acid; 12,13(S)-EOT, 12,13(S)-epoxy-9(Z),11,15(Z)-octadecatrienoic acid; 12-oxo-PDA, 12-oxo-10,15(Z)-phytodienoic acid.

0006-291X/88 $1.50
Copyright © 1988 by Academic Press, Inc.
All rights of reproduction in any form reserved.

medium into stable α-ketols, which had been isolated in earlier work (3,4). Confirmation of the formation and structures of fatty acid allene oxides was very recently provided by Brash et al., who isolated the methyl esters of a number of allene oxides and characterized them by eg. NMR spectrometry (5).

12-Oxo-10,15(Z)-phytodienoic acid (12-oxo-PDA) and pre-clavulone A are cyclopentenone derivatives which are formed from fatty acid hydroperoxides in plants and lower marine organisms, respectively. Allene oxides have been proposed to serve as the immediate precursors of 12-oxo-PDA and pre-clavulone A (6-10), eg. because of the well established chemical conversion of allene oxides into cyclopentenones (11,12), and because of the fact that formation of 12-oxo-PDA and pre-clavulone A is accompanied by the formation of α-ketols, non-enzymatic hydrolysis products of allene oxides. Direct evidence for the concept of allene oxides serving as precursors of cyclopentenones of plant and marine origin was recently provided by the finding that the allene oxide 12,13(S)-EOD, in the presence of bovine serum albumin, underwent cyclization into a cyclopentenone related to 12-oxo-PDA (9), and by the finding that degradation of the methyl ester of 12,13(S)-EOT in buffer led to formation of the methyl ester of 12-oxo-PDA (5).

The present paper is concerned with the mechanism of formation of 12-oxo-PDA and, specifically, with the presence in corn homogenate of a soluble allene oxide cyclase that catalyzes the conversion of the allene oxide 12,13(S)-EOT into optically pure 12-oxo-PDA.

EXPERIMENTAL

[1-^{14}C]13(S)-HPOD and [1-^{14}C]13(S)-HPOT (specific radioactivities, 1.4 kBq/μmol and 6.3 kBq/μmol, respectively) were prepared as described (13). Pronase was purchased from Sigma Chemical Co.

Defatted meal of corn (Bear X8632, Noble Bear Hybrid Corn, Inc., Decatur, IL) was homogenized in 0.1 M potassium phosphate buffer pH 6.7 (1:5, w/v) at 0° with a Polytron. The homogenate was centrifuged at 9,300xg for 15 min and the resulting supernatant was centrifuged at 105,000xg for 60 min. The 105,000xg supernatant was removed and kept on ice. The 105,000xg particle fraction was either used directly, or washed by resuspension in buffer and recentrifugation at 105,000xg. The following enzyme preparations were used for the incubations: 105,000xg supernatant (1.7 mg protein/ml), 105,000xg particle fraction resuspended in buffer (1.0 mg protein/ml), washed 105,000xg particle fraction in buffer (1.0 mg protein/ml), and washed 105,000xg particle fraction resuspended in 105,000xg supernatant (particle protein, 1.0 mg/ml, soluble protein, 1.7 mg/ml). Endogenous 12-oxo-PDA was undetectable (less than 0.2 μM) in the preparations used.

Hydroperoxide dehydrase activity was determined by a spectrophotometric method in which dilutions of enzyme preparations were treated with either 13(S)-HPOD or 13(S)-HPOT in a cuvette at 20°. The initial rate of decrease in absorption at 236 nm was monitored.

Incubations of [1-^{14}C]13(S)-HPOT were carried out at 0°. In trapping experiments, 10-150 μM 13(S)-HPOT was incubated with 10 ml of enzyme preparation (either 105,000xg supernatant or 105,000xg particle fraction) and 1 ml aliquots were removed at 15, 30, 45, and 60 sec and added to 20 ml of methanol. In studies of 12-oxo-PDA formation, 3-150 μM 13(S)-HPOT was incubated with 10 ml of enzyme preparation (washed particle fraction, resuspended in either buffer or 105,000xg super-

natant) for 10 min and added to 30 ml of methanol. When using low concentrations of substrate, several such incubations were pooled in order to produce sufficient amounts of 12-oxo-PDA for identification and for steric analysis. The incubation mixtures were acidified and extracted twice with diethyl ether. The esterified product was subjected to TLC (solvent system, ethyl acetate/toluene (15:85, v/v)).

Steric analysis of 12-oxo-PDA as well as the instrumental methods used were as described in detail (9,14).

RESULTS

Detection of 12,13(S)-epoxy-9(Z),11,15(Z)-octadecatrienoic acid. Corn homogenates were fractionated by differential centrifugation and hydroperoxide dehydrase activity was measured by a spectrophotometric method using 13(S)-HPOD as the substrate (initial concentration, 34 μM). Dehydrase was present in the 105,000xg particle and supernatant fractions, catalyzing the consumption of 1.9 and 0.2 μmol of 13(S)-HPOD/min·mg of protein, respectively.

As expected from recent work (1), the product formed from 13(S)-HPOT by action of hydroperoxide dehydrase was an unstable allene oxide, 12,13(S)-epoxy-9(Z),11,15(Z)-octadecatrienoic acid (12,13(S)-EOT). The structure of this compound was established as described for the related allene oxide 12,13(S)-EOD (1). Thus, incubation of 10-150 μM 13(S)-HPOT at 0° for 10-60 sec with either the 105,000xg particle fraction in buffer or the 105,000xg supernatant followed by treatment with 20 vol of methanol led to the appearance of a trapping product, 12-oxo-13-methoxy-9(Z),15(Z)-octadecadienoic acid. The half-life of 12,13(S)-EOT at 0° and pH 6.7 as determined by the trapping technique (1) was 26 sec (earlier found for 12,13(S)-EOD and 9(S),10-EOD at 0° and pH 7.4, 33 and 34 sec, respectively (1,2)).

The ultraviolet spectrum of 12,13(S)-EOT showed an absorption band with λ_{max} = 236 nm and was virtually identical to that of 12,13(S)-EOD (1), thus proving the presence in 12,13(S)-EOT of one pair of conjugated double bonds. As was earlier observed for 12,13(S)-EOD (1), stability of 12,13(S)-EOT was significantly enhanced in non-hydroxylic solvents. For example, the half-life of 12,13(S)-EOT in 90% aqueous acetonitrile at 15° was 39 sec (earlier found for 12,13(S)-EOD at 15°, 35 sec). Finally, degradation of 12,13(S)-EOT in aqueous acetonitrile did not lead to the formation of the α-ketol derivative but to two isomeric macrolactones, 12-oxo-9(Z),15(Z)-octadecadien-11-olide and 12-oxo-9(Z),15(Z)-octadecadien-13-olide. These findings were in complete agreement with results recently obtained with 12,13(S)-EOD (15) and 9(S),10-EOD (2).

Detection of an allene oxide cyclase in corn homogenate. In order to study the further transformations of the allene oxide 12,13(S)-EOT, this compound was generated by incubation of [1-^{14}C]13(S)-HPOT with hydroperoxide dehydrase contained in the washed 105,000xg particle fraction. The dehydrase activity in the preparation used was sufficient to catalyze complete conversion of more than 150 μM 13(S)-HPOT into 12,13(S)-EOT in 20 sec at 0°. A total incubation time of 10 min at 0° was used in order to allow complete conversion of the allene oxide into stable end products. Fig. 1A shows a radio-TLC analysis of the esterified product isolated after incubation of

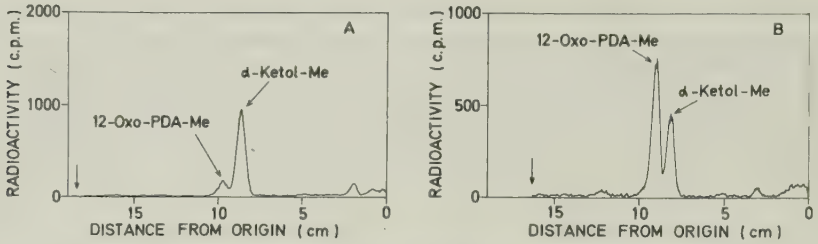

Fig. 1. TLC radiochromatograms of esterified products formed by incubation of 25 μM [1-^{14}C]13(S)-HPOT with (A) washed 105,000xg particle fraction resuspended in 10 ml of buffer, and (B) washed 105,000xg particle fraction resuspended in 10 ml of 105,000xg supernatant. Solvent system, ethyl acetate/toluene, 15:85 (v/v).

[1-^{14}C]13(S)-HPOT with washed 105,000xg particle fraction resuspended in buffer. Two labeled compounds, together forming about 80% of the recovered radioactivity, appeared. The minor compound was identified as methyl 12-oxo-10,15(Z)-phytodienoate (methyl ester of 12-oxo-PDA; R_f = 0.54) and the major one as the α-ketol derivative methyl 12-oxo-13-hydroxy-9(Z),15(Z)-octadecadienoate (R_f = 0.48) by UV and IR spectrometry, GC-MS, and chemical conversions as described in detail (1,9). Interestingly, when 13(S)-HPOT was incubated with the 105,000xg particle fraction resuspended in the 105,000xg supernatant, the generated 12,13(S)-EOT was preferentially converted into 12-oxo-PDA at the expense of α-ketol (Fig. 1B). Formation of 12-oxo-PDA and α-ketol at different concentrations of 13(S)-HPOT (and hence of 12,13(S)-EOT) is shown in Fig. 2. As seen, in the absence of 105,000xg supernatant, the amounts of 12-oxo-PDA produced were modest and were directly proportional to the substrate concentration. Furthermore, 12-oxo-PDA and α-ketol, the non-enzymatically produced hydrolysis product of allene oxide, appeared in a fixed ratio (about 0.14), irrespective

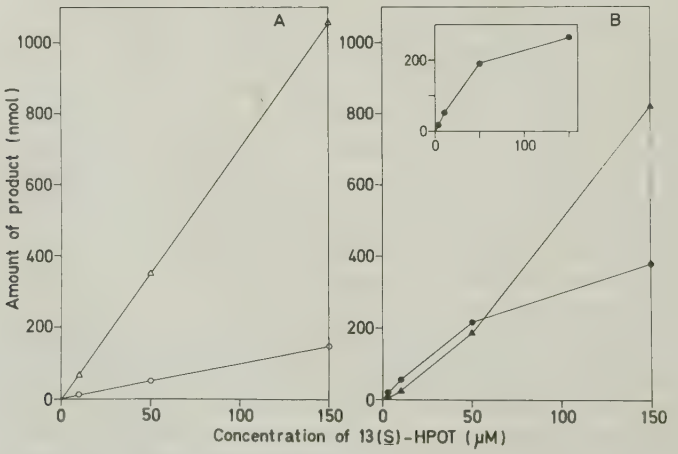

Fig. 2. Amounts of 12-oxo-PDA and α-ketol formed at different concentrations of 13(S)-HPOT. A: 13(S)-HPOT incubated with washed 105,000xg particle fraction in 10 ml of buffer. 12-Oxo-PDA, -○-○-; α-ketol, -△-△-. B: 13(S)-HPOT incubated with washed 105,000xg particle fraction resuspended in 10 ml of 105,000xg supernatant. 12-Oxo-PDA, -●-●-; α-ketol, -▲-▲-. Inset in panel B: amounts of enzymatically formed 12-oxo-PDA calculated from total amounts of 12-oxo-PDA and correction for 12-oxo-PDA formed by a non-enzymatic reaction.

TABLE I

Ratio 12-oxo-PDA/α-ketol and enantiomeric composition of 12-oxo-PDA

Incubation[a]	Concentration of 13(S)-HPOT (μM)	Ratio of 12-oxo-PDA/α-ketol	Enantiomers of 12-oxo-PDA (9S,13S/9R,13R)
A	10	0.17	51:49
A	50	0.14	50:50
A	150	0.14	51:49
B	3	2.88	98: 2
B	10	2.18	97: 3
B	50	1.17	95: 5
B	150	0.46	88:12
C	10	0.16	-
D	10	0.15	-

[a] Incubations consisted of washed 105,000xg particle fraction resuspended in: A, buffer; B, 105,000xg supernatant; C, 105,000xg supernatant heated at 90° for 10 min; D, 105,000xg supernatant preincubated at 37° for 1 h with 8 mg of pronase.

of substrate concentration. In the presence of 105,000xg supernatant, formation of 12-oxo-PDA was enhanced (Fig. 2B). In this case, the ratios 12-oxo-PDA/α-ketol were high at low substrate concentrations and dropped when substrate concentration was increased. These results suggested that, in the absence of 105,000xg supernatant, formation of 12-oxo-PDA occurred by a non-enzymatic, chemical cyclization of the allene oxide, whereas 12-oxo-PDA formation observed in the presence of 105,000xg supernatant occurred by action of a saturable activity, that selectively catalyzed formation of 12-oxo-PDA, as well as by non-enzymatic cyclization.

Further evidence for the formation of 12-oxo-PDA by both enzymatic and non-enzymatic routes was provided by steric analysis of 12-oxo-PDA (Table I). As seen, 12-oxo-PDA formed in the absence of 105,000xg supernatant was racemic, irrespective of the substrate concentration used. On the other hand, 12-oxo-PDA produced in the presence of 105,000xg supernatant was enriched with respect to the 9(S),13(S)-enantiomer. This enrichment was especially pronounced at low substrate concentrations. For example, incubation of 3 μM 13(S)-HPOT led to the formation of essentially optically pure 12-oxo-PDA (ratio between 9(S),13(S)- and 9(R),13(R)-enantiomers, 98:2).

Partial characterization of allene oxide cyclase. As seen in Table I, the stimulatory effect of the 105,000xg supernatant on the formation of 12-oxo-PDA was abolished by heat treatment (90°, 10 min) as well as by treatment with pronase. In further experiments with ammonium sulfate-fractionated supernatant, the fraction precipitated at 30-55% saturation was found to contain 90-95% of the allene oxide cyclase activity, whereas fractions collected at 0-30% and 55-80% saturation contained little or no activity.

In order to further characterize the allene oxide cyclase, ammonium sulfate precipitate of 105,000xg supernatant (30-55% saturation) was subjected to gel filtration (Fig. 3). Aliquots of the fractions were assayed for hydroperoxide dehydrase activity by the spectrophotometric

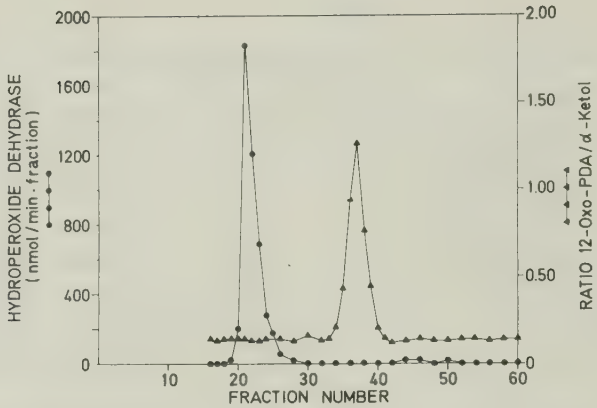

Fig. 3. Separation of hydroperoxide dehydrase and allene oxide cyclase by gel filtration. Ammonium sulfate precipitate obtained from 50 ml of 105,000xg supernatant (30-55% saturation; 40 mg of protein) was applied to a column of AcA 44 (LKB-Produkter AB, Bromma, Sweden; 88 x 2.6 cm). The column was eluted with 0.1 M potassium phosphate buffer pH 6.7 at a flow rate of 0.6 ml/min. Fraction size, 8.6 ml. Hydroperoxide dehydrase, -●-●-; ratio 12-oxo-PDA/α-ketol, -▲-▲-. As described in the text, non-enzymatic cyclization of allene oxide produced 12-oxo-PDA and α-ketol in a ratio of about 0.14:1.

method, and for allene oxide cyclase activity by incubation with [1-^{14}C]13(S)-HPOT in the presence of 105,000xg particle fraction followed by determination of 12-oxo-PDA and α-ketol by radio-TLC. The hydroperoxide dehydrase activity was excluded from the gel, indicating a molecular weight in excess of 130,000. In this context, it may be mentioned that reported molecular weights of cotton and spinach hydroperoxide dehydrases are 250,000 and 220,000, respectively (16,7). The allene oxide cyclase, detected by an increased formation of 12-oxo-PDA relative to the background level caused by non-enzymatic cyclization of allene oxide, appeared with an effluent volume of 292-344 ml (Fig. 3). As expected, 12-oxo-PDA generated by incubation of 13(S)-HPOT with the 105,000xg particle fraction plus fractions containing the allene oxide cyclase was enriched with respect to the 9(S),13(S)-enantiomer (eg., peak fraction, ratio between 9(S),13(S)- and 9(R),13(R)-enantiomers, 95:5), whereas similar incubations using fractions eluted before and after the allene oxide cyclase-containing fractions led to the formation of racemic 12-oxo-PDA. By using appropriate standard proteins to calibrate the column, it was found that the chromatographic behaviour of the cyclase was the same as that of a protein with a molecular weight of about 45,000.

DISCUSSION

The present paper is concerned with the mechanism of formation of the plant cyclopentenone, 12-oxo-10,15(Z)-phytodienoic acid (12-oxo-PDA) from α-linolenic acid 13-hydroperoxide (13(S)-HPOT). Transformation was initiated by hydroperoxide dehydrase-catalyzed conversion of the hydroperoxide into the unstable allene oxide derivative, 12,13(S)-EOT. Formation of 12-oxo-PDA from allene oxide was found to occur by non-enzymatic, chemical cyclization, as well as by an allene oxide cyclase-catalyzed reaction (Fig. 4). In the first

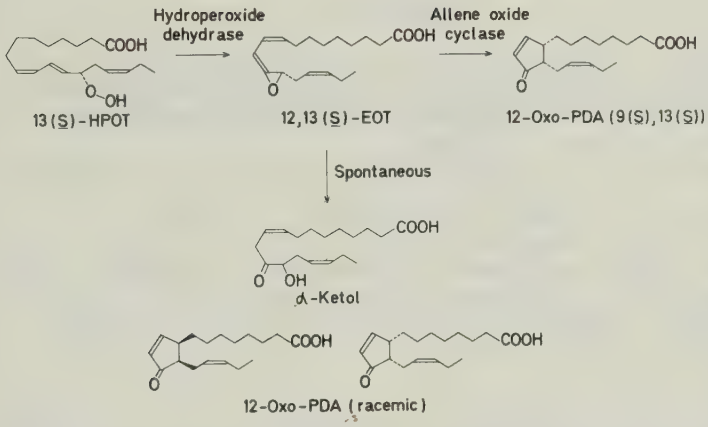

Fig. 4. Formation of 9(S),13(S)-12-oxo-PDA from 13(S)-HPOT by sequential actions of hydroperoxide dehydrase and allene oxide cyclase. Competing non-enzymatic conversion of allene oxide 12,13(S)-EOT into α-ketol and racemic 12-oxo-PDA is also shown.

case, the yield of 12-oxo-PDA relative to α-ketol, a non-enzymatically produced hydrolysis product of 12,13(S)-EOT, was relatively low, and the 12-oxo-PDA formed was racemic. In the second case, 12-oxo-PDA was the only product formed from allene oxide, and consisted of the pure 9(S),13(S)-enantiomer. The allene oxide cyclase activity appeared in the soluble fraction of corn homogenate, was destroyed by heating and proteolytic digestion, was precipitable by ammonium sulfate, and migrated like a protein with a molecular weight of about 45,000 on gel filtration.

In recent studies, 12-oxo-PDA obtained by incubation of 13(S)-HPOT with preparations of corn (14) and flaxseed (17) was found to be only partially optically pure and racemic, respectively. The present work, demonstrating the existence of a plant allene oxide cyclase, suggests that the incomplete optical purity of 12-oxo-PDA observed was due to low (14) or missing (17) allene oxide cyclase activity in the preparations used. It is postulated that the *in vivo* biosynthesis of 12-oxo-PDA occurs by sequential actions of ω6-lipoxygenase, hydroperoxide dehydrase, and allene oxide cyclase, resulting in the formation of optically pure 12-oxo-PDA. In this context it should be noted that the stereochemistry of 12-oxo-PDA formed in the presence of allene oxide cyclase described in the present paper is the same as that of (+)-7-iso-jasmonic acid, a growth-regulating hormone which is biosynthesized from 12-oxo-PDA in plant tissue (18).

Further studies on the kinetic and molecular properties of the corn allene oxide cyclase are in progress and will be reported later.

ACKNOWLEDGMENTS

The expert technical assistance of Mrs. G. Hamberg is gratefully acknowledged. This work was supported by a grant from the Swedish Medical Research Council (project No. 03X-05170).

REFERENCES

1. Hamberg, M. (1987) Biochim. Biophys. Acta 920, 76-84.
2. Hamberg, M., and Hughes, M.A. (1988) Proceedings of the Taipei Conference on Prostaglandin and Leukotriene Research, Raven Press, New York. In press.
3. Zimmerman, D.C. (1966) Biochem. Biophys. Res. Commun. 23, 398-402.
4. Gardner, H.W. (1970) J. Lipid Res. 11, 311-321.
5. Brash, A.R., Baertschi, S.W., Ingram, C.D., and Harris, T.M. (1988) Proc. Natl. Acad. Sci. USA 85, 3382-3386.
6. Corey, E.J., d'Alarcao, M., Matsuda, S.P.T., Lansbury, P.T., and Yamada, Y. (1987) J. Am. Chem. Soc. 109, 289-290.
7. Vick, B.A., and Zimmerman, D.C. (1987) Plant Physiol. 85, 1073-1078.
8. Brash, A.R., Baertschi, S.W., Ingram, C.D., and Harris, T.M. (1987) J. Biol. Chem. 262, 15829-15839.
9. Hamberg, M., and Hughes, M.A. (1988) Lipids 23, 469-475.
10. Crombie, L., and Morgan, D.O. (1988) J. Chem. Soc., Chem. Commun., 558-560.
11. Grimaldi, J., and Bertrand, M. (1969) Tetrahedron Lett. 38, 3269-3272.
12. Malacria, M., and Roumestant, M.L. (1977) Tetrahedron 33, 2813-2817.
13. Hamberg, M., and Gotthammar, B. (1973) Lipids 8, 737-744.
14. Hamberg, M., Miersch, O., and Sembdner, G. (1988) Lipids 23, 521-524.
15. Hamberg, M. (1988) Chem. Phys. Lipids 46, 235-243.
16. Vick, B.A., and Zimmerman, D.C. (1981) Plant Physiol. 67, 92-97.
17. Baertschi, S.W., Ingram, C.D., Harris, T.M., and Brash, A.R. (1988) Biochemistry 27, 18-24.
18. Vick, B.A., and Zimmerman, D.C. (1983) Biochem. Biophys. Res. Commun. 111, 470-477.

Vol. 156, No. 1, 1988 BIOCHEMICAL AND BIOPHYSICAL RESEARCH COMMUNICATIONS
October 14, 1988 Pages 551-556

ENTEROTOXIN OF *Clostridium perfringens* TYPE A FORMS ION-PERMEABLE CHANNELS IN A LIPID BILAYER MEMBRANE

Nakaba Sugimoto[1], Masayuki Takagi[2], Kunihiro Ozutsumi[1], Shigeko Harada[1], Morihiro Matsuda[1]

[1]Research Institute for Microbial Diseases, Osaka University, Suita, Osaka 565, Japan
[2]College of General Education, Osaka University, Toyonaka, Osaka 560, Japan

Received September 2, 1988

SUMMARY: The enterotoxin of *Clostridium perfringens* type A was found to form ion-permeable channels in a lipid bilayer. A patch clamp technique was used to detect channel activities in an asolectin bilayer with incorporated enterotoxin. About 20% of the lipid bilayer patches examined showed rectangular or stepwise shift of membrane current. The shifts indicated the gating of ion-permeable channels in the patches. The channels showed high conductance (40-450 pS), no rectification in current-voltage curves and occasional long-lasting events. The significance of these findings is discussed in relation to the mechanism of action of the toxin. © 1988 Academic Press, Inc.

The enterotoxin produced by certain strains of *Clostridium perfringens* type A is a simple protein with a molecular weight of about 35,000 and is a causative agent of food poisoning by this organism. It is cytotoxic to certain cells in culture(1) and causes disturbances of amino acid transportations(2), morphological alterations(3) and leakage of intracellular macromolecules(4) of the cells. The mechanism of the cytotoxic action of the enterotoxin can be divided into two groups of steps on the basis of their requirement for calcium in the extracellular fluid, Ca-independent early steps and Ca-dependent late steps, as we reported previously(5) and as confirmed recently by others(6, 7). Intoxicated cells show influx of Na and efflux of K and Mg(8, 9). Recently, we demonstrated that these ionic fluxes occur in the Ca-independent early steps, and that addition of substances with molecular

Mailing Address: Morihiro Matsuda, Department of Tuberculosis Research I, Research Institute for Microbial Diseases, Osaka University, 3-1, Yamadaoka, Suita, Osaka 565, JAPAN

0006-291X/88 $1.50
Copyright © 1988 by Academic Press, Inc.
All rights of reproduction in any form reserved.

weights of more than about 200 to the extracellular fluid prevented induction of morphological alterations of HeLa and Vero cells by the enterotoxin(10). These results suggested that the enterotoxin formed 'holes' in the cell membrane through which substances with molecular (or atomic) weights of less than about 200, such as Na and K, passed across the cell membrane. However, the molecular mechanism of the formation of 'holes' in the cell membrane by the enterotoxin is unknown.

In this study, we used lipid bilayer membranes of asolectin to examine the action of the enterotoxin on the membrane in a simpler system than cellular membranes. We applied the patch clamp technique, which has been used for analyses of single channel activities, to examine the changes elicited by the enterotoxin. Here we report that the enterotoxin of Clostridium perfringens type A forms ion-permeable gating channels in lipid bilayers of asolectin and discuss the significance of this finding in relation to the molecular mechanism of the action of the enterotoxin.

MATERIALS AND METHODS: The enterotoxin of C. perfringens was produced and purified to homogeneity as described previously(11). The purified preparation of enterotoxin had a lethal activity of about 470 mouse minimum lethal dose per mg of protein and a cytotoxicity of about 320 ng/ml of the 50% effective dose to HeLa S_3 in the trypan blue dye exclusion test.

Asolectin (soybean lecithin; Daigo Eiyo, Osaka, Japan) was suspended at a concentration of 9 mg/ml in 4 mM Tris-Hepes buffer, pH 6.4, containing 130 mM NaCl and 4 mM $CaCl_2$ by sonication under continuous bubbling with N_2 gas. Then 200 µl of the suspension was mixed with an equal volume of a solution of 300 ng/ml of the enterotoxin in the same buffer and sonicated at 37℃ for 2 min. Test mixtures were made by adding 5 µl of the sonicate to 0.2 ml of the buffer. The formation of lipid monolayers on the aqueous surface of the test mixtures was confirmed by observing drops of water running over the surface.

Patch pipettes were made of hard glass capillaries of 1.5 mm diameter and filled with the buffer. The electrical resistance of the patch pipettes was 20-50 MΩ. A lipid bilayer was formed at the tip of the patch pipettes by the method of Suarez-Isla et al.(12) by dipping the tip into the test mixture twice. The formation of a lipid bilayer at the tip of the patch pipette was confirmed by demonstrating increase in the electrical resistance of the patch pipette. The voltage of the inside of the patch pipette against the bath electrode was clamped, and current passed through the lipid bilayer at the tip of the patch pipette was amplified with a patch clamp amplifier (CEZ-2200, Nihonkoden, Tokyo, Japan), monitored with a pen recorder (WR-3701, Graphtec, Tokyo, Japan) and recorded with an FM data recorder (MR-10, TEAC, Tokyo, Japan).

RESULTS AND DISCUSSION

1. Formation of ion-permeable channels in a lipid bilayer by the enterotoxin: In all, 102 lipid bilayer patches of asolectin membranes with incorporated enterotoxin were studied. Of these, 21 lipid bilayer patches showed definite channel activities in records of their membrane currents. Figure 1 shows an example of the current records. The level of the membrane current shifted abruptly rectangularly or stepwise. These abrupt shifts of the membrane current indicate gating of the ion-permeable channel(s) in the lipid bilayer patch. As seen in the figure, the channel activities showed at least 4 conductance levels of 125, 250, 380 and 490 pS, respectively. This multiplicity in conductance levels of channel activities can be explained by supposing that the patch of the lipid bilayer used in this experiment contained 4 ion-permeable channels with similar conductances of about 125 pS. The channels activities of 14 patches of lipid bilayers showed multiple conductance levels. In 11 of these 14 lipid bilayer patches, the values of conductance were integrals of the minimum value in each lipid bilayer patch, and the frequencies and durations of channel events with larger conductances were much less than those of events with smaller conductances. Therefore, we conclude that the multiple conductances of channel activities in these lipid bilayer patches were summations of the activities of several channels that had similar conductances. The minimum conductance value in each lipid bilayer

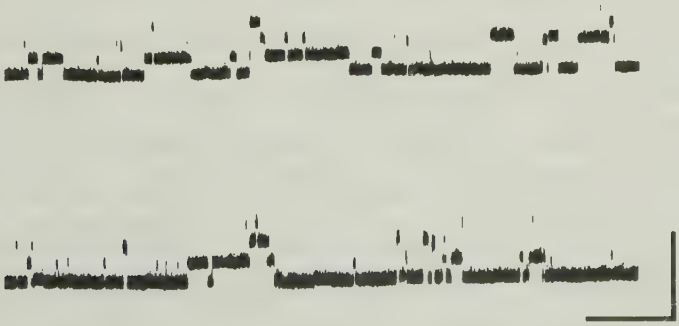

Figure 1. An example of the membrane current showing channel activities. A patch of lipid bilayer was formed at the tip of a patch pipette as described in Materials and Methods. The resistance of the lipid bilayer was 0.53 GΩ. The membrane potential was clamped at +11.5 mV. Calibration bars indicate 30 sec (abscissa) and 7.5 pA (ordinate).

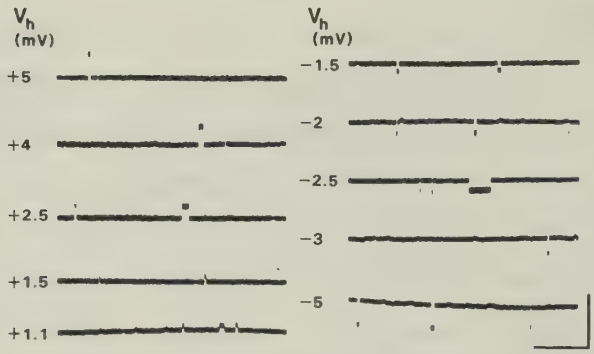

Figure 2. Records of membrane current obtained from a lipid bilayer patch at different holding potentials(Vh). The holding potential of each trace of the current record is shown on the left of the trace. Calibration bars indicate 30 sec (abscissa) and 5 pA (ordinate).

patch ranged from 40 to 450 pS. This variation of the values for minimum conductance may be due to minor differences in experimental conditions. But in all cases, the values for the conductance of ion-permeable channels formed by the enterotoxin are from about ten to several hundred times higher than the values of conductances reported for Na channels(13) and Ca channels(14, 15).

2. Characterization by single channel recording of the 'enterotoxin-channels' formed in the lipid bilayer: For further analysis of the channels formed in the lipid bilayer by the enterotoxin, we selected patches of lipid bilayer with single conductance levels. Figure 2 shows a series of current records obtained at various holding potentials from a patch of this type. The trace at a holding potential of −2.5 mV in Fig. 2 shows an event that lasted as long as 19 sec. Events with durations of at least a few seconds were frequently seen in this experiment. Records from other membrane patches also indicated that the 'enterotoxin-channels' sometimes opened for several seconds, though the numbers of events decreased exponentially with increase of the duration time. The results showed that the events of the 'enterotoxin-channels' sometimes have very long durations, though gating of the channels seemed to occur randomly. The current-voltage curve (Fig. 3) obtained from the same patch as that for Fig. 2 indicates that the conductances of the 'enterotoxin-channels' at different holding potentials give the same value of 415 pS. All the 'enterotoxin-channels' in this study gave linear current-voltage relationships and no rectification of the current was observed. These

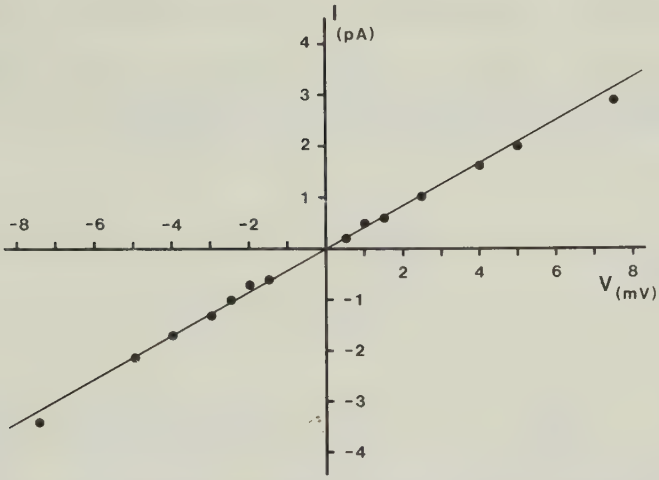

Figure 3. Current-voltage relationship of an 'enterotoxin-channel' obtained from the same lipid bilayer patch as for Fig. 2. Amplitudes of events are plotted against the holding potentials. The line was drawn by eye.

results indicated that the 'enterotoxin-channels' pass ions evenly in both directions, from outside to inside and from inside to outside.

The present results clearly showed that the enterotoxin of Clostridium perfringens type A formed characteristic ion-permeable channels in a lipid bilayer of asolectin. This finding provides a molecular basis for the mechanism of action of the enterotoxin. From our previous results in experiments on whole cells, we expected that the enterotoxin would form a static 'hole'. But on the contrary, the 'enterotoxin-channels' found in this study showed dynamic gating. Nevertheless, the characteristics of the 'enterotoxin-channels' are consistent with the results of previous studies. The large conductance of the 'enterotoxin-channels' may explain the fact that substances with molecular weights of less than ca. 200 appeared to pass through the 'holes' in the cell membrane of enterotoxin-treated cells. The bidirectional characteristic of the 'enterotoxin-channels' in the lipid membrane is consistent with bidirectional movement of cations in enterotoxin-treated cells: influx of Na and Ca, and efflux of K and Mg. The extraordinarilly long-lasting events in the channels of lipid membranes could explain the apparent 'hole' formation in intoxicated cells. Further characterization of the 'enterotoxin-channels' in lipid bilayers and studies

on the memberanes of intoxicated cells by the technique of single channel recording are now in progress to clarify the exact role of formation of ion-permeable channels by the enterotoxin in the mechanism of its cytotoxic action.

ACKNOWLEDGMENT: This work was supported in part by a grant from Ohyama Health Foundation Inc.

REFERENCES

1. Keusch, G.T. & Donta, S.T. (1975) J. Infect. Dis., 131, 58-63.
2. Giger, O. & Pariza, M.W. (1978) Biochem. Biophys. Res. Commun., 82, 378-383.
3. McClane, B.A. & McDonel, J.L. (1979) J. Cell. Physiol., 99, 191-200.
4. Skjelkvale, H., Tolleshaug, H. & Jarmund, T. (1980) Acta Path. Microbiol. Scand. Sect. B., 88, 95-102.
5. Matsuda, M. & Sugimoto, N. (1979) Biochem. Biophys. Res. Commun., 91, 629-636.
6. Horiguchi, Y., Uemura, T., Kozaki, S. & Sakaguchi, G. (1986) Biochim. Biophys. Acta, 889, 65-71.
7. McClane, B.A., Wnek, A.P., Hulkower, K.I. & Hanna, P.C. (1988) J. Biol. Chem., 263, 2423-2435.
8. Giger, O. & Pariza, M.W. (1980) Biochim. Biophys. Acta, 595, 264-276.
9. Sugimoto, N., Ozutsumi, K. & Matsuda, M. (1985) Eur. J. Epidemiol., 1, 264-273.
10. Matsuda, M., Ozutsumi, K., Iwahashi, H. & Sugimoto, N. (1986) Biochem. Biophys. Res. Commun., 141, 704-710.
11. Sugimoto, N., Ozutsumi, K. & Matsuda, M. (1985) Eur. J. Epidemiol., 1, 131-138.
12. Suarez-Isla, B.A., Wan, K., Lindstrom, J. & Montal, M. (1983) Biochemistry, 22, 2319-2323.
13. Oiki, S., Danho, W. & Montal, M. (1988) Proc. Natl. Acad. Sci. USA, 85, 2393-2397.
14. Coyne, M.D., Dagan, D. & Levitan, I.B. (1987) J. Memb, Biol., 97, 205-213.
15. Nakao, S., Hamamoto, T., Kagawa, Y., Shimizu, R., Mori, H. & Hirata, H. (1988) Biochem. Biophys. Res. Commun., 152, 1255-1267.

Vol. 156, No. 1, 1988 BIOCHEMICAL AND BIOPHYSICAL RESEARCH COMMUNICATIONS
October 14, 1988 Pages 557-562

EXCISION REPAIR IN XERODERMA PIGMENTOSUM GROUP C CELLS IS REGULATED DIFFERENTLY IN TRANSFORMED CELLS AND PRIMARY FIBROBLASTS

James E. Cleaver

Laboratory of Radiobiology and Environmental Health
University of California, San Francisco, CA 94143-0750

Received September 7, 1988

Excision repair in xeroderma pigmentosum group C cells occurs at about 20-30% of normal levels. In confluent fibroblasts a unique characteristic of this low repair is that it is clustered, representing very efficient repair in a small region of the genome. In SV40-transformed fibroblasts and Epstein-Barr virus-transformed lymphocytes of complementation group C, however, excision repair is randomly distributed. This may be a consequence of the high rate of proliferation of both of these cell types, because random repair is also observed in rapidly proliferating group C fibroblasts. The distribution of sites that can be mended in group C cells, therefore, varies according to the transformed and proliferative state of the cells, demonstrating that transformed cells do not always exhibit repair characteristics identical to those of primary fibroblasts. © 1988 Academic Press, Inc.

Xeroderma pigmentosum (XP) is a human disorder caused by defects in a family of genes, represented by complementation groups A through I, that control repair of ultraviolet (UV) damage to DNA (1-3). In XP complementation group C, repair of UV damage to DNA is reduced to about 20-30% of normal. Several previous studies have indicated that this residual repair is highly clustered in plateau phase group C cells (4-9). To facilitate investigation of the multiple genetic defects in this disease, a series of SV40-transformed fibroblasts and Epstein-Barr virus-transformed lymphocytes have been developed for various complementation groups (10-15). It is important to know how faithfully these transformed lines reflect the repair of UV damage that occurs in untransformed cells of the same group, because other kinds of repair are known to be altered by transformation (16). In previous experiments, I showed that XP group C cells in exponential growth (6) or exposed to the polymerase alpha inhibitor aphidicolin (7) no longer repair UV damage in clusters. In light of these results, the rapid proliferation and absence of a nonproliferative plateau phase in transformed cells might preclude detection of clustered repair, even at high cell densities.

Abbreviations: XP, xeroderma pigmentosum; UV, ultraviolet; dThd, thymidine; BrdUrd, bromodeoxyuridine; FdUrd, fluorodeoxyuridine.

0006-291X/88 $1.50
Copyright © 1988 by Academic Press, Inc.
All rights of reproduction in any form reserved.

In this study, I have determined the intragenome distribution of repair in XP group C cell lines transformed by two different methods and find that neither displays the clustered repair characteristic of primary group C fibroblasts.

Materials and Methods

Normal (FS1), XP group C (XP17ME), and SV40-transformed group C (XP4PA) (15) fibroblasts were grown in Eagle's minimal essential medium with 10% fetal calf serum. An Epstein-Barr virus-transformed lymphoblastoid cell line of complementation group C (GM2249A) was grown in RPMI medium plus 10% fetal calf serum. To obtain uniformly labeled DNA, cultures were incubated for at least 3 days with 0.01 to 0.05 μCi/ml [^{14}C]thymidine ([^{14}C]dThd) (spec. act., 53 mCi/mmol). The medium was changed regularly until normal and XP fibroblast cultures were confluent, and they were then maintained in 1% serum for 2 to 7 days to ensure that they were nonproliferating. XP4PA was grown similarly to confluence, but because of its transformed phenotype, proliferation continued and mitotic figures were always evident. GM2249A was grown to saturation density (2 x 10^6 cells/ml) and maintained with daily complete changes of medium. At this density, the cell number remained constant for at least 4 days, although cells remained capable of synthesizing DNA (17).

To obtain DNA labeled in repair sites, [^{14}C]dThd-labeled cultures were first grown in bromodeoxyuridine (BrdUrd) (10 μM) and fluorodeoxyuridine (FdUrd) (2 μM) for 60 min to start synthesis of density-labeled DNA and then irradiated with UV light (6.5, 13, or 26 J/m^2; 1.3 J/m^2/sec; 254 nm) and incubated with [^{3}H]dThd (10 μCi/ml; 80 Ci/mmol), BrdUrd (10 μM), FdUrd (2 μM), and hydroxyurea (2 mM) for 6 h. Hydroxyurea was included to suppress ^{3}H incorporation by semiconservative replication and thereby improve resolution of repair. At the end of the labeling period, cultures were harvested, washed in phosphate-buffered saline, centrifuged, and drained, and DNA was isolated as previously described (18). The repaired DNA of normal density was separated from hybrid-density DNA labeled by semiconservative DNA synthesis in isopycnic gradients at neutral pH (18). The average single-strand molecular weight (weight average) from isopycnic gradients was 1.50 ± 0.14 (SD) x 10^7 daltons (6).

Repaired DNA from normal-density regions of neutral isopycnic gradients was dialyzed against a buffer (20 mM Tris, 2 mM EDTA, 40 mM NaCl, pH 8.0) suitable for UV endonuclease treatment. DNA (200 μl) was incubated with 20 μl of purified UV endonuclease extract from *Micrococcus luteus* at 37°C for 2 h. At the end of digestion, DNA was centrifuged in alkaline sucrose gradients at 25,000 rev/min in an SW28 rotor for 5 h. DNA radioactivity was then determined and molecular weights were calculated for ^{3}H- and ^{14}C-labeled DNA (18). For DNA isolated from normal and XP cells immediately after a UV dose of 13 J/m^2, UV endonuclease treatment produced weight-average molecular weights of 4.68 ± 0.22 x 10^6 and 4.35 ± 0.16 x 10^6, respectively (6). These values represent the production of 62.0 ± 7.1 pyrimidine dimers per 2 x 10^8 daltons by a dose of 13 J/m^2 in human fibroblasts. The radioactivity in each fraction of the gradient was displayed as a percentage of radioactivity in the whole gradient to facilitate comparisons between ^{3}H and ^{14}C distributions.

Results

Repaired DNA, isolated from neutral isopycnic gradients, was digested with UV endonuclease to cleave it at all unrepaired cyclobutane pyrimidine dimers, making it possible to determine the size distribution of unrepaired and repaired DNA. This method, first used by Mansbridge and Hanawalt (4), depends on the principle that if cells are allowed to repair after irradiation, ^{3}H label will be inserted into repair patches and the distribution of ^{3}H will depend on the distribution of the repaired sites in relation to flanking unrepaired dimers in

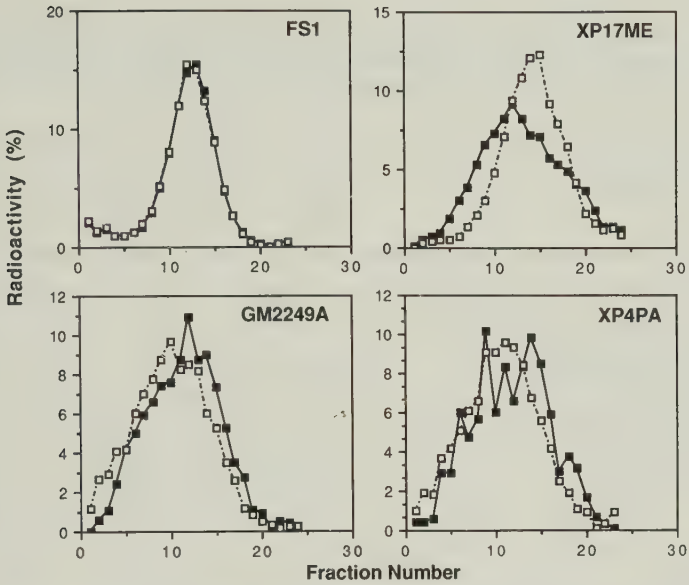

Figure 1. Alkaline sucrose gradient profiles of DNA purified from normal-density DNA in isopycnic gradients and digested with *M. luteus* UV endonuclease. XP group C cells were labeled uniformly with [^{14}C]dThd (0.05 μCi/ml, 53 mCi/mmol), irradiated with UV light (13 J/m^2), and labeled with [^{3}H]dThd (10 μCi/ml, 80 Ci/mmol), BrdUrd (10 μM), FdUrd (2 μM), and hydroxyurea (2 mM) for 6 h. Top left: FS1, normal primary fibroblasts. Top right: XP17ME, XP group C primary fibroblasts irradiated as confluent monolayers. Bottom left: GM2249A, Epstein-Barr virus-transformed lymphoblastoid cells. Bottom right: XP4PA, SV40-transformed fibroblasts. □, ^{14}C; ■, ^{3}H. Centrifugation was from right to left at 25,000 rev/min for 5 h.

the genome. The clustering of repair patches will yield ^{3}H-labeled molecules significantly larger than the majority of the DNA, which will be cleaved into lengths corresponding to the spacing of unrepaired DNA lesions. If, on the other hand, the repair patches and the unrepaired lesions are distributed similarly throughout the DNA, the ^{3}H in the repair patches and the ^{14}C label will give similar size distributions in alkaline sucrose gradients. Because repair of (6-4) photoproducts proceeds much more rapidly than that of cyclobutane dimers (19, 20), the distribution of ^{3}H-labeled patches will be biased toward the distribution of repaired (6-4) photoproducts with respect to unrepaired cyclobutane dimers after short labeling times of a few hours.

Repaired DNA from normal cells showed no difference between the distributions of ^{3}H-labeled repaired DNA and ^{14}C-labeled DNA. Repaired DNA from a primary XP group C fibroblast line (XP17ME) showed the profile characteristic of group C (Fig. 1) (4-6). Repaired DNA was distributed with a size distribution larger than that of the ^{14}C-labeled bulk DNA, indicating that the repair patches were clustered along the DNA fragments. Neither the SV40-transformed group C fibroblast line (XP4PA) nor the lymphoblastoid group C cell line (GM2249A) exhibited such profiles. For these cell types, the ^{3}H-labeled repaired DNA was similar to the ^{14}C-labeled bulk DNA, indicating that repair was not distributed in a clustered manner (Fig. 1). Analysis of a series of experiments on the basis of the ^{3}H and ^{14}C

Table 1. Ratios of ^3H (repaired DNA) and ^{14}C (bulk DNA) weight-average molecular weights in normal and XP group C cells labeled with [^3H]dThd after irradiation with 6.5 to 26 J/m^2 UV light*

Cell line and condition	Dose (J/m^2)	Time (h)	$^3H/^{14}C$ mol. wt.
Normal (FS)			0.97 - 1.03†
XP group C (confluent fibroblasts)			1.34 - 1.93‡
XP group C (exponentially growing)			0.80 - 1.40‡
XP4PA (SV40-transformed)	13	6	0.85
	26	6	1.04
GM2249A (Epstein-Barr virus-transformed)	6.5	6	0.79
	6.5	24	0.74
	26	6	0.69
	26	24	0.84

*In previous studies these ratios were found to be independent of the UV doses between 6.5 and 13 J/m^2 for labeling times between 6 and 42 h. For normal and XP group C fibroblasts, therefore, values for these doses and labeling times were pooled from the previous studies to provide a context with which to compare the results obtained in this study for XP4PA and GM2249A.

†Range of values reported by Karentz and Cleaver (5) and Cleaver (6,7). The value for the XP17ME profile in Fig. 1 was 1.44.

‡Range of values reported by Cleaver (6).

molecular weight ratios confirmed that neither XP4PA nor GM2249A exhibited clustered repair, unlike that seen in numerous investigations of XP group C fibroblasts (Table 1). The $^3H/^{14}C$ molecular weight ratios for transformed cells were on average below 1.0, as expected of molecules containing less than one ^3H-labeled patch, on average, whereas the ^{14}C label was uniformly distributed (6, 7).

Discussion

The clustering of repair in confluent XP group C fibroblasts has become a diagnostic characteristic of these cells. Every fibroblast culture representative of this group that has been investigated has shown such nonuniform distribution of repair. These include the original cell lines studied by Mansbridge and Hanawalt (4); four studied by Mullenders *et al.* (8,9); one by Player and Kantor (21); and a total of six lines studied in our own laboratory (5-7). A sufficient number of cell lines have now been described by independent investigators to regard clustering as a consistent feature of repair in confluent untransformed fibroblasts from XP group C. The present study, however, shows that transformed group C cells, even at high density, do not show clustered repair.

The reason for the absence of clustered repair in transformed group C cells depends on the interpretation of the clustered repair itself. Clustered repair may be due either to repair

of specific transcriptionally active genes (22, 23) or to a restricted diffusion of a low number of repair enzyme complexes (6, 7). An increase in the gene-specific mode of repair was not observed in XP group C cells in one investigation (24). Preferential repair of certain genes can, however, occur even in normal cells without causing clustered repair (Fig. 1) (23). The two kinds of nonuniform distributions of repair, therefore, occur at different levels of resolution and do not represent the same process.

Repair in transformed XP group C cells will most closely correspond to that observed in XP group C fibroblasts stimulated to enter the DNA synthesis phase (Table 1) (6); in neither of these cases is clustered repair observed. Clustered repair may be inconsistent with the rapidly proliferating state. I previously suggested that clustered repair may be the result of a regulatory role for DNA polymerases that exercise a dual role in repair and replication (6, 7). Inhibition of DNA polymerase by aphidicolin has previously been shown to eliminate clustered repair in confluent primary fibroblasts, which further identifies the polymerase step of excision repair as a site of regulation of repair in XP group C (7).

These results therefore indicate that transformation of XP group C cells, which alters the regulatory controls that lead to a nonproliferative state at high cell density, leads to a condition in which clustered repair can no longer be observed. Such differences may be important in understanding the precise defect in XP group C cells and must be borne in mind when using transformed cells because they are consequently not equivalent to primary fibroblasts in all aspects of excision repair.

Acknowledgments

I am grateful to Mr. W.C. Charles for technical assistance in isopycnic and alkaline sucrose gradient sedimentation and to Dr. E.C. Friedberg for the XP4PA cell culture originally transformed in Dr. A. Sarasin's laboratory. The GM2249A lymphoblastoid cell line was obtained from the Institute for Medical Research, Camden, New Jersey. This work was supported by the Office of Health and Environmental Research, U.S. Department of Energy (contract no. DE-AC03-76-SF01012).

References

1. Robbins, J.H., Kraemer, K.H., Lutzner, M.A., Festoff, B.W., and Coon, H.G. (1974) Ann. Intern. Med. 80, 221-248.
2. Cleaver, J.E. (1983) In The Metabolic Basis of Inherited Disease (J.B. Stanbury, J.B. Wyngaarden, D.S. Frederickson, J.L. Goldstein and M.S. Brown, Eds.), 5th ed., pp. 1227-1248. McGraw-Hill, New York.
3. Cleaver, J.E. (1987) In Photomedicine (E. Ben-Hur and I. Rosenthal, Eds.), pp. 31-62. CRC Press, Boca Raton, Fla.
4. Mansbridge, J.N., and Hanawalt, P.C. (1983) In Cellular Responses to DNA Damage (E.C. Friedberg and B.A. Bridges, Eds.), pp. 195-207. Alan R. Liss, New York.
5. Karentz, D., and Cleaver, J.E. (1986) Mutat. Res. 165, 165-174.
6. Cleaver, J.E. (1986) Nucleic Acids Res. 14, 8155-8165.
7. Cleaver, J.E. (1987) Cancer Res. 47, 2393-2396.
8. Mullenders, L.H.F., van Kesteren, A.C., Bussmann, C.J.M., van Zeeland, A.A., and Natarajan, A.T. (1984) Mutat. Res. 141, 75-82.

9. Mullenders, L.H.F., van Kesteren, A.C., Bussmann, C.J.M., van Zeeland, A.A., and Natarajan, A.T. (1986) Carcinogenesis 7, 995-1002.
10. Barbis, D.P., Schultz, R.A., and Friedberg, E.C. (1986) Mutat. Res. 165, 175-184.
11. Canaani, D., Naiman, T., Teitz, T., and Berg, P. (1986) Somat. Cell Genet. 12, 13-20.
12. Hashimoto, T., Nakano, Y., Owada, M.K., Kakunaga, T., and Furuyama, J. (1986) Mutat. Res. 166, 215-220.
13. Protić-Sabljić, M., Seetharam, S., Seidman, M.M., and Kraemer, K.H. (1986) Mutat. Res. 166, 287-294.
14. Vuillaume, M., Calvayrac, R., Best-Belpomme, M., Tarroux, P., Hubert, M., Decroix, Y., and Sarasin, A. (1986) Cancer Res. 46, 538-544.
15. Daya-Grosjean, L., James, M.R., Drougard, C., and Sarasin, A. (1987) Mutat. Res. 183, 185-196.
16. Day, R.S., III, Ziolkowski, C.H.J., Scudiero, D.A., Meyer, S.A., and Mattern, M.R. (1980) Carcinogenesis 1, 21-32.
17. Milam, K.M., Thomas, G.H., and Cleaver, J.E. (1986) Exp. Cell Res. 165, 260-268.
18. Cleaver, J.E. (1984) In Handbook of Mutagenicity Test Procedures (B.J. Kilbey, M. Legator, W. Nichols and C. Ramel, Eds.), 2nd ed., pp. 33-69. Elsevier, Amsterdam.
19. Clarkson, J.M., Mitchell, D.L., and Adair, G.M. (1983) Mutat. Res. 112, 287-299.
20. Mitchell, D.L., Haipek, C.A., and Clarkson, J.M. (1985) Mutat. Res. 143, 109-112.
21. Player, A.N., and Kantor, G.J. (1987) Mutat. Res. 184, 169-178.
22. Bohr, V.A., Smith, C.A., Okumoto, D.S., and Hanawalt, P.C. (1985) Cell 40, 359-369.
23. Mellon, I., Bohr, V.A., Smith, C.A., and Hanawalt, P.C. (1986) Proc. Natl. Acad. Sci. USA 83, 8878-8882.
24. Bohr, V.A., Okumoto, D.S., and Hanawalt, P.C. (1986) Proc. Natl. Acad. Sci. USA 83, 3830-3833.

Vol. 156, No. 1, 1988 BIOCHEMICAL AND BIOPHYSICAL RESEARCH COMMUNICATIONS
October 14, 1988 Pages 563-569

EVIDENCE FOR THE EXPRESSION OF A PRIMITIVE INTESTINAL-LIKE ALKALINE PHOSPHATASE IN THE INTESTINAL 407 CELL LINE

Kazuyuki Hirano[1,*], Tomikazu Kusano[1], Kentaro Asai[1], Kyozo Hayashi[1], Torgny Stigbrand[2], Shiro Iino[3] and Jose L Millan[4]

[1]Gifu Pharmaceutical University, 6-1 Mitahorahigashi 5-chome, Gifu 502, Japan,

[2] Department of Physiological Chemistry, University of Umea, S-901 87 Umea, Sweden,

[3]Department of Internal Medicine, Faculty of Medicine, University of Tokyo, Tokyo 113, Japan

[4]Cancer Research Center, La Jolla Cancer Research Foundation, La Jolla, California 92037

Received July 25, 1988

SUMMARY: Intestinal-like alkaline phosphatase was found to be expressed in the intestinal 407 cell line. This enzyme was identified by use of monoclonal antibodies specific for human placental (H_7 and HPMS-1) and intestinal alkaline phosphatase (2HIMS-1 and 2HIMS-3) separately. Purification of this isozyme by use of two different monoclonal antibody immunoaffinity chromatographies demonstrates a single protein band on SDS-polyacrylamide gel electrophoresis indicating that this enzyme is not formed as a heterodimer. The apparent monomer subunit molecular weight and the dimer molecular weight of this isozyme were determined to 70000 and 160000, respectively. The enzyme is a homodimer according to molecular weight determinations. Furthermore, this isozyme is neuraminidase sensitive and comparatively heat stable, properties also characteristic for the placental enzyme.

Our data suggest that the intestinal-like alkaline phosphatase in the intestinal 407 cell line displays properties intermediate of the intestinal and placental isozymes which may reflect the existence and reexpression of a new primitive isozyme. © 1988 Academic Press, Inc.

INTRODUCTION: Human alkaline phosphatases (E.C.3.1.3.1) comprise a complex group of isozymes encoded for by at least four different genes (1). cDNA's encoding three isozymes have been cloned and sequenced (2-5) as well as the gene coding for germ cell alkaline phosphatase (6), revealing 52% homology between the

Abbreviation used: MICA, monoclonal immunocatalytical assay.

* To whom correspondence should be addressed.

0006-291X/88 $1.50
Copyright © 1988 by Academic Press, Inc.
All rights of reproduction in any form reserved.

tissue-unspecific and placental alkaline phosphatase molecules, and 80% homology between the intestinal and the placental alkaline phosphatases at the amino acid level. The placental alkaline phosphatase shows a unique degree of allelic polymorphism and a number of alleles have been described at the placental gene locus (7). Random combinations of subunits result in more than 40 phenotypes (8). Placental alkaline phosphatase was one of the first proteins found to be ectopically expressed by cancer cells (9). Intestinal alkaline phosphatase also appears in at least two different forms: one is the adult intestinal alkaline phosphatase and the other is the fetal intestinal alkaline phosphatase (10).

In the past decade, two reports have been presented dealing with hybrid types of alkaline phosphatases as primitive isozymes (11, 12). It is however not yet confirmed that hybrid enzymes exist as long as polyclonal antibodies for placental or intestinal alkaline phosphatases are used to characterize the hybrid enzymes because these enzymes have been shown to share several antigenic determinants. In this paper, we present evidence for existence of a primitive intestinal-like alkaline phosphatase expressed in a intestinal 407 cell line.

MATERIALS AND METHODS

Monoclonal antibody : Monoclonal antibodies were prepared according to the method of Köhler and Milstein (13). H_7 and HPMS-1 monoclonal antibodies are specific for the placental alkaline phosphatase, 2HIMS-1 for the adult and fetal intestinal alkaline phosphatases, 2HIMS-3 for the adult intestinal alkaline phosphatase and HLMS-1 for tissue-unspecific alkaline phosphatase (14-16). The monoclonal antibodies were used after Protein A-Sepharose CL-4B purification, as earlier described (14).
Purification of the intestinal-like alkaline phosphatase : Cultured intestinal 407 cells were homogenized in 1 volume of butanol and 3 volumes of Tris-HCl buffer, pH 7.5, containing 10 μM $MgCl_2$ and $ZnCl_2$ and 0.02% NaN_3. The water-phase was dialyzed against the above buffer. After centrifugation, the dialyzed sample was applied on a HPMS-1 column and washed with 50 mM of Tris-HCl, pH 8.0, containing 0.9% NaCl. The enzyme was eluted with 0.2 M Na_2CO_3 containing 0.5 M NaCl. The active fractions were neutralized by addition of 0.1 M acetic acid and dialyzed against 50 mM Tris-HCl buffer, pH 8.0, containing 0.5 M NaCl. The enzyme was then, in a second cycle, applied on a 2HIMS-1 column and the intestinal-like alkaline phosphatase was eluted by use of the same procedure.

Monoclonal immunocatalytical assays (MICAs) : MICAs were performed as described previously (15, 16). Briefly, each monoclonal antibody bound to paper discs was used to trap the isozyme and the activity on the paper disc was determined using phenylphosphate or 4-methylumbelliferyl phosphate as substrate.
SDS-polyacrylamide gel electrophoresis : 9% polyacrylamide gel was used according to Laemmli (17).

RESULTS AND DISCUSSION

The intestinal 407 cells were expected to express the fetal intestinal alkaline phosphatase. However this cell line expresses several phosphatase isozymes including the intestinal-like alkaline phosphatase as well as the placental and tissue-unspecific alkaline phosphatase as judged from the electophoretic mobility and the reactivity with the monoclonal antibodies. The levels of expressed alkaline phosphatase isozymes were determined by the MICAs as shown in Table I. The intestinal-like alkaline phosphatase is the main enzyme in terms of activity and this enzyme reacts with the monoclonal antibody 2HIMS-1 but not with 2HIMS-3. Furthermore, the electrophoretic mobility of the intestinal-like enzyme is clearly different from that of the adult and fetal intestinal alkaline phosphatases, suggesting the existence of a new type of intestinal-like alkaline phosphatase in this cell line. Existence of hybrid-type alkaline phosphatases (heterodimers) has been reported in KB-cells, FL-cells and the fetal intestine, respectively (11, 12). However, the mixture of placental and intestinal-like alkaline phosphatases presents the same immunochemical reactivity with polyclonal antibodies as those of the hybrid enzymes if not monoclonal antibodies specific for each isozyme are used as discriminatory tools. Purification of this new type of

Table I. Alkaline phosphatase isozymes in Intestine 407 cells

Isozyme	Antibody	Activity (IU/mg protein)
Placental alkaline phosphatase	HPMS-1	0.449
Liver alkaline phosphatase	HLMS-1	0.165
Intestinal alkaline phosphatase	2HIMS-1	6.830
Intestinal alkaline phosphatase	2HIMS-3	0.600

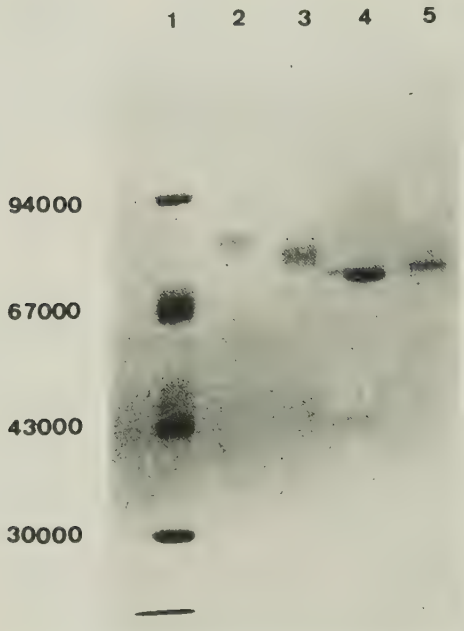

Figure 1. SDS-polyacrylamide gel electrophoresis of different purified alkaline phosphatases.
9% polyacrylamide gel was used and the proteins were stained by Coomassie Brilliant Blue R-250. Lane 1; marker proteins, lane 2; intestinal alkaline phosphatase, lane 3; meconial alkaline phosphatase, lane 4; placental alkaline phosphatase, lane 5; intestinal-like alkaline phosphatase in the intestinal 407 cells.

intestinal-like alkaline phosphatase is necessary to further elucidate the structure of this enzyme. The new enzyme was purified by use of two different monoclonal antibodies coupled to CH-Sepharose 4B columns. Fig. 1 shows the SDS-polyacrylamide gel electrophoretic pattern of the purified intestinal-like alkaline phosphatase from the intestinal 407 cells. The fractions which bind to the two monoclonal antibody columns demonstrate a single protein band (Mr 70000), clearly different from the placental and intestinal enzyme and the molecular weight of this intestinal-like alkaline phosphatase was calculated to 160000 from Sephadex G-200 gel filtration data. These results strongly suggest that the new type of intestinal-like alkaline phosphatase in the 407 cells may be a primitive enzyme and not a hybrid-type alkaline phosphatase. This intestinal-like alkaline phosphatase was furthermore confirmed to be neuraminidase sensitive (data not shown). The immunoreactivity data of the new intestinal-like

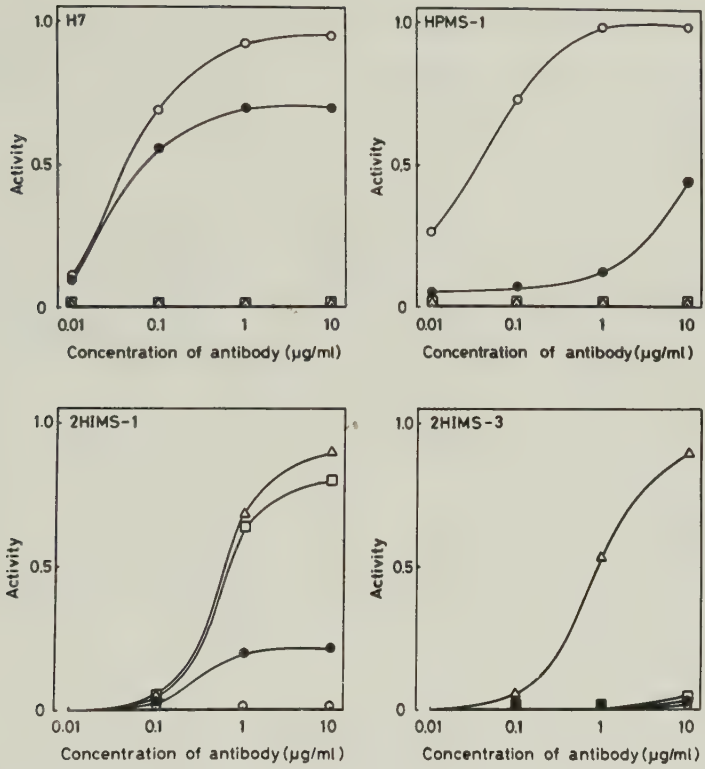

Figure 2. Reactivities with different monoclonal antibodies with the intestinal-like alkaline phosphatase from intestinal 407 cells.
100 microliter of an anti-mouse IgG antibody was coated in the 96 wells immunoplate at 37°C for 3 h followed by washing three times with phosphate-buffered saline (PBS) containing 0.05% Tween 20 and 0.05% sodium merthiolate (PBS-Tween). The wells were blocked with 300 μl of 1% bovine serum albumin dissolved in PBS containing 0.05% sodium merthiolate at 4°C overnight and then the wells were washed with 400 μl of PBS-Tween 20. 100 μl of the indicated monoclonal antibody, dissolved in 0.1%-PBS, was added to each well and allowed to stand for 3 h at 37°C. The wells were washed three times with 10 mM sodium phosphate buffer, pH 7.4, containing 0.15 M NaCl 0.05% Tween 20 and 0.05% sodium merthiolate. 100 μl of alkaline phosphatase (70 IU/L) dissolved in 0.1% BSA-10 mM Tris-HCl buffer, pH 7.4, containing 0.02% sodium azide was added to each well and allowed to stand for 3 h at 37°C. The activity was determined in 200 μl of 2.7 mM p-nitrophenylphosphate dissolved in 0.1 M ethanolamine-HCl buffer, pH 9.8, containing 0.1 mM $MgCl_2$.
○: placental alkaline phosphatase, △: intestinal alkaline phosphatase, □: meconial alkaline phosphatase, ●: intestinal-like alkaline phosphatase.

alkaline phosphatase with the monoclonal antibodies indicated that this enzyme reacts with both the placental and intestinal specific monoclonal antibodies (H_7, HPMS-1 and 2HIMS-1), but not with the adult intestinal specific monoclonal antibody (2HIMS-3) as shown in Fig. 2. Therefore the new enzyme probably contains structures reminding of human placental and fetal intestinal

alkaline phosphatases but not of adult intestinal alkaline phosphatase. The heat stability of the new enzyme is also intermediate to the placental and fetal lintestinal alkaline phosphatases.

The above results may give rise to speculations that the intestinal-like enzyme in intestinal 407 cells is a primitive alkaline phosphatase with common determinants of both the human placental and fetal intestinal alkaline phosphatases and the translational product of a gene intermediate in the evolution of the placental and fetal intestinal alkaline phosphatase genes. It is still unknown which regulatory mechanisms are involved in the expression of this enzyme. The identification of potential remnants of evolutionary products is of significant importance for the elucidation of the development of the complex phosphatase isozyme group in man.

ACKNOWLEDGMENT

This work was supported in part by a Grant-in-Aids for General Scientific Research from the Ministry of Education, Science and Culture, Japan.

REFERENCES

1. Fishman, W.H. (1974) Am. J. Med. **56**, 617-650.
2. Kam, W., Clauser, E., Kim, Y.S., Kan, Y.W. and Rutter, W.J. (1985) Proc. Natl. Acad. Sci. U.S.A. **82**, 8715-8719.
3. Millan, J.L. (1986) J. Biol. Chem. **261**, 3112-3115.
4. Berger, J., Garattini, E., Hua, J.-C. and Udenfriend, S. (1987) Proc. Natl. Acad. Sci. U.S.A. **84**, 695-698.
5. Weiss, M.J., Henthorn, P.S., Lafferty, M.A., Slaughter, C., Raducha, M. and Harris, H. (1986) Proc. Natl. Acad. Sci. U.S.A. **83**, 7182-7186.
6. Millan, J.L. and Manes, T. (1988) Proc. Natl. Acad. Sci. U.S.A. in press.
7. Stigbrand, T., Millan, J.L. and Fishman, W.H. (1982) The geneticbasis of alkaline phosphatase isozyme expression. In Isozymes: Current Topics in Biological and Medical Reserch. Vol. 6, A.R. Liss, pp 93-117.
8. Beckman, L., Bjorling, G. and Christodoulou, C. (1966) Acta Genet. Basel **16**, 59-73.
9. Fishman, W.H., Inglis, N.R., Green, S., Anstiss, C.L., Gosh, N.K., Reif, A.E., Rustigian, R., Krant, M.J. and Stolbach, L.L. (1968) Nature **219**, 697-699.
10. Sugiura, M., Hirano, K., Iiizumi, Y., Miyazaki, J., Miki, K., Iino, S., Suzuki, H. and Oda, T. (1981) Chem. Pharm. Bull. **29**, 3660-3666.

11. Singer, R.M. and Herz, F. (1978) J. Natl. Cancer **60**, 573-577.
12. Behrens, C.M., Enns, C.A. and Sussman, H.H. (1983) Bichem. J. **211**, 553-558.
13. Köhler, G. and Milstein, C. (1975) Nature **256**, 495-497.
14. Millan, J.L. and Stigbrand, T. (1983) Eur. J. Biochem. **136**, 1-7.
15. Hirano, K., Iiizumi, Y., Hayashi, Y., Tanaka, T., Sugiura, M., Hayashi, K., Lu, Z-D. and Iino, S. (1986) Anal. Biochem. **154**, 624-631.
16. Hirano, K., Matsumoto, H., Tanaka, T., Hayashi, Y., Iino, S., Domar, U. and Stigbrand, T. (1987) Clin. Chim. Acta **166**, 265-273.
17. Laemmli, U.K. (1970) Nature **222**, 680-681.

Vol. 156, No. 1, 1988 BIOCHEMICAL AND BIOPHYSICAL RESEARCH COMMUNICATIONS
October 14, 1988 Pages 570-575

INSULIN AND GLUCOSE MODULATE PROTEIN KINASE C ACTIVITY IN RAT ADIPOCYTES

Boris Draznin, J. Wayne Leitner, Karl E. Sussman, and Nancy A. Sherman

Medical Research Service, Veterans Administration Medical Center, and Department of Medicine, University of Colorado Health Sciences Center, Denver, Colorado 80220

Received August 8, 1988

In the presence of 1 mM glucose, insulin (10 ng/ml) increases both catalytic and receptor-binding properties of adipocyte cytosolic protein kinase C (PKC). Preincubation of adipocytes with 10 mM glucose raises basal PKC catalytic activity and prevents further stimulation of this enzyme by insulin. The effect of hyperglycemia is likely to be mediated by direct conversion of glucose into diacylglycerol. Thus, an incorporation of ^{14}C-glucose into diacylglycerol is enhanced 10-fold in the presence of 10 mM glucose. These observations indicate that, in normal adipocytes, both insulin and glucose activate PKC; hyperglycemia eliminates the ability of insulin to stimulate this enzyme, thereby interfering with insulin action. © 1988 Academic Press, Inc.

Recent studies of Bollag, et. al. (1) demonstrated that protein kinase C (PKC) directly phosphorylates the insulin receptor and reduces receptor protein-tyrosine kinase (TK) activity by 65%. Takayama, et. al. (2) have observed that activation of PKC by phorbol ester resulted in stimulated phosphorylation of serine residues and a 50% reduction in insulin-stimulated tyrosine phosphorylation. These receptors also exhibited a reduced TK activity *in vivo* and *in vitro*. Since activation of insulin receptor involves TK as one of the initial steps in transduction of insulin-generated signals (3), reduction in TK activity may result in decreased magnitude of insulin action. If insulin is capable of activating PKC in its target tissues, then PKC effect on TK activity of insulin receptor may provide for an elegant feedback system diminishing or even terminating insulin action.

In this study, the effect of insulin on PKC in normal rat adipocytes was examined. We also investigated the possibility

0006-291X/88 $1.50
Copyright © 1988 by Academic Press, Inc.
All rights of reproduction in any form reserved.

that hyperglycemia may modulate the effect of insulin on PKC activation.

METHODS

Isolated rat adipocytes were preincubated for 24 hrs with 1 or 10 mM glucose in the presence or in the absence of insulin (10 ng/ml). After the preincubation, the cells were washed three times and incubated for 40 min in glucose- and insulin-free medium to eliminate any possible influence of high glucose or insulin present during 24 hr preincubation (4). The cells were resuspended in Krebs-Ringer bicarbonate buffer and one half of the cells was then exposed to 10 ng/ml of insulin for 20 min at 37°C (insulin-stimulated PKC activity), while the remaining cells were incubated without insulin (basal PKC activity). At the end of the incubation, the cells were washed and sonicated for differential centrifugation (5). Plasma membrane and cytosolic fractions were isolated and used immediately in histone III-S phosphorylation assay to estimate PKC activity (6,7). The activity was determined by the difference in the pmoles of ^{32}P incorporation per mg protein per min in the presence of Ca^{+} (1 mM), diolein (8 μM), and phosphatidylserine (60 μM), and in the absence of these agents (but in the presence of 1 mM EGTA).

^{3}H-PDB (New England Nuclear, Boston, MA) binding to cytosolic and membrane-associated PKC was carried out as described by Uchida, et. al. (8) and Cambier, et. al. (9). The cells were isolated and preincubated for 24 hr as described above, except that insulin was absent from preincubation media. ^{3}H-PDB binding was performed using 20 nM ^{3}H-PDB as a ligand, 1.5 μM 4β-phorbol 12 β myristate 13 α acetate (TPA) to assess non-specific binding, and filtration through 2.4 cm Whatman GF/C glass filter to remove any unbound ligand. Both basal and insulin-stimulated ^{3}H-PDB binding were determined.

Determinations of [$U^{14}C$]-glucose (sp. activity 304.7 μCi/μMole) incorporation into diacylglycerol in isolated adipocytes was performed as described by Tamarit-Rodriguez, et. al. (10), using thin layer chromatography. The position of DAG was detected under the UV light after spraying the plates with 2',7'-dichlorofluoresclin. The spots corresponding to DAG markers were scraped into scintillation vials and counted for radioactivity present.

RESULTS AND DISCUSSION

In adipocytes pre-incubated with 1 mM glucose, insulin enhanced both cytosolic PKC catalytic activity (Fig 1) and ^{3}H-PDB binding (Fig 2). The magnitude of insulin action was approximately the same in both assays, suggesting that enhancement of PKC activity may be secondary to an increase in enzyme concentration. The origin of the PKC contributing to the increase in ^{3}H-PDB binding is unknown. Recently, Pershadsingh, et. al. (11) have reported an insulin-induced decrease (27%) in ^{3}H-PBu_2 (phorbol 12,13 dibutyrate) binding to

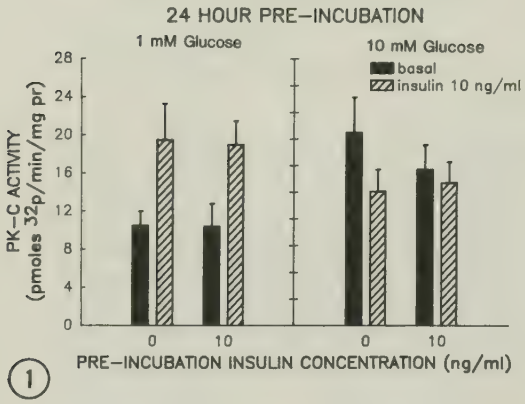

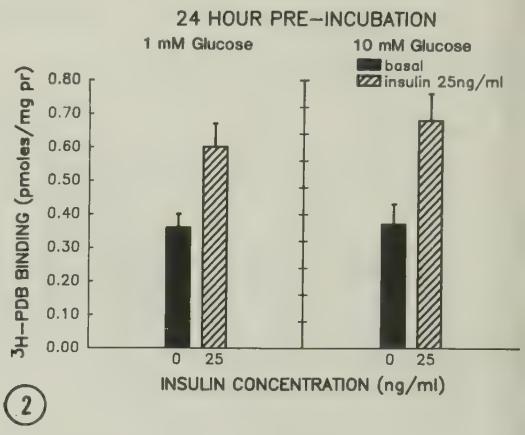

Figure 1: Effect of glucose and insulin on cytosolic PKC activity in rat adipocytes. Results represent mean ± SEM of 5 experiments, each performed in duplicate.

Figure 2: The effect of glucose and insulin on ^{3}H-PDB binding to cytosolic PKC in rat adipocytes. Results represent specific ^{3}H-PDB binding expressed as mean ± SEM of 3 experiments, each performed in triplicate. Insulin-stimulated ^{3}H-PDB binding was significantly ($p < 0.01$) greater than basal under both conditions (1 and 10 mM glucose). Results of ^{3}H-PDB binding to plasma membrane fractions are reported in the text.

the adipocyte PM, which could partially account for a 42% increase observed in the cytosol. In the present experiments, insulin induced a 20% decrease in ^{3}H-PDB binding to the PM and a 65% increase in cytosolic binding. It is conceivable that PKC from other cellular organelles was translocated to the cytosol.

We did not observe insulin-induced changes in PKC activity (determined by HP assay) in the PM fraction (data not shown). This is in agreement with several previous observations (5,12-14), indicating that insulin does not cause translocation of PKC to the plasma membrane. The presence of 10 ng/ml insulin in the 24 hr preincubation medium (1 mM glucose) did not alter either basal or subsequent insulin-stimulated PKC activity (Fig 1).

In contrast, preincubation of adipocytes with 10 mM glucose significantly effected basal PKC activity and the response to insulin. Basal activity of cytosolic PKC was significantly increased ($p < 0.05$) regardless of whether or not insulin was present in the culturing media (Fig 1). Despite this augmentation in basal PKC catalytic activity (HP assay), the basal concentration of the enzymes was unchanged (PDB binding)

Table 1. Effect of 10 mM glucose on cytosolic PKC activity in normal adipocytes

	PKC activity pmoles ^{32}P/min/mg protein	P
1 mM Glucose		
a) alone	11.08 ± 1.05	
b) + insulin (10 ng/ml)	7.34 ± 2.77	< .05 vs. a
10 mM Glucose		
c) 2 min (alone)	9.74 ± 2.11	NS vs. a
d) 2 min (+ insulin 10 ng/ml)	28.86 ± 7.02	< .05 vs. c
e) 2 hrs (alone)	20.80 ± 4.47	< .01 vs. a
f) 2 hrs (+ insulin 10 ng/ml)	21.27 ± 5.28	NS vs. e
g) 24 hrs (alone)	21.25 ± 2.56	NS vs. e
h) 24 hrs (+ insulin 10 ng/ml)	15.20 ± 1.54	NS vs. g

Adipocytes were preincubated with 10 mM glucose for 2 min, 2 or 24 hrs. PKC activity was determined by HP assay as described in Figure 1 legend. The results represent mean ± SEM of 3 to 5 experiments, each conducted in duplicate or triplicate.

and remained similar to that observed in adipocytes cultured with 1 mM glucose. Twenty-four hour preincubation with 10 mM glucose completely abolished insulin-induced increases in PKC catalytic activity (Fig 1) without altering insulin-stimulated increase in PKC concentrations (Fig 2). Finally, the presence of insulin in the 24 hour preincubation medium did not alter the response to acute addition of insulin (Fig 1). The activity of PKC in the PM fraction remained unchanged in all experiments (not shown).

These observations suggest that glucose (10 mM) stimulates selectively the catalytic subunit of PKC. Under these circumstances, insulin continues to increase the amount of binding subunit, but provides no further stimulation of the catalytic subunit. This effect of 10 mM glucose was evident after 2 hrs of incubation but not after 2 min (Table 1).

The mechanism whereby glucose activates the catalytic activity of PKC is unknown. Glucose-induced increases in $[Ca^{2+}]i$ and in diacylglycerol (DAG) production are among the possibilities. To examine the first possibility, we preincubated adipocytes as described above in the presence of

Table 2. [U ^{14}C] Glucose Incorporation into Diacylglycerol in Isolated Adipocytes*

Time	with 1 mM glucose (pmoles/mg protein)	with 10 mM glucose (pmoles/mg protein)
4 min (n=4)	41.33 ± 3.06	385.95 ± 39.03
20 min (n=6)	46.30 ± 5.43	348.57 ± 38.45
2 hr (n=6)	37.44 ± 5.47	352.93 ± 40.69

*[U ^{14}C] glucose specific activity 304.7 μCi/μMole incorporation into DAG was assessed by thin layer chromatography as described by Tamarit-Rodriguez, et. al. (10).

the Ca^{2+} channel blocker, verapamil (30 μM). In adipocytes preincubated with 10 mM glucose, verapamil reduced cytosolic free calcium concentration from 162 ± 11 to 99 ± 13 nM, $p < 0.05$ (measured with fura-2 as previously described, 15). However, verapamil failed to affect the augmentation of PKC activity induced by 10 mM glucose (18 ± 3 pmoles/^{32}P/min/mg protein vs. 21.2 ± 3 with 10 mM glucose alone). This suggested that the effect of glucose on PKC activity was not calcium mediated.

We then addressed the possibility of glucose being converted into DAG and the rate of such conversion being increased in the presence of high glucose concentrations. The higher rate of ^{14}C-glucose incorporation into DAG reflects increased DAG production, but does not indicate the source of newly formed DAG. DAG can be derived in the process of triphosphoinositide hydrolysis or as a result of de-novo synthesis, largely from glycerol-3-phosphate via phosphatidic acid (see 16 for review).

The effect of glucose concentration on [U ^{14}C]-glucose carbon incorporation into DAG was examined at 4 and 20 min of incubation and at 2 hrs (Table 2). In the presence of 10 mM glucose, there was 8 to 10-fold increase in amount of ^{14}C-glucose incorporation into DAG at 4, 20 min and 2 hr of incubation. Although these data do not directly distinguish between the sources of DAG, they indicate that in the presence of hyperglycemia, increasing amounts of glucose are converted into DAG and may thereby activate PKC. Since insulin has been shown to rapidly activate de novo DAG synthesis (17), the process of DAG formation is likely to represent the point of convergence of insulin and glucose influence on signal transduction system of insulin target cells.

Taking these observations in conjunction with the ability of PKC to reduce TK activity of insulin receptors (1,2), one may postulate that activation of PKC by hyperglycemia may result in diminution of insulin receptor TK activity and impaired insulin action. Furthermore, activation of PKC may, at least in part, explain post-receptor defect(s) in insulin target tissues induced by hyperglycemia and/or hyperinsulinemia.

ACKNOWLEDGMENTS

We thank Gloria Smith for her excellent secretarial help.

REFERENCES

1. Bollag, G.E., Roth, R.A., Beaudoin, J., Mochly-Rosen, D., and Koshland, D.E. (1986) Proc. Natl. Acad. Sci. U.S.A. **83**, 5822-5824.
2. Takayama, S., White, M.F., and Kahn, C.R. (1988) J. Biol. Chem. **263**, 3440-3447.
3. Kahn, C.R. (1985) Ann. Rev. Med. **36**, 429-451.
4. Garvey, W.T., Olefsky, J.M., Matthaei, S., and Marshall, S. (1987) J. Biol. Chem. **262**, 189-197.
5. Karnieli, E., Zarnowski, M.J., Hissin, P.J., Simpson, I.A., Salans, L.B., and Cushman, S.W. (1981) J. Biol. Chem. **256**, 4772-4777.
6. Kikkawa, U., Minakuchi, R., Takai, Y., and Nishizuka, Y. (1983) Methods Enzymol. **99**, 288-298.
7. Cooper, D.R., Konda, T.S., Standaert, M.L., Davis, J.S., Pollet, R.J., and Farese, R.V. (1987) J. Biol. Chem. **262**, 3633-3639.
8. Uchida, T. and Filburn, C.R. (1984) J. Biol. Chem. **259**, 12311-12314.
9. Cambier, J.C., Newell, M.K., Justement, L.B., McGuire, J.C., Leach, K.L., and Chen, Z.Z. (1987) Nature **327**, 629-632.
10. Tamarit-Rodriguez, J., Vara, E., and Tamarit, J. (1984) Biochem. J. **221** 317-324.
11. Pershadsingh, H.A., Shade, D.L., and McDonald, J.M. (1987) Biochem. Biophys. Res. Commun. **145**, 1384-1389.
12. Glynn, B.P., Colliton, J.W., McDermott, J.M., and Witters, L.A. (1986) Biochem. Biophys. Res. Commun. **135**, 1119-1125.
13. Vaartjes, W.J., de Haas, C.G.M., and Van den Bergh, S.G. (1986) Biochem. Biophys. Res. Commun. **138**, 1328-1333.
14. Walaas, S.I., Horn, R.S., Adler, A., Albert, K.A., and Walaas, O. (1987) FEBS Letters **220**, 311-318.
15. Draznin, B, Sussman, K.E., Kao, M., Lewis, D., and Sherman, N. (1987) J. Biol. Chem. **262**, 14385-14388.
16. Farese, R.V. (1987) in Phospholipids and Cellular Regulation (Kuo, J.F., ed) pp. 207-228, CRC Press Inc., Florida.
17. Farese, R.V., Konda, T.S., Davis, J.S., Standaert, M.L., Pollet, R.J., and Cooper, D.R. (1987) Science **236**, 586-589.

Vol. 156, No. 1, 1988 BIOCHEMICAL AND BIOPHYSICAL RESEARCH COMMUNICATIONS
October 14, 1988 Pages 576-580

THE COMPLETE NUCLEOTIDE SEQUENCE OF HUMAN LIVER CYTOCHROME b_5 mRNA

Min Yoo and Alan W. Steggles

Department of Biochemistry and Molecular Pathology, Northeastern Ohio Universities College of Medicine, P.O. Box 95, Rootstown, OH 44272

Received August 11, 1988

We have isolated and sequenced a cDNA clone corresponding to human liver cytochrome b_5 mRNA. The 760 base pair (bp) sequence contains the complete coding and 3' non-translated regions plus 52 bp of 5' non-translated sequence. The derived amino acid sequence showed that the previous assignment of several amino acids was in error. In addition, the sequence of the previously unknown COOH hydrophobic region has been obtained. © 1988 Academic Press, Inc.

The amino acid sequences of the soluble portions of both the human liver and erythrocyte cytochrome b_5's have been available for some time (1,2). The two proteins show the same sequence except at positions 98 which are thr and pro for the liver and erythrocyte proteins respectively. In the former the thr is followed by a hydrophobic region of unknown length or sequence, whereas in the later the pro is the terminal amino acid (1,2). Based on data from other species, the hydrophobic region of cytochrome b_5 should contain about 36 amino acids (3-7), and function as the membrane binding domain for the liver protein.

There are three intriguing questions that relate to human liver cytochrome b_5 and its corresponding mRNA. First, what is the hydrophobic sequence of human liver cytochrome b_5? Second, what is the relationship between the liver and the erythrocyte proteins? Are they derived from two mRNAs from two different genes, or from

0006-291X/88 $1.50
Copyright © 1988 by Academic Press, Inc.
All rights of reproduction in any form reserved.

two mRNAs from one gene by some alternative mRNA processing mechanism? Last, what is the molecular defect in the cytochrome b_5 gene(s) that leads to one of the forms of inherited methemoglobinemia (8). Any attempts to study these questions must start with the isolation and characterization of a suitable cDNA probe corresponding to either of the liver or erythrocyte cytochrome b_5 mRNA's.

MATERIALS AND METHODS

The human liver λgt11 cDNA libraries were obtained from Clontech Ltd. (Palo Alto, CA) and Dr. S.L.C. Woo (Baylor, TX). Enzymes were purchased from Bethesda Research Labs (Bethesda, MD), Pharmacia (Piscataway, NJ) and U.S. Biochemicals (Cleveland, OH). Radioisotopes were from ICN Ltd. (Irvine, CA). Nitrocellulose filters were purchased from Schleicher and Schuell (Keene, NH) and Millipore (Bedford, MA), and nylon membranes from New England Nuclear (Boston, MA). Low melt agarose was from FMC Co. (Rockland, ME). The plasmid vector "Bluescript" was obtained from Stratagene (San Diego, CA). All other reagents and chemicals were of the best quality available.

The λgt11 phage from the Clontech library were used to infect Y1088 cells (9) prior to plating at a density of ca. 15000 pfu/ 15 cm petri dish. Nitrocellulose filter lifts were made, amplified, denatured and baked (10,11). After prehybridization (10), the filters were placed into hybridization solution (10) containing 2 x 10^6 cpm/filter of [^{32}P] labelled DNA probe (12).

The probe was the EcoRI - DraI insert isolated from the plasmid pR1 and contains the complete coding sequence for rabbit liver cytochrome b_5 mRNA (13). After an overnight hybridization at 37°C, the filters were washed once with 6 x SSC, 0.1% SDS at room temperature for 10', then, once with 1 x SSC, 0.1% SDS for 30' at 37°C and once with 0.2xSSC, 0.1% SDS for 30' at 42°C. The filters were air dried and used to expose Kodak XAR5 film at -70°C. One Quanta III intensifying screen was used. In the initial screen of ca. 500,000 plaques, five positive signals were identified, only one was subsequently plaque purified. The insert from this phage λHa was subcloned into the EcoR I cut dephosphorylated Bluescript vector. This insert (Ha) was subsequently shown to be a partial copy of human liver cytochrome b_5 mRNA. Ha was radiolabelled (12) and then used as a probe to screen the second cDNA library at high stringency (10). From this screening of ca. 500,000 phage, twelve positive signals were identified, and all were subsequently plaque purified (10). Two phage ($\lambda Hb_{5.1}$ and $\lambda Hb_{5.2}$) were studied in detail. The inserts were subcloned, and mapped with restriction enzymes (10,14). Selected DNA fragments were isolated from low melt agarose gels and again subcloned (14).

The complete nucleotide sequences of $Hb_{5.1}$ and $Hb_{5.2}$ were determined, using both double and single stranded DNA sequencing protocols (15,16).

RESULTS AND DISCUSSION

The restriction maps of pH1 and pH2 were used to determine the DNA sequencing strategy (Fig. 1). The nucleotide sequence (Fig. 2) of pH2 contains 52, 402 and 308 bp in the 5', coding and 3' regions, respectively. The derived amino acid sequence (Fig. 2) is the same as the published sequence and confirms the reassignments at six positions (1,2). Four of these are the initial met and the three adjacent amino acids; the other two are gln for glu at position 18, and asn for asp at position 62. In addition there is a transposition of the lys and arg at positions 89 and 91. The latter were probably due to protein sequencing errors (17). The amino acids at positions 89 and 91 now agree with the majority of the published sequences (3-7,18). It will be interesting to see if the equivalent monkey sequence of lys-pro-arg (19) is changed to arg-pro-lys when the monkey liver cytochrome b_5 cDNA nucleotide sequence is obtained. From the nucleotide sequence we have obtained the previously unknown hydrophobic COOH region. This thirty-six amino acid sequence is similar to those described for rabbit, cow, pig, rat and horse (3-7). The trp trp thr asn trp sequence at positions 109-113 is conserved (3-7), except for the chicken (18). The chicken liver cytochrome b_5 sequence is also unusual in that it contains six extra amino acids at the NH_2 terminus, and one less amino acid at the COOH terminus (18). It is

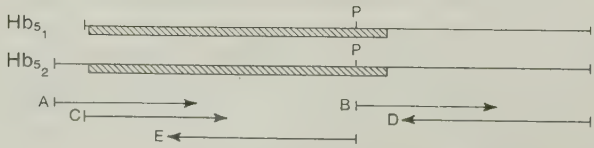

Figure 1. The sequencing strategy for human liver cytochrome b_5 cDNA. A, B, and C were double stranded, D and E were single stranded DNA sequencing. All sequences were repeated at least four times.

```
CAGCCAGCTCGACGGGGCTGTGTGTGCTGGGCCTGGCTCGCGGCGAACCGAG  52

ATG GCA GAG CAG TCG GAC GAG GCC GTG AAG TAC TAC ACC   91
Met Ala Glu Gln Ser Asp Glu Ala Val Lys Tyr Tyr Thr  (13)

CTA GAG GAG ATT CAG AAG CAC AAC CAC AGC AAG AGC ACC  130
Leu Glu Glu Ile Gln Lys His Asn His Ser Lys Ser Thr  (26)

TGG CTG ATC CTG CAC CAC AAG GTG TAC GAT TTG ACC AAA  169
Trp Leu Ile Leu His His Lys Val Tyr Asp Leu Thr Lys  (39)

TTT CTG GAA GAG CAT CCT GGT GGG GAA GAA GTT TTA AGG  208
Phe Leu Glu Glu His Pro Gly Gly Glu Glu Val Leu Arg  (52)

GAA CAA GCT GGA GGT GAC GCT ACT GAG AAC TTT GAG GAT  247
Glu Gln Ala Gly Gly Asp Ala Thr Glu Asn Phe Glu Asp  (65)

GTC GGG CAC TCT ACA GAT GCC AGG GAA ATG TCC AAA ACA  286
Val Gly His Ser Thr Asp Ala Arg Glu Met Ser Lys Thr  (78)

TTC ATC ATT GGG GAG CTC CAT CCA GAT GAC AGA CCA AAG  325
Phe Ile Ile Gly Glu Leu His Pro Asp Asp Arg Pro Lys  (91)

TTA AAC AAG CCT CCG GAA ACT CTT ATC ACT ACT ATT GAT  364
Leu Asn Lys Pro Pro Glu Thr Leu Ile Thr Thr Ile Asp (104)

TCT AGT TCC AGT TGG TGG ACC AAC TGG GTG ATC CCT GCC  403
Ser Ser Ser Ser Trp Trp Thr Asn Trp Val Ile Pro Ala (117)

ATC TCT GCA GTG GCC GTC GCC TTG ATG TAT CGC CTA TAC  442
Ile Ser Ala Val Ala Val Ala Leu Met Tyr Arg Leu Tyr (130)

ATG GCA GAG GAC TGA ACACCTCCTCAGAAGTCAGCGCAGGAAGAGC  488
Met Ala Glu Asp xxx                                 (134)

CTGCTTTGGACACGGGAGAAAAGAAGCCATTGCTAACTACTTCAACTGACA  539

GAAACCTTCACTTGAAAACAATGATTTTAATATATCTCTTTCTTTTTCTTC  590

CGACATTAGAAACAAAACAAAAAGAACTGTCCTTTCTGCGCTCAAATTTTT  641

CGAGTGTGCCTTTTTATTCATCTACTTTATTTTGATGTTTCCTTAATGTGT  692

AATTTACTTATTATAAGCATGATCTTTTAAAAATATATTTGGCTTTTAAAG  743

TAAAAAAAAAAAAAAAAAA                                  762
```

Figure 2. The complete nucleotide sequence of human liver cytochrome b_5 cDNA and the derived amino acid sequence.

possible that these differences will be restricted to avian cytochrome b5's.

We do not know whether the cDNA clone pH_2 is missing either a stretch of 3' poly A sequence, some 5' non-translated sequence, or both. The 5' non-translated sequence has the consensus ribosome binding site at nucleotides 20-30 (20), in agreement with the majority of eucaryote mRNAs.

The isolation and characterization of a cDNA for human liver cytochrome b_5 mRNA will enable studies on the one gene-two gene

question and on the molecular basis of certain inherited methemoglobinemias to be initiated (8).

ACKNOWLEDGEMENTS

This study was supported by the State of Ohio Academic and Research Challenge Funds and by a grant from the Ohio Heart Association.

REFERENCES

1. Ozols J. (1972) J. Biol. Chem. 247, 2242-2254.
2. Abe K., Kimura S., Kizawa R., Anan F.K., and Sugita Y. (1985) J. Biochem. 97, 1659-1668.
3. Takahagi Y., Gerber G.E., Nihei K. and Khorana H.A. (1980) J. Biol. Chem. 255, 1536-1541.
4. Fleming P.J., Dailey H.A., Corcoran D. and Strittmatter P. (1978) J. Biol. Chem. 253, 5369-5372.
5. Ozols J. and Gerard G. (1977) Proc. Natl. Acad. Sci. (USA) 74, 3725-3729.
6. Ozols J. and Heinemann F.S. (1982) Biochim Biophys Acta 704, 163-172.
7. Ozols J. and Gerard C. (1977) J. Biol. Chem. 252, 8549-8553.
8. Hegesh E., Hegesh J. and Kaftory A. (1986) N. Engl. J. Med. 314, 757-761.
9. Young R.A. and Davis R.W. (1983) Science 222, 778-782.
10. Maniatis T., Fritsch E.F. and Sambrook J. (1982) Molecular Cloning. A Laboratory Manual, Cold Spring Harbor.
11. Woo, SLC (1979) Methods in Enzymol. 68, 389-395.
12. Feinberg A. and Vogelstein B. Anal Biochem (1984) 137, 266-267.
13. Dariush N., Fisher C.W. and Steggles A.W. Prot. Seq. Data Analysis (1988) In press.
14. Struhl K. (1985) Biotechniques 3, 452-453.
15. Sanger F. and Coulson A.R. (1975) J. Mol. Biol. 94, 441-448.
16. Chen E.Y. and Seeberg P.H. (1985) DNA 4, 165-170.
17. Naoki A., Mayumi Y., Yoshitaka G. and Taro O. (1988) Biochem. Biophys. Res. Commun. 152, 1395-1400.
18. Zhang H. and Somerville C. (1988) Arch. Biochem. Biophys. 264, 343-347.
19. Nobrega F.A. and Ozols T. (1971) J. Biol. Chem. 246, 1706-1717.
20. Kozak M. (1987) Nucl. Acids Res. 15, 8125-8132.

Vol. 156, No. 1, 1988 BIOCHEMICAL AND BIOPHYSICAL RESEARCH COMMUNICATIONS
October 14, 1988 Pages 581-587

APOLIPOPROTEIN B-100 IS THE MAJOR FORM OF THIS APOLIPOPROTEIN SECRETED BY HUMAN INTESTINAL Caco-2 CELLS

Diana M. Lee[†‡], Nassrin Dashti and Tina Mok

Lipoprotein and Atherosclerosis Research Program, Oklahoma Medical Research Foundation and [†]the Department of Biochemistry and Molecular Biology, University of Oklahoma Health Sciences Center, Oklahoma City, OK 73104

Received August 15, 1988

SUMMARY: Although the discovery of stop codon has explained the mechanism for the formation of the intestinal marker, apolipoprotein B-48, the dispute regarding the presence of apolipoprotein B-100 in the intestine is still unsettled. To further investigate the characteristics of intestinal apolipoprotein B, the newly developed human colonic adenocarcinoma Caco-2 cells which express functional properties of the differentiated enterocytes, were used. SDS-polyacrylamide gel electrophoresis analyses of the intact culture medium or its lipoproteins of d < 1.23 g/ml showed the presence of only a single protein band of apolipoprotein B-100 with no detectable apolipoprotein B-48. After immunoblotting with oligoclonal antibodies to the amino-terminal peptide of apolipoprotein B, a trace amount of apolipoprotein B-48 was observed in the isolated lipoproteins, but not in the intact culture medium. These results suggest that apolipoprotein B-100 is the major form of apolipoprotein B secreted by human intestinal cells. © 1988 Academic Press, Inc.

Apolipoprotein B (ApoB) is the major carrier for triacylglycerol and cholesterol in the circulation. It is an essential structural component of chylomicrons, very-low-density (VLDL) and low-density lipoproteins (LDL). Human ApoB, as currently viewed by most investigators, exists in two major forms: the ApoB-100 from liver and the ApoB-48 from intestine.

Recent studies on cDNA clones of ApoB-100 have indicated that the gene for ApoB-100 is present in both liver and intestine of man, monkey and rat (1-4), suggesting the possibility of synthesis and secretion of ApoB-100 by intestine.

The abbreviations used are: ApoB, apolipoprotein B; VLDL, very low density lipoproteins (d < 1.006 g/ml); LDL, low density lipoproteins (d 1.006-1.063 g/ml); HDL, high density lipoproteins (d 1.063-1.23 g/ml); DMEM, Dulbecco's Modified Eagle Medium; N-terminal, amino-terminal; C-terminal, carboxyl-terminal; SDS-PAGE, polyacrylamide gel electrophoresis in the presence of sodium dodecyl sulfate.

[‡]Address correspondence and reprint requests to this author at the Lipoprotein and Atherosclerosis Research Program, Oklahoma Medical Research Foundation, 825 N.E. 13th St., Oklahoma City, OK 73104.

0006-291X/88 $1.50
Copyright © 1988 by Academic Press, Inc.
All rights of reproduction in any form reserved.

This is supported by our previous observation that ApoB-100 was found in rat mesenteric chyle when analyzed immediately after collection of chyle (5). ApoB-100 was also found to be the only form of ApoB in human chylomicrons when analyzed promptly after plasma collection (6).

Most recently, an inframe stop codon was discovered in human intestinal mRNA of ApoB resulting from a C to U substitution in the codon CAA encoding Gln-2153 to UAA, which is a termination codon for ApoB-48 (7-9). This discovery of stop codon explains the mechanism of ApoB-48 formation. If the stop codon is present in all the intestinal ApoB mRNAs, one should not be able to detect ApoB-100 in the intestine. Our previous studies (5,6), as well as those by others (10), do not support this hypothesis. To further investigate the characteristics of intestinal ApoB, we have utilized the newly developed human colonic adenocarcinoma Caco-2 cell line. Caco-2 cells undergo in vitro differentiation and express structural characteristics (11) and functional properties (12-14) typical of the small intestinal enterocytes. Thus, the ApoB secreted into the medium by Caco-2 represents the intestinal form of this apolipoprotein with no contribution from plasma or the liver. Results from this study further support the hypothesis that ApoB-100 is the major ApoB form synthesized and secreted by human intestinal cells.

MATERIALS AND METHODS

Cell culture. The human colonic adenocarcinoma cell line Caco-2 were obtained from American Type Culture Collection (Rockville, MD). The cells were grown in Dulbecco's Modified Eagle Medium (DMEM) supplemented with 2 mM glutamine, 1% nonessential amino acids, kanamycin sulfate (50 μg/ml), and 10% fetal calf serum at 37°C in a 5% CO_2, 95% air atmosphere. The culture medium was changed daily after the cells reached confluency. All experiments were conducted with 10-14-days post confluence cells at which time the differentiation-dependent expression of their functional properties typical of small intestinal enterocytes is maximal (11). At the start of each experiment, the maintenance medium was removed, monolayers were washed twice with phosphate-buffered saline and serum-free DMEM was added. After a 20 hour incubation, culture medium was removed and centrifuged at 2000 rpm for 30 min to remove cell debris.

Isolation of lipoproteins. Preservative cocktail (D) containing antibiotics/EDTA/protease inhibitor/antioxidants (15) was added to the pooled medium. The medium was divided in half and to one half, leupeptin at 1 mM final concentration was added. Lipoproteins of d < 1.23 g/ml were isolated by a one-step ultracentrifugation at 40,000 rpm for 36 hours at 4°C. The lipoproteins were dialyzed against 0.02 M Tris-buffered saline (pH 7.4) containing the corresponding preservatives at 4°C under N_2 and concentrated with Amicon membrane cone before analyses.

To determine the distribution of ApoB in various density classes, the medium was also fractionated into VLDL, LDL and high density lipoprotein (HDL) as previously described (16). The concentration of ApoB in density classes was measured by electroimmunoassay with antibodies to lipoprotein B (17).

Preparation of antibodies. Amino-terminal peptide of ApoB consisting of H_2N-Glu-Glu-Glu-Met-Leu-Glu-Asn-Val-Ser-Leu-Val-Cys-Pro-Lys-Asp-Ala-Thr-Arg-COOH

Table 1. Amino acid composition of the synthesized N-terminal peptide of ApoB after HPLC purification (moles/mole of peptide)

Amino Acids	Found	Expected
Asp	1.9	2
Thr	1.0	1
Ser	0.9	1
Glu	4.1	4
Pro	1.2	1
Gly	0	0
Ala	1.0	1
Cys	N.D.[a]	1
Val	2.0	2
Met	0.7	1
Ile	0	0
Leu	1.9	2
Tyr	0	0
Phe	0	0
His	0	0
Lys	1.2	1
Arg	1.1	1
Total		18

[a]N.D., not determined.

(18) was synthesized using Applied Biosystem Model 430A peptide synthesizer (Foster City, CA) according to the method described by Barany and Merrifield (19). The synthesized product was analyzed by reversed-phase HPLC. Two major peaks were found and both showed identical amino acid composition (Table 1). The difference in elution position possibly was due to dehydroserine. Edman degradation of the crude peptide yielded a single correct sequence as described above.

The N-terminal peptide of ApoB was cross-linked to rabbit albumin (Sigma) with glutaraldehyde (Sigma) (20). After extensive dialysis against phosphate buffered saline, the peptide-albumin was mixed with equal volume of Freund's complete adjuvant and inoculated into rabbit lymph nodes (21). A second intradermal injection was given on the back after a month. Blood was drawn 7 weeks later. Positive immunoreaction was shown by ELISA with the peptide only. A booster shot was given every 7-8 weeks. Positive immunoreactions with ApoB, LDL and whole plasma were shown after the third booster shot.

Monoclonal antibodies to ApoB, MB47, a generous gift of Dr. L. Curtiss (La Jolla, CA), were used as anti-C-terminal portion of ApoB. MB47 was shown to inhibit the LDL-receptor interaction and bind an epitope on thrombin fragment T_2, a carboxyl-terminal portion of ApoB-100 (22).

Polyacrylamide gel electrophoresis in sodium dodecyl sulfate. The lipoproteins of d < 1.23 g/ml or the concentrated intact culture medium were analyzed by 3.3% polyacrylamide gel electrophoresis in the presence of SDS (SDS-PAGE), according to the method of Fairbanks *et al*. (23) as modified previously (5), including recrystallization of the acrylamide and inclusion of 0.02% thiodiglycol as antioxidant in the running buffer.

Immunoblotting. Electrophoresis of lipoproteins or intact culture medium was carried out in a 3.3% polyacrylamide slab gel containing SDS using the same buffer system described above. The proteins were transferred to Immobilon transfer membrane (Millipore, Bedford, MA) by electroblotting, according to Towbin *et al*. (24) and immunoblotted as described previously (6). The oligoclonal antibodies to N-terminal peptide of ApoB and monoclonal anti-ApoB

(C-terminal portion) were diluted 1:1000 and 1:2000, respectively for immunoblotting.

RESULTS AND DISCUSSION

Quantitation of ApoB in lipoprotein density fractions isolated from Caco-2 cell culture medium from four experiments showed that 0-4.6% of total ApoB was recoverred in VLDL, 95-100% was in the LDL and only trace amount was found in HDL (Table 2). Since ApoB-48 was observed in HDL of Caco-2 cell culture medium (10), the analyses of ApoB were performed on the total lipoproteins of d < 1.23 g/ml or on the concentrated intact medium. As shown in Fig. 1 (gel 2), the SDS-PAGE analysis of freshly prepared lipoproteins of d < 1.23 g/ml from Caco-2 culture medium contained only a single band with mobility corresponding to ApoB-100. The ApoB-48 band was not detectable by Coomassie blue staining. After immunoblotting, a trace amount of ApoB-48 was observed with anti-N-terminal peptide of ApoB which could not easily be photographed (Fig. 1, pattern 3). Thus, ApoB-100 remained the predominant band, as illustrated by immunoblotting (Fig. 1). In comparison to a reference VLDL which contained a small amount of ApoB-48, the immunoblot showed the presence of ApoB-48 band with the oligoclonal antibodies to N-terminal peptide of ApoB (Fig. 1, pattern 5) and the absence of ApoB-48 band with anti-C-terminal portion of ApoB (MB47) (Fig. 1, pattern 6). These results validate that the anti-N-terminal peptide of ApoB is effective in detecting the authentic ApoB-48, if present, and that the anti-C-terminal portion of ApoB should react only with ApoB-100 and not with the ApoB-48, as described previously (22). To avoid the manipulation of lipoprotein isolation, concentrated intact culture medium was analyzed. Fig. 2 shows that when the concentrated medium was analyzed immediately after collection, ApoB-100 was the only form of ApoB detected by SDS-PAGE (gel 8) as well as by immunoblotting (patterns 6 and 7). When the isolated lipoproteins of d < 1.23 g/ml from the same medium, with or without leupeptin, were analyzed, a trace

Table 2. Concentration and distribution of apolipoprotein B in culture medium and lipoprotein density classes

Total medium	Fraction		
	VLDL	LDL	HDL
(μg/g cell protein/h)	(Percent distribution)[a]		
63.32 ± 8.49[b]	0-4.6	95.4-100	Trace

[a]Mean of 4 experiments.

[b]Mean ± SEM of 8 experiments.

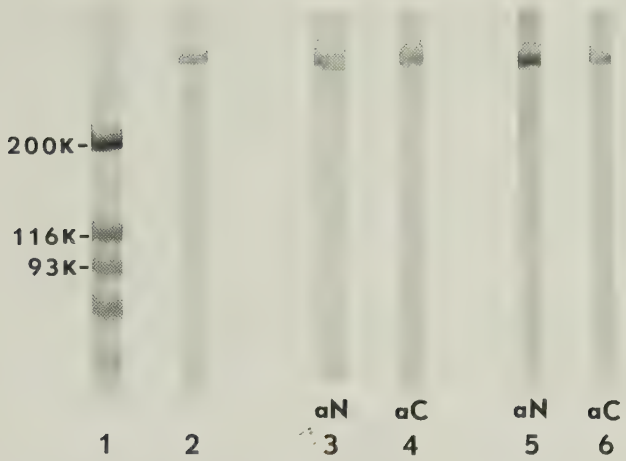

Fig. 1. Analyses of lipoproteins of d < 1.23 g/ml from Caco-2 cell culture medium by electrophoresis and immunoblotting. Gels 1 and 2, electropherograms of calibration proteins (gel 1) and lipoproteins of d < 1.23 g/ml from Caco-2 cell culture medium (gel 2) in 3.3% polyacrylamide gel slabs containing SDS. Patterns 3 and 4, immunoblots with antisera after transferring proteins from gel 2 to Immobilon transfer membrane. Patterns 5 and 6, immunoblots of a reference VLDL which contained ApoB-48. aN, oligoclonal antibodies to N-terminal peptide of ApoB; aC, monoclonal antibodies to C-terminal half of ApoB, MB47 (22).

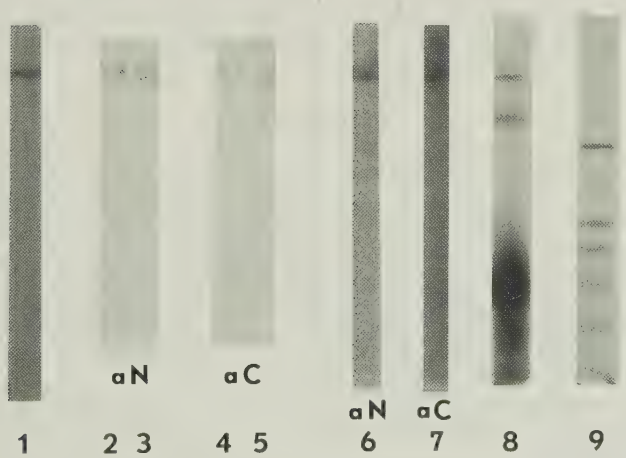

Fig. 2. Analyses of Caco-2 cell culture medium and its lipoproteins of d < 1.23 g/ml by electrophoresis and immunoblotting. Gels 1, 8 and 9, electropherograms on 3.3% polyacrylamide gel slab containing SDS. Sample in gel 1, lipoproteins of d < 1.23 g/ml from Caco-2 cell culture medium; gel 8, concentrated intact culture medium from Caco-2 cell; gel 9, calibration standards same as in Fig. 1. Patterns 2-7, immunoblots with antisera after transferring proteins from gels to Immobilon transfer membrane. Samples in patterns 2-5, lipoproteins of d < 1.23 g/ml from Caco-2 cell culture medium, with leupeptin (patterns 2 and 4) and without leupeptin (patterns 3 and 5). Samples in patterns 6 and 7, intact culture medium of Caco-2 cells with leupeptin. aN, oligoclonal antibodies to N-terminal peptide of ApoB; aC, monoclonal antibodies to C-terminal half of ApoB, MB47 (22).

amount of ApoB-48 was detected by immunoblotting for both preparations (patterns 2 and 3); thus, ApoB-100 remained the predominant band. However, by SDS-PAGE alone, again only ApoB-100 was observed, with no detectable ApoB-48 band (Fig. 2, gel 1).

Analyses of three additional preparations of lipoproteins from Caco-2 cell media confirmed the same observations. These results suggest that ApoB-100 is the major, if not the only ApoB form secreted by the intestinal Caco-2 cells under the present culture condition. Hughes et al. (10) have also shown that ApoB-100 was the only ApoB form present in VLDL and LDL secreted by Caco-2 cells. Furthermore, the authors observed that ApoB-48 was the minor and ApoB-100 the major form of ApoB in HDL of the culture medium. If the presence of stop codon in ApoB mRNA is the only mechanism for the presence of ApoB-48 in Caco-2 cell culture medium, either the number of mRNA containing stop codon is very small so that the "authentic" ApoB-48 derived from stop codon is minimal, or the majority of the ApoB-48 synthesized by Caco-2 cells is not secreted.

ACKNOWLEDGMENTS

We would like to express our appreciation to Ms. E. Carter for expert technical assistance, to Dr. K. Jackson of Saint Francis Hospital of Tulsa Medical Research Institute, Oklahoma City, OK, for synthesis of N-terminal peptide of ApoB. We are grateful to Dr. L. Curtiss of La Jolla, CA, for her generous gift of monoclonal antibody, and to Ms. J. Pilcher for typing the manuscript. This work was supported in part by grant HL-23181 from the National Heart, Lung, and Blood Institute of the National Institutes of Health, and by the resources of the Oklahoma Medical Research Foundation.

REFERENCES

1. Lusis, A.J., West, R., Mahrabian, M., Reuben, M.A., LeBouef, R.C., Kaptein, J.S., Johnson, D.F., Schumaker, V.N., Yahasz, M.P., Schotz, M.C., and Elovson, J. (1985) Proc. Natl. Acad. Sci. USA 82, 4597-4601.
2. Knott, T.J., Rall, S.C., Jr., Innerarity, T.L., Jacobson, S.F., Urdea, M.S., Levy-Wilson, B., Powell, L.M., Pease, R.J., Eddy, R., Nakai, H., Byers, M., Preistly, L.M., Robertson, E., Rall, L.B., Betsholtz, C., Shows, T.B., Mahley, R.W., and Scott, J. (1985) Science 230, 37-43.
3. Deeb, S.S., Disteche, C., Motulsky, A.G., Lebo, R.V., and Kan, Y.W. (1986) Proc. Natl. Acad. Sci. USA 83, 419-422.
4. Law, S.W., Lackner, K.J., Hospattankar, A.V., Anchors, J.M., Sakaguchi, A.Y., Naylor, S.L., and Brewer, H.R., Jr. (1985) Proc. Natl. Acad. Sci. USA 82, 8340-8344.
5. Lee, D.M., Koren, E., Singh, S., and Mok, T. (1984) Biochem. Biophys. Res. Commun. 123, 1149-1156.
6. Lee, D.M., and Singh, S. (1988) Biochim. Biophys. Acta 960, 148-156.
7. Powell, L.M., Wallis, S.C., Pease, R.J., Edwards, Y.H., Knott, T.J., and Scott, J. (1987) Cell 50, 831-840.
8. Chen, S.-H., Habib, G., Yang, C.-Y., Gu, Z.-W., Lee, B.R., Weng, S.-A., Silberman, S.R., Cai, S.-J., Deslypere, J.P., Rosseneu, M., Gotto, A.M., Jr., Li, W.-H., and Chan, L. (1987) Science 238, 363-366.
9. Hospattankar, A.V., Higuchi, K., Law, S.W., Meglin, N., and Brewer, H.B., Jr. (1987) Biochem. Biophys. Res. Commun. 148, 279-285.
10. Hughes, T.E., Sasak, W.V., Ordovas, J.M., Forte, T.M., Lamon-Fava, S., and Schaefer, E.J. (1987) J. Biol. Chem. 262, 3762-3767.

11. Pinto, M., Robine-Leon, S., Appay, M.D., Kedinger, M., Triadou, N., Dussaulx, E., Lacroix, B., Simon-Assmann, P., Haffen, K., Fogh, J., and Zweibaum, A. (1983) Biol. Cell 47, 323-330.
12. Hauri, H.P., Sterchi, E.E., Bienz, D., Franzen, J.A.M., and Marxer, A. (1985) J. Cell Biol. 101, 838-851.
13. Grasset, E., Bernabeu, J., and Pinto, M. (1985) Am. J. Physiol. 248, C410-C418.
14. Vincent, M.L., Russell, R.M., and Sasak, V. (1985) Hum. Nutr. Clin. Nutr. 39C, 355-360.
15. Lee, D.M., Valente, A.J., Kuo, W.H., and Maeda, H. (1981) Biochim. Biophys. Acta 666, 133-146.
16. Alaupovic, P., Lee, D.M., and McConathy, W.J. (1972) Biochim. Biophys. Acta 260, 689-707.
17. Curry, M.D., Gustafson, A., Alaupovic, P., and McConathy, W.J. (1978) Clin. Chem. 24, 280-286.
18. Knott, T.J., Wallis, S.C., Powell, L.M., Pease, R.J., Lusis, A.J., Blackhart, B., McCarthy, B.J., Mahley, R.W., Levy-Wilson, B., and Scott, J. (1986) Nucleic Acids Res. 14, 7501-7503.
19. Barany, G., and Merrifield, R.B. (1979) in The Peptides, Analysis, Synthesis, Biology, Gross, E., and Meienhoser, J., eds., vol. 2, pp. 1-284, Academic Press, New York.
20. Reichlin, M. (1980) Methods Enzymol. 70, 159-165.
21. Sigel, M.B., Sinha, Y.N., and VanderLaan, W.P. (1983) Methods Enzymol. 93, 3-12.
22. Young, S.G., Witztum, J.L., Casal, D.C., Curtiss, L.K., and Bernstein, S. (1986) Arteriosclerosis 6, 178-188.
23. Fairbanks, G., Steck, T.L., and Wallach, D.F.H. (1971) Biochemistry 10, 2606-2617.
24. Towbin, H., Staehlin, T., and Gordon, J. (1979) Proc. Natl. Acad. Sci. USA 76, 4350-4354.

Vol. 156, No. 1, 1988 BIOCHEMICAL AND BIOPHYSICAL RESEARCH COMMUNICATIONS
October 14, 1988 Pages 588-594

HETEROLOGOUS UP-REGULATION OF THE 1,25-DIHYDROXYVITAMIN D_3 RECEPTOR BY PARATHYROID HORMONE (PTH) AND PTH-LIKE PEPTIDE IN OSTEOBLAST-LIKE CELLS

H.A.P. Pols, J.P.T.M. van Leeuwen, J.P. Schilte, T.J. Visser and J.C. Birkenhäger

Department of Internal Medicine III,
Erasmus University Medical School, Rotterdam, The Netherlands

Received September 2, 1988

1,25-Dihydroxyvitamin D_3 (1,25-$(OH)_2D_3$) receptor content in cultured osteogenic sarcoma cells (UMR-106) was found to be increased after treatment with both bovine and human PTH and human PTH-like peptide (hPLP). The dose dependent increase of receptors was preceded by a dose dependent stimulation of cAMP production. This suggests a role for cAMP as mediator of the PTH- and hPLP-induced 1,25-$(OH)_2D_3$ receptor up-regulation. Furthermore, evidence was obtained that new mRNA and de novo receptor synthesis is involved in this heterologous 1,25-$(OH)_2D_3$ receptor up-regulation. © 1988 Academic Press, Inc.

Parathyroid hormone (PTH) and 1,25-dihydroxyvitamin D_3 (1,25-$(OH)_2D_3$ are important regulators of calcium and bone metabolism. From both in vivo and in vitro studies evidence was obtained indicating an interaction between PTH and 1,25-$(OH)_2D_3$ on their major targets (1-4). In bone, receptors for both calcitrophic hormones are only found in osteoblasts (5). Recently, we and others reported that exposure of osteoblast-like cells to 1,25-$(OH)_2D_3$ decreased their cAMP response to PTH (6). This phenomenon has been referred as heterologous desensitization. At present it is not known whether PTH in return is also capable to influence 1,25-$(OH)_2D_3$ action in osteoblasts.

0006-291X/88 $1.50
Copyright © 1988 by Academic Press, Inc.
All rights of reproduction in any form reserved.

In the rat osteogenic sarcoma cell line UMR-106 we have recently shown that 1,25-$(OH)_2D_3$ elicits a homologous up-regulation of its receptor (7). UMR-106 cells are also responsive to PTH by showing a cAMP response (8). Therefore, we used these cells to analyze the effects of both human and bovine PTH on 1,25-$(OH)_2D_3$ receptor level. Furthermore, we examined the effect of human PTH-like peptide (hPLP), a hormone involved in the pathogenesis of humoral hypercalcemia of malignancy (9,10). In the current study we have observed that both PTH and hPLP up-regulates the 1,25-$(OH)_2D_3$ receptor.

MATERIALS AND METHODS

The rat osteogenic sarcoma cell line UMR-106 was supplied by Dr. M.P.M. Herrmann-Erlee (Laboratory of Cell Biology, University of Leiden, Leiden, The Netherlands). [23,24-^{3}H]1,25-$(OH)_2D_3$ (102 Ci/mmol) was obtained from Amersham and nonradioactive 1,25-$(OH)_2D_3$ was generously provided by LEO Pharmaceuticals. Cycloheximide, actinomycin D, bovine and human PTH(1-34) (bPTH(1-34), hPTH(1-34)) were from Sigma, while synthetic human PTH-like peptide(1-34) (hPLP(1-34)) was a generous gift of Dr. C.W.G.M. Löwik (Clinical Investigation Unit, University Hospital Leiden, The Netherlands). Fetal calf serum (FCS), MEM medium, penicillin, streptomycin and glutamine were purchased from Flow Laboratories.

Cell culture conditions: UMR-106 cells were seeded at 0.6×10^5 cells/cm^2 and cultured in MEM supplemented with 2 mM glutamine, 100 U/ml penicillin, 100 ug/ml streptomycin and 10% FCS. After an additional 16 h preincubation in MEM with 2 % charcoal-treated FCS, the confluent cultures were incubated in serum-free MEM with or without the compounds indicated. The incubations were carried out for 0-6 h at 37° C with the culture flasks placed on a slightly angled slowly rotating plate. At the end of the incubation the cells were rinsed with ice-cold Hanks medium, trypsinized and,after inactivation of trypsine, centrifuged.

Preparation of cell extracts and [^{3}H]1,25-$(OH)_2D_3$ binding assay: For single point assays, conditions were employed which were previously shown to provide valid estimates of total receptor content in cytosolic extracts (7). The cell pellet was extracted on ice in a hypertonic buffer consisting of 300 mM KCl, 10 mM Tris-HCl (pH 7.4), 1 mM EDTA, 5 mM dithiothreitol, 10 mM sodium molybdate and 0.1 % Triton X-100. High-speed supernatants were obtained and 200 ul aliquots were incubated at 0° C overnight with 0.5 nM [^{3}H]1,25-$(OH)_2D_3$ in the presence or absence of a 200-fold molar excess of unlabeled hormone. Receptor-bound 1,25-$(OH)_2D_3$ was separated from unbound sterol by charcoal adsorption

(11). The protein concentration was measured according to the method of Bradford (12).

Cyclic AMP assay: The cells were incubated for 3 min (maximal effect) at 37° C in Hanks-Hepes buffer with 0.5 % BSA and supplemented with the peptides to be tested (8). cAMP was measured by the protein binding assay of Lust et al (13). The DNA content was determined fluorimetrically by the method of Johnson-Wint (14).

RESULTS

In Fig. 1 the time-course of the effect of 10^{-8} M bPTH(1-34) on the cellular level of 1,25-$(OH)_2D_3$ receptors is shown. The increase in 1,25-$(OH)_2D_3$ binding following treatment with PTH was found to reach a maximum at 4 h. In vehicle-treated cultures no change in cellular 1,25-$(OH)_2D_3$ receptor level was found. Scatchard analysis after 4 h incubation with PTH showed no significant change in the apparent dissociation constant (≈20 pM) of the 1,25-$(OH)_2D_3$ receptor (results not shown).

To determine whether the observed increase in receptors reflected changes in translation and/or transcription, we examined the ability

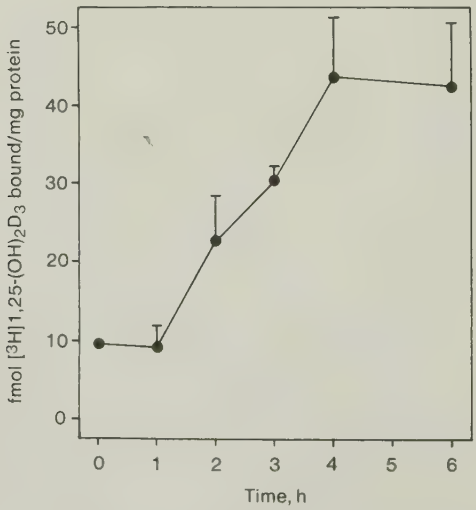

Fig. 1: Time course of the PTH-induced 1,25-$(OH)_2D_3$ receptor up-regulation. At the start of the experiment the medium was changed from MEM with 2 % charcoal-treated FCS to serum-free MEM without or with 10^{-8} M bovine PTH(1-34). At the times indicated 1,25-$(OH)_2D_3$ receptor content was assayed in cytosolic extracts as described in "Materials and Methods". Values are the means ± SD of 2 experiments.

Table I: Effect of cycloheximide and actinomycin D on the ability of bPTH(1-34) to up-regulate the 1,25-$(OH)_2D_3$ receptor level in UMR-106 cells

TREATMENT	Vehicle	bPTH(1-34)
Vehicle	10.6 ± 0.8	35.9 ± 8.0
Cycloheximide	5.9 ± 0.4	6.8 ± 1.7
Actinomycin D	6.8 ± 0.5	8.8 ± 0.9

After the medium was changed from MEM with 2 % charcoal-treated FCS to serum-free MEM, UMR-106 cells were treated for 4 h with vehicle or bPTH(1-34) in the absence or presence of cycloheximide (10 ug/ml) or actinomycin D (1 ug/ml). 1,25-$(OH)_2D_3$ receptor concentration was determined in cytosolic extracts as described in "Materials and Methods". Results are expressed in fmol [^{3}H]1,25-$(OH)_2D_3$ bound per mg protein. Values are the means ± SD of triplicate determinations.

of cycloheximide and actinomycin D, respectively, to block the increase in receptors induced by bPTH(1-34). As shown in Table I, the cells simultaneously treated with bPTH(1-34) and cycloheximide or actinomycin D fail to exhibit the up-regulation of the receptor found in the absence of these inhibitors.

The effect of various concentrations of bovine and human PTH(1-34) on 1,25-$(OH)_2D_3$ receptor up-regulation are depicted in Fig. 2. Although we observed a similar ED_{50} for both peptides (approximately 10^{-9} M), the maximum achieved in the presence of bPTH(1-34) seems somewhat higher. The maximum response to hPLP is comparable to that obtained with the PTH fragments. However, the dose response curve is shifted to the left with an ED_{50} of about 10^{-10} M.

Both PTH fragments and hPLP also produced a dose-dependent stimulation of the cAMP production in UMR-106 cells (Fig. 3). However, compared to the effect on 1,25-$(OH)_2D_3$ receptor up-regulation approximately 10 times higher concentrations of the peptides were required to elicit a half maximum effect.

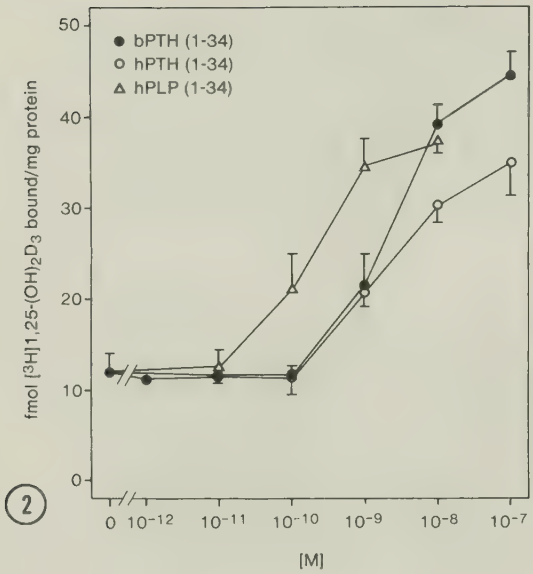

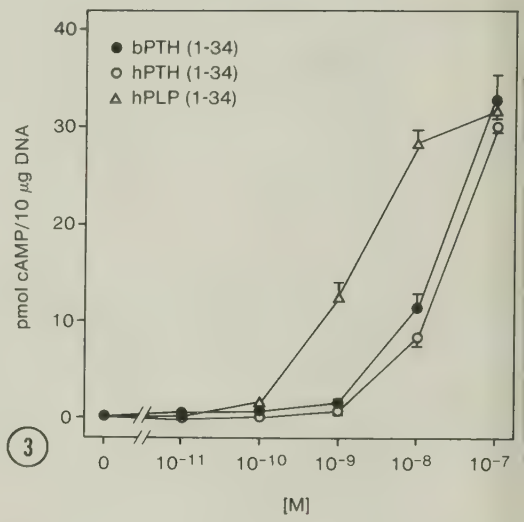

Fig. 2: Effect of bPTH, hPTH and hPLP on 1,25-$(OH)_2D_3$ receptor concentration. After the medium was changed from MEM with 2 % FCS to serum-free MEM the UMR-106 cells were incubated for 4 h with various concentrations of bPTH, hPTH and hPLP. 1,25-$(OH)_2D_3$ receptor content was assayed in cytosolic extracts as described in "Materials and Methods" Values are the means ± SD of 2 experiments.

Fig. 3: Effect of bPTH, hPTH and hPLP on cAMP accumulation. cAMP production in response to various concentrations bPTH, hPTH and hPLP was determined as described in "Materials and Methods". Values are the means ± of 2 experiments.

DISCUSSION

To our knowledge this is the first report describing a dose-dependent heterologous up-regulation of the 1,25-$(OH)_2D_3$ receptor by PTH fragments and hPLP in an osteoblast-like cell line. Based on the current results this represents an increase in the number of functional receptors since Scatchard analysis data indicated a single class of binding sites with equivalent affinity contants for 1,25-$(OH)_2D_3$ in vehicle and PTH-treated cultures. Furthermore, the inhibition of the PTH-stimulated receptor up-regulation by actinomycin D support the hypothesis that this process is dependent upon new RNA synthesis.

Although there seems to exist some difference between the maximum effects achieved in the presence of the peptides tested, the lower

ED_{50} for hPLP as compared to human and bovine PTH is remarkable. For the cAMP responses a similar phenomenon was observed. Other investigators also obtained evidence that hPLP is more potent than PTH in stimulating cAMP formation and also in generating a biological response (plasminogen activator activity) in clonal osteogenic sarcoma cells (9,10).

As shown in Figs. 2 and 3 the dose-dependent increase of 1,25-$(OH)_2D_3$ receptors by PTH and hPLP parallels the dose-dependent stimulation of cAMP generation. This suggests an involvement of cAMP as a second messenger in the observed up-regulation of binding sites for 1,25-$(OH)_2D_3$. The fact that low concentrations of PTH and hPLP induce an increment of 1,25-$(OH)_2D_3$ receptors, but do not stimulate cAMP generation, do not directly implicate the involvement of another second messenger. For instance other studies also showed that small increases in cAMP production, not detectable by the methods used, can be sufficient to fully activate cellular response units (15). The difference in the ED_{50} for induction of receptor up-regulation and stimulation of cAMP production is not unique for the biological response examined in the present study. Recently, a comparable difference in de ED_{50} between stimulation of ornithine decarboxylase activity and cAMP production in UMR-106 cells was described (8).

The maximum 1,25-$(OH)_2D_3$ receptor up-regulation by PTH and hPLP is lower than the homologous up-regulation induced by 1,25-$(OH)_2D_3$ itself (7). It remains to be established whether this difference reflects the recent finding that homologous up-regulation of the 1,25-$(OH)_2D_3$ receptor not only results from an increase in receptor synthesis, but also from a prolongation of receptor half-life (16).

The physiological significance of our findings that PTH and hPLP exhibit up-regulation of the 1,25-$(OH)_2D_3$ receptor is not yet clear. However, preliminary observations in our laboratory indicate a higher 1,25-$(OH)_2D_3$ inducible 24-hydroxylase activity after pretreatment of

the cultures with PTH. We interpret this finding to indicate that the PTH-induced increase in 1,25-$(OH)_2D_3$ receptors apparently results in a greater biological response of the cell to 1,25-$(OH)_2D_3$. Whether cAMP is indeed the second messenger involved in the PTH- and hPLP-induced 1,25-$(OH)_2D_3$ receptor up-regulation or that other intracellular messengers are involved remains to be established. Our recent observation that the cAMP analog dibutyryl cAMP is capable of mimicking the described effect on 1,25-$(OH)_2D_3$ receptor level (results not shown) does support a role for cAMP . From a physiological point of view it is interesting that 1,25-$(OH)_2D_3$ attenuates the PTH-stimulated cAMP response in osteoblasts (6), because this could be a potential mechanism in counteracting the heterologous up-regulation of 1,25-$(OH)_2D_3$ receptors by PTH.

REFERENCES

1. Forte, L.R., Nickols, G.A. and Anast, C.S. (1976) J. Clin. Invest. 57:559-68.
2. Nseir, N.J., Szramowski, J. and Puschett, J.B. (1978) Min. Electrolyte Metab. 1:48-56.
3. Wong, G.L., Luben, R.A. and Cohn D.V. (1977) Science 197:663-65.
4. Rubin, J. and Catherwood, B.D. (1984) Biochem. Biophys. Res. Commun. 123:210-15.
5. Rodan, G.A. and Rodan S.B. (1984) In: Bone and Mineral Research, Annual 2. Ed: Peck W.A. Elsevier, Amsterdam, pp 244-85.
6. Pols, H.A.P., Schilte, J.P., Herrmann-Erlee, M.P.M., Visser, T.J. and Birkenhäger, J.C. (1986) Bone and Mineral 1:397-405.
7. Pols, H.A.P., Birkenhäger, J.C. Schilte, J.P. and Visser, T.J. (1988) Biochim. Biophys. Acta 970:122-29.
8. van Leeuwen, J.P.T.M., Bos M.P. and Herrmann-Erlee M.P.M. (1988) J. Cell. Physiol. 135:488-94.
9. Moseley, J.M., Kubota, M., Diefenbach-Jagger, H., Wettenhall, R.E.H., Kemp, B.E., Suva, L.J., Rodda, C.P., Ebeling, P.R., Hudson, P.J., Zajac, J.D. and Martin, T.J. (1987) Proc. Natl. Acad. Sci. USA 84:5048-52.
10. Kemp, B.E., Stapleton, D., Rodda, C.P., Michelangeli, V.P., Ebeling, P.R., Moseley J.M., Simmons, H.A., Raisz L.G. and Martin T.J. (1987) Science 238:1568-70.
11. Feldman, D., McCain, T.A., Hirst, M.A., Chen, T.L. and Colston, K.W. (1979) J. Biol. Chem. 200:10378-82.
12. Bradford, M.M. (1976) Anal. Biochem. 72:248-254.
13. Lust, W.D., Dye, E., Deaton, A.V., and Passoneau J.V. (1976) Anal. Biochem. 72:8-15.
14. Johnson-Wint B. and Hollis S. (1982) Anal. Biochem. 122:338-44.
15. Saez, J.M., Morera, A.M. and Dazoid A. (1981) Adv. Cyclic Nucleotide Res. 14:563-79.
16. Costa, E.M. and Feldman, D. (1987) Endocrinology 120:1173-78.

Vol. 156, No. 1, 1988 BIOCHEMICAL AND BIOPHYSICAL RESEARCH COMMUNICATIONS
October 14, 1988 Pages 595-601

ISOLATION OF THE HUMAN PLATELET GLYCOPROTEIN IIb GENE AND CHARACTERIZATION OF THE 5' FLANKING REGION

Prandini M.H., Denarier E., Frachet P., Uzan G. and Marguerie G.

Laboratoire d'Hématologie, INSERM U.217,
Fédération des Laboratoires de Biologie, CENG. 85X, 38041 Grenoble Cedex, France

Received September 6, 1988

SUMMARY: Platelet membrane glycoprotein (GP) IIbIIIa complex functions as a receptor for fibrinogen, von Willebrand factor and fibronectin, and mediates adhesive reactions of platelets. The gene for the GPIIb subunit is only active in megakaryocytic cell type. We have isolated this gene from a genomic library. The GPIIb gene was characterized by restriction mapping and sequencing of the 5' and 3' regions containing the first and the last exons. The transcription start site and the polyadenylation signal were identified. From these data we deduced that the gene spans a region of 22 kb and that the mRNA contains a leader sequence of 32 nucleotides. At the 3' end the last exon encodes the 19 amino acids corresponding to the cytoplasmic domain of the GPIIb light chain. Upstream the transcription start site, two sequences are homologous to consensus binding sites of the nuclear factors SP1 and CP2. Two inverted repeats were also identified in this region.
© 1988 Academic Press, Inc.

Cell-cell contact and interaction between cells and extracellular matrices are mediated by a broadly distributed family of adhesion receptors which has recently been named integrins (1) . Each member of this superfamily is a non covalently bound heterodimer with α and β subunits containing membrane spaning domains. The superfamily of integrins, is composed of the different groups of adhesion receptors, including the leucocyte adhesion molecule (Leu-CAM), the VLA family and the cytoadhesins (for review see 1 and 2). Within each subfamily the same β subunit is associated with variable α subunits forming different heterodimers with specific structural and functional features. During the past two years most of the subunits of the different integrins have been cloned and their amino acid sequences were deduced from the cDNA sequence (3-8). A central question now emerging, concerns the identification of the mechanisms implicating the different integrins in cell-differenciation and phenotypic selection.

With available cDNA clones for these receptors it is now feasible to compare the structure of the corresponding genes and to identify the mechanisms that control their tissue specific expression. Two members of the cytoadhesin family have been identified : GPIIbIIIa from platelets and megakaryocytes and the vitronectin receptor which is expressed in endothelial cells (9,10). The two receptors have an RGD recognition specificity (11,12) and share the same β subunit (GPIIIa). While the β subunit is expressed in different cellular systems, the α subunits appear to be cell specific. Thus GPIIb

0006-291X/88 $1.50
Copyright © 1988 by Academic Press, Inc.
All rights of reproduction in any form reserved.

expression seems to be restricted to the megakaryocytic lineage and consequently constitutes a suitable marker for the studies of the mechanisms governing megakaryocytopoiesis. In this paper we describe the isolation of genomic clones containing the entire GPIIb gene and the characterization of the 5' flanking domain of this gene.

METHODS

Screening of human genomic library and characterization of DNAs. A genomic library constructed in λEMBL4 phage from partially Mbo I digested human leucocyte DNA was generously provided by Dr A. Kahn (Paris). It was screened with different human GPIIb cDNA, that have already been described (4,13). Three specific cDNA clones were used for the screening : λIIb_2, corresponding to the 3' region, λIIb_3 corresponding to approximately 80% of the GPIIb cDNA and λIIb_4 corresponding to the 5' end of the cDNA (Fig. 1A). In addition an 18 bases oligonucleotide corresponding to the 5' end of the cDNA in position +37 to +54 (Fig. 3) was synthesized using the phosphoramidite method with an Applied Biosystem DNA synthesizer and used to further align the genomic clones. λIIb_3 was used as probe for Southern blot analysis of genomic DNA and of the DNA from the positive clones (14). DNA sequencing was performed by the dideoxynucleotide chain termination method (15). DNA fragments were subcloned in PGEM1 plasmid (Promega biotec, Madison WI. U.S.A.) and the sequence was obtained on both strands using synthetic oligonucleotides.
Primer extension. Total RNA was extracted from human megakaryocytes (16) using the thiocyanate-guanidinium method (17) and the poly A^+ mRNA were purified by chromatography on oligo (dT) cellulose column (18). The 5' end labelled oligonucleotide (7.10^6 cpm) was hybridized to poly A^+ mRNA and elongated using the protocol and reagents of the first strand cDNA synthesis kit (Amersham England).
RNase mapping. RNase mapping with Sp6 probes was carried out essentially as previously described (19). The templates used for the generation of the anti-sens RNA probes were obtained by cloning a 1.4 kb Nco I-Eco RI fragment and a 1 kb Bgl I-Bgl I fragment isolated from the 1.9 kb 5' subclone, in the appropriate orientation, in the PGEM1 plasmid. For synthesis of the Sp6 probes, the templates were linearized by Dde I and Pvu II respectively. Total RNA (50 μg) was hybridized overnight to 5.10^6 cpm of probe at 45°C and digested with RNase T1 and RNase A. The RNase resistant products were subsequently analysed on 6% acrylamide sequencing gel.

RESULTS

Isolation and characterization of the human GPIIb gene. Approximatively 10^6 recombinants from the amplified genomic library were screened using different human GPIIb cDNA clones as hybridization probes (Fig.1 A). Five independent clones were identified, isolated and purified. Alignement of these clones was achieved by restriction enzyme digestion and Southern blotting analysis using 3' and 5' restriction fragments from the cDNA probes. Two overlapping genomic clones spaning about 30 Kb were found to contain the boundaries of the gene. A partial restriction map of the GPIIb gene is shown in Fig. 1B. Comparison of the size of the restriction fragment predicted from the isolated genomic clones with that of the fragments obtained by the digestion of the genomic DNA indicates that there is only one copy of the GPIIb gene in the human genome (data not shown).

Characterization of the 3' end of the gene. A Hind III-Eco RI 125 bp fragment generated by the digestion of the λIIb_3 cDNA clone and corresponding to the 3' non coding region of

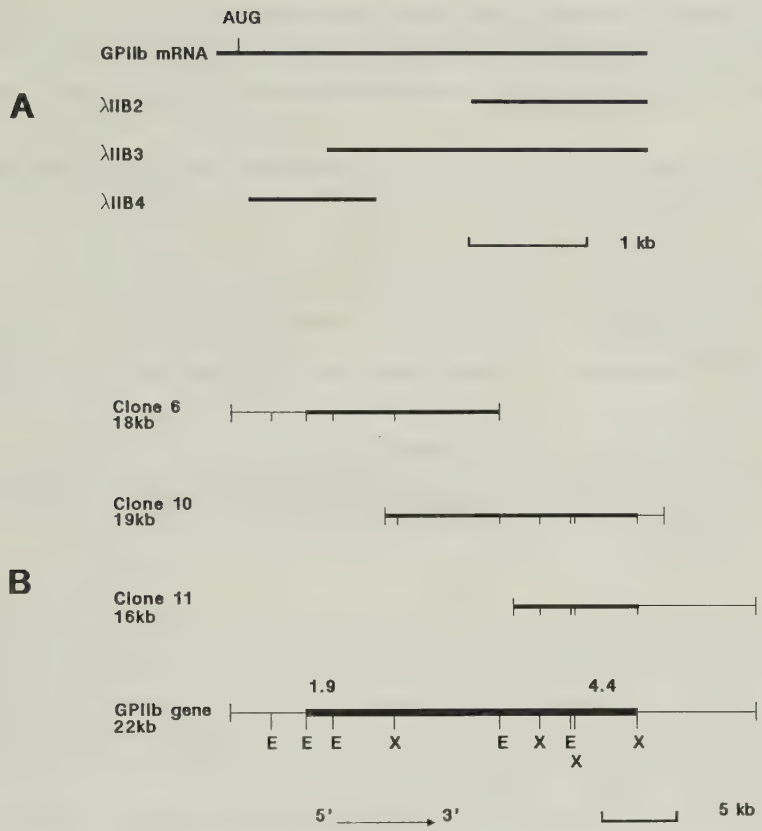

Fig. 1 A : Location of the different cDNA probes used for screening of the genomic library in relation to the GPIIb mRNA.
B : Position of three genomic DNA clones and restriction map of GPIIb gene. The thick line represents genomic fragments which hybridize with cDNA.

the mRNA was purified and used as probe to further localize the 3' end of the gene. This probe hybridized with an Xho I-Xho I 4.4 Kb fragment of genomic clones 10 and 11 (Fig. 1B). This fragment was subcloned in PGEM1 plasmid and sequenced. A partial sequence containing an exon encoding the 19 C-terminal amino acid residues of GPIIb and 196 nucleotides of the 3' untranslated region present in the mRNA is shown in Fig. 2. Only one polyadenylation site with the consensus sequence AATAAA was found 15 bases before the end of the exon. No other polyadenylation sites were found within 200 bases downstream.

Characterization of the 5' end of the gene and localization of the transcriptionnal start site. An 18 bases long oligonucleotide corresponding to the sequence of the 5' end of the GPIIb cDNA (20) was used to define more precisely the 5' region of the gene. This probe hybridized with a 1.9 Kb Eco RI-Eco RI fragment from the genomic clone 6 (Fig. 1B). This fragment was subcloned in the PGEM1 plasmid and sequenced. The complete sequence is shown in Fig. 3. Comparison with the cDNA sequence (20) and the N-terminal domain of GPIIb (21) indicates that this fragment contains the putative translation initiation codon

```
AAAACTCAGGAAGAAACAAACCCACCAATCGTTCCAGGCATATCTCAAATGCAAAAGGCATCCATTGTGAGTACAGTGGG   80
CTTTCATGTTCTGCGCTGGTCCAGGGAGGTGCTCATAGCTACTTCCTCACATGTGCTCTGGGGCCAGCAAATCATCTGTA  160

TACCCTGACCTTGGCCCCCGTGTACCCCCAG GTC GGC TTC TTC AAG CGG AAC CGG CAC ACC CTG GAA   227
                                Val Gly Phe Phe Lys Arg Asn Arg His Thr Leu Glu

GAA GAT GAT GAA GAG GGG GAG TGATGGTGCAGCCTACACTATTCTAGCAGGAGGGTTGGGCGTGCTACCTGCA  301
Glu Asp Asp Glu Glu Gly Glu

CCGCCCCTTCTCCAACAAGTTGCCTCCAAGCTTTGGGTTGGAGCTGTTCCATTGGGTCCTCTTGGTGTCGTTTCCCTCCC  381

                                                          *
AACAGAGCTGGGCTACCCCCCCTCCTGCTGCCTAATAAAGAGACTGAGCCCTGATGCTGAGCATGCTGCCTCCTTTTGGG  461

GCCAGAGAAGAGAGTACCGAAGAATGTTTTGGACGGGGACCTAGGGCTGGTGGAAGTATGAACGAGAGAGTCACTGCCAG  541
GGCGAAGTTTGCAAATCACTGTCTTTGGGGAGTGTCAGGGAGTACAGAGTTGGGGTGGTAGGTGTAACAGAAGACGGAGA  621
GCC                                                                                623
```

Fig. 2 DNA sequence of the 3' end of the human GPIIb gene.
The sequence shown covers the exon encoding the 19 C-terminal amino acids and a 3' untranslated region. The polyadenylation signal is boxed. The asterisk indicates the last nucleotide of the gene. Dotted line indicates the 3'splice site.

ATG, the entire signal peptide and 31 N-terminal amino acid residues of GPIIb. This exon is followed by an intron extending up to the end of this 1.9 Kb fragment. The exon-intron boundary sequence is consistent with the consensus sequence GT (A/G) AGT (22).
To identify the transcription initiation site for human GPIIb mRNA, a combination of primer extension and RNase mapping analysis was used. The primer extension experiments were performed with two oligonucleotides (A and B) corresponding to different positions on the exon (see Fig. 3). The extended products were resolved on a 6% denaturing polyacrylamide gel. After autoradiography, two fragments of 217 and 76 bases long respectively were visualized (Fig. 4). The RNase mapping analysis were performed using two anti-sens RNA probes hybridized with total RNA from megacaryocytes. The protected fragments extend 212 bases from the Nco I site and 170 bases from the Bgl I site (Fig. 5). All of the RNases mapping and primer extension analysis indicated similar 5' terminus, suggesting that the exon is the first one in the GPIIb gene and that its 5' end corresponds to the transcriptionnal start site indicated as +1 in Fig.3 .

DISCUSSION

The screening of a human genomic library has enable us to identify DNA segments containing the gene coding for the platelet glycoprotein IIb. From the positions of the transcription initiation site as determined by primer extension and RNases mapping, and the polyadenylation site corresponding to the cDNA, the GPIIb gene spans a region of 22 kb in length. The restriction map of this gene is in agreement with the size of the restriction fragment obtained from the digestion of genomic DNA indicating that there is only one copy of this gene. Results obtained from both primer extension and RNases mapping were compatible and identified a single transcription initiation start corresponding to an A in the 5' DNA sequence (Fig.3).

```
                                GAATTCCCCGGATCAGAAAATAGAAATCAAAAGGAAAATGTGGCTATGGTTAC-1201
CCCTAGCGGACCTCTTAAATCTTCCTGAGAACCTGCTTTTTTGGGAAGGCATGAGTGCCAGTAAGACTTGGCACTCCTCC-1121
TCTTCCGCTTACCGAGAGAAAATGACTTTGCCTTTCTGCTCAAAACTCATCCCTTCACTTTGTCACCCTATGTTTGCATC-1041
TTCCATCCTTAGTGTGTGTTTCCATCCAGTCTTTCAGCAATACACGTACTACACATTGGACTCTTGGGTAGTCTCTAGGG -961
CTGTAGCAAGGAGCCTTGCTCCCAAGGGACTCATTTACACAATCCTGTGAACGGACCAAGAGTAAACAGTGTGCTCAATG -881
                          Bgl I
CTGTGCCTACGTGTGTTAGCCCACGCGGCCAGCCTGAGGAGTCAGGGAAGGCTCCCCTAGGCAAAGCCCCAACCAGAATC -801
AAGTCTTAATGGTTAAAGAGCTCCATCACCCAAAAAGGATTGAGGGCCTACCTTCAACTGAACAGCTAATGCATAATCTC -721
AGAAACTGTGAGTCAAAATTCCCTGGAATAACTCCACTTTATCCCCAATCTCCTTGCCACCTAGACCAAGGTCCATTCAC -641

CACCCTGTCCCCAGCACTGACTGCACTGCTGTGGCCACACTAAAGCTTGGCTCAAGACGGAGGAGGAGTGAGGAAGCTGC -561
                                                                          IR1
TGCACCAATATGGCTGGTTGAGGCCGCCCAAGGTCCTAGAAGGAGGAAGTGGGTAAATGCCATATCCAAAAAGATACAGA -481
                                                                        PvuII
AGCCTCAGGTTTTATCGGGGGCAGCAGCTTCCTTCTCCTTCCCCGACCTGTGGCCAAGTCACAAAGCACCACAGCTGTAC -401
                          IR1
AGCCAGATGGGGGAAGGGAGGAGATTAGAACTGTAGGCTAGAGTAGACAAGTATGGACCAGTTCACAATCACGCTATCCC -321
AAGCCAGAAAGTGATGGTGGCTTGGACTAGCACGGTGGTAGTAGAGATGGGGTAAAGATTCAAGAGACATCATTGATAGG -241

CAGAACCAATAGGACATGGTAATAAATCTATTCTCAGGAAAGGGGAGGAGTCATGGCTTTCAGCCATGAGCATCCACCCT -161
                                    IR2                                   DdeI
CTGGGTGGCCTCACCCACTTCCTGGCAATTCTAGCCACCATGAGTCCAGGGGCTATAGCCCTTTGCTCTGCCCGTTGCTC  -81
          IR2
AGCAAGTTACTTGGGGTTCCAGTTTGATAAGAAAAGACTTCCTGTGGAGGAATCTGAAGGGAAGGAGGAGGAGCTGGCCC   -1
                                                                    (B)
+1
ATTCCTGCCTGGGAGGTTGTGGAAGAAGGAAG ATG GCC AGA GCT TTG TGT CCA CTG CAA GCC CTC TGG   68
                                 Met Ala Arg Ala Leu Cys Pro Leu Gln Ala Leu Trp

CTT CTG GAG TGG GTG CTG CTG CTC TTG GGA CCT TGT GCT GCC CCT CCA GCC TGG GCC TTG  128
Leu Leu Glu Trp Val Leu Leu Leu Leu Gly Pro Cys Ala Ala Pro Pro Ala Trp Ala Leu
                                                      Bgl I
AAC CTG GAC CCA GTG CAG CTC ACC TTC TAT GCA GGC CCC AAT GGC AGC CAG TTT GGA TTT  188
Asn Leu Asp Pro Val Gln Leu Thr Phe Tyr Ala Gly Pro Asn Gly Ser Gln Phe Gly Phe
            (A)                   NcoI
TCA CTG GAC TTC CAC AAG GAC AGC CAT GGG AG GTGAGCCGTAAGGGAAGTTGGGGTATTGGGAGAGAGC  258
Ser Leu Asp Phe His Lys Asp Ser His Gly

AGGACCCCTCCCCATCACTGCTTCTGGGGGCTTCGAGTTTCCCATTTGCGATAGCAGTTGAGCAAGGTGACTTGTGGGGG  338
CCTATTCAGGTTGATTTCTTGTCAAGATGTGGGTCCCAGGGACTGGCTCAGGTGAAGGTATAAGGGCAGGGCACATGTGG  418
GCTGATGGGCACTGAAAACTACAGCAAGAACAAAGGGAAGACAATAGTTGATGCTTTATTTTTTCCCAAGGGTCAGTTGT  498
ATGAACCACTCCACCCTCAACACCTTGAAATGCAGAGAGGAGGCCGGGCGCGGTGCTCATGCCTGTAATCCCAGCACTTT  578
GGGAGGCCGAGGCGGGCAGATCACCTGAGGTCGAGAATT                                           616
```

Fig. 3 DNA sequence of the first exon and 5'flanking region of the human GPIIb gene. The 1.9 kbp Eco RI fragment of genomic clone 6 was subcloned in PGEM1 and complete sequence was obtained using various synthetic oligonucleotides as sequencing primers. The A designated as +1 is the putative transcription start site, the arrow below shows the direction of transcription. Potential regulatory elements discussed in the text are boxed. Horizontal arrows show inverted repeats. The 5' splice site is indicated with a dotted line. A and B are oligonucleotides used for primer extension experiments.

The only ATG between +1 and the codon corresponding to the amino terminal Leucine of the mature protein is at position +33 and is in the correct reading frame. The deduced signal sequence is in total agreement with the sequence derived from the cDNA which was previously published by Poncz et al. (20). Thus the exon encoding the signal peptide is the first exon of the gene. In addition this exon contains 31 amino acid residues from the N-terminus of the mature protein. At the 3' end of the gene the last exon encodes

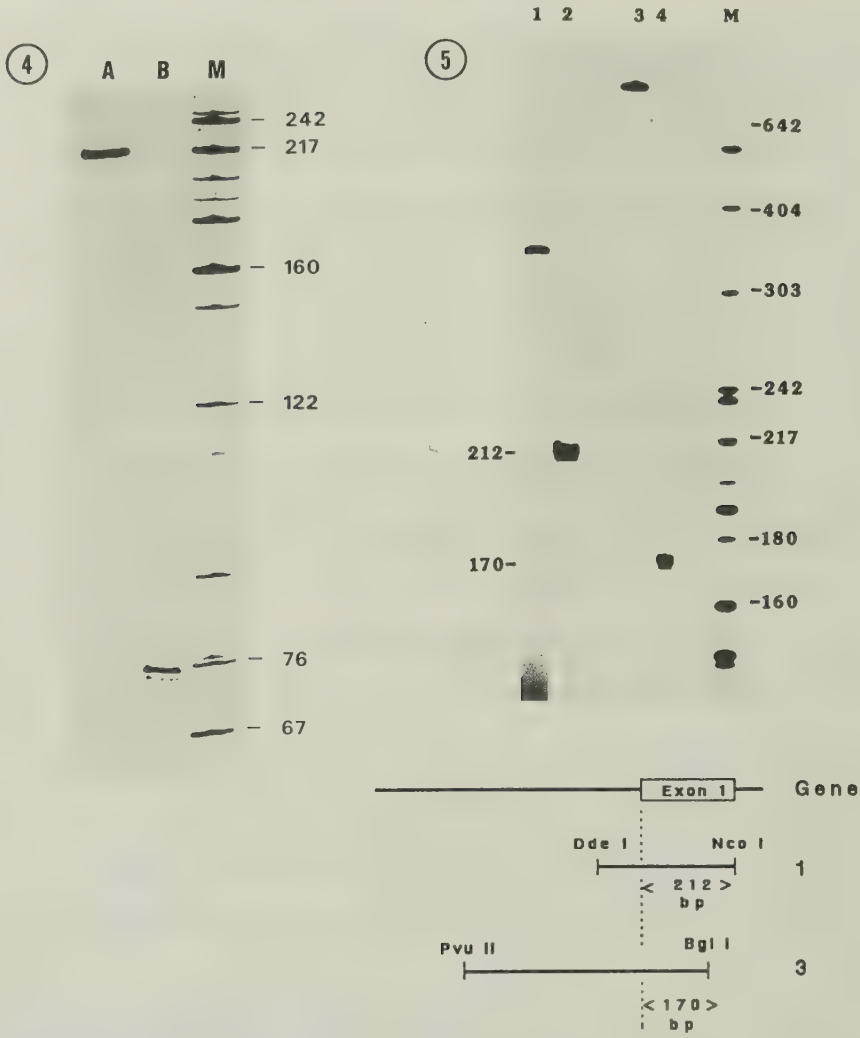

Fig. 4 Primer extension analysis.
Two oligonucleotides A and B (40 and 30 mers respectively) complementary to GPIIb mRNA were ^{32}P-end labelled and elongated with AMV reverse transcriptase after hybridization with poly A^{+} mRNA from megakaryocytes.
The 40 mers oligonucleotide extended to produce a 217 bases product (lane A), whereas the 30 mers primer produced a 76 bases product (lane B). The molecular weight marker (lane M) is an Hpa II digest of pBR 322.

Fig. 5 RNase mapping experiments.
Complementary RNA transcript were synthesized with Sp6 RNA polymerase using genomic fragment subcloned in PGEM1. Two probes were used, the first one extending between the Nco I and Dde I sites (lane 1), the second extending between Bgl I and Pvu II sites (lane 3). After hybridization with total megakaryocyte RNA and digestion with ribonucleases, protected fragments were analysed on 6% sequencing gels (lane 2 and 4). The molecular weight marker (lane M) is an Hpa II digest of pBR 322.

the complete sequence of the cytoplasmic domain of the GPIIb light chain and the 3' untranslated region of the mRNA including the polyadenylation site. Thus the data presented confirm that the N-terminal methionin published by Poncz et al (20) is the first aminoacid of the pro-GPIIb and further indicate that the mRNA contains a leader

sequence of 32 bases. The limit of the gene is therefore compatible with a mRNA of 3336 bases long (poly-A tail excepted).

Analysis of the 5' flanking sequence indicates that there is no canonical consensus sequence corresponding to the TATA box (22) between -30 to -60, unless the sequence GAATCT at position -31 or the sequence AATAAA at position -55 may serve as TATA box for this gene. In addition there is no CAAT box in the usual domain between -60 to -120 (23). An AGAACCAAT sequence corresponding to the sequence identified as binding site for the CAAT binding protein CP2 (24) is however located at position -228. A sequence CCGCCC is found at position -534 which corresponds to the consensus sequence for the binding of the transcription factor SP1 (25). In addition several inverted repeats can be identified, one of them flanking the CCGCCC consensus sequence (Fig.3).

The knowledge of the sequence surrounding the transcription initiation start site will now allow the study of the regulation of GPIIb during the megakaryocytopoiesis.

REFERENCES

1. Hynes R.O. (1987) Cell 48, 549-554
2. Phillips D.R., Charo I.F., Parise L.V. and Fitzgerald L.A. (1988) Blood 71, 831-843
3. Fitzgerald L.A., Poncz M., Steiner B., Rall S.C., Bennett J.S. and Phillips D.R. (1987) Biochemistry 26, 8158-8165
4. Uzan G., Frachet P., Lajmanovich A., Prandini M.-H., Denarier E., Duperray A., Loftus J., Ginsberg M., Plow E. and Marguerie G. (1988) Eur. J. Biochem. 171, 87-93
5. Fitzgerald L.A., Steiner B., Rall S.C., Lo S.-S. and Phillips D.R. (1987) J. Biol. Chem.262, 3936-3939
6. Kishimoto T.K., O'Connor K., Lee A., Roberts T.M. and Springer T.A. (1987) Cell 48, 681-690
7. Corbi A.L., Miller L.J. O'Connor K., Larson R.S. and Springer T.A. (1987) EMBO J. 6, 4023-4028
8. Arnaout M.A., Remold-O'Donnel E., Pierce M.W., Harris P. and Tenen D.G. (1988) Proc. Natl. Acad. Sci. USA 85, 2776-2780
9. Ginsberg M.H., Loftus J., Ryckwaert J.-J., Pierschbacher M., Pytela R., Ruoslahti E. and Plow E.F. (1987) J. Biol. Chem. 262, 5437-5440
10. Zimrin A.B., Eisman R., Vilaire G., Schwartz E., Bennett J.S. and Poncz M. (1988) J. Clin. Invest. 81, 1470-1475
11. Pytela R., Pierschbacher M. and Ruoslahti E. (1985) Cell 40, 191-196
12. Ruoslahti E. and Pierschbacher M.D. (1986) Cell 44, 517-518
13. Frachet P., Uzan G. and Marguerie G. (1988) in Biochemistry and physiopathology of platelet membrane. Ed Marguerie G., Zwaal R.F.A. Colloque INSERM/John Libbey Eurotext Ltd. 158, 155-161
14. Southern E.M. (1975) J. Mol. Biol. 98, 503-517
15. Sanger F., Nicklen S. and Coulson A.R.(1977) Proc. Natl. Acad. Sci. USA 74, 5463-5467
16. Berthier R., Marin M., Duperray A., Prenant M., Newton I., Schweitzer A., Hollard D. and Marguerie G. (1987) Exp. Hematol. 15, 750-758
17. Chomczynski P. and Sacchi N. (1987) Anal. Biochem. 162, 156-159
18. Aviv H. and Leder P. (1972) Proc Natl Acad Sci USA 69, 1408-1412
19. Melton D.A., Krieg P.A., Rebagliati M.R., Maniatis T., Zinn K. and Green M.R. (1984) Nucl. Acids Res. 12, 7035-7056
20. Poncz M., Eisman R., Heidenreich R., Silver S.M., Vilaire G., Surrey S., Schwartz E. and Bennet J.S. (1987) J. Biol. Chem. 262, 8476-8482
21. Charo I.F., Fitzgerald L.A., Steiner B., Rall S.C., Bekeart L.S. and Phillips D.R. (1986) Proc. Natl. Acad. Sci. USA 83, 8351-8355
22. Breathnach R. and Chambon P. (1981) Annu. Rev. Biochem. 50, 349-383
23. Benoist C. and Chambon P. (1981) Nature 290, 304-310
24. Chodosh L.A., Baldwin A.S., Carthew R.W. and Sharp P.A. (1988) Cell 53, 11-24
25. Briggs M.R., Kadonaga J.T., Bell S.P. Tjian R. (1986) Science 234, 47-52

Vol. 156, No. 1, 1988 BIOCHEMICAL AND BIOPHYSICAL RESEARCH COMMUNICATIONS
October 14, 1988 Pages 602-609

PURIFICATION OF THE D-2 DOPAMINE RECEPTOR FROM BOVINE STRIATUM

Zvulun Elazar, Hannah Kanety, Carol David and Sara Fuchs

Department of Chemical Immunology
The Weizmann Institute of Science
Rehovot, 76100, Israel

Received September 6, 1988

The D-2 dopamine receptor has been purified 21500 fold from bovine striatal membranes. Solubilized receptor preparation was partially purified by affinity chromatography on a haloperidol adsorbent followed by gel filtration on a Sephacryl S-300 column. The fractions eluted from this column which contained the ligand binding activity were further chromatographed on wheat germ agglutinin conjugated to Sepharose. The resulting receptor preparation displays a major polypeptide band of an apparent molecular weight of 92 kDa, and exhibits a specific binding activity of 2490 pmol spiperone per mg protein. This purified receptor preparation can readsorb specifically to the haloperidol affinity column indicating that the 92 kDa polypeptide represents the ligand binding unit of the D-2 dopamine receptor. © 1988 Academic Press, Inc.

The D-2 dopamine receptor has recently been solubilized from membranes of pituitary gland and striatum by use of various detergents and its pharmacology is well defined (reviewed in 1,2). This receptor is a glycoprotein as indicated by its specific adsorption to and elution from wheat germ agglutinin-Sepharose (3). In order to elucidate the molecular mechanisms by which dopaminergic signal transduction correlates with dopaminergic functions, it is essential to isolate and fully characterize this receptor. Purification of the D-2 dopamine receptor has been impeded both by the minute quantities available and by the lack of specific ligands suitable for affinity purification. Affinity resins based on several dopaminergic antagonists of the butyrophenone family have been prepared recently and employed for the isolation of ligand-specific antibodies and of the dopamine receptor itself (4-7). Photoaffinity labeling of the D-2 dopamine receptor has indicated that, in a variety of mammalian tissues and species, a 92-94 kDa polypeptide is probably the ligand binding unit of the receptor (8-11). In this report we describe a

0006-291X/88 $1.50
Copyright © 1988 by Academic Press, Inc.
All rights of reproduction in any form reserved.

purification procedure of the D-2 dopamine receptor yielding a preparation which exhibits a single major band on SDS-polyacrylamide gel electrophoresis, with an apparent molecular weight of 92 kDa and a specific binding activity of 2490 pmol spiperone per mg protein.

MATERIALS AND METHODS

Materials: [^{3}H]-spiperone (24.8 Ci/mmol) and [^{3}H]-haloperidol (18.7 Ci/mmol) were purchased from New England Nuclear (Boston). Haloperidol and spiperone were gifts from Janssen Pharmaceuticals (Beerse). Butaclamol [(+) and (-)] and mianserine were obtained from Research Biochemicals Inc. (Wayland, MA). 3-[(3-cholamidopropyl) -dimethylammonio]-1 propanesulfonate (CHAPS), N-acetylglucosamine, phenylmethylsulfonyl fluoride (PMSF) and leupeptin were obtained from Sigma. Sepharose-wheat germ agglutinin (Sepharose-WGA), Sephacryl S-300 and molecular weight standards were purchased from Pharmacia.

Membrane preparation and solubilization: Bovine striatal membranes were prepared and solubilized essentially as described previously (12), with the addition of leupeptin (20 μg/ml) in the solubilization buffer.

Purification procedure: Affi-gel 10 (Bio-Rad) conjugated with haloperidol glycine ester (HGE) was prepared as described previously (13). Before use, the gel was washed with deionized water and mixed with an equal volume of Sepharose 4B. This adsorbent, designated affi-gel-HGE, was washed with 10 bed volumes of a buffer containing 50 mM HEPES pH 7.4, 5 mM $MgCl_2$ and 1 mM EDTA (HME buffer), supplemented with 1 mM CHAPS, 150 mM NaCl, 1 mM DTT and 1 mM PMSF (wash buffer). The washed adsorbent was mixed with 5 volumes of the solubilized membrane preparation that had been diluted 1:1 with HME buffer, and the mixture was incubated with gentle shaking for 16 hr at 4°C, or for 1 h at 22°C. The supernatant was removed and the gel was washed three times, each with 5 bed volumes of wash buffer. Elution was carried out with 10 μM spiperone in wash buffer for 40 min at 22°C, and the eluted solution was concentrated by centricon 10 (Amicon) and designated eluate I.

Eluate I (0.5 ml, 0.1 mg protein/ml) was chromatographed on a Sephacryl S-300 column (0.5 x 60 cm) and eluted with wash buffer at a flow rate of 4 ml/h. Fractions of 1.4 ml were collected and samples were analyzed by SDS polyacrylamide gel (7-15%) electrophoresis (SDS-PAGE) (14) or by [^{3}H]-spiperone binding. For the SDS-PAGE analysis, an aliquot of eluate I was radioiodinated (15) and mixed with unlabeled preparation prior to chromatography on Sephacryl S-300. Following gel filtration, the fractions containing the [^{3}H]-spiperone binding activity were pooled and added to Sepharose-WGA in a ratio of 7/1 (v/v). The adsorbed material was eluted with 0.2M N-acetylglucosamine in wash buffer. The eluted material (eluate II) was concentrated and assayed for [^{3}H]-spiperone binding or by SDS-PAGE.

Reconstitution of D-2 receptor activity: Reconstitution of D-2 receptor activity was performed as described by Cerione et al. (16) for the β-adrenergic receptor, with some modifications. The tested samples (50-200 μl) were incubated with HME buffer containing 100 mM NaCl, bovine serum albumin (2 mg/ml), sonicated phosphatidylcholine (0.7 mM) and octyl-β-D- glucoside (0.8%), in a final volume of 0.5 ml for 15 min at 4°C and then dialyzed against 1000 volumes of HME buffer containing 1 mM PMSF, 100 mM NaCl and Bio-Beads SM-2 resin (2 g/l) for 16 hr at 4°C.

Binding assays: Specific binding of [^{3}H]-spiperone and [^{3}H]-haloperidol to receptor preparations was determined as described previously (12).

Protein determination: Protein concentrations were determined by Bradford micro assay (17), fluorescamine assay (18), and/or trace radioiodination.

RESULTS

The first step of purification of the D-2 dopamine receptor was affinity chromatography on an adsorbent of haloperidol glycine ester coupled to affi-gel 10 (affi-gel-HGE). This adsorbent was found to adsorb 70-80% of the [^{3}H]-spiperone binding activity and less than 5% of the total proteins from a CHAPS solubilized membrane preparation. Adsorption of the [^{3}H]-spiperone binding activity was inhibited by preincubation of the solubilized preparation with spiperone or (+)-butaclamol and to a lesser extent by haloperidol, apomorphine or dopamine. (-)-Butaclamol and the serotonergic antagonist mianserine had no significant effect (Fig. 1). This profile demonstrates that the affinity matrix displays the predicted specificity for the D-2 dopamine receptor. Approximately, 0.1% of the total protein applied to the affi-gel-HGE matrix was eluted with 10 μM spiperone (Table I). Elution with spiperone was more efficient than that obtained with other dopaminergic antagonists such as

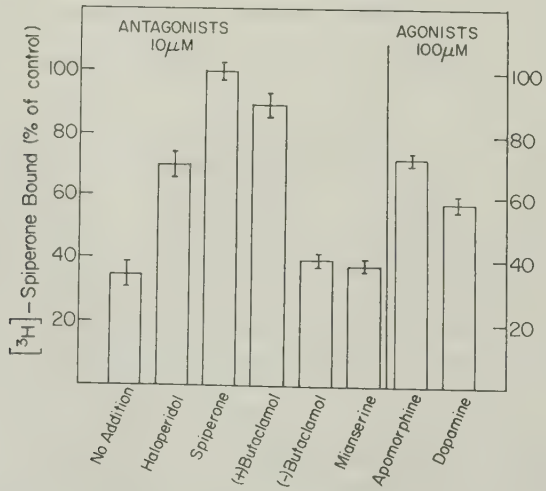

Fig. 1: Specificity of adsorption of solubilized D-2 dopamine receptor to affi-gel-HGE. Two milliliters of solubilized receptor preparation were preincubated with the indicated ligands for 40 min at 22°C and applied to 0.4 ml of affi-gel-HGE for 1 h at 22°C. The effluent was desalted on Sephadex G-50 mini columns and assayed for [^{3}H]-spiperone binding. The results are expressed as the percent of a control in which the solubilized receptor was incubated with affi-gel-ethanolamine. Parallel experiments were also performed to correct for the incomplete removal of the ligands by desalting.

TABLE I: Purification of D-2 dopamine receptor from bovine striatum

Step	Volume (ml)	Protein conc. (mg/ml)	Specific activity (pmole[^{3}H]-spiperone/ mg protein)	Purification (fold)	Recovery (%)
Membranes	25	10	0.116	1	100
CHAPS extract	25	2.45	0.20	1.72	42
Affi-gel-HGE (eluate I)	5	0.01	96.7[a]	833	17
Sephacryl	4.2	0.002	330[a]	2840	9.6
Sepharose-WGA (eluate II)	0.5	<0.0002	2490[a]	21460	0.9

[a] [^{3}H]-spiperone binding was measured following reconstitution into phosphatidylcholine liposomes.

haloperidol and (+)-butaclamol (data not shown). The eluted material (eluate I) had to be reconstituted by insertion into artificial phosphatidylcholine liposomes before assaying for [^{3}H]-spiperone binding activity. This step resulted in a 500 fold purification, and about 40% of the binding activity applied to the affi-gel-HGE was recovered (Table I).

Eluate I retained the dopaminergic antagonist specificity and stereospecificity (Fig. 2). Spiperone and (+)-butaclamol inhibited the [^{3}H]-spiperone binding to eluate I with IC_{50} values of 0.8 nM and 1.6 nM, respectively, while the IC_{50} of (-)-butaclamol was at least 3 orders of magnitude higher. The affinities of [^{3}H]-haloperidol and [^{3}H]-spiperone (K_D values of 1.32 $\pm$ 0.29 and 0.63 $\pm$ 0.17 nM, respectively) for eluate I were similar to their affinities (1.26 $\pm$ 0.25 and 0.52 $\pm$ 0.15 nM, respectively) for the solubilized preparation.

Radioiodinated eluate I exhibited several protein bands on SDS-PAGE (Fig. 3A, lane 1). To elucidate which protein(s) corresponds to the D-2 dopamine receptor, the solubilized receptor preparation was preincubated with spiperone (10 μM) prior to application on affi-gel-HGE, and subsequently eluted with spiperone. These conditions, in which the D-2 dopamine receptor does not bind

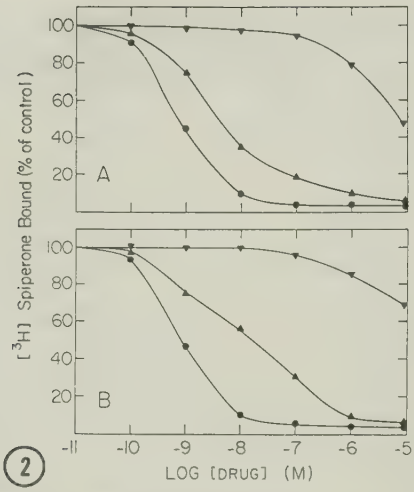

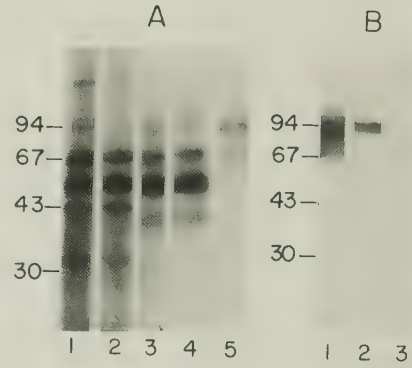

Fig. 2: Binding specificity of reconstituted affinity-purified receptor preparation. Solubilized receptor (A) or affinity purified-reconstituted receptor (B) were incubated in HME buffer with [^{3}H]-spiperone (3-5 nM) and increasing concentrations of spiperone (●), (+)-butaclamol (▲) and (-)-butaclamol (▼). The 100% [^{3}H]-spiperone bound corresponds to 160-180 pM (in A) and 150-170 pM (in B).

Fig. 3: A). SDS-PAGE analysis of radioiodinated D-2 receptor preparations. 1, eluate I; 2, eluate obtained when the solubilized receptor preparation was preincubated with 10 μM spiperone prior to chromatography on affi-gel-HGE; 3, pooled fractions 23-25 from the Sephacryl-300 column; 4, unbound material following adsorption of fractions 23-25 on Sepharose-WGA; 5, eluate II.
B). Readsorption of eluate II on affi-gel-HGE. Radiolabeled eluate II (1) was applied to affi-gel-HGE (2) or to affi-gel-ethanolamine (3) and eluted with Laemmli sample buffer.

to affi-gel-HGE (Fig. 1), resulted in a depletion of protein bands of 92 kDa and 140 kDa, and also in a decrease in the amount of additional bands of 30 and 14 kDa (Fig. 3A, lane 2).

The affinity purified receptor preparation (eluate I) was further chromatographed on a Sephacryl S-300 column, resulting in an additional enrichment of the receptor binding activity (Table I). The fractions eluted from this column were analyzed by ligand binding activity or by SDS-PAGE (Fig. 4). The fractions which included the binding activity were devoid of several major proteins present in eluate I and contained the aforementioned 92 kDa band. Fractions 23-25, which contained the ligand binding activity, were pooled, concentrated and loaded onto Sepharose-WGA. Most of the proteins were not adsorbed to the Sepharose-WGA resin, whereas the 92 kDa polypeptide was adsorbed and specifically eluted with N-acetylglucosamine (Fig. 3A, lanes

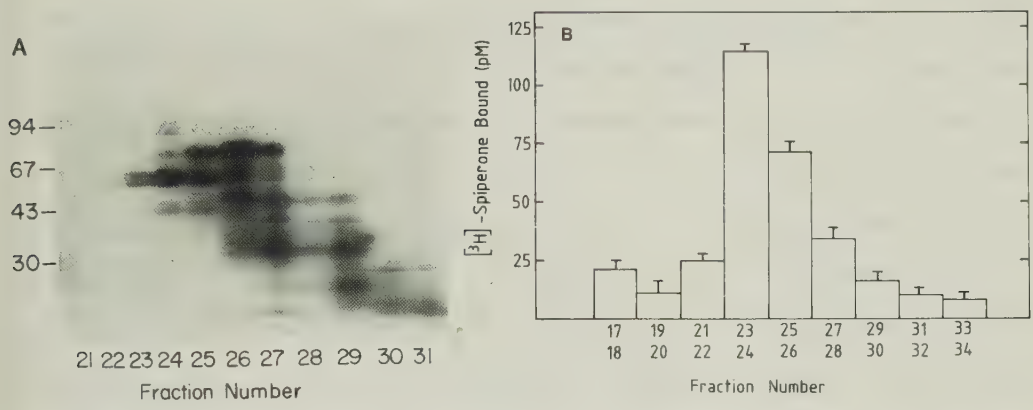

Fig. 4: Gel filtration of eluate I. A). Radiolabeled eluate I was mixed with the same volume of concentrated unlabeled eluate I and chromatographed on a Sephacryl S-300 column. Fractions were concentrated and electrophoresed on a 7-15% SDS-polyacrylamide gel. B). Unlabeled eluate I was chromatographed on Sephacryl S-300. Fractions were pooled, concentrated, reconstituted and [^{3}H]-spiperone binding was determined.

3-5). When radioiodinated, this purified preparation (eluate II) exhibited a single band on SDS-PAGE. When assayed for [^{3}H]-spiperone binding activity, following reconstitution into artificial vesicles, eluate II bound 2490 pmoles spiperone per mg protein (Table I). This binding was specifically inhibited by excess of either spiperone, haloperidol or (+)-butaclamol. In addition, samples of radiolabeled eluate II were shown to specifically readsorb to affi-gel-HGE (Fig. 3B). This further identifies the 92 kDa protein as the D-2 dopamine receptor binding unit.

DISCUSSION

This paper describes a purification procedure for the D-2 dopamine receptor from bovine striatum. The affinity chromatography step on affi-gel-HGE led to partial purification of the receptor. Mainly the 92, and occasionally 140 kDa protein bands were specifically depleted from the eluate by preincubation with spiperone. The nature of the 140 kDa polypeptide is unknown. It might represent a complex of the 92 kDa protein with another polypeptide or a precursor of the D-2 receptor binding unit. Some of the other proteins which elute with spiperone might represent functional components, e.g. G-proteins, which may be specifically coupled to the receptor complex. Indeed, preliminary experi-

ments indicate that eluate I contains G_i and G_o proteins that are functionally associated with the D-2 dopamine receptor (19).

Several lines of evidence provided in this report indicate that the purified 92 kDa polypeptide is the D-2 receptor binding unit. Firstly, the peak of [^{3}H]-spiperone binding activity eluted from the Sephacryl column correlates with the presence of the 92 kDa polypeptide (Fig. 4) and, of the proteins present in this peak, only the 92 kDa band could readsorb to the haloperidol affinity resin (unpublished data). Secondly, the specific binding activity in eluate II, is 20-30% of the theoretical value, assuming one ligand binding site per receptor molecule. Taking into account some inactivation during the purification and reconstitution, and possible incorrect insertion of the receptor into artificial liposomes, this specific activity is consistent with the expected value. Finally, the purified 92 kDa protein from Sepharose-WGA can specifically readsorb to the affi-gel-HGE matrix (Fig. 3B).

The combination of ligand affinity chromatography together with gel filtration and chromatography on Sepharose-WGA provides an improved procedure for purification of the D-2 dopamine receptor. We are now attempting to improve the yields in the various purification steps so as to obtain sufficient amounts of purified D-2 receptor for the production of specific antibodies, as well as for structural analysis of the receptor.

ACKNOWLEDGMENTS: We wish to thank Mrs. S. Carmon for excellent technical assistance. This research was supported by grants from the Chief Scientist's Office, Ministry of Health, Israel, from Enosh and Harry Stern Foundations, and from the Henry and Francoise Glasberg Foundation for Research on Cellular Diseases.

REFERENCES

1. Seeman, P. (1980) Pharmacol. Rev. 32, 229-313.
2. Niznik, H.B. (1987) Mol. Cell. Endocrinol. 54, 1-22.
3. Lew, J.Y., and Goldstein, M. (1984) J. Neurochem. 42, 1298-1305.
4. Schreiber, M., Fogelfeld, L., Souroujon, M., Kohen, F., and Fuchs, S. (1983) Life Science 33, 1514-1526.
5. Senogles, S.E., Amlaiky, N., Johnson, A.L., and Caron, M.G. (1986) Biochemistry 25, 749-753.
6. Antonian, L., Antonian, E., Randall, B.M., and Schuster, D.I. (1986) Life Science 38, 1847-1858.
7. Ramwani, J., and Mishra, R.K. (1986) J. Biol. Chem. 261, 8894-8898.
8. Lew, J.Y., Meller, E., and Goldstein, M. (1985) Eur. J. Pharmacol. 113, 145-146.

9. Amlaiky, N., and Caron, M.G. (1986) J. Neurochem. 47, 196-204.
10. Seeman, P. and Niznik, H.B. (1986) Eur. J. Pharmacol. 127, 297-299.
11. Kanety, H. and Fuchs, S. (1988) Biochem. Biophys. Res. Commun. (in press).
12. Elazar Z., Kanety, H., Schreiber, M. and Fuchs, S. (1988) Life Sci. 42, 1987-1993.
13. Kanety, H., Schreiber, M., Elazar, Z. and Fuchs, S. (1988) J. Neuroimmunol. 18, 25-36.
14. Laemmli, U.K. (1970) Nature 227, 680-685.
15. Greenwood, F.C., Hunter, W.M., and Glover, J.S. (1963) Biochem. J. 89, 114-123.
16. Cerione, R.A., Strulovici, B., Benovic, J.L., Lefkowitz, R.J., and Caron, M.G. (1983) Nature (London) 306, 562-566.
17. Bradford, M.M. (1976) Anal. Biochem. 72, 247-248.
18. Udenfriend, S., Stein, S., Bohlen, P., Dairman, W., Leimgruber, W., and Weigele, M. (1972) Science 178, 871-872.
19. Elazar, Z., Siegel, G., David, C., Kanety, H. and Fuchs, S. (1988) Soc. Neurosci. Abst. (in press).

ERRATUM

Volume 154, Number 2, July 29, 1988

In the article "DNA Repair in Lymphocytes from Humans and Rats with Chronic Iron Overload," by A. Pietrangelo, A. Cossarizza, D. Monti, E. Ventura, and C. Franceschi, pages 698-704:

The authors' affiliation should read "Istitutes of Clinica Medica III and Patologia Generale #, University of Modena, Modena, Italy."

On page 703, acknowledgment of grant support was omitted and should read "This work was supported by a grant from the National Research Council of Italy."

0006-291X/88 $1.50
Copyright © 1988 by Academic Press, Inc.
All rights of reproduction in any form reserved.

Information for Contributors

BIOCHEMICAL AND BIOPHYSICAL RESEARCH COMMUNICATIONS is devoted to the rapid dissemination of timely and significant observations in the diverse fields of modern experimental biology. Manuscripts submitted should be so written as to emphasize clearly the novel aspects of the information reported.

Authors submitting a manuscript do so on the understanding that if it is accepted for publication, copyright in the article, including the right to reproduce the article in all forms and media, shall be assigned exclusively to the Publisher. The Publisher will not refuse any reasonable request by the author for permission to reproduce any of his or her contributions to the journal.

Original papers only will be considered. Manuscripts are accepted for review with the understanding that the same work has not been submitted to another Editor of this journal and also that it has not been published, that it is not under consideration for publication elsewhere, and that its submission for publication has been approved by all of the authors and by the institution where the work was carried out; further, that any person cited as a source of personal communications has approved such citation. Written authorization may be required at the Editor's discretion. Articles and any other material published in BIOCHEMICAL AND BIOPHYSICAL RESEARCH COMMUNICATIONS represent the opinions of the author(s) and should not be construed to reflect the opinions of the Editor(s) and the Publisher.

Manuscripts in duplicate may be sent to any one of the editors whose names and addresses are listed on the inside front cover. To assist us in ensuring rapid processing of your article, please submit a signed photocopy of the copyright assignment form which appears as page 3 of this "Information" along with your manuscript. (This form will not be binding if your manuscript is not accepted for publication in BBRC.) *In the case of rejected manuscripts only one copy of the manuscript will be returned to the author.*

To ensure rapid and accurate publication, it is essential that manuscripts conform to the instructions which follow. Manuscripts which are not in accordance with these specifications may be returned.

Preparation of Manuscripts

Article length should not exceed 5 typewritten pages, using one-and-a-half (1½) spacing (W spacing) on 8.5 x 11-in. high-quality paper (the complete manuscript, including space occupied by figures and tables, should not exceed 8 pages).

Summary. Each article must be preceded by a brief summary, typed single-spaced, not exceeding 10 lines (approximately 100–150 words). This paragraph should adequately summarize the pertinent findings of the paper.

Typing. Articles are reproduced directly from the submitted manuscript as camera-ready copy. Manuscripts must therefore be typewritten on good quality white bond paper. A black silk or carbon typewriter ribbon should be used. Special care should be taken to ensure a sharp clean impression of letters throughout. Use of an electric typewriter is strongly recommended. Erasures should be avoided. Care must also be taken to avoid errors in spelling, word division, and punctuation. **No changes may be made in manuscripts after acceptance.**

Manuscripts should be 1½-spaced on one side of the sheet: **methods, references, footnotes, tables, and figure legends should be single-spaced.** Typing area of the page must be as close as possible to 6.5 in. wide and 9.5 in. long.

Symbols and Abbreviations defined in the IUPAC-IUB Document No. 1 (*Arch. Biochem. Biophys.* (1966) **115**, 1–12) may be used without definition. Use of all other abbreviations and symbols is to be avoided. When abbreviations are essential, they should be consistent with the form and style of the above document and **must be defined in a single footnote and typed on a separate page**, rather than in the text. Such abbreviations **must not** be used in the Summary.

Enzyme names should not be abbreviated except when the substrate has an approved abbreviation (e.g., ATPase). Use the Enzyme Commission ("EC") code number when available.

Isotopes should be styled following the recommendations of the IUB Commission of Editors of Biochemical Journals. The symbol of the isotope introduced should be placed in square brackets directly attached to the front of the name (e.g., [^{32}P]CMP). Note that the isotope number should only be used as a (superior) prefix to the atomic symbol, not to an abbreviation.

Submission of data to protein or genetic databases. The Editors of this Journal encourage the use of databases as repositories for detailed data on protein structure (e.g., x-ray crystallographic coordinates) and on DNA sequences and mapping assignments. Authors are requested to complete data entry and annotation forms (which can be obtained from the Journal Editorial Office or from the databases) and to submit these summaries and database entries (in floppy disc, tape, or hard-copy form) to the database at the time the manuscript is accepted for publication. This will assure that mapping or sequencing work can be accessed by data retrieval methods.

In the Methods section, authors should draw attention to any particular chemical or biological hazards that may be involved in carrying out the experiments described. Any relevant safety precautions should be described; if an accepted code of practice has been followed, a reference to the relevant standards should be given.

For further information regarding nomenclature authors are advised to consult the Instructions to Authors of the **Archives of Biochemistry and Biophysics** (1987) **252**, vii-xxv. Reprints are available from the Publisher.

Footnotes, references, tables, and figure legends should be typed single-spaced on separate pages.

Illustrations and Tables. **Do not attempt to insert figures, figure legends, or tables into the text.** This will be done by the Publisher.

All drawings should be clearly labeled in black ink in a manner suitable for direct reproduction (Leroy lettering size 120 or 140). Do not use press-on lettering: typewritten lettering is not acceptable.

Figures will be reduced to fit within the type area of the page (approximately 5 x 8 in.); the original drawings should be no larger than 8.5 x 11 in.

Glossy photographs of drawings are acceptable provided they are sharp, clear prints with an even *black* density. Illustrations in color can be accepted only if the authors defray the cost.

Mathematical or chemical symbols that cannot be typed should be inked in carefully in black. Structural formulas should be drawn in black ink.

Illustrations and tables should be submitted on separate sheets.

Page Numbers and Headings. Page numbers should be typed at the top of the page.

The title of the paper should be typed in capital letters near the top of the first page, with the name(s) and affiliation(s) of the author(s) typed just below. Headings within the article should be arranged according to their relative importance.

References to the literature should be cited by the number in parentheses in the text and listed in numerical order in a single-spaced typed list placed at the end of the manuscript. Abbreviations of journals should conform to those of *Chemical Abstracts Service Source Index*, 1985. Note the following examples.

1. Graan, T., and Ort, D. R. (1986) Arch. Biochem. Biophys. 248, 445–451.

2. Metzler, D. E. (1977) Biochemistry: The Chemical Reaction of Living Cells, p. 298. Academic Press, New York.

3. Rosenfeld, R. G., and Hintz, R. L. (1986) In The Receptors (P. M. Conn, Ed.), Vol. III, pp. 281–329. Academic Press, Orlando, FL.

Note that inclusive pagination must be given.

Acknowledgment of Receipt. Authors desiring acknowledgment of receipt of manuscript should enclose a stamped self-addressed card.

Reprints. Reprint order forms, with price lists, are sent to the authors immediately upon acceptance of their manuscript.

BIOCHEMICAL AND BIOPHYSICAL RESEARCH COMMUNICATIONS

Manuscript Title _____

_____

Authors _____

I hereby confirm the assignment of all copyrights in and to the manuscript named above in all forms and media to Academic Press effective if and when it is accepted for publication by Academic Press. (For U.S. government employee authors, this provision applies only to the extent to which copyright is transferable.) I also confirm that the manuscript contains no material the publication of which would violate any copyright or other personal or proprietary right of any person or entity, and I acknowledge that Academic Press is relying on this letter in publishing this manuscript.

_____ Date

_____ Signed

_____ Name (and title if not author)

To be signed by at least one of the authors (who has obtained the assent of the others, if any). In the case of a "work made for hire" (a work prepared by an employee within the scope of his or her employment or commissioned as a work for hire under a written agreement), an authorized representative of the employer should sign.

Please note: Manuscripts cannot be processed for publication until the Publisher has received this signed form.

If the manuscript is not published by Academic Press, this letter will not take effect.

(Continued from following page)

Site-Directed Mutagenesis at the Regulatory Site of Fructose-6-phosphate 1-Kinase from *Bacillus stearothermophilus* *B. C. Valdez, S. H. Chang, and E. S. Younathan* 537
Biosynthesis of 12-Oxo-10,15(Z)-phytodienoic Acid: Identification of an Allene Oxide Cyclase *Mats Hamberg* 543
Enterotoxin of *Clostridium perfringens* Type A Forms Ion-Permeable Channels in a Lipid Bilayer Membrane *Nakaba Sugimoto, Masayuki Takagi, Kunihiro Ozutsumi, Shigeko Harada, and Morihiro Matsuda* 551
Excision Repair in Xeroderma Pigmentosum Group C Cells Is Regulated Differently in Transformed Cells and Primary Fibroblasts *James E. Cleaver* 557
Evidence for the Expression of a Primitive Intestinal-like Alkaline Phosphatase in the Intestinal 407 Cell Line *Kazuyuki Hirano, Tomikazu Kusano, Kentaro Asai, Kyozo Hayashi, Torgny Stigbrand, Shiro Iino, and Jose L. Millan* 563
Insulin and Glucose Modulate Protein Kinase C Activity in Rat Adipocytes *Boris Draznin, J. Wayne Leitner, Karl E. Sussman, and Nancy A. Sherman* 570
The Complete Nucleotide Sequence of Human Liver Cytochrome b_5 mRNA *Min Yoo and Alan W. Steggles* 576
Apolipoprotein B-100 Is the Major Form of This Apolipoprotein Secreted by Human Intestinal Caco-2 Cells *Diana M. Lee, Nassrin Dashti, and Tina Mok* 581
Heterologous Up-Regulation of the 1,25-Dihydroxyvitamin D_3 Receptor by Parathyroid Hormone (PTH) and PTH-like Peptide in Osteoblast-like Cells *H. A. P. Pols, J. P. T. M. van Leeuwen, J. P. Schilte, T. J. Visser, and J. C. Birkenhäger* 588
Isolation of the Human Platelet Glycoprotein IIb Gene and Characterization of the 5′ Flanking Region *M. H. Prandini, E. Denarier, P. Frachet, G. Uzan, and G. Marguerie* 595
Purification of the D-2 Dopamine Receptor from Bovine Striatum *Zvulun Elazar, Hannah Kanety, Carol David, and Sara Fuchs* 602
ERRATUM
Volume 154, Number 2, July 29, 1988: A. Pietrangelo, A. Cossarizza, D. Monti, E. Ventura, and C. Franceschi, "DNA Repair in Lymphocytes from Humans and Rats with Chronic Iron Overload," pp. 698–704 610

(Continued from following page)

Structure of the Human Blood Platelet Membrane Glycoprotein Ibα Gene
Roland H. Wenger, Nelly Kieffer, Andreas N. Wicki, and Kenneth J. Clemetson 389
Different Roles of the Diphosphate Moieties of Allylic and Homoallylic Diphosphates in Prenyltransferase Reaction *Takeshi Gotoh, Tanetoshi Koyama, and Kyozo Ogura* 396
Saposin D: A Sphingomyelinase Activator
Satoshi Morimoto, Brian M. Martin, Yasuo Kishimoto, and John S. O'Brien 403
Lectins Inhibit Cell Binding and Spreading on a Laminin Substrate
John W. Dean III, S. Chandrasekaran, and Marvin L. Tanzer 411
Slipped DNA Structures within the Enhancer Region of the Moloney Murine Leukemia Virus *Miguel A. Gama Sosa, Jessica C. Hall, and Ruth M. Ruprecht* 417
Cyclic AMP Decreases LDL Catabolism and Cholesterol Synthesis in the Human Hepatoma Cell Line HepG2 *Cécile Maziere, Jean-Claude Maziere, Suzanne Salmon, Martine Auclair, Liliana Mora, Martine Moreau, and Jacques Polonovski* 424
Antisera to an Amino-Terminal Peptide Detect the Amyloid Protein Precursor of Alzheimer's Disease and Recognize Senile Plaques
Mark R. Palmert, Marcia Berman Podlisny, Dennis S. Witker, Tilman Oltersdorf, Linda H. Younkin, Dennis J. Selkoe, and Steven G. Younkin 432
An Investigation of Human Oxyhemoglobin β Tetramer Dissociation Using Haptoglobin Binding *Linda A. Michalski and Melisenda J. McDonald* 438
Partial Amino Acid Sequence Analysis of Human Placenta Monoamine Oxidase A and Bovine Liver Monoamine Oxidase B *Shiuan Chen and Walter Weyler* 445
Ribulose 1,5-Bisphosphate-Dependent CO_2 Fixation in the Halophilic Archaebacterium, *Halobacterium mediterranei* *Nenoo Rawal, S. M. Kelkar, and Wijaya Altekar* 451
Unregulated Secretion of an Exogenous Glycotripeptide by Rat Islets and HIT Cells
Gerald Gold, Felix T. Wieland, and Gerold M. Grodsky 457
IL1/ETAF Activity and Undetectable IL1β mRNA and Minimal IL1α mRNA Levels in Normal Adult Heat-Separated Epidermis *Stephen Demczuk* 463
In Vitro Demonstration by the Rate Assay of the Presence of Small Pores in the Outer Membrane of *Pseudomonas aeruginosa*
Eisaku Yoshihara, Naomasa Gotoh, and Taiji Nakae 470
Fibrinogen Association with Human Monocytes: Evidence for Constitutive Expression of Fibrinogen Receptors and for Involvement of Mac-1 (CD18, CR3) in the Binding
Cristina Trezzini, Thomas W. Jungi, Peter Kuhnert, and Ernst Peterhans 477
Transient Accumulation of Inositol (1,3,4,5)-Tetrakisphosphate in Response to α_1-Adrenergic Stimulation in Adult Cardiac Myocytes
Guy P. Heathers, Peter B. Corr, and Leona J. Rubin 485
Evidence for a Differential Physiological Modulation of Brown Fat Iodothyronine 5′-Deiodinase Activity in the Perinatal Period
M. Giralt, I. Martin, T. Mampel, F. Villarroya, R. Iglesias, and O. Viñas 493
Characterization of Epitopes on the Cationic Peanut Peroxidase by Four Monoclonal Antibodies *Chunfang Hu and Robert B. van Huystee* 500
Paradoxical Protection of Both Protein-Free and High Protein Diets against Acute Ammonium Intoxication *Vicente Felipo, María-Dolores Miñana, and Santiago Grisolía* 506
Abscisic Acid Enhances Aggregation and Fusion of Phospholipid Vesicles
William Stillwell, Blair Brengle, and Stephen R. Wassall 511
Molecular Cloning of the Nosiheptide Resistance Gene from *Streptomyces actuosus* ATCC 25421 *Donald C. Dosch, William R. Strohl, and Heinz G. Floss* 517
15-Hydroxyeicosatetraenoic Acid Dehydrogenase Activity in Microsomal Fraction of Mouse Liver Homogenate *Dai-Eun Sok, Jun Bu Kang, and Hong Dae Shin* 524
Sites of Modification of Human Angiogenin by Bromoacetate at pH 5.5
Robert Shapiro, Daniel J. Strydom, Stanislawa Weremowicz, and Bert L. Vallee 530

(Continued from inside back cover)

Effect of Retinoic Acid on cAMP-Dependent Protein Phosphorylation in Psoriatic Fibroblasts *F. Raynaud, C. Liapi, P. Gerbaud, W. B. Anderson, and D. Evain-Brion* 263

The Transcription of the Interleukin 1β Gene Is Induced with PMA and Inhibited with Dexamethasone in U937 Cells *Tsutomu Nishida, Masaaki Takano, Takuma Kawakami, Naoki Nishino, Satoru Nakai, and Yoshikatsu Hirai* 269

Thyroid Hormone Action on Glucose Transporter Activity in Astrocytes *Lois M. Roeder, Irene B. Hopkins, Jeffrey R. Kaiser, Lea Hanukoglu, and J. Tyson Tildon* 275

Purification and Characterization of a Cytochrome P450 Isozyme Isolated from the Liver of Rats Pretreated with Clofibrate *Liliane Kiffel, Chantal Célier, and Jean-Paul Leroux* 282

An Insulin Mediator Preparation Serves to Stimulate the Cyclic GMP Activated Cyclic AMP Phosphodiesterase Rather than Other Purified Insulin-Activated Cyclic AMP Phosphodiesterases *Nigel J. Pyne and Miles D. Houslay* 290

HIV-1 Protease Specificity of Peptide Cleavage Is Sufficient for Processing of gag and pol Polyproteins *Paul L. Darke, Ruth F. Nutt, Stephen F. Brady, Victor M. Garsky, Terrence M. Ciccarone, Chih-Tai Leu, Patricia K. Lumma, Roger M. Freidinger, Daniel F. Veber, and Irving S. Sigal* 297

Amino Acid Composition and Proteolytic Generated Domains of Higher Plant Tubulin *Pascal Picquot, Marylin Vantard, Iradj Amiri, Luc Fausser, and Anne-Marie Lambert* 304

Does Endothelin Mobilize Calcium from Intracellular Store Sites in Rat Aortic Vascular Smooth Muscle Cells in Primary Culture? *Nobuco Miasiro, Hiromichi Yamamoto, Hideo Kanaide, and Motoomi Nakamura* 312

Characterization of Two Glycoproteins of Human Pancreatic Juice: P35, a Truncated Protease E, and P19, Precursor of Protein X *O. Guy-Crotte, C. Barthe, D. Basso, B. Fournet, and C. Figarella* 318

N-Acylated Pentapeptide Antagonists of Substance P on Guinea Pig Ileum *Pascal Schmitt, Michel Mayer, Sylviane Magneney, Robert Michelot, and Pierre Potier* 323

Evidence that a GTP Binding Protein Regulates Phosphorylation of the CD3 Antigen in Human T Lymphocytes *Adelina A. Davies, J. Mark Hexham, Doreen A. Cantrell, and Michael J. Crumpton* 328

A Novel Action of Activin A: Stimulation of Insulin Secretion in Rat Pancreatic Islets *Yasuo Totsuka, Mari Tabuchi, Itaru Kojima, Hiroshiro Shibai, and Etsuro Ogata* 335

RNA Mediated Formation of a Phosphorothioate Diester Bond *Jamal M. Buzayan, Paul A. Feldstein, George Bruening, and Fritz Eckstein* 340

Interaction between α1 and β1 Subunits of Human Hemoglobin *Yasuko Kawamura-Konishi and Haruo Suzuki* 348

Isolation and Structural Determination of Rat Neuromedin U *Naoto Minamino, Kenji Kangawa, Mayumi Honzawa, and Hisayuki Matsuo* 355

Different Types of ADP-Ribose Protein Bonds Formed by Botulinum C2 Toxin, Botulinum ADP-Ribosyltransferase C3, and Pertussis Toxin *Klaus Aktories, Ingo Just, and Walter Rosenthal* 361

Identification of Glutathione *S*-Transferase as a Substrate and Glutathione as an Inhibitor of *in Vitro* Calmodulin-Stimulated Protein Methylation in Rat Liver Cytosol *Tom L. Neal, Lynda S. Wright, and Frank L. Siegel* 368

Discrepancies between the Affinities of Binding and Action of the Novel β-Adrenergic Agonist BRL 37344 in Rat Brown Adipose Tissue *Patrick Muzzin, Josiane Seydoux, Jean-Paul Giacobino, John-Craig Venter, and Claire Fraser* 375

Plasminogen Activator Inhibitor 2: Isolation and Characterization of the Promoter Region of the Gene *E. K. O. Kruithof and E. Cousin* 383

(Continued from outside back cover)

Almost Total Conversion of Pancreas to Liver in the Adult Rat: A Reliable Model to Study Transdifferentiation *M. S. Rao, R. S. Dwivedi, V. Subbarao, M. I. Usman, D. G. Scarpelli, M. R. Nemali, A. Yeldandi, S. Thangada, S. Kumar, and J. K. Reddy* 131

On the Mechanism of the Chromate Reduction by Glutathione: ESR Evidence for the Glutathionyl Radical and an Isolable Cr(V) Intermediate *Xianglin Shi and N. S. Dalal* 137

Rapid Purification of Inositol Monophosphate Phosphatase from Beef Brain *James L. Meek, Timothy J. Rice, and Elizabeth Anton* 143

Spacial Isolation of Protein Kinase C Activation in Thrombin Stimulated Human Platelets *Michael F. Crouch and Eduardo G. Lapetina* 149

A Lecithin:Retinol Acyltransferase Activity in Human and Rat Liver *Paul N. MacDonald and David E. Ong* 157

Brush Border Membrane Vesicles Formed from Human Duodenal Biopsies Exhibit Na^+-Dependent Concentrative L-Leucine and D-Glucose Uptake *James M. Harig, Konrad H. Soergel, Jeanne Barry, and Krishnamurthy Ramaswamy* 164

Three Growth Hormone- and Two Prolactin-Related Novel Peptides of M_r 13,000–18,000 Identified in the Anterior Pituitary *Y. N. Sinha and B. P. Jacobsen* 171

Domain Structure of Cellobiohydrolase II as Studied by Small Angle X-Ray Scattering: Close Resemblance to Cellobiohydrolase I *Peter M. Abuja, Ingrid Pilz, Marc Claeyssens, and Peter Tomme* 180

Endothelin and Ca^{2+} Agonist Bay K 8644: Different Vasoconstrictive Properties *Michel Auguet, Sylvie Delaflotte, Pierre-Etienne Chabrier, Eduardo Pirotzky, François Clostre, and Pierre Braquet* 186

Calcimedin, Calelectrin: Correlation of Relatedness *Pamela B. Moore* 193

Growth Hormone-Dependent Insulin-like Growth Factor (IGF) Binding Protein Both Inhibits and Potentiates IGF-I-Stimulated DNA Synthesis in Human Skin Fibroblasts *John S. M. De Mellow and Robert C. Baxter* 199

Synthesis of Nuclear Lamins in BHK-21 Cells Synchronized with Aphidicolin *Sylvain Foisy and Viviane Bibor-Hardy* 205

Potassium Ion-Dependent Proton Efflux and Depolarization from Spleen Lysosomes *Yoshinori Moriyama* 211

Release of Peptide Leukotrienes from Rat Kupffer Cells *Yoshihide Sakagami, Yasuhiro Mizoguchi, Shuichi Seki, Kenzo Kobayashi, Seiji Morisawa, and Sukeo Yamamoto* 217

DNA-Binding Proteins in Protein Kinase C Preparations *Alessandro Testori, Charles S. T. Hii, Agnes Fournier, Leigh A. Burgoyne, and Andrew W. Murray* 222

Water Immersion Increases the Concentration of the Immunoreactive N-Terminal Fragment of Proatrial Natriuretic Factor in Human Plasma *Alexander L. Gerbes and Angelika M. Vollmar* 228

The Effect of Cyclosporin A on the Growth and Prolactin Binding to Nb-2 Rat Lymphoma Cells *Shobha Varma and Kurt E. Ebner* 233

Norepinephrine Stimulates the Production of Inositol Trisphosphate and Inositol Tetrakisphosphate in Rat Aorta *Vivian Pijuan and Irene Litosch* 240

Yeast *KEX2* Gene Encodes an Endopeptidase Homologous to Subtilisin-like Serine Proteases *Kensaku Mizuno, Tomoko Nakamura, Takehiro Ohshima, Shoji Tanaka, and Hisayuki Matsuo* 246

The Calcium Channel Antagonist ω-Conotoxin Inhibits Secretion from Peptidergic Nerve Terminals *G. Dayanithi, N. Martin-Moutot, S. Barlier, D. A. Colin, M. Kretz-Zaepfel, F. Couraud, and J. J. Nordmann* 255

BIOCHEMICAL AND BIOPHYSICAL RESEARCH COMMUNICATIONS

CONTENTS

Volume 156, Number 1, October 14, 1988

AUTHOR INDEX, Volume 156, Number 1, October 14, 1988 iii

HL-60 Cells Become Resistant toward Antitumor Ether-Linked Phospholipids following Differentiation into a Granulocytic Form *David S. Vallari, Zigrida L. Smith, and Fred Snyder* 1

Bis-Pyridoxal Polyphosphates: A New Class of Specific Intramolecular Crosslinking Agents for Hemoglobin *Ruth E. Benesch and Suzanna Kwong* 9

Physiological Concentrations of Atrial Natriuretic Factor Stimulate Human Erythroid Progenitors *in Vitro* *Eero Niskanen and Alex J. Baertschi* 15

Physicochemical Characterization of [^{3}H]DHEA Binding in Rat Liver *Mohammed Kalimi and William Regelson* 22

Proteolytic Activity in the Insulin Receptor *Eleazar C. Vega-SaenzdeMiera and Boanerges Rubalcava* 30

A Genuine Organ Specific Alcohol Dehydrogenase from Hamster Testes: Isolation, Characterization, and Developmental Changes *Wing-Ming Keung* 38

Anti-HLA Class I Monoclonal Antibody Effect on PKC Kinetics in PHA Activated Human Peripheral Blood Mononuclear and E^+ Cells *Licia Poltronieri, Edon Melloni, Michele Rubini, Rita Selvatici, Cristina Mazzilli, Roberto Baricordi, and Enrico Gandini* 46

Reconstitution of Partially Purified Opioid Receptors with a GTP-Binding Protein *Toshiyuki Fujioka, Fumiko Inoue, Sachiyo Sumita, and Masayuki Kuriyama* 54

Identification of a High-Affinity Receptor for Interleukin-1β in Rat Brain *Goro Katsuura, Paul E. Gottschall, and Akira Arimura* 61

Exon–Intron Organization of a Gene for Pregnancy-Specific β_1-Glycoprotein, a Subfamily Member of CEA Family: Implications for Its Characteristic Repetitive Domains and C-Terminal Sequences *Shinzo Oikawa, Chikako Inuzuka, Goro Kosaki, and Hiroshi Nakazato* 68

High Affinity Receptors for Atrial Natriuretic Factor in PC12 Cells *A. Rathinavelu and G. E. Isom* 78

Evidence for Light-Induced Lysine Conformational Changes during the Primary Event of the Bacteriorhodopsin Photocycle *Earl McMaster and Aaron Lewis* 86

Affinity Purification of Human Deoxycytidine Kinase: Avoidance of Structural and Kinetic Artifacts Arising from Limited Proteolysis *Min-Young Kim, Seiichiro Ikeda, and David H. Ives* 92

A Consensus Sequence in the N-Terminus of Exported Proteins: Resemblance with Metal Binding Domains and Implications in Protein Translocation across Membranes *Panagiotis A. Tsonis, Janusz M. Sowadski, and Paul F. Goetinck* 99

Mitogenic Activity in Ovine Uterine Fluids: Characterization of a Growth Factor Activity Which Specifically Stimulates Myoblast Proliferation *R. Curtis Bird, Frank F. Bartol, Harlow Daron, David A. Stringfellow, and M. Gatz Riddell* 108

Chemical Characterization by Protein Sequence Analysis of the Bovine Estrogen Receptor *Thomas Ratajczak, Martine J. Brockway, Roland Hähnel, Robert L. Moritz, and Richard J. Simpson* 116

Dermorphin Analogs: Resistance to *in Vitro* Enzymatic Degradation Is Not Always Increased by Additional D-Amino Acid Substitutions *Krzysztof Darlak, Deanne E. Benovitz, Arno F. Spatola, and Zbigniew Grzonka* 125

(Continued on inside back cover)